Scientific and Technical Aerospace Reports

Volume 40
January 11, 2002

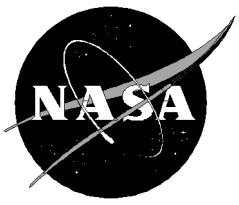

National Aeronautics and Space Administration
Langley Research Center

Scientific and Technical Information Program Office

The NASA STI Program Office . . . in Profile

Since its founding, NASA has been dedicated to the advancement of aeronautics and space science. The NASA Scientific and Technical Information (STI) Program Office plays a key part in helping NASA maintain this important role.

The NASA STI Program Office is operated by Langley Research Center, the lead center for NASA's scientific and technical information. The NASA STI Program Office provides access to the NASA STI Database, the largest collection of aeronautical and space science STI in the world. The Program Office is also NASA's institutional mechanism for disseminating the results of its research and development activities. These results are published by NASA in the NASA STI Report Series, which includes the following report types:

- TECHNICAL PUBLICATION. Reports of completed research or a major significant phase of research that present the results of NASA programs and include extensive data or theoretical analysis. Includes compilations of significant scientific and technical data and information deemed to be of continuing reference value. NASA's counterpart of peer-reviewed formal professional papers but has less stringent limitations on manuscript length and extent of graphic presentations.

- TECHNICAL MEMORANDUM. Scientific and technical findings that are preliminary or of specialized interest, e.g., quick release reports, working papers, and bibliographies that contain minimal annotation. Does not contain extensive analysis.

- CONTRACTOR REPORT. Scientific and technical findings by NASA-sponsored contractors and grantees.

- CONFERENCE PUBLICATION. Collected papers from scientific and technical conferences, symposia, seminars, or other meetings sponsored or cosponsored by NASA.

- SPECIAL PUBLICATION. Scientific, technical, or historical information from NASA programs, projects, and missions, often concerned with subjects having substantial public interest.

- TECHNICAL TRANSLATION. English-language translations of foreign scientific and technical material pertinent to NASA's mission.

Specialized services that complement the STI Program Office's diverse offerings include creating custom thesauri, building customized databases, organizing and publishing research results . . . even providing videos.

For more information about the NASA STI Program Office, see the following:

- Access the NASA STI Program Home Page at ***http://www.sti.nasa.gov***

- E-mail your question via the Internet to help@sti.nasa.gov

- Fax your question to the NASA STI Help Desk at (301) 621-0134

- Telephone the NASA STI Help Desk at (301) 621-0390

- Write to:
  NASA STI Help Desk
  NASA Center for AeroSpace Information
  7121 Standard Drive
  Hanover, MD 21076-1320

Introduction

Scientific and Technical Aerospace Reports (STAR) is an electronic abstract journal, listing citations with abstracts for aerospace-related reports obtained from worldwide sources. It is electronically published biweekly and announces documents that have recently been entered into the NASA Scientific and Technical Information (STI) Database. The documents are of the following types:

- NASA, NASA contractor, and NASA grantee reports;
- Reports issued by other U.S. Government agencies, domestic and foreign institutions, universities, and private firms;
- Translations in report form;
- NASA-owned patents and patent applications
- Other U.S. Government agency and foreign patents and patent applications
- Domestic and foreign dissertations and theses.

Also included are two indexes, Subject Term and Personal Author. The Subject Term Index is generated from the *NASA Thesaurus* terms associated and listed with each document.

STAR subject coverage includes all aspects of aeronautics and space research and development, supporting basic and applied research, and applications. Aerospace aspects of Earth resources, energy development, conservation, oceanography, environmental protection, urban transportation, and other topics of high national priority are also covered.

Abstracts in *STAR* are categorized by 10 major subject divisions that are divided further into 76 specific subject categories. The subject divisions and categories are listed in the Table of Contents together with a note for each that defines its scope and provides any cross-references.

SCAN Goes Electronic!

If you have electronic mail or if you can access the Internet, you can view biweekly issues of *SCAN* from your desktop absolutely free!

Electronic SCAN takes advantage of computer technology to inform you of the latest worldwide, aerospace-related, scientific and technical information that has been published.

No more waiting while the paper copy is printed and mailed to you. You can view *Electronic SCAN* the same day it is released—up to 191 topics to browse at your leisure. When you locate a publication of interest, you can print the announcement. You can also go back to the *Electronic SCAN* home page and follow the ordering instructions to quickly receive the full document.

Start your access to *Electronic SCAN* today. Over 1,000 announcements of new reports, books, conference proceedings, journal articles...and more—available to your computer every two weeks.

For Internet access to *E-SCAN*, use any of the following addresses:

http://www.sti.nasa.gov
ftp.sti.nasa.gov
gopher.sti.nasa.gov

Determine the SCAN topics you wish to receive and send an e-mail to **listserv@sti.nasa.gov**. Leave the subject line blank and enter a subscribe command, denoting which topic you want and your name in the message area, formatted as follows:

Subscribe SCAN–02–01 Jane Doe

For additional information, e-mail a message to **help@sti.nasa.gov**.

Phone: (301) 621-0390

Fax: (301) 621-0134

Write: NASA STI Help Desk
NASA Center for AeroSpace Information
7121 Standard Drive
Hanover, MD 21076-1320

Looking just for *Aerospace Medicine and Biology* reports?

Although hard copy distribution has been discontinued, you can still receive these vital announcements through your *E-SCAN* subscription. Just **Subscribe SCAN-AEROMED Jane Doe** in the message area of your e-mail to **listserv@sti.nasa.gov**.

Table of Contents

Subject Divisions

Document citations are grouped first by the following divisions. Select a division title to view the category-level Table of Contents.

A. Aeronautics
B. Astronautics
C. Chemistry and Materials
D. Engineering
E. Geosciences
F. Life Sciences
G. Mathematical and Computer Sciences
H. Physics
I. Social and Information Sciences
J. Space Sciences
K. General

Indexes

Two indexes are available. You may use the find command under the tools menu while viewing the PDF file for direct match searching on any text string. You may also select either of the two indexes provided for searching on *NASA Thesaurus* subject terms and personal author names.

Subject Term Index
Personal Author Index

Document Availability

Select **Availability Info** for important information about NASA Scientific and Technical Information (STI) Program Office products and services, including registration with the NASA Center for AeroSpace Information (CASI) for access to the NASA CASI TRS (Technical Report Server), and availability and pricing information for cited documents.

Subject Categories of the Division A. Aeronautics

Select a category to view the collection of records cited. N.A. means no abstracts in that category.

01 Aeronautics (General) 1

Includes general research topics related to manned and unmanned aircraft and the problems of flight within the Earth's atmosphere. Also includes manufacturing, maintenance, and repair of aircraft. For specific topics in aeronautics see *categories 02 through 09*. For information related to space vehicles see *12 Astronautics*.

02 Aerodynamics 1

Includes aerodynamics of flight vehicles, test bodies, airframe components and combinations, wings, and control surfaces. Also includes aerodynamics of rotors, stators, fans and other elements of turbomachinery. For related information, see also *34 Fluid Mechanics and Heat Transfer.*

03 Air Transportation and Safety 3

Includes passenger and cargo air transport operations; aircraft ground operations; flight safety and hazards; and aircraft accidents. Systems and hardware specific to ground operations of aircraft and to airport construction are covered in *09 Research and Support Facilities (Air)*. Air traffic control is covered in *04 Aircraft Communications and Navigation*. For related information see also *16 Space Transportation and Safety*; and *85 Technology Utilization and Surface Transportation*.

04 Aircraft Communications and Navigation 9

Includes all modes of communication with and between aircraft; air navigation systems (satellite and ground based); and air traffic control. For related information see also *06 Avionics and Aircraft Instrumentation*; *17 Space Communications; Spacecraft Communications, Command and Tracking*, and *32 Communications and Radar.*

05 Aircraft Design, Testing and Performance 9

Includes all stages of design of aircraft and aircraft structures and systems. Also includes aircraft testing, performance, and evaluation, and aircraft and flight simulation technology. For related information, see also *18 Spacecraft Design, Testing and Performance* and *39 Structural Mechanics*. For land transportation vehicles, see *85 Technology Utilization and Surface Transportation*.

06 Avionics and Aircraft Instrumentation 12

Includes all avionics systems, cockpit and cabin display devices, and flight instruments intended for use in aircraft. For relatead information see also *04 Aircraft Communications and Navigation; 08 Aircraft Stability and Control; 19 Spacecraft Instrumentation and Astrionics; and 35 Instrumentation and Photography.*

07 Aircraft Propulsion and Power 12

Includes prime propulsion systems and systems components, e.g., gas turbine engines and compressors; and onboard auxiliary power plants for aircraft. For related information see also *20 Spacecraft Propulsion and Power, 28 Propellants and Fuels*, and *44 Energy Production and Conversion*.

09 Research and Support Facilities (Air) 13

Includes airports, runways, hangers, and aircraft repair and overhaul facilities, wind tunnels, water tunnels, and shock tubes; flight simulators; and aircraft engine test stands. Also includes airport ground equipment and systems. For airport ground operation see *03 Air Transportation and Safety.* For astronautical facilities see *14 Ground Support Systems and Facilities (Space).*

Subject Categories of the Division B. Astronautics

Select a category to view the collection of records cited. N.A. means no abstracts in that category.

14 Ground Support Systems and Facilities (Space) 15

Includes launch complexes, research and production facilities; ground support equipment, e.g., mobile transporters; and test chambers and simulators. Also includes extraterrestrial bases and supporting equipment. For related information see also *09 Research and Support Facilities (Air).*

15 Launch Vehicles and Launch Operations 15

Includes all classes of launch vehicles, launch/space vehicle systems, and boosters; and launch operations. For related information see also *18 Spacecraft Design, Testing, and Performance; and 20 Spacecraft Propulsion and Power.*

16 Space Transportation and Safety 17

Includes passenger and cargo space transportation, e.g., shuttle operations; and space rescue techniques. For related information, see also *03 Air Transportation and Safety* and *15 Launch Vehicles and Launch Vehicles,* and *18 Spacecraft Design, Testing and Performance*. For space suits, see *54 Man/System Technology and Life Support*.

18 Spacecraft Design, Testing and Performance 21

Includes satellites; space platforms; space stations; spacecraft systems and components such as thermal and environmental controls; and spacecraft control and stability characteristics. For life support systems, see *54 Man/System Technology and Life Support.* For related information, see also *05 Aircraft Design, Testing and Performance, 39 Structural Mechanics, and 16 Space Transportation and Safety.*

19 Spacecraft Instrumentation and Astrionics 23

Includes the design, manufacture, or use of devices for the purpose of measuring, detecting, controlling, computing, recording, or processing data related to the operation of space vehicles or platforms. For related information, see also *06 Aircraft Instrumentation and Avionics;* For spaceborne instruments not integral to the vehicle itself see *35 Instrumentation and Photography*; For spaceborne telescopes and other astronomical instruments see *89 Astronomy, Instrumentation and Photography*; For spaceborne telescopes and other astronomical instruments see *89 Astronomy.*

20 Spacecraft Propulsion and Power 23

Includes main propulsion systems and components, e.g., rocket engines; and spacecraft auxiliary power sources. For related information, see also *07 Aircraft Propulsion and Power; 28 Propellants and Fuels; 15 Launch Vehicles and Launch Operations;* and *44 Energy Production and Conversion*.

Subject Categories of the Division C. Chemistry and Materials

Select a category to view the collection of records cited. N.A. means no abstracts in that category.

23 Chemistry and Materials (General) 27

Includes general research topics related to the composition, properties, structure, and use of chemical compounds and materials as they relate to aircraft, launch vehicles, and spacecraft. For specific topics in chemistry and materials see *categories 24 through 29*. For astrochemistry see category *90 Astrophysics*.

24 Composite Materials 39

Includes physical, chemical, and mechanical properties of laminates and other composite materials.

25 Inorganic, Organic, and Physical Chemistry 42

Includes the analysis, synthesis, and use inorganic and organic compounds; combustion theory; electrochemistry; and photochemistry. For related information see also *34 Fluid Dynamics and Thermodynamics, For astrochemistry see category 90 Astrophysics*.

26 Metals and Metallic Materials 68

Includes physical, chemical, and mechanical properties of metals and metallic materials; and metallurgy.

27 Nonmetallic Materials 83

Includes physical, chemical, and mechanical properties of plastics, elastomers, lubricants, polymers, textiles, adhesives, and ceramic materials. For composite materials see *24 Composite Materials.*

28 Propellants and Fuels 97

Includes rocket propellants, igniters and oxidizers; their storage and handling procedures; and aircraft fuels. For nuclear fuels see *73 Nuclear Physics*. For related information see also *07 Aircraft Propulsion and Power, 20 Spacecraft Propulsion and Power*, and *44 Energy Production and Conversion*.

29 Space Processing 115

Includes space-based development of materials, compounds, and processes for research or commercial application. Also includes the development of materials and compounds in simulated reduced–gravity environments. For legal aspects of space commercialization see *84 Law, Political Science and Space Policy.*

Subject Categories of the Division D. Engineering

Select a category to view the collection of records cited. N.A. means no abstracts in that category.

31 Engineering (General) 116

Includes general research topics to engineering and applied physics, and particular areas of vacuum technology, industrial engineering, cryogenics, and fire prevention. For specific topics in engineering see *categories 32 through 39*.

32 Communications and Radar 123

Includes radar; radio, wire, and optical communications; land and global communications; communications theory. For related information see also *04 Aircraft Communications and Navigation;* and *17 Space Communications, Spacecraft Communications, Command and Tracking;* for search and rescue see *03 Air Transportation and Safety,* and *16 Space Transportation and Safety.*

33 Electronics and Electrical Engineering 129

Includes development, performance, and maintainability of electrical/electronic devices and components; related test equipment. and microelectronics and integrated circuitry. For related information see also *60 Computer Operations and Hardware;* and *76 Solid-State Physics*. For communications equipment and devices see *32 Communications and Radar.*

34 Fluid Mechanics and Thermodynamics 141

Includes fluid dynamics and kinematics and all forms of heat transfer; boundary layer flow; hydrodynamics; hydraulics; fluidics; mass transfer and ablation cooling. For related information see also *02 Aerodynamics.*

35 Instrumentation and Photography 154

Includes remote sensors; measuring instruments and gauges; detectors; cameras and photographic supplies; and holography. For aerial photography see *43 Earth Resources and Remote Sensing*. For related information see also *06 Avionics and Aircraft Instrumentation;* and *19 Spacecraft Instrumentation*.

36 Lasers and Masers 159

Includes lasing theory, laser pumping techniques, maser amplifiers, laser materials, and the assessment of laser and maser outputs. For cases where the application of the laser or maser is emphasized see also the specific category where the application is treated. For related information see also *76 Solid-State Physics*.

37 Mechanical Engineering 164

Includes mechanical devices and equipment; machine elements and processes. For cases where the application of a device or the host vehicle is emphasized see also the specific category where the application or vehicle is treated. For robotics see *63 Cybernetics, Artificial Intelligence, and Robotics*; and *54 Man/System Technology and Life Support*.

38 Quality Assurance and Reliability 169

Includes approaches to, and methods for reliability analysis and control, inspection, maintainability, and standardization.

39 Structural Mechanics 173

Includes structural element design, analysis and testing; dynamic responses of structures; weight analysis; fatigue and other structural properties; and mechanical and thermal stresses in structure. For applications see *05 Aircraft Design, Testing and Performance* and *18 Spacecraft Design, Testing and Performance*.

Subject Categories of the Division E. Geosciences

Select a category to view the collection of records cited. N.A. means no abstracts in that category.

42 Geosciences (General) 178

Includes general research topics related to the Earth sciences, and the specific areas of petrology, minerology, and general geology. For other specific topics in geosciences see *categories 42 through 48*.

43 Earth Resources and Remote Sensing 187

Includes remote sensing of earth features, phenomena and resources by aircraft, balloon, rocket, and spacecraft; analysis or remote sensing data and imagery; development of remote sensing products; photogrammetry; and aerial photographs. For instrumentation see *35 Instrumentation and Photography.*

44 Energy Production and Conversion 190

Includes specific energy conversion systems, e.g., fuel cells; and solar, geothermal, windpower, and waterwave conversion systems; energy storage; and traditional power generators. For technologies related to nuclear energy production see *73 Nuclear Physics*. For related information see also *07 Aircraft Propulsion and Power; 20 Spacecraft Propulsion and Power,* and *28 Propellants and Fuels*.

45 Environment Pollution 210

Includes atmospheric, water, soil, noise, and thermal pollution.

46 Geophysics 233

Includes earth structure and dynamics, aeronomy; upper and lower atmosphere studies; ionospheric and magnetospheric physics; and geomagnetism. For related information see *47 Meteorology and Climatology;* and *93 Space Radiation*.

47 Meteorology and Climatology 240

Includes weather observation forecasting and modification.

48 Oceanography 255

Includes the physical, chemical and biological aspects of oceans and seas; ocean dynamics, and marine resources. For related information see also *43 Earth Resources and Remote Sensing*.

Subject Categories of the Division F. Life Sciences

Select a category to view the collection of records cited. N.A. means no abstracts in that category.

51 Life Sciences (General) 260

Includes general research topics related to plant and animal biology (non–human); ecology; microbiology; and also the origin, development, structure, and maintenance, of animals and plants in space and related environmental conditions. For specific topics in life sciences see *categories 52 through 55*.

52 Aerospace Medicine 262

Includes the biological and physiological effects of atmospheric and space flight (weightlessness, space radiation, acceleration, and altitude stress) on the human being; and the prevention of adverse effects on those environments. For psychological and behavioral effects of aerospace environments see *53 Behavioral Sciences*. For the effects of space on animals and plants see *51 Life Sciences*.

53 Behavioral Sciences 263

Includes psychological factors; individual and group behavior; crew training and evaluation; and psychiatric research.

54 Man/System Technology and Life Support 264

Includes human factors engineering; bionics, man–machine, life support, space suits and protective clothing. For related information see also *16 Space Transportation* and *52 Aerospace Medicine*..

55 Exobiology 266

Includes astrobiology; planetary biology; and extraterrestrial life. For the biological effects of aerospace environments on humans see *52 Aerospace medicine*; on animals and plants see *51 Life Sciences*. For psychological and behavioral effects of aerospace environments see *53 Behavioral Science*.

Subject Categories of the Division G. Mathematical and Computer Sciences

Select a category to view the collection of records cited. N.A. means no abstracts in that category.

59 Mathematical and Computer Sciences (General) 352

Includes general topics and overviews related to mathematics and computer science. For specific topics in these areas see *categories 60 through 67*.

60 Computer Operations and Hardware 355

Includes hardware for computer graphics, firmware and data processing. For components see *33 Electronics and Electrical Engineering*. For computer vision see *63 Cybernetics, Artificial Intelligence and Robotics*.

61 Computer Programming and Software 357

Includes software engineering, computer programs, routines, algorithms, and specific applications, e.g., CAD/CAM. For computer software applied to specific applications, see also the associated category.

62 Computer Systems 370

Includes computer networks and distributed processing systems. For information systems see *82 Documentation and Information Science*. For computer systems applied to specific applications, see the associated category.

63 Cybernetics, Artificial Intelligence and Robotics 371

Includes feedback and control theory, information theory, machine learning, and expert systems. For related information see also *54 Man/System Technology and Life Support.*

64 Numerical Analysis 375

Includes iteration, differential and difference equations, and numerical approximation.

65 Statistics and Probability 377

Includes data sampling and smoothing; Monte Carlo method; time series and analysis; and stochastic processes.

66 Systems Analysis and Operations Research 379

Includes mathematical modeling of systems; network analysis; mathematical programming; decision theory; and game theory.

67 Theoretical Mathematics 379

Includes algebra, functional analysis, geometry, topology set theory, group theory and and number theory.

Subject Categories of the Division H. Physics

Select a category to view the collection of records cited. N.A. means no abstracts in that category.

70 Physics (General) 380

Includes general research topics related to mechanics, kinetics, magnetism, and electrodynamics. For specific areas of physics see *categories 71 through 77*. For related instrumentation see *35 Instrumenta-*

tion and Photography; for geophysics, astrophysics or solar physics see *46 Geophysics, 90 Astrophysics,* or *92 Solar Physics*.

71 Acoustics **417**

Includes sound generation, transmission, and attenuation. For noise pollution see *45 Environment Pollution.* For aircraft noise see also *02 Aerodynamics* and *07 Aircraft Propulsion Propulsion and Power.*

72 Atomic and Molecular Physics **418**

Includes atomic and molecular structure, electron properties, and atomic and molecular spectra. For elementary particle physics see *73 Nuclear Physics*.

73 Nuclear Physics **428**

Includes nuclear particles; and reactor theory. For space radiation see *93 Space Radiation*. For atomic and molecular physics see *72 Atomic and Molecular Physics*. For elementary particle physics see *77 Physics of Elementary Particles and Fields*. For nuclear astrophysics see *90 Astrophysics*.

74 Optics **443**

Includes light phenomena and the theory of optical devices. For lasers see *36 Lasers and Masers*.

75 Plasma Physics **460**

Includes magnetohydrodynamics and plasma fusion. For ionospheric plasmas see *46 Geophysics.* For space plasmas see *90 Astrophysics*.

76 Solid-State Physics **470**

Includes condensed matter physics, crystallography, and superconductivity. For related information see also *33 Electronics and Electrical Engineering* and *36 Lasers and Masers*.

77 Physics of Elementary Particles and Fields **495**

Includes quantum mechanics; theoretical physics; and statistical mechanics. For related information see also *72 Atomic and Molecular Physics, 73 Nuclear Physics, and 25 Inorganic, Organic and Physical Chemistry.*

Subject Categories of the Division I. Social and Information Sciences

Select a category to view the collection of records cited. N.A. means no abstracts in that category.

81 Administration and Management **507**

Includes management planning and research.

82 Documentation and Information Science 516

Includes information management; information storage and retrieval technology; technical writing; graphic arts; and micrography. For computer documentation see *61 Computer Programming and Software*.

84 Law, Political Science and Space Policy 519

Includes aviation law; space law and policy; international law; international cooperation; and patent policy.

85 Technology Utilization and Surface Transportation 520

Includes aerospace technology transfer; urban technology; surface and mass transportation. For related information see also *03 Air Transportation and Safety, 16 Space Transportation and Safety, and 44 Energy Production and Conversion.* For specific technology transfer applications see also the category where the subject is treated.

Subject Categories of the Division J. Space Sciences

Select a category to view the collection of records cited. N.A. means no abstracts in that category.

88 Space Sciences (General) 520

Includes general research topics related to the natural space sciences. For specific topics in space sciences see *categories 89 through 93*.

89 Astronomy 521

Includes observations of celestial bodies, astronomical instruments and techniques; radio, gamma-ray, x–ray, ultraviolet, and infrared astronomy; and astrometry.

90 Astrophysics 523

Includes cosmology; celestial mechanics; space plasmas; and interstellar and interplanetary gases and dust.

91 Lunar and Planetary Science and Exploration 528

Includes planetology; selenology; meteorites; comets; and manned and unmanned planetary and lunar flights. For spacecraft design or space stations see *18 Spacecraft Design, Testing and Performance*.

92 Solar Physics 533

Includes solar activity, solar flares, solar radiation and sunspots. For related information see *93 Space Radiation.*

93 Space Radiation 536

Includes cosmic radiation; and inner and outer Earth radiation belts. For biological effects of radiation on plants and animals see *52 Aerospace Medicine*. For theory see *73 Nuclear Physics.*

Subject Categories of the Division K. General

Select a category to view the collection of records cited. N.A. means no abstracts in that category.

99 General 537

Includes aeronautical, astronautical, and space science related histories, biographies, and pertinent reports too broad for categorization; histories or broad overviews of NASA programs such as Apollo, Gemini, and Mercury spacecraft, Earth Resources Technology Satellite (ERTS), and Skylab; NASA appropriations hearings.

Document Availability Information

The mission of the NASA Scientific and Technical (STI) Program Office is to quickly, efficiently, and cost-effectively provide the NASA community with desktop access to STI produced by NASA and the world's aerospace industry and academia. In addition, we will provide the aerospace industry, academia, and the taxpayer access to the intellectual scientific and technical output and achievements of NASA.

Eligibility and Registration for NASA STI Products and Services

The NASA STI Program offers a wide variety of products and services to achieve its mission. Your affiliation with NASA determines the level and type of services provided by the NASA STI Program. To assure that appropriate level of services are provided, NASA STI users are requested to register at the NASA Center for AeroSpace Information (CASI). Please contact NASA CASI in one of the following ways:

E-mail:	help@sti.nasa.gov
Fax:	301-621-0134
Phone:	301-621-0390
Mail:	ATTN: Registration Services NASA Center for AeroSpace Information 7121 Standard Drive Hanover, MD 21076-1320

Limited Reproducibility

In the database citations, a note of limited reproducibility appears if there are factors affecting the reproducibility of more than 20 percent of the document. These factors include faint or broken type, color photographs, black and white photographs, foldouts, dot matrix print, or some other factor that limits the reproducibility of the document. This notation also appears on the microfiche header.

NASA Patents and Patent Applications

Patents owned by NASA are announced in the STI Database. Printed copies of patents (which are not microfiched) are available for purchase from the U.S. Patent and Trademark Office.

When ordering patents, the U.S. Patent Number should be used, and payment must be remitted in advance, by money order or check payable to the Commissioner of Patents and Trademarks. Prepaid purchase coupons for ordering are also available from the U.S. Patent and Trademark Office.

Patents and patent applications owned by NASA are available for licensing. Requests for licensing terms and further information should be addressed to:

National Aeronautics and Space Administration
Associate General Counsel for Intellectual Property
Code GP
Washington, DC 20546-0001

Sources for Documents

One or more sources from which a document announced in the STI Database is available to the public is ordinarily given on the last line of the citation. The most commonly indicated sources and their acronyms or abbreviations are listed below, with an Addresses of Organizations list near the back of this section. If the publication is available from a source other than those listed, the publisher and his address will be displayed on the availability line or in combination with the corporate source.

Avail: NASA CASI. Sold by the NASA Center for AeroSpace Information. Prices for hard copy (HC) and microfiche (MF) are indicated by a price code following the letters HC or MF in the citation. Current values are given in the NASA CASI Price Code Table near the end of this section.

Note on Ordering Documents: When ordering publications from NASA CASI, use the document ID number or other report number. It is also advisable to cite the title and other bibliographic identification.

Avail: SOD (or GPO). Sold by the Superintendent of Documents, U.S. Government Printing Office, in hard copy.

Avail: BLL (formerly NLL): British Library Lending Division, Boston Spa, Wetherby, Yorkshire, England. Photocopies available from this organization at the price shown. (If none is given, inquiry should be addressed to the BLL.)

Avail: DOE Depository Libraries. Organizations in U.S. cities and abroad that maintain collections of Department of Energy reports, usually in microfiche form, are listed in Energy Research Abstracts. Services available from the DOE and its depositories are described in a booklet, *DOE Technical Information Center—Its Functions and Services* (TID-4660), which may be obtained without charge from the DOE Technical Information Center.

Avail: ESDU. Pricing information on specific data, computer programs, and details on ESDU International topic categories can be obtained from ESDU International.

Avail: Fachinformationszentrum Karlsruhe. Gesellschaft für wissenschaftlich-technische Information mbH 76344 Eggenstein-Leopoldshafen, Germany.

Avail: HMSO. Publications of Her Majesty's Stationery Office are sold in the U.S. by Pendragon House, Inc. (PHI), Redwood City, CA. The U.S. price (including a service and mailing charge) is given, or a conversion table may be obtained from PHI.

Avail: Issuing Activity, or Corporate Author, or no indication of availability. Inquiries as to the availability of these documents should be addressed to the organization shown in the citation as the corporate author of the document.

Avail: NASA Public Document Rooms. Documents so indicated may be examined at or purchased from the National Aeronautics and Space Administration (JBD-4), Public Documents Room (Room 1H23), Washington, DC 20546-0001, or public document rooms located at NASA installations, and the NASA Pasadena Office at the Jet Propulsion Laboratory.

Avail: NTIS. Sold by the National Technical Information Service. Initially distributed microfiche under the NTIS SRIM (Selected Research in Microfiche) are available. For information concerning this service, consult the NTIS Subscription Section, Springfield, VA 22161.

Avail: Univ. Microfilms. Documents so indicated are dissertations selected from Dissertation Abstracts and are sold by University Microfilms as xerographic copy (HC) and microfilm. All requests should cite the author and the Order Number as they appear in the citation.

Avail: US Patent and Trademark Office. Sold by Commissioner of Patents and Trademarks, U.S. Patent and Trademark Office, at the standard price of $1.50 each, postage free.

Avail: (US Sales Only). These foreign documents are available to users within the United States from the National Technical Information Service (NTIS). They are available to users outside the United States through the International Nuclear Information Service (INlS) representative in their country, or by applying directly to the issuing organization.

Avail: USGS. Originals of many reports from the U.S. Geological Survey, which may contain color illustrations, or otherwise may not have the quality of illustrations preserved in the microfiche or facsimile reproduction, may be examined by the public at the libraries of the USGS field offices whose addresses are listed on the Addresses of Organizations page. The libraries may be queried concerning the availability of specific documents and the possible utilization of local copying services, such as color reproduction.

Addresses of Organizations

British Library Lending Division
Boston Spa, Wetherby, Yorkshire
England

Commissioner of Patents and Trademarks
U.S. Patent and Trademark Office
Washington, DC 20231

Department of Energy
Technical Information Center
P.O. Box 62
Oak Ridge, TN 37830

European Space Agency–
Information Retrieval Service ESRIN
Via Galileo Galilei
00044 Frascati (Rome) Italy

ESDU International
27 Corsham Street
London
N1 6UA
England

Fachinformationszentrum Karlsruhe
Gesellschaft für wissenschaftlich–technische
Information mbH
76344 Eggenstein–Leopoldshafen, Germany

Her Majesty's Stationery Office
P.O. Box 569, S.E. 1
London, England

NASA Center for AeroSpace Information
7121 Standard Drive
Hanover, MD 21076-1320

(NASA STI Lead Center)
National Aeronautics and Space Administration
Scientific and Technical Information Program Office
Langley Research Center – MS157
Hampton, VA 23681

National Technical Information Service
5285 Port Royal Road
Springfield, VA 22161

Pendragon House, Inc.
899 Broadway Avenue
Redwood City, CA 94063

Superintendent of Documents
U.S. Government Printing Office
Washington, DC 20402

University Microfilms
A Xerox Company
300 North Zeeb Road
Ann Arbor, MI 48106

University Microfilms, Ltd.
Tylers Green
London, England

U.S. Geological Survey Library National Center
MS 950
12201 Sunrise Valley Drive
Reston, VA 22092

U.S. Geological Survey Library
2255 North Gemini Drive
Flagstaff, AZ 86001

U.S. Geological Survey
345 Middlefield Road
Menlo Park, CA 94025

U.S. Geological Survey Library
Box 25046
Denver Federal Center, MS914
Denver, CO 80225

NASA CASI Price Tables — Effective October 1, 2001
Prices are subject to change without notice

Hardcopy & Microfiche Prices			
Code	*NASA*	*U.S.**	*International**
A01	$9.50	$9.50	$19.00
A02	$13.50	$14.50	$29.00
A03	$24.50	$27.50	$55.00
A04	$27.00	$30.50	$61.00
A05	$28.50	$32.50	$65.00
A06	$31.00	$35.50	$71.00
A07	$34.50	$39.50	$79.00
A08	$37.50	$43.00	$86.00
A09	$42.50	$49.00	$98.00
A10	$45.50	$53.00	$106.00
A11	$48.50	$56.50	$113.00
A12	$52.50	$61.00	$122.00
A13	$55.50	$65.00	$130.00
A14	$57.50	$67.00	$134.00
A15	$59.50	$69.50	$139.00
A16	$61.50	$72.00	$144.00
A17	$63.50	$74.50	$149.00
A18	$67.00	$78.50	$157.00
A19	$69.00	$81.00	$162.00
A20	$71.00	$83.50	$167.00
A21	$73.00	$86.00	$172.00
A22	$78.50	$92.50	$185.00
A23	$80.50	$95.00	$190.00
A24	$82.50	$97.00	$194.00
A25	$84.50	$99.50	$199.00
A99	Contact NASA CASI		

Exception Prices			
Code	*NASA*	*U.S.**	*International**
E01	$102.50	$121.00	$242.00
E02	$111.00	$131.50	$263.00
E03	$120.50	$143.00	$286.00
E04	$130.00	$154.00	$308.00
E05	$139.50	$165.50	$331.00
E06	$148.00	$176.00	$352.00
E07	$157.50	$187.00	$374.00
E08	$167.00	$198.50	$397.00
E09	$175.50	$209.00	$418.00
E10	$185.00	$220.00	$440.00
E11	$194.50	$231.50	$463.00
E12	$202.50	$241.00	$482.00
E13	$212.00	$252.50	$505.00
E14	$221.50	$264.00	$528.00
E15	$231.00	$275.50	$551.00
E16	$239.50	$285.50	$571.00
E17	$249.00	$297.00	$594.00
E18	$258.50	$308.50	$617.00
E19	$267.00	$318.50	$637.00
E20	$276.50	$330.00	$660.00
E21	$286.00	$341.50	$683.00
E22	$294.50	$351.50	$703.00
E23	$304.00	$363.00	$726.00
E24	$313.50	$374.50	$749.00
E99	Free	Free	Free

NASA Prices:
For NASA libraries, NASA Employees & NASA contractors registered at NASA CASI.

U.S. Prices:
For users within the U.S.

International Prices:
For users outside the U.S. and International Embassies within the U.S.

Processing
Standard N/A
(most orders are processed within three (3) business days, then shipped)

Rush
$10.00 per item
(orders are processed within one (1) business day, then shipped)

Shipping & Handling Fees: per item
Standard (USPS Priority)
$2.00 U.S.
(delivered within 2-3 business days)

$7.00 International
(delivered within 4-7 business days)

USPS Express (U.S. only)
$13.00
(1-day delivery service to most destinations)

Fax (Up to 30 pages,
$16.50 U.S.
$24.00 International

Federal Express
User's Account Only _____

Federal Depository Library Program

In order to provide the general public with greater access to U.S. Government publications, Congress established the Federal Depository Library Program under the Government Printing Office (GPO), with 53 regional depositories responsible for permanent retention of material, inter-library loan, and reference services. At least one copy of nearly every NASA and NASA-sponsored publication, either in printed or microfiche format, is received and retained by the 53 regional depositories. A list of the Federal Regional Depository Libraries, arranged alphabetically by state, appears at the very end of this section. These libraries are not sales outlets. A local library can contact a regional depository to help locate specific reports, or direct contact may be made by an individual.

Public Collection of NASA Documents

An extensive collection of NASA and NASA-sponsored publications is maintained by the British Library Lending Division, Boston Spa, Wetherby, Yorkshire, England for public access. The British Library Lending Division also has available many of the non-NASA publications cited in the STI Database. European requesters may purchase facsimile copy or microfiche of NASA and NASA-sponsored documents FIZ–Fachinformation Karlsruhe–Bibliographic Service, D-76344 Eggenstein-Leopoldshafen, Germany and TIB–Technische Informationsbibliothek, P.O. Box 60 80, D-30080 Hannover, Germany.

Submitting Documents

All users of this abstract service are urged to forward reports to be considered for announcement in the STI Database. This will aid NASA in its efforts to provide the fullest possible coverage of all scientific and technical publications that might support aeronautics and space research and development. If you have prepared relevant reports (other than those you will transmit to NASA, DOD, or DOE through the usual contract- or grant-reporting channels), please send them for consideration to:

ATTN: Acquisitions Specialist
NASA Center for AeroSpace Information
7121 Standard Drive
Hanover, MD 21076-1320.

Reprints of journal articles, book chapters, and conference papers are also welcome.

You may specify a particular source to be included in a report announcement if you wish; otherwise the report will be placed on a public sale at the NASA Center for AeroSpace Information. Copyrighted publications will be announced but not distributed or sold.

Federal Regional Depository Libraries

ALABAMA

AUBURN UNIV. AT MONTGOMERY LIBRARY
Documents Dept.
7300 University Dr.
Montgomery, AL 36117–3596
(205) 244–3650 Fax: (205) 244–0678

UNIV. OF ALABAMA
Amelia Gayle Gorgas Library
Govt. Documents
P.O. Box 870266
Tuscaloosa, AL 35487–0266
(205) 348–6046 Fax: (205) 348–0760

ARIZONA

DEPT. OF LIBRARY, ARCHIVES, AND PUBLIC RECORDS
Research Division
Third Floor, State Capitol
1700 West Washington
Phoenix, AZ 85007
(602) 542–3701 Fax: (602) 542–4400

ARKANSAS

ARKANSAS STATE LIBRARY
State Library Service Section
Documents Service Section
One Capitol Mall
Little Rock, AR 72201–1014
(501) 682–2053 Fax: (501) 682–1529

CALIFORNIA

CALIFORNIA STATE LIBRARY
Govt. Publications Section
P.O. Box 942837 – 914 Capitol Mall
Sacramento, CA 94337–0091
(916) 654–0069 Fax: (916) 654–0241

COLORADO

UNIV. OF COLORADO – BOULDER
Libraries – Govt. Publications
Campus Box 184
Boulder, CO 80309–0184
(303) 492–8834 Fax: (303) 492–1881

DENVER PUBLIC LIBRARY
Govt. Publications Dept. BSG
1357 Broadway
Denver, CO 80203–2165
(303) 640–8846 Fax: (303) 640–8817

CONNECTICUT

CONNECTICUT STATE LIBRARY
231 Capitol Avenue
Hartford, CT 06106
(203) 566–4971 Fax: (203) 566–3322

FLORIDA

UNIV. OF FLORIDA LIBRARIES
Documents Dept.
240 Library West
Gainesville, FL 32611–2048
(904) 392–0366 Fax: (904) 392–7251

GEORGIA

UNIV. OF GEORGIA LIBRARIES
Govt. Documents Dept.
Jackson Street
Athens, GA 30602–1645
(706) 542–8949 Fax: (706) 542–4144

HAWAII

UNIV. OF HAWAII
Hamilton Library
Govt. Documents Collection
2550 The Mall
Honolulu, HI 96822
(808) 948–8230 Fax: (808) 956–5968

IDAHO

UNIV. OF IDAHO LIBRARY
Documents Section
Rayburn Street
Moscow, ID 83844–2353
(208) 885–6344 Fax: (208) 885–6817

ILLINOIS

ILLINOIS STATE LIBRARY
Federal Documents Dept.
300 South Second Street
Springfield, IL 62701–1796
(217) 782–7596 Fax: (217) 782–6437

INDIANA

INDIANA STATE LIBRARY
Serials/Documents Section
140 North Senate Avenue
Indianapolis, IN 46204–2296
(317) 232–3679 Fax: (317) 232–3728

IOWA

UNIV. OF IOWA LIBRARIES
Govt. Publications
Washington & Madison Streets
Iowa City, IA 52242–1166
(319) 335–5926 Fax: (319) 335–5900

KANSAS

UNIV. OF KANSAS
Govt. Documents & Maps Library
6001 Malott Hall
Lawrence, KS 66045–2800
(913) 864–4660 Fax: (913) 864–3855

KENTUCKY

UNIV. OF KENTUCKY
King Library South
Govt. Publications/Maps Dept.
Patterson Drive
Lexington, KY 40506–0039
(606) 257–3139 Fax: (606) 257–3139

LOUISIANA

LOUISIANA STATE UNIV.
Middleton Library
Govt. Documents Dept.
Baton Rouge, LA 70803–3312
(504) 388–2570 Fax: (504) 388–6992

LOUISIANA TECHNICAL UNIV.
Prescott Memorial Library
Govt. Documents Dept.
Ruston, LA 71272–0046
(318) 257–4962 Fax: (318) 257–2447

MAINE

UNIV. OF MAINE
Raymond H. Fogler Library
Govt. Documents Dept.
Orono, ME 04469–5729
(207) 581–1673 Fax: (207) 581–1653

MARYLAND

UNIV. OF MARYLAND – COLLEGE PARK
McKeldin Library
Govt. Documents/Maps Unit
College Park, MD 20742
(301) 405–9165 Fax: (301) 314–9416

MASSACHUSETTS

BOSTON PUBLIC LIBRARY
Govt. Documents
666 Boylston Street
Boston, MA 02117–0286
(617) 536–5400, ext. 226
Fax: (617) 536–7758

MICHIGAN

DETROIT PUBLIC LIBRARY
5201 Woodward Avenue
Detroit, MI 48202–4093
(313) 833–1025 Fax: (313) 833–0156

LIBRARY OF MICHIGAN
Govt. Documents Unit
P.O. Box 30007
717 West Allegan Street
Lansing, MI 48909
(517) 373–1300 Fax: (517) 373–3381

MINNESOTA

UNIV. OF MINNESOTA
Govt. Publications
409 Wilson Library
309 19th Avenue South
Minneapolis, MN 55455
(612) 624–5073 Fax: (612) 626–9353

MISSISSIPPI

UNIV. OF MISSISSIPPI
J.D. Williams Library
106 Old Gym Bldg.
University, MS 38677
(601) 232–5857 Fax: (601) 232–7465

MISSOURI

UNIV. OF MISSOURI – COLUMBIA
106B Ellis Library
Govt. Documents Sect.
Columbia, MO 65201–5149
(314) 882–6733 Fax: (314) 882–8044

MONTANA

UNIV. OF MONTANA
Mansfield Library
Documents Division
Missoula, MT 59812–1195
(406) 243–6700 Fax: (406) 243–2060

NEBRASKA

UNIV. OF NEBRASKA – LINCOLN
D.L. Love Memorial Library
Lincoln, NE 68588–0410
(402) 472–2562 Fax: (402) 472–5131

NEVADA

THE UNIV. OF NEVADA LIBRARIES
Business and Govt. Information Center
Reno, NV 89557–0044
(702) 784–6579 Fax: (702) 784–1751

NEW JERSEY

NEWARK PUBLIC LIBRARY
Science Div. – Public Access
P.O. Box 630
Five Washington Street
Newark, NJ 07101–7812
(201) 733–7782 Fax: (201) 733–5648

NEW MEXICO

UNIV. OF NEW MEXICO
General Library
Govt. Information Dept.
Albuquerque, NM 87131–1466
(505) 277–5441 Fax: (505) 277–6019

NEW MEXICO STATE LIBRARY
325 Don Gaspar Avenue
Santa Fe, NM 87503
(505) 827–3824 Fax: (505) 827–3888

NEW YORK

NEW YORK STATE LIBRARY
Cultural Education Center
Documents/Gift & Exchange Section
Empire State Plaza
Albany, NY 12230–0001
(518) 474–5355 Fax: (518) 474–5786

NORTH CAROLINA

UNIV. OF NORTH CAROLINA – CHAPEL HILL
Walter Royal Davis Library
CB 3912, Reference Dept.
Chapel Hill, NC 27514–8890
(919) 962–1151 Fax: (919) 962–4451

NORTH DAKOTA

NORTH DAKOTA STATE UNIV. LIB.
Documents
P.O. Box 5599
Fargo, ND 58105–5599
(701) 237–8886 Fax: (701) 237–7138

UNIV. OF NORTH DAKOTA
Chester Fritz Library
University Station
P.O. Box 9000 – Centennial and University Avenue
Grand Forks, ND 58202–9000
(701) 777–4632 Fax: (701) 777–3319

OHIO

STATE LIBRARY OF OHIO
Documents Dept.
65 South Front Street
Columbus, OH 43215–4163
(614) 644–7051 Fax: (614) 752–9178

OKLAHOMA

OKLAHOMA DEPT. OF LIBRARIES
U.S. Govt. Information Division
200 Northeast 18th Street
Oklahoma City, OK 73105–3298
(405) 521–2502, ext. 253
Fax: (405) 525–7804

OKLAHOMA STATE UNIV.
Edmon Low Library
Stillwater, OK 74078–0375
(405) 744–6546 Fax: (405) 744–5183

OREGON

PORTLAND STATE UNIV.
Branford P. Millar Library
934 Southwest Harrison
Portland, OR 97207–1151
(503) 725–4123 Fax: (503) 725–4524

PENNSYLVANIA

STATE LIBRARY OF PENN.
Govt. Publications Section
116 Walnut & Commonwealth Ave.
Harrisburg, PA 17105–1601
(717) 787–3752 Fax: (717) 783–2070

SOUTH CAROLINA

CLEMSON UNIV.
Robert Muldrow Cooper Library
Public Documents Unit
P.O. Box 343001
Clemson, SC 29634–3001
(803) 656–5174 Fax: (803) 656–3025

UNIV. OF SOUTH CAROLINA
Thomas Cooper Library
Green and Sumter Streets
Columbia, SC 29208
(803) 777–4841 Fax: (803) 777–9503

TENNESSEE

UNIV. OF MEMPHIS LIBRARIES
Govt. Publications Dept.
Memphis, TN 38152–0001
(901) 678–2206 Fax: (901) 678–2511

TEXAS

TEXAS STATE LIBRARY
United States Documents
P.O. Box 12927 – 1201 Brazos
Austin, TX 78701–0001
(512) 463–5455 Fax: (512) 463–5436

TEXAS TECH. UNIV. LIBRARIES
Documents Dept.
Lubbock, TX 79409–0002
(806) 742–2282 Fax: (806) 742–1920

UTAH

UTAH STATE UNIV.
Merrill Library Documents Dept.
Logan, UT 84322–3000
(801) 797–2678 Fax: (801) 797–2677

VIRGINIA

UNIV. OF VIRGINIA
Alderman Library
Govt. Documents
University Ave. & McCormick Rd.
Charlottesville, VA 22903–2498
(804) 824–3133 Fax: (804) 924–4337

WASHINGTON

WASHINGTON STATE LIBRARY
Govt. Publications
P.O. Box 42478
16th and Water Streets
Olympia, WA 98504–2478
(206) 753–4027 Fax: (206) 586–7575

WEST VIRGINIA

WEST VIRGINIA UNIV. LIBRARY
Govt. Documents Section
P.O. Box 6069 – 1549 University Ave.
Morgantown, WV 26506–6069
(304) 293–3051 Fax: (304) 293–6638

WISCONSIN

ST. HIST. SOC. OF WISCONSIN LIBRARY
Govt. Publication Section
816 State Street
Madison, WI 53706
(608) 264–6525 Fax: (608) 264–6520

MILWAUKEE PUBLIC LIBRARY
Documents Division
814 West Wisconsin Avenue
Milwaukee, WI 53233
(414) 286–3073 Fax: (414) 286–8074

Typical Report Citation and Abstract

❶ **19970001126** NASA Langley Research Center, Hampton, VA USA
❷ **Water Tunnel Flow Visualization Study Through Poststall of 12 Novel Planform Shapes**
❸ Gatlin, Gregory M., NASA Langley Research Center, USA Neuhart, Dan H., Lockheed Engineering and Sciences Co., USA;
❹ Mar. 1996; 130p; In English
❺ Contract(s)/Grant(s): RTOP 505-68-70-04
❻ Report No(s): NASA-TM-4663; NAS 1.15:4663; L-17418; No Copyright; Avail: CASI; A07, Hardcopy; A02, Microfiche
❼ To determine the flow field characteristics of 12 planform geometries, a flow visualization investigation was conducted in the Langley 16- by 24-Inch Water Tunnel. Concepts studied included flat plate representations of diamond wings, twin bodies, double wings, cutout wing configurations, and serrated forebodies. The off-surface flow patterns were identified by injecting colored dyes from the model surface into the free-stream flow. These dyes generally were injected so that the localized vortical flow patterns were visualized. Photographs were obtained for angles of attack ranging from 10’ to 50’, and all investigations were conducted at a test section speed of 0.25 ft per sec. Results from the investigation indicate that the formation of strong vortices on highly swept forebodies can improve poststall lift characteristics; however, the asymmetric bursting of these vortices could produce substantial control problems. A wing cutout was found to significantly alter the position of the forebody vortex on the wing by shifting the vortex inboard. Serrated forebodies were found to effectively generate multiple vortices over the configuration. Vortices from 65’ swept forebody serrations tended to roll together, while vortices from 40’ swept serrations were more effective in generating additional lift caused by their more independent nature.
❽ Author
❾ *Water Tunnel Tests; Flow Visualization; Flow Distribution; Free Flow; Planforms; Wing Profiles; Aerodynamic Configurations*

Key

1. Document ID Number; Corporate Source
2. Title
3. Author(s) and Affiliation(s)
4. Publication Date
5. Contract/Grant Number(s)
6. Report Number(s); Availability and Price Codes
7. Abstract
8. Abstract Author
9. Subject Terms

SCIENTIFIC AND TECHNICAL AEROSPACE REPORTS

A Biweekly Publication of the National Aeronautics and Space Administration

VOLUME 40, JANUARY 11, 2002

01
AERONAUTICS (GENERAL)

Includes general research topics related to manned and unmanned aircraft and the problems of flight within the Earth's atmosphere. Also includes manufacturing, maintenance, and repair of aircraft. For specific topics in aeronautics see categories 02 through 09. For information related to space vehicles see 12 Astronautics.

20020002772 Argonne National Lab., IL USA

Newton-Krylov-Schwarz methods for aerodynamics problems: compressible and incompressible flows on unstructured grids

Kaushik, D. K.; Keyes, D. E.; Smith, B. F.; Feb. 24, 1999; 10p; In English

Report No.(s): DE2001-12411; ANL/MCS/CP-98468; No Copyright; Avail: Department of Energy Information Bridge, Microfiche

We review and extend to the compressible regime an earlier parallelization of an implicit incompressible unstructured Euler code, and solve for flow over an M6 wing in subsonic, transonic, and supersonic regimes. While the parallelization philosophy of the compressible case is identical to the incompressible, we focus here on the nonlinear and linear convergence rates, which vary in different physical regimes, and on comparing the performance of currently important computational platforms. Multiple-scale problems should be marched out at desired accuracy limits, and not held hostage to often more stringent explicit stability limits. In the context of inviscid aerodynamics, this means evolving transient computations on the scale of the convective transit time, rather than the acoustic transit time, or solving steady-state problems with local CFL (Courant-Friedrichs-Lewy) numbers approaching infinity. Whether time-accurate or steady, we employ Newton's method on each (pseudo-) timestep. The coupling of analysis with design in aerodynamic practice is another motivation for implicitness. Design processes that make use of sensitivity derivatives and the Hessian matrix require operations with the Jacobian matrix of the state constraints (i.e., of the governing PDE (partial differential equation) system); if the Jacobian is available for design, it may be employed with advantage in a nonlinearly implicit analysis, as well.

NTIS

Aerodynamics; Compressible Flow; Incompressible Flow; Euler Equations of Motion; Computational Fluid Dynamics

02
AERODYNAMICS

Includes aerodynamics of flight vehicles, test bodies, airframe components and combinations, wings, and control surfaces. Also includes aerodynamics of rotors, stators, fans and other elements of turbomachinery. For related information, see also 34 Fluid Mechanics and Heat Transfer.

20020001438 NASA Langley Research Center, Hampton, VA USA

Isolated Performance at Mach Numbers From 0.60 to 2.86 of Several Expendable Nozzle Concepts for Supersonic Applications

Re, Richard J., NASA Langley Research Center, USA; Berrier, Bobby L., NASA Langley Research Center, USA; Abeyounis, William K., NASA Langley Research Center, USA; November 2001; 199p; In English

Contract(s)/Grant(s): RTOP 706-17-21-05

Report No.(s): NASA/TP-2001-211259; L-17877; NAS 1.60:211259; No Copyright; Avail: CASI; A09, Hardcopy; A03, Microfiche

Investigations have been conducted in the Langley 16-Foot Transonic Tunnel (at Mach numbers from 0.60 to 1.25) and in the Langley Unitary Plan Wind Tunnel (at Mach numbers from 2.16 to 2.86) at an angle of attack of 0 deg to determine the isolated performance of several expendable nozzle concepts for supersonic nonaugmented turbojet applications. The effects of centerbody base shape, shroud length, shroud ventilation, cruciform shroud expansion ratio, and cruciform shroud flap vectoring were investigated. The nozzle pressure ratio range, which was a function of Mach number, was between 1.9 and 11.8 in the 16-Foot Transonic Tunnel and between 7.9 and 54.9 in the Unitary Plan Wind Tunnel. Discharge coefficient, thrust-minus-drag, and the forces and moments generated by vectoring the divergent shroud flaps (for Mach numbers of 0.60 to 1.25 only) of a cruciform nozzle configuration were measured. The shortest nozzle had the best thrust-minus-drag performance at Mach numbers up to 0.95 but was approached in performance by other configurations at Mach numbers of 1.15 and 1.25. At Mach numbers above 1.25, the cruciform nozzle configuration having the same expansion ratio (2.64) as the fixed geometry nozzles had the best thrust-minus-drag performance. Ventilation of the fixed geometry divergent shrouds to the nozzle external boattail flow generally improved thrust-minus-drag performance at Mach numbers from 0.60 to 1.25, but decreased performance above a Mach number of 1.25.

Author

Nozzle Flow; Nozzle Geometry; Supersonic Nozzles; Wind Tunnel Tests; Performance Tests; Nozzle Thrust Coefficients; Nozzle Design

20020002328 Army Research Lab., Vehicle Technology Center, Hampton, VA USA

Wind Tunnel Evaluation of a Model Helicopter Main-Rotor Blade With Slotted Airfoils at the Tip

Noonan, Kevin W., Army Aviation and Missile Command, USA; Yeager, William T., Jr., Army Research Lab., USA; Singleton, Jeffrey D., Army Research Lab., USA; Wilbur, Matthew L., Army Research Lab., USA; Mirick, Paul H., Army Research Lab., USA; December 2001; 132p; In English

Contract(s)/Grant(s): RTOP 581-10-11-01

Report No.(s): NASA/TP-2001-211260; L-17776; NAS 1.60:211260; AMCOM/AFDD/TR-00-A-003; ARL-TR-2154; No Copyright; Avail: CASI; A07, Hardcopy; A02, Microfiche

Data for rotors using unconventional airfoils are of interest to permit an evaluation of this technology's capability to meet the U.S. Army's need for increased helicopter mission effectiveness and improved safety and survivability. Thus, an experimental investigation was conducted in the Langley Transonic Dynamics Tunnel (TDT) to evaluate the effect of using slotted airfoils in the rotor blade tip region (85 to 100 percent radius) on rotor aerodynamic performance and loads. Four rotor configurations were tested in forward flight at advance ratios from 0.15 to 0.45 and in hover in-ground effect. The hover tip Mach number was 0.627, which is representative of a design point of 4000-ft geometric altitude and a temperature of 95 F. The baseline rotor configuration had a conventional single-element airfoil in the tip region. A second rotor configuration had a forward-slotted airfoil with a -6 deg slat, a third configuration had a forward-slotted airfoil with a -10 slat, and a fourth configuration had an aft-slotted airfoil with a 3 deg flap (trailing edge down). The results of this investigation indicate that the -6 deg slat configuration offers some performance and loads benefits over the other three configurations.

Author

Wind Tunnel Tests; Slots; Rotary Wings; Rotor Aerodynamics; Blade Tips; Aerodynamic Loads

20020005126 NASA Langley Research Center, Hampton, VA USA

Base Passive Porosity for Drag Reduction

Bauer, Steven X. S., Inventor, NASA Langley Research Center, USA; Wood, Richard M., Inventor, NASA Langley Research Center, USA; Sep. 11, 2001; 8p; In English; Continuation-in-part of abandoned US-Patent-Appl-SN-327061, Filed 19 Oct. 1994 Patent Info.: Filed 1 Nov. 1996; NASA-Case-LAR-15601-1; US-Patent-6,286,892; US-Patent-Appl-SN-744414; US-Patent-Appl-SN-327061; No Copyright; Avail: CASI; A02, Hardcopy; A01, Microfiche

A device for controlling drag on a ground vehicle. The device consists of a porous skin mounted on the trailing surface of the ground vehicle. The porous skin may be separated from the vehicle surface by a distance of at least the thickness of the porous skin. Alternately, the trailing surface of the ground vehicle may be porous. The device minimizes the strength of the separation in the base and wake regions of the ground vehicle, thus reducing drag.

Official Gazette of the U.S. Patent and Trademark Office

Aerodynamic Drag; Drag Reduction; Porosity

03
AIR TRANSPORTATION AND SAFETY

Includes passenger and cargo air transport operations; aircraft ground operations; flight safety and hazards; and aircraft accidents. Systems and hardware specific to ground operations of aircraft and to airport construction are covered in 09 Research and Support Facilities (Air). Air traffic control is covered in 04 Aircraft Communications and Navigation. For related information see also 16 Space Transportation and Safety; and 85 Technology Utilization and Surface Transportation.

20020001179 NASA Langley Research Center, Hampton, VA USA
Aircraft Wake Vortex Spacing System (AVOSS) Performance Update and Validation Study
Rutishauser, David K., NASA Langley Research Center, USA; OConnor, Cornelius J., NASA Langley Research Center, USA; October 2001; 25p; In English
Contract(s)/Grant(s): RTOP 728-40-30-01
Report No.(s): NASA/TM-2001-211240; L-18124; NAS 1.15:211240; No Copyright; Avail: CASI; A03, Hardcopy; A01, Microfiche

An analysis has been performed on data generated from the two most recent field deployments of the Aircraft Wake VOrtex Spacing System (AVOSS). The AVOSS provides reduced aircraft spacing criteria for wake vortex avoidance as compared to the FAA spacing applied under Instrument Flight Rules (IFR). Several field deployments culminating in a system demonstration at Dallas Fort Worth (DFW) International Airport in the summer of 2000 were successful in showing a sound operational concept and the system's potential to provide a significant benefit to airport operations. For DFW, a predicted average throughput increase of 6% was observed. This increase implies 6 or 7 more aircraft on the ground in a one-hour period for DFW operations. Several studies of performance correlations to system configuration options, design options, and system inputs are also reported. The studies focus on the validation performance of the system.
Author
Aircraft Approach Spacing; Aircraft Wakes; Vortex Avoidance; Air Traffic Control

20020001192 Nebraska Univ., Aviation Inst., Omaha, NE USA
The Airline Quality Rating 2000
Bowen, Brent D., Nebraska Univ., USA; Headley, Dean E., Wichita State Univ., USA; 2000; 58p; In English
Report No.(s): UNOAI-2000-2; Copyright; Avail: Issuing Activity

The Airline Quality Rating (AQR) was developed and first announced in early 1991 as an objective method of comparing airline quality on combined multiple performance criteria. This current report, Airline Quality Rating 2000, reflects monthly Airline Quality Rating scores for 1999. AQR scores for the calendar year 1999 are based on 14 elements that focus on airline performance areas important to air travel consumers. The Airline Quality Rating 2000 is a summary of month-by-month quality ratings for the ten major U.S. airlines operating during 1999. Using the Airline Quality Rating system of weighted averages and monthly performance data in the areas of on-time arrivals, involuntary denied boardings, mishandled baggage, and a combination of 11 customer complaint categories, major airlines comparative performance for the calendar year of 1999 is reported. This research monograph contains a brief summary of the AQR methodology, detailed data and charts that track comparative quality for major airlines domestic operations for the 12 month period of 1999, and industry average results. Also, comparative Airline Quality Rating data for 1998, are included for each airline to provide historical perspective regarding performance quality in the industry.
Author
Airline Operations; Air Transportation; Ratings; Total Quality Management; Commercial Aircraft

20020001448 Lawrence Livermore National Lab., Livermore, CA USA
Crash Hit Frequency Analysis of Aircraft Overflights of the Nevada Test Site (NTS) and the Device Assembly Facility (DAF)
Kimura, C. Y.; Sanzo, D. L.; Sharirli, M.; Apr. 01, 1999; 10p; In English
Report No.(s): DE2001-8799; UCRL-JC-131259; No Copyright; Avail: Department of Energy Information Bridge, Microfiche

Aircraft crashes are an element of external events required to be analyzed and documented in Facility Safety Analysis Reports (SARs) and Nuclear Explosive Safety Studies (NESS). Aircraft crashes into Department of Energy facilities are of concern due to effects related to impact and fire that can potentially lead to penetration of the facility, disruption of operations, and the potential release of radioactive and/or hazardous materials subsequent to the aircraft impact. This paper discusses the review and analysis of aircraft crash hit frequency on the Device Assembly Facility (DAF) within the Nevada Test Site (NTS). The frequency of an aircraft crashing and hitting the DAF is in the 1 E-7 to E-8 range. While this is considered to be acceptably small, it is not considered

an upper bound. The results of the analysis are highly dependent on the assumptions made and the available data. There is considerable uncertainty in the number of overflights which are taking place over the NTS. to reduce this uncertainty, additional follow-on work will be done to monitor the level of air activity over the NTS and to recalculate the aircraft crash hit frequency on the DAF when better overflight estimates are obtained.
NTIS
Aircraft Accidents; Crashes; Frequencies

20020001774 National Aerospace Lab., Amsterdam, Netherlands
External Risk Around Airports. A Model Update
Pikaar, A. J.; Piers, M. A.; Ale, B.; Aug. 2000; 16p; In English; Based on a presentation held at the International Conference (5th) International Conference on Probabilistic Safety Assessment and Management, Osaka, Japan, November 27-December 1, 2000
Report No.(s): PB2001-108824; NLR-TP-2000-400; No Copyright; Avail: CASI; A03, Hardcopy; A01, Microfiche

Typical third party risk analysis methods consist of three submodels: an accident probability model, an accident location probability model and an accident consequence model. In 1992, the National Research Laboratory (NRL), developed a method for the calculation of third party risk levels around airports. This report discusses the changes made to the models and a comparison of the result of calculations with the old model and the new model.
NTIS
Airports; Accidents; Risk

20020001782 Federal Aviation Administration, William J. Hughes Technical Center, Atlantic City, NJ USA
Project Plan: Web-Based Assessment of Screener Competency
Morgan, S. B.; May 13, 2001; 18p; In English
Report No.(s): PB2001-108598; DOT/FAA/AR-01/93; No Copyright; Avail: CASI; A03, Hardcopy; A01, Microfiche

This project plan describes the development of a web-based On-the-Job Training test and Screener Multi-faceted Assessment Recurrent Test to assess checkpoint screener X-ray image interpretation skills.
NTIS
Internets; Tests; Scanners; Personnel Development

20020001959 Lockheed Martin Aeronautics Co., Fort Worth, TX USA
JSF Perspective
Cappuccio, Frank, Lockheed Martin Aeronautics Co., USA; May 12, 2001; 7p; In English; Proceedings from Armaments for the 3rd Simulation Based Acquisition 3rd Simulation Based AcquisConference, 15-17 May 2001, USA; Original contains color images
Report No.(s): AD-A394594; No Copyright; Avail: CASI; A02, Hardcopy; A01, Microfiche

No abstract.
Author
Military Aircraft; Procurement

20020002248 L-3 Communications Corp., Mesa, AZ USA
Visual Interface Unit: A Modern Approach to Integrating Image Generators in a DIS and HLA Environment ***Final Report, Apr. 1999 - Jan. 2000***
Call, Lance R.; Jul. 2000; 12p; In English
Contract(s)/Grant(s): F41624-97-D-5000; AF Proj. 1123
Report No.(s): AD-A391815; AFRL-HE-AZ-TR-1999-0254; No Copyright; Avail: Defense Technical Information Center (DTIC)

This paper explores how simulators and image generators (IGs) may be integrated and presents a historical perspective of how hosts and IGs have traditionally been connected. How a Visual Interface Unit (VIU) may be used to integrate several different kinds of hosts (F-16, A-10, etc.) with multiple kinds of IGs while lowering the host/IG integration, maintenance, and upgraded costs is also discussed. An architecture using a Standard Host IG interface and a 'network-enabled' IG capable of connecting to a 'public' network to get most of its information is suggested. A network-enabled IG significantly reduces the amount of information that must be exchanged between a host and its IG. Using the Standard Host IG interface protocol would allow a 'plug-and-plan' IG connection regardless of the vendor.
DTIC
Protocol (Computers); Display Devices; Flight Simulators; Architecture (Computers); Systems Integration; Image Processing

20020002258 General Accounting Office, Washington, DC USA

Financial Management: Assessment of the Airline Industry's Estimated Losses Arising from the Events of September 11

Oct. 05, 2001; 26p; In English

Report No.(s): PB2002-100186; GAO-02-133R; No Copyright; Avail: CASI; A03, Hardcopy; A01, Microfiche

In the wake of the September 11, 2001, terrorist attacks on the United States, the airline industry has estimated significant losses resulting from the temporary shutdown of the nation's airspace and the sever drop in passenger traffic since the attacks. In response, on September 22, 2001, the President signed the Air Transportation Safety and System Stabilization Act which provides $5 billion in emergency assistance to compensate the nation's air carriers for these losses. Specifically, the law stipulates that an amount equal to $5 billion will be made available to compensate air carriers for direct losses incurred beginning September 11 as a result of any federal ground stop order issued by the Secretary of Transportation, and incremental losses incurred beginning September 11 through December 31, 2001, as a direct result of terrorist attacks. We performed an analysis of the data and methodologies used by the airline industry to estimate the losses through December 31, 2001, stemming from the terrorist attacks to determined whether there is a reasonable basis for the estimate, and assess the overall reasonableness of the $5 billion compensation package. This letter summarizes the information we provided during our September 28, 2001, briefing pursuant to these requests.

NTIS

Financial Management; Losses; Air Transportation

20020002261 General Accounting Office, Washington, DC USA

Drug Control: State Department Provides Required Aviation Program Oversight, but Safety and Security Should Be Enhanced

Sep. 2001; 26p; In English

Report No.(s): PB2002-100159; GAO-01-1021; No Copyright; Avail: CASI; A03, Hardcopy; A01, Microfiche

According to the Department of State, the Andean region continues to cultivate, produce, and export almost all of the world's cocaine and an increasing amount of heroin. Colombia is the source of 90 percent of the cocaine entering the USA and approximately two-thirds of the heroin found on the East Coast. While coca cultivation estimates have decreased by approximately two-thirds in Bolivia and Peru since 1996, increases in coca cultivation in Colombia have offset much of these successes. Your office raised concerns about reports you had received that the Office of Aviation might not be providing adequate oversight of its aviation program and might not be ensuring that the program operates safely. In response to these concerns, we determined whether the Office of Aviation (1) oversaw and evaluated DynCorp's performance in accordance with applicable requirements and (2) ensured the safe operation of its aircraft and the physical security of its operational sites. to address your concerns, we discussed these matters with cognizant U.S. officials at the Department of State, Washington, D.C., and the U.S. Embassy in Bogota, Colombia; and U.S. and DynCorp officials at the Office of Aviation's main operating base in Florida and operational sites in Colombia. We reviewed pertinent contract evaluation reports and related documentation and followed up on several recent operational and safety reviews of the Office of Aviation's program. Although we examined relevant documentation for Bolivia and Peru, we focused our review on the Office's program in Colombia.

NTIS

Drugs; Narcotics; Safety

20020002271 Veridian Engineering, Inc., Egg Harbor, NJ USA

Phase IIB Qualification Test Plan and Procedures of Commercially Available Radio Frequency Identification (RFID) Systems for Baggage Identification, Tracking and Security Applications. Continental Airlines Trial

Cerino, A. T.; Sep. 1999; 60p; In English

Report No.(s): PB2002-100255; No Copyright; Avail: CASI; A04, Hardcopy; A01, Microfiche

The Operational Test for the Continental Airlines Trial will be used to evaluate those RFID systems that have the potential to accomplish baggage identification, tracking and security requirements in an operational environment utilizing handheld readers, and belt/ramp readers.

NTIS

Baggage; Security; Airline Operations; Identifying

20020002272 Veridian Engineering, Inc., Egg Harbor, NJ USA

Phase IIB Operational Test Report of Commercially Available Radio Frequency Identification (RFID) Systems for Baggage Identification, Tracking and Security Applications. Continental Airlines Trial

Cerino, A. T.; Jan. 2000; 60p; In English

Report No.(s): PB2002-100254; No Copyright; Avail: CASI; A04, Hardcopy; A01, Microfiche

The following is a test report describing the results of the Phase IIB Operational RFID Test conducted with Continental Airlines in San Antonio and Houston, Texas to demonstrate the feasibility of conducting baggage tracking in a complete, real-time end-to-end mode using RFID Technology.

NTIS

Baggage; Airline Operations

20020002315 General Accounting Office, Washington, DC USA

Aviation Security: Commercially Available Advanced Explosives Detection Devices

Apr. 24, 1997; 20p; In English

Report No.(s): PB2002-100157; GAO/RCED-97-119R; No Copyright; Avail: CASI; A03, Hardcopy; A01, Microfiche

In August and September 1996, we testified on aviation security issues before the Senate Commerce, Science, and Transportation Committee and provided the Committee with information about devices that were currently available or under development for detecting explosives and the devices' operational capabilities. As requested, we are providing you with updated information on the advanced explosives detection devices that are commercially available and can be used to screen checked baggage, carry-on items, passengers, and cargo and mail. You also asked that we review the financial, airport-related, and operational issues associated with deploying detection technology at U.S. airports. Many security initiatives have been undertaken since the July 1996 crash of TWA Flight 800. In its final report of February 1997, the Gore Commission said that it expected that the National Civil Aviation Review Commission would consider a variety of options to pay for security measures; a report on funding is expected to be made in the fall of 1997. In addition, FAA has directed that the contractors installing the explosive detection devices gather data on the effect that deploying these devices has on airport-related and operational issues. As discussed with your office, we agreed to reassess the need for us to do further work on the financial and operational issues associated with deploying detection technology at U.S. airports on the basis of the final outcome of these two initiatives.

NTIS

Explosives Detection; Airport Security; Airports; Contractors

20020002338 Veridian Engineering, Inc., Egg Harbor, NJ USA

Phase IIB Qualification Test Plan and Procedure of Commercially Available Radio Frequency Identification (RFID) Systems for Baggage Identification, Tracking and Security Applications. Continental Airlines Trial; San Antonio and Houston, Texas

Cerino, A. T.; Jul. 19, 1999; 44p; In English

Report No.(s): PB2002-100253; No Copyright; Avail: CASI; A03, Hardcopy; A01, Microfiche

This document describes the Qualification Test Plan/Procedures for the Phase IIB Qualification RFID Test to be conducted prior to the Operational RFID Test with Continental Airlines in San Antonio and Houston, Texas.

NTIS

Baggage; Airline Operations; Performance Tests

20020002339 Veridian Engineering, Inc., Egg Harbor, NJ USA

Phase IIB Qualification Test of Commercially Available Radio Frequency Identification (RFID) Systems for Baggage Identification, Tracking and Security Applications. Alaska Airlines/Singapore Airlines Trial

Cerino, A. T.; Jun. 2000; 78p; In English

Report No.(s): PB2002-100252; No Copyright; Avail: CASI; A05, Hardcopy; A01, Microfiche

The Operational test for the Alaska and Singapore Airlines Trial was used to evaluate those RFID systems that have the potential to accomplish baggage identification, tracking and security requirements in an operational environment, utilizing RFID handheld, belt and ramp readers, and with interline baggage transfers.

NTIS

Baggage; Airline Operations

20020002342 General Accounting Office, Washington, DC USA

Aviation Security: Implementation of Recommendations Is Under Way, but Completion Will Take Several Years

Apr. 1998; 66p; In English

Report No.(s): PB2002-100462; GAO/RCED-98-102; No Copyright; Avail: CASI; A04, Hardcopy; A01, Microfiche

As the threat of terrorist activities has increased in the USA, the need to improve domestic aviation security has grown. Currently, the Federal Aviation Administration (FAA), other federal agencies, and the aviation industry are implementing 31 recommendations on aviation security made by the White House Commission on Aviation Safety and Security. Some of these recommendations are similar to legislative mandates enacted by the Congress under the Federal Aviation Reauthorization Act of 1996. The expeditious implementation of these recommendations1 by federal agencies and the aviation industry is crucial to strengthening the security of the domestic aviation system. This report responds to your request for information on the tracking, monitoring, and coordinating activities undertaken by the agencies responsible for implementing the recommendations made by the Commission and on FAA's progress in implementing eight of these recommendations, five of which are similar to mandates contained in the Reauthorization Act of 1996. As agreed with your offices, this report addresses the following specific questions: (1) How do the federal agencies responsible for implementing aviation security recommendations track, monitor, and coordinate their activities; (2) What progress has FAA made in implementing three of the Commission's aviation security recommendations that were scheduled to be completed in fiscal year 1997 and have all implementation issues been resolved; (3) What progress has FAA made in implementing five recommendations that were both recommended by the Commission and mandated by the Congress in 1996, and what major issues need to be addressed before they can be fully implemented.

NTIS

Civil Aviation; Security; Flight Safety; Aircraft Industry

20020002355 Federal Aviation Administration, Washington, DC USA

Notices to Airmen, Domestic/International, August 9, 2001

2001; 312p; In English

Report No.(s): PB2001-108173; No Copyright; Avail: CASI; A14, Hardcopy; A03, Microfiche

Table of Contents: Airway NOTAMS; Airport, Facilities, and Procedural NOTAMs; General NOTAMs; Revisions to Minimum en Route IFR Altitudes and Changeover Points; Part 3. International NOTAMS; Part 4. Graphic Notes.

NTIS

National Airspace System; Airports; Air Navigation

20020002849 NASA Ames Research Center, Moffett Field, CA USA

Handling Qualities Influences on Civil Tiltrotor Terminal Operating Procedure Development

Decker, William A., NASA Ames Research Center, USA; Simmons, Rickey C., NASA Ames Research Center, USA; Tucker, George E., NASA Ames Research Center, USA; [1994]; 8p; In English; 51st Annual Forum, 9-11 May 1995, Washington, DC, USA; Sponsored by American Helicopter Society, Inc., USA

Contract(s)/Grant(s): RTOP 538-07-15; No Copyright; Avail: CASI; A02, Hardcopy; A01, Microfiche

The potential for tiltrotor aircraft as civil transports has been well recognized. Realization of that potential requires development of operating procedures tailored to take advantage of the tiltrotor's capabilities, including thrust vectoring independent of body pitch attitude and good low-speed control. While the tiltrotor shares flight characteristics with both fixed wing airplanes and helicopters, it must convert between those flight modes, typically within the context of precise terminal operations. A series of piloted simulation experiments has been conducted on the NASA Ames Research Center Vertical Motion Simulator (VMS) to investigate the influence of tiltrotor cockpit design features on developing certification and operating criteria for civil tiltrotor transports. Handling qualities evaluations have shaped cockpit design guidelines and operating procedure development for a civil tiltrotor. In particular, four topics demonstrate the interplay of handling qualities and operations profile in the development of terminal operating procedures and cockpit or control equipment for a civil tiltrotor: conversion (airplane to helicopter mode), final approach path angle, operating profile speeds and speed changes (particularly under instrument conditions), and one engine inoperative operational considerations.

Author

Tilting Rotors; Controllability; Aircraft Control

20020004663 Sandia National Labs., Albuquerque, NM USA

Combustion Model for the TWA 800 Center-Wing Fuel Tank Explosion

Baer, M. R.; Gross, R. J.; Oct. 02, 1998; 52p; In English

Report No.(s): DE2001-702; SAND98-2043; No Copyright; Avail: Department of Energy Information Bridge

In support of the National Transportation Safety Board investigation of the TWA Flight 800 accident, a combined experimental/computational effort was conducted that focused on quarter-scale testing and simulation of the fuel-air explosion in the Boeing 747 center wing fuel tank. This report summarizes the modeling approach used at Sandia National Laboratories. In this approach approximations are introduced that capture the essential physics associated with turbulent flame propagation in multiple compartment fuel tanks. This model efficiently defines the pressure loading conditions during a jet-fuel air explosion in a fuel tank confinement. Modeling calculations compare favorably with a variety of experimental quarter-scale tests conducted in rigid confinement. The modeling describes well the overpressure history in several geometry configurations. Upon demonstrating a reasonable comparison to experimental observations, a parametric study of eight possible ignition sources is then discussed. Model calculations demonstrate that different loading conditions arise as the location of the ignition event is varied. by comparing the inferred damage and calculated impulses to that seen in the recovered tank, it maybe possible to reduce the number of likely sources. A possible extension of this work to better define tank damage includes coupling the combustion model as a pressure loading routine for structural failure analysis.
NTIS
Aerial Explosions; Aircraft Accident Investigation; Aircraft Accidents; Jet Engine Fuels; Fuel Tanks; Combustion Physics; Failure Analysis; Safety Management; Turbulent Flames

20020005128 NASA Langley Research Center, Hampton, VA USA
Airborne Use of Traffic Intent Information in a Distributed Air-Ground Traffic Management Concept: Experiment Design and Preliminary Results
Wing, David J., NASA Langley Research Center, USA; Adams, Richard J., Booz-Allen and Hamilton, Inc., USA; Duley, Jacqueline A., Booz-Allen and Hamilton, Inc., USA; Legan, Brian M., Booz-Allen and Hamilton, Inc., USA; Barmore, Bryan E., Titan Systems, USA; Moses, Donald, Science Applications International Corp., USA; November 2001; 31p; In English
Contract(s)/Grant(s): RTOP 727-01-26-01
Report No.(s): NASA/TM-2001-211254; NAS 1.15:211254; L-18135; No Copyright; Avail: CASI; A03, Hardcopy; A01, Microfiche

A predominant research focus in the free flight community has been on the type of information required on the flight deck to enable pilots to ”autonomously” maintain separation from other aircraft. At issue are the relative utility and requirement for information exchange between aircraft regarding the current ”state” and/or the ”intent” of each aircraft. This paper presents the experimental design and some initial findings of an experimental research study designed to provide insight into the issue of intent information exchange in constrained en-route operations and its effect on pilot decision making and flight performance. Two operational modes for autonomous operations were compared in a piloted simulation. The tactical mode was characterized primarily by the use of state information for conflict detection and resolution and an open-loop means for the pilot to meet operational constraints. The strategic mode involved the combined use of state and intent information, provided the pilot an additional level of alerting, and allowed a closed-loop approach to meeting operational constraints. Potential operational benefits of both modes are illustrated through several scenario case studies. Subjective data results are presented that generally indicate pilot consensus in favor of the strategic mode.
Author
Air Traffic Control; Decision Making; Feedback Control; Autonomy; Flight Operations

20020005889 NASA Ames Research Center, Moffett Field, CA USA
Pre-Departure Clearance (PDC): An Analysis of Aviation Safety Reporting System Reports Concerning PDC Related Errors
Montalyo, Michael L., NASA Ames Research Center, USA; [1994]; 1p; In English; 8th International Symposium on Aviation Psychology, 23-27 Apr. 1995, Columbus, OH, USA
Contract(s)/Grant(s): RTOP 538-04-11; No Copyright; Avail: Issuing Activity; Abstract Only

Airlines operating in the USA are required to operate under instrument flight rules (EFR). Typically, a clearance is issued via voice transmission from clearance delivery at the departing airport. In 1990, the Federal Aviation Administration (FAA) began deployment of the Pre-Departure Clearance (PDC) system at 30 U.S. airports. The PDC system utilizes aeronautical datalink and Aircraft Communication and Reporting System (ACARS) to transmit departure clearances directly to the pilot. An objective of the PDC system is to provide an immediate reduction in voice congestion over the clearance delivery frequency. Participating airports report that this objective has been met. However, preliminary analysis of 42 Aviation Safety Reporting System (ASRS) reports has revealed problems in PDC procedures and formatting which have caused errors in the proper execution of the clearance. It must be acknowledged that this technology, along with other advancements on the flightdeck, is adding more responsibility to the crew and increasing the opportunity for error. The present study uses these findings as a basis for further

coding and analysis of an additional 82 reports obtained from an ASRS database search. These reports indicate that clearances are often amended or exceptions are added in order to accommodate local ATC facilities. However, the onboard ACARS is limited in its ability to emphasize or highlight these changes which has resulted in altitude and heading deviations along with increases in ATC workload. Furthermore, few participating airports require any type of PDC receipt confirmation. In fact, 35% of all ASRS reports dealing with PDC's include failure to acquire the PDC at all. Consequently, this study examines pilots' suggestions contained in ASRS reports in order to develop recommendations to airlines and ATC facilities to help reduce the amount of incidents that occur.
Author
Airline Operations; Instrument Flight Rules; Aircraft Communication

04
AIRCRAFT COMMUNICATIONS AND NAVIGATION

Includes all modes of communication with and between aircraft; air navigation systems (satellite and ground based); and air traffic control. For related information see also 06 Avionics and Aircraft Instrumentation; 17 Space Communications; Spacecraft Communications, Command and Tracking, and 32 Communications and Radar.

20020004352 NASA Goddard Space Flight Center, Greenbelt, MD USA
Temperature Humidity and Sea Level Pressure Increments Induced by 1DVAR Analysis of GPS Refractivity
Poli, Paul, NASA Goddard Space Flight Center, USA; Joiner, Joanna, NASA Goddard Space Flight Center, USA; Kursinski, Emil Robert, Jet Propulsion Lab., California Inst. of Tech., USA; [2001]; 1p; In English; 2001 AGU Spring Meeting, 29 May - 2 Jun. 2001, Boston, MA, USA; Sponsored by American Geophysical Union, USA; No Copyright; Avail: Issuing Activity; Abstract Only

The Global Positioning System (GPS) transmitted signals are affected by the atmosphere. Using the radio occultation technique, where a receiver is placed on a low-Earth-orbiting platform. it is possible to perform soundings. by measuring the bending angles of the rays. The information can be converted into atmospheric refractivity. We have developed a one dimensional variational (1DVAR) analysis that uses GPS/MET 1995 refractivity and 6-hour FVDAS (Finite Volume Data Assimilation System) forecasts as background information to constrain the retrievals. The analysis increments are defined as 1DVAR minus background temperature, humidity and sea level pressure. Before assimilating the 1DVAR profiles into the FVDAS. the increments need to be understood. First, some bias could be induced in the retrievals when confronted with actual biased data: second. bias in the back-round could create undesired bias in the retrievals. Anv bias in the analyses will ultimately change the climatology of the model the retrievals will be assimilated into. We relate the increments to the reduction of the difference between observed minus computed refractivity profiles. We also point out the difference in the mean increments using backgrounds which have assimilated either NESDIS TIROS Operational Vertical Sounder (TOVS) operational retrievals or Data Assimilation Office (DAO) TOVS interactive retrievals. The climatology of the model in terms of refractivity is significantly different and this impacts the GPS 1DVAR increments. This testifies that changing the basic load of assimilated data has an influence on the impact the GPS data may have in a DAS.
Author
Global Positioning System; Humidity; Refractivity; Sea Level; Climatology; Mathematical Models; Pressure; Atmospheric Temperature

05
AIRCRAFT DESIGN, TESTING AND PERFORMANCE

Includes all stages of design of aircraft and aircraft structures and systems. Also includes aircraft testing, performance, and evaluation, and aircraft and flight simulation technology. For related information, see also 18 Spacecraft Design, Testing and Performance and 39 Structural Mechanics. For land transportation vehicles, see 85 Technology Utilization and Surface Transportation.

20020001062 Lawrence Livermore National Lab., Livermore, CA USA
Experimental Investigations of Material Models for Ti-6A1-4V and 2024-T3
Leseur, D.; May 03, 1999; 36p; In English
Contract(s)/Grant(s): W-7405-ENG-48
Report No.(s): DE2001-11977; UCRL-ID-134691; No Copyright; Avail: Department of Energy Information Bridge, Microfiche

This report describes studies of the deformation and failure behavior of Ti-6Al-4V and 2024-T3 aluminum. Data was obtained at high strain rates and large strains using the split Hopkinson pressure bar technique. This information, plus additional data from the literature, was used to critically evaluate the ability of the Johnson Cook material model to represent the deformation and failure response of Ti-6AMV and 2024-T3 under conditions relevant to simulations of engine containment and the influence of uncontained engine debris on aircraft structures. This model is being used in the DYNA3D finite element code, which is being developed/validated for evaluating aircraft/engine designs relative to the federal airworthiness standards and for improving mitigation/containment technology. The results of the experimental work reported here were used to define a new set of material constants for the strength component of the Johnson Cook model for Ti-6Al-4V and 2024-T3. The capabilities and limitations of the model are reviewed. The model can accurately represent the stress-strain response of the materials. The major concern with the Johnson Cook material model is its ability to accurately represent the stress - strain rate response at strain rates greater than 10(sup 3)-10(sup 4) s(sup (minus)1). Additional work is also needed to adequately account for failure via shear localization, which was the dominant failure mode at high strain rates in both materials. Failure modeling in both Ti-6Al-N and 2024-T3 will be considered further in future reports.
NTIS
Aluminum; Deformation; Mathematical Models; Failure Modes; Stress-Strain Relationships; Structural Failure

20020001553 Sandia National Labs., Albuquerque, NM USA
Full-Scale Structural and NDI Validation Tests of Bonded Composite Doublers for Commercial Aircraft Applications
Roach, D.; Walkington, P.; Feb. 01, 1999; 244p; In English
Report No.(s): DE2001-4368; SAND98-1015; No Copyright; Avail: Department of Energy Information Bridge, Microfiche

Composite doublers, or repair patches, provide an innovative repair technique which can enhance the way aircraft are maintained. Instead of riveting multiple steel or aluminum plates to facilitate an aircraft repair, it is possible to bond a single Boron-Epoxy composite doubler to the damaged structure. Most of the concerns surrounding composite doubler technology pertain to long-term survivability, especially in the presence of non-optimum installations, and the validation of appropriate inspection procedures. This report focuses on a series of full-scale structural and nondestructive inspection (NDI) tests that were conducted to investigate the performance of Boron-Epoxy composite doublers. Full-scale tests were conducted on fuselage panels cut from retired aircraft. These full-scale tests studied stress reductions, crack mitigation, and load transfer capabilities of composite doublers using simulated flight conditions of cabin pressure and axial stress. Also, structures which modeled key aspects of aircraft structure repairs were subjected to extreme tension, shear and bending loads to examine the composite laminate's resistance to disbond and delamination flaws. Several of the structures were loaded to failure in order to determine doubler design margins. Nondestructive inspections were conducted throughout the test series in order to validate appropriate techniques on actual aircraft structure. The test results showed that a properly designed and installed composite doubler is able to enhance fatigue life, transfer load away from damaged structure, and avoid the introduction of new stress risers (i.e. eliminate global reduction in the fatigue life of the structure). Comparisons with test data obtained prior to the doubler installation revealed that stresses in the parent material can be reduced 30%--60% through the use of the composite doubler. Tests to failure demonstrated that the bondline is able to transfer plastic strains into the doubler and that the parent aluminum skin must experience significant yield strains before any damage to the doubler will occur.
NTIS
Composite Materials; Full Scale Tests; Nondestructive Tests; Aircraft Structures; Debonding (Materials)

20020002845 General Accounting Office, Washington, DC USA
Joint Strike Fighter Acquisition: Mature Critical Technologies Needed to Reduce Risks
Oct. 2001; 28p; In English
Report No.(s): PB2002-100607; GAO-02-39; No Copyright; Avail: CASI; A03, Hardcopy; A01, Microfiche

The Joint Strike Fighter Program is the most expensive aircraft program in the Department of Defense (DOD). It is intended to produce affordable, next-generation aircraft to replace aging aircraft in the military services inventories. As currently planned, the program will cost about $200 billion to develop and procure about 3,000 aircraft and related support equipment. Two contractor teams, led by the Boeing Company and by the Lockheed Martin Aeronautics Company, are competing for the engineering and manufacturing development phase. This phase of the program is projected to last about 8 years and cost about $20 billion and typically involves large, fixed investments in human capital, facilities, and materials. This document reports that a key objective of the programs acquisition strategy is affordability and that a part of that strategy-- entering into engineering and manufacturing development with low technical risk--would not be achieved because technologies critical to meeting the programs

cost and requirement objectives were projected to be at low levels of technical maturity in April 2001, the date then scheduled for awarding the engineering and manufacturing development contract.
NTIS
Fighter Aircraft; Defense Program; Product Development

20020005092 NASA Ames Research Center, Moffett Field, CA USA
Optimization on a Network-based Parallel Computer System for Supersonic Laminar Wing Design
Garcia, Joseph A., NASA Ames Research Center, USA; Cheung, Samson, MCAT Inst., USA; [1995]; 1p; In English; NASA Computational Aerosciences (CAS) Workshop, 7-9 Mar. 1995, Moffett Field, CA, USA; Sponsored by NASA Ames Research Center, USA
Contract(s)/Grant(s): RTOP 509-10-00; No Copyright; Avail: Issuing Activity; Abstract Only

A set of Computational Fluid Dynamics (CFD) routines and flow transition prediction tools are integrated into a network based parallel numerical optimization routine. Through this optimization routine, the design of a 2-D airfoil and an infinitely swept wing will be studied in order to advance the design cycle capability of supersonic laminar flow wings. The goal of advancing supersonic laminar flow wing design is achieved by wisely choosing the design variables used in the optimization routine. The design variables are represented by the theory of Fourier series and potential theory. These theories, combined with the parallel CFD flow routines and flow transition prediction tools, provide a design space for a global optimal point to be searched. Finally, the parallel optimization routine enables gradient evaluations to be performed in a fast and parallel fashion.
Author
Parallel Computers; Supersonic Flow; Computational Fluid Dynamics; Airfoils; Swept Wings; Laminar Flow

20020005142 NASA Langley Research Center, Hampton, VA USA
Flight Investigation of the Effects of Pressure-Belt Tubing Size on Measured Pressure Distributions
Rivers, Natale A., NASA Langley Research Center, USA; vanDam, Cornielious P., California Univ., USA; Brown, Phillip W., NASA Langley Research Center, USA; Rivers, Robert A., NASA Langley Research Center, USA; November 2001; 46p; In English
Contract(s)/Grant(s): RTOP 706-62-21-03
Report No.(s): NASA/TM-2001-209857; L-18078; NAS 1.15:209857; No Copyright; Avail: CASI; A03, Hardcopy; A01, Microfiche

The pressure-belt technique is commonly used to measure pressure distributions on lifting and nonlifting surfaces where flush, through-the-surface measurements are not possible. The belts, made from strips of small-bore, flexible plastic tubing, are surface-mounted by a simple, nondestructive method. Additionally, the belts require minimal installation time, thus making them much less costly to install than flush-mounted pressure ports. Although pressure belts have been used in flight research since the early 1950s, only recently have manufacturers begun to produce thinner, more flexible tubing, and thin, strong adhesive tapes that minimize the installation-induced errors on the measurement of surface pressures. The objective of this investigation was to determine the effects of pressure-belt tubing size on the measurement of pressure distributions. For that purpose, two pressure belts were mounted on the right wing of a single-engine, propeller-driven research airplane. The outboard pressure belt served as a baseline for the measurement and the comparison of effects. Each tube had an outer diameter (OD) of 0.0625 in. The inboard belt was used to evaluate three different tube sizes: 0.0625-, 0.1250-, and 0.1875-in. OD. A computational investigation of tube size on pressure distribution also was conducted using the two-dimensional Multielement Streamtube Euler Solver (MSES) code.
Author
In-Flight Monitoring; Pressure Measurement; Pressure Distribution; Fasteners

20020005836 NASA Ames Research Center, Moffett Field, CA USA
Design of Flight Vehicle Management Systems
Meyer, George, NASA Ames Research Center, USA; [1994]; 1p; In English; 33rd IEEE CDC Meeting, 12-14 Dec. 1994, Lake Buena Vista, FL, USA; Sponsored by Institute of Electrical and Electronics Engineers, USA
Contract(s)/Grant(s): RTOP 505-64-52; No Copyright; Avail: Issuing Activity; Abstract Only

As the operation of large systems becomes ever more dependent on extensive automation, the need for an effective solution to the problem of design and validation of the underlying software becomes more critical. Large systems possess much detailed structure, typically hierarchical, and they are hybrid. Information processing at the top of the hierarchy is by means of formal logic and sentences; on the bottom it is by means of simple scalar differential equations and functions of time; and in the middle it is by an interacting mix of nonlinear multi-axis differential equations and automata, and functions of time and discrete events. The

lecture will address the overall problem as it relates to flight vehicle management, describe the middle level, and offer a design approach that is based on Differential Geometry and Discrete Event Dynamic Systems Theory.
Author
Management Systems; Flight Vehicles; Program Verification (Computers)

06
AVIONICS AND AIRCRAFT INSTRUMENTATION

Includes all stages of design of aircraft and aircraft structures and systems. Also includes aircraft testing, performance, and evaluation, and aircraft and flight simulation technology. For related information, see also 18 Spacecraft Design, Testing and Performance and 39 Structural Mechanics. For land transportation vehicles, see 85 Technology Utilization and Surface Transportation.

20020002861 Research Inst. for Advanced Computer Science, Moffett Field, CA USA
Particle Filters for Real-Time Fault Detection in Planetary Rovers
Dearden, Richard, Research Inst. for Advanced Computer Science, USA; Clancy, Dan, Research Inst. for Advanced Computer Science, USA; [2001]; 8p; In English; ESA Workshop on On-Board Autonomy; n; Avail: CASI; A02, Hardcopy; A01, Microfiche

Planetary rovers provide a considerable challenge for robotic systems in that they must operate for long periods autonomously, or with relatively little intervention. to achieve this, they need to have on-board fault detection and diagnosis capabilities in order to determine the actual state of the vehicle, and decide what actions are safe to perform. Traditional model-based diagnosis techniques are not suitable for rovers due to the tight coupling between the vehicle's performance and its environment. Hybrid diagnosis using particle filters is presented as an alternative, and its strengths and weakeners are examined. We also present some extensions to particle filters that are designed to make them more suitable for use in diagnosis problems.
Author
Fault Detection; Robotics; Roving Vehicles

07
AIRCRAFT PROPULSION AND POWER

Includes prime propulsion systems and systems components, e.g., gas turbine engines and compressors; and onboard auxiliary power plants for aircraft. For related information see also 20 Spacecraft Propulsion and Power, 28 Propellants and Fuels, and 44 Energy Production and Conversion.

20020001559 Siemens Westinghouse Power Corp., USA
Advanced Thermal Barrier Coating System Development
Mar. 31, 1999; 6p; In English
Report No.(s): DE2001-6614; No Copyright; Avail: Department of Energy Information Bridge

The objectives of the program are to provide an improved Thermal Barrier Coating (TBC) system with increased temperature capability and improved reliability relative to current state of the art TBC systems. The development of such a coating system is essential to the ATS (Advanced Turbine System) engine meeting its objectives. The base program consists of three phases: Phase I: Program Planning - Complete; Phase II: Development; and Phase III: Selected Specimen. Bench Test Work is being performed in Phase II and III of the program.
NTIS
Heat Resistant Alloys; Protective Coatings; Thermal Insulation; Thermal Control Coatings; Systems Engineering

20020005064 Federal Energy Technology Center, Morgantown, WV USA
Advanced gas turbine systems research ***Quarterly Report, 1 Jan. - 31 Mar. 1999***
Apr. 01, 1999; 14p; In English
Report No.(s): DE2001-769310; DE-FC21-92MC29061-16; No Copyright; Avail: Department of Energy Information Bridge, Microfiche

No abstract available.
NTIS
Gas Turbines; Electric Power Plants

20020005065 Federal Energy Technology Center, Morgantown, WV USA
Advanced gas turbine systems research ***Quarterly Report, 1 Apr. - 30 Jun. 1999***
Jul. 01, 1999; 9p; In English
Report No.(s): DE2001-769312; DE-FC21-92MC29061-17; No Copyright; Avail: Department of Energy Information Bridge, Microfiche

The activities of the AGTSR Program during this reporting period are described in this report. As has become tradition, the report is divided into discussions on Membership, Administration, Technology Transfer (Workshop/Education) and Research. Items worthy are highlighted below with additional explanation in the text of the report.
NTIS
Gas Turbines; Technology Transfer

09
RESEARCH AND SUPPORT FACILITIES (AIR)

Includes airports, runways, hangars, and aircraft repair and overhaul facilities; wind tunnels, water tunnels, and shock tubes; flight simulators; and aircraft engine test stands. Also includes airport ground equipment and systems. For airport ground operations see 03 Air Transportation and Safety. For astronautical facilities see 14 Ground Support Systems and Facilities (Space).

20020000766 Department of the Navy, Washington, DC USA
Corrosion Sensor
Lucas, Keith, Inventor; Mar. 26, 2001; 35p; In English
Patent Info.: Filed 26 Mar. 2001; US-Patent-Appl-SN-09816148
Report No.(s): AD-D019965; No Copyright; Avail: Issuing Activity (Defense Technical Information Center (DTIC)), Microfiche

A system using tank corrosion sensors to provide for an overall assessment and monitoring of the electro-chemical corrosion and coatings condition in ships' tanks, and particularly in ships' seawater or compensated fuel tanks, The system includes reference half cells mounted along a suspended cable and one instrumented sacrificial anode at the end of the cable to provide optimal sensing capability within a tank structure. The reference half-cells and the sacrificial anode measure a potential and current output, respectively. Together the measurements provide objective information that can be used to predict corrosion damage and coating deterioration occurring throughout the structure of the tank. The system may be used for an overall assessment and monitoring of the electro-chemical corrosion and coatings condition.. In a preferred embodiment, the measurements are stored in a data-logger that is optimally contained within an associated instrument housing. If used with other systems in other tanks, the system may be used to monitor the relative tank condition, trend tank condition changes over time, range tank behavior into three categories and provide a direct analysis methodology for making tank maintenance decisions.
DTIC
Corrosion; Detection

20020000942 NASA Ames Research Center, Moffett Field, CA USA
Low-Disturbance Flow Characteristics of the NASA-Ames Laminar Flow Supersonic Wind Tunnel
Wolf, Stephen W. D., MCAT Inst., USA; Laub, James A., NASA Ames Research Center, USA; [1994]; 9p; In English; AIAA 13th Applied Aerodynamics Conference, 19-22 Jun. 1995, San Diego, CA, USA; Sponsored by American Inst. of Aeronautics and Astronautics, USA
Contract(s)/Grant(s): RTOP 537-03-23; No Copyright; Avail: CASI; A02, Hardcopy; A01, Microfiche

A unique, low-disturbance (quiet) supersonic wind tunnel has been commissioned at the NASA-Ames Fluid Mechanics Laboratory (FML) to support Supersonic Laminar Flow Control (SLFC) research. Known as the Laminar Flow Supersonic Wind Tunnel (LFSWT), this tunnel is designed to operate at potential cruise Mach numbers and unit Reynolds numbers (Re) of the High Speed Civil Transport (HSCT). The need to better understand the receptivity of the transition phenomena on swept (HSCT) wings to attachment-line contamination and cross-flows has provided the impetus for building the LFSWT. Low-disturbance or "quiet" wind tunnels are known to be an essential part of any meaningful boundary layer transition research. In particular, the receptivity of supersonic boundary layers to wind tunnel disturbances can significantly alter the transition phenomena under investigation on a test model. Consequently, considerable effort has gone into the design of the LFSWT to provide quiet flow. The paper describes efforts to quantify the low-disturbance flows in the LFSWT operating at Mach 1.6, as a precursor to transition research on wing models. The research includes: (1) Flow measurements in both the test section and settling chamber of the LFSWT, using a full range of measurement techniques; (2) Study of the state of the test section boundary layer so far by using a single hot-wire

mounted above the floor centerline, with and without boundary layer trips fitted at the test section entrance; (3) The effect of flow quality of unsteady supersonic diffuser flow, joint steps and gaps, and wall vibration.
Derived from text
Flow Characteristics; Laminar Flow; Supersonic Wind Tunnels; Wind Tunnel Models; Boundary Layer Control; Supersonic Diffusers

20020001772 National Aerospace Lab., Amsterdam, Netherlands
Basic Flight Simulation Tool for Rigid Airships
Lemmers, A. J. J. J.; Marsman, A. P. L. A.; Aug. 2000; 23p; In English
Report No.(s): PB2001-108828; NLR-TP-2000-443; No Copyright; Avail: CASI; A03, Hardcopy; A01, Microfiche
The National Aerospace Laboratory NLR is developing a basic flight simulation tool of a rigid airship. This tool will allow simulation of a generic large rigid airship and it will support the fundamentals of Flight Mechanics and Stability and Control. The tool will run in a PC-based environment using MATLAB/Simulink. The basic simulation will support six degrees of freedom and will cover the complete flight envelope. A modular approach is used for the design, which gives the possibility for an easy upgrade when new or modified equipment is available.
NTIS
Flight Simulators; Airships; Flight Envelopes

20020004023 NASA Ames Research Center, Moffett Field, CA USA
Diverse Studies in the Reactivated NASA/Ames Radiation Facility: From Shock Layer Spectroscopy to Thermal Protection System Impact
Miller, Robert J., NASA Ames Research Center, USA; [1994]; 1p; In English; Aerobalistic Range Association 45th Meeting, 10-14 Oct. 1994, Huntsville, AL, USA; Sponsored by Aerobalistic Range Association, USA
Contract(s)/Grant(s): RTOP 478-26-01; No Copyright; Avail: Issuing Activity; Abstract Only
NASA/Ames' Hypervelocity Free-Flight Radiation Facility has been reactivated after having been decommissioned for some 15 years, first tests beginning in early 1994. This paper discusses two widely different studies from the first series, one involving spectroscopic analysis of model shock-layer radiation, and the other the production of representative impact damage in space shuttle thermal protection tiles for testing in the Ames arc-jet facilities. These studies emphasize the interorganizational and interdisciplinary value of the facility in the newly-developing structure of NASA.
Author
Shock Layers; Radiation; Thermal Protection; Space Shuttles; NASA Space Programs; Impact Damage; Spectroscopic Analysis

20020005120 NASA Ames Research Center, Moffett Field, CA USA
Computational Modeling of the Ames 11-Ft Transonic Wind Tunnel in Conjunction with IofNEWT
Djomehri, M. Jahed, Calspan Corp., USA; Buning, Pieter G., NASA Ames Research Center, USA; Erickson, Larry L., NASA Ames Research Center, USA; [1995]; 2p; In English; NASA Computational Aerosciences Workshop, 7-9 Mar. 1995, Moffett Field, CA, USA; Sponsored by NASA Ames Research Center, USA
Contract(s)/Grant(s): RTOP 505-59-20; No Copyright; Avail: Issuing Activity; Abstract Only
Technical advances in Computational Fluid Dynamics have now made it possible to simulate complex three-dimensional internal flows about models of various size placed in a Transonic Wind Tunnel. TWT wall interference effects have been a source of error in predicting flight data from actual wind tunnel measured data. An advantage of such internal CFD calculations is to directly compare numerical results with the actual tunnel data for code assessment and tunnel flow analysis. A CFD capability has recently been devised for flow analysis of the NASA/Ames 11-Ft TWT facility. The primary objectives of this work are to provide a CFD tool to study the NASA/Ames 11-Ft TWT flow characteristics, to understand the slotted wall interference effects, and to validate CFD codes. A secondary objective is to integrate the internal flowfield calculations with the Pressure Sensitive Paint data, a surface pressure distribution capability in Ames' production wind tunnels. The effort has been part of the Ames IofNEWT, Integration of Numerical and Experimental Wind Tunnels project, which is aimed at providing further analytical tools for industrial application. We used the NASA/Ames OVERFLOW code to solve the thin-layer Navier-Stokes equations. Viscosity effects near the model are captured by Baldwin-Lomax or Baldwin-Barth turbulence models. The solver was modified to model the flow behavior in the vicinity of the tunnel longitudinal slotted walls. A suitable porous type wall boundary condition was coded to account for the cross-flow through the test section. Viscous flow equations were solved in generalized coordinates with a three-factor implicit central difference scheme in conjunction with the Chimera grid procedure. The internal flow field about the model and the tunnel walls were descretized by the Chimera overset grid system. This approach allows the application of efficient grid generation codes about individual components of the configuration; separate minor grids were developed to resolve the model

and overset onto a main grid which discretizes the interior of the tunnel test section. Individual grid components axe not required to have mesh boundaries joined in any special way to each other or to the main tunnel grid. Programs have been developed to rotate the model about the tunnel pivot point and rotation axis, similar to that of the tunnel turntable mechanism for adjusting the pitch of the physical model in the test section.
Author
Computational Fluid Dynamics; Transonic Wind Tunnels; Flow Distribution; Aerodynamic Interference; Walls; Wind Tunnel Tests

14
GROUND SUPPORT SYSTEMS AND FACILITIES (SPACE)

Includes launch complexes, research and production facilities; ground support equipment, e.g., mobile transporters; and test chambers and simulators. Also includes extraterrestrial bases and supporting equipment. For related information see also 09 Research and Support Facilities (Air).

20020002753 NASA Kennedy Space Center, Cocoa Beach, FL USA
The Advanced Technology Development Center (ATDC)
Clements, G. R., NASA Kennedy Space Center, USA; [2001]; 10p; In English; STAIF-2002, 3-7 Feb. 2002, Albuquerque, NM, USA; No Copyright; Avail: CASI; A02, Hardcopy; A01, Microfiche

NASA is building the Advanced Technology Development Center (ATDC) to provide a 'national resource' for the research, development, demonstration, testing, and qualification of Spaceport and Range Technologies. The ATDC will be located at Space Launch Complex 20 (SLC-20) at Cape Canaveral Air Force Station (CCAFS) in Florida. SLC-20 currently provides a processing and launch capability for small-scale rockets; this capability will be augmented with additional ATDC facilities to provide a comprehensive and integrated in situ environment. Examples of Spaceport Technologies that will be supported by ATDC infrastructure include densified cryogenic systems, intelligent automated umbilicals, integrated vehicle health management systems, next-generation safety systems, and advanced range systems. The ATDC can be thought of as a prototype spaceport where industry, government, and academia, in partnership, can work together to improve safety of future space initiatives. The ATDC is being deployed in five separate phases. Major ATDC facilities will include a Liquid Oxygen Area; a Liquid Hydrogen Area, a Liquid Nitrogen Area, and a multipurpose Launch Mount; 'Iron Rocket' Test Demonstrator; a Processing Facility with a Checkout and Control System; and Future Infrastructure Developments. Initial ATDC development will be completed in 2006. Author
Launching Bases; Management Systems

15
LAUNCH VEHICLES AND LAUNCH OPERATIONS

Includes all classes of launch vehicles, launch/space vehicle systems, and boosters; and launch operations. For related information see also 18 Spacecraft Design, Testing, and Performance; and 20 Spacecraft Propulsion and Power.

20020000873 California Univ., Santa Barbara, CA USA
Atmospheric radiation measurement: unmanned aerospace vehicle. Final technical report
Gautier, C.; Mar. 01, 2000; 76p; In English
Report No.(s): DE2001-764576; No Copyright; Avail: Department of Energy Information Bridge

Our most important contribution to the ARM-UAV (Atmospheric Radiation Measurement - Unmanned Aerospace Vehicle) program is our analysis of the aircraft observations taken during the Atmospheric Radiation Measurement Enhanced Shortwave Experiment (ARESE). We analyzed aircraft measurements and compared these to computations made from a 3-D radiative transfer model (SB3D) that was partially developed under the UAV program. The 3-D radiative transfer model was enhanced and modified to be a research tool for analysis of future UAV missions. The enhancement includes extending the spectral range of the model from 0.25 to 50 ums. Additionally, an ocean surface component has been added to that includes ocean waves, foam, and ocean column microphysics. This component provides a much more accurate characterization of the ocean BDRF for analyzing reflectance measurements over the ocean made by the UAV. A copy of the user manual is attached. The first part of this analysis was to determine if theoretical calculations of atmospheric column absorption of solar radiation in the presence of clouds matched observations. This analysis included both spectral and broadband fluxes. The second part of the analysis was to analyze the spectral signature of the absorption in order to develop potential physical processes that could explain-the discrepancy between

observations and models. Our primary findings for the data analyzed is that broadband solar radiation absorption is underestimated in theoretical models. The difference we found when using the spectral measurements as a, guide for our broadband computations is about 20 W m-2. This value is much less than that found by investigators using broadband measurements, but still significant. From the spectral comparison, we identified three potential causes for the discrepancy we found. The most dominant is related to the difficulty of parameterizing aerosols in radiative transfer models. by reducing the single scattering albedo and asymmetry factor of aerosols in our model we were able match the spectral observations in the visible. A second cause is that the silicon detectors used in instruments underestimate the flux near 1.06 urn leading to erroneous estimates of atmospheric absorption. Our analysis showed that unresolved 02-02 dimers in this spectral range could not account for the discrepancy. Finally, we demonstrated that cloud droplets required a three-fold increase in cloud albedo to match spectral measurements in near-infrared region. We modified the droplets by introducing soot in the droplets showed that the absorption in the visible would be to high for soot to provide explanation for the cloud absorption anomaly.
NTIS
Aerospace Vehicles; Atmospheric Radiation; Pilotless Aircraft; Radiation Measurement; Atmospheric Attenuation; Mathematical Models; Radiative Heat Transfer

20020003360 Los Alamos National Lab., NM USA
Four years of operations and results with forte
Roussel-Dupre, D.; Klingner, P.; Carlson, L.; Jun. 01, 2001; 18p; In English
Report No.(s): DE2001-783152; LA-UR-01-2955; No Copyright; Avail: Department of Energy Information Bridge, Microfiche
The FORTE (Fast Onboard Recording Transient Events) satellite was launched on 29 August 1997 and has been in continuous operation since that time. FORTE was placed in a nearly circular, 825-km-altitude, 70 degrees inclination orbit by a Pegasus rocket funded by Air Force Space Test Program. The Department of Energy funded the FORTE satellite, which was designed and built at Los Alamos. FORTE's successful launch and engineered robustness were a result of several years of dedicated work by the joint Los Alamos National Laboratory/Sandia National Laboratory project team, led through mission definition, payload and satellite development, and launch by Dr. Stephen Knox. The project is now led to Dr. Abram Jacobson. FORTE carries a suite of instruments, an optical system and a rf system, for the study of lightning and anthropogenic signals. As a result of this effort, new understandings of lightning events have emerged as well as a more complete understanding of the relationship between optical and rf lightning events. This paper will provide an overview of the FORTE satellite and will discuss the on orbit performance of the subsystems.
NTIS
Performance; Payloads; Radio Frequencies; Launching; Lightning

20020005137 Army Research Lab., Aberdeen Proving Ground, MD USA
Numerical Simulations of the Slingatron, *Jul. - Dec. 2000*
Cooper, Gene R., Army Research Lab., USA; Tidman, Derek A., ALCorp., USA; Bundy, Mark L., Army Research Lab., USA; Wilkerson, Stephen, Army Research Lab., USA; Proceedings of the 10th US Army Gun Dynamics Symposium; September 2001; 32p; In English; 10th US Army Gun Dynamics Symposium, 23-26 Apr. 2001, Austin, TX, USA
Contract(s)/Grant(s): DA Proj. 1L1-62618-AH-80
Report No.(s): ARL-RP-30; No Copyright; Avail: CASI; A03, Hardcopy; A01, Microfiche
The slingatron mass accelerator is described for several track configurations (shapes), and numerical simulations of this accelerating mass traversing a given track configuration are presented. The sled is modeled as a point mass that interacts with the slingatron track using both a conventional and a new empirical velocity dependent friction law. The closed loop circular slingatron was found to produce high maximum sled velocities provided the gyration angular speed is always increasing. In contrast several spiral shaped slingatron tracks reveal that high maximum sled velocities are obtainable with the gyration speed held constant. In fact, a slingatron constructed out of semi-circles is shown capable of generating high velocity sleds in such a way that no initial sled injection is necessary. Choosing the proper initial gyration phase with an empirically determined friction model allows the mass sled to gain ever-increasing velocities when placed in a semi-circle slingatron. The sled bearing pressure and its total acceleration are examined and presented.
Author
Angular Velocity; Feedback Control; Gyration; Acceleration (Physics)

16
SPACE TRANSPORTATION AND SAFETY

Includes passenger and cargo space transportation, e.g., shuttle operations; and space rescue techniques. For related information, see also 03 Air Transportation and Safety and 15 Launch Vehicles and Launch Vehicles, and 18 Spacecraft Design, Testing and Performance. For space suits, see 54 Man/System Technology and Life Support.

20020000737 NASA Marshall Space Flight Center, Huntsville, AL USA
Space Transportation: Past, Present, and Future
1998; In English; CD-ROM contains a multimedia presentation compatible with Windows and Macintosh Operating Systems
Report No.(s): NONP-NASA-CD-2001163537; No Copyright; Avail: CASI; C01, CD-ROM

This CD-ROM contains a multimedia presentation produced by NASA Marshall Space Flight Center. The production recounts the history of space transportation research from the early 20th Century to the present, including the current NASA/Orbital X-34 project. The CD includes motion pictures, animation and sound.
CASI
Space Transportation; Rocket Vehicles; NASA Space Programs; Scientists

20020001348 NASA Johnson Space Center, Houston, TX USA
STS-108 Flight Day 2 Highlights
Dec. 07, 2001; In English; Videotape: 9 min. 19 sec. playing time, in color, with sound
Report No.(s): NONP-NASA-VT-2001206813; BRF-1431B; No Copyright; Avail: CASI; B01, Videotape-Beta; V01, Videotape-VHS

On this second day of the STS-108, Endeavour continues to approach the International Space Station. A camera on the end of the Remote Manipulator System robotic arm scans the side of Endeavour and shows the Rafaello Multipurpose Logistics Module.
CASI
Endeavour (Orbiter); Remote Manipulator System; Crew Procedures (Inflight)

20020002232 NASA Johnson Space Center, Houston, TX USA
STS-108 Flight Day 7 Highlights
Dec. 12, 2001; In English; Videotape: 35 min. 10 sec. playing time, in color, with sound
Report No.(s): NONP-NASA-VT-2001216283; BRF-1431G; No Copyright; Avail: CASI; B03, Videotape-Beta; V03, Videotape-VHS

On this seventh day of the STS-108 mission, NASA Ground Control, STS-108 crew (Commander Dominic Gorie, Pilot Mark Kelly, and Mission Specialists Linda Godwin and Daniel Tani), Expedition 3 crew (Commander Frank Culbertson, Jr. and Flight Engineers Mikhail Turin and Vladimir Dezhurov), and Expedition 4 crew (Commander Yuri Onufrienko and Flight Engineers Carl Walz and Daniel Bursch) are seen during a ceremony of remembrance on the three-month anniversary of the September 11th tragedy. The three crews also answer questions from the press on their missions. They are seen as they transfer supplies and equipment from the Rafaello Multipurpose Logistics Module.
CASI
Spacecrews; International Space Station; Crew Procedures (Inflight); Loading Operations

20020002326 NASA Johnson Space Center, Houston, TX USA
STS-104 Mission Highlights Resource Tape, Part 2 of 4
Dec. 12, 2001; In English; Videotape: 59 min. 25 sec. playing time, in color, with sound
Report No.(s): NONP-NASA-VT-2001214902; JSC-1891; No Copyright; Avail: CASI; B03, Videotape-Beta; V03, Videotape-VHS

A continuation of 'STS-104 Mission Highlights Resource Tape, Part 1 of 4' (internal ID 2001214904), this video shows footage from flight days four through seven of the STS-104 mission. Mission Specialists Mike Gernhardt and Jim Reilly are seen during their spacewalks, Pilot Charles Hobaugh and Mission Specialists Janet Kavandi, Mike Gernhardt, and Jim Reilly, and Expedition 2 Flight Engineer Susan Helms work inside the newly installed Quest Airlock. Expedition 2 Flight Engineer Jim Voss is seen as he works to outfit the vestibule between the Unity Module and Quest and opening the hatch between the two components of the International Space Station. Flight days seven (continued) though twelve can be found on the videos 'STS-104 Mission

Highlights Resource Tape, Part 3 of 4' (internal ID 2001214906) and 'STS-104 Mission Highlights Resource Tape, Part 4 of 4' (internal ID 2001214905).
CASI
Air Locks; Extravehicular Activity; International Space Station; Spacecrews; Crew Procedures (Inflight)

20020002331 NASA Johnson Space Center, Houston, TX USA
STS-108 Flight Day 6 Highlights
Dec. 11, 2001; In English; Videotape: 39 min. playing time, in color, with sound
Report No.(s): NONP-NASA-VT-2001217633; BRF-1431F; No Copyright; Avail: CASI; B03, Videotape-Beta; V03, Videotape-VHS

On this sixth day of the STS-108 mission, Mission Specialists Linda Godwin and Daniel Tani perform their spacewalks, where they place insulating blankets on the two Beta Gimbal Assemblies.
CASI
Extravehicular Activity; International Space Station; Crew Procedures (Inflight)

20020002375 NASA Kennedy Space Center, Cocoa Beach, FL USA
A Fully Redundant On-Line Mass Spectrometer System Used to Monitor Cryogenic Fuel Leaks on the Space Shuttle
Griffin, Timothy P., DYNACS Engineering Co., Inc., USA; Naylor, Guy R., DYNACS Engineering Co., Inc., USA; Haskell, William D., DYNACS Engineering Co., Inc., USA; Breznik, Greg S., NASA Kennedy Space Center, USA; Mizell, Carolyn A., NASA Kennedy Space Center, USA; Helms, William R., NASA Kennedy Space Center, USA; Oct. 18, 2001; 31p; In English
Contract(s)/Grant(s): NAS10-98001; No Copyright; Avail: CASI; A03, Hardcopy; A01, Microfiche

An on-line gas monitoring system was developed to replace the older systems used to monitor for cryogenic leaks on the Space Shuttles before launch. The system uses a mass spectrometer to monitor multiple locations in the process, which allows the system to monitor all gas constituents of interest in a nearly simultaneous manner. The system is fully redundant and meets all requirements for ground support equipment (GSE). This includes ruggedness to withstand launch on the Mobile Launcher Platform (MLP), ease of operation, and minimal operator intervention. The system can be fully automated so that an operator is notified when an unusual situation or fault is detected. User inputs are through personal computer using mouse and keyboard commands. The graphical user interface is very intuitive and easy to operate. The system has successfully supported four launches to date. It is currently being permanently installed as the primary system monitoring the Space Shuttles during ground processing and launch operations. Time and cost savings will be substantial over the current systems when it is fully implemented in the field. Tests were performed to demonstrate the performance of the system. Low limits-of-detection coupled with small drift make the system a major enhancement over the current systems. Though this system is currently optimized for detecting cryogenic leaks, many other gas constituents could be monitored using the Hazardous Gas Detection System (HGDS) 2000.
Author
On-Line Systems; Mass Spectroscopy; Leakage; Cryogenic Rocket Propellants; Real Time Operation

20020002378 NASA Johnson Space Center, Houston, TX USA
STS-108 Flight Day 8 Highlights
Dec. 13, 2001; In English; Videotape: 22 min. 50 sec. playing time, in color, with sound
Report No.(s): NONP-NASA-VT-2001216282; BRF-1431H; No Copyright; Avail: CASI; B02, Videotape-Beta; V02, Videotape-VHS

On this eighth day of the STS-108 mission, the STS-108 crew (Commander Dominic Gorie, Pilot Mark Kelly, and Mission Specialists Linda Godwin and Daniel Tani), Expedition 3 crew (Commander Frank Culbertson, Jr. and Flight Engineers Mikhail Turin and Vladimir Dezhurov), and Expedition 4 crew (Commander Yuri Onufrienko and Flight Engineers Carl Walz and Daniel Bursch) work to reload the Rafaello Multipurpose Logistics Module. Commander Culbertson is seen on the International Space Station's treadmill.
CASI
International Space Station; Crew Procedures (Inflight); Loading Operations

20020002385 NASA Johnson Space Center, Houston, TX USA
STS-108 Flight Day 4 Highlights
Dec. 10, 2001; In English; Videotape: 33 min. 45 sec. playing time, in color, with sound
Report No.(s): NONP-NASA-VT-2001214921; BRF-1431D; No Copyright; Avail: CASI; B03, Videotape-Beta; V03, Videotape-VHS

On this fourth day of the STS-108 mission, the robotic arm is seen as it moves towards the Rafaello Multipurpose Logistics Module to prepare for the grapple and transfer of the module from Endeavour to the International Space Station (ISS). Expedition 4 Flight Engineer Carl Walz and STS-108 Mission Specialist Linda Godwin are shown during preparations to open the hatch between ISS and Rafaello. Expedition 3 Commander Frank Culbertson, Expedition 4 Commander Yuri Onufrienko, and STS-108 Pilot Mark Kelly are seen during an on-orbit press conference, where they answer questions about the supply transfer between Rafaello and ISS and share their thoughts about the September 11th tragedy.
CASI
Endeavour (Orbiter); International Space Station; Crew Procedures (Inflight)

20020002387 NASA Johnson Space Center, Houston, TX USA
STS-108 Flight Day 3 Highlights
Dec. 08, 2001; In English; Videotape: 28 min. 59 sec. playing time, in color, with sound
Report No.(s): NONP-NASA-VT-2001214917; BRF-1431C; No Copyright; Avail: CASI; B02, Videotape-Beta; V02, Videotape-VHS

On this third day of the STS-108 mission, the Endeavour Orbiter is seen docking with the International Space Station. The crew of STS-108 (Commander Dominic Gorie, Pilot Mark Kelly, and Mission Specialists Linda Godwin and Daniel Tani) and Expedition 4 (Commander Yuri Onufrienko and Flight Engineers Carl Walz and Daniel Bursch) greet the Expedition 3 crew (Commander Frank Culbertson, Jr. and Flight Engineers Mikhail Turin and Vladimir Dezhurov) in the Destiny Laboratory Module.
CASI
Endeavour (Orbiter); International Space Station; Spacecraft Docking; Spacecrews; Crew Procedures (Inflight)

20020002389 NASA Johnson Space Center, Houston, TX USA
STS-108 Flight Day 5 Highlights
Dec. 10, 2001; In English; Videotape: 18 min. playing time, in color, with sound
Report No.(s): NONP-NASA-VT-2001214915; BRF-1431E; No Copyright; Avail: CASI; B02, Videotape-Beta; V02, Videotape-VHS

On this fifth day of the STS-108 mission, the STS-108 crew (Commander Dominic Gorie, Pilot Mark Kelly, and Mission Specialists Linda Godwin and Daniel Tani), Expedition 3 crew (Commander Frank Culbertson, Jr. and Flight Engineers Mikhail Turin and Vladimir Dezhurov), and Expedition 4 crew (Commander Yuri Onufrienko and Flight Engineers Carl Walz and Daniel Bursch) join in an on-orbit conference to honor those who lost loved ones in the September 11th tragedy. They are also seen moving equipment from the Rafaello Multipurpose Logistics Module to the International Space Station.
CASI
International Space Station; Spacecrews; Crew Procedures (Inflight)

20020002390 NASA Johnson Space Center, Houston, TX USA
STS-104 Mission Highlights Resource Tape, Part 1 of 4
Dec. 11, 2001; In English; Videotape: 59 min. 16 sec. playing time, in color, with sound
Report No.(s): NONP-NASA-VT-2001214904; JSC-1891; No Copyright; Avail: CASI; B03, Videotape-Beta; V03, Videotape-VHS

An overview of the STS-104 mission is given through footage of each flight day. Scenes from flight days one through three show activities such as astronaut prelaunch procedures (breakfast, suit-up, and boarding Atlantis), launch, and on-orbit activities such as the opening of the payload bay doors, rendezvous and docking of the Orbiter to the International Space Station (ISS), and the opening of the hatches separating the Orbiter from ISS. The STS-104 crew (Commander Steven Lindsey, Pilot Charles Hobaugh, and Mission Specialists Mike Gernhardt, Jim Reilly, and Janet Kavandi) greets the Expedition 2 crew (Commander Yuriy Usachev and Flight Engineers James Voss and Susan Helms). Footage from flight days four through twelve can be found on the following videos: 'STS-104 Mission Highlights Resource Tape, Part 2 of 4' (internal ID 2001214902), 'STS-104 Mission Highlights Resource Tape, Part 3 of 4' (internal ID 2001214906), and 'STS-104 Mission Highlights Resource Tape, Part 4 of 4' (internal ID 2001214905).
CASI
International Space Station; Spacecraft Launching; Orbital Rendezvous; Spacecraft Docking; Crew Procedures (Inflight); Crew Procedures (Preflight)

20020002391 NASA Johnson Space Center, Houston, TX USA

STS-104 Mission Highlights Resource Tape, Part 4 of 4

Dec. 12, 2001; In English; Videotape: 47 min. playing time, in color, with sound

Report No.(s): NONP-NASA-VT-2001214905; JSC-1891; No Copyright; Avail: CASI; B03, Videotape-Beta; V03, Videotape-VHS

A continuation of 'STS-104 Mission Highlights Resource Tape, Part 1 of 4' (internal ID 2001214904), 'STS-104 Mission Highlights Resource Tape, Part 2 of 4' (internal ID 2001214902), and 'STS-104 Mission Highlights Resource Tape, Part 3 of 4' (internal ID 2001214906), this video shows footage from flight days ten (continued from part three) through twelve. The Atlantis Orbiter undocks from the International Space Station and performs the fly-around before landing back on Earth. Various unspecified views of Earth are seen from space.

CASI

Atlantis (Orbiter); International Space Station; Spacecraft Docking; Spacecraft Landing

20020002392 NASA Johnson Space Center, Houston, TX USA

STS-104 Mission Highlights Resource Tape

Dec. 12, 2001; In English; Videotape: 56 min. 16 sec. playing time, in color, with sound

Report No.(s): NONP-NASA-VT-2001214906; JSC-1891; No Copyright; Avail: CASI; B03, Videotape-Beta; V03, Videotape-VHS

A continuation of 'STS-104 Mission Highlights Resource Tape, Part 1 of 4' (internal ID 2001214904) and 'STS-104 Mission Highlights Resource Tape, Part 2 of 4' (internal ID 2001214902), this video shows footage from flight days seven (continued from part two) through ten. Mission Specialists Mike Gernhardt and Jim Reilly are seen during their spacewalks, and Expedition 2 Flight Engineer Jim Voss and STS-104 Commander Steven Lindsey replace a leaking intermodular valve in the vestibule between the Unity Module and Quest Airlock. Voss is seen checking for further leaks the next day. Flight day ten is continued on 'STS-104 Mission Highlights Resource Tape, Part 4 of 4' (internal ID 2001214905), which also shows flight days eleven and twelve.

CASI

Extravehicular Activity; Valves; Crew Procedures (Inflight); International Space Station

20020003351 NASA Kennedy Space Center, Cocoa Beach, FL USA

A Quadrupole Ion Trap Mass Spectrometer for Quantitative Analysis of Nitrogen-Purged Compartments within the Space Shuttle

Ottens, Andrew K., Florida Univ., USA; Griffin, Timothy P., DYNACS Engineering Co., Inc., USA; Helms, William R., NASA Kennedy Space Center, USA; Yost, Richard A., Florida Univ., USA; [2001]; 2p; In English; ASMS Conference, 28-31 May 2001, Chicago, IL, USA; Sponsored by American Society of Mechanical Engineers, USA

Contract(s)/Grant(s): NAS10-98001; No Copyright; Avail: CASI; A01, Hardcopy; A01, Microfiche

To enter orbit the Space Shuttle burns 1.8 million liters of liquid hydrogen combined with 0.8 million liters of liquid oxygen through three rocket engines mounted in the aft. NASA monitors the nitrogen-purged aft compartment for increased levels of hydrogen or oxygen in order to detect and determine the severity of a cryogenic fuel leak. Current monitoring is accomplished with a group of mass spectrometer systems located as much as 400 feet away from the shuttle. It can take up to 45 seconds for gas to reach the mass spectrometer, which precludes monitoring for leaks in the final moments before liftoff (the orbiter engines are started at T-00:06 seconds). to remedy the situation, NASA is developing a small rugged mass spectrometer to be used as point-sources around the Space Shuttle.

Author

Mass Spectrometers; Monitors; Quadrupoles; Quantitative Analysis; Space Shuttles

20020005644 NASA Johnson Space Center, Houston, TX USA

STS-108 Flight Day 11 Highlights

Dec. 15, 2001; In English; Videotape: 35 min. 10 sec. playing time, in color, with sound

Report No.(s): NONP-NASA-VT-2001220094; BRF-1431K; No Copyright; Avail: CASI; B03, Videotape-Beta; V03, Videotape-VHS

On this eleventh day of the STS-108 mission, the Expedition 3 crew (Commander Frank Culbertson, Jr. and Flight Engineers Mikhail Turin and Vladimir Dezhurov), Expedition 4 crew (Commander Yuri Onufrienko and Flight Engineers Carl Walz and Daniel Bursch), and STS-108 crew (Commander Dominic Gorie, Pilot Mark Kelly, and Mission Specialists Linda Godwin and Daniel Tani) are seen as the E3 crew bids farewell to the International Space Station (ISS) that has been their home for the previous

several months. Endeavour undocks from ISS and performs the customary flyaround. The STS-108 crew and Commander Culbertson answer questions from the press in an on-orbit interview.
CASI
International Space Station; Crew Procedures (Inflight); Endeavour (Orbiter); Spacecraft Docking

20020005646 NASA Johnson Space Center, Houston, TX USA
STS-108 Flight Day 10 Highlights
Dec. 15, 2001; In English; Videotape: 24 min. 40 sec. playing time, in color, with sound
Report No.(s): NONP-NASA-VT-2001220096; BRF-1431J; No Copyright; Avail: CASI; B02, Videotape-Beta; V02, Videotape-VHS

On this tenth day of the STS-108 mission, STS-108 Mission Specialist Linda Godwin is seen during unloading operations in the Rafaello Multipurpose Logistics Module (MPLM). The exterior of Endeavour and the International Space Station are shown as the Canadarm grapples the MPLM and transfers it to the payload bay of the orbiter.
CASI
International Space Station; Loading Operations; Crew Procedures (Inflight); Space Station Modules

20020005890 NASA Johnson Space Center, Houston, TX USA
STS-108 Flight Day 9 Highlights
Dec. 14, 2001; In English; Videotape: 13 min. playing time, in color, with sound
Report No.(s): NONP-NASA-VT-2001218089; BRF-1431I; No Copyright; Avail: CASI; B01, Videotape-Beta; V01, Videotape-VHS

On this ninth day of the STS-108 mission, the Expedition 3 crew (Commander Frank Culbertson, Jr. and Flight Engineers Mikhail Turin and Vladimir Dezhurov), Expedition 4 crew (Commander Yuri Onufrienko and Flight Engineers Carl Walz and Daniel Bursch), and STS-108 crew (Commander Dominic Gorie, Pilot Mark Kelly, and Mission Specialists Linda Godwin and Daniel Tani) are seen during a ceremony where the E3 crew officially hands over the control of the International Space Station of the E4 crew. Kelly, Godwin, and Tani are seen on the middeck of Endeavour stowing equipment.
CASI
International Space Station; Spacecrews; Loading Operations; Crew Procedures (Inflight)

20020005897 NASA Johnson Space Center, Houston, TX USA
STS-108 Flight Day 12 Highlights
Dec. 17, 2001; In English; Videotape: 26 min. 37 sec. playing time, in color, with sound
Report No.(s): NONP-NASA-VT-2001220095; BRF-1431L; No Copyright; Avail: CASI; B02, Videotape-Beta; V02, Videotape-VHS

On this twelfth day of the STS-108 mission, the deployment of the Starship-3 satellite is shown. Expedition 3 Commander Frank Culbertson, STS-108 Commander Dominic Gorie, Expedition 3 Flight Engineers Mikhail Turin and Vladimir Dezhurov, and STS-108 Pilot Mark Kelly are seen in an on-orbit interview, where they answer questions about their missions. Gorie, Kelly, and STS-108 Mission Specialist Linda Godwin are seen as they stow equipment on the middeck of Endeavour.
CASI
Crew Procedures (Inflight); Spacecrews

18
SPACECRAFT DESIGN, TESTING AND PERFORMANCE

Includes satellites; space platforms; space stations; spacecraft systems and components such as thermal and environmental controls; and spacecraft control and stability characteristics. For life support systems, see 54 Man/System Technology and Life Support. For related information, see also 05 Aircraft Design, Testing and Performance, 39 Structural Mechanics, and 16 Space Transportation and Safety.

20020001443 NASA Marshall Space Flight Center, Huntsville, AL USA
Simple Thermal Environment Model (STEM) User's Guide
Justus, C.G., Computer Sciences Corp., USA; Batts, G. W., Computer Sciences Corp., USA; Anderson, B. J., NASA Marshall Space Flight Center, USA; James, B. F., NASA Marshall Space Flight Center, USA; October 2001; 91p; In English
Report No.(s): NASA/TM-2001-211222; NAS 1.15:211222; M-1026; No Copyright; Avail: CASI; A05, Hardcopy; A01, Microfiche

This report presents a Simple Thermal Environment Model (STEM) for determining appropriate engineering design values to specify the thermal environment of Earth-orbiting satellites. The thermal environment of a satellite, consists of three components: (1) direct solar radiation, (2) Earth-atmosphere reflected shortwave radiation, as characterized by Earth's albedo, and (3) Earth-atmosphere-emitted outgoing longwave radiation (OLR). This report, together with a companion "guidelines" report provides methodology and guidelines for selecting "design points" for thermal environment parameters for satellites and spacecraft systems. The methods and models reported here are outgrowths of Earth Radiation Budget Experiment (ERBE) satellite data analysis and thermal environment specifications discussed by Anderson and Smith (1994). In large part, this report is intended to update (and supersede) those results.

Author

Thermal Environments; Satellite Temperature; Spacecraft Environments; User Manuals (Computer Programs)

20020002376 NASA Goddard Space Flight Center, Greenbelt, MD USA

Design of the Thermal Control System for the Space Technology 5 Microsatellite

Douglas, Donya, NASA Goddard Space Flight Center, USA; Michalek, Ted, NASA Goddard Space Flight Center, USA; Swanson, Ted, NASA Goddard Space Flight Center, USA; [2001]; 9p; In English; 31st International Conference on Environmental Systems (ICES), 9-12 Jul. 2001, Orlando, FL, USA; Sponsored by Society of Automotive Engineers, Inc., USA

Report No.(s): SAE-01ICES-7; Copyright; Avail: Issuing Activity

The New Millennium Program's (NMP) Space Technology 5 (ST-5) Project, currently in Phase B of the design process, is slated to launch three 20-kg class spin stabilized microsatellites in late 2003. The proposed orbit is highly elliptical and could result in an earth shadow eclipse of almost 2 hours. Although ST-5's maximum eclipse is only 2 hours, future missions could involve eclipses as long as 8 hours. As spacecraft size, mass, and available resources decrease and eclipse duration increases, thermal engineers will be challenged to design simple but robust thermal control systems that meet temperature requirements for all phases of the mission. This paper presents the results of a study of three design concepts and preliminary analysis of the design selected for ST-5.

Author

Temperature Control; Control Systems Design; Microsatellites

20020004360 NASA Marshall Space Flight Center, Huntsville, AL USA

Guidelines for the Selection of Near-Earth Thermal Environment Parameters for Spacecraft Design

Anderson, B. J., NASA Marshall Space Flight Center, USA; Justus, C. G., Computer Sciences Corp., USA; Batts, G. W., Computer Sciences Corp., USA; October 2001; 32p; In English

Report No.(s): NASA/TM-2001-211221; NAS 1.15:211221; M-1025; No Copyright; Avail: CASI; A03, Hardcopy; A01, Microfiche

Thermal analysis and design of Earth orbiting systems requires specification of three environmental thermal parameters: the direct solar irradiance, Earth's local albedo, and outgoing longwave radiance (OLR). In the early 1990s data sets from the Earth Radiation Budget Experiment were analyzed on behalf of the Space Station Program to provide an accurate description of these parameters as a function of averaging time along the orbital path. This information, documented in SSP 30425 and, in more generic form in NASA/TM-4527, enabled the specification of the proper thermal parameters for systems of various thermal response time constants. However, working with the engineering community and SSP-30425 and TM-4527 products over a number of years revealed difficulties in interpretation and application of this material. For this reason it was decided to develop this guidelines document to help resolve these issues of practical application. In the process, the data were extensively reprocessed and a new computer code, the Simple Thermal Environment Model (STEM) was developed to simplify the process of selecting the parameters for input into extreme hot and cold thermal analyses and design specifications. In the process, greatly improved values for the cold case OLR values for high inclination orbits were derived. Thermal parameters for satellites in low, medium, and high inclination low-Earth orbit and with various system thermal time constraints are recommended for analysis of extreme hot and cold conditions. Practical information as to the interpretation and application of the information and an introduction to the STEM are included. Complete documentation for STEM is found in the user's manual, in preparation.

Author

Earth Radiation Budget Experiment; Environment Models; Spacecraft Design; Thermal Environments; Irradiance; Solar Radiation

19
SPACECRAFT INSTRUMENTATION AND ASTRIONICS

Includes the design, manufacture, or use of devices for the purpose of measuring, detecting, controlling, computing, recording, or processing data related to the operation of space vehicles or platforms. For related information, see also 06 Aircraft Instrumentation and Avionics; For spaceborne instruments not integral to the vehicle itself see 35 Instrumentation and Photography; For spaceborne telescopes and other astronomical instruments see 89 Astronomy, Instrumentation and Photography; For spaceborne telescopes and other astronomical instruments see 89 Astronomy.

20020002251 Sandia National Labs., Albuquerque, NM USA
Chemical Microsensor and Micro-Instrument Technology at Sandia National Laboratories
Butler, M. A.; Frye-Mason, G. C.; Hughes, R. C.; Osbourn, G. C.; Mar. 26, 1999; 6p; In English
Report No.(s): DE2001-5048; SAND99-0713C; No Copyright; Avail: Department of Energy Information Bridge, Microfiche

Important factors in the application of chemical sensing technology to space applications are low mass, small size, and low power. All of these attributes are enabled by the application of microelectromechanical systems (MEMS) and micro-fabrication technology to chemical sensing. Several Sandia projects that apply these technologies to the development of new chemical sensing capabilities with the potential for space applications will be described. The Polychromator project is a joint project with Honeywell and MIT to develop an electrically programmable diffraction grating that can be programmed to synthesize the spectra of molecules. This grating will be used as the reference cell in a gas correlation radiometer to enable remote chemical detection of most chemical species. Another area of research where micro-fabrication is having a large impact is the development of a lab on a chip. Sandia's efforts to develop the (mu)ChemLab(trademark) will be described including the development of microfabricated pre-concentrators, chromatographic columns, and detectors. Chemical sensors are evolving in the direction of sensor arrays with pattern recognition methods applied to interpret the pattern of response. Sandia's development of micro-fabricated chemiresistor arrays and the VERI pattern recognition technology to interpret the sensor response will be described.
NTIS
Detection; Microinstrumentation; Sensors; Chemical Indicators

20020005788 NASA Glenn Research Center, Cleveland, OH USA
Adaptive Vibration Reduction Controls for a Cryocooler With a Passive Balancer
Kopasakis, George, NASA Glenn Research Center, USA; Cairelli, James E., NASA Glenn Research Center, USA; Traylor, Ryan M., Purdue Univ., USA; October 2001; 14p; In English; 2001 Cryogenic Engineering Conference, 16-20 July, 2001, Madison, WI, Madison, WI, USA, USA; Sponsored by Cryogenic Society of America, USA
Contract(s)/Grant(s): RTOP 783-82-00
Report No.(s): NASA/TM-2001-211094; E-12937; NAS 1.15:211094; No Copyright; Avail: CASI; A03, Hardcopy; A01, Microfiche

In this paper an adaptive vibration reduction control (AVRC) design is described for a Stirling cryocooler combined with a passive balancer. The AVRC design was based on a mass-spring model of the cooler and balancer, and the AVRC algorithm described in this paper was based on an adaptive binary search. Results are shown comparing the baseline uncontrolled cooler with no balancer, the cooler with the balancer, and, finally, the cooler with the balancer and the AVRC. The comparison shows that it may be possible to meet stringent vibration reduction requirements without an active balancer.
Author
Adaptive Control; Vibration Damping; Balancing; Coolers

20
SPACECRAFT PROPULSION AND POWER

Includes main propulsion systems and components, e.g., rocket engines; and spacecraft auxiliary power sources. For related information, see also 07 Aircraft Propulsion and Power; 28 Propellants and Fuels; 15 Launch Vehicles and Launch Operations; and 44 Energy Production and Conversion.

20020001166 Lawrence Livermore National Lab., Livermore, CA USA
Space Shuttle Cleaning Verification Applications of the Contamination Analysis Unit to Reusable Solid Rocket Motor Production Scenarios
Koester, C.; Meltzer, M.; Ross, S.; Dec. 01, 1998; 58p; In English
Report No.(s): DE2001-8701; UCRL-CR-132900; EW02MM09B; No Copyright; Avail: Department of Energy Information Bridge, Microfiche

This report describes work to date on a project to test the capabilities of a mass spectrometer-based system for analyzing in-situ organic compounds on a variety of substrates. The system is termed the 'Contamination Analysis Unit' (CAU) and employs vacuum and thermal desorption of surface residues, followed by ionization and analysis with a Leybold Inficon Transpector mass spectrometer. The agreement covering this project was made between the USA government, represented by the Department of Energy (DOE) and Thiokol Aerospace and Industrial Technologies (Thiokol) under contract number M89R020. Work on the project has been performed by Lawrence Livermore National Laboratory (LLNL).
NTIS
Mass Spectrometers; Organic Compounds; Contamination; Cleaning

20020002286 Los Alamos National Lab., NM USA
Heatpipe-operated Mars Exploration Reactor (HOMER)
Poston, D. I.; Oct. 01, 2000; 11p; In English
Report No.(s): DE2001-766062; LA-UR-00-5209; No Copyright; Avail: Department of Energy Information Bridge, Microfiche
The Heatpipe Power System (HPS) is a near-term low-cost, space fission power system that has been under development at Los Alamos National Laboratory (LANL) for 5 years. The goal of the HPS project is to devise an attractive space fission system that can be developed quickly and affordably. The primary ways of doing this are by using existing technology and by designing the system for inexpensive testing. If the system can be designed to allow highly prototypic testing with electrical heating, then an exhaustive test program can be carried out inexpensively and quickly and thorough testing of the actual flight unit can be performed which is a major benefit to reliability. Over the past 4 years, LANL has conducted three HPS proof-of-concept technology demonstrations each has been highly successful. The Heatpipe-Operated Mars Exploration Reactor (HOMER) is a derivative of the HPS designed especially for producing electricity on the surface of Mars. The key attributes of the HOMER are described in this paper, as well as a 20-kWe point design system scalability, and the current technology status.
NTIS
Heat Pipes; Space Power Reactors; Fission; Fabrication; Design Analysis; Performance Tests; Mars Exploration

20020002292 Prairie View Agricultural and Mechanical Coll., TX USA
Local Heat Transfer and CHF for Subcooled Flow Boiling ***Final Report, 15 Sep. 1992 - 14 May 1998***
Boyd, R.; Aug. 01, 1998; 12p; In English
Report No.(s): DE2001-765713; No Copyright; Avail: Department of Energy Information Bridge, Microfiche
The Heatpipe Power System (HPS) is a near-term low-cost, space fission power system that has been under development at Los Alamos National Laboratory (LANL) for 5 years. The goal of the HPS project is to devise an attractive space fission system that can be developed quickly and affordably. The primary ways of doing this are by using existing technology and by designing the system for inexpensive testing. If the system can be designed to allow highly prototypic testing with electrical heating, then an exhaustive test program can be carried out inexpensively and quickly and thorough testing of the actual flight unit can be performed which is a major benefit to reliability. Over the past 4 years, LANL has conducted three HPS proof-of-concept technology demonstrations each has been highly successful. The Heatpipe-Operated Mars Exploration Reactor (HOMER) is a derivative of the FIRS designed especially for producing electricity on the surface of Mars. The key attributes of the HOMER are described in this paper, as well as a 20-kWe point design system scalability, and the current technology status.
NTIS
Heat Flux; Heat Transfer; Boiling; Cooling; Critical Flow

20020002698 NASA Kennedy Space Center, Cocoa Beach, FL USA
Rocket Launch-Induced Vibration and Ignition Overpressure Response
Caimi, Raoul, NASA Kennedy Space Center, USA; Margasahayam, Ravi, DYNACS Engineering Co., Inc., USA; Nayfeh, Jamal, University of Central Florida, USA; [2001]; 8p; In English; International Congress on Sound and Vibration, 2-6 Jul. 2001, Hong Kong; No Copyright; Avail: CASI; A02, Hardcopy; A01, Microfiche
Rocket-induced vibration and ignition overpressure response environments are predicted in the low-frequency (5 to 200 hertz) range. The predictions are necessary to evaluate their impact on critical components, structures, and facilities in the immediate vicinity of the rocket launch pad.
Author
Rocket Launching; Ignition; Overpressure; Vibration Effects

20020002856 DYNACS Engineering Co., Inc., Cocoa Beach, FL USA

The Launch of Bumper 8 from the Cape: The End of an Era and the Beginning of Another

Starr, Stanley O., DYNACS Engineering Co., Inc., USA; [2001]; 11p; In English; IAF Congress, 1-4 Oct. 2001, Toulouse, France; Sponsored by International Astronautical Federation, Switzerland

Contract(s)/Grant(s): NAS10-98001; Copyright; Avail: Issuing Activity

On July 24, 1950, Bumper 8 was launched from a small concrete launch pad north of the Cape Canaveral lighthouse, becoming the first launch from the Long Range Proving Ground. The Bumper missiles, six launched from White Sands and two from Cape Canaveral, were a combination of a German V-2 first stage and a WAC Corporal unguided, liquid fuel rocket as a second stage. The Bumper missions achieved great advances in altitude and velocity, demonstrated the first successful ignition of a second stage liquid rocket, and explored the boundaries of aerodynamic heating and complex missile control systems. They also engaged public interest during a time when weapons developments were largely secret. The fledgling Long Range Proving, Ground had just embarked on a multiyear program to build a thousand mile, over ocean missile range when it was tasked with supporting the complex launching and tracking requirements of the last two Bumper launches. The LRPG quickly created facilities to support the Bumper launches, under harsh environmental conditions and with a hastily assembled team, and successfully met the Bumper launch schedule. Although announced to the press and widely remembered as successful, the two Bumper launches did not meet their technical objectives.

Author

Missiles; Missile Control; Missile Ranges

20020005117 NASA Marshall Space Flight Center, Huntsville, AL USA

Rocket Engine Thrust Chamber Assembly

Cornelius, Charles S., Inventor, NASA Marshall Space Flight Center, USA; Counts, Richard H., Inventor, NASA Marshall Space Flight Center, USA; Myers, W. Neill, Inventor, NASA Marshall Space Flight Center, USA; Lackey, Jeffrey D., Inventor, NASA Marshall Space Flight Center, USA; Peters, Warren, Inventor, NASA Marshall Space Flight Center, USA; Shadoan, Michael, Inventor, NASA Marshall Space Flight Center, USA; Sparks, David L., Inventor, NASA Marshall Space Flight Center, USA; Lawrence, Timothy W., Inventor, NASA Marshall Space Flight Center, USA; Mar. 06, 2001; 8p; In English

Patent Info.: Filed 10 Dec. 1998; NASA-Case-MFS-31138-1; US-Patent-6,195,984; US-Patent-Appl-SN-228034; No Copyright; Avail: CASI; A02, Hardcopy; A01, Microfiche

A thrust chamber assembly for liquid fueled rocket engines and the method of making it wherein a two-piece mandrel having the configuration of an assembly having a combustion chamber portion connected to a nozzle portion through a throat portion is wrapped with a silica tape saturated with a phenolic resin, the tape extending along the mandrel and covering the combustion chamber portion of the mandrel to the throat portion. The width of the tape is positioned at an angle of 30 to 50 deg. to the axis of the mandrel such that one edge of the tape contacts the mandrel while the other edge is spaced from the mandrel. The phenolic in the tape is cured and the end of the wrap is machined to provide a frusto-conical surface extending at an angle of 15 to 30 deg. with respect to the axis of the mandrel for starting a second wrap on the mandrel to cover the throat portion. The remainder of the mandrel is wrapped with a third silica tape having its width positioned at a angle of 5 to 20 deg. from the axis of the mandrel. The resin in the third tape is cured and the assembly is machined to provide a smooth outer surface. The entire assembly is then wrapped with a tow of graphite fibers wetted with an epoxy resin and, after the epoxy resin is cured, the graphite is machined to final dimensions.

Official Gazette of the U.S. Patent and Trademark Office

Combustion Chambers; Epoxy Resins; Graphite; Rocket Engines; Thrust Chambers

20020005123 NASA Marshall Space Flight Center, Huntsville, AL USA

Combustion Chamber/Nozzle Assembly and Fabrication Process Therefor

Myers, W. Neill, Inventor, NASA Marshall Space Flight Center, USA; Cornelius, Charles S., Inventor, NASA Marshall Space Flight Center, USA; Dec. 26, 2000; 6p; In English; Provisional of US-Patent-Appl-SN-057004, filed 18 Aug. 1997

Patent Info.: Filed 14 Aug. 1998; US-Patent-6,164,060; US-Patent-Appl-SN-134703; US-Patent-Appl-SN-057004; No Copyright; Avail: CASI; A02, Hardcopy; A01, Microfiche

An integral lightweight combustion chamber/nozzle assembly for a rocket engine has a refractory metal shell defining a chamber of generally frusto-conical contour. The shell communicates at its larger end with a rocket body, and terminates at its smaller end in a tube of generally cylindrical contour, which is open at its terminus and which serves as a nozzle for the rocket engine. The entire inner surface of the refractory metal shell has a thermal and oxidation barrier layer applied thereto. An ablative silica phenolic insert is bonded to the exposed surface of the thermal and oxidation barrier layer. The ablative phenolic insert provides a chosen inner contour for the combustion chamber and has a taper toward the open terminus of the nozzle. A process

for fabricating the integral, lightweight combustion chamber/nozzle assembly is simple and efficient, and results in economy in respect of both resources and time.
Official Gazette of the U.S. Patent and Trademark Office
Combustion Chambers; Fabrication; Nozzle Design; Metal Shells

20020005130 NASA Glenn Research Center, Cleveland, OH USA
Reduced Toxicity Fuel Satellite Propulsion System Including Fuel Cell Reformer with Alcohols Such as Methanol
Schneider, Steven J., Inventor, NASA Glenn Research Center, USA; Nov. 13, 2001; 30p; In English
Patent Info.: Filed 17 Apr. 2001; NASA-Case-LEW-16636-3; US-Patent-6,314,718; US-Patent- Appl-SN-837819; US-Patent-Appl-SN-291883; No Copyright; Avail: CASI; A03, Hardcopy; A01, Microfiche

A reduced toxicity fuel satellite propulsion system including a reduced toxicity propellant supply for consumption in an axial class thruster and an ACS class thruster. The system includes suitable valves and conduits for supplying the reduced toxicity propellant to the ACS decomposing element of an ACS thruster. The ACS decomposing element is operative to decompose the reduced toxicity propellant into hot propulsive gases. In addition the system includes suitable valves and conduits for supplying the reduced toxicity propellant to an axial decomposing element of the axial thruster. The axial decomposing element is operative to decompose the reduced toxicity propellant into hot gases. The system further includes suitable valves and conduits for supplying a second propellant to a combustion chamber of the axial thruster, whereby the hot gases and the second propellant auto-ignite and begin the combustion process for producing thrust.
Official Gazette of the U.S. Patent and Trademark Office
Fuel Systems; Propellant Consumption; Propellants; Toxicity; Spacecraft Propulsion

20020005645 NASA Glenn Research Center, Cleveland, OH USA
Investigation of Keeper Erosion in the NSTAR Ion Thruster
Domonkos, Matthew T., NASA Glenn Research Center, USA; Foster, John E., NASA Glenn Research Center, USA; Patterson, Michael J., NASA Glenn Research Center, USA; Williams, George J., Jr., Ohio Aerospace Inst., USA; December 2001; 28p; In English; 27th; 27th International Electric Propulsion Conference, 14-19 October, 2001, Pasadena, CA, USA; Sponsored by NASA Glenn Research Center, USA
Contract(s)/Grant(s): RTOP 755-B4-04
Report No.(s): NASA/TM-2001-211280; E-13080; IEPC-01-308; NAS 1.15:211280; No Copyright; Avail: CASI; A03, Hardcopy; A01, Microfiche

The goal of the present investigation was to determine the cause for the difference in the observed discharge keeper erosion between the 8200 hr wear test of a NASA Solar Electric Propulsion Technology Applications Readiness (NSTAR) engineering model thruster and the ongoing extended life test (ELT) of the NSTAR flight spare thruster. During the ELT, the NSTAR flight spare ion thruster experienced unanticipated erosion of the discharge cathode keeper. Photographs of the discharge keeper show that the orifice has enlarged to slightly more than twice the original diameter. Several differences between the ELT and the 8200 hr wear test were initially identified to determine any effects which could lead to the erosion in the ELT. In order to identify the cause of the ELT erosion, emission spectra from an engineering model thruster were collected to assess the dependence of keeper erosion on operating conditions. Keeper ion current was measured to estimate wear. Additionally, post-test inspection of both a copper keeper-cap was conducted, and the results are presented. The analysis indicated that the bulk of the ion current was collected within 2-mm radially of the orifice. The estimated volumetric wear in the ELT was comparable to previous wear tests. Redistribution of the ion current on the discharge keeper was determined to be the most likely cause of the ELT erosion. The change in ion current distribution was hypothesized to caused by the modified magnetic field of the flight assemblies.
Author
Erosion; Ion Currents; Ion Engines; Solar Electric Propulsion; Wear Tests

20020005820 Los Alamos National Lab., NM USA
Chemical analysis of plutonium-238 for space applications
Wong, A.; Aug. 01, 2000; 8p; In English
Report No.(s): DE2001-768727; LA-UR-00-3849; No Copyright; Avail: Department of Energy Information Bridge

Los Alamos National Laboratory (LANL) has produced general-purpose heat sources (GPHS) containing plutonium-238 oxide for space and terrestrial uses over the past two decades. Power Source Technologies Group (NMT-9) has fill capabilities to both recover and purify (238)PuO2 from scrap and aged fuels and to fabricate oxides into fuel pellets for heat sources.
NTIS
Plutonium 238; Chemical Analysis; Technology Utilization; Fabrication; Plutonium Oxides

23
CHEMISTRY AND MATERIALS (GENERAL)

Includes general research topics related to the composition, properties, structure, and use of chemical compounds and materials as they relate to aircraft, launch vehicles, and spacecraft. For specific topics in chemistry and materials see categories 24 through 29. For astrochemistry see category 90 Astrophysics.

20020000742 Tennessee Technological Univ., Cookeville, TN USA
Separation and Analytical Chemistry of the Actinides
Ensor, D. D.; Jun. 30, 1998; 15p; In English
Report No.(s): DE2001-763051; LA-SUB-99-26; No Copyright; Avail: Department of Energy Information Bridge, Microfiche

The determination of low levels of actinides from water samples and aqueous waste streams involves a lengthy and complicated process which is characterized by low recoveries and poor precision. The objective of this work was to evaluate the use of a Photon Electron Rejecting Alpha Liquid Scintillation Spectrometer (PERALS(reg-sign)), in combination with extractive scintillators, for the detection of actinides. The results of the application of this method to aqueous samples containing uranium, thorium, plutonium, and americium, both individually and in mixtures showed promising results. Using a commercially available extractant, ALPHAEX(reg-sign), recoveries of plutonium and americium were approx. 98.4% in individual samples and in mixtures with activities ranging from 6 pci to 500 pci. The separation of these two elements was accomplished by selective extraction after adjusting the acidity of the aqueous sample. The application of this technique to a raw waste sample showed reasonable recoveries when combined with classical anion exchange separation techniques. Efforts to develop an extractive scintillator using a recently synthesized tetradentate extractant were only moderately successful since solubility problems limit the extractant's efficiency in the scintillator. The application of a curve fitting program, PEAKFIT(reg-sign), to spectra obtained using the PERALS(reg-sign) spectrometer provided useful isotropic information.
NTIS
Analytical Chemistry; Actinide Series; Wastes; Alpha Particles; Solvent Extraction

20020000746 Combustion Specialists, Inc., Maple Valley, WA USA
Detection and Control of Deposition on Pendant Tubes
Kychakoff, G.; Apr. 24, 2000; 5p; In English
Report No.(s): DE2001-764452; DOE/GO/10375-Q; No Copyright; Avail: Department of Energy Information Bridge

The project objective is to develop a deposition sensing system and to demonstrate that it can be used to help extend the time between boiler shutdowns and ameliorate other problems associated with deposit formation.
NTIS
Deposition; Detection; Tubes; Control Theory

20020000891 Argonne National Lab., IL USA
Magnetic properties and crystal structure of RENiAl and UNiAl hydrides
Bordallo, H. N.; Drulis, H.; Havela, L.; Iwasieczko, W.; Kolomiets, A. V.; Aug. 11, 1999; 14p; In English
Report No.(s): DE2001-11924; ANL/IPNS/CP-99744; No Copyright; Avail: Department of Energy Information Bridge, Microfiche

RENiAl (RE = rare-earth metal) and UNiAl compounds crystallizing in the hexagonal ZrNiAl-type structure (space group P(bar 6)2m) can absorb up to 2 and 3 hydrogen (deuterium) atoms per formula unit, respectively. Hydrogenation leads to a notable lattice expansion and modification of magnetic properties. However, the impact of hydrogenation on magnetism is the opposite for 4f- and 5f-materials: TN(T(sub c))is lowered in the case of rare-earth hydrides, while for UNiAlH(D)(sub x) it increases by an order of magnitude. Here we present results of magnetic and structure studies performed of these compounds, focusing on the correlation between magnetic and structural variations and discussing possible reasons of the striking difference in effect of hydrogenation on rare-earth and actinide intermetallics.
NTIS
Crystal Structure; Magnetic Properties; Nickel Alloys; Rare Earth Alloys; Aluminum Alloys; Uranium Alloys; Hydrides

20020000895 Argonne National Lab., IL USA
Cerium, uranium, and plutonium behavior in glass-bonded sodalite, a ceramic nuclear waste form
Lewis, M. A.; Lexa, D.; Morss, L. R.; Richmann, M. K.; Sep. 03, 1999; 18p; In English
Report No.(s): DE2001-11916; ANL/CMT/CP-99703; No Copyright; Avail: Department of Energy Information Bridge, Microfiche

Glass-bonded sodalite is being developed as a ceramic waste form (CWF) to immobilize radioactive fission products, actinides, and salt residues from electrometallurgical treatment of spent nuclear reactor fuel. The CWF consists of about 75 mass % sodalite, 25 mass % glass, and small amounts of other phases. This paper presents some results and interpretation of physical measurements to characterize the CWF structure, and dissolution tests to measure the release of matrix components and radionuclides from the waste form. Tests have been carried out with specimens of the CWF that contain rare earths at concentrations similar to those expected in the waste form. Parallel tests have been carried out on specimens that have uranium or plutonium as well as the rare earths at concentrations similar to those expected in the waste forms; in these specimens UCl(sub 3) forms UO(sub 2) and PuCl(sub 3) forms PuO(sub 2). The normalized releases of rare earths in dissolution tests were found to be much lower than those of matrix elements (B, Si, Al, Na). When there is no uranium in the CWF, the release of cerium is two to ten times lower than the release of the other rare earths. The low release of cerium may be due to its tetravalent state in uranium-free CWF. However, when there is uranium in the CWF, the release of cerium is similar to that of the other rare earths. This trivalent behavior of cerium is attributed to charge transfer or covalent interactions among cerium, uranium, and oxygen in (U,Ce)O(sub 2).
NTIS
Radioactive Wastes; Sodalite; Containment; Glass; Ceramics

20020000900 Argonne National Lab., IL USA
Interaction of polymer with clays
Auvray, L.; Lal, J.; Jul. 02, 1999; 19p; In English
Report No.(s): DE2001-11881; ANL/IPNS/CP-99416; No Copyright; Avail: Department of Energy Information Bridge, Microfiche

Normally synthetic well defined monodisperse discotic laponite clays are known to form a gel phase at mass concentrations as low as a few percent in distilled water. Hydrosoluble polymer polyethylene oxide was added to this intriguing clay system, it was observed that it either prevents gelation or slows it down extremely depending on the polymer weight, concentration or the laponite concentration. Small Angle Neutron scattering (SANS) was used to study these systems because only by isotopic labelling can the structure of the adsorbed polymer layers be determined. The contrast variation technique is specifically used to determine separately the different partial structure factors of the clay and polymer. In this way the signal of the adsorbed chains is separated from the signal of the free chains.
NTIS
Clays; Gelation; Polymers; Glycols; Polyethylenes; Fluid-Solid Interactions

20020000906 Argonne National Lab., IL USA
Elemental mercury removal using a wet scrubber
Gonzalez, E.; Livengood, C. D.; Martin, K.; Mendelsohn, M. H.; Zhou, C. Q.; May 19, 1999; 9p; In English
Report No.(s): DE2001-11821; ANL/ES/CP-99072; No Copyright; Avail: Department of Energy Information Bridge, Microfiche

Mercury (Hg) is a toxic metal that is emitted into the environment by both natural and human activities. Acute and chronic exposure to mercury and methyl mercury in humans results in central nervous system damage, kidney damage, and even death. Although some Hg emission sources have been regulated, coal-fired utilities have not been. In anticipation of federal regulations on mercury emissions from coal-fired power plants, Argonne National Laboratory (ANL) has designed a flue gas simulation system to study the removal of elemental mercury. The simulated flue gas enters the system and combines with the inlet mercury vapor (from a calibrated permeation tube), carried by nitrogen gas. This combined gas continues past the flow meter and the pressure gage to the reactor inlet. Inside the reactor chamber, the flue gas is sprayed with NOXSORB(reg-sign), a chloric acid solution, which reacts with elemental mercury. The amount of reaction (oxidation) of elemental mercury is important since mercury in an oxidized form is highly soluble, In this form, the Hg can be picked up downstream by a wet scrubber from fossil-fuel burning utilities. Experiments on mercury removal from flue gases have been conducted at ANL, with the participation of a senior design team from Purdue University Calumet. Temperature variations ranging from room temperature to 350 F have been studied. Other parameters, such as the concentration of NOXSORB(reg-sign), were also tested. Furthermore, pump speed and sprayer droplet sizes of the NOXSORB(reg-sign) solution were studied. A literature survey on the current and proposed mercury control legislation, along with the existing control technologies, has been performed as part of the senior design project. With guidance from ANL, an understanding of the simulation system has been developed. This information has been used to determine the mass transfer. Another literature survey was performed on the reaction kinetics of mercury. The information obtained was used to postulate probable behavior of elemental mercury in flue gas. The experimental results obtained at Argonne will be related to

existing wet scrubber technology to determine the economic feasibility of mercury removal. A cost per pound of mercury analysis will be utilized.
NTIS
Scrubbers; Mercury Vapor; Toxicity; Mercury (Metal)

20020000911 Texas Univ., Dallas, TX USA
Synthesis of Compounds for Los Alamos National Laboratory
Ferraris, J. P.; Jul. 20, 1999; 27p; In English
Report No.(s): DE2001-763055; LA-SUB-99-20; No Copyright; Avail: Department of Energy Information Bridge, Microfiche
As part of contract 6709U0015-3C, the compounds listed were synthesized and transferred to LANL for evaluation. Work on these has resulted in several papers, manuscripts and talks bearing LANL and UTD co-authorship. The detailed synthetic procedures are described and the chemical structure of the mentioned compounds are shown in a table. Synthetic procedures: (1) 2-Methoxy-5-(2(prime)-ethyl hexyloxy)-1,4-distyrylbenzene--see synthesis of compound V in the reference. (2) MEHPPV : 1.000 g 1,4-methoxyethylhexyloxy- 2,5-dibromomethylbenzene + 0.0042 g (1 mol %) anthracene were dissolved in 35 ml dry THF and 1.0 M solution of t-BuOK in THF was added slowly during 60 min and stirred at room temperature for 20 hours. The red suspension was precipitated in 200 ml cold MeOH, the solid was filtered, washed by MeOH and dried in vacuum. The red-orange solid was extracted by boiling hexane for 24 hours. Insolublein hexane red polymer was extracted by boiling xylene for 24 hours, soluble in xylene fraction was dissolved in THF and precipitated in MeOH. After filtration and drying in vacuum 0.220 g(36% yield) of red polymer with M(sub W)=357000 and absorption maximum at 496 nm (chloroform) was obtained. (3)1,4-distyrylbenzene - see synthesis of compound 1 in the reference. (star)(star) xy-5-(2(prime) -ethylhexyloxy)benzene: This compound was obtained in 51% yield according the general procedure for the Wittig reaction described in the reference (from 2- methoxy-5(2(prime)- ethylhexyloxy) -1,4-xylylene-bis (triphenylphosphonium chloride) and (star)(star) m.p.49-51 C. (5) Films of aromatic copolyamides with fragments of 9,10-bis(p-carboxyphenyl) anthracene and bis(m-aminophenyl) -9,10-anthracene--see synthesis of copolyamides XXI and XXII in the reference.(6,7) Films of the solid solution of 9,10-diphenylanthracene in poly(m- phenyleneisophtalamide) (PMPI) were obtained from the 5.0% solution of mixture 0.231 g PMPI and 0.0319 g 9.10-diphenylanthracene in N-MP at conditions described in the reference. (8) 2,5-Didodecyloxy-1,4-distyrylbenzene--see synthesis of compoundIV in the reference. (9) 2,5- Dioctyloxy-1, 4-distyrylbenzene--see synthesis of compound Ill in the reference. (10) 2,5-Dimethoxy-1, 4-distyrylbenzene--see synthesis of compound II in the reference. (11) Films with the compositions of polystyrene (PS) + 2,5-didodecyloxy-1,4- distyrylbenzene (8) (40:60 w/w) and PS + 2,5-dioctyloxy-1,4-distyrylbenzene (9) (40:60 w/w) were obtained by evaporation of 10% solution of components in chloroform at room temperature. (12) FATs and other (omega)-substituted alkane thiols including -CN, -CHO, -OH, -NH2.
NTIS
Chemical Composition; Synthesis (Chemistry); Ethyl Compounds; Methoxy Systems

20020000917 Lawrence Livermore National Lab., Livermore, CA USA
Solid phase microextraction analysis of B83 SLTS and Core B compatibility test units
Chambers, D. M.; Ithaca, J.; King, H. A.; Malcolm, S.; Mar. 26, 1999; 6p; In English
Report No.(s): DE2001-12129; UCRL-JC-133766; No Copyright; Avail: Department of Energy Information Bridge, Microfiche
Solid phase microextraction has permitted the efficient collection and analysis of a broad range of volatile and semivolatile compounds outgassed from materials. In 1998, we implemented a microextraction protocol at Mason and Hanger, Pantex Plant, for the analysis of weapons and compatibility test units. The chemical information that was obtained from this work is interpreted by determining the source and outgas mechanism for each compound in the weapon signature, which is a task only accomplished by analysis of material standards.
NTIS
Compatibility; Solid Phases; Protocol (Computers)

20020000939 Sandia National Labs., Albuquerque, NM USA
Porosity in Polysilsesquioxane Xerogels
Baugher, B. M.; Loy, D. A.; Rahimian, K.; Aug. 17, 1999; 8p; In English
Report No.(s): DE2001-14104; SAND99-2751C; No Copyright; Avail: Department of Energy Information Bridge, Microfiche
Polymerization of organotrialkoxysilanes is a convenient method for introducing organic functionality into hybrid organic-inorganic materials. However, not much is known about the effects of the organic substituent on the porosity of the resulting xerogels. In this study, we prepared a series of polysilsesquioxane xerogels from organotrialkoxysilanes, RSi(OR(sup 1))(sub 3), with different organic groups (R = H, Me, Et dodecyl, hexadecyl, octadecyl, vinyl, chloromethyl, (p-chloromethyl)

phenyl, cyanoethyl). Polymerizations of the monomers were carried out under a variety of conditions, varying monomer concentration, type of catalyst, and alkoxide substituent. The effect of the organic substituent on the sol-gel process was often dramatic. In many cases, gels were formed only at very high monomer concentration and/or with only one type of catalyst. All of the gels were processed as xerogels and characterized by scanning electron microscopy and nitrogen sorption porosimetry to evaluate their pore structure.
NTIS
Xerogels; Organic Materials; Porosity; Organic Silicon Compounds

20020001072 Argonne National Lab., IL USA
REF1-horizontal-surface reflectometer-reference instrument WBS 1.7.10
Crawford, R. K.; Jan. 18, 1999; 12p; In English
Report No.(s): DE2001-12079; ANL/SNS/98-6; No Copyright; Avail: Department of Energy Information Bridge, Microfiche
REF1 is designed to study the reflectivity of horizontal surfaces, such as a free liquid surface. A schematic representation of REF1 the parameters for this instrument are provided. The instrument will be useful for a wide range of science, including interfacial studies in polymers and surface chemistry involving thin layers of surfactants or other materials on the surfaces of liquids. The instrument geometry will be flexible so that other capabilities (e.g., polarized neutrons) can be added at a later date. Data rates will be sufficiently high to permit kinetic studies on many systems.
NTIS
Surface Properties; Reflectance; Liquid Surfaces; Reflectometers

20020001170 Lawrence Livermore National Lab., Livermore, CA USA
Emission Spectra Land Particle Ejection During Visible-Laser Ablation of Graphite for Diamond-Like Coatings
Chang, J. J.; Gragon, E. P.; McLean, W.; Warner, B. E.; Feb. 01, 1999; 12p; In English
Report No.(s): DE2001-8777; UCRL-JC-131300; No Copyright; Avail: Department of Energy Information Bridge, Microfiche
The authors have investigated the emission spectra of a carbon plume generated from graphite by a visible pulsed laser for diamond-like coatings (DLC). The laser utilized was a 300-watt class copper vapor laser with a pulse duration of approximately 40 ns. to better understand the laser-target interaction, they have visualized plume dynamics near the graphite ejection during pulsed laser deposition (PLD). The ejection of material started at about 500 ns after the onset of laser pulse and lasted for about 10 micrometers. The material ejection is very directional and introduced larger amounts of micro particulates in the DLC film. The authors have found that the use of a random phase plate to smooth the laser intensity profile effectively eliminated this ejection of material with additional advantage of higher coating rate. The spectra in the visible and ultraviolet of the plume emission were analyzed to correlate with DLC quality and coating rate. They have characterized the carbon plasma based on emissions from C, C2, C+ and C++ for laser peak intensities between 0.1 - 5 GW/sq cm. They authors have produced high-quality DLC with its coating rate optimized at laser peak power densities between 0.5 GW/sq cm and 0.8 GW/sq cm. The kinetic energy of C+ was estimated to be approximately 20 eV at this optimized coating condition. They found that greater C+ kinetic energy at higher laser intensity does not necessarily produce better DLC. This process optimization enabled them to demonstrate a coating rate as high as 2000 micrometers/hr. The c2 swan-band emission from the plume was most pronounced in the optimized coating condition and was used as a process diagnostic tool.
NTIS
Carbon; Emission Spectra; Graphite; Laser Target Interactions; Plumes

20020001240 Michigan State Univ., Dept. of Chemistry, East Lansing, MI USA
Direct Examination of Separation Processes in Chromatography by Laser-Induced Fluorescence ***Final Report, 1 Sep. 1989 - 28 Feb. 1999***
McGuffin, V. L.; Feb. 28, 1999; 71p; In English
Report No.(s): DE2001-766061; DOE/ER/14056-64; No Copyright; Avail: Department of Energy Information Bridge
This report summarizes the progress September 1, 1989 to February 28, and accomplishments of this research project from 1999. During this period, we have developed an experimental system for the direct examination of the chromatographic or electrophoretic column by laser-induced fluorescence. This system has been utilized to examine and to characterize the retention of model solutes on octadecylsilica, the most common stationary phase for reversed-phase liquid chromatography. Thermodynamic quantities such as the molar free energy, molar enthalpy, molar volume, enthalpyentropy compensation temperature, and enthalpy-volume compensation pressure, as well as the kinetic rate constants for solute distribution between the mobile and stationary phases have been systematically measured as a function of bonding density, temperature (10 to 70 C), pressure (400 to 4500 psi), and mobile phase composition. In each of these studies, substantial knowledge has been gained

regarding the fundamental thermodynamic and kinetic processes that are responsible for chromatographic separations. We have also initiated the development and validation of a three-dimensional computer simulation of chromatographic and electrophoretic separations. In this simulation, the trajectories of individual molecules are monitored through the transport processes of diffusion, convection by laminar, electroosmotic, or electrophoretic flow, and surface interaction by a partition or adsorption mechanism. The molecular distribution and the corresponding zone profile may be examined and characterized by means of statistical solute zones have been determined as a function of the distribution coefficient along the column as well as in regions of spatial and temporal transition (e.g., injection and elution). In addition to these primary research objectives, we have made significant progress toward the development of systematic optimization methods for chromatography and electrophoresis. In these optimization methods, the theoretical knowledge gained through experimental and computer simulation studies has been applied to practical problems. Finally, we have developed novel detection methods based on laser-induced fluorescence, fluorescence quenching, and photoionization for environmental, forensic, and biomedical applications.
NTIS
Chromatography; Computerized Simulation; Electrophoresis; Three Dimensional Models; Laser Induced Fluorescence

20020001569 Argonne National Lab., IL USA
Effect of Source Gas Chemistry on Tribological Performance of Diamond-Like Carbon Films
Erdemir, A.; Eryilmaz, O. L.; Fenske, G. R.; Nilufer, I. B.; Aug. 23, 1999; 17p; In English
Report No.(s): DE2001-11834; ANL/ET/CP-99151; No Copyright; Avail: Department of Energy Information Bridge
In this study, we investigated the effects of various source gases (i. e., methane, ethane, ethylene, acetylene and methane + hydrogen) on friction and wear performance of diamond-like carbon (DLC) films. Specifically, we described the anomalous nature and fundamental friction and wear mechanisms of DLC films derived from gas discharge plasmas with very low to very high hydrogen content. The films were deposited on steel substrates by a plasma enhanced chemical vapor deposition process at room temperature and the tribological tests were performed in dry nitrogen. The results of tribological tests revealed a close correlation between the friction and wear coefficients of the DLC films and the source gas chemistry. Specifically, films grown in source gases with higher hydrogen-to-carbon ratios had much lower friction coefficients and wear rates than the films derived from source gases with lower hydrogen-to-carbon ratios. The lowest friction coefficient (0.002) was achieved with a film derived from 25% methane-75% hydrogen while the films derived from acetylene had a coefficient of 0.15. Similar correlations were observed on wear rates. Specifically, the films derived from hydrogen rich plasmas had the least wear while the films derived from pure acetylene suffered the highest wear. We used a combination of scanning and transmission electron microscopy and Raman spectroscopy to characterize the structural chemistry of the resultant DLC films.
NTIS
Coefficient of Friction; Tribology; Wear; Films

20020001775 Technical Research Centre of Finland, Jyvaskyla, Finland
Electrodeposition of PbS, PbSe and PbTe Thin Films
Saloniemi, H.; Dec. 15, 2000; 145p; In English
Report No.(s): PB2001-108734; VTT/PUB-423; Copyright; Avail: National Technical Information Service (NTIS), Microfiche
Lead chalcogenides (PbS, PbSe, PbTe) are narrow band gap semiconductors which are largely used in infrared applications. In the present study lea chalcogenide thin films were deposited electrochemically from aqueous solutions. Two different electrodeposition methods were used; PbSe and PbTe thin films were prepared at constant potential while PbS was deposited by cycling the potential.
NTIS
Semiconductor Devices; Thin Films; Electrodeposition

20020001857 Maryland Univ., College Park, MD USA
Molecular simulation of phase equilibria for complex fluids
Panagiotopoulos, A. Z.; Feb. 13, 1999; 13p; In English
Report No.(s): DE2001-764614; No Copyright; Avail: Department of Energy Information Bridge
The general area of this project is the development and application of molecular simulation methods for prediction of equilibrium properties of complex fluids. In earlier project periods, we have developed the Gibbs ensemble methodology for direct determination of phase equilibria. The technique has met with considerable success and is now in widespread use throughout the world. In the most recent project period, we focused on polar/ionic, polymeric, and surfactant systems. We have made considerable

progress in developing novel algorithms to meet the computational challenges presented by the strong interactions in these systems, and have generated data for well-defined models that can be used to test theories and compare to experimental data.
NTIS
Simulation; Surfactants; Equilibrium; Phase Stability (Materials); Complex Compounds; Fluids

20020001863 ARCADIS Geraghty and Miller, Inc., Research Triangle Park, NC USA
Innovative Approach for Measuring Ammonia and Methane Fluxes from a Hog Farm Using Open-Path Fourier Transform Infrared Spectroscopy
Harris, D. B.; Thompson, E. L.; Vogel, C. A.; Hashmonay, R. A.; Natschke, D.; Jan. 01, 2000; 12p; In English
Report No.(s): PB2002-100040; No Copyright; Avail: CASI; A03, Hardcopy; A01, Microfiche

The paper describes a new approach to quantify emissions from area air pollution sources. The approach combines path-integrated concentration data acquired with any path-integrated optical remote sensing (PI-ORS) technique and computed tomography (CT) technique. In this study, and open-path Fourier transform infrared (OP-FTIR) instrument sampled path-integrated concentrations along five radial beam paths, in a vertical plane downwind from an area source. The innovative CT technique, which applies the smooth basis function minimization (SBFM) method to the beam data in conjunction with measured wind data, was used to estimate the total flux from the area source. Results are presented from a field experiment designed for quantifying ammonia and methane emissions before and after a bioactive cover was added to control odors from a hog farm waste lagoon near Jacksonville, NC. This field study provides a new insight to the processes taking place in these facilities. The suggested technologies may provide robust and real-time estimates of gaseous emission fluxes and near-field dispersion parameters for near-ground level area sources.
NTIS
Ammonia; Methane; Air Pollution

20020001984 Argonne National Lab., IL USA
Analytical Chemistry Laboratory *Progress Report, FY 1998*
Boparai, A. S.; Bowers, D. L.; Graczyk, D. G.; Green, D. W.; Lindahl, P. C.; Mar. 29, 1999; 64p; In English
Report No.(s): DE2001-12021; ANL/ACL-98/2; No Copyright; Avail: Department of Energy Information Bridge

This report summarizes the activities of the Analytical Chemistry Laboratory (ACL) at Argonne National Laboratory (ANL) for Fiscal Year (FY) 1998 (October 1997 through September 1998). This annual progress report, which is the fifteenth in this series for the ACL, describes effort on continuing projects, work on new projects, and contributions of the ACL staff to various programs at ANL.
NTIS
Analytical Chemistry; Reaction Kinetics

20020001993 Surmet Corp., Burlington, MA USA
Insulating Coating Development for Vanadium Alloys. Phase I Technical Report
Gunda, N.; Sastri, S.; Jayaraman, M.; Karandikar, P.; May 11, 2000; 14p; In English
Report No.(s): DE2001-763935; No Copyright; Avail: Department of Energy Information Bridge

Self-cooled liquid-lithium/vanadium blanket offers many advantages for fusion power systems. Liquid metals moving through a magnetic field are subjected to magnetohydrodynamic (MHD) effects that can increase the pressure drop and affect the flow profiles and heat transfer. Insulating coatings are required to eliminate this effect. Based on the thermodynamic stability data five different coatings were selected PVD and CVD processes were developed to deposit these coatings. All coatings have resistivities much higher than the minimum required. Liquid lithium testing at Argonne National Laboratory indicates that one of the coatings showed only partial spalling. Thus, further refinement of this coating has significant potential to satisfy the requirements for Li/V blanket technology.
NTIS
Vanadium Alloys; Vapor Deposition; Liquid Metals; Protective Coatings; Magnetohydrodynamics; Reactor Materials; Thermonuclear Reactions; Lithium Alloys; Blankets (Fusion Reactors)

20020002004 Sandia National Labs., Albuquerque, NM USA
Finite Element Modeling of a Micro hotplate for Microfluidic Applications
Benson, D. A.; Frye-Mason, G. C.; Manginell, R. P.; Rosato, D. A.; Mar. 09, 1999; 6p; In English
Report No.(s): DE2001-4272; SAND99-0576C; No Copyright; Avail: Department of Energy Information Bridge, Microfiche

A hand-held chemical laboratory ((mu)ChemLab) is being developed that utilizes a silicon-nitride-supported microhotplate in the front-end, gas sampling and preconcentration stage. Device constraints include low-power (200mW at 5V), rapid heating (20msec), and a relatively uniform temperature distribution throughout the heated area ((approximately)3mm(sup 2)). to optimize for these criteria, the electro-thermal behavior of the microhotplate was modeled using Thermal Analysis System (TAS). Predicted steady-state and transient behavior agree well with infrared (IR) microscope data and measured transient response for a low-stress silicon nitride thermal conductivity of k(sub n) = 6.4 x 10(sup (minus)2) W x (cm x (degree)C)(sup (minus)1) and a convection coefficient of h(sub cv) = 3.5 x 10(sup (minus)3) W x (cm(sup 2) x (degree)C)(sup (minus)1). The magnitude of h(sub cv) is framed in the context of vacuum measurements and empirical data. Details and limitations of the IR measurement are discussed. Finally, the efficacy of methods for reducing thermal gradients in the microhotplate's active area is presented.
NTIS
Finite Element Method; Mathematical Models; Thermal Conductivity; Fluids; Microanalysis

20020002255 Sandia National Labs., Albuquerque, NM USA
Oxidation Effects on the Friction of Lubricants and Self-Lubricating Materials in the Enduring Stockpile
Dugger, M. T.; Peebles, D. E.; Ohlhausen, J. A.; Robinson, J. A.; Sorroche, E. H.; Mar. 18, 1999; 7p; In English
Report No.(s): DE2001-4713; SAND99-0650C; No Copyright; Avail: Department of Energy Information Bridge, Microfiche

Predictive models of solid lubricant performance are needed to determine the dynamic behavior of electromechanical devices after long periods of storage. X-ray photoelectron spectroscopy has been used to determine the kinetics of oxidation and sulfate formation for solid lubricants and self-lubricating materials containing MoS2, exposed to a variety of oxidation conditions. The frictional performance of the lubricant has then been determined as a function of its surface chemistry and the ambient environment in which sliding takes place. Results indicate that surface sulfate formation governs the initial or start-up friction coefficient of MoS2-containing films, while the composition of the ambient gas determines the steady-state friction coefficient. The dependence of the steady-state friction coefficient on the environment in which sliding takes place has been examined, and the results show that dynamic oxidation of surfaces having exposed metal has a major impact on friction. Surface oxidation is also shown to influence the frictional behavior of a self-lubricating composite material containing MoS2.
NTIS
Coefficient of Friction; Dynamic Characteristics; Friction Factor; Oxidation; Solid Lubricants

20020002360 Harvard Univ., Cambridge, MA USA
Fundamental spectroscopic studies of carbenes and hydrocarbon radicals
Mar. 12, 1999; 20p; In English
Report No.(s): DE2001-765943; No Copyright; Avail: Department of Energy Information Bridge, Microfiche

Determination of bond dissociation energies and heats of formation of hydrocarbon radicals and carbenes requires knowledge of their structures, but this is not provided by standard mass spectrometric studies; what is needed is high-resolution spectroscopy, often best achieved at centimeter and millimeter wavelengths. Nearly 60 reactive organic molecules were investigated in the period from 1988-1998.
NTIS
Carbenes; Radicals; Spectroscopy; Hydrocarbons

20020002707 Sandia National Labs., Albuquerque, NM USA
Simulation of Sintering of Layered Structures
Olevsky,; Tikare,; Garino,; Braginsky,; Nov. 22, 2000; 6p; In English
Report No.(s): DE2001-768065; SAND2000-2920C; No Copyright; Avail: Department of Energy Information Bridge

An integrated approach, combining the continuum theory of sintering and Potts model based mesostructure evolution analysis, is used to solve the problem of bi-layered structure sintering. Two types of bi-layered structures are considered: layers of the same material with different initial porosity, and layers of two different materials. The effective sintering stress for the bi-layer powder sintering is derived, both at the meso- and the macroscopic levels. Macroscopic shape distortions and spatial distributions of porosity are determined as functions of the dimensionless specific time of sintering. The effect of the thickness of the layers on shrinkage, warpage, and pore-grain structure is studied. Ceramic ZnO powders are employed as a model experimental system to assess the model predictions.
NTIS
Ceramics; Porosity; Powder Metallurgy; Sintering

20020002713 California Univ., Lawrence Berkeley Lab., Berkeley, CA USA

Ideal strength and mechanical hardness of solids

Krenn, C.; Apr. 01, 2000; 94p; In English

Report No.(s): DE2001-767573; LBNL-45246; No Copyright; Avail: Department of Energy Information Bridge

Relationships between intrinsic mechanical hardness and atomic-scale properties are reviewed, Hardness scales closely and linearly with shear modulus for a given class of material (covalent, ionic or metallic). A two-parameter fit and a Peierls-stress model produce a more universal scaling relationship, but no model can explain differences in hardness between the transition metal carbides and nitrides. Calculations of 'ideal strength' (defined by the limit of elastic stability of a perfect crystal) are proposed. The ideal shear strengths of fcc aluminum and copper are calculated using ab initio techniques and allowing for structural relaxation of all five strain components other than the imposed strain. The strengths of Al and Cu are similar (8-9% of the shear modulus), but the geometry of the relaxations in Al and Cu is very different. The relaxations are consistent with experimentally measured third-order elastic constants. The general thermodynamic conditions of elastic stability that set the upper limits of mechanical strength are derived. The conditions of stability are shown for cubic (hydrostatic), tetragonal (tensile) and monoclinic (shear) distortions of a cubic crystal. The implications of this stability analysis to first-principles calculations of ideal strength are discussed, and a method to detect instabilities orthogonal to the direction of the applied stress is identified. The relaxed ideal shear and tensile strengths of bcc tungsten are also calculated using ab initio techniques and are favorably compared to recent nano-indentation measurements. The (l-brace)100(r-brace) tensile strength (29.5 GPa) is governed by the Bain instability. The shear strengths in the weak directions on (l-brace)110(r-brace), (l-brace)112(r-brace), and (l-brace)123(r-brace) planes are very nearly equal ((approx) 18 GPa) and occur at approximately the same strain (17-18%). This isotropy is a function of the linear elastic isotropy for shear in directions containing (l-angle)111(r-angle) in bcc and of the atomic configurations of energetic saddle points reached during shear. This isotropy may also explain the prevalence of the pencil glide of dislocations in bcc metals. A final chapter presents some recent ideal strength calculations of TiC and TiN and discusses future directions for research.

NTIS

Hardness; Solids; Mechanical Properties; Modulus of Elasticity; Transition Metals

20020002803 Los Alamos National Lab., NM USA

Explosive compaction of clad graphite powders and obtaining of coatings on their base

Peikrishvili, A. B.; Japaridze, L. A.; Oct. 01, 2000; 13p; In English

Report No.(s): DE2001-766125; LA-UR-00-5226; No Copyright; Avail: Department of Energy Information Bridge, Microfiche

In order to consolidate graphite based powders and in order to obtain coatings with density values near to the theoretical ones clad graphite powders of the C(graphite), - Ni (C - Ni) compositions were explosively compacted under different loading conditions. Theoretical calculations revealed that for assessing the stress-deformed state of C- Ni compositions and computing the normal and tangent stress components (when V is less than C(longitudinal) and VD<C(transversal))itisrecommnded to apply the dynamic problem's solution model while the pressure impulse P = f(x) is being uniformly spread with constant rate along the boundary of a semi-infinite elastic body. The results of our experiments showed that it is possible to obtain high dense coatings from CE-Ni compositions bonded by an intermediate layer to the substrate material. The structure and properties of the coatings depends on the intensity of the shock loading and temperature. The effect of the shock loading conditions (temperature, loading intensity) on the structure, properties and structure/properties relationships for the C-Ni coatings are discussed.

NTIS

Coatings; Explosives; Graphite; Compacting; Elastic Bodies

20020003393 Los Alamos National Lab., NM USA

Precision cleaning of semiconductor surfaces using carbon dioxide-based fluids

Rubin, J.; Sivils, L.; Busnaina, A.; Jul. 01, 1999; 29p; In English

Report No.(s): DE2001-768231; LA-UR-99-2370; No Copyright; Avail: Department of Energy Information Bridge, Microfiche

The Los Alamos National Laboratory, on behalf of the Hewlett-Packard Company, is conducting tests of a closed-loop CO2-based supercritical fluid process, known as Supercritical CO2 Resist Remover (SCORR). We have shown that this treatment process is effective in removing hard-baked, ion-implanted photoresists, and appears to be fully compatible with metallization systems. We are now performing experiments on production wafers to assess not only photoresist removal, but also residual surface contamination due to particulate and trace metals. Dense-phase (liquid or supercritical) CO2, since it is non-polar, acts like an organic solvent and therefore has an inherently high volubility for organic compounds such as oils and greases. Also, dense CO2 has a low-viscosity and a low dielectric constant. Finally, CO2 in the liquid and supercritical fluid states can solubilize metal completing agents and surfactants. This combination of properties has interesting implications for the removal not only of organic

films, but also trace metals and inorganic particulate. In this paper we discuss the possibility of using CO2 as a precision-cleaning solvent, with particular emphasis on semiconductor surfaces.
NTIS
Cleaning; Semiconductors (Materials); Carbon Dioxide; Supercritical Fluids

20020004025 NASA Ames Research Center, Moffett Field, CA USA
The Origins of Polycyclic Aromatic Hydrocarbons: Are They Everywhere?
Allamandola, L. J., NASA Ames Research Center, USA; [1994]; 1p; In English; NATO Advanced Studies Workshop, 6-17 Jun. 1994, Erice, Italy; Sponsored by North Atlantic Treaty Organization, Unknown
Contract(s)/Grant(s): RTOP 399-20-10-05; No Copyright; Avail: Issuing Activity; Abstract Only

During the past 15 years considerable progress in observational techniques has been achieved in the middle-infrared region (5000-500 per centimeter, 2-20 micron), the region where most diagnostic molecular vibrations occur. Spectra of many different astronomical infrared sources, some deeply embedded in dark molecular clouds and others at their edges, are now available. These spectra provide a powerful probe, not only for the identification of interstellar molecules in both the gas and solid phases, but also of the physical and chemical conditions which prevail in these two very different domains. The two lectures will focus on the evidence that polycyclic aromatic hydrocarbons (PAHs) are an important, ubiquitous and abundant interstellar species. PAHs are. extremely stable species which can range in size from a few angstroms across to several hundred angstroms (PAHs are also the building blocks of amorphous carbon particles). This identification rests on the suggestive agreement between the laboratory spectra of PAHs with a set of IR emission bands which emanate from many different sources where ultraviolet starlight impinges on a ”dusty” region. The picture is that individual PAHs are first pumped into highly vibrationally excited states and relax by fluorescence at their fundamental vibrational frequencies. That PAHs are a ubiquitous interstellar component has serious ramifications in other spectral regions as well, including the strong extinction in the ultraviolet, and the classic visible diffuse interstellar bands discovered more than 50 years ago (but unexplained to this day) The first part of the course will focus on the interpretation of astronomical spectra. The second lecture will start by showing how recent laboratory data on PAHs taken under realistic interstellar conditions has con borated the PAH hypothesis and led to great insight into the conditions in the PAH containing regions. This lecture will end by reviewing the ever-increasing evidence for interstellar PAHs in meteorites and interplanetary dust particles. This in conjunction with the recent suggestion that PAHs are abundant in Jupiter’s atmosphere will make the point that ”PAHs are Everywhere”.
Author
Infrared Radiation; Interstellar Matter; Polycyclic Aromatic Hydrocarbons; Infrared Sources (Astronomy); Molecular Clouds

20020004919 Federal Energy Technology Center, Morgantown, WV USA
Functionally Graded Alumina/Mullite Coatings for Protection of Silicon Carbide Ceramic Components from Corrosion
Sotirchos, S. V.; Apr. 01, 1997; 20p; In English
Report No.(s): DE2001-3832; DE-FG22-96PC96208-1; No Copyright; Avail: Department of Energy Information Bridge, Microfiche

During the six months of this reporting period, we accomplished the following: Preparatory work was done on the development of the feed supply system (for mixtures of AlCl(sub 3), SiCl(sub 4), H(sub 2) and CO(sub 2)) and effluent treatment section for the CVD system we plan to employ for coating preparation. A comprehensive literature survey of past work done on the chemical vapor deposition of silica, alumina and aluminosilicates (mullite) was carried out, and work was initiated on the study of thermochemical equilibrium in the Al/Si/Cl/C/O/H system so as to identify the boundaries of the region of the space of operating parameters and conditions where preparation of functionally graded mullite/ alumina coatings through CVD from metal chloride, CO(sub 2), and H(sub 2) is feasible. Since the alumina/mullite films that are proposed to be developed can also be applied to carbon matrix composites provided that a layer that bridges the gap that exists between the thermal expansion coefficient of carbon and that of mullite is employed, experiments were conducted on the preparation of compositionally graded carbon/silicon carbide coatings. Deposition from mixtures of ethylene and methyltrichlorosilane or tetrachlorosilane (silicon tetrachloride) in hydrogen was used for the preparation of SiC/C coatings, and our experiments focused on the study of the occurrence of multiple steady states in the deposition process and the effects of the type of chlorosilane on the deposition rate and the deposit composition and their variation along the length of the reactor. The results showed that when operation is carried out outside the multiplicity region, codeposition of SiC and C from ethylene and chlorosilanes is a feasible route for preparation of SiC/C graded coatings.
NTIS
Aluminum Oxides; Ceramics; Coating; Silicon Carbides; Mullites; Carbon; Corrosion Prevention

20020005061 Los Alamos National Lab., NM USA

Equation of state and hugoniot locus for porous materials: p-alpha model revisited

Menikoff, R.; Aug. 01, 1999; 5p; In English

Report No.(s): DE2001-769210; LA-UR-99-2364; No Copyright; Avail: Department of Energy Information Bridge, Microfiche

Foams, porous solids and granular materials have a characteristic Hugoniot locus that for weak shocks is concave in the (particle velocity, shock velocity)-plane. An equation of state (EOS) that has this property can be constructed implicitly from a Helmholtz free energy of the form (Psi)(sub s)(V,T,(phi)) = (Psi)(sub s)(V,T)+B((phi)) where the equilibrium volume fraction (phi)(sub eq) is determined by minimizing (Psi), i.e., the condition (partial derivative)(sub (psi)) (Psi) = 0. For many cases, a Hayes EOS for the pure solid (Psi)(sub s)(V,T) is adequate. This provides a thermodynamically consistent framework for the P-(alpha) model. For this form of EOS the volume fraction has a similar effect to an endothermic reaction in that the partial Hugoniot loci with fixed (psi) are shifted to the left in the (V,P)-plane with increasing f. The equilibrium volume fraction can then be chosen to match the concavity of the principal Hugoniot locus. An example is presented for the polymer estane. A small porosity of only 1.4 percent is required to match the experimental concavity in the Hugoniot data. This type of EOS can also be used to obtain the so-called ”universal” Hugoniot for liquids.

NTIS

Granular Materials; Porous Materials; Equations of State

20020005111 Thomas Jefferson National Accelerator Facility, Newport News, VA USA

Energetic Deposition in Vacuum

Wu, G.; Phillips, L.; Sundelin, R.; Goodman, T.; Sep. 01, 2001; 5p; In English

Report No.(s): DE2001-786146; JLAB-OTP-01-03; DOE/ER/40150-1900; No Copyright; Avail: Department of Energy Information Bridge, Microfiche

In hoping to improve Niobium deposition on Copper cavity, a vacuum deposition system has been built to test the idea of Nb energetic condensation on copper substrate. The system directly uses microwave power to create the pure Nb plasma, which can be used to extract energetic Nb ion flux to do direct deposition on copper substrate. In this paper, we briefly describe the system, discuss the potential benefit of this technique and report the initial result of Nb plasma creation and Niobium thin film deposition.

NTIS

Vacuum Deposition; Niobium; Plasmas (Physics); Metal Films

20020005168 Sandia National Labs., Albuquerque, NM USA

DOE Laboratory Catalysis Research Symposium: Abstracts

Dunham, T.; Feb. 01, 1999; 53p; In English

Report No.(s): DE2001-4148; SAND99-0418; No Copyright; Avail: Department of Energy Information Bridge, Microfiche

The conference consisted of two sessions with the following subtopics: (1) Heterogeneous Session: Novel Catalytic Materials; Photocatalysis; Novel Processing Conditions; Metals and Sulfides; Nuclear Magnetic Resonance; Metal Oxides and Partial Oxidation; Electrocatalysis; and Automotive Catalysis. (2) Homogeneous Catalysis: H-Transfer and Alkane Functionalization; Biocatalysis; Oxidation and Photocatalysis; and Novel Medical, Methods, and Catalyzed Reactions.

NTIS

Catalysis; Conferences; Research and Development; Electrocatalysts

20020005169 Sandia National Labs., Albuquerque, NM USA

Detection of Biological Materials Using Ion Mobility Spectroscopy

Rodacy, P. J.; Sterling, J. P.; Butler, M. A.; Mar. 01, 1999; 17p; In English

Report No.(s): DE2001-4164; SAND99-0467; No Copyright; Avail: Department of Energy Information Bridge, Microfiche

Traditionally, Ion Mobility Spectroscopy has been used to examine ions of relatively low molecular weight and high ion mobility. In recent years, however, biomolecules such as bradykinin, cytochrome c, bovine pancreatic trypsin inhibitor (BPTI), apomyoglobin, and lysozyme, have been successfully analyzed, but studies of whole bio-organisms have not been performed. In this study an attempt was made to detect and measure the mobility of two bacteriophages, (lambda)-phage and MS2 using electrospray methods to inject the viruses into the ion mobility spectrometer. Using data from Yeh, et al., which makes a comparison between the diameter of non-biologic particles and the specific particle mobility, the particle mobility for the MS2 virus was estimated to be 10(sup (minus)2) cm(sup 2)/volt-sec. From this mobility the drift time of these particles in our spectrometer was calculated to be approximately 65 msec. The particle mobility for the (lambda)-phage virus was estimated to be 10(sup (minus)3) cm(sup 2)/volt-sec. which would result in a drift time of 0.7 sec. Spectra showing the presence of a viral peak at the expected drift time were not observed. However, changes in the reactant ion peak that could be directly attributed to the

presence of the viruses were observed. Virus clustering, excessive collisions, and the electrospray injection method limited the performance of this IMS. However, we believe that an instrument specifically designed to analyze such bioagents and utilizing other injection and ionization methods will succeed in directly detecting viruses and bacteria.
NTIS
Detection; Ion Mobility Spectroscopy; Biochemistry; Microorganisms

20020005199 Sandia National Labs., Albuquerque, NM USA
Strength Testing and Fractography of MEMS Materials
Glass, S. J.; Lavan, D.; Buchheit, T. E.; Jackson, K.; Nov. 28, 2000; 16p; In English
Report No.(s): DE2001-769052; SAND2000-0081C; No Copyright; Avail: Department of Energy Information Bridge

The safe, secure, and reliable application of microelectromechanical systems (MEMS) devices requires knowledge about the MEMS materials' strength distributions and strength-limiting flaws. Sandia has developed a microtensile testing technique that uses the lateral force capabilities of a computer-controlled Nanoindenter to quantify the strength distribution of MEMS materials such as silicon and amorphous diamond. The sample sizes reflect the critical dimensions and features typical of MEMS devices.
NTIS
Amorphous Materials; Fractography; Mechanical Properties; Microelectromechanical Systems

20020005205 Sandia National Labs., Albuquerque, NM USA
Lifetime Predictions for Elastomers from Accelerated Aging Experiments
Gillen,; Clough,; Dec. 06, 2000; 4p; In English
Report No.(s): DE2001-769086; SAND2000-3037C; No Copyright; Avail: Department of Energy Information Bridge, Microfiche

Prediction of polymer lifetimes is an important challenge for the polymer industry, particularly for materials expected to perform reliably for extended time periods (e.g., decades). It is also critically important for comparing new material formulations during their development. This paper briefly reviews some of the state-of-the-art lifetime prediction methods available for commercially formulated clastomers exposed to oxygen, humidity, and/or high-energy radiation environments. Important complications and pitfalls associated with such methods are highlighted.
NTIS
Elastomers; Service Life; Experimentation; Accelerated Life Tests; Aging (Materials); Prediction Analysis Techniques

20020005224 National Renewable Energy Lab., Golden, CO USA
Use of Uniformly Distributed Concentrated Sunlight for Highly Accelerated Testing of Coatings
Jorgensen, G.; Bingham, C.; King, D.; Lewandowski, A.; Netter, J.; Dec. 14, 2000; 20p; In English
Report No.(s): DE2001-772423; NREL/CP-520-28579; No Copyright; Avail: Department of Energy Information Bridge

NREL (National Renewable Energy Laboratory) has developed a new ultraviolet (UV) light concentrator that allows material samples to be subjected to uniform intensity levels of 50-100X solar UV (ultraviolet) at closely controlled sample exposure temperatures. In collaboration with industry, representative coating systems have been exposed without introducing unrealistic degradation mechanisms. Furthermore, correlations have been derived between these highly accelerated test conditions and results obtained at 1-2 suns. Such information is used to predict the degradation of materials in real-world applications. These predictions are compared with measured in-service performance losses to validate the approach. This allows valuable information to be obtained in greatly reduced timeframes, which can provide tremendous competitive advantage in the commercial marketplace.
NTIS
Ultraviolet Radiation; Coatings; Accelerated Life Tests; Radiation Damage

20020005825 Oak Ridge National Lab., TN USA
Optimization of the Ion-Cut Process in Si and SiC
Holland, O. W.; Jan. 05, 2001; 10p; In English; Fall 2000 Materials Research Society Meeting, 11/27/2000--12/01/2000, Boston, MA, USA
Report No.(s): DE2001-774479; P00-109467; No Copyright; Avail: Department of Energy Information Bridge, Microfiche

H(sup plus)-implantation is the basis for an ion-cut process, which combines hydrophilic wafer bonding, to produce heterostructures over a wide range of materials. This process has been successfully applied in Si to produce a commercial silicon-on-insulator material. The efficacy of implantation to produce thin-film separation was studied by investigation of H(sup plus)-induced exfoliation in Si and SiC. Experiments were done to isolate the effects of the hydrogen chemistry from that of

implant damage. Damage is manipulated independently of H+ dosage by a variety of techniques ranging from elevated temperature irradiation to a two-step implantation scheme in Si, and the use of channeled-ion implantation in SiC. The results will demonstrate that such schemes can significantly reduce the critical dose for exfoliation.
NTIS
Ion Implantation; SOI (Semiconductors); Thin Films

20020005826 Oak Ridge National Lab., TN USA
Micro-Structuring of Silicon by Pulsed-Laser Ablation Under Reactive Atmospheres
Jesse, S.; Jan. 18, 2001; 6p; In English; Fall 2000 Materials Research Society Meeting, 11/27/2000--12/01/2000, Boston, MA, USA
Contract(s)/Grant(s): AC05-96OR22464
Report No.(s): DE2001-774480; P01-109563; No Copyright; Avail: Department of Energy Information Bridge, Microfiche

Micro-holes hundreds of microns-deep below the initial surface surrounded by 40- micron-tall micro-cones protruding over the initial surface form in silicon as a response to multiple UV pulsed-laser irradiation in an SF(sub 6) atmosphere. The micro-holes and micro-cones are arranged in a characteristic ensemble displaying a self-organized pattern. Similarly, deep-holes and micro-column ensembles form when the irradiation is performed in an oxygen-rich atmosphere. The formation mechanism of micro-columns and micro-cones in these reactive atmospheres has been studied using scanning electron microscopy, profilometry and x-ray diffraction. The growth of cones under SF(sub 6) atmospheres was studied in-situ using an ICCD gated camera coupled to a long distance microscope. The images obtained with the ICCD camera show that the fluorescent plume is correlated with the amount of ablated material. There is also a strong correlation between the plume and the growth of the cones. The cones grow in the region where the laser-generated plume is intense. When the flux of silicon-rich material ceases because the holes are very deep the balance between redeposition and ablation is tilted toward the latter and the cones begin to recede. Laser ablation is not only a function of the nominal fluence but also of the surface roughness and microstructure. These results strongly support the growth mechanism whereby laser-ablated silicon-rich molecules and clusters are transported to the tip and side of the cones by the laser-generated plasma.
NTIS
Silicon; Microstructure

20020005875 Montana State Univ., Dept. of Chemistry, Bozeman, MT USA
Composite Materials for Optical Limiting ***Final Report, 1 May 1998-30 Apr. 2001***
Spangler, Lee; Apr. 2001; 17p; In English
Contract(s)/Grant(s): DAAG55-98-1-0271
Report No.(s): AD-A395335; ARO-37782.1-CH-DPS; No Copyright; Avail: CASI; A03, Hardcopy; A01, Microfiche

This project funded two principle investigators to explore materials for optical limiting. Dr. Charles Spangle's research group synthesized organic and dendritic materials designed to optically limit via reverse saturable absorption (RSA) via photoinduced formation of charged states. Dr. Lee Spangle's research group investigated the spectroscopy, mechanism, and efficiency of photo-induced states in these, and related compounds. Thus, the technical part of the report will be divided into two sections, synthesis and characterization.
DTIC
Composite Materials; Organic Materials; Synthesis (Chemistry); Spectroscopy; Nonlinear Optics

20020005880 Arizona Univ., Tucson, AZ USA
Synthesis and Characterization of Supramolecular Composites ***Final Report, 15 Jun. 1998-14 Jun 2001***
O'Brien, David F.; Sep. 13, 2001; 7p; In English
Contract(s)/Grant(s): DAAG55-98-1-0394
Report No.(s): AD-A395357; ARO-37695.1-CH; No Copyright; Avail: CASI; A02, Hardcopy; A01, Microfiche

The concept of an area-minimizing surface has been used extensively to describe the morphologies of hydrated amphiphiles and block copolymers. These morphologies include lamellar, hexagonal, and the more complex bicontinuous cubic phases. In spite of the morphological similarities between certain block copolymers and hydrated amphiphiles there are of course some major differences. The stability of the two systems can be widely different This distinction is now minimized by the successful introduction of methods to polymerize and even crosslink the phases of hydrated amphiphiles to greatly enhance their stability. The presence of the water domains in the polymerized nonlamellar phases, in particular the inverted hexagonal phase, are regions of well defined size and shape. This research is examining methods to create novel materials by selective use of these to (1) deposit metals and minerals or (2) isolate rod-like polymers. The major focus of the ongoing research is to extend the current state of the

science to ascertain the potential and limits of a fundamentally new method for the synthesis of high value supramolecular composites.
DTIC
Block Copolymers; Synthesis (Chemistry); Composite Materials; Polymerization; Minerals

24
COMPOSITE MATERIALS

Includes physical, chemical, and mechanical properties of laminates and other composite materials.

20020000762 Lawrence Livermore National Lab., Livermore, CA USA
Elastic properties of large tow 2-D braided composites by numerical and analytical methods
Nguyen, T. D.; Zywicz, E.; Sep. 01, 1998; 27p; In English
Report No.(s): DE2001-8427; UCRL-ID-131921; No Copyright; Avail: Department of Energy Information Bridge, Microfiche
The homogenized extensional and flexural properties of a large tow, two- dimensional, braided carbon-fiber composite lamina were evaluated using analytical and numerical methods. The plane-stress composite lamina was assumed to be periodic in its plane and was modeled with a single representative volume element. The homogenized elastic properties were analytically estimated using beam-theory concepts and upper and lower bound techniques as well as using three-dimensional finite element analyses. The homogenized extensional and bending lamina properties are, in general, distinct properties and are not simply related to each other as in monolithic beams and plates or in composites with very fine and highly periodic microstructures. The importance and cause of distinct homogenized extensional and flexural elastic properties is briefly discussed.
NTIS
Elastic Properties; Braided Composites; Carbon Fibers

20020001228 Argonne National Lab., IL USA
Novel thermal properties of nanostructured materials
Eastman, J. A.; Jan. 13, 1999; 9p; In English
Report No.(s): DE2001-10862; ANL/MSD/CP-96711; No Copyright; Avail: Department of Energy Information Bridge
A new class of heat transfer fluids, termed nanofluids, has been developed by suspending nanocrystalline particles in liquids. Due to the orders-of-magnitude larger thermal conductivities of solids compared to those of liquids such as water, significantly enhanced thermal properties are obtained with nanofluids. For example, an approximately 20% improvement in effective thermal conductivity is observed when 5 vol.% CuO nanoparticles are added to water. Even more importantly, the heat transfer coefficient of water under dynamic flow conditions is increased more than 15% with the addition of less than 1 vol.% CuO particles. The use of nanofluids could impact many industrial sectors, including transportation, energy supply and production, electronics, textiles, and paper production by, for example, decreasing pumping power needs or reducing heat exchanger sizes. In contrast to the enhancement in effective thermal transport rates that is obtained when nanoparticles are suspended in fluids, nanocrystalline coatings are expected to exhibit reduced thermal conductivities compared to coarse-grained coatings. Reduced thermal conductivities are predicted to arise because of a reduction in the mean free path of phonons due to presence of grain boundaries. This behavior, combined with improved mechanical properties, makes nanostructured zirconia coatings excellent candidates for future applications as thermal barriers. Yttria-stabilized zirconia (YSZ) thin films are being produced by metal-organic chemical vapor deposition techniques. Preliminary results have indicated that the thermal conductivity is reduced by approximately a factor-of-two at room temperature in 10 nm grain-sized YSZ compared to coarse-grained or single crystal YSZ.
NTIS
Thermodynamic Properties; Nanostructure (Characteristics); Dispersions; Working Fluids; Thin Films; Conductive Heat Transfer

20020002014 TPL, Inc., Albuquerque, NM USA
Barium Titanate/Polymer Nanoscale Composites with Controllable Architectures ***Final Report, 2 Sep. 1998 - 8 Apr. 1999***
Luther, E.; Slenes, K.; Law, K.; Labanowski, C.; Romero, T.; Jul. 06, 1999; 13p; In English
Report No.(s): DE2001-765520; TPL-AD14-FR; No Copyright; Avail: Department of Energy Information Bridge, Microfiche
Final report of Phase I SBIR grant. A study of processing methods for barium titanate/polymer nanocomposites for use in dielectric applications.
NTIS
Barium Titanates; Dielectrics; Nanocomposites; Polymers; Control Theory

20020002735 Gamma Engineering Corp., Rockville, MD USA

Continuous Fiber Wound Ceramic Composite (CFCC) for Commercial Water Reactor Fuel ***Progress Report, Period ending 1 Apr. 2000***

Apr. 01, 2000; 44p; In English

Report No.(s): DE2001-762123; No Copyright; Avail: Department of Energy Information Bridge

Our program began on August 1, 1999. As of April 1, 2000, the progress has been in materials selection and test planning. Three subcontracts are in place (McDermott Technologies Inc. for continuous fiber reinforced ceramic tubing fabrication, Swales Aerospace for LOCA testing of tubes, and Massachusetts Institute of Technology for In Reactor testing of tubes). With regard to materials selection we visited McDermott Technologies Inc. a number of times, including on February 23, 2000 to discuss the Draft Material Selection and Fabrication Report. The changes discussed at this meeting were implemented and the final version of this report is attached. McDermott Technologies Inc. will produce one type of tubing: Alumina oxide (Nextel 610) fiber, a carbon coating (left in place), and alumina-yttria matrix. A potentially desirable Continuous Fiber Ceramic Composites (CFCC) material of silicon carbide fiber with spinel matrix was discussed. That material selection was not adopted primarily due to material availability and cost. Gamma Engineering is exploring the available tube coatings at Northwestern University as a mechanism for reducing the permeability of the tubes, and thus, will use coating as a differentiating factor in the testing of tubing in the LOCA test as well as the In-Reactor Test. The conclusion of the Material Selection and Fabrication Report lists the possible coatings under evaluation. With regard to Test Planning, the MIT and Swales Aerospace have submitted draft Test Plans. MIT is attempting to accommodate an increased number of test specimens by evaluating alternative test configurations. Swales Aerospace held a design review at their facilities on February 24, 2000 and various engineering alternatives and safety issues were addressed. The final Test Plans are not expected until just before testing begins to allow for incorporation of changes during 'dry runs.'

NTIS

Ceramic Matrix Composites; Fiber Composites; Materials Selection

20020002736 Gamma Engineering Corp., Rockville, MD USA

Nuclear Energy Research Initiative (NERI) Program Continuous Fiber Wound Ceramic Composite (CFCC) for Commercial Water Reactor Fuel ***Progress Report, Period ending 30 Jun. 2000***

Jul. 11, 2000; 8p; In English

Report No.(s): DE2001-762083; No Copyright; Avail: Department of Energy Information Bridge, Microfiche

This project began on August 1, 1999. As of July 1, 2000, the progress has been in materials production, test planning, testing facility design and instruction, and calibration. One new subcontractor was added to provide a solution to the Continuous Fiber Ceramic Composites (CFCC) material permeability issue (Northwestern University). This is in addition to the three subcontracts that were previously in place (McDermott Technologies Inc. for continuous fiber reinforced ceramic tubing fabrication, Swales Aerospace for LOCA testing of tubes, and Massachusetts Institute of Technology for In Reactor testing of tubes).

NTIS

Calibrating; Ceramic Matrix Composites; Fiber Composites; Permeability

20020002853 Gamma Engineering Corp., Rockville, MD USA

Nuclear Energy Research Initiative (NERI) Program Continuous Fiber Wound Ceramic Composite (CFCC) for Commercial Water Reactor Fuel ***Progress Report***

Feinroth, H.; Jan. 01, 2000; 6p; In English

Report No.(s): DE2001-762094; No Copyright; Avail: Department of Energy Information Bridge

Our program began on August 1, 1999. As of January 1, 2000, the progress has been in contracting, materials selection, and test planning. All three subcontracts are now in place (McDermott Technologies Inc. for ceramic fabrication, Swales Aerospace for LOCA testing, and Massachusetts Institute of Technology for in Reactor testing). With regard to material selection, we visited McDermott Technologies on December 6, 1999 to discuss the progress on Materials Selection and issues regarding Permeability Reduction in Continuous Fiber Ceramic Composites (CFCC) materials. We are evaluating several options for reducing the permeability of the CFCC materials, including Chemical Vapor Infiltration. McDermott Technologies is approximately two months late on their scheduled delivery to Gamma of Materials Selection reports. They have indicated by letter that they plan to deliver a draft and then final Materials Selection Report to Gamma by January 15 and February 1st, 2000, respectively. With regard to Test Planning, Swales Aerospace is proceeding with engineering the test chamber. The power supply selection for the Kanthal furnace was changed from AC to DC current to simplify equipment and operation. The mechanism for opening the 'sliding door' on bottom of furnace has been changed from air cylinder to stainless steel spring/cord to provide inherent simplicity and failsafe operation. Alumina tubing for apparatus calibration was obtained from Coors Ceramics; 0.5 x 1/16 foot wall x 16 inches, grade

AD-998, 99.8% Al2O3, density 3.9 gr/cc. This will be cut into 3 inch specimen and very closely matches the expected test specimens from McDermott. Swales and Gamma are currently selecting extension springs from Associated Spring to provide a tension on furnace 'bottom door'. Swales and Gamma are currently evaluating sample of Alumina board from Zircar for the furnace 'door'.
NTIS
Fiber Composites; Materials Selection; Ceramic Matrix Composites; Water Cooled Reactors

20020004018 Los Alamos National Lab., NM USA
Mechanical response of boron carbide-aluminum composites during compressive loading
Palfey, W.; Aug. 01, 2000; 9p; In English
Report No.(s): DE2001-768887; LA-UR-00-3408; No Copyright; Avail: Department of Energy Information Bridge, Microfiche

The compressive stress-strain and failure behavior of 80'XOB4C-Al and 65'XOB4C-Al composites has been examined at room temperature and at strain rates of 10(exp -4)and 10(exp 3) s-1. The composite structure has been processed to consist of dual continuous phases such that the B4C and the aluminum are mutually constrained by their physical proximity. Being nearly incompressible, the aluminum supports the B4C skeleton by limiting bending in the B4C ligaments, while the B4C constrains shear in the aluminum and inhibits its plastic flow. Thus, owing to the mutual constraint of the constituents, the compressive fracture strength of the composite is more than a factor of two greater than that of the B4C skeleton with fracture stresses in excess of 2000 MPa in the 65DG/0 B4C-Al and greater than 3800 MPa in the 80DG/0 B4C-Al. The characteristics of the compressive stress-strain response as well as the ratios of transverse strains to longitudinal strains (i.e. the 'Poisson' ratios) indicate that failure of the 65% B4C-Al composite is controlled by the Al, but that the 80DG/0 B4C-Al is dominated by the B4C.
NTIS
Boron Carbides; Aluminum; Composite Materials; Mechanical Properties; Compression Loads

20020005059 Los Alamos National Lab., NM USA
Size effects in the tensile strength of unidirectional fiber composites
Sivasambu, M.; Aug. 01, 1999; 53p; In English
Report No.(s): DE2001-769207; LA-UR-99-2353; No Copyright; Avail: Department of Energy Information Bridge, Microfiche

Monte Carlo simulation and theoretical modeling are used to study the statistical failure modes in unidirectional composites consisting of elastic fibers in an elastic matrix. Both linear and hexagonal fiber arrays are considered, forming 2D and 3D composites, respectively. Failure is idealized using the chain-of-bundles model in terms of (delta)-bundles of length (delta), which is the length-scale of fiber load transfer. Within each (delta)-bundle, fiber load redistribution is determined by local load-sharing models that approximate the in-plane fiber load redistribution from planar break clusters as predicted from 2D and 3D shear-lag models. As a result these models are 1D and 2D, respectively. Fiber elements have random strengths following either the Weibull or the power-law distribution with shape and scale parameters (rho) and (sigma)(sub (delta)), respectively. Simulations of (delta)-bundle failure, reveal two regimes. When fiber strength variability is low (roughly (rho) > 2) the dominant failure mode is by growing clusters of fiber breaks up to instability. When this variability is high (roughly 0 < (rho) < 1) cluster formation is suppressed by a dispersed fiber failure mode. For these two cases, closed-form approximations to the strength distribution of a (delta)-bundle are developed under the local load-sharing model and an equal load-sharing model of Daniels, respectively. The results compare favorably with simulations on (delta)-bundles with up to 1500 fibers. The location of the transition in terms of (rho) is affected by the upper tail properties of the fiber strength distributions as well as the number of fibers.
NTIS
Fiber Composites; Tensile Strength; Failure Modes

20020005118 NASA Marshall Space Flight Center, Huntsville, AL USA
Method of Making a Composite Tank
DeLay, Thomas K., Inventor, NASA Marshall Space Flight Center, USA; Feb. 27, 2001; 3p; In English; Division of US-Patent-Appl-SN-218652, filed 22 Dec. 1998
Patent Info.: Filed 19 Jun. 2000; NASA-Case-MFS-31379-2-DIV; US-Patent-6,193,917; US-Patent-Appl-SN-606109; US-Patent-Appl-SN-218652; No Copyright; Avail: CASI; A01, Hardcopy; A01, Microfiche

A composite tank for containing liquid oxygen and the method of making the same wherein a water-soluble mandrel having the desired tank configuration and a cylindrical A method of making a composite tank for containing liquid oxygen configuration of the mandrel and an outer boss conforming to the configuration of the inner boss, the bosses each having a tubular portion for receiving the protuberance on the mandrel and a spherical portion. The mandrel and the bosses are first coated with a nickel coating. The mandrel is then wrapped with graphite fibers wetted with an epoxy resin and this resin is cured. A layer of insulating

foam is then applied to the tank and cured. The insulating foam is machined to a desired configuration and a layer of aramid fibers wetted with a second epoxy resin is wrapped around the tank. The second resin is cured and the water soluble mandrel is washed from inside the tank.
Official Gazette of the U.S. Patent and Trademark Office
Mandrels; Graphite-Epoxy Composites; Epoxy Resins

20020005192 Los Alamos National Lab., NM USA
Measuring spatial variation of residual stresses in a MMC using crack compliance
Prime, M.; Apr. 01, 2000; 5p; In English
Report No.(s): DE2001-768973; LA-UR-00-2084; No Copyright; Avail: Department of Energy Information Bridge

We present a novel measurement of the spatial variation of residual stresses in a metal matrix composite (MMC). Failures in MMCs are sensitive to localized residual stresses. For example, the interface bond strength depends on the radial residual stress at the fiber-matrix interface. Unfortunately, most residual stress measurements in MMCs are spatial averages rather than values. Neutron diffraction measurements average over the whole sample, although they do provide separate stresses in the fiber and matrix. Layer removal methods similarly provide a spatial average over a large volume. X-ray diffraction can measure a local stress value but only on the surface. The measurement on spatially resolved residual stresses is also crucial for validating predictive models. Models with different predictions for local residual stresses can lead to the same averaged values. Therefore, the practice of validating models using only average values. Therefore, the practice of validating models using only average stresses can lead to false confirmations.
NTIS
Residual Stress; Metal Matrix Composites; Cracks

20020005807 Sandia National Labs., Albuquerque, NM USA
Maleimide Functionalized Siloxane Resins
Shaltout, R. M.; Loy, D. A.; Wheeler, D. R.; Apr. 21, 1999; 8p; In English
Report No.(s): DE2001-5921; SAND99-1002C; No Copyright; Avail: Department of Energy Information Bridge, Microfiche

In-situ filling through hydrolysis and condensation of silicon alkoxides has been utilized to generate nanocomposites in which the filler phase can be intimately associated with the polymer on relatively small length scales. One problem of the method has been achieving useful fill volumes without bulk phase separation of the reacting silicon monomer from the polymer. In this paper, we describe the preparation of a new class of nanocomposite materials in which the inorganic filler phase is pre-assembled before copolymerization with an organic species. Maleimide monomers, prepared from alkoxysilylpropyl amines and maleic anhydride, were protected against side reactions by forming the oxonorbornene Diels-Alder adduct with furan. The monomers were then reacted under sol-gel conditions to form oligomers or polymers-the filler phase. The material was activated by thermal deprotection of the maleimide and reacted with organic monomers or polymers to form the filled nanocomposite.
NTIS
Monomers; Siloxanes; Composite Materials; Hydrolysis; Condensation

25
INORGANIC, ORGANIC AND PHYSICAL CHEMISTRY

Includes the analysis, synthesis, and use inorganic and organic compounds; combustion theory; electrochemistry; and photochemistry. For related information see also 34 Fluid Dynamics and Thermodynamics, For astrochemistry see category 90 Astrophysics.

20020000753 National Petroleum Technology Office, Tulsa, OK USA
In-Situ Combustion Handbook: Principles and Practices
Sarathi, P. S.; Jan. 28, 1999; 423p; In English
Report No.(s): DE2001-3175; DOE/PC/91008-0374; No Copyright; Avail: Department of Energy Information Bridge

For nearly 90 years in-situ combustion technique has been used in the U.S. in attempts to improve recovery from oil reservoirs. Despite its long history and commercial success of many field projects, the process has not found widespread acceptance among operators due to the excessive number of failures of many early field trails. Most of these failures can be traced to the inappropriate application of the process in poorer prospects. Analysis of the successful projects, however, indicates that the process is applicable

to a wide range of reservoirs, and the chances of failures can be minimized by careful selection of the reservoir and adopting prudent engineering practices.
NTIS
Combustion; Oil Recovery; In Situ Resource Utilization; Crude Oil; Energy Conversion Efficiency

20020000757 Los Alamos National Lab., NM USA
Interactions of Plutonium Dioxide with Water and Oxygen-Hydrogen Mixtures
Haschke, J. M.; Allen, T. H.; Jan. 01, 1999; 32p; In English
Report No.(s): DE2001-3509; LA-13537-MS; No Copyright; Avail: Department of Energy Information Bridge

Pressure-volume-temperature data and mass spectrometric results obtained during exposure of PuO(sub 2) to D(sub 2)O show that the dioxide reacts with water at room temperature to produce a higher oxide (PuO(sub 2+x))and H(sub 2). Results demonstrate that PuO(sub 2+x) is the thermodynamically stable oxide in air. The absence of O(sub 2) at detectable levels in the gas phase implies that radiolytic decomposition of water to the elements is not a significant reaction. The rate of the PuO(sub 2)+H(sub 2)O reaction is 6(+-)4 nmol H(sub 2)/m(sup 2) day, a value that is independent of the H(sub 2)O concentration on the oxide over a range that extends from fractional monolayer coverage to saturation by liquid water. Evaluation of literature data shows that oxide compositions in excess of PuO(sub 2.25) are attained, but the maximum value of x is unknown. During exposure of PuO(sub 2) to a 2:1 D(sub 2):O(sub 2) mixture at room temperature, the elements combine by a process consistent with a surface-catalyzed reaction. Water is simultaneously formed by the H(sub 2) + O(sub 2) reaction and consumed by the PuO(sub 2) + H(sub 2)O reaction and accumulates until the opposing rates are equal. Thereafter, PuO(sub 2 + x) is formed at a constant rate by the water-catalyzed PuO(sub 2) + O(sub 2) reaction. The failure of earlier attempts to prepare higher oxides of plutonium is discussed and the catalytic cycle that promotes the reaction of PuO(sub 2) with O(sub 2) is described. Implications of the results for extended storage and environmental chemistry of oxide are examined. Moisture-catalyzed oxidation of PuO(sub 2) accounts for observation of both pressure increases and decreases in oxide storage containers with air atmospheres. Application of the experimental rate results indicates that the reaction of a typical oxide with 0.5 mass % of adsorbed water may be complete after 25 to 50 years at room temperature.
NTIS
Chemical Reactions; Plutonium Oxides; Deuterium; Activation Energy

20020000767 Lawrence Livermore National Lab., Livermore, CA USA
Simulation of damage evolution and accumulation in vanadium
Alonso, E.; Caturla, M. J.; Diaz De La Rubia, T.; Perlado, M. J.; Feb. 08, 1999; 32p; In English
Report No.(s): DE2001-8434; UCRL-ID-133389; AT6020000; No Copyright; Avail: Department of Energy Information Bridge, Microfiche

Energetic atoms which have been knocked off their lattice sites by neutron or ion irradiation leave a trail of vacancies and interstitials in their wake. Most of these defects recombine with their opposites within their own collision cascade. Some fraction, however, escape to become freely migrating defects (FMD) in the bulk of the material. The interaction of FMD with the microstructure has long been linked to changes in the macroscopic properties of materials under irradiation. We calculate the fraction of FMD in pure vanadium for a wide range of temperatures and primary knock-on atom (PKA) energies. The collision cascade database is obtained from molecular dynamics (MD) simulations with an embedded atom method (EAM) potential. The actual FMD calculation is carried out by a kinetic Monte Carlo (kMC) code with a set of parameters extracted either from the experimental literature or from MD simulations. We take two different approaches to the problem and compare them. The first consists of an idealized simulation for single cascades. Annealing each cascade at different temperatures allows the mobile species to escape and account for FMD. The second analyzes bulk diffusion and damage.
NTIS
Vanadium; Damage; Neutron Irradiation; Ion Irradiation

20020000771 Lawrence Livermore National Lab., Livermore, CA USA
Fire risk analysis for the NIF capacitor containment design
Alvares, N.; Newton, M.; Staggs, K.; Feb. 22, 1999; 30p; In English
Report No.(s): DE2001-8502; UCRL-ID-133180; No Copyright; Avail: Department of Energy Information Bridge, Microfiche

No abstract prepared.
NTIS
Capacitors; Containment

20020000863 Los Alamos National Lab., NM USA

GASFLOW: a computational fluid dynamics code for gases, aerosols, and combustion, Volume 1, theory and computational model

Nichols, B. D.; Mueller, C.; Necker, G. A.; Travis, J. R.; Spore, J. W.; Oct. 01, 1998; 159p

Report No.(s): DE2001-1218; LA-13357-M-VOL-1; No Copyright; Avail: Department of Energy Information Bridge, Microfiche

Los Alamos National Laboratory (LANL) and Forschungszentrum Karlsruhe (FzK) are developing GASFLOW, a three-dimensional (3D) fluid dynamics field code as a best-estimate tool to characterize local phenomena within a flow field. Examples of 3D phenomena include circulation patterns; flow stratification; hydrogen distribution mixing and stratification; combustion and flame propagation; effects of noncondensable gas distribution on local condensation and evaporation; and aerosol entrainment, transport, and deposition. An analysis with GASFLOW will result in a prediction of the gas composition and discrete particle distribution in space and time throughout the facility and the resulting pressure and temperature loadings on the walls and internal structures with or without combustion. A major application of GASFLOW is for predicting the transport, mixing, and combustion of hydrogen and other gases in nuclear reactor containments and other facilities. It has been applied to situations involving transporting and distributing combustible gas mixtures. It has been used to study gas dynamic behavior (1) in low-speed, buoyancy-driven flows, as well as sonic flows or diffusion dominated flows; and (2) during chemically reacting flows, including deflagrations. The effects of controlling such mixtures by safety systems can be analyzed. The code version described in this manual is designated GASFLOW 2.1, which combines previous versions of the USA Nuclear Regulatory Commission code HMS (for Hydrogen Mixing Studies) and the Department of Energy and FzK versions of GASFLOW. The code was written in standard FORTRAN 90. This manual comprises three volumes. Volume I describes the governing physical equations and computational model. Volume II describes how to use the code to set up a model geometry, specify gas species and material properties, define initial and boundary conditions, and specify different outputs, especially graphical displays. Sample problems are included. Volume III contains some of the assessments performed by LANL and FzK. GASFLOW is under continual development, assessment, and application by LANL and FzK. This manual is considered a living document and will be updated as warranted. NTIS

Computational Fluid Dynamics; Computer Programs; Three Dimensional Models; Computerized Simulation; Gas Flow; User Manuals (Computer Programs)

20020000871 Rutgers - The State Univ., Piscataway, NJ USA

Final Report: Carbon-Hydrogen Bond Functionalization Catalyzed by Transition Metal Systems, June 1, 1990-May 31, 1993

Goldman, A. S.; May 31, 1993; 9p; In English

Report No.(s): DE2001-764582; DOE/ER/14124-1-VOL-1; No Copyright; Avail: Department of Energy Information Bridge

The selective catalytic functionalization of hydrocarbons, particularly alkanes, is one of the most important and challenging goals in catalysis science. Alkane derivatives (e.g. alcohols, olefins) invariably contain C-H bonds weaker than those of the parent molecule. Thus methods for alkane conversion that involve simple cleavage of a C-H bond (either homolytic or heterolytic) will generally show selectivity for the initial product, thereby preventing build-up of significant concentrations of that product. During the past grant cycle, we have made particularly significant breakthroughs toward the goal of development of practical catalytic systems for alkane dehydrogenation. This includes (i) development of the first efficient 'acceptorless' systems, and (ii) development of transfer-dehydrogenation systems that are the first to regioselectively dehydrogenate n-alkanes to give appreciable yields of alpha-olefins (terminal linear alkenes).

NTIS

Catalysis; Transition Metals; Hydrocarbons; Systems Engineering; Chemical Bonds

20020000899 Argonne National Lab., IL USA

Chemical dynamics in the gas phase: quantum mechanics of chemical reactions

Gray, S. K.; Jul. 02, 1999; 5p; In English

Report No.(s): DE2001-11883; ANL/CHM/CP-99425; No Copyright; Avail: Department of Energy Information Bridge, Microfiche

This research program focuses on both the development and application of accurate quantum mechanical methods to describe gas phase chemical reactions and highly excited molecules. Emphasis is often placed on time-dependent or integrative approaches that, in addition to computational simplifications, yield useful mechanistic insights. Applications to systems of current experimental and theoretical interest are emphasized. The results of these calculations also allow one to gauge the quality of the

underlying potential energy surfaces and the reliability of more approximate theoretical approaches such as classical trajectories and transition state theories.
NTIS
Chemical Reactions; Gases; Quantum Mechanics; Combustion Physics; Reaction Kinetics

20020000901 Argonne National Lab., IL USA
Solution structure of detergent micelles at conditions relevant to membrane protein crystallization
Littrell, K.; Thiyagarajan, P.; Tiede, D.; Urban, V.; Jul. 02, 1999; 21p; In English
Report No.(s): DE2001-11879; ANL/IPNS/CP-99414; No Copyright; Avail: Department of Energy Information Bridge, Microfiche

In this study small angle neutron scattering was used to characterize the formation of micelles in aqueous solutions of the detergents DMG and SPC as a function of detergent concentration and ionic strength of the solvent. The effects on the micelle structure of the additives glycerol and PEG, alone as well as in combination typical for actual membrane protein crystallization, were also explored. This research suggests that the micelles are cigar-like in form at the concentrations studied. The size of the micelles was observed to increase with increasing ionic strength but decrease with the addition of glycerol or PEG.
NTIS
Crystallization; Micelles; Glycerols; Protein Crystal Growth

20020000902 Argonne National Lab., IL USA
Optical determination of incipient soot particle concentrations in ethene laminar diffusion flames
Gupta, S. B.; Santoro, R. J.; Jul. 06, 1999; 8p; In English
Report No.(s): DE2001-11876; ANL/ES/CP-99394; No Copyright; Avail: Department of Energy Information Bridge, Microfiche

Recent studies in premixed flames have shown the existence of 'transparent particles.' These particles, 2 nm in size and in high number densities are considered to be a phase transitional between the gas phase PAH species and particulate soot. In the present study, various optical diagnostics were evaluated for measuring the concentration of these particles in situ, Through such evaluations, a technique using extinction at two wavelengths was found to be ideal. While employing such a technique, the volume fractions of these particles in an ethene laminar diffusion flame were measured. Low in the flame, these particles were found to be concentrated in the fuel rich core, while at higher locations, they could be found with appreciable volume fractions even in the soot laden regions. Having given due consideration for the errors due to uncertainties in the optical constants, we report the existence of these particles in an ethene flame with volume fractions comparable to those of soot. Also, similar measurements performed in a low sooting ethene/methanol flame show the concentration of these particles to be of the same order of magnitude as in a pure ethene flame.
NTIS
Soot; Ethylene; Optical Equipment; Flames; Combustion Physics

20020000913 Auburn Univ., AL USA
Enhancement of Dilute-Acid Total-Hydrolysis Process for High-Yield Saccharification of Cellulosic Biomass
Lee, Y. Y.; Xiang, Q.; Kim, T. H.; Kim, J.; Jul. 24, 2000; 19p; In English
Report No.(s): DE2001-763027; DOE/GO/10475-Q; No Copyright; Avail: Department of Energy Information Bridge, Microfiche

The primary emphasis of the project work during this period was again placed on the Task I. The experimental kinetic investigations were continued using batch reactors (the experimental set-up previously reported) and the bed-shrinking flow-through (BSFT) reactors. From the experimental findings accumulated to this point, we have confirmed that the earlier research work of NREL that the BSFT reactor provides glucose yield in the vicinity of 90DG/0. We have obtained yields of 87.54%, 90.32%, and 90.78% respectively at 205, 220 C. We have acquired data that farther support that the yields far above the theoretical glucose yield of 70% are achievable. This indeed represents a breakthrough and a milestone event in the acid hydrolysis technology dilute-acid hydrolysis technologies. We are in the process of laying the foundation of the kinetics of dilute-acid hydrolysis of cellulosic biomass. Our goal is to gain fundamental understanding of the reactions and other rate processes involved in this complex process. The recent progress on the work along theses lines is summarized in this report.
NTIS
Biomass; Hydrolysis; Dilution; Acids; Cellulose

20020001041 Lawrence Livermore National Lab., Livermore, CA USA

Ignitability of DMSO vapors at elevated temperature and reduced pressure

Bergman, W.; Ural, E. A.; Weisgerber, W.; Mar. 08, 1999; 56p; In English

Report No.(s): DE2001-8522; UCRL-CR-132949; No Copyright; Avail: Department of Energy Information Bridge, Microfiche

Ignitability of DMSO vapors have been evaluated at 664 mm Hg pressure. The minimum temperature at which the DMSO vapors that are in equilibrium with liquid DMSO has been determined using two types of strong ignition sources. This temperature is 172 F for chemical igniters, and 178 F for spark ignition. Numerous tests have been conducted using controlled intensity sparks to define the shape of the minimum ignition energy curve as a function of temperature. The ignition energies spanned four orders of magnitude (approximately from 20,000 to 2 mJ) while the DMSO vapor mixture temperature varied from 185 to 207 F. The Sandia Generator was used to simulate worst case electrostatic sparks that can be produced by the human body. Although it was not designed for air discharges, this device had been used by LLNL for 1 mm spark gap and the resultant spark energy had been measured to fall within the range from 3.2 to 8.8 mJ. CRC tests using this device showed that the minimum ignition temperature strongly depends on the spark gap. The minimum ignition temperature was 207 F at 1 mm spark gap, 203 F at 3 mm spark gap, and 197 F at 6 mm spark gap. This strong dependence on the spark gap is believed to be partly due to the changes in the spark energy as the spark gap changes.

NTIS

Dimethyl Compounds; Sulfur Oxides; Vapors; Ignition

20020001045 Lawrence Livermore National Lab., Livermore, CA USA

Delocalization and New Phase in Americium: Theory

Soderlind, P.; Apr. 23, 1999; 17p; In English

Report No.(s): DE2001-8544; UCRL-ID-134321; DP0101031; No Copyright; Avail: Department of Energy Information Bridge, Microfiche

Density-functional electronic structure calculations have been used to investigate the high pressure behavior of Am. At about 80 kbar (8 GPa) calculations reveal a monoclinic phase similar to the ground state structure of plutonium (alpha-Pu). The experimentally suggested alpha-U structure is found to be substantially higher in energy. The phase transition from fcc to the low symmetry structure is shown to originate from a drastic change in the nature of the electronic structure induced by the elevated pressure. A calculated volume collapse of about 25% is associated with the transition. For the low density phase, an orbital polarization correction to the local spin density (LSD) theory was applied. Gradient terms of the electron density were included in the calculation of the exchange/correlation energy and potential, according to the generalized gradient approximation (GGA). The results are consistent with a Mott transition; the 5f electrons are delocalized and bonding on the high density side of the transition and chemically inert and non-bonding (localized) on the other. Theory compares rather well with recent experimental data which implies that electron correlation effects are reasonably modeled in our orbital polarization scheme.

NTIS

Electronic Structure; High Pressure; Phase Transformations; Americium

20020001056 Argonne National Lab., IL USA

Theoretical investigations of silver clusters and silver-ligand systems

Jellinek, J.; Salian, U.; Srinivas, S.; May 19, 1999; 41p; In English

Report No.(s): DE2001-11816; ANL/CHM/CP-99056; No Copyright; Avail: Department of Energy Information Bridge, Microfiche

Studies directed at understanding structural and electronic properties of silver clusters have been and remain the subject of an active theoretical (1-22) and experimental (23-38) effort. One of the reasons is the (still) important role these systems play in the photographic process. Investigations of interactions of silver clusters with different atoms and molecules are motivated primarily by a possible utility of these clusters in catalytic processes. The important role of silver in the selective oxidation of ethylene into ethylene oxide, the feedstock for polyester production, is well-known (39). Possible variations in chemical reactivity with the cluster size and understanding of the mechanisms of interactions with different ligands may lead to new and more efficient applications. Investigations of cluster-ligand systems also contribute a great deal to a better understanding of gas-surface interactions. Accordingly, theoretical studies of silver clusters and cluster-ligand systems (40-44) fall into two categories, those that use clusters as models for silver surfaces (40), and those that target clusters and cluster-ligand interactions as subjects in their own right (41-44). The common goal of all these studies is to elucidate the nature of the interatomic interactions and bonding at

the microscopic level and thereby arrive at a fundamental understanding and description of the various structural and electronic properties.
NTIS
Silver Compounds; Electronic Structure; Atomic Interactions; Gas-Solid Interactions

20020001161 Lawrence Livermore National Lab., Livermore, CA USA
Residual Stresses in Mo/Si and Mo2C/Si Multilayers
Barbee, T. W.; Nguyen, T. D.; Apr. 01, 1999; 10p; In English
Report No.(s): DE2001-8583; UCRL-JC-134021; No Copyright; Avail: Department of Energy Information Bridge, Microfiche

The authors report a study of the residual stresses and residual stress relaxation in Mo/Si and Mo2C/Si extreme ultraviolet (EUV) multilayers. The multilayers were fabricated by magnetron sputter deposition, and stress measured using the substrate curvature laser scanning technique. It was found that Mo2C/Si multilayers exhibit higher compressive stress than Mo/Si of comparable period and layer thickness ratio. The multilayers sputtered at 0.5 mT Ar pressure have higher compressive stress than those sputtered at 2 mT Ar pressure. The data indicate that the residual stresses in the multilayers are primarily determined by the Si layers. Annealing of the multilayers at a heating rate of 5 C/minute as well as at a fixed temperature (isothermal) results in a reduction of the compressive stresses. Near zero stress is achieved after annealing at 300 C. The time dependence of the residual stress decrease during isothermal annealing was found to fit best to a bimolecular viscous flow model of defect annihilation in the amorphous Si layers. The relationships between the effects of annealing on the multilayer microstructure and the observed stress reduction are discussed.
NTIS
Annealing; Residual Stress; Sputtering; Stress Relaxation; Microstructure

20020001164 California Univ., Lawrence Berkeley Lab., Berkeley, CA USA
Oxidative Weathering Chemical Migration Under Variably Saturated Conditions and Supergene Copper Enrichment
Xu, T.; Pruess, K.; Brimhall, G.; Apr. 01, 1999; 45p; In English
Report No.(s): DE2001-8698; LBNL-43129; No Copyright; Avail: Department of Energy Information Bridge, Microfiche

Transport of oxygen gas from the land surface through an unsaturated zone has a strong influence on oxidative weathering processes. Oxidation of sulfide minerals such as pyrite (FeS2), one of the most common naturally occurring minerals, is the primary source of acid drainage from mines and waste rock piles. Here we present a detailed numerical model of supergene copper enrichment that involves the oxidative weathering of pyrite (FeS2) and chalcopyrite (CuFeS2), and acidification that causes mobilization of metals in the unsaturated zone, with subsequent formation of enriched ore deposits of chalcocite (CuS) and covellite (Cu2S) in the reducing conditions below the water table. We examine and identify some significant conceptual and computational issues regarding the oxidative weathering processes through the modeling tool. The dissolution of gaseous oxygen induced by the oxidation reduces oxygen partial pressure, as well as the total pressure of the gas phase. As a result, the gas flow is modified, then the liquid phase flow. Results indicate that this reaction effect on the fluid flow may not be important under ambient conditions, and gas diffusion can be a more important mechanism for oxygen supply than gas or liquid advection. Acidification, mobilization of metals, and alteration of primary minerals mostly take place in unsaturated zone (oxidizing), while precipitation of secondary minerals mainly occurs in saturated zone (reducing). The water table may be considered as an interface between oxidizing and reducing zones. Moving water table due to change of infiltration results in moving oxidizing zone and redistributing aqueous chemical constitutes and secondary mineral deposits. The oxidative weathering processes are difficult to model numerically, because concentrations of redox sensitive chemical species such as O2(aq), SO4(2-) and HS(-) may change over tens of orders of magnitude between oxidizing and reducing conditions. In order to simulate substantial reaction progress over geologic time, one can benefit from the quasi-stationary state (QSS) approximation. A significant saving of computing time using QSS is demonstrated through the example. In addition, changes in porosity and permeability due to mineral dissolution and precipitation are also addressed in some degree. Even though oxidative weathering is sensitive to many factors, this work demonstrates that our model provides a comprehensive suite of process modeling capabilities, which could serve as a prototype for oxidative weathering processes with broad significance for geoscientific, engineering, and environmental applications.
NTIS
Copper Sulfides; Mathematical Models; Minerals; Oxidation; Weathering

20020001207 Argonne National Lab., IL USA
Solvent reorganization energies measured by an electron transfer reaction in supercritical ethane
Feng, W.; Jonah, C. D.; Sawamura, S.; Takahashi, K.; Apr. 14, 1997; 6p; In English
Report No.(s): DE2001-12351; ANL/CHM/CP-92836; No Copyright; Avail: Department of Energy Information Bridge, Microfiche

The intermolecular electron transfer reaction between a biphenyl anion and pyrene in supercritical ethane was studied using pulse radiolysis. Second-order electron transfer rates were found to be of the order of 10(exp 11) M(sup -1) s(sup -1). The rate constants appear to be approximately constant over the pressure range 55-133 bar. Two possibilities are discussed that could explain the present results: solvent clustering; or a dependence of the solvent reorganization energy on pressure. Reorganization energies E(sub r) of non-polar supercritical ethane were estimated from the observed rate constant using the modified Marcus equation. E(sub r) may be larger than normally expected for non-polar solvents because of density fluctuations.
NTIS
Electron Transfer; Ethane; Molecular Interactions

20020001211 Argonne National Lab., IL USA
Photoionization-photoelectron research
Ruscic, B.; Mar. 06, 1998; 6p; In English
Report No.(s): DE2001-12346; ANL/CHM/CP-95838; No Copyright; Avail: Department of Energy Information Bridge, Microfiche

In the broad sense of a general definition, the fundamental goal of this research program is to explore, understand, and utilize the basic processes of interaction of vacuum UV light with atoms and molecules. In practical terms, this program uses photoionization mass spectrometry and other related techniques to study chemically relevant transient and metastable species that are intimately connected to energy-producing processes, such as combustion, or play-prominent roles in the associated environmental issues. Some recent examples of species that have been studied are: CH3, CH2, CH3O, CH2OH, CH3S, CH2SH, HCS, HNCO, NCO, HNCS, NCS, the isomers of C2H5O, HOBr, CF3 and CF3OH. The ephemeral species of interest are produced in situ using various suitable techniques, such as sublimation, pyrolysis, microwave discharge, chemical abstraction reactions with H or F atoms, laser photodissociation, on-line synthesis, and others. The desired information is obtained by applying a variety of suitable photoionization methods, which use both conventional and coherent light sources in the vacuum W region. The spiritus movens of our studies is the need to provide the chemical community with essential information on the species of interest, such as accurate and reliable thermochemical, spectroscopic and structural data, and thus contribute to the global comprehension of the underlying chemical processes. The scientific motivation is also fueled by the necessity to unveil useful generalities, such as bonding patterns within a class of related compounds, or systematic behavior in the ubiquitous autoionization processes. In addition, the nature of the results obtained in this program is such that it generates a significant impetus for further theoretical work. The experimental work of this program is coordinated with other related experimental and theoretical efforts of the Chemical Dynamics Group to provide a broad perspective on this area of science.
NTIS
Photoionization; Photoelectrons; Far Ultraviolet Radiation

20020001220 Lawrence Livermore National Lab., Livermore, CA USA
Nutrient limitation and microbially mediated chemistry: studies using tuff inoculum obtained from the Exploratory Studies Facility, Yucca Mountain
Chen, C. I.; Chuu, Y. J.; Meike, A.; Ringelberg, D.; Sawvel, A.; Oct. 30, 1998; 10p; In English
Report No.(s): DE2001-2833; UCRL-JC-131039; No Copyright; Avail: Department of Energy Information Bridge, Microfiche

Flow-through bioreactors are used to investigate the relationship between the supply (and limitation) of major nutrients required by microorganisms (C, N, P, S) and effluent chemistry to obtain data that can be useful to develop models of microbially mediated aqueous chemistry. The bioreactors were inoculated with crushed tuff from Yucca Mountain. Six of the 14 bioreactor experiments currently in operation have shown growth, which occurred in as few as five days and as much as a few months after initiation of the experiment. All of the bioreactors exhibiting growth contained glucose as a carbon source, but other nutritional components varied. Chemical signatures of each bioreactor were compared to each other and selected results were compared to computer simulations of the equivalent abiotic chemical reactions. At 21 C, the richest medium formulation produced a microbial community that lowered the effluent pH from 6.4 to as low as 3.9. The same medium formulation at 50 C produced no significant change in pH but caused a significant increase in Cl after a period of 200 days. Variations in concentrations of other elements, some of which appear to be periodic (Ca, Mg, etc.) also occur. Bioreactors fed with low C, N, P, S media showed growth, but had stabilized at lower cell densities. The room temperature bioreactor in this group exhibited a phospholipid fatty acid (PLFA) signature of sulfur- or iron-reducing bacteria, which produced a significant chemical signature in the effluent from that bioreactor. Growth had not been observed yet in the alkaline bioreactors, even in those containing glucose. The value of combining detailed chemical and community (e.g., ester-linked PLFA) analyses, long-duration experiments, and abiotic chemical models to distinguish chemical patterns is evident. Although all of the bioreactors contain the same initial microorganisms and mineral constituents, PLFA analysis demonstrates that both input chemistry and temperature determine the character of the long-term

population of microorganisms. Where microbial growth occurs, that community can impact the chemistry of water significantly. These principles are well known, but we note their relevance to modeling microbially mediated chemistry. We recognize, in addition to microbial growth, three categories of chemical effects, each of which will require a different approach and constitutive equation(s): (1) unidirectional bacterial modification of the chemistry (i.e., pH) that is directly related to the dominance of particular species, (2) secondary impact of direct microbial modifications (i.e., increased dissolution of solids as a result of reduced pH), and (3) cyclical effects that may be attributed to internal regulation (e.g., osmoregulation or internal pH regulation) or evolution of the microbial community.
NTIS
Bioreactors; Microorganisms; Fatty Acids; Effluents; Waste Treatment

20020001226 Argonne National Lab., IL USA
Density functional and neutron diffraction studies of lithium polymer electrolytes
Baboul, A. G.; Jun. 26, 1998; 13p; In English
Report No.(s): DE2001-10866; ANL/MSD/CP-96742; No Copyright; Avail: Department of Energy Information Bridge

The structure of PEO (polyethylene oxide) doped with lithium perchlorate has been determined using neutron diffraction on protonated and deuterated samples. The experiments were done in the liquid state. Preliminary analysis indicates the Li-O distance is about 2.0 (angstrom). The geometries of a series of gas phase lithium salts LiCF(sub 3)SO(sub 3), Li(CF(sub 3)SO(sub 2))(sub 2)N, Li(CF(sub 3)SO(sub 2))(sub 2)CH, LiClO(sub 4), LiPF(sub 6), LiAsF(sub 6) used in polymer electrolytes have been optimized at B3LYP/6-31G(d) density functional level of theory. All local minima have been identified. For the triflate, imide, methanide, and perchlorate anions, the lithium cation is coordinated to two oxygens and have binding energies of ca. 141 kcal/mol at the B3LYP/6-311+G(3df, 2p)/B3LYP/6-31G(star) level of theory. For the hexafluoroarsenate and hexafluorophosphate the lithium cation is coordinated to three oxygens and have binding energies of ca. 136 kcal/mol.
NTIS
Electrolytes; Lithium Compounds

20020001233 Argonne National Lab., IL USA
High-resolution electron microscopy studies of the precipitation of copper under neutron irradiation in an Fe-1.3WT % Cu alloy
Nicol, A. C.; Dec. 21, 1998; 12p; In English
Report No.(s): DE2001-10850; ANL/MSD/CP-96674; No Copyright; Avail: Department of Energy Information Bridge

We have studied by electron microscopy the copper-rich precipitates in an Fe-1.3wt%Cu model alloy irradiated with neutrons to doses of 8.61 x 10(sup (minus)3) dpa and 6.3 x 10(sup (minus)2) dpa at a temperature of (approximately)270 C. In the lower dose material a majority (ca. 60%) of the precipitates visible in high-resolution electron microscopy were timed 9R precipitates of size (approximately)2-4 nm, while ca. 40% were untwinned. In the higher dose material, a majority (ca. 75%) of visible precipitates were untwinned although many still seemed to have a 9R structure. The average angle (alpha) between the herring-bone fringes in the twin variants was measured as 125(degree), not the 129(degree) characteristic of precipitates in thermally-aged and electron-irradiated material immediately after the bcc(r-arrow)9R martensitic transformation. We argue that these results imply that the bcc(r-arrow)9R transformation of small (4 nm) precipitates under neutron irradiation takes place at the irradiation temperature of 270 C rather than after subsequent cooling. Preliminary measurements showed that precipitate sizes did not depend strongly on dose, with a mean diameter of 3.4 +/- 0.7 nm for the lower dose material, and 3.0 +/- 0.5 nm for the higher dose material. This result agrees with the previous assumption that the lack of coarsening in precipitates formed under neutron irradiation is a consequence of the partial dissolution of larger precipitates by high-energy cascades.
NTIS
Copper Alloys; Electron Microscopy; Neutron Irradiation

20020001294 Lawrence Livermore National Lab., Livermore, CA USA
Next generation experiments and models for shock initiation and detonation of solid explosives
Tarver, C. M.; Jun. 01, 1999; 7p; In English
Report No.(s): DE2001-12159; UCRL-JC-134558; DP0101011; No Copyright; Avail: Department of Energy Information Bridge, Microfiche

Current phenomenological hydrodynamic reactive flow models, such as Ignition and Growth and Johnson-Tang-Forest, when normalized to embedded gauge and laser velocimetry data, have been very successful in predicting shock initiation and detonation properties of solid explosives in most scenarios. However, since these models use reaction rates based on the compression and pressure of the reacting mixture, they can not easily model situations in which the local temperature, which

controls the local reaction rate, changes differently from the local pressure. With the advent of larger, faster, parallel computers, microscopic modeling of the hot spot formation processes and Arrhenius chemical kinetic reaction rates that dominate shock initiation and detonation can now be attempted. Such a modeling effort can not be successful without nanosecond or better time resolved experimental data on these processes. The experimental and modeling approaches required to build the next generation of physically realistic reactive flow models are discussed.
NTIS
Detonation; Explosives; Mathematical Models; Pyrotechnics; Shock Waves

20020001295 Lawrence Livermore National Lab., Livermore, CA USA
Experimental and theoretical progress on an All-Arrhenius model of solid explosive shock initiation
Forbes, J. W.; Tarver, C. M.; Urtiew, P. A.; Jun. 01, 1999; 8p; In English
Report No.(s): DE2001-12157; UCRL-JC-134603; DP0101011; No Copyright; Avail: Department of Energy Information Bridge, Microfiche

Phenomenological shock initiation models, such as Ignition and Growth (I and G) and Johnson-Tang-Forest (JTF), have been very successful in predicting the vast majority of reactive flow states produced during shock initiation and detonation of solid explosives. However, because their reaction rates are pressure and compression dependent and their equations of state are not complete enough to describe all of the available experimental data, these models can not be expected to describe all explosive initiation phenomena. For example, the effects of initial particle size distributions and initial temperature can not be modeled without defining a separate set of model coefficients for each condition. Therefore a new shock initiation model is being developed in the ALE3D and LS-DYNA2D/3D hydrodynamic codes, in which heat transfer and detailed chemical kinetic mechanisms are directly coupled into the hydrodynamic equations. This model creates 'hot spots' by various postulated mechanisms (void collapse, friction, shear, etc.), determines whether these hot spots are large and hot enough to react and grow, and then calculates the spreading rates of the growing reaction sites. The reactions are propagated as they are in nature: by heat transfer using Arrhenius kinetics. The chemical decomposition mechanisms are based on thermal explosion experimental data. The most difficult problem encountered thus far involves modeling the physical mechanisms that produce the large increases in reactive surface area necessary to produce the rapid pressure buildups measured during transitions to detonation. Current research on reaction rates, equations of state, mixture rules, etc. are discussed. The experimental techniques and measurements required for model normalization are also discussed.
NTIS
Explosives; Mathematical Models; Shock Waves; Reaction Kinetics; Solids

20020001510 Sandia National Labs., Albuquerque, NM USA
Multistage Infrared Emitters Based on InAsSb Strained Layers Grown by Metal-Organic Chemical Vapor Deposition
Allerman, A. A.; Baucom, K. C.; Biefeld, R. M.; Kurtz, S. R.; Jan. 04, 1999; 9p; In English
Report No.(s): DE2001-2825; SAND98-1996C; No Copyright; Avail: Department of Energy Information Bridge, Microfiche

We report on the metal-organic chemical vapor deposition (MOCVD) of mid-infrared InAaSb multistage emitters using a high speed rotating disk reactor. The devices contain AlAsSb cladding and strained InAsSb active regions. These emitters have multistage, type I InAsSb/InAsP quantum well active regions. A semi-metal GaAsSb/InAs layer acts as an internal electron source for the multistage injection lasers and AlAsSb is the electron confinement layer. These structures are the first MOCVD multistage devices. Broadband LEDs (light emitting diode) produced 2 mW average power at 3.7 (micro)m and 80 K and 0.1 mW at 4.3 (micro)m and 300K. A multistage, 3.8-3.9 (micro)m laser structure operated up to T=180 K. At 80 K, peak-power approximately equals 100 mW/facet and a high slope-efficiency (48%) were observed in these gain guided lasers.
NTIS
Lasers; Indium Compounds; Metalorganic Chemical Vapor Deposition

20020001533 TPL, Inc., Albuquerque, NM USA
Micromachined Silicon Sensor for DNA Sequencing by Hybridization ***Final Report, 2 Sep. 1998 - 17 Mar. 1999***
Kepley, L. J.; Sep. 16, 1999; 15p; In English
Report No.(s): DE2001-765422; No Copyright; Avail: Department of Energy Information Bridge, Microfiche

Final report of a Phase I SBIR contractor investigation of a porous silicon platform for ultrasonic DNA sensing applications.
NTIS
Deoxyribonucleic Acid; Micromachining; Porous Silicon; Microbiology

20020001541 Sandia National Labs., Albuquerque, NM USA

Chemical Solution Processing of Strontium Bismuth Tantalate Films

Boyle, T. J.; Lakeman, C. D. E.; Dec. 21, 1998; 11p; In English

Report No.(s): DE2001-2818; SAND98-2837C; No Copyright; Avail: Department of Energy Information Bridge, Microfiche

We describe Chemical Solution Deposition (CSD) processes by which Strontium Bismuth Tantalate (SBT) thin films can be prepared at temperatures as low as 550 C. In this paper, we will present strategies used to optimize the properties of the films including solution chemistry, film composition, the nature of the substrate (or bottom electrode) used, and the thermal processing cycle. Under suitable conditions, (approximately) 1700 (angstrom) films can be prepared which have a large switchable polarization (2P(sub r) 10(micro)C/square cm), and an operating voltage, defined as the voltage at which 0.80 x 2P(sub r) max is switched, 2.0V. We also describe an all-alkoxide route to SBT films from which SBT can be crystallized at 550 C.

NTIS

Tantalum Compounds; Strontium; Bismuth; Deposition; Thin Films

20020001565 Argonne National Lab., IL USA

Mesoporous Synthetic Clays: Synthesis, Characterization, and Use as HDS Catalyst Supports

Bloomquist, C. A. A.; Carrado, K. A.; Marshall, C. L.; Seifert, S.; Wei, D.; Aug. 10, 1999; 10p; In English

Report No.(s): DE2001-11853; ANL/CHM/CP-99251; No Copyright; Avail: Department of Energy Information Bridge

Mesoporous synthetic clays (MSCs) are obtained when polymer-containing silicate gels are hydrothermally crystallized to form layered magnesium silicate hectorite clays containing polymers that are incorporated in situ. Polyvinylpyrrolidone (PVP) of several average molecular weights ranging from 10 K to 1.3 M, in gel loadings varying from 5-30 wt%, were used. The organic polymer template molecules were removed from synthetic polymer-clay complexes via calcination. Pore radii, surface areas, and pore volumes of the resulting porous inorganic networks were then measured. For the most part there is a direct correlation between both PVP molecular weight and polymer loading on the diameter of the average pore. In addition to conventional techniques, the polymer-clay materials were also characterized by small angle x-ray scattering to ascertain the disposition of the polymeric matrix. The MSC materials after calcination were examined as potential supports for hydrodesulfurization (HDS). They were loaded with a bimetallic Co/Mo catalyst system for comparison with a commercial Co/Mo alumina catalyst. Dibenzothiophene (DBT) diluted with hexadecane (0.75 wt% S) was utilized as a liquid feed for the HDS tests. This feed was chosen as a deep HDS test of a heavy model oil. The pore diameters of the MSC catalysts were found to have a strong effect on both the HDS activity and selectivity.

NTIS

Catalysts; Characterization; Clays

20020001594 Lawrence Livermore National Lab., Livermore, CA USA

Kinetic modeling of non-ideal explosives

Fried, L. E.; Howard, W. M.; Souers, P. C.; Mar. 01, 1999; 12p; In English

Report No.(s): DE2001-12572; UCRL-JC-132512; No Copyright; Avail: Department of Energy Information Bridge, Microfiche

We have implemented a Wood-Kirkwood kinetic detonation model based on multi-species equations of state and multiple reaction rate laws. Finite rate laws are used for the slowest chemical reactions, while other reactions are given infinite rates and are kept in constant thermodynamic equilibrium. We model a wide range of ideal and non-ideal composite energetic materials. In addition, we develop an exp-6 equation of state for the product fluids that reproduces a wide range experimental shock Hugoniot and static compression data. For unreacted solids, including solid and liquid Al and Al(sub 2)O(sub 3), we use a Murnaghan form for the equation of state. We find that we can replicate experimental detonation velocities to within a few per cent for a wide range of explosives, while obtaining good agreement with estimated reaction zone lengths. The detonation velocity as a function of charge radius is also correctly reproduced.

NTIS

Explosions; Reaction Kinetics

20020001837 Argonne National Lab., IL USA

Study of nitrogenation of a NdFe12xMox compound by in situ neutron powder diffraction

Ding, Y.; Lin, J.; Loong, C. K.; Short, S. M.; Nov. 18, 1997; 16p; In English

Report No.(s): DE2001-8882; ANL/IPNS/CP-94847; No Copyright; Avail: Department of Energy Information Bridge, Microfiche

The effects on the crystal lattice of a NdFe(sub 12(minus)x)Mo(sub x)(x (approx equal) 1.7) compound which contained (approximately)12 vol% of bcc (body centered cubic)-Fe were studied by neutron powder diffraction during controlled

nitrogenation over the 25-600 C temperature range. The sample inside the furnace was connected to a closed volume of ultra-pure nitrogen gas while neutron data were collected over regular time intervals during sequential heating. Substantial nitrogen absorption occurred between 500 to 600 C. During the nitrogenation process the NdFe(sub 12(minus)x)Mo(sub x)N(sub y) lattice expanded while the bcc-Fe lattice contracted. An increasing decomposition of the compound into bcc-Fe at 600 C was observed. The average size of the NdFe(sub 12(minus)x)Mo(sub x)N(sub y) crystalline grains decreased starting at (approximately)300 C, reaching a minimum at (approximately)500 C and then increased markedly at higher temperatures. The development of lattice strains, on the other hand, showed an opposite trend, i.e., a maximum at 500 C. A correlation of structural modification of the crystalline phases and the nitrogenation process is discussed.
NTIS
Neutron Diffraction; Crystal Lattices; Nitrogenation; Ternary Alloys

20020001851 Florida Univ., Gainesville, FL USA
Time-resolved far-infrared experiments at the National Synchrotron Light Source
Tanner, D. B.; Reitze, D. H.; Carr, G. L.; Oct. 12, 1999; 17p; In English
Report No.(s): DE2001-764708; No Copyright; Avail: Department of Energy Information Bridge

A facility for time-resolved infrared and far-infrared spectroscopy has been built and commissioned at the National Synchrotron Light Source. This facility permits the study of time dependent phenomena over a frequency range from 2-8000 per-cm (0.25 meV-1 eV). Temporal resolution is approximately 200 psec and time dependent phenomena in the time range out to 100 nsec can be investigated.
NTIS
Infrared Spectroscopy; Light Sources; Synchrotrons

20020001860 Toronto Univ., Dept. of Civil Engineering, Ontario Canada
Prediction of Chloride Penetration in Concrete ***Final Report, Sep. 1997 - Sep. 00***
Hooton, R. D.; Stanish, T. K.; Oct. 2001; 436p; In English
Report No.(s): PB2002-100056; No Copyright; Avail: CASI; A19, Hardcopy; A04, Microfiche

This report presents the results of a study conducted for the Federal Highway Administration to identify or develop a test method to predict the chloride penetration resistance of concrete in a short time frame (less than 35 days). The test was to be applicable for evaluating new mixes, for accepting or rejecting new concrete, and for evaluating in-place concrete. This report will be of interest to materials engineers and others who are involved in design, construction, and evaluation of concrete susceptible to corrosion.
NTIS
Chlorides; Corrosion; Concretes

20020001861 National Inst. of Building Sciences, Buiding Seismic Safety Council, Washington, DC USA
NEHRP Recommended Provisions for Seismic Regulations for New Buildings and Other Structures. Part 1. Provisions. 2000 Edition
Mar. 2001; 398p; In English
Report No.(s): PB2002-100053; FEMA-368; No Copyright; Avail: CASI; A17, Hardcopy; A04, Microfiche

The report presents criteria for the design and construction of structures to resist earthquake ground motions. The purposes of the Provisions are as follows: 1. to provide minimum design criteria for structures appropriate to their primary function and use considering the need to protect the health, safety, and welfare of the general public by minimizing the earthquake-related risk to life and 2. to improve the capability of essential facilities and structures containing substantial quantities of hazardous materials to function during and after design earthquakes.
NTIS
Corrosion Prevention; Design Analysis; Buildings

20020001881 Argonne National Lab., IL USA
Neutron scattering characterization of pure and rare-earth modified zirconia catalysis
Loong, C. K.; Ozawa, M.; Richardson, J. W.; Suzuki, S.; Thiyagarajan, P.; Nov. 18, 1997; 12p; In English
Report No.(s): DE2001-8881; ANL/IPNS/CP-94846; No Copyright; Avail: Department of Energy Information Bridge, Microfiche

The combined application of neutron powder diffraction, small angle neutron scattering and neutron inelastic scattering has led to improved understanding of the crystal phases, defect structure, microstructure and hydroxyl/water dynamics in pure and

lanthanide-modified zirconia catalysts. Powder diffraction experiments quantified the degree of stabilization and provided evidence for static, oxygen vacancy-induced atomic displacements in stabilized zirconia. Quantitative assessment of Bragg peak breadths led to measurements 'grain size' representing coherency length of long-range ordered atomic arrangements (crystals). Small angle neutron scattering provided a separate measurement of 'grain size' representing the average size of the primary particles in the aggregates, and the evolution of porosity (micro- versus meso-) and surface roughness caused by RE modification and heat treatment. Finally, the dynamics of hydrogen atoms associated with surface hydroxyls and adsorbed water were investigated by neutron-inelastic scattering, revealing changes in frequency and band breadth of O-H stretch, H-O-H bend, and librational motion of water molecules.
NTIS
Zirconium Oxides; Catalysis; Neutron Scattering; Neutron Diffraction; Rare Earth Elements

20020001888 Argonne National Lab., IL USA
New method for oxidation of gaseous, elemental mercury
Livengood, C. D.; Mendelsohn, M. H.; Aug. 23, 1999; 15p; In English
Report No.(s): DE2001-12435; ANL/ES/CP-98436; No Copyright; Avail: Department of Energy Information Bridge, Microfiche
Elemental mercury (Hg) is difficult to remove from flue-gas streams using existing wet-scrubber technology, primarily because of its limited volubility in water. We have proposed and tested a concept for enhancing gaseous Hg(sup 0)removal in wet scrubber systems by altering the chemical form of the Hg(sup 0) to a water-soluble oxidized species. Recently, we have discovered a new method for injection of the oxidizing species that dramatically improves reactant utilization and at the same time gives significant nitric oxide (NO) oxidation as well. Our method uses a diluted oxidizing solution containing chloric acid and sodium chlorate (sold commercially as NOXSORB(trademark)). When this solution is injected into a gas stream containing Hg(sup 0) at about 300 F, we found that nearly 100% of the Hg(sup 0) was removed from the gas phase and was recovered in liquid samples from the test system. At the same time, approximately 80% of the added NO was also removed (oxidized). The effect of sulfur dioxide (SO(sub 2)) on this method was also investigated, and it appears to decrease slightly the amount of Hg oxidized. We are currently testing the effect of variations in oxidizing solution concentration, SO(sub 2) concentration, NO concentration, and reaction time (residence time).
NTIS
Oxidation; Flue Gases; Gas Streams; Mercury (Metal)

20020001961 Lawrence Livermore National Lab., Livermore, CA USA
Laser-generated metallic hydrogen
Nellis, W. J.; Pollaine, S. M.; Aug. 27, 1999; 4p; In English
Report No.(s): DE2001-14569; UCRL-JC-135176; No Copyright; Avail: Department of Energy Information Bridge, Microfiche
Hydrogen reaches the minimum conductivity of a metal at 140 GPa (1.4 Mbar) and 3000 K. These conditions were achieved using a two-stage light-gas gun. The authors have investigated computationally the use of a laser-heated hohlraum to shock compress hydrogen to these conditions in samples sufficiently thin that the metallic fluid might be quenched metastably on release of dynamic pressure. A configuration was found such that the duration of maximum pressure is sufficiently long that the hydrogen film cools by thermal conduction before pressure is released.
NTIS
Metallic Hydrogen; Conductive Heat Transfer; Light Gas Guns

20020001996 Louisiana State Univ., Baton Rouge, LA USA
Gallium Zeolites for Light Paraffin Aromatization
Price, G. L.; Dooley, K. M.; Feb. 10, 1999; 12p; In English
Report No.(s): DE2001-6588; No Copyright; Avail: Department of Energy Information Bridge
The primary original goal of this project was to investigate the active state of gallium-containing MFI catalysts for light paraffin aromatization, in particular the state of gallium in the active material. Our original hypothesis was that the most active and selective materials were those which contained gallium zeolitic cations, and that previously reported conditions for the activation of gallium-containing catalysts served to create these active centers. We believed that in high silica materials such as MFI, ion-exchange is most effectively accomplished with metals in their 1+ oxidation state, both because of the sparsity of the anionic ion-exchange sites associated with the zeolite, and because the large hydration shells associated with aqueous 3+ cations hinder transport. Metals such as Ga which commonly exist in higher oxidation states need to be reduced to promote ion-exchange and this is the reason that reduction of gallium-containing catalysts for light paraffin aromatization often yields a dramatic enhancement in catalytic activity. We have effectively combined reduction with ion-exchange and we term this combined process

reductive solid-state ion-exchange. Our hypothesis has largely been proven true, and a number of the papers we have published directly address this hypothesis.
NTIS
Paraffins; Gallium; Zeolites

20020002222 NASA Ames Research Center, Moffett Field, CA USA
Theoretical Study of the First Transition Row Oxides and Sulfides
Bauschlicher, Charles W., Jt., NASA Ames Research Center, USA; Maitre, Philippe, NASA Ames Research Center, USA; [1994]; 1p; In English
Contract(s)/Grant(s): RTOP 232-01-04; No Copyright; Avail: Issuing Activity; Abstract Only

The first transition row oxides and sulfides are studied using several different levels of theory. The calculations show the bonding mechanism in the sulfides and oxides to be very similar. For the oxides, accurate experimental data allow the theoretical methods to be calibrated. The same level of theory is used to study the sulfides where there is far less experimental information. For ScO through MnO and CuO the coupled cluster singles and doubles technique including a perturbational estimate of the unliked triple excitations [CCSD(T)] yields spectroscopic constants ((tau)e, (omega)e, and D0) in good agreement with experiment. The triple excitations are found to be very important in achieving this accuracy. For FeO to NiO, the single determinant self-consistent-field (SCF) approach yields pi orbitals that are localized on the metal or oxygen. This appears to cause problems for the single reference techniques; this is discussed in detail for NiO. The complete-active-space SCF/internally contracted averaged coupled pair functional approach (CASSCF/ICACPF) works well for FeO to NiO. The calculation of accurate dipole moments is found to be very difficult.
Author
Sulfides; Transition Metals; Metal Oxides; Self Consistent Fields

20020002275 Oak Ridge National Lab., TN USA
Estimation of Flammability Limits of Selected Fluorocarbons with F2 and CIF3
Trowbridge, L. D.; Sep. 01, 1999; 78p; In English
Report No.(s): DE2001-12455; ORNL/TM-1999/184; No Copyright; Avail: Department of Energy Information Bridge, Microfiche

During gaseous diffusion plant operations, conditions leading to the formation of flammable gas mixtures may occasionally arise. Currently, these could consist of the evaporative coolant CFC-114 and fluorinating agents such as F2 and CIF3. Replacement of CFC-114 with non-ozone-depleting substitutes such as c-C4F8 and C4F(10) is planned. Consequently, in the future, these too must be considered potential 'fuels' in flammable gas mixtures. Two questions of practical interest arise: (1) can a particular mixture sustain and propagate a flame if ignited, and (2) what is the maximum pressure that can be generated by the burning (and possibly exploding) gas mixture, should ignite. Experimental data on these systems are limited. to assist in answering these questions, a literature search for relevant data was conducted, and mathematical models were developed to serve as tools for predicting potential detonation pressures and estimating (based on empirical correlations between gas mixture thermodynamics and flammability for known systems) the composition limits of flammability for these systems. The models described and documented in this report are enhanced versions of similar models developed in 1992.
NTIS
Flammability; Estimating; Fluorocarbons; Fluorination; Gaseous Diffusion

20020002283 Federal Energy Technology Center, Morgantown, WV USA
Functionally graded alumina/mullite coatings for protection of silicon carbide ceramic components from corrosion
Oct. 01, 1997; 23p; In English
Report No.(s): DE2001-8827; DE-FG22-96PC96208-02; No Copyright; Avail: Department of Energy Information Bridge, Microfiche

The main objective of this research project is the formulation of processes that can be used to prepare compositionally graded alumina/mullite coatings for protection from corrosion of silicon carbide components (monolithic or composite) used or proposed to be used in coal utilization systems (e.g., combustion chamber liners, heat exchanger tubes, particulate removal filters, and turbine components) and other energy-related applications. Mullite will be employed as the inner (base) layer and the composition of the film will be continuously changed to a layer of pure alumina, which will function as the actual protective coating of the component. Chemical vapor deposition reactions of silica, alumina, and aluminosilicates (mullite) through hydrolysis of aluminum and silicon chlorides in the presence of CO2 and H2 will be employed to deposit compositionally graded films of mullite and alumina. Our studies will include the kinetic investigation of the silica, alumina, and aluminosilicate deposition processes,

characterization of the composition, microstructure, surface morphology, and mechanical behavior of the prepared films, and modeling of the various deposition processes. During this reporting period, the construction and development of the chemical vapor deposition system was completed, and experiments were conducted on the deposition of alumina, silica, and aluminosilicates (such as mullite) from mixtures of AlCl3 and CH3SiCl3 in CO2 and H2. Work was mainly done on the investigation of the effects of the reaction temperature on the deposition kinetics. It was found that the temperature had a positive effect on the single oxides deposition rates and the codeposition rate. The apparent activation energy values extracted from the deposition rate vs. temperature curves in the high temperature region were similar for the three deposition processes, having a value around 20 kcal/mol. The codeposition rates were higher, by a more than a factor of 2 in some cases, than the sum of the deposition rates of the two oxides in the independent experiments at the same operating conditions, and this result led to the conclusion that there should exist additional surface reaction steps in the codeposition process, that lead to solid formation and involve both silicon-containing and aluminum-containing species. The elemental analysis (EDXA) of films deposited from MTS-AlCl3-CO2-H2 mixtures showed that silicon oxide was the main component, and comparison of the deposition rates of SiO2 and Al2O3 during codeposition with those seen in single species deposition experiments at the same conditions revealed that the codeposition process was characterized by a dramatic enhancement of the deposition of SiO2 and an equally dramatic reduction in the rate of Al2O3 deposition. Since the enhanced codeposition rate was caused by increased silicon oxide deposition, it was concluded that the main deposition product of the additional surface reaction steps in codeposition must be silicon oxide. A comprehensive investigation of the effects of the other operating parameters on the kinetics of the codeposition process will be carried out in the next reporting period.

NTIS

Protective Coatings; Silicon Carbides; Ceramics; Corrosion Resistance; Aluminum Oxides; Mullites

20020002284 Federal Energy Technology Center, Morgantown, WV USA

Functionally graded alumina/mullite coatings for protection of silicon carbide ceramic components from corrosion

Mar. 01, 1998; 25p; In English

Report No.(s): DE2001-8823; DE-FG22-96PC96208-03; No Copyright; Avail: Department of Energy Information Bridge, Microfiche

The main objective of this research project is the formulation of processes that can be used to prepare compositionally graded alumina/mullite coatings for protection from corrosion of silicon carbide components (monolithic or composite) used or proposed to be used in coal utilization systems (e.g., combustion chamber liners, heat exchanger tubes, particulate removal filters, and turbine components) and other energy-related applications. Mullite will be employed as the inner (base) layer and the composition of the film will be continuously changed to a layer of pure alumina, which will function as the actual protective coating of the component. Chemical vapor deposition reactions of silica, alumina, and aluminosilicates (mullite) through hydrolysis of aluminum and silicon chlorides in the presence of CO2 and H2 will be employed to deposit compositionally graded films of mullite and alumina. Our studies will include the kinetic investigation of the silica, alumina, and aluminosilicate deposition processes, characterization of the composition, microstructure, surface morphology, and mechanical behavior of the prepared films, and modeling of the various deposition processes. During this reporting period, the construction and development of the chemical vapor deposition system was completed, and experiments were conducted on the deposition of alumina, silica, and aluminosilicates (such as mullite) from mixtures of AlCl3 and CH3SiCl3 in CO2 and H2. Work was mainly done on the investigation of the effects of the reaction temperature on the deposition kinetics. It was found that the temperature had a positive effect on the single oxides deposition rates and the codeposition rate. The apparent activation energy values extracted from the deposition rate vs. temperature curves in the high temperature region were similar for the three deposition processes, having a value around 20 kcal/mol. The codeposition rates were higher, by a more than a factor of 2 in some cases, than the sum of the deposition rates of the two oxides in the independent experiments at the same operating conditions, and this result led to the conclusion that there should exist additional surface reaction steps in the codeposition process, that lead to solid formation and involve both silicon-containing and aluminum-containing species. The elemental analysis (EDXA) of films deposited from MTS-AlCl3-CO2-H2 mixtures showed that silicon oxide was the main component, and comparison of the deposition rates of SiO2 and Al2O3 during codeposition with those seen in single species deposition experiments at the same conditions revealed that the codeposition process was characterized by a dramatic enhancement of the deposition of SiO2 and an equally dramatic reduction in the rate of Al2O3 deposition. Since the enhanced codeposition rate was caused by increased silicon oxide deposition, it was concluded that the main deposition product of the additional surface reaction steps in codeposition must be silicon oxide. A comprehensive investigation of the effects of the other operating parameters on the kinetics of the codeposition process will be carried out in the next reporting period.

NTIS

Protective Coatings; Silicon Carbides; Ceramics; Corrosion Resistance; Aluminum Oxides; Mullites

20020002288 Los Alamos National Lab., NM USA

Combustion in porous media

Dillon, J.; Sep. 01, 1999; 27p; In English

Report No.(s): DE2001-765956; LA-SUB-99-56; No Copyright; Avail: Department of Energy Information Bridge, Microfiche

A 2.8-liter tube-shaped combustion vessel was constructed to study flame propagation and quenching in porous media. For this experiment, hydrogen-air flames propagating horizontally into abed of 6 mm diameter glass beads were studied. Measurements of pressure and temperature along the length of the tube were used to observe flame propagation of quenching. The critical hydrogen concentration for Hz-air mixtures was found to be 11.5%, corresponding to a critical Peclet number of Pe* = 37. This value is substantially less than the value of Pe* = 65 quoted in the literature, for example Babkin et al. (1991). It is hypothesized that buoyancy and a dependence of Pe on the Lewis number account for the discrepancy between these two results. NTIS

Combustion; Porous Materials; Buoyancy; Flame Propagation; Peclet Number

20020002300 Brown Univ., Providence, RI USA

High pressure/high temperature thermogravimetric apparatus ***Final Report***

Calo, J. M.; Suuberg, E. M.; Dec. 01, 1999; 40p; In English

Report No.(s): DE2001-765239; No Copyright; Avail: Department of Energy Information Bridge

The purpose of this instrumentation grant was to acquire a state-of-the-art, high pressure, high temperature thermogravimetric apparatus (HP/HT TGA) system for the study of the interactions between gases and carbonaceous solids for the purpose of solving problems related to coal utilization and applications of carbon materials. The instrument that we identified for this purpose was manufactured by DMT (Deutsche Montan Technologies), Institute of Cokemaking and Coal Chemistry of Essen, Germany. Particular features of note include: Two reactors: a standard TGA reactor, capable of 1100 C at 100 bar; and a high temperature (HT) reactor, capable of operation at 1600 C and 100 bar; A steam generator capable of generating steam to 100 bar; Flow controllers and gas mixing system for up to three reaction gases, plus a separate circuit for steam, and another for purge gas; and an automated software system for data acquisition and control. The HP/TP DMT-TGA apparatus was purchased in 1996 and installed and commissioned during the summer of 1996. The apparatus was located in Room 128 of the Prince Engineering Building at Brown University. A hydrogen alarm and vent system were added for safety considerations. The system has been interfaced to an Ametek quadruple mass spectrometer (MS 100), pumped by a Varian V250 turbomolecular pump, as provided for in the original proposal. With this capability, a number of gas phase species of interest can be monitored in a near-simultaneous fashion. The MS can be used in a few different modes. During high pressure, steady-state gasification experiments, it is used to sample, measure, and monitor the reactant/product gases. It can also be used to monitor gas phase species during nonisothermal temperature programmed reaction (TPR) or temperature programmed desorption (TPD) experiments.
NTIS

Coal; Gases; Thermogravimetry; High Pressure; Solids; High Temperature Tests

20020002313 Federal Energy Technology Center, Morgantown, WV USA

Attrition resistant iron-based fischer-tropsch catalysts

Goodwin, J. G.; Spivey, J. J.; Jothimurugesan, K.; Gangwal, S. K.; Mar. 29, 1999; 11p; In English

Report No.(s): DE2001-8834; DE-FG22-96PC96217-05; No Copyright; Avail: Department of Energy Information Bridge, Microfiche

The Fischer-Tropsch (F-T) reaction provides a way of converting coal-derived synthesis gas (CO+H2) to liquid fuels. Since the reaction is highly exothermic, one of the major problems in control of the reaction is heat removal. Recent work has shown that the use of slurry bubble column reactors (SBCRs) can largely solve this problem. Iron-based (Fe) catalysts are preferred catalysts for F-T when using low CO/H2 ratio synthesis gases derived from modern coal gasifiers. This is because in addition to reasonable F-T activity, the F-T catalysts also possess high water gas shift (WGS) activity. However, a serious problem with the use of Fe catalysts in a SBCR is their tendency to undergo attrition. This can cause fouling/plugging of downstream filters and equipment, making the separation of catalyst from the oil/wax product very difficult if not impossible, and results in a steady loss of catalyst from the reactor. The objectives of this research are to develop a better understanding of the parameters affecting attrition resistance of Fe F-T catalysts suitable for use in SBCRs and to incorporate this understanding into the design of novel Fe catalysts having superior attrition resistance. Catalyst preparations will be based on the use of spray drying and will be scalable using commercially available equipment. The research will employ among other measurements, attrition testing and F-T synthesis, including long duration slurry reactor runs in order to ascertain the degree of success of the various preparations. The goal is to develop an Fe catalyst which can be used in a SBCR having only an internal filter for separation of the catalyst from the liquid product, without sacrificing F-T activity and selectivity. The effect of silica addition via coprecipitation and as a binder

to a doubly promoted Fischer-Tropsch synthesis iron catalyst (100 Fe/5 Cu/4.2 K) was studied. The catalysts were prepared by coprecipitation, followed by binder addition and drying in a 1 m diameter, 2 m tall spray dryer. The binder silica content was varied from 0 to 20 wt %. A catalyst with 12 wt % binder silica was found to have the highest attrition resistance. F-T reaction studies over 100 hours in a fixed-bed reactor showed that this catalyst maintained around 95% CO conversion with a methane selectivity of less than 7 wt % and a C5 + selectivity of greater than 73 wt %. The effect of adding precipitated silica from 0 to 20 parts by weight to this catalyst (containing 12 wt % binder silica) was also studied. Addition of precipitated silica was found to be detrimental to attrition resistance and resulted in increased methane and reduced wax formation. An HPR series of proprietary catalysts was prepared to further improve the attrition resistance. Based on the experience gained, a proprietary HPR-43 catalyst has been successfully spray dried in 500 g quantity. This catalyst showed 95% CO conversion over 125 h and had less than 4% methane selectivity. Its attrition resistance was one of the highest among the catalyst tested.
NTIS
Catalysts; Fischer-Tropsch Process; Iron

20020002316 Texas Univ., Austin, TX USA
New Architectures for Integrated Photoelectrochemical Systems ***Final Report, 1 Sep. 1994 - 31 Aug. 1999***
Fox, M. A.; Oct. 01, 1998; 13p; In English
Report No.(s): DE2001-765745; No Copyright; Avail: Department of Energy Information Bridge, Microfiche

This work seeks to prepare new macromolecular and supramolecular architectures that attach oriented light-sensitive organic materials to metal and semiconductor surfaces. We use these integrated materials to define the photophysical principles that control vectorial energy and electron migration over distances that are large on a molecular scale, while developing synthetic methodology for spatial definition of these catalytic arrays on the nanometer to micrometer scale. Chemically modified surfaces are envisioned as important vehicles for conversion of incident photons to chemical or electrical energy. In practice, this work involves: (1) synthesis and characterization of new polymeric and supramolecular arrays for directional electron transfer, involving both linear and nonlinear macromolecules and new liquid crystals; (2) optical imaging in self-assembled monolayers on metals and on modified semiconductor surfaces; (3) fundamental studies of long range electronic coupling along rigid molecular backbones and in organic-inorganic composite materials.
NTIS
Photoelectrochemistry; Organic Materials; Electron Transfer; Macromolecules

20020002344 Texas Univ., Austin, TX USA
Corrosion Performance of Epoxy-Coated Reinforcement: Summary, Findings, and Guidelines ***Final Report***
Vaca-Cortes, E.; Kahhaleh, K. Z.; Jirsa, J. O.; Wheat, H. G.; Carrasquillo, R. L.; Jul. 1998; 104p; In English
Report No.(s): PB2002-100242; No Copyright; Avail: CASI; A06, Hardcopy; A02, Microfiche

The integrity and corrosion performance of epoxy-coated reinforcement in aggressive environments was investigated through a series of experimental studies. The effects of coating condition and amount of damage, repaired vs. unrepaired damage, bar fabrication, and concrete cracking were studied. It was found that regardless of coating condition, the performance of epoxy-coated bars was better than that of uncoated bars. The approach for the corrosion performance evaluation of epoxy-coated reinforcement included in this report should serve as an aid to engineers involved in the specification, design, construction, inspection, and maintenance of concrete bridge and other transportation structures. Findings have been transmitted to TXDOT throughout the project to permit implementation of practices that will extend the service life of transportation structures. Guidelines for quality control, design, and construction practice of concrete structures with epoxy-coated reinforcement are included. A test procedure to evaluate the adhesive strength of the epoxy coating was developed and is recommended for quality control.
NTIS
Coatings; Concrete Structures; Epoxy Resins

20020002345 Kansas Univ., Dept. of Civil and Environmental Engineering, Lawrence, KS USA
Performance and Constructability of Silica Fume Bridge Deck Overlays ***Final Report, Jan. 1998 - Jan. 00***
Miller, G. G.; Darwin, D.; Jan. 2000; 452p; In English
Report No.(s): PB2002-100239; No Copyright; Avail: CASI; A20, Hardcopy; A04, Microfiche

The effects of construction practices and material properties on the performance of concrete bridge decks are evaluated. Emphasis is placed on comparing bridge decks with silica fume and conventional concrete overlays and determining if the silica fume overlays commonly used on bridges in Kansas are performing at a level that justifies the extra cost and construction precautions. Forty continuous steel girder bridges, 20 with silica fume overlays, 16 with conventional overlays and four with

monolithic bridge decks are included in the study. Field surveys were conducted to document cracking patterns and crack density and to obtain samples for chloride content and rapid chloride permeability (RCPT) analysis.
NTIS
Concretes; Silicon Dioxide; Bridges (Structures); Construction

20020002352 Brookhaven National Lab., Upton, NY USA
Effect of Chromate Concentration on the Repassivation of Corroding Aluminum
Jeffcoate, C. S.; Isaacs, H. S.; Hawkins, J.; Thompson, G. E.; Feb. 09, 1999; 14p; In English
Report No.(s): DE2001-6247; BNL-66152; KC-02-01-02; No Copyright; Avail: Department of Energy Information Bridge, Microfiche

Current density maps of anodically polarized pure aluminum in chloride solutions were measured and the effect of chromate/dichromate buffer additions monitored. The higher the polarized potential the more chromate was required to repassivate the corroding surface. Small pits repassivated easily, crevice corrosion events were the last to repassivate. Open circuit potential measurements showed the presence of meta-stable pitting at chloride concentrations of 0.3M. The lifetime and magnitude of these metastable pits was reduced on the addition of 0.05M chromate buffer.
NTIS
Chromates; Current Density; Aluminum

20020002704 Sandia National Labs., Albuquerque, NM USA
Coupled Thermal-Chemical-Mechanical Modeling of Validation Cookoff Experiments
Erikson,; Schmitt,; Atwood,; Curran,; Nov. 27, 2000; 15p; In English
Report No.(s): DE2001-768084; SAND2000-2926C; No Copyright; Avail: Department of Energy Information Bridge

The cookoff of energetic materials involves the combined effects of several physical and chemical processes. These processes include heat transfer, chemical decomposition, and mechanical response. The interaction and coupling between these processes influence both the time-to-event and the violence of reaction. The prediction of the behavior of explosives during cookoff, particularly with respect to reaction violence, is a challenging task. to this end, a joint DoD/DOE program has been initiated to develop models for cookoff, and to perform experiments to validate those models. In this paper, a series of cookoff analyses are presented and compared with data from a number of experiments for the aluminized, RDX-based, Navy explosive PBXN-109. The traditional thermal-chemical analysis is used to calculate time-to-event and characterize the heat transfer and boundary conditions. A reaction mechanism based on Tarver and McGuire's work on RDX(sup 2) was adjusted to match the spherical one-dimensional time-to-explosion data. The predicted time-to-event using this reaction mechanism compares favorably with the validation tests. Coupled thermal-chemical-mechanical analysis is used to calculate the mechanical response of the confinement and the energetic material state prior to ignition. The predicted state of the material includes the temperature, stress-field, porosity, and extent of reaction. There is little experimental data for comparison to these calculations. The hoop strain in the confining steel tube gives an estimation of the radial stress in the explosive. The inferred pressure from the measured hoop strain and calculated radial stress agree qualitatively. However, validation of the mechanical response model and the chemical reaction mechanism requires more data. A post-ignition burn dynamics model was applied to calculate the confinement dynamics. The burn dynamics calculations suffer from a lack of characterization of the confinement for the flaw-dominated failure mode experienced in the tests. High-pressure burning rates are needed for more detailed post-ignition studies. Sub-models for chemistry, mechanical response and burn dynamics need to be validated against data from less complex experiments. The sub-models can then be used in integrated analysis for comparison with experimental data taken during integrated tests.
NTIS
Boundary Conditions; Chemical Reactions; Heat Transfer; Coupling; Models; Proving; Thermal Analysis

20020002710 California Univ., Lawrence Berkeley Lab., Berkeley, CA USA
Photoisomerization and photodissociation dynamics of reactive free radicals
Bise, R. T.; Aug. 24, 2000; 198p; In English
Report No.(s): DE2001-767628; LBNL-46763; No Copyright; Avail: Department of Energy Information Bridge

The photofragmentation pathways of chemically reactive free radicals have been examined using the technique of fast beam photofragment translational spectroscopy. Measurements of the photodissociation cross-sections, product branching ratios, product state energy distributions, and angular distributions provide insight into the excited state potential energy surfaces and nonadiabatic processes involved in the dissociation mechanisms. Photodissociation spectroscopy and dynamics of the predissociative (tilde A)(sup 2)A(sub 1) and (tilde B)(sup 2)A(sub 2) states of CH(sub 3)S have been investigated. At all photon energies, CH(sub 3) + S((sup 3)P(sub j)), was the main reaction channel. The translational energy distributions reveal resolved

structure corresponding to vibrational excitation of the CH(sub 3) umbrella mode and the S((sup 3)P(sub j)) fine-structure distribution from which the nature of the coupled repulsive surfaces is inferred. Dissociation rates are deduced from the photofragment angular distributions, which depend intimately on the degree of vibrational excitation in the C-S stretch. Nitrogen combustion radicals, NCN, CNN and HNCN have also been studied. For all three radicals, the elimination of molecular nitrogen is the primary reaction channel. Excitation to linear excited triplet and singlet electronic states of the NCN radical generates resolved vibrational structure of the N(sub 2) photofragment. The relatively low fragment rotational excitation suggests dissociation via a symmetric C(sub 2V) transition state. Resolved vibrational structure of the N(sub 2) photofragment is also observed in the photodissociation of the HNCN radical. The fragment vibrational and rotational distributions broaden with increased excitation energy. Simple dissociation models suggest that the HNCN radical isomerizes to a cyclic intermediate (c-HCNN) which then dissociates via a tight cyclic transition state. In contrast to the radicals mentioned above, resolved vibrational structure was not observed for the ICNN radical due to extensive fragment rotational excitation, suggesting that intermediate bent states are strongly coupled along the dissociation pathway. The measurements performed in this Thesis have additionally refined the heats of formation and bond dissociation energies of these radicals and have unambiguously confirmed and added to the known electronic spectroscopy.

NTIS

Photolysis; Dissociation; Isomerization; Angular Distribution; Atomic Energy Levels

20020002717 Federal Energy Technology Center, Morgantown, WV USA

Investigation of heat transfer and combustion in the advanced Fluidized Bed Combustor (FBC)

Lee, S. W.; Oct. 01, 1998; 180p; In English

Report No.(s): DE2001-766746; DE-FG22-93MT93006-15; No Copyright; Avail: Department of Energy Information Bridge

The objective of this project is to predict the heat transfer and combustion performance in newly-designed fluidized bed combustor (FBC) and to provide the design guide lines and innovative concept for small-scale boiler and furnace. The major accomplishments are summarized.

NTIS

Combustion; Heat Transfer; Fluidized Bed Processors; Reaction Kinetics

20020002720 Texas Univ., Austin, TX USA

Catalytic Hydrocarbon Reactions over Supported Metal Oxides, August 1, 1995-July 31, 1999 ***Final Report, 1 Aug. 1995 - 31 Jul. 1999***

Ekerdt, J. G.; Jul. 31, 1999; 9p; In English

Report No.(s): DE2001-765710; No Copyright; Avail: Department of Energy Information Bridge, Microfiche

The research program focused on the catalysis of hydrodesulfurization (HDS) over molybdenum-based catalysts and how catalyst composition, redox ability, structure and neighboring sites control the catalytic properties of metal oxides. We sought to understand the catalytic features/sites that control hydrogenation, hydrogenolysis, and isomerization during HDS. Unprompted silica-supported molybdenum oxides and molybdenum sulfides were studied. Model catalyst systems were prepared from organometallic precursors or cluster compounds to generate supported structures that feature Mo(II) and Mo(IV) cations that are isolated or in ensembles and that have either Mo-O or Mo-S bonds. Conventional MoS2 catalysts, which contain both edge and rim sites, were be studied. Finally, single-layer MOSMoS2 structures were also prepared from 2H-MoS2 powder so that the model systems could be compared against a disulfide catalyst that only involves rim sites. Catalytic reactions for thiophene and tetrahydrothione were studied over the various catalysts. Oxidation states were determined using X-ray photoelectron spectroscopy. X-ray crystallography was used to characterize and follow changes in the MoS2 structures. The program on metal oxides prepared supported oxides that have a specific structure and oxidation state to serve as model templates for the more complex commercial catalysts and then employed these structures in reaction studies. This focus area examined the relationships between structure and cation redox characteristics in oxidation catalysis. Infrared and Raman spectroscopy were used to characterize the cations and reaction intermediates.

NTIS

Catalysis; Metal Oxides; Desulfurizing; Hydrogenation; Hydrogenolysis; Isomerization

20020002721 California State Univ., San Diego, CA USA

Fundamental Studies of Spray Combustion, March 15, 1987-July 14, 1999 ***Final Report, 15 Mar. 1987 - 14 Jul. 1999***

Li, S. C.; Libby, P.; Williams, F.; Jul. 14, 1999; 5p; In English

Report No.(s): DE2001-765704; No Copyright; Avail: Department of Energy Information Bridge, Microfiche

The authors research on spray combustion, involving both experimental and theoretical components, has addressed droplet and spray characteristics in laminar counterflowing streams, laminar counterflow spray diffusion flames, and impingement of sprays on hot surfaces, both with and without a flame present, and flame structure and flame chemistry.
NTIS
Sprayers; Combustion

20020002738 California Inst. of Tech., Pasadena, CA USA
Computational Study of Electron Tunneling in Proteins ***Final Report***
Regan, J. J.; Mar. 03, 1999; 3p; In English
Report No.(s): DE2001-761899; No Copyright; Avail: Department of Energy Information Bridge, Microfiche

Electron transfer (ET) processes in proteins are characterized by the motion of a single electron between centers of localization (such as the chlorophyll dimer in photosynthetic reaction centers). An electronic donor state D is created by the injection of an electron or by photo-excitation, after which the system makes a radiationless transition to an acceptor state A., resulting in the effective transfer of an electron over several angstroms. The experimental and theoretical understanding of the rate of this process has been the focus of much attention in physics, chemistry, and biology.
NTIS
Electron Tunneling; Proteins

20020002770 Argonne National Lab., IL USA
Higher order photon transitions in H-like and He-like ions
Berry, H. G.; Cheng, S.; Curtis, L. J.; Dunford, R. W.; Kanter, E. P.; Mar. 08, 1999; 16p; In English
Report No.(s): DE2001-12415; ANL/PHY/CP-98529; No Copyright; Avail: Department of Energy Information Bridge, Microfiche

Higher order photon transitions such as M1, M2 and two-photon decay are conveniently studied using highly-charged electron ions. Here we discuss two examples from recent experiments which were done using the ATLAS (Argonne Tandem Linac Accelerator System) facility at Argonne National Laboratory. The first is a test of Relativistic Quantum Mechanics involving a precision measurement of the spectral shape of the two-photon decay of the 1s2s(sup 1)S(sub 0) state in He-like nickel and the second is a test of the theory of damping in quantum mechanics involving observation of E1-M1 interference in the electric field quenching of metastable H-like ions.
NTIS
Photons; Quantum Mechanics; Linear Accelerators; Hydrogen Ions

20020002792 Argonne National Lab., IL USA
H + CH2 CO Yields CH3 + CO at High Temperature: A High Pressure Chemical Activation Reaction with Positive Barrier
Hranisavljevic, J.; Kumaran, S. S.; Michael, J. V.; Dec. 08, 1997; 22p; In English
Report No.(s): DE2001-8910; ANL/CHM/CP-95085; No Copyright; Avail: Department of Energy Information Bridge, Microfiche

The Laser Photolysis-Shock Tube (LP-ST) technique coupled with H-atom atomic resonance absorption spectrometry (ARAS) has been used to study the reaction H + CH2CO yields CH3 + CO over the temperature range of 863-1400 K. The results can be represented by the Arrhenius expression, k = (4.85 +/- 0.70) x 10(exp -11) exp(-2328 +/- 155 K/T) cc/molecule/s. The present data have been combined with the earlier low temperature flash photolysis-resonance fluorescence measurements to yield a joint three parameter expression, k = 5.44 x 10(exp -14) T(sup 0.8513) exp(-1429 K/T) cc/molecule/s. This is a chemical activation process that proceeds through vibrationally excited acetyl radicals. However, due to the presence of a low lying forward dissociation channel to CH3 + CO, the present results refer to the high pressure limiting rate constants. Hence, transition state theory with Eckart tunneling is used to explain the data.
NTIS
Chemical Reactions; Reaction Kinetics; Carbon Monoxide; Methyl Compounds

20020002806 Kansas City Plant, Kansas City, MO USA
Epoxidation of Plant Oils
Lula, J. W.; Jun. 13, 2000; 7p; In English
Report No.(s): DE2001-756510; KCP-613-6347; No Copyright; Avail: Department of Energy Information Bridge

This paper briefly describes the methods used to epoxy bond PZT ceramic to stators used in 8-mm piezoelectric motors. It also includes a discussion of the advantages of metallic bonds over epoxy, and beginning work with metallic bonds made by silver diffusion bonding and tin lead soldering.
NTIS
Epoxidation; Oils; Stators; Industrial Plants; Metal Bonding

20020002847 Northwestern Univ., Evanston, IL USA
Novel Approaches for the Preparation of Sulfur-Tolerant Three-Way Catalysts. Third Annual Report, August 15, 2000 - July 14, 2001
Kim, D. H.; Kozlov, A.; Kung, M. C.; Kung, H. H.; Andersen, P.; 2001; 32p; In English
Report No.(s): PB2002-100377; No Copyright; Avail: CASI; A03, Hardcopy; A01, Microfiche

The oxygen storage capacity of a three-way catalyst is strongly linked to its catalytic performance. The current generation of oxygen storage component is a mixed oxide of ceria and zirconia. A deeper understanding of how the oxygen storage capacity of a solid is related to its preparative procedure should lead to the development of more active catalysts. H2 temperature programmed reduction and CO pulse reactions were used to measure the redox properties of CeZrO2 supported on Al2O3. It was observed that the redox properties of these mixed oxides are a strong function of the preparation variables of the sample. In particular, preparation procedures that enhance intimate mixing of ceria and zirconia result in catalysts that have better reducibility at low temperatures. The redox properties of these samples could be modified by reduction-oxidation treatments. There exists an optimal temperature for the re-oxidation process. At low temperatures, not all CeO2 was re-oxidized and at high temperatures, sintering of the mixed oxides took place.
NTIS
Catalysts; Cerium Compounds; Aluminum Oxides; Oxidation-Reduction Reactions

20020003378 Federal Energy Technology Center, Morgantown, WV USA
Evaluation of Methods for Application of Epitaxial Buffer and Superconductor Layers
Mar. 30, 1999; 76p; In English
Report No.(s): DE2001-8942; DE-AC22-95PC95231-19; No Copyright; Avail: Department of Energy Information Bridge, Microfiche

The recent achievements of critical currents exceeding million amperes per square centimeter at 77K in YBCO deposited over suitably textured substrate have stimulated interest in the potential applications of coated conductors at high temperatures and in high magnetic fields. Currently, ion-beam assisted deposition (IBAD), and rolling assisted bi-axially textured substrate (RABiTS), represent two available options for obtaining textured substrates. For applying suitable coatings of buffer and high temperature superconductor (HTS) material over textured substrates, several options are available which include sputtering, electron-beam evaporation, laser ablation, electrophoresis, chemical vapor deposition (including metal organics chemical vapor deposition), sol-gel, metal organics decomposition, electrodeposition and aerosol/spray pyrolysis. A commercial continuous long-length wire/tape manufacturing scheme developed out of any suitable combination of the above techniques would consist of operations involving preparation of the substrate and application of buffer, HTS and passivation/insulation materials and special treatment steps such as post-annealing. These operations can be effected by various process parameters that can be classified into chemistry, materials, engineering, and environmental related parameters. Under the Department of Energy-sponsored program, to carry out an engineering evaluation, first, the process flow schemes were developed for various candidate options identifying the major operating steps, process conditions, and process streams. Next, to evaluate quantifiable parameters such as process severity (e.g., temperature and pressure), coating thickness and deposition rate for HTS material, achieved maximum J(sub c) value (for 1 micrometer thick) and cost of chemical and material utilization efficiency, the multi-attribute method was used to determine attributes/merits for various parameters and candidate options. to determine similar attribute values for the non-quantifiable parameters, a subjective evaluation was used. Results of the two evaluations were then combined to calculate the overall merit/utility of a given option using weighting factors. to evaluate the effect of arbitrarily determined weighting factors, a sensitivity analysis was carried out by using three different sets of weighting factors. In the end, the results of the overall utility/merit values calculated using different sets of weighting factors were utilized to determine the preliminary ranking among the candidate options. As a result of this study, MOD, Sol-Gel, MOCVD, Electron-Beam, and PLD options have been identified as the leading candidates for continuous, long-length processing of coated HTS conductors. However, there are several technical concerns related to each of these which need to be addressed first before a commercially viable option can be developed out of any one of them.
NTIS
Deposition; Epitaxy; Substrates; YBCO Superconductors

20020003414 Lawrence Livermore National Lab., Livermore, CA USA

Chemical Dynamics at the Advanced Light Source

Baer, T.; Berrah, N.; Fadley, C.; Moore, C. B.; Neumark, D. M.; Feb. 02, 1999; 24p; In English

Report No.(s): DE2001-6536; LBNL-42816; No Copyright; Avail: Department of Energy Information Bridge

A day-long retreat was held January 15, 1999 to chart the future directions for chemical dynamics studies at the Advanced Light Source. This represents an important period for the Chemical Dynamics Beamline, as the hardware is well-developed, most of the initial experimental objectives have been realized and the mission is now to identify the future scientific priorities for the beamline and attract users of the highest caliber. to this end, we have developed a detailed scientific program for the near term; identified and prioritized the long range scientific opportunities, identified essential new hardware, and outlined an aggressive outreach program to involve the chemical physics community.

NTIS

Light Sources; Reaction Kinetics; Chemical Reactions

20020003420 Los Alamos National Lab., NM USA

Actinide chemistry in the emic/a1c13 room temperature ionic liquid

Costa, D.; Smith, W.; Oct. 01, 1999; 36p; In English

Report No.(s): DE2001-768242; LA-UR-99-5521; No Copyright; Avail: Department of Energy Information Bridge, Microfiche

Room temperature ionic liquids (RTIL) area relatively new class of solvents whose unique set of chemical and physical properties hold the promise of making revolutionary changes in many traditional chemical processes. We have previously reported on the redox behavior of uranyl chloride in room temperature acidic 1- ethyl-3-methyl imidazolium chloride by electrochemical and spectroscopic techniques.The uranyl moiety is unstable to oxygen loss in this melt with the concomitant growth of a uranium (V) chloride species. We proposed that an equilibrium is established between the Lewis acidic A12C17and the uranium oxy-chloride species. Similar behavior may be expected for plutonium oxide species. We have demonstrated that a basic EMIC/AICl3 solution of PuC13displays one reversible oxidation and an irreversible reduction. The reversible wave has been confirmed to be associated with the Pu (111)/Pu(IV) redox couple by comparison with the CV of an authentic sample of Cs2PuCl6. The irreversible reduction wave is believed to come from the reduction of a plutonium oxide contaminant. In this talk we will focus on our work on the chemistry of plutonium complexes in room temperature ionic liquids (i.e. EMIC/AlC13and EMIBF4).

NTIS

Chemical Reactions; Oxidation-Reduction Reactions; Plutonium Oxides; Methyl Chloride

20020003567 Argonne National Lab., IL USA

Engineering the Use of Green Plants to Reduce Produced Water Disposal Volume

Hinchman, R.; Mollock, G. N.; Negri, M. C.; Settle, T.; Jan. 29, 1998; 9p; In English

Report No.(s): DE2001-8921; ANL/ES/CP-95137; No Copyright; Avail: Department of Energy Information Bridge, Microfiche

In 1990, the Laboratory began an investigation into biological approaches for the reduction of water produced from oil and gas wells. In the spring of 1995, the Company began an on-site experiment at an oil/gas lease in Oklahoma using one of these approaches. The process, known as phytoremediation, utilizes the ability of certain salt tolerant plants to draw the produced water through their roots, transpire the water from their leaves, and thereby reduce overall water disposal volumes and costs. At the Company experimental site, produced water flows through a trough where green plants (primarily cordgrass) have been planted in pea gravel. The produced water is drawn into the plant through its roots, evapotranspirates and deposits a salt residue on the plant leaves. The plant leaves are then harvested and used by a local rancher as cattle feed. The produced water is tested to assure it contains nothing harmful to cattle. In 1996, the Company set up another trough to compare evaporation rates using plants versus using an open container without plants. Data taken during all four seasons (water flow rate, temperature, pH, and conductivity) have shown that using plants to evapotranspirate produced water is safe, more cost effective than traditional methods and is environmentally sound.

NTIS

Residues; Water; Evaporation; Plants (Botany)

20020003808 Los Alamos National Lab., NM USA

Accurate quantification of dried residue thin films using x-ray fluorescence

Worley, C.; Havrilla, G.; Sep. 01, 2000; 9p; In English

Report No.(s): DE2001-768772; LA-UR-00-4155; No Copyright; Avail: Department of Energy Information Bridge, Microfiche

An XRF specimen preparation method was developed to quantify the concentration of gallium in plutonium metal while minimizing the risk of contaminating the instrument with radioactive material. to ensure that homogeneous specimens are

examined, plutonium is dissolved in dilute HCl and HNO(sub 3) prior to analysis. In the preliminary work here, non-radioactive aqueous gallium standards were prepared, and zinc was added as an internal standard to improve the accuracy and precision. Aliquots from these solutions were cast on Mylar XRF films and air dried prior to analysis. Two methods of casting the solutions were evaluated: (1) casting as a thin layer using a surfactant to wet the support film and (2) casting multiple small spots on the support film. Aqueous gallium standards were prepared and cast as dried residue specimens using each method. These specimens were then analyzed, and calibration curves were prepared. Highly linear calibrations were obtained for each preparation method when zinc was used as the internal standard (RMS values (le)1% of the standards concentration range in both cases). Based on this preliminary work, this dried residue process appears very promising for the accurate quantification of gallium in plutonium.
NTIS
Fluorescence; Radioactive Materials; Mylar (Trademark); Calibrating; Mean Square Values

20020003814 Los Alamos National Lab., NM USA
Catalysis science and technology
Abrams, M.; Baker, R.; Aug. 01, 2000; 10p; In English
Report No.(s): DE2001-768735; LA-UR-00-3984; No Copyright; Avail: Department of Energy Information Bridge, Microfiche

This is the final report of a three-year, Laboratory-Directed Research and Development (LDRD) project at the Los Alamos National Laboratory (LANL). Our objectives were to develop a multidisciplinary team and capabilities to develop a fundamental understanding of homogeneous, heterogeneous, and heterogenized catalysts. With the aid of theoretical chemistry approaches we explored and characterized the chemical reactivity and physical properties of a large number of catalytic systems.
NTIS
Chemical Reactions; Heterogeneity; Catalysts

20020004356 NASA Ames Research Center, Moffett Field, CA USA
General Model for Multicomponent Ablation Thermochemistry
Milos, Frank S., NASA Ames Research Center, USA; Marschall, Jochen, National Academy of Sciences - National Research Council, USA; [1994]; 1p; In English; AIAA 29th Thermophysics Conference, 19-22 Jun. 1995, San Diego, CA, USA; Sponsored by American Inst. of Aeronautics and Astronautics, USA
Contract(s)/Grant(s): RTOP 232-01-04; No Copyright; Avail: Issuing Activity; Abstract Only

A previous paper (AIAA 94-2042) presented equations and numerical procedures for modeling the thermochemical ablation and pyrolysis of thermal protection materials which contain multiple surface species. This work describes modifications and enhancements to the Multicomponent Ablation Thermochemistry (MAT) theory and code for application to the general case which includes surface area constraints, rate limited surface reactions, and non-thermochemical mass loss (failure). Detailed results and comparisons with data are presented for the Shuttle Orbiter reinforced carbon-carbon oxidation protection system which contains a mixture of sodium silicate (Na2SiO3), silica (SiO2), silicon carbide (SiC), and carbon (C).
Author
Ablation; Mathematical Models; Thermochemistry; Carbon-Carbon Composites

20020004916 Federal Energy Technology Center, Morgantown, WV USA
Engineering development of coal-fired high performance power systems
Oct. 01, 1998; 25p; In English
Report No.(s): DE2001-7741; DE-AC22-95PC95143-10; No Copyright; Avail: Department of Energy Information Bridge, Microfiche

A High Performance Power System (HIPPS) is being developed. This system is a coal-fired, combined cycle plant with indirect heating of gas turbine air. Foster Wheeler Development Corporation and a team consisting of Foster Wheeler Energy Corporation, Bechtel Corporation, University of Tennessee Space Institute and Westinghouse Electric Corporation are developing this system. In Phase 1 of the project, a conceptual design of a commercial plant was developed. Technical and economic analyses indicated that the plant would meet the goals of the project which include a 47 percent efficiency (HHV) and a 10 percent lower cost of electricity than an equivalent size PC plant. The concept uses a pyrolyzation process to convert coal into fuel gas and char. The char is fired in a High Temperature Advanced Furnace (HITAF). The HITAF is a pulverized fuel-fired boiler/air heater where steam is generated and gas turbine air is indirectly heated. The fuel gas generated in the pyrolyzer is then used to heat the gas turbine air further before it enters the gas turbine. The project is currently in Phase 2 which includes engineering analysis, laboratory testing and pilot plant testing. Research and development is being done on the HIPPS systems that are not commercial or being developed on other projects. Pilot plant testing of the pyrolyzer subsystem and the char combustion subsystem are being done separately, and after each experimental program has been completed, a larger scale pyrolyzer will be tested at the Power Systems

Development Facility (PSDF) in Wilsonville, Al. The facility is equipped with a gas turbine and a topping combustor, and as such, will provide an opportunity to evaluate integrated pyrolyzer and turbine operation. This report addresses the areas of technical progress for this quarter. Preliminary process design was started with respect to the integrated test program at the PSDF. All of the construction tasks at Foster Wheeler's Combustion and Environmental Test Facility (CETF) have been completed in preparation for the char combustion test program, this includes installation of the char burner, and the on-line mass spectrometer. A test matrix has been defined, utilizing a statistical design of experiment (SDOE) methodology, for the char combustion program. The first phase of the CETF shakedown has been completed, and all analog devices (thermocouples, transmitters, etc.) have been calibrated.
NTIS
Coal; Gas Heating; Gas Turbines; Pilot Plants

20020005070 Federal Energy Technology Center, Morgantown, WV USA
Mossbauer spectroscopy studies of iron catalysts used in slurry phase fischer-tropsch synthesis
Huffman, G. P.; Rao, K. R. P. M.; Huggins, F. E.; Feb. 01, 1998; 14p; In English
Report No.(s): DE2001-769337; DE-AC22-94PC93066-01; No Copyright; Avail: Department of Energy Information Bridge, Microfiche

Iron and cobalt are the two principal choices as catalysts for Fischer-Tropsch (F-T) synthesis. As discussed in a recent review by Wender each metal has certain advantages and disadvantages. Davis and co-workers have recently discussed the advantages of iron-based F-T catalysts in some detail. In order to understand the catalytic reaction mechanisms of iron during F-T synthesis, it is critical to identify the active catalytic phases. Moreover, from a practical point of view, it is equally important to identify the reactions and transformations that deactivate the catalysts. (sup 57)Fe Moessbauer spectroscopy is perhaps the best technique available for quantitative characterization of the iron phases in complex samples. For the past several years, our group has been using Moessbauer spectroscopy to characterize the iron-based catalysts prepared and tested for F-T synthesis in a number of DOE-sponsored programs. The results of this investigation have been summarized in detail in DOE reports and in a number of publications released over the past few years. A list of the principal publications resulting from this work is given. A brief summary of the highlights of the results presented in these papers is presented in the current report.
NTIS
Catalysts; Fischer-Tropsch Process; Iron

20020005071 Federal Energy Technology Center, Morgantown, WV USA
Technology development for iron fischer-tropsch catalysis
Davis, B. H.; Apr. 01, 1998; 18p; In English
Report No.(s): DE2001-769339; DE-AC22-94PC94055-15; No Copyright; Avail: Department of Energy Information Bridge, Microfiche

The goal of the proposed work is the development of iron-based Fischer-Tropsch catalysts that combined high activity, selectivity and life with physical robustness for slurry phase reactors that will produce either low-alpha or high-alpha products. The catalyst that is developed will be suitable for testing at the Advanced Fuels Development Facility at LaPorte, Texas or similar sized plant. Previous work by the offerer has produced a catalyst formulation that is 1.5 times as active as the 'standard-catalyst' developed by German workers for slurry phase synthesis. The proposed work will optimize the catalyst composition and pretreatment operation for this low-alpha catalyst. In parallel, work will be conducted to design a high-alpha iron catalyst that is suitable for slurry phase synthesis. Studies will be conducted to define the chemical phases present at various stages of the pretreatment and synthesis stages and to define the course of these changes. The oxidation/reduction cycles that are anticipated to occur in large, commercial reactors will be studied at the laboratory scale. Catalyst performance will be determined for catalysts synthesized in this program for activity, selectivity and aging characteristics.
NTIS
Fischer-Tropsch Process; Catalysts; Iron

20020005083 Argonne National Lab., IL USA
Modeling corrosion and constituent release from a metal waste form
Bauer, T. H.; Fink, J. K.; Abraham, D. P.; Johnson, I.; Johnson, S. G.; Dec. 04, 2000; 12p; In English
Report No.(s): DE2001-772117; ANL/RAE/CP-103572; No Copyright; Avail: Department of Energy Information Bridge, Microfiche

Several ANL ongoing experimental programs have measured metal waste form (MWF) corrosion and constituent release. Analysis of this data has initiated development of a consistent and quantitative phenomenology of uniform aqueous MWF

corrosion. The effort so far has produced a preliminary fission product and actinide release model based on measured corrosion rates and calibrated by immersion test data for a 90 C J-13 and concentrated J-13 solution environment over 1-2 year exposure times. Ongoing immersion tests of irradiated and unirradiated MWF samples using more aggressive test conditions and improved tracking of actinides will serve to further validate, modify, and expand the application base of the preliminary model-including effects of other corrosion mechanisms. Sample examination using both mechanical and spectrographic techniques will better define both the nature and durability of the protective barrier layer. It is particularly important to assess whether the observations made with J-13 solution at 900 C persist under more aggressive conditions. For example, all the multiplicative factors in Table 1 implicitly assume the presence of protective barriers. Under sufficiently aggressive test conditions, such protective barriers may very well be altered or even eliminated.
NTIS
Corrosion; Calibrating; Fission Products

20020005106 Department of Energy, Aiken, SC USA
Radiolytic Reduction of Uranyl Ion
Hyder, M. L.; Aug. 29, 2001; 15p; In English
Report No.(s): DE2001-786068; DP-MS-68-62; No Copyright; Avail: Department of Energy Information Bridge, Microfiche
Uranyl ion was reduced by ionizing radiation in deoxygenated solutions containing organic solutes. This reduction is effected by free radical species formed from the organics and perhaps in part by H atoms from water decomposition. This reports details results of that study.
NTIS
Ionizing Radiation; Free Radicals

20020005164 Federal Energy Technology Center, Morgantown, WV USA
Low Temperature VOC Combustion Over Manganese, Cobalt and Zinc AlPO4 Molecular Sieves
Szostak, R.; Mar. 31, 1997; 12p; In English
Report No.(s): DE2001-3828; DE-FG22-95PC95218-03; No Copyright; Avail: Department of Energy Information Bridge, Microfiche
The objective of this project is to prepare manganese, cobalt and zinc containing AlPO4 molecular sieves and evaluate their catalytic activities for the removal of low levels of volatile organic compounds (VOCs) from gas streams. This report highlights our research activities for period October 1,1996 to March 31, 1997.
NTIS
Low Temperature; Manganese; Volatile Organic Compounds; Absorbents; Zinc; Cobalt; Phosphorus Compounds; Aluminum

20020005165 Federal Energy Technology Center, Morgantown, WV USA
EM 14: Bubbleless Gas Transfer Technology for the In Situ Remediation of Chlorinated Hydrocarbons
Gallaher, J. R.; Kurz, M. D.; Nov. 01, 1998; 12p; In English
Report No.(s): DE2001-3837; DE-FC21-94MC31388-21; No Copyright; Avail: Department of Energy Information Bridge, Microfiche
The primary objective of this project is to demonstrate the ability of hydrogen to supply reducing equivalents for the reductive dehalogenation of PCE. This objective will be accomplished by two types of activities. First, laboratory experiments will compare the kinetics of hydrogen-mediated dehalogenation with natural routes of loss (hydrolysis and natural attenuation). Secondly, bench-scale column experiments will be performed to demonstrate hydrogen-mediated reductive dehalogenation in aquifer sediments.
NTIS
Halogenation; Hydrogen; Carbon Tetrachloride; Aquifers; Chlorocarbons

20020005394 Federal Energy Technology Center, Morgantown, WV USA
Temperature, velocity and species profile measurements for reburning in a pulverized, entrained flow, coal combustor
Tree, D. R.; Mar. 01, 1999; 77p; In English
Report No.(s): DE2001-775039; DE-FG22-95PC95223-07; No Copyright; Avail: Department of Energy Information Bridge, Microfiche
Nitrogen oxide emissions from pulverized coal combustion have been and will continue to be a regulated pollutant for electric utility boilers burning pulverized coal. Full scale combustion models can help in the design of new boilers and boiler retrofits which meet emissions standards, but these models require validation before they can be used with confidence. The objective of

this work was to obtain detailed combustion measurements of pulverized coal flames which implement two NO reduction strategies, namely reburning and advanced reburning, to provide data for model validation. The data were also compared to an existing comprehensive pulverized coal combustion model with a reduced mechanism for NO reduction under reburning and advanced reburning conditions. The data were obtained in a 0.2 MW, cylindrical, down-fired, variable swirl, pulverized coal reactor. The reactor had a diameter of 0.76 m and a length of 2.4 m with access ports along the axial length. A Wyodak, sub-bituminous coal was used in all of the measurements. The burner had a centrally located primary fuel and air tube surrounded by heated and variably swirled secondary air. Species of NO, NO(sub x), CO, CO(sub 2) and O(sub 2) were measured continuously. Aqueous sampling was used to measure HCN and NH(sub 3) at specific reactor locations. Samples were drawn from the reactor using water quenched suction probes. Velocity measurements were obtained using two component laser doppler anemometry in back-scatter mode. Temperature measurements were obtained using a shielded suction pyrometer. A series of six or more radial measurements at six or more axial locations within the reactor provided a map of species, temperature, and velocity measurements. In total, seven reactor maps were obtained. Three maps were obtained at baseline conditions of 0, 0.5 and 1.5 swirl and 10% excess air. Two maps were obtained under reburning conditions of 0.78 stoichiometric ratio and 1.5 swirl and 0.9 stoichiometric ratio and 0.5 swirl. and finally, two maps were obtained under advanced reburning conditions both at the same operating condition of 1.05 stoichiometric ratio in the reburning zone followed by ammonia injection. Numerous effluent measurements were obtained to study the affect of natural gas injection location, stoichiometric ratio, and injection velocity on effluent NO. For advanced reburning, effluent measurements were obtained for a similar matrix of operating conditions with the additional variable of ammonia nitrogen to nitrogen in NO or nitrogen stoichiometric ratio (NSR).
NTIS
Coal; Combustion Chambers; Air Pollution; Pollution Control; Nitrogen Oxides; Mathematical Models

20020005416 NASA Ames Research Center, Moffett Field, CA USA
A Coupled-Cluster Study of the Molecular Structure, Vibrational Spectrum, and Relative Energies of the XCN and XNC (X=F, Cl) Isomers
Lee, Timothy J., NASA Ames Research Center, USA; Racine, Stephen C., NASA Ames Research Center, USA; [1994]; 1p; In English
Contract(s)/Grant(s): RTOP 537-02-20; No Copyright; Avail: Issuing Activity; Abstract Only

The XCN and XNC (X=F, Cl) isomers have been investigated using the CCSD and CCSD(T) methods in conjunction with a TZ2P basis set. Equilibrium geometries, dipole moments, harmonic frequencies, IR intensities and relative energies have been evaluated. The CCSD(T) geometries and vibrational frequencies for the XCN isomers are in good agreement with the available experimental data. The CCSD(T) results for FCN and FNC are in good agreement with the CEPA calculations of Botshwina et al., with the exception of the energy difference, which the CEPA method underestimates by about 1.2 kcal/mol. FCN and CICN are shown to be lower in energy than the FNC and ClNC isomers by 69.511.0 and 42.711.0 kcal/mol (0 K), respectively.
Author
Isomers; Vibrational Spectra; Molecular Structure

20020005829 Federal Energy Technology Center, Morgantown, WV USA
Technology development for iron and cobalt Fischer-Tropsch catalysts= *Quarterly Report, 1 Jul. - 30 Sep. 1999*
Davis, B. H.; Nov. 01, 1999; 83p; In English
Report No.(s): DE2001-775014; DE-FC26-98FT40308-04; No Copyright; Avail: Department of Energy Information Bridge, Microfiche

The impact of deuterium on the Fischer-Tropsch (FT) synthesis was studied with a precipitated iron catalyst in the slurry phase. Deuterium has been used by several research groups to better understand the mechanism of CO hydrogenation. Inverse (k(sub H)/k(sub D) 1), normal (k(sub H)/k(sub D) 1) and no isotope effect (k(sub H)/k(sub D) = 1) have been reported. The conflicting results are thought to arise because rate of reaction is a combination of kinetic and equilibrium factors. In summary, the presence of boron produced only minor changes on the properties of the cobalt catalyst. In earlier studies, it was shown that the presence of boron made the catalyst less susceptible to poisoning by sulfur. Steady-state supercritical Fischer-Tropsch synthesis was studied in the work using a fixed-bed reactor and an unpromoted Co/SiO(sub 2) catalyst. This serves as the baseline for promoted catalyst studies. A pentane-hexane mixture was used as the supercritical solvent. Overall reactor pressure, syngas partial pressure and contact time were kept constant to obtain a valid comparison of the impact of solvent density in the catalytic activity and selectivity. Three different partial pressures of the mixture were chosen based on the density-pressure curve in order to investigate the pressure tuning effect to Fischer-Tropsch synthesis near critical region.
NTIS
Catalysts; Cobalt; Iron; Fischer-Tropsch Process

20020005831 Federal Energy Technology Center, Morgantown, WV USA

Reduction of inherent mercury emissions in pc combustion ***Semiannual Report, 1 Jul. - 31 Dec. 1997***

Kramlich, J. C.; Sliger, R. N.; Going, D. J.; Aug. 19, 1998; 7p; In English

Report No.(s): DE2001-775017; DE-FG22-95PC95216-05; No Copyright; Avail: Department of Energy Information Bridge, Microfiche

Mercury emission compliance is one of the major potential challenges raised by the 1990 Clean Air Act Amendments. Simple ways of controlling emissions have not been identified. The variability in the field data suggests that inherent mercury emissions may be reduced if the source of this inherent capture can be identified and controlled. The key mechanisms appear to involve the oxidation of the mercury to Hg(sup 2), generally producing the more reactive HgCl(sub 2), followed by its capture by certain components of the fly ash or char. This research focuses on identifying the rate-limiting steps associated with the oxidation step. Work in this reporting period focused on the development of oxidation data as a function of temperature and HCl concentration. The temperature range was 800-1200 C. The results show a lower level of oxidation than indicated by the earlier data of Hall et al. One possible reason for this discrepancy was the preheating of the HCl stream in the Hall experiment, leading to the partial decomposition of the HCl into reactive species. In the present experiments, the HCl was injected as a cold stream. The measured oxidation at these conditions was substantially above that predicted by equilibrium, indicating the dominance of finite rate chemistry. This is to be explored in subsequent work.

NTIS

Combustion; Exhaust Emission; Mercury (Metal); Air Pollution

20020005853 Oak Ridge National Lab., TN USA

Dynamic Particle Growth Testing: Phase I Studies

Hu, M. Z. C.; May 17, 2001; 106p; In English

Report No.(s): DE2001-786478; ORNL/TM-2001/100; No Copyright; Avail: Department of Energy Information Bridge, Microfiche

In this study, we investigated the formation of aluminosilicate solids/particles from caustic (4-6 M NaOH) solutions that contained dissolved silicon and aluminum (typically 0.004-0.3 M) at elevated temperatures (40-110degC). Solid formation was found to occur both in bulk solutions and on submerged substrate surfaces. The solids underwent a complicated crystalline phase transformation and solid/particle morphology evolution with time. X-ray diffraction (XRD) analyses showed that at equilibrium the aluminosilicate solids were predominantly sodalite with a formula of Na8(A1SiO4)6(NO3)2.4H2O, whose stoichiometric reactive formation seems to be relatively unaffected by the concentration or the (Si)/(A1) ratio in solution. The bulk solids or scales microscopically resembled aggregrated, connected, or fused microspheres within which there were finer, primary crystalline particles. A real-time DLS technique was employed to monitor the particle-growth dynamics (i.e., determination of induction period for solid-phase formation) in quiescent solutions, while SEM was used to examine heterogeneous surface growth of particles and formation of surface solids (i.e., scales) on stainless steel surfaces.

NTIS

Solutions; X Ray Diffraction; Phase Transformations; Stainless Steels

20020005855 Oak Ridge National Lab., TN USA

Hiroshima Air-Over-Ground Analysis: Comparison of DORT and MCNP Calculations

Santoro, R. T.; Sep. 04, 2001; 28p; In English

Report No.(s): DE2001-786481; ORNL/TM-2001/160; No Copyright; Avail: Department of Energy Information Bridge, Microfiche

Monte Carlo (MCNP4B) and Discrete Ordinates (DORT) calculations were carried out to estimate 60Co and 152Eu activation as a function of ground range due to neutrons emitted from the Hiroshima A-bomb. Results or ORNL DORT and MCNP calculations using RZ cylindrical air-over-ground models are compared with LANL MCNP results obtained with an XYZ air-over-ground model. All of the calculations were carried out using ENDF/B-VI cross-section data and detailed angle and energy resolved neutron emission spectra from the weapon. Favorable agreement was achieved for the 60Co and 152Eu activation for ground ranges out to 1000m from the three calculations.

NTIS

Gamma Rays; Neutrons; Cylindrical Bodies; Neutron Emission; Energy Spectra

20020005879 Queens Coll., Flushing, NY USA
Film Synthesized Rare Earth Transition Metal Permanent Magnet Systems ***Final Report, 1 Apr. 1998-30 Jun. 2001***
Cadieu, Fred J.; Sep. 18, 2001; 38p; In English
Contract(s)/Grant(s): DAAG55-98-1-0172
Report No.(s): AD-A395355; ARO-37186.7-MS; No Copyright; Avail: CASI; A03, Hardcopy; A01, Microfiche

Specific results of this research include five unique results. (1) The elucidation of the concept of a growth coherence region as being pivotal for the growth of textured polycrystalline films. This concept allows the prediction of what texture modes would be possible for any new system that may be discovered. (2) For the very first time it was demonstrated that pulsed laser deposition can be used to grow highly textured high coercivity rare earth transition metal films with magnetic properties comparable to the best sputtered films. (3) It was shown that the simultaneous use of sputtering and pulsed laser deposition methods can be used to grow nanophase dispersed films with special magnetic and other properties. (4) A new type of magnetoresistive magnetic memory element operable at room temperature was demonstrated for specially deposited La-manganite films when used in conjunction with another magnetic film element. (5) A method was invented whereby particulate free films of a great many substances can be deposited by pulsed laser deposition.

DTIC
Magnetic Films; Permanent Magnets; Synthesis (Chemistry); Coercivity; Transition Metals; Rare Earth Elements

26
METALS AND METALLIC MATERIALS

Includes physical, chemical, and mechanical properties of metals and metallic materials; and metallurgy.

20020000741 Los Alamos National Lab., NM USA
Effects of Joints in Two Beryllium Hemispheres Used to Form an Ignition Capsule for the National Ignition Facility
Bel'kov, S. A.; Bondarenko, S. V.; Ilkaeva, L. A.; Kochemasov, G. G.; Mkhitarian, L. S.; Feb. 02, 1998; 18p; In English
Report No.(s): DE2001-763048; LA-SUB-99-44; B70040006-35-TASK-19; No Copyright; Avail: Department of Energy Information Bridge, Microfiche

2-D numerical results under the program 'MTMOZA' were presented in the report for the first stage. These results were obtained from solution of the problems of the shock ware passage through a joint between two flat beryllium plates which is filled with Al. Two problems have been considered with varying joint (gap) width. It was demonstrated, that the intrinsic oscillations, arising in a narrow gap have an amplitude comparable with the gap width, therefore they must have essentially nonlinear character, resulting in fast mixing with the surrounding matter.

NTIS
Beryllium; Ignition; Two Dimensional Models; Numerical Analysis

20020000760 Oak Ridge Y-12 Plant, TN USA
Hydroforming Applications at Oak Ridge
Bird, E. L.; Ludtka, G. M.; Mar. 10, 1999; 14p; In English
Report No.(s): DE2001-3743; Y/DV-1606; No Copyright; Avail: Department of Energy Information Bridge

Hydroforming technology is a robust forming process that produces components with high precision and complexity. The goal of this paper is to present a brief description of the sheet hydroforming process with respect to the authors' experience and capabilities. Following the authors' discussion of the sheet-metal forming application, the tubular hydroforming process is described in the context of one of our technology development programs with an automotive industrial partner. After that is a summary of the tubular hydroforming advisor (expert system) development activity, which was a significant part of this overall program based on previous experience in developing a design and manufacturing support hydroforming advisor for the Oak Ridge Y-12 Plant's weapons-component manufacturing needs. Therefore, this paper is divided into three sections: (1) Hydroforming of Stainless Steel Parts, (2) Tubular Hydroforming, and (3) Components of a Tubular Hydroforming Advisor.

NTIS
Stainless Steels; Hydroforming

20020000888 Argonne National Lab., IL USA
Rolling-contact fatigue resistance of hard coatings on bearing steels
Erdemir, A.; Aug. 18, 1999; 24p; In English
Report No.(s): DE2001-11942; ANL/ET/CP-99845; No Copyright; Avail: Department of Energy Information Bridge, Microfiche

Ball- and roller-bearings of the 21st Century are expected to perform better and last longer while operating under more stringent conditions than before. to meet these great expectations, researchers have been constantly exploring new bearing designs or refining existing ones, optimizing microstructure and chemistry of bearing materials, and alternatively, they have been considering the use of thin hard coatings for improved bearing performance and durability. Already, some laboratory tests have demonstrated that hard nitride, carbide (such as TiN, TiC, etc.) and diamondlike carbon (DLC) coatings can be very effective in prolonging the fatigue lives of bearing steels. This paper provides an overview of the recent developments in hard coatings for bearing applications. Previous studies have demonstrated that thin, hard coatings can effectively prolong the fatigue lives of bearing steel substrates. In particular, thinner hard coatings (i.e., 0.2 - 1 (micro)m thick) provide exceptional improvements in the fatigue lives of bearing steel substrates. In contrast, thicker hard coatings suffer micro fracture and delamination when tested under high contact stresses, hence are ineffective and may even have a negative effect on bearing life. Overall, it was concluded that thin hard coatings may offer new possibilities for bearing industry in meeting the performance and durability needs of the 21st Century.
NTIS
Coatings; Steels; Stresses; Fatigue (Materials); Contact Resistance; Roller Bearings

20020000936 Atomic Energy Commission, Idaho Operations Office, Idaho Falls, ID USA
Ferrite Measurement in Austenitic and Duplex Stainless Steel Castings. Literature Review
Lundin, C. D.; Zhou, G.; Ruprecht, W.; Aug. 01, 1999; 87p; In English
Report No.(s): DE2001-14580; DOE/ID/13734-2; No Copyright; Avail: Department of Energy Information Bridge, Microfiche
The ability to determine ferrite rapidly, accurately and directly on a finished casting, in the solution annealed condition, can enhance the acceptance, save on manufacturing costs and ultimately improve service performance of duplex stainless steel cast products. If the suitability of a non-destructive ferrite determination methodology can be demonstrated for standard industrial measurement instruments, the production of cast secondary standards for calibration of these instruments is a necessity. With these concepts in mind, a series of experiments were carried out to demonstrate, in a non-destructive manner, the proper methodology for determining ferrite content. The literature was reviewed, with regard to measurement techniques and vagaries, an industrial ferrite measurement round-robin was conducted, the effects of casting surface finish, preparation of the casting surface for accurate measurement and the evaluation of suitable means for the production of cast secondary standards for calibration were systematically investigated. The data obtained from this research program provides recommendations to ensure accurate, repeatable and reproducible ferrite measurement and qualifies the Feritscope for field use on production castings.
NTIS
Castings; Austenitic Stainless Steels; Ferrites; Nondestructive Tests; Measuring Instruments

20020000937 Atomic Energy Commission, Idaho Operations Office, Idaho Falls, ID USA
Ferrite Measurement in Austenitic and Duplex Stainless Steel Castings *Final Report*
Lundin, C. D.; Zhou, G.; Ruprecht, W.; Aug. 01, 1999; 140p; In English
Report No.(s): DE2001-14577; DOE/ID/13734-1; No Copyright; Avail: Department of Energy Information Bridge, Microfiche
The ability to determine ferrite rapidly, accurately and directly on a finished casting, in the solution annealed condition, can enhance the acceptance, save on manufacturing costs and ultimately improve service performance of duplex stainless steel cast products. If the suitability of a non-destructive ferrite determination methodology can be demonstrated for standard industrial measurement instruments, the production of cast secondary standards for calibration of these instruments is a necessity. With these concepts in mind, a series of experiments were carried out to demonstrate, in a non-destructive manner, the proper methodology for determining ferrite content. The literature was reviewed, with regard to measurement techniques and vagaries, an industrial ferrite measurement round-robin was conducted, the effects of casting surface finish, preparation of the casting surface for accurate measurement and the evaluation of suitable means for the production of cast secondary standards for calibration were systematically investigated. The data obtained from this research program provide recommendations to ensure accurate, repeatable, and reproducible ferrite measurement and qualifies the Feritscope for field use on production castings.
NTIS
Ferrites; Castings; Measuring Instruments; Austenitic Stainless Steels; Nondestructive Tests

20020000938 Atomic Energy Commission, Idaho Operations Office, Idaho Falls, ID USA
Development of Lead-Free Copper Alloy-Graphite Castings
Oct. 01, 1999; 72p; In English
Report No.(s): DE2001-14366; DOE/ID/13236-4; No Copyright; Avail: Department of Energy Information Bridge, Microfiche

In this project, graphite is used as a substitute for lead in order to maintain the machinability of plumbing components at the level of leaded brass. Graphite dispersed in Cu alloy was observed to impart good machinability and reduce the sizes of chips during machining of plumbing components in a manner similar to lead. Copper alloys containing dispersed graphite particles could be successfully cast in several plumbing fixtures which exhibited acceptable corrosion rate, solderability, platability, and pressure tightness. The power consumption for machining of composites was also lower than that of the matrix alloy. In addition, centrifugally cast copper alloy cylinders containing graphite particles were successfully made. These cylinders can therefore be used for bearing applications, as substitutes for lead-containing copper alloys. The results indicate that copper graphite alloys developed under this DOE (Department of Energy) project have a great potential to substitute for lead copper alloys in both plumbing and bearing applications.
NTIS
Cast Alloys; Castings; Copper Alloys; Graphite; Mechanical Properties

20020000944 Argonne National Lab., IL USA
Effects of neutron irradiation on fracture toughness of austenitic stainless steels
Chopra, O. K.; Gruber, E. E.; Shack, W. J.; May 21, 1999; 16p; In English
Report No.(s): DE2001-11822; ANL/ET/CP-99074; No Copyright; Avail: Department of Energy Information Bridge, Microfiche
Austenitic stainless steels are used extensively as structural alloys in reactor pressure vessel internal components because of their superior fracture toughness properties. However, exposure to high levels of neutron irradiation for extended periods leads to significant reduction in the fracture resistance of these steels. This paper presents results of fracture toughness J-R curve tests on four heats of Type 304 stainless steel that were irradiated to fluence levels of (approx)0.3 and 0.9 x 10(sup 21) n cm(sup (minus)2) (E is greater than 1 MeV) at (approx)288 C in a helium environment in the Halden heavy water boiling reactor. The tests were performed on 1/4-T compact tension specimens in air at 288 C; crack extensions were determined by both DC potential and elastic unloading compliance techniques.
NTIS
Neutron Irradiation; Austenitic Stainless Steels; Fracture Strength

20020000949 Oak Ridge National Lab., TN USA
Proceedings of the IEA Workshop/Working Group Meeting on Ferritic/Martensitic Steels
Klueh, R. L.; Oct. 01, 1998; 393p; In English
Report No.(s): DE2001-2699; ORNL/M-6627; No Copyright; Avail: Department of Energy Information Bridge, Microfiche
The International Energy Agency(IEA) Working Group on Ferritic/Martensitic Steels for Fusion held a workshop at ECN Nuclear Research Petten, The Netherlands, 1-2 October 1998. The Working Group, consisting of researchers from Japan, the European Union, the USA, and Switzerland met to review research that has been completed since the previous meeting and to continue planning and coordinating an international collaborative test program on reduced-activation ferritic/martensitic steels for fusion applications. At the workshop, data were presented from the continuing research on the IEA heats of steel that are being studied in the collaboration. Data on these and other reduced-activation steels in the irradiated and unirradiated condition were presented. Other subjects that were discussed included effects of a ferromagnetic steel in a fusion machine, the effect of helium on properties, and the development and application of oxide dispersion-strengthened steels for fusion. A Working Group status-review meeting is planned in conjunction with the International Conference on Fusion Reactor Materials (ICFRM-9) in Colorado Springs, Colorado, USA 10-15 October 1999, at which time plans for a workshop to be held 2000 will be finalized.
NTIS
Conferences; Ferromagnetic Materials; Nuclear Research; Martensitic Stainless Steels

20020001040 Lawrence Livermore National Lab., Livermore, CA USA
Galvanic corrosion-effect of environmental and experimental variables
Fleming, D. L.; Lum, B. Y.; Roy, A. K.; Nov. 01, 1998; 10p; In English
Report No.(s): DE2001-8518; UCRL-JC-132374; No Copyright; Avail: Department of Energy Information Bridge, Microfiche
Galvanic corrosion behavior of A 516 steel coupled to alloy C-22 and Ti Gr-12, respectively was evaluated in an acidic brine (pH approximately 2.75) at 30 C, 60 C and 80 C using zero resistance ammeter method. A limited number of experiments were also performed in a neutral brine involving A 516 steel/alloy C-22 couple. The steady-state galvanic current and galvanic potential were measured as functions of anode-to-cathode (A/C) area ratio and electrode distance. Results indicate that the galvanic current was gradually reduced as the A/C area ratio was increased. No systematic trend on the effect of A/C area ratio on the galvanic potential was observed. Also, no significant effect of electrode distance on the galvanic current and galvanic potential was evident. In general, increased galvanic current was noticed with increasing temperature. The limited data obtained in the neutral brine

indicate that the galvanic current was reduced in this environment, compared to that in the acidic brine. Optical microscopic examination was performed on all tested specimens to evaluate the extent of surface damage resulting from galvanic interaction. A 516 steel suffered from general corrosion and crevice corrosion in all environments tested. Very light crevice corrosion mark was observed with alloy C-22 and Ti Gr-12 in the acidic brine at 60 C and 80 C. However, this mark appears to be a surface discoloration and no actual crevice was detected.
NTIS
Steels; Electrochemical Corrosion

20020001057 Argonne National Lab., IL USA
In-situ observations of adsorption and film formation on metal electrodes by synchrotron far infrared reflectance spectroscopy
Bowmaker, G. A.; Hahn, F.; Leger, J. M.; Melendres, C. A.; May 17, 1999; 9p; In English
Report No.(s): DE2001-11817; ANL/CMT/CP-99057; No Copyright; Avail: Department of Energy Information Bridge, Microfiche

Adsorption and film formation are key processes associated with the passivation and inhibition of metallic corrosion. New experimental approaches are needed to advance our knowledge in these areas. We have developed the technique of Synchrotron Far Infrared Reflectance Spectroscopy (SFIRS) for in situ investigations of the structure and composition of surface films and adsorbed layers on metals. We demonstrate its application to the determination of the nature of surface films on copper in aqueous solutions and the adsorption of anions on gold. The anodic corrosion films on copper in alkaline solution were found to consist of Cu(sub 2)O in the passive region at about (minus)0.05 V vs SCE and CUO, together with CU(OH)(sub 2), at 0.30 V. We have also observed for the first time the adsorption of anions at monolayer coverage on the surface of a gold electrode in perchloric acid solution. Halides (CL-, Br-), nitrate, sulfate, and phosphate have been studied. When two different anions are present in solution, the more strongly adsorbed species determines the corrosion behavior of the metal. This is illustrated in the competitive adsorption of bromide and phosphate on gold.
NTIS
Metals; Adsorption; Electrodes; Synchrotrons; Infrared Spectroscopy

20020001165 Lawrence Livermore National Lab., Livermore, CA USA
Tailoring Material Properties of Sputtered Beryllium
McEachern, R. M.; Mar. 01, 1999; 6p; In English
Report No.(s): DE2001-8700; UCRL-ID-133589; DP0210000,REPT-97-ERD-129; No Copyright; Avail: Department of Energy Information Bridge, Microfiche

Doped beryllium is a material of considerable interest to both the ICF and the weapons communities, as well as finding application in specialized industrial settings (e.g., x-ray windows and mirrors). Some of these uses require conformal coating of thin films on (possibly) irregularly-shaped surfaces. Physical vapor deposition (PVD) is often used to accomplish this, and sputtering is often the technique of choice. Among its advantages are that the depositing atoms are relatively energetic, leading to more compact films. Moreover, by simply applying a voltage bias to the substrate, ambient noble gas ions will bombard the growing film, which can cause further densification and other modifications to the microstructure. Sputtering is also well suited to the introduction of dopants, even those that are insoluble. Most applications of these novel materials will require fundamental knowledge of their properties. Because so many can be devised, such information is generally unavailable. The objective of the effort has been to systematically study the properties of films produced under different conditions, with an emphasis on surface finish and permeability. They have made extensive use of atomic force microscopy (AFM) and electron microscopy to determine the microstructure of the films, along with composition probes (mainly x-ray fluorescence) to quantify the chemical structure. The studies can be roughly divided into three categories. First, there are those in which the properties of pure or Cu-doped Be films have been investigated, especially on randomly-agitated spherical capsules. Included are studies of the effects of a constant substrate bias ranging from 0 to 120 v and application of an intermittent bias during deposition. Second, there are experiments in which the structure of the depositing films has been modified via the incorporation of dopants, primarily boron. Finally, there have been numerous attempts to characterize the permeability of Be coatings at temperatures ranging from 200 to 500 C.
NTIS
Beryllium; Doped Crystals; Sputtering; Thin Films; Surface Properties

20020001178 Argonne National Lab., IL USA

Crack initiation in smooth fatigue specimens of austenitic stainless steel in light water reactor environments

Chopra, O. K.; Smith, J. L.; Apr. 08, 1999; 10p; In English; ASME/JSME Joint Pressure Vessel and Piping Conference, 1-5 Aug. 1999, Boston, MA, USA

Contract(s)/Grant(s): W-31109-ENG-38

Report No.(s): DE2001-12388; ANL/ET/CP-98400; No Copyright; Avail: Department of Energy Information Bridge, Microfiche

The fatigue design curves for structural materials specified in Section III of the ASME Boiler and Pressure Vessel Code are based on tests of smooth polished specimens at room temperature in air. The effects of light water reactor (LWR) coolant environments are not explicitly addressed by the Code design curves; however, recent test data illustrate the detrimental effects of LWR coolant environments on the fatigue resistance of austenitic stainless steels (SSs). Certain loading and environmental conditions have led to test specimen fatigue lives that are significantly shorter than those obtained in air. Results of fatigue tests that examine the influence of reactor environments on crack initiation and crack growth of austenitic SSs are presented. Block loading was used to mark the fracture surface to determine crack length as a function of fatigue cycles in water environments, Crack lengths were measured by scanning electron microscopy. The mechanism for decreased fatigue life in LWR environments is discussed, and crack growth rates in the smooth fatigue specimens are compared with existing data from studies of crack growth rates.

NTIS

Austenitic Stainless Steels; Crack Initiation; Fatigue (Materials); Fracture Strength; Light Water Reactors

20020001195 Argonne National Lab., IL USA

Phonon density of states in Fe/Cr (001) superlattices and Tb-Fe thin-film alloys

Alp, E. E.; Keune, W.; Roehlsberger, R.; Ruckert, T.; Schror, H.; Feb. 15, 1999; 12p; In English; International Conference on Magnetic Multilayers, 15-16 June 1998, Vancouver, British Columbia, Canada

Contract(s)/Grant(s): W-31109-ENG-38

Report No.(s): DE2001-12391; ANL/XFD/CP-98412; No Copyright; Avail: Department of Energy Information Bridge, Microfiche

Inelastic nuclear scattering of X-rays from the 14.413 keV nuclear resonance of (sup 57)Fe was employed to measure directly the Fe-projected phonon density of states (DOS) in MBE-grown Fe/Cr(00l) superlattices on MgO(001). The Moessbauer-inactive (sup 56)Fe isotope was used in the Fe layers. A 1(angstrom) thick Moessbauer-active (sup 57)Fe-probe layer (95% enriched) was placed at different locations within the Fe layers. This procedure permits one to distinguish phonon density of states at the Fe-Cr-interface from that at the center of the Fe-film. Distinct differences have been observed in the DOS of our samples. The phonon DOS of an amorphous Tb(sub 33)Fe(sub 67) alloy film was found to be a broad and structureless hump, contrary to that of an epitaxial TbFe(sub 2) film, which exhibits characteristic features.

NTIS

Superlattices; Thin Films; Phonons; Metal Films; Inelastic Scattering

20020001199 Argonne National Lab., IL USA

Microstructure Evolution in Low-Temperature, Ion-implanted AlxGa1-xAs

Coleman, J. J.; Lagow, B. W.; Rehn, L. E.; Robertson, I. M.; Mar. 10, 1999; 15p; In English; Materials Research Society Meeting, 30 Nov. - 4 Dec. 1998, Boston, MA, USA

Contract(s)/Grant(s): W-31109-ENG-38

Report No.(s): DE2001-12381; ANL/MSD/CP-98542; No Copyright; Avail: Department of Energy Information Bridge, Microfiche

The accumulation of ion implantation damage in Al(sub x)Ga(sub 1(minus)x)As/GaAs heterostructures (0 (le) x (le) 0.85) at 77 K has been investigated by using a combination of RBS (at 77 K and 293 K) and TEM (at 293 K). Recovery, as seen by a decrease in the channeling yield, occurs on warming to room temperature unless the material has been driven amorphous or x (ge) 0.85. Depending on the implantation condition, the recovered structure consists of either planar defects or dislocation loops. Planar defects were also observed in alloys with x = 0.85, although they were confined to a narrow band that separated the amorphous from the crystalline material. by implanting with ions of different energy it was shown that amorphization can initiate within the layer away from the interfaces, showing that interfaces are not needed for amorphization. Implantations with 500 keV Krions were performed at 50 K in-situ in the Intermediate-Voltage Electron Microscope--Accelerator facility at Argonne National Laboratory. Planar defects were produced on warmup, showing that they are not necessary for amorphization. We propose that amorphization

initiates because of an accumulation of damage and that the dependence of the amorphization dose on Al content is related to differences in cascade dynamics.
NTIS
Aluminum Gallium Arsenides; Microstructure; Defects; Ion Implantation

20020001286 Lawrence Livermore National Lab., Livermore, CA USA
Surface topographies of one-year weight-loss coupons of alloy C-22 from long-term corrosion testing
Bedrossian, P. J.; Jun. 11, 1999; 37p; In English
Report No.(s): DE2001-12205; UCRL-ID-134649; No Copyright; Avail: Department of Energy Information Bridge, Microfiche
We have used an atomic force microscope (AFM) to characterize the surface topographies of weight-loss coupons of Alloy C-22 which had been exposed to two different environments in the Long-Term Corrosion Test Facility at LLNL for one year. We have observed a silicate deposit on these coupons, with the most extensive coverage occurring on the coupon immersed in an acidified bath. We have not detected localized corrosion on these coupons.
NTIS
Alloys; Corrosion Tests

20020001561 Virginia Commonwealth Univ., Richmond, VA USA
Electronic Structure and Geometries of Small Compound Metal Clusters
Apr. 14, 1999; 15p; In English
Report No.(s): DE2001-6607; No Copyright; Avail: Department of Energy Information Bridge
During the tenure of the DOE (Department of Energy) grant DE-FG05-87EI145316 we have concentrated on equilibrium geometries, stability, and the electronic structure of transition metal-carbon clusters (met-cars), clusters designed to mimic the chemistry of atoms, and reactivity of homo-nuclear metal clusters and ions with various reactant molecules. It is difficult to describe all the research the authors have accomplished as they have published 38 papers. In this report, they outline briefly the salient features of their work on the following topics: (1) Designer Clusters: Building Blocks for a New Class of Solids; (2) Atomic Structure, Stability, and Electronic Properties of Metallo-Carbohedrenes; (3) Reactivity of Metal Clusters with H(sub 2) and NO; and (4) Anomalous Spectroscopy of Li(sub 4) Clusters.
NTIS
Electronic Structure; Electrical Properties; Metal Clusters; Atomic Structure

20020001587 Lawrence Livermore National Lab., Livermore, CA USA
Influence of severe plastic deformation on the structure and properties of ultrahigh carbon steel wire
Leseur, D. R.; Sherby, O. D.; Syn, C. K.; Jul. 01, 1999; 13p; In English
Report No.(s): DE2001-12731; UCRL-JC-133137; GJ0902000,REPT-96-ERD-026; No Copyright; Avail: Department of Energy Information Bridge, Microfiche
Ultrahigh-carbon steel wire can achieve very high strength after severe plastic deformation, because of the fine, stable substructures produce. Tensile strengths approaching 6000 MPa are predicted for UHCS containing 1.8% C. This paper discusses the microstructural evolution during drawing of UHCS wire, the resulting strength produced and the factors influencing fracture. Drawing produces considerable alignment of the pearlite plates. Dislocation cells develop within the ferrite plates and, with increasing strain, the size normal to the axis (lambda) decreases. These dislocation cells resist dynamic recovery during wire drawing and thus extremely fine substructures can be developed ((lambda) < 10 nm). Increasing the carbon content reduces the mean free ferrite path in the as-patented wire and the cell size developed during drawing. For UHCS, the strength varies as (lambda)(sup -5). Fracture of these steels was found to be a function of carbide size and composition. The influence of processing and composition on achieving high strength in these wires during severe plastic deformation is discussed.
NTIS
Carbon Steels; Plastic Deformation; Wire; Substructures

20020001590 Lawrence Livermore National Lab., Livermore, CA USA
General and localized corrosion of the drip shield
Estill, J. C.; Farmer, J. C.; McCright,; Aug. 20, 1999; 53p; In English
Report No.(s): DE2001-12726; UCRL-ID-135423; No Copyright; Avail: Department of Energy Information Bridge, Microfiche
Ti Gr 7 is an extremely corrosion resistant material, with a very stable passive film. Based upon exposures in the LTCTF, it has been determined that the general corrosion and oxidation rates of Ti Gr 7 are essentially below the level of detection. In any event, over the 10,000 year life of the repository, general corrosion and oxidation should not be life limiting. The large separation

between measured corrosion and threshold potentials indicate that localized breakdown of the passive film is unlikely under plausible conditions, even in SSW at 120 C. In the future, the pH and current in crevices formed from Ti Gr 7 should be determined experimentally. With exposures of two years, no significant evidence of crevice corrosion has been observed with Ti Gr 16 in SDW, SCW, and SAW at temperatures up to 90 C, though many of the samples have a beautiful green patina. An abstracted model has been presented, with parameters determined experimentally, that should enable performance assessment to account for the general and localized corrosion of this material. A feature of this model is the use of the materials specification to limit the range of corrosion and threshold potentials, thereby making sure that substandard materials prone to localized attack are avoided.
NTIS
Titanium; Corrosion Resistance; Cracks

20020001665 Atomic Energy Commission, Idaho Falls, ID USA
Relationship Between Casting Distortion, Mold Filling, and Interfacial Heat Transfer in Sand Molds
Parker, J. K.; Woodbury, K. A.; Piwonka, T. S.; Owusu, Y.; Sep. 30, 1999; 329p; In English
Report No.(s): DE2001-12625; DOE/ID/13363; No Copyright; Avail: Department of Energy Information Bridge, Microfiche
This project sought to determine the relationship between casting dimensions and interfacial heat transfer in aluminum alloy sand castings. The program had four parts; measurement of interfacial heat transfer coefficients in resin bonded and green sand molds, the measurement of gap formation in these molds, the analysis of castings made in varying gratings, orientations and thicknesses, and the measurement of residual stresses in castings in the as-cast and gate removed condition. New values for interfacial heat transfer coefficients were measured, a novel method for gap formation was developed, and the variation of casting dimensions with casting method, gating, and casting orientation in the mold was documented.
NTIS
Aluminum Alloys; Castings; Cast Alloys; Heat Transfer; Heat Transfer Coefficients

20020001842 Los Alamos National Lab., NM USA
Long term instability growth of radiatively driven thin planar shells
Mason, R. J.; Hollowell, D. E.; Oct. 01, 2000; 19p; In English
Report No.(s): DE2001-765638; LA-UR-00-5069; No Copyright; Avail: Department of Energy Information Bridge, Microfiche
The authors study Rayleigh-Taylor instability of radiatively driven thin copper foils under pure ablation, as well as with beryllium tampers to provide additional pressure drive. Modeling was done with the RAGE adaptive mesh refinement code of experiments done on the NOVA and OMEGA lasers. The copper foils were typically 11.5 (micro)m thick with 0.45 (micro)m amplitude, 45 (micro)m wavelength cosine surface perturbations. The beryllium layer was 5 (micro)m thick. The drive was a P26-like laser pulse delivering a peak 160-185 eV radiation temperatures. Good agreement between experiment and simulation has been obtained out to 4.5 ns. Mechanisms for late time agreement are discussed.
NTIS
Copper; Metal Foils; Pulsed Lasers

20020001965 Lawrence Livermore National Lab., Livermore, CA USA
Lifetime studies of Mo/Si and Mo/Be multilayer coatings for extreme ultraviolet lithography
Bajt, S.; Clift, W. M.; Folta, J. A.; Gullikson, E. M.; Klebanoff, L. E.; Aug. 05, 1999; 10p; In English
Report No.(s): DE2001-12565; UCRL-JC-132916; No Copyright; Avail: Department of Energy Information Bridge, Microfiche
Extreme Ultraviolet Lithography (EUVL) is a candidate for future application by the semiconductor industry in the production of sub-100 nm feature sizes in integrated circuits. Using multilayer reflective coatings optimized at wavelengths ranging from 11 to 14 nm, EUVL represents a potential successor to currently existing optical lithography techniques. In order to assess lifetimes of the multilayer coatings under realistic conditions, a series of radiation stability tests has been performed. In each run a dose of EUV radiation equivalent to several months of lithographic operation was applied to Mo/Si and MO/Be multilayer coatings within a few days. Depending on the residual gas concentration in the vacuum environment, surface deposition of carbon during the exposure lead to losses in the multilayer reflectivity. However, in none of the experimental runs was structural damage within the bulk of the multilayers observed. Mo/Si multilayer coatings recovered their full original reflectivity after removal of the carbon layer by an ozone cleaning method. Auger depth profiling on MO/Be multilayers indicate that carbon penetrated into the Be top layer during illumination with high doses of EUV radiation. Subsequent ozone cleaning fully removed the carbon, but revealed enhanced oxidation of the area illuminated, which led to an irreversible loss in reflectance on the order

of 1%. Keywords: Extreme ultraviolet (EUV) lithography, multilayer reflective coatings, radiation stability, surface contamination
NTIS
Lithography; Reflectance

20020001966 Lawrence Livermore National Lab., Livermore, CA USA
Shock compressed solids on the Nova laser
Colvin, J. D.; Gold, D. M.; Kalantar, D. H.; Mikaelian, K. O.; Remington, B. A.; Aug. 03, 1999; 7p; In English
Report No.(s): DE2001-12564; UCRL-JC-132687; No Copyright; Avail: Department of Energy Information Bridge, Microfiche

Experiments are being developed to shock compress metal foils in the solid state to study the material strength under high compression. The x-ray drive has been characterized and hydrodynamics experiments performed to study growth of the Rayleigh-Taylor (RT) instability in Al foils at a peak pressure of about 1.8 Mbar. Pre-imposed modulations with an initial wavelength of lo-50 pm, and amplitude of 0.5 pm show growth. Variation in the growth factors may be a result of shot-shot variation in preheating of the Al sample due to emission from the plasma in the hohlraum target
NTIS
Metal Foils; Lasers

20020001973 Argonne National Lab., IL USA
In situ examination of moving crack tips in ordered intermetallics
Heuer, J.; Lam, N. Q.; Okamoto, P. R.; Stubbins, J. F.; Jan. 25, 1999; 9p; In English
Report No.(s): DE2001-12368; ANL/MSD/CP-98330; No Copyright; Avail: Department of Energy Information Bridge, Microfiche

Recent studies have shown that high stress concentrations at moving crack tips in the intermetallic compound NiTi can induce a crystalline-to-amorphous (C-A) transformation of the crack tip region. This stress-induced C-A transformation has a temperature dependence and crystallization behavior similar to those of ion irradiation-induced C-A transformation of NiTi. The present study examines if these similarities between stress- and irradiation-induced amorphization hold true for two other intermetallic compounds, CuTi and Ni(sub 3)Ti. In situ straining was performed in an intermediate-voltage transmission electron microscope. The presence or absence of an amorphous phase was determined by dark field imaging and selected area diffraction of crack tip regions. Crack tips in both CuTi and Ni(sub 3)Ti were found to remain crystalline upon fracture. The observed absence of stress-induced amorphization in Ni(sub 3)Ti is consistent with its known absence during irradiation, but the absence in CuTi differs from its known irradiation-induced amorphization behavior. Reasons for the similarity and difference are discussed.
NTIS
Crack Propagation; Stress Concentration; Temperature Dependence; Intermetallics

20020002238 Lawrence Livermore National Lab., Livermore, CA USA
Role of interfacial dislocations on creep of a fully lamellar tial
Hsiung, L. M.; Nieh, T. G.; Aug. 16, 1999; 10p; In English
Report No.(s): DE2001-12553; UCRL-JC-135382; KC0201050; No Copyright; Avail: Department of Energy Information Bridge

Deformation mechanisms of a fully lamellar TiAl ((gamma) lamellae: 100 (approximately) 300 nm thick, (alpha)(sub 2) lamellae: 10 (approximately) 50 nm thick) crept at 760 C have been investigated. It was found that, as a result of a fine structure, the motion and multiplication of dislocations within both (gamma) and (alpha)(sub 2) lamellae are limited at low creep stresses (>400 MPa). Thus, the glide and climb of lattice dislocations have insignificant contribution to creep deformation. In contrast, the motion of interfacial dislocations on (gamma)(alpha)(sub 2) and (gamma)(gamma) interfaces (i.e. interface sliding) dominates the deformation at low stresses. The major obstacles impeding the motion of interfacial dislocations was found to be lattice dislocations impinging on lamellar interfaces. The number of impinging lattice dislocations increases as the applied stress increases and, subsequently, causes the pileup of interfacial dislocations on the interfaces. The pileup further leads to the formation of deformation twins. Deformation twinning activated by the pileup of interfacial dislocations is suggested to be the dominant deformation mechanism at high stresses (is less than 400 MPa).
NTIS
Deformation; Titanium Aluminides; Creep Properties

20020002290 Washington State Univ., Pullman, WA USA
Coarsening in Multicomponent Multiphase Systems ***Final Report, 1 Nov. 1995 - 31 Oct. 1998***
Hoyt, J. J.; Oct. 22, 1999; 7p; In English
Report No.(s): DE2001-765803; No Copyright; Avail: Department of Energy Information Bridge, Microfiche

The goal of the project was to extend the theory of particle coarsening, which is well established for binary systems, to the case of multicomponent and multiphase alloys. The theoretical approach involved three stages: (1) a mean field description based on the Lifshitz-Slyozov-Wagner (LSW) formulation (recently published in Acta Mater.), (2) an analytical description of coarsening valid at small volume fractions where the Marqusee and Ross model was employed and (3) a numerical simulation of three phase coarsening where the boundary integral method of Akaiwa and Voorhees was implemented. The main result of the mean field analysis can be stated as follows. The growth rate of a particle from a particular phase in a multiphase system is precisely the same as that derived for a single phase, multicomponent system. Also, it was found that the scaled particle size distribution for each phase in the system has exactly the same form as that originally derived by LSW. Since it neglects particle interactions, the mean field theory is clearly unrealistic and as such the formulation of coarsening in low volume fraction multiphase systems was undertaken.
NTIS
Alloys; Particle Interactions; Numerical Analysis

20020002303 Sandia National Labs., Albuquerque, NM USA
Soldering of Thin Film-Metallized Glass Substrates
Hosking, F. M.; Hernandez, C. L.; Glass, S. J.; Mar. 31, 1999; 8p; In English
Report No.(s): DE2001-5675; SAND98-2081; No Copyright; Avail: Department of Energy Information Bridge, Microfiche
The ability to produce reliable electrical and structural interconnections between glass and metals by soldering was investigated. Soldering generally requires premetallization of the glass. As a solderable surface finish over soda-lime-silicate glass, two thin films coatings, Cr-Pd-Au and NiCr-Sn, were evaluated. Solder nettability and joint strengths were determined. Test samples were processed with Sn60-Pb40 solder alloy at a reflow temperature of 210 C. Glass-to-cold rolled steel single lap samples yielded an average shear strength of 12 MPa. Solder fill was good. Control of the Au thickness was critical in minimizing the formation of AuSn4 intermetallic in the joint, with a resulting joint shear strength of 15 MPa. Similar glass-to-glass specimens with the Cr-Pd-Au finish failed at 16.5 MPa. The NiCr-Sn thin film gave even higher shear strengths of 20-22.5 MPa, with failures primarily in the glass.
NTIS
Glass; Soldering; Substrates; Thin Films

20020002318 Lawrence Livermore National Lab., Livermore, CA USA
Experimental investigation of beryllium-based multilayer coatings for extreme ultraviolet lithography
Bajit, S.; Behymer, R. D.; Folta, J.; Mirkarimi, P. B.; Montcalm, C.; Jul. 30, 1999; 16p; In English
Report No.(s): DE2001-12561; UCRL-JC-132917; No Copyright; Avail: Department of Energy Information Bridge, Microfiche
The performance of beryllium-based multilayer coatings designed to reflect light of wavelengths near 11 nm, at normal incidence, is presented. These multilayer coatings are of special interest for extreme ultraviolet lithography (EUVL). The beryllium-based multilayers investigated were Mo/Be, Ru/Be and a new material combination Mo,CiBe. The highest reflectivity achieved so far is 70% at 11.3 mn with 70 bilayers of Mo/Be. However, even though high reflectivity is very important, there are other parameters to satisfy the requirements for an EUVL production tool. Multilayer stress, thermal stability, radiation stability and long term reflectance stability are of equal or greater importance. An experimental characterization of several coatings was carried out to determine the reflectivity, stress, microstructure, and long term stability of these coatings. Theoretically calculated reflectivities are compared with experimental results for different material pairs; differences between experimental and theoretical reflectivities and bandwidths are addressed.
NTIS
Lithography; Microstructure; Thermal Stability; Reflectance

20020002701 Los Alamos National Lab., NM USA
Modular steady state glow discharge quadrupole mass spectrometer system for the at-line analysis of plutonium metal
Steiner, R.; Wayne, D.; Dec. 01, 1998; 6p; In English
Report No.(s): DE2001-768226; LA-UR-98-5697; No Copyright; Avail: Department of Energy Information Bridge
Historically, glow discharge mass and optical spectrometric techniques have been used in industry for the characterization of processed metals, such as steels and other alloys. This technique is especially well suited for this type of product analysis because the glow discharge ionization source accommodates solid conducting samples with minimal or no sample preparation.

This characteristic along with minimal matrix effect considerations makes the glow discharge source well suited for these types of applications.
NTIS
Glow Discharges; Mass Spectrometers; Plutonium; Steels

20020002752 Argonne National Lab., IL USA
Spring magnet films
Bader, S. D.; Fullerton, E. E.; Gornakov, V. S.; Inomata, A.; Jiang, J. S.; Mar. 29, 1999; 8p; In English
Report No.(s): DE2001-12421; ANL/MSD/CP-98200; No Copyright; Avail: Department of Energy Information Bridge, Microfiche

The properties of exchange-spring-coupled bilayer and superlattice films are highlighted for Sm-Co hard magnet and Fe or Co soft magnet layers. The hexagonal Sm-Co is grown via magnetron sputtering in a- and b-axis epitaxial orientations. In both cases the c-axis, in the film plane, is the easy axis of magnetization. Trends in coercivity with film thickness are established and related to the respective microstructure of the two orientations. The magnetization reversal process for the bilayers is examined by magnetometry and magneto-optical imaging, as well as by simulations that utilize a one-dimensional model to provide the spin configuration for each atomic layer. The Fe magnetization is pinned to that of the Sm-Co at the interface, and reversal proceeds via a progressive twisting of the Fe magnetization. The Fe demagnetization curves are reversible as expected for a spring magnet. Comparison of experiment and simulations indicates that the spring magnet behavior can be understood from the intrinsic properties of the hard and soft layers. Estimates are made of the ultimate gain in performance that can potentially be realized in this system.
NTIS
Magnetic Films; Superlattices

20020003391 Los Alamos National Lab., NM USA
Synthesis and fabrication of Mo-W components for neutron resonance spectroscopy temperature measurement
Bingert, S.; Desch, P.; Trujillo, E.; Sep. 01, 1999; 38p; In English
Report No.(s): DE2001-768228; LA-UR-99-3877; No Copyright; Avail: Department of Energy Information Bridge, Microfiche

A Molybdenum Tungsten-182 (MoW-182) alloy was specified for an application that would ultimately result in the measurement of temperature and particle velocity during the steady state time following the shock loading of various materials. The W-182 isotope provides a tag for the analysis of neutron resonance line shape from which the temperature may be calculated. The material was specified to have 1.8 atom percent W, with W-rich regions no larger than 1 micrometer in size. Both the composition and W distribution were critical to the experiment. Another challenge to the processing was the very small quantity of W-182 material available for the synthesis of the alloy. Therefore, limited fabrication routes were available for evaluation. Several synthesis and processing routes were explored to fabricate the required alloy components. First, precipitation of W onto Mo powder using ammonium metatungstate was investigated for powder synthesis followed by uniaxial hot pressing. Second, mechanical alloying (MA) followed by hot isostatic pressing (HIP) and warm forging was attempted. Finally, arc-melting techniques followed by either hot rolling or crushing the alloyed button into powder and consolidation were pursued. The results of the processing routes and characterization of the materials produced will be discussed.
NTIS
Molybdenum Alloys; Tungsten Isotopes; Temperature Measurement; Fabrication

20020003399 Los Alamos National Lab., NM USA
Effect of repeated compressive dynamic loading on the stress-induced martensitic transformation in niti shape memory alloys
Miller, D.; Thissell, W.; Aug. 01, 2000; 10p; In English
Report No.(s): DE2001-768250; LA-UR-00-3684; No Copyright; Avail: Department of Energy Information Bridge, Microfiche

It has been shown that quasi-static, cyclic, isothermal mechanical loading influences the mechanical response of the stress-induced martensitic transformation in fully annealed NiTi Shape Memory Alloys (SMAs). As the cycle number increases, hardening of the stress-strain response during the martensitic phase transformation is seen along with a decrease in the threshold stress for initiation of stress-induced martensite. Also, the amount of plastic strain and detwinned martensitic strain decreases as the cycle number increases. However, NiTi SMAs have not been experimentally explored under high compressive strain rates. This research explores the cyclic near-adiabatic stress-induced martensitic loading using a Split Hopkinskin Pressure Bar (SHPB). The results of the dynamic loading tests are presented with emphasis on the loading rate, stress-strain response, specimen temperature and post-test microstructural evaluation. The results from the high strain rate tests show similarities with the

quasi-static results in the hardening of the stress-strain response and shifting of the threshold stress for initiation of stress-induced martensite.
NTIS
Compression Loads; Dynamic Loads; Martensitic Transformation; Shape Memory Alloys

20020003561 Lawrence Livermore National Lab., Livermore, CA USA
High power laser for peening of metals enabling production technology
Daly, J.; Dane, C. B.; Hackel, L. A.; Harrison, J.; Jun. 18, 1998; 26p; In English
Report No.(s): DE2001-2851; UCRL-JC-131104-REV-1; DP0212000; No Copyright; Avail: Department of Energy Information Bridge

Cryogenic energy-dispersive x-ray detectors are being developed because of their superior energy resolution (less than or equal to 10 eV FWHM for keV x rays) compared to semiconductor EDS systems. So far, their range of application is limited due to their comparably small size and low count rate. We present data on the development of superconducting tunnel junction (STJ) detector arrays to address both of these issues. A single STJ detector has a resolution around 10 eV below 1 keV and can be operated at count rates of order 10,000 counts/s. We show that the simultaneous operation of several STJ detectors does not diminish their energy resolution significantly, while increasing the detector area and the maximum count rate by a factor given by the total number of independent channels.
NTIS
High Power Lasers; Metals; Shot Peening; Radiant Heating

20020003812 Los Alamos National Lab., NM USA
State-variable approach for predicting the time required for 50% recrystallization
Stout, M.; Aug. 01, 2000; 9p; In English
Report No.(s): DE2001-768739; LA-UR-00-3812; No Copyright; Avail: Department of Energy Information Bridge, Microfiche

It is important to be able to model the recrystallization kinetics in aluminum alloys during hot deformation. The industrial relevant process of hot rolling is an example of where the knowledge of whether or not a material recrystallizes is critical to making a product with the correct properties. Classically, the equations that describe the kinetics of recrystallization predict the time to 50% recrystallization. These equations are largely empirical; they are based on the free energy for recrystallization, a Zener-Holloman parameter, and have several adjustable exponents to fit the equation to engineering data. We have modified this form of classical theory replacing the Zener-Hollomon parameter with a deformation energy increment, a free energy available to drive recrystallization. The advantage of this formulation is that the deformation energy increment is calculated based on the previously determined temperature and strain-rate sensitivity of the constitutive response. We modeled the constitutive response of the AA5182 aluminum using a state variable approach, the value of the state variable is a function of the temperature and strain-rate history of deformation. Thus, the recrystallization kinetics is a function of only the state variable and free energy for recrystallization. There are no adjustable exponents as in classical theory. Using this approach combined with engineering recrystallization data we have been able to predict the kinetics of recrystallization in AA5182 as a function of deformation strain rate and temperature.
NTIS
Free Energy; Recrystallization; Aluminum Alloys

20020003815 Argonne National Lab., IL USA
Characterization of oxidation products on a ZrFe2-type laves intermetallic exposed to 200 C steam
Abraham, D. P.; Dietz, N.; Finnegan, N.; Nov. 20, 2000; 7p; In English
Report No.(s): DE2001-768627; ANL/CMT/CP-103450; No Copyright; Avail: Department of Energy Information Bridge

The release of radioactive elements from the stainless steel-15 wt% zirconium (SS-15Zr) metal waste form will be governed by the corrosion behavior of ZrFe(sub 2)-type intermetallics phases present in the alloy. In this article, oxidation products that formed on a ZrFe(sub 2)-type intermetallic sample exposed to 200 C steam were characterized by Auger Electron Spectroscopy (AES) and Transmission Electron Microscopy (TEM). The data revealed two oxide layers on the sample surface: an outer crystalline iron-oxide layer and an inner amorphous zirconium-rich layer believed to be zirconium oxide. Thermodynamic considerations indicate that the zirconium-rich layer formed first. The iron-oxide layer appears to have resulted from the diffusion of iron through the zirconium-rich layer to the oxide-vapor interface.
NTIS
Oxidation; Corrosion; Intermetallics; Waste Management; Containment

20020003825 Argonne National Lab., IL USA

Disorder-driven hysteresis-loop criticality in Co/CoO-films

Berger, A.; Inomata, A.; Jiang, J. S.; Pearson, J. E.; Bader, S. D.; Nov. 01, 2000; 16p; In English

Report No.(s): DE2001-768582; ANL/MSD/CP-102423; No Copyright; Avail: Department of Energy Information Bridge, Microfiche

The effect of magnetic disorder on the magnetization reversal process in thin Co/CoO-films has been investigated. The antiferromagnetic CoO layer allows a reversible tuning of the magnetic disorder by simple temperature variation. For temperatures above a critical temperature T(sub c), we observe a discontinuous magnetization reversal, whereas smooth magnetization loops occur for T greater than T(sub c). Our measurements establish the existence of a disorder-driven critical point in the non-equilibrium phase diagram. In addition, we observe scaling behavior in the vicinity of the critical point and determine the critical exponents to (beta) = 0.022 +/- 0.006 and (beta)(delta) = 0.30 +/- 0.03.

NTIS

Critical Temperature; Magnetization; Cobalt; Cobalt Oxides; Thin Films

20020003829 Argonne National Lab., IL USA

Preparation of nickel substrates for coated conductors

Truchan, T. G.; Rountree, F. H.; Lanagan, M. T.; McClellan, S. M.; Miller, D. J.; Nov. 01, 2000; 7p; In English

Report No.(s): DE2001-768570; ANL/ET/CP-99359; No Copyright; Avail: Department of Energy Information Bridge, Microfiche

Polycrystalline Ni has been used as a substrate for high-current, coated YBa2Cu3O(sub x) superconductors. For many conductors, Ni is rolled to large deformation and annealed to produce a cube texture. In this study, Ni was rolled to greater than 95% reduction and annealed in 5% H2/95% He at 300-1000 C for various times. The resulting substrates were examined by scanning electron microscopy, X-ray and electron diffraction, and surface interferometry. Key determinations for the Ni were extent of in-plane and out-of-plane texture, surface smoothness, and grain size. The extent of texture was approximately independent of annealing temperature and increased slightly with annealing time. Annealing at temperatures greater than 600 C increased surface roughness, primarily due to grain-boundary grooving. Grain growth was fastest at 1000 C and was proportional to time to the 0.1 power.

NTIS

Nickel; Substrates; YBCO Superconductors

20020004003 Los Alamos National Lab., NM USA

Examination of 304L stainless steel to 6061-T6 aluminum inertia welded transition joints after irradiation in a spallation neutron spectrum

Dunn, K.; May 01, 2000; 14p; In English

Report No.(s): DE2001-768994; LA-UR-00-2313; No Copyright; Avail: Department of Energy Information Bridge

The Savannah River Technology Center (SRTC) designed and fabricated tritium target/blanket assemblies which were irradiated for six months at the Los Alamos Neutron Science Center (LANSCE). Cooling water was supplied to the assemblies through 1 inch diameter 304L Stainless Steel (SS) tubing. to attach the 304L SS tubing to the modules a 304L SS to 6061-T6 Aluminum (Al) inertia welded transition joint was used. These SS/Al inertia weld transition joints simulate expected transition joints in the Accelerator Production of Tritium (APT) Target/Blanket whereas many as a thousand SS/Al weld transition joints will be used. Materials compatibility between the 304L SS and the 6061 -T6 Al in the spallation neutron environment is a major concern as well as the corrosion associated with the cooling water flowing through the piping. The irradiated inertia weld examination will be discussed.

NTIS

Irradiation; Stainless Steels; Welded Joints; Aluminum

20020004005 Los Alamos National Lab., NM USA

Retention of very high levels of helium and hydrogen generated in various structural alloys by 800 MeV protons and spallation neutrons

Oliver, B.; May 01, 2000; 18p; In English

Report No.(s): DE2001-768992; LA-UR-00-2315; No Copyright; Avail: Department of Energy Information Bridge

A series of irradiations were conducted in the Los Alamos Neutron Science Center as part of the test program supporting the Accelerator Production of Tritium Program sponsored by US-DOE. In this irradiation campaign, a variety of candidate structural alloys were placed in various particle spectra, ranging from 800 MeV protons, to mixed energy distributions of both protons and

spallation neutrons, and to primarily high energy neutrons. At proton energies on the order of hundreds of MeV, exceptionally high levels of gas atoms are generated in all elemental constituents of typical structural alloys, with helium typically at -150 appm per dpa and hydrogen at approximately an order of magnitude greater. Since neither of these gases are considered to have a good effect on structural properties of interest, their retention after both recoil and diffusional losses is of strong interest. Helium is essentially immobile at all temperatures of interest, but hydrogen has some limited temperature-dependent mobility. to assess the degree of retention, each gas was measured in a number of highly irradiated specimens of different alloy compositions and dpa levels. The results show that helium production is relatively insensitive to composition and its retention is nearly total. The retained hydrogen levels, however, are somewhat sensitive to composition, reflecting different levels of diffusional loss, but are still at very large concentrations. There is some speculation that co-generation of helium and hydrogen assists in the trapping of hydrogen, and results in relatively high levels of hydrogen retention even at higher irradiation temperatures.
NTIS
Helium; Hydrogen; Spallation; Alloys; Neutrons; Protons; Irradiation; Cogeneration

20020004662 Sandia National Labs., Albuquerque, NM USA
PdMn and PdFe: New Materials for Temperature Measurement Near 2K
Aselage, T. L.; Duncan, R. V.; Klemme, B. J.; Sergatskov, D. A.; Adriaans, M. J.; Feb. 01, 1999; 18p; In English
Report No.(s): DE2001-3931; SAND99-0342; No Copyright; Avail: Department of Energy Information Bridge, Microfiche

Interest in the critical dynamics of superfluid He in microgravity conditions has motivated the development of new high resolution thermometry technology for use in space experiments near 2K. The current material commonly used as the temperature sensing element for high resolution thermometers (HRTs) is copper ammonium bromide (Cu(NH(sub 4))(sub 2)Br(sub 4)2H(sub 2)O) or CAB, which undergoes a ferromagnetic phase transition at 1.8K. HRTs made from CAB have demonstrated low drift (<10fK/s) and a temperature resolution of 0.1nK. Unfortunately, paramagnetic salts such as CAB are difficult to prepare and handle, corrosive to most metals, and become dehydrated if kept under vacuum conditions at room temperature. We have developed a magnetic thermometer using dilute magnetic alloys of Mn or Fe dissolved in a pure Pd matrix. These metallic thermometers are easy to fabricate, chemically inert, and mechanically robust. Unlike salts, they may be directly soldered to the stage to be measured. Also, the Curie temperature can be varied by changing the concentration of Fe or Mn, making them available for use in a wide temperature range. Susceptibility measurements, as well as preliminary noise and drift measurements, show them to have sub-nK resolution with a drift of less than 10(sup (minus)13) K/s.
NTIS
Temperature Measurement; Superfluidity; Helium; Ferromagnetic Materials; Manganese Alloys; Palladium Alloys

20020004666 Sandia National Labs., Albuquerque, NM USA
Fusion Welding of AerMet 100 Alloy
Englehart, D. A.; Michael, J. R.; Novotny, P. M.; Robino, C. V.; Aug. 01, 1999; 66p; In English
Report No.(s): DE2001-12656; SAND99-1833; No Copyright; Avail: Department of Energy Information Bridge, Microfiche

A database of mechanical properties for weldment fusion and heat-affected zones was established for AerMet(reg-sign)100 alloy, and a study of the welding metallurgy of the alloy was conducted. The properties database was developed for a matrix of weld processes (electron beam and gas-tungsten arc) welding parameters (heat inputs) and post-weld heat treatment (PWHT) conditions. In order to insure commercial utility and acceptance, the matrix was commensurate with commercial welding technology and practice. Second, the mechanical properties were correlated with fundamental understanding of microstructure and microstructural evolution in this alloy. Finally, assessments of optimal weld process/PWHT combinations for cotildent application of the alloy in probable service conditions were made. The database of weldment mechanical properties demonstrated that a wide range of properties can be obtained in welds in this alloy. In addition, it was demonstrated that acceptable welds, some with near base metal properties, could be produced from several different initial heat treatments. This capability provides a means for defining process parameters and PWHT's to achieve appropriate properties for different applications, and provides useful flexibility in design and manufacturing. The database also indicated that an important region in welds is the softened region which develops in the heat-affected zone (HAZ) and analysis within the welding metallurgy studies indicated that the development of this region is governed by a complex interaction of precipitate overaging and austenite formation. Models and experimental data were therefore developed to describe overaging and austenite formation during thermal cycling. These models and experimental data can be applied to essentially any thermal cycle, and provide a basis for predicting the evolution of microstructure and properties during thermal processing.
NTIS
Data Bases; Fusion Welding; Gas Tungsten Arc Welding; Mechanical Properties

20020005052 Argonne National Lab., IL USA

Orthoclase Surface Structure Dissolution Measured In Situ by X-Ray Reflectivity and Atomic Force Microscopy

Sturchio, N. C.; Fenter, P.; Cheng, L.; Teng, H.; Nov. 28, 2000; 7p; In English

Report No.(s): DE2001-768634; ANL/ER/CP-103540; No Copyright; Avail: Department of Energy Information Bridge

Orthoclase surface topography and interface structure were measured during dissolution by using in situ atomic force microscopy (AFM) and synchrotrons X-ray reflectivity at pH 1.1-12.9 and T = 25-84 C. Terrace roughening at low pH and step motion at high pH were the main phenomena observed, and dissolution rates were measured precisely. Contrasting dissolution mechanisms are inferred for low- and high-pH conditions. These observations clarify differences in alkali feldspar dissolution mechanisms as a function of pH, demonstrate a new in situ method for measuring face-specific dissolution rates on single crystals, and improve the fundamental basis for understanding alkali feldspar weathering processes.

NTIS

Dissolving; pH; Topography; Single Crystals; Surface Properties

20020005053 Argonne National Lab., IL USA

Probing the Electrical Double-Layer Structure at the Rutile-Water Interface with X-Ray Standing Waves

Fenter, P.; Cheng, L.; Rihs, S.; Machesky, M.; Bedzyk, M. J.; Nov. 28, 2000; 7p; In English

Report No.(s): DE2001-768635; ANL/ER/CP-103541; No Copyright; Avail: Department of Energy Information Bridge

We demonstrate that the X-ray standing wave (XSW) technique is a powerful probe of the electrical double-layer (EDL) structure. Measurements were made of SR adsorption at the rutile-water interface from aqueous solutions. Our results show that Bragg XSW, using small-period standing waves generated by Bragg diffraction from the substrate, precisely probes the location of ions within the condensed layer, and the in situ partitioning of ions between the condensed and diffuse layers. Such measurements can provide important constraints for the development and verification of theoretical models that describe ion adsorption at the solid-water interface.

NTIS

Adsorption; Rutile; Water; Liquid-Liquid Interfaces; Standing Waves

20020005058 Bechtel National, Inc., Oak Ridge, TN USA

Nondestructive and Localized Measurements of Stress-Strain Curves and Fracture Toughness of Ferritic Steels at Various Temperatures Using Innovative Stress-Strain Microprobe Technology ***Final Report, 13 Aug. 1996 - 16 Jun. 1999***

Haggag, F. M.; Oct. 29, 1999; 49p; In English

Report No.(s): DE2001-769202; DOE/ER/82115-2; No Copyright; Avail: Department of Energy Information Bridge, Microfiche

The results presented in this report demonstrate the capabilities of Advanced Technology Corporation's patented Portable/In Situ Stress-Strain Microprobe (TM) (SSM) System and its Automated Ball Indentation (ABI) test techniques to nondestructively measure the yield strength, the stress-strain curve, and the fracture toughness of ferritic steel samples and components in a reliable and accurate manner.

NTIS

Ferritic Stainless Steels; Nondestructive Tests

20020005166 Oak Ridge National Lab., TN USA

Metals and Ceramics Division History 1946-1996

Craig, D. F.; Sep. 27, 1998; 153p; In English

Report No.(s): DE2001-4073; ORNL/M-6589; No Copyright; Avail: Department of Energy Information Bridge, Microfiche

The division was formed in 1946 at the suggestion of Dr. Eugene P. Wigner to attack the problem of the distortion of graphite in the early reactors due to exposure to reactor neutrons, and the consequent radiation damage. It was called the Metallurgy Division and assembled the metallurgical and solid state physics activities of the time which were not directly related to nuclear weapons production. During this period the Division evolved into three organizational areas: basic research, applied research in nuclear reactor materials, and reactor programs directly related to a specific reactor(s) being designed or built.

NTIS

Ceramics; Solid State Physics; Metallurgy; Nuclear Reactors

20020005167 Lawrence Livermore National Lab., Livermore, CA USA

Interaction between point defects and edge dislocation in BCC iron

DiazdelaRubia, T.; Shastry, V.; Oct. 12, 1998; 10p; In English

Report No.(s): DE2001-4119; UCRL-JC-132378; KC0202020; No Copyright; Avail: Department of Energy Information Bridge, Microfiche

We present results of atomistic simulations of the interaction between self interstitial atoms and vacancies with edge dislocations in BCC iron. The calculations are carried out using molecular dynamics with an energy minimization scheme based on the quasi-Newton approach and use the Finnis-Sinclair interatomic potential for BCC iron developed by Ackland et al. Large anisotropy in the strain field of self interstitials is observed and it causes strong interaction with edge dislocations even when the defect is located on the dislocation glide plane. For vacancies, the relaxation volume is smaller and much more isotropic, which results in a far weaker interaction with the dislocation. A temperature dependent capture radius for vacancies and self interstitials is extracted from the simulations. The difference between the capture radii of vacancies and self interstitials is used to define the sink strength of the dislocation. Large deviations are observed from the predictions of elasticity based on treating point defects as isotropic dilatational centers. Further, the capture radius of edge dislocations in BCC iron is observed to be small and is of the order of l-3 nm for self interstitials.

NTIS

Body Centered Cubic Lattices; Edge Dislocations; Iron; Point Defects; Interstitials; Anisotropy

20020005267 Lawrence Livermore National Lab., Livermore, CA USA

Hydrogen-Induced Cracking of Drip Shield

Lu, S. C.; Aug. 01, 1999; 38p; In English

Report No.(s): DE2001-12724; UCRL-ID-135630; No Copyright; Avail: Department of Energy Information Bridge, Microfiche

A simple and conservative model has been developed to evaluate the effects of hydrogen-induced cracking (HIC) on the drip shield. The basic premise of the model is that failure will occur once the hydrogen content exceeds a certain limit or critical value, HC. This model is very conservative because it assumes that, once the environmental and material conditions can support that particular corrosion process, failure will be effectively instantaneous. In the description of the HIC model presented, extensive evidence has been provided to support a qualitative assessment of Ti-7 as an excellent choice of material for the drip shield with regard to degradation caused by hydrogen-induced cracking. LTCTF test data observed at LLNL, although unqualified, provides additional indication beyond a qualitative level that hydrogen concentration appears to be low in titanium materials. Quantitative evaluation based on the HIC model described indicates that the hydrogen concentration does not exceed the critical value. It is concluded that drip shield material (Ti-7) is able to sustain the effects of hydrogen-induced cracking.

NTIS

Hydrogen; Cracking (Chemical Engineering); Corrosion; Shielding

20020005405 Los Alamos National Lab., NM USA

Effects of xe ion irradiation and subsequent annealing on the properties of magnesium-aluminate spinel

Afanasyev, I.; Apr. 01, 2000; 6p; In English

Report No.(s): DE2001-769044; LA-UR-00-2399; No Copyright; Avail: Department of Energy Information Bridge, Microfiche

Single crystals of magnesium-aluminate spinel MgAl(sub 2)O(sub 4) were irradiated with 340 keV Xe(sup 2) ions at (minus)173 C ((approximately) 100 K). A fluence of 1 x 10(sup 20) Xe/m(sup 2) created an amorphous layer at the surface of the samples. The samples were annealed for 1 h at different temperatures ranging from 130 C to 880 C. Recrystallization took place in the temperature interval between 610 C and 855 C. Transmission electron microscopy (TEM) images show two distinct layers near the surface: (1) a polycrystalline layer with columnar grain structure; and (2) a buried damaged layer epitaxial with the substrate. After annealing at 1100 C for 52 days, the profile of implanted Xe ions did not change, which means that Xe ions are not mobile in the spinel structure up to 1100 C. The thickness of the buried damaged layer decreased significantly in the 1100 C annealed sample comparing to the sample annealed for 1 h at 855 C.

NTIS

Annealing; Recrystallization; Xenon; Ion Irradiation; Magnesium; Single Crystals; Aluminum Oxides

20020005407 Los Alamos National Lab., NM USA

Contour method: simple 2-d mapping of residual stresses

Prime, M.; Gonzales, A.; Jun. 01, 2000; 9p; In English

Report No.(s): DE2001-769066; LA-UR-00-1900; No Copyright; Avail: Department of Energy Information Bridge, Microfiche

We present an entirely new method for measuring residual stress that is extremely simple to apply yet more powerful than existing techniques. In this method, a part is carefully cut in two. The contour of the resulting new surface is measured to determine the displacements normal to the surface caused by the release of the residual stresses. Analytically, the opposite of these measured displacements are applied as boundary conditions to the surface in a finite element model. by Bueckner's superposition principle, this gives the original residual stresses normal to the plane of the cut. Unlike other relaxation methods for measuring residual stress, the measured data can be used to solve directly for the stresses without a tedious inversion technique. At the same time, an arbitrary two-dimensional variation in stresses can be determined. We demonstrate the method on a steel specimen with a known residual stress profile.
NTIS
Steels; Mathematical Models; Residual Stress; Measuring Instruments

20020005818 Argonne National Lab., IL USA
Spallation studies on alumina-forming model alloys
Rieck, T.; Majumdar, S.; Natesan, K.; Sep. 15, 2000; 41p; In English
Report No.(s): DE2001-768567; ANL/FE-00/01; No Copyright; Avail: Department of Energy Information Bridge
Experimental and analytical studies were conducted on the spallation behavior of alumina oxide scales on two Ni-based model alloys and one Fe-based model alloy. Oxide thicknesses of up to 5.0 pm were successfully grown on the Ni- based and Fe-based alloys, respectively, at an oxidation temperature of up to 1200C. Four-point bend tests were conducted on these specimens at room temperature and at 1000C to determine the critical strain energy release rates for delamination of oxide scales.
NTIS
Aluminum Oxides; Spallation; Iron Alloys; Fabrication; Nickel Alloys; Mathematical Models

20020005856 Oak Ridge National Lab., TN USA
Oxide-Dispersion-Strengthened Fe3Al-Based Alloy Tubes: Application-Specific Development for the Power Generation Industry
Kad, B. K.; Jul. 20, 2001; 35p; In English
Report No.(s): DE2001-786484; ORNL/SUB/97-SY009/2; No Copyright; Avail: Department of Energy Information Bridge, Microfiche
A detailed and comprehensive research and development methodology is being prescribed to produce Oxide Dispersion Strengthened (ODS)-Fe3Al thin walled tubes, using powder extrusion methodologies, for eventual use at operating temperatures of up to 1100degC in the power generation industry. A particular 'in service application' anomaly of Fe3Al-based alloys is that the environmental mechanical resistance is maintained up to 1200degC, well beyond where such alloys retain sufficient mechanical strength. Grain boundary creep processes at such high temperatures are anticipated to be the dominant failure mechanism.
NTIS
Grain Boundaries; High Temperature; Electric Generators

27
NONMETALLIC MATERIALS

Includes physical, chemical, and mechanical properties of plastics, elastomers, lubricants, polymers, textiles, adhesives, and ceramic materials. For composite materials see 24 Composite Materials.

20020000740 Los Alamos National Lab., NM USA
Behaviour of Implanted Xenon in Yttria-Stabilised Zirconia as Inert Matrix of a Nuclear Fuel
Gegueldre, C.; Pouchon, M.; Do, M.; Sep. 21, 2000; 17p; In English
Report No.(s): DE2001-763041; LA-UR-00-4468; No Copyright; Avail: Department of Energy Information Bridge, Microfiche
A zirconia-based fuel is studied for use of plutonium in light water reactors. Among the relevant properties for a nuclear fuel, efficient retention of fission products is required since the fuel matrix constitutes the first barrier against fission product release.
NTIS
Nuclear Fuels; Xenon; Yttrium Oxides; Zirconium Oxides

20020000780 DYNACS Engineering Co., Inc., Cocoa Beach, FL USA

Aerogel Beads as Cryogenic Thermal Insulation System

Fesmire, J. E., NASA Kennedy Space Center, USA; Augustynowicz, S. D., DYNACS Engineering Co., Inc., USA; Rouanet, S., Cabot Corp., USA; [2001]; 8p; In English; Joint CEC and ICMC, 16-20 Jul. 2001, Madison, WI, USA

Contract(s)/Grant(s): NAS10-98001; No Copyright; Avail: CASI; A02, Hardcopy; A01, Microfiche

An investigation of the use of aerogel beads as thermal insulation for cryogenic applications was conducted at the Cryogenics Test Laboratory of NASA Kennedy Space Center. Steady-state liquid nitrogen boiloff methods were used to characterize the thermal performance of aerogel beads in comparison with conventional insulation products such as perlite powder and multilayer insulation (MLI). Aerogel beads produced by Cabot Corporation have a bulk density below 100 kilograms per cubic meter (kg/cubic m) and a mean particle diameter of 1 millimeter (mm). The apparent thermal conductivity values of the bulk material have been determined under steady-state conditions at boundary temperatures of approximately 293 and 77 kelvin (K) and at various cold vacuum pressures (CVP). Vacuum levels ranged from 10(exp -5) torr to 760 torr. All test articles were made in a cylindrical configuration with a typical insulation thickness of 25 mm. Temperature profiles through the thickness of the test specimens were also measured. The results showed the performance of the aerogel beads was significantly better than the conventional materials in both soft-vacuum (1 to 10 torr) and no-vacuum (760 torr) ranges. Opacified aerogel beads performed better than perlite powder under high-vacuum conditions. Further studies for material optimization and system application are in progress.

Author

Aerogels; Cryogenics; Thermal Insulation

20020001036 NASA Goddard Space Flight Center, Greenbelt, MD USA

Effects of Manufacturing and Deployment on Thin Films for the NGTS Sunshade

Wooldridge, Eve M., NASA Goddard Space Flight Center, USA; Powers, Charles E., NASA Goddard Space Flight Center, USA; Townsend, Jacqueline A., NASA Goddard Space Flight Center, USA; Peters, Wanda C., Swales Aerospace, USA; Cadogan, David P., ILC Dover, USA; Lin, John K. H., ILC Dover, USA; [2001]; 13p; In English; 42nd AIAA Structures, Structural Dynamics and Material Conference, 16-19 Apr. 2001, Seattle, WA, USA; Sponsored by American Inst. of Aeronautics and Astronautics, USA

Report No.(s): AIAA Paper 2001-1349; No Copyright; Avail: CASI; A03, Hardcopy; A01, Microfiche

The Next Generation Space Telescope (NGST) is being developed as an advanced astronomical observatory. The NGST proposes to utilize several thin film membrane layers to create a shield for protection of the telescope from solar thermal energy and stray light, The shield will take the form of a polygon, approximately 15 x 30 m, with individual membrane layers positioned so that they do not come in contact with one another. The membrane shield will be deployed and supported by a series of booms, which will be packed into a small volume for launch. Finally, the shield will be deployed on orbit. Several film materials are being considered for the membrane shield, including CPI, Kapton E, Kapton RN, and Upilex. Each of these polyimide materials was tested to determine their durability over the 10-year mission. New facets of materials testing have been introduced in this study to develop performance data with greater realism to actual use, particularly that of degradation from packing, launch and deployment processing. Materials were exposed to handling that simulated the life of the materials from manufacture through deployment with standardized fixtures and then exposed to a simulated, L2, 10-year radiation environment. Mechanical and thermal radiative properties were measured before and after each phase of testing. This paper summarizes the program and test results.

Author

Spaceborne Telescopes; Thin Films; Sun; Thermal Energy; Polyimides; Protection

20020001069 Argonne National Lab., IL USA

Corrosion behavior of environmental assessment glass in product consistency tests of extended duration

Bates, J. K.; Buck, E. C.; Ebert, W. L.; Luo, J. S.; Tam, S. W.; Nov. 18, 1998; 75p; In English

Report No.(s): DE2001-12003; ANL-98/27; No Copyright; Avail: Department of Energy Information Bridge, Microfiche

We have conducted static dissolution tests to study the corrosion behavior of the Environmental Assessment (EA) glass, which is the benchmark glass for high-level waste glasses being produced at US Department of Energy facilities. These tests were conducted to evaluate the behavior of the EA glass under the same long-term and accelerated test conditions that are being used to evaluate the corrosion of waste glasses. Tests were conducted at 90 C in a tuff groundwater solution at glass surface area/solution volume (WV) ratios of about 2000 and 20,000 m(sup (minus)1). The glass dissolved at three distinct dissolution rates in tests conducted at 2000 m(sup (minus)1). Based on the release of boron, dissolution within the first seven days occurred at a rate of about 0.65 g/(m(sup 2) (center dot) d). The rate between seven and 70 days decreased to 0.009 g/(m(sup 2) (center dot) d). An

increase in the dissolution rate occurred at longer times after the precipitation of zeolite phases analcime, gmelinite, and an aluminum silicate base. The dissolution rate after phase formation was about 0.18 g/(m(sup 2) (center dot) d). The formation of the same zeolite alteration phases occurred after about 20 days in tests at 20,000 m(sup (minus)). The average dissolution rate over the first 20 days was 0.5 g/(m(sup 2) (center-dot) d) and the rate after phase formation was about 0.20 g/(m(sup 2) (center-dot) d). An intermediate stage with a lower rate was not observed in tests at 20,000 m(sup (minus)1). The corrosion behavior of EA glass is similar to that observed for other high-level waste glasses reacted under the same test conditions. The dissolution rate of EA glass is higher than that of other high-level waste glasses both in 7-day tests and after alteration phases form.
NTIS
Glass; Corrosion; Minerals; Petrology; Dissolving; Environmental Tests

20020001206 Argonne National Lab., IL USA
Crystallization pathway in the bulk metallic glass Zr41.2Ti13.8Cu12.5Ni10Be22.5
Geyer, U.; Johnson, W. L.; Schneider, S.; Thiyagarajan, P.; Jun. 24, 1997; 9p; In English
Report No.(s): DE2001-12352; ANL/IPNS/CP-93578; No Copyright; Avail: Department of Energy Information Bridge, Microfiche

A new family of multicomponent metallic alloys exhibits an excellent glass forming ability at moderate cooling rates of about 10K/s and a wide supercooled liquid region. These glasses are eutectic or nearly eutectic, thus far away from the compositions of competing crystalline phases. The nucleation of crystals from the homogeneous amorphous phase requires large thermally activated composition fluctuations for which the time scale is relatively long, even in the supercooled liquid. In the Zr(sub 41.2)Ti(sub 13.8)Cu(sub 12.5)Ni(sub 10)Be(sub 22.5) alloy therefore a different pathway to crystallization is observed. The initially homogeneous alloy separates into two amorphous phases. In the decomposed regions, crystallization probability increases and finally polymorphic crystallization occurs. The evolution of decomposition and succeeding primary crystallization in the bulk amorphous Zr(sub 41.2)Ti(sub 13.8)Cu(sub 12.5)Ni(sub 10)Be(sub 22.5), alloy have been studied by small angle neutron. Samples annealed isothermally in the supercooled liquid and in the solid state exhibit interference peaks indicating quasiperiodic inhomogeneities in the scattering length density. The related wavelengths increase with temperature according to the linear Cahn-Hilliard theory for spinodal decomposition. Also the time evolution of the interference peaks in the early stages is consistent with this theory. At later stages, X-ray diffraction and transmission electron microscopy investigations confirm the formation of nanocrystals in the decomposed regions.
NTIS
Crystallization; Metallic Glasses; Eutectic Alloys

20020001232 Argonne National Lab., IL USA
Erosion of magnesium potassium phosphate ceramic waste forms
Goretta, K. C.; Nov. 20, 1998; 11p; In English
Report No.(s): DE2001-10851; ANL/ET/CP-96677; No Copyright; Avail: Department of Energy Information Bridge

Phosphate-based chemically bonded ceramics were formed from magnesium potassium phosphate (MKP) binder and either industrial fly ash or steel slag. The resulting ceramics were subjected to solid-particle erosion by a stream of either angular Al(sub 2)O(sub 3) particles or rounded SiO(sub 2) sand. Particle impact angles were 30 or 90(degree) and the impact velocity was 50 m/s. Steady-state erosion rates, measured as mass lost from a specimen per mass of impacting particle, were dependent on impact angle and on erodent particle size and shape. Material was lost by a combination of fracture mechanisms. Evolution of H(sub 2)O from the MKP phase appeared to contribute significantly to the material loss.
NTIS
Ceramics; Magnesium Compounds; Wastes

20020001552 Sandia National Labs., Albuquerque, NM USA
Effect of Thick Film Firing Conditions on the Solderability and Structure of Au-Pt-Pd Conductor for Low-Temperature, Co-Fired Ceramic Substrates
Hernandez, C. L.; Vianco, P. T.; Mar. 16, 1999; 7p; In English
Report No.(s): DE2001-4504; SAND98-2165C; No Copyright; Avail: Department of Energy Information Bridge, Microfiche

Low-temperature, co-fired ceramics (LTCC) are the substrate material-of-choice for a growing number of multi-chip module (MCM) applications. Unlike the longer-standing hybrid microcircuit technology based upon alumina substrates, the manufacturability and reliability of thick film solder joints on LTCC substrates have not been widely studied. An investigation was undertaken to fully characterize such solder joints. A surface mount test vehicle with Daisy chain electrical connections was designed and built with Dupont(trademark) 951 tape. The Dupont(trademark) 4569 thick film ink (Au76-Pt21-Pd3 wt.%) was

used to establish the surface conductor pattern. The conductor pattern was fired onto the LTCC substrate in a matrix of process conditions that included: (1) double versus triple prints, (2) dielectric frame versus no frame, and (3) three firing temperatures (800 C, 875 C and 950 C). Pads were examined from the test vehicles. The porosity of the thick film layers was measured using quantitative image analysis in both the transverse and short transverse directions. A significant dependence on firing temperature was recorded for porosity. Solder paste comprised of Sn63-Pb37 powder with an RMA flux was screen printed onto the circuit boards. The appropriate components, which included chip capacitors of sizes 0805 up to 2225 and 50 mil pitch, leadless ceramic chip carriers having sizes of 16 I/O to 68 I/O, were then placed on the circuit boards. The test vehicles were oven reflowed under a N(sub 2) atmosphere. The solderability of the thick film pads was also observed to be sensitive to the firing conditions. Solderability appeared to degrade by the added processing steps needed for the triple print and dielectric window depositions. However, the primary factor in solderability was the firing temperature. Solderability was poorer when the firing temperature was higher.
NTIS
Microelectronics; Solders; Thick Films; Ceramics; Capacitors; Low Temperature; Metals

20020001572 Argonne National Lab., IL USA
Recovery of flexible polyurethane foam from shredder residue
Daniels, E. J.; Jody, B. J.; Jun. 29, 1999; 70p; In English
Report No.(s): DE2001-12052; ANL/ESD/TM-152; No Copyright; Avail: Department of Energy Information Bridge
Argonne National Laboratory has developed a patented, continuous process for the recovery of flexible polyurethane foam (PUF) from auto shredder residue (ASR). to test the process, Argonne researchers conceived of, designed, and built a continuous foam washing and drying system that was pilot-tested at a shredder facility for six months. Economic analysis of the process, using manufacturers' quotes and operating data from Argonne's pilot plant, indicates a payback of less than two years for a plant producing about 1,000 ton/yr of foam. Samples of clean foam were shipped to three major foam reprocessors; all three indicated that the quality of the PUF recovered by the Argonne process met their requirements. Tests of the recovered foam by an independent testing laboratory showed that the recycled foam met the specifications for several automotive applications, including carpet padding, headliner, and sound-suppression support materials. Recovery of foam reduces the mass and the volume of material going to the landfill by about 5% and 30%, respectively. Annually, recovery will save about 1.2 x 10(exp 12) Btu of energy, cut the amount of solid waste being landfilled by about 150,000 tons, and eliminate the emission of about 250 tons of volatile organic compounds (VOCs) into the air.
NTIS
Materials Recovery; Polyurethane Foam; Waste Management; Automobiles

20020001591 Lawrence Livermore National Lab., Livermore, CA USA
Imaging shocked sapphire at 200-460 KBAR: the effect of crystal orientation on optical emission
Hare, D. E.; Holmes, N. C.; Webb, D. J.; Aug. 25, 1999; 6p; In English
Report No.(s): DE2001-12725; UCRL-JC-135520; No Copyright; Avail: Department of Energy Information Bridge, Microfiche
We have taken 12-50 ns exposure duration images of 200-460 kbar shock loaded, single crystal sapphire (Al2O3) windows of the c-cut (0001), r-cut (1,-1,0,2) and a-cut (1,1,-2,0) orientations. We find that the spectra of the emission are broad and relatively featureless, extending at least from 760 to 280 nm. Images of this emission at the lower end of the stress range (200-220 kbar) show that it is spatially very heterogeneous, coming from a few seemingly-randomly distributed locations within the crystal. This emission heterogeneity becomes more fine-grained with increasing shock stress. Finally, the r-cut orientation produces significantly less emission than the other two orientations at the same stress.
NTIS
Single Crystals; Crystallography; Sapphire; Light Emission

20020001662 Argonne National Lab., IL USA
Mixed-conducting dense ceramics for gas separation applications
Balachandran, U.; Dorris, S. E.; Dusek, J. T.; Guan, J.; Liu, M.; Jun. 22, 1999; 18p; In English
Report No.(s): DE2001-12424; ANL/ET/CP-98236; No Copyright; Avail: Department of Energy Information Bridge, Microfiche
Mixed-conducting (electronic and ionic conducting) dense ceramics are used in many applications, including fuel cells, gas separation membranes, batteries, sensors, and electrocatalysis. This paper describes mixed-conducting ceramic membranes that are being developed to selectively remove oxygen and hydrogen from gas streams in a nongalvanic mode of operation (i.e., with no electrodes or external power supply). Ceramic membranes made of SR-Fe-Co oxide (SFC), which exhibits high combined electronic and oxygen ionic conductivities, can be used for high-purity oxygen separation and/or partial oxidation of methane to

synthesis gas (syngas, a mixture of CO and H(sub 2)). The electronic and ionic conductivities of SFC were found to be comparable in magnitude. Steady-state oxygen permeability of SFC has been measured as a function of oxygen-partial-pressure gradient and temperature. For an (approx)3-mm-thick membrane, the oxygen permeability was (approx)2.5 scc(center-dot)cm(sup (minus)2)(center-dot)min(sup (minus)1) at 900 C. Oxygen permeation increases as membrane thickness decreases. Tubular SFC membranes have been fabricated and operated at 900 C for (approx)1000 h in converting methane into syngas. The oxygen permeated through the membrane reacted with methane in the presence of a catalyst and produced syngas. We also studied the transport properties of yttria-doped BaCeO(sub 3(minus)(delta)) (BCY) by impedance spectroscopy and open-cell voltage (OCV) measurement. Total conductivity of the BCY sample increased from (approx)5 x 10(sup (minus)3) (Omega)(sup (minus)1)(center-dot)cm(sup (minus)1) to (approx)2x 10(sup (minus)2) (Omega)(sup (minus)1)(center-dot)cm(sup (minus)1), whereas the protonic transference number decreased from 0.87 to 0.63 and the oxygen transference number increased from 0.03 to 0.15 as temperature increased from 600 to 800 C. Unlike SFC, in which the ionic and electronic conductivities are nearly equivalent BCY exhibits protonic conductivity that is significantly higher than its electronic conductivity. to enhance the electronic conductivity and therefore to increase hydrogen permeation, metal powder was combined with the BCY to form a cermet membrane, Nongalvanic permeation of hydrogen through the BCY-cermet membranes was demonstrated and characterized as a function of membrane thickness.
NTIS
Ceramics; Conductivity; Fabrication; Gas Mixtures; Synthesis (Chemistry); Membranes; Ferroelectric Materials

20020001886 Los Alamos National Lab., NM USA
Elementary approach to self-assembly and elastic properties of random copolymers
Chitanvis, S. M.; Oct. 01, 2000; 28p; In English
Report No.(s): DE2001-765584; LA-UR-00-5003; No Copyright; Avail: Department of Energy Information Bridge, Microfiche
The authors have mapped the physics of a system of random copolymers onto a time-dependent density functional-type field theory using techniques of functional integration. Time in the theory is merely a label for the location of a given monomer along the extent of a flexible chain. We derive heuristically within this approach a non-local constraint which prevents segments on chains in the system from straying too far from each other, and leads to self-assembly. The structure factor is then computed in a straightforward fashion. The long wave-length limit of the structure factor is used to obtain the elastic modulus of the network. It is shown that there is a surprising competition between the degree of micro-phase separation and the elastic moduli of the system.
NTIS
Copolymers; Phase Transformations; Self Assembly; Elastic Properties

20020002228 Department of Energy, Aiken, SC USA
Durability Testing of Heavy-Ion Irradiated Crystalline Ceramics
Crawford, C.; Sep. 29, 1999; 77p; In English
Report No.(s): DE2001-12508; WSRC-TR-99-00263; No Copyright; Avail: Department of Energy Information Bridge, Microfiche
The purpose of this report is to assess the effects of heavy-ion irradiation on the durability of pyrochlore-rich baseline ceramics and single-phase pyrochlore, zirconolite and brannerite ceramics.
NTIS
Ceramics; Performance Tests; Ion Irradiation

20020002264 Technische Univ., Delft, Netherlands
Formation and Stability of Blends with a Co-Continuous Morphology
Willemse, R. C.; Nov. 23, 1998; 161p; In English
Report No.(s): PB2002-100091; Copyright; Avail: National Technical Information Service (NTIS), Microfiche
Contents include the following: Introduction; Morphology Development in Immiscible Polymer Blends: the Initial Morphology; Co-Continuous Morphologies in Polymer Blends: A New Model; Co-Continuous Morphologies in Polymer Blends: the Influence of the Interfacial Tension; Stability of the Polymer Blend Morphology: the Role of the Initial Morphology; Tensile Properties of Immiscible Polymer Blends; Multi-Component Blends: Recycling; Concluding Remarks; and Summary.
NTIS
Polymer Blends; Interfacial Tension; Mixtures

20020002277 Sandia National Labs., Albuquerque, NM USA

Modeling and Imaging Flexural Plate Wave Devices

Adkins, D. R.; Butler, M. A.; Chu, A. S.; Schubert, W. K.; Jul. 09, 1999; 7p; In English

Report No.(s): DE2001-8865; SAND99-1012C; No Copyright; Avail: Department of Energy Information Bridge, Microfiche

Sandia National Laboratories is developing a new form of flexural plate wave device (FPW) for sensor applications. In this device, Lorentz forces cause out of plane vibrations in a silicon nitride membrane. Current induced in transducer lines on the membrane provides information about the amplitude and phase of these surface vibrations. by tracking the large amplitude vibrations that occur at resonant frequencies, it is possible to infer information about loading on the membrane. In fabricating FPWs, it is important to understand the impact that minor defects can have on operation. Through modeling and testing, they are developing resilient designs that provide large amplitude signals with a high tolerance to defects. A finite element model has been developed to perform design trade-off studies, and results from the model are being verified with a unique measurement system that can image Angstrom scale displacements at vibrational frequencies up to 800 kHz. Results from FPW modeling and imaging efforts are presented in this paper.

NTIS

Imaging Techniques; Lorentz Force; Silicon Nitrides; Display Devices

20020002278 Sandia National Labs., Albuquerque, NM USA

Thermal Degradation Studies of A Polyurethane Propellant Binder

Assink, R. A.; Celina, M.; Gillen, K. T.; Graham, A. C.; Minier, L. M.; Jun. 12, 1999; 33p; In English

Report No.(s): DE2001-8863; SAND99-0566C; No Copyright; Avail: Department of Energy Information Bridge, Microfiche

The thermal oxidative aging of a crosslinked hydroxy-terminated polybutadiene (HTPB)/isophorone diisocyanate (IPDI) based polyurethane rubber, used as a polymeric binder in solid propellant grain, was investigated at temperatures from 25 C to 125 C. The changes in tensile elongation, polymer network properties and chain dynamics, mechanical hardening and density were determined with a range of techniques including modulus profiling, solvent swelling, NMR relaxation and O2 permeability measurements. We critically evaluated the Arrhenius methodology that is commonly used with a linear extrapolation of high temperature aging data using extensive data superposition and highly sensitive oxygen consumption experiments. The effects of other constituents in the propellant formulation on aging were also investigated. We conclude that crosslinking is the dominant process at higher temperatures and that the degradation involves only limited hardening in the bulk of the material. Significant curvature in the Arrhenius diagram of the oxidation rates was observed. This is similar to results for other rubber materials.

NTIS

Thermal Degradation; Polyurethane Resins; Propellant Binders; Aging (Materials)

20020002294 Tennessee Univ., Knoxville, TN USA

Effect of pressure, isotopic (H/D) substitution, and other variables on miscibility in polymer-solvent systems. The nature of the demixing process; dynamic light scattering and small angle neutron scattering studies ***Final Report***

VanHook, W. A.; Jan. 01, 2000; 14p; In English

Report No.(s): DE2001-765324; No Copyright; Avail: Department of Energy Information Bridge

A research program examining the effects of pressure, isotope substitution and other variables on miscibility in polymer solvent systems is described. The techniques employed included phase equilibrium measurements and dynamic light scattering and small angle neutron scattering.

NTIS

Solubility; Solvents; Isotopes; Pressure Effects; Independent Variables

20020002354 Sandia National Labs., Albuquerque, NM USA

Better Methods for Predicting Lifetimes of Seal Materials

Celina, M.; Gillen, K. T.; Keenan, M. R.; Mar. 16, 1999; 7p

Report No.(s): DE2001-4502; SAND99-0623C; No Copyright; Avail: Department of Energy Information Bridge, Microfiche

We have been working for many years to develop better methods for predicting the lifetimes of polymer materials. Because of the recent interest in extending the lifetimes of nuclear weapons and the importance of environmental seals (o-rings, gaskets) for protecting weapon interiors against oxygen and water vapor, we have recently turned our attention to seal materials. Perhaps the most important environmental o-ring material is butyl rubber, used in various military applications. Although it is the optimum choice from a water permeability perspective, butyl can be marginal from an aging point-of-view. The purpose of the present work

was to derive better methods for predicting seal lifetimes and applying these methods to an important butyl material, Parker compound B6 12-70.
NTIS
Military Technology; Life (Durability); Nuclear Weapons; Polymers; O Ring Seals

20020002699 NASA Kennedy Space Center, Cocoa Beach, FL USA
Thermal Insulation Performance of Flexible Piping for Use in HTS Power Cables
Fesmire, James E., NASA Kennedy Space Center, USA; Augustynowicz, S. D., DYNACS Engineering Co., Inc., USA; Demko, J. A., Oak Ridge National Lab., USA; [2001]; 9p; In English; Joint CEC and ICMC, 16-20 Jul. 2001, Madison, WI, USA
Contract(s)/Grant(s): NAS10-98001; DE-AI05-00OR-22814; No Copyright; Avail: CASI; A02, Hardcopy; A01, Microfiche

High-temperature superconducting (HTS) cables that typically operate at temperatures below 80 K are being developed for power transmission. The practical application of HTS power cables will require the use of flexible piping to contain the cable and the liquid nitrogen coolant. A study of thermal performance of multilayer insulation (MLI) was conducted in geometries representing both rigid and flexible piping. This experimental study performed at the Cryogenics Test Laboratory of NASA Kennedy Space Center provides a framework for the development of cost-effective, efficient thermal insulation systems that will support these long-distance flexible lines containing HTS power cables. The overall thermal performance of the insulation system for a rigid configuration and for a flexible configuration, simulating a flexible HTS power cable, was determined by the steady-state liquid nitrogen boiloff method under the full range of vacuum levels. Two different cylindrically rolled material systems were tested: a standard MLI and a layered composite insulation (LCI). Comparisons of ideal MLI, MLI on rigid piping, and MLI between flexible piping are presented.
Author
High Temperature Superconductors; Multilayer Insulation; Thermal Insulation; Power Lines; Performance Tests

20020002706 Sandia National Labs., Albuquerque, NM USA
Formation of PS-b-PEO/Silica Films with Flat or Curved Multi-Bilayer Mesostructures of Large-Characteristic Length Scales Prepared by Solvent Evaporation-Induced Self-Assembly
Yu,; Brinker,; Hurd,; Eisenberg,; Nov. 22, 2000; 4p; In English
Report No.(s): DE2001-768066; SAND2000-2921C; No Copyright; Avail: Department of Energy Information Bridge

Diblock/silica films with multi-bilayer vesicular mesostructures of large characteristic length scales were synthesized through evaporation-induced self-assembly of PS-b-PEO. The present system is believed to be the first to yield diblock/silica films with multi-bilayer vesicular mesostructures through solvent evaporation-induced self-assembly (EISA). The ready formation in the present system is argued to be the polydispersity of polymer chains.
NTIS
Copolymers; Solvents; Silicon Dioxide; Molecular Chains

20020002708 Sandia National Labs., Albuquerque, NM USA
PS-b-PEO/Silica Films with Regular and Reverse Mesostructures of Large Characteristic Length Scales Prepared by Solvent Evaporation-Induced Self-Assembly
Yu,; Brinker,; Hurd,; Eisenberg,; Nov. 22, 2000; 4p; In English
Report No.(s): DE2001-768063; SAND2000-2918C; No Copyright; Avail: Department of Energy Information Bridge

Since the discovery of surfactant-templated silica by Mobil scientists in 1992, mesostructured silica has been synthesized in various forms including thin films, powders, particles, and fibers. In general, mesostructured silica has potential applications, such as in separation, catalysis, sensors, and fluidic microsystems. In respect to these potential applications, mesostructured silica in the form of thin films is perhaps one of the most promising candidates. The preparation of mesostructured silica films through preferential solvent evaporation-induced self-assembly (EISA) has recently received much attention in the laboratories. However, no amphiphile/silica films with reverse mesophases have ever been made through this EISA procedure. Furthermore, templates employed to date have been either surfactants or poly(ethylene oxide)-b-poly(propylene oxide)-b-poly(ethylene oxide) triblock copolymers, such as pluronic P-123, both of which are water-soluble and alcohol-soluble. Due to their relatively low molecular weight, the templated silica films with mesoscopic order have been limited to relatively small characteristic length scales. In the present communication, the authors report a novel synthetic method to prepare mesostructured amphiphilic/silica films with regular and reverse mesophases of large characteristic length scales. This method involves evaporation-induced self-assembly (EISA) of amphiphilic polystyrene-block-poly(ethylene oxide) (PS-b-PEO) diblock copolymers. In the present study, the PS-b-PEO diblocks are denoted as, for example, PS(215)-b-PEO(100), showing that this particular sample contains 215 S repeat units and 100 EO repeat units. This PS(215)-b-PEO(100) diblock possesses high molecular weight and does not directly mix with

water or alcohol. to the authors knowledge, no studies have reported the use of water-insoluble and alcohol-insoluble amphiphilic diblocks as structure-directing agents in the synthesis of mesostructured silica films through EISA. It is believed that the present system is the first to yield amphiphile/silica films with regular and reverse mesophases, as well as curved multi-bilayer mesostructures, through EISA. The ready formation of the diblock/silica films with multi-bilayer vesicular mesostructures is discussed.
NTIS
Copolymers; Molecular Weight; Silicon Dioxide; Thin Films

20020002716 Federal Energy Technology Center, Morgantown, WV USA
Oxygen transport ceramic membranes
Bandopadhyay, S.; Nagabhushana, N.; Oct. 01, 2000; 34p; In English
Report No.(s): DE2001-767396; DE-FC26-99FT40054-01; No Copyright; Avail: Department of Energy Information Bridge

This is the third quarterly report on oxygen Transport Ceramic Membranes. In the following, the report describes the progress made by our university partners in Tasks 1 through 6, experimental apparatus that was designed and built for various tasks of this project, thermodynamic calculations, where applicable and work planned for the future. (Task 1) Design, fabricate and evaluate ceramic to metal seals based on graded ceramic powder/metal braze joints. (Task 2) Evaluate the effect of defect configuration on ceramic membrane conductivity and long term chemical and structural stability. (Task 3) Determine materials mechanical properties under conditions of high temperatures and reactive atmospheres. (Task 4) Evaluate phase stability and thermal expansion of candidate perovskite membranes and develop techniques to support these materials on porous metal structures. (Task 5) Assess the microstructure of membrane materials to evaluate the effects of vacancy-impurity association, defect clusters, and vacancy-dopant association on the membrane performance and stability. (Task 6) Measure kinetics of oxygen uptake and transport in ceramic membrane materials under commercially relevant conditions using isotope labeling techniques.
NTIS
Ceramics; Oxygen; Thermal Expansion; Thermodynamics; Mechanical Properties; Fabrication

20020002751 Argonne National Lab., IL USA
Microstructure and nonstoichiometry of barium strontium titanate thin films for dram applications
Browning, N. D.; Kingon, A. I.; Stemmer, S.; Streiffer, S. K.; Apr. 23, 1999; 9p; In English
Report No.(s): DE2001-12422; ANL/MSD/CP-98293; No Copyright; Avail: Department of Energy Information Bridge, Microfiche

In this paper we investigate the microstructural accommodation of nonstoichiometry in (Ba(sub x)SR(sub 1(minus)x)Ti(sub 1+y)O(sub 3+z)) (BST) thin films grown by chemical vapor deposition. Films with three different (Ba+SR)/Ti ratios of 49/51 (y=0.04 in the notation of the formula above), of 48/52 (y=0.08) and of 46.5/53.5 (y=O.15), were studied. High resolution electron microscopy (HREM) is used to study the microstructure of the BST films. High spatial resolution electron energy-loss spectroscopy (EELS) is used to reveal changes in chemistry and local atomic environment both at grain boundaries and within grains as a function of titanium excess. We find an amorphous phase at the grain boundaries and grain boundary segregation of excess titanium in the samples with y=0.15. In addition, EELS is also used to show that excess titanium is being partially accommodated in the grain interior. Implications for the film's electrical and dielectric properties are outlined.
NTIS
Vapor Deposition; Electron Microscopy; Microstructure; Thin Films

20020002793 Argonne National Lab., IL USA
Radiation Damage of a Glass-Bonded Zeolite Waste Form Using Ion Irradiation
Allen, T. R.; Storey, B. G.; Dec. 05, 1997; 9p; In English
Report No.(s): DE2001-8908; ANL/ED/CP-95067; No Copyright; Avail: Department of Energy Information Bridge, Microfiche

Glass-bonded zeolite is being considered as a candidate ceramic waste form for storing radioactive isotopes separated from spent nuclear fuel in the electrorefining process. to determine the stability of glass-bonded zeolite under irradiation, transmission electron microscope samples were irradiated using high energy helium, lead, and krypton. The major crystalline phase of the waste form, which retains alkaline and alkaline earth fission products, loses its long range order under both helium and krypton irradiation. The dose at which the long range crystalline structure is lost is about 0.4 dpa for helium and 0.1 dpa for krypton. Because the damage from lead is localized in such a small region of the sample, damage could not be recognized even at a peak

damage of 50 dpa. Because the crystalline phase loses its long range structure due to irradiation, the effect on retention capacity needs to be further evaluated.
NTIS
Glass; Ion Irradiation; Radiation Damage; Zeolites; Waste Management

20020002842 Argonne National Lab., IL USA
Determining Thermal Diffusivity and Defect Attributes in Ceramic Matrix Composites by Infrared Imaging
Ahuja, S.; Ellingson, W. A.; Koehl, E. R.; Stuckey, J.; Dec. 05, 1997; 11p; In English
Report No.(s): DE2001-8905; ANL/ET/CP-95050; No Copyright; Avail: Department of Energy Information Bridge, Microfiche

Ceramic matrix composites are being developed for numerous high temperature applications, including rotors and combustors for advanced turbine engines, heat exchanger and hot-gas filters for coal gasification plants. Among the materials of interest are silicon-carbide- fiber-reinforced silicon-carbide (SiC(f)/SiC), silicon-carbide- fiber-reinforced silicon-nitride (SiC(f)/Si3N4), aluminum-oxide-reinforced-alumina ((Al2O(3f))/Al2O3), etc. In the manufacturing of these ceramic composites, the conditions of the fiber/matrix interface are critical to the mechanical and thermal behavior of the component. Defects such as delaminations and non-uniform porosity can directly effect the performance. A nondestructive evaluation (NDE) method, developed at Argonne National Laboratory has proved beneficial in analyzing as-processed conditions and defect detection created during manufacturing. This NDE method uses infrared thermal imaging for fill-field quantitative measurement of the distribution of thermal diffusivity in large components. Intensity transform algorithms have been used for contrast enhancement of the output image. Nonuniformity correction and automatic gain control are used to dynamically optimize video contrast and brightness, providing additional resolution in the acquired images. Digital filtering, interpolation, and least-squares-estimation techniques have been incorporated for noise reduction and data acquisition. The Argonne NDE system has been utilized to determine thermal shock damage, density variations, and variations in-fiber coating in a full array of test specimens.
NTIS
Ceramic Matrix Composites; Defects; Fiber Composites; Fiber-Matrix Interfaces; Nondestructive Tests; Thermal Diffusivity; Infrared Imagery

20020003375 Los Alamos National Lab., NM USA
Management of Silica in Los Alamos National Laboratory Tap Water: A Study of Silica Solubility
Wohlberg, C.; Worland, V. P.; Kozubal, M. A.; Erickson, G. F.; Jacobson, H. M.; Jul. 01, 1999; 390p; In English
Report No.(s): DE2001-8938; LA-13171; No Copyright; Avail: Department of Energy Information Bridge, Microfiche

Well water at Los Alamos National Laboratory (LANL) has a silica (SiO2) content of 60 to 100 mg/L, with 4 mg/L of magnesium, 13 mg/L calcium, and lesser concentrations of other ions. On evaporation in cooling towers, when the silica concentration reaches 150 to 220 mg/L, silica deposits on heat transfer surfaces. When the high silica well water is used in the reprocessing of plutonium, silica remains in solution at the end of the process and creates a problem of removal from the effluent prior to discharge or evaporation. The work described in this report is divided into two major parts. The first part describes the behavior of silica when the water is evaporated at various conditions of pH and in the presence of different classes of anions: inorganic and organic. In the second part of this work it was found that precipitation (floccing) of silica was a function of solution pH and mole ratio of metal to silica.
NTIS
Silicon Dioxide; Solubility; Evaporation; Precipitation (Chemistry)

20020003383 Argonne National Lab., IL USA
Applications of disorder-induced concept to critical-solute-accumulation-processes
Lam, N. Q.; Okamoto, P. R.; Heuer, J. K.; Oct. 10, 2000; 19p; In English
Report No.(s): DE2001-766320; ANL/MSD/CP-103023; No Copyright; Avail: Department of Energy Information Bridge, Microfiche

A generalized version of the Lindemann melting criterion has recently been used to develop a unified thermodynamic description of disorder-induced amorphization and heat-induced melting. This concept of amorphization as a melting process is based on the fact that the melting temperature of a defective crystal driven far from equilibrium will decrease relative to that of its defect-free equilibrium state. The broader view of melting provides a new perspective of damage-accumulation processes such as radiation damage, ion implantation, ion beam mixing, plastic deformation, and fracture. For example, within this conceptual framework, disorder-induced amorphization is simply polymorphous melting of a critically disordered crystal at temperatures

below the glass transition temperature. In the present communication, we discuss the application of the concept to two specific cases: amorphous phase formation during ion implantation and solute segregation-induced intergranular fracture.
NTIS
Deformation; Glass; Amorphous Materials; Melting Points; Thermodynamics

20020003385 Argonne National Lab., IL USA
Nynthesis of superlow friction carbon films from highly nydrogenated methane plasmas
Erdemir, A.; Eryilmaz, O. L.; Nilufer, I. B.; Fenske, G. R.; Oct. 13, 2000; 20p; In English
Report No.(s): DE2001-766338; ANL/ET/CP-103083; No Copyright; Avail: Department of Energy Information Bridge, Microfiche

In this study, we investigated the friction and wear performance of diamondlike carbon films (DLC) derived from increasingly hydrogenated methane plasmas. The films were deposited on steel substrates by a plasma-enhanced chemical vapor deposition process at room temperature and the tribological tests were performed in dry nitrogen. Tests results revealed a close correlation between the hydrogen in source gas plasma and the friction and wear coefficients of the DLC films. Specifically, films grown in plasmas with higher hydrogen-to-carbon ratios had much lower friction coefficients and wear rates than did films derived from source gases with lower hydrogen-to-carbon ratios. The lowest friction coefficient (0.003) was achieved with a film derived from 25% methane--75% hydrogen, while a coefficient of 0.015 was found for films derived from pure methane. Similar correlations were observed for wear rates. Films derived from hydrogen-rich plasmas had the least wear, while films derived from pure methane suffered the highest wear. We used a combination of surface analytical methods to characterize the structure and chemistry of the DLC films and worn surfaces.
NTIS
Carbon; Methane; Thin Films; Friction; Vapor Deposition; Hydrogen Plasma; Hydrogenation

20020003411 California Univ., Lawrence Berkeley Lab., Berkeley, CA USA
Plasma synthesis of high temperature ceramic films
Brown, I. G.; Monteiro, O. R.; Nov. 01, 1998; 33p; In English
Report No.(s): DE2001-6531; LBNL-42492; No Copyright; Avail: Department of Energy Information Bridge

Thin films of alumina, chromia, mullite, yttria and zirconia have been synthesized using a plasma-based method called metal plasma immersion ion implantation and deposition (Mepiiid)--a highly versatile plasma deposition technique with ion energy control. Monolithic films (a single ceramic component) and multilayer films (individual layers of different ceramic materials) were formed. The films were characterized for their composition and structure in a number of different ways, and the high temperature performance of the films was explored, particularly for their ability to maintain their integrity and adhesion when subjected to repetitive high temperature thermal cycling up 1100 C. We found that the films retain their adhesion and quality without any apparent degradation with time, even after a large number of cycles; (the tests were extended out to a total of 40 cycles each of 24 hours duration). After repetitive high temperature thermal cycling, the film-substrate adhesion was greater than approximately 70 Mpa, the instrumental limit of measurement, and the interface toughness was approximately 0.8 MPa m(exp 1/2).
NTIS
Synthesis (Chemistry); Ceramics; Thin Films; Ion Implantation; Metal Ions

20020003733 Rockwell International Science Center, Thousand Oaks, CA USA
Subcritical Crack Growth in Ceramic Composites at High Temperature Measured Using Digital Image Correlation
Mumm, D. R.; Morris, W. L.; Dadkhah, M. S.; Cox, B. N.; Jan. 11, 1996; 14p; In English
Report No.(s): DE2001-3042; No Copyright; Avail: Department of Energy Information Bridge

An in situ experimental technique is described that allows high resolution, high sensitivity determination of displacements and full-field strains during high temperature mechanical testing. The technique is used to investigate elevated temperature crack growth in SiC/Nicalon sub f composites. At 1150 degrees C, the reinforcing fibers have a higher creep susceptibility than the matrix. Fiber creep leads to relaxation of crack bridging tractions, resulting in subcritical crack growth. Differential image analysis is used to measure the crack opening displacement profile u(x) of an advancing, bridged crack. With appropriate modeling, such data can be used to determine the traction law, from which the mechanics of cracking and failure may be determined.
NTIS
Crack Propagation; Ceramic Matrix Composites; High Temperature

20020003802 Atomic Energy Commission, Idaho Falls, ID USA

Preparation and Characterization of INTEC Phase 2b Composition Variation Study Glasses

Staples, B. A.; Scholes, B. A.; Torres, L. L.; Musick, C. A.; Boyle, B. R.; Feb. 01, 2000; 92p; In English

Report No.(s): DE2001-768819; INEEL/EXT-99-01322; No Copyright; Avail: Department of Energy Information Bridge, Microfiche

The second phase of the composition variation study (CVS) for the development of glass compositions to immobilize Idaho Nuclear Technology and Engineering Center (INTEC) high level wastes (HLW) is complete. This phase of the CVS addressed waste composition of high activity waste fractions (HAW) from the initial separations flowsheet. Updated estimates if INTEC calcined HLW compositions and of high activity waste fractions proposed to be separated from dissolved calcine were used as the waste component for this CVS phase. These wastes are of particular interest because high aluminum, calcium, zirconium, fluorine, potassium, and low iron and sodium content places them outside the vitrification experience in the Department of Energy complex. Because of the presence of calcium and fluorine, two major zirconia calcine components not addressed in Phase I, a series of scooping tests, designated Phase 2a, were performed. The results of these tests provided information on the effects of calcium and fluoride solubility and their impacts on product properties and composition boundary information for Phase 2b. Details and results of Phase 2a are reported separately. Through application of statistical techniques and the results of Phase 2a, a test matrix was defined for Phase 2b of the CVS. From this matrix, formulations were systematically selected for preparation and characterization with respect to visual and optical homogeneity, viscosity as a function of melt temperature, liquidus temperature (TL), and leaching properties based on response to the product consistency test. The results of preparing and characterizing the Phase 2b glasses are presented in this document. Based on the results, several formulations investigated have suitable properties for further development. A full analysis of the composition-product characteristic relationship of glasses being developed for immobilizing INTEC wastes will be performed at the completion of composition-property relationship phases of the CVS.

NTIS

Glass; Reactor Technology; Statistical Analysis; Radioactive Wastes; Composition (Property); Solubility

20020003819 Argonne National Lab., IL USA

Science and technology of Ultrananocrystalline Diamond (UNCD) thin films for multifunctional devices

Auciello, O.; Gruen, D. M.; Krauss, A. R.; Jayatissa, A.; Sumant, A.; Nov. 15, 2000; 14p; In English

Report No.(s): DE2001-768621; ANL/MSD/CP-103393; No Copyright; Avail: Department of Energy Information Bridge

MEMS (microelectromechanical systems) devices are currently fabricated primarily in silicon because of the available surface machining technology. However, Si has poor mechanical and tribological properties, and practical MEMS devices are currently limited primarily to applications involving only bending and flexural motion, such as cantilever accelerometers and vibration sensors, However, because of the poor flexural strength and fracture toughness of Si, and the tendency of Si to adhere to hydrophyllic surfaces, even these simple devices have limited dynamic range. Future MEMS applications that involve significant rolling or sliding contact will require the use of new materials with significantly improved mechanical and tribological properties, and the ability to perform well in harsh environments. Diamond is a superhard material of high mechanical strength, exceptional chemical inertness, and outstanding thermal stability. The brittle fracture strength is 23 times that of Si, and the projected wear life of diamond MEMS moving mechanical assemblies (MEMS-MMAS) is 10,000 times greater than that of Si MMAs. However, as the hardest known material, diamond is notoriously difficult to fabricate. Conventional CVD (chemical vapor deposition) thin film deposition methods offer an approach to the fabrication of ultra-small diamond structures, but the films have large grain size, high internal stress, poor intergranular adhesion, and very rough surfaces, and are consequently ill-suited for MEMS-MMA applications. A thin film deposition process has been developed that produces phase-pure ultrananocrystalline diamond (UNCD) with morphological and mechanical properties that are ideally suited for MEMS applications in general, and MMA use in particular. We have developed lithographic techniques for the fabrication of diamond microstructure including cantilevers and multi-level devices, acting as precursors to micro-bearings and gears, making UNCD a promising material for the development of high performance MEMS devices.

NTIS

Diamonds; Mechanical Properties; Thin Films; Tribology; Microelectromechanical Systems

20020003972 Lawrence Livermore National Lab., Livermore, CA USA

Impact studies of five ceramic materials and Pyrex

Cunningham, B. J.; Holt, A. C.; Hord, B. L.; Kusubov, A. S.; Reaugh, J. E.; May 22, 1998; 25p; In English

Report No.(s): DE2001-2862; UCRL-100717-Rev-1; DP0101022; No Copyright; Avail: Department of Energy Information Bridge

We measured the ballistic performance of five ceramic materials (alumina, silicon carbide, boron carbide, aluminum nitride, and titanium diboride) and Pyrex, when they are backed by thick steel plates. The projectile for all tests was a right-circular cylinder of tungsten sinter-alloy W2 with length 25.4 mm and diameter 6.35 mm, fired at velocities from 1.35 to 2.65 km/s. For this threat we determined the minimum areal density of each material that is needed to keep the projectile from penetrating the backup steel. For all of the facing materials studied here, this performance measure increases approximately linearly with projectile velocity. However, the rate of increase is significantly lower for aluminum nitride than for the other materials studied. Indeed, aluminum nitride is a poor performer at the lowest velocity tested, but is clearly the best at the highest velocity. Our computer simulations show the significant influence of the backing material on ceramic performance, manifested by a transition region extending two projectile diameters upstream from the material interface. Experiments with multiple material layers show that this influence also manifests itself through a significant dependence of ballistic performance on the ordering of the material
NTIS
Impact Tests; Ceramics; Thick Plates; Borosilicate Glass

20020003992 Argonne National Lab., IL USA
Development of mixed-conducting dense ceramic membranes for hydrogen separation
Balachandran, U.; Bose, A. C.; Guan, J.; Stiegel, G. J.; Apr. 17, 1998; 7p; In English
Report No.(s): DE2001-8891; ANL/ET/CP-94969; No Copyright; Avail: Department of Energy Information Bridge, Microfiche

The electronic transference numbers of BCY were relatively low when compared with the protonic numbers. At 800 C, a hydrogen flux of only 0.02 cm(sup 3)/min/cm(sup 2) was obtained in an (approx) 2-rnm-thick BCY sample by short-circuiting the two Pt electrodes. We have developed a novel composite system with improved electronic transport, and preliminary measurements indicate that the new membrane materials can be used in a nongalvanic mode to separate hydrogen from gas mixtures. A maximum flux of 0.12 cm(sup 3)/min/cm(sup 2) has been measured at 800 C in the composite material operated in the nongalvanic mode. Currently, work is underway to further enhance the hydrogen flux in the composite membrane materials.
NTIS
Ceramics; Hydrogen; Composite Materials; Membranes

20020004915 Sandia National Labs., Albuquerque, NM USA
Superposition and Wear-Out Approaches Applied to Polymer Lifetime Prediction
Celina,; Gillen,; Dec. 06, 2000; 4p; In English
Report No.(s): DE2001-769081; SAND2000-3036C; No Copyright; Avail: Department of Energy Information Bridge

The objective of this paper is to present novel approaches for the lifetime prediction of polymeric materials. Time-temperature superposition principles using sensitive oxygen uptake (oxidation rate) measurements have been established as a methodology for material lifetime predictions. We first review some of the existing data and discuss the various issues when correlating such data with other degradation parameters, i.e. the need for sufficient overlap in superpositions, the required minimum temperature ranges and the establishment is failure criteria.
NTIS
Polymers; Service Life; Wear

20020005077 Oak Ridge National Lab., TN USA
Statistical characterization of three grades of large billet-graphites: Stackpole 2020, Union Carbide TS1792, and Toyo Tanso IG11
Kennedy, C. R.; Sep. 01, 1987; 77p; In English
Report No.(s): DE2001-770926; DOE-HTGR-87-010; ORNL/TM-10457; No Copyright; Avail: Department of Energy Information Bridge

Large billets of three fine-grained, isostatically molded graphites (three billets each of grade TS1792 from Union Carbide Corporation, six billets of grade IG11 from Toyo Tanso, and thirteen billets of grade 2020 from Stackpole Corporation) were evaluated by nondestructive methods, and the results were analyzed. The results of sonic testing were shown to be interrelated to both the mean and variance of strength obtained from destructive testing. The virtue of the nondestructive evaluation is clearly illustrated by the practical ability to evaluate up to 100% of the billet volume, thus giving a more accurate description of the materials mechanical properties. It was shown that the randomness of the mean strength in these billets makes it very unlikely that test results from small-sample volumes removed from the billet will be representative of the billet as a whole. In critical

applications requiring a high level of quality assurance, a more complete nondestructive evaluation of the billet appears to be required.
NTIS
Graphite; Mechanical Properties; Carbides; Billets; Variance (Statistics)

20020005176 California Univ., Lawrence Berkeley Lab., Berkeley, CA USA
Energy and daylight performance of angular selective glazings
Sullivan, R.; Beltran,; Lee, E. S.; Rubin, M.; Selkowitz, S. E.; Nov. 01, 1998; 22p; In English
Report No.(s): DE2001-7325; LBNL-41694; BS-384; No Copyright; Avail: Department of Energy Information Bridge

This paper presents the results of a study investigating the energy and daylight performance of anisotropic angular selective glazings. The DOE-2.1E energy simulation program was used to determine the annual cooling, lighting and total electricity use, and peak electric demand. RADIANCE, a lighting simulation program, was used to determine daylight illuminance levels and distribution. We simulated a prototypical commercial office building module located in Blythe, California. We chose three hypothetical conventional windows for comparison: a single-pane tinted window, a double-pane low-E window, and a double-pane spectrally selective window. Daylighting controls were used. No interior shades were modeled in order to isolate the energy effects of the angular selective glazing. Our results show that the energy performance of the prototype angular selective windows is about the same as conventional windows for a 9.14 m (30 ft) deep south-facing perimeter zone with a large-area window in the hot, sunny climate of Blythe. It is theoretically possible to tune the angular selectivity of the glazing to achieve annual cooling energy reductions of 18%, total electricity use reductions of 15%, and peak electric demand reductions of 11% when compared to a conventional glazing with the same solar-optical properties at normal incidence. Angular selective glazings can provide more uniformly distributed daylight, particularly in the area next to the window, which will result in a more visually comfortable work environment.
NTIS
Buildings; Computerized Simulation; Daytime; Cooling; Illuminance; Illuminating

20020005210 Federal Energy Technology Center, Morgantown, WV USA
Separation of fischer-tropsch wax from catalyst by supercritical extraction
Thies, M. C.; Joyce, P. C.; Oct. 31, 1998; 17p; In English
Report No.(s): DE2001-7697; DE-FG22-94PC94219-16; No Copyright; Avail: Department of Energy Information Bridge, Microfiche

The objective of this research project is to evaluate the potential of supercritical fluid (SCF) extraction for the recovery and fractionation of the wax product from the slurry bubble column (SBC) reactor of the Fischer-Tropsch (F-T) process. The wax, comprised mostly of branched and linear alkanes with a broad molecular weight distribution up to C(sub 100), will be extracted with a hydrocarbon solvent that has a critical temperature near the operating temperature of the SBC reactor, i.e., 200-300 C. Initial work is being performed using n-hexane as the solvent. The success of the project depends on two factors. First, the supercritical solvent must be able to dissolve the F-T wax; furthermore, this must be accomplished at conditions that do not entrain the solid catalyst. Second, the extraction must be controlled so as not to favor the removal of the low molecular weight wax compounds. That is, a constant carbon-number distribution in the wax slurry must be maintained at steady-state column operation. Three major tasks are being undertaken to evaluate our proposed SCF extraction process. Task 1: Equilibrium solubility measurements for model F-T wax components in supercritical fluids at conditions representative of those in a SBC reactor. Task 2: Thermodynamic modeling of the measured VLE data for extending our results to real wax systems. Task 3: Process design studies of our proposed process. Additional details of the task structure are given.
NTIS
Waxes; Catalysts; Synthesis (Chemistry); Fischer-Tropsch Process; Low Molecular Weights

20020005263 Sandia National Labs., Albuquerque, NM USA
Using Designed Residual Stress Profiles to Produce Flaw-Tolerant Glass
Beauchamp, E. K.; Glass, S. J.; Green, D. J.; Sglavo, M.; Sep. 02, 1999; 10p; In English
Report No.(s): DE2001-12714; SAND99-0303C; No Copyright; Avail: Department of Energy Information Bridge, Microfiche

A processing approach has been identified and reduced to practice in which a residual stress profile can be designed such that cracks in a brittle material are arrested or grow in a stable fashion. In the procedure, cracks in the body encounter an increase in the magnitude of residual compression as the crack propagates. If correctly designed, the process increases strength, significantly decreases strength variability, and gives rise to multiple cracking. This approach is demonstrated for an ion-exchanged silicate

glass using four-point and biaxial flexure strength testing. Optical microscopy was used to study the morphology and development of the multiple cracking that precedes the final failure.
NTIS
Brittle Materials; Cracks; Morphology; Stress Distribution; Fracture Mechanics; Crack Propagation

20020005843 Los Alamos National Lab., NM USA
Dynamics of polymers at interfaces
Smith, G. S.; Majewski, J.; Nov. 01, 1999; 8p; In English
Report No.(s): DE2001-785036; LA-UR-99-2853; No Copyright; Avail: Department of Energy Information Bridge

This is the final report of a three-year, Laboratory-Directed Research and Development (LDRD) project at the Los Alamos National Laboratory (LANL). This project addresses fundamental questions concerning the behavior of polymers at interfaces: (1) What processes control the formation of an adsorbed layer on a clean surface; (2) What processes control the displacement of preadsorbed polymers; (3) Can one accurately predict the structure of polymer layers. To answer these questions, using neutron reflectivity, we have studied adsorbed layers of the polymer poly(methyl methacrylate) PMMA onto a quartz substrate. The polymer density profiles were derived from the neutron reflectivity data. We have shown that dry films exhibit behavior predicted by mean-field theory in that the equilibrated layer thickness scales with the molecular weight of the polymer. Also, we find that the profiles of the polymers in solution qualitatively agree with those predicted by reflected random walk (RRW) theories, yet the profiles are not in quantitative agreement.
NTIS
Polymers; Interfaces; Molecular Weight; Neutrons; Acrylates

20020005854 Oak Ridge National Lab., TN USA
Evidence of Collisional Coherences in the Transport of Hydrogenic Krypton through Amorphous Carbon Foils
Minami, T.; Aug. 24, 2001; 15p; In English
Report No.(s): DE2001-786479; P01-111677; No Copyright; Avail: Department of Energy Information Bridge, Microfiche

We study theoretically and experimentally the population dynamics of the internal state of 60MeV/u Dr35+ ions traversing amorphous carbon foils. A quantum transport theory is developed that incorporates the state mixing induced by the wake field of the ion as well as all the coherences generated by the collisional and radiative redistribution of states. We show that the internal state of the ion is sensitive to collisional coherences and the wake field. The results of the full simulations are found to be in good agreement with experimental data.
NTIS
Amorphous Materials; Carbon; Foils (Materials); Quantum Theory

20020005862 NASA Glenn Research Center, Cleveland, OH USA
Slow Crack Growth Analysis of Advanced Structural Ceramics Under Combined Loading Conditions: Damage Assessment in Life Prediction Testing
Choi, S. R., Ohio Aerospace Inst., USA; Gyekenyesi, J. P., NASA Glenn Research Center, USA; Journal of Engineering for Gas Turbines and Power; April 2001; Volume 123, pp. 277-287; In English; International Gas Turbine and Aeroengine Congress and Exhibition, 8-11 May 2000, Munich, Germany
Report No.(s): Paper-00-GT-062; Copyright; Avail: Issuing Activity

Slow crack growth analysis was performed with three different loading histories including constant stress- rate/constant stress-rate testing (Case I loading), constant stress/constant stress-rate testing (Case II loading), and cyclic stress/constant stress-rate testing (Case III loading). Strength degradation due to slow crack growth and/or damage accumulation was determined numerically as a function of percentage of interruption time between the two loading sequences for a given loading history. The numerical solutions were examined with the experimental data determined at elevated temperatures using four different advanced ceramic materials, two silicon nitrides, one silicon carbide and one alumina for the Case I loading history, and alumina for the Case II loading history. The numerical solutions were in reasonable agreement with the experimental data, indicating that notwithstanding some degree of creep deformation presented for some test materials slow crack growth was a governing mechanism associated with failure for all the rest materials.
Author
Crack Propagation; Ceramics; Life (Durability); Damage Assessment

28
PROPELLANTS AND FUELS

Includes rocket propellants, igniters and oxidizers; their storage and handling procedures; and aircraft fuels. For nuclear fuels see 73 Nuclear Physics. For related information see also 07 Aircraft Propulsion and Power, 20 Spacecraft Propulsion and Power, and 44 Energy Production and Conversion.

20020000743 CALSTART, Burbank, CA USA
ARPA TRP Turboalternator Development. Quarterly Report, October 1-December 31, 1996
May 01, 1998; 10p; In English
Report No.(s): DE2001-763053; DOE/GO/10016-10; No Copyright; Avail: Department of Energy Information Bridge, Microfiche

This is a quarterly report of CALSTART's progress with their programs. For the last quarter, CALSTART has performed the following work in support of the Allied Signal turbogenerator project: We have taken prime turbogenerator marketing information, in the form of data sheets, posters and a new touch-screen computer interactive information program to two industry conferences that provided significant visibility and outreach for the AlliedSignal product. The first conference was EVS-13 (Electric Vehicle Symposium 13) October 11-18 in Osaka, Japan, the world's largest conference dedicated solely to electric vehicles and technology. AlliedSignal's turbogenerator display and information occupied the premier front location in the APU (auxiliary power unit) tower of the CALSTART industry exhibit and received substantial notice at a focused conference of more than 1,600 attendees. The exhibit was heavily attended and the turbogenerator received much interest. The second industry conference where CALSTART showcased the turbogenerator for marketing support was the NAEVI (North American Electric Vehicle and Infrastructure) Conference in San Diego, California, December 11-13. In addition to holding the premier spot in the display exhibit, CALSTART transported the turbogenerator itself to augment the display location. This conference represented the biggest American conference on EVS in 1996 and was well attended. The AlliedSignal display and information were utilized by several hundred people directly and by several hundred more as a central part of the exhibit they visited, creating a favorable impression of the technology.

NTIS
Efficiency; Marketing; Turbogenerators; Auxiliary Power Sources

20020000744 CALSTART, Burbank, CA USA
ARPA TRP Turboalternator Development. Quarterly Report, April 1-June 30, 1997
May 12, 1998; 46p; In English
Report No.(s): DE2001-763054; DOE/GO/10016-12B; No Copyright; Avail: Department of Energy Information Bridge, Microfiche

This is a quarterly report of CALSTART's progress with their programs. Their overall objectives remain: (1) efficiently and responsible management of the program and; (2) assist in the commercialization of the technology by doing the following: identifying potential strategic partners; explaining need and value of turbogenerator; reach important audiences for AlliedSignal; showcase technology at key conferences/briefings; raise technology profile via custom Web information; and extend AlliedSignal turbogenerator outreach efforts.

NTIS
Efficiency; Management; Commercialization; Turbogenerators

20020000754 National Petroleum Technology Office, Tulsa, OK USA
COA User's Guide
Fox, B.; Pautz, J.; Sellers, C.; Jan. 28, 1999; 123p; In English
Report No.(s): DE2001-3180; DOE/PC/91008-0151; No Copyright; Avail: Department of Energy Information Bridge

The Department of Energy (DOE) has one of the largest and most complete collections of information on crude oil composition that is available to the public. The computer program that manages this database of crude oil analyses has recently been rewritten to allow easier access to this information. This report describes how the new system can be accessed and how the information contained in the Crude Oil Analysis Data Bank can be obtained.

NTIS
Crude Oil; Data Bases; Computer Programs; Data Base Management Systems; User Manuals (Computer Programs)

20020000770 Lawrence Livermore National Lab., Livermore, CA USA

Characterization of Russian ballistic furnace shells

Fearon, E.; Feb. 18, 1999; 19p; In English

Report No.(s): DE2001-8497; UCRL-ID-133927; DP0211000; No Copyright; Avail: Department of Energy Information Bridge, Microfiche

The authors received another batch of polystyrene ballistic furnace shells on December 4, 1998. Assigned the batch number of LSC012, it consisted of three cassettes containing 36 shells in each cassette. A group of 27 of the shells were selected for characterization that ranged in diameter from 1880 to 1780 micrometers. There were two shells with a diameter above 1900 micrometers, but they were too fragile and did not survive initial handling. For characterization, they examined the shells through a stereo microscope, measured diameter and sphericity on RACI, and weighed a subset of the 27 shells that did not have large particles or polymer shards adhered to the outside in order to calculate wall thickness. They then selected the cleanest and most spherical shells for Sphere Mapping. This batch of shells has about the same physical appearance as the one they documented August 26, 1998. There were some shells with polymer shards adhered to the outside, a few large vacuoles or large particle embedded in the polymer wall, and some with a scattering of small black particles on the outside. There were no swirls in the shell walls. As mentioned in the previous report, each shell is measured with the RACI system in three orthogonal views. They now have new analysis software on RACI that returns the mode two amplitude of the sphere radius vs. angle of rotation around the edge of the shadowgram of the shell. From this they report the maximum radius out-of-round, the largest of the three different orientations.

NTIS

Furnaces; Shells (Structural Forms)

20020000880 Argonne National Lab., IL USA

Gas-to-liquids Synthetic Fuels for Use in Fuel Cells: Reformability, Energy density, and Infrastructure Compatibility

Ahmed, S.; Kopasz, J. P.; Russell, B. J.; Tomlinson, H. L.; Sep. 08, 1999; 8p; In English; 3rd; 3rd International Fuel Cell Conference, 11/30/1999--12/03/1999, Nagoya, Japan

Contract(s)/Grant(s): W-31109-ENG-38

Report No.(s): DE2001-11959; ANL/CMT/CP-99986; No Copyright; Avail: Department of Energy Information Bridge, Microfiche

The fuel cell has many potential applications, from power sources for electric hybrid vehicles to small power plants for commercial buildings. The choice of fuel will be critical to the pace of its commercialization. This paper reviews the various liquid fuels being considered as an alternative to direct hydrogen gas for the fuel cell application, presents calculations of the hydrogen and carbon dioxide yields from autothermal reforming of candidate liquid fuels, and reports the product gas composition measured from the autothermal reforming of a synthetic fuel in a micro-reactor. The hydrogen yield for a synthetic paraffin fuel produced by a cobalt-based Fischer-Tropsch process was found to be similar to that of retail gasoline. The advantages of the synthetic fuel are that it contains no contaminants that would poison the fuel cell catalyst, is relatively benign to the environment, and could be transported in the existing fuel distribution system.

NTIS

Fuel Cells; Liquid Fuels; Synthetic Fuels

20020000890 Argonne National Lab., IL USA

Alternatives to conventional diesel fuel-some potential implications of California's TAC decision on diesel particulate

Eberhardt, J. J.; Rote, D. M.; Saricks, C. L.; Stodolsky, F.; Aug. 10, 1999; 16p; In English

Report No.(s): DE2001-11927; ANL/ES/CP-99771; No Copyright; Avail: Department of Energy Information Bridge, Microfiche

Limitations on the use of petroleum-based diesel fuel in California could occur pursuant to the 1998 declaration by California's Air Resources Board (CARB) that the particulate matter component of diesel exhaust is a carcinogen, therefore a toxic air contaminant (TAC) subject to provisions of the state's Proposition 65. It is the declared intention of CARB not to ban or restrict diesel fuel, per se, at this time. Assuming no total ban, Argonne National Laboratory (ANL) explored two feasible 'mid-course' strategies. (1) Increased penetration of natural gas and greater gasoline use in the transportation fuels market, to the extent that some compression-ignition (CI) applications revert to spark-ignition (SI) engines. (2) New specifications requiring diesel fuel reformulation based on exhaust products of individual diesel fuel constituents. Each of these alternatives results in some degree of (conventional) diesel displacement. In the first case, diesel fuel is assumed admissible for ignition assistance as a pilot fuel in natural gas (NG)-powered heavy-duty vehicles, and gasoline demand in California increases by 32.2 million liters per day overall, about 21 percent above projected 2010 baseline demand. Natural gas demand increases by 13.6 million diesel liter equivalents per day, about 7 percent above projected (total) consumption level. In the second case, compression-ignition engines utilize

substitutes for petroleum-based diesel having similar ignition and performance properties. For each case we estimated localized air emission plus generalized greenhouse gas and energy changes. Economic implications of vehicle and engine replacement were not evaluated.
NTIS
Diesel Fuels; Clean Fuels; Air Pollution

20020001042 Department of Energy, Tulsa, OK USA
Improved Oil Recovery in Mississippian Carbonate Reservoirs of Kansas: Near-Term, Class 2
Carr, T. R.; Green, D. W.; Willhite, G. P.; Jul. 08, 1999; 68p; In English
Report No.(s): DE2001-8525; DOE/BC/14987-12; No Copyright; Avail: Department of Energy Information Bridge, Microfiche

This report describes progress during the third year of the project entitled 'Improved Oil Recovery in Mississippian Carbonate Reservoirs in Kansas'. This project funded under the Department of Energy's Class 2 program targets improving the reservoir performance of mature oil fields located in shallow shelf carbonate reservoirs. The focus of this project is development and demonstration of cost-effective reservoir description and management technologies to extend the economic life of mature reservoirs in Kansas and mid-continent. The project introduced a number of potentially useful technologies, and demonstrated these technologies in actual oil field operations. Advanced technology was tailored specifically to the scale appropriate to the operations of Kansas producers. An extensive technology transfer effort is ongoing. Traditional technology transfer methods (e.g., publications and workshops) are supplemented with a public domain relational database and an online package of project results that is available through the Internet. The goal is to provide the independent complete access to project data, project results and project technology on their desktop. Included in this report is a summary of significant project results at the demonstration site (Schaben Field, Ness County, Kansas). The value of cost-effective techniques for reservoir characterization and simulation at Schaben Field were demonstrated to independent operators. All major operators at Schaben have used results of the reservoir management strategy to locate and drill additional infill locations. At the Schaben Demonstration Site, the additional locations resulted in incremental production increases of 200 BOPD from a smaller number of wells.
NTIS
Carbonates; Oil Fields; Kansas; Oil Recovery

20020001051 Lawrence Livermore National Lab., Livermore, CA USA
Improving the Penetration of Commercial Shaped Charge Perforators
Glenn, L. A.; Apr. 01, 1999; 6p; In English
Report No.(s): DE2001-8568; UCRL-JC-134157; DP0301010; No Copyright; Avail: Department of Energy Information Bridge, Microfiche

Computational analysis demonstrated that the penetration of a shaped charge jet could be substantially enhanced by imploding the liner in a high pressure light gas atmosphere. The gas pressure helps confine the jet on the axis of penetration in the latter stages of formation. A light gas, such as helium or hydrogen, is required in order to keep the gas density low enough so as not to inhibit liner collapse. The computational analysis has now been experimentally confirmed.
NTIS
Penetration; Shaped Charges; Explosives

20020001076 National Renewable Energy Lab., Golden, CO USA
Life Cycle Assessment of Coal-fired Power Production
Spath, P. L.; Mann, M. K.; Kerr, D. R.; Sep. 01, 1999; 172p; In English
Report No.(s): DE2001-12100; NREL/TP-570-25119; No Copyright; Avail: Department of Energy Information Bridge, Microfiche

Coal has the largest share of utility power generation in the US, accounting for approximately 56% of all utility-produced electricity. Therefore, understanding the environmental implications of producing electricity from coal is an important component of any plan to reduce total emissions and resource consumption. A life cycle assessment (LCA) on the production of electricity from coal was performed in order to examine the environmental aspects of current and future pulverized coal boiler systems. Three systems were examined: (1) a plant that represents the average emissions and efficiency of currently operating coal-fired power plants in the US (this tells us about the status quo; (2) a new coal-fired power plant that meets the New Source Performance Standards (NSPS); and (3) a highly advanced coal-fired power plant utilizing a low emission boiler system (LEBS).
NTIS
Environment Effects; Coal; Electricity

20020001171 Lawrence Livermore National Lab., Livermore, CA USA

Multigrid Strategy for Accelerating Steady-State Computations of Waves Propagating with Curvature Dependent Speeds

Rochez, J. C.; Dec. 16, 1998; 11p; In English

Report No.(s): DE2001-8780; UCRL-JC-132809; No Copyright; Avail: Department of Energy Information Bridge, Microfiche

A multigrid strategy is developed for accelerating the steady state computations of waves propagating with curvature dependent speeds. This will allow the rapid computation of a burn table. In a high explosive material, the creation of a burn table will allow the elimination of solving chemical reaction ODEs and feed in source terms to the reactive flow equations for solution of the system of ignition of the high explosive material. Standard iterative methods show a quick reduction of the residual followed by a slow final convergence to the solution at high iterations. Such systems are excellent choices for the use of multigrid methods to speed up convergence, even on a nonlinear system such as this. Numerical steady-state solutions to the eikonal equation on a rectangular grid are conducted. Results are presented for a square grid in 2D and a cubic grid in 3D using a Runge-Kutta time iteration for the smoothing operator until steady-state is reached.

NTIS

Iterative Solution; Multigrid Methods; Numerical Analysis; Wave Propagation; Chemical Explosions

20020001236 Sandia National Labs., Albuquerque, NM USA

Hypervelocity Impact of Spaced Plates by a Mock Kill Vehicle

Weir, R. J.; Hertel, E. S.; Wilbeck, J.; Herwig, S.; Kilpatrick, J.; Oct. 23, 2000; 29p; In English

Report No.(s): DE2001-766569; SAND2000-2601C; No Copyright; Avail: Department of Energy Information Bridge

In support of the National Missile Defense (NMD) program, a series of Light Gas Gun (LGG) lethality tests were conducted at the Arnold Engineering Development Center (AEDC). A new projectile was designed for this test series that would be representative of aspects of a generic NMD system kill vehicle. A series of projectile development tests were performed during the design phase of the projectile. This paper reports the results from the second development show in which the projectile impacted normally against two thin aluminum target plates, spaced approximately 5.5 diameters apart. Results reported include the documentation of the damage to the first and second plates, the debris generated behind the first plate, and correlation of these with analytical and numerical predictions. Hydrocodes used for analyses included ALE3D, run by the Lawrence Livermore National Laboratory, and CTH, run by the Sandia National Laboratories. The purpose of the hydrocode analyses was to help in assessing the ability of these codes to predict the debris formation process and the target damage.

NTIS

Hypervelocity Impact; Lethality; Projectiles; Impact Strength

20020001237 Sandia National Labs., Albuquerque, NM USA

Advanced Transient Simulator for Studying Shallow Gas Blowouts

Rath, J. S.; Podio, A. L.; Oct. 24, 2000; 25p; In English

Report No.(s): DE2001-766556; SAND99-2784C; No Copyright; Avail: Department of Energy Information Bridge

Two wellbore hydraulics simulators (KICK' and COMBOF2'3) were modified to simulate high flow rate from overpressured high permeability formations in order to study the necessary reaction time to avoid a blowout event. This paper describes the computational approaches and results of calculations using these two different numerical wellbore hydraulic simulators. The coupling of the wellbore and the reservoir model is an important aspect of these simulators. The wellbore is coupled to an overpressured highly permeable zone through the use of an infuence function. An influence function is an externally generated linear system whereby a change in pseudo-pressure yields a change in cumulative gas influx (or mass flow rate). This influence function can be generated from a suitable two-phase flow reservoir simulator, prior to the wellbore hydraulic simulator calculations. The KICK numerical simulator uses a moving boundary approach to more accurately describe the multi-phase fluid mixing and transport during drilling activities. Both simulators were tied to analyze potential blowout scenarios at the Waste Isolation Pilot Plant (WIPP) transuranic waste (TRUW) repository.

NTIS

Blowouts; Boreholes; Reaction Time; Simulators; Wells

20020001238 Federal Energy Technology Center, Morgantown, WV USA

Bench-Scale Demonstration of Hot-Gas Desulfurization Technology

Gangwal, S. K.; Portzer, J. W.; Jan. 01, 2000; 15p; In English

Report No.(s): DE2001-766244; DE-AC21-93MC30010-29; No Copyright; Avail: Department of Energy Information Bridge

The US Department of Energy (DOE), Federal Energy Technology Center (FETC), is sponsoring research in advanced methods for controlling contaminants in hot coal gasifier gas (coal-derived fuel-gas) streams of integrated gasification

combined-cycle (IGCC) power systems. The hot gas cleanup work seeks to eliminate the need for expensive heat recovery equipment, reduce efficiency losses due to quenching, and minimize wastewater treatment costs.
NTIS
Coal Derived Gases; Contaminants; Desulfurizing; High Temperature Gases

20020001280 Lawrence Livermore National Lab., Livermore, CA USA
Resource recovery and reuse (R3) of explosives by conversion to higher value products
Coburn, M. D.; Lee, G. S.; Mitchell, A. R.; Pagoria, P. F.; Schmidt, R. D.; Apr. 28, 1999; 11p; In English
Report No.(s): DE2001-12230; UCRL-JC-134059; No Copyright; Avail: Department of Energy Information Bridge, Microfiche

Five million pounds of Explosive D (ammonium picrate) are available from demilitarization inventories for use in Resource Recovery and Reuse (R3) activities. Investigations on the direct conversion of Explosive D to picramide (2,4,6-trinitroaniline) are described. Studies leading to improved conversions of picramide to TATB (1,3,5- triamino-2,4,6-trinitrobenzene) using Vicarious Nucleophilic Substitution (VNS) chemistry are reported.
NTIS
Explosives; Materials Recovery; Reuse

20020001283 National Renewable Energy Lab., Golden, CO USA
Survey of the Economics of Hydrogen Technologies
Padro, C. E. G.; Putsche, V.; Sep. 14, 1999; 57p; In English
Report No.(s): DE2001-12212; NREL/TP-570-27079; No Copyright; Avail: Department of Energy Information Bridge, Microfiche

A survey of the economics of hydrogen production, storage, transport, and end-use technologies has been completed. More than 100 publications concerning the economics of current and near-term hydrogen technologies were surveyed. Technologies more than 20 years from commercialization were not considered.
NTIS
Hydrogen Production; Economics

20020001284 Pacific Northwest National Lab., Richland, WA USA
Regeneration of Hydrotreating and FCC Catalysts
Wai, C. M.; Frye, J. G.; Fulton, J. L.; Bowman, L. E.; Silva, L. J.; Sep. 30, 1999; 58p; In English
Report No.(s): DE2001-12208; PNNL-13025; No Copyright; Avail: Department of Energy Information Bridge, Microfiche

Hydrotreating, hydrocracking, and fluid catalytic cracking (FCC) catalysts are important components of petroleum refining processes. Hydrotreating and hydrocracking catalysts are used to improve the yield of high-quality light oil fractions from heavier crude oil and petroleum feedstocks containing high levels of impurities. FCC catalysts improve the yield of higher octane gasoline from crude oil. Residuum hydrotreating and cracking catalysts are susceptible to irreversible deactivation caused by adsorption of sulfur and by metals impurities, such as vanadium and nickel. The gradual buildup of these impurities in a hydrotreating catalyst eventually plugs the pores and deactivates it. Nickel and vanadium adversely affect the behavior of cracking catalysts, reducing product yield and quality. Replacing deactivated catalysts represents a significant cost in petroleum refining. Equally important are the costs and potential liabilities associated with treating and disposing spent catalysts. For example, recent US Environmental Protection Agency rulings have listed spent hydrotreating and hydrorefining catalysts as hazardous wastes. FCC catalysts, though more easily disposed of as road-base or as filler in asphalt and cement, are still an economic concern mainly because of the large volumes of spent catalysts generated. New processes are being considered to increase the useful life of catalysts or for meeting more stringent disposal requirements for spent catalysts containing metals. This report discusses a collaborative effort between Pacific Northwest National Laboratory (PNNL) and Phillips Petroleum, Inc., to identify promising chemical processes for removing metals adhered to spent hydrodesulfurization (HDS, a type of hydrotreating catalyst) and FCC catalysts. This study, conducted by PNNL, was funded by the US Department of Energy's Bartlesville Project Office. Fresh and spent catalysts were provided by Phillips Petroleum. The FCC catalyst was a rare-earth exchanged Y zeolite in a silica-alumina matrix. X-ray fluorescence analyses showed that the rare earths used in preparing the catalysts were a mixture of lanthanum and cerium. Antimony found in the spent catalyst was added during operation of the FCC unit as a way to suppress the adverse effects of deposited nickel. The fresh HDS samples consisted of sulfided nickel and molybdenum on an alumina support. The spent catalyst showed nearly 10% vanadium on the catalyst and a modest increase in nickel and sulfur on the catalyst as a result of operations. Hydrocracking catalysts were not available for this study.
NTIS
Hydrocracking; Catalysts; Crude Oil; Impurities; Deactivation

20020001285 Lawrence Livermore National Lab., Livermore, CA USA

CRT compatibility evaluation of LX-16 and Halthane 73-18

Foltz, M. F.; Foster, P. A.; Mar. 26, 1999; 7p; In English

Report No.(s): DE2001-12207; UCRL-JC-133765; No Copyright; Avail: Department of Energy Information Bridge, Microfiche

A preliminary compatibility study was carried out between the plastic-bonded PETN- based high explosive LX-16 and the adhesive Halthane 73-l 8. The work, based on the Chemical Reactivity Test (CRT), used non-standard times and temperatures to find conditions corresponding to accelerated decomposition. This study is a prequel to a more comprehensive isothermal and thermal cycling study that will include both material evaluation and test tire.

NTIS

Adhesives; Explosives; Decomposition

20020001571 Argonne National Lab., IL USA

Impactt5a model: Enhancements and modifications since December 1994 with special reference to the effect of tripled-fuel-economy vehicles on fuel-cycle energy and emissions

Mintz, M. M.; Saricks, C. L.; Aug. 28, 1999; 85p; In English

Report No.(s): DE2001-12053; ANL/ESD/TM-154; No Copyright; Avail: Department of Energy Information Bridge

Version 5A of the Integrated Market Penetration and Anticipated Cost of Transportation Technologies (IMPACTT5A) model is a spreadsheet-based set of algorithms that calculates the effects of advanced-technology vehicles on baseline fuel use and emissions. Outputs of this Argonne National Laboratory-developed model include estimates of (1) energy use and emissions attributable to conventional-technology vehicles under a baseline scenario and (2) energy use and emissions attributable to advanced- and conventional-technology vehicles under an alternative market-penetration scenario. Enhancements to IMPACTT made after its initial documentation in December 1994 have enabled it to deal with a wide range of fuel and propulsion system technologies included in Argonne's GREET model in a somewhat modified three-phased approach. Vehicle stocks are still projected in the largely unchanged STOCK module. Vehicle-miles traveled, fuel use, and oil displacement by advanced-technology vehicles are projected in an updated USAGE module. Now, both modules can incorporate vehicle efficiency and fuel share profiles consistent with those of the Partnership for a New Generation of Vehicles. Finally, fuel-cycle emissions of carbon monoxide, volatile organic compounds, nitrogen oxides, toxics, and greenhouse gases are computed in the EMISSIONS module via an interface with the GREET model that was developed specifically to perform such calculations. Because of this interface, results are now more broadly informative than were results from earlier versions of IMPACTT.

NTIS

Fuel Consumption; Automobiles; Fuel Systems

20020001575 Argonne National Lab., IL USA

Assessment of PNGV fuels infrastructure phase 2 report: Additional capital needs and fuel-cycle energy and emissions impacts

Johnson, L.; Mintz, M.; Singh, M.; Stork, K.; Vyas, A.; Oct. 14, 1998; 184p; In English

Report No.(s): DE2001-12046; ANL/ESD-37; No Copyright; Avail: Department of Energy Information Bridge

This report documents the methodologies and results of Argonne National Laboratory's assessment of additional capital needs and fuel-cycle energy and emission impacts associated with using various fuels in vehicles that are three times as fuel-efficient as today's typical light-duty vehicles. These "3X vehicles" are being developed in the Partnership for a New Generation of Vehicles (PNGV) program. In 1994, the National Research Council's Peer Review Committee on the PNGV program called for an assessment of the potential impacts of 3X vehicles on the fuel infrastructure. In response, the U.S. Department of Energy (DOE) tasked Argonne National Laboratory (ANL) to investigate these impacts. In August 1995, the results of the first phase of Argonne's analysis were published. The second phase of Argonne's analysis, which covers additional fuels and issues identified during the phase 1 effort, is documented in this report.

NTIS

Fuels; Automobiles; Energy Conversion Efficiency

20020001832 Argonne National Lab., IL USA

Stable Isotope Investigations of Chlorinated Aliphatic Hydrocarbons

Abrajano, T.; Heraty, L. J.; Holt, B. D.; Huang, L.; Sturchio, N. C.; Jun. 01, 1999; 7p; In English

Report No.(s): DE2001-11823; ANL/ER/CP-99091; No Copyright; Avail: Department of Energy Information Bridge

Stable isotope ratio measurements for carbon and chlorine can be used to elucidate the processes affecting transformation and transportation of chlorinated aliphatic hydrocarbons (CAHs) in the environment. Methods recently developed in our

laboratory for isotopic analysis of CAHs have been applied to laboratory measurements of the kinetic isotope effects associated with aerobic degradation of dichloromethane (DCM) and with both anaerobic and aerobic cometabolic degradation of trichlomethene (TCE) in batch and column microbial cultures. These experimental determinations of fractionation factors are crucial for understanding the behavior of CAHs in complex natural systems, where the extent of biotransformation can be masked by dispersion and volatilization. We have also performed laboratory investigations of kinetic isotope effects accompanying evaporation of CAHs, as well as field investigations of natural attenuation and in situ remediation of CAHs in a number of contaminated shallow aquifers at sites operated by the federal government and the private sector.
NTIS
Chemical Fractionation; Isotope Effect; Aliphatic Hydrocarbons; Isotope Ratios

20020001890 Argonne National Lab., IL USA
Gasoline-Fueled Hybrid Versus Conventional Vehicle Emissions and Fuel Economy
Anderson, J.; Bharathan, D.; He, J.; Plotkin, S.; Santini, D.; Jun. 18, 1999; 24p; In English
Report No.(s): DE2001-11854; ANL/ES/CP-99264; No Copyright; Avail: Department of Energy Information Bridge

This paper addresses the relative fuel economy and emissions behavior, both measured and modeled, of technically comparable, contemporary hybrid and conventional vehicles fueled by gasoline, in terms of different driving cycles. Criteria pollutants (hydrocarbons, carbon monoxide, and nitrogen oxides) are discussed, and the potential emissions benefits of designing hybrids for grid connection are briefly considered. In 1997, Toyota estimated that their grid-independent hybrid vehicle would obtain twice the fuel economy of a comparable conventional vehicle on the Japan 10/15 mode driving cycle. This initial result, as well as the fuel economy level (66 mpg), made its way into the US press. Criteria emissions amounting to one-tenth of Japanese standards were cited, and some have interpreted these results to suggest that the grid-independent hybrid can reduce criteria emissions in the US more sharply than can a conventional gasoline vehicle. This paper shows that the potential of contemporary grid-independent hybrid vehicle technology for reducing emissions and fuel consumption under US driving conditions is less than some have inferred. The importance (and difficulty) of doing test and model assessments with comparable driving cycles, comparable emissions control technology, and comparable performance capabilities is emphasized. Compared with comparable-technology conventional vehicles, grid-independent hybrids appear to have no clear criteria pollutant benefits (or disbenefits). (Such benefits are clearly possible with grid-connectable hybrids operating in zero emissions mode.) However, significant reductions in greenhouse gas emissions (i.e., fuel consumption) are possible with hybrid vehicles when they are used to best advantage.
NTIS
Exhaust Emission; Exhaust Gases; Fuel Consumption; Electric Hybrid Vehicles

20020002279 Sandia National Labs., Albuquerque, NM USA
Analysis of Subsidence Data for the Big Hill Site, Texas
Bauer, S. J.; Jun. 01, 1999; 22p; In English
Report No.(s): DE2001-8849; SAND99-1478; No Copyright; Avail: Department of Energy Information Bridge, Microfiche

The elevation change data measured at the Big Hill SPR site over the last 10 years has been studied and a model utilized to project elevation changes into the future. The subsidence rate at Big Hill is low in comparison with other Strategic Petroleum Reserve sites and has decreased with time due to the maintenance of higher operating pressures and the normal decrease in creep closure rate of caverns with time. However, the subsidence at the site is projected to continue. A model was developed to project subsidence values 20 years into the future; no subsidence related issues are apparent from these projections.
NTIS
Crude Oil; Creep Properties; Elevation; Subsidence

20020002718 Federal Energy Technology Center, Morgantown, WV USA
Oxidative coupling of methane using inorganic membrane reactors
Ma, Y. H.; Moser, W. R.; Dixon, A. G.; Ramachandra, A. M.; Lu, Y.; Apr. 01, 1998; 365p; In English
Report No.(s): DE2001-766717; DE-AC22-92PC92113-22; No Copyright; Avail: Department of Energy Information Bridge

The objective of this research is to study the oxidative coupling of methane in catalytic inorganic membrane reactors. A specific target is to achieve conversion of methane to C2 hydrocarbons at very high selectivity and higher yields than in conventional non-porous, co-feed, fixed bed reactors by controlling the oxygen supply through the membrane. A membrane reactor has the advantage of precisely controlling the rate of delivery of oxygen to the catalyst. This facility permits balancing the rate of oxidation and reduction of the catalyst. In addition, membrane reactors minimize the concentration of gas phase oxygen thus reducing non selective gas phase reactions, which are believed to be a main route for the formation of COx products. Such

gas phase reactions are a cause of decreased selectivity in the oxidative coupling of methane in conventional flow reactors. Membrane reactors could also produce higher product yields by providing better distribution of the reactant gases over the catalyst than the conventional plug flow reactors. Membrane reactor technology also offers the potential for modifying the membranes both to improve catalytic properties as well as to regulate the rate of the permeation/diffusion of reactants through the membrane to minimize by-product generation. Other benefits also exist with membrane reactors, such as the mitigation of thermal hot-spots for highly exothermic reactions such as the oxidative coupling of methane. The application of catalytically active inorganic membranes has potential for drastically increasing the yield of reactions which are currently limited by either thermodynamic equilibria, product inhibition, or kinetic selectivity.
NTIS
Exothermic Reactions; Membranes; Methane; Oxidation; Reactor Technology; Coupling

20020003390 Federal Energy Technology Center, Morgantown, WV USA
Novel CO2 separation system
Copeland, R. J.; Alptekin, G.; Cesario, M.; Gebhard, S.; Gershanovich, Y.; Jan. 01, 1999; 133p; In English
Report No.(s): DE2001-766698; DE-AC26-98FT40421-01; No Copyright; Avail: Department of Energy Information Bridge, Microfiche

Because of concern over global climate change, new systems are needed that produce electricity from fossil fuels and emit less CO2. The fundamental problem with current CO2 separation systems is the need to separate dilute CO2 and pressurize it for storage or sequestration. This is an energy intensive process that can reduce plant efficiency by 9-37% and double the cost of electricity.
NTIS
Fossil Fuels; Carbon Dioxide; Electricity; Climate Change

20020003823 Argonne National Lab., IL USA
Rate-limiting step for alkane dehydrogenation in zeolite H-ZSM-5
Zygmunt, S. A.; Bootz, B. L.; Miller, A. W.; Curtiss, L. A.; Iton, L. E.; Nov. 01, 2000; 4p; In English
Report No.(s): DE2001-768593; ANL/MSD/CP-103180; No Copyright; Avail: Department of Energy Information Bridge, Microfiche

We have carried out a computational study of protolytic cracking, dehydrogenation, and H/D exchange of ethane, propane, and butane using a cluster model of H-ZSM-5. Our previous work has demonstrated that quantum-chemical techniques can give quantitatively accurate activation energies for alkane cracking in zeolites. Experimental kinetic studies have shown that the apparent activation energies for cracking and H/D exchange decrease with n-alkane chain length, while for dehydrogenation the energies increase. Our goal is to study the dependence of the activation energy on the alkane chain length in these reactions and to understand why the dehydrogenation reaction behaves so differently.
NTIS
Alkanes; Dehydrogenation; Zeolites; Reaction Kinetics

20020003824 Argonne National Lab., IL USA
Toward a reliable computational description of hydrocarbon activation in zeolites: a study of cracking, dehydrogenation, and H/D Exchange of alkanes in H-ZSM-5
Zygmunt, S. A.; Bootz, B. L.; Miller, A. W.; Curtiss, L. A.; Iton, L. E.; Nov. 01, 2000; 4p; In English
Report No.(s): DE2001-768592; ANL/MSD/CP-103177; No Copyright; Avail: Department of Energy Information Bridge, Microfiche

During the past decade, quantum-chemical calculations have been used to model hydrocarbon reactions in zeolite acid catalysts. In the interest of computational feasibility, the zeolite has often been represented by a very small cluster model, at times including only one tetrahedrally-coordinated atom (a 1T cluster). The results of such calculations have given important qualitative insights such as possible reaction pathways and transition state geometries, but the calculated activation energies for hydrocarbon reactions have usually been 50 percent or more higher than experimental values. In our recent work we developed a methodology of quantum-chemical techniques and corrections that allowed us to calculate a quantitatively accurate activation energy for protolytic cracking of ethane in H-ZSM-5. In order to test the limits of our computational method, we have carried out a study of protolytic cracking, dehydrogenation, and H/D exchange of the n-alkanes ethane, propane, and butane using a cluster model

of H-ZSM-5. Our goal is to study the dependence of the activation energy on the alkane chain length in these reactions and to determine whether this method can produce results in quantitative agreement with available experimental results (2-5).
NTIS
Hydrocarbons; Zeolites; Dehydrogenation; Cracking (Chemical Engineering)

20020003987 Florida Solar Energy Center, Cape Canaveral, FL USA
Sustainable hydrogen production ***Final Report***
Linkous, C.; Slattery, D.; Kopitzke, R.; Muradov, N.; Jun. 30, 1999; 165p; In English
Report No.(s): DE2001-763086; FSEC-CR-1093-99; DOE/GO/10062-F; No Copyright; Avail: Department of Energy Information Bridge, Microfiche

Our objective in this work was to develop an efficient, affordable, direct photoconversion scheme for generating Hz from water using sunlight. We sought to find an alternative to the traditional photoelectrochemical cell configuration, with the idea of maintaining low module construction costs. Our approach was to use semiconductor powders in a dud bed configuration, breaking down the energy requirement for water splitting into a 2-photon process, and enabling separate production of H2 and O2. The photocatalytic system would employ two modules, each consisting of a shallow, flat, sealed container, in which micron-sized photocatalytic particles are immobilized. An aqueous solution containing a redox mediator is pumped between the two chambers. Different photoparticles and catalysts are chosen for their respective modules so as to effect oxidative water-splitting in one vessel to evolve oxygen gas, and reductive water-splitting in the other to evolve hydrogen.
NTIS
Hydrogen Production; Catalysts; Microparticles; Oxidation-Reduction Reactions; Photoelectrochemical Devices; Sunlight; Water Splitting

20020003988 Oklahoma Univ., Norman, OK USA
Novel catalytic approaches for hydrogen production (Photocatalytic water splitting) ***Final Report, 16 May 1997 - 15 May 1999***
Mallinson, R. G.; Resasco, D. E.; Nicholas, K. M.; Lobban, L. L.; May 15, 1999; 119p; In English
Report No.(s): DE2001-763081; DOE/GO/10141-F; No Copyright; Avail: Department of Energy Information Bridge, Microfiche

Efficient hydrogen production via photolysis of water has been the focus of the current study. Water splitting experiments have been performed under visible and ultraviolet irradiation. Experiments under ultraviolet irradiation involved metal-semiconductor photocatalysts and visible irradiation experiments were performed with sensitized photocatalysts.
NTIS
Photolysis; Hydrogen Production; Water

20020003997 Federal Energy Technology Center, Morgantown, WV USA
Pillared clays as superior catalysts for selective catalytic reduction of nitric oxide
Long, R. Q.; Yang, R. T.; Sep. 30, 1998; 38p
Contract(s)/Grant(s): FG22-96PC96206
Report No.(s): DE2001-7736; DE-FG22-96PC96206-04; No Copyright; Avail: Department of Energy Information Bridge, Microfiche

Selective catalytic reduction (SCR) of NO(sub x) by hydrocarbons was investigated on Pt doped MCM-41 and copper ion and/or cerium ion-exchanged Al-MCM-41 in the presence of excess oxygen. It was found that Pt/MCM-41 provided the highest specific NO reduction rates as compared with other Pt doped catalysts reported in the literature, such as Pt/Al(sub 2)O(sub 3) and Pt/ZSM-5. For different hydrocarbons, the catalytic activity decreased according to the sequence of C(sub 3)H(sub 6) (approx) C(sub 2)H(sub 4) C(sub 3)H(sub 8)CH(sub 4). This catalyst was also stable in the presence of H(sub 2)O and SO(sub 2). Cu exchanged Al-MCM-41 and cerium promoted Cu-Al-MCM-41 (i.e., Ce-Cu-Al-MCM-41) were also found to be active in this reaction. Higher NO(sub x) conversions to N2 were obtained on the Ce-Cu-Al-MCM-41 as compared with Cu-Al-MCM-41. The activity of Ce-Cu-Al-MCM-41 was approximately the same as that of Cu-ZSM-5; but the former had a wider temperature window. TPR results indicated that only isolated Cu(sup 2+) and Cu(sup +) ions were detected in the Cu(sup 2+)-exchanged Al-MCM-41 samples, which may play an important role in the selective catalytic reduction of NO(sub x) to N(sub 2). After some cerium ions were introduced into Cu-Al-MCM-41, Cu(sup 2+) in the molecular sieve became more easily reducible by H(sub 2). This may be related to the increase of catalytic activity of NO(sub x) reduction by ethylene.
NTIS
Catalysts; Clays; Nitric Oxide; Reduction (Chemistry)

20020004000 Federal Energy Technology Center, Morgantown, WV USA

Development of advanced hot-gas desulfurization processes

Jothimurugesan, K.; Apr. 26, 1999; 14p; In English

Report No.(s): DE2001-773441; FG26-97FT97276-03; No Copyright; Avail: Department of Energy Information Bridge, Microfiche

Advanced integrated gasification combined cycle (IGCC) power plants nearing completion, such as Sierra-Pacific, employ a circulating fluidized-bed (transport) reactor hot-gas desulfurization (HGD) process that uses 70-180 (micro)m average particle size (aps) zinc-based mixed-metal oxide sorbent for removing H(sub 2)S from coal gas down to less than 20 ppmv. The sorbent undergoes cycles of absorption (sulfidation) and air regeneration. The key barrier issues associated with a fluidized-bed HGD process are chemical degradation, physical attrition, high regeneration light-off (initiation) temperature, and high cost of the sorbent. Another inherent complication in all air-regeneration-based HGD processes is the disposal of the problematic dilute SO(sub 2) containing regeneration tail-gas. Direct Sulfur Recovery Process (DSRP), a leading first generation technology, efficiently reduces this SO(sub 2) to desirable elemental sulfur, but requires the use of 1-3% of the coal gas, thus resulting in an energy penalty to the plant. Advanced second-generation processes are under development that can reduce this energy penalty by modifying the sorbent so that it could be directly regenerated to elemental sulfur. The objective of this research is to support the near and long term DOE efforts to commercialize the IGCC-HGD process technology. Specifically we aim to develop: optimized low-cost sorbent materials with 70-80 (micro)m average aps meeting all Sierra specs; attrition resistant sorbents with 170 (micro)m aps that allow greater flexibility in the choice of the type of fluidized-bed reactor e.g. they allow increased throughput in a bubbling-bed reactor; and modified fluidizable sorbent materials that can be regenerated to produce elemental sulfur directly with minimal or no use of coal gas. The effort during the reporting period has been devoted to development of optimized low-cost zinc-oxide-based sorbents for Sierra-Pacific. The sorbent surface were modified to prevent sintering during pure air regeneration. Modifications were made to the sorbent to increase its ability to withstand high temperature and prevent loss of capacity by utilizing various textural promoters. Also several modified zinc-based sorbents prepared that can be regenerated to produce elemental sulfur directly with minimal use of coal gas.

NTIS

Coal Derived Gases; Desulfurizing; Fluidized Bed Processors

20020004665 Weyerhaeuser Co., Tacoma, WA USA

Biomass Gasification Combined Cycle

Kieffer, J. A.; Jul. 01, 2000; 184p; In English

Report No.(s): DE2001-769196; DOE/GO/10173; No Copyright; Avail: Department of Energy Information Bridge, Microfiche

Gasification combined cycle continues to represent an important defining technology area for the forest products industry. The 'Forest Products Gasification Initiative', organized under the Industry's Agenda 2020 technology vision and supported by the DOE "Industries of the Future" program, is well positioned to guide these technologies to commercial success within a five-to ten-year timeframe given supportive federal budgets and public policy. Commercial success will result in significant environmental and renewable energy goals that are shared by the Industry and the Nation. The Battelle/FERCO LIVG technology, which is the technology of choice for the application reported here, remains of high interest due to characteristics that make it well suited for integration with the infrastructure of a pulp production facility. The capital cost, operating economics and long-term demonstration of this technology area key input to future economically sustainable projects and must be verified by the 200 BDT/day demonstration facility currently operating in Burlington, Vermont. The New Bern application that was the initial objective of this project is not currently economically viable and will not be implemented at this time due to several changes at and around the mill which have occurred since the inception of the project in 1995. The analysis shows that for this technology, and likely other gasification technologies as well, the first few installations will require unique circumstances, or supportive public policies, or both to attract host sites and investors.

NTIS

Biomass; Cycles; Forests; Gasification

20020004667 Oak Ridge National Lab., TN USA

Systems Studies

Graham, R. L.; Mar. 17, 1998; 15p; In English

Report No.(s): DE2001-772465; P00-108385; No Copyright; Avail: Department of Energy Information Bridge, Microfiche

The Systems Studies Activity had two objectives: (1) to investigate nontechnical barriers to the deployment of biomass production and supply systems and (2) to enhance and extend existing systems models of bioenergy supply and use. For the first objective, the Activity focused on existing bioenergy markets. Four projects were undertaken: a comparative analysis of bioenergy

in Sweden and Austria; a one-day workshop on nontechnical barriers jointly supported by the Production Systems Activity; the development and testing of a framework for analyzing barriers and drivers to bioenergy markets; and surveys of wood pellet users in Sweden, Austria and the US. For the second objective, two projects were undertaken. First, the Activity worked with the Integrated BioEnergy Systems (IBS) Activity of TEA Bioenergy Task XIII to enhance the BioEnergy Assessment Model (BEAM). This model is documented in the final report of the IBS Activity. The Systems Studies Activity contributed to enhancing the feedstock portion of the model by developing a coherent set of willow, poplar, and switchgrass production modules relevant to both the US and the UK. The Activity also developed a pretreatment module for switchgrass. Second, the Activity sponsored a three-day workshop on modeling bioenergy systems with the objectives of providing an overview of the types of models used to evaluate bioenergy and promoting communication among bioenergy modelers. There were nine guest speakers addressing different types of models used to evaluate different aspects of bioenergy, ranging from technoeconomic models based on the ASPEN software to linear programming models to develop feedstock supply curves for the US. The papers from this workshop have been submitted to Biomass and Bioenergy and are under editorial review.
NTIS
Biomass; Biomass Energy Production; Models

20020004670 Oak Ridge National Lab., TN USA
Bioenergy Status and Expansion in the USA
Wright, L. L.; Jan. 10, 2001; 10p; In English; 1999 Meeting of International Energy Agency - Task 17: Production of Short Rotation Biomass Crops, 6-9 Sept. 1999, Auburn, AL, USA
Contract(s)/Grant(s): AC05-96OR22464
Report No.(s): DE2001-774470; P00-107157; No Copyright; Avail: Department of Energy Information Bridge, Microfiche

The U.S. is a large consumer and producer of energy. Current energy consumption is about 100 EJ with bioenergy providing 3 percent of the total. The U.S. President has charged the Departments of Energy and Agriculture and the Environmental Protection Agency to modify and coordinate their programs to promote an increase by 3 times the amount of biobased products and bioenergy produced in 2010. Legislative actions are also supporting increased bioenergy research and modification of tax incentives to encourage increased bioenergy commercialization. Development of biomass power production technologies and biomass liquid fuels production is being pursued through separate programs with the U.S. Department of Energy (DOE). Each program has differing needs and expectations for biomass feedstock research. The Bioenergy Feedstock Development Program (BFDP) integrates the feedstock needs of both programs. Research is addressing near-term, mid-term and long-term goals simultaneously. Development of new crops and cropping technology comprises the largest component of the current program. More emphasis is being placed on residues, both agricultural and urban, to meet near-term bioenergy goals.
NTIS
Fuels; Fuel Production; Bioconversion; Biomass

20020004917 Atomic Energy Commission, Idaho Falls, ID USA
Thermal Conversion of Methane to Acetylene Final Report
Fincke, J. R.; Anderson, R. P.; Hyde, T.; Wright, R.; Bewley, R.; Jan. 31, 2000; 69p; In English
Report No.(s): DE2001-774309; INEEL/EXT-99-01378; No Copyright; Avail: Department of Energy Information Bridge, Microfiche

This report describes the experimental demonstration of a process for the direct thermal conversion of methane to acetylene. The process utilizes a thermal plasma heat source to dissociation products react to form a mixture of acetylene and hydrogen. The use of a supersonic expansion of the hot gas is investigated as a method of rapidly cooling (quenching) the product stream to prevent further reaction or thermal decomposition of the acetylene which can lower the overall efficiency of the process.
NTIS
Energy Conversion; Methane; Acetylene

20020004918 National Renewable Energy Lab., Golden, CO USA
SuperShuttle CNG Fleet Evaluation *Final Report*
Eudy, L.; Dec. 07, 2000; 52p; In English
Report No.(s): DE2001-772435; NREL/TP-540-29226; No Copyright; Avail: Department of Energy Information Bridge

The mission of the US Department of Energy's (DOE) Office of Transportation Technologies is to promote the development and deployment of transportation technologies that reduce US dependence on foreign oil, while helping to improve the nation's air quality and promoting US competitiveness. In support of this mission, DOE has directed the National Renewable Energy Laboratory (NREL) to conduct projects to evaluate the performance and acceptability of alternative fuel vehicles (AFV). NREL

has undertaken several fleet study projects, which seek to provide objective real-world fleet experiences with AFVs. For this type of study we collect, analyze, and report on operational, cost, emissions, and performance data from AFVs being driven in a fleet application. The primary purpose of such studies is to make real-world information on AFVs available to fleet managers and other potential AFV purchasers. For this project, data was collected from 13 passenger vans operating in the Boulder/Denver, Colorado area. The study vehicles were all 1999 Ford E-350 passenger vans based at SuperShuttle's Boulder location. Five of the vans were dedicated CNG (compressed natural gas), five were bi-fuel CNG/gasoline, and three were standard gasoline vans that were used for comparison.
NTIS
Air Quality; Clean Fuels; Renewable Energy; Natural Gas; Automobiles

20020005139 Oak Ridge National Lab., TN USA
Economic Analysis of Energy Crop Production in the U.S.: Location, Quantities, Price, and Impacts on Traditional Agricultural Crops
Walsh, M. E.; De La Torre Ugarte, D.; Slinsky, S.; Graham, R. L.; Shapouri, H.; Oct. 04, 1998; 10p; In English
Report No.(s): DE2001-772462; P00-108388; No Copyright; Avail: Department of Energy Information Bridge, Microfiche

POLYSYS is used to estimate US locations where, for any given energy crop price, energy crop production can be economically competitive with conventional crops. POLYSYS is a multi-crop, multi-sector agricultural model developed and maintained by the University of Tennessee and used by the USDA (US Department of Agriculture)-Economic Research Service. It includes 305 agricultural statistical districts (ASD) which can be aggregated to provide state, regional, and national information. POLYSYS is being modified to include switchgrass, hybrid poplar, and willow on all land suitable for their production. This paper summarizes the preliminary national level results of the POLYSYS analysis for selected energy crop prices for the year 2007 and presents the corresponding maps (for the same prices) of energy crop production locations by ASD. Summarized results include: (1) estimates of energy crop hectares (acres) and quantities (dry Mg, dry tons), (2) identification of traditional crops allocated to energy crop production and calculation of changes in their prices and hectares (acres) of production, and (3) changes in total net farm returns for traditional agricultural crops. The information is useful for identifying areas of the US where large quantities of lowest cost energy crops can most likely be produced.
NTIS
Biomass; Agriculture; Economic Analysis; Computer Programs; Evaluation; Models

20020005175 California Univ., Lawrence Berkeley Lab., Berkeley, CA USA
Melvin Calvin: Fuels from Plants
Taylor, S. E.; Otvos, J. W.; Nov. 24, 1998; 22p; In English
Report No.(s): DE2001-7286; LBNL-41469; No Copyright; Avail: Department of Energy Information Bridge

A logical extension of his early work on the path of carbon during photosynthesis, Calvin's studies on the production of hydrocarbons by plants introduced many in the scientific and agricultural worlds to the potential of renewable fuel and chemical feedstocks. He and his co-workers identified numerous candidate compounds from plants found in tropical and temperate climates from around the world. His travels and lectures concerning the development of alternative fuel supplies inspired laboratories worldwide to take up the investigation of plant-derived energy sources as an alternative to fossil fuels.
NTIS
Hydrocarbons; Photosynthesis; Fuels; Biomass

20020005211 Federal Energy Technology Center, Morgantown, WV USA
Synthesis of methyl methacrylate from coal-derived syngas
Jang, B. W. L.; Choi, G. N.; Spivey, J. J.; Zoeller, J. R.; Colberg, R. D.; Oct. 20, 1998; 16p; In English
Report No.(s): DE2001-7702; DE-AC22-94PC94065-17; No Copyright; Avail: Department of Energy Information Bridge, Microfiche

Research Triangle Institute (RTI), Eastman Chemical Company, and Bechtel collectively are developing a novel three-step process for the synthesis of methyl methacrylate (MMA) from coal-derived syngas that consists of the steps of synthesis of a propionate, its condensation with formaldehyde to form methacrylic acid (MAA), and esterification of MAA with methanol to produce MMA. RTI has completed the research on the three-step methanol-based route to MMA. Under an extension to the original contract, RTI is currently evaluating a new DME-based process for MMA. The key research need for DME route is to develop catalysts for DME partial oxidation reactions and DME condensation reactions. Over the last quarter (July-September, 1998), the project team has completed the continuous condensation of formaldehyde with propionic acid over 10% Nb2O5/SiO2 at 300 C. Six activity and five regeneration cycles have been completed. The results show that 10% Nb2O5/SiO2 deactivates

slowly with time but can be regenerated to its original activity with 2% O2 in nitrogen over night at 400 C. We have investigated the effects of regeneration, propionic acid/formaldehyde ratio (PA/HCHO = 4.5/1 to 1.5/1) and reaction temperature(280-300 C) on reaction activity and product selectivity over 20% Nb2O5/SiO2 catalysts. The regeneration effect on 20% Nb2O5/SiO2 is similar to the effect on 10% Nb2O5/SiO2. The regeneration can bring the deactivated catalyst to its original activity. However, the selectivity to MAA decreases with regeneration while the selectivity to DEK and CO2 increases. When PA/HCHO ratio is decreased from 4.5/1 to 2.25/1 then to 1.5/1 at 300 C the MAA yield decreases but the MAA selectivity first increases then decreases. Decreasing the reaction temperature from 300 C to 280 C decreases the MAA yield from 39.5% to 30.7% but increases the MAA selectivity from 73.7% to 82.2%. The results indicate that both temperature and PA/HCHO ratio are important parameters to optimize the economic of the condensation between propionic acid and formaldehyde.
NTIS
Esters; Synthesis (Chemistry); Methyl Compounds; Technology Assessment; Propionic Acid

20020005212 Federal Energy Technology Center, Morgantown, WV USA
Engineering evaluation of hot-gas desulfurization with sulfur recovery
Roberts, G. W.; Portzer, J. W.; Kozup, S. C.; Gangwal, S. K.; May 31, 1998; 161p; In English
Report No.(s): DE2001-7703; DE-AC21-94MC31258-19; No Copyright; Avail: Department of Energy Information Bridge, Microfiche

Engineering evaluations and economic comparisons of two hot-gas desulfurization (HGD) processes with elemental sulfur recovery, being developed by Research Triangle Institute, are presented. In the first process, known as the Direct Sulfur Recovery Process (DSRP), the SO(sub 2) tail gas from air regeneration of zinc-based HGD sorbent is catalytically reduced to elemental sulfur with high selectivity using a small slipstream of coal gas. DSRP is a highly efficient first-generation process, promising sulfur recoveries as high as 99% in a single reaction stage. In the second process, known as the Advanced Hot Gas Process (AHGP), the zinc-based HGD sorbent is modified with iron so that the iron portion of the sorbent can be regenerated using SO(sub 2). This is followed by air regeneration to fully regenerate the sorbent and provide the required SO(sub 2) for iron regeneration. This second-generation process uses less coal gas than DSRP. Commercial embodiments of both processes were developed. Process simulations with mass and energy balances were conducted using ASPEN Plus. Results show that AHGP is a more complex process to operate and may require more labor cost than the DSRP. Also capital costs for the AHGP are higher than those for the DSRP. However, annual operating costs for the AHGP appear to be considerably less than those for the DSRP with a potential break-even point between the two processes after just 2 years of operation for an integrated gasification combined cycle (IGCC) power plant using 3 to 5 wt% sulfur coal. Thus, despite its complexity, the potential savings with the AHGP encourage further development and scaleup of this advanced process.
NTIS
Sulfur; Regeneration (Engineering); High Temperature Gases; Catalytic Activity

20020005216 National Renewable Energy Lab., Golden, CO USA
Overview of Biodiesel and Petroleum Diesel Life Cycles
Sheehan, J.; Camobreco, V.; Duffield, J.; Shapouri, H.; Graboski, M.; Apr. 27, 2000; 60p; In English
Report No.(s): DE2001-771560; NREL/TP-580-24772; No Copyright; Avail: Department of Energy Information Bridge

This report presents the findings from a study of the life cycle inventories for petroleum diesel and biodiesel. It presents information on raw materials extracted from the environment, energy resources consumed, and air, water, and solid waste emissions generated.
NTIS
Solid Wastes; Diesel Fuels; Crude Oil

20020005219 California Univ., Lawrence Berkeley Lab., Berkeley, CA USA
Biomass power and state renewable energy policies under electric industry restructuring
Porter, K.; Wiser, R.; Aug. 01, 2000; 12p; In English
Report No.(s): DE2001-771940; LBNL-46948; No Copyright; Avail: Department of Energy Information Bridge

Several states are pursuing policies to foster renewable energy as part of efforts to restructure state electric power markets. The primary policies that states are pursuing for renewables are system benefits charges (SBCs) and renewable portfolio standards (RPSs). However, the eligibility of biomass under state RPS and SBC policies is in question in some states. Eligibility restrictions may make it difficult for biomass power companies to access these policies. Moreover, legislative language governing the eligibility of biomass power is sometimes vague and difficult to interpret. This paper provides an overview of state RPS and SBC

policies and focuses on the eligibility of biomass power. For this paper, the authors define biomass power as using wood and agricultural residues and landfill methane, but not waste-to-energy, to produce energy.
NTIS
Biomass; Energy Policy; Renewable Energy; Industries

20020005225 National Renewable Energy Lab., Golden, CO USA
Environmental Life Cycle Implications of Using Bagasse-Derived Ethanol as a Gasoline Oxygenate in Mumbai (Bombay)
Kadam, K.; Dec. 07, 2000; 89p; In English
Report No.(s): DE2001-772426; NREL/TP-580-28705; No Copyright; Avail: Department of Energy Information Bridge

Bagasse is the fibrous residue generated during sugar production and can be a desirable feedstock for fuel ethanol production. About 15%-25% of the bagasse is left after satisfying the mills energy requirements, and this excess bagasse can be used in a bioconversion process to make ethanol. It is estimated that a 23 million L/yr ((approximately) 6 million gal/yr) ethanol facility is feasible by combining excess bagasse from three larger sugar mills in Maharashtra state. The plant could supply about half of the ethanol demand in Mumbai, assuming that all gasoline is sold as an E10 fuel, a blend of 90% gasoline and 10% ethanol by volume. The life cycle assessment (LCA) performed in this study demonstrated the potentially significant benefits of diverting excess bagasse in Maharashtra to ethanol production, as opposed to disposing it by burning. In particular, lower net values for the ethanol production scenario were observed for the following: fossil energy consumption, and emissions of carbon monoxide, hydrocarbons (except methane), SOx, NOx, particulates, carbon dioxide, and methane. The lower greenhouse potential of the ethanol scenario is also important in the context of Clean Development Mechanism and Joint Implementation because India is a developing country.
NTIS
Biomass Energy Production; Gasoline; Ethyl Alcohol; Bioconversion; India

20020005226 National Renewable Energy Lab., Golden, CO USA
Biomass Energy Production in California: The Case for a Biomass Policy Initiative ***Final Report***
Morris, G.; Dec. 14, 2000; 99p; In English
Report No.(s): DE2001-772427; NREL/SR-570-28805; No Copyright; Avail: Department of Energy Information Bridge

During the 1980s California developed the largest and most diverse biomass energy industry in the world. Biomass energy production has become an important component of the state's environmental infrastructure, diverting solid wastes from open burning and disposal in landfills to a beneficial use application.
NTIS
Biomass Energy Production; California; Waste Utilization

20020005230 National Renewable Energy Lab., Golden, CO USA
Biofuels News: Fall 2000; Volume 3, Number 2
Brown, H.; Nov. 28, 2000; 4p; In English
Report No.(s): DE2001-772439; NREL/BR-580-29330; DOE/GO-102000-1149; No Copyright; Avail: Department of Energy Information Bridge, Microfiche

Newsletter for DOE (Department of Energy) Biofuels Program. Articles on recent DOE grants and contracts under Bioenergy Initiative and related programs; also on creation of National Bioenergy Center at NREL (National Renewable Energy Laboratory).
NTIS
Synthetic Fuels; Biomass Energy Production; Energy Policy; USA

20020005231 National Renewable Energy Lab., Golden, CO USA
Siting Evaluation for Biomass-Ethanol Production in Hawaii
Kinoshita, C. M.; Zhou, J.; Oct. 15, 2000; 113p; In English
Report No.(s): DE2001-772440; NREL/SR-580-29414; No Copyright; Avail: Department of Energy Information Bridge, Microfiche

This report examines four Hawaiian islands, Oahu, Hawaii, Maui, and Kauai, to identify three best combinations of potential sites and crops for producing dedicated supplies of biomass for conversion to ethanol. Key technical and economic factors considered in the siting evaluation include land availability (zoning and use), land suitability (agronomic conditions), potential

quantities and costs of producing biomass feedstocks, infrastructure (including water and power supplies), transportation, and potential bioresidues to supplement dedicated energy crops.
NTIS
Biomass Energy Production; Biomass; Ethyl Alcohol

20020005235 Oak Ridge National Lab., TN USA
Predicting Switchgrass Farmgate and Delivered Costs: An 11-State Analysis
Graham, R. L.; English, B. C.; Noon, C. E.; Jager, H. I.; Daly, M. J.; Aug. 24, 1997; 10p; In English
Report No.(s): DE2001-772461; P00-108389; No Copyright; Avail: Department of Energy Information Bridge, Microfiche

A GIS (Global Information System)-based modeling system was developed for analyzing the geographic variation in potential switchgrass feedstock supplies and prices. The modeling system is designed for analyzing individual US states; parameters for six southern states (Alabama, Florida, Georgia, Missouri, South Carolina, Tennessee) and five midwestern states (Iowa, Minnesota, Nebraska, North Dakota, South Dakota). Potential switchgrass supplies are estimated for each state under two switchgrass technology adoption scenarios.
NTIS
Biomass; Grasses; Estimating

20020005236 Oak Ridge National Lab., TN USA
Factors for Bioenergy Market Development
Roos, A.; Hektor, B.; Graham, R. L.; Rakos, C.; Oct. 04, 1998; 10p; In English
Report No.(s): DE2001-772463; P00-108386; No Copyright; Avail: Department of Energy Information Bridge, Microfiche

Focusing on the development of the whole bioenergy market rather than isolated projects, this paper contributes to the identification of barriers and drivers behind bioenergy technology implementation. It presents a framework for the assessment of the potentials for bioenergy market growth to be used by decision makers in administration and industry. The conclusions are based on case studies of operating bioenergy markets in Austria, US and Sweden. Six important factors for bioenergy market growth have been identified: (1) Integration with other business, e.g. for biomass procurement, (2) Scale effects of bioenergy market, (3) Competition on bioenergy market, (4) Competition with other business, (5) National policy, (6) Local policy and local opinion. Different applications of the framework are discussed.
NTIS
Biomass; Commerce; Biomass Energy Production; Energy Policy

20020005255 Federal Energy Technology Center, Morgantown, WV USA
High Temperature High Pressure Thermodynamic Measurements for Coal Model Compounds
Kabadi, V. N.; Feb. 20, 1999; 19p; In English
Report No.(s): DE2001-8977; DE-FG22-95PC95214-04; No Copyright; Avail: Department of Energy Information Bridge, Microfiche

It is well known that the fluid phase equilibria can be represented by a number of gamma-models, but unfortunately most of them do not function well under high temperature. In this calculation, we mainly investigate the performance of UNIQUAC and NRTL models under high temperature, using temperature dependent parameters rather than using the original formulas. The other feature of this calculation is that we try to relate the excess Gibbs energy, G(sup E), and enthalpy of mixing, H(sup E), simultaneously. In other words, we will use the high temperature and pressure, G(sup E), and H(sup E) data to regress the temperature dependent parameters to find out which model and what kind of temperature dependent parameters should be used.
NTIS
Enthalpy; Thermodynamics; High Temperature Tests; Temperature Dependence; Gibbs Free Energy; Models

20020005256 Federal Energy Technology Center, Morgantown, WV USA
High Temperature High Pressure Thermodynamic Measurements for Coal Model Compounds
Kabadi, V. N.; Feb. 24, 1999; 41p
Report No.(s): DE2001-8978; DE-FG22-95PC95214-05; No Copyright; Avail: Department of Energy Information Bridge, Microfiche

The enthalpy of a fluid measured with respect to some reference temperature and pressure (enthalpy increment or Cp) is required for many engineering designs. Different techniques for determining enthalpy increments include direct measurement, integration of heat capacity as a function of temperature at constant pressure, and calculation from accurate density measurements as a function of temperature and pressure with ideal-gas enthalpies. Techniques have been developed for measurement of heat

capacities using differential scanning calorimeters, but routine measurements with a precision better than 3% are rare. For thermodynamic model development, excess enthalpies or enthalpies of mixing of binary and ternary systems are generally required. Although these data can be calculated from measured values of incremental enthalpies of mixtures and corresponding pure components, the method of calculation involves subtraction of large numbers, and it is impossible to obtain accurate results from relatively accurate incremental enthalpy data. Directly measured heats of mixing provide better data for model development. In what follows, we give a brief literature survey of experimental methods available for measurement of incremental enthalpies as well as heats of mixing.
NTIS
Enthalpy; Heat Measurement; Thermodynamics; Models

20020005257 Federal Energy Technology Center, Morgantown, WV USA
Economical Production of Alcohol Fuels from Coal-Derived Synthesis Gas
Jan. 01, 1997; 16p; In English
Report No.(s): DE2001-8982; DE-AC22-91PC91034-21; No Copyright; Avail: Department of Energy Information Bridge, Microfiche

Langmuir-Hinshelwood-type kinetic schemes were derived for the formation of methanol through butanol and total hydrocarbons over a Co-K-MoS2/C catalyst. Reduced Mo-Ni-K/C materials continue to be considered as promising catalysts for HAS. A kinetic study of this catalyst has been started. TPR results on alkali-substituted Mo/C are beginning to be amenable to a systematic quantitative analysis. The characterization studies of transition-metal-oxide catalysts has ended. Consideration of various models for the performance of a packed-bed membrane reactor in the synthesis of methanol indicates that a model involving large (but finite) permeances of CO and MeOH may be optimal. Comparison of the membrane reactor with a packed-bed tubular reactor indicates that the former may be advantageous at low total flow rates.
NTIS
Alcohols; Coal Derived Gases; Methyl Alcohol; Mathematical Models

20020005258 Federal Energy Technology Center, Morgantown, WV USA
Economical Production of Alcohol Fuels from Coal-Derived Synthesis Gas
Apr. 01, 1997; 17p; In English
Report No.(s): DE2001-8983; DE-AC22-91PC91034-22; No Copyright; Avail: Department of Energy Information Bridge, Microfiche

The kinetic data for a Mo-Ni-K/C catalyst were completed. Kinetic schemes were derived for the formation of methanol and ethanol over this catalyst. TPR results on alkali-substituted Mo/C are beginning to be amenable to a systematic quantitative analysis.
NTIS
Alcohols; Catalysts; Fuels

20020005259 Federal Energy Technology Center, Morgantown, WV USA
Economical Production of Alcohol Fuels from Coal-Derived Synthesis Gas
Jun. 01, 1997; 10p; In English
Report No.(s): DE2001-8984; DE-AC22-91PC91034-23; No Copyright; Avail: Department of Energy Information Bridge, Microfiche

During this time period, we finished the kinetic study on the reduced Mo-Ni-K/C catalyst. Experimental work on this project is essentially over. We are continuing the development of kinetic models for this catalyst. We are also continuing with the quantitative analyses of TPR spectra from K-Mo/C catalysts. We request a meeting with US Department of Energy to consider plans to follow up the current work.
NTIS
Alcohols; Catalysts; Fuels; Quantitative Analysis; Kinetics

20020005260 Sandia National Labs., Albuquerque, NM USA
Aluminum-Enhanced Underwater Electrical Discharges for Steam Explosion Triggering
Hogeland, S. R.; Nelson, L. S.; Roth, T. C.; Jul. 01, 1999; 58p; In English
Report No.(s): DE2001-12653; SAND99-0796; No Copyright; Avail: Department of Energy Information Bridge, Microfiche

For a number of years, we have been initiating steam explosions of single drops of molten materials with pressure and flow (bubble growth) transients generated by discharging a capacitor bank through gold bridgewires placed underwater. Recent

experimental and theoretical advances in the field of steam explosions, however, have made it important to substantially increase these relatively mild transients in water without using high explosives, if possible. To do this with the same capacitor bank, we have discharged similar energies through tiny strips of aluminum foil submerged in water. by replacing the gold wires with the aluminum strips, we were able to add the energy of the aluminum-water combustion to that normally deposited electrically by the bridgewire explosion in water. The chemical enhancement of the explosive characteristics of the discharges was substantial: when the same electrical energies were discharged through the aluminum strips, peak pressures increased as much as 12-fold and maximum bubble volumes as much as five-fold above those generated with the gold wires. For given weights of aluminum, the magnitudes of both parameters appeared to exceed those produced by the underwater explosion of equivalent weights of high explosives.
NTIS
Aluminum; Underwater Explosions; Metal Foils

20020005393 Federal Energy Technology Center, Morgantown, WV USA
Separation of fischer-tropsch wax from catalyst by supercritical extraction
Joyce, P. C.; Thies, M. C.; Mar. 31, 1999; 47p; In English
Report No.(s): DE2001-775038; DE-FG22-94PC94219-17; No Copyright; Avail: Department of Energy Information Bridge, Microfiche

The objective of this research project was to evaluate the potential of supercritical fluid (SCF) extraction for the recovery and fractionation of the wax product from the slurry bubble column (SBC) reactor of the Fischer-Tropsch (F-T) process. The wax, comprised mostly of branched and linear alkanes with a broad molecular weight distribution up to C(sub 100), is to be extracted with a hydrocarbon solvent that has a critical temperature near the operating temperature of the SBC reactor, i.e., 200-300 C. Aspen Plus(trademark) was used to perform process simulation studies on the proposed extraction process, with Redlich-Kwong-Soave (RKS) being used for the thermodynamic property model. In summary, we have made comprehensive VLE (vapor-liquid equilibrium) measurements for short alkane + long alkane systems over a wide range of pressures and temperatures, dramatically increasing the amount of high quality data available for these simple yet highly relevant systems. In addition, our work has demonstrated that, surprisingly, no current thermodynamic model can adequately predict VLE behavior for these systems. Thus, process simulations (such as those for our proposed SCF extraction process) that incorporate these systems can currently only give results that are qualitative at best. Although significant progress has been made in the past decade, more experimental and theoretical work remains to be done before the phase equilibria of asymmetric alkane mixtures can be predicted with confidence.
NTIS
Catalysts; Supercritical Fluids; Waxes; Fischer-Tropsch Process; Extraction

20020005642 National Energy Technology Lab., Pittsburgh, PA USA
Minimization of no emissions from multi-burner coal-fired boilers ***Semiannual Report, March-September 1999***
Eddings, E. G.; Molina, A.; Pershing, D. W.; Sarofim, A. F.; Davis, K. A.; Apr. 01, 2000; 32p; In English
Report No.(s): DE2001-786524; FG26-97FT97275-04; No Copyright; Avail: Department of Energy Information Bridge, Microfiche

The focus of this program is to provide insight into the formation and minimization of NO-x in multi-burner arrays, such as those that would be found in a typical utility boiler. Most detailed studies are performed in single-burner test facilities, and may not capture significant burner-to-burner interactions that could influence NO-x emissions.
NTIS
Nitrogen Oxides; Boilers; Coal

20020005827 Federal Energy Technology Center, Morgantown, WV USA
Engineering development of coal-fired high-performance power systems, ***Jun. 1999***
Oct. 01, 1999; 28p; In English
Report No.(s): DE2001-775011; DE-AC22-95PC95143-16; No Copyright; Avail: Department of Energy Information Bridge, Microfiche

A High Performance Power System (HIPPS) is being developed. This system is a coal-fired, combined cycle plant with indirect heating of gas turbine air. Foster Wheeler Development Corporation and a team consisting of Foster Wheeler Energy Corporation, Bechtel Corporation, University of Tennessee Space Institute and Westinghouse Electric Corporation are developing this system. In Phase 1 of the project, a conceptual design of a commercial plant was developed. Technical and economic analyses indicated that the plant would meet the goals of the project which include a 47 percent efficiency (HHV) and a 10 percent lower cost of electricity than an equivalent size PC plant. The concept uses a pyrolysis process to convert coal into fuel gas and char.

The char is fired in a High Temperature Advanced Furnace (HITAF). The HITAF is a pulverized fuel-fired boiler/air heater where steam is generated and gas turbine air is indirectly heated. The fuel gas generated in the pyrolyzer is then used to heat the gas turbine air further before it enters the gas turbine. The project is currently in Phase 2 which includes engineering analysis, laboratory testing and pilot plant testing. Research and development is being done on the HIPPS systems that are not commercial or being developed on other projects. Pilot plant testing of the pyrolyzer subsystem and the char combustion subsystem are being done separately, and after each experimental program has been completed, a larger scale pyrolyzer will be tested at the Power Systems Development Facility (PSDF) in Wilsonville, AL. The facility is equipped with a gas turbine and a topping combustor, and as such, will provide an opportunity to evaluate integrated pyrolyzer and turbine operation. This report addresses the areas of technical progress for this quarter. Analysis of the arch-fired burner continued during this quarter. Unburned carbon and NOx performance are included in this report. Construction commenced this quarter to modify the CETF for horizontal firing. A new indirect feed system will be required to provide a more stable fuel feed to the new wall-fired burner. The conceptual design of the char transfer system for the PSDF is complete. Final detailed design will commence after FETC (Federal Energy Technology Center) has completed all cold model testing. DOE (Department of Energy)-FETC is utilizing an existing experimental facility to evaluate the performance of the proposed char transfer system.
NTIS
Coal; Energy Technology; Electric Power Plants

20020005828 Federal Energy Technology Center, Morgantown, WV USA
Technology development for iron and cobalt Fischer-Tropsch catalysts ***Quarterly Report, 1 Apr. - 30 Jun. 1999***
Davis, B. H.; Jul. 31, 1999; 86p; In English
Report No.(s): DE2001-775013; DE-FC26-98FT40308-03; No Copyright; Avail: Department of Energy Information Bridge, Microfiche

The simple polymerization mechanism for the Fischer-Tropsch synthesis produces products which follows an Anderson-Schulz-Flory distribution. Thus, plotting the logarithm of the mole fraction versus carbon number will produce a straight line whose slope is related to alpha which is determined by the chain termination and propagation probabilities. In contrast, the products from laboratory and large commercial plants exhibit a two-alpha plot. Vapor-liquid calculations show that product accumulation cannot be responsible for the two-alpha plot when the alpha value is large enough to produce liquid products at the reaction temperature. Only in the case where alpha is small and all products are in the vapor phase, allowing evaporation of the startup solvent and a drying out of the reactor can a product accumulation produce a two-alpha plot. Results of filtration successes and failures from runs with the CSTR (Continuous Stirred Tank Reactor) are described.
NTIS
Catalysts; Cobalt; Iron; Fischer-Tropsch Process; Polymerization

20020005857 National Energy Technology Lab., Pittsburgh, PA USA
Advanced biomass reburning for high efficiency nox control and biomass reburning: modeling/engineering studies joint final report
Zamansky, V. M.; Sheldon, M. S.; Lissianski, V. V.; Maly, P. M.; Moyeda, D. K.; Oct. 01, 2000; 101p; In English
Report No.(s): DE2001-786516; FC26-97FT97270-12; No Copyright; Avail: Department of Energy Information Bridge, Microfiche

The focus of this program is to provide insight into the formation and minimization of NO-x in multi-burner arrays, such as those that would be found in a typical utility boiler. Most detailed studies are performed in single-burner test facilities, and may not capture significant burner-to-burner interactions that could influence NO-x emissions.
NTIS
Biomass; Nitrogen Oxides; Boilers

20020005858 National Energy Technology Lab., Pittsburgh, PA USA
Minimization of no emissions from multi-burner coal-fired boilers
Eddings, E. G.; Molina, A.; Pershing, D. W.; Sarofim, A. F.; Davis, K. A.; Apr. 01, 2000; 35p; In English
Report No.(s): DE2001-786519; FG26-97FT97275-01; No Copyright; Avail: Department of Energy Information Bridge, Microfiche

The focus of this program is to provide insight into the formation and minimization of NO-x in multi-burner arrays, such as those that would be found in a typical utility boiler. Most detailed studies are performed in single-burner test facilities, and may not capture significant burner-to-burner interactions that could influence NO-x emissions.
NTIS
Biomass; Nitrogen Oxides; Boilers

29
SPACE PROCESSING

Includes space-based development of materials, compounds, and processes for research or commercial application. Also includes the development of materials and compounds in simulated reduced-gravity environments. For legal aspects of space commercialization see 84 Law, Political Science and Space Policy.

20020001030 DYNACS Engineering Co., Inc., Cocoa Beach, FL USA
Chemical Engineering in Space
Lobmeyer, Dennis A., DYNACS Engineering Co., Inc., USA; Meneghelli, Barry J., DYNACS Engineering Co., Inc., USA; [2001]; 8p; In English; 2001 SCW, 11-13 Jul. 2001, Milwaukee, WI, USA
Contract(s)/Grant(s): NAS10-98001; No Copyright; Avail: CASI; A02, Hardcopy; A01, Microfiche

The state of the art in launch systems uses chemical propulsion systems, primarily liquid hydrogen and liquid oxygen, to provide the energy necessary to achieve orbit and escape the bonds of Earth's gravity. In the future there may be other means available; however, currently few of these alternatives can compare to the speed or the ease of use provided by cryogenic chemical propulsion agents. Cryogenics, the science and art of producing cold operating conditions, has become increasingly important to our ability to travel within our solar system. The production and transport of cryogenic fuels as well as the long-term storage of these fluids are necessary for mankind to travel within our solar system. It is with great care and at a significant cost that gaseous compounds such as hydrogen and oxygen are liquified and become dense enough to use for rocket fuel. As our explorations move farther away from Earth, we need to address how to produce the necessary fuels to make a complete round-trip. The cost and the size of any expedition to another celestial body are extreme. If we are constrained by the need to take everything necessary (fuel, life support, etc.) for our survival and return, we greatly increase the risk of being able to go. As with the early explorers on Earth, we will need to harvest much of our energy and our life support from the celestial bodies. The in situ production of these energy sources is paramount to success. Due to the current propulsion system designs, the in-situ processes will require liquefaction and the application of cryogenics. The challenge we face for the near future is to increase our understanding of cryogenic long-term storage and off-world production of cryogenic fluids. We must do this all within the boundaries of very restricted size, weight, and robustness parameters so that we may launch these apparatus from Earth and utilize them elsewhere. Miniaturization, efficiency, and physically robust systems will all play a part in making space exploration possible; however, it is cryogenics that will enable all of this to occur.
Author
Chemical Engineering; Cryogenics; Space Exploration; Cryogenic Fluids

20020005086 Argonne National Lab., IL USA
Aerodynamic levitation: an approach to microgravity
Glorieux, B.; Saboungi, M. L.; Millot, F.; Enderby, J.; Rifflet, J. C.; Dec. 05, 2000; 12p; In English
Report No.(s): DE2001-772122; ANL/MSD/CP-103588; No Copyright; Avail: Department of Energy Information Bridge, Microfiche

Measurements of the thermophysical and structural properties of liquid materials at high temperature have undergone considerable development in the past few years. Following improvements in electromagnetic levitation, aerodynamic levitation associated with laser heating has shown promise for assessing properties of different molten materials (metals, oxides, and semiconductors), preserving sample purity over a wide range of temperatures and under different gas environments. The density, surface tension and viscosity are measured with a high-speed video camera and an image analysis system. Results on nickel and alumina show that small droplets can be considered in the first approximation to be under microgravity conditions. Using a non-invasive contactless technique recently developed to measure electrical conductivity, results have been extended to variety of materials ranging from liquid metals and liquid semiconductors to ionically conducting materials. The advantage of this technique is the feasibility of monitoring changes in transport occurring during phase transitions and in deeply undercooled states.
NTIS
Microgravity; Aerodynamics; Levitation

20020005116 DYNACS Engineering Co., Inc., Information and Applied Technology, Cocoa Beach, FL USA

Chemical Engineering in Space

Lobmeyer, Dennis A., DYNACS Engineering Co., Inc., USA; Meneghelli, Barry, DYNACS Engineering Co., Inc., USA; [2001]; 7p; In English; 6th World Congress of Chemical Engineering, 23-27 Sep. 2001, Melbourne, Australia; No Copyright; Avail: CASI; A02, Hardcopy; A01, Microfiche

The aerospace industry has long been perceived as the domain of both physicists and mechanical engineers. This perception has endured even though the primary method of providing the thrust necessary to launch a rocket into space is chemical in nature. The chemical engineering and chemistry personnel behind the systems that provide access to space have labored in the shadows of the physicists and mechanical engineers. As exploration into the cosmos moves farther away from Earth, there is a very distinct need for new chemical processes to help provide the means for advanced space exploration. The state of the art in launch systems uses chemical propulsion systems, primarily liquid hydrogen and liquid oxygen, to provide the energy necessary to achieve orbit. As we move away from Earth, there are additional options for propulsion. Unfortunately, few of these options can compare to the speed or ease of use provided by the chemical propulsion agents. It is with great care and significant cost that gaseous compounds such as hydrogen and oxygen are liquefied and become dense enough to use for rocket fuel. These low-temperature liquids fall within a specialty area known as cryogenics. Cryogenics, the science and art of producing cold operating conditions for use on Earth, in orbit, or on some other nonterrestrial body, has become increasingly important to our ability to travel within our solar system. The production of cryogenic fuels and the long-term storage of these fluids are necessary for travel. As our explorations move farther away from Earth, we need to address how to produce the necessary fuels to make a round-trip. The cost and the size of these expeditions are extreme at best. If we take everything necessary for our survival for the round-trip, we invalidate any chance of travel in the near future. As with the early explorers on Earth, we need to harvest much of our energy and our life support from the celestial bodies. The in situ production of these energy sources is paramount to success. We are currently working on several processes to produce the propellants that would allow us to visit and explore the surface of Mars. The capabilities currently at our disposal for launching and delivering equipment to another planet or satellite dictate that the size and scale of any hardware must be extremely small. The miniaturization of the processes needed to prepare the in situ propellants and life support commodities is a real challenge. Chemical engineers are faced with the prospect of reproducing an entire production facility in miniature so the complex can be lifted into space and delivered to our destination. Another area that does not normally concern chemical engineers is the extreme physical aspects payloads are subjected to with the launch of a spacecraft. Extreme accelerations followed by the sudden loss of nearly all gravitational forces are well outside normal equipment design conditions. If the equipment cannot survive the overall trip, then it obviously will not be able to yield the needed products upon arrival. These launch constraints must be taken into account. Finally, we must consider both the effectiveness and efficiencies of the processes. A facility located on the Moon or Mars will not have an unlimited supply of power or other ancillary utilities. For a Mars expedition, the available electric power is severely limited. The design of both the processes and the equipment must be considered. With these constraints in mind, only the most efficient designs will be viable. Cryogenics, in situ resource utilization, miniaturization, launchability, and power/process efficiencies are only a few of the areas that chemical engineers provide support and expertise for the exploration of space.

Author

Aerospace Industry; Chemical Engineering; Space Exploration

31
ENGINEERING (GENERAL)

Includes general research topics to engineering and applied physics, and particular areas of vacuum technology, industrial engineering, cryogenics, and fire prevention. For specific topics in engineering see categories 32 through 39.

20020000765 Lawrence Livermore National Lab., Livermore, CA USA

Principles and techniques for designing precision machines

Hale, L. C.; Feb. 01, 1999; 493p; In English

Report No.(s): DE2001-8431; UCRL-LR-133066; No Copyright; Avail: Department of Energy Information Bridge, Microfiche

This thesis is written to advance the reader's knowledge of precision-engineering principles and their application to designing machines that achieve both sufficient precision and minimum cost. It provides the concepts and tools necessary for the engineer to create new precision machine designs. Four case studies demonstrate the principles and showcase approaches and solutions to specific problems that generally have wider applications. These come from projects at the Lawrence Livermore National Laboratory in which the author participated: the Large Optics Diamond Turning Machine, Accuracy Enhancement of High-Productivity Machine Tools, the National Ignition Facility, and Extreme Ultraviolet Lithography. Although broad in scope, the

topics go into sufficient depth to be useful to practicing precision engineers and often fulfill more academic ambitions. The thesis begins with a chapter that presents significant principles and fundamental knowledge from the Precision Engineering literature. Following this is a chapter that presents engineering design techniques that are general and not specific to precision machines. All subsequent chapters cover specific aspects of precision machine design. The first of these is Structural Design, guidelines and analysis techniques for achieving independently stiff machine structures. The next chapter addresses dynamic stiffness by presenting several techniques for Deterministic Damping, damping designs that can be analyzed and optimized with predictive results. Several chapters present a main thrust of the thesis, Exact-Constraint Design. A main contribution is a generalized modeling approach developed through the course of creating several unique designs. The final chapter is the primary case study of the thesis, the Conceptual Design of a Horizontal Machining Center.
NTIS
Machine Tools; Computer Aided Design; Precision

20020000768 Sandia National Labs., Albuquerque, NM USA
Surface Micromachine Microfluidics: Design, Fabrication, Packaging, and Characterization
Galambos, P.; Eaton, W. P.; Shul, R.; Willison, C. G.; Sniegowski, J. J.; Jun. 30, 1999; 10p; In English
Report No.(s): DE2001-8469; SAND99-1638C; No Copyright; Avail: Department of Energy Information Bridge, Microfiche
The field of microfluidics is undergoing rapid growth in terms of new device and system development. Among the many methods of fabricating microfluidic devices and systems, surface micromachining is relatively underrepresented due to difficulties in the introduction of fluids into the very small channels produced, packaging problems, and difficulties in device and system characterization. The potential advantages of using surface micromachining including compatibility with the existing integrated circuit tool set, integration of electronic sensing and actuation with microfluidics, and fluid volume minimization. In order to explore these potential advantages we have developed first generation surface micromachined microfluidic devices (channels) using an adapted pressure sensor fabrication process to produce silicon nitride channels, and the SUMMiT process to produce polysilicon channels. The channels were characterized by leak testing and flow rate vs. pressure measurements. The fabrication processes used and results of these tests are reported in this paper.
NTIS
Micromachining; Fabrication; Microelectromechanical Systems; Packaging

20020001038 Lawrence Livermore National Lab., Livermore, CA USA
Six degrees of freedom end effector places 8000 lbs robotic canisters in the National Ignition Facility
McMahon, D.; Tiszauer, D.; Yakuma, S.; Jan. 28, 1999; 11p; In English
Report No.(s): DE2001-8513; UCRL-JC-133042; No Copyright; Avail: Department of Energy Information Bridge, Microfiche
The National Ignition Facility (NIF), currently under design and construction at Lawrence Livermore National Laboratory, will be the world's largest laser when complete. The NIF will use about 8000 large optics of 26 different types to focus up to 192 laser beams on a dime-size target. A system of auto-guided robotic vehicles transports opto-mechanical packages, called line replaceable units (LRUs), for installation and maintenance operations. Most LRUs are transported inside a portable clean room, or canister, containing robotic mechanisms that insert each LRU into its respective location in the laser. Together the LRU and canister can weigh up to 8000 lb. Due to precision-alignment requirements of the LRU and because the canister internal mechanisms operate in the canister reference frame, the canisters themselves must be precisely located relative to the laser support structure. In many instances precise location is obtained with the aid of precision canister locating points, called docking points, some of which are on the laser bay ceiling at 19 feet off the floor. The robotic vehicle transporting the LRU and canister is tasked with positioning these 8000 lb. Canisters at 19-foot elevation with less than one inch offset error. The final positioning of the canister in six degrees of freedom is accomplished with an actively controlled three degree of freedom end effector coupled to a passive three degrees of freedom canister lift system.
NTIS
Degrees of Freedom; Robotics; Clean Rooms; End Effectors

20020001163 California Univ., Lawrence Berkeley Lab., Berkeley, CA USA
Berkeley Lab to Help Build Straw Bale Building
Worsham, S. A.; Van Mechelen, G.; Dec. 01, 1998; 11p; In English
Report No.(s): DE2001-8672; LBNL-42660; No Copyright; Avail: Department of Energy Information Bridge, Microfiche
The Shorebird Environmental Learning Center (SELC) is a new straw bale building that will showcase current and future technologies and techniques that will reduce the environmental impacts of building construction and operations. The building will also serve as a living laboratory to test systems and monitor their performance. The project will be the model for a building process

that stops using our precious resources and reduces waste pollution. The rice straw that will be used for the bale construction is generally waste material that is typically burned--millions of tons of it a year--especially in California's San Joaquin Valley. Buildings have significant impacts on the overall environment. Building operations, including lighting, heating, and cooling, consume about 30% of the energy used in the USA. Building construction and the processes into making building materials consume an additional 8% of total energy. Construction also accounts for 39% of wood consumed in the US, while 25% of solid waste volume is construction and demolition (CD) debris. The SELC will incorporate a variety of materials and techniques that will address these and other issues, while providing a model of environmentally considered design for Bay Area residents and builders. Environmental considerations include energy use in construction and operations, selection of materials, waste minimization, and indoor air quality. We have developed five major environmental goals for this project: (1) Minimize energy use in construction and operations; (2) Employ material sources that are renewable, salvaged, recycled, and/or recyclable; (3) Increase building lifespan with durable materials and designs that permit flexibility and modification with minimal demolition; (4) Reduce and strive to eliminate construction debris; and (5) Avoid products that create toxic pollutants and make a healthy indoor environment.
NTIS
Construction Materials; Environment Effects; Hay

20020001540 Sandia National Labs., Albuquerque, NM USA
Micrometer-Scale Machining of Metals and Polymers Enabled by Focused Ion Beam Sputtering
Adams, D. P.; Benavides, G. L.; Vasile, M. J.; Dec. 22, 1998; 7p; In English
Report No.(s): DE2001-2819; SAND98-2843C; No Copyright; Avail: Department of Energy Information Bridge, Microfiche
This work combines focused ion beam sputtering and ultra-precision machining for microfabrication of metal alloys and polymers. Specifically, micro-end mills are made by Ga ion beam sputtering of a cylindrical tool shank. Using an ion energy of 20keV, the focused beam defines the tool cutting edges that have submicrometer radii of curvature. We demonstrate 25 micrometers diameter micromilling tools having 2, 4 and 5 cutting edges. These tools fabricate fine channels, 26-28 microns wide, in 6061 aluminum, brass, and polymethyl methacrylate. Micro-tools are structurally robust and operate for more than 5 hours without fracture.
NTIS
Ion Beams; Sputtering; Machining; Alloys; Organometallic Polymers

20020001785 AFAB Technologies, Inc., Loxahatchee, FL USA
A Low Cost, Self Acting, Liquid Hydrogen Boil-Off Recovery System ***Final Report, 23 Feb. 1998 - 23 Jun. 2000***
Pelfrey, Joy W., AFAB Technologies, Inc., USA; Jun. 23, 2001; 96p; In English
Contract(s)/Grant(s): NAS13-98018
Report No.(s): AT98007-8; No Copyright; Avail: CASI; A05, Hardcopy; A01, Microfiche
The purpose of this research was to develop a prototype liquid hydrogen boll-off recovery system. Perform analyses to finalize recovery system cycle, design detail components, fabricate hardware, and conduct sub-component, component, and system level tests leading to the delivery of a prototype system. The design point and off-design analyses identified cycle improvements to increase the robustness of the system by adding a by-pass heat exchanger. Based on the design, analysis, and testing conducted, the recovery system will liquefy 31% of the gaseous boil off from a liquid hydrogen storage tank. All components, including a high speed, miniature turbocompressor, were designed and manufacturing drawings were created. All hardware was fabricated and tests were conducted in air, helium, and hydrogen. Testing validated the design, except for the turbocompressor. A rotor-to-stator clearance issue was discovered as a result of a concentricity tolerance stack-up.
Author
Cryogenics; Turbocompressors; Liquid Hydrogen; Materials Recovery

20020001977 Argonne National Lab., IL USA
Potential impacts of 316(B) regulatory controls on economics, electricity reliability, and the environment
Veil, J. A.; Mar. 19, 1999; 14p; In English
Report No.(s): DE2001-12360; ANL/EA/CP-98623; No Copyright; Avail: Department of Energy Information Bridge, Microfiche
Nearly half of the US utility-owned steam electric generating capacity is cooled by once-through cooling systems. These plants withdraw cooling water primarily from surface water bodies. Section 316(b) of the Clean Water Act requires that the location, design, construction, and capacity of cooling water intake structures reflect the best technology available (BTA) for minimizing adverse environmental impacts. At present, the US Environmental Protection Agency (EPA) has not yet promulgated

applicable implementing regulations governing intake structures; however, the Agency is required by a Consent Decree to develop such regulations. EPA has presented a draft tiered regulatory framework approach that, depending on site-specific factors, may impose various regulatory burdens on affected utilities. Potential new requirements could range from compiling and submitting existing data to demonstrate that existing conditions at each unit represent BTA to retrofitting plants with closed-cycle cooling systems (primarily cooling towers). If the final regulations require installation of cooling towers or implementation of other costly plant modifications, utilities may elect to close some generating units rather than invest the finds necessary to upgrade them to meet the Section 316(b) requirements. Potentially, some regions of the country may then have a higher proportion of closed units than others, leading to a concern over the reliability of those regions' electricity supply. If a significant number of plants convert from once-through cooling systems to cooling towers, the environment will face secondary adverse impacts, such as additional fuel usage, air emissions, and water evaporation, and utilities will need to construct additional generating capacity. This paper describes a study that Argonne National Laboratory will conduct for the US Department of Energy to explore some of the potential outcomes of EPA's Section 316(b) regulatory process and their impact on economics, electricity supply reliability, and the environment.
NTIS
Economics; Electricity; Cooling Systems; Environment Protection; Environmental Control

20020002356 National Inst. of Standards and Technology, (BFRL), Gaithersburg, MD USA
State-of-the-Art Review of CO2 Demand Controlled Ventilation Technology and Application
Emmerich, S. J.; Persily, A. K.; July 2001; 58p; In English
Report No.(s): PB2001-108141; NISTIR-6729; No Copyright; Avail: CASI; A04, Hardcopy; A01, Microfiche
The control of outdoor air intake rates in mechanically ventilated buildings based on indoor carbon dioxide (CO2) levels, often referred to as CO2 demand controlled ventilation (DCV), has the potential for reducing the energy consumption associated with building ventilation in some commercial and institutional buildings. Carbon dioxide DCV has been discussed, promoted, studied and demonstrated for about twenty years, but questions still remain regarding the actual energy savings potential as a function of climate, ventilation system features, and building occupancy. In addition, questions exist as to the indoor air quality (IAQ) impacts of the approach and the best way to implement CO2 DCV in general and in a given building. This report presents a state-of-the-art review of CO2 DCV technology and application including discussion of the concept and its application, and a literature review. In addition the regulatory and standard requirements impacting CO2 DCV are also examined.
NTIS
Carbon Dioxide; Ventilation; Air Intakes; Indoor Air Pollution

20020002696 Idaho Univ., Moscow, ID USA
Catalytic Reactor Studies ***Final Report, (Jul. 2000 - Aug. 2001)***
Steciak, J.; Beyerlein, S.; Jones, H.; Klein, M.; Kramer, S.; Sep. 2001; 50p; In English
Report No.(s): PB2002-100281; NIATT-N01-17; No Copyright; Avail: CASI; A03, Hardcopy; A01, Microfiche
A literature search identified design and safety concerns for plug flow, pressurized reactors. A modular plug flow reactor was designed. The vaporizer and mixing section were constructed. Thermodynamic calculations show the influence of the water-gas shift reaction on the increased oxidation of carbon monoxide with increased fuel water content. The impact of water on NO formation can be roughly explained by the sensitivity of the thermal NO mechanism to decreasing combustion temperature with increasing water-fuel content. Three major pathways exist for gas-phase ethanol combustion based on the three radicals formed with an H atom is stripped from one of the three backbone atoms in the molecule (C1, C2, or O). Acetaldehyde, ethene, and formaldehyde are stable intermediate products depending on the pathway, with the acetaldehyde path dominating. In the presence of the catalyst, hydrogen atoms are stripped off the ethanol molecule because of the proximity effect of the platinum surface. Pt surface reactions produce stable products, radicals, and heat. Products, radicals and heat diffuse from the surface to promote the initiation of gas-phase ethanol. HCT, a finite-difference code that calculates one-dimensional time-dependent problems involving gas hydrodynamics, transport, and detailed chemical kinetics, has been ported from UNIX to a Windows environment.
NTIS
Reaction Kinetics; Hydrodynamics; Catalysts; Vapor Phases

20020002697 NASA Kennedy Space Center, Cocoa Beach, FL USA
Quick Cooling and Filling Through a Single Port for Cryogenic Transfer Operations
Jones, J. R., NASA Kennedy Space Center, USA; Fesmire, James E., NASA Kennedy Space Center, USA; [2001]; 7p; In English; Joint CEC and ICMC, 16-20 Jul. 2001, Madison, WI, USA
Contract(s)/Grant(s): NAS10-98001; No Copyright; Avail: CASI; A02, Hardcopy; A01, Microfiche

Improved technology for the efficient transfer of cryogens is needed for future on-orbit fueling and remote Lunar/Mars operations. The cooling and filling of a liquid nitrogen (LN2) test vessel through a single port were investigated in a series of experiments. A new 'in-space' transfer tube design concept was used to demonstrate the ability to quickly cool and load cryogens through a single feed-through connection. Three different fill tube configurations with three different diameters were tested. The tubes providing the quickest cooldown time and the quickest fill time for the test article tank were determined. The results demonstrated a clear trade-off between cooling time and filling time for the optimum tube design. This experimental study is intended to improve technology for future flight tank designs by reducing fill system size, complexity, heat leak rate, and operations time. These results may be applied to Space Shuttle Power Reactant Storage and Distribution (PRSD) System upgrades and other future applications. Further study and experimental analysis for optimization of the fill tube design are in progress.
Author
Liquid Cooling; Pipes (Tubes); Liquid Nitrogen

20020002779 Argonne National Lab., IL USA
Two-phase pressure drop of refrigerants during flow boiling in small channels: an experimental investigation and correlation development
Chyu, M. C.; France, D. M.; Tran, T. N.; Wambsganss, M. W.; Jan. 19, 1999; 19p; In English
Report No.(s): DE2001-12396; ANL/ET/CP-98230; No Copyright; Avail: Department of Energy Information Bridge, Microfiche
Two-phase flow pressure drop measurements were made during a phase-change heat transfer process with three refrigerants (R-134a, R-12, and R-113) at six different pressures ranging from 138 kPa to 856 kPa, and in two sizes of round tubes (2.46 mm and 2.92 mm inside diameters) and one rectangular channel (4.06 x 1.7 mm). State-of-the-art large-tube correlations failed to satisfactorily predict the experimental data. The data were used to develop a new correlation for two-phase pressure drop during flow boiling in small channels. The correlation was then tested against the experimental data for the three refrigerants; the error was +/- 20%.
NTIS
Boiling; Refrigerants; Two Phase Flow

20020003408 California Univ., Lawrence Berkeley Lab., Berkeley, CA USA
Residential equipment part load curves for use in DOE-2
Henderson, H.; Huang, Y. J.; Parker, D.; Feb. 01, 1999; 14p; In English
Report No.(s): DE2001-6519; LBNL-42175; No Copyright; Avail: Department of Energy Information Bridge
DOE-2 (DOE2 90) includes several correlation curves that predict the energy use of systems underpart load conditions. DOE-2 simulates systems on an hour-by-hour basis, so the correlations are intended to predict part load energy use (and efficiency) as a function of the part load ratio (PLR) for each hour, where PLR = Hourly Load/Available Capacity. Generally residential and small commercial HVAC equipment meets the load at off-design conditions by cycling on and off. Therefore, the part load correlations must predict the degradation due to this on and off operation over an hourly interval.
NTIS
Air Conditioning; Energy Conservation; Space Heating (Buildings); Ventilation

20020003999 Department of Energy, Chicago Operations Office, Argonne, IL USA
Generic approach to improved semi-solid forming of metals
Klier, E. M.; May 04, 2000; 13p
Report No.(s): DE2001-773540; DOE/ER/82763-1; No Copyright; Avail: Department of Energy Information Bridge, Microfiche
Lack of technology for the production of large inexpensive feedstock, with uniform spherical primary phase throughout as required for semi-solid forming, has restricted realization of the full potential for the semi-solid forming process. Furthermore, narrow process windows and alloy chemistry restrictions increase process costs and limit performance attributes possible with existing semi-solid metal systems. Successful semi-solid forming trials utilizing Chesapeake Composites Corporation's DSC(trademark) Metals for feedstock indicate that this represents a generic approach to providing a permanent highly uniform, spherical solid phase, without electromagnetic or mechanical shearing. This approach also provides for further growth of semi-solid forming by providing for: low cost large diameter billet stock, reduced semi-solid forming costs, extension of semi-solid forming to new alloy systems, and semi-solid formed components with substantially enhanced physical and mechanical properties. In Phase I, Chesapeake utilized DSC(trademark) Aluminum to successfully demonstrate: the low cost production of large diameter feedstock with uniform permanent spherical solid phase, an expansion of the semi-solid forming process window, and semi-solid formed material with substantially enhanced physical and mechanical properties versus existing semi-solid forming materials. In Phase II, the production of 6 inch diameter billets suitable for semi-solid forming (SSF) and the

design, fabrication, and testing of SSF DSC(trademark) Aluminum engine components will be demonstrated. Primary billet processing costs, SSF costs, heat and mass transport during SSF, and material behavior will be modeled. Basic and application specific microstructural--mechanical--thermal property databases will be developed. Finally, 4 inch billet SSF capability will be established and the formability map for DSC(trademark) Aluminum above the melting point will be established.
NTIS
Forming Techniques; Metal Working; Semisolids; Mechanical Properties

20020004664 Los Alamos National Lab., NM USA
Design of small automation work cell system demonstrations
Turner, C.; Pehl, J.; Dec. 01, 2000; 15p; In English
Report No.(s): DE2001-769096; LA-UR-00-5859; No Copyright; Avail: Department of Energy Information Bridge, Microfiche

The introduction of automation systems into many of the facilities dealing with the production, use and disposition of nuclear materials has been an ongoing objective. Many previous attempts have been made, using a variety of monolithic and, in some cases, modular technologies. Many of these attempts were less than successful, owing to the difficulty of the problem, the lack of maturity of the technology, and over optimism about the capabilities of a particular system. Consequently, it is not surprising that suggestions that automation can reduce worker Occupational Radiation Exposure (ORE) levels are often met with skepticism and caution. The development of effective demonstrations of these technologies is of vital importance if automation is to become an acceptable option for nuclear material processing environments. The University of Texas Robotics Research Group (UTRRG) has been pursuing the development of technologies to support modular small automation systems (each of less than 5 degrees-of-freedom) and the design of those systems for more than two decades. Properly designed and implemented, these technologies have a potential to reduce the worker ORE associated with work in nuclear materials processing facilities. Successful development of systems for these applications requires the development of technologies that meet the requirements of the applications. These application requirements form a general set of rules that applicable technologies and approaches need to adhere to, but in and of themselves are generally insufficient for the design of a specific automation system. For the design of an appropriate system, the associated task specifications and relationships need to be defined. These task specifications also provide a means by which appropriate technology demonstrations can be defined. Based on the requirements and specifications of the operations of the Advanced Recovery and Integrated Extraction System (ARIES) pilot line at Los Alamos National Laboratory (LANL), which are considered to be representative of nuclear material handling glove box operations, the UTRRG has developed three task demonstration concepts to evaluate modular small automation systems. These demonstrations, utilizing 2 to 3 degree-of-freedom systems, include container movement, material transfer via pouring, and container loading. Based on an analysis of the ARIES pilot line specifications, these three simple demonstrations are considered to be similar to approximately 50% of the tasks in the ARIES pilot line. Since these task demonstrations functionally represent basic tasks, they are representative of the current potential of modular small automation technology to a wide spectrum of hazardous applications extending beyond the ARIES pilot line. The selection of these three demonstrations, their design and their effectiveness in demonstrating the potential of modular small automation technology are discussed.
NTIS
Automatic Control; Materials Handling; Radioactive Materials; Robotics

20020005178 Oak Ridge National Lab., TN USA
Aging of Polyurethane Foam Insulation in Simulated Refrigerator Panels: One-Year Results with Third-Generation Blowing Agents
Gabbard, W. A.; Weaver, F. J.; Wilkes, K. E.; Sep. 27, 1999; 11p; In English
Report No.(s): DE2001-7405; ORNL/CP-104224; EC-12-03-00-0; No Copyright; Avail: Department of Energy Information Bridge

Laboratory data are presented on the effect of constant-temperature aging on the apparent thermal conductivity of polyurethane foam insulation for refrigerators and freezers. The foam specimens were blown with HCFC-141b and with three of its potential replacements--HFC-134a, HFC-245fa, and cyclopentane. Specimens were aged at constant temperatures of 90 F, 40 F, and -10 F. Thermal conductivity measurements were made on two types of specimens: full-thickness simulated refrigerator panels containing foam enclosed between solid plastic sheets, and thin slices of core foam cut from similar panels. Results are presented for the first year of a multi-year study for the full-thickness panels and for about 1-1/2 years of aging for the core-foam specimens.
NTIS
Aging (Metallurgy); Blowing; Cyclic Hydrocarbons; Insulation; Polyurethane Foam; Refrigerators; Panels; Temperature Effects

20020005207 Corporation for Solar Technology and Renewable Resources, Las Vegas, NV USA
Development of Markets for Solar Water Heating Systems ***Final Report***
Sep. 29, 2000; 139p; In English
Report No.(s): DE2001-769150; DOE/GO/10355/F; No Copyright; Avail: Department of Energy Information Bridge, Microfiche

The SWH concept reborn in the mid-seventies has undergone significant advancements under the leadership of the DOE and their predecessor agencies. Advancements have included new, improved, materials, designs, and system integration concepts. Attempts to introduce the new designs into the residential markets during the late seventies and early eighties with the aid of federal and state tax incentives were largely unsuccessfull. for a number reasons:

NTIS
Market Research; Solar Heating; Water Heating

20020005810 Department of Energy, Office of Environmental Managment, Washington, DC USA
Light duty utility arm
Dec. 01, 1998; 22p; In English
Report No.(s): DE2001-6064; DOE/EM-0406; OST-REF-850; No Copyright; Avail: Department of Energy Information Bridge, Microfiche

The Light-Duty Utility Arm (LDUA) System is a mobile, multi-axis positioning system capable of deploying tools and sensors (end effecters) inside radioactive waste tanks for tank wall inspection, waste characterization, and waste retrieval. The LDUA robotic manipulator enters a tank through existing openings (risers) in the tank dome of the underground tanks. Using various end effecters, the LDUA System is a versatile system for high-level waste tank remediation. The LDUA System provides a means to deploy tools, while increasing the technology resources available to the U.S. Department of Energy (DOE). Ongoing end effectors development will provide additional capabilities to remediate the waste tanks.

NTIS
Tools; Characterization; Radioactive Wastes; End Effectors; Deployment

20020005834 Federal Energy Technology Center, Morgantown, WV USA
Experimental and theoretical investigations of new power cycles and advanced falling film heat exchangers
Razani, A.; Kim, K. J.; Oct. 28, 2000; 99p; In English
Report No.(s): DE2001-775032; DE-FG26-98FT40148-02; No Copyright; Avail: Department of Energy Information Bridge, Microfiche

The annual progress report for the period of October 1, 1999 to September 30, 2000 on DOE (Department of Energy)/UNM (University of New Mexico) grant number DE-FG26-98FT40148 discusses the progress on both the theoretical analysis of advanced power cycles and the experimental investigation of advanced falling film heat exchangers. The previously developed computer program for the triple cycle, based on the air standard cycle assumption, was modified to include actual air composition (%77.48 N(sub 2), %20.59 O(sub 2), %1.9 H(sub 2)O, and %0.03 CO(sub 2)). The actual combustion products were used in exergy analysis of the triple cycle. The effect of steam injection into the combustion chamber on its irreversibility, and the irreversibility of the entire cycle, was evaluated. A more practical fuel inlet condition and a better position of the feedwater heater in the steam cycle were used in the modified cycle. The effect of pinch point and the temperature difference between the combustion products, as well as the steam in the heat recovery steam generator on irreversibility of the cycle were evaluated. Design, construction, and testing of the multitube horizontal falling film condenser facility were completed. Two effective heat transfer additives (2-ethyl-1-hexanol and alkyl amine) were identified and tested for steam condensation. The test results are included. The condenser was designed with twelve tubes in an array of three horizontals and four verticals, with a 2-inch horizontal and 1.5-inch vertical in-line pitch. by using effective additives, the condensation heat transfer rate can be augmented as much as 30%, as compared to a heat transfer that operated without additives under the same operating condition. When heat transfer additives function effectively, the condensate-droplets become more dispersed and have a smaller shape than those produced without additives. These droplets, unlike traditional turbulence, start at the top portion of the condenser tubes and cover most of the tubes. Such a flow behavior can be explained by the Marangoni effect (in terms of thermodynamic equilibrium) in connection with obtained surface tension data. In our experiments, we noted that the use of heat transfer additives such as 2-ethyl-1-hexanol for steam condensation was highly effective.

NTIS
Heat Exchangers; Thermodynamics; Exergy; Waste Energy Utilization

32
COMMUNICATIONS AND RADAR

Includes radar; radio, wire, and optical communications; land and global communications; communications theory. For related information see also 04 Aircraft Communications and Navigation; and 17 Space Communications, Spacecraft Communications, Command and Tracking; for search and rescue see 03 Air Transportation and Safety, and 16 Space Transportation and Safety.

20020001084 Lawrence Livermore National Lab., Livermore, CA USA
Accurately measuring MPI broadcasts in a computational grid
Karonis, N. T.; de Supinski, B. R.; May 06, 1999; 12p; In English
Report No.(s): DE2001-12133; UCRL-JC-133177-REV-1; No Copyright; Avail: Department of Energy Information Bridge, Microfiche

An MPI library's implementation of broadcast communication can significantly affect the performance of applications built with that library. In order to choose between similar implementations or to evaluate available libraries, accurate measurements of broadcast performance are required. As we demonstrate, existing methods for measuring broadcast performance are either inaccurate or inadequate. Fortunately, we have designed an accurate method for measuring broadcast performance, even in a challenging grid environment. Measuring broadcast performance is not easy. Simply sending one broadcast after another allows them to proceed through the network concurrently, thus resulting in inaccurate per broadcast timings. Existing methods either fail to eliminate this pipelining effect or eliminate it by introducing overheads that are as difficult to measure as the performance of the broadcast itself. This problem becomes even more challenging in grid environments. Latencies a long different links can vary significantly. Thus, an algorithm's performance is difficult to predict from it's communication pattern. Even when accurate pre-diction is possible, the pattern is often unknown. Our method introduces a measurable overhead to eliminate the pipelining effect, regardless of variations in link latencies. choose between different available implementations. Also, accurate and complete measurements could guide use of a given implementation to improve application performance. These choices will become even more important as grid-enabled MPI libraries (6, 7) become more common since bad choices are likely to cost significantly more in grid environments. In short, the distributed processing community needs accurate, succinct and complete measurements of collective communications performance. Since successive collective communications can often proceed concurrently, accurately measuring them is difficult. Some benchmarks use knowledge of the communication algorithm to predict the timing of events and, thus, eliminate concurrency between the collective communications that they measure. However, accurate event timing predictions are often impossible since network delays and local processing overheads are stochastic. Further, reasonable predictions are not possible if source code of the implementation is unavailable to the benchmark. We focus on measuring the performance of broadcast communication.
NTIS
Algorithms; Computational Grids; Pipelining (Computers); Broadcasting

20020001162 Department of Energy, Richland, WA USA
Bechtel Hanford Inc. Network Security Plan for the Environmental Restoration Contract
Slade, B. E.; Jun. 30, 1999; 22p; In English
Report No.(s): DE2001-8587; BHI-00998-REV-4; No Copyright; Avail: Department of Energy Information Bridge, Microfiche

As part of the Computer Protection Plan, this Network Security Plan identifies the specific security measures used to protect Bechtel Hanford, Inc.'s (BHI's) enterprise network. The network consists of the communication infrastructure and information systems used by BHI to perform work related to the Environmental Restoration Contract (ERC) at the Hanford Site. It provides electronic communication between the ERC-leased facilities in Richland, Washington, and facilities located on the Hanford Site. Network gateways to other site and offsite networks provide electronic communication with the remainder of the Hanford community.
NTIS
Information Systems; Computer Information Security; Computer Networks

20020001451 Argonne National Lab., IL USA
Communication Services for Advanced Network Applications
Bresnahan, J.; Foster, I.; Insley, J.; Toonen, B.; Tuecke, S.; Jun. 10, 1999; 9p; In English
Report No.(s): DE2001-11843; ANL/MCS/CP-99212; No Copyright; Avail: Department of Energy Information Bridge

Advanced network applications such as remote instrument control, collaborative environments, and remote I/O are distinguished by traditional applications such as videoconferencing by their need to create multiple, heterogeneous flows with different characteristics. For example, a single application may require remote I/O for raw datasets, shared controls for a

collaborative analysis system, streaming video for image rendering data, and audio for collaboration. Furthermore, each flow can have different requirements in terms of reliability, network quality of service, security, etc. They argue that new approaches to communication services, protocols, and network architecture are required both to provide high-level abstractions for common flow types and to support user-level management of flow creation and quality. They describe experiences with the development of such applications and communication services.
NTIS
Reliability; Remote Control; Telecommunication; Video Data; Computer Networks

20020001508 Argonne National Lab., IL USA
IBM SP high-performance networking with a GRF
Navarro, J. P.; May 27, 1999; 11p; In English
Report No.(s): DE2001-12064; ANL/MCS-P747-1298; No Copyright; Avail: Department of Energy Information Bridge, Microfiche

Increasing use of highly distributed applications, demand for faster data exchange, and highly parallel applications can push the limits of conventional external networking for IBM SP sites. In technical computing applications we have observed a growing use of a pipeline of hosts and networks collaborating to collect, process, and visualize large amounts of realtime data. The GRF, a high-performance IP switch from Ascend and IBM, is the first backbone network switch to offer a media card that can directly connect to an SP Switch. This enables switch attached hosts in an SP complex to communicate at near SP Switch speeds with other GRF attached hosts and networks.
NTIS
Computer Networks; Data Transmission; Real Time Operation

20020001771 National Inst. of Standards and Technology, Gaithersburg, MD USA
Video Transmission over CDMA-2000 System
Gharavi, H.; 2001; 6p; In English
Report No.(s): PB2001-108883; No Copyright; Avail: CASI; A02, Hardcopy; A01, Microfiche

The paper presents a twin-class unequal protected video transmission over mobile channels. As a transport vehicle, we have considered CDMA-2000. A dual priority transmission has been invoked in CDMA-2000 by adopting a relative gain adjustment strategy for transmitting the partitioned video signal. The most challenging aspect of this investigation has been to maintain full compatibility with the CDMA-2000 standard. In particular, for the reverse link where the power allocation is tightly controlled, this strategy has been successfully deployed by taking advantage of the flexibility of its link budget. Finally, we will demonstrate that this strategy can result in a significantly higher quality of the reconstructed video data when transmitted over time-varying multipath fading of IMT-2000 channels.
NTIS
Code Division Multiple Access; Deployment

20020002005 Sandia National Labs., Albuquerque, NM USA
Lynx: A High-Resolution Synthetic Aperture Radar
Doerry, A. W.; Hensley, W. H.; Pace, F.; Stence, J.; Tsunoda, S. I.; Mar. 08, 1999; 10p; In English
Report No.(s): DE2001-4263; SAND99-0562C; No Copyright; Avail: Department of Energy Information Bridge, Microfiche

Lynx is a high resolution, synthetic aperture radar (SAR) that has been designed and built by Sandia National Laboratories in collaboration with General Atomics (GA). Although Lynx may be operated on a wide variety of manned and unmanned platforms, it is primarily intended to be fielded on unmanned aerial vehicles. In particular, it may be operated on the Predator, I-GNAT, or Prowler II platforms manufactured by GA Aeronautical Systems, Inc. The Lynx production weight is less than 120 lb. and has a slant range of 30 km (in 4 mm/hr rain). It has operator selectable resolution and is capable of 0.1 m resolution in spotlight mode and 0.3 m resolution in stripmap mode. In ground moving target indicator mode, the minimum detectable velocity is 6 knots with a minimum target cross-section of 10 dBsm. In coherent change detection mode, Lynx makes registered, complex image comparisons either of 0.1 m resolution (minimum) spotlight images or of 0.3 m resolution (minimum) strip images. The Lynx user interface features a view manager that allows it to pan and zoom like a video camera. Lynx was developed under corporate finding from GA and will be manufactured by GA for both military and commercial applications. The Lynx system architecture will be presented and some of its unique features will be described. Imagery at the finest resolutions in both spotlight and strip modes have been obtained and will also be presented.
NTIS
Architecture (Computers); High Resolution; Synthetic Aperture Radar; Military Technology; Imaging Techniques

20020002357 Research Inst. of National Defence, Div. of Sensor Technology, Linkoeping, Sweden

Modeling of the Radar Signature of Objects on a Rough Surface ***Modellering av Radarsignatur foer Objekt pa Skrovlig Yta***

Fagerstroem, J.; Oct. 1999; ISSN 1104-9154; 24p; In Swedish; Original contains color illustrations

Report No.(s): PB2001-108135; FOA-R-99-01234-615-SE; No Copyright; Avail: CASI; A03, Hardcopy; A01, Microfiche

A computational model based on statistically generated rough surfaces, physical optics (PO), and Synthetic Aperture Radar (SAR) imaging has been developed. The model is applied to the study of radar clutter caused by rough surfaces. The modeled normalized radar cross section of the surfaces, can be described by the exponential probability density function. This is in agreement with experimental results of several natural surfaces, and is also reasonable from a theoretical point of view. The radar signature of objects on ground is modeled using SAR imaging of three straight cylinders placed on surfaces with varying degrees of roughness. A smooth surface tends to increase the radar signature distinctness of the cylinders. This is due to corner reflector effects between the side faces of the cylinders and the smooth surface. The cylinder signatures become more indistinct as the roughness of the surface increases. This is due to (1) a decreasing 'corner reflector effect' and (2) the formation and increase of distinct scattering centra on the surface. In this study the subjective concepts 'distinct' (tydlig) and 'indistinct' (otydling) are employed as measures of the radar signature. This approach has some weaknesses, and points at the need for more quantitative measures to be used in similar studies in the future. The report is intended for research scientists in the field of radar signature analysis.

NTIS

Radar Signatures; Mathematical Models; Clutter; Radar Detection; Signature Analysis

20020002754 General Accounting Office, Washington, DC USA

Information Sharing: Practices That Can Benefit Critical Infrastructure Protection

Oct. 2001; 42p; In English

Report No.(s): PB2002-100605; GAO-02-24; No Copyright; Avail: CASI; A03, Hardcopy; A01, Microfiche

This report responds to your May 2001 request that we study the practices of organizations that successfully share sensitive or time-critical information. Information sharing and coordination are key elements in developing comprehensive and practical approaches to defending against computer-based, or cyber, attacks, which could threaten the national welfare. Such attacks could severely disrupt computer-supported operations, compromise the confidentiality of sensitive information, and diminish the integrity of critical data. Computer-based incidents, such as the ILOVEYOU virus in May 2000 and the recent Code Red, Sir Cam, and Nimda attacks, have caused significant disruptions and damage. In addition, the terrorist attacks of September 11 illustrate the importance of having timely information from others on threats and possible precursors to an attack.

NTIS

Computer Techniques; Time Dependence; Viruses

20020002812 Kansas City Plant, Kansas City, MO USA

Remote Environmental Monitoring System CRADA

Hensley, R. D.; Mar. 30, 2000; 10p; In English

Report No.(s): DE2001-752802; KCP-613-6311; CRADA-98KCP1065; No Copyright; Avail: Department of Energy Information Bridge

The goal of the project was to develop a wireless communications system, including communications, command, and control software, to remotely monitor the environmental state of a process or facility. Proof of performance would be tested and evaluated with a prototype demonstration in a functioning facility. AR Designs' participation provided access to software resources and products that enable network communications for real-time embedded systems to access remote workstation services such as Graphical User Interface (GUI), file I/O, Events, Video, Audio, etc. in a standardized manner. This industrial partner further provided knowledge and links with applications and current industry practices. FM and T's responsibility was primarily in hardware development in areas such as advanced sensors, wireless radios, communication interfaces, and monitoring and analysis of sensor data. This role included a capability to design, fabricate, and test prototypes and to provide a demonstration environment to test a proposed remote sensing system. A summary of technical accomplishments is given.

NTIS

Systems Engineering; Environmental Monitoring; Command and Control; Remote Sensing; Prototypes

20020003395 Los Alamos National Lab., NM USA

Optimal configuration of a command and control network: balancing performance and reconfiguration constraints

Dowell, L.; Jul. 01, 1999; 22p; In English

Report No.(s): DE2001-768238; LA-UR-99-2394; No Copyright; Avail: Department of Energy Information Bridge, Microfiche

The optimization of the configuration of communications and control networks is important for assuring the reliability and performance of the networks. This paper presents techniques for determining the optimal configuration for such a network in the presence of communication and connectivity constraints.
NTIS
Configuration Management; Communication Networks; Command and Control

20020003413 California Univ., Lawrence Berkeley Lab., Berkeley, CA USA
Three-dimensional transient electromagnetic modeling in the Laplace Domain
Mizunaga, H.; Lee, K. H.; Kim, H. J.; Sep. 01, 1998; 22p; In English
Report No.(s): DE2001-6535; LBNL-42677; No Copyright; Avail: Department of Energy Information Bridge
In modeling electromagnetic responses, Maxwell's equations in the frequency domain are popular and have been widely used (Nabighian, 1994; Newman and Alumbaugh, 1995; Smith, 1996, to list a few). Recently, electromagnetic modeling in the time domain using the finite difference (FDTD) method (Wang and Hohmann, 1993) has also been used to study transient electromagnetic interactions in the conductive medium. This paper presents a new technique to compute the electromagnetic response of three-dimensional (3-D) structures. The proposed new method is based on transforming Maxwell's equations to the Laplace domain. For each discrete Laplace variable, Maxwell's equations are discretized in 3-D using the staggered grid and the finite difference method (FDM). The resulting system of equations is then solved for the fields using the incomplete Cholesky conjugate gradient (ICCG) method. The new method is particularly effective in saving computer memory since all the operations are carried out in real numbers. For the same reason, the computing speed is faster than frequency domain modeling. The proposed approach can be an extremely useful tool in developing an inversion algorithm using the time domain data.
NTIS
Electromagnetic Interactions; Maxwell Equation; Three Dimensional Models; Laplace Equation; Finite Difference Time Domain Method

20020003418 California Univ., Lawrence Berkeley Lab., Berkeley, CA USA
Initial results of the CD-1 reliable multicast experiment
Agarwal, D.; Stead, R.; Coan, B.; Burns, J. E.; Shah, N.; Sep. 29, 2000; 9p; In English
Report No.(s): DE2001-767641; LBNL-46957; No Copyright; Avail: Department of Energy Information Bridge, Microfiche
During the past year, an experiment has been underway to test use of reliable multicast capabilities for transmission of continuous data in the Global Communication Infrastructure. For the experiment a version of the CD-1 protocol was multicast enabled. The experiment has demonstrated the feasibility of transmitting data in a multicast mode over the GCI. In the case of the Comprehensive Nuclear Test-Ban Treaty the sender could be the station and the receivers the International Data Center (IDC) and one or more National Data Centers (NDC). The potential advantages of multicasting include (a) the timely receipt of the data by the IDC and the host NDC and (b) the simultaneous availability of the raw station data at, at least, two locations. The latter, by introducing redundant data paths, decreases the probability of loss of station data due to a potential failure of a single data receiver. This experiment is only one element of a needed more thorough assessment of the reliability and cost-effectiveness of introducing redundancies in the data transmission paths and the data sinks of the IMS. The next stage of the multicast experiment planned is installation of the multicast-enabled CD-1 software at the GERES IMS station, at the German NDC and at the IDC for further experiments with actual IMS station data. This stage of the experiment is waiting on installation of a GCI link to the German NDC. Negotiations regarding price for this installation have been on going between the Global Communication Infrastructure (GCI) contractor and the German NDC with no resolution. Current development of the CD-x protocol is proceeding in two complementary directions. Along with the work on a multicast enabled version of CD-1 there is also work to develop CD-1.1, which will add end-to-end reliability to the CD-1 protocol among other things. A possible future activity would be to combine the reliable multicast and the end-to-end reliability mechanisms into one CD-x protocol version.
NTIS
Reliability; Cost Effectiveness; Information Systems; Data Transmission

20020003429 Los Alamos National Lab., NM USA
Failure of TCP in high-performance computational grids
Feng, W.; Aug. 01, 2000; 13p; In English
Report No.(s): DE2001-768821; LA-UR-00-3765; No Copyright; Avail: Department of Energy Information Bridge
Distributed computational grids depend on TCP (Transport Control Protocol) to ensure reliable end-to-end communication between nodes across the wide-area network (WAN). Unfortunately, TCP performance can be abysmal even when buffers on the end hosts are manually optimized. Recent studies blame the self-similar nature of aggregate network traffic for TCP's poor

performance because such traffic is not readily amenable to statistical multiplexing in the Internet, and hence computational grids. In this paper we identify a source of self-similarity previously ignored, a source that is readily controllable: TCP. Via an experimental study, we examine the effects of the TCP stack on network traffic using different implementations of TCP. We show that even when aggregate application traffic ought to smooth out as more applications; traffic are multiplexed, TCP induces burstiness into the aggregate traffic loud, thus adversely impacting network performance. Furthermore, our results indicate that TCP performance will worsen as WAN speeds continue to increase.
NTIS
Data Transmission; Protocol (Computers); Wide Area Networks; Performance Tests

20020003575 Sandia National Labs., Albuquerque, NM USA
Input Impedance of Antennas in High Frequency Cavities
Warne, L. K.; Hudson, H. G.; Johnson, W. A.; Jorgenson, R. E.; Stronach, S. L.; Dec. 01, 2000; 75p; In English
Contract(s)/Grant(s): AC04-94AL85000
Report No.(s): DE2001-773909; SAND2000-3112; No Copyright; Avail: Department of Energy Information Bridge, Microfiche
This report models and measurements of antenna input impedance in resonant cavities at high frequencies. The behavior of input impedance is useful in determining the transmission and reception characteristics of an antenna (as well as the transmission characteristics of certain apertures). Results are presented for both the case where the cavity is undermoded (modes with separate and discrete spectra) as well as the overmoded case (modes with overlapping spectra). A model series is constructed and analyzed to determine the impedance statistical distribution. Both an electrically small dipole as well as an electrically longer resonant dipole and wall mounted monopole are analyzed. Measurements in a large mode stirred chamber cavity are compared with calculations. Finally a method based on power arguments is given, yielding simple formulas for the impedance distribution.
NTIS
Cavity Resonators; Impedance; Antennas

20020003807 Los Alamos National Lab., NM USA
Novel signal processing with nonlinear transmission lines
Reagor, D.; Aug. 01, 2000; 21p; In English
Report No.(s): DE2001-768777; LA-UR-00-3988; No Copyright; Avail: Department of Energy Information Bridge, Microfiche
Nonlinear dielectrics offer uniquely strong and tunable nonlinearities that make them attractive for current devices (for example, frequency-agile microwave filters) and for future signal-processing technologies. The goal of this project is to understand pulse propagation on nonlinear coplanar waveguide prototype devices. We have performed time-domain and frequency-domain experimental studies of simple waveguide structures and pursued a theoretical understanding of the propagation of signals on these nonlinear waveguides. To realistically assess the potential applications, we used a time-domain measurement and analysis technique developed during this project to perform a broadband electrodynamics characterization in terms of nonlinear, dispersive, and dissipative effects. We completed a comprehensive study of coplanar waveguides made from high-temperature superconducting thin-film YBa(sub 2)Cu(sub 3)O(sub 7(minus)(delta)) electrodes on nonlinear dielectric single-crystal SRTiO(sub 3) substrates. by using parameters determined from small-signal (linear) transmission characteristics of the waveguides, we develop a model equation that successfully predicts and describes large-signal (nonlinear) behavior.
NTIS
High Temperature Superconductors; Transmission Lines; Dielectrics; Electrodynamics

20020003930 Decision Systems, Inc., USA
Collaboration in Controller-Pilot Communication
Morrow, Daniel, Decision Systems, Inc., USA; [1994]; 18p; In English; NASA/FAA/Air Force Methods and Metrics of Voice Communication Workshop, May 1994, San Antonio, TX, USA; Sponsored by NASA, USA
Contract(s)/Grant(s): NCC2-832; 2000-00342240; NIAAA-AA07035; No Copyright; Avail: CASI; A03, Hardcopy; A01, Microfiche
Like other forms of dialogue, air traffic control (ATC) communication is an act of collaboration between two or more people. Collaboration progresses more or less smoothly depending on speaker and listener strategies. For example, we have found that the way controllers organize and deliver messages influences how easily pilots understand these messages, which in turn determines how much time and effort is needed to successfully complete the transaction. In this talk, I will introduce a collaborative framework for investigating controller-pilot communication and then describe a set of studies that investigate ATC communication from two complementary directions. First, we focused on the impact of ATC message factors (e.g., length, speech rate) on the cognitive processes involved in ATC: communication. Second, we examined pilot factors that influence the amount

of cognitive resources available for these communication processes. These studies also illustrate how the collaborate framework can help analyze the impact of proposed visual data link systems on ATC communication. Examining the joint effects of communication medium, message factors, and pilot/controller factors on performance should help improve air safety and communication efficiency. Increased efficiency is important for meeting the growing demands on the National Air System.
Author
Air Traffic Control; Messages; Voice Communication; Visual Signals

20020005060 Los Alamos National Lab., NM USA
Optimal configuration of a command and control network: balancing performance and reconfiguration constraints
Dowell, L.; Nov. 01, 1999; 6p; In English
Report No.(s): DE2001-769208; LA-UR-99-2394; No Copyright; Avail: Department of Energy Information Bridge, Microfiche

The optimization of the configuration of communications and control networks is important for assuring the reliability and performance of the networks. This paper presents techniques for determining the optimal configuration for such a network in the presence of communication and connectivity constraints. Reconfiguration to restore connectivity to a data-fusion network following the failure of a network component.
NTIS
Configuration Management; Command and Control; Communication Networks

20020005129 NASA Marshall Space Flight Center, Huntsville, AL USA
Lidar Remote Sensing System
Kavaya, Michael J., Inventor, NASA Marshall Space Flight Center, USA; Amzajerdian, Farzin, Inventor, NASA Marshall Space Flight Center, USA; Nov. 14, 2000; 6p; In English; Provisional US-Patent-Appl-SN-060001, filed 22 Aug. 1997
Patent Info.: Filed 14 Aug. 1998; NASA-Case-MFS-26395; US-Patent-6,147,747; US-Patent-Appl-SN-134704; US-Patent-Appl-SN-060001; No Copyright; Avail: CASI; A02, Hardcopy; A01, Microfiche

A lidar remote sensing system wherein a laser signal is transmitted along an optical path through a telescope having a primary and secondary mirrors and a rotating prism at the telescope output. When the reflected signal from the target is received it is passed back through the system to a detector, where it is heterodyned with a signal from a local oscillator to detect Doppler frequency shifts in the returned signal. Since the prism is rotating, the prism will be at one position when the signal is transmitted and at another when the returned signal is received. This causes the reflected signal to be off the optical path, reducing the power of the returned signal. to correct this problem a de-rotator or prism is mounted for rotation, in synchronism with the rotating prism. about the optical path in a position to intersect the returned beam and refract it back onto the optical path to reduce the power loss in the returned signal.
Official Gazette of the U.S. Patent and Trademark Office
Optical Paths; Prisms; Rotation; Synchronism

20020005197 Los Alamos National Lab., NM USA
Application of high temperature superconductors to underground communications
Reagor, D.; Oct. 01, 2000; 18p; In English
Report No.(s): DE2001-769002; LA-UR-00-3986; No Copyright; Avail: Department of Energy Information Bridge

The best approach for underground communication electromagnetic waves that are deeply earth penetrating known for some time, but the low frequency receivers have been the limiting factor. The state-of-the-art receivers use wire wound on an air or ferrite core. These receivers are rather insensitive to low frequency magnetic fields when configured into a small package and used over a wide bandwidth. High-temperature SQUID (Superconducting Quantum Interference Device) technology is far more sensitive to low frequency magnetic fields. Receivers based on high temperature SQUID technology can be placed in small packages that can be easily carried by personnel moving in an underground environment. The receivers possess the sensitivity and bandwidth to carry voice and data in a configuration that is easier to install and maintain than hard-wired technology. The receivers may also be used with autonomous equipment such as remotely operated mining equipment or sensor systems. These receivers will increase mine productivity and worker safety.
NTIS
High Temperature Superconductors; Underground Communication; Squid (Detectors); Wire

33
ELECTRONICS AND ELECTRICAL ENGINEERING

Includes development, performance, and maintainability of electrical/electronic devices and components; related test equipment. and microelectronics and integrated circuitry. For related information see also 60 Computer Operations and Hardware; and 76 Solid-State Physics. For communications equipment and devices see 32 Communications and Radar.

20020000915 Technology Service Corp., Los Angeles, CA USA
Signal based motion compensation for synthetic aperture radar
Kirk, J.; Jun. 07, 1999; 98p; In English
Report No.(s): DE2001-764587; No Copyright; Avail: Department of Energy Information Bridge

The purpose of the Signal Based Motion Compensation (SBMC) for Synthetic Aperture Radar (SAR) effort is to develop a method to measure and compensate for both down range and cross range motion of the radar in order to provide high quality focused SAR imagery in the absence of precision measurements of the platform motion. Currently SAR systems require very precise navigation sensors for motion compensation. These sensors are very expensive and are often supplied in pairs for reliability. In the case of GPS they can be jammed, further degrading performance. This makes for a potentially very expensive and possibly vulnerable SAR system. SBMC can eliminate or reduce the need for these expensive navigation sensors thus reducing the cost of budget minded SAR systems. The results on this program demonstrated the capability of the SBMC approach.
NTIS
Global Positioning System; Radar Imagery; Synthetic Aperture Radar; Navigation Instruments; Sensors

20020000940 Sandia National Labs., Albuquerque, NM USA
Integratible Process for Fabrication of Fluidic Microduct Networks on a Single Wafer
Matzke, C. M.; Ashby, C. I.; Bridges, M. M.; Griego, L.; Wong, C. C.; Sep. 07, 1999; 11p; In English
Report No.(s): DE2001-13994; SAND99-2323C; No Copyright; Avail: Department of Energy Information Bridge, Microfiche

We present a microelectronics fabrication compatible process that comprises photolithography and a key room temperature SiON thin film plasma deposition to define and seal a fluidic microduct network. Our single wafer process is independent of thermomechanical material properties, particulate cleaning, global flatness, assembly alignment, and glue medium application, which are crucial for wafer fusion bonding or sealing techniques using a glue medium. From our preliminary experiments, we have identified a processing window to fabricate channels on silicon, glass and quartz substrates. Channels with a radius of curvature between 8 and 50 (micro)m, are uniform along channel lengths of several inches and repeatable across the wafer surfaces. to further develop this technology, we have begun characterizing the SiON film properties such as elastic modulus using nanoindentation, and chemical bonding compatibility with other microelectronic materials.
NTIS
Wafers; Microelectronics; Photolithography; Thin Films

20020001213 Argonne National Lab., IL USA
Preparation of ultralow-friction surface films on vanadium diboride
Erdemir, A.; Fenske, G. R.; Halter, M.; Oct. 14, 1996; 18p; In English
Report No.(s): DE2001-12342; ANL/ET/CP-90202; No Copyright; Avail: Department of Energy Information Bridge, Microfiche

In this paper, we present a simple annealing procedure (which we refer to as ”flash-annealing” because of short duration) that results in the formation of an ultralow friction surface film on vanadium diboride (VB2) surfaces. This annealing is done in a box furnace at 800 C for a period of 5 min. During annealing, the exposed surface of the VB2 undergoes oxidation and forms a layer of boron oxide (B2O3). In open air, the B2O3 layer reacts spontaneously with moisture and forms a boric acid (H3BO3) film. The friction coefficient of a 440C steel pin against this H3BO3 film is approximately 0.05, compared to 0.8 against the as-received VB2. Based on Raman spectroscopy and electron microscopy studies, we elucidate the ultralow friction mechanism of the flash-annealed VB2 surfaces.
NTIS
Vanadium; Borides; Annealing; Friction Reduction

20020001460 Argonne National Lab., IL USA
Signal trend identification with fuzzy methods
Reifman, J.; Tsoukalas, L. H.; Wang, X.; Wei, T. Y. C.; Aug. 19, 1999; 12p; In English
Report No.(s): DE2001-11931; ANL/RE/CP-99798; No Copyright; Avail: Department of Energy Information Bridge, Microfiche

A fuzzy-logic-based methodology for on-line signal trend identification is introduced. Although signal trend identification is complicated by the presence of noise, fuzzy logic can help capture important features of on-line signals and classify incoming power plant signals into increasing, decreasing and steady-state trend categories. In order to verify the methodology, a code named PROTREN is developed and tested using plant data. The results indicate that the code is capable of detecting transients accurately, identifying trends reliably, and not misinterpreting a steady-state signal as a transient one.
NTIS
Fuzzy Systems; Signal Analysis; Trend Analysis; On-Line Systems

20020001532 Sandia National Labs., Albuquerque, NM USA
Performance of the Polar Formatting Algorithm for SAR Image Formation on Wide Aperture Collections
Jakowatz, C. V.; Thompson, P. A.; Doran, N. E.; Oct. 12, 2000; 8p; In English
Report No.(s): DE2001-765247; SAND2000-2531C; No Copyright; Avail: Department of Energy Information Bridge, Microfiche

In this paper we describe the performance of the well-known polar formatting algorithm (PFA) for formation of spotlight-mode synthetic aperture imagery from phase history data, under conditions of large-angle synthetic apertures. Such conditions typically occur when the SAR center frequency is low and/or the azimuthal resolution is is very high. Traditional wisdom states that PFA is not desirable for large aperture angles (say on the order of 60 degrees) because either: 1) the polar-to-Cartesian interpolation step is typically implemented as two separate one-dimensional filters and the resulting interpolation errors lead to unacceptable quality in the reconstructed image; or 2) the polar-to-Cartesian conversion is implemented as a fully two-dimensional interpolation and ends up consuming excessive computation time. Here we show that the traditional wisdom is incorrect, i.e., we show that the conventional polar-to-Cartesian interpolation implemented as two separable 1-D steps does yield acceptable image quality even for very wide-angle aperture collections. In addition, we dispel a second notion that PFA is inadequate in imaging scenarios wherein range curvature effects are significant. In fact, the defocus induced by range curvature in PFA in many situations can be corrected via post-filtering of the formed SAR image, and convolution back projection time for the refocus is quite reasonable. We will demonstrate these results by way of PFA formation of SAR imagery from synthetic target data and will contrast the PFA results with those from the CBP (convolution/back-projection) algorithm. CBP is often considered to be superior to PFA for wide-aperture or near-field imaging scenarios, because CBP avoids the step of 2-D interpolation of phase history data and also can be easily modified to account for curved wavefronts in the near-field scenario. The downside of CBP is that it is generally much less efficient computationally than PFA. Our conclusion is that PFA with post-filtering for correction of near-field effects is the algorithm of choice.
NTIS
Algorithms; Apertures; Synthetic Aperture Radar; Mathematical Models; Interpolation

20020001732 National Defence Research Establishment, Linkoeping, Sweden
Classification of Buried Land Mines using 3D Templates on GPR Data Sequences
Lauberts, A.; Dec. 2000; 30p; In English
Report No.(s): PB2001-108162; FOA-R-00-01683-310-SE; No Copyright; Avail: CASI; A03, Hardcopy; A01, Microfiche

A series of experiments have been carried out using a ground penetrating radar (GPR) in order to detect and classify anti-tank (AT) and anti-personnel (AP) mine like objects buried in sand. Two different antennas were operated with pulsed or stepped frequency radar emitter. The classification methods is based on 3D templates extracted from data regions known to contain prototype mines. Various modifications of these templates were matched to full data volumes using normalized correlation. Depending on sand moisture, successful recognition was achieved for both AT mines (dry sand sufficient) and AP mines (wet sand).
NTIS
Ground Penetrating Radar; Mines

20020001878 Sandia National Labs., Albuquerque, NM USA
Range Imaging for Underwater Vision Enhancement
Rish, J. W.; Blume, B.; Nellums, B.; Sackos, J.; Foster, J.; Apr. 19, 1999; 13p; In English
Report No.(s): DE2001-5836; SAND99-0974C; No Copyright; Avail: Department of Energy Information Bridge

This paper presents results from a series of preliminary tests to evaluate a scannerless range-imaging device as a potential sensory enhancement tool for divers and as a potential identification sensor for deployment on small unmanned underwater vehicles. The device, developed by Sandia National Laboratories, forms an image on the basis of point-to-point range to the target rather than an intensity map. The range image is constructed through a classical continuous wave phase detection technique in

which the light source is amplitude modulated at radio frequencies. The receiver incorporates a gain-modulated image intensifier, and range information is calculated on the basis of the phase difference between the transmitted and reflected signal. The initial feasibility test at the Coastal Systems Station showed the device to be effective at imaging low-contrast underwater targets such as concertina wire. It also demonstrated success at imaging a 21-inch sphere at a depth of 10 feet in the water column through a wavy air-water interface.
NTIS
Images; Radar; Underwater Vehicles; Performance Tests; Evaluation

20020001880 Sandia National Labs., Albuquerque, NM USA
IMAP: Interferometry for Material Property Measurement in MEMS
Jensen, B. D.; Miller, S. L.; deBoer, M. P.; Mar. 10, 1999; 5p; In English
Report No.(s): DE2001-4275; SAND99-0586C; No Copyright; Avail: Department of Energy Information Bridge, Microfiche

An interferometric technique has been developed for non-destructive, high-confidence, in-situ determination of material properties in MEMS. by using interferometry to measure the full deflection curves of beams pulled toward the substrate under electrostatic loads, the actual behavior of the beams has been modeled. No other method for determining material properties allows such detailed knowledge of device behavior to be gathered. Values for material properties and non-idealities (such as support post compliance) have then been extracted which minimize the error between the measured and modeled deflections. High accuracy and resolution have been demonstrated, allowing the measurements to be used to enhance process control.
NTIS
Interferometry; Microelectromechanical Systems; Mechanical Properties; Electrostatics; Loads (Forces)

20020002002 Sandia National Labs., Albuquerque, NM USA
Design and Experimental Evaluation of a 3rd Generation Addressable CMOS Piezoresistive Stress Sensing Test Chip
Sweet, J. N.; Peterson, D. W.; Hsia, A. H.; Apr. 13, 1999; 10p; In English
Report No.(s): DE2001-5745; SAND99-0523C; No Copyright; Avail: Department of Energy Information Bridge

Piezoresistive stress sensing chips have been used extensively for measurement of assembly related die surface stresses. Although many experiments can be performed with resistive structures which are directly bonded, for extensive stress mapping it is necessary to have a large number of sensor cells which can be addressed using CMOS logic circuitry. Our previous test chip, the ATC04, has 100 cells, each approximately 0.012 in. on a side, on a chip with a side dimension of 0.45 in. When a cell resistor is addressed, it is connected to a four terminal measurement bus through CMOS transmission gates. In theory, the gate resistances do not affect the measurement. In practice, there may be subtle effects which appear when very high accuracy is required. At high temperatures, gate leakage can increase to a point at which the resistor measurement becomes inaccurate. For ATC04 this occurred at or above 50 C. Here, we report on the first measurements obtained with a new prototype test chip, the ATC06. This prototype was fabricated in a 0.5 micron feature size silicided CMOS process using the MOSIS prototyping facility. The cell size was approximately 0.004 in. on a side. In order to achieve piezoresistive behavior for the implanted resistors it was necessary to employ a non-standard silicide blocking process. The stress sensitivity of both implanted and polysilicon blocked resistors is discussed. Using a new design strategy for the CMOS logic, it was possible to achieve a design in which only 5 signals had to be routed to a cell for addressing vs. 9 for ATC04. With our new design, the resistor under test is more effectively electrically isolated from other resistors on the chip, thereby improving high temperature performance. We present data showing operation up to 140 C.
NTIS
Pressure Sensors; Sensitivity; Stresses; Resistors; Design Analysis; Evaluation

20020002006 Sandia National Labs., Albuquerque, NM USA
Fabrication, Packaging, and Performance of VCSELs and Photodetectors for Space Applications
Armendariz, M. G.; Briggs, R. D.; Choquette, K. D.; Geib, K. M.; Serkland, D. K.; Mar. 09, 1999; 9p; In English
Report No.(s): DE2001-4258; SAND99-0308C; No Copyright; Avail: Department of Energy Information Bridge, Microfiche

Optocouplers are used for a variety of applications aboard spacecraft including electrical isolation, switching and power transfer. Commercially available light emitting diode (LED)-based optocouplers have experienced severe degradation of light output due to extensive displacement damage occurring in the semiconductor lattice caused by energetic proton bombardment. A new optocoupler has been designed and fabricated which utilizes vertical cavity surface emitting laser (VCSEL) and resonant cavity photodetector (RCPD) technologies for the optocoupler emitter and detector, respectively. Linear arrays of selectively oxidized GaAs/AlGaAs VCSELS and RCPDS, each designed to operate at a wavelength of 850nm, were fabricated using an airbridge contacting scheme. The airbridged contacts were designed to improve packaging yields and device reliability by eliminating the use of a polyimide planarizing layer which provided poor adhesion to the bond pad metallization. Details of the

airbridged optocoupler fabrication process are reported. Discrete VCSEL and RCPD devices were characterized at temperatures between (minus)100 to 100 C. Devices were packaged in a face-to-face configuration to form a single channel optocoupler and its performance was evaluated under conditions of high-energy proton bombardment.
NTIS
Cavity Resonators; Fabrication; Packaging; Semiconductors (Materials); Surface Emitting Lasers; Technology Utilization; Polyimides

20020002007 Sandia National Labs., Albuquerque, NM USA
MEMS functional validation using the configuration space approach to simulation and analysis
Allen, J.; Sacks, E.; Mar. 09, 1999; 5p; In English
Report No.(s): DE2001-4257; SAND99-0006C; No Copyright; Avail: Department of Energy Information Bridge, Microfiche
We have developed an interactive computer-aided design program that supports mechanical design of devices fabricated in surface micro-machining processes. The program automates kinematic analysis via a novel configuration space computation code, performs real-time simulation, and supports functional parametric design. Designers can visualize system function under a range of operating conditions, can find and correct design flaws, and can optimize performance. We used the program to detect and correct a design flaw in a micro-mechanical indexing mechanism fabricated at Sandia with the SUMMiT process.
NTIS
Computerized Simulation; Fabrication; Mechanical Engineering; Microelectromechanical Systems; Automatic Control

20020002291 Los Alamos National Lab., NM USA
Properties of a prototype Bi-based HTS composite with a high resistivity sheath for resistive fault current limiting applications
Diehl, R. C.; Fleshler, S.; Oct. 01, 2000; 7p; In English
Report No.(s): DE2001-765750; LA-UR-00-5093; No Copyright; Avail: Department of Energy Information Bridge, Microfiche
Prototype Bi-2223 based composite conductors have been fabricated to provide inherent passive fault current limiting functionality in devices. An HTS insert strand possessing a high resistivity sheath (HRS) was laminated to two metallic strips to provide additional capacity to absorb the heat generated during a fault. Sheath resistivities up to 45 times that of pure Ag were achieved. We summarize the electrical response of 10 to 100 cm straight sections of conductor to pulsed dc and ac currents several times the critical current. DC pulsed I-V characteristics have been obtained over 7 to 8 orders of magnitude of voltage. For electric field levels around 10 V/m, the I-V curves demonstrate the advantage of the HRS conductor in facilitating fault current limiting over the conventional Ag-sheathed Bi-2223 approach. The recovery time for ac faults of 10 V/m was mapped out for various fault hold times. Instantaneous operational recovery was observed for fault hold times up to 3 seconds.
NTIS
Bismuth Alloys; Superconductors (Materials); Critical Current; Electrical Resistivity; Fabrication

20020002363 Vrije Univ., Amsterdam, Netherlands
Azimuthal Asymmetries in Hard Scattering Processes
Boer, D.; Sep. 15, 1998; 164p; In English
Report No.(s): PB2002-100084; No Copyright; Avail: CASI; A08, Hardcopy; A02, Microfiche
Contents include the following: Introduction; Unraveling higher twist; Properties of correlation functions; Spin asymmetries in the Drell-Yan process; Asymmetries in electron-positron annihilation; Leading asymmetries in electron-positron annihilation at the Z peak; Technical aspects of hard scattering processes; Summary, conclusion and outlook; Bibliography.
NTIS
Asymmetry; Positron Annihilation; Scattering

20020002733 Cape Cod Research, Inc., East Falmouth, MA USA
Solid-State Ultracapacitors for Electric Vehicles and Consumer Electronics *Final Report*
Dixon, B. G.; Jun. 01, 1999; 31p; In English
Report No.(s): DE2001-762520; DOE/ER/82138; No Copyright; Avail: Department of Energy Information Bridge
Advanced ultracapacitors are described that are based upon conducting polymer technology. Both Type 1 and Type 2 capacitors were constructed in single cell and stacked arrays that had superior electrochemical properties. More specifically nanophase clay electrode supports were fabricated and the conducting polymers solvent deposited upon them. Both liquid phase and solid polymer electrolytes were evaluated as well. Both single cell and multiple cell capacitors were prepared that exceeded

the 15 Wh/kg, 1500 W/kg goals set by the USA Department of Energy. In addition, it was shown that different conducting polymer electrode configurations could be constructed that showed promise.
NTIS
Capacitors; Conducting Polymers; Solid State Devices

20020002742 Nanomaterials Research Corp., Longmont, CO USA
Pulse Capacitors for Next Generation Linear Colliders ***Final Report***
Hooker, M. W.; Mar. 03, 2000; 26p; In English
Report No.(s): DE2001-761355; No Copyright; Avail: Department of Energy Information Bridge, Microfiche

During this Phase 1 SBIR research program, Nanomaterials Research Corporation (NRC) successfully demonstrated high-voltage multilayer capacitors produced from sub-100 nm ceramic powders. The devices produced by NRC exhibited properties that make them particularly useful for pulse power applications. These properties include: (1) high capacitance; (2) low loss; (3) high breakdown voltage; (4) high insulation resistance; and (5) rapid discharge characteristics. Furthermore, the properties of the nanostructured capacitors were consistently found to exceed those of components that represent the state of the art within the industry. Encouraged by these results, NRC is planning to submit a Phase 2 proposal with the objective of securing seed capital to continue this development effort.
NTIS
Capacitors; Nanostructures (Devices)

20020002745 Oak Ridge National Lab., TN USA
Ion Implantation Processing Technologies for Telecommunications Electronics
Haynes, T. E.; May 01, 2000; 53p; In English
Report No.(s): DE2001-755647; C/ORNL94-0270; No Copyright; Avail: Department of Energy Information Bridge, Microfiche

The subject Cooperative Research and Development Agreement (CRADA) was a collaboration between Oak Ridge National Laboratory and Bell Laboratories, Lucent Technologies (formerly AT&T Bell Laboratories) to explore the development of ion implantation technologies for silicon integrated circuit (IC) manufacturing.
NTIS
Integrated Circuits; Ion Implantation; Manufacturing

20020002775 Argonne National Lab., IL USA
In situ mass spectroscopy of recoiled ion studies of degradation processes in SRBi2Ta2O9 thin films during hydrogen gas annealing
Auciello, O.; Chang, R. P. H.; Gruen, D. M.; Im, J.; Kim, S. H.; Mar. 10, 1999; 10p; In English
Report No.(s): DE2001-12408; ANL/MSD/CP-98538; No Copyright; Avail: Department of Energy Information Bridge, Microfiche

It is known that the forming gas (N(sub 2)-H(sub 2) mixture) annealing process required for microcircuit fabrication results in an unacceptable electrical degradation of SRBi(sub 2)Ta(sub 2)O(sub 9) (SBT) ferroelectric capacitors due mainly to the interaction of H(sub 2) with the ferroelectronic layer of the capacitor. We have found a strong relationship between changes in the surface composition of the ferroelectric layer and the electrical properties of SBT capacitors as a result of hydrogen annealing. Mass spectroscopy of recoiled ions (MSRI) analysis revealed a strong reduction in the Bi signal as a function of exposure to hydrogen at high temperatures ((approximately) 500 C). The Bi signal reduction correlates with Bi depletion in the SBT surface region. Subsequent annealing in oxygen at temperatures in the range of 700-800 C resulted in the recovery of the MSRI Bi signal, corresponding to the replenishment of Bi in the previously Bi-depleted surface region. XRD (x ray diffraction) analysis (probing the whole SBT film thickness) showed little difference in the XRD spectra of the SBT fti before and after hydrogen and oxygen-recovery annealing. The combined results of the MSRI and XRD analyses can be interpreted as an indication that the degradation of the electrical properties of the SBT capacitors, after hydrogen annealing, is mainly due to the degradation of the near surface region of the SBT layer.
NTIS
Annealing; Thin Films; Ions; Electrical Properties; Capacitors

20020002784 Sandia National Labs., Albuquerque, NM USA
Photoconductive Semiconductor Switch Technology for Short Pulse Electromagnetics and Lasers
Denison, G. J.; Helgeson, W. D.; Hjalmarson, H. P.; Loubriel, G. M.; Mar, A.; Aug. 05, 1999; 6p; In English
Report No.(s): DE2001-9696; SAND99-2049C; No Copyright; Avail: Department of Energy Information Bridge, Microfiche

High gain photoconductive semiconductor switches (PCSS) are being used to produce high power electromagnetic pulses foc (1) compact, repetitive accelerators, (2) ultra-wide band impulse sources, (3) precision gas switch triggers, (4) optically-activated firesets, and (5) high power optical pulse generation and control. High power, sub-nanosecond optical pulses are used for active optical sensors such as compact optical radars and range-gated hallistic imaging systems. Following a brief introduction to high gain PCSS and its general applications, this paper will focus on PCSS for optical pulse generation and control. PCSS technology can be employed in three distinct approaches to optical pulse generation and control: (1) short pulse carrier injection to induce gain-switching in semiconductor lasers, (2) electro-optical Q-switching, and (3) optically activated Q-switching. The most significant PCSS issues for these applications are switch rise time, jitter, and longevity. This paper will describe both the requirements of these applications and the most recent results from PCSS technology. Experiments to understand and expand the limitations of high gain PCSS will also be described.
NTIS
Photoconductivity; Electromagnetic Pulses; Semiconductors (Materials); Switches

20020002807 Kansas City Plant, Kansas City, MO USA
Ceramic Element Bonding For Piezoelectric Motors
Yerganian, S. S.; Jun. 13, 2000; 23p; In English
Report No.(s): DE2001-756503; KCP-613-6342; No Copyright; Avail: Department of Energy Information Bridge
This collaborative research program between Aerodyne Research, Inc. and Boston College (AR.UBC) has studied the heterogeneous gas-liquid interactions related to ozone formation and destruction processes in the atmosphere. This involves laboratory determination of gas/liquid mass transport rates using bubble column and droplet apparatuses capable of measuring both fast and slow heterogeneous processes. The research plan was to study heterogeneous chemistry of nitrogen containing species, including ammonia NH, and so-called 'NO' gas phase species (including NO, NO(2), NO(3), HNO(2), and CH(2)O) on atmospherically relevant aqueous solutions (including sulfuric acid and nitrosyl sulfuric acid).
NTIS
Bonding; Ceramics; Piezoelectric Motors; Heterogeneity; Nitrogen

20020002808 Kansas City Plant, Kansas City, MO USA
Review of 8-mm Piezoelectric Motor Connection Methods
Barben, C. L.; Yerganian, S. S.; Jun. 08, 2000; 31p
Report No.(s): DE2001-756315; KCP-613-6331; No Copyright; Avail: Department of Energy Information Bridge
This report presents the design and evaluation of electrical connection methods for driving an 8-millimeter traveling wave piezoelectric ring motor. This proved to be a difficult problem because many of the electrical leads and the bonds attaching them to the PZT ceramic were subject to breaking due to resonant vibrations as the motor was run. Methods investigated to provide electrical leads to the PZT ceramic ring included discrete wires, custom-designed cables, and a fixed ceramic ring. Bonds to the ceramic ring were made using three conductive adhesives, thermosonically bonded gold jumper wires, and soldering. A scanning laser Doppler vibrometer was used to evaluate the resonance in the electrical leads. Finite element analysis was used to help guide the design of a new cable to eliminate the resonance problems.
NTIS
Electric Connectors; Lead Zirconate Titanates; Piezoelectric Motors; Millimeter Waves

20020002839 Sandia National Labs., Albuquerque, NM USA
Doped Contacts for High-Longevity Optically Activated, High Gain GaAs Photoconductive Semiconductor Switches
Baca, A. G.; Brown, D. J.; Donaldson, R. D.; Helgeson, W. D.; Hjalmarson, H. P.; Aug. 05, 1999; 6p; In English
Report No.(s): DE2001-9698; SAND99-2051C; No Copyright; Avail: Department of Energy Information Bridge, Microfiche
The longevity of high gain GaAs photoconductive semiconductor switches (PCSS) has been extended to over 50 million pulses. This was achieved by improving the ohmic contacts through the incorporation of a doped layer beneath the PCSS contacts which is very effective in the suppression of filament formation and alleviating current crowding to improve the longevity of PCSS. Virtually indefinite, damage-free operation is now possible at much higher current levels than before. The inherent damage-free current capacity of the switch depends on the thickness of the doped layers and is at least 100A for a dopant diffusion depth of 4pm. The contact metal has a different damage mechanism and the threshold for damage (approximately 40A) is not further improved beyond a dopant diffusion depth of about 2 micrometers. In a diffusion-doped contact switch, the switching performance is not degraded when contact metal erosion occurs. This paper will compare thermal diffusion and epitaxial growth

as approaches to doping the contacts. These techniques will be contrasted in terms of the fabrication issues and device characteristics.
NTIS
Semiconductors (Materials); Switches; Photoconductivity; High Gain; Gallium Arsenides

20020002840 Pepco, Inc., Snyderville, UT USA
Technical Progress Report for PEPCO: Turbo-Z Battery Charging System
Jul. 22, 1999; 8p; In English
Report No.(s): DE2001-767383; No Copyright; Avail: Department of Energy Information Bridge, Microfiche

The authors are entering the final phase of development for this project. Work has been imparted to define the components of the flexible battery charger control board. Detailed analog and digital circuits are complete. Improved analog to digital and digital to analog converters have been selected for use with the control board. The control board schematics are complete and construction of the hardware is in progress. The programming of the circuit board modules is underway. The documentation and circuit schematic drawings are in process. The test stand has added the integration of a dedicated fast computer/microprocessor to control the test stand. This will allow measurements to be taken and recorded more often. This has required modification of the software. The software is being debugged. The modules to be controlled by the test stand microprocessor include the charger module, the battery simulator, the discharge pulse, and discharger. Integrating these components will greatly enhance design and testing. An SCR charger power module has been has been designed, built, and debugged. The circuits for the battery simulator and discharge pulse have been detailed and debugged. The discharge pulse characteristics have been defined and designed. The charger power and discharge pulse modules can be used with either the test stand or the flexible control board. This work is the result of extensive catalog and internet research for the test stand and control board components. The documentation for the project is underway. It is important to have this documentation for reference purposes. Also, the drawing schematics will help with future projects, and they will help with flow-charting the projects for all parties involved. The drawings and some output parameters as of June 1999 are attached.
NTIS
Battery Chargers; Electric Batteries; Digital Electronics; Logic Circuits

20020003381 Sandia National Labs., Albuquerque, NM USA
3-D Silicon Photonic Lattices: Cornerstone of an Emerging Photonics Revolution
Fleming, J. G.; Lin, S. Y.; Jul. 08, 1999; 12p; In English
Report No.(s): DE2001-8950; SAND99-1707C; No Copyright; Avail: Department of Energy Information Bridge, Microfiche

Three-dimensional photonic lattices are engineered materials which are the photonic analogues of semiconductors. These structures were first proposed and demonstrated in the mid-to-late 1980's. However, due to fabrication difficulties, lattices active in the infrared are only just emerging. Wide ranges of structures and fabrication approaches have been investigated. The most promising approach for many potential applications is a diamond-like structure fabricated using silicon microprocessing techniques. This approach has enabled the fabrication of 3-D silicon photonic lattices active in the infrared. The structures display band gaps centered from 12 microns down to 1.55 microns.
NTIS
Fabrication; Photonics; Crystal Lattices

20020003419 Los Alamos National Lab., NM USA
Transverse stress and fatigue effects in YBCO-coated IBAD tapes
Ekin, J.; Bray, S.; Nov. 21, 2000; 7p; In English
Report No.(s): DE2001-767923; LA-UR-00-5557; No Copyright; Avail: Department of Energy Information Bridge, Microfiche

Measurements of the effects of static and cyclic (fatigue) transverse stress on the critical current of YBCO-coated IBAD tapes are reported at 76 K in self magnetic field. YBCO films (approx. 1 um thick) on Inconel substrates (125 um thick) with IBAD buffer layers had critical-current densities (jc) exceeding 1 MA/cm2 and n values of about 50 (where n is an index of the sharpness of the superconductor-normal transition). Under static loads of 100 Mpa, the Jc degradation was less than 5% (7% at 120 Mpa). When subjected to cyclic loading, there was less than 2& additional Jc degradation after 2000 fatigue cycles. Microscopic examination of the samples indicates that this limited Jc degradation may have arisen from longitudinal cracks forming near the edges of the sample after being subjected to these high transverse pressures. This fracture mode would indicate that longitudinal

side support from high-yield substrates or epoxy impregnation of the magnet structure may provide additional tolerance against Jc degradation from transverse stress.
NTIS
Barium Oxides; Cyclic Loads; Epoxy Resins; Superconducting Films; Magnetic Fields

20020003423 Los Alamos National Lab., NM USA
Frequency response measurements of leda rf control system
Rohlev, T.; Aug. 01, 2000; 6p; In English
Report No.(s): DE2001-768258; LA-UR-00-3729; No Copyright; Avail: Department of Energy Information Bridge, Microfiche
A VXI based control system is currently used to maintain constant field amplitude and phase in the Low Energy Demonstration Accelerator (LEDA) RFQ under various beam loading conditions. The control system uses both digital feedback for low frequency disturbances and analog feedback for higher frequency disturbances. This paper discusses the measured frequency response of the control systems.
NTIS
Frequency Response; Feedback; Control

20020003969 Lawrence Livermore National Lab., Livermore, CA USA
Microtechnology engineering at Lawrence Livermore National Laboratory
Langland, B.; Feb. 01, 1998; 28p; In English
Report No.(s): DE2001-2871; UCRL-ID-129545; No Copyright; Avail: Department of Energy Information Bridge
The capability of cooling laser diode bars in an architecture that allows the construction of a high-irradiance pump source for solid-state lasers, together with a beam path that exploits the very beneficial average-power thermomechanical properties of crystalline solid-state laser materials, makes high-repetition-rate, diode-pumped slab lasers ideally suited for high-repetition-rate, small-single-pulse-energy, average-power applications. We have built a 1-kW version of this laser design to verify the basic concepts of high-average-power diode packaging and wave-front control in the new zig-zag architecture. With what we have learned in the process, it is quite straightforward to build versions that exceed 2 kW and have very-near-diffraction-limited beam quality. Such lasers will have numerous applications in the military as well as the civil sector.
NTIS
Semiconductor Lasers; Diodes; Solid State Lasers

20020003986 Northrop Grumman Corp., Electronic Sensors and Systems Div., Baltimore, MD USA
2000 Dollar Electric Powertrain Option-1 Program ***Final Report***
Jun. 01, 1999; 91p; In English
Report No.(s): DE2001-763087; DOE/GO/10017-17; No Copyright; Avail: Department of Energy Information Bridge, Microfiche
This report describes the tasks accomplished as part of Northrop Grumman's TRP $2000 Electric Powertrain Option-1 program. Northrop Grumman has strived to achieve technology advances and development considered as high priority to the success of future electric vehicles. Northrop Grumman has achieved the intent of the program by taking several steps toward reducing the cost of the electric vehicle powertrain, demonstrating technologies in the form of hardware and introducing enhancements into production that are consistent with the needs of the market.
NTIS
Technology Assessment; Electric Motor Vehicles

20020004911 Sandia National Labs., Albuquerque, NM USA
Infrastructure, Technology and Applications of Micro-Electro-Mechanical Systems (MEMS)
Allen, J. J.; Jakubczak, J. F.; Krygowski, T. W.; Miller, S. L.; Montague, S.; Jul. 09, 1999; 8p; In English
Report No.(s): DE2001-8955; SAND99-1734C; No Copyright; Avail: Department of Energy Information Bridge, Microfiche
A review is made of the infrastructure, technology, and capabilities of Sandia National Laboratories for the development of micromechanical systems. By incorporating advanced fabrication processes, such as chemical mechanical polishing, and several mechanical polysilicon levels, the range of micromechanical systems that can be fabricated in these technologies is virtually limitless. Representative applications include a micro-engine driven mirror, and a micromachined lock. Using a novel integrated microelectromechanical systems (MEMS)/complementary metal oxide semiconductor (CMOS) technology, a six

degree-of-freedom accelerometer/gyroscope system has been designed by researchers at U.C. Berkeley and fabricated on the same silicon chip as the CMOS control circuits to produce an integrated micro-navigational unit.
NTIS
CMOS; Fabrication; Microelectromechanical Systems; Micromachining; Micromechanics

20020005081 Sandia National Labs., Albuquerque, NM USA
Recent Advances in AC-DC Transfer Measurements Using Thin-Film Thermal Converters
Wunsch,; Kinard,; Manginell,; Lipe,; Solomon,; Dec. 08, 2000; 13p; In English
Report No.(s): DE2001-771534; SAND2000-3059C; No Copyright; Avail: Department of Energy Information Bridge

New standards for ac current and voltage measurements, thin-film multifunction thermal converters (MJTCS), have been fabricated using thin-film and micro-electro-mechanical systems (MEMS) technology. Improved sensitivity and accuracy over single-junction thermoelements and targeted performance will allow new measurement approaches in traditionally troublesome areas such as the low frequency and high current regimes. A review is presented of new microfabrication techniques and packaging methods that have resulted from a collaborative effort at Sandia National Laboratories and the National Institute of Standards and Technology (MHZ).
NTIS
Microelectromechanical Systems; Thin Films; Current Converters (AC to DC); Electrical Measurement; Fabrication

20020005103 Bechtel Nevada Corp., Las Vegas, NV USA
Using Multispectral Imaging to Measure Temperature Profiles and Emissivity of Large Thermionic Dispenser, Cathodes
Simmons, D. F.; Fortgang, C. M.; Holtkamp, D. B.; Sep. 01, 2001; 16p; In English
Report No.(s): DE2001-785549; DOE/NV/11718-572; No Copyright; Avail: Department of Energy Information Bridge, Microfiche

Thermionic dispenser cathodes are widely used in modern high-power microwave tubes. Use of these cathodes has led to significant improvement in performance. In recent years these cathodes have been used in electron linear accelerators (LINACs), particularly in induction LINACs, such as the Experimental Test Accelerator at Lawrence Livermore National Laboratory. For induction LINACs, the thermionic dispenser cathode provides greater reproducibility, longer pulse lengths, and lower emittance beams than dpes a field emission cathode.
NTIS
Thermionic Emission; Linear Accelerators; Electron Beams; Thermionic Cathodes; Cathodes

20020005113 Thomas Jefferson National Accelerator Facility, Newport News, VA USA
Far-IR/THz Radiation from the Jefferson Lab FEL Energy Recovered Linac
Williams, G. P.; Sep. 01, 2001; 12p; In English
Report No.(s): DE2001-786148; JLAB-ACC-01-15; DOE/ER/40150-1902; No Copyright; Avail: Department of Energy Information Bridge, Microfiche

The Free Electron Laser at Jefferson Lab is based on a photo-injected energy recovered linac, and currently uses a 40 MeV electron beam with an average current of 5 mA. The electron bunches are extremely short with FWHM values that are in the few hundred femtosecond regime. These electron bunches pass a chicane around the optical cavity, and therefore emit synchrotron radiation. In the far-IR region, the wavelength of light being emitted quickly approaches that of the electron bunch length, giving rise to multiparticle coherent enhancement. The result is a broadband spectrum more than 5 orders of magnitude brighter than can be obtained from incoherent synchrotron IR sources. We will discuss preliminary measurements of this radiation, and applications to spectroscopy and imaging.
NTIS
Radiation; Electron Beams; Free Electron Lasers; Synchrotron Radiation; Far Infrared Radiation

20020005121 NASA Marshall Space Flight Center, Huntsville, AL USA
Arc-Tangent Circuit for Continuous Linear Output
Alhorn, Dean C., Inventor, NASA Marshall Space Flight Center, USA; Howard, David E., Inventor, NASA Marshall Space Flight Center, USA; Smith, Dennis A., Inventor, NASA Marshall Space Flight Center, USA; Oct. 24, 2000; 10p; In English
Patent Info.: Filed 27 Nov. 1998; NASA-Case-MFS-31219-1; US-Patent-6,138,131; US-Patent-Appl-SN-208400; No Copyright; Avail: CASI; A02, Hardcopy; A01, Microfiche

A device suitable for determining arc-tangent of an angle theta is provided. Circuitry generates a first square wave at a frequency omega(t) and a second square wave at the frequency omega(t) but shifted by a phase difference equal to the angle theta.

A pulse width modulation signal generator processes the first and second square waves to generate a pulse width modulation signal having a frequency of omega(t) and having a pulse width that is a function of the phase difference theta. The pulse width modulation signal is converted to a DC voltage that is a linear representation of the phase difference theta.
Official Gazette of the U.S. Patent and Trademark Office
Pulse Duration Modulation; Square Waves; Tangents; Measuring Instruments

20020005131 NASA Ames Research Center, Moffett Field, CA USA
Evolutionary Optimization of Yagi-Uda Antennas
Lohn, Jason D., NASA Ames Research Center, USA; Kraus, William F., NASA Ames Research Center, USA; Linden, Derek S., Linden Innovation Research, USA; Colombano, Silvano P., NASA Ames Research Center, USA; [2001]; 8p; In English; 4th International Conference on Evoluable Systems, USA; No Copyright; Avail: CASI; A02, Hardcopy; A01, Microfiche

Yagi-Uda antennas are known to be difficult to design and optimize due to their sensitivity at high gain, and the inclusion of numerous parasitic elements. We present a genetic algorithm-based automated antenna optimization system that uses a fixed Yagi-Uda topology and a byte-encoded antenna representation. The fitness calculation allows the implicit relationship between power gain and sidelobe/backlobe loss to emerge naturally, a technique that is less complex than previous approaches. The genetic operators used are also simpler. Our results include Yagi-Uda antennas that have excellent bandwidth and gain properties with very good impedance characteristics. Results exceeded previous Yagi-Uda antennas produced via evolutionary algorithms by at least 7.8% in mainlobe gain. We also present encouraging preliminary results where a coevolutionary genetic algorithm is used. Author
Antenna Design; Genetic Algorithms; Yagi Antennas; Design Optimization

20020005173 Sandia National Labs., Albuquerque, NM USA
Role of Interfacial Properties on MEMS Performance and Reliability
de Boer, M. P.; Knapp, J. A.; Mayer, T. M.; Michalske, T. A.; May 21, 1999; 16p; In English
Report No.(s): DE2001-7264; SAND99-1294C; No Copyright; Avail: Department of Energy Information Bridge

We have constructed a humidity-controlled chamber in which deflections of polysilicon cantilever beams are observed by interferometry, resulting in in-situ adhesion measurements within a fracture mechanics framework. From adhesion energy measurements for uncoated hydrophilic beams, we demonstrate an exponential dependence of adhesion on relative humidity (RH). We can explain this trend with a single-asperity model for capillary condensation. For coated hydrophobic beams, adhesion is independent of RH up to a threshold value which depends on the coating used. However, we have found that exposure to very high RH ((ge)90%) ambients can cause a dramatic increase in adhesion, surprisingly with a stronger effect for perfluorodecyltrichlorosilane (FDTS, C10H4F17SiCl3) than octadecyltrichlorosilane (ODTS, C18H37SiCl3). Newly developed computational mechanics to measure adhesion in the presence of an applied load allow us to explore how the adhesion increase develops. We believe that water adsorption at silanol sites at the FDTS/substrate interface, possibly exacerbated by coupling agent migration, leads to water islanding and the subsequent adhesion increase at very high RH levels.
NTIS
Interfaces; Fracture Mechanics; Microelectromechanical Systems; Component Reliability; Miniaturization; Cantilever Beams; Silicon Polymers

20020005203 Sandia National Labs., Albuquerque, NM USA
Novel Thin Film Dispenser Cathode for Thermionic Emission
Zavadil, K. R.; King, D. B.; Ruffner, J. A.; Dec. 04, 2000; 8p; In English
Report No.(s): DE2001-769077; SAND2000-3026C; No Copyright; Avail: Department of Energy Information Bridge

A thin film dispenser or micro-dispenser cathode can be generated using standard rf sputtering deposition technology. These films are compositionally modulated structures based on W and a multi-component Ba oxide. Annealing to temperatures horn 900 to 1300K results in Ba reduction, transport and diffusion across the emitter surface. A finite temperature range exists(is less than 1200K)where a uniform Re coating can be retained at the emitter surface. The metallic coating results in a nearly homogeneous work function based on emission characteristics. These films Produce stable emission at higher temperatures(> 1200K) where the uniform Re coating is lost. Analysis of emission properties yield a work function of 2.2 eV and an apparent emission coefficient of 6 A/sq (cm.K) after annealing to 1200K.This high apparent emission coefficient yields a film suitable for milliwatt power generation applications. Microminiature Thermionic Converters(MTCS) are one potential application for these films.
NTIS
Cathodes; Thin Films; Microminiaturization; Radio Frequencies; Sputtering; Deposition; Thermionic Emitters; Metal Coatings

20020005251 Sandia National Labs., Albuquerque, NM USA

W-Coating for MEMS

Fleming, J. G.; Mani, S. S.; Sniegowski, J. J.; Jul. 08, 1999; 10p; In English

Report No.(s): DE2001-8951; SAND99-1708C; No Copyright; Avail: Department of Energy Information Bridge, Microfiche

The integration of miniaturized mechanical components has spawned a new technology known as microelectromechanical systems (MEMS). Surface micromachining, defined as the fabrication of micromechanical structures from deposited thin films, is one of the core technological processes underlying MEMS. Surface micromachined structures have a large ratio of surface area to volume which makes them particularly vulnerable to adhesion to the substrate or adjacent structures during release or in use - a problem called stiction. Since microactuators can have surfaces in normal or sliding contact, function and wear are critical issues for reliable operation of MEMS devices. Surface modifications are needed to reduce adhesion and friction in micromechanical structures. In this paper, we will present a process used to selectively coat MEMS devices with Tungsten using a CVD (Chemical Vapor Deposition) process. We will discuss the effect of wet and vapor phase cleans along with different process variables. Endurance of the W coating is important, especially in applications where wear due to repetitive contacts with the film may occur. Further, tungsten is hard and chemically inert, Tungsten CVD is used in the integrated-circuit industry, which makes this approach manufacturable.

NTIS

Coating; Microelectromechanical Systems; Microinstrumentation; Friction Factor

20020005264 Sandia National Labs., Albuquerque, NM USA

Equivalent-Circuit Model for the TSM Resonator with a Viscoelastic Layer

Bandey, H. L.; Cernosek, R. W.; Hillman, A. R.; Martin, S. J.; Sep. 16, 1999; 6p; In English

Report No.(s): DE2001-12716; SAND99-0725C; No Copyright; Avail: Department of Energy Information Bridge, Microfiche

This paper describes a new equivalent-circuit model for the thickness shear mode resonator with a surface viscoelastic layer operating near film resonance. The electrical impedance of the film is represented by a simple three-element parallel circuit containing a resistor, a capacitor, and an inductor. These elements describe the film's viscous power dissipation, elastic energy storage, and kinetic energy storage, respectively. Resonator response comparisons between this lumped-element model and the general transmission-line model show good agreement over a range of film phase conditions and not just near film resonance.

NTIS

Electrical Impedance; Equivalent Circuits; Resonators

20020005269 Argonne National Lab., IL USA

Experimental Demonstration of Dielectric Structure Based Two Beam Acceleration

Gai, W.; Conde, M. E.; Konecny, R.; Power, J. G.; Schoessow, P.; Nov. 2000; 9p; In English

Report No.(s): DE2001-768632; ANL-HEP-CP-00-125; No Copyright; Avail: Department of Energy Information Bridge

We report on the experimental results of the dielectric based two beam accelerator (step-up transformer). by using a single high charge beam, we have generated and extracted a high power radio frequency pulse from a 7.8 GHz primary dielectric structure and then subsequently transferred to a second accelerating structure with higher dielectric constant and smaller transverse dimensions. We have measured the energy change of a second (witness) beam passing through the acceleration stage. The measured gradient is greater than four times the deceleration gradient. The detailed experiment of set-up and results of the measurements are dimmed. Future plans for the development of a 100 MeV demonstration accelerator based on this technique is presented.

NTIS

Dielectrics; Gradients

20020005403 Los Alamos National Lab., NM USA

Utilizing results from insar to develop seismic location benchmarks and implications for seismic source studies

Begnaud, M.; Sep. 01, 2000; 11p; In English

Report No.(s): DE2001-768890; LA-UR-00-3529; No Copyright; Avail: Department of Energy Information Bridge, Microfiche

Obtaining accurate seismic event locations is one of the most important goals for monitoring detonations of underground nuclear teats. This is a particular challenge at small magnitudes where the number of recording stations may be less than 20. Although many different procedures are being developed to improve seismic location, most procedures suffer from inadequate testing against accurate information about a seismic event. Events with well-defined attributes, such as latitude, longitude, depth and origin time, are commonly referred to as ground truth (GT). Ground truth comes in many forms and with many different levels of accuracy. Interferometric Synthetic Aperture Radar (InSAR) can provide independent and accurate information (ground truth)

regarding ground surface deformation and/or rupture. Relating surface deformation to seismic events is trivial when events are large and create a significant surface rupture, such as for the M(sub w) = 7.5 event that occurred in the remote northern region of the Tibetan plateau in 1997. The event, which was a vertical strike slip even appeared anomalous in nature due to the lack of large aftershocks and had an associated surface rupture of over 180 km that was identified and modeled using InSAR. The east-west orientation of the fault rupture provides excellent ground truth for latitude, but is of limited use for longitude. However, a secondary rupture occurred 50 km south of the main shock rupture trace that can provide ground truth with accuracy within 5 km. The smaller, 5-km-long secondary rupture presents a challenge for relating the deformation to a seismic event. The rupture is believed to have a thrust mechanism; the dip of the field allows for some separation between the secondary rupture trace and its associated event epicenter, although not as much as is currently observed from catalog locations. Few events within the time period of the InSAR analysis are candidates for the secondary rupture. of these, we have identified six possible secondary rupture events (mb range = 3.7-4.8, with two magnitudes not reported), based on synthetic tests and residual analysis. All of the candidate events are scattered about the main and secondary rupture. A Joint Hypocenter Determination (JHD) approach applied to the aftershocks using global picks was not able to identify the secondary event. We added regional data and used propagation path corrections to reduce scatter and remove the 20-km bias seen in the main shock location. A&r preliminary analysis using several different velocity models, none of the candidate events proved to relocate on the surface trace of the secondary rupture. However, one event (mb = not reported) moved from a starting distance of (approximately)106 km to a relocated distance of (approximately)28 km from the secondary rupture, the only candidate event to relocate in relative proximity to the secondary rupture.
NTIS
Explosions; Underground Explosions; Monitors; Seismology; Ground Truth

20020005404 Los Alamos National Lab., NM USA
Structural analysis of superconducting accelerator cavities
Schrage, D.; Aug. 01, 2000; 6p; In English
Report No.(s): DE2001-768897; LA-UR-00-3624; No Copyright; Avail: Department of Energy Information Bridge, Microfiche
The static and dynamic structural behavior of superconducting cavities for various projects was determined by finite element structural analysis. The (beta) = 0.61 cavity shape for the Neutron Science Project was studied in detail and found to meet all design requirements if fabricated from five millimeter thick material with a single annular stiffener. This 600 MHz cavity will have a Lorentz coefficient of (minus)1.8 Hz/(Mv/sq meter) and a lowest structural resonance of more than 100 Hz. Cavities at (beta) = 0.48, 0.61, and 0.77 were analyzed for a Neutron Science Project concept which would incorporate 7-cell cavities. The medium and high beta cavities were found to meet all criteria but it was not possible to generate a (beta) = 0.48 cavity with a Lorentz coefficient of less than (minus)3 Hz/(Mv/sq meter).
NTIS
Superconducting Devices; Cavities; Linear Accelerators; Structural Analysis

20020005789 California Univ., Lawrence Berkeley Lab., Berkeley, CA USA
Studies of the magnetic structure at the ferromagnet - antiferromagnet interface
Scholl, A.; Nolting, F.; Stohr, J.; Luning, J.; Seo, J. W.; Jan. 02, 2001; 20p; In English
Report No.(s): DE2001-775128; LBNL-45807; No Copyright; Avail: Department of Energy Information Bridge, Microfiche
Antiferromagnetic layers are a scientifically challenging component in magneto-electronic devices such as magnetic sensors in hard disk heads, or magnetic RAM (random access memory) elements. In this paper we show that photo-electron emission microscopy (PEEM) is capable of determining the magnetic structure at the interface of ferromagnets and antiferromagnets with high spatial resolution (down to 20 nm). Dichroism effects at the L edges of the magnetic 3d transition metals, using circularly or linearly polarized soft x-rays from a synchrotron source, give rise to a magnetic image contrast. Images, acquired with the PEEM2 experiment at the Advanced Light Source, show magnetic contrast for antiferromagnetic LaFeO(sub 3), microscopically resolving the magnetic domain structure in an antiferromagnetically ordered thin film for the first time. Magnetic coupling between LaFeO(sub 3) and an adjacent Co layer results in a complete correlation of their magnetic domain structures. From field dependent measurements a unidirectional anisotropy resulting in a local exchange bias of up to 30 Oe in single domains could be deduced. The elemental specificity and the quantitative magnetic sensitivity render PEEM a perfect tool to study magnetic coupling effects in multi-layered thin film samples.
NTIS
Ferromagnetic Materials; Antiferromagnetism; Magnetic Films; Interfaces

20020005809 Sandia National Labs., Albuquerque, NM USA
Comparison of 1 T(Omega) and 10 T (Omega) High Resistance Standards Between NIST and Sandia
Jarrett, D. G.; Dziuba, R. F.; Kraft, M. E.; Apr. 23, 1999; 10p; In English
Report No.(s): DE2001-5950; SAND98-2847C; No Copyright; Avail: Department of Energy Information Bridge, Microfiche

NIST-built 10 T(Omega) and commercial 1 T(Omega) standard resistors were hand carried between NIST and Sandia for a high resistance comparison. The comparison tested the ruggedness of the new NIST-built standard resistors, provided a check of the scaling between the two laboratories, supported measurements to reestablish NIST calibration services at 10 T(Omega) and 100 T(Omega), and demonstrated the possibility of establishing a NIST high resistance measurement assurance program (MAP). The comparison has demonstrated agreement on the order of 0.07% which is within the expanded uncertainties (coverage factor = 2) of NIST and Sandia at 1 T(Omega) and 10 T(Omega).
NTIS
Standards; Electrical Resistivity; Resistors

20020005871 Stanford Univ., Stanford Electronics Labs., Stanford, CA USA
Stanford Electronics Lab JSEP Contract *Final Report, 1 May 1997-31 Mar. 2001*
Harris, J. S.; Mar. 31, 2001; 45p; In English
Contract(s)/Grant(s): DAAG55-97-1-0115
Report No.(s): AD-A395328; ARO-36290.1-EL-JSE; No Copyright; Avail: CASI; A03, Hardcopy; A01, Microfiche

This is the final report of the research conducted at Stanford Electronics Laboratories under the sponsorship of the Joint Services Electronics Program from March 1 1997 through March 31 2001. This report summarizes the areas of research, identifies the most significant results and lists the dissertations, publications and presentations.
DTIC
Research Projects; Education; Documents; Quantum Electronics

34
FLUID MECHANICS AND THERMODYNAMICS

Includes fluid dynamics and kinematics and all forms of heat transfer; boundary layer flow; hydrodynamics; hydraulics; fluidics; mass transfer and ablation cooling. For related information see also 02 Aerodynamics.

20020000756 Sandia National Labs., Albuquerque, NM USA
Density Functional Theory for Classical Fluids at Complex Interfaces: (TRAMONTO 1.0: Methods, Applications, and User's Guide)
Frink, L. J. D.; Salinger, A. G.; Jan. 01, 1999; 78p; In English
Report No.(s): DE2001-3193; SAND98-2840; No Copyright; Avail: Department of Energy Information Bridge

This report contains a summary of work on a 2 and 3-dimensional (2D/3D) parallel density functional theory (DFT) code for inhomogeneous fluids. The behavior of fluids near surfaces or macromolecules is critically important in a wide range of physical systems including adsorbants, colloidal dispersions, sensors, and self-assembled systems. One of the premier tools for studying inhomogeneous fluids at the molecular length scale is DFT. However, until this LDRD (Laboratory-Directed Research and Development) was undertaken, no general purpose 2D or 3D codes existed. The state of the art was to perform 1D calculations, and then attempt to generalize the results (by using superposition approximations for example) to more complex systems. While this approach is useful, 2D and 3D calculations will necessarily give a much deeper insight into the structure and behavior of fluids near surfaces that are complex either in their geometry or surface chemical patterns. In this report we summarize the development of a general multipurpose 2D/3D capability that can be easily extended to a wide range of surfaces from zeolites to polymers.
NTIS
Fluid Mechanics; Interfaces; Colloids; Complex Systems; Macromolecules; Zeolites; Computerized Simulation

20020000759 Federal Energy Technology Center, Morgantown, WV USA
Study of the Electromedics Autotransfusion System, CRADA PC93-010 *Final Report*
Shaffer, F.; Shahnam, M.; Mar. 31, 1995; 11p; In English
Report No.(s): DE2001-3716; DOE/FETC-99/1089; CRADA PC93-010; No Copyright; Avail: Department of Energy Information Bridge

This report describes the work at PETC (Process Engineering Technology Center) to evaluate flow dynamics in the Electromedics autotransfusion system. First, a literature survey was conducted for flow studies in centrifuge systems. Although

no flow studies were identified for Latham-type bowls, pertinent literature for general centrifugal separation was found and reviewed. Sample measurements were taken with Laser Doppler Velocimetry (LDV). The data indicates that LDV is a useful tool in flow analysis. Velocity, turbulence intensity, and bowl vibration are all accurately measured with LDV. For optical imaging of particle separation it is necessary to use fluorescent doped particles and color separation. This allows each type of particle to be observed in a mixture. A market survey was completed and sources for fluorescent dyed particles of three different emission wavelengths and corresponding optical bandpass filters were identified.
NTIS
Separators; Laser Doppler Velocimeters; Blood Plasma; Medical Equipment

20020000772 Lawrence Livermore National Lab., Livermore, CA USA
3D unstructured mesh ALE hydrodynamics with the upwind discontinuous galerkin method
Kershaw, D. S.; Milovich, J. L.; Prasad, M. K.; Shaw, M. J.; Shestakov, A. I.; May 07, 1999; 8p; In English
Report No.(s): DE2001-8507; UCRL-JC-132987; DP0101031; No Copyright; Avail: Department of Energy Information Bridge, Microfiche

The authors describe a numerical scheme to solve 3D Arbitrary Lagrangian-Eulerian (ALE) hydrodynamics on an unstructured mesh using a discontinuous Galerkin method (DGM) and an explicit Runge-Kutta time discretization. Upwinding is achieved through Roe's linearized Riemann solver with the Harten-Hyman entropy fix. For stabilization, a 3D quadratic programming generalization of van Leer's 1D minmod slope limiter is used along with a Lapidus type artificial viscosity. This DGM scheme has been tested on a variety of hydrodynamic test problems and appears to be robust making it the basis for the integrated 3D inertial confinement fusion modeling code (ICF3D). For efficient code development, they use C++ object oriented programming to easily separate the complexities of an unstructured mesh from the basic physics modules. ICF3D is fully parallelized using domain decomposition and the MPI message passing library. It is fully portable. It runs on uniprocessor workstations and massively parallel platforms with distributed and shared memory.
NTIS
Unstructured Grids (Mathematics); Hydrodynamics; Galerkin Method; Lagrangian Function; Runge-Kutta Method

20020000865 Los Alamos National Lab., NM USA
Solutions of the Noh Problem for Various Equations of State Using Lie Groups
Axford, R. A.; Aug. 01, 1998; 23p; In English
Report No.(s): DE2001-1167; LA-13497; No Copyright; Avail: Department of Energy Information Bridge, Microfiche

A method for developing invariant equations of state for which solutions of the Noh problem will exist is developed. The ideal gas equation of state is shown to be a special case of the general method. Explicit solutions of the Noh problem in planar, cylindrical and spherical geometry are determined for a Mie-Gruneisen and the stiff gas equation of state.
NTIS
Equations of State; Lie Groups; Ideal Gas

20020000874 Los Alamos National Lab., NM USA
Some Recent Developments for Moving-Least-Squares Particle Methods
Dilts, G. A.; Sep. 01, 2000; 16p; In English
Report No.(s): DE2001-764461; LA-UR-00-4596; No Copyright; Avail: Department of Energy Information Bridge

Dilts has introduced an extension of smoothed-particle hydrodynamics (SPH) using moving-least-squares interpolants (MLSPH) that in certain variations provides linear completeness and improved tension stability at the cost of a loss of local conservation, or local flux balance. Local conservation has been found a highly desirable property of the original formulation of SPH. Reference also showed that local conservation could be regained satisfactorily at the cost of a loss of linear completeness, due to the inadequacy of the nodal quadrature scheme. In the course of regaining local conservation, it was found that it is necessary to introduce boundary conditions into the scheme in natural way, and that to do so required a means of identifying precisely which particles formed the boundary. A two-dimensional 'exposure method' for doing so was introduced. We shall here describe a three-dimensional exposure method that performs to the same level of satisfaction.
NTIS
Interpolation; Least Squares Method; Two Dimensional Models; Hydrodynamics

20020000876 Argonne National Lab., IL USA

Dynamic Signatures of Driven Vortex Motion

Crabtree, G. W.; Kwok, W. K.; Lopez, D.; Olsson, R. J.; Paulius, L. M.; Sep. 16, 1999; 19p; In English; 2nd; 2nd Polish-US Conference on High Temperature Superconductivity Wroclam and Kudowa, 17-21 Aug. 1998, Warsaw, Poland

Contract(s)/Grant(s): W-31109-ENG-38

Report No.(s): DE2001-11965; ANL/MSD/CP-100037; No Copyright; Avail: Department of Energy Information Bridge, Microfiche

We probe the dynamic nature of driven vortex motion in superconductors with a new type of transport experiment. An inhomogeneous Lorentz driving force is applied to the sample, inducing vortex velocity gradients that distinguish the hydrodynamic motion of the vortex liquid from the elastic and-plastic motion of the vortex solid. We observe elastic depinning of the vortex lattice at the critical current, and shear induced plastic slip of the lattice at high Lorentz force gradients.

NTIS

Vortices; Hydrodynamics; High Temperature Superconductors

20020000889 Argonne National Lab., IL USA

Hairpin vortex formation, a case study for unsteady visualization

Fischer, P. F.; Papka, M. E.; Szymanski, M.; Tufo, H. M.; Aug. 10, 1999; 14p; In English

Report No.(s): DE2001-11928; ANL/MCS/CP-99772; No Copyright; Avail: Department of Energy Information Bridge, Microfiche

To better understand the vortex dynamics of coherent structures in turbulent and transitional boundary layers, we consider direct numerical simulation of the interaction between a flat-plate boundary-layer flow and an isolated hemispherical roughness element. of principal interest is the evolution of hairpin vortices that form an interlacing pattern in the wake of the hemisphere, lift away from the wall, and are stretched by the shearing action of the boundary layer. Using animations of unsteady three-dimensional representations of this flow, produced by the vtk toolkit and enhanced to operate in a CAVE virtual environment, we identify and study several key features in the evolution of this complex vortex topology not previously observed in other visualization formats.

NTIS

Vortices; Flow Visualization; Computerized Simulation; Unsteady Flow

20020000930 Lawrence Livermore National Lab., Livermore, CA USA

Final report for CAFDA project entitled, Experimental and numerical investigation of accelerated fluid interface

Greenough, J. A.; Jacobs, J. W.; Marcus, D. L.; Mar. 26, 1997; 25p; In English

Report No.(s): DE2001-2565; UCRL-CR-126749; SC-B295120,DP0102011; No Copyright; Avail: Department of Energy Information Bridge, Microfiche

The main thrust of this collaborative effort can be summarized as an attempt to use the strengths of physical experiments and numerical simulations in understanding the dynamics of accelerated interfaces. Laboratory experiments represent the true nature of the physical processes and the simulations represent a model of these processes. We have taken the first steps toward this goal through development and calibration of new experimental techniques as well as validation and direct, systematic, and quantitative comparison with computational results. This report summarizes accomplishments made towards these goals. More detailed information is provided in reprints appended to this document.

NTIS

Experimentation; Numerical Analysis; Fluid Boundaries; Fluid Dynamics

20020000941 Sandia National Labs., Albuquerque, NM USA

Experimental Investigation of the Flow in a Virtual Cyclone

Torczynski, J. R.; O'Hern, T. J.; Rader, D. J.; Brockmann, J. E.; Grasser, T. W.; Sep. 01, 1998; 45p; In English

Report No.(s): DE2001-1315; SAND98-2004; YN010000000; No Copyright; Avail: Department of Energy Information Bridge, Microfiche

An experimental investigation has confirmed the predicted flow pattern in a prototype virtual cyclone, a novel device for nonimpact particle separation proposed by Torcdzynski and Rader based solely on computational simulations. The virtual cyclone differs from an ordinary cyclone in that the flow is turned by a virtual wall composed of an eddy rather than by a solid wall. A small-scale version of the computationally simulated geometry has been fabricated out of Lucite. The working fluid is ambient air, which is drawn through the apparatus and flow-metering equipment using a wind-tunnel vacuum source. The flow is seeded with smoke or water droplets produced by a nebulizer so that flow visualization techniques and particle-imaging velocimetry

could be applied. Experiments have been performed on this apparatus for flows with Reynolds numbers from 200 up to 40,000 (a Mach number of 0.3). Flow visualization using a laser light sheet passing through the mid-plane of the apparatus verified that the computationally predicted flow is obtained over the entire range of flow rates. The shear layer between the main and recirculating flow is observed to become turbulent around a Reynolds number of 4000. While not changing the flow structure, the turbulent mixing produced by shear-layer roll-up limits particle concentration at the higher flow rates. In order to achieve highly efficient particle separation using a virtual cyclone, turbulence must be suppressed or mitigated. If laminar flow cannot be achieved for macroscopic-scale virtual cyclones, it should be achievable for a small-scale (low Reynolds number) virtual cyclone fabricated using MEMS (microelectromechanical systems)-related technologies. This approach could lead to a chip-scale particle concentrator.
NTIS
Air Flow; Centrifuges; Computational Fluid Dynamics; Separators

20020001025 Los Alamos National Lab., NM USA
Three-Dimensional Computational Fluid Dynamics
Haworth, D. C.; O'Rourke, P. J.; Ranganathan, R.; Sep. 01, 1998; 56p; In English
Report No.(s): DE2001-1186; LA-13427-MS; No Copyright; Avail: Department of Energy Information Bridge, Microfiche
Computational fluid dynamics (CFD) is one discipline falling under the broad heading of computer-aided engineering (CAE). CAE, together with computer-aided design (CAD) and computer-aided manufacturing (CAM), comprise a mathematical-based approach to engineering product and process design, analysis and fabrication. In this overview of CFD for the design engineer, our purposes are three-fold: (1) to define the scope of CFD and motivate its utility for engineering, (2) to provide a basic technical foundation for CFD, and (3) to convey how CFD is incorporated into engineering product and process design.
NTIS
Three Dimensional Models; Computational Fluid Dynamics; Production Engineering

20020001068 Argonne National Lab., IL USA
Large eddy simulation and its implementation in the COMMIX code
Sun, J.; Yu, D. H.; Feb. 15, 1999; 26p; In English
Report No.(s): DE2001-11994; ANL-97/16; No Copyright; Avail: Department of Energy Information Bridge, Microfiche
Large eddy simulation (LES) is a numerical simulation method for turbulent flows and is derived by spatial averaging of the Navier-Stokes equations. In contrast with the Reynolds-averaged Navier-Stokes equations (RANS) method, LES is capable of calculating transient turbulent flows with greater accuracy. Application of LES to differing flows has given very encouraging results, as reported in the literature. In recent years, a dynamic LES model that presented even better results was proposed and applied to several flows. This report reviews the LES method and its implementation in the COMMIX code, which was developed at Argonne National Laboratory. As an example of the application of LES, the flow around a square prism is simulated, and some numerical results are presented. These results include a three-dimensional simulation that uses a code developed by one of the authors at the University of Notre Dame, and a two-dimensional simulation that uses the COMMIX code. The numerical results are compared with experimental data from the literature and are found to be in very good agreement.
NTIS
Large Eddy Simulation; Navier-Stokes Equation; Reynolds Averaging; Applications Programs (Computers); Two Dimensional Models

20020001087 Lawrence Livermore National Lab., Livermore, CA USA
Accuracy evaluation for the Madejski splat-quench solidification model
Aceves, S. M.; Sahai, V.; Shapiro, A. B.; Mar. 01, 1999; 29p; In English
Report No.(s): DE2001-12138; UCRL-JC-133757; No Copyright; Avail: Department of Energy Information Bridge, Microfiche
Development of methods to spray form materials by precisely controlled deposition of droplets can result in new manufacturing processes which offer improved metallurgical performance and reduced production costs. These processes require a more detailed knowledge of the fluid mechanics, heat transfer and solidification that occur during droplet spreading. Previous work using computer simulations of this process have been difficult to implement and have required long running times. This paper examines the use of an alternative, simplified, method developed by Madjeski for solving for the problem of droplet spreading and solidification. These simplifications reduce the overall splat spreading and solidification problem to a closed-form differential equation. This differential equation is then solved under various conditions as reported from recent publications of experimental and numerical results of drop analysis. The results from the model are compared in terms of maximum spl at diameter, minimum splat thickness, and time for the droplet spreading to reach 95% of the maximum diameter. The results indicate

that the accuracy of the model can be improved by accounting for energy losses in the initial rate of droplet spreading. The model results show that the predictions of experimental results are improved to within 30% over a wide range of conditions.
NTIS
Heat Transfer; Computerized Simulation; Drops (Liquids); Energy Dissipation

20020001203 Argonne National Lab., IL USA
Hydrodynamic simulation of a lithium chloride salt system
Eberle, C. S.; Herrmann, S. D.; Knighton, G. C.; Feb. 12, 1999; 24p; In English
Report No.(s): DE2001-12358; ANL/ED/CP-98418; No Copyright; Avail: Department of Energy Information Bridge, Microfiche

A fused lithium chloride salt system's constitutive properties were evaluated and compared to a number of fluid properties, and water was shown to be an excellent simulant of lithium chloride salt. With a simple flow model, the principal scaling term was shown to be a function of the kinematic viscosity. A water mock-up of the molten salt was also shown to be within a +/- 3% error in the scaling analysis. This made it possible to consider developing water scaled tests of the molten salt system. Accurate flow velocity and pressure measurements were acquired by developing a directional velocity probe. The device was constructed and calibrated with a repeatable accuracy of +/- 15%. This was verified by a detailed evaluation of the probe. Extensive flow measurements of the engineering scale mockup were conducted, and the results were carefully compared to radial flow patterns of a straight blade stirrer. The flow measurements demonstrated an anti-symmetric nature of the stirring, and many additional effects were also identified. The basket design was shown to prevent fluid penetration into the fuel baskets when external stirring was the flow mechanism.
NTIS
Hydrodynamics; Lithium Chlorides; Molten Salts; Simulation

20020001351 Institute for Computer Applications in Science and Engineering, Hampton, VA USA
Blending Methodology of Linear Parameter Varying Control Synthesis of F-16 Aircraft System ***Final Report***
Shin, Jong-Yeob, Institute for Computer Applications in Science and Engineering, USA; Balas, Gary J., Minnesota Univ., USA; Kaya, Alpay M., California Univ., USA; October 2001; 26p; In English
Contract(s)/Grant(s): NAS1-97046; RTOP 505-90-52-01
Report No.(s): NASA/CR-2001-211237; NAS 1.26:211237; ICASE-Rept-2001-33; No Copyright; Avail: CASI; A03, Hardcopy; A01, Microfiche

This paper presents the design of a linear parameter varying (LPV) controller for the F-16 longitudinal axes over the entire flight envelope using a blending methodology which lets an LPV controller preserve performance level over each parameter subspace and reduces computational costs for synthesizing an LPV controller. Three blending LPV controller synthesis methodologies are applied to control F-16 longitudinal axes. Using a function substitution method, a quasi-LPV model of the F-16 longitudinal axes is constructed from the nonlinear equations of motion over the entire flight envelope, including non-trim regions, to facilitate synthesis of LPV controllers for the F-16 aircraft. The nonlinear simulations of the blending LPV controller show that the desired performance and robustness objectives are achieved across all altitude variations.
Author
Aircraft Control; Controllers; Control Systems Design; Liapunov Functions; Control Simulation; Longitudinal Control

20020001352 Institute for Computer Applications in Science and Engineering, Hampton, VA USA
Analysis of Linear Parameter Varying System Models Based on Reachable Sets ***Final Report***
Shin, Jong-Yeob, Institute for Computer Applications in Science and Engineering, USA; October 2001; 22p; In English
Contract(s)/Grant(s): NAS1-97046; RTOP 505-90-52-01
Report No.(s): NASA/CR-2001-211231; NAS 1.26:211231; ICASE-2001-30; No Copyright; Avail: CASI; A03, Hardcopy; A01, Microfiche

This paper presents the analysis method of quasi-Linear Parameter Varying (LPV) models, comparing the ellipsoid set which contains the reachable set of a nonlinear system to define which quasi-LPV model is less conservative to represent the nonlinear dynamics. Three quasi-LPV models are constructed from a nonlinear model using three different methods, to facilitate synthesis of an LPV controller for the nonlinear system. The comparison results of closed-loop system performance with synthesized LPV controllers correspond to the analysis results of quasi-LPV models.
Author
Controllers; Feedback Control; Nonlinear Systems; Mathematical Models; Independent Variables

20020001780 Center for Mathematics and Computer Science, Amsterdam Netherlands

Godunov-Type Scheme with Applications in Hydrodynamics. Modelling, Analysis and Simulation

van Brummelen, E. H.; Dec. 1998; 24p; In English

Report No.(s): PB2001-108616; MAS-R9829; Copyright; Avail: National Technical Information Service (NTIS), Microfiche

In spite of the absence of shock waves in most hydrodynamic applications, sufficient reason remains to employ Godunov-type schemes in this field. In the instance of two-phase flow, the shock capturing ability of these schemes may serve to maintain robustness and accuracy at the interface. Moreover, approximate Riemann solvers have greatly relieved the initial drawback of computational expensiveness of Godunov-type schemes. In the present work the authors develop an Osher-type flux-difference splitting approximate Riemann solver and they examine its application in hydrodynamics. Actual computations are left to future research.

NTIS

Hydrodynamics; Robustness (Mathematics); Flux Difference Splitting; Shock Waves

20020001846 Los Alamos National Lab., NM USA

Optimal control formulation for inviscid incompressible ideal fluid flow

Bloch, A. M.; Crouch, P. E.; Oct. 01, 2000; 9p

Report No.(s): DE2001-765583; LA-UR-00-5005; No Copyright; Avail: Department of Energy Information Bridge, Microfiche

In this paper we consider the Hamiltonian formulation of the equations of incompressible ideal fluid flow from the point of view of optimal control theory. The equations are compared to the finite symmetric rigid body analyzed earlier by the authors. We discuss various aspects of the Hamiltonian structure of the Euler equations and show in particular that the optimal control approach leads to a standard formulation of the Euler equations, the so-called impulse equations in the Lagrangian form. We discuss various other aspects of the Euler equations from a pedagogical point of view. We show that the Hamiltonian in the maximum principle is given by the pairing of the Eulerian impulse density with the velocity. We provide a comparative discussion of the flow equations in their Eulerian and Lagrangian form and describe how these forms occur naturally in the context of optimal control. We demonstrate that the extremal equations corresponding to the optimal control problem for the flow have a natural canonical symplectic structure.

NTIS

Fluid Flow; Incompressible Flow; Control Theory

20020001957 California Univ., Lawrence Radiation Lab., Livermore, CA USA

The Status of Transport Properties of Air

Schrock, V. E.; Sep. 25, 1962; 32p; In English

Contract(s)/Grant(s): W-7405-eng-48

Report No.(s): AD-A395188; UCRL-7052; No Copyright; Avail: CASI; A03, Hardcopy; A01, Microfiche

No abstract.

Author

Transport Properties; Air; Thermal Conductivity; Viscosity

20020002335 Institute for Computer Applications in Science and Engineering, Hampton, VA USA

Three-dimensional Flow in Cavity at Yaw *Final Report*

Povitsky, Alex, Institute for Computer Applications in Science and Engineering, USA; October 2001; 23p; In English

Contract(s)/Grant(s): NAS1-97046; RTOP 505-90-52-01

Report No.(s): NASA/CR-2001-211232; NAS 1.26:211232; ICASE-2001-31; AIAA Paper 2001-2847; No Copyright; Avail: CASI; A03, Hardcopy; A01, Microfiche

This study is motivated by 3-D flows about protrusions and cavities with an arbitrary angle between the external flow and rigid elements. The novel type of a ”building block” cavity flow is proposed where the cavity lid moves along its diagonal (Case A). The proposed case is taken as a typical representative of essentially 3-D highly separated vortical flows having simple single-block rectangular geometry of computational domain. Computational results are compared to the previous studies where the lid moves parallel to the cavity side walls (Case B). These 3-D lid-driven cavity flows are studied by numerical modeling using second-order upwind schemes for convective terms. The volume and plane integrals of primary and transversal momentum are introduced to compare cases in a quantitative way. For the laminar flow in the cubic cavity, the integral momentum of the secondary flow (which is perpendicular to the lid direction) is about an order of magnitude larger than that in Case B. In Case A, the number of secondary vortices substantially depends on the Re number. The secondary vortices in the central part of the cavity in Case A distinguishes it from Case B, where only corner secondary vortices appear. For a rectangular 3-D 3:1:1 cavity the integral

momentum of the secondary flow in Case A is an order of magnitude larger than that in the benchmark cases. The flow field in Case A includes a curvilinear separation line and non-symmetrical vortices which are discussed in the paper. The estimated Gortler number is approximately 4.5 times larger in Case A than that in Case B for the same Re number. This indicates that in Case A the flow becomes unsteady for smaller Re numbers than in Case B. For developed turbulent flow in the cubic cavity, the yaw effect on amplification of secondary flow is as strong as that for the laminar flow despite the more complex vortical flow pattern in benchmark case B.
Author
Computational Fluid Dynamics; Cavity Flow; Mathematical Models; Separated Flow; Three Dimensional Flow; Turbulent Flow

20020002722 California Univ., Santa Barbara, CA USA
First Annual Meeting of the Institute of Multifluid Science and Technology (IMUST)
Feb. 28, 1998; 6p; In English
Report No.(s): DE2001-765703; No Copyright; Avail: Department of Energy Information Bridge, Microfiche
This report consists of summaries of the 6 Action Items from the first annual meeting. The 6 Action Items are: (1) to aggressively pursue ”Education” in multiphase flow; (2) to pursue the work on dispersed flows presented in the last meeting to conclusions; (3) to focus the next meeting on flow regimes; (4) to pursue cooperative efforts toward identifying and settling key flow regime issues; (5) to pursue cooperative efforts towards the understanding and development of design tools, for multiphase stirred vessels (including sparged, slurry liquids); and (6) to continue to refine the TAC efforts towards useful conclusions.
NTIS
Multiphase Flow; Fluid Mechanics

20020002729 Prism Corp., Washington, DC USA
Development of X-Ray Tracer Diagnostics for Radiatively-Driven Ablator Experiments ***Annual Report, FY 1998***
MacFarlane, J. J.; Cohen, D. H.; Wang, P.; Moses, G. A.; Peterson, R. R.; May 1999; 22p; In English
Report No.(s): DE2001-765022; PCS-R-003; No Copyright; Avail: Department of Energy Information Bridge
This report covers fiscal year 1998 of our ongoing project to develop tracer X-ray spectroscopic diagnostics for hohlraum environments. This effort focused on an experimental campaign carried out at OMEGA on 25-27 August 1998. This phase of the project heavily emphasized experimental design, diagnostic development, and target fabrication, as well as building up numerical models for the experiments. The spectral diagnostic under development involves using two thin (few 1000 angstroms) mid-Z tracers in two witness plates mounted on the side of a hohlraum with the tracers’ K(sub a) absorption features seen against an X-ray backlighter. The absorption data are used to sample the time-dependent, localized properties of each witness plate as a radiation wave ablates it. The experiments represented the first application of this diagnostic, in this case to side-by-side doped and undoped plastic to investigate the effects of capsule ablator dopants.
NTIS
Ablative Materials; Experiment Design; Hohlraums; X Ray Spectroscopy

20020002777 Argonne National Lab., IL USA
Application of computational fluid dynamics (CFD) to nuclear applications
Brewster, R. A.; Jonnavithula, S.; RizwanUddin,; Rock, D. T.; Weber, D. P.; Feb. 08, 1999; 25p; In English
Report No.(s): DE2001-12401; ANL/RE/CP-98394; No Copyright; Avail: Department of Energy Information Bridge, Microfiche
Detailed analysis of a quarter channel was performed using VIPRE (Virtual Indicated Performance of Reciprocating Engines) and CFX. Results show that VIPRE and CFX agree closely in both cross-sectionally averaged axial temperature and cross-sectionally averaged axial velocity profiles. Detailed temperature distributions in the radial direction over 1 mm from the clad surface towards the center of the channel were calculated using CFX, showing significant local variation. This information can be used for example, to determine if this temperature will lead to bubble nucleation. Quarter subassembly calculations were made with both VIPRE and STAR-CD. Comparison between the solutions show that the two codes yield very similar solutions under comparable conditions. However, the STAR-CD CFD (computational fluid dynamics) calculation provides the analyst with much more detailed flow and temperature distributions than can be predicted by a one-dimensional code such as VIPRE. In addition, a 60 million cell one-eighth reactor core calculation was made using STAR-CD. This analysis showed the importance of accurately predicting the flow and temperature fields in all assemblies simultaneously with modern parallel processing technology, practical turnaround for these types of calculation can be obtained.
NTIS
Fluid Mechanics; Computational Fluid Dynamics; Computer Programs; Nuclear Reactions

20020002782 Sandia National Labs., Albuquerque, NM USA

Sensitivity Analysis and Uncertainty Propagation in a General-Purpose Thermal Analysis Code

Blackwell, B. F.; Dowding, K. J.; Aug. 04, 1999; 29p; In English

Report No.(s): DE2001-9700; SAND99-2058C; No Copyright; Avail: Department of Energy Information Bridge, Microfiche

Methods are discussed for computing the sensitivity of field variables to changes in material properties and initial/boundary condition parameters for heat transfer problems. The method we focus on is termed the ”Sensitivity Equation Method” (SEM). It involves deriving field equations for sensitivity coefficients by differentiating the original field equations with respect to the parameters of interest and numerically solving the resulting sensitivity field equations. Uncertainty in the model parameters are then propagated through the computational model using results derived from first-order perturbation theory; this technique is identical to the methodology typically used to propagate experimental uncertainty. Numerical results are presented for the design of an experiment to estimate the thermal conductivity of stainless steel using transient temperature measurements made on prototypical hardware of a companion contact conductance experiment. Comments are made relative to extending the SEM to conjugate heat transfer problems.

NTIS

Sensitivity Analysis; Thermal Analysis; Heat Transfer; Perturbation Theory

20020002858 Prism Corp., Washington, DC USA

Development of X-ray Tracer Diagnostics for Radiatively-Driven Copper-Doped Beryllium Ablators, *FY 1999*

Cohen, D. H.; MacFarlane, J. J.; Wang, P.; Jaanimagi, P. A.; Oertel, J.; May 01, 2000; 13p; In English

Report No.(s): DE2001-762795; PCS-R-009; No Copyright; Avail: Department of Energy Information Bridge

This report covers the fiscal year 1999 portion of our ongoing project to develop tracer spectral diagnostics of ablator conditions in the hohlraum radiation environment. The overall goal of the experimental campaign is to measure the turn-on times of K(sub a) absorption features from tracers buried in planar witness plates. The tracers are thin and at a specific, known depth in the witness plates so that the turn-on times are indicators of the arrival of the Marshak wave at the specified depths. Ultimately, we intend to compare the delay in the turn-on times of the tracer signals between doped and undoped ablator materials, and thus study the effect of ablator dopants on the Marshak wave velocity. During FY 1999, our primary goal was to simply measure an absorption signal, matching tracer depth to drive temperature and testing the overall feasibility of our experimental scheme. In indirect-drive inertial confinement fusion (ICF) energy is deposited rapidly on the outside of a spherical capsule, ablating the outer layers of the capsule and compressing the interior. If this process is carefully controlled, then hydrogen fuel at the center of the capsule can be compressed and heated such that fusion reactions may proceed. The efficiency of the compression depends crucially on the time-dependent energy deposition onto the ablator material on the outside of the capsule. The nature of this coupling can be controlled through the use of ablator dopants, which modify the density and opacity of the ablator layer. Clearly, it is crucial to the success of indirect-drive ICF to have a means for testing the effects of ablator dopants, and more generally for having a diagnostic that is capable of determining time-dependent ablator properties. To this end, we are adapting tracer spectroscopy techniques to make time-dependent measurements of the ionization state of planar ablator materials mounted on the sides of hohlraums. Specifically, we are doing backlighter point-projection spectroscopy of K(sub a) features from tracers placed in the interiors of planar witness plates made of ablator materials. As the radiation wave, or Marshak wave, diffuses into the ablator material it drives a shock ahead of it. When the shock arrives at a given point in the witness plate it heats the tracer to roughly 20 eV. Soon after, the radiation wave arrives, heating the tracer to well above 100 eV nearly instantaneously. Thus, the ’turn-on’ of tracer absorption from high ionization states is an indicator that the radiation wave has arrived at the tracer. Furthermore, the time-dependent ionization balance in the tracer is, our simulations show, indicative of the efficiency with which the radiation field couples to the ablator material. Note that this technique holds out the possibility of making a determination of the instantaneous impact of the radiation field on the ablator physics, as opposed to something like a shock breakout measurement, in which the observed signal reflects the integrated time-history of the impact of the radiation field on the ablator.

NTIS

Ablative Materials; Doped Crystals; Ionization

20020002859 NASA Ames Research Center, Moffett Field, CA USA

Time-Dependent Simulation of Incompressible Flow in a Turbopump Using Overset Grid Approach

Kiris, Cetin, NASA Ames Research Center, USA; Kwak, Dochan, NASA Ames Research Center, USA; [2001]; 15p; In English; ECCOMAS 2001, 4-7 Sep. 2001, Swasea, UK; No Copyright; Avail: CASI; A03, Hardcopy; A01, Microfiche

This paper reports the progress being made towards complete unsteady turbopump simulation capability by using overset grid systems. A computational model of a turbo-pump impeller is used as a test case for the performance evaluation of the MPI, hybrid MPI/Open-MP, and MLP versions of the INS3D code. Relative motion of the grid system for rotor-stator interaction was

obtained by employing overset grid techniques. Unsteady computations for a turbo-pump, which contains 114 zones with 34.3 Million grid points, are performed on Origin 2000 systems at NASA Ames Research Center. The approach taken for these simulations, and the performance of the parallel versions of the code are presented.
Author
Turbine Pumps; Computerized Simulation; Performance Tests; Incompressible Flow

20020003373 Argonne National Lab., IL USA
Automatic Differentiation and Navier-Stokes
Bischof, C.; Hovland, P.; Mohammadi, B.; Dec. 17, 1997; 24p; In English
Report No.(s): DE2001-8919; ANL/MCS/CP-95126; No Copyright; Avail: Department of Energy Information Bridge, Microfiche

We describe the use of automatic differentiation (AD) to enhance a compressible Navier-Stokes model. With the solver, AD is used to accelerate convergence by more than an order of magnitude. Outside the solver, AD is used to compute the derivatives needed for optimization. We emphasize the potential for performance gains if the programmer does not treat AD as a black box, but instead utilizes high-level knowledge about the nature of the application.
NTIS
Navier-Stokes Equation; Convergence; Mathematical Models

20020003415 California Univ., Lawrence Berkeley Lab., Berkeley, CA USA
Ohm's Law, Fick's Law, Joule's Law, and Ground Water Flow
Narasimhan, T. N.; Feb. 01, 1999; 18p; In English
Report No.(s): DE2001-6537; LBNL-42824; No Copyright; Avail: Department of Energy Information Bridge

Starting from the contributions of Ohm, Fick and Joule during the nineteenth century, an integral expression is derived for a steady-state groundwater flow system. In general, this integral statement gives expression to the fact that the steady-state groundwater system is characterized by two dependent variables, namely, flow geometry and fluid potential. As a consequence, solving the steady-state flow problem implies the finding of optimal conditions under which flow geometry and the distribution of potentials are compatible with each other, subject to the constraint of least action. With the availability of the digital computer and powerful graphics software, this perspective opens up possibilities of understanding the groundwater flow process without resorting to the traditional differential equation. Conceptual difficulties arise in extending the integral expression to a transient groundwater flow system. These difficulties suggest that the foundations of groundwater hydraulics deserve to be reexamined.
NTIS
Ground Water; Ohms Law; Unsteady Flow; Water Flow; Hydrology; Flow Geometry; Ficks Equation

20020003576 Lawrence Livermore National Lab., Livermore, CA USA
Geometry of two-dimensional slices of irregular level sets in turbulent flows
Catrakis, H. J.; Cook, A. W.; Dimotakis, P. E.; Patton, J. M.; Mar. 20, 1998; 16p; In English
Report No.(s): DE2001-2861; UCRL-JC-131726; DP0101031; No Copyright; Avail: Department of Energy Information Bridge

Isoscalar surfaces in turbulent flows are found to be more complex than (self-similar) fractals, in both the far field of liquid-phase turbulent jets and in a realization of Rayleigh-Taylor-instability flow. In particular, they exhibit a scale-dependent coverage dimension, D(sub 2)((lambda)), for 2-D slices of scalar level sets, that increases with scale, from unity, at small scales, to 2, at large scales. For the jet flow and Reynolds numbers investigated, the isoscalar-surface geometry is both scalar-threshold- and Re-dependent; the level-set (coverage) length decreases with increasing Re, indicating enhanced mixing with increasing Reynolds number; and the size distribution of closed regions is well described by lognormal statistics at small scales. A similar D(sub 2)((lambda)) behavior is found for level-set data of 3-D density-interface behavior in recent direct numerical-simulation studies of Rayleigh-Taylor-instability flow. A comparison of (spatial) spectral and isoscalar coverage statistics will be discussed.
NTIS
Turbulent Flow; Fluid Mechanics; Taylor Instability; Turbulent Jets

20020003729 Lawrence Livermore National Lab., Livermore, CA USA
CFD Simulation of Infiltration Heat Recovery
Buchanan, C. R.; Sherman, M. H.; Jul. 01, 1998; 14p; In English
Report No.(s): DE2001-6425; LBNL-42098; No Copyright; Avail: Department of Energy Information Bridge

Infiltration has traditionally been assumed to affect the energy load of a building by an amount equal to the product of the infiltration flow rate and the sensible enthalpy difference between inside and outside. Results from detailed computational fluid

dynamics simulations of five wall geometries over a range of infiltration rates show that heat transfer between the infiltrating air and walls can be substantial, reducing the impact of infiltration. Factors affecting the heat recovery are leakage path length, infiltration flow rate, and wall construction. The classical method for determination of the infiltration energy load was found to over-predict the amount by as much as 95 percent and by at least 10 percent. However, the air flow paths typical of building envelopes give over-predictions at the low end of this range.
NTIS
Air Flow; Computational Fluid Dynamics; Heat Transfer; Infiltration; Waste Energy Utilization; Recovery; Computerized Simulation; Buildings

20020003978 Lawrence Livermore National Lab., Livermore, CA USA
New computational method for non-LTE, the linear response matrix
Fournier, K. B.; Grasiani, F. R.; Harte, J. A.; Libby, S. B.; More, R. M.; Nov. 02, 1998; 23p; In English
Report No.(s): DE2001-2848; UCRL-JC-132407; DP0102012; No Copyright; Avail: Department of Energy Information Bridge

My coauthors have done extensive theoretical and computational calculations that lay the ground work for a linear response matrix method to calculate non-LTE (local thermodynamic equilibrium) opacities. I will give briefly review some of their work and list references. Then I will describe what has been done to utilize this theory to create a computational package to rapidly calculate mild non-LTE emission and absorption opacities suitable for use in hydrodynamic calculations. The opacities are obtained by performing table look-ups on data that has been generated with a non-LTE package. This scheme is currently under development. We can see that it offers a significant computational speed advantage. It is suitable for mild non-LTE, quasi-steady conditions. and it offers a new insertion path for high-quality non-LTE data. Currently, the linear response matrix data file is created using XSN. These data files could be generated by more detailed and rigorous calculations without changing any part of the implementation in the hydro code. The scheme is running in Lasnex and is being tested and developed.
NTIS
Local Thermodynamic Equilibrium; Matrix Methods; Opacity

20020004179 Bionetics Corp., Moffett Field, CA USA
Development of a General Method for Determining Leak Rates from Limiting Enclosures
Zografos, A. I., Bionetics Corp., USA; Blackwell, C. C., Bionetics Corp., USA; [1994]; 1p; In English; 24th International Conference on Environmental Systems, 20-23 Jun. 1994, Friedrichshafen, Germany
Contract(s)/Grant(s): RTOP 106-20-07; No Copyright; Avail: Issuing Activity; Abstract Only

This paper discusses the development of a general method for the determination of very low leak rates from limiting enclosures. There are many methods that can be used to detect and repair leaks from enclosures. Many methods have also been proposed that allow the estimation of actual leak rates, usually expressed as enclosure volume turnover. The proposed method combines measurements of the state variables (pressure, temperature, and volume) as well as the change in the concentration of a tracer gas to estimate the leak rate. The method was applied to the containment enclosure of the Engineering Development Unit of the CELSS Test Facility, currently undergoing testing at the NASA Ames Research Center.
Author
Leakage; Test Facilities

20020005085 Argonne National Lab., IL USA
Spatiotemporal dynamics of a shallow fluidized bed
Aranson, I. S.; Tsimring, L. S.; Clark, D. K.; Dec. 05, 2000; 7p; In English
Report No.(s): DE2001-772121; ANL/MSD/CP-103587; No Copyright; Avail: Department of Energy Information Bridge, Microfiche

An experimental and theoretical study of the dynamics of an air-fluidized thin granular layer is presented. Near the threshold of instability, the system exhibits critical behavior with remarkably long transient dynamics. Above the threshold of fluidization the system undergoes a Hopf bifurcation as the layer starts to oscillate at a certain frequency due to a feedback between the layer dilation and the airflow rate. Based on our experimental data, we formulate a the simple dynamical model which describes the transition in a shallow fluidized bed.
NTIS
Granular Materials; Air Flow

20020005093 Stanford Univ., Dept. of Aeronautics and Astronautics, Stanford, CA USA

A Numerical Investigation of the Burnett Equations Based on the Second Law

Comeaux, Keith A., Stanford Univ., USA; Chapman, Dean R., Stanford Univ., USA; MacCormack, Robert W., Stanford Univ., USA; [1995]; 1p; In English; 29th AIAA Thermophysics Conference, 19-22 Jun. 1995, San Diego, CA, USA; Sponsored by American Inst. of Aeronautics and Astronautics, USA

Contract(s)/Grant(s): RTOP 232-01-04; No Copyright; Avail: Issuing Activity; Abstract Only

The Burnett equations have been shown to potentially violate the second law of thermodynamics. The objective of this investigation is to correlate the numerical problems experienced by the Burnett equations to the negative production of entropy. The equations have had a long history of numerical instability to small wavelength disturbances. Recently, Zhong corrected the instability problem and made solutions attainable for one dimensional shock waves and hypersonic blunt bodies. Difficulties still exist when attempting to solve hypersonic flat plate boundary layers and blunt body wake flows, however. Numerical experiments will include one-dimensional shock waves, quasi-one dimensional nozzles, and expanding Prandlt-Meyer flows and specifically examine the entropy production for these cases.

Author

Burnett Equations; Numerical Analysis; Entropy

20020005127 NASA Ames Research Center, Moffett Field, CA USA

Viscous Incompressible Flow Computations for 3-D Steady and Unsteady Flows

Kwak, Dochan, NASA Ames Research Center, USA; [2001]; 86p; In English; Viscous Incompressible Flow Computations For 3-D Steady and Unsteady Flows, 8-12 Oct. 2001, Seoul, Korea, Democratic People's Republic of; No Copyright; Avail: CASI; A05, Hardcopy; A01, Microfiche

This viewgraph presentation gives an overview of viscous incompressible flow computations for three-dimensional steady and unsteady flows. Details are given on the use of computational fluid dynamics (CFD) as an engineering tool, solution methods for incompressible Navier-Stokes equations, numerical and physical characteristics of the primitive variable approach, and the role of CFD in the past and in current engineering and research applications.

CASI

Computational Fluid Dynamics; Three Dimensional Flow; Unsteady Flow; Viscous Flow; Incompressible Flow

20020005177 Los Alamos National Lab., NM USA

Heat Pipe Development for Advanced Energy Transport Concepts Phase II Final Report Covering the Period October 1, 1997, to September 30, 1998

Martinez, A. L.; Sena, J. T.; Merrigan, M. A.; Elder, M. G.; Reid, R. S.; Feb. 01, 1999; 143p; In English

Report No.(s): DE2001-7384; LA-13549-PR; No Copyright; Avail: Department of Energy Information Bridge

This report summarizes progress in the Heat Pipe Technology Development for Advanced Energy Transport Concepts (Phase II) program for the year October 1, 1997, to September 30, 1998. Significant accomplishments during the year include the processing and testing of a 1.8-m long Mo-Li heat pipe, development of a thermochemical model for the sodium-Haynes 230 material system, fabrication of a series of heat pipes to assess the compatibility of several materials with sodium, and the execution of a test measuring the response of a sodium heat pipe to the penetration of water.

NTIS

Heat Pipes; Performance Tests; Design Analysis; Technology Assessment

20020005179 Lawrence Livermore National Lab., Livermore, CA USA

Turbulence Structure and Implications for Dispersion: Insights from Large-Eddy Simulations

Calhoun, R.; Cederwall, R.; Street, R.; Oct. 04, 1999; 7p; In English

Report No.(s): DE2001-756951; UCRL-JC-135954; No Copyright; Avail: Department of Energy Information Bridge

We have presented two flows where detailed knowledge of the fluid mechanics would appear to be crucial for accurate dispersion modeling. We expect that Large-eddy simulations (LES) will complement traditional dispersion modeling by providing both the ability to discern between cases where traditional models work well and cases where more complicated characterizations are necessary, and a method to investigate potentially unique flow features and turbulence structure for specific flow problems.

NTIS

Fluid Mechanics; Large Eddy Simulation; Turbulent Flow

20020005194 Los Alamos National Lab., NM USA

Energy landscape of 2D fluid forms

Jiang, Y.; Apr. 01, 2000; 11p; In English

Report No.(s): DE2001-768977; LA-UR-00-2049; No Copyright; Avail: Department of Energy Information Bridge

The equilibrium states of 2D non-coarsening fluid foams, which consist of bubbles with fixed areas, correspond to local minima of the total perimeter. (1) The authors find an approximate value of the global minimum, and determine directly from an image how far a foam is from its ground state. (2) For (small) area disorder, small bubbles tend to sort inwards and large bubbles outwards. (3) Topological charges of the same sign repel while charges of opposite sign attract. (4) They discuss boundary conditions and the uniqueness of the pattern for fixed topology.

NTIS

Foams; Fluid Mechanics; Bubbles

20020005195 Los Alamos National Lab., NM USA

Theoretical description of inhomogeneous turbulence

Turner, L.; Mar. 01, 2000; 13p; In English

Report No.(s): DE2001-768978; LA-UR-00-1997; No Copyright; Avail: Department of Energy Information Bridge

This is the final report of a three-year, Laboratory-Directed Research and Development (LDRD) project at the Los Alamos National Laboratory (LANL). In this LDRD, we have developed a highly compact and descriptive formalism that allows us to broach the theoretically formidable morass of inhomogeneous turbulence. Our formalism has two novel aspects: (1) an adaptation of helicity basis functions to represent an arbitrary incompressible channel flow and (2) the invocation of a hypothesis of random phase. A result of this compact formalism is that the mathematical description of inhomogeneous turbulence looks much like that of homogeneous turbulence--at the moment, the most rigorously explored terrain in turbulence research. As a result, we can explore the effect of boundaries on such important quantities as the gradients of mean flow, mean pressure, triple-velocity correlations and pressure velocity correlations, all of which vanish under the conventional, but artificial, assumption that the turbulence is statistically spatially uniform. Under suitable conditions, we have predicted that a mean flow gradient can develop even when none is initially present.

NTIS

Turbulence; Inhomogeneity; Formalism

20020005198 Los Alamos National Lab., NM USA

Influence of CFD analysis on the design of cooling channels for the CCL cavity for the spallation neutron source

Konecni, S.; Jun. 01, 2000; 9p; In English

Report No.(s): DE2001-769034; LA-UR-00-2549; No Copyright; Avail: Department of Energy Information Bridge

Water flow in cooling channels was simulated using the computational fluid dynamics (CFD) code CFX4. Pressure drop in the cooling channels of the coupled-cavity linac (CCL) cavity was calculated. The effects of the manifold on the pressure drop were studied also. Reducing the pressure drop was a primary goal of the exercise that led to changing the cooling channel entrance regions. Results of this analysis were used in sizing pumps required for the cooling system.

NTIS

Computational Fluid Dynamics; Linear Accelerators; Neutron Sources; Spallation; Water Flow; Cooling Systems

20020005241 Bettis Atomic Power Lab., West Mifflin, PA USA

Study of interfacial area transport and sensitivity analysis for air-water bubbly flow

Kim, S.; Sun, X.; Ishii, M.; Beus, S. G.; Sep. 01, 2000; 30p; In English

Report No.(s): DE2001-774249; B-T-3324; No Copyright; Avail: Department of Energy Information Bridge, Microfiche

The interfacial area transport equation applicable to the bubbly flow is presented. The model is evaluated against the data acquired by the state-of-the-art miniaturized double-sensor conductivity probe in an adiabatic air-water co-current vertical test loop under atmospheric pressure condition. In general, a good agreement, within the measurement error of plus/minus 10%, is observed for a wide range in the bubbly flow regime. The sensitivity analysis on the individual particle interaction mechanisms demonstrates the active interactions between the bubbles and highlights the mechanisms playing the dominant role in interfacial area transport. The analysis employing the drift flux model is also performed for the data acquired. Under the given flow conditions, the distribution parameter of 1.076 yields the best fit to the data.

NTIS

Two Phase Flow; Bubbles; Air Flow; Water Flow

20020005242 Purdue Univ., West Lafayette, IN USA

Interfacial structures of confined air-water two-phase bubbly flow

Kim, S.; Ishii, M.; Wu, Q.; McCreary, D.; Beus, S. G.; Aug. 01, 2000; 27p; In English

Report No.(s): DE2001-774251; B-T-3291; No Copyright; Avail: Department of Energy Information Bridge, Microfiche

The interfacial structure of the two-phase flows is of great importance in view of theoretical modeling and practical applications. In the present study, the focus is made on obtaining detailed local two-phase parameters in the air-water bubbly flow in a rectangular vertical duct using the double-sensor conductivity probe. The characteristic wall-peak is observed in the profiles of the interfacial area concentration and the void fraction. The development of the interfacial area concentration along the axial direction of the flow is studied in view of the interfacial area transport and bubble interactions. The experimental data is compared with the drift flux model with C(sub 0) = 1.35.

NTIS

Two Phase Flow; Air Flow; Water Flow; Bubbles

20020005243 Bettis Atomic Power Lab., West Mifflin, PA USA

New assessment of RELAP5-3D using a General Electric level swell problem

Aumiller, D. L.; Tomlinson, E. T.; Clarke, W. G.; Sep. 01, 2000; 19p; In English

Report No.(s): DE2001-774255; B-T-3320; No Copyright; Avail: Department of Energy Information Bridge, Microfiche

The RELAP5-3D (version bt) computer program was used to assess a GE level swell experiment. The primary goal of the new assessment models was to faithfully represent the experimental facility and instrumentation. In developing the new models, a non-physical representation of the vessel heads in a previous assessment was found. This distortion resulted in predictions that closely matched the experimental data, but were in error. The new assessment also highlighted an instability in the calculation of interfacial drag. To explore this issue, analyses were performed using three different interfacial drag correlations appropriate for large diameter pipes and/or vessels. The results of this study show that the Kataoka-Ishii correlation, which is currently used in RELAP5-3D, compares most favorably with the experimental data. Additionally, a numerical instability was uncovered with the analysis performed using the Gardner correlation and was traced to the calculation of bubble diameter in the bubbly flow regime.

NTIS

Computer Programs; Software Reliability; Two Phase Flow

20020005415 Computer Sciences Corp., Moffett Field, CA USA

Scientific Visualization of Large Scale Unsteady Fluid Flow

Lane, David A., Computer Sciences Corp., USA; [1994]; 1p; In English

Contract(s)/Grant(s): RTOP 536-01-11; No Copyright; Avail: Issuing Activity; Abstract Only

In a numerical flow simulation. it is common to generate several thousand time steps of unsteady (time-dependent) flow data. Each time step may require tens to hundreds of megabytes for disk storage, and the total disk requirement for storing the unsteady flow data may be hundreds of gigabytes. Interactive visualization of unsteady flow data of this magnitude is presently impossible with the current hardware technology. This chapter describes the current approaches for unsteady flow visualization. An effective particle tracing technique for unsteady flow is also described. First, the life cycle of a typical numerical flow simulation is outlined. Several unsteady flow data sets from real-world problems are then given. The current approaches for visualizing unsteady flow are then described. There are many existing systems for flow visualization, and some of them are discussed. Streaklines depict time-varying phenomena that are sometimes difficult or impossible to see with other visualization techniques. The algorithms for computing streaklines are described. Several unsteady flow data sets have been visualized using streaklines, and the results are presented. Finally, some current issues in unsteady flow visualization are discussed.

Author

Numerical Flow Visualization; Unsteady Flow; Fluid Flow; Computational Fluid Dynamics

20020005837 NASA Ames Research Center, Moffett Field, CA USA

Calibration of Axisymmetric and Quasi-1D Solvers for High Enthalpy Nozzles

Papadopoulos, P. E., Thermoscience Inst., USA; Gochberg, L. A., National Academy of Sciences - National Research Council, USA; Tokarcik-Polsky, S., Sterling Software, Inc., USA; Venkatapathy, E., Thermoscience Inst., USA; Deiwert, G. S., NASA Ames Research Center, USA; [1994]; 1p; In English; 29th AIAA Thermophysics Conference, 19-22 Jun. 1995, San Diego, CA, USA; Sponsored by American Inst. of Aeronautics and Astronautics, USA

Contract(s)/Grant(s): RTOP 505-70-62; No Copyright; Avail: Issuing Activity; Abstract Only

The proposed paper will present a numerical investigation of the flow characteristics and boundary layer development in the nozzles of high enthalpy shock tunnel facilities used for hypersonic propulsion testing. The computed flow will be validated against existing experimental data. Pitot pressure data obtained at the entrance of the test cabin will be used to validate the numerical simulations. It is necessary to accurately model the facility nozzles in order to characterize the test article flow conditions. Initially the axisymmetric nozzle flow will be computed using a Navier Stokes solver for a range of reservoir conditions. The calculated solutions will be compared and calibrated against available experimental data from the DLR HEG piston-driven shock tunnel and the 16-inch shock tunnel at NASA Ames Research Center. The Reynolds number is assumed to be high enough at the throat that the boundary layer flow is assumed turbulent at this point downstream. The real gas affects will be examined. In high Mach number facilities the boundary layer is thick. Attempts will be made to correlate the boundary layer displacement thickness. The displacement thickness correlation will be used to calibrate the quasi-1D codes NENZF and LSENS in order to provide fast and efficient tools of characterizing the facility nozzles. The calibrated quasi-1D codes will be implemented to study the effects of chemistry and the flow condition variations at the test section due to small variations in the driver gas conditions.

Author

Flow Characteristics; Boundary Layers; Shock Tunnels; Computerized Simulation; Axisymmetric Flow; Calibrating

20020005882 California Univ., Radiation Lab., Livermore, CA USA

Shock Hydrodynamics

Wilkins, Mark L.; Feb. 19, 1962; 26p; In English

Contract(s)/Grant(s): W-7405-eng-48

Report No.(s): AD-A395375; UCRL-6797; No Copyright; Avail: CASI; A03, Hardcopy; A01, Microfiche

The Hugoniot relations, which express conservation of mass, momentum, and energy across a discontinuity, are derived. The relations are applied to a perfect gas for illustration, and graphical methods of solving shock problems are presented.

DTIC

Hydrodynamics; Shock Loads; Hugoniot Equation of State

20020005886 State Univ. of New York, Stony Brook, NY USA

Turbulent Mixing and Solid Impact: Studies in Multiscale Modeling ***Final Report, 1 Jul. 1998-30 Jun. 2001***

Glimm, James; Plohr, Bradley J.; Jun. 30, 2001; 16p; In English

Contract(s)/Grant(s): DAAG55-98-1-0313

Report No.(s): AD-A395387; ARO-38338.20-MA; No Copyright; Avail: CASI; A03, Hardcopy; A01, Microfiche

The principal directions of the research reported were fluid interface instabilities, multiphase flow, solid dynamics, flow in porous media, uncertainty quantification and photonics. Our Front Tracking code, FronTier, has been extended to three dimensions, and is now functioning robustly for the simulation of three-dimensional complex fluid mixing flows. We have made a major effort in the study of multiphase flow, including a proposed model of averaged multiphase flow equations which seem to avoid most of the well known pitfalls for such equations. Validation studies for the Front Tracking code, FronTier Solid have been performed. Photonics, a new project for this work, is conducted in collaboration with C. Bowden of Redstone Arsenel, and a group of his collaborators. We have developed a parallelized FDTD code to allow simulations in complex 3D geometries for photonic crystals and other photonic devices.

DTIC

Turbulent Flow; Multiphase Flow; Turbulent Mixing; Liquid-Liquid Interfaces; Interface Stability

35
INSTRUMENTATION AND PHOTOGRAPHY

Includes remote sensors; measuring instruments and gauges; detectors; cameras and photographic supplies; and holography. For aerial photography see 43 Earth Resources and Remote Sensing. For related information see also 06 Avionics and Aircraft Instrumentation; and 19 Spacecraft Instrumentation.

20020000870 MetroLaser, Irvine, CA USA

Holographic memory module with ultra-high capacity and throughput

Markov, V. A.; Jun. 04, 2000; 29p; In English

Report No.(s): DE2001-764589; No Copyright; Avail: Department of Energy Information Bridge

High capacity, high transfer rate, random access memory systems are needed to archive and distribute the tremendous volume of digital information being generated, for example, the human genome mapping and online libraries. The development of multi-gigabit per second networks underscores the need for next-generation archival memory systems. During Phase I we conducted the theoretical analysis and accomplished experimental tests that validated the key aspects of the ultra-high density holographic data storage module with high transfer rate. We also inspected the secure nature of the encoding method and estimated the performance of full-scale system. Two basic architectures were considered, allowing for reversible compact solid-state configuration with limited capacity, and very large capacity write once read many memory system.
NTIS
Holography; Modules; Computer Networks; Random Access Memory

20020001445 Lawrence Livermore National Lab., Livermore, CA USA
Multilayer Coatings of 10x Projection for Extreme-Ultraviolet Lithography
Folta, J. A.; Montcalm, C.; Spiller, E.; Wedowski, M.; Mar. 09, 1999; 9p; In English
Report No.(s): DE2001-8781; UCRL-JC-132560; No Copyright; Avail: Department of Energy Information Bridge, Microfiche
Two new sets of projections optics for the prototype 10X reduction extreme ultraviolet (EUV) lithography system were coated with Mo/Si multilayers. The coating thickness was graded across the optics by using shadow masks to ensure maximum throughput at all incidence angles in the camera. The overall deviation of the (normalized) wavelength response across the clear aperture of each mirror is below 0.01% RMS. However, the wavelength mismatch between two optics coated in different runs is up to 0.07 nm. Nevertheless, this is still within the allowed tolerances, and the predicted optical throughput loss in the camera due to such wavelength mismatch is about 4%. EUV reflectances of 63-65% were measured around 13.40 nm for the secondary optics, which is in good agreement with the expected reflectance based on the substrate finish as measured with AFM.
NTIS
Coatings; Extreme Ultraviolet Radiation; Lithography

20020001884 Colorado State Univ., Fort Collins, CO USA
Global Change Research with Unmanned Aerospace Vehicles UAV Applications for Studying the Radiation and Optical Properties of Upper Tropospheric Clouds, *1 Feb. 1995 - 31 Mar. 1998*
Stephens, G. L.; Jan. 31, 1998; 7p; In English
Report No.(s): DE2001-765421; No Copyright; Avail: Department of Energy Information Bridge, Microfiche
This paper describes the design and characteristics of a scanning spectral polarimeter which is capable of measuring spectral radiances and fluxes in the range between 0.4 rm to 4.0 pm. The instrument characteristics are described and a discussion of the procedures to calibrate the unpolarized radiances and fluxes are prescribed along the detailed error analyses of this calibration.
NTIS
Optical Properties; Troposphere; Clouds (Meteorology); Remote Sensing; Pilotless Aircraft; Radiance

20020002359 Office of Air Quality Planning and Standards, Research Triangle Park, NC USA
Economic Impact Analysis for the Proposed Municipal Solid Waste Landfills
Sorrels, L.; Bradley, L.; September 2000; 24p; In English
Report No.(s): PB2001-107704; EPA/452/D-00/005; No Copyright; Avail: CASI; A03, Hardcopy; A01, Microfiche
The calibration and irradiation of instruments that measure x-rays and gamma-rays are performed in terms of the physical quantity air-kerma. The calibrations listed in the NIST Special Publication 250 Calibration Services Users Guide as calibrations 46010C through 46050S. The process for establishing calibration or correction factors for radiation detectors, charge sensitivity tests for high-gain electrometers, and irradiations of passive dosimeters is explained in this document. Calibrations are performed by comparing the instrument to a NIST primary standard, which include four free-air chambers for x-rays and cavity ionization chambers for cesium-137 and cobalt-60 gamma rays. Details of the design and use of these standards are presented in this document, as well as, a description of the quality assurance checks, which are performed to assure the constancy of the standards and the accuracy of the calibrations and irradiations. The overall uncertainty with a significance of a 95% confidence limit is given as 0.9% for the air-kerma rate in the NIST beams, 1% for the calibration of a cable-connected chamber and irradiation of passive dosimeters, and 1.5% for the calibration of a condenser chamber.
NTIS
Calibrating; X Rays; Gamma Rays; Dosimeters; Electrometers

20020002714 Lawrence Livermore National Lab., Livermore, CA USA

Moisture proof columnar Cesium Iodide (CsI) layers for gas avalanche microdetectors

Park, I. J.; Cho, H. S.; Hong, W. S.; Perez-Mendez, V.; Kadyk, J.; May 05, 1999; 5p; In English

Report No.(s): DE2001-767507; LBNL-42566; No Copyright; Avail: Department of Energy Information Bridge

Cesium iodide columnar layers having a diameter of 3 (micro)m, and wall spacing of (approx) 1 (micro)m act as secondary electron emitters and can be used for detection of radiation: charged particles, X-rays and gamma rays. With a large enough electric field across the columnar layers, (approx) 400 (micro)m in thickness, gas avalanche gain is evident when placed in a suitable gas, such as P10 or argon-ethane mixtures. The cesium iodide columns are damaged by ambient moisture. This damage can be prevented by evaporating protective layers of insoluble, low boiling point inorganic materials, such as mercuric iodide. Columnar layers with 20 nm coatings of mercuric iodide yield more than 30,000 electrons on average when traversed by electrons from a (sup 90)SR beta source.

NTIS

Cesium Iodides; Gas Mixtures; Moisture; Protective Coatings; Radiation Detectors; Electron Avalanche

20020003344 NASA Goddard Space Flight Center, Greenbelt, MD USA

New Instrumentation, Patterns and Their Effects on TID Testing of Antifuse-Based FPGAs

Kleyner, Igor, Orbital Sciences Corp., USA; Katz, Rich, NASA Goddard Space Flight Center, USA; Wang, J. J., Actel Corp., USA; [2001]; 22p; In English; 2001 MAPLD International Conference, Sep. 2001, Laurel, MD, USA; No Copyright; Avail: CASI; A03, Hardcopy; A01, Microfiche

TID-induced leakage currents for some families of antifuse-based Field Programmable Gate Array (FPGA) devices are significantly affected by the state of bias of a device's internal nodes; proper consideration of this effect is essential for proper testing of these devices and interpretation of test results. Variations in TID performance based on utilization of different internal logic modules for implementing identical circuits may be utilized by circuit designers for improvement in TID performance by tailoring the placement algorithm. Propagation delays are significantly affected by TID-induced damage for the devices of 54SX32S family.

Derived from text

Leakage; Field-Programmable Gate Arrays; Electromagnetic Wave Transmission

20020003352 NASA Goddard Space Flight Center, Greenbelt, MD USA

Development of Low-Noise High Value Chromium Silicide Resistors for Cryogenic Detector Applications

Jhabvala, Murzy, NASA Goddard Space Flight Center, USA; Babu, Sachi, Ball Aerospace and Technologies Corp., USA; Monroy, Carlos, Raytheon Information Technology and Scientific Services, USA; Darren, C., California Inst. of Tech., USA; [2001]; 15p; In English; No Copyright; Avail: CASI; A03, Hardcopy; A01, Microfiche

Extremely high sensitivity detectors, such as silicon bolometers are required in many NASA missions for detection of photons from the x-ray to the far infrared regions. Typically, these detectors are cooled to well below the liquid helium (LHe) temperature (4.2 K) to achieve the maximum detection performance. As photoconductors, they are generally operated with a load resistor and a pre-set bias voltage, which is then coupled to the input gate of a source-follower Field Effect Transistor (FET) circuit. It is imperative that the detector system signal to noise performance be limited by the noise of the detector and not by the noise of the external components. The load resistor value is selected to optimize the detector performance. These two criteria tend to be contradictory in that these detectors require load resistors in the hundreds of megaohms, which leads to a higher Johnson noise. Additionally, the physical size of the resistor must be small for device integration as required by such missions as the NASA High Resolution Airborne Wide-Band Camera (HAWC) instrument and the Submillimeter High Angular Resolution Camera (SHARC) for the Caltech Submillimeter Observatory (CSO). We have designed, fabricated and characterized thin film resistors using a CrSi/TiW/Al metal system on optical quality quartz substrates. The resistor values range from 100 megaohms to over 650 megaohms and are Johnson noise limited at LHe temperatures. The resistor film is sputtered with a sheet resistance ranging from 300 ohms to 1600 ohms and the processing sequence developed for these devices allows for chemically fine tuning the sheet resistance in-situ. The wafer fabrication process was of sufficiently high yield (>80%) providing clusters of good resistors for integrated multiple detector channels, a very important feature in the assembly of these two instruments.

Author

Cryogenics; Radiation Counters; Resistors

20020003998 Bechtel Nevada Corp., Las Vegas, NV USA

Image Tool

Baker, S. A.; Gardner, S. D.; Rogers, M. L.; Sanders, F.; Tunnell, T. W.; Jan. 01, 2001; 10p; In English

Report No.(s): DE2001-773560; DOE/NV/11718-466; No Copyright; Avail: Department of Energy Information Bridge, Microfiche

ImageTool is a software package developed at Bechtel Nevada, Los Alamos Operations. This team has developed a set of analysis tools, in the form of image processing software used to evaluate camera calibration data. Performance measures are used to identify capabilities and limitations of a camera system, while establishing a means for comparing systems. The camera evaluations are designed to provide system performance, camera comparison and system modeling information. This program is used to evaluate digital camera images. ImageTool provides basic image restoration and analysis features along with a special set of camera evaluation tools which are used to standardize camera system characterizations. This process is started with the acquisition of a well-defined set of calibration images. Image processing algorithms provide a consistent means of evaluating the camera calibration data. Performance measures in the areas of sensitivity, noise, and resolution are used as a basis for comparing camera systems and evaluating experimental system performance. Camera systems begin with a charge-coupled device (CCD) camera and optical relay system and may incorporate image intensifiers, electro-static image tubes, or electron bombarded charge-coupled devices (EBCCDs). Electro-optical components provide fast shuttering and/or optical gain to camera systems. Camera types evaluated include gated intensified cameras and multi-frame cameras used in applications ranging from X-ray radiography to visible and infrared imaging. It is valuable to evaluate the performance of a camera system in order to determine if a particular system meets experimental requirements. In this paper we highlight the processing features of ImageTool.

NTIS

Cameras; Image Processing; Pattern Recognition; Image Analysis; Calibrating

20020005097 DYNACS Engineering Co., Inc., Cocoa Beach, FL USA

UV-IR Hydrogen Fire Detector

Medelius, Pedro J., DYNACS Engineering Co., Inc., USA; [2001]; 15p; In English; Sensors Expo, 4-7 Jun. 2001, Chicago, IL, USA

Contract(s)/Grant(s): NAS10-98001; No Copyright; Avail: CASI; A03, Hardcopy; A01, Microfiche

The objective of this project is to design a sensor than can accurately determine the presence of a hydrogen fire within its field of view and to eliminate the main cause of false alarms: reflections from the flare stack. Details are given in viewgraph presentation form on the technical approach, initial testing, sensor testing, intellectual property, patented technology, and licensing.

Derived from text

Fires; Gas Detectors; Performance Tests

20020005119 NASA Marshall Space Flight Center, Huntsville, AL USA

Non-Contact Linear Actuator Position Sensor Having a PID-Compensating Controller

Alhorn, Dean C., Inventor, NASA Marshall Space Flight Center, USA; Howard, David E., Inventor, NASA Marshall Space Flight Center, USA; Jun. 12, 2001; 10p; In English

Patent Info.: Filed 27 Nov. 1998; NASA-Case-MFS-31218; US-Patent-6,246,228; US-Patent-Appl-SN-209363; No Copyright; Avail: CASI; A02, Hardcopy; A01, Microfiche

A position sensor or controller generates a response signal in existing armature windings of an actuator and detects the response signal to determine the position of the armature. to generate the response signal, the actuator includes a sensor excitation winding near the armature. Two sensor excitation windings can be provided, above and below the armature, to cancel out z components and thus allow for a variable gap. The sensor excitation winding or windings are supplied with an excitation signal to induce the response signal in the armature windings. The response signal is derived by differentially amplifying and frequency filtering a raw output of the armature windings. The response signal is demodulated to determine position. If a position controller rather than a mere sensor is desired, the position signal can be buffered, PID compensated, amplified, and fed back to the armature windings.

Official Gazette of the U.S. Patent and Trademark Office

Actuators; Armatures; Controllers; Excitation; Winding

20020005125 NASA Marshall Space Flight Center, Huntsville, AL USA

Position Sensor with Integrated Signal-Conditioning Electronics on a Printed Wiring Board

Alhorn, Dean C., Inventor, NASA Marshall Space Flight Center, USA; Howard, David E., Inventor, NASA Marshall Space Flight Center, USA; Smith, Dennis A., Inventor, NASA Marshall Space Flight Center, USA; Nov. 06, 2001; 9p; In English

Patent Info.: Filed 27 Nov. 1998; NASA-Case-MFS-31238-1; US-Patent-6,313,624; US-Patent-Appl-SN-208401; No Copyright; Avail: CASI; A02, Hardcopy; A01, Microfiche

A position sensor, such as a rotary position sensor, includes the signal-conditioning electronics in the housing. The signal-conditioning electronics are disposed on a printed wiring board, which is assembled with another printed wiring board including the sensor windings to provide a sub-assembly. A mu-metal shield is interposed between the printed wiring boards to prevent magnetic interference. The sub-assembly is disposed in the sensor housing adjacent to an inductor board which turns on a shaft. The inductor board emanates an internally or externally generated excitation signal that induces a signal in the sensor windings. The induced signal represents the rotary position of the inductor board relative to the sensor winding board.

Official Gazette of the U.S. Patent and Trademark Office

Signal Processing; Sensors; Printed Circuits

20020005184 Lawrence Livermore National Lab., Livermore, CA USA

Extreme Ultraviolet Lithography for 0.1 micro-m Devices

Vaidya, S.; Sweeney, D. W.; Stulen, R.; Attwood, D.; Jul. 07, 1999; 6p; In English

Report No.(s): DE2001-757420; UCRL-JC-133192-REV-1; No Copyright; Avail: Department of Energy Information Bridge

Extreme Ultraviolet Lithography (EUVL) has emerged as one of the leading successors to optics for 0.1 micro-m IC fabrication. Its strongest attribute is the potential to scale to much finer resolution at high throughput. As such, this technique could meet the lithography needs for Si ULSI down to fundamental device limits. In the US, Lawrence Livermore, Sandia, and Lawrence Berkeley National Laboratories are participating in an industry funded research effort to evolve EUV technology and build a prototype camera for lithographic exposure. More recently, both Europe and Japan have initiated government/industry sponsored programs in EUVL development. This talk will focus on our program successes to date, and highlight some of the challenges that still lie ahead.

NTIS

Extreme Ultraviolet Radiation; Photolithography; Fabrication

20020005201 Exponent, Boulder, CO USA

Restoration Monitoring: A Simple Photo Monitoring Method

Nelson, J. K.; Feb. 14, 2000; 10p; In English

Report No.(s): DE2001-769075; RFP-5322; No Copyright; Avail: Department of Energy Information Bridge

Through the use of a simple photo monitoring design, it is possible to visually document, with both landscape and ground views, the progression of a restoration/revegetation project in a repeatable, cost-effective manner. The use of web browser technology can display the results in a simple, informative, professional manner, suitable for presentations and displays.

NTIS

Restoration; Vegetation; Topography; Photography

20020005252 Sandia National Labs., Albuquerque, NM USA

Multispectral Thermal Imager (MTI) Payload Overview

Bender, S. C.; Brock, B. C.; Bullington, D. M.; Byrd, D. A.; Claassen, P. J.; Jul. 07, 1999; 14p; In English

Report No.(s): DE2001-8953; SAND99-1723C; No Copyright; Avail: Department of Energy Information Bridge, Microfiche

MTI is a comprehensive research and development project that includes up-front modeling and analysis, satellite system design, fabrication, assembly and testing, on-orbit operations, and experimentation and data analysis. The satellite is designed to collect radiometrically calibrated, medium resolution imagery in 15 spectral bands ranging from 0.45 to 10.70 pm. The payload portion of the satellite includes the imaging system components, associated electronics boxes, and payload support structure. The imaging system includes a three-mirror anastigmatic off-axis telescope, a single cryogenically cooled focal plane assembly, a mechanical cooler, and an onboard calibration system. Payload electronic subsystems include image digitizers, real-time image compressors, a solid state recorder, calibration source drivers, and cooler temperature and vibration controllers. The payload support structure mechanically integrates all payload components and provides a simple four point interface to the spacecraft bus. All payload components have been fabricated and tested, and integrated.

NTIS

Imaging Techniques; Payloads; Multispectral Photography; Systems Engineering

36
LASERS AND MASERS

Includes lasing theory, laser pumping techniques, maser amplifiers, laser materials, and the assessment of laser and maser outputs. For cases where the application of the laser or maser is emphasized see also the specific category where the application is treated. For related information see also 76 Solid-State Physics.

20020000751 Lawrence Livermore National Lab., Livermore, CA USA
Plasma electrode pockels cell for the National Ignition Facility
Alger, T.; Biltoft, P.; Boley, C. D.; Fochs, S.; Funkhouser, B.; Jul. 28, 1998; 6p; In English
Report No.(s): DE2001-2768; UCRL-JC-129710; No Copyright; Avail: Department of Energy Information Bridge, Microfiche

The National Ignition Facility (NIF), now under construction at Lawrence Livermore National Laboratory, will be the largest laser fusion facility ever built. The NIF laser architecture is based on a multi-pass power amplifier to reduce cost and maximize performance. A key component in this laser design is an optical switch that closes to trap the optical pulse in the cavity for four gain passes and then opens to divert the optical pulse out of the amplifier cavity. The switch is comprised of a Pockels cell and a polarizer and is unique because it handles a beam that is 40 cm x 40 cm square and allows close horizontal and vertical beam spacing. Conventional Pockels cells do not scale to such large apertures or the square shape required for close packing. Our switch is based on a Plasma-Electrode Pockels Cell (PEPC). In a PEPC, low-pressure helium discharges (1-2 kA) are formed on both sides of a thin slab of electro-optic material. Typically, we use KH(sub 2)PO(sub 4) crystals (KDP). The discharges form highly conductive, transparent sheets that allow uniform application of a high-voltage pulse (17 kV) across the crystal. A 37 cm x 37 cm PEPC has been in routine operation for two years on the 6 k.J Beamlet laser at LLNL. For the NIF, a module four apertures high by one wide (4x1) is required. However, this 4x1 mechanical module will be comprised electrically of a pair of 2x1 sub-modules. Last year (FY 97), we demonstrated full operation of a prototype 2x1 PEPC. In this PEPC, the plasma spans two KDP crystals. A major advance in the 2x1 PEPC over the Beamlet PEPC is the use of anodized aluminum construction that still provides sufficient insulation to allow formation of the planar plasmas.
NTIS
Plasma Electrodes; Power Amplifiers; Modules; Crystals; Birefringence

20020000886 Argonne National Lab., IL USA
Multi-dimensional free-electron laser simulation codes: a comparison study
Biedron, S. G.; Chae, Y. C.; Dejus, R. J.; Faatz, B.; Freund, H. P.; Aug. 23, 1999; 19p; In English
Report No.(s): DE2001-11946; ANL/ASD/CP-99877; No Copyright; Avail: Department of Energy Information Bridge, Microfiche

A self-amplified spontaneous emission (SASE) free-electron laser (FEL) is under construction at the Advanced Photon Source (APS). Five FEL simulation codes were used in the design phase: GENESIS, GINGER, MEDUSA, RON, and TDA3D. Initial comparisons between each of these independent formulations show good agreement for the parameters of the APS SASE FEL.
NTIS
Free Electron Lasers; Computerized Simulation

20020000887 Argonne National Lab., IL USA
Rf-gun-driven recirculated linac as injector and FEL driver
Andersson, A.; Biedron, S.; Eriksson, M.; Freund, H.; Werin, S.; Aug. 23, 1999; 11p; In English
Report No.(s): DE2001-11945; ANL/ASD/CP-99876; No Copyright; Avail: Department of Energy Information Bridge, Microfiche

A new pre-injector for the MAX-Laboratory is under design and construction. A thermionic rf gun, designed to operate at medium currents with low back bombardment power, is under construction. The gun will, via a magnetic compressor and energy filter, feed a recirculated linac consisting of two SLED-equipped structures giving 125 MeV each. The first will be delivered in 1999. The system is aimed as a pre-injector for the existing storage rings at MAX-Lab, but will also open up possibilities for a SASE FEL in the UV reaching above 100 MW below 100 run.
NTIS
Design Analysis; Fabrication; Radio Frequencies; Storage Rings (Particle Accelerators); Electron Guns

20020001530 Arizona Univ., Optical Sciences Center, Tucson, AZ USA

A Femtosecond Laser Source for the Study and Development of Organic Photonic Materials ***Final Report, 1 Apr. 2000 - 31 Mar. 2001***

Kippelen, Bernard; Mar. 31, 2001; 2p; In English

Contract(s)/Grant(s): F49620-00-1-0208

Report No.(s): AD-A388150; AFRL-SR-BL-TR-01-0199; No Copyright; Avail: Defense Technical Information Center (DTIC)

This report is to certify the acquisition of a Spectra Physics femtosecond Ti:Sapp laser source comprised of a pump source Millennia XsP that delivers 10W of optical power, and a Tsunami femtosecond laser (Model: 3960X1BB. S/N: 2019) with broadband optics (700 nm-1000 nm) and a birefringent filter to pump an OPAL for the amount ff $154.000. The laser was installed at the end of August of 2000 and has been running properly since then. This acquisition was complemented with that of an anti-vibration optical table, a high voltage power supply, a spectrometer, a computer for data acquisition, a source meter, and various optical and optomechanical components with matching funds provided by the University of Arizona.

DTIC

Organic Materials; Photonics; Birefringence; Laser Outputs

20020002237 Lawrence Livermore National Lab., Livermore, CA USA

Measurements of deep heating generated by ultra-intense laser-plasma interactions

Hatchett, S. P.; Key, M. H.; Koch, J. A.; Lee, R. W.; Pennington, D.; Aug. 25, 1999; 19p; In English

Report No.(s): DE2001-12554; UCRL-JC-133686; No Copyright; Avail: Department of Energy Information Bridge

We measure 300 eV thermal temperatures at near-solid densities by x-ray spectroscopy of tracer layers buried up to 30 pm inside CH slabs which are irradiated by a 0.5 kJ, 5 ps laser. X-ray imaging data suggest that collimated electron transport produces comparable temperatures as deep as 200 pm, and unexpectedly show the heated regions to be 50-120 pm-diameter rings. The data indicate that intense lasers can directionally heat solid matter to high temperatures over large distances; the results are relevant for fast-ignition inertial-confinement fusion and hot, dense plasma research

NTIS

Heating; Measure and Integration; High Temperature Plasmas; Electron Transfer

20020002364 National Defence Research Establishment, Linkoeping, Sweden

Fiber Laser Hydrophones, an Introductory Survey

Kullander, F.; Knuthammar, B.; Dec. 2000; 34p; In English

Report No.(s): PB2002-100058; FOA-R-00-01779-409-SE; No Copyright; Avail: CASI; A03, Hardcopy; A01, Microfiche

This report is the results of a limited study of fiber laser sensors in defense applications. Fiber laser sensors have characteristics such as extreme strain sensitivity and small size which are useful in certain military applications. Among these, towed array sonar systems for underwater surveillance have been found to be of special interest and this report focuses on aspects related to hydroacoustics. The potentially very lightweight and small-size sensor cable, including up to 100 acoustic elements should be useful not only in special applications within this field but also generally in various kinds of towed array applications.

NTIS

Hydrophones; Surveillance; Sonar

20020002723 Colorado State Univ., Fort Collins, CO USA

Ultra Fast Regeneratively Amplified Titanium Sapphire Laser System ***Final Report, 1 Apr. 1995 - 31 Mar. 1997***

Schenck, C. C.; Mar. 31, 1997; 3p; In English

Report No.(s): DE2001-765652; No Copyright; Avail: Department of Energy Information Bridge, Microfiche

A regeneratively-amplified picosecond laser system for studying light-activatable energy-transducing molecules has been constructed with the equipment finds in this multiuser shared equipment grant. Manuscripts describing the use of this apparatus to study the transient release of heat by biomolecules using transient thermal gratings are in preparation.

NTIS

Lasers; Sapphire; Titanium

20020002726 Wisconsin Univ., Fusion Technology Inst., Madison, WI USA

Development of X-ray tracer diagnostics for radiatively-driven ablator experiments, November 1, 1997-October 31, 1998 ***Final Report, 1 Nov. 1997 - 31 Oct. 1998***

MacFarlane, J. J.; Cohen, D. H.; Ping Wang, G. A.; Moses, R. R.; Peterson, P. A.; Jun. 01, 1999; 22p; In English

Report No.(s): DE2001-765573; No Copyright; Avail: Department of Energy Information Bridge, Microfiche

This is a combined experimental and theoretical analysis of tracer layers as spectral diagnostics for radiation burn-through of ablator materials. German-doped plastic is attached as a witness plate to a laser driven hohlraum. Backlit absorption spectroscopy is used as a diagnostic. Target shots were performed on the OMEGSA laser at UR/LLE.
NTIS
Ablative Materials; X Rays; Thermonuclear Reactions; Absorption Spectroscopy

20020002743 Sandia National Labs., Albuquerque, NM USA
Antimonide-Based Long-Wavelength Lasers on GaAs Substrates
Klem,; Blum,; Aug. 17, 2000; 8p; In English
Report No.(s): DE2001-761056; SAND2000-1695C; No Copyright; Avail: Department of Energy Information Bridge, Microfiche

We have investigated the use of GaAsSb in edge-emitting laser active regions, in order to obtain lasing near 1.3 micrometers. Single quantum well GaAsSb devices display electroluminescence at wavelengths as long as 1.34 micrometers, but substantial blueshifts occur under high injection conditions. GaAsSb single quantum well edge emitters have been obtained which lase at 1.275 micrometers with a room-temperature threshold current density as low as 535 A/sq cm. Modification of the basic GaAsSb/GaAs structure with the addition of InGaAs layers results in a strongly type-2 band alignment which can be used to further extend the emission wavelength of these devices. Using GaAsSb/InGaAs active regions, lasers emitting at 1.17 micrometers have been obtained with room-temperature threshold current densities of 120 A/sq cm, and devices operating at 1.29 micrometers have displayed thresholds as low as 375 A/sq cm. Characteristic temperatures for devices employing various GaAsSb-based active regions have been measured to be 60-73 K.
NTIS
Gallium Arsenides; Threshold Currents; Semiconductor Lasers

20020002766 Argonne National Lab., IL USA
FEL development at the Advanced Photon Source
Arnold, N. D.; Benson, C.; Berg, S.; Berg, W.; Biedron, S. G.; Mar. 15, 1999; 13p; In English
Report No.(s): DE2001-12419; ANL/ASD/CP-98592; No Copyright; Avail: Department of Energy Information Bridge, Microfiche

Construction of a single-pass free-electron laser (FEL) based on the self-amplified spontaneous emission (SASE) mode of operation is nearing completion at the Advanced Photon Source (APS) with initial experiments imminent. The APS SASE FEL is a proof-of-principle fourth-generation light source. As of January 1999 the undulator hall, end-station building, necessary transfer lines, electron and optical diagnostics, injectors, and initial undulatory have been constructed and, with the exception of the undulatory, installed. All preliminary code development and simulations have also been completed. The undulator hall is now ready to accept first beam for characterization of the output radiation. It is the project goal to push towards full FEL saturation, initially in the visible, but ultimately to W and VUV, wavelengths.
NTIS
Photons; Free Electron Lasers; Light Sources

20020002804 Lawrence Livermore National Lab., Livermore, CA USA
Time-Resolved Studies of Laser Damage Processes in DKDP Crystals
Jiang, H.; McNary, R.; Tom, H.; Yan, M.; Radousky, H.; Feb. 12, 2000; 7p; In English
Report No.(s): DE2001-756895; UCRL-JC-137641; No Copyright; Avail: Department of Energy Information Bridge

The authors have used a 3-color imaging technique to obtain time-resolved series of images during nanosecond laser damage in bulk DKDP crystals. In contrast to single-pump, single-probe time-resolved imaging techniques, they are able to correlate behavior during single damage events. This enables us to observe a range of morphological dynamics that is otherwise difficult to study, including: the propagation of elastic sound waves and the liquid/solid melt front from the damage nucleation site and the dynamics of crack formation and propagation.
NTIS
Crystals; Morphology; Nucleation; Time Series Analysis; Laser Damage

20020003979 Lawrence Livermore National Lab., Livermore, CA USA
Domain decomposition methods for parallel laser-tissue models with Monte Carlo transport
Alme, H. J.; Rodrique, G.; Zimmerman, G.; Oct. 19, 1998; 14p; In English
Report No.(s): DE2001-2847; UCRL-JC-132595; DP0101031; No Copyright; Avail: Department of Energy Information Bridge

Achieving parallelism in simulations that use Monte Carlo transport methods presents interesting challenges. For problems that require domain decomposition, load balance can be harder to achieve. The Monte Carlo transport package may have to operate with other packages that have different optimal domain decompositions for a given problem. to examine some of these issues, we have developed a code that simulates the interaction of a laser with biological tissue; it uses a Monte Carlo method to simulate the laser and a finite element model to simulate the conduction of the temperature field in the tissue. We will present speedup and load balance results obtained for a suite of problems decomposed using a few domain decomposition algorithms we have developed.
NTIS
Finite Element Method; Mathematical Models; Monte Carlo Method; Tissues (Biology); Computerized Simulation; Laser Beams

20020004913 Sandia National Labs., Albuquerque, NM USA
5.2 mW Single-Mode Power from a Coupled-Resonator Vertical-Cavity Laser
Fischer, A. J.; Choquette, K. D.; Chow, W. W.; Allerman, A. A.; Geib, K. M.; Nov. 28, 2000; 5p; In English
Report No.(s): DE2001-769062; SAND2000-2964C; No Copyright; Avail: Department of Energy Information Bridge
We have achieved 5.2 mW of single fundamental-mode power from a coupled-resonator 'vertical-cavity' laser. The enhanced mode selectivity is due to gain profiling combined with current-induced changes in cavity coupling.
NTIS
Laser Cavities; Resonators; Lasers

20020005183 Lawrence Livermore National Lab., Livermore, CA USA
High-Power Reliable Operation of InGaAsP/InP Laser Bars at 1.73 micro-m
Skidmore, J.; Page, R. H.; Freitas, B. L.; Reinhardt, C. E.; Utterback, E. J.; Feb. 16, 1999; 1p; In English
Report No.(s): DE2001-757413; UCRL-JC-133216; No Copyright; Avail: Department of Energy Information Bridge
InGaAsP/InP laser bars with an emission wavelength of 1.73 micro-m have been fabricated using compressively-strained multiple-quantum-well separate-confinement heterostructures. One-cm-wide, 0.7-fill-factor, diode bars are bonded onto Si microchannel heatsinks. A maximum cw power of 16 W was produced from a one-cm bar. Derated to SW cw, the extrapolated lifetime is 10,000 hours of operation with a 20% degradation in output power. A 10-bar microlensed diode array with a one-square-cm aperture produced 200 W of peak power and was focused onto a Cr:ZnSe slab laser. Over 3 watts of pulsed power and xxmw of average power was generated at a wavelength of 2.5 micro-m.
NTIS
Gallium Arsenide Lasers; Indium Gallium Arsenides; Indium Phosphides; Semiconductor Lasers; Fabrication; Continuous Radiation

20020005186 Lawrence Livermore National Lab., Livermore, CA USA
Tabletop Transient Collisional Excitation X-Ray Lasers
Dunn, J.; Li, Y.; Osterheld, A. L.; Nilsen, J.; Moon, S. J.; Sep. 03, 1999; 10p; In English
Report No.(s): DE2001-757465; UCRL-JC-136567; REPT-97-ERD-105; No Copyright; Avail: Department of Energy Information Bridge
Recent transient collisional excitation x-ray laser experiments are reported using the COMET tabletop laser driver at the Lawrence Livermore National Laboratory (LLNL). Ne-like and Ni-like ion x-ray laser schemes have been investigated with a combination of long 600 ps and short approximately 1 ps high power laser pulses with 5-10 J total energy. We show small signal gain saturation for x-ray lasers when a reflection echelon traveling wave geometry is utilized. A gain length product of 18 has been achieved for the Ni-like Pd 4d --> 4p J=0-1 line at 147 angstrom, with an estimated output of approximately 10 micro-J. Strong lasing on the 119 angstrom Ni-like Sn line has also been observed. to our knowledge this is the first time gain saturation has been achieved on a tabletop laser driven scheme and is the shortest wavelength tabletop x-ray laser demonstrated to date. In addition, we present preliminary results of the characterization of the line focus uniformity for a Ne-like ion scheme using L-shell spectroscopy.
NTIS
Excitation; X Ray Lasers; High Power Lasers; Laser Pumping; Lasing

20020005811 Lawrence Livermore National Lab., Livermore, CA USA

High pressure solid state experiments on the NOVA laser

Chandler, E. A.; Colvin, J. D.; Gold, D. M.; Hauer, A. A.; Kalantar, D. H.; Nov. 01, 1998; 14p; In English

Report No.(s): DE2001-6149; UCRL-JC-129810; DP0210000; No Copyright; Avail: Department of Energy Information Bridge, Microfiche

An x-ray drive has been developed to shock compress metal foils in the solid state in order to study the material strength under high compression. The drive has been characterized and hydrodynamics experiments designed to study growth of the Rayleigh-Taylor (RT) instability in Cu foils at 3 Mbar peak pressures have been started. Pre-imposed modulations with an initial wavelength of 20-50 (micro)m, and amplitudes of 1.0-2.5 (micro)m show growth consistent with simulations. In this parameter regime, the fluid and solid states are expected to behave similarly for Cu. An analytic stability analysis is used to motivate an experimental design with an Al foil where the effects of material strength on the RT growth are significantly enhanced. Improved x-ray drive design will allow the material to stay solid under compression throughout the experiment, and dynamic diffraction techniques are being developed to verify the compressed state.

NTIS

Lasers; Copper; X Ray Apparatus; Fabrication; Stability Tests; Materials Tests; Compressive Strength

20020005845 Brookhaven National Lab., Upton, NY USA

High gain harmonic generation x-ray free electron laser

Wu,; Yu,; Jun. 18, 2001; 5p; In English

Report No.(s): DE2001-785359; BNL-68542; No Copyright; Avail: Department of Energy Information Bridge

We present the calculation on the performance of a High Gain Harmonic Generation (HGHG) X-ray Free Electron Laser (FEL) based on the high quality electron beam from the proposed Photoinjected Energy Recovery Linac (PERL) at the NSLS. We consider several sets of e-beam parameters. The calculation indicates that it is possible to produce a fully coherent FEL with a wavelength around 10 Angstrom, with a peak power of several GW. The high order harmonics will also be produced with a significant amount of peak power. One further attractive feature is the possibility to produce ultra short radiation pulses of about 10n fs based on such HGHG scheme.

NTIS

Free Electron Lasers; Linear Accelerators; X Ray Lasers

20020005864 NASA Ames Research Center, Moffett Field, CA USA

Contributions of a Tunable Diode Laser Instrument (ATLAS) to the Stratospheric Ozone Depletion Question

Loewenstein, Max, NASA Ames Research Center, USA; [1994]; 1p; In English; 4th International Symposium on Monitoring of Gaseous Pollutants by Tunable Diode Lasers, 19-20 Oct. 1994, Freiburg, Germany

Contract(s)/Grant(s): RTOP 464-14-11; No Copyright; Avail: Issuing Activity; Abstract Only

The Airborne Tunable Laser Absorption Spectrometer - ATLAS - was designed and built at the NASA Ames Research Center and operates on the NASA ER-2 high altitude research aircraft. ATLAS has taken part in a number of important polar and mid-latitude research campaigns, since 1987, focused on various aspects of stratospheric ozone chemistry and dynamics. The chief measurement carried out by the ATLAS second harmonic diode laser spectrometer is of the important atmospheric tracer N2O. Using N2O as an inert tracer we have been able to gain significant new information on polar vortex dynamics and on the correlations of several important long-lived tracers in the stratosphere. The correlation of N2O with NOy (total reactive nitrogen) has been shown to be linear for a great variety of unperturbed stratospheric conditions, and the breakdown of this correlation has been used to detect denitrification by PSCs in the polar vortex, especially in the Antarctic spring. Denitrification is an important step in the process of ozone hole formation in the austral spring. Correlations of N2O with CFCs and CH4 have led to improved estimates of atmospheric lifetimes of these important molecules. Finally the correlation of N2O with CO2, the latter now being measured with great precision by a new instrument on the ER-2, has led to a significant new tool for studying horizontal and vertical mixing in the lower stratosphere, a tool which is very useful in assessing the potential effects of high speed civil transport aircraft in the lower stratosphere. A new, light-weight version of ATLAS is currently being built for unmanned high altitude aircraft, specifically the new Perseus vehicle. We will give a brief description of this effort.

Author

Tunable Lasers; Diodes; Absorption Spectroscopy; Airborne Lasers; Nitrogen Oxides

37
MECHANICAL ENGINEERING

Includes mechanical devices and equipment; machine elements and processes. For cases where the application of a device or the host vehicle is emphasized see also the specific category where the application or vehicle is treated. For robotics see 63 Cybernetics, Artificial Intelligence, and Robotics; and 54 Man/System Technology and Life Support.

20020001562 Pennsylvania State Univ., University Park, PA USA
Spark Ignited Turbulent Flame Kernel Growth
Santavicca, D. A.; Jun. 01, 1995; 16p; In English
Report No.(s): DE2001-6605; No Copyright; Avail: Department of Energy Information Bridge

An experimental study of the effects of spark power and of incomplete fuel-air mixing on spark-ignited flame kernel growth was conducted in turbulent propane-air mixtures at 1 atm, 300K conditions. The results showed that increased spark power resulted in an increased growth rate, where the effect of short duration breakdown sparks was found to persist for times of the order of milliseconds. The effectiveness of increased spark power was found to be less at high turbulence and high dilution conditions. Increased spark power had a greater effect on the 0-5 mm burn time than on the 5-13 mm burn time, in part because of the effect of breakdown energy on the initial size of the flame kernel. and finally, when spark power was increased by shortening the spark duration while keeping the effective energy the same there was a significant increase in the misfire rate, however when the spark power was further increased by increasing the breakdown energy the misfire rate dropped to zero. The results also showed that fluctuations in local mixture strength due to incomplete fuel-air mixing cause the flame kernel surface to become wrinkled and distorted; and that the amount of wrinkling increases as the degree of incomplete fuel-air mixing increases. Incomplete fuel-air mixing was also found to result in a significant increase in cyclic variations in the flame kernel growth. The average flame kernel growth rates for the premixed and the incompletely mixed cases were found to be within the experimental uncertainty except for the 33%-RMS (root mean square)-fluctuation case where the growth rate was significantly lower. The premixed and 6%-RMS-fluctuation cases had a 0% misfire rate. The misfire rates were 1% and 2% for the 13%-RMS-fluctuation and 24%-RMS-fluctuation cases, respectively; however, it drastically increased to 23% in the 33%-RMS-fluctuation case.
NTIS
Ignition; Sparks; Turbulent Flames; Gas Mixtures

20020001883 Kansas City Plant, Kansas City, MO USA
Mechanical Testing Development for Reservoir Forgings
Wenski, E. G.; May 22, 2000; 37p; In English
Report No.(s): DE2001-755481; KCP-613-6330; No Copyright; Avail: Department of Energy Information Bridge, Microfiche

The goal of this project was to determine the machining techniques and testing capabilities required for mechanical property evaluation of commercially procured reservoir forgings. Due to the small size of these specific forgings, specialized methods are required to adequately machine and test these sub-miniature samples in accordance with the requirements of ASTM-E8 and ASTM-E9. At the time of project initiation, no capability existed at Federal Manufacturing & Technologies (FM&T) to verify the physical properties of these reservoirs as required on the drawing specifications. The project determined the sample definitions, machining processes, and testing procedures to verify the physical properties of the reservoir forgings; specifically, tensile strength, yield strength, reduction of area, and elongation. In addition, a compression test method was also developed to minimize sample preparation time and provide a more easily machined test sample while maintaining the physical validation of the forging.
NTIS
Machining; Mechanical Properties; Forging

20020001887 Pennsylvania State Univ., University Park, PA USA
In-Cylinder Study of Soot and NO in a DI Diesel Engine ***Final Report***
Litzinger, T. A.; Oct. 18, 1995; 61p; In English
Report No.(s): DE2001-6600; No Copyright; Avail: Department of Energy Information Bridge

Clearly the reduction of NOx and particulate emissions remains a major challenge to diesel engine manufacturers due to increasingly stringent emission standards in the US and other countries. The well documented NOx/particulate trade-off observed in diesel engines makes the simultaneous reduction of both emissions particularly difficult for manufacturers to achieve. In an effort to provide an improved understanding of the fundamental processes which result in this trade-off, a program was carried out at Penn State to develop the appropriate engine facilities and laser diagnostics to permit in-cylinder studies of diesel combustion and emissions production with the support of the Department of Energy Advanced Industrial Technology Division

. This work has also been supported by the Cummins Engine Company, Lubrizol Corporation and the National Science Foundation. An optically accessible, direct injection, diesel engine was constructed for these studies. The major objective of the design of the engine was to maximize optical access under conditions representative of diesel engine combustion in small bore, commercial engines. Intake air is preheated and boosted in pressure to make the in-cylinder conditions of heat release and pressure as realistic as possible. Another important objective of the design was flexibility in combustion chamber geometry to permit a variety of head and bowl geometries to be studied. In all the results reported in this report a square bowl was used to simplify the introduction of laser light sheets into the engine.
NTIS
Combustion Chambers; Diesel Engines; Engine Design; Exhaust Emission; Combustion Products

20020001972 Argonne National Lab., IL USA
Thermal management in heavy vehicles: a review identifying issues and research requirements
Wambsganss, M. W.; Jan. 15, 1999; 17p; In English
Report No.(s): DE2001-12369; ANL/ET/CP-98208; No Copyright; Avail: Department of Energy Information Bridge, Microfiche
Thermal management in heavy vehicles is cross-cutting because it directly or indirectly affects engine performance, fuel economy, safety and reliability, engine/component life, driver comfort, materials selection, emissions, maintenance, and aerodynamics. It follows that thermal management is critical to the design of large (class 6-8) trucks, especially in optimizing for energy efficiency and emissions reduction. Heat rejection requirements are expected to increase, and it is industry's goal to develop new, innovative, high-performance cooling systems that occupy less space and are lightweight and cost-competitive. The state of the art in heavy vehicle thermal management is reviewed, and issues and research areas are identified.
NTIS
Temperature Control; Trucks; Design Analysis; Cost Effectiveness; Materials Selection; Engine Parts

20020003374 Oak Ridge National Lab., TN USA
Heavy Vehicle Propulsion System Materials Program Semiannual Progress Report for October 1998 Through March 1999
Johnson, R. D.; Jun. 01, 1999; 157p; In English
Report No.(s): DE2001-8924; ORNL/TM-1999/95; No Copyright; Avail: Department of Energy Information Bridge, Microfiche
The purpose of the Heavy Vehicle Propulsion System Materials Program is the development of materials: ceramics, intermetallics, metal alloys, and metal and ceramic coatings, to support the dieselization of class 1-3 trucks to realize a 35% fuel-economy improvement over current gasoline-fueled trucks and to support commercialization of fuel-flexible LE-55 low-emissions, high-efficiency diesel engines for class 7-8 trucks. The Office of Transportation Technologies, Office of Heavy Vehicle Technologies (OIT OHVT) has an active program to develop the technology for advanced LE-55 diesel engines with 55% efficiency and low emissions levels of 2.0 g/bhp-h NOX and 0.05 g/bhp-h particulate. The goal is also for the LE-55 engine to run on natural gas with efficiency approaching that of diesel fuel. The LE-55 program is being completed in FY 1997 and, after approximately 10 years of effort, has largely met the program goals of 55% efficiency and low emissions. However, the commercialization of the LE-55 technology requires more durable materials than those that have been used to demonstrate the goals. Heavy Vehicle Propulsion System Materials will, in concert with the heavy duty diesel engine companies, develop the durable materials required to commercialize the LE-55 technologies. OIT OHVT also recognizes a significant opportunity for reduction in petroleum consumption by dieselization of pickup trucks, vans, and sport utility vehicles. Application of the diesel engine to class 1,2, and 3 trucks is expected to yield a 35% increase in fuel economy per vehicle. The foremost barrier to diesel use in this market is emission control. Once an engine is made certifiable, subsequent challenges will be in cost; noise, vibration, and harshness (NVH); and performance. The design of advanced components for high-efficiency diesel engines has, in some cases, pushed the performance envelope for materials of construction past the point of reliable operation. Higher mechanical and tribological stresses and higher temperatures of advanced designs limit the engine designer; advanced materials allow the design of components that may operate reliably at higher stresses and temperatures, thus enabling more efficient engine designs. Advanced materials also offer the opportunity to improve the emissions, NVH, and performance of diesel engines for pickup trucks, vans, and sport utility vehicles. The principal areas of research are: (1) Cost Effective High Performance Materials and Processing; (2) Advanced Manufacturing Technology; (3)Testing and Characterization; and (4) Materials and Testing Standards.
NTIS
Diesel Engines; Engine Design; Propulsion; Trucks

20020003387 Federal Energy Technology Center, Morgantown, WV USA

Utility advanced turbine systems (ATS) technology readiness testing phase 3 restructured (3r)

Mar. 17, 2000; 49p; In English

Report No.(s): DE2001-766360; DE-FC21-95MC31176-26; No Copyright; Avail: Department of Energy Information Bridge, Microfiche

This scope document defines the work scope for accomplishing the design of the GE MS7001H and MS9001H (7H and 9H) combined-cycle power systems under the original ATS Phase 3 DOE Cooperative Agreement No. DE-FC21-95MC31176, and incorporates changes in scope required to convert Phase 3 to the 'restructured' Phase 3R as defined in Amendment A012 to the Cooperative Agreement.

NTIS

Turbines; Technology Assessment; Performance Tests

20020003388 Federal Energy Technology Center, Morgantown, WV USA

Utility advanced turbine systems (ats) technology readiness testing

Apr. 01, 1999; 79p; In English

Report No.(s): DE2001-766689; DE-FC21-95MC31176-22; No Copyright; Avail: Department of Energy Information Bridge, Microfiche

The overall objective of the Advanced Turbine System (ATS) Phase 3 Cooperative Agreement between GE and the U.S. Department of Energy (DOE) is the development of the GE 7H and 9H combined cycle power systems. The major effort will be expended on detail design. Validation of critical components and technologies will be performed, including: hot gas path component testing, sub-scale compressor testing, steam purity test trials, and rotational heat transfer conflation testing. Processes will be developed to support the manufacture of the first system, which was to have been sited and operated in Phase 4 but will now be sited and operated commercially by GE. This change has resulted from DOE's request to GE for deletion of Phase 4 in favor of a restructured Phase 3 (as Phase 3R) to include full speed, no load (FSNL) testing of the 7H gas turbine. Technology enhancements that are not required for the first machine design but will be critical for future ATS advances in performance, reliability, and costs will be initiated. Long-term tests of materials to confirm design life predictions will continue. The objective of this task is to design 7H and 9H compressor rotor and stator structures with the goal of achieving high efficiency at lower cost and greater durability by applying proven GE Power Systems (GEPS) heavy-duty use design practices. The designs will be based on the GE Aircraft Engines (GEAE) CF6-80C2 compressor. Transient and steady-state thermo-mechanical stress analyses will be run to ensure compliance with GEPS life standards. Drawings will be prepared for forgings, castings, machining, and instrumentation for full speed, no load (FSNL) tests of the first unit on both 9H and 7H applications.

NTIS

Gas Turbines; Technology Assessment; Performance Tests; Cycles

20020003732 Oak Ridge National Lab., TN USA

Microwave Nitridation of Sintered Reaction Bonded Silicon Parts for Natural Gas Fueled Diesel Engines

Edler, J.; Kiggans, J. O.; Suman, A. W.; Tiegs, T. N.; Jan. 01, 1999; 18p; In English

Report No.(s): DE2001-3140; ORNL/M-6664; C/ORNL97-0465; No Copyright; Avail: Department of Energy Information Bridge

This cooperative project was a joint development program between Eaton Corporation and Lockheed Martin Energy Research (LMER). Cooperative work was of benefit to both parties. ORNL was able to assess up-scale of the microwave nitridation process using a more intricate-shaped part designed for application in advanced diesel engines. Eaton Corporation mined access to microwave facilities and expertise for the nitridation of SRBSN materials. The broad objective of the CRADA established with Eaton Corporation and ORNL was to develop cost-effective silicon nitride ceramics compared to the current materials available. The following conclusions can be made from the work performed under the CRADA: (1) Demonstrated that the binder burnout step can be incorporated into the SRBSN processing in the microwave furnace. (2) Scale-up of the microwave nitridation process using Eaton Corporation parts showed that the nitridation weight gains were essentially identical to those obtained by conventional heating. (3) Combined nitridation and sintering processes using silicon nitride beads as packing powders results in degradation of the mechanical properties. (4) Gelcasting of silicon nitride materials using Eaton Si mixtures was demonstrated.

NTIS

Nitriding; Silicon Nitrides; Diesel Engines; Microwaves

20020004674 Federal Energy Technology Center, Morgantown, WV USA

Engineering development of advanced coal-fired low emission boiler systems

Jan. 01, 1996; 5p; In English

Report No.(s): DE2001-769333; DE-AC22-92PC92158-01; No Copyright; Avail: Department of Energy Information Bridge, Microfiche

As a result of technical and cost evaluations in this period, a decision has been made to redirect a portion of the experimental program. The 8/94 Phase II Test Plan included the following experimental tasks: (1) Reburn development at a scale of 15 million Btu/hr, at the University of Utah; (2) large burner testing at 100 million Btu/hr, slag tap firing with reburning, at the DB Riley Research Center; (3) Bench scale copper oxide tests at Tecogen; (4) Copper oxide moving bed reactor testing at 5 million Btu/hr, at the Illinois Coal Development Park (ICDP); and (5) Copper oxide reactor testing on a 30 million Btu/hr (approximately 3 MW(sub e) equivalent) slip stream at the DB Riley Research Center. A design for the 30 million Btu/hr copper oxide slipstream was completed in sufficient detail for cost and schedule quotations on major components. Both cost and construction time estimates were significantly higher than planned, a major factor being foundation and structural requirements specific to the available site. A further technical consideration was the limited, continuous test time available, due to operating restrictions, relative to the solids residence time within the reactor.

NTIS

Product Development; Coal; Boilers

20020004920 NASA Marshall Space Flight Center, Huntsville, AL USA

Passive Capture Joint with Three Degrees of Freedom

Cloyd, Richard A., Inventor, NASA Marshall Space Flight Center, USA; Weddendorf, Bruce, Inventor, NASA Marshall Space Flight Center, USA; Feb. 13, 2001; 6p; In English

Patent Info.: Filed 7 Dec. 1998; NASA-Case-MFS-31146-1; US-Patent-6,186,693; US-Patent-Appl-SN-206146; No Copyright; Avail: CASI; A02, Hardcopy; A01, Microfiche

A passive capture joint with three degrees of freedom is presented wherein two structural elements are joined together solely by moving the two elements into position, and which when joined together have rotation in all three axes. The inventive apparatus is comprised of two halves: (1) a joint ball mounted on a stem as in a common trailer hitch, and; (2) a socket. The socket consists of a base having an exterior wall and forming an interior chamber, the chamber having a top end and a bottom end, and an interior wall. The chamber is open at the top end, and forms a spherical cup at the bottom end. The socket base's interior chamber is sized to accept the joint ball. The base also forms at least one bore at an acute angle away from the interior chamber's open end. The bores have a first opening in the interior wall of the chamber, and a second opening in the exterior wall of the base. Retaining balls sized to fit within the bores, but to only partially pass through the first opening, are moveably housed within the bores. The retaining balls are moveably held in the first opening by a compression spring housed in the bore. As the joint ball is inserted in the chamber it forces the retaining balls back into the bore until the equator of the joint ball passes. Because the bore is at an acute angle to the chamber the joint ball cannot exit the chamber without the joint being unlocked. The joint is unlocked by rotating a locking ring which encircles the base and covers the second opening. The locking ring has a radial slot for each retaining ball, disposed angularly from the base, and sized to allow passage of the retaining ball in the radial direction when the locking ring is rotated to align the radial slot with the second opening.

Official Gazette of the U.S. Patent and Trademark Office

Cavities; Joints (Junctions); Balls

20020005124 NASA Marshall Space Flight Center, Huntsville, AL USA

Load Transfer Mechanism for a Turbine Disk

Effinger, Michael R., Inventor, NASA Marshall Space Flight Center, USA; Dec. 19, 2000; 6p; In English

Patent Info.: Filed 12 Nov. 1998; NASA-Case-MFS-31270-1; US-Patent-6,162,019; US-Patent-Appl-SN-190784; No Copyright; Avail: CASI; A02, Hardcopy; A01, Microfiche

A load transferring system wherein a composite turbine disk mounted on a shaft is in contact with a backup disk which is secured to the shaft. The turbine disk is made of layers of woven carbon fibers held in a rigid configuration in a ceramic matrix. The composite disk has a plurality of lugs which have trapezoidal cross sections when cut by planes which are perpendicular to each other, with both planes being normal to the disk. The backup disk is provided with recesses which are the negative of the trapezoidal lugs to lock the two disks together. A second backup disk may be secured to the shaft to secure the composite turbine disk between the backup disks.

Official Gazette of the U.S. Patent and Trademark Office

Loads (Forces); Turbines; Disks (Shapes)

20020005132 NASA Marshall Space Flight Center, Huntsville, AL USA

Gasket Assembly for Sealing Mating Surfaces

Bryant, Melvin A., III, Inventor, NASA Marshall Space Flight Center, USA; Nov. 07, 2000; 6p; In English

Patent Info.: Filed 21 Sep. 1998; NASA-Case-MFS-31175-1; US-Patent-6,142,483; US-Patent-Appl-SN-160205; No Copyright; Avail: CASI; A02, Hardcopy; A01, Microfiche

A gasket assembly for securing a pair of surface together wherein an electrically conductive gasket base having a central opening is provided with a pair of layers secured to opposite sides of the gasket base, with the layers being a fusible alloy, a brazing alloy or a synthetic, thermoplastic material which will melt, without degrading, when the gasket base is heated. The surfaces may be secured to each other by a plurality of bolts to squeeze the gasket assembly there between or by some other clamping means. An electrical current is passed through the gasket base to heat it to a temperature sufficient to melt the layers to seal the surfaces to opposite sides of the gasket base.

Official Gazette of the U.S. Patent and Trademark Office

Bonding; Gaskets; Sealing

20020005163 Federal Energy Technology Center, Morgantown, WV USA

Advanced Gas Turbine Systems Research *Quarterly Report*

Sep. 30, 1998; 13p; In English

Report No.(s): DE2001-3807; DE-FC21-92MC29061-14; No Copyright; Avail: Department of Energy Information Bridge, Microfiche

Major Accomplishments by Advanced Gas Turbine Systems Research (AGTSR) during this reporting period are highlighted below and amplified in later sections of this report: AGTSR distributed 50 proposals from the 98RFP to the IRB for review, evaluation and rank-ordering during the summer; AGTSR conducted a detailed program review at DOE-FETC on July 24; AGTSR organized the 1998 IRB proposal review meeting at SCIES on September 15-16; AGTSR consolidated all the IRB proposal scores and rank-orderings to facilitate the 98RFP proposal deliberations; AGTSR submitted meeting minutes and proposal short-list recommendation to the IRB and DOE for the 98RFP solicitation; AGTSR reviewed two gas turbine related proposals as part of the CU RFP State Project for renovating the central energy facility; AGTSR reviewed and cleared research papers with the IRB from the University of Pittsburgh, Wisconsin, and Minnesota; AGTSR assisted GTA in obtaining university stakeholder support of the ATS program from California, Pennsylvania, and Colorado; AGTSR assisted GTA in distributing alert notices on potential ATS budget cuts to over 150 AGTSR performing university members; AGTSR submitted proceedings booklet and organizational information pertaining to the OAI hybrid gas turbine workshop to DOE-FETC; For DOE-FETC, AGTSR updated the university consortium poster to include new members and research highlights; For DOE-FETC, the general AGTSR Fact Sheet was updated to include new awards, workshops, educational activity and select accomplishments from the research projects; For DOE-FETC, AGTSR prepared three fact sheets highlighting university research supported in combustion, aero-heat transfer, and materials; For DOE-FETC, AGTSR submitted pictures on materials research for inclusion in the ATS technology brochure; For DOE-FETC, AGTSR submitted a post-2000 roadmap showing potential technology paths AGTSR could pursue in the next decade; AGTSR distributed the ninth newsletter UPDATE to DOE, the IRB: and two interested partners involved in ATS; AGTSR submitted information on its RFP's, workshops, and educational activities for the 1999 ASMWIGTI technology report for worldwide distribution; AGTSR coordinated university poster session titles and format with Conference Management Associates (CMA) for the 98 ATS Annual; and AGTSR submitted 2-page abstract to CMA for the 98 ATS Review titled: 'AGTSR: A Virtual National Lab'.

NTIS

Gas Turbines; Power Plants; Education; Conferences

20020005874 Army Research Inst. for the Behavioral and Social Sciences, Alexandria, VA USA

Human Factors and Safety Observations Regarding the Air Powered Tool Set (APTS)

Nystrom, Charles O.; Smith, Norman D.; Dec. 01, 1989; 4p; In English

Report No.(s): AD-A395334; ARI-WPFH89-03; No Copyright; Avail: CASI; A01, Hardcopy; A01, Microfiche

This paper presents various questions and comments regarding the Air Powered Tool Set (APTS).

CASI

Human Factors Engineering; Safety; Mechanical Engineering; Tools

38
QUALITY ASSURANCE AND RELIABILITY

Includes approaches to, and methods for reliability analysis and control, inspection, maintainability, and standardization.

20020001037 NASA Goddard Space Flight Center, Greenbelt, MD USA
Reliability Assessment for COTS Components in Space Flight Applications
Krishnan, G. S., NASA Goddard Space Flight Center, USA; Mazzuchi, Thomas A., George Washington Univ., USA; [2001]; 5p; In English; 2001 Military and Space Conference, 17-20 Sep. 2001, Nice, France; No Copyright; Avail: CASI; A01, Hardcopy; A01, Microfiche

Systems built for space flight applications usually demand very high degree of performance and a very high level of accuracy. Hence, the design engineers are often prone to selecting state-of-art technologies for inclusion in their system design. The shrinking budgets also necessitate use of COTS (Commercial Off-The-Shelf) components, which are construed as being less expensive. The performance and accuracy requirements for space flight applications are much more stringent than those for the commercial applications. The quantity of systems designed and developed for space applications are much lower in number than those produced for the commercial applications. With a given set of requirements, are these COTS components reliable? This paper presents a model for assessing the reliability of COTS components in space applications and the associated affect on the system reliability. We illustrate the method with a real application.
Author
Commercial Off-The-Shelf Products; Systems Engineering; Component Reliability

20020001067 Lawrence Livermore National Lab., Livermore, CA USA
Image recovery techniques for x-ray computed tomography in limited data environments
Aufderheide, M. B.; Goodman, D. M.; Jackson, J. A.; Johansson, E. M.; Mar. 01, 1999; 32p; In English
Report No.(s): DE2001-11988; UCRL-ID-133380; REPT-97-ERD-085; No Copyright; Avail: Department of Energy Information Bridge, Microfiche

There is an increasing requirement throughout LLNL for nondestructive evaluation using X-ray computed tomography (CT). In many cases, restrictions on data acquisition time, imaging geometry, and budgets make it unfeasible to acquire projection data over enough views to achieve desired spatial resolution using conventional CT methods. In particular, conventional CT methods are non-iterative algorithms that have the advantage of low computational effort, but they are not sufficiently adaptable to incorporate prior information or non-Gaussian statistics. Most currently existing iterative tomography algorithms are based on methods that are time consuming because they converge very flowingly, if at all. The goal of the work was to develop a set of limited data CT reconstruction tools and then demonstrate their usefulness by applying them to a variety of problems of interest to LLNL. In this project they continued their development of reconstruction tools and they have demonstrated their effectiveness on several important problems.
NTIS
Imaging Techniques; Nondestructive Tests; Computer Aided Tomography; Algorithms; X Rays

20020001088 Lawrence Livermore National Lab., Livermore, CA USA
Calibration of manganin pressure gauges at 250 C
Forbes, J. W.; Garcia, F.; Tarver, C. M.; Uttiew, P. A.; Jun. 01, 1999; 6p; In English
Report No.(s): DE2001-12145; UCRL-JC-132715; No Copyright; Avail: Department of Energy Information Bridge, Microfiche

During the past several decades manganin gauges have been used extensively for making in-situ high pressure measurements in materials under dynamic loading conditions. Prior to their use manganin gauges were calibrated but only under normal ambient temperatures. Recent interest in the behavior of both reactive and inert materials, when they were subjected to dynamic loading while being at high initial temperature, required a re-visit of the calibration procedure and reconfirmation of the gauges' proper behavior in such an extreme thermal environment. The paper describes the procedure of making such new calibrations of the existing manganin gauges and reports on the new findings. The Hugoniot for 6061-T6 aluminum at 250*C is also given.
NTIS
Calibrating; Manganin (Trademark); Dynamic Loads; High Pressure; In Situ Measurement; Thermal Environments

20020001168 Department of Energy, Savannah River Site, Aiken, SC USA
Accident Fault Trees for Defense Waste Processing Facility
Sarrack, A. G.; Jun. 22, 1999; 659p; In English
Report No.(s): DE2001-8705; No Copyright; Avail: Department of Energy Information Bridge, Microfiche

The purpose of this report is to document fault tree analyses which have been completed for the Defense Waste Processing Facility (DWPF) safety analysis. Logic models for equipment failures and human error combinations that could lead to flammable gas explosions in various process tanks, or failure of critical support systems were developed for internal initiating events and for earthquakes. These fault trees provide frequency estimates for support systems failures and accidents that could lead to radioactive and hazardous chemical releases both on-site and off-site. Top event frequency results from these fault trees will be used in further APET analyses to calculate accident risk associated with DWPF facility operations. This report lists and explains important underlying assumptions, provides references for failure data sources, and briefly describes the fault tree method used. Specific commitments from DWPF to provide new procedural/administrative controls or system design changes are listed in the 'Facility Commitments' section. The purpose of the 'Assumptions' section is to clarify the basis for fault tree modeling, and is not necessarily a list of items required to be protected by Technical Safety Requirements.

NTIS

Failure; Fault Trees; Gas Explosions; Support Systems; Systems Engineering; Waste Management

20020001235 Argonne National Lab., IL USA

Fault detection service for wide area distributed computations

Stelling, P.; Jun. 09, 1998; 13p; In English

Report No.(s): DE2001-10848; ANL/MCS/CP-96665; No Copyright; Avail: Department of Energy Information Bridge

The potential for faults in distributed computing systems is a significant complicating factor for application developers. While a variety of techniques exist for detecting and correcting faults, the implementation of these techniques in a particular context can be difficult. Hence, we propose a fault detection service designed to be incorporated, in a modular fashion, into distributed computing systems, tools, or applications. This service uses well-known techniques based on unreliable fault detectors to detect and report component failure, while allowing the user to trade off timeliness of reporting against false positive rates. We describe the architecture of this service, report on experimental results that quantify its cost and accuracy, and describe its use in two applications, monitoring the status of system components of the GUSTO computational grid testbed and as part of the NetSolve network-enabled numerical solver.

NTIS

Fault Detection; Distributed Processing; Component Reliability; Computer Programs

20020001549 Sandia National Labs., Albuquerque, NM USA

Reliability Testing of Polysilicon For MEMs Devices

LaVan, D. A.; Buchheit, T. E.; Apr. 05, 1999; 6p; In English

Report No.(s): DE2001-5689; SAND99-0810C; No Copyright; Avail: Department of Energy Information Bridge

Mission critical applications of MEMS devices require knowledge of the distribution in their material properties and long-term reliability of the small-scale structures. This project reports on a new testing program at Sandia to quantify the strength distribution using samples that reflect the dimensions of critical MEMS components. The strength of polysilicon fabricated with Sandia's SUMMiT 4-layer process was successfully measured using samples with gage sections 2.5 (micro)m thick by 1.7 (micro)m wide and lengths of 15 and 25 (micro)m. These tensile specimens have a freely moving pivot on one end that anchors the sample to the silicon die and prevents off axis loading during testing. Each sample is loaded in uniaxial tension by pulling laterally with a flat tipped diamond in a computer-controlled Nanoindenter. The stress-strain curve is calculated using the specimen cross section and gage length dimensions verified by measuring against a standard in the SEM. The first 48 samples had a means strength of 2.24 (+/-) 0.35 GPa. Fracture strength measurements grouped into three strength levels, which matched three failure modes observed in post mortem examinations. The seven samples in the highest strength group failed in the gage section (strength of 2.77 (+/-) 0.04 GPa), the moderate strength group failed at the gage section fillet and the lowest strength group failed at a dimple in the hub. With this technique, multiple tests can be programmed at one time and performed without operator assistance at a rate of 20-30 per day allowing the collection of significant populations of data. Since the new test geometry has been proven, the project is moving to test the distributions seen from real geometric features typical to MEMS such as the effect of gage length, fracture toughness, bonding between layers, etch holes, dimples and shear of gear teeth.

NTIS

Microelectromechanical Systems; Polycrystals; Reliability; Silicon Polymers; Computer Aided Design; Materials Tests; Numerical Control

20020002739 Rockwell International Corp., Thousand Oaks, CA USA

Investigation of the Mechanism of IGA/SCC of Alloy 600 in Corrosion Accelerating Heated Crevice Environments ***Progress Report***

Lumsden, J.; Nov. 01, 1999; 10p; In English

Report No.(s): DE2001-761827; No Copyright; Avail: Department of Energy Information Bridge, Microfiche

This program focuses on understanding mechanisms causing corrosion damage to steam generator tubes in a pressurized water reactor (PWR). The crevice formed by the tube/tube support plate (T/TSP) intersection in a PWR steam generator is a concentration site for nonvolatile impurities (referred to as hideout) in the steam generator water. The restricted mass transport in the small crevice volume prevents the species, which concentrate during the generation of steam, from quickly dispersing into the bulk water. The concentrated solutions in crevices have been a contributing cause of several forms of corrosion of steam generator tubes including intergranular attack/stress corrosion cracking (IGA/SCC), pitting, and wastage.

NTIS

Boilers; Corrosion; Damage; Pressurized Water Reactors; Stress Corrosion Cracking

20020002811 Kansas City Plant, Kansas City, MO USA

Metrology Measurement Capabilities

Barnes, L. M.; Mar. 23, 2000; 60p; In English

Report No.(s): DE2001-753923; KCP-613-6317; No Copyright; Avail: Department of Energy Information Bridge

This document contains descriptions of Federal Manufacturing and Technologies (FM and T) Metrology capabilities, traceability flow charts, and the measurement uncertainty of each measurement capability. Metrology provides NIST traceable precision measurements or equipment calibration for a wide variety of parameters, ranges, and state-of-the-art uncertainties in laboratories that conform to the requirements of the Department of Energy Development and Production Manual Chapter 8.4, and ANSI/NCSL Z540-1 (equivalent to ISO Guide 25). FM and T Metrology laboratories are accredited by NVLAP for the parameters, ranges, and uncertainties listed in the specific scope of accreditation under NVLAP Lab code 200108-0. These parameters are summarized.

NTIS

Manufacturing; Metrology; Data Acquisition; Flow Charts

20020003341 Atomic Energy Commission, Idaho Falls, ID USA

Mixed Waste Focus Area/Characterization Monitoring Sensor Technology Nondestructive Waste Assay Capability Evaluation Project End-User Summary Report

Becker, G. K.; McIlwain, M. E.; Connolly, M. J.; Nov. 01, 1998; 64p; In English

Report No.(s): DE2001-768860; INEEL/EXT-98-01108; No Copyright; Avail: Department of Energy Information Bridge, Microfiche

The Mixed Waste Focus Area (MWFA) in conjunction with the Characterization Monitoring and Sensor Technology (CMST) crosscut program identified the need to objectively evaluate the capability of nondestructive waste assay (NDA) technologies. This was done because of a general lack of NDA technology performance data with respect to a representative cross section of waste form configurations comprising the Department of Energy (DOE) contact-handled alpha contaminated (e.g., transuranic (TRU) waste). The overall objective of the Capability Evaluation Project (CEP) was to establish a known and unbiased NDA data and information base that can be used to support end-user decisions with regards to technology system selection and to support technology development organizations in identifying technology system deficiencies. The primary performance parameters evaluated in the CEP were measurement bias and relative precision. The performance of a given NDA technology is a direct function of the attributes represented by the waste matrix configuration. Such attributes include matrix density, matrix elemental composition, radionuclidic composition, radionuclide mass loading, and the spatial variation of these components. Analyzing the manner in which bias and precision vary as a function of test sample attribute and NDA technology provides a foundation for deriving performance capability and limitation statements and determines which waste matrix attributes, or combinations of attributes, are compatible or incompatible with existing technologies. The CEP achieved the stated end-user objective. The data indicate that the nondestructive waste assay systems evaluated have a definite capability to perform assay of contact-handled TRU waste packaged in 55-gallon drums. There is, however, a performance envelope where this capability exists, an area near the envelope boundaries where it is questionable, and a realm outside the envelope where the technologies do not perform. Therefore, the end user must be aware of this envelope and ensure the appropriate technology is selected. This program provides the end user with waste type specific performance data to assist in the assessment and selection of a given waste NDA technology. Additionally, the CEP afforded the private sector participants the opportunity to evaluate system performance using National Institute of

Standards and Technology traceable radioactive significant enhancements to their respective systems and supported all participants in attaining DOE-CAO certification. Ultimately, the DOE end users will benefit from these enhancements.
NTIS
Radioactive Wastes; Nondestructive Tests; Technology Assessment; Hazardous Materials; Assaying; Radioactivity

20020003371 Argonne National Lab., IL USA
Modeling the behavior of an earthquake base-isolated building
Coveney, V. A.; Jamil, S.; Johnson, D. E.; Kulak, R. F.; Uras, R. A.; Nov. 26, 1997; 21p; In English
Report No.(s): DE2001-8899; ANL/RE/CP-95005; No Copyright; Avail: Department of Energy Information Bridge, Microfiche
Protecting a structure against earthquake excitation by supporting it on laminated elastomeric bearings has become a widely accepted practice. The ability to perform accurate simulation of the system, including FEA of the bearings, would be desirable--especially for key installations. In this paper attempts to model the behavior of elastomeric earthquake bearings are outlined. Attention is focused on modeling highly-filled, low-modulus, high-damping elastomeric isolator systems; comparisons are made between standard triboelastic solid model predictions and test results.
NTIS
Buildings; Earthquakes; Mathematical Models; Elastomers

20020003985 Los Alamos National Lab., NM USA
Fiber Optic Calorimetry
Rudy, C.; Bayliss, S.; Bracken, D.; Bush, J.; Davis, P.; Dec. 12, 1997; 14p; In English
Report No.(s): DE2001-763148; LA-UR-97-4176; No Copyright; Avail: Department of Energy Information Bridge, Microfiche
A twin-bridge calorimeter using optical fiber as the sensor element was constructed and tested. This system demonstrates the principle and capability of using optical fibers for heat-flow measurements of special nuclear material. This calorimeter uses piezoelectric-generated phase-carrier modulation with subsequent electronic signal processes to allow phase shifts as small as 1 microradian ((micro)rad) to be measured. The sensing element consists of 21-m lengths of single-mode optical fiber wrapped around sample and reference chambers. The sensitivity of the calorimeter was determined to be 74 radians (rad) of phase shift per milliwatt of thermal power. One milliwatt of thermal power is equivalent to 400 mg of plutonium (6% Pu-240). The system noise base was about 0.2 rad, equivalent to about 1 mg of plutonium.
NTIS
Fiber Optics; Fabrication; Performance Tests; Calorimeters; Heat Measurement

20020005105 Department of Energy, Aiken, SC USA
Californium-252: A New Isotopic Source for Neutron Radiography
Reinig, W. C.; Aug. 29, 2001; 8p; In English
Report No.(s): DE2001-786062; DP-MS-68-48; No Copyright; Avail: Department of Energy Information Bridge, Microfiche
This report discusses a new isotopic source for neutron radiography, Californium-252. Nuclear reactors are the usual source of neutrons for radiography, primarily because of their intense neutron beams. If neutron radiography is to have widespread use, intense transportable neutron sources are required that can be used in plants, in laboratories and in the field.
NTIS
Neutron Radiography; Isotopes; Nuclear Reactors; Californium Isotopes

20020005408 Los Alamos National Lab., NM USA
Monte carlo error estimation applied to nondestructive assay methods
Estep, R.; Jun. 01, 2000; 13p; In English
Report No.(s): DE2001-769070; LA-UR-00-2164; No Copyright; Avail: Department of Energy Information Bridge, Microfiche
Monte Carlo randomization of nuclear counting data into N replicate sets is the basis of a simple and effective method for estimating error propagation through complex analysis algorithms such as those using neural networks or tomographic image reconstructions. The error distributions of properly simulated replicate data sets mimic those of actual replicate measurements and can be used to estimate the std. dev. for an assay along with other statistical quantities. We have used this technique to estimate the standard deviation in radionuclide masses determined using the tomographic gamma scanner (TGS) and combined thermal/epithermal neutron (CTEN) methods. The effectiveness of this approach is demonstrated by a comparison of our Monte Carlo error estimates with the error distributions in actual replicate measurements and simulations of measurements. We found that the std. dev. estimated this way quickly converges to an accurate value on average and has a predictable error distribution

similar to N actual repeat measurements. The main drawback of the Monte Carlo method is that N additional analyses of the data are required, which may be prohibitively time consuming with slow analysis algorithms.
NTIS
Monte Carlo Method; Error Analysis; Neutron Counters; Data Processing; Nondestructive Tests

39
STRUCTURAL MECHANICS

Includes structural element design, analysis and testing; dynamic responses of structures; weight analysis; fatigue and other structural properties; and mechanical and thermal stresses in structure. For applications see 05 Aircraft Design, Testing and Performance and 18 Spacecraft Design, Testing and Performance.

20020000896 Argonne National Lab., IL USA
Tetrahedral element shape optimization via the Jacobian determinant and condition number
Freitag, L. A.; Knupp, P. M.; Jul. 30, 1999; 14p; In English
Report No.(s): DE2001-11915; ANL/MCS/CP-99689; No Copyright; Avail: Department of Energy Information Bridge, Microfiche

We present a new shape measure for tetrahedral elements that is optimal in the sense that it gives the distance of a tetrahedron from the set of inverted elements. This measure is constructed from the condition number of the linear transformation between a unit equilateral tetrahedron and any tetrahedron with positive volume. We use this shape measure to formulate two optimization objective functions that are differentiated by their goal: the first seeks to improve the average quality of the tetrahedral mesh; the second aims to improve the worst-quality element in the mesh. Because the element condition number is not defined for tetrahedral with negative volume, these objective functions can be used only when the initial mesh is valid. Therefore, we formulate a third objective function using the determinant of the element Jacobian that is suitable for mesh untangling. We review the optimization techniques used with each objective function and present experimental results that demonstrate the effectiveness of the mesh improvement and untangling methods. We show that a combined optimization approach that uses both condition number objective functions obtains the best-quality meshes.
NTIS
Grid Generation (Mathematics); Tetrahedrons; Hypergeometric Functions

20020001172 Minnesota Univ., Dept. of Geology and Geophysics, Minneapolis, MN USA
Superplastic Deformation of ice: Experimental Observations
Goldsby, D. L., Minnesota Univ., USA; Kohlstedt, D. L., Minnesota Univ., USA; Journal of Geophysical Research; Jun. 10, 2001; ISSN 0148-0227; Volume 106, No. B6, pp. 11,017-11,030; In English
Contract(s)/Grant(s): NAG5-6797
Report No.(s): Paper-2000JB900336; Copyright; Avail: Issuing Activity

Creep experiments on fine-grained ice reveal the existence of three creep regimes: (1) a dislocation creep regime; (2) a superplastic flow regime in which grain boundary sliding is an important deformation process; and (3) a basal slip creep regime in which the strain rate is limited by basal slip. Dislocation creep in ice is likely climb-limited, is characterized by a stress exponent of 4.0, and is independent of grain size. Superplastic flow is characterized by a stress exponent of 1.8 and depends inversely on grain size to the 1.4 power. Basal slip limited creep is characterized by a stress exponent of 2.4 and is independent of grain size. A fourth creep mechanism, diffusional flow, which usually occurs at very low stresses, is inaccessible at practical laboratory strain rates even for our finest grain sizes of approximately 3 micrometers. A constitutive equation based on these experimental results that includes flow laws for these four creep mechanisms is described. This equation is in excellent agreement with published laboratory creep data for coarse-grained samples at high temperatures. Superplastic flow of ice is the rate-limiting creep mechanism over a wide range of temperatures and grain sizes at stresses less than or equal to 0.1 MPa, conditions which overlap those occurring in glaciers, ice sheets, and icy planetary interiors.
Author
Deformation; Ice; Creep Properties; Grain Size

20020001511 Argonne National Lab., IL USA
Proceedings of the 18th Symposium on Energy Engineering Sciences
Sep. 26, 2000; 262p; In English
Report No.(s): DE2001-766270; CONF-2000/1; No Copyright; Avail: Department of Energy Information Bridge

Damage nucleation, growth, and failures of metallic structural components that operate at high temperature are overviewed. Damage nucleation usually begins with the development of small voids at a size level at the high end of the nanoscale (50 to 500 nm). These voids begin to grow via diffusion mechanisms along the grain boundaries along with dislocation creep within the grains. Voids eventually link-up to produce micro-cracks (size 2 to 20 micrometers). Micro-cracks then link-up to produce macro-cracks, which eventually leads to component failure. Here we overview the high temperature damage development process, especially with regard to cyclic loading, which has received little attention to date. It is seen that damage development under cyclic loading develops in a fashion quite different from the constant load situation.
NTIS
Cracks; Damage; Grain Boundaries; Microcracks; Cracking (Fracturing)

20020001844 Los Alamos National Lab., NM USA
Forum discussion on probabilistic structural analysis methods
Rodriguez, E. A.; Girrens, S. P.; Oct. 01, 2000; 5p; In English
Report No.(s): DE2001-765636; LA-UR-00-5033; No Copyright; Avail: Department of Energy Information Bridge, Microfiche
The use of Probabilistic Structural Analysis Methods (PSAM) has received much attention over the past several decades due in part to enhanced reliability theories, computational capabilities, and efficient algorithms. The need for this development was already present and waiting at the door step. Automotive design and manufacturing has been greatly enhanced because of PSAM and reliability methods, including reliability-based optimization. This demand was also present in the US Department of Energy (DOE) weapons laboratories in support of the overarching national security responsibility of maintaining the nations nuclear stockpile in a safe and reliable state.
NTIS
Probability Theory; Structural Analysis

20020001847 Los Alamos National Lab., NM USA
Probabilistic structural response with geometric shape uncertainties under collapse loading
Pepin, J. E.; Rodriguez, E. A.; Oct. 01, 2000; 10p; In English
Report No.(s): DE2001-765582; LA-UR-00-5008; No Copyright; Avail: Department of Energy Information Bridge, Microfiche
Engineers at Los Alamos National Laboratory (LANL) are currently developing the capability to provide a reliability-based structural evaluation technique for performing weapon reliability assessments. to enhance the analyst's confidence with these new methods, an integrated experiment and analysis project has been developed. The uncertainty associated with the collapse response of commercially available spherical marine float is evaluated with the aid of the non-liner explicit dynamics code DYNA3D coupled with the probabilistic code NESSUS (Numerical Evaluation of Stochastic Structures Under Stress). Variations in geometric shape parameters and uncertainties in material parameters are characterized and included in the probabilistic model.
NTIS
Probability Theory; Dynamic Loads; Shapes; Dynamic Structural Analysis; Reliability Analysis

20020001848 Los Alamos National Lab., NM USA
Probabilistic structural response of a valve assembly to high impact loading
Rodriguez, E. A.; Thacker, B. H.; Oct. 01, 2000; 10p; In English
Report No.(s): DE2001-765581; LA-UR-00-5009; No Copyright; Avail: Department of Energy Information Bridge, Microfiche
Engineers at Los Alamos National Laboratory (LANL) are currently developing capabilities, in cooperation with Southwest Research Institute, to provide reliability-based structural evaluation techniques for performing weapon component and system reliability assessments. The development and applications of Probabilistic Structural Analysis Methods (PSAM) is an important ingredient in the overall weapon reliability assessments. Focus, herein, is placed on the uncertainty associated with the structural response of an explosive actuated valve-piston assembly. The probabilistic dynamic response of the piston upon impact is evaluated through the coupling of the probabilistic code NESSUS (Numerical Evaluation of Stochastic Structures Under Stress) with the non-linear structural dynamics code, ABAQUS/Explicit. The probabilistic model includes variations in piston mass and geometry, and mechanical properties, such as Young's Modulus, yield strength, and flow characteristics. Finally, the probability of exceeding a specified strain limit, which is related to piston fracture, is determined.
NTIS
Pistons; Probability Theory; Valves; Dynamic Structural Analysis; Component Reliability; Impact Loads

20020001958 California Univ., Lawrence Radiation Lab., Livermore, CA USA
Calculation of Elastic-Plastic Flow
Wilkins, Mark L.; Apr. 19, 1963; 66p; In English
Contract(s)/Grant(s): W-7405-eng-48
Report No.(s): AD-A395185; UCRL-7322; No Copyright; Avail: CASI; A04, Hardcopy; A01, Microfiche
No abstract.
Author
Elastic Properties; Plastic Properties; Plastic Flow

20020001990 New Hampshire Univ., Durham, NH USA
Quantitative determination of the effects of yield strength, mode mixity, and crack length on crack face interactions during shear loading. An experimental and analytical investigation of the effect of fracture surface interference in shear.
Gross, T. S.; Mendelsohn, D. A.; Dec. 31, 1997; 22p; In English
Report No.(s): DE2001-764183; No Copyright; Avail: Department of Energy Information Bridge
A collaborative project to continue our studies of the effect of fracture surface interference on the driving force for shear crack growth is proposed. Specifically, we will use in situ. phase shifted speckle interferometry techniques to measure the displacement field around a Mode I fatigue pre-crack loaded in shear as a function of load. The effective Mode II stress intensity factor and the induced Mode I stress intensity factor will be determined by fitting the displacement fields to near tip analytical expressions. The crack face shear and normal traction distribution will be estimated by using the experimentally observed crack face displacement as boundary conditions to boundary element and finite element models of the specimen.
NTIS
Crack Propagation; Finite Element Method; Fracturing; Cracks; Yield Strength; Fatigue (Materials); Strain Distribution

20020002009 Sandia National Labs., Albuquerque, NM USA
Some Effects of Specimen and Loading Variables on the Fracture Toughness of Epoxy-to-Substrate Interfaces
Guess, T. R.; Reedy, E. D.; Stavig, M. E.; Dec. 23, 1998; 4p; In English
Report No.(s): DE2001-2823; SAND98-2874C; No Copyright; Avail: Department of Energy Information Bridge, Microfiche
The nucleation and growth of cracks at critical interfaces can degrade electrical and mechanical performance of electronic assemblies. Sandia National Laboratories is working to develop a fracture mechanics-based approach for assessing the reliability of components containing interfaces and subjected to thermal/mechanical fatigue. Models are being developed to predict the nucleation of a crack-like flaw in the vicinity of an interface, the path of crack propagation (along interface or into substrate), and the conditions for crack propagation. In addition, interfacial fracture toughness data are being generated to support model development. This paper summarizes an experimental study aimed at measuring the fracture toughness of epoxy-to-substrate interfaces that are representative of those found in bonded and encapsulated electronic components.
NTIS
Fracture Strength; Crack Propagation; Epoxy Resins; Fracture Mechanics

20020002709 Sandia National Labs., Albuquerque, NM USA
Synthesis of Structural Responses Using Experimentally Measured Frequency Response Functions and Field Test Data
Cap,; Nelson,; Nov. 17, 2000; 12p; In English
Report No.(s): DE2001-768062; SAND2000-1726C; No Copyright; Avail: Department of Energy Information Bridge
This paper presents an analysis technique used to generate the structural response at locations not measured during the ejection of a captive-carried store. The ejection shock event is complicated by the fact that forces may be imparted to the store at eight distinct locations. The technique derives forcing functions by combining the initial field test data for a limited number of measurement locations with Frequency Response Functions (FRFs) measured using a traditional modal-type impact (tap) test at the same locations. The derived forcing functions were then used with tap test FRFs measured at additional locations of interest to produce the desired response data.
NTIS
Field Tests; Responses; Frequency Distribution

20020003357 Sandia National Labs., Albuquerque, NM USA
Physics-based Modeling of Brittle Fracture: Cohesive Formulations and the Application of Meshfree Methods
Klein, P. A.; Foulk, J. W.; Chen, E. P.; Wimmer, S. A.; Gao, H.; Dec. 01, 2000; 114p; In English
Report No.(s): DE2001-772347; SAND2001-8099; No Copyright; Avail: Department of Energy Information Bridge, Microfiche

Simulation of generalized fracture and fragmentation remains an ongoing challenge in computational fracture mechanics. There are difficulties associated not only with the formulation of physically-based models of material failure, but also with the numerical methods required to treat geometries that change in time. The issue of fracture criteria is addressed in this work through a cohesive view of material, meaning that a finite material strength and work to fracture are included in the material description. In this study, we present both surface and bulk cohesive formulations for modeling brittle fracture, detailing the derivation of the formulations, fitting relations, and providing a critical assessment of their capabilities in numerical simulations of fracture. Due to their inherent adaptivity and robustness under severe deformation, meshfree methods are especially well-suited to modeling fracture behavior. We describe the application of meshfree methods to both bulk and surface approaches to cohesive modeling. We present numerical examples highlighting the capabilities and shortcomings of the methods in order to identify which approaches are best-suited to modeling different types of fracture phenomena.
NTIS
Mechanical Properties; Brittleness; Fracture Mechanics; Cohesion

20020003426 Los Alamos National Lab., NM USA
Knots and random walks in vibrated granular chains
Ben-Naim, E.; Aug. 01, 2000; 7p; In English
Report No.(s): DE2001-768816; LA-UR-00-3704; No Copyright; Avail: Department of Energy Information Bridge
The authors study experimentally statistical properties of the opening times of knots in vertically vibrated granular chains. Our measurements are in good qualitative and quantitative agreement with a theoretical model involving three random walks interacting via hard core exclusion in one spatial dimension. In particular, the knot survival probability follows a universal scaling function which is independent of the chain length, with a corresponding diffusive characteristic time scale. Both the large-exit-time and the small-exit-time tails of the distribution are suppressed exponentially, and the corresponding decay coefficients are in excellent agreement with the theoretical values.
NTIS
Statistical Analysis; Probability Theory; Models; Molecular Chains

20020004673 Sandia National Labs., Albuquerque, NM USA
Representation of Random Shock via the Karhunen Loeve Expansion
Paez,; Hunter,; Dec. 08, 2000; 10p; In English
Report No.(s): DE2001-771524; SAND2000-3053C; No Copyright; Avail: Department of Energy Information Bridge
Shock excitations are normally random process realizations, and most of our efforts to represent them either directly or indirectly reflect this fact. The most common indirect representation of shock sources is the shock response spectrum. It seeks to establish the damage-causing potential of random shocks in terms of responses excited in linear, single-degree-of-freedom systems. This paper shows that shock sources can be represented directly by developing the probabilistic and statistical structure that underlies the random shock source. Confidence bounds on process statistics and probabilities of specific excitation levels can be established from the model. Some numerical examples are presented.
NTIS
Karhunen-Loeve Expansion; Random Processes; Mathematical Models; Excitation; Mechanical Shock

20020005200 Sandia National Labs., Albuquerque, NM USA
Damping Investigations of a Simplified Frictional Shear Joint
Smallwood, D. O.; Gregory, D. L.; Coleman, R. G.; Dec. 05, 2000; 12p
Report No.(s): DE2001-769057; SAND2000-1929C; No Copyright; Avail: Department of Energy Information Bridge
The inability to include accurate damping models for bolted connections limits the accuracy of structural models to predict dynamic response. Experiments utilizing a system simulating a bolted shear joint to investigate frictional damping associated with micro-slip are discussed. Measurement and three computational techniques to quantify the energy dissipation as a function of the applied force to the shear joint are described. Parameters of the shear joint include the normal force amplitude and distribution, input force, frequency, material type, and surface characteristics. An underlying power law relationship between the energy dissipated per cycle and the applied input force is revealed and explored for the simplified shear joint. Methods to directly observe and measure the damping force at resonance are also discussed. This is a continuation of the work that was presented last year.
NTIS
Bolted Joints; Dynamic Response; Friction Factor; Structural Vibration; Vibration Damping; Shear Stress

20020005244 Bettis Atomic Power Lab., West Mifflin, PA USA

Measurement of residual stresses using fracture mechanics weight functions

Fan, Y.; Oct. 01, 2000; 15p; In English

Report No.(s): DE2001-774257; B-T-3331; No Copyright; Avail: Department of Energy Information Bridge, Microfiche

A residual stress measurement method has been developed to quantify through-the-thickness residual stresses. Accurate measurement of residual stresses is crucial for many engineering structures. Fabrication processes such as welding and machining generate residual stresses that are difficult to predict. Residual stresses affect the integrity of structures through promoting failures due to brittle fracture, fatigue, stress corrosion cracking, and wear. In this work, the weight function theory of fracture mechanics is used to measure residual stresses. The weight function theory is an important development in computational fracture mechanics. Stress intensity factors for arbitrary stress distribution on the crack faces can be accurately and efficiently computed for predicting crack growth. This paper demonstrates that the weight functions are equally useful in measuring residual stresses. In this method, an artificial crack is created by a thin cut in a structure containing residual stresses. The cut relieves the residual stresses normal to the crack-face and allows the relieved residual stresses to deform the structure. Strain gages placed adjacent to the cut measure the relieved strains corresponding to incrementally increasing depths of the cut. The weight functions of the cracked body relate the measured strains to the residual stresses normal to the cut within the structure. The procedure details, such as numerical integration of the singular functions in applying the weight function method, will be discussed.

NTIS

Residual Stress; Stress Measurement; Fracture Mechanics

20020005819 Los Alamos National Lab., NM USA

Identification of nonlinearities in an 8-DOF system through spectral feedback

Arcand, B.; Wait, J.; Aug. 01, 2000; 10p; In English

Report No.(s): DE2001-768722; LA-UR-00-3903; No Copyright; Avail: Department of Energy Information Bridge

The accurate detection and characterization of nonlinearities associated with damage in structural systems is an area of vibration analysis that is being widely researched. In this paper, nonlinear behavior is considered a potential indicator of damage. Most conventional damage detection methods, such as those based on resonant frequencies and mode shapes, do not accurately identify the location and extent of nonlinearities present in a given structural system. As an extension of previous work at LANL, an effort is made to validate a damage detection method proposed by Adams. This method states that the frequency response function (FRF) matrix obtained from a low-level vibration test approximates the underlying linear FRF matrix of the system. The nonlinear systems' responses to high level excitation are combined with the linear FRF in a classic feedback loop to obtain the contributions of nonlinear internal forces. The temporal and spatial characteristics of the nonlinearities present in a structural system are identified. An 8-DOF system is used as a test case to validate the aforementioned method. Results of the tests and important issues concerning the method are presented.

NTIS

Feedback; Nonlinearity; Degrees of Freedom; Frequency Response; Spectra; Structural Vibration

20020005822 Los Alamos National Lab., NM USA

Dynamic ductile evolution and tensile fracture: New experimental insights for models evaluation

Zurek, A.; Aug. 01, 2000; 14p; In English

Report No.(s): DE2001-768738; LA-UR-00-3811; No Copyright; Avail: Department of Energy Information Bridge

Under dynamic loading conditions, the rapid nature of the fracture process may simultaneously activate a considerable number of nucleation sites for void formation at the region of the tensile stress field. The growth and coalescence of these voids forms the deformation plane and eventually the fracture surface. Attempts to quantify damage evolution during fracture using microstructural observations, specifically for spallation, were pioneered by Seaman and his coworkers. They performed incipient spallation experiments in which they imposed a peak stress below the spall strength of the material, thereby developing an incipient spallation zone rather than complete separation. When this experimental methodology is applied, recovery techniques are utilized to recover the deformed samples without introducing any additional damage. Seaman and his coworkers, and later Lacomme, et al., developed damage quantification techniques based on area measurements of incipient fracture. However, measuring the area of a fracture opening with a certain degree of precision from a two dimensional image can be extremely inaccurate due to the irregular shape of the image. In recent years several techniques have been developed, or improved, that may allow a better and more accurate quantification of image features observed in metallographic analyses in incipient damage of

fracture surfaces. Many of these measured quantities are essential towards developing a solid, robust understanding necessary for a good constitutive model.
NTIS
Ductility; Mathematical Models; Tensile Stress; Mechanical Properties; Fracture Mechanics; Spallation

42
GEOSCIENCES (GENERAL)

Includes general research topics related to the Earth sciences, and the specific areas of petrology, mineralogy, and general geology. For other specific topics in geosciences see categories 41 through 48.

20020000761 Lawrence Livermore National Lab., Livermore, CA USA
Preliminary definition of geophysical regions for the Middle East and North Africa
Sweeney, J. J.; Walter, B.; Dec. 01, 1998; 43p; In English
Report No.(s): DE2001-8425; UCRL-ID-132899; GC0402000; No Copyright; Avail: Department of Energy Information Bridge, Microfiche

The ability to calibrate seismic stations to improve the monitoring of the Comprehensive Test Ban Treaty is partially limited by the availability of seismic events with known locations and source properties. to confidently extrapolate from these events to aseismic regions, and to properly account for discontinuities in seismic properties requires accurate geophysical models. This paper lays out a preliminary, first-order, regionalization of the Middle East and North African (MENA) region. The model specifies boundaries and velocity structures based on the geology and tectonics of the region, previously published studies, and empirical data observations by the LLNL group. This model is a starting point and is expected to be improved and refined by comparisons with ongoing tomography efforts and the collection of new data. We anticipate that this model and its successors will prove useful as a background model in the process of forming station calibration maps based on intelligent interpolation techniques such as kriging. We also hope the model, as it improves and demonstrates some predictive power, will provide a reference model for broader CTBT research efforts in detection, location and discrimination as well as other aspects of earth science.
NTIS
Geophysics; Middle East; Africa; Geology; Seismology

20020000773 Lawrence Livermore National Lab., Livermore, CA USA
Automatic registering receptacle safety design for bottom loading system used in National Ignition Facility
Leung, K. K.; Tiszauer, D. H.; Jan. 26, 1999; 6p; In English
Report No.(s): DE2001-8510; UCRL-JC-133045; No Copyright; Avail: Department of Energy Information Bridge, Microfiche

The National Ignition Facility (NIF) is a high power laser facility for fusion research. The project's design philosophy modularizes the laser's optical subsystem components into Line Replaceable Units (LRU) for ease in maintenance over its expected 30 year life. The LRUs are transported between the Optics Assembly Building (OAB) and the laser structure by a robotic material handling system. A major component of part of this handling system is a portable clean room or canister, which protects the optics of the LRU during transport between the OAB and the laser. The canister itself contains robotic systems that move the LRU into position inside the clean laser cavity, once the canister is docked to the laser's enclosure. The bottom loading canister carries a variety of different LRUs for placement in different portions of the laser. With this canister docking is accomplished from underneath the laser enclosure. Once docked, the canister becomes the reference from which the robotic insertion mechanisms inside the canister load the LRUs into the laser. Three concave downward conical cavities, mounted on the bottom of the laser enclosure are the receptacles which guide a set of kinematic pins on top of the canister to achieve a precise canister position. Because the canister with LRU can weigh up to 8000 pounds, each receptacle is subject to several thousand pounds of three-dimensional seismic loads during a seismic event. This paper presents an approach developed for the application of the three dimensional seismic loads with consideration of time-phasing to obtain both an upper and lower bound solution to the combined stress on each receptacle. The contacting seismic loads for a bottom loading canister, dock to the laser enclosure, are obtained by other NIF groups. They obtained the loading on the kinematic mounting pins by a nonlinear time-domain seismic analysis using a site-specific seismic acceleration time history. This paper focuses on the application of these loads to determine the seismic effects on the complex stress distribution in each steel receptacle. Finite element analysis is performed to predict stresses in various

parts of the receptacle. The net stress state, includes the combined stress from the mounting threads, bending stress in the thin section on the cone and the surface compressive stresses.
NTIS
Safety; Laser Fusion; Clean Rooms; Seismology; Laser Cavities

20020001043 Lawrence Livermore National Lab., Livermore, CA USA
New C-14 calibration data set for the last deglaciation based on marine varves
Hughen, K. A.; Kashgarian, M.; Lehman, S. J.; Overpeck, J. T.; Peterson, L. C.; Feb. 22, 1999; 14p; In English
Report No.(s): DE2001-8542; UCRL-JC-133356; YN010000; No Copyright; Avail: Department of Energy Information Bridge, Microfiche

Varved sediments of the tropical Cariaco basin provide a new C-14 calibration data set for the period of deglaciation (10,000 to 14,500 years before present: 10-14.5 cal ka BP). Independent evaluations of the Cariaco Basin calendar and C-14 chronologies were based on the agreement of varve ages with the GISP2 ice core layer chronology for similar high-resolution paleoclimate records, in addition to C-14 age agreement with terrestrial C-14 dates, even during large climatic changes. These assessments indicate that the Cariaco Basin C-14 reservoir age remained stable throughout the Younger Dryas and late Alleroed climatic events and that the varve and C-14 chronologies provide an accurate alternative to existing calibrations based on coral U/Th dates. The Cariaco Basin calibration generally agrees with coral-derived calibrations but is more continuous and resolves century-scale details of C-14 change not seen in the coral records. C-14 plateaus can be identified at 9.6, 11.4, and 11.7 C-14 ka BP, in addition to a large, sloping plateau during the Younger Dryas (approximately10 to 11 C-14 ka BP). Accounting for features such as these is crucial to determining the relative timing and rates of change during abrupt global climate changes of the last deglaciation.
NTIS
Carbon 14; Climate Change; Calibrating

20020001046 Lawrence Livermore National Lab., Livermore, CA USA
Tracing Waste-Water in River and Ground Water of Orange County Using Boron Isotopes and General Geochemistry
Bullen, T.; Davisson, M. L.; Vengosh, A.; Mar. 26, 1999; 14p; In English
Report No.(s): DE2001-8552; UCRL-ID-133529; No Copyright; Avail: Department of Energy Information Bridge, Microfiche

Surface water runoff within the Santa Ana River (SAR) watershed is generated from a variety of sources, including a mountain snowmelt, urban waste-water discharge, and dairy feedlots. During summer baseflow periods, the persistent flow of approximately 200 cubic feet per second (cfs) consists almost entirely of tertiary-treated waste-water from upstream urban discharge. The Orange County Water District (OCWD) artificially recharges the majority of flow from the SAR during high and low flow periods into the Forebay region to augment groundwater pumping demands. Proposed regulations for reclaimed water recharge into portable use aquifers have direct impact on how OCWD manages groundwater recharge from the SAR. Knowledge of how much treated waste-water recharges into the Forebay area of the Orange County Groundwater Basin has direct benefit to future management and regulatory activities. This project attempted to trace the inorganic components of waste-water dissolved in the SAR and local groundwater in the Forebay by applying geochemical and boron isotopic systematics. The objectives were to characterize the chemical and boron isotropic compositions of recharged surface water and groundwater, to delineate typical mixing end-members, and to examine if recharge water from the SAR has a different isotopic signature relative to non-anthropogenically-influenced groundwater. The overall goal is to test whether a combination of boron isotopes and water chemistry will provide an accurate means to quantifiably distinguish waste-water from non-waste water sources in surface and groundwater of the Forebay.
NTIS
Boron Isotopes; Ground Water; Rivers; Waste Water

20020001078 Los Alamos National Lab., NM USA
Volcanism Studies: Final Report for the Yucca Mountain Project
Crowe, B. M.; Perry, F. V.; Valentine, G. A.; Bowker, L. M.; Dec. 01, 1998; 554p; In English
Report No.(s): DE2001-12111; LA-13478; No Copyright; Avail: Department of Energy Information Bridge, Microfiche

This report synthesizes the results of volcanism studies conducted by scientists at the Los Alamos National Laboratory and collaborating institutions on behalf of the Department of Energy's Yucca Mountain Project. An assessment of the risk of future volcanic activity is one of many site characterization studies that must be completed to evaluate the Yucca Mountain site for potential long-term storage of high-level radioactive waste. The presence of several basaltic volcanic centers in the Yucca Mountain region of Pliocene and Quaternary age indicates that there is a finite risk of a future volcanic event occurring during the 10,000-year isolation period of a potential repository. Chapter 1 introduces the volcanism issue for the Yucca Mountain site

and provides the reader with an overview of the organization, content, and significant conclusions of this report. The risk of future basaltic volcanism is the primary topic of concern including both events that intersect a potential repository and events that occur near or within the waste isolation system of a repository. Future volcanic events cannot be predicted with certainty but instead are estimated using formal methods of probabilistic volcanic hazard assessment (PVHA). Chapter 2 describes the volcanic history of the Yucca Mountain region (YMR) and emphasizes the Pliocene and Quaternary volcanic record, the interval of primary concern for volcanic risk assessment. The distribution, eruptive history, and geochronology of Plio-Quaternary basalt centers are described by individual center emphasizing the younger postcaldera basalt (Ma). The Lathrop Wells volcanic center is described in detail because it is the youngest basalt center in the YMR. The age of the Lathrop Wells center is now confidently determined to be about 75 thousand years old. Chapter 3 describes the tectonic setting of the YMR and presents and assesses the significance of multiple alternative tectonic models. The Crater Flat volcanic zone is defined and described as one of many alternative models of the structural controls of the distribution of Plio-Quaternary basalt centers in the YMR. Geophysical data are described for the YMR and are used as an aid to understand the distribution of basaltic volcanic centers. Chapter 4 discusses the petrologic and geochemical features of basaltic volcanism in the YMR, the southern Great Basin and the Basin and Range province. Geochemical and isotopic data are presented for post-Miocene basalts of the Yucca Mountain region. Alternative petrogenetic models are assessed for the formation of the Lathrop Wells volcanic center. Based on geochemical data, basaltic ash in fault trenches near Yucca Mountain is shown to have originated from the Lathrop Wells center. Chapter 5 synthesizes eruptive and subsurface effects of basaltic volcanism on a potential repository and summarizes current concepts of the segregation, ascent, and eruption of basalt magma. Chapter 6 synthesizes current knowledge of the probability of disruption of a potential repository at Yucca Mountain. In 1996, an Expert Elicitation panel was convened by DOE that independently conducted PVHA for the Yucca Mountain site. Chapter 6 does not attempt to revise this PVHA; instead, it further examines the sensitivity of variables in PVHA.
NTIS
Volcanoes; Volcanology; Waste Disposal; Radioactive Wastes

20020001359 NASA Goddard Space Flight Center, Greenbelt, MD USA
Standards, Aligned Lessons, and Content of Earth Science
Meeson, Blanche W., NASA Goddard Space Flight Center, USA; [2001]; 1p; In English; NSTA National Convention, 21-25 Mar. 2001, Saint Louis, MO, USA; Sponsored by National Science Teachers Association, USA; No Copyright; Avail: Issuing Activity; Abstract Only

Never before have we been able to see so clearly how Earth breathes, moves, and lives. Global change and how we are affecting it are hot topics, and NASA is putting the necessary tools to work to collect the global data and monitor it over time. Plenty of NASA materials will be distributed free to attendees for use in their classrooms or learning centers.
Author
Earth Sciences; NASA Programs; Climatology

20020001446 Lawrence Livermore National Lab., Livermore, CA USA
Thermomechanical Effects on Permeability for a 3-D Model of YM Rock
Berge, P. A.; Blair, S. C.; Wang, H. F.; Jan. 12, 1999; 8p; In English
Report No.(s): DE2001-8789; UCRL-JC-132065; No Copyright; Avail: Department of Energy Information Bridge, Microfiche

The authors estimate how thermomechanical processes affect the spatial variability of fracture permeability for a three dimensional model representing Topopah Spring tuff at the nuclear-waste repository horizon in Yucca Mountain, Nevada. Using a finite-difference code, they compute thermal stress changes. They evaluate possible permeability enhancement resulting from shear slip along various mapped fracture sets after 50 years of heating, for rock in the near-field environment of the proposed repository. The results indicate permeability enhancement of a factor of two for regions about 10 to 30 m above drifts, for north-south striking vertical fractures. Shear slip and permeability increases of a factor of four can occur in regions just above drifts, for east-west striking vertical fractures. Information on how permeability may change over the lifetime of a geologic repository is important to the prediction and evaluation of repository performance.
NTIS
Crustal Fractures; Permeability; Thermal Stresses; Thermodynamics; Three Dimensional Models; Igneous Rocks

20020001576 Argonne National Lab., IL USA
Long-term evapotranspiration estimates in the Walnut River Watershed in Kansas
Coulter, R. L.; Klazura, G. E.; Lesht, B. M.; Wesely, M. L.; Aug. 04, 1999; 12p; In English
Report No.(s): DE2001-12043; ANL/ER/RP-99715; No Copyright; Avail: Department of Energy Information Bridge

This project focuses on improving and testing a simple method for using reflectance data obtained from satellites to infer the effects on evapotranspiration of variations in soil moisture availability. The major advantage to the method, which is based on the parameterization of subgrid-scale surface fluxes (PASS) model, is that it can be applied to areas having diverse surface characteristics where direct surface flux measurements either do not exist or are not feasible and where meteorological data are available from only a limited number of ground stations. The emphasis of the PASS model is on improving: (1) methods for using high-resolution satellite remote sensing data to derive the essential parameters for individual types of surfaces overlarge areas; (2) algorithms for describing the interactions of near-surface atmospheric conditions with surface processes; and (3) algorithms for computing surface energy and water vapor flux at a scale close to the size of a satellite pixel. An operational modeling system is being developed. Testing of the system is accomplished by applying it to the Walnut River Wak-shed (WRW), instrumented watershed of moderate area (5,000 square km) located just east of Wichita, Kansas. Data from field experiments such as the intensive field campaign in 1997 by the Cooperative Atmosphere-Surface Exchange Study (CASES) and from routine operation of the Atmospheric Boundary Layer Experiments (ABLE) in the WRW are used to evaluate the ability of the PASS model to estimate accumulated water loss over a growing season. The research goals of the project areas follow: (1) Improve the existing satellite-data interfacing modules, especially the parameterization of soil moisture availability and water vapor flux; (2) Apply and evaluate the methods by using measurements at ground stations distributed within the WRW; and (3) Develop an operational version of the modeling system, and apply it to derive long-term evapotranspiration estimates at the WRW.
NTIS
Evapotranspiration; Watersheds; Kansas; Reflectance; Satellite Imagery

20020001767 California Univ., Dept. of Land, Air, and Water Resources, Davis, CA USA
Characteristic Solution to Nitrate Transport and Fate in Ground Water in Agricultural Watersheds
Hantush, M. M.; Marino, M. A.; Jan. 01, 2000; 14p; In English
Report No.(s): PB2002-100038; No Copyright; Avail: CASI; A03, Hardcopy; A01, Microfiche

Ground-water contamination by nonpoint source pollutants is recognized as a major environmental threat to human and the sustainability of healthy ecosystems. In this paper, the authors advective-reactive models that describe transport and fate of pollutants in inclined unconfined aquifers subject to a variable source. The models have implication on nitrate transport and denitrification at depth in aquifers, and the impact this has on attenuating nitrate discharge to streams in agricultural watersheds. The objectives of the models are: (1) to predict the impact of geochemical and physical controls on baseflow loadings in agricultural watersheds; and (2) to develop an index that measures the capacity for nitrate removal in ground water in agricultural watersheds. First, the steady-state ground-water flow problem is solved in two-layered unconfined aquifers with impervious inclined beds. Approximate closed-form expressions are also developed for ground-water fluxes in a two-layer inclined unconfined aquifer. Second, the transport and fate problem is formulated for the two-geochemically distinct layers, and solved in a Lagrangian framework using a regular perturbation technique.
NTIS
Aquifers; Watersheds; Nitrates; Denitrogenation; Pollution Transport

20020001777 Winand Staring Centre, Wageningen, Netherlands
Emerald: A Stochastic Modelling Approach for Rapid Assessment of Groundwater Dynamics
Walvoort, D. J. J.; Bierkens, M. F. P.; 1999; 86p; In English
Report No.(s): PB2001-108654; No Copyright; Avail: CASI; A05, Hardcopy; A01, Microfiche

A simple one-dimensional stochastic model was developed for quantifying groundwater dynamics and model accuracy. Due to its soil physical backbone, the model is somewhere between pure empirical models on the one hand, and complex physical-mechanistic models on the other. Hence, it is envisaged that it is more effective in scenario studies than pure empirical models, and more easily to operate than complex physical-mechanistic models. A case study showed that the model was capable of predicting various groundwater characteristics.
NTIS
Ground Water; Mathematical Models; Hydrology Models; Predictions

20020001969 Department of Energy, Tulsa, OK USA
Detailed Gravity and Magnetic Survey of the Taylorsville Triassic Basin
Leftwich, J.; Nowroozi, A. A.; Oct. 01, 1999; 21p; In English
Report No.(s): DE2001-12439; DOE/BC/15022-1; No Copyright; Avail: Department of Energy Information Bridge, Microfiche

This work reports the progress on collecting existing gravity data in a rectangular area covering the Richmond and Taylorsville Basins and its vicinity. The area covers one-degree latitude and one degree longitude, starting at 37 North, 77 West

and ending at 38 North, 78 West. Dr. David Daniels of the United State Geological Survey supplied us with more than 4900 Bouguer gravity anomalies in this area. The purpose of this report is to present the data in form of several maps and discuss its relation to the geology of the Triassic Basins and its vicinity. Johnson and others (1985) also presented a map of the Bouguer gravity anomaly of this area. However, their map covers a smaller area, and it is based on smaller number of observations.
NTIS
Gravity Anomalies; Magnetic Surveys; Structural Basins; Geological Surveys

20020001995 Princeton Univ., Plasma Physics Lab., NJ USA
Grand Challenge Problems in Environmental Modeling and Remediation: Groundwater Contaminant Transport (Partnerships in Computational Science)
Celia, M. A.; Mar. 11, 1999; 11p; In English
Report No.(s): DE2001-6601; No Copyright; Avail: Department of Energy Information Bridge

The over-reaching goal of the Groundwater Grand Challenge component of the Partnership in Computational Science (PICS) was to develop and establish the massively parallel approach for the description of groundwater flow and transport and to address the problem of uncertainties in the data and its interpretation. This necessitated the development of innovative algorithms and the implementation of massively parallel computational tools to provide a suite of simulators for groundwater flow and transport in heterogeneous media. This report summarizes the activities and deliverables of the Princeton University component of the Groundwater Grand Challenge project funded through the High Performance Computing (HPC) grand challenge program of the Department of Energy from 1995 through 1998. Seven institutions were primarily involved in this project: Brookhaven National Laboratory, Oak Ridge National Laboratory, Princeton University, SUNY at Stony Brook, Texas A and M University, The University of South Carolina, and the University of Texas at Austin, with contributing efforts from the Westinghouse Savannah River Technology Center. Each institution had primary responsibility for specific research components, but strong collaboration among all institutions was essential for the success of the project and in producing the final deliverables. PICS deliverables include source code for the suite of research simulators and auxiliary HPC tools, associated documentation, and test problems. These materials will be available as indicated from each institution's web page or from the Center for Computational Sciences Oak Ridge National Laboratory in January 1998.
NTIS
Pollution Control; Transport Properties; Ground Water; Environment Pollution; Environment Models; Computer Techniques

20020001997 South Carolina Univ., Columbia, SC USA
Grand Challenge Problems in Environmental Modeling and Remediation: Groundwater Contaminant Transport (Partnerships in Computational Science)
Sharpley, R. C.; Dec. 01, 1997; 11p; In English
Report No.(s): DE2001-6580; DOE/ER/25266-2; No Copyright; Avail: Department of Energy Information Bridge

The over-reaching goal of the Groundwater Grand Challenge component of the Partnership in Computational Science (PICS) was to develop and establish the massively parallel approach for the description of groundwater flow and transport and to address the problem of uncertainties in the data and its interpretation. This necessitated the development of innovative algorithms and the implementation of massively parallel computational tools to provide a suite of simulators for groundwater flow and transport in heterogeneous media. This report summarizes the activities and deliverables of the University of South Carolina component of the Groundwater Grand Challenge project funded through the High Performance Computing grand challenge program of the Department of Energy from 1995 through 1997. Seven institutions were primarily involved in this project: Brookhaven National Laboratory, Oak Ridge National Laboratory, Princeton University, SUNY at Stony Brook, Texas A and M University, The University of South Carolina, and the University of Texas at Austin, with contributing efforts from the Westinghouse Savannah River Technology Center. Each institution had primary responsibility for specific research components, but strong collaboration among all institutions was essential for the success of the project and in producing the final deliverables. PICS deliverables include source code for the suite of research simulators and auxiliary HPC (high power computing) tools, associated documentation, and test problems. These materials will be available as indicated from each institution's web page or from the Center for Computational Sciences Oak Ridge National Laboratory in January 1998.
NTIS
Fluid Flow; Ground Water; Environment Models; Contaminants; Parallel Processing (Computers); Environment Pollution

20020002229 Sandia National Labs., Albuquerque, NM USA
Sandia National Laboratories/New Mexico Geographic Data Atlas
Bleakly, D. R.; Eshelman, L.; Sep. 01, 1999; 254p; In English
Report No.(s): DE2001-12490; SAND99-1775; No Copyright; Avail: Department of Energy Information Bridge, Microfiche

The Geographic Data Atlas is published jointly by the Environmental Geographic Information System (EGIS) and the Facilities Geographic Information System (FGIS) to support the data-gathering efforts of Sandia National Laboratories/New Mexico (SNL/NM) for the Sitewide Environmental Impact Statement (SWEIS). This atlas provides the SWEIS staff and contractors with an up-to-date set of maps that accurately portray the types of geographic data available through the Geographic Information Systems (GIS) systems at SNL/NM. The EGIS provides environmentally related scientific data support and analysis through the implementation of an integrated GIS, relational database management systems (RDBMS) and associated analytical software. EGIS maintains an ARC/INFO GIS database containing more than 2,000 cartographic data layers that represent the environmental and physical characteristics of entities within the Kirtland Air Force Base (KAFB), the whole Kirtland Federal Complex (KFC), and other areas where SNL/NM has responsibility. EGIS creates customized maps that show customer data with respect to the topographic and environmental settings, and themes such as geology, soil types, vegetation, wells, and contaminant sources. The Facilities Geographic Information System (FGIS) provides facilities-related information on utilities and the utility infrastructure, buildings, roads, and survey monumentation, and any geographically related information on the base mapping of the SNL/NM site. The FGIS updates and maintains the base maps and current digital orthophotography. All of this data is maintained on an INTERGRAPH Modular GIS Environment (MGE) platform.
NTIS
Geology; Information Systems; Data Base Management Systems; Environmental Surveys; Surveys; Orthophotography

20020002244 Texas Univ., Austin, TX USA
Grand challenge problems in environmental modeling and remediation: groundwater contaminant transport
Arbogast, T.; Bryant, S.; Dawson, C. N.; Wheeler, M. F.; Aug. 31, 1998; 27p; In English
Report No.(s): DE2001-765660; No Copyright; Avail: Department of Energy Information Bridge, Microfiche

This report describes briefly the work of the Center for Subsurface Modeling (CSM) of the University of Texas at Austin (and Rice University prior to September 1995) on the Partnership in Computational Sciences Consortium (PICS) project entitled Grand Challenge Problems in Environmental Modeling and Remediation: Groundwater Contaminant Transport.
NTIS
Environment Models; Ground Water; Contaminants

20020002343 Geological Survey, Reston, VA USA
Vegetative Resistance to Flow in South Florida: Summary of Vegetation Sampling in Taylor Slough, Everglades National Park, September 1997-July 1998
Rybicki, N. B.; Reel, J. T.; Ruhl, H. A.; Gammon, P. T.; Carter, V.; Jan. 01, 2001; 132p; In English
Report No.(s): PB2002-100320; USGS/OFR-01/102; No Copyright; Avail: CASI; A07, Hardcopy; A02, Microfiche

The U.S. Geological Survey is one of many agencies providing scientific support to the effort to restore the South Florida Everglades. In September and November 1997 and July 1998, vegetation was sampled at selected sites in the Everglades as part of a study to quantify vegetative resistance to flow. The objectives of the vegetation sampling are (1) to provide detailed information on species composition, vegetation characteristics, and biomass for quantification of the effect of vegetation on water flow, and (2) to use these data in the future to infer flow resistance from vegetation information. Forty-two vegetation quadrats were sampled in Taylor Slough to determine the number and width of stems and leaves and the biomass of live and dead standing sawgrass, rush, and other plants, and the biomass of dead litter and periphyton. The samples were grouped into ten vegetation classes based on species composition and total biomass minus periphyton biomass.
NTIS
Vegetation; Biomass; Hydrology; Geological Surveys

20020002358 Forest Service, Pacific Northwest Research Station, Portland, OR USA
Summary Estimates of Forest Resources on Unreserved Lands of the Chatham Inventory Unit, Tongass National Forest, Southeast Alaska, 1998
van Hees, W. W. S.; June 2001; 22p; In English
Report No.(s): PB2001-108031; FSRB-PNW-234; No Copyright; Avail: CASI; A03, Hardcopy; A01, Microfiche

Summary estimates are presented of forest resource area, timber volume, and growth and mortality of timber on unreserved national forest land in the Chatham inventory unit of the Tongass National Forest. Pacific Northwest Research Station, Forest

Inventory and Analysis crews collected inventory data from 1995 to 2000. Productive forest land area (timberland) was estimated at 1,302 thousand acres, cubic-foot volume on timberland at 7,561 million cubic feet, and net annual growth and mortality at 31,613 and 28,341 thousand cubic feet, respectively.
NTIS
Forests; Inventories; Alaska

20020003801 Atomic Energy Commission, Idaho Falls, ID USA
Development of Probabilistic Design Basis Earthquake (DBE) Parameters for Moderate and High Hazard Facilities at INEEL
Payne, S. M.; Gorman, V. W.; Jensen, S. A.; Nitzel, M. E.; Russell, M. J.; Mar. 01, 2000; 201p; In English
Report No.(s): DE2001-768827; INEEL/EXT-99-00775; No Copyright; Avail: Department of Energy Information Bridge, Microfiche

Design Basis Earthquake (DBE) horizontal and vertical response spectra are developed for moderate and high hazard facilities or Performance Categories (PC) 3 and 4, respectively, at the Idaho National Engineering and Environmental Laboratory (INEEL). The probabilistic DBE response spectra will replace the deterministic DBE response spectra currently in the U.S. Department of Energy Idaho Operations Office (DOE-ID) Architectural Engineering Standards that govern seismic design criteria for several facility areas at the INEEL. Probabilistic DBE response spectra are recommended to DOE Naval Reactors for use at the Naval Reactor Facility at INEEL. The site-specific Uniform Hazard Spectra (UHS) developed by URS Greiner Woodward Clyde Federal Services are used as the basis for developing the DBE response spectra. In 1999, the UHS for all INEEL facility areas were recomputed using more appropriate attenuation relationships for the Basin and Range province. The revised UHS have lower ground motions than those produced in the 1996 INEEL site-wide probabilistic ground motion study. The DBE response spectra were developed by incorporating smoothed broadened regions of the peak accelerations, velocities, and displacements defined by the site-specific UHS. Portions of the DBE response spectra were adjusted to ensure conservatism for the structural design process.
NTIS
Earthquakes; Hazards; Structural Design; Probability Theory

20020004019 Los Alamos National Lab., NM USA
Lithospheric processes
Baldridge, W.; Dec. 01, 2000; 18p; In English
Report No.(s): DE2001-768862; LA-UR-00-5439; No Copyright; Avail: Department of Energy Information Bridge

The authors used geophysical, geochemical, and numerical modeling to study selected problems related to Earth's lithosphere. We interpreted seismic waves to better characterize the thickness and properties of the crust and lithosphere. In the southwestern US and Tien Shari, crust of high elevation is dynamically supported above buoyant mantle. In California, mineral fabric in the mantle correlate with regional strain history. Although plumes of buoyant mantle may explain surface deformation and magmatism, our geochemical work does not support this mechanism for Iberia. Generation and ascent of magmas remains puzzling. Our work in Hawaii constrains the residence of magma beneath Hualalai to be a few hundred to about 1000 years. In the crust, heat drives fluid and mass transport. Numerical modeling yielded robust and accurate predictions of these processes. This work is important fundamental science, and applies to mitigation of volcanic and earthquake hazards, Test Ban Treaties, nuclear waste storage, environmental remediation, and hydrothermal energy.
NTIS
Lithosphere; Earth Planetary Structure; Earth Crust; Structural Properties (Geology); Numerical Analysis

20020004921 Lawrence Livermore National Lab., Livermore, CA USA
Role of Lame (lambda) in estimating porosity and saturation from seismic velocities
Berryman, J. G.; Berg, P. A.; Bonner, B. P.; Mar. 12, 1999; 13p; In English
Report No.(s): DE2001-757418; UCRL-JC-133587; KC0403030; No Copyright; Avail: Department of Energy Information Bridge

No abstract.
NTIS
Porosity; Saturation; Seismology; Velocity Distribution; Elastic Waves

20020005069 Pacific Northwest National Lab., Richland, WA USA

Groundwater Monitoring Plan for the Solid Waste Landfill

Lindberg, J. W.; Chou, C. J.; Dec. 14, 2000; 93p; In English

Report No.(s): DE2001-769335; PNNL-13014; No Copyright; Avail: Department of Energy Information Bridge, Microfiche

The Solid Waste Landfill (SWL) is regulated by the Washington State Department of Ecology under WAC 173-304. Between 1973 and 1976, the landfill received primarily paper waste and construction debris, but it also received asbestos, sewage, and catch tank liquid waste. Groundwater monitoring results indicate the SWL has contaminated groundwater with volatile organic compounds and possibly metals at levels that exceed regulatory limits. DynCorp, Tri-Cities, Inc. operates the facility under an interim closure plan (final closure plan will be released shortly). Pacific Northwest National Laboratory (PNNL) monitors groundwater at the site. This monitoring plan includes well and constituent lists, and summarizes sampling, analytical, and quality control requirements. Changes from the previous monitoring plan include elimination of two radionuclides from the analyte list and some minor changes in the statistical analysis. Existing wells in the current monitoring network only monitor the uppermost portion of the upper-most aquifer. Therefore, two new downgradient wells and one existing upgradient well are proposed to determine whether groundwater waste constituents have reached the lower portion of the uppermost aquifer. The proposed well network includes three upgradient wells and ten downgradient wells. The wells will be sampled quarterly for 14 analytes required by WAC 173-304-490 plus volatile organic compounds and filtered arsenic as site-specific analytes.

NTIS

Solid Wastes; Ground Water; Aquifers; Wells; Sampling

20020005074 Federal Energy Technology Center, Morgantown, WV USA

Riverton dome gas exploration and stimulation technology demonstration, Wind River Basin, Wyoming

Surdam, R. C.; Jiao, Z.; Boyd, N. K.; Nov. 01, 1999; 26p; In English

Report No.(s): DE2001-769347; DE-FC26-97FT34181; No Copyright; Avail: Department of Energy Information Bridge

The new exploration technology for basin center gas accumulations developed by R.C. Surdam and Associates at the Institute for Energy Research, University of Wyoming, was applied to the Riverton Dome 3-D seismic area. Application of the technology resulted in the development of important new exploration leads in the Frontier, Muddy, and Nugget formations. The new leads are adjacent to a major north-south trending fault, which is downdip from the crest of the major structure in the area. In a blind test, the drilling results from six new Muddy test wells were accurately predicted. The initial production values, IP, for the six test wells ranged from one mmcf/day to four mmcf/day. The three wells with the highest IP values (i.e., three to four mmcf/day) were drilled into an intense velocity anomaly (i.e., anomalously slow velocities). The well drilled at the end of the velocity anomaly had an IP value of one mmcf/day, and the two wells drilled outside of the velocity anomaly had IP values of one mmcf/day and are presently shut in. Based on these test results, it is concluded that the new IER exploration strategy for detecting and delineating commercial, anomalously pressured gas accumulation is valid in the southwestern portions of the Wind River Basin, and can be utilized to significantly reduce exploration risk and to increase profitability of so called basin center gas accumulations.

NTIS

Energy Technology; River Basins; Stimulation; Wyoming; Natural Gas

20020005075 Geological Survey, Idaho Falls, ID USA

Hydrologic Conditions and Distribution of Selected Constituents in Water, Snake River Plain Aquifer, Idaho National Engineering and Environmental Laboratory, Idaho, 1996 through 1998

Bartholomay, R. C.; Tucker, B. J.; Davis, L. C.; Greene, M. R.; Sep. 01, 2000; 60p; In English

Report No.(s): DE2001-769365; DOE/ID-22167; No Copyright; Avail: Department of Energy Information Bridge

Radiochemical and chemical wastewater discharged since 1952 to infiltration ponds and disposal wells at the Idaho National Engineering and Environmental Laboratory (INEEL) has affected water quality in the Snake River Plain aquifer. The US Geological Survey, in cooperation with the US Department of Energy, maintains a monitoring network at the INEEL to determine hydrologic trends and to delineate the movement to radiochemical and chemical wastes in the aquifer. This report presents an analysis of water-level and water-quality data collected from the Snake River Plain aquifer during 1996-98. Detectable concentrations of radiochemical constituents in water samples from wells in the Snake River Plain aquifer at the INEEL decreased or remained constant during 1996-98. Decreased concentrations are attributed to reduced rates of radioactive-waste disposal, sorption process, radioactive decay, and changes in waste-disposal practices. Detectable concentrations of chemical constituents in water from the Snake River Plain aquifer at the INEEL were variable during 1996-98.

NTIS

Aquifers; Radiochemistry; Rivers; Hydrology; Geological Surveys

20020005084 Argonne National Lab., IL USA

Continuum description of avalanches in granular media

Aranson, I. S.; Tsimring, L. S.; Dec. 05, 2000; 7p; In English

Report No.(s): DE2001-772120; ANL/MSD/CP-103586; No Copyright; Avail: Department of Energy Information Bridge, Microfiche

A continuum theory of partially fluidized granular flows is proposed. The theory is based on a combination of the mass and momentum conservation equations with the order parameter equation which describes the transition between flowing and static components of the granular system. We apply this model to the dynamics of avalanches in chutes. The theory provides a quantitative description of recent observations of granular flows on rough inclined planes (Daerr and Douady 1999): layer bistability, and the transition from triangular avalanches propagating downhill at small inclination angles to balloon-shaped avalanches also propagating uphill for larger angles.

NTIS

Avalanches; Momentum Theory; Continuums

20020005182 Lawrence Livermore National Lab., Livermore, CA USA

Laboratory Velocity Measurements Used for Recovering Soil Distributions from Field Seismic Data

Berge, P. A.; Bertete-Aguirre, H.; Oct. 20, 1999; 15p; In English

Report No.(s): DE2001-756954; UCRL-JC-135132; EW4090100; No Copyright; Avail: Department of Energy Information Bridge

Recent advances in field methods make it possible to obtain high quality compressional (P) and shear (S) velocity data for the shallow subsurface. Environmental and engineering problems require new methods for interpreting the velocity data in terms of sub-surface soil distribution. Recent advances in laboratory measurement techniques have provided high quality velocity data for soils at low pressures that can be used to improve interpretation of field data. We show how laboratory data can be used to infer lithology from field data. We use laboratory ultrasonic velocity measurements from artificial soils made by combining various amounts of sand and peat moss.

NTIS

Lithology; Soils; Velocity Measurement

20020005824 Oak Ridge National Lab., TN USA

Mercury and Methylmercury Relationships in Contaminated Streams in the Southwestern U.S.A

Southworth, G. R.; Jan. 10, 2001; 5p; In English; 25th; 25th Annual International Conference on Heavy Metals in the Environment, 6-8 August, 2000, Ann Arbor, MI, USA

Contract(s)/Grant(s): AC05-96OR22464

Report No.(s): DE2001-774476; P00-108073; No Copyright; Avail: Department of Energy Information Bridge, Microfiche

Field and laboratory studies have demonstrated that concentrations of methylmercury in freshwater systems are influenced by the concentrations of precursor inorganic mercury. Because the production of methylmercury from inorganic mercury is influenced by a large number of chemical and ecological factors, extrapolation of observed relationships between precursor mercury and methlymercury in specific aquatic systems to other systems generally fail. However, in chemically and ecologically similar lakes and streams, generalizations concerning the relationship between inorganic mercury and methylmercury in water may be more universal. We measured total mercury and methylmercury in filtered and unfiltered water samples from 28 sites in 13 freshwater streams in Tennessee, Kentucky, Virginia, and North Carolina. All sites were sampled under warm weather baseflow conditions. Seven of the streams had a previous or ongoing history of mercury contamination from point sources, while three others were suspected to be contaminated based on concentrations of mercury in fish. Three were presumed to be influenced primarily by atmospheric and geologic sources of mercury. Total mercury concentrations varied more among the 28 sites than did methylmercury concentrations, and regression of methylmercury versus total mercury did not yield evidence of a strong relationship. However, when data from contaminated sites receiving discharges from Dept. of Energy facilities in Oak Ridge, TN were excluded, there was a much stronger relationship. We hypothesize that some chemical characteristic of these streams associated with the industrial discharges lessens the net methylation rate of inorganic mercury.

NTIS

Streams; Water Pollution; Mercury (Metal); Contamination; Water Sampling

43
EARTH RESOURCES AND REMOTE SENSING

Includes remote sensing of earth features, phenomena and resources by aircraft, balloon, rocket, and spacecraft; analysis or remote sensing data and imagery; development of remote sensing products; photogrammetry; and aerial photographs. For instrumentation see 35 Instrumentation and Photography.

20020000775 Colorado Univ., Colorado Center for Astrodynamics Research, Boulder, CO USA
Using GPS Reflections for Satellite Remote Sensing
Mickler, David, Colorado Univ., USA; [2000]; 16p; In English
Contract(s)/Grant(s): NAG1-1927
Report No.(s): AAS-00-142; No Copyright; Avail: CASI; A03, Hardcopy; A01, Microfiche

GPS signals that have reflected off of the ocean's surface have shown potential for use in oceanographic and atmospheric studies. The research described here investigates the possible deployment of a GPS reflection receiver onboard a remote sensing satellite in low Earth orbit (LEO). The coverage and resolution characteristics of this receiver are calculated and estimated. This mission analysis examines using reflected GPS signals for several remote sensing missions. These include measurement of the total electron content in the ionosphere, sea surface height, and ocean wind speed and direction. Also discussed is the potential test deployment of such a GPS receiver on the space shuttle. Constellations of satellites are proposed to provide adequate spatial and temporal resolution for the aforementioned remote sensing missions. These results provide a starting point for research into the feasibility of augmenting or replacing existing remote sensing satellites with spaceborne GPS reflection-detecting receivers. Author

Global Positioning System; Ocean Surface; Remote Sensing; Low Earth Orbits

20020001350 NASA Goddard Space Flight Center, Greenbelt, MD USA
Remote Sensing of Aerosol and their Radiative Properties from the MODIS Instrument on EOS-Terra Satellite: First Results and Evaluation
Kaufman, Yoram, NASA Goddard Space Flight Center, USA; Tanre, Didier, NASA Goddard Space Flight Center, USA; Remer, Lorraine, NASA Goddard Space Flight Center, USA; Holben, Brent, NASA Goddard Space Flight Center, USA; [2001]; 1p; In English; International Summer School, 22-28 Sep. 2001, La Londe-les-Maures, France; No Copyright; Avail: Issuing Activity; Abstract Only

The MODIS instrument was launched on the NASA Terra satellite in Dec. 1999. Since last Oct., the sensor and the aerosol algorithm reached maturity and provide global daily retrievals of aerosol optical thickness and properties. MODIS has 36 spectral channels in the visible to IR with resolution down to 250 m. This allows accurate cloud screening and multi-spectral aerosol retrievals. We derive the aerosol optical thickness over the ocean and most of the land areas, distinguishing between fine (mainly man-made aerosol) and coarse aerosol particles. The information is more precise over the ocean where we derive also the effective radius and scattering asymmetry parameter of the aerosol. New methods to derive the aerosol single scattering albedo are also being developed. These measurements are use to track different aerosol sources, transport and the radiative forcing at the top and bottom of the atmosphere. The AErosol RObotic NETwork of ground based radiometers is used for global validation of the satellite derived optical thickness, size parameters and single scattering albedo and measure additional aerosol parameters that cannot be derived from space.
Author

Aerosols; Algorithms; Imaging Spectrometers; Ocean Surface; Remote Sensing; Terra Spacecraft

20020001589 Lawrence Livermore National Lab., Livermore, CA USA
Regional hydrology of the Dixie Valley geothermal field, Nevada: preliminary interpretations of chemical and isotopic data
Counce, D.; Dunlap, C.; Goff, F.; Huebner, M.; Janik, C.; Aug. 16, 1999; 11p; In English
Report No.(s): DE2001-12727; UCRL-JC-135417; No Copyright; Avail: Department of Energy Information Bridge, Microfiche

Chemical and isotopic analyses of Dixie Valley regional waters indicate several distinct groups ranging in recharge age from Pleistocene (less than 20 ka) to recent (less than 50 ka). Valley groundwater is older than water from perennial springs and artesian wells in adjacent ranges, with Clan Alpine range (east) much younger (most less than 50 ka) than Stillwater range (west; most greater than 1000a). Geothermal field fluids (approximately 12-14 ka) appear derived from water similar in composition to non-thermal groundwater observed today in valley artesian wells (also -14 ka). Geothermal fluid interaction with mafic rocks (Humboldt Lopolith) appears to be common, and significant reaction with granodiorite may also occur. Despite widespread occurrence of carbonate rocks, large scale chemical interaction appears minor. Age asymmetry of the ranges, more extensive

interaction with deep-seated waters in the west, and distribution of springs and artesian wells suggest the existence of a regional upward hydrologic gradient with an axis in proximity to the Stillwater range.
NTIS
Hydrology; Nevada; Geochronology; Isotope Ratios; Geotemperature

20020002711 California Univ., Lawrence Berkeley Lab., Berkeley, CA USA
Water resources development in Santa Clara Valley, California: Insights into the human-hydrologic relationship
Reynolds, J. L.; Narasimhan, T. N.; Jun. 01, 2000; 158p; In English
Report No.(s): DE2001-767622; LBNL-46598; No Copyright; Avail: Department of Energy Information Bridge

Groundwater irrigation is critical to food production and, in turn, to humankind's relationship with its environment. The development of groundwater in Santa Clara Valley, California during the early twentieth century is instructive because (1) responses to unsustainable resource use were largely successful; (2) the proposals for the physical management of the water, although not entirely novel, incorporated new approaches which reveal an evolving relationship between humans and the hydrologic cycle; and (3) the valley serves as a natural laboratory where natural (groundwater basin, surface watershed) and human (county, water district) boundaries generally coincide. Here, I investigate how water resources development and management in Santa Clara Valley was influenced by, and reflective of, a broad understanding of water as a natural resource, including scientific and technological innovations, new management approaches, and changing perceptions of the hydrologic cycle. Market demands and technological advances engendered reliance on groundwater. This, coupled with a series of dry years and laissez faire government policies, led to overdraft. Faith in centralized management and objective engineering offered a solution to concerns over resource depletion, and a group dominated by orchardists soon organized, fought for a water conservation district, and funded an investigation to halt the decline of well levels. Engineer Fred Tibbetts authored an elaborate water salvage and recharge plan that optimized the local water resources by integrating multiple components of the hydrologic cycle. Informed by government investigations, groundwater development in Southern California, and local water law cases, it recognized the limited surface storage possibilities, the spatial and temporal variability, the relatively closed local hydrology, the interconnection of surface and subsurface waters, and the value of the groundwater basin for its storage, transportation, and treatment abilities. The proposal was typically described as complementing an already generous nature, not simply subduing it. Its implementation was limited by political tensions, and fifteen years later, a scaled-down version was constructed. Well levels recovered, but within a decade were declining due to increasing withdrawals. I assert that the approach in Santa Clara Valley was a forerunner to more recent innovations in natural resource management in California and beyond.
NTIS
Hydrological Cycle; Water Resources; California; Valleys

20020002850 Atomic Energy Commission, Idaho Falls, ID USA
Fracture Permeability and in Situ Stress in the Dixie Valley, Nevada, Geothermal Reservoir
Zoback, M. D.; Mar. 08, 1999; 15p; In English
Report No.(s): DE2001-12560; DOE/ID/13452; No Copyright; Avail: Department of Energy Information Bridge

We have collected and analyzed fracture and fluid flow data from wells both within and outside the producing geothermal reservoir at Dixie Valley. Data from wellbore imaging and flow tests in wells outside the producing field that are not sufficiently hydraulically connected to the reservoir to be of commercial value provide both the necessary control group of fracture populations and an opportunity to test the concepts proposed in this study on a regional, whole-reservoir scale. Results of our analysis indicate that fracture zones with high measured permeabilities within the producing segment of the fault are parallel to the local trend of the Stillwater fault and are optimally oriented and critically stressed for frictional failure in the overall east-southeast extensional stress regime measured at the site. In contrast, in the non-producing (i.e., relatively impermeable:) well 66-21 the higher ratio of S(sub h min) to S(sub v) acts to decrease the shear stress available to drive fault slip. Thus, although many of the fractures at this site (like the Stillwater fault itself) are optimally oriented for normal faulting they are not critically stressed for frictional failure. Although some of the fractures observed in the non-producing well 45-14 are critically stressed for frictional failure, the Stillwater fault zone itself is frictionally stable. Thus, the high horizontal differential stress (i.e., S(sub Hmax)-S(sub hmin)) together with the severe misorientation of the Stillwater fault zone for normal faulting at this location appear to dominate the overall potential for fluid flow.
NTIS
Geothermal Resources; Permeability; Stress Analysis; Data Acquisition; Reservoirs; Fractures (Materials)

20020004187 NASA Langley Research Center, Hampton, VA USA

A Comparison of GPS and Scatterometer Sensing of Ocean Wind Speed and Direction

Armatys, Michael, Colorado Univ., USA; Komjathy, Attila, Colorado Univ., USA; Axelrad, Penina, Colorado Univ., USA; Katzberg, Stephen J., NASA Langley Research Center, USA; [2000]; 2p; In English

Contract(s)/Grant(s): NAG1-1927; No Copyright; Avail: CASI; A01, Hardcopy; A01, Microfiche

Initial estimates of ocean surface wind speed and direction based on observations of reflected Global Positioning System (GPS) signals are presented and compared to QuikSCAT wind fields. The two wind speed estimates are generally in agreement to within 2-3 m/s, and under favorable conditions of well developed seas and stable winds, direction estimates agree to within 10 deg. An overview of the GPS technique is presented as well as a presentation and discussion of these first results.

Author

Estimates; Global Positioning System; Ground Wind; Wind Velocity; Remote Sensing

20020004347 NASA Langley Research Center, Hampton, VA USA

Sea Ice Remote Sensing Using Surface Reflected GPS Signals

Komjathy, Attila, Colorado Univ., USA; Maslanik, James, Colorado Univ., USA; Zavorotny, Valery U., National Oceanic and Atmospheric Administration, USA; Axelrad, Penina, Colorado Univ., USA; Katzberg, Stephen J., NASA Langley Research Center, USA; [2000]; 4p; In English; IEEE International Geoscience and Remote Sensing Symposium, 24-28 Jul. 2000, Honolulu, HI, USA; Sponsored by Institute of Electrical and Electronics Engineers, USA

Contract(s)/Grant(s): NAG1-1927; No Copyright; Avail: CASI; A01, Hardcopy; A01, Microfiche

This paper describes a new research effort to extend the application of Global Positioning System (GPS) signal reflections, received by airborne instruments, to cryospheric remote sensing. Our experimental results indicate that reflected GPS signals have potential to provide information on the presence and condition of sea and freshwater ice as well as the freeze/thaw state of frozen ground. In this paper we show results from aircraft experiments over the ice pack near Barrow, Alaska indicating correlation between forward-scattered GPS returns and RADARSAT backscattered measurements.

Author

Remote Sensing; Global Positioning System; Signal Reflection

20020004361 NASA Marshall Space Flight Center, Huntsville, AL USA

National Environmental Change Information System Case Study ***Final Report***

Goodman, S. J., NASA Marshall Space Flight Center, USA; Ritschard, R., Alabama Univ., USA; Estes, M. G., Jr., Universities Space Research Association, USA; Hatch, U., Auburn Univ., USA; November 2001; 54p; In English

Contract(s)/Grant(s): RTOP 428-50-09

Report No.(s): NASA/TM-2001-211410; NAS 1.15:211410; M-1034; No Copyright; Avail: CASI; A04, Hardcopy; A01, Microfiche

The Global Hydrology and Climate Center and NASA's Marshall Space Flight Center conducted a fact-finding case study for the Data Management Working Group (DMWG), now referred to as the Data and Information Working Group (DIWG), of the U.S. Global Change Research Program (USGCRP) to determine the feasibility of an interagency National Environmental Change Information System (NECIS). In order to better understand the data and information needs of policy and decision makers at the national, state, and local level, the DIWG asked the case study team to choose a regional water resources issue in the southeastern United States that had an impact on a diverse group of stakeholders. The southeastern USA was also of interest because the region experiences interannual climatic variations and impacts due to El Nino and La Nina. Jointly, with input from the DIWG, a focus on future water resources planning in the Apalachicola-Chattahoochee-Flint (ACF) River basins of Alabama, Georgia, and Florida was selected. A tristate compact and water allocation formula is currently being negotiated between the states and U.S. Army Corps of Engineers (COE) that will affect the availability of water among competing uses within the ACF River basin. All major reservoirs on the ACF are federally owned and operated by the U.S. Army COE. A similar two-state negotiation is ongoing that addresses the water allocations in the adjacent Alabama-Coosa-Tallapoosa (ACT) River basin, which extends from northwest Georgia to Mobile Bay. The ACF and ACT basins are the subject of a comprehensive river basin study involving many stakeholders. The key objectives of this case study were to identify specific data and information needs of key stakeholders in the ACF region, determine what capabilities are needed to provide the most practical response to these user requests, and to identify any limitations in the use of federal data and information. The NECIS case study followed the terms of reference developed by the interagency DIWG. The case study "lessons learned" and "key findings" offer guidelines and considerations

to the DMWG for the development and implementation of a NECIS that would support the data and information needs of policy and decision makers at the national, state, and local level.
Author
Information Systems; Climate Change; Data Management; River Basins; Water Resources; Resources Management; Case Histories

20020005104 Bechtel Nevada Corp., Las Vegas, NV USA
Aerial Radiological Survey of Abandoned Uranium Mines in the Navajo Nation
Hendricks, T. J.; Aug. 01, 2001; 31p; In English
Report No.(s): DE2001-785590; DOE/NV/11718-602; No Copyright; Avail: Department of Energy Information Bridge, Microfiche

Aerial radiological surveys of forty-one geographical areas in the Navajo Nation were conducted during the period of October 1994 through October 1999. The surveys were conducted at the request of the U.S. Environmental Protection Agency (EPA) Region 9 and were performed by personnel of the Remote Sensing Laboratory (RSL) located in Las Vegas, Nevada, a facility of the U.S. Department of Energy, National Nuclear Security Administration Nevada Operations Office. The aerial survey and subsequent processing characterized the overall radioactivity levels and excess bismuth 214 activity (indicator of uranium ore deposits and/or uranium mines) within the surveyed areas. A total of 772,000 aerial gamma spectra and associated position parameters were obtained and analyzed during the multi-year operation. The survey determined that only 15 square miles (39 square kilometers) of the 1,144 square miles (2,963 square kilometers) surveyed (approximately 1.3 %) had excess bismuth indications above the minimum reportable activity, thus reducing thearea requiring further investigation by a nominal factor of 76.Radiation contour data files, produced by RSL, were converted to Geographic Information System-compatible digital files and provided to EPA and EPA contractors for inclusion in numerous reports and graphics products.
NTIS
Uranium; Mineral Deposits; Remote Sensing; Radioactive Isotopes

20020005202 Pacific Northwest National Lab., Richland, WA USA
Chemical Emission Scenarios and Detection Limits for Active Infrared Remote Sensing
Blake, T. A.; Probasco, K. M.; Dec. 08, 2000; 225p; In English
Report No.(s): DE2001-769076; PNNL-13382; No Copyright; Avail: Department of Energy Information Bridge

This report presents results from the calculation of chemical emission rates from various military and human activities: diesel electric generator exhaust, diesel exhaust from a missile transport vehicle, evaporation of light organic compounds from stored diesel, evaporation of spilled SCUD missile fuel, burning ammunition, burning sarin, human breath, cook stove exhaust, septic system and landfill emissions. Also presented are the results of Gaussian puff dispersion calculations of the different chemical compounds in each of the plume scenarios. These calculations allow concentration-pathlengths for the compounds to be determined, and, using this information, estimates are made of the infrared absorption cross sections for the compounds. Calculated infrared absorbance spectra of the compounds are also presented along with the absorbance spectra of compounds found in the atmosphere that may interfere with detection of the target compounds.
NTIS
Remote Sensing; Contaminants; Infrared Radiation; Exhaust Emission; Exhaust Gases; Infrared Absorption; Infrared Detectors

44
ENERGY PRODUCTION AND CONVERSION

Includes specific energy conversion systems, e.g., fuel cells; and solar, geothermal, windpower, and waterwave conversion systems; energy storage; and traditional power generators. For technologies related to nuclear energy production see 73 Nuclear Physics. For related information see also 07 Aircraft Propulsion and Power; 20 Spacecraft Propulsion and Power, and 28 Propellants and Fuels.

20020000875 AWS Scientific, Inc., Albany, NY USA
NY/NJ Distributed Wind Power Field Verification Project
May 01, 2000; 5p; In English
Report No.(s): DE2001-764460; No Copyright; Avail: Department of Energy Information Bridge

During the 1st Quarter, AWS successfully executed an Agreement for Professional and Technical Services with Bob Bechtold, the host for the Webster, NY installation. The Agreement officially commits host organization cost sharing for the project, and describes the specific responsibilities of each party. AWS continues to work with the other host organizations to

develop similar Agreements and to prepare for the host site installations. Testing at the National Wind Technology Center (NWTC) continues to be monitored.
NTIS
Windpower Utilization; Energy Technology; New York; New Jersey

20020000912 Atomic Energy Commission, Idaho Operations Office, Idaho Falls, ID USA
Electrical Generating Capacities of Geothermal Slim Holes
Pritchett, J. W.; Oct. 01, 1998; 203p; In English
Report No.(s): DE2001-13786; DOE/ID/13455; No Copyright; Avail: Department of Energy Information Bridge, Microfiche

Theoretical calculations are presented to estimate the electrical generating capacity of the hot fluids discharged from individual geothermal wells using small wellhead generating equipment over a wide range of reservoir and operating conditions. The purpose is to appraise the possibility of employing slim holes (instead of conventional production-size wells) to power such generators for remote off-grid applications such as rural electrification in developing countries. Frequently, the generating capacity desired is less than one megawatt, and can be as low as 100 kilowatts; if slim holes can be usefully employed, overall project costs will be significantly reduced. This report presents the final results of the study. Both self-discharging wells and wells equipped with downhole pumps (either of the 'lineshaft' or the 'submersible' type) are examined. Several power plant designs are considered, including conventional single-flash backpressure and condensing steam turbines, binary plants, double-flash steam plants, and steam turbine/binary hybrid designs. Well inside diameters from 75 mm to 300 mm are considered; well depths vary from 300 to 1200 meters. Reservoir temperatures from 100 C to 240 C are examined, as are a variety of reservoir pressures and CO2 contents and well productivity index values.
NTIS
Thermal Energy; Geothermal Energy Extraction; Geothermal Energy Conversion; Geothermal Resources; Electric Generators

20020000923 Argonne National Lab., IL USA
Hydrogen-fueled polymer electrolyte fuel cell systems for transportation
Ahluwalia, R.; Doss, E. D.; Kumar, R.; Oct. 19, 1998; 42p; In English
Report No.(s): DE2001-11997; ANL-98/16; No Copyright; Avail: Department of Energy Information Bridge, Microfiche

The performance of a polymer electrolyte fuel cell (PEFC) system that is fueled directly by hydrogen has been evaluated for transportation vehicles. The performance was simulated using a systems analysis code and a vehicle analysis code. The results indicate that, at the design point for a 50-kW PEFC system, the system efficiency is above 50%. The efficiency improves at partial load and approaches 60% at 40% load, as the fuel cell operating point moves to lower current densities on the voltage-current characteristic curve. At much lower loads, the system efficiency drops because of the deterioration in the performance of the compressor, expander, and, eventually, the fuel cell. The results also indicate that the PEFC system can start rapidly from ambient temperatures. Depending on the specific weight of the fuel cell (1.6 kg/kW in this case), the system takes up to 180s to reach its design operating conditions. The PEFC system has been evaluated for three mid-size vehicles: the 1995 Chrysler Sedan, the near-term Ford AIV (Aluminum Intensive Vehicle) Sable, and the future P2000 vehicle. The results show that the PEFC system can meet the demands of the Federal Urban Driving Schedule and the Highway driving cycles, for both warm and cold start-up conditions. The results also indicate that the P2000 vehicle can meet the fuel economy goal of 80 miles per gallon of gasoline (equivalent).
NTIS
Electrolytic Cells; Fuel Cells; Hydrogen; Polymers; Urban Transportation

20020000932 Federal Energy Technology Center, Morgantown, WV USA
Biomass Reburning: Modeling/Engineering Studies
Zamansky, V. M.; Jan. 20, 1998; 15p; In English
Report No.(s): DE2001-2133; DE-FC26-97FT97270-01; No Copyright; Avail: Department of Energy Information Bridge, Microfiche

Reburning is a mature fuel staging NO(sub x) control technology which has been successfully demonstrated at full scale by Energy and Environmental Research Corporation (EER) and others on numerous occasions. Based on chemical kinetic modeling and experimental combustion studies, EER is currently developing novel concepts to improve the efficiency of the basic gas reburning process and to utilize various renewable and waste fuels for NO(sub x) control. This project is designed to develop engineering and modeling tools for a family of NO(sub x) control technologies utilizing biomass as a reburning fuel. Basic and advanced biomass reburning have the potential to achieve 60-90+% NO(sub x) control in coal fired boilers at a significantly lower cost than SCR (sector combustion rig). The scope of work includes modeling studies (kinetic, CFD (computational fluid

dynamics), and physical modeling), experimental evaluation of slagging and fouling associated with biomass reburning, and economic study of biomass handling requirements. Project participants include: EER, FETC (Federal Energy Technology Center) R (research) and D (development) group, Niagara Mohawk Power Corporation and Antares, Inc. Most of the combustion experiments on development of biomass reburning technologies are being conducted in the scope of coordinated SBIR (Small Business Innovative Research) program funded by USDA (USA Department of Agriculture). The first reporting period (October 1-December 31, 1997) included preparation of project management plan and organization of project kick-off meeting at DOE (Department of Energy) FETC. The quarterly report briefly describes the management plan and presents basic information about the kick-off meeting.
NTIS
Biomass; Nitrogen Oxides; Air Pollution

20020001023 Sandia National Labs., Albuquerque, NM USA
Vshot measurements of distal II dish concentrators
Jones, S. A.; Dec. 14, 1998; 8p; In English
Report No.(s): DE2001-2362; SAND98-2778C; No Copyright; Avail: Department of Energy Information Bridge, Microfiche

The Video Scanning Hartmann Optical Tester (VSHOT) is a laser ray-trace tool for measuring the slope error of solar concentrator mirrors. The VSHOT measurements made on two, 8.5-m diameter, Distal II dishes represent its first use on a concentrator installed and operating in the field. A number of valuable lessons were learned regarding the use of the VSHOT for outdoor testing. The two dishes were found to have overall figure-of-merit RMS (root mean square) slope errors from an ideal parabola of 2.99 and 3.18 milliradians. The VSHOT measurements compare well qualitatively with distant observer photographs made using a colored concentric ring target.
NTIS
Parabolic Reflectors; Optical Scanners

20020001024 Federal Energy Technology Center, Morgantown, WV USA
Biomass Reburning: Modeling/Engineering Studies
Maly, P. M.; Lissianski, V. V.; Zamansky, V. M.; Apr. 30, 1998; 36p; In English
Report No.(s): DE2001-2134; DE-FC26-97FT97270-02; No Copyright; Avail: Department of Energy Information Bridge, Microfiche

This project is designed to develop engineering and modeling tools for a family of NO(sub x) control technologies utilizing biomass as a reburning fuel. The second reporting period (January 1- March 31) included kinetic modeling of the reburning process while firing natural gas and biomass. Modeling was done with a kinetic mechanism that combined reactions relevant to reburning from GRI (Gas Research Institute)-Mech 2.11 with SNCR (selective non-catalytic reduction) reactions. Experimental data obtained in a 1 MMBtu/h Boiler Simulator Facility (BSF) for reburning with natural gas and biomass were modeled using the ODF (oriented distribution function) kinetic code. System was treated as a series of four one-dimensional reactors. Modeling of natural gas reburning qualitatively agrees with experimental data for a wide range of initial conditions. Modeling of furniture waste reburning does not qualitatively match experimental data due to a number of model simplifications. Future work will concentrate on improving the basic reburning model to give quantitative agreement with experiments and on search for better representation of biomass composition in kinetic modeling. Experimental data on biomass reburning are included in Appendix 3. These data were obtained during the reporting period in the scope of a coordinated program funded by the U.S. Department of Agriculture.
NTIS
Biomass; Chemical Reactions; Reaction Kinetics; Biomass Burning; Mathematical Models

20020001050 Lawrence Livermore National Lab., Livermore, CA USA
Microseismicity Survey of the El Hoyo-Monte Galan Geothermal Region in Nicaragua
Hutchings, L.; Kasamayer, P.; Smith, A. T.; Apr. 01, 1999; 9p; In English
Report No.(s): DE2001-8563; UCRL-ID-133825; No Copyright; Avail: Department of Energy Information Bridge, Microfiche

The project's objective is to use conceptual and mathematical models of geothermal fields as a basis for interpreting multiple datasets of geophysical data and for improving geothermal exploration techniques. The objective of this effort is to collect and interpret microseismicity data. The technical objectives are: plan and carry out a joint seismic deployment in Nicaragua, recording microseismicity activity at magnitude 1.5 or less; analyze microseismicity data to define possible fracture zones/geothermal

conduits; determine the velocity and possibly the attenuation structure in the El Hoyo-Monte Galan area; and work with the staff of the Trans-Pacific Geothermal Company to evaluate existing geological and geophysical data.
NTIS
Geophysics; Seismology

20020001055 Argonne National Lab., IL USA
Magnetic resonance imaging of polymer electrolytes and insertion electrodes
Gerald, R. E.; Klingler, R. J.; Rathke, J. W.; May 19, 1999; 6p; In English
Report No.(s): DE2001-11815; ANL/CMT/CP-99053; No Copyright; Avail: Department of Energy Information Bridge, Microfiche

This program seeks to better define electrode-electrolyte interfaces and solid-state ion transport mechanisms that are a central feature of fuel cells and advanced electrochemical systems. The goal is to develop a new generation of materials with enhanced energy efficiency and reduced tendency toward dendrite or passive film formation at the electrode-electrolyte interface.
NTIS
Electrolytes; Fuel Cells; Magnetic Resonance; Electrodes; Imaging Techniques; Electrochemistry

20020001071 Argonne National Lab., IL USA
GCtool for fuel cell systems design and analysis: user documentation
Ahluwalia, R. K.; Geyer, H. K.; Jan. 15, 1999; 128p; In English
Report No.(s): DE2001-12005; ANL-98/8; No Copyright; Avail: Department of Energy Information Bridge, Microfiche

GCtool is a comprehensive system design and analysis tool for fuel cell and other power systems. A user can analyze any configuration of component modules and flows under steady-state or dynamic conditions. Component models can be arbitrarily complex in modeling sophistication and new models can be added easily by the user. GCtool also treats arbitrary system constraints over part or all of the system, including the specification of nonlinear objective functions to be minimized subject to nonlinear, equality or inequality constraints. This document describes the essential features of the interpreted language and the window-based GCtool environment. The system components incorporated into GCtool include a gas flow mixer, splitier, heater, compressor, gas turbine, heat exchanger, pump, pipe, diffuser, nozzle, steam drum, feed water heater, combustor, chemical reactor, condenser, fuel cells (proton exchange membrane, solid oxide, phosphoric acid, and molten carbonate), shaft, generator, motor, and methanol steam reformer. Several examples of system analysis at various levels of complexity are presented. Also given are instructions for generating two- and three-dimensional plots of data and the details of interfacing new models to GCtool.
NTIS
Fuel Cells; Systems Engineering; Gas Turbines; Mathematical Models; Design Analysis

20020001077 National Renewable Energy Lab., Golden, CO USA
Predicting Ultimate Loads for Wind Turbine Design
Nov. 23, 1998; 12p; In English
Report No.(s): DE2001-12109; NREL/CP-500-25787; No Copyright; Avail: Department of Energy Information Bridge, Microfiche

This paper addresses the statistical uncertainty of loads prediction using structural dynamics simulation codes and the requirements for the number and duration of simulations for obtaining robust load estimates.
NTIS
Wind Turbines; Loads (Forces); Dynamic Structural Analysis

20020001081 Pacific Northwest National Lab., Richland, WA USA
Hanford Site National Environmental Policy Act (NEPA) Characterization
Rohay, A. C.; Fosmire, C. J.; Neitzel, D. A.; Hoitink, D. J.; Harvey, D. W.; Sep. 28, 1999; 203p; In English
Report No.(s): DE2001-12122; PNNL-6415-REV-11; EW3130040; No Copyright; Avail: Department of Energy Information Bridge, Microfiche

This document describes the US Department of Energy's (DOE) Hanford Site environment. It is updated each year and is intended to provide a consistent description of the Hanford Site environment for the many NEPA documents being prepared by DOE contractors. No conclusions or recommendations are provided. This year's report is the eleventh revision of the original document published in 1988 and is (until replaced by the 12th revision) the only version that is relevant for use in the preparation of Hanford NEPA; SEPA and CERCLA documents. The two chapters included in this document (Chapters 4 and 6) are numbered to correspond to the chapters where such information is presented in environmental impact statements (EISs) and other

Site-related NEPA or CERCLA documentation. Chapter 4.0 (Affected Environment) describes Hanford Site climate and meteorology, geology, hydrology, ecology, cultural, archaeological and historical resources, socioeconomic; occupational safety, and noise. Sources for extensive tabular data related to these topics are provided in the chapter. Most subjects are divided into a general description of the characteristics of the Hanford Site, followed by site-specific information, where available, of the 100,200,300, and other Areas. This division allows the reader to go directly to those sections of particular interest. When specific information on each of these separate areas is not complete or available, the general Hanford Site description should be used. Chapter 6.0 (Statutory and Regulatory Requirements) is essentially a definitive NEPA Chapter 6.0, which describes applicable federal and state laws and regulations, DOE directives and permits, and environmental standards directly applicable to the NEPA documents on the Hanford Site. People preparing environmental assessments and EISs should also be cognizant of the document entitled 'Recommendations for the Preparation of Environmental Assessments and Environmental Impact Statements' published by the DOE Office of NEPA Oversight. Pacific Northwest National Laboratory (PNNL) staff prepared individual sections of this document, with input from other Site contractors. More detailed data are available from reference sources cited or from the authors. The following sections of the document were reviewed by the authors and updated with the best available information through June 1999: Climate and Meteorology; Ecology; Cultural, Archaeological, and Historical Resources; Socioeconomics; and All of Chapter 6.

NTIS

Environment Management; Environmental Surveys; Cultural Resources

20020001085 Lawrence Livermore National Lab., Livermore, CA USA

Evaluation of insulated pressure vessels for cryogenic hydrogen storage

Aceves, S. M.; Garcia-Villazana, O.; Martinez-Frias, J.; Mar. 01, 1999; 33p; In English

Report No.(s): DE2001-12135; UCRL-JC-133755; EB4200000; No Copyright; Avail: Department of Energy Information Bridge, Microfiche

This paper presents an analytical and experimental evaluation of the applicability of insulated pressure vessels for hydrogen-fueled light-duty vehicles. Insulated pressure vessels are cryogenic-capable pressure vessels that can be fueled with liquid hydrogen (LH) or ambient-temperature compressed hydrogen (CH2). Insulated pressure vessels offer the advantages of liquid hydrogen tanks (low weight and volume), with reduced disadvantages (lower energy requirement for hydrogen liquefaction and reduced evaporative losses). The purpose of this work is to verify that commercially available aluminum-lined, fiber- wrapped vessels can be used for cryogenic hydrogen storage. The paper reports on previous and ongoing tests and analyses that have the purpose of improving the system design and assure its safety.

NTIS

Cryogenics; Pressure Vessels; Compressed Gas; Liquid Hydrogen

20020001086 National Renewable Energy Lab., Golden, CO USA

Photovoltaic Energy Program Contract Summary; Fiscal Year 1998

Surek, T.; Feb. 16, 1999; 227p; In English

Report No.(s): DE2001-12136; NREL/BK-520-25781; No Copyright; Avail: Department of Energy Information Bridge, Microfiche

This document provides individual summaries of some 200 photovoltaics research projects performed in house and by subcontractors to Department of Energy national laboratories and field offices, including the National Renewable Energy Laboratory, Sandia National Laboratories, Golden Field Office, Brookhaven National Laboratory, Albuquerque Field Office, and Boston Support Office. The document is divided into the following sections: research and development, technology development, and systems engineering and applications. Three indexes are included: performing organizations by name, performing organizations by state, and performing organizations by technology area.

NTIS

Photovoltaic Conversion; Renewable Energy; Systems Engineering

20020001173 Argonne National Lab., IL USA

Composite electrodes for lithium batteries

Hackney, S. A.; Johnson, C. S.; Kahaian, A. J.; Kepler, K. D.; Shao-Horn, Y.; Feb. 03, 1999; 21p; In English

Report No.(s): DE2001-12357; ANL/CMT/CP-98352; No Copyright; Avail: Department of Energy Information Bridge, Microfiche

The stability of composite positive and negative electrodes for rechargeable lithium batteries is discussed. Positive electrodes with spinel-type structures that are derived from orthorhombic-LiMnO2 and layered-MnO2 are significantly more stable than

standard spinel LiMn2O4 electrodes when cycled electrochemically over both the 4-V and 3-V plateaus in lithium cells. Transmission electron microscope data of cycled electrodes have indicated that a composite domain structure accounts for this greater electrochemical stability. The performance of composite Cu(sub x)Sn materials as alternative negative electrodes to amorphous SnO(sub x) electrodes for lithium-ion batteries is discussed in terms of the importance of the concentration of the electrochemically inactive copper component in the electrode.
NTIS
Electrodes; Lithium Batteries

20020001225 National Renewable Energy Lab., Golden, CO USA
Mongolia wind resource assessment project
Chadraa, B.; Elliott, D.; Natsagdorj, L.; Sep. 07, 1998; 8p; In English
Report No.(s): DE2001-1316; NREL/CP-500-25148; WF7C0201; No Copyright; Avail: Department of Energy Information Bridge, Microfiche

The development of detailed, regional wind-resource distributions and other pertinent wind resource characteristics (e.g., assessment maps and reliable estimates of seasonal, diurnal, and directional) is an important step in planning and accelerating the deployment of wind energy systems. This paper summarizes the approach and methods being used to conduct a wind energy resource assessment of Mongolia. The primary goals of this project are to develop a comprehensive wind energy resource atlas of Mongolia and to establish a wind measurement program in specific regions of Mongolia to identify prospective sites for wind energy projects and to help validate some of the wind resource estimates. The Mongolian wind resource atlas will include detailed, computerized wind power maps and other valuable wind resource characteristic information for the different regions of Mongolia.
NTIS
Mongolia; Windpower Utilization; Resources Management

20020001229 Argonne National Lab., IL USA
Greenhouse gases in the corn-to-fuel ethanol pathway
Wang, M. Q.; Jun. 18, 1998; 21p; In English
Report No.(s): DE2001-10855; ANL/ES/CP-96692; No Copyright; Avail: Department of Energy Information Bridge

Argonne National Laboratory (ANL) has applied its Greenhouse gas, Regulated Emissions and Energy in Transportation (GREET) full-fuel-cycle analysis model to examine greenhouse gas (GHG) emissions of corn-feedstock ethanol, given present and near-future production technology and practice. On the basis of updated information appropriate to corn farming and processing operations in the four principal corn- and ethanol-producing states (Illinois, Iowa, Minnesota, and Nebraska), the model was used to estimate energy requirements and GHG emissions of corn farming; the manufacture, transportation to farms, and field application of fertilizer and pesticide; transportation of harvested corn to ethanol plants; nitrous oxide emissions from cultivated cornfields; ethanol production in current average and future technology wet and dry mills; and operation of cars and light trucks using ethanol fuels. For all cases examined on the basis of mass emissions per travel mile, the corn-to-ethanol fuel cycle for Midwest-produced ethanol used in both E85 and E10 blends with gasoline outperforms conventional (current) and reformulated (future) gasoline with respect to energy use and GHG production. Also, GHG reductions (but not energy use) appear surprisingly sensitive to the value chosen for combined soil and leached N-fertilizer conversion to nitrous oxide. Co-product energy-use attribution remains the single key factor in estimating ethanol's relative benefits because this value can range from 0 to 50%, depending on the attribution method chosen.
NTIS
Greenhouse Effect; Ethyl Alcohol; Fuels; Biomass

20020001230 Argonne National Lab., IL USA
Studies of electrolyte penetration in carbon anodes by NMR techniques
Sandi, G.; Dec. 09, 1998; 10p; In English
Report No.(s): DE2001-10854; ANL/CHM/CP-96690; No Copyright; Avail: Department of Energy Information Bridge

A toroid cavity nuclear magnetic resonance (NMR) detector capable of recording radial concentration profiles, diffusion constants, and displacements of charge carriers was employed to investigate the lithium ion distribution in an electrochemical cell containing a carbonaceous material synthesized from pyrene and pillared clays as inorganic templates. A carbon rod was used in a control experiment to assign the Li(sup +) spectrum and to calibrate the one dimensional radial images.
NTIS
Electric Batteries; Anodes; Electrolytes; Nuclear Magnetic Resonance

20020001231 Argonne National Lab., IL USA

Carbons for lithium ion cells prepared using sepiolite as an inorganic template

Sandi, G.; Dec. 09, 1998; 11p; In English

Report No.(s): DE2001-10853; ANL/CHM/CP-96689; No Copyright; Avail: Department of Energy Information Bridge

Carbon anodes for Li ion cells have been prepared by the in situ polymerization of olefins such as propylene and ethylene in the channels of sepiolite clay mineral. Upon dissolution of the inorganic framework, a disordered carbon was obtained. The carbon was tested as anode in coin cells, yielding a reversible capacity of 633 mAh/g, 1.70 times higher than the capacity delivered by graphitic carbon, assuming 100% efficiency. The coulombic efficiency was higher than 90%.

NTIS

Electric Batteries; Carbon; Anodes; Clays

20020001281 National Renewable Energy Lab., Golden, CO USA

Workshop on Satellites for Solar Energy Assessments (2nd)

Renne, D.; Jun. 28, 1999; 297p; In English

Report No.(s): DE2001-12227; NREL/CP-560-26563; No Copyright; Avail: Department of Energy Information Bridge, Microfiche

A Collection of Presentations on new techniques for developing climatological estimates of the solar resource at all locations on earth at a resolution of 100 km, and of developing estimates at half-hour intervals at resolutions of 10 km or less in specific locations.

NTIS

Artificial Satellites; Solar Energy

20020001287 National Renewable Energy Lab., Golden, CO USA

Validation of a Photovoltaic Module Energy Ratings Procedure at NREL

Emery, K.; Kroposki, B.; Marion, B.; Myers, D.; Osterwald, C.; Aug. 11, 1999; 97p; In English

Report No.(s): DE2001-12187; NREL/TP-520-26909; No Copyright; Avail: Department of Energy Information Bridge, Microfiche

The procedure determines the energy production of a PV module for five reference days. The reference days represent possible operating environments and are qualitatively described as Hot Sunny, Cold Sunny, Hot Cloudy, Cold Cloudy, and Nice. Based on statistical weather criteria, these days were selected from the National Solar Radiation Database (NSRDB). Besides the hourly solar radiation and meteorological data from the NSRDB, the reference days include air mass, angle of incidence, plane of array, and spectral irradiance for a south-facing PV module at latitude tilt, battery-charging voltage, and parameters f1 and f2 for determining PV module temperature. Indoor I-V curve measurements over a range of temperatures and irradiances characterize the electrical performance of a PV module and are used to determine factors to correct for non-linear performance when irradiance and temperature vary. They also serve as a matrix of reference I-V curves for translating to reference-day conditions. The sensitivity of a PV module to variations in the spectral distribution of the incident radiation is accounted for by using an incident irradiance. Differences in PV module thermal characteristics are accounted for by using a PV module's installed nominal operating cell temperature (INOCT) for input to the Fuentes temperature model. The procedure does not consider radiation and transmittance losses at large incident angles. These losses were judged too small, and not sufficiently different, for various PV modules to justify the complexity of their measurement and inclusion in the procedure. PV performance measurements from NREL's Outdoor Test Facility during calendar-year 1998 were used to validate the procedure by comparing modeled and measured maximum power values for seven flat-plate PV modules representing different technologies. On an annual basis, modeled values compared within 5% of measured values. Taking into account reproducibility errors from ratings being performed by different facilities and the modeling errors, the following statement applies to the ability of this procedure to show relative differences in the energy production of two PV modules: "Because of errors in measurements and energy rating methodology, differences of 8% or less in the energy ratings of two PV modules are not significant. If one of the PV modules is amorphous silicon, differences of 13% or less in the energy ratings of two PV modules are not significant." This work was performed to develop and validate a PV module energy rating procedure for incorporation into IEEE PAR1479, "Recommended Practice for the Evaluation of Photovoltaic Module Energy Production."

NTIS

Photovoltaic Conversion; Solar Radiation; Meteorological Parameters; Weather

20020001293 National Renewable Energy Lab., Golden, CO USA

Photovoltaics for Buildings Cutting-Edge PV

Hayter, S. J.; Martin, R. L.; Nov. 05, 1998; 11p; In English

Report No.(s): DE2001-12167; NREL/CP-550-25764; No Copyright; Avail: Department of Energy Information Bridge, Microfiche

Photovoltaic (PV) technology development for building-integrated applications (commonly called PV for Buildings) is one of the fastest growing areas in the PV industry. Buildings represent a huge potential market for photovoltaics because they consume approximately two-thirds of the electricity consumed in the US. The PV and buildings industries are beginning to work together to address issues including building codes and standards, integration, after-market servicing, education, and building energy efficiency. One of the most notable programs to encourage development of new PV-for-buildings products is the PV:BONUS program, supported by the US Department of Energy. Demand for these products from building designers has escalated since the program was initiated in 1993. This paper presents a range of PV-for-buildings issues and products that are currently influencing today's PV and buildings markets.

NTIS

Buildings; Technology Assessment; Photovoltaic Conversion; Electricity

20020001297 Lawrence Livermore National Lab., Livermore, CA USA

Testing of solid-oxide fuel cells for micro to macro power generation

Graff, R. T.; Hayes, J. P.; Jankowski, A. F.; Morse, J. D.; May 01, 1999; 7p; In English

Report No.(s): DE2001-12149; UCRL-JC-134198; No Copyright; Avail: Department of Energy Information Bridge, Microfiche

Thin film, solid-oxide fuel cells (TFSOFCs) are developed using photolithographic patterning and physical vapor deposition. In this study, both electrode layers of nickel (Ni) and silver (Ag) as well as the solid-oxide electrolyte layer of yttria-stabilized zirconia (YSZ) are synthesized on the micrometer scale for thickness. The anode layer enables combination of the reactive gases, is conductive to pass the electric current, and provides mechanical support to the electrolyte and cathode layers. The morphology desired for both the anode and cathode layers facilitates generation of maximum current density from the fuel cell. For these purposes, the parameters of the deposition process and post- deposition patterning are optimized for continuous porosity across both electrode layers. The electrodes are characterized using scanning electron microscopy and the power output generated through current-voltage measurement. We find that a TFSOFC based on Ni-YSZ-Ag can be operate d with dilute fuel mixtures at temperatures below 300 C.

NTIS

Electrolytes; Photolithography; Solid Oxide Fuel Cells; Vapor Deposition; Solid State Physics; Microanalysis; Electrodes; Thin Films

20020001506 National Renewable Energy Lab., Golden, CO USA

Workshop on Basic Research Opportunities in Photovoltaics

Deb, S.; Benner, J.; McConnell, R.; Aug. 25, 1999; 108p; In English

Report No.(s): DE2001-12188; NREL/BK-590-26952; No Copyright; Avail: Department of Energy Information Bridge, Microfiche

The Basic Research Opportunities in Photovoltaics Workshop was held on May 3, 1999, in Seattle, Washington, in conjunction with the 195th Meeting of the Electrochemical Society. The workshop was structured into eight topics. Each topic area opened with a presentation in which the participants were asked to address the following: a brief introduction of the area of research; key research issues that were identified in an earlier workshop in 1992; what fundamental research has been done since then or is currently being done to address those issues; what are the research issues that are still relevant in light of advances made since the first workshop; identification of new fundamental research opportunities that will lead to important advances and innovations; and identification of significant commonalities and common research issues that have a cross-cutting impact, such as logically exist in silicon-based thin films, II-VI, and related materials. The topic areas discussed included amorphous and microcrystalline silicon, crystalline silicon, cadmium telluride, copper indium diselenide; III-V materials; novel materials and energy conversion approaches, semiconducting oxides, and characterization. After the meeting, participants in each working topic continued discussions by electronic means, completing journal articles that are to be published as a separate section in the ECS Proceedings of the "PV for the 21st Century" Symposium.

NTIS

Photovoltaic Conversion; Conferences

20020001539 Sandia National Labs., Albuquerque, NM USA

Electrical and Electrochemical Performance Characteristics of Small Commercial Li-Ion Cells

Ingersoll, D.; Nagasubramanian, G.; Roth, E. P.; Dec. 22, 1998; 8p; In English

Report No.(s): DE2001-2821; SAND98-2844C; No Copyright; Avail: Department of Energy Information Bridge, Microfiche

Advanced rechargeable lithium-ion batteries are presently being developed and commercialized worldwide for use in consumer electronics, military and space applications. At Sandia National Laboratories we have used different electrochemical techniques such as impedance and charge/discharge at ambient and subambient temperatures to probe the various electrochemical processes that are occurring in Li-ion cell. The purpose of this study is to identify the component that reduces the cell performance at subambient temperatures. Our impedance data suggest that while the variation in the electrolyte resistance between room temperature and -20 C is negligible the anode electrolyte interfacial resistance increases by an order of magnitude in the same temperature regime. We believe that the solid electrolyte interface (SEI) layer on the carbon anode may be responsible for the increase in cell impedance. We have also evaluated the cells in hybrid mode with capacitors. High-current operation in the hybrid mode allowed fill usage of the Li-ion cell capacity at 25 C and showed a factor of 5 improvement in delivered capacity at -20 C. NTIS

Lithium Batteries; Solid Electrolytes; Electrochemistry; Electrical Properties

20020001547 Sandia National Labs., Albuquerque, NM USA

New Mexico's Pioneering Steps in Commercializing Solar Power

Hill, R. R.; Apr. 09, 1999; 6p; In English

Report No.(s): DE2001-5695; SAND99-0891C; No Copyright; Avail: Department of Energy Information Bridge

Over the past two years, New Mexico has been engaged in a significant new approach to implement large purchases of solar power. This effort followed a regulatory process that treated solar power generation similar to conventional generation obtained by an investor-owned utility under the regulation of a public utility commission. In 1997, Public Service Company of New Mexico (PNM) gained approval to purchase power from a 100-MW combustion turbine facility that would be owned and operated by a wholesale generator. At the same time it issued the approval, and following discussions with the utility, the New Mexico Public Utility Commission (NMPUC) also required PNM to issue a request for proposal for a 5-MW central station solar facility, a major step for solar technologies in the state, in what would be the world's largest of its technology type. In cooperation with the staff of the NMPUC, PNM reviewed the proposals received, and Applied Power Corporation was selected for the photovoltaic portion of the proposed plan; retaining ownership of the plant, assuming the risks connected with the technology, and operating the plant in exchange for a power purchase agreement in a first-of-its-kind contract for photovoltaics. During the NMPUC hearings, various parties raised significant opposition to the cost-recovery mechanism that was proposed and voiced issues about the type of solar plant, its size, cost and the tiding approaches to building it. Because of these issues, alternative proposals were put forth that reduced the size and costs of the plant and had implied changes in ownership and risks. The order issued by the NMPUC on October 21, 1998, requires PNM to impose a charge of 0.5% on its retail electric customers' monthly bills to be used to acquire the solar facilities, but also to obtain other renewable electric power resources, both on a pay-as-you-go basis. This paper identifies the issues and their resolution that similar projects are expected to encounter. NTIS

New Mexico; Solar Energy; Commerce; Cost Reduction; Photovoltaic Conversion

20020001555 Los Alamos National Lab., NM USA

Catalysts for improved fuel processing

Borup, R. L.; Inbody, M. A.; Sep. 01, 2000; 8p; In English

Report No.(s): DE2001-763246; LA-UR-00-4458; No Copyright; Avail: Department of Energy Information Bridge

This report covers our technical progress on fuel processing catalyst characterization for the specific purpose of hydrogen production for proton-exchange-membrane (PEM) fuel cells. These development efforts support DOE activities in the development of compact, transient capable reformers for on-board hydrogen generation starting from candidate fuels. The long-term objective includes increased durability and lifetime, in addition to smaller volume, improved performance, and other specifications required meeting fuel processor goals. The technical barriers of compact fuel processor size, transient capability, and compact, efficient thermal management all are functions of catalyst performance. Significantly, work at LANL now tests large-scale fuel processors for performance and durability, as influenced by fuels and fuel constituents, and complements that testing with micro-scale catalyst evaluation which is accomplished under well controlled conditions. NTIS

Catalysts; Fuels; Fuel Cells; Manufacturing

20020001570 Argonne National Lab., IL USA

Altering the Equilibrium Condition in SR-Doped Lanthanum Manganite

Carter, J. D.; Krumpelt, M.; Vaughey, J.; Wang, X.; May 28, 1999; 11p; In English

Report No.(s): DE2001-11832; ANL/CMT/CP-99141; No Copyright; Avail: Department of Energy Information Bridge

The material of choice for a solid oxide fuel cell cathode based on a yttria-stabilized zirconia (YSZ) electrolyte is doped lanthanum manganite, (La,SR)MnO3. It excels at many of the attributes necessary for a system to work at the required operating temperature and is flexible enough to allow for materials optimization. Although strontium-doping increases the electronic conductivity of the material, the ionic conductivity of the material remains negligible under operating conditions. Studies have shown that the internal equilibrium of the material heavily favors oxidation of the manganese and rather than the loss of lattice oxygen as a charge compensation mechanism. This lack of oxygen vacancies in the structure retards the ability of the material to conduct oxygen ions; thus the optimized system requires a large number of engineered triple point boundary locations to work efficiently. We have successfully doped the host LSM lattice to alter the interred equilibrium of the material to increase its ionic conductivity and thus lower the cathodic overpotential of the system. Our presentation will discuss these new materials, the results of cell tests, and a number of characterization experiments performed.

NTIS

Cell Cathodes; Doped Crystals; Electrolytes; Solid Oxide Fuel Cells; Yttria-Stabilized Zirconia

20020001581 Argonne National Lab., IL USA

Greenhouse-gas emissions from biofuel use in Asia

Streets, D. G.; Waldhoff, S. T.; Jul. 06, 1999; 10p; In English

Report No.(s): DE2001-12428; ANL/DIS/CP-98264; No Copyright; Avail: Department of Energy Information Bridge, Microfiche

Biomass is a primary fuel for much of the world's population. In some developing countries it can contribute 80-90% of total primary energy consumption. In Asia as a whole we estimate that biomass contributes about 22 EJ, almost 24% of total energy use. Much of this biomass is combusted in inefficient domestic stoves and cookers, enhancing the formation of products of incomplete combustion (PIC), many of which are greenhouse gases. An inventory of the combustion of biofuels (fuelwood, crop residues, and dried animal waste) in Asia is used to develop estimates of the emissions of carbon-containing greenhouse gases (CO(sub 2),CO, CH(sub 4), and NMHC) in Asian countries. The data are examined from two perspectives: total carbon released and total global warming potential (GWP) of the gases. We estimate that blofuels contributed 573 Tg-C in 1990, about 28% of the total carbon emissions from energy use in Asia. China (259 Tg-C) and India (187 Tg-C) were the largest emitting countries by far. The majority of the emissions, 504 Tg-C, are in the form of CO(sub 2); however, emissions of non-CO(sub 2) greenhouse gases are significant: 57 Tg-C as CO, 6.4 Tg-C as CH(sub 4), and 5.9 Tg-C as NMHC. Because of the high rate of incomplete combustion in typical biofuel stoves and the high GWP coefficients of the products of incomplete combustion, biofuels comprise an even larger share of energy-related emissions when measured in terms of global warming potential (in CO(sub 2) equivalents): 38% over a 20-year time frame and 31% over 100 years. Even when the biofuel is assumed to be harvested on a completely sustainable basis (all CO(sub 2) emissions are reabsorbed in the following growing season), PIC emissions from biofuel combustion account for almost 5% of total carbon emissions and nearly 25% of CO(sub 2) equivalents in terms of short-term (20-year) GWP.

NTIS

Exhaust Emission; Exhaust Gases; Global Warming; Greenhouse Effect; Asia; Biomass Burning

20020001585 Argonne National Lab., IL USA

Overview of electrochemical power sources for electric and hybrid-electric vehicles

Dees, D. W.; Feb. 12, 1999; 5p; In English

Report No.(s): DE2001-12374; ANL/CMT/CP-98422; No Copyright; Avail: Department of Energy Information Bridge, Microfiche

Electric and hybrid-electric vehicles are being developed and commercialized around the world at a rate never before seen. These efforts are driven by the prospect of vehicles with lower emissions and higher fuel efficiencies. The widespread adaptation of such vehicles promises a cleaner environment and a reduction in the rate of accumulation of greenhouse gases, Critical to the success of this technology is the use of electrochemical power sources such as batteries and fuel cells, which can convert chemical energy to electrical energy more efficiently and quietly than internal combustion engines. This overview will concentrate on the work being conducted in the US to develop advanced propulsion systems for the electric and hybrid vehicles, This work is spearheaded by the US Advanced Battery Consortium (USABC) for electric vehicles and the Partnership for a New Generation of Vehicle (PNGV) for hybrid-electric vehicles, both of which can be read about on the world wide web (www.uscar.tom). As is

commonly known, electric vehicles rely strictly on batteries as their source of power. Hybrid-electric vehicles, however, have a dual source of power. An internal combustion engine or eventually a fuel cell supplies the vehicle with power at a relatively constant rate. A battery pack (much smaller than a typical electric-vehicle battery pack) provides the vehicle with its fast transient power requirements such as during acceleration. This hybrid arrangement maximizes vehicle fuel efficiency. Electric and hybrid-electric vehicles will also be able to convert the vehicle's change in momentum during braking into electrical energy and store it in its battery pack (instead of lose the energy as heat). This process, known as regenerative braking, will add to the vehicle's fuel efficiency in an urban environment.
NTIS
Fuel Cells; Electrochemical Cells; Electric Motor Vehicles; Electric Hybrid Vehicles

20020001661 Sandia National Labs., Albuquerque, NM USA
Solar Heat-Pipe Receiver Wick Modeling
Andraka, C. E.; Dec. 21, 1998; 10p; In English
Report No.(s): DE2001-2816; SAND98-2836; No Copyright; Avail: Department of Energy Information Bridge, Microfiche

Stirling-cycle engines have been identified as a promising technology for the conversion of concentrated solar energy into usable electrical power. In previous experimented work, we have demonstrated that a heat pipe receiver can significantly improve system performance-over a directly-illuminated heater head. The design and operating conditions of a heat pipe receiver differ significantly from typical laboratory heat pipes. New wick structures have been developed to exploit the characteristics of the solar generation system. Typically, these wick structures allow vapor generation within the wick. Conventional heat pipe models do not handle this enhancement yet it can more than double the performance of the wick. In this study, I develop a steady-state model of a boiling-enhanced wick for a solar heat pipe receiver. The model is used for design-point calculations and is written in FORTRAN90. Some limited comparisons have been made with actual test data.
NTIS
Stirling Engines; Heat Pipes; Solar Energy Conversion; Wicks

20020001829 Argonne National Lab., IL USA
Improved MCFC Performance with Li/Na/Ba/Ca Carbonate Electrolyte
Centeno, C. J.; Kaun, T. D.; Krumpelt, M.; Schoeler, A.; Jul. 21, 1999; 12p; In English
Report No.(s): DE2001-11830; ANL/CMT/CP-99123; No Copyright; Avail: Department of Energy Information Bridge

Earlier electrolyte segregation tests of Li/Na carbonate used chemical analysis such as inductively coupled plasma/atomic emission spectroscopy (ICP/AES) of matrix strips wetted with carbonate and exposed to 5- to 20-V potential gradients. A segregation factor was correlated to the Li/Na carbonate composition. While fairly substantial segregation occurs at the eutectic composition of 52% Li, it is minimal at 60% to 75% Li. Such lithium-rich Li/Na carbonates may not be practical because the melting points are too high (i.e., liquidus point is 625 C). by adding calcium and barium to the lithium/sodium carbonates, we were able to lower the melting point and maintain nonsegregating behavior. This work is directed at examining the long-term stability of the quaternary Li/Na/Ba/Ca electrolytes. Electrolyte optimization work evaluates Li/Na ratio and Ba/Ca level to improve cell performance at 320 mA/sq cm and reduce temperature sensitivity. A number of cells with quaternary Li/Na/Ba/Ca electrolytes ranging from 3 to 5% Ba/Ca have operated well with stable, long-term performance. Congruent melting carbonate is important for commercial development. The best so far is 3.5% Ba/Ca/Na/Li (3.5 mol%/3.5 mol% Ba/Ca) carbonate (m.p. 440 C). Performance at 160 mA/sq cm is increased up to 150 mV as compared with the baseline cell containing the Li/Na eutectic composition. Life stability has been reproduced by a number of bench-scale MCFC test with operations of 2000-4300 h and the electrolyte composition across the matrix little changed.
NTIS
Electrolytes; Lithium; Melting Points; Sodium Carbonates

20020001979 Argonne National Lab., IL USA
Surface water discharges from onshore stripper wells
Veil, J. A.; Jan. 16, 1998; 12p; In English
Report No.(s): DE2001-12034; ANL/EA/RP-95358; No Copyright; Avail: Department of Energy Information Bridge

Under current US Environmental Protection Agency (EPA) rules, small onshore oil producers are allowed to discharge produced water to surface waters with approval from state agencies; but small onshore gas producers, however, are prohibited from discharging produced water to surface waters. The purpose of this report is to identify those states that allow surface water discharges from small onshore oil operations and to summarize the types of permitting controls they use. It is intended that the

findings of this report will serve as a rationale to encourage the EPA to revise its rules and to remove the prohibition on surface water discharges from small gas operations.
NTIS
Oils; Wells; Surface Water

20020001988 California Univ., Lawrence Berkeley Lab., Berkeley, CA USA
Promises and problems with metallic interconnects for reduced temperature solid oxide fuel cells
Hou, P. Y.; Huang, K.; Bakker, W. T.; May 01, 1999; 12p; In English
Report No.(s): DE2001-764339; LBNL-43185; No Copyright; Avail: Department of Energy Information Bridge
The oxidation kinetics and electrical properties of oxide scales thermally grown on the surface of a commercial iron-based alloy have been investigated up to 1000 C. The effect of surface coating to improve performance was studied, and it was found that a double coating of Y and Ni oxide was most beneficial. While the Y oxide reduced the oxidation rate, the Ni oxide increased the Cr2O3 scale conductivity. Different electrodes were applied to the alloy or to pre-oxidized samples. Some of the electrodes, such as LaSRCoO3 (LSCo), reacted strongly with the alloy upon oxidation by increasing the oxidation rate and forming a mixed Fe/Co/Cr interlayer that impeded conduction. Application of these electrodes to a pre-oxidized surface eliminated these problems.
NTIS
Solid Oxide Fuel Cells; Iron Alloys; Electrical Properties; Chromium Oxides; Electrodes

20020002010 Sandia National Labs., Albuquerque, NM USA
Sandwich Construction Solar Structural Facets
Diver, R. B.; Grossman, J. W.; Dec. 22, 1998; 8p; In English
Report No.(s): DE2001-2822; SAND98-2845C; No Copyright; Avail: Department of Energy Information Bridge, Microfiche
Silver/glass mirrors have excellent optical properties but need a method of support in order to be used in concentrating solar thermal systems. In collaboration with the Cummins dish/Stirling development program, they started investigating sandwich construction as a way to integrate silver/glass mirrors into solar optical elements. In sandwich construction, membranes such as sheet metal or plastic are bonded to the front and back of a core (like a sandwich). For solar optical elements, a glass mirror is bonded to one of the membranes. This type of construction has the advantages of a high strength-to-weight ratio, and reasonable material and manufacturing cost. The inherent stiffness of sandwich construction mirror panels also facilitates large panels. This can have cost advantages for both the amount of hardware required as well as reduced installation and alignment costs. In addition, by incorporating the panels into the support structure reductions in the amount of structural support required are potentially possible.
NTIS
Sandwich Structures; Mirrors; Solar Energy Conversion

20020002016 Physical Optics Corp., Torrance, CA USA
Autonomous and Intelligent Neurofuzzy Decision Maker for Smart Drilling Systems, September 2, 1998-March 17, 1999
Final Report, 2 Sep. 1998 - 17 Mar. 1999
Kim, D. H.; Jun. 17, 1999; 37p; In English
Report No.(s): DE2001-765242; No Copyright; Avail: Department of Energy Information Bridge, Microfiche
Human error -- missing or misinterpreting data -- can have significant technical and cost impacts on the drilling and completion of an oil/gas well. Therefore, intelligent drilling control is needed to autonomously and intelligently analyze and interpret data from sensing and monitoring units, and to recommend action to the driller or drilling engineer. Such intelligent drilling control can lower overall drilling cost, reduce drilling time, and increase rate of success.
NTIS
Autonomy; Decision Making; Drilling; Fuzzy Systems; Artificial Intelligence

20020002253 Sandia National Labs., Albuquerque, NM USA
Novel InGaAsN pn Junction for High-Efficiency Multiple-Junction Solar Cells
Allerman, A. A.; Chang, P. C.; Gee, J. M.; Hammons, B. E.; Hou, H. Q.; Mar. 26, 1999; 5p; In English
Report No.(s): DE2001-5031; SAND99-0437C; No Copyright; Avail: Department of Energy Information Bridge, Microfiche
We report the application of a novel material, InGaAsN, with bandgap energy of 1.05 eV as a junction in an InGaP/GaAs/InGaAsN/Ge four-junction design. Results of the growth and structural, optical, and electrical properties were

demonstrated, showing the promising perspective of this material for ultra high efficiency solar cells. Photovoltaic properties of an as-grown pn diode structure and improvement through post growth annealing were also discussed.
NTIS
Electrical Properties; Gallium Phosphides; Optical Properties; Solar Cells

20020002254 Pacific Northwest National Lab., Richland, WA USA
Overview of Stationary Fuel Cell Technology
Brown, D. R.; Jones, R.; Mar. 23, 1999; 57p; In English
Report No.(s): DE2001-4717; PNNL-12147; No Copyright; Avail: Department of Energy Information Bridge, Microfiche

Technology developments occurring in the past few years have resulted in the initial commercialization of phosphoric acid (PA) fuel cells. Ongoing research and development (R and D) promises further improvement in PA fuel cell technology, as well as the development of proton exchange membrane (PEM), molten carbonate (MC), and solid oxide (SO) fuel cell technologies. In the long run, this collection of fuel cell options will be able to serve a wide range of electric power and cogeneration applications. A fuel cell converts the chemical energy of a fuel into electrical energy without the use of a thermal cycle or rotating equipment. In contrast, most electrical generating devices (e.g., steam and gas turbine cycles, reciprocating engines) first convert chemical energy into thermal energy and then mechanical energy before finally generating electricity. Like a battery, a fuel cell is an electrochemical device, but there are important differences. Batteries store chemical energy and convert it into electrical energy on demand, until the chemical energy has been depleted. Depleted secondary batteries may be recharged by applying an external power source, while depleted primary batteries must be replaced. Fuel cells, on the other hand, will operate continuously, as long as they are externally supplied with a fuel and an oxidant.
NTIS
Chemical Energy; Fuel Cells; Primary Batteries; Storage Batteries

20020002281 Federal Energy Technology Center, Morgantown, WV USA
Technical Progress Report for UTSI/CFFF MHD Program Completion and Related Activity for the Period April 1-June 30, 1998
Jul. 01, 1998; 15p; In English
Report No.(s): DE2001-8840; DE-AC22-95PC95231-16; No Copyright; Avail: Department of Energy Information Bridge, Microfiche

Routine preventive maintenance of the DOE Coal Fired Flow Facility (CFFF) is being performed. Modernization programs, funded under subcontract from Foster Wheeler Development Corporation by the DOE HIPPS Program, have been completed on the coal processing system, the data acquisition and control system and the control room. Environmental restoration actions continued with monitoring of groundwater wells and holding pond effluent. Progress is reported on the approved groundwater remediation plan. Actions are underway to dispose of spent seed/ash mixtures and excess coal remaining from the MHD POC program. The status of five (5) High Temperature Superconductor (HTS) projects is reported.
NTIS
Magnetohydrodynamics; Preventive Maintenance; Coal

20020002282 Federal Energy Technology Center, Morgantown, WV USA
Technical Progress Report for UTSI/CFFF MHD Program Completion and Related Activity for the Period October 1-December 31, 1998
Jan. 01, 1999; 22p; In English
Report No.(s): DE2001-8838; DE-AC22-95PC95231-18; No Copyright; Avail: Department of Energy Information Bridge, Microfiche

Maintenance of the DOE CFFF facility was suspended, due to a stop work order issued in September 1998. Property accounting actions were continued on a minimum basis with university funding. No work was done on the environmental management and environmental restoration for the facility. Continued progress is reported on the five (5) high temperature superconductivity projects under Task 6. A cooperative group has been formed to facilitate the development of chemical processes for the manufacture of HTS superconductor wire. The group includes EURUS Technologies, Incorporated, Sandia National Laboratory, Clemson University, University of Houston and the National Magnet Laboratory. The ac loss project continues laboratory work in an effort to determine the optimum configuration for multiple conductor cables to minimize the ac loss. The cost/performance analysis concentrated on addressing comments on the draft Topical Report on the life cycle cost analysis of coated conductor manufacture by electron beam and PLD. Work on diagnostics for real time process control reported includes

surface smoothness measurement by scatterometry, Raman scattering for real time determination of crystalline structure and oxygen content and atomic absorption measurements for control of stoichiometry in MOCVD deposition of YBCO.
NTIS
Magnetohydrodynamics; Life Cycle Costs; High Temperature Superconductors; Chemical Reactions

20020002786 Sandia National Labs., Albuquerque, NM USA
Review of Back Contact Silicon Solar Cells for Low-Cost Application
Smith, D. D.; Aug. 04, 1999; 11p; In English
Report No.(s): DE2001-9692; SAND99-2025C; No Copyright; Avail: Department of Energy Information Bridge, Microfiche

Back contact solar cells hold significant promise for increased performance in photovoltaics for the near future. Two major advantages which these cells possess are a lack of grid shading loss and coplanar interconnection. Front contacted cells can have up to 10% shading loss when using screen printed metal grids. A front contact cell must also use solder connections which run from the front of one cell to the back of the next for series interconnection. This procedure is more difficult to automate than the case of co-planar contacts. The back contact cell design is not a recent concept. The earliest silicon solar cell developed by Bell Labs was a back contact device. There have been many design modifications to the basic concept over the years. to name a few, there is the Interdigitated Back Contact (IBC) cell, the Stanford Point contact solar cell, the Emitter Wrap Through (EWT), and its many variations. A number of these design concepts have demonstrated high efficiency. The SunPower back contact solar cell holds the efficiency record for silicon concentrator cells. The challenge is to produce a high efficiency cell at low cost using high throughput techniques. This has yet to be achieved with a back contact cell design. The focus of this paper will be to review the relevant features of back contact cells and progress made toward the goal of a low cost version of this device.
NTIS
Solar Cells; Photovoltaic Conversion

20020002799 Donovan, Hamester and Rattien, Inc., Washington, DC USA
Materials research needs to improve the performance and durability of solar heating and cooling systems
Herzenberg, S.; Silberglitt, R.; LaPorta, C.; Mar. 11, 1981; 152p; In English
Report No.(s): DE2001-766273; No Copyright; Avail: Department of Energy Information Bridge, Microfiche

This report describes the results of aimed at identifying the major materials a detailed study research needs associated with improving the durability and efficiency of active and passive solar heating and cooling (SHAC).systems. It represents the first part of a larger study which will assess the extent and effectiveness with which these research needs are being pursued and recommend effective DOE solar materials R&D strategies. The methodology for this effort has been: (1) in-depth study of the field performance and durability problems encountered with existing SHAC systems; (2) specification of the most significant materials characteristics likely to effect potential solutions of these problems; and (3) a detailed comparison of the properties of commercially available and developmental materials with the specifications of step (2).
NTIS
Solar Heating; Solar Energy Conversion; Phase Change Materials; Heating Equipment; Air Conditioning Equipment

20020002801 Los Alamos National Lab., NM USA
Solar electric thermal hydronic (SETH) product development project
Stickney, B. L.; Sindelar, A.; Oct. 01, 2000; 13p; In English
Report No.(s): DE2001-766185; LA-SUB-00-80; No Copyright; Avail: Department of Energy Information Bridge, Microfiche

Positive Energy, Inc. received a second Technology Maturation and Commercialization Project Subcontract during the 1999 round of awards. This Subcontract is for the purpose of further aiding Positive Energy, Inc. in preparing its Solar Electric Thermal Hydronic (SETH) control and distribution package for market introduction. All items of this subcontracted project have been successfully completed. This Project Report contains a summary of the progress made during the SETH Development Project (the Project) over the duration of the 1999 Subcontract. It includes a description of the effort performed and the results obtained in the pursuit of intellectual property protection and development of product documentation for the end users. This report also summarizes additional efforts taken by and for the SETH project outside of the Subcontract. It presents a chronology of activities over the duration of the Subcontract, and includes a few selected sample copies of documents offered as evidence of their success.
NTIS
Solar Energy; Temperature Control; Product Development; Chronology

20020003354 National Renewable Energy Lab., Golden, CO USA

Energia Renovable para Centros de Salud Rurales (Renewable Energy for Rural Health Clinics)

Jimenez, T.; Olson, K.; Jul. 28, 1999; 52p; In English

Report No.(s): DE2001-757057; NREL/BK-500-26224; No Copyright; Avail: Department of Energy Information Bridge, Microfiche

Esta es la primera de una serie de guias de aplicaciones que el Programa de Energia de Villas de NREL esta comisionando para acoplar sistemas comerciales renovables con aplicaciones rurales, incluyendo agua, escuelas rurales y micro empresas. La guia esta complementada por las actividades de desarrollo del Programa de Energia de Villas de NREL, proyectos pilotos internacionales y programas de visitas profesionales.

NTIS

Energy Sources; Renewable Energy; Medical Services; Clinical Medicine

20020003389 Federal Energy Technology Center, Morgantown, WV USA

Molten carbonate fuel cell product design improvement

Jan. 01, 2000; 29p; In English

Report No.(s): DE2001-766690; DE-FC21-95MC31184-33; No Copyright; Avail: Department of Energy Information Bridge, Microfiche

The FCE PDI program is designed to advance the carbonate fuel cell technology from the current full-size field test to the commercial design. The specific objectives selected to attain the overall program goal are: Define power plant requirements and specifications; Establish the design for a multifuel, low-cost, modular, market-responsive power plant; Resolve power plant manufacturing issues and define the design for the commercial-scale manufacturing facility; Define the stack and balance-of-plant (BOP) equipment packaging arrangement, and module designs; Acquire capability to support developmental testing of stacks and critical BOP equipment to prepare for commercial design; and Resolve stack and BOP equipment technology issues, and design, build and field test a modular prototype power plant to demonstrate readiness for commercial entry.

NTIS

Carbonates; Fuel Cells; Manufacturing; Molten Carbonate Fuel Cells

20020003402 California Univ., Lawrence Berkeley Lab., Berkeley, CA USA

Wind Generation in the Future Competitive California Power Market

Sezgen, O.; Marnay, C.; Bretz, S.; Mar. 01, 1998; 76p; In English

Report No.(s): DE2001-6467; LBNL-41134; No Copyright; Avail: Department of Energy Information Bridge

The goal of this work is to develop improved methods for assessing the viability of wind generation in competitive electricity markets. The viability of a limited number of possible wind sites is assessed using a geographic information system (GIS) to determine the cost of development, and Elfin, an electric utility production costing and capacity expansion model, to estimate the possible revenues and profits of wind farms at the sites. This approach improves on a simple profitability calculation by using a site-specific development cost calculation and by taking the effect of time varying market prices on revenues into account. The first component of the work is to develop data characterizing wind resources suitable for use in production costing and capacity expansion models, such as Elfin, that are capable of simulating competitive electricity markets. An improved representation of California wind resources is built, using information collected by the California Energy Commission (CEC) in previous site evaluations, and by using a GIS approach to estimating development costs at 36 specific sites. These sites, which have been identified as favorable for wind development, are placed on Digital Elevation Maps (DEMs) and development costs are calculated based on distances to roads and transmission lines. GIS is also used to develop the potential capacity at each site by making use of the physical characteristics of the terrain, such as ridge lengths. In the second part of the effort, using a previously developed algorithm for simulating competitive entry to the California electricity market, the Elfin model is used to gauge the viability of wind farms at the 36 sites. The results of this exercise are forecasts of profitable development levels at each site and the effects of these developments on the electricity system as a whole. Under best guess assumptions, including prohibition of new nuclear and coal capacity, moderate increase in gas prices and some decline in renewable capital costs, about 7.35 GW of the 10 GW potential capacity at the 36 specific sites is profitably developed and 62 TWh of electricity produced per annum by the year 2030. Most of the development happens during the earlier years of the forecast. Sensitivity of these results to future gas price scenarios is also presented. This study also demonstrates that an analysis based on a simple levelized profitability calculation approach does not sufficiently capture the implications of time varying prices in a competitive market.

NTIS

Market Research; Windpower Utilization; California; Windpowered Generators

20020003416 California Univ., Lawrence Berkeley Lab., Berkeley, CA USA
Induction Accelerator Efficiency at 5 Hz
Molvik, A. W.; Faltens, A.; Oct. 05, 2000; 17p; In English
Report No.(s): DE2001-767594; LBNL-45683; HIFAN 1037; No Copyright; Avail: Department of Energy Information Bridge, Microfiche

We simulate fusion power plant driver efficiency by pulsing small induction cores at 5 Hz (a typical projected power plant repetition rate), with a resistive load in the secondary winding that is scaled to simulate the beam loading for induction acceleration. Starting from a power plant driver design that is based on other constraints, we obtain the core mass and acceleration efficiency for several energy ranges of the driver accelerator and for three magnetic alloys. The resistor in the secondary is chosen to give the same acceleration efficiency, the ratio of beam energy gain to energy input to the core module (core plus acceleration gap), as was computed for the driver. The pulser consists of a capacitor switched by FETs, Field Effect Transistors, which are gated on for the desired pulse duration. The energy to the resistor is evaluated during the portion of the pulse that is adequately flat. We present data over a range of 0.6 to 5 (mu)s pulse lengths. With 1 (mu)s pulses, the acceleration efficiency at 5 Hz is measured to be 75%, 52%, and 32% for thin-tape-wound cores of nanocrystalline, amorphous, and 3% silicon steel materials respectively, including only core losses. The efficiency increases for shorter pulse durations.
NTIS
Accelerators; Induction; Power Plants; Pulse Generators

20020004349 NASA Goddard Space Flight Center, Greenbelt, MD USA
Development of a 10 Ah, Prismatic, Lithium-Ion Cell for NASA/GSFC
Stein, Brian, Mine Safety Appliances Co., USA; Baker, John W., Mine Safety Appliances Co., USA; George, Douglas S., Mine Safety Appliances Co., USA; Isaacs, Nathan D., Mine Safety Appliances Co., USA; Shah, Pinakin M., Mine Safety Appliances Co., USA; Rao, Gopalakrishna M., NASA Goddard Space Flight Center, USA; [2001]; 20p; In English; Space Power Workshop, 2-5 Apr. 2001, Redondo Beach, CA, USA; Original contains color illustrations
Contract(s)/Grant(s): NAS5-97171; No Copyright; Avail: CASI; A03, Hardcopy; A01, Microfiche

MSA's 10 Ah Li-ion cell is a rugged design suitable for the stringent requirements of aerospace applications. Eighteen cells demonstrate consistent cycling performance over a wide range of rates and temperatures. The cell passes qualification requirements for vibration survivability technology improvements at MSA continue to enhance cell performance.
Derived from text
Lithium Batteries; Metal Ions; Qualifications; Design Analysis

20020005066 Federal Energy Technology Center, Morgantown, WV USA
Advanced gas turbine systems research ***Quarterly Report, 1 Jul. - 30 Sep. 1999***
Oct. 01, 1999; 22p; In English
Report No.(s): DE2001-769313; DE-FC21-92MC29061-18; No Copyright; Avail: Department of Energy Information Bridge, Microfiche

The activities of the AGTSR Program during this reporting period are described in this quarterly report. The report text is divided into discussions on Membership, Administration, Technology Transfer (Workshop/Education) and Research. Items worthy of note are highlighted below with additional detail following in the text of the report.
NTIS
Technology Transfer; Gas Turbines

20020005068 Federal Energy Technology Center, Morgantown, WV USA
Utility advanced turbine systems (ATS) technology readiness testing
Oct. 01, 1999; 95p; In English
Report No.(s): DE2001-769331; DE-FC21-95MC31176-24; No Copyright; Avail: Department of Energy Information Bridge, Microfiche

The overall objective of the Advanced Turbine System (ATS) Phase 3 Cooperative Agreement between GE and the U.S. Department of Energy (DOE) is the development of a highly efficient, environmentally superior, and cost-competitive utility ATS for base-load utility-scale power generation, the GE 7H (60 Hz) combined cycle power system, and related 9H (50 Hz) common technology. The major effort will be expended on detail design. Validation of critical components and technologies will be performed, including: hot gas path component testing, sub-scale compressor testing, steam purity test trials, and rotational heat transfer confirmation testing. Processes will be developed to support the manufacture of the first system, which was to have been sited and operated in Phase 4 but will now be sited and operated commercially by GE. This change has resulted from DOE's request

to GE for deletion of Phase 4 in favor of a restructured Phase 3 (as Phase 3R) to include full speed, no load (FSNL) testing of the 7H gas turbine. Technology enhancements that are not required for the first machine design but will be critical for future ATS advances in performance, reliability, and costs will be initiated. Long-term tests of materials to confirm design life predictions will continue. Information specifically related to 9H production is presented for continuity in H program reporting, but lies outside the ATS program. This report summarizes work accomplished from 4Q98 through 3Q99. The most significant accomplishments are listed.
NTIS
Turbines; Technology Assessment; Reliability

20020005076 Los Alamos National Lab., NM USA
Carbon Dioxide Extraction from Air: Is It An Option
Lackner, K.; Ziock, H. J.; Grimes, P.; Feb. 01, 1999; 15p; In English
Report No.(s): DE2001-770509; LA-UR-99-583; No Copyright; Avail: Department of Energy Information Bridge

Controlling the level of carbon dioxide in the atmosphere without limiting access to fossil energy resources is only possible if carbon dioxide is collected and disposed of away from the atmosphere. While it may be cost-advantageous to collect the carbon dioxide at concentrated sources without ever letting it enter the atmosphere, this approach is not available for the many diffuse sources of carbon dioxide. Similarly, for many older plants a retrofit to collect the carbon dioxide is either impossible or prohibitively expensive. For these cases we investigate the possibility of collecting the carbon dioxide directly from the atmosphere. We conclude that there are no fundamental obstacles to this approach and that it deserves further investigation. Carbon dioxide extraction directly from atmosphere would allow carbon management without the need for a completely changed infrastructure. In addition it eliminates the need for a complex carbon dioxide transportation infrastructure, thus at least in part offsetting the higher cost of the extraction from air.
NTIS
Carbon Dioxide; Extraction; Earth Atmosphere; Atmospheric Composition

20020005078 Atomic Energy Commission, Idaho Falls, ID USA
Field Operations Program Chevrolet S-10 (Lead-Acid) Accelerated Reliability Testing *Final Report*
Francfort, J.; Argueta, J.; Wehrey, M.; Karner, D.; Tyree, L.; Jul. 01, 1999; 51p; In English
Report No.(s): DE2001-771511; INEEL/EXT/99-00650; No Copyright; Avail: Department of Energy Information Bridge

This report summarizes the Accelerated Reliability testing of five lead-acid battery-equipped Chevrolet S-10 electric vehicles by the US Department of Energy's Field Operations Program and the Program's testing partners, Electric Transportation Applications (ETA) and Southern California Edison (SCE). ETA and SCE operated the S-10s with the goal of placing 25,000 miles on each vehicle within 1 year, providing an accelerated life-cycle analysis. The testing was performed according to established and published test procedures. The S-10s' average ranges were highest during summer months; changes in ambient temperature from night to day and from season-to-season impacted range by as much as 10 miles. Drivers also noted that excessive use of power during acceleration also had a dramatic effect on vehicle range. The spirited performance of the S-10s created a great temptation to inexperienced electric vehicle drivers to 'have a good time' and to fully utilize the S-10s acceleration capability. The price of injudicious use of power is greatly reduced range and a long-term reduction in battery life. The range using full-power accelerations followed by rapid deceleration in city driving has been 20 miles or less.
NTIS
Electric Motor Vehicles; Lead Acid Batteries; Reliability Analysis; Urban Transportation; Accelerated Life Tests

20020005080 Sandia National Labs., Albuquerque, NM USA
Diffraction Grating Structures in Solar Cells
Zaidi,; Gee,; Ruby,; Dec. 01, 2000; 6p; In English
Report No.(s): DE2001-771530; SAND2000-3057C; No Copyright; Avail: Department of Energy Information Bridge

Sub-wavelength periodic texturing (gratings) of crystalline-silicon (c-Si) surfaces for solar cell applications can be designed for maximizing optical absorption in thin c-Si films. We have investigated c-Si grating structures using rigorous modeling, hemispherical reflectance, and internal quantum efficiency measurements. Model calculations predict almost (approximately)100% energy coupling into obliquely propagating diffraction orders. by fabrication and optical characterization of a wide range of 1D and 2D c-Si grating structures, we have achieved broad-band, low ((approximately) 5%) reflectance without an anti-reflection film. by integrating grating structures into conventional solar cell designs, we have demonstrated short-circuit current density enhancements of 3.4 and 4.1 mA/cm(sup 2) for rectangular and triangular 1D grating structures compared to planar

controls. The effective path length enhancements due to these gratings were 2.2 and 1.7, respectively. Optimized 2D gratings are expected to have even better performance.
NTIS
Crystallinity; Diffraction; Gratings (Spectra); Solar Cells; Mathematical Models; Fabrication; Silicon

20020005087 Argonne National Lab., IL USA
Commuter simulation of lithium-ion battery performance in hybrid electric vehicles
Nelson, P. A.; Henriksen, G. L.; Amine, K.; Dec. 04, 2000; 14p; In English
Report No.(s): DE2001-772123; ANL/CMT/CP-103592; No Copyright; Avail: Department of Energy Information Bridge, Microfiche

In this study, a lithium-ion battery was designed for a hybrid electric vehicle, and the design was tested by a computer program that simulates driving of a vehicle on test cycles. The results showed that the performance goals that have been set for such batteries by the Partnership for a New Generation of Vehicles are appropriate. The study also indicated, however, that the heat generation rate in the battery is high, and that the compact lithium-ion battery would probably require cooling by a dielectric liquid for operation under conditions of vigorous vehicle driving.
NTIS
Electric Batteries; Electric Motor Vehicles

20020005171 Sandia National Labs., Albuquerque, NM USA
Instability of Polyvinylidene Fluoride-Based Polymeric Binder in Lithium-Ion Cells ***Final Report***
Garcia, M.; Nagasubramanian, G.; Tallant, D. R.; Roth, E. P.; May 01, 1999; 46p; In English
Report No.(s): DE2001-7020; SAND99-1164; No Copyright; Avail: Department of Energy Information Bridge

Thermal instabilities were identified in SONY-type lithium-ion cells and correlated with interactions of cell constituents and reaction products. Three temperature regions of interaction were identified and associated with the state of charge (degree of Li intercalation) of the cell. Anodes were shown to undergo exothermic reactions as low as 100 C involving the solid electrolyte interface (SEI) layer and the LiPF(6) salt in the electrolyte (EC-PC:DEC/IM LiPF(6)). These reactions could account for the thermal runaway observed in these cells beginning at 100 C. Exothermic reactions were also observed in the 200 degree C to 300 C region between the intercalated lithium anodes, the LiPF(6) salt, and the PVDF. These reactions were followed by a high-temperature reaction region, 300 to 400 C, also involving the PVDF binder and the intercalated lithium anodes. The solvent was not directly involved in these reactions but served as a moderator and transport medium. Cathode exothermic reactions with the PVDF binder were observed above 200 degree C and increased with the state of charge (decreasing Li content). The stability of the PVDF binder as a function of electrochemical cycling was studied using FTIR. The infrared spectra from the extracts of both electrodes indicate that PVDF is chemically modified by exposure to the lithium cell electrolyte (as well as electrochemical cycling) in conjunction with NMP extraction. Preconditioning of PVDF to dehydrohalogenation, which may be occurring by reaction with LiPf(6), makes the PVDF susceptible to attack by a range of nucleophiles.
NTIS
Solid Electrolytes; Vinylidene; Lithium; Metal Ions; Electrochemical Cells; Electrolytic Cells; Thermal Instability; Vinyl Polymers

20020005204 Sandia National Labs., Albuquerque, NM USA
Extreme Load Estimation for Wind Turbines: Issues and Opportunities for Improved Practice
Veers, P. S.; Butterfield, S.; Dec. 06, 2000; 12p; In English
Report No.(s): DE2001-769079; SAND2000-3035C; No Copyright; Avail: Department of Energy Information Bridge

Current design load estimation procedures for wind turbines often do not accurately treat the statistical nature of loads. Current practice for wind turbine load analysis is reviewed. The authors' opinions on the shortcomings of these practices are discussed. Experience gained from recent research on statistical load extrapolation methods is reviewed. Statistical modeling techniques are presented. Open questions on current techniques are summarized and critical issues that need to be resolved for an accurate statistical load extrapolation method are discussed.
NTIS
Mathematical Models; Statistical Analysis; Wind Turbines; Load Distribution (Forces)

20020005206 Technology Management, Inc., Cleveland, OH USA
Fuel Cell and Reversible Fuel Cell Modules for Grid-Independent Electric Power Systems
Ruhl, R. C.; Sep. 30, 2000; 28p; In English
Report No.(s): DE2001-769149; DOE/GO/10455; No Copyright; Avail: Department of Energy Information Bridge, Microfiche
Highly reliable, grid independent, electric power systems with average AC power outputs of 300 Watts and higher are often preferred for a variety of remote applications, including residences. Requirements for a selected example are given. Propane is the assumed primary fuel available.
NTIS
Fuel Cells; Electric Power Supplies; Alternating Current

20020005217 National Renewable Energy Lab., Golden, CO USA
Renewable Energy for Microenterprise
Allderdice, A.; Rogers, J. H.; Nov. 28, 2000; 80p; In English
Report No.(s): DE2001-771562; NREL/BK-500-26188; No Copyright; Avail: Department of Energy Information Bridge
This guide provides readers with a broad understanding of the potential benefits that current renewable energy technologies can offer rural microenterprises. It also introduces the institutional approaches that have been developed to make RE technologies accessible to microentrepreneurs and the challenges that these entrepreneurs have encountered.
NTIS
Energy Technology; Renewable Energy

20020005223 National Renewable Energy Lab., Golden, CO USA
Wind Power Plant Evaluation Naval Auxiliary Landing Field, San Clemente Island, California, *24 Sep. 1999 - 15 Dec. 2000*
Olsen, T. L.; Gulman, P. J.; McKenna, E.; Dec. 11, 2000; 105p; In English
Report No.(s): DE2001-772421; NREL/SR-500-27527; No Copyright; Avail: Department of Energy Information Bridge
The purpose of this report is to evaluate the wind power benefits and impacts to the San Clement Island (SCI) wind power system, including energy savings, emissions reduction, system stability, and decreased naval dependence on fossil fuel at the island. The primary goal of the SCI wind power system has been to operate with the existing diesel power plant and provide equivalent or better power quality and system reliability than the existing diesel system. The wind system is intended to reduce, as far as possible, the use of diesel fuel and the inherent generation of nitrogen oxide emissions and other pollutants.
NTIS
California; Diesel Fuels; Windpower Utilization; Electric Power Plants

20020005227 National Renewable Energy Lab., Golden, CO USA
Philippines Wind Energy Resource Atlas Development
Elliott, D.; Nov. 29, 2000; 12p; In English
Report No.(s): DE2001-772429; NREL/CP-500-28903; No Copyright; Avail: Department of Energy Information Bridge
This paper describes the creation of a comprehensive wind energy resource atlas for the Philippines. The atlas was created to facilitate the rapid identification of good wind resource areas and understanding of the salient wind characteristics. Detailed wind resource maps were generated for the entire country using an advanced wind mapping technique and innovative assessment methods recently developed at the National Renewable Energy Laboratory.
NTIS
Philippines; Windpower Utilization; Renewable Energy; Wind (Meteorology); Wind Measurement

20020005228 National Renewable Energy Lab., Golden, CO USA
Solar-Based Rural Electrification and Micro-Enterprise Development in Latin America: A Gender Analysis
Smith, J.; Nov. 16, 2000; 29p; In English
Report No.(s): DE2001-772433; NREL/SR-550-28995; No Copyright; Avail: Department of Energy Information Bridge
Worldwide, an estimated 1.5 to 2 billion people do not have access to electricity, including 100 million in the Latin America region. Depending on the country, 30 to 90% of this unelectrified Latin American population lives in rural areas where geographic remoteness and low energy consumption patterns may preclude the extension of the conventional electricity grid. Women are heavily impacted by the energy scarcity given their role as primary energy procurers and users for the household, agricultural and small industrial subsectors in developing countries. As a result, women spend disproportionately more time engaged in energy-related activities like carrying water and searching for cooking fuel. This paper describes the use of decentralized renewable energy systems as one approach to meet the energy needs of rural areas in Latin America. It outlines the advantages

of a decentralized energy paradigm to achieve international development goals, especially as they relate to women. The paper studies Enersol Associates, Inc.'s Solar-Based Rural Electrification model as an example of a decentralized energy program which has merged energy and development needs through the local involvement of energy entrepreneurs, non-governmental organizations and community members.
NTIS
Electricity; Energy Consumption; Solar Energy Conversion; Developing Nations; Electrification

20020005229 National Renewable Energy Lab., Golden, CO USA
Validation Testing of Procedures for Determining the Performance of Stand-Alone Photovoltaic Systems
McNutt, P.; Kroposki, B.; Hansen, R.; DeBlasio, R.; Lynn, K.; Nov. 27, 2000; 69p; In English
Report No.(s): DE2001-772434; NREL/TP-520-29185; No Copyright; Avail: Department of Energy Information Bridge

Standard test procedures have been developed to assess the performance of stand-alone PV (photovoltaic) systems tested outdoors under prevailing conditions. A copy of the procedures is included in Appendix E. This report presents an overview of the procedures and results from three validation tests conducted between January 1999 and September 2000 at one European and four US test sites. There was good measurement agreement between the results measured at different test sites on similar systems. to date, most PV system performance test procedures have looked at the performance of the individual components and have not addressed how the integrated system works as a whole. The performance test procedures described in this report verify that the system and load operate as expected, ensure that the PV array and system are capable of recharging the battery, determine the usable battery capacity (UBC), and determine if there is any significant change in the UBC measured three different times during the procedures. The procedures have been submitted to both IEEE (International Electric, Electronic and Electromechanical) SCC (Standards Coordinating Committee)21 and IEC (International Electrotechnical Commission) TC (Technical Committee) 82 for use in developing standards. The IEEE SCC21 has initiated P1526, 'Recommended Practice for Testing the Performance of Stand-Alone Photovoltaic Systems' and the IEC TC82 has initiated Standard 62124, 'Photovoltaic Stand-Alone Systems Design Qualification and Type Approval. The IEC document also addresses indoor testing.
NTIS
Electric Batteries; Photovoltaic Conversion; Standards

20020005805 Sandia National Labs., Albuquerque, NM USA
Solar-Powered Systems for Environmental Remediation
Miralles, C.; Jensen, B.; Flack, A.; Yelin, B.; Cromwell, J.; Apr. 01, 1999; 93p; In English
Report No.(s): DE2001-5902; SAND99-0936; No Copyright; Avail: Department of Energy Information Bridge, Microfiche

This study assesses the market and specific applications for solar-powered environmental remediation. to assist in the assessment, system specifications and a mathematical model of system performance and life-cycle cost were developed for the most promising markets and remediation technologies. An overview of existing remediation technologies, and an evaluation of the blower technology used to create the mathematical system model are provided. A review of the potential markets for environmental remediation showed that the single most promising target market is Department of Defense sites. Results indicate that solar-powered systems can compete most effectively with grid-connected systems for low-power applications in remote locations. However, the results indicated that for certain applications solar-powered systems could compete with grid-connected systems when grid extensions as short as 100 feet are required. These initial results are promising enough that field-testing of four types of solar-powered remediation systems is recommended. It is thought that successful field demonstrations would open additional markets in the private sector.
NTIS
Solar Energy; Mathematical Models; Performance Prediction

20020005830 Federal Energy Technology Center, Morgantown, WV USA
UTSI/CFFF MHD program completion and related activities
Muehlhauser, J. W.; Chapman, J. N.; Apr. 30, 1999; 42p; In English
Report No.(s): DE2001-775016; DE-AC22-95PC95231-22; No Copyright; Avail: Department of Energy Information Bridge, Microfiche

Maintenance work on the DOE (Department of Energy) CFFF (Coal Fired Flow Facility) facility remained in suspension for the entire quarter in accordance with the stop work order issued the previous quarter. Work resumed on the environmental restoration activities during the quarter and work performed is summarized. Progress continued on the five high temperature superconductivity projects under Task 6. On the sol-gel process, improvement is reported in application of buffer layers to single crystals. Problems are discussed in applying buffer layers to nickel substrates. The status of cost performance studies is

summarized. The status of diagnostic measurements directed toward real time control of manufacturing processes is reported with emphasis on measurement of surface smoothness. The results of atomic absorption measurement of MOCVD (metalorganic chemical vapor deposition) precursors are reported.
NTIS
Coal; Superconductivity; Sol-Gel Processes; Single Crystals

20020005841 Los Alamos National Lab., NM USA
Evaluation of a fast-response urban wind model: Comparison to single-building wind tunnel data
Pardyjak, E. R.; Brown, M. J.; Aug. 01, 2001; 7p; In English
Report No.(s): DE2001-784472; LA-UR-01-4028; No Copyright; Avail: Department of Energy Information Bridge

Prediction of the 3-dimensional flow field around buildings and other obstacles is important for a number of applications, including urban air quality studies, and tracking of plumes from accidental releases of toxic air contaminants, indoor/outdoor air pollution problems, and thermal comfort assessments. Various types of computational fluid dynamics (CFD) models have been used to determining the flow fields around buildings (e.g., Reisner et al., 1998; Eichhorn et al., 1988). Comparisons to measurements show that these models work reasonably well for the most part (e.g., Ehrhard et al., 2000; Johnson and Hunter, 1998; Murakami, 1997). However, CFD models are computationally intensive and for some applications turn-around time is of the essence. For example, planning and assessment studies in which hundreds of cases must be analyzed or emergency response scenarios in which plume transport must be computed quickly.
NTIS
Buildings; Flow Distribution; Three Dimensional Flow; Wind (Meteorology)

20020005873 West Virginia Univ., Dept. of Mechanical and Aerospace Engineering, Morgantown, WV USA
Free-Piston Diesel-Fueled Linear Alternator for Auxiliary Power Unit Applications ***Final Report, 15 Jul. 1996-14 Jul 2001***
Atkinson, Christopher; Famouri, Parviz; Clark, Nigel; Jan. 1999; 62p; In English
Contract(s)/Grant(s): DAAH04-96-1-0328
Report No.(s): AD-A395333; EMS-10-01; ARO-36200.3-RT-DPS; No Copyright; Avail: CASI; A04, Hardcopy; A01, Microfiche

Present day internal combustion engines have been proven to be a successful means of converting linear reciprocating motion into rotary motion through the use of a slider-crank mechanism. However, a substantial portion of the mechanical work produced is lost in internal friction due to the presence of moving parts, like the crankshaft. The use of a linear engine to eliminate the crankshaft and other rotating components would eliminate these sources of friction, and hence improve the overall efficiency of the engine. Further advantages of this engine configuration are those of reduced weight and cost, from the reduction of components required. Previous studies of free-piston engine designs have indicated that they would be useful where linear power delivery could be used, such as in fluid power delivery, or in electrical energy applications.
DTIC
Auxiliary Power Sources; Diesel Engines; Linear Alternators; Diesel Fuels; Free-Piston Engines

45
ENVIRONMENT POLLUTION

Includes atmospheric, water, soil, noise, and thermal pollution.

20020000750 Lawrence Livermore National Lab., Livermore, CA USA
Quantifying magnitudes and distributions of CO sources
Dignon, J.; Penner, J. E.; Walton, J. J.; Mar. 01, 1998; 12p; In English
Report No.(s): DE2001-2767; UCRL-JC-130375; No Copyright; Avail: Department of Energy Information Bridge, Microfiche

We use a simplified version of the GRANTOUR chemical tracer model to analyze emissions of CO from various sources. The GRANTOUR model has been simplified to include the eigenvalue chemistry solution method of Prather (1994). The analysis includes fossil fuel combustion, biomass burning, hydrocarbon oxidation, ocean, and terrestrial sources of CO. We also present a 1(degree) x 1(degree) emissions inventory of CO from fossil fuel combustion.
NTIS
Biomass Burning; Fossil Fuels; Hydrocarbons; Magnitude; Atmospheric Models; Carbon Monoxide

20020001034 NASA Goddard Space Flight Center, Greenbelt, MD USA

Baseline Maritime Aerosol: Methodology to Derive the Optical Thickness and Scattering Properties

Kaufman, Yoram J., NASA Goddard Space Flight Center, USA; Smirnov, Alexander, Science Systems and Applications, Inc., USA; Holben, Brent N., NASA Goddard Space Flight Center, USA; Dubovik, Oleg, Science Systems and Applications, Inc., USA; [2001]; 4p; In English; Original contains color illustrations; No Copyright; Avail: CASI; A01, Hardcopy; A01, Microfiche

Satellite Measurements of the global distribution of aerosol and their effect on climate should be viewed in respect to a baseline aerosol. In this concept, concentration of fine mode aerosol particles is elevated above the baseline by man-made activities (smoke or urban pollution), while coarse mode by natural processes (e.g. dust or sea-spray). Using 1-3 years of measurements in 10 stations of the Aerosol Robotic network (ACRONET we develop a methodology and derive the optical thickness and properties of this baseline aerosol for the Pacific and Atlantic Oceans. Defined as the median for periods of stable optical thickness (standard deviation is less than 0.02) during 2-6 days, the median baseline aerosol optical thickness over the Pacific Ocean is 0.052 at 500 am with Angstrom exponent of 0.77, and 0.071 and 1.1 respectively, over the Atlantic Ocean. Author

Aerosols; Smoke; Scattering; Optical Thickness; Dust; Climate

20020001082 Pacific Northwest National Lab., Richland, WA USA

Assessment of Unabated Facility Emission Potentials for Evaluating Airborne Radionuclide Monitoring Requirements at Pacific Northwest National Laboratory, 1999

Edwards, D. L.; Shields, K. D.; Sula, M. J.; Ballinger, M. Y.; Sep. 28, 1999; 37p; In English

Report No.(s): DE2001-12123; PNNL-10855-REV-1; No Copyright; Avail: Department of Energy Information Bridge, Microfiche

Assessments were performed to evaluate compliance with the airborne radionuclide emission monitoring requirements in the National Emission Standards for Hazardous Air Pollutants (NESHAP--US Code of Federal Regulations, Title 40 Part 61, Subpart H). In these assessments, potential unabated offsite doses were evaluated for emission locations at facilities owned by the US Department of Energy and operated by Pacific Northwest National Laboratory (Pacific Northwest) on the Hanford Site. Two of the facilities evaluated, 325 Building Radiochemical Processing Laboratory, and 331 Building Life Sciences Laboratory met state and federal criteria for continuous sampling of airborne radionuclide emissions. One other building, the 3720 Environmental Sciences Laboratory, was recognized as being in transition with the potential for meeting the continuous sampling criteria.

NTIS

Environmental Laboratories; Exhaust Emission; Pollution Control; Air Pollution

20020001212 Argonne National Lab., IL USA

Validating the role of AFVs in voluntary mobile source emission reduction programs

Santini, D. J.; Saricks, C. L.; Mar. 17, 1999; 16p; In English

Report No.(s): DE2001-12345; ANL/ES/CP-98620; No Copyright; Avail: Department of Energy Information Bridge, Microfiche

Late in 1997, EPA announced new allowances for voluntary emission control programs. As a result, the US Department of Energy's (DOE) Clean Cities and other metro areas that have made an ongoing commitment to increasing participation by alternative fuel vehicles (AFVs) in local fleets have the opportunity to estimate the magnitude and obtain emission reduction credit for following through on that commitment. Unexpectedly large reductions in key ozone precursor emissions in key locations and times of the day can be achieved per vehicle-mile by selecting specific light duty AFV offerings from original equipment manufacturers (OEMs) in lieu of their gasoline-fueled counterparts. Additional benefit accrues from the fact that evaporative emissions of non-methane hydrocarbons (generated in the case of CNG, LNG, and LPG by closed fuel-system AFV technology) can be essentially negligible. Upstream emissions from fuel storage and distribution with the airshed of interest are also reduced. This paper provides a justification and outlines a method for including AFVs in the mix of strategies to achieve local and regional improvements in ozone air quality, and for quantifying emission reduction credits. At the time of submission of this paper, the method was still under review by the US EPA Office of Mobile Sources, pending mutually satisfactory resolution of several of its key points. Some of these issues are discussed in the paper.

NTIS

Air Pollution; Pollution Control; Fuel Systems; Alternatives

20020001279 Department of Energy, Aiken, SC USA

Well Installation and Sampling Report for Monitoring Wells TCM6 TCM7, and TNX 28D - 40D and GeoSiphon Cell TGSC-2

Nichols, R. L.; Sep. 20, 1999; 43p; In English

Report No.(s): DE2001-12334; WSRC-TR-99-00226; No Copyright; Avail: Department of Energy Information Bridge, Microfiche

The shallow groundwater and sediments beneath the TNX Area are contaminated with both dissolved and residual chlorinated volatile organic compounds (CVOCs) such as trichloroethylene (TCE), carbon tetrachloride and perchloroethylene (PCE). The Savannah River Technology Center (SRTC) is studying a new technology for remediating CVOCs known as GeoSiphon.

NTIS

Wells; Water Pollution; Volatile Organic Compounds; Ground Water; Sampling

20020001360 NASA Wallops Flight Center, Wallops Island, VA USA

Vertical Distribution and Variability of Ozone During July 1999 Over Andenes, Norway

Schmidlin, F. J., NASA Wallops Flight Center, USA; Northam, E. T., NASA Wallops Flight Center, USA; Ross, E. D., NASA Wallops Flight Center, USA; [2001]; 1p; In English; European Geophysical Society Meeting, 23-31 Mar. 2001, Payerne, Switzerland; Sponsored by European Geophysical Society, Unknown; No Copyright; Avail: Issuing Activity; Abstract Only

Ozonesonde measurements of the polar atmosphere obtained at Andenes, Norway during July 1999 showed unusual characteristics when compared with mid- or low-latitude ozone profiles. A minimum of two ozonesondes each day were released, one in late afternoon and one in early evening. A very well-defined ledge in the ozone profile corresponding to the tropopause appears to form as a result of transport. The ozone amount increases four to five times, from about 30 nb at the tropopause to 120 nb at a pressure about 10-20 hPa lower. The typical peak ozone value, although at a higher altitude than the ledge, appears at a much lower pressure (approx. 140 hPa) than found in midor low-latitudes (approx. 18-25 hPa), Total column ozone amounts are consistently higher than 300 DU. Analysis of the variation with regard to wind conditions will be discussed.

Author

Ozone; Vertical Distribution; Wind (Meteorology); Meteorological Parameters; Tropical Regions; Variability

20020001449 Federal Energy Technology Center, Morgantown, WV USA

Investigation of Mixed Metal Sorbent/Catalysts for the Simultaneous Removal of Sulfur and Nitrogen Oxides

Akyurtlu, A.; Akyurtlu, J. F.; Mar. 31, 1999; 23p; In English

Report No.(s): DE2001-8818; DE-FG22-96PC96216-05; No Copyright; Avail: Department of Energy Information Bridge

Simultaneous removal of SO2 and NO(x) using a regenerable solid sorbent will constitute an important improvement over the use of separate processes for the removal of these two pollutants from stack gases and possibly eliminate several shortcomings of the individual SO2 and NO(x) removal operations. The work done at PETC and the Department of Energy-funded investigation of the investigators on the sulfation and regeneration of alumina-supported cerium oxide sorbents have shown that they can perform well at relatively high temperatures (823-900 K) as regenerable desulfurization sorbents. Survey of the recent literature shows that addition of copper oxide to ceria lowers the sulfation temperature of ceria down to 773 K, sulfated ceria-based sorbents can function as selective SCR catalysts even at elevated temperatures, SO2 can be directly reduced to sulfur by CO on CuO-ceria catalysts, and ceria-based catalysts may have a potential for selective catalytic reduction of NO(x) by methane. These observations indicate a possibility of developing a ceria-based sorbent/catalyst which can remove both SO2 and NO(x) from flue gases within a relatively wide temperature window, produce significant amounts of elemental sulfur during regeneration, and use methane for the selective catalytic reduction of NO(x). The objective of this research is to conduct kinetic and parametric studies of the selective catalytic reduction of NO(x) with NH3 and CH4 over alumina-supported cerium oxide and copper oxide-cerium oxide sorbent/catalysts; investigate SO2 removal at lower temperatures by supported copper oxide-cerium oxide sorbents; and investigate the possibility of elemental sulfur production during regeneration with CO or with CH4-air mixtures.

NTIS

Catalysts; Cerium Oxides; Sorbents; Sulfur Dioxides; Removal

20020001538 Lawrence Livermore National Lab., Livermore, CA USA

Radiological background levels found on glass fiber filters used for low-level environmental surveillance air sampling

Althouse, P. E.; Sep. 16, 1998; 10p; In English

Report No.(s): DE2001-2774; UCRL-JC-131844; No Copyright; Avail: Department of Energy Information Bridge, Microfiche

Environmental surveillance of low-level radioactive particles in air requires a thorough understanding of low-level techniques and air sample collection media. High-volume air sampling for radioactive particles around Lawrence Livermore National Laboratory (LLNL) employs glass-fiber filters that are analyzed for gross alpha and gross beta activity and for specific isotopes. This study was conducted to determine the activities of radionuclides contained in blank glass-fiber filters. Data from this study provided a partial explanation of differences between current reported concentrations of radionuclides in air and those reported historically when cellulose filters were used in the LLNL monitoring effort.
NTIS
Actinide Series Compounds; Glass Fibers; Air Sampling; Radioactive Contaminants

20020001557 Department of Energy, Carlsbad, NM USA
Cost analysis of NO(x) control alternatives for stationary gas turbines
Major, B.; Nov. 05, 1999; 48p; In English
Report No.(s): DE2001-761922; No Copyright; Avail: Department of Energy Information Bridge
The use of stationary gas turbines for power generation has been growing rapidly with continuing trends predicted well into the future. Factors that are contributing to this growth include advances in turbine technology, operating and siting flexibility and low capital cost. Restructuring of the electric utility industry will provide new opportunities for on-site generation. In a competitive market, it maybe more cost effective to install small distributed generation units (like gas turbines) within the grid rather than constructing large power plants in remote locations with extensive transmission and distribution systems. For the customer, on-site generation will provide added reliability and leverage over the cost of purchased power One of the key issues that is addressed in virtually every gas turbine application is emissions, particularly NO(x) emissions. Decades of research and development have significantly reduced the NO(x) levels emitted from gas turbines from uncontrolled levels. Emission control technologies are continuing to evolve with older technologies being gradually phased-out while new technologies are being developed and commercialized. The objective of this study is to determine and compare the cost of NO(x) control technologies for three size ranges of stationary gas turbines: 5 MW, 25 MW and 150 MW. The purpose of the comparison is to evaluate the cost effectiveness and impact of each control technology as a function of turbine size. The NO(x) control technologies evaluated in this study include: Lean premix combustion, also known as dry low NO(x) (DLN) combustion; Catalytic combustion; Water/steam injection; Selective catalytic reduction (SCR)--low temperature, conventional, high temperature; and SCONO(x)(TM).
NTIS
Cost Analysis; Combustion; Gas Turbines; Nitrogen Oxides

20020001573 Argonne National Lab., IL USA
Emissions and fuel economy of a vehicle with a spark-ignition, direct-injection engine: Mitsubishi Legnum GDI(trademark)
Cole, R. L.; Poola, R. B.; Sekar, R.; Apr. 08, 1999; 104p; In English
Report No.(s): DE2001-12050; ANL/ESD/TM-149; No Copyright; Avail: Department of Energy Information Bridge
A 1997 Mitsubishi Legnum station wagon with a 150-hp, 1.8-L, spark-ignition, direct-injection (SIDI) engine was tested for emissions by using the FTP-75, HWFET, SC03, and US06 test cycles and four different fuels. The purpose of the tests was to obtain fuel-economy and emissions data on SIDI vehicles and to compare the measurements obtained with those of a port-fuel-injection (PFI) vehicle. The PFI vehicle chosen for the comparison was a 1995 Dodge Neon, which meets the Partnership for a New Generation of Vehicles (PNGV) emissions goals of nonmethane hydrocarbons (NMHC) less than 0.125 g/mi, carbon monoxide (CO) less than 1.7 g/mi, nitrogen oxides (NO(sub x)) less than 0.2 g/mi, and particulate matter (PM) less than 0.01 g/mi. The Mitsubishi was manufactured for sale in Japan and was not certified to meet current US emissions regulations. Results show that the SIDI vehicle can provide up to 24% better fuel economy than the PFI vehicle does, with correspondingly lower greenhouse gas emissions. The SIDI vehicle as designed does not meet the PNGV goals for NMHC or NO(sub x) emissions, but it does meet the goal for CO emissions. Meeting the goal for PM emissions appears to be contingent upon using low-sulfur fuel and an oxidation catalyst. One reason for the difficulty in meeting the NMHC and NO(sub x) goals is the slow (200 s) warm-up of the catalyst. Catalyst warm-up time is primarily a matter of design. The SIDI engine produces more NMHC and NO(sub x) than the PFI engine does, which puts a greater burden on the catalyst to meet the emissions goals than is the case with the PFI engine. Oxidation of NMHC is aided by unconsumed oxygen in the exhaust when the SIDI engine operates in stratified-charge mode, but the same unconsumed oxygen inhibits chemical reduction of NO(sub x) . Thus, meeting the NO(sub x) emissions goal is likely to be the greatest challenge for the SIDI engine.
NTIS
Automobile Engines; Automobile Fuels; Combustion Efficiency; Exhaust Emission; Fuel Injection

20020001574 Argonne National Lab., IL USA

Membrane-based air composition control for light-duty diesel vehicles: A benefit and cost assessment

Poola, R.; Stork, K.; Nov. 09, 1998; 48p; In English

Report No.(s): DE2001-12047; ANL/ESD/TM-144; No Copyright; Avail: Department of Energy Information Bridge

This report presents the methodologies and results of a study conducted by Argonne National Laboratory (Argonne) to assess the benefits and costs of several membrane-based technologies. The technologies evaluated will be used in automotive emissions-control and performance-enhancement systems incorporated into light-duty diesel vehicle engines. Such engines are among the technologies that are being considered to power vehicles developed under the government-industry Partnership for a New Generation of Vehicles (PNGV). Emissions of nitrogen oxides (NO(sub x)) from diesel engines have long been considered a barrier to use of diesels in urban areas. Recently, particulate matter (PM) emissions have also become an area of increased concern because of new regulations regarding emissions of particulate matter measuring 2.5 micrometers or less (PM2.5). Particulates are of special concern for diesel engines in the PNGV program; the program has a research goal of 0.01 gram per mile (g/mi) of particulate matter emissions under the Federal Test Procedure (FTP) cycle. This extremely low level (one-fourth the level of the Tier II standard) could threaten the viability of using diesel engines as stand-alone powerplants or in hybrid-electric vehicles. The techniques analyzed in this study can reduce NO(sub x) and particulate emissions and even increase the power density of the diesel engines used in light-duty diesel vehicles. For nearly a decade, Argonne has been evaluating membrane-based methods to control the composition of air used in combustion. Membranes are the only practical method of modifying air composition for on-board use. The applicability of the technique depends strongly on both the technical and economic feasibility of implementing it on a vehicle. Over the past 10 years, significant technical advances have been made in the development of air-separation membranes. Researchers have developed and commercialized novel membrane materials that can efficiently separate air at the concentrations required for vehicle applications and have developed compact membrane modules that can be incorporated into vehicle design. Previous analysis by Argonne and others has demonstrated the effectiveness of oxygen enrichment at reducing PM, smoke, hydrocarbon (HC), and carbon monoxide (CO) emissions while increasing engine power output. Under appropriate oxygen-enriched operating conditions, diesel engines have achieved a net increase of 10-20% in power density and a decrease of 30-60% in PM emissions. Nitrogen-enriched air can be used as an alternative to exhaust gas recirculation to control NO(sub x) emissions and can also be used to generate a monatomic nitrogen plasma for exhaust post-treatment to reduce emissions of NO(sub x). Argonne has recently identified an operating regime that can simultaneously reduce NO(sub x) and PM while increasing power output when oxygen-enriched combustion air is used. This promising technique, which will be verified by additional experimental work at Argonne (using a range of engine sizes), will require the use of membranes similar to those analyzed in this study.

NTIS

Air Pollution; Pollution Control; Diesel Engines; Exhaust Emission

20020001577 Argonne National Lab., IL USA

Atmospheric Radiation Measurement Program Facilities Newsletter

Sisterson, D. L.; Jul. 30, 1999; 4p; In English

Report No.(s): DE2001-12042; ANL/ER/RP-99693; No Copyright; Avail: Department of Energy Information Bridge

Summer research efforts continue in July with the SGP99 Hydrology Campaign headed by the US Department of Agriculture, Agricultural Research Service. Other participants are the National Aeronautics and Space Administration (NASA), the National Oceanic and Atmospheric Administration, and the ARM Program. This campaign focuses on measuring soil moisture by using satellite-based instruments and takes place July 7-22, 1999. Soil moisture is an important component of Earth's hydrologic cycle and climate, but the understanding of it and the ability to measure it accurately are limited. Scientists need to understand soil moisture better so that it can be incorporated correctly into general circulation models. As an important factor in growing crops, soil moisture dictates a farmer's success or failure. Too much soil moisture can drown out croplands and cause flooding, whereas too little can lead to drought conditions, robbing crops of their life-supporting water. Decisions about which crops to plant and other land use issues depend on the understanding of soil moisture patterns. Soil moisture can be measured in various ways. ARM employs several direct methods using soil moisture probes buried from 1 inch to 6.5 feet below the surface. One type of probe has two stainless steel screens separated by a piece of fiberglass. Electrical resistance, which is a function of soil moisture content, is measured between the screens. Another type of probe measures soil temperature and the increase in temperature after the soil is heated by small heating element. From this measurement, the volume of water in the soil can be calculated.

NTIS

Soil Moisture; Hydrology; Moisture Content

20020001733 Office of Air Quality Planning and Standards, Research Triangle Park, NC USA

User's Manual for the RACT/BACT/LAER Clearinghouse (RBLC) Web: Volume 1 - Web Basics

Jun. 2001; 68p; In English; Original contains color illustrations

Report No.(s): PB2002-100302; EPA/456/B-01/001A; No Copyright; Avail: CASI; A04, Hardcopy; A01, Microfiche

This user's manual was prepared for and funded by the New Source Review RACT/BACT/LAER Clearinghouse (RBLC), U.S. Environmental Protection Agency (EPA). The RBLC has been established and is maintained by the Clean Air Technology Center (CATC) to assist State and local air pollution control personnel in making control technology determinations and in sharing technology information. The RBLC provides data on prevention and control technology determinations made primarily by State and local permitting agencies. The Clearinghouse contains over 4,000 determinations that can help the user to identify appropriate technologies to mitigate or treat most air pollutant emission streams. The RBLC was designed to help permit applicants and reviewers make pollution prevention and control technology decisions for stationary air pollution sources and includes data submitted by 50 states and territories in the U.S. on over 200 different air pollutants and 1,000 industrial processes. The Clearinghouse also has a rule data base that summarizes all emission standards issued by EPA's Office of Air Quality Planning and Standards (OAQPS). This includes New Source Performance Standards (NSPS), National Emission Standards for Hazardous Air Pollutants (NESHAP), and Maximum Achievable Control Technology (MACT) standards. The rule data base also includes prevention and control technology cost information related to each rule and references to supporting documentation.

NTIS

Pollution Control; Air Pollution; Air Quality; Contaminants; Environment Protection; Exhaust Emission

20020001766 Environmental Protection Agency, Cincinnati, OH USA

Effect of Water (Vapor-Phase and Carbon) on Elemental Mercury Removal in a Flow Reactor

Serre, S. D.; Gullett, B. K.; Li, Y. H.; Jan. 01, 2000; 18p; In English; Presented at AWMA Annual Conference, Orlando, FL., 6/24-28/01

Report No.(s): PB2002-100039; EPA/600/A-01/061; No Copyright; Avail: CASI; A03, Hardcopy; A01, Microfiche

The paper gives results of studying the effect of vapor-phase moisture on elemental mercury (Hgo) removal by activated carbon (AC) in a flow reactor. Tests involved injecting AC into both a dry and a 4% moisture nitrogen (N2)/Hgo gas stream. A bituminous-coal-based AC (Calgon WPL) was injected into an Hgo-laden gas stream (124 ppbv) at 150 C at carbon-to-mercury ratios (C:Hg) between 1300 and 4400 :l. Adding 4% (vol.) water (H2O) into the gas resulted in about a 10% drop in removal (21-80%), compared to tests in dry N2 (26-89%). The H2O molecules probably form hydrogen bonds with the AC, reducing the number of active sites available for Hgo. The effect of AC moisture content on Hgo removal was also studied. Darco FGD (lignit-based) AC was injected at 100 C and 86 ppbv Hgo.

NTIS

Mercury (Metal); Activated Carbon; Water Vapor; Vapor Phases

20020001768 ARCADIS Geraghty and Miller, Inc., Research Triangle Park, NC USA

Particulate Matter Measurements using Open-Path Fourier Transform Infrared Spectroscopy

Hashmonay, R. A.; Harris, D. B.; Jan. 01, 2001; 14p; In English

Report No.(s): PB2002-100037; No Copyright; Avail: CASI; A03, Hardcopy; A01, Microfiche

Open-path Fourier transform infrared (OP-FTIR) spectroscopy is an accepted technology for measuring gaseous air contaminants. OP-FTIR absorbance spectra acquired during changing aerosols conditions reveal related changes in very broad baseline features. Usually, this shearing of a spectrum's baseline is viewed as undesirable because it interferes with quantifying gases. However, the paper shows that this wavelength-dependent absorbance can be used to measure particulate matter (PM). It describes a developed inversion algorithm for retrieving the size distribution of the PM in the beam path. It gives preliminary results from OP-FTIR inversion algorithm and measured optical properties, the calculated extinction spectra were fitted to the measured extinction, using the Mile theory for spherical particles. Time series data reveal significant rapid shifts in size distribution of the PM in the OP-FTIR. Results indicate that size distribution parameters may be retrieved from OP-FTIR spectra acquired over an open optical path. The suggested method may provide real-time concentrations of gaseous and PM contaminants simultaneously. Emission flux estimate of PM may be generated for near-ground-level (roads) and area sources when several beam paths are deployed downwind.

NTIS

Air Pollution; Gases; Infrared Spectrometers; Aerosols; Particulates

20020001776 Winand Staring Centre, Wageningen, Netherlands
Calibration of the Model SMART2 in the Netherlands, using Data Available at the European Scale
Mol-Dijkstra, J. P.; Kros, J.; 1999; 50p; In English
Report No.(s): PB2001-108655; No Copyright; Avail: CASI; A03, Hardcopy; A01, Microfiche

This report describes the calibration of the soil acidification model SMART2 and the derivation of the calibration data in accordance of the EC-project 'Assessment of 'cumulative' uncertainty in Spatial Decision Support Systems' (UNCERDSS) (contract ENV4-CT95-0070). This EC-project was performed in order to quantify the cumulative uncertainty in Spatial Decision Support Systems due to model and data errors. The contribution of DLO Winand Staring Centre to this project was the application of the model SMART2 in order to predict the risk of contamination of groundwater through nitrates and aluminium linked to atmospheric deposition. In order to reduce the model error, SMART2 was calibrated, using data that were available at European scale. This study is performed in 1997 and 1998.

NTIS
Calibrating; Regression Analysis; Soils; Acidity

20020001783 Environmental Protection Agency, Air Pollution Prevention and Control Div., Research Triangle Park, NC USA
Mercury CEMs: Technology Update
Ryan, J. V.; Kilgroe, J. D.; Jan. 01, 2000; 10p; In English; Presented at Annual North American Conference (9th), Miami, FL. 5/6-9/01
Report No.(s): PB2001-108525; EPA/600/A-01/036; No Copyright; Avail: CASI; A02, Hardcopy; A01, Microfiche

Continuous emission monitors (CEMs) for mercury (Hg) are receiving increased attention and focus. Their potential use as a compliance assurance tool is of particular interest. While Hg CEMs are currently used in Europe for compliance purposes, use of Hg CEMs in the Untied States (U.S.) has focused on combustion research and Hg control technology evaluation applications. Hg CEMs are now receiving increased attention as compliance assurance tools. Several program exist to evaluate Hg CEM measurement performance. It is through these efforts that application-specific measurement issues are investigated. Collectively, these efforts have served to advance the state-of-the-art of the technology as evidenced by the number and types of CEMs now available and the various applications in use.

NTIS
Mercury (Metal); Air Pollution; Combustion Control

20020001859 Office of Air Quality Planning and Standards, Research Triangle Park, NC USA
Quality Management Plan for the PM Supersites Program
2001; 78p; In English
Report No.(s): PB2002-100301; EPA/454/R-01/011; No Copyright; Avail: CASI; A05, Hardcopy; A01, Microfiche

The document is a Quality Management Plan (QMP) for the environmental data operations of the PM Supersites Research Monitoring Program. The Office of Air Quality Planning and Standards (OAQPS) staff developed this QMP to outline the roles of organizations involved in the Supersites Particle Monitoring Program. This QMP was generated using the EPA Quality Assurance (QA) regulations and guidance as described in EPA QA/R-2, EPA Requirements for Quality Management Plans and the accompanying document, EPA QA/G-2, Guidance for Developing, Reviewing and Implementing Quality Management Plans. All pertinent elements of the QMP regulations and guidance are addressed in this document.

NTIS
Management Planning; Data Processing; Quality Control; Regulations; Air Quality

20020001862 Midwest Research Inst., Cary, NC USA
Low-Concentration NOx Emissions Measurement
Clapsaddle, C. A.; Trenholm, A. R.; Marshall, A. M.; Jan. 01, 2001; 16p; In English
Report No.(s): PB2002-100046; No Copyright; Avail: CASI; A03, Hardcopy; A01, Microfiche

The paper gives results of a recent series of low-concentration nitrogen oxides (NO-x) emission measurements, made by Midwest Research Institute (MRI) a NO-x control system called Xonon(trademark) Cool Combustion. (NOTE: Some in industry question the capability of certain existing EPA Reference Methods to accurately and precisely make low-concentration emission measurements, noting that the methods were not developed for such low-concentration applications). The Cool Combustion systems produced between 1 and 2 ppmv of NO-x emissions. Because the Cool Combustion system was installed on a gas turbine, EPA Method 20 was followed to measure the NO-x and oxygen (O2) concentrations in the turbine exhaust. The measurement range for the Thermo Environmental Instruments (TEI) Model 42H NO-x analyzer was 0 to 20 ppmv. All Method 20 quality control (QC) procedures were followed strictly. Test program results indicated that low-concentration NO-x emission

measurements can be made accurately. The paper details the test program and sampling system used to make the low-concentration NO-x emission measurements. Results of the QC checks and the mean and 95% confidence interval of the mean of 12 test runs are reported.
NTIS
Nitrogen Oxides; Measurement; Air Pollution; Concentration (Composition); Environment Models

20020001980 Argonne National Lab., IL USA
Ozone Risk Assessment Utilities (ORAMUS) user's manual and tutorial, Volume 2, Chronic Health Endpoints
Clemmons, M. A.; Jusko, M. J.; Whitfield, R. G.; Dec. 16, 1998; 57p; In English
Report No.(s): DE2001-12030; ANL/DIS/TM-44-Vol-2; No Copyright; Avail: Department of Energy Information Bridge, Microfiche

The primary purpose of this manual is to provide instructions on how to install and use the ORAMUS (Ozone Risk AssessMent UtilitieS) software. ORAMUS is a DOS-based software system that allows you to calculate and view risk estimates for health effects attributable to short- and long-term exposure to tropospheric ozone. The system combines exposure estimates with exposure-response relationships and then calculates and displays estimates of the overall risk in the form of probability distributions. ORAMUS allows you to select from three basic models: headcount risk, benchmark risk, and hospital admissions. It calculates a wide range of risk results for 27 air quality scenarios, 9 urban areas, 33 acute health endpoints, 4 chronic health endpoints, and 3 populations of interest. This manual is a tutorial designed to guide you through a series of steps that will familiarize you with the features of the system. The manual consists of two volumes. Volume 1 addresses acute health endpoints, and Volume 2 covers chronic health endpoints. Acute results were used during the National Ambient Air Quality Standards review process for ozone. Chronic results were not used.
NTIS
Ozone; User Manuals (Computer Programs); Computer Programs; Health; Air Pollution; Risk

20020001981 Argonne National Lab., IL USA
Ozone Risk Assessment Utilities (ORAMUS) user's manual and tutorial, Volume 1, Acute Health Endpoints
Clemmons, M. A.; Jusko, M. J.; Whitfield, R. G.; Dec. 16, 1998; 73p; In English
Report No.(s): DE2001-12029; ANL/DIS/TM-44-Vol-1; No Copyright; Avail: Department of Energy Information Bridge

The primary purpose of this manual is to provide instructions on how to install and use the ORAMUS (Ozone Risk AssessMent UtilitieS) software. ORAMUS is a DOS-based software system that allows you to calculate and view risk estimates for health effects attributable to short- and long-term exposure to tropospheric ozone. The system combines exposure estimates with exposure-response relationships and then calculates and displays estimates of the overall risk in the form of probability distributions. ORAMUS allows you to select from three basic models: headcount risk, benchmark risk, and hospital admissions. It calculates a wide range of risk results for 27 air quality scenarios, 9 urban areas, 33 acute health endpoints, 4 chronic health endpoints, and 3 populations of interest. This manual is a tutorial designed to guide you through a series of steps that will familiarize you with the features of the system. The manual consists of two volumes. Volume 1 addresses acute health endpoints, and Volume 2 covers chronic health endpoints. Acute results were used during the National Ambient Air Quality Standards review process for ozone. Chronic results were not used.
NTIS
Ozone; Computer Programs; Air Pollution; User Manuals (Computer Programs); Health

20020001991 Arkenol Holdings, Inc.,, Mission Viejo, CA USA
Creation of greenhouse gas benefits via biobased fuel and chemical production within the country of Guyana
Fatigati, M. A.; Sumait, N.; Carver, M.; Mar. 01, 1998; 74p; In English
Report No.(s): DE2001-764177; No Copyright; Avail: Department of Energy Information Bridge

The goal of this investigation is to complete feasibility studies necessary to advance the development of a biorefinery in the agricultural regions of Guyana located along its coastal strip which will reduce and sequester greenhouse gases through the production of cleaner burning fuels or chemicals from renewable materials. Completion of these pre-development activities has provided more specific information for use in calculating the baseline and greenhouse gas emissions reduced or sequestered by the biorefinery to supplement information submitted in Arkenol's proposal to USIJI on June 30, 1997. As stated above, the results of this study will be used to seek project financing for the detailed development and construction of the Guyana biorefinery project.
NTIS
Fuel Production; Greenhouse Effect; Exhaust Emission; Combustion

20020001992 Aerodyne Research, Inc., Billerica, MA USA

Heterogeneous chemistry affecting upper tropospheric and stratospheric ozone. Final report, April, 1994-January, 1998

Worsnop, D. R.; Jayne, J. T.; Kolb, C. E.; Davidovits, P.; Aug. 01, 1999; 56p; In English

Report No.(s): DE2001-763953; ARI 3834; No Copyright; Avail: Department of Energy Information Bridge

This collaborative research program between Aerodyne Research, Inc. and Boston College (AR.UBC) has studied the heterogeneous gas-liquid interactions related to ozone formation and destruction processes in the atmosphere. This involves laboratory determination of gas/liquid mass transport rates using bubble column and droplet apparatuses capable of measuring both fast and slow heterogeneous processes. The research plan was to study heterogeneous chemistry of nitrogen containing species, including ammonia, NH3, and so-called #NO# gas phase species (including NO, NO2, NO3, HNO2 and CH2O) on atmospherically relevant aqueous solutions (including sulfuric acid and nitrosyl sulfuric acid). The project comprised four tasks involving laboratory measurements of gadliquid kinetics: (1) Uptake of CH,O into aqueous solution utilizing the ARUBC bubbler apparatus. This included upgrading the bubbler to a horizontal flow design. This work was the fust direct measurement of acid and base catalyzed CH,O hydrolysis over the full range of pH (0 to 14) in aqueous solution. (2) Uptake of CH2O into concentrated sulfuric and nitric acid solution over the temperature range 245-275K. This work utilized the ARI/BC droplet apparatus modified for generation of acid solution. This work confirmed and quanttiled previous reports of enhanced CH2O uptake in acid solution. (3) Reaction of CH2O with HNO3 in concentrated sulfuric acid solution. This involved the design and construction of mixed liquid reaction vessel coupled to the mass spectrometric detection system for monitoring the evolution of product gases from solution. This work showed that the autocatalytic reaction of CH2O with HONO (in HNO3 mixtures) is acid catalyzed in H2SO4 solution. However, the rate is likely too slow to be atmospherically important. (4) Uptake of NH, into aqueous and sulfuric acid solution over the temperature range 245-290K. This work showed that the accommodation coefficient (alpha) of NH3 depends on relative humidity, with alpha = 1 on water increasing to cz=l for H2SO4 concentration is greater than 50wt%. Combined with re-analysis of previous aerosol neutralization studies, this work shows that NH~ uptake coefficients under atmospheric conditions will be less than unity and thus potentially rate-limiting for atmospheric aerosol nucleation and growth. The results (with the exception of Task 3) have been published (or submitted for publication) and thus will only be summarized here. The abstracts of the published manuscripts are attached as appendices. Appendix D contains the entire submitted manuscript describing in detail Task 4.

NTIS

Atmospheric Composition; Stratosphere; Troposphere; Ozone; Air Pollution; Climate Change; Atmospheric Chemistry; Aqueous Solutions; Ammonia

20020002220 NASA Goddard Space Flight Center, Greenbelt, MD USA

TOMS Tropical Tropospheric Ozone Data Sets at the University of Maryland Website

Kochhar, A. K., Maryland Univ., USA; Thompson, A. M., NASA Goddard Space Flight Center, USA; Hudson, R. D., Maryland Univ., USA; Frolov, A. D., Maryland Univ., USA; Witte, J. C., Science Systems and Applications, Inc., USA; [2001]; 1p; In English; AGU Spring Meeting, 29 May - 2 Jun. 2001, Boston, MA, USA; Sponsored by American Geophysical Union, USA; No Copyright; Avail: Issuing Activity; Abstract Only

Since 1997, shortly after the launch of the Earth-Probe TOMS (Total Ozone Mapping Spectrometer) satellite instrument, we have been processing data in near-real time to post maps of tropical tropospheric ozone at a website: metosrv2.umd.edu/-tropo. Daily, 3-day and 9-day averages of tropical tropospheric ozone column depth (TTO) are viewable from 10N to 10S. Data can be downloaded (running 9-day means) from 20N-30S. Pollution events are trackable along with dynamically-induced variations in tropospheric ozone column. TOMS smoke aerosol (toms.gsfc.nasa.gov) can be used to interpret biomass burning ozone, as for example, during the extreme ozone and smoke pollution period during the ENSO-related fires of August November 1997. During that time plumes of ozone and smoke were frequently decoupled and ozone from Indonesian fires and from Africa merged in one large feature by late October 1997. In addition to the Earth-Probe TOMS record, data as half-month averages and as daily 9-day means from the Nimbus 7 TOMS instrument are at the metosrv2.umd.edu/-tropo website. A guide to the website and examples of ozone time-series and maps will be shown.

Author

Ozone; Satellite Instruments; Total Ozone Mapping Spectrometer; Tropical Regions; Troposphere; Meteorological Parameters

20020002250 Pacific Northwest National Lab., Richland, WA USA

Airborne Effluent Monitoring System Certification for New Canister Storage Building Ventilation Exhaust Stack

Glissmeyer, J. A.; Maughan, A. D.; Apr. 01, 1999; 67p; In English

Report No.(s): DE2001-5086; PNNL-12166; No Copyright; Avail: Department of Energy Information Bridge, Microfiche

Pacific Northwest National Laboratory conducted three of the six tests needed to verify that the effluent monitoring system for the new Canister Storage Building ventilation exhaust stack meets applicable regulatory performance criteria for air sampling

systems at nuclear facilities. These performance criteria address both the suitability of the location for the air-sampling probe and the transport of the sample to the collection devices. The criteria covering the location for the air-sampling probe ensure that the contaminants in the stack are well mixed with the airflow at the probe location such that the extracted sample represents the whole. The sample-transport criteria ensure that the sampled contaminants are quantitatively delivered to the collection device. The specific performance criteria are described in detail in this report. The tests reported here cover the contaminant tracer uniformity and particle delivery performance criteria. These criteria were successfully met. The other three tests were conducted by the start-up staff of Duke Engineering and Services Hanford Inc. (DESH) and reported elsewhere. The Canister Storage Building is located in the 200 East Area of the US Department of Energy's Hanford Site near Richland, Washington. The new air-exhaust system was built under the W379 Project. The air sampling system features a probe with a single shrouded sampling nozzle, a sample delivery line, and a filter holder to collect the sample.
NTIS
Air Sampling; Contaminants; Exhaust Systems; Air Pollution; Monitors

20020002296 Duke Univ., Durham, NC USA
Science and technology reviews of FACE (Free Air Carbon Enrichment) ***Final Report***
Strain, B. R.; Mar. 23, 1998; 16p; In English
Report No.(s): DE2001-765305; No Copyright; Avail: Department of Energy Information Bridge

The purpose of this grant was to bring together the principals of all known facilities that had been developed, principals who had submitted proposals to develop FACE (free air carbon enrichment) facilities, and principals who want to develop proposals for facilities. In addition, critical program personnel from potential funding agencies and a few high level science administrators were invited to observe the proceedings and to visit a working FACE facility. The objectives of this study are to conduct a three-day international meeting on scientific aspects of research with the new and developing free air carbon enrichment (FACE) technology. Immediately following the science meeting, conduct a two-day international meeting on experimental protocols to be applied in FACE research. to conduct a four day international meeting on the assessment of the responses of forest ecosystems to elevated atmospheric carbon dioxide. The three meetings supported by this grant were all highly successful meetings and resulted in the formation of an organized and identified working group with the acronym InterFACE (International Free-Air Carbon Dioxide Enrichment) working group.
NTIS
Research Management; Carbon; Conferences

20020002304 Versar, Inc., Columbia, MD USA
Sediment Concentrations of Radionuclides Released by Calvert Cliffs Nuclear Power Plant. Volume 2: Appendices
Jan. 2001; 442p; In English
Report No.(s): PB2002-100244; No Copyright; Avail: CASI; A19, Hardcopy; A04, Microfiche

Operation of the Calvert Cliffs Nuclear Power Plant (CCNPP) generates gaseous and liquid radioactive wastes that are ultimately discharged to the atmosphere and Chesapeake Bay. While atmospheric releases are chiefly radioactive noble gases with little environmental significance, aqueous discharges to Chesapeake Bay contain radionuclides that can be accumulated by aquatic and estuarine biota or become associated with sediments. Sediments potentially serve as a sink for selected radionuclides. This accumulation in the sediments could increase the availability of these radionuclides. This accumulation in the sediments could increase the availability of these radionuclides to aquatic biota and through food chain transport to a radiation dose to man. Development of mass balance for individual radionuclides allows an estimation of their increased bioavailability. The Maryland Power Plant Research Program (PPRP) collects and analyzes various environmental samples in order to assess the radioecological impact of CCNPP. PPRP has conducted a quarterly sediment monitoring program to determine the actual level of impact within the ecosystem components since 1975. This report describes the development and application of a sediment inventory of radionuclides released by the CCNPP and accumulated in Chesapeake Bay sediments.
NTIS
Nuclear Power Plants; Sediments; Liquid Wastes

20020002321 Boston Coll., Chestnut Hill, MA USA
Measurement of heterogeneous chemical processes relevant to aerosol surfaces and trace gases active in the marine environment ***Final Report, 1 Aug. 1991 - 30 Jun. 1998***
Davidovits, P.; Worsnop, D. R.; Jayne, J. T.; Kolb, C. E.; Jul. 01, 1998; 10p; In English
Report No.(s): DE2001-765306; DOE/ER/61208; No Copyright; Avail: Department of Energy Information Bridge

Ocean produced reduced sulfur compounds including dimethylstilde (DMS), hydrogen sulfide (H2S) carbon disulfide (CS2), methyl memaptan (CH3CH) and carbonyl sulfide (OCS) deliver a sulfur burden to the atmosphere which is roughly equal to sulfur oxides produced by fossil fuel combustion. These species and their oxidation products dimethyl sulfoxide (DMSO), dimethyl sulfone (DMSOZ) and methane sulfonic acid (MSA) dominate aerosol and CCN production in clean marine air. Furthermore, oxidation of reduced sulfur species will be strongly influenced by NOx/O3 chemistry as well as halogen and ammonia chemistry in marine atmospheres. The multiphase chemical processes for these species must be understood in order to study the evolving role of combustion produced sulfur oxides over the oceans.
NTIS
Aerosols; Gases; Trace Elements; Sulfur Compounds; Chemical Reactions

20020002329 NASA Ames Research Center, Moffett Field, CA USA
Suitability of Gray Water for Hydroponic Crop Production Following Biological and Physical Chemical and Biological Subsystems
Bubenheim, David L., NASA Ames Research Center, USA; Harper, Lynn D., NASA Ames Research Center, USA; Wignarajah, Kanapathipillai, NASA Ames Research Center, USA; Greene, Catherine, NASA Ames Research Center, USA; [1994]; 1p; In English; 30th COSPAR Scientific Assembly, 11-21 Jul. 1994, Hamburg, Germany; Sponsored by Committee on Space Research, Unknown
Contract(s)/Grant(s): RTOP 199-61-12; No Copyright; Avail: Issuing Activity; Abstract Only

The water present in waste streams from a human habitat must be recycled in Controlled Ecological Life Support Systems (CELSS) to limit resupply needs and attain self-sufficiency. Plants play an important role in providing food, regenerating air, and producing purified water via transpiration. However, we have shown that the surfactants present in hygiene waste water have acute toxic effects on plant growth (Bubenheim et al. 1994; Greene et al., 1994). These phytotoxic affects can be mitigated by allowing the microbial population on the root surface to degrade the surfactant, however, a significant suppression (several days) in crop performance is experienced prior to reaching sub-toxic surfactant levels and plant recovery. An effective alternative is to stabilize the microbial population responsible for degradation of the surfactant on an aerobic bioreactor and process the waste water prior to utilization in the hydroponic solution (Wisniewski and Bubenheim, 1993). A sensitive bioassay indicates that the surfactant phytotoxicity is suppressed by more than 90% within 5 hours of introduction of the gray water to the bioreactor; processing for more than 12 hours degrades more than 99% of the phytotoxin. Vapor Compression Distillation (VCD) is a physical / chemical method for water purification which employees sequential distillation steps to separate water from solids and to volatilize contaminants. The solids from the waste water are concentrated in a brine and the pure product water (70 - 90% of the total waste water volume depending on operating conditions) retains non of the phytotoxic effects. Results of the bioassay were used to guide evaluations of the suitability of recovered gray water following biological and VCD processing for hydroponic lettuce production in controlled environments. Lettuce crops were grown for 28 days with 100% of the input water supplied with recovered water from the biological processor or VCD. When compared with the growth of plants in control hydroponic solution containing pure deionized water, no growth difference could be measured resulting from any of the recovered water treatments. Both biological treatment and VCD offer alternative technology approaches to recovering water from waste streams appropriate for input into a crop production system. A high level of crop performance (food, air, and water production) can be maintained with either processor; selection decisions can be based on other factors regarding system integration.
Author
Aerobes; Closed Ecological Systems; Farm Crops; Hydroponics; Waste Water; Crop Growth

20020002332 NASA Goddard Space Flight Center, Greenbelt, MD USA
Retrieval of Polar Stratospheric Cloud Microphysical Properties From Lidar Measurements: Dependence on Particle Shape Assumptions
Reichardt, Susanne, NASA Goddard Space Flight Center, USA; Reichardt, Jens, NASA Goddard Space Flight Center, USA; Yang, Ping, NASA Goddard Space Flight Center, USA; McGee, Thomas J., NASA Goddard Space Flight Center, USA; [2001]; 2p; In English; AGU Spring Meeting, 29 May - 2 Jun. 2001, Boston, MA, USA; Sponsored by American Geophysical Union, USA; No Copyright; Avail: Issuing Activity; Abstract Only

Knowledge of particle sizes and number densities of polar stratospheric clouds (PSCs) is highly important, because they are critical parameters for the modeling of the ozone chemistry of the stratosphere. In situ measurements of PSC particles are rare. the main instrument for the accumulation of PSC data are lidar systems. Therefore the derivation of some microphysical properties of PSCS from the optical parameters measured by lidars would be highly beneficial for ozone research. Inversion of lidar data obtained in the presence of PSCs formed from crystalline particles type 11 and the various nitric acid tri Ydrrate (NAT) types cannot be easily accomplished, because a suitable scattering theory for small faceted crystals has not been readily available tip

to now. As a consequence, the T-matrix method is commonly used for the interpretation of these PSC lidar data. Here the assumption is made that the optical properties of an ensemble of spheroids resemble those of crystalline PSCs, and microphysical properties of the PSC are inferred from the optical signatures of the PSC at two or more wavelengths. The problem with the T-matrix approach is that the assumption of spheroidal instead of faceted particles can lead to dramatically wrong results: Usually cloud particle properties are deduced from analysis of lidar profiles of backscatter ratio and depolarization ratio. The particle contribution to the backscatter ratio is given by the product of the particle number density and the backscattering cross section. The latter is proportional to the value of the particle's scattering phase function at 180 degrees scattering angle. At 180 degrees however, the phase functions of rough, faceted crystals and of spheroids with same maximum dimension differ by a factor of 6. From this it follows that for a PSC consisting of faceted crystals, the particle number density is underestimated by roughly the same factor if spheroidal particles are unrealistically assumed. We are currently developing a retrieval technique for determining the microphysical parameters of crystalline PSCs that takes into account the faceted shape of the PSC particles. This approach utilizes finite-difference time-domain (FDTD) calculations of particle optical properties. The accuracy and the free choice of the shape of the scattering particle make the FDTD technique a promising tool for the inversion of PSC lidar data. A first comparison of FDTD and T-matrix calculations will be presented.
Author
Cloud Physics; In Situ Measurement; Stratosphere; Optical Radar; Mathematical Models

20020002340 Versar, Inc., Columbia, MD USA
Sediment Concentrations of Radionuclides Released by Calvert Cliffs Nuclear Power Plant. Volume 1: Narrative Discussion
Jones, T. S.; McLean, R. I.; Jan. 2001; 60p; In English
Report No.(s): PB2002-100243; No Copyright; Avail: CASI; A04, Hardcopy; A01, Microfiche

Operation of the Calvert Cliffs Nuclear Power Plant (CCNPP) generates gaseous and liquid radioactive wastes that are ultimately discharged to the atmosphere and Chesapeake Bay. While atmospheric releases are chiefly radioactive noble gases with little environmental significance, aqueous discharges to Chesapeake Bay contain radionuclides that can be accumulated by aquatic and estuarine biota or become associated with sediments. Sediments potentially serve as a sink for selected radionuclides. This accumulation in the sediments could increase the availability of these radionuclides. This accumulation in the sediments could increase the availability of these radionuclides to aquatic biota and through food chain transport to a radiation dose to man. Development of mass balance for individual radionuclides allows an estimation of their increased bioavailability. The Maryland Power Plant Research Program (PPRP) collects and analyzes various environmental samples in order to assess the radioecological impact of CCNPP. PPRP has conducted a quarterly sediment monitoring program to determine the actual level of impact within the ecosystem components since 1975. This report describes the development and application of a sediment inventory of radionuclides released by the CCNPP and accumulated in Chesapeake Bay sediments.
NTIS
Nuclear Power Plants; Sediments; Mass Distribution; Liquid Wastes

20020002369 NASA Goddard Space Flight Center, Greenbelt, MD USA
Tropical Tropospheric Ozone and Smoke Interactions: Satellite Observations During the 1997 Indonesian Fires
Thompson, A. M., NASA Goddard Space Flight Center, USA; Witte, J. C., Science Systems and Applications, Inc., USA; Herman, J. R., NASA Goddard Space Flight Center, USA; Hudson, R. D., Maryland Univ., USA; Frolov, A. D., Maryland Univ., USA; Kochhar, A. K., Maryland Univ., USA; Fujiwara, M., Hokkaido Univ., Japan; [2001]; 1p; In English; AGU Spring Meeting, 29 May - 2 Jun. 2001, Boston, MA, USA; Sponsored by American Geophysical Union, USA; No Copyright; Avail: Issuing Activity; Abstract Only

Biomass burning generates hydrocarbons, nitrogen oxides and carbon monoxide that lead to tropospheric ozone pollution. Other combustion products form soot and various aerosol particles that make up smoke. Since early 1997 smoke and tropospheric ozone have been monitored in real-time from TOMS (Total Ozone Mapping Spectrometer) at toms.gsfc.nasa.gov (smoke aerosol) and metosrv2.umd.edu/-tropo (tropospheric ozone). The striking increase in smoke and tropospheric ozone observed during the 1997 Indonesian fires was the first extreme episode observed. During the August-November period, plumes of excess ozone and smoke coincided at times but were decoupled at other times, a phenomenon followed with trajectories. Thus, trans-boundary evolution of smoke and ozone differed greatly. The second discovery of the 1997 TOMS record was a dynamical interaction of ozone with the strong El Nino Southern Oscillation (ENSO) and Indian Ocean Dipole (IOD) that led to a jump in tropospheric ozone in March 1997 over the entire Indian Ocean, well ahead of the intense burning period. A climatology of smoke and

tropospheric ozone from a 1980's TOMS instrument shows offsets in the timing of these pollutants - further evidence that factors other than biomass burning exert a strong influence on tropical tropospheric ozone.
Author
Fires; Indian Ocean; Ozone; Satellite Observation; Smoke; Southern Oscillation; Tropical Regions; Climatology

20020002370 NASA Goddard Space Flight Center, Greenbelt, MD USA
Highlights from the 1998-2000 SHADOZ (Southern Hemisphere Additional Ozonesondes) Satellite Validation Project
Witte, J. C., Science Systems and Applications, Inc., USA; Thompson, A. M., NASA Goddard Space Flight Center, USA; Fortuin, P., Royal Netherlands Meteorological Inst., Netherlands; [2001]; 1p; In English; AGU Spring Meeting, 29 May - 2 Jun. 2001, Boston, MA, USA; Sponsored by American Geophysical Union, USA; No Copyright; Avail: Issuing Activity; Abstract Only

There are three years of data (more than 1000 individual ozone profiles) available from a network of 10 southern hemisphere tropical and subtropical stations, designated the Southern Hemisphere ADditional OZonesondes (SHADOZ) project. Since late 1999, a tropical station in the northern hemisphere (Paramaribo, Surinam; lat/long) joined SHADOZ, providing coordinated weekly ozone and radiosonde data from the surface to approx. 7 hPa for satellite validation, process studies, and model evaluation. Profiles are also collected at: Ascension Island; Nairobi, Kenya; Irene, South Africa; R (union Island; Watukosek, Java; Fiji; Tahiti; American Samoa; San Cristobal, Galapagos; Natal, Brazil. The archive, station characteristics and photos are available at http://code9l6.gsfc.nasa.gov/Data_ services/shadoz>. SHADOZ ozone time-series and profiles in 1998-2000 display highly variable tropospheric ozone, a zonal wave-one pattern in total (and tropospheric) column ozone, and signatures of the Quasi-Biennial Oscillation (QBO) in stratospheric ozone. Total, stratospheric and tropospheric column ozone amounts peak between August and November and are lowest between March and May. Integrated total ozone column amounts from the sondes are lower than independent measurements from a ground-based network and from the TOMS (Total Ozone Mapping Spectrometer) satellite (version 7 data).
Author
Ozone; Quasi-Biennial Oscillation; Southern Hemisphere; Total Ozone Mapping Spectrometer; Stratosphere; Radiosondes

20020002371 NASA Goddard Space Flight Center, Greenbelt, MD USA
Evidence of Stratosphere-to-Troposphere Transport Within a Mesoscale Model and TOMS Total Ozone
Olsen, Mark A., NASA Goddard Space Flight Center, USA; Stanford, John L., NASA Goddard Space Flight Center, USA; [2001]; 1p; In English; AGU Spring Meeting, 29 May - 2 Jun. 2001, Boston, MA, USA; Sponsored by American Geophysical Union, USA; No Copyright; Avail: Issuing Activity; Abstract Only

We present evidence for stratospheric mass transport into, and remaining in, the troposphere in an intense midlatitude cyclone. Mesoscale forecast model analysis fields from the Mesoscale Analysis and Prediction System (MAPS) were compared with total ozone observations from the Total Ozone Measurement Spectrometer (TOMS). Coupled with parcel back-trajectory calculations, the analyses suggest two mechanisms contributed to the mass exchange: (1) A region of dynamical ly-induced exchange occurred on the cyclone's southern edge. Parcels originally in the stratosphere crossed the jet core and experienced dilution by turbulent mixing with tropospheric air. (2) Diabatic effects reduced parcel potential vorticity (PV) for trajectories traversing precipitation regions, resulting in a "PV-hole" signature in the cyclone center. Air with lower-stratospheric values of ozone and water vapor was left in the troposphere. The strength of the latter process may be atypical. These results, combined with other research, suggest that precipitation-induced diabatic effects can significantly modify, (either decreasing or increasing) parcel potential vorticity, depending on parcel trajectory configuration with respect to jet core and maximum heating regions. In addition, these results underscore the importance of using not only PV but also chemical constituents for diagnoses of stratosphere-troposphere exchange (STE).
Author
Mesometeorology; Mesoscale Phenomena; Ozone; Weather Forecasting

20020002769 Argonne National Lab., IL USA
Air compliance through pollution prevention at Air Force Materiel Command facilities
Kolpa, R.; Ryckman, S. J.; Smith, A. E.; Mar. 19, 1999; 16p; In English
Report No.(s): DE2001-12416; ANL/EA/CP-98634; No Copyright; Avail: Department of Energy Information Bridge, Microfiche

Options for air compliance through pollution prevention (P2) have been identified at 14 facilities of the US Air Force Material Command, ranging from depots with significant light industrial activity to laboratories. Previous P2 efforts concentrated on reducing hazardous and solid wastes, with any reduction in air impacts generally being a collateral benefit. This work focused on reducing air emissions and air compliance vulnerabilities. P2 options were identified in three stages. First, potentially

applicable P2 options were identified from Internet and published information. Attention was given to identifying the types of sources to which an option could be applied, the option's state of development, and constraints that could limit its application. Traditional P2 options involving technology or equipment changes and material substitution were considered. In addition, newer approaches based on administrative 'controls' were considered. These included inserting P2 into operating permits in exchange for administrative relief, privatization, derating boilers, and reducing an installation's potential to emit and compliance vulnerability by separating sources not under the Air Force's 'common control.' Next, criteria and toxic emissions inventories by source category were prepared from inventory data supplied by facilities. The major problems at this stage were differences in the levels of detail provided by facilities and in the categories used by different installations. Emitting categories were matched to P2 option categories to identify candidate options. Candidates were screened to account for local regulations and technical information about sources in the inventories. When possible, emission reductions were estimated to help facility personnel prioritize options. Some options identified are being actively pursued by facilities to determine their site-specific feasibility. Although much work has been done to implement material substitution programs, this work indicates that different priorities and additional opportunities might result from using air emissions and compliance vulnerability as driving metrics.
NTIS
Air Pollution; Pollution Control; Regulations; Prevention

20020002771 Argonne National Lab., IL USA
Fuel and emission impacts of heavy hybrid vehicles
An, F.; Eberhardt, J. J.; Stodolsky, F.; Mar. 02, 1999; 12p; In English
Report No.(s): DE2001-12412; ANL/ES/CP-98502; No Copyright; Avail: Department of Energy Information Bridge, Microfiche

Hybrid powertrains for certain heavy vehicles may improve fuel economy and reduce emissions. of particular interest are commercial vehicles, typically in Classes 3-6, that travel in urban areas. Hybrid strategies and associated energy/emissions benefits for these classes of vehicles could be significantly different from those for passenger cars. A preliminary analysis has been conducted to investigate the energy and emissions performance of Class 3 and 6 medium-duty trucks and Class 6 school buses under eight different test cycles. Three elements are associated with this analysis: (1) establish baseline fuel consumption and emission scenario's from selected, representative baseline vehicles and driving schedules; (2) identify sources of energy inefficiency from baseline technology vehicles; and (3) assess maximum and practical potentials for energy savings and emissions reductions associated with heavy vehicle hybridization under real-world driving conditions. Our analysis excludes efficiency gains associated with such other measures as vehicle weight reduction and air resistance reduction, because such measures would also benefit conventional technology vehicles. Our research indicates that fuel economy and emission benefits of hybridization can be very sensitive to different test cycles. We conclude that, on the basis of present-day technology, the potential fuel economy gains average about 60-75% for Class 3 medium-duty trucks and 35% for Class 6 school buses. The fuel economy gains can be higher in the future, as hybrid technology continues to improve. The practical emissions reduction potentials associated with vehicle hybridization are significant as well.
NTIS
Trucks; Automobiles; Fuel Consumption; Electric Hybrid Vehicles; Energy Consumption

20020002773 Argonne National Lab., IL USA
Managing environmental information in the age of outsourcing
Perkins, S.; Smith, K.; Whorton, M.; Williams, G.; Mar. 08, 1999; 8p; In English
Report No.(s): DE2001-12410; ANL/EA/CP-98535; No Copyright; Avail: Department of Energy Information Bridge, Microfiche

As more data gathering, analysis, and tracking tasks are outsourced the need for multiple contractors and military personnel to input, update, access, store, and track information is becoming critical to efficient functioning and managing of environmental projects and programs at military installations. This paper presents two case studies detailing the way two organizations, the Rocky Mountain Arsenal (RMA) in Colorado, and the 611th Air Support Group (611 ASG) in Alaska, are managing complex data using web-based technology. RMA is involved in one of the largest environmental cleanup programs in the Department of Defense. As such, large volumes of environmental data and documents must be generated, stored, and tracked. Often these documents are prepared by multiple contractors and are reviewed by several parties or groups. to manage environmental information and to ensure that it meets compliance requirements more efficiently, RMA has developed an electronic document tracking and distribution system. This system allows access to up-to-date information, including a detailed review of all pertinent regulatory and other requirements at RMA. The dynamic system includes milestones, review deadlines, submission deadlines, and other requirements for managing the environmental program. The 611 ASG manages more than 30 remote installations in Alaska, many of which are operated by contractor personnel. These installations contain hundreds of buildings that are constantly being

modified because of exposure to harsh arctic climates; some of them have been determined to be eligible for the National Register of Historic Places. to meet regulatory requirements for cultural resources management as well as engineering requirements for upkeep of buildings, a database was developed to store and analyze building data. The database has a web-based interface that allows anyone with the correct access codes to input new data, modify existing data, or query the database using a number of standard reports. This system allows the 611 ASG to centrally manage its building information while also permitting installation contractors to update and use data through the Internet from their remote locations.
NTIS
Data Management; Organizations; Information Resources Management

20020002790 Argonne National Lab., IL USA
Visibility Assessment: Monte Carlo Characterization of Temporal Variability
Laulainen, N.; Shannon, J.; Trexler, E. C.; Dec. 12, 1997; 16p; In English
Report No.(s): DE2001-8913; ANL/ER/CP-95093; No Copyright; Avail: Department of Energy Information Bridge, Microfiche
Current techniques for assessing the benefits of certain anthropogenic emission reductions are largely influenced by limitations in emissions data and atmospheric modeling capability and by the highly variant nature of meteorology. These data and modeling limitations are likely to continue for the foreseeable future, during which time important strategic decisions need to be made. Statistical atmospheric quality data and apportionment techniques are used in Monte-Carlo models to offset serious shortfalls in emissions, entrainment, topography, statistical meteorology data and atmospheric modeling. This paper describes the evolution of Department of Energy (DOE) Monte-Carlo based assessment models and the development of statistical inputs. A companion paper describes techniques which are used to develop the apportionment factors used in the assessment models.
NTIS
Atmospheric Models; Monte Carlo Method; Variability

20020002841 Argonne National Lab., IL USA
Visibility Assessment: Coping with Incomplete Emissions and Modeling
Laulainen, N.; Shannon, J.; Trexler, E. C.; Dec. 12, 1997; 15p; In English
Report No.(s): DE2001-8914; ANL/ER/CP-95094; No Copyright; Avail: Department of Energy Information Bridge, Microfiche
The availability of complete emissions and entrainment data, topographic data and statistical meteorology data, and the modeling to account for all aerosol constituents presently found in our atmospheres, is not likely to improve substantially in the foreseeable future. This inability to model all of the transformation and transport processes which result in visibility-impairing aerosol species arriving at a point of interest, does not necessarily prevent our assessment of the benefits of reducing emissions from sources that can be modeled. We must, however, have an adequate statistical record of the concentrations of these materials and we must have a reliable means to apportion the concentration into controllable (i.e., those we can quantify and model) and uncontrollable fractions. Statistical concentration data, for remote scenic regions, are available for relevant aerosol species from the IMPROVE Network, for years beginning in 1988. A comparable network is unfortunately not available for urban areas. Here we describe the evolution of our source apportionment assumptions for two remote sites of much current interest, Grand Canyon and Shenandoah National Parks. Ingenuity and in some cases additional field investigations are necessary to improve such apportionment assumptions. to that end we briefly summarize promising approaches, such as receptor analysis and characterization of the particulate loading of on-shore flows, and current Department of Energy research relevant to the issue.
NTIS
Aerosols; Meteorology; Atmospheric Chemistry; Mathematical Models

20020003342 Atomic Energy Commission, Idaho Falls, ID USA
October 1999 Groundwater Sampling and Data Analysis, Distler Brickyard Site, Hardin County, Kentucky
Peterson, L. N.; Martin, J. P.; Taylor, C. J.; Mar. 01, 2000; 51p; In English
Report No.(s): DE2001-768868; INEEL/EXT-2000-00198-REV-0; No Copyright; Avail: Department of Energy Information Bridge, Microfiche
This report describes the results of a sampling event conducted at the Distler Brickyard Superfund Site, Hardin County, Kentucky, October 1999. The purpose of the sampling event was to evaluate the extent of natural biodegradation of chlorinated aliphatic hydrocarbons (CAH) occurring at the Site. Sampling locations were selected to evaluate three areas of the suspected CAH plume: the source area, an axial cross-section, and a downgradient transect. Due to inadequate recharge to and the poor physical condition of some monitoring wells at the Site, the sampling approach was modified to reflect wells that could be sampled. Results indicate that natural anaerobic degradation of chlorinated aliphatic hydrocarbons is occurring in the presumed source area around monitoring well GW-11. The primary contaminant of concern, trichloroethene, migrates downgradient from

the source area into the Coarse Grained Alluvium Aquifer at concentrations slightly greater than the Maximum Contaminant Level (MCL). Based on the available, the following hypothesis is proposed: the source area has been remediated through soil removal activities and subsequent anaerobic reductive dechlorination. If this is the case, this Site may be a good candidate for implementation of a monitored natural attenuation remedy. However, more data are necessary before this hypothesis can be confirmed.
NTIS
Kentucky; Biodegradation; Aliphatic Hydrocarbons; Data Processing; Contaminants; Chlorocarbons; Ground Water; Sampling

20020003346 NASA Goddard Space Flight Center, Greenbelt, MD USA
Results from Global Land-Surface Data Assimilation Methods
Radakovich, Jon D., General Sciences Corp., USA; Houser, Paul R., NASA Goddard Space Flight Center, USA; daSilva, Arlindo, NASA Goddard Space Flight Center, USA; Bosilovich, Michael G., NASA Goddard Space Flight Center, USA; [2001]; 1p; In English; Spring AGU 2001 Meeting, 29 May - 2 Jun. 2001, Boston, MA, USA; Sponsored by American Geophysical Union, USA Contract(s)/Grant(s): NAS5-00167; No Copyright; Avail: Issuing Activity; Abstract Only

Realistic representation of the land surface is crucial in global climate modeling (GCM). Recently, the Mosaic land-surface Model (LSM) has been driven off-line using GEOS DAS (Goddard Earth Observing System Data Assimilation System) atmospheric forcing, forming the Off-line Land-surface Global Assimilation (OLGA) system. This system provides a computationally efficient test bed for land surface data assimilation. Here, we validate the OLGA simulation of surface processes and the assimilation of ISCCP surface temperatures. Another component of this study as the incorporation of the Physical-space Statistical Analysis System (PSAS) into OLGA, in order to assimilate surface temperature observations from the International Satellite Cloud Climatology Project (ISCCP). to counteract the subsequent forcing of the analyzed skin temperature back to the initial state following the analysis. incremental bias correction (IBC) was included in the assimilation. The IBC scheme effectively removed the time mean bias, but did not remove him in the mean diurnal cycle. Therefore, a diurnal him correction (DBC) scheme was developed, where the time-dependent bias was modeled with a sine wave parameterization. In addition, quality control of the ISCCP data and anisotropic temperature correction were implemented in PSAS. Preliminary results showed a substantial impact from the inclusion of PSAS and DBC that was visible in the surface meteorology fields and energy budget. Also, the monthly mean diurnal cycle from the experiment closely matched the diurnal cycle from the observations.
Author
Earth Observing System (EOS); Land Surface Temperature; Climatology; Data Systems; ISCCP Project; Assimilation

20020003348 NASA Goddard Space Flight Center, Greenbelt, MD USA
Variations and Trends in Global and Regional Precipitation Based on the 22-Year GPCP (Global Precipitation Climatology Project) and Three-Year TRMM (Tropical Rainfall Measuring Mission) Data Sets
Adler, Robert F., NASA Goddard Space Flight Center, USA; Curtis, Scott, Maryland Univ. Baltimore County, USA; Huffman, George, Science Systems and Applications, Inc., USA; Bolvin, David, Science Systems and Applications, Inc., USA; Nelkin, Eric, Science Systems and Applications, Inc., USA; [2001]; 2p; In English; Spring AGU 2001 Meeting, 29 May - 2 Jun. 2001, Boston, MA, USA; Sponsored by American Geophysical Union, USA; No Copyright; Avail: Issuing Activity; Abstract Only

This paper gives an overview of the analysis of global precipitation over the last few decades and the impact of the new TRMM precipitation observations. The 20+ year, monthly, globally complete precipitation analysis of the World Climate Research Program's (WCRP/GEWEX) Global Precipitation Climatology Project (GPCP) is used to study global and regional variations and trends and is compared to the much shorter TRMM(Tropical Rainfall Measuring Mission) tropical data set. The GPCP data set shows no significant trend in global precipitation over the twenty years, unlike the positive trend in global surface temperatures over the past century. The global trend analysis must be interpreted carefully, however, because the inhomogeneity of the data set makes detecting a small signal very difficult, especially over this relatively short period. The relation of global (and tropical) total precipitation and ENSO events is quantified with no significant signal when land and ocean are combined. Identifying regional trends in precipitation may be more practical. From 1979 to 2000 the tropics have pattern of regional rainfall trends that has an ENSO-like pattern with features of both the El Nino and La Nina. This feature is related to a possible trend in the frequency of ENSO events (either El Nino or La Nina) over the past 20 years. Monthly anomalies of precipitation are related to ENSO variations with clear signals extending into middle and high latitudes of both hemispheres. The El Nino and La Nina mean anomalies are near mirror images of each other and when combined produce an ENSO signal with significant spatial continuity over large distances. A number of the features are shown to extend into high latitudes. Positive anomalies extend in the Southern Hemisphere (S.H.) from the Pacific southeastward across Chile and Argentina into the south Atlantic Ocean. In the Northern Hemisphere (N.H.) the counterpart feature extends across the southern U.S. and Atlantic Ocean into Europe. Further to the west a negative anomaly extends southeastward again from the Maritime Continent across the South Pacific and through the Drake

Passage. In the Southern Hemisphere an anomaly feature is shown to spiral into the Antarctica land mass. The extremes of ENSO-related anomalies are also examined and indicate that globally, during both El Nino and La Nina, more extremes of precipitation (both wet and dry) occur than during the ”neutral” regime, with the El Nino regime showing larger magnitudes. The distribution is different for the globe as a whole and when the area is restricted to just land. The recent (1998-present) TRMM observations are compared with the similar period of GPCP analyses with very good agreement in terms of pattern and generally good agreement with regard to magnitude. However, there still are differences among the individual TRMM products using passive and active microwave techniques and these need to be resolved before longer-term products such as the GPCP analyses can be validated.
Author
Climatology; Precipitation (Meteorology); Trmm Satellite; Tropical Regions; Annual Variations; Anomalies

20020003563 California Univ., Lawrence Berkeley Lab., Berkeley, CA USA
Impacts of cool cities on air quality: A preliminary modeling assessment for Nashville TN, Dallas TX and Atlanta GA
Taha, H.; Jun. 15, 1998; 27p; In English
Report No.(s): DE2001-6522; LBNL-42256; No Copyright; Avail: Department of Energy Information Bridge

Previous atmospheric modeling efforts that concentrated on the Los Angeles Basin suggested beneficial and significant air quality impacts from cool cities strategies. This paper discusses an extension of similar modeling efforts to three regions, Atlanta GA, Dallas - Ft. Worth TX, and Nashville TN, that experience smog and air quality problems. According to the older ozone air quality standard (120 ppb), these regions were classified as serious, moderate, and marginal, respectively, but may be out of compliance with respect to the newer, 80-ppb/8-hours standard. Results from this exploratory modeling work suggest a range of possible impacts on meteorological and air quality conditions. For example, peak ozone concentrations during each region’s respective episode could be decreased by 1-6 ppb (conservative and optimistic scenarios, respectively) in Nashville, 5-15 ppb in Dallas - Fort Worth, and 5-12 ppb in Atlanta following implementation of cool cities. The reductions are generally smaller than those obtained from simulating the Los Angeles Basin but are still significant. In all regions, the simulations suggest, the net, domain-wide effects of cool cities are reductions in ozone mass and improvements in air quality. In Atlanta, Nashville, and Dallas, urban areas benefiting from reduced smog reach up to 8460, 7350, and 12870 sq km in area, respectively. Results presented in this paper should be taken as exploratory and preliminary. These will most likely change during a more comprehensive modeling study to be started soon with the support of the US Environmental Protection Agency. The main purpose of the present project was to obtain the initial data (emission inventories) for these regions, simulate meteorological conditions, and perform preliminary sensitivity analysis. In the future, additional regions will be simulated to assess the potential of cool cities in improving urban air quality.
NTIS
Air Quality; Sensitivity Analysis; Gas Composition; Simulation; Weather; Environment Protection; Atmospheric Models; Cities

20020003982 Institute of Gas Technology, Chicago, IL USA
Development of METHANE de-NOX (Trade Name) Reburning Process ***Quarterly Report, 1 Jul. - 30 Sep. 1999***
Sep. 30, 1999; 7p; In English
Report No.(s): DE2001-763160; DOE/GO/10418-Q; No Copyright; Avail: Department of Energy Information Bridge, Microfiche

The use of biomass and wood waste solids and sludges as fuel is often hampered by their low heating values and the presence of bound nitrogen that result in inefficient combustion and high NO(x) emissions. Cofiring supplemental fuel through auxiliary burners helps with improving the combustion effectiveness and NOx reduction, but the benefits are limited to the fractional heat input of the auxiliary fuel. IGT has developed a recess called METHANE de-NOX(reg-sign) , which has shown substantially greater economic, energy and environmental benefits than traditional cofiring methods in demonstrations with both MSW- and coal-fired stoker boilers. In this process, auxiliary fuel such as natural gas or oil is injected directly into the lower region of the primary flame zone just above the grate. This increases and stabilizes the average combustion temperature, which improves combustion of high-moisture fuels, provides more uniform temperature profiles and reduced peak temperature, and reduces the availability of oxygen to reduce NOx formation. This is in contrast to conventional reburning, where natural gas is injected above the primary combustion zone after the majority of NOx has already been formed.
NTIS
Pollution Control; Efficiency; Air Pollution; Methane; Procedures; Burners; Combustion Products

20020004188 Lamont-Doherty Geological Observatory, Palisades, NY USA

Modeling South Pacific Ice-Ocean Interactions in the Global Climate System ***Final Report, 1 Mar. 1997 - 28 Feb. 2001***

Holland, David M., Lamont-Doherty Geological Observatory, USA; Jenkins, Adrian, Lamont-Doherty Geological Observatory, USA; Jacobs, Stanley S., Lamont-Doherty Geological Observatory, USA; [2001]; 118p; In English

Contract(s)/Grant(s): NAG5-4028; LDEO Contrib. 6034; No Copyright; Avail: CASI; A06, Hardcopy; A02, Microfiche

The objective of this project has been to improve the modeling of interactions between large Antarctic ice shelves and adjacent regions of the Southern Ocean. Our larger goal is to gain a better understanding of the extent to which the ocean controls ice shelf attrition, thereby influencing the size and dynamics of the Antarctic Ice Sheet. Melting and freezing under ice shelves also impacts seawater properties, regional upwelling and sinking and the larger-scale ocean circulation. Modifying an isopycnal coordinate general circulation model for use in sub-ice shelf cavities, we found that the abrupt change in water column thickness at an ice shelf front does not form a strong barrier to buoyancy-driven circulation across the front. Outflow along the ice shelf base, driven by melting of the thickest ice, is balanced by deep inflow. Substantial effort was focused on the Filchner-Ronne cavity, where other models have been applied and time-series records are available from instruments suspended beneath the ice. A model comparison indicated that observed changes in the production of High Salinity Shelf Water could have a major impact on circulation within the cavity. This water propagates into the cavity with an asymmetric seasonal signal that has similar phasing and shape in the model and observations, and can be related to winter production at the sea surface. Even remote parts of the sub-ice shelf cavity are impacted by external forcing on sub-annual time scales. This shows that cavity circulations and products, and therefore cavity shape, will respond to interannual variability in sea ice production and longer-term climate change. The isopycnal model gives generally lower net melt rates than have been obtained from other models and oceanographic data, perhaps due to its boundary layer formulation, or the lack of tidal forcing. Work continues on a manuscript describing the Ross cavity results.

Author

Cavities; Land Ice; Computerized Simulation; Fluid-Solid Interactions; Environment Models; Water Flow

20020004669 California Univ., Lawrence Berkeley Lab., Berkeley, CA USA

Evaluating Chemical Persistence in a Multimedia Environment: ACART Analysis

Bennett, D. H.; McKone, T. E.; Kastenberg, W. E.; Feb. 01, 1999; 38p; In English

Report No.(s): DE2001-7370; LBNL-42897; No Copyright; Avail: Department of Energy Information Bridge

For the thousands of chemicals continuously released into the environment, it is desirable to make prospective assessments of those likely to be persistent. Persistent chemicals are difficult to remove if adverse health or ecological effects are later discovered. A tiered approach using a classification scheme and a multimedia model for determining persistence is presented. Using specific criteria for persistence, a classification tree is developed to classify a chemical as 'persistent' or 'non-persistent' based on the chemical properties. In this approach, the classification is derived from the results of a standardized unit world multimedia model. Thus, the classifications are more robust for multimedia pollutants than classifications using a single medium half-life. The method can be readily implemented and provides insight without requiring extensive and often unavailable data. This method can be used to classify chemicals when only a few properties are known and be used to direct further data collection. Case studies are presented to demonstrate the advantages of the approach.

NTIS

Air Pollution; Chemical Properties; Contaminants; Atmospheric Chemistry

20020005067 Federal Energy Technology Center, Morgantown, WV USA

Bench-Scale Demonstration of Hot-Gas Desulfurization Technology

Apr. 01, 1999; 18p; In English

Report No.(s): DE2001-769317; DE-AC21-93MC30010-28; No Copyright; Avail: Department of Energy Information Bridge, Microfiche

The U.S. Department of Energy (DOE), Federal Energy Technology Center (FETC), is sponsoring research in advanced methods for controlling contaminants in hot coal gasifier gas (coal derived fuel-gas) streams of integrated gasification combined-cycle (IGCC) power systems. The hot gas cleanup work seeks to eliminate the need for expensive heat recovery equipment, reduce efficiency losses due to quenching, and minimize wastewater treatment costs. Hot-gas desulfurization research has focused on regenerable mixed-metal oxide sorbents that can reduce the sulfur in coal-derived fuel-gas to less than 20 ppmv and can be regenerated in a cyclic manner with air for multicycle operation. Zinc titanate (Zn2TiO4 or ZnTiO3), formed by a solid-state reaction of zinc oxide (ZnO) and titanium dioxide (TiO2), is currently one of the leading sorbents.

NTIS

Desulfurizing; High Temperature Gases; Coal Derived Gases; Contaminants

20020005072 Federal Energy Technology Center, Morgantown, WV USA

Membrane system for recovery of volatile organic compounds from remediation off-gases

Wijmans, J. G.; Daniels, R.; Olsen, R.; Jan. 13, 2000; 4p; In English

Report No.(s): DE2001-769341; DE-AR21-96MC33081; No Copyright; Avail: Department of Energy Information Bridge, Microfiche

In situ vacuum extraction, air or steam sparging, and vitrification are widely used methods of remediating soil contaminated with volatile organic compounds (VOCs). All of these processes produce a VOC.-laden air stream from which the VOC must be removed before the air can be discharged or recycled to the generating process. Treatment of these off-gases is often a major portion of the cost of the remediation project. Carbon adsorption and catalytic incineration, the most common methods of treating these gas streams, suffer from significant drawbacks. Membrane Technology and Research, Inc. (NITR) proposes an alternative treatment technology, based on permselective membranes that separate the organic components from the gas stream, producing a VOC-free air stream. The technology we propose to develop can be applied to all of these off-gas streams and is not tied to a particular off-gas generating source. We propose to develop a completely self-contained system because remediation projects are frequently in remote locations where access to trained operators and utilities is limited. The system will be a turnkey unit, skid-mounted and completely automatic, requiring power but no other utilities. The system will process the off-gas, producing a concentrated liquid VOC stream and a purified gas containing less than 10 ppm VOC that can be discharged or recycled to the gas-generating process.

NTIS

Gas Streams; Volatile Organic Compounds; Membranes

20020005073 Federal Energy Technology Center, Morgantown, WV USA

High productivity vacuum blasting system

Ebadian, M. A.; Jan. 13, 2000; 4p; In English

Report No.(s): DE2001-769342; DE-AR26-98FT40367; No Copyright; Avail: Department of Energy Information Bridge

The purpose of the project is to increase the productivity and economics of existing vacuum blasting technology. This technology is used to remove radioactive contamination, PCB's and lead-base paint and provides worker and environmental protection by continuously recycling the blast media and the full containment of the dust generated in the process.

NTIS

Economics; Vacuum Systems; Radioactivity; Abrasives

20020005174 Lawrence Livermore National Lab., Livermore, CA USA

Indoor Environment Program: 1996 Annual Report

Nov. 01, 1996; 11p; In English

Report No.(s): DE2001-7283; LBNL-41072; No Copyright; Avail: Department of Energy Information Bridge

The forty-five chemists, physicists, biologists, architects, engineers, staff, and students of the Indoor Environment Program are all working to solve the problems of indoor air quality, health, comfort, and energy use associated with the indoor environment. A common thread throughout this work is the importance of ventilation--both for its role in supporting human health and comfort as well as for its liability in requiring large amounts of energy to heat and cool it. The importance of understanding these interactions can be illustrated by two examples: the health and productivity of workers and the performance of sensitive equipment in clean room environments. During the past year, we estimated the magnitudes of health and productivity gains that may be obtained by providing better indoor environments. The ratio of the potential financial benefits of improving indoor environments to the costs of the improvements ranges between 20 and 50. A second example is from our Clean Room Energy Efficiency Study: Clean rooms utilize large amounts of electricity to operate fans that recirculate air at very high flow rates through particle filters. Usually, the fans operate continuously at full speed, even when the clean room is unused. to reduce the energy use in a research clean room, the rate of air recirculation was controlled in response to real-time measurements of particle concentration. With this new control system, fan energy use decreased by 65% to 85% while maintaining particle concentrations below the allowable limits except during occasional one-minute periods. The estimated payback period for this technology is one to four years.

NTIS

Indoor Air Pollution; Air Quality; Environment Management

20020005249 Oak Ridge National Lab., TN USA

Net Carbon Sequestration in Agriculture: A National Assessment

West, T. O.; Jan. 10, 2001; 6p; In English; Energy 2000, 23-28 July 2000, Las Vegas, NV, USA

Contract(s)/Grant(s): AC05-96OR22464

Report No.(s): DE2001-774471; P00-107540; No Copyright; Avail: Department of Energy Information Bridge, Microfiche

Agricultural ecosystems have the potential to sequester carbon dioxide from the atmosphere and partially mitigate global climatic change. A full carbon cycle analysis of predominant cropping systems is being conducted to determine potential net carbon sequestration in those systems. Carbon sequestration rates calculated from the full cycle analysis are being used in conjunction with existing land use data sets to determine current and potential carbon storage in the USA. The full cycle analysis completed for a continuous corn crop indicated that there is little difference in the energy used and the carbon emitted between conventional tillage and no-till practices. While the use of farm machinery produces less carbon emissions when using no-till, less carbon is emitted from crop inputs used in conjunction with conventional tillage. No-till practices sequester a larger gross amount of carbon than other tillage intensities, and may sequester a larger net amount of carbon depending on crop type. Preliminary results from a national assessment of 32 long-term experiments indicated an increase in gross carbon sequestration of approximately 168 kg/ha/yr when changing from conventional to no-till practices. Updated rates of carbon sequestration based on analyses of multiple factors (e.g., crop management practices and environmental variables) coupled with a full carbon cycle analysis are expected to provide an accurate basis for policy decisions regarding carbon sequestration initiatives.
NTIS
Carbon Cycle; Carbon Dioxide; Agriculture

20020005411 NASA Goddard Space Flight Center, Greenbelt, MD USA
Cloud Slicing: A New Technique to Derive Upper Tropospheric Ozone from Satellite Measurements
Ziemke, J. R., NASA Goddard Space Flight Center, USA; Chandra, S., NASA Goddard Space Flight Center, USA; Bhartia, P. K., NASA Goddard Space Flight Center, USA; [2001]; 1p; In English; AGU Spring Meeting, 29 May - 2 Jun. 2001, Boston, MA, USA; Sponsored by American Geophysical Union, USA; No Copyright; Avail: Issuing Activity; Abstract Only

A new technique denoted cloud slicing has been developed for measuring upper tropospheric ozone. Cloud slicing takes advantage of the opaque property of water vapor clouds to ultraviolet wavelength radiation. Measurements of above-cloud column ozone from the Nimbus 7 total ozone mapping spectrometer (TOMS) instrument are combined together with Nimbus 7 temperature humidity and infrared radiometer (THIR) cloud-top pressure data to derive ozone column amounts in the upper troposphere. In this study tropical TOMS and THIR data for the period 1979-1984 are analyzed. by combining total tropospheric column ozone (denoted TCO) measurements from the convective cloud differential (CCD) method with 100-400 hPa upper tropospheric column ozone amounts from cloud slicing, it is possible to estimate 400-1000 hPa lower tropospheric column ozone and evaluate its spatial and temporal variability. Results for both the upper and lower tropical troposphere show a year-round zonal wave number 1 pattern in column ozone with largest amounts in the Atlantic region (up to 15 DU in the 100-400 hPa pressure band and around 25-30 DU in the 400-1000 hPa pressure band). Upper tropospheric ozone derived from cloud slicing shows maximum column amounts in the Atlantic region in the June-August and September-November seasons which is similar to the seasonal variability of CCD derived TCO in the region. For the lower troposphere, largest column amounts occur in the September-November season over Brazil in South America and also southern Africa. Localized increases in the tropics in lower tropospheric ozone are found over the northern region of South America around August and off the west coast of equatorial Africa in the March-May season. Time series analysis for several regions in South America and Africa show an anomalous increase in ozone in the lower troposphere around the month of March which is not observed in the upper troposphere. The eastern Pacific indicates weak seasonal variability of upper, lower, and total tropospheric ozone compared to the western Pacific which shows largest TCO amounts in both hemispheres around spring months. Ozone variability in the western Pacific is expected to have greater variability caused by strong convection, pollution and biomass burning, land/sea contrast and monsoon developments.
Author
Troposphere; Ozone; Ultraviolet Radiation; Water Vapor; Ozonometry

20020005832 Federal Energy Technology Center, Morgantown, WV USA
Reduction of inherent mercury emissions in pc combustion. Semi-annual report, January 1-June 30, 1998 ***Semiannual Report, 1 Jan. - 30 Jun. 1998***
Kramlich, J. C.; Sliger, R. N.; Going, D. J.; Aug. 06, 1999; 9p; In English
Report No.(s): DE2001-775018; DE-FG22-95PC95216-06; No Copyright; Avail: Department of Energy Information Bridge, Microfiche

Mercury emission compliance is one of the major potential challenges raised by the 1990 Clean Air Act Amendments. Simple ways of controlling emissions have not been identified. The variability in the field data suggests that inherent mercury emissions may be reduced if the source of this inherent capture can be identified and controlled. The key mechanisms appear to involve the oxidation of the mercury to Hg(sup 2), generally producing the more reactive HgCl(sub 2) , followed by its capture by certain components of the fly ash or char. This research focuses on identifying the rate-limiting steps associated with the oxidation step. Work in this reporting period focused on the development and application of a kinetics model to the oxidation data developed in

the present program and literature data under MSW (municipal solid waste) conditions. The results indicate that the pathway Hg + Cl = HgCl followed by HgCl + HCl = HgCl(sub 2) + H predominates over Hg + Cl(sub 2) under high-temperature conditions. This primarily occurs because Cl(sub 2) concentrations are too low under the present conditions to contribute significantly.
NTIS
Mercury (Metal); Oxidation; Mercury Compounds; Air Pollution; Combustion Products; Pollution Control

20020005833 Federal Energy Technology Center, Morgantown, WV USA
Reduction of inherent mercury emissions in pc combustion. Semi-annual technical report, January 1-June 30, 1999 ***Semiannual Report, 1 Jan. - 30 Jun. 1999***
Kramlich, J. C.; Sliger, R. N.; Going, D. J.; Aug. 06, 1999; 6p; In English
Report No.(s): DE2001-775020; DE-FG22-95PC95216-08; No Copyright; Avail: Department of Energy Information Bridge, Microfiche

Mercury emission compliance presents one of the major potential challenges raised by the 1990 Clean Air Act Amendments. Simple ways of controlling emissions have not been identified. The variability in the field data suggest that inherent mercury emissions may be reduced if the source of this inherent capture can be identified and controlled. The key mechanisms appear to involve the oxidation of mercury to Hg(sup 2), generally producing the more reactive HgCl(sub 2), followed by its capture by certain components of the fly ash or char, or in the air pollution control equipment. This research focuses on identifying the rate-limiting steps associated with the oxidation step. Work in this reporting period focused on testing of the kinetic mechanism reported in the previous semiannual report, and the interpretation of data (both ours and literature). This model yields good qualitative agreement with the data and indicates that mercury oxidation occurs during the thermal quench of the combustion gases. The model also suggests that atomic chlorine is the key oxidizing species. The oxidation is limited to a temperature window between 700-400 C that is defined by the overlap of (1) a region of significant superequilibrium Cl concentration, and (2) a region where oxidized mercury is favored by equilibrium. Above 700 C reverse reactions effectively limit oxidized mercury concentrations. Below 400 C, atomic chlorine concentrations are too low to support further oxidation. The implication of these results are that homogeneous oxidation is governed primarily by (1) HCl concentration, (2) quench rate, and (3) background gas composition. Work conducted under the present grant has been the subject of one journal paper that was accepted for publication during the reporting period.
NTIS
Combustion Products; Mercury (Metal); Mercury Compounds; Air Pollution; Oxidation; Reaction Kinetics

20020005835 Federal Energy Technology Center, Morgantown, WV USA
Validation of mercury cems when cofiring biomass at madison electric's blount station
Laudal, D. L.; Thompson, J. S.; Sep. 30, 2000; 42p; In English
Report No.(s): DE2001-775033; DE-FC26-98FT40321-13; No Copyright; Avail: Department of Energy Information Bridge, Microfiche

The state of Wisconsin has been concerned about mercury deposition into its lakes and streams and has been evaluating strategies to reduce mercury emissions. As part of this effort, the Blount Station, owned and operated by Madison Gas and Electric Company (MGE), has undergone a project to evaluate the effects and potential mercury emissions reduction of cofiring preconsumer waste. MGE owns and operates the Blount Generating Station located in central Madison, Wisconsin. At present, Blount operates with nine boilers and six turbine generators. The two largest boilers at Blount produce 400,000 pounds of steam per hour at 950 F and 1250 psi. These larger boilers, MGE's Boiler Nos. 8 and 9, have the capability of cofiring both paper and plastic. MGE's Blount Generating Station was one of the first electric generating stations in the USA to retrofit its existing steam boilers to successfully burn refuse-derived fuel and other alternate fuels including waste paper and wood. It is the No. 9 boiler that was the focus of this project to determine the effect of cofiring PDF (plastic- and paper-derived fuel) on speciated mercury emissions. The project was laid out to compare four different fuel combinations: (1) coal feed only, (2) coal with plastic, (3) coal with paper, and (4) coal with paper and plastic. The design was to run the boiler for 2 days at each condition, thus allowing four samples to be taken at each condition. This plan was aimed at getting at least three representative samples at each condition and allowed for difficulties in sampling and boiler operation. The following objectives were accomplished as part of the project to determine the effects of cofiring PDF on mercury emissions and speciation at MGE Blount Station: Successfully completed all of the mercury sampling for each of the four boiler/PDF conditions using the Ontario Hydro (OH) mercury speciation method; Determined mercury concentrations at the stack location using mercury continuous emission monitors (CEMs) for each of the four boiler/PDF conditions; Calculated the overall mercury mass balance for each of the runs; Determined chlorine concentrations

at the stack location using EPA Method 26A for each of the four boiler/PDF conditions; and calculated speciated mercury flow to determine removal and/or transformations before its exiting the unit at the stack for each of the four boiler/PDF conditions.
NTIS
Biomass; Mercury (Metal); Waste Utilization; Exhaust Emission; Electric Power Plants; Solid Wastes; Biomass Energy Production

20020005842 Los Alamos National Lab., NM USA
Temperature measurements collected from an instrumented van in Salt Lake City, Utah as part of URBAN 2000
Brown, M. J.; Pardyjak, E. R.; Aug. 01, 2001; 7p; In English
Report No.(s): DE2001-784473; LA-UR-01-4029; No Copyright; Avail: Department of Energy Information Bridge

Measurements of temperature and position were collected during the night from an instrumented van on routes through Salt Lake City and the rural outskirts. The measurements were taken as part of the Department of Energy Chemical and Biological National Security Program URBAN 2000 Field Experiment conducted in October 2000 (Shinn et al., 2000 and Allwine et al., 2001a). The instrumented van was driven over three primary routes, two including downtown, residential, and rural areas and a third that went by a line of permanently fixed temperature probes (Allwine et al., 2001b) for cross-checking purposes. Each route took from 45 to 60 minutes to complete. Based on four nights of data, initial analyses indicate that there was a temperature difference of 2-5degC between the urban core and nearby rural areas. Analyses also suggest that there were significant fine scale temperature differences over distances of tens of meters within the city and in the nearby rural areas. The temperature measurements that were collected are intended to supplement the meteorological measurements taken during the URBAN2000 Field Experiment, to assess the importance of the urban heat island phenomenon in Salt Lake City, and to test the urban canopy parameterizations that have been developed for regional scale meteorological codes as part of the DOE CBNP program.
NTIS
Temperature; Meteorological Parameters; Data Processing; Data Reduction

20020005859 National Energy Technology Lab., Pittsburgh, PA USA
Minimization of no emissions from multi-burner coal-fired boilers. Semi-annual Report, September 1998-February 1999
Eddings, E. G.; Molina, A.; Pershing, D. W.; Sarofim, A. F.; Davis, K. A.; Apr. 01, 2000; 32p; In English
Report No.(s): DE2001-786522; FG26-97FT97275-03; No Copyright; Avail: Department of Energy Information Bridge, Microfiche

The focus of this program is to provide insight into the formation and minimization of NO-x in multi-burner arrays, such as those that would be found in a typical utility boiler. Most detailed studies are performed in single-burner test facilities, and may not capture significant burner-to-burner interactions that could influence NO-x emissions.
NTIS
Nitrogen Oxides; Coal; Boilers; Optimization

20020005888 NASA Goddard Space Flight Center, Greenbelt, MD USA
Evaluation of Stratospheric Transport in New 3D Models Using the Global Modeling Initiative Grading Criteria
Strahan, Susan E., NASA Goddard Space Flight Center, USA; Douglass, Anne R., NASA Goddard Space Flight Center, USA; [2001]; 1p; In English; AGU Spring Meeting, 29 May - 2 Jun. 2001, Boston, MA, USA; Sponsored by American Geophysical Union, USA; No Copyright; Avail: Issuing Activity; Abstract Only

The Global Modeling Initiative (GMI) Team developed objective criteria for model evaluation in order to identify the best representation of the stratosphere. This work created a method to quantitatively and objectively discriminate between different models. In the original GMI study, 3 different meteorological data sets were used to run an offline chemistry and transport model (CTM). Observationally-based grading criteria were derived and applied to these simulations and various aspects of stratospheric transport were evaluated; grades were assigned. Here we report on the application of the GMI evaluation criteria to CTM simulations integrated with a new assimilated wind data set and a new general circulation model (GCM) wind data set. The Finite Volume Community Climate Model (FV-CCM) is a new GCM developed at Goddard which uses the NCAR CCM physics and the Lin and Rood advection scheme. The FV-Data Assimilation System (FV-DAS) is a new data assimilation system which uses the FV-CCM as its core model. One year CTM simulations of 2.5 degrees longitude by 2 degrees latitude resolution were run for each wind data set. We present the evaluation of temperature and annual transport cycles in the lower and middle stratosphere in the two new CTM simulations. We include an evaluation of high latitude transport which was not part of the original GMI criteria.

Grades for the new simulations will be compared with those assigned during the original GMT evaluations and areas of improvement will be identified.
Author
Three Dimensional Models; Climate Models; Stratosphere

20020005892 NASA Goddard Space Flight Center, Greenbelt, MD USA
Stratospheric Age Spectra and Mean Ages From In Situ Observations of Carbon Dioxide
Andrews, Arlyn E., NASA Goddard Space Flight Center, USA; Boering, Kristie A., California Univ., USA; Daube, Bruce C., Jr., Harvard Univ., USA; Wofsy, Steven C., Harvard Univ., USA; [2001]; 1p; In English; AGU Spring Meeting, 29 May - 2 Jun. 2001, Boston, MA, USA; Sponsored by American Geophysical Union, USA; No Copyright; Avail: Issuing Activity; Abstract Only

Tropospheric CO2 mixing ratios exhibit latitudinally varying seasonal and interannual oscillations superimposed on the long-term positive trend due to fossil fuel combustion. In situ observations of CO2 obtained from 1992-2000 using the NASA ER-2 aircraft and high-altitude balloons show that these time-varying signals propagate into the stratosphere, providing information about the transport history of sampled air. We have used these data to derive age spectra and mean ages that can be compared with results from models of the stratospheric circulation. Age spectra have been derived for altitudes below approximately 20 km for the tropics and for northern midlatitudes, where there is sufficient data and where the amplitudes of the seasonal and interannual oscillations are large enough to be detected. The midlatitude CO2 data are consistent with bimodal age spectra, which may result from a subtropical ”barrier” to horizontal exchange. Seasonally resolved mean ages are available with nearly pole-to-pole coverage below 20 km and in the tropics and at middle and high northern latitudes up to the maximum altitude reached by the balloons (approximately 30 km). The oldest air sampled was in the Arctic polar vortex with a mean age of 6.5 +/- 0.5 years.
Author
Stratosphere; Carbon Dioxide; In Situ Measurement; Mixing Ratios; Atmospheric Circulation

20020005893 NASA Goddard Space Flight Center, Greenbelt, MD USA
Measurement of the Vertical Distribution of Aerosol by Globally Distributed MP Lidar Network Sites
Spinhirne, James, NASA Goddard Space Flight Center, USA; Welton, Judd, Maryland Univ. Baltimore County, USA; Campbell, James, Science Systems and Applications, Inc., USA; [2001]; 1p; In English; IEEE IGARSS 2001 Meeting, 9-13 Jul. 2001, Sydney, Australia; Sponsored by Institute of Electrical and Electronics Engineers, USA; No Copyright; Avail: Issuing Activity; Abstract Only

The global distribution of aerosol has an important influence on climate through the scattering and absorption of shortwave radiation and through modification of cloud optical properties. Current satellite and other data already provide a great amount of information on aerosol distribution. However there are critical parameters that can only be obtained by active optical profiling. For aerosol, no passive technique can adequately resolve the height profile of aerosol. The aerosol height distribution is required for any model for aerosol transport and the height resolved radiative heating/cooling effect of aerosol. The Geoscience Laser Altimeter System (GLAS) is an orbital lidar to be launched by 2002. GLAS will provide global measurements of the height distribution of aerosol. The sampling will be limited by nadir only coverage. There is a need for local sites to address sampling, and accuracy factors. Full time measurements of the vertical distribution of aerosol are now being acquired at a number of globally distributed MP (micro pulse) lidar sites. The MP lidar systems provide profiling of all significant cloud and aerosol to the limit of signal attenuation from compact, eye safe instruments. There are currently six sites in operation and over a dozen planned. At all sites there are a complement of passive aerosol and radiation measurements supporting the lidar data. Four of the installations are at Atmospheric Radiation Measurement program sites. The aerosol measurements, retrievals and data products from the network sites will be discussed. The current and planned application of data to supplement satellite aerosol measurements is covered.
Author
Vertical Distribution; Aerosols; Remote Sensing; Laser Altimeters; Optical Radar

20020005895 Federal Energy Technology Center, Morgantown, WV USA
Reduction of inherent mercury emissions in pc combustion. Semi-annual technical report, July 1-December 31, 1998 ***Semiannual Report, 1 Jul. - 31 Dec. 1998***
Kramlich, J. C.; Sliger, R. N.; Going, D. J.; Aug. 06, 1999; 7p; In English
Report No.(s): DE2001-775019; DE-FG22-95PC95216-07; No Copyright; Avail: Department of Energy Information Bridge, Microfiche

Mercury emission compliance presents one of the major potential challenges raised by the 1990 Clean Air Act Amendments. Simple ways of controlling emissions have not been identified. The variability in the field data suggest that inherent mercury emissions may be reduced if the source of this inherent capture can be identified and controlled. The key mechanisms appear to involve the oxidation of mercury to Hg(sup 2), generally producing the more reactive HgCl(sub 2), followed by its capture by certain components of the fly ash or char, or in the air pollution control equipment. This research focuses on identifying the rate-limiting steps associated with the oxidation step. Work in this reporting period focused on the refinement of the rate constants used in the kinetic mechanism for mercury oxidation. The possible reactions leading to mercury oxidation are reviewed. Rate constants for these reactions are discussed, using both literature sources and detailed estimates. The resulting mechanism represents the best present picture of the overall chlorine homogeneous oxidation chemistry. Application of this mechanism to the data will be explored in the subsequent reporting period. Work conducted under the present grant has been the subject of two meeting papers presented during the reporting period.
NTIS
Combustion Products; Mercury (Metal); Mercury Compounds; Oxidation; Reaction Kinetics; Air Pollution

46
GEOPHYSICS

Includes earth structure and dynamics, aeronomy; upper and lower atmosphere studies; ionospheric and magnetospheric physics; and geomagnetism. For related information see 47 Meteorology and Climatology; and 93 Space Radiation.

20020000925 Minnesota Univ., Dept. of Geology and Geophysics, Minneapolis, MN USA
Rheology of Diabase: Implications for Tectonics on Venus and Mars ***Final Report, 1 Apr. 1998 - 31 Mar. 2001***
Kohlstedt, David L., Minnesota Univ., USA; [2001]; 4p; In English
Contract(s)/Grant(s): NAG5-6797; No Copyright; Avail: CASI; A01, Hardcopy; A01, Microfiche

Two important goals of our experimental investigation of the rheological behavior of diabase rocks were: (1) to determine flow laws describing their creep behavior over wide ranges of temperature, stress and strain rate and (2) to develop an understanding of the physical mechanisms by which these rocks flow under laboratory conditions. With this basis, a primary objective then was to construct constitutive equations that can be used to extrapolate from laboratory to planetary conditions. We specifically studied the rheological properties of both natural rock samples and synthetic aggregates. The former provided constraints for geologic systems, while the latter defined the relative contributions of the constituent mineral phases and avoided the influence of glass/melt found in natural samples. In addition, partially molten samples of crustal rock composition were deformed in shear to large strains (greater than 200%) important in crustal environments. The results of this research yielded essential rheological properties essential for models of crustal deformation on terrestrial planets, specifically Venus and Mars, as well as on the geodynamical evolution of these planets. Over the past three years, we also completed our investigation of the creep behavior of water ice with applications to the glaciers, ice sheets and icy satellites. Constitutive equations were determined that describe flow over a wide ranged of stress, strain rate, grain size and temperature. In the case of ice, three creep regimes were delineate. Extrapolation demonstrates that dislocation glide and grain boundary sliding processes dominate flow in ice I under planetary conditions and that diffusion creep is not an important deformation mechanism either in the laboratory or on icy satellites. These results have already been incorporated by other investigators into models describing, for example, the thickness and stability of the ice shell on Europa and to unravel long-standing discrepancies between field observations on glaciers and laboratory results.
Author
Planetary Geology; Rheology; Creep Properties; Rocks; Crustal Fractures; Terrestrial Planets

20020001191 Search for Extraterrestrial Intelligence Inst., Moffett Field, CA USA
Charge Generation and Propagation in Igneous Rocks
Freund, Friedemann, Search for Extraterrestrial Intelligence Inst., USA; [2000]; 1p; In English; European Seismological Commission Meeting 2000, 11-15 Sep. 2000, Lisbon, Portugal; No Copyright; Avail: Issuing Activity; Abstract Only

Resistivity changes, ground potentials, electromagnetic (EM) and luminous signals prior to or during earthquakes have been reported, in addition to ground uplift and tilt, and to changes in the seismic wave propagation parameters. However, no physical model exists that ties these diverse phenomena together. Through time-resolved impacts experiments it has been observed that, when igneous rocks (gabbro, diorite, granite) are impacted at low velocities (approx. 100 m/sec), highly mobile electronic charge carriers are generated, spreading from a small volume near the impact point, causing electric potentials, EM and light emission. The rock becomes momentarily conductive. When impacted at higher velocities (approx. 1.5 km/sec), the propagation of the P

and S waves is registered through the transient piezoelectric response of quartz. At the same time, the rock volume is filled with mobile charge carriers, and a positive surface potential is registered. During the next 1-2 msec the surface potential oscillates, due to electron injection from ground. These observations are consistent with positive holes, e.g. defect electrons in the O(2-) sublattice, that can travel via the O 2p-dominated valence band of the silicate minerals at the speed of a phonon-mediated charge transfer. Before activation, the positive hole charge carriers lay dormant in form of positive hole pairs, PHP, electrically inactive, chemically equivalent to peroxy links in the structures of constituent minerals. PHPs are introduced by way of hydroxyl (O3Si-OH) incorporated into nominally anhydrous minerals when they crystallize in water-laden environments. Given that sound waves of even relatively low intensity appear to cause PHPs dissociation, thus generating mobile positive holes, it is proposed that microfracturing during rock deformation cause PHP dissociation. Depending on where and how much the rock volume is stressed, the positive holes are expected to form fluctuating charge clouds in the earthquake source region that may account for earthquake-related electrical phenomena and the reported low frequency EM signals.
Author
Earthquakes; Electrical Resistivity; Charge Transfer; Seismic Waves; Wave Propagation; Charge Carriers; Light Emission

20020001248 NASA Wallops Flight Center, Wallops Island, VA USA
Validating the use of Satellite SAR for Measuring Small-Scale Surface Wind Variations
Vandemark, Douglas, NASA Wallops Flight Center, USA; Mourad, P., NASA Wallops Flight Center, USA; Crawford, T., NASA Wallops Flight Center, USA; Sun, J., NASA Wallops Flight Center, USA; [2001]; 1p; In English; OAI Conference, 3-5 Apr. 2001, Miami, FL, USA; No Copyright; Avail: Issuing Activity; Abstract Only

We present aircraft measurements of near-surface atmospheric boundary layer roll signatures and radar-derived sea surface roughness. The open-ocean data were collected at an altitude of 20 m using NOAA's Long-EZ aircraft. In addition, the flight was coincident with a RADARSAT SAR overpass where presumed boundary layer roll impacts are prevalent in the SAR backscatter image. The Long-EZ air and sea data are completely coincident in space and time and this unique feature allows us to validate the supposed link between SAR backscatter signatures and organized large eddy surface impacts. We find remarkable correlation between measured modulations in the along-wind component of wind speed and radar backscatter for the atmospheric eddy scale of 1 to 1.5 km. Close agreement between normalized modulation amplitudes suggests the radar-inferred surface slope variance is changing linearly with wind speed. Implications for SAR usage in coastal regions and for boundary layer study will be discussed.
Author
Atmospheric Boundary Layer; Ocean Surface; Surface Roughness; Wind (Meteorology); Wind Variations; Synthetic Aperture Radar

20020001353 Toronto Univ., Dept. of Physics, Ontario Canada
Ice-age Ice-sheet Rheology: Constraints from the Last Glacial Maximum Form of the Laurentide Ice Sheet
Peltier, W. Richard, Toronto Univ., Canada; Goldsby, David L., Minnesota Univ., USA; Kohlstedt, David L., Minnesota Univ., USA; Tarasov, Lev, Toronto Univ., Canada; Annals of Glaciology; [2000]; Volume 30, pp. 163-176; In English
Contract(s)/Grant(s): NAG5-4956; NSERC-A9627; Copyright; Avail: Issuing Activity

State-ot-the-art thermomechanical models of the modern Greenland ice and the ancient Laurenticle ice sheet that covered Canada at the Last Glacial Maximum (LGM) are not able to explain simultaneously the observed forms of these cryospheric structures when the same, anisotropy-enhanced, version of the conventional Glen flow law is employed to describe their rheology. The LGM Laurenticle ice sheet. predicted to develop in response to orbital climate forcing, is such that the ratio of its thickness to its horizontal extent is extremely large compared to the aspect ratio inferred on the basis of surface-geomorphological and solid-earth-geophysical constraints. We show that if the Glen flow law representation of the rheology is replaced with a new rheology based upon very high quality laboratory measurements of the stress-strain-rate relation, then the aspect ratios of both the modern Greenland ice sheet and the Laurenticle ice sheet, that existed at the LGM, are simultaneously explained with little or no retuning of the flow law.
Author
Rheology; Glaciers; Thermodynamics; Greenland

20020001784 NASA Goddard Space Flight Center, Greenbelt, MD USA
A 7.5-Year Dataset of SSM/I-Derived Surface Turbulent Fluxes Over Global Oceans
Chou, Shu-Hsien, NASA Goddard Space Flight Center, USA; Shie, Chung-Lin, Maryland Univ. Baltimore County, USA; Atlas, Robert M., NASA Goddard Space Flight Center, USA; Adizzone, Joe, General Sciences Corp., USA; Nelkin, Eric, Science Systems and Applications, Inc., USA; [2001]; 4p; In English; WCRP/SCOR Workshop, 21-24 May 2001, Washington, DC, USA; No Copyright; Avail: CASI; A01, Hardcopy; A01, Microfiche

The global air-sea turbulent fluxes are needed for driving ocean models and validating coupled ocean-atmosphere global models. A method was developed to retrieve surface air humidity from the radiances measured by the Special Sensor Microwave/Imager (SSM/I) Using both SSM/I-retrieved surface wind and air humidity, they computed daily turbulent fluxes over global oceans with a stability-dependent bulk scheme. Based on this method, we have produced Version 1 of Goddard Satellite-Based Surface Turbulent Fluxes (GSSTF) dataset from the SSM/I data and other data. It provides daily- and monthly-mean surface turbulent fluxes and some relevant parameters over global oceans for individual F8, F10, and F11 satellites covering the period July 1987-December 1994. It also provides 1988-94 annual- and monthly-mean climatologies of the same variables, using only F8 and F1 1 satellite data. It has a spatial resolution of 2.0 degrees x 2.5 degrees lat-long and is archived at the NASA/GSFC DAAC. The purpose of this paper is to present an updated assessment of the GSSTF 1.0 dataset.
Author
Microwave Imagery; Turbulence; Air Water Interactions; Atmospheric Models; Ocean Models; Remote Sensing

20020001968 Lawrence Livermore National Lab., Livermore, CA USA
Iron sound velocities in shock wave experiments
Holmes, N. C.; Nguyen, J. H.; Aug. 20, 1999; 6p; In English
Report No.(s): DE2001-12444; UCRL-JC-133194; No Copyright; Avail: Department of Energy Information Bridge, Microfiche
We have performed a series of sound velocity measurements in iron at earth's core pressures. Experiments were carried out at shock pressures as high as 400 GPa, with particular emphasis on the pressure range between 175 GPa and 275 GPa. The measured sound velocities of iron at elevated pressures exhibit a single discontinuity near 250 GPa, corresponding to the vanishing of shear strength as the iron melts. A second discontinuity reported by Brown and McQueen in their previous iron sound velocity studies was not observed in our study. Our results are consistent with their data otherwise. Experimental details and error propagation techniques essential to determining the melting point will also be discussed.
NTIS
Acoustic Velocity; Iron; Shock Waves; Velocity Measurement; Wave Propagation

20020002240 Lawrence Livermore National Lab., Livermore, CA USA
Detection of explosive events by monitoring acoustically-induced geomagnetic perturbations
Lewis, J. P.; Rock, D. R.; Shaeffer, D. L.; Warshaw, S. I.; Oct. 07, 1999; 64p; In English
Report No.(s): DE2001-12544; UCRL-ID-133240; REPT-97-ERD-003; No Copyright; Avail: Department of Energy Information Bridge
The Black Thunder Coal Mine (BTCM) near Gillette, Wyoming was used as a test bed to determine the feasibility of detecting explosion-induced geomagnetic disturbances with ground-based induction magnetometers. Two magnetic observatories were fielded at distances of 50 km and 64 km geomagnetically north from the northernmost edge of BTCM. Each observatory consisted of three separate but mutually orthogonal magnetometers, Global Positioning System (GPS) timing, battery and solar power, a data acquisition and storage system, and a three-axis seismometer. Explosions with yields of 1 to 3 kT of TNT equivalent occur approximately every three weeks at BTCM. We hypothesize that explosion-induced acoustic waves propagate upward and interact collisionally with the ionosphere to produce ionospheric electron density (and concomitant current density) perturbations which act as sources for geomagnetic disturbances. These disturbances propagate through an ionospheric Alfven waveguide that we postulate to be leaky (due to the imperfectly conducting lower ionospheric boundary). Consequently, wave energy may be observed on the ground. We observed transient pulses, known as Q-bursts, with pulse widths about 0.5 s and with spectral energy dominated by the Schumann resonances. These resonances appear to be excited in the earth-ionosphere cavity by Alfven solitons that may have been generated by the explosion-induced acoustic waves reaching the ionospheric E and F regions and that subsequently propagate down through the ionosphere to the atmosphere. In addition, we observe late time (> 800 s) ultra low frequency (ULF) geomagnetic perturbations that appear to originate in the upper F region ((approximately)300 km) and appear to be caused by the explosion-induced acoustic wave interacting with that part of the ionosphere. We suggest that explosion-induced Q-bursts may be discriminated from naturally occurring Q-bursts by association of the former with the late time explosion-induced ULF perturbations. We also present evidence for an acoustically-induced magnetic signal at both magnetic observatories, indicating that magnetometers act as highly sensitive detectors of acoustically-induced ground motion. Further experimental and theoretical work are required to improve confidence in these conclusions.
NTIS
Magnetometers; Explosions; Acoustic Excitation; Perturbation; Geomagnetism; Monitors; Magnetic Disturbances

20020002379 NASA Goddard Space Flight Center, Greenbelt, MD USA

The Effect of Deep, Tropical Convection on the Tropical Tropopause Layer

Dessler, A. E., NASA Goddard Space Flight Center, USA; [2001]; 1p; In English; AGU Spring Meeting, 29 May - 2 Jun. 2001, Boston, MA, USA; Sponsored by American Geophysical Union, USA; No Copyright; Avail: Issuing Activity; Abstract Only

There is evidence that most convective detrainment occurs below 355-K potential temperature (14 km). On the other hand, it is also generally accepted that convection does occasionally reach the altitude of the tropopause, typically approx. 16 km, or higher. The question is whether the relatively infrequent penetrations above 14 km are sufficient to influence the composition of the atmosphere above 14 km. Using measurements of O3 and CO as tracers of convective activity, I quantify the height distribution of mass detraining from convection near the tropopause by means of a simple mixing model similar to those used to calculate mixing into the stratospheric ”tropical pipe”. I calculate that significant detrainment from convection is occurring as high as approx. 380 K (16 km), an altitude typical of the tropopause. Further, I calculate that as much as 40% of the mass crossing the 380-K surface at this time detrained above 370 K. I conclude that the ”mixing barrier” at 14 km is more porous than previously thought.

Author

Convection; Tropical Regions; Tropopause; Stratosphere

20020002705 Sandia National Labs., Albuquerque, NM USA

Ratdamper: a numerical model for coupling mechanical and hydrological properties within the disturbed rock zone at the waste isolation pilot plant

Rath,; Pfeifle,; Hunsche,; Nov. 27, 2000; 10p; In English

Report No.(s): DE2001-768083; SAND99-2785C; No Copyright; Avail: Department of Energy Information Bridge

A numerical model for predicting damage and permeability in the disturbed rock zone (DRZ) has been developed. The semi-empirical model predicts damage based on a function of stress tensor invariant. For a wide class of problems hydrologic/mechanical coupling is necessary for proper analysis. The RATDAMPER model incorporates dilatant volumetric strain and permeability. The RATDAMPER model has been implemented in a weakly coupled code, which combines a finite element structural code and a finite difference multi-phase fluid flow code. Using the development of inelastic volumetric strain, a value of permeability can be assigned. This flexibility allows empirical permeability functional relationships to be evaluated.

NTIS

Multiphase Flow; Permeability; Rock Mechanics; Mathematical Models; Couplings; Mechanical Properties; Radioactive Wastes

20020002712 California Univ., Lawrence Berkeley Lab., Berkeley, CA USA

Single well seismic imaging: Status report

Daley, T. M.; Majer, E. L.; Gritto, R.; Mar. 01, 2000; 59p; In English

Report No.(s): DE2001-767580; LBNL-45342; No Copyright; Avail: Department of Energy Information Bridge

This reports updates the status of LBNL’s SWSI project, including all data acquisition completed in 1999 and initial analysis of the various data sets.

NTIS

Data Acquisition; Seismology; Imaging Techniques; Wells

20020002731 Desert Research Inst., Reno, NV USA

Simulated Effects of Elevated CO2 on Nitrogen Cycling using the NuCM Model

Johnson, D. W.; Oct. 14, 1998; 26p; In English

Report No.(s): DE2001-762876; No Copyright; Avail: Department of Energy Information Bridge

The interactions between elevated CO2 and N cycling were explored using simulations generated by the Nutrient Cycling Model (NuCM) for a Pinus taeda site at Duke, North Carolina and a mixed deciduous site at Walker Branch, Tennessee. The simulations tested whether N limitation would prevent growth increase in response to elevated CO2 and whether growth response to CO2 in N-limited systems could be facilitated by increased biomass/N (reduced concentration) and/or increased litter N mineralization. Nitrogen limitation precluded additional growth when target growth rates and litterfall were increased (simulating potential response to elevated CO2) at the Duke site. At the Walker Branch site, increasing target growth and litterfall caused a slight (790) increases in growth. Reducing foliar N concentrations caused reduced growth because of N limitation created by reduced litter quality (C/N ratio), reduced decomposition and N accumulation in forest floor. These effects were most pronounced at the Duke site, where the forest floor N turnover rate was lower than at the Walker Branch site. Reducing wood N concentration allowed prolonged increases in growth because of greater biomass/N; however, N uptake was reduced, allowing greater N

immobilization in the forest floor and soil. Increased N mineralization caused increased growth at the Duke site but not at Walker Branch.
NTIS
Carbon Dioxide; Cycles; Forests; Nitrogen; Environment Effects

20020003345 NASA Goddard Space Flight Center, Greenbelt, MD USA
Are Droughts in the USA Great Plains Predictable on Seasonal and Longer Time Scales?
Schubert, Siegfried D., NASA Goddard Space Flight Center, USA; Suarez, M., NASA Goddard Space Flight Center, USA; Pegion, P., NASA Goddard Space Flight Center, USA; Kistler, M., NASA Goddard Space Flight Center, USA; [2001]; 1p; In English; Spring AGU 2001 Meeting, 29 May - 2 Jun. 2001, Boston, MA, USA; Sponsored by American Geophysical Union, USA; No Copyright; Avail: Issuing Activity; Abstract Only

The USA Great Plains has experienced numerous episodes of unusually dry conditions lasting anywhere from months to several years, In this presentation, we will examine the predictability of such episodes and the physical mechanisms controlling the variability of the summer climate of the continental USA. The analysis is based on ensembles of multi-year simulations and seasonal hindcasts generated with the NASA Seasonal to-Interannual Prediction Project (NSIPP-1) General Circulation Model.
Author
Climatology; Drought; Great Plains Corridor (North America); Atmospheric General Circulation Models; Annual Variations

20020003347 NASA Goddard Space Flight Center, Greenbelt, MD USA
Wind and Rotation Enhanced Escape from the Early Terrestrial Atmospheres
Hartle, Richard E., NASA Goddard Space Flight Center, USA; [2001]; 1p; In English; Spring AGU 2001 Meeting, 29 May - 2 Jun. 2001, Boston, MA, USA; Sponsored by American Geophysical Union, USA; No Copyright; Avail: Issuing Activity; Abstract Only

The earliest atmospheres of the terrestrial planets are thought to have been hotter, have stronger winds and rotate faster than atmospheres of today. Since these primitive atmospheres were weakly bound, they evolved rapidly because atmospheric escape was very strong, often referred to as ”blowoff.” Such escape has been treated as hydrodynamic, transonic flow; similar to solar wind flow dynamics. However, in many cases, although the outward flow is hydrodynamic at low altitudes, it becomes collisionless at higher altitudes, before sonic speeds are ever attained. Recent models dealing with the transition from fluid to kinetic flow have applied the Jeans escape flux at the exobase. This approach leads to escape rates that are too low, because thermospheric winds and planetary rotation are known to increase the escape flux above the corresponding Jeans flux. In particular, for a given density and temperature at the exobase, the escape flux increases as the wind speed and/or the rotation rate increase. Also, for a given wind speed and rotation rate, the escape flux enhancement over the Jeans flux increases as the mass of an escaping constituent increases, an important factor in isotope fractionation, especially the enrichment of deuterium on Mars. Accounting for a range of possible temperatures, thermospheric wind speeds and planetary rotation rates in the primitive atmospheres of the terrestrial planets, estimates are made of light constituent escape flux increases over the corresponding Jeans fluxes.
Author
Wind (Meteorology); Planetary Atmospheres; Rotation; Solar Wind Velocity; Thermosphere

20020003350 NASA Goddard Space Flight Center, Greenbelt, MD USA
Response to Comment on ”Does the Earth Have an Adaptive Infrared Iris?”
Bell, Thomas L., NASA Goddard Space Flight Center, USA; Chou, Ming-Dah, NASA Goddard Space Flight Center, USA; Lindzen, Richard S., Massachusetts Inst. of Tech., USA; Hou, Arthur Y., NASA Goddard Space Flight Center, USA; [2001]; 6p; In English; No Copyright; Avail: CASI; A02, Hardcopy; A01, Microfiche

In his comment on Lindzen et al., Harrison found that the amount of high-level clouds, A, and the sea-surface temperature beneath clouds, T, averaged over a large oceanic domain in the western Pacific have secular linear trends of opposite signs over a period of 20 months. He found that when the linear trends are subtracted from the data, the correlation between the residual A and T is much reduced. His estimates of the confidence levels for the correlation indicate, moreover, that this correlation is not statistically significant. The domain-averaged A and, to a lesser degree, T, have distinct intra-seasonal and seasonal variations. These variations are influenced by the large-scale wind and temperature distributions and by the seasonal variation of insolation. to separate the local effect from the effect of slowly changing large-scale conditions, rather than subtracting 20-month linear trends from the series, which has the potential to spuriously extrapolate intra-seasonal and seasonal variations to even longer time scales,

we subtracted 30-day running means of A and T from each time series; in effect, the data were high-pass filtered. The number of points (days), N, is reduced by this process from the original value of 510 to 480.
Derived from text
Annual Variations; Atmospheric Temperature; Sea Surface Temperature; Temperature Distribution; Clouds (Meteorology)

20020003831 Los Alamos National Lab., NM USA
Eddy resolving nutrient ecodynamics in the global parallel ocean program and connections with trace gases in the sulfur, halogen and nmhc cycles
Chu, S.; Elliott, S.; Aug. 01, 2000; 9p; In English
Report No.(s): DE2001-768251; LA-UR-00-3699; No Copyright; Avail: Department of Energy Information Bridge, Microfiche

Ecodynamics and the sea-air transfer of climate relevant trace gases are intimately coupled in the oceanic mixed layer. Ventilation of species such as dimethyl sulfide and methyl bromide constitutes a key linkage within the earth system. We are creating a research tool for the study of marine trace gas distributions by implementing coupled ecology-gas chemistry in the high resolution Parallel Ocean Program (POP). The fundamental circulation model is eddy resolving, with cell sizes averaging 0.15 degree (lat/long). Here we describe ecochemistry integration. Density dependent mortality and iron geochemistry have enhanced agreement with chlorophyll measurements. Indications are that dimethyl sulfide production rates must be adjusted for latitude dependence to match recent compilations. This may reflect the need for phytoplankton to conserve nitrogen by favoring sulfurous osmolytes. Global simulations are also available for carbonyl sulfide, the methyl halides and for nonmethane hydrocarbons. We discuss future applications including interaction with atmospheric chemistry models, high resolution biogeochemical snapshots and the study of open ocean fertilization.
NTIS
Atmospheric Chemistry; Gases; Remote Sensing; Seas; Trace Contaminants

20020004350 G and A Technical Software, Inc., Newport News, VA USA
HALOE Algorithm Improvements for Upper Tropospheric Sounding ***Final Report, Mar. 1998 - Sep. 2001***
Thompson, Robert Earl, G and A Technical Software, Inc., USA; McHugh, Martin J., G and A Technical Software, Inc., USA; Gordley, Larry L., G and A Technical Software, Inc., USA; Hervig, Mark E., G and A Technical Software, Inc., USA; Russell, James M., III, Hampton Univ., USA; Dec. 07, 2001; 34p; In English
Contract(s)/Grant(s): NAS5-98076
Report No.(s): GATS-120701; NRA-97-MTPE-04; No Copyright; Avail: CASI; A03, Hardcopy; A01, Microfiche

This report details the ongoing efforts by GATS, Inc., in conjunction with Hampton University and University of Wyoming, in NASA's Mission to Planet Earth Upper Atmospheric Research Satellite (UARS) Science Investigator Program entitled 'HALOE Algorithm Improvements for Upper Tropospheric Sounding.' The goal of this effort is to develop and implement major inversion and processing improvements that will extend Halogen Occultation Experiment (HALOE) measurements further into the troposphere. In particular, O3, H2O, and CH4 retrievals may be extended into the middle troposphere, and NO, HCl and possibly HF into the upper troposphere. Key areas of research being carried out to accomplish this include: pointing/tracking analysis; cloud identification and modeling; simultaneous multichannel retrieval capability; forward model improvements; high vertical-resolution gas filter channel retrievals; a refined temperature retrieval; robust error analyses; long-term trend reliability studies; and data validation. The current (first year) effort concentrates on the pointer/tracker correction algorithms, cloud filtering and validation, and multichannel retrieval development. However, these areas are all highly coupled, so progress in one area benefits from and sometimes depends on work in others.
Author
Algorithms; Halogen Occultation Experiment; Troposphere; Remote Sensing

20020004351 NASA Goddard Space Flight Center, Greenbelt, MD USA
On the Origin of Polar Vortex Air
Rosenfield, J. E., NASA Goddard Space Flight Center, USA; Schoeberl, M. R., NASA Goddard Space Flight Center, USA; [2001]; 1p; In English; Spring AGU 2001 Meeting, 29 May - 2 Jun. 2 2001, Boston, MA, USA; Sponsored by American Geophysical Union, USA
Report No.(s): AGU-04194323; No Copyright; Avail: Issuing Activity; Abstract Only

The existence of the multi-year HALOE CH4 data set, together with some comparisons of forward with back trajectory calculations which we have carried out, has motivated us to reexamine the question of polar vortex descent. Three-dimensional diabatic trajectory calculations have been carried out for the seven month fall to spring period in both the northern hemisphere (NH) and southern hemisphere (SH) polar stratosphere for the years 1992-1999. These computations are compared to fixed

descent computations where the parcels were fixed at their latitude-longitude locations and allowed to descend without circulating. The forward trajectory computed descent is always less than the fixed descent due to horizontal parcel motions and variations in heating rates with latitude and longitude. Although the forward calculations estimate the maximum amount of descent that can occur, they do not necessarily indicate the actual origin of springtime vortex air. This is because more equator-ward air can be entrained within the vortex during its formation. to examine the origin of the springtime vortex air, the trajectory model was run backward for seven months from spring to fall. The back trajectories show a complex distribution of parcels in which one population originates in the upper stratosphere and mesosphere and experiences considerable descent in the polar regions, while the remaining parcels originate at lower altitudes of the middle and lower stratosphere and are mixed into the polar regions during vortex formation without experiencing as much vertical transport. The amount of descent experienced by the first population shows little variability from year to year, while the computed descent and mixing of the remaining parcels show considerable interannual variability due to the varying polar meteorology. Because of this complex parcel distribution it is not meaningful to speak of a net amount of descent experienced over the entire winter period. Since the back trajectories indicate that much of the air can come from lower altitudes than would be implied by the forward calculations, using a comparison between pre-winter and post-winter tracer profiles to estimate the amount of descent over this period will give erroneous descent amounts. In order to evaluate the computed descent, spring methane amounts were computed by mapping HALOE fall observations onto the final latitude-altitude locations of the back trajectories. These locations indicate the origin of the spring vortex air. The agreement between the computed means and the spring HALOE means is generally within 0.1-0.2 ppmv in the NH and 0.1-0.4 ppmv in the SH.
Author
Halogen Occultation Experiment; Polar Meteorology; Polar Regions; Vortices; Northern Hemisphere; Earth Atmosphere

20020004357 NASA Ames Research Center, Moffett Field, CA USA
A Study of High Altitude Hypersonic Flow-Field Radiation
Moreau, Stephane, Stanford Univ., USA; Park, Chul, NASA Ames Research Center, USA; [1994]; 1p; In English
Contract(s)/Grant(s): RTOP 232-01-04; No Copyright; Avail: Issuing Activity; Abstract Only

This paper presents the results of the works carried out jointly at Stanford University and Ames Research Center under a grant from the Ballistic Missile Defense Organization (BMDO) (formerly the Strategic Defense Initiative Organization) to explain and understand the results of the two flight experiments, Bow Shock Ultra-Violet 1 and Bow Shock Ultra-Violet 2, carried out by the Organization. A portion of the material contained in this paper has been reported elsewhere in open literature. However, this paper provides (1) the details of scientific contents not available in those literature, (2) the links among those and the logical order of the efforts involved, and (3) some materials not contained in any open literature. The first author is responsible for execution of the work; the second author directed the work of the first author. In the two flight experiments mentioned above, the spectra of radiation in the ultraviolet wavelength range incident on the stagnation point of a blunt body were measured at the flight speeds of 3.8 and 5.2 km/sec over a wide range of altitudes. The results were compared first with the calculations made using the original version of the NEQAIR/STRAP codes written earlier by the second author. At low altitudes, the calculations agreed with the measurement. However, at high altitudes, the calculations underestimated the intensity of the radiation by several orders of magnitudes. A shock tube experiment was carried out at CALSPAN and a plasma-torch experiment was carried out at Stanford University to produce experimental data to help explain the discrepancy. In addition, the shock tube experiment at Ames Research Center carried out independently of the BMDO was also found to be relevant to this question. In this paper, several theoretical models are developed and calculations using the models were carried out to explain the results not only of the flight experiments but also of the CALSPAN, Stanford, and Ames experiments. The are: (1) the diffusion model for the rotational mode to explain the slowness of rotational excitation, (2) assignment of different vibrational temperatures and different relaxation rates for different molecules, and (3) the modification of the NEQAIR code to accommodate the new experimental data. This paper shows that the discrepancy between the flight data and calculation is smaller with the present model, but is still substantial.
Author
Ballistic Missiles; Flow Distribution; High Altitude; Hypersonics; Mathematical Models; Radiation

20020005412 NASA Goddard Space Flight Center, Greenbelt, MD USA
An Overview of Modeling Middle Atmospheric Odd Nitrogen
Jackman, Charles H., NASA Goddard Space Flight Center, USA; Kawa, S. Randolph, NASA Goddard Space Flight Center, USA; [2001]; 1p; In English; AGU Spring Meeting, 29 May - 2 Jun. 2001, Boston, MA, USA; Sponsored by American Geophysical Union, USA; No Copyright; Avail: Issuing Activity; Abstract Only

Odd nitrogen (N, NO, NO2, NO3, N2O5, HNO3, HO2NO2, ClONO2, and BrONO2) constituents are important components in the control of middle atmospheric ozone. Several processes lead to the production of odd nitrogen (NO(sub y)) in the middle

atmosphere (stratosphere and mesosphere) including the oxidation of nitrous oxide (N2O), lightning, downflux from the thermosphere, and energetic charged particles (e.g., galactic cosmic rays, solar proton events, and energetic electron precipitation). The dominant production mechanism of NO(sub y) in the stratosphere is N2O oxidation, although other processes contribute. Mesospheric NO(sub y) is influenced by N2O oxidation, downflux from the thermosphere, and energetic charged particles. NO(sub y) is destroyed in the middle atmosphere primarily via two processes: 1) dissociation of NO to form N and O followed by N + NO yielding N2 + O to reform even nitrogen; and 2) transport to the troposphere where HNO3 can be rapidly scavenged in water droplets and rained out of the atmosphere. There are fairly significant differences among global models that predict NO(sub y). NO(sub y) has a fairly long lifetime in the stratosphere (months to years), thus disparate transport in the models probably contributes to many of these differences. Satellite and aircraft measurement provide modeling tests of the various components of NO(sub y). Although some recent reaction rate measurements have led to improvements in model/measurement agreement, significant differences do remain. This presentation will provide an overview of several proposed sources and sinks of NO(sub y) and their regions of importance. Multi-dimensional modeling results for NO(sub y) and its components with comparisons to observations will also be presented.
Author
Nitrogen Oxides; Middle Atmosphere; Ozone; Atmospheric Composition

20020005887 Sonoquest/Advanced Ultrasonics Research, Wellesley Hills, MA USA
Effect of Water Content and Sea Salt on Seismoacoustic Waves in Beach Sand ***Final Report, May 2000-Sep. 2001***
Chamuel, Jacques R.; Sep. 2001; 27p; In English
Contract(s)/Grant(s): N00014-00-C-0386
Report No.(s): AD-A395391; JRC-42-2001; No Copyright; Avail: CASI; A03, Hardcopy; A01, Microfiche

New findings are presented providing physical insight on the effect of moisture and sea salt on high-frequency seismoacoustic waves in beach sand. Quantitative results reveal that the velocity of high-frequency compressional waves increases by about 8% as the water content is decreased by 18% from full saturation. This increase in velocity is in contrast with the Biot-Gassmann theory which predicts that the velocity of low-frequency compressional waves decreases by 85% as the water content is decreased by only 1% from saturation. Velocity plots as function of water saturation are compared for different sands and spherical glass beads. The effect of sea salt on grain to grain acoustic coupling is demonstrated. Salt crystallization and transport can lead to the formation of hard sand/salt layers with a compressional velocity increasing from 200 m/s to 2887 m/s, and a shear velocity increasing from 10 m/s to 1885 m/s. A hypothesis is discussed with preliminary results on the potential existence of a suction-cup effect increasing the rigidity of unconsolidated compacted sediments, in the absence of roughness, due to the formation of cavitation microbubbles as the tensile strength of the thin capillary water film between compressed sand grains is exceeded.
DTIC
Water Waves; Seismic Waves; Underwater Acoustics; Ocean Bottom; Sodium Chlorides; Sands

47
METEOROLOGY AND CLIMATOLOGY

Includes weather observation forecasting and modification

20020000778 NASA Goddard Space Flight Center, Greenbelt, MD USA
Cloud Microphysics Budget in the Tropical Deep Convective Regime
Li, Xiao-Fan, NASA Goddard Space Flight Center, USA; Sui, C.-H., NASA Goddard Space Flight Center, USA; Lau, K.-M., NASA Goddard Space Flight Center, USA; March 2001; 46p; In English; No Copyright; Avail: CASI; A03, Hardcopy; A01, Microfiche

Cloud microphysics budgets in the tropical deep convective regime are analyzed based on a 2-D cloud resolving simulation. The model is forced by the large-scale vertical velocity and zonal wind and large-scale horizontal advections derived from TOGA COARE for a 20-day period. The role of cloud microphysics is first examined by analyzing mass-weighted mean heat budget and column-integrated moisture budget. Hourly budgets show that local changes of mass-weighted mean temperature and column-integrated moisture are mainly determined by the residuals between vertical thermal advection and latent heat of condensation and between vertical moisture advection and condensation respectively. Thus, atmospheric thermodynamics depends on how cloud microphysical processes are parameterized. Cloud microphysics budgets are then analyzed for raining conditions. For cloud-vapor exchange between cloud system and its embedded environment, rainfall and evaporation of raindrop are compensated by the condensation and deposition of supersaturated vapor. Inside the cloud system, the condensation of supersaturated vapor balances conversion from cloud water to raindrop, snow, and graupel through collection and accretion

processes. The deposition of supersaturated vapor balances conversion from cloud ice to snow through conversion and riming processes. The conversion and riming of cloud ice and the accretion of cloud water balance conversion from snow to graupel through accretion process. Finally, the collection of cloud water and the melting of graupel increase raindrop to compensate the loss of raindrop due to rainfall and the evaporation of raindrop.
Author
Cloud Physics; Tropical Regions; Heat Budget; Moisture

20020000872 Harvard Univ., Cambridge, MA USA
Assessment strategies for global environmental change. Final report
Parson, E. A.; Clark, W. C.; Nov. 15, 1999; 23p; In English
Report No.(s): DE2001-764579; No Copyright; Avail: Department of Energy Information Bridge

The objective of this project has been to investigate how scientific and technical assessments of global environmental issues have been designed, implemented and used to investigate what strategies of assessment have been most useful in informing policy and decision. Drawing on both relevant theoretical literatures and detailed systematic review of assessment experience to date, the project has sought generalizable insights into the origins, conduct and consequences of assessment and into how each of these is shaped by the policy and knowledge context in which assessments are conducted. The project has sought to advance intellectual understanding of assessment as a political and knowledge-based process, to enhance communication among scholars and practitioners of global environmental assessments, and to provide practical insights into how to design and implement assessment and scientific advisory processes, to better integrated scientific understanding and decision making. We believe that achieving this integration is one of the most fundamental challenges that must be met for societies to more effectively manage, and live with global environmental change.
NTIS
Technology Assessment; Greenhouse Effect; Climatology; Environments

20020000878 Argonne National Lab., IL USA
Science of Climate Change
Doctor, R. D.; Sep. 10, 1999; 11p; In English; Power-Gen International ’99, 30 Nov. - 2 Dec. 1999, New Orleans, LA, USA
Report No.(s): DE2001-11961; ANL/ES/CP-100002; No Copyright; Avail: Department of Energy Information Bridge, Microfiche

A complex debate is underway on climate change linked to proposals for costly measures that would reshape our power grid. This confronts technical experts outside of the geophysical disciplines with extensive, but unfamiliar, data both supporting and refuting claims that serious action is warranted. For example, evidence is brought to the table from one group of astrophysicists concerned with sunspots--this group believes there is no issue man can manage; while another group of oceanographers concerned with the heat balance in the world’s oceans are very alarmed at the loss of arctic ice. What is the evidence. In an effort to put some of these issues in perspective for a technical audience, without a background in geophysics, a brief survey will consider (1) an overview of the 300 years of scientific inquiry on man’s relationship to climate; (2) a basic discussion of what is meant by the ’greenhouse’ and why there are concerns which include not only CO(sub 2), but also CH(sub 4), N(sub 2)O, and CFC’s; (3) the geological record on CO(sub 2)--which likely was present at 1,000 times current levels when life began; (4) the solar luminosity and sunspot question; and (5) the current evidence for global climate change. We are at a juncture where we are attempting to understand the earth as an integrated dynamic system, rather than a collection of isolated components.
NTIS
Climate Change; Atmospheric Composition; Man Environment Interactions; Paleoclimatology

20020001033 NASA Goddard Space Flight Center, Greenbelt, MD USA
Snow-Cover Variability in North America in the 2000-2001 Winter as Determined from MODIS Snow Products
Hall, Dorothy K., NASA Goddard Space Flight Center, USA; Salomonson, Vincent V., NASA Goddard Space Flight Center, USA; Riggs, George A., Science Systems and Applications, Inc., USA; Chien, Janet Y. L., General Sciences Corp., USA; [2001]; 4p; In English; IGARSS 2001, 9-13 Jul. 2001, Sydney, Australia; No Copyright; Avail: CASI; A01, Hardcopy; A01, Microfiche

Moderate Resolution Imaging Spectroradiometer (MODIS) snow-cover maps have been available since September 13, 2000. These products, at 500 m spatial resolution, are available through the National Snow and Ice Data Center Distributed Active Archive Center in Boulder, Colorado. by the 2001-02 winter, 5 km climate-modeling grid (CMG) products will be available for presentation of global views of snow cover and for use in climate models. All MODIS snow-cover products are produced from

automated algorithms that map snow in an objective manner. In this paper, we describe the MODIS snow products, and show snow maps from the fall of 2000 in North America.
Author
Spectroradiometers; Snow Cover; Mapping; North America

20020001234 Argonne National Lab., IL USA
Place for sodars in a high-technology environment
Coulter, R. L.; Jun. 12, 1998; 10p; In English
Report No.(s): DE2001-10849; ANL/ER/CP-96667; No Copyright; Avail: Department of Energy Information Bridge

In an era of increasingly complex technology, some of the atmospheric quantities most difficult to measure and observe are yielding their secrets to increasingly complex instruments and combinations of instruments. For example, water vapor profiles, a long-time nemesis to detailed examination, have become measurable with the use of Raman lidar; temperature profile measurements are becoming relatively routine with radio acoustic sounding systems (RASSs) or infrared Fourier transform instrumentation such as the atmospheric emitted radiance interferometer (AERI); and radar, lidar, or combinations of the two are enabling wind profile measurements to increasing altitudes. What, then, is the role of the relatively pedestrian sodar in such an era? Because the sodar's propagation speed in the atmosphere is six orders of magnitude smaller than that of its electromagnetic counterparts (3 x 10(sup 2) vs. 3 x 10(sup 8) m/s), severely limiting its rate of interrogation, and because the sodar's signal limit frequency modulation techniques, many high-technology advances associated with enormous increases in computation speed and available memory have had relatively little direct impact on acoustic remote sensing. However, the principal elements of acoustic remote sensing continue to make it a useful, even essential, tool for obtaining a better understanding of the physics of the lower atmosphere. The sodar's 'slow' propagation speed provides relatively easy access to the region between 10 m and several hundred meters above the surface that is often inaccessible to other instruments. This is the region of the atmosphere where conditions often change radically with height, the 'matching' region between large-scale forcing and small-scale surface heterogeneities that can have large effects on human activity. The atmosphere provides signals for sodars that are rich in content because the phase speed of sound is dependent on the atmosphere itself and is tied directly to the atmosphere's temperature and wind structure. Hence, the signals from acoustic remote sensing instruments can provide boundary conditions crucial for the proper operation of numerical models of the atmosphere whose output is becoming increasingly important in individual and business decision making.
NTIS
Meteorological Instruments; Sodar; Sound Detecting and Ranging; Earth Atmosphere

20020001242 State Univ. of New York, Albany, NY USA
Treatment of Cloud Radiative Effects in General Circulation Models ***Final Report***
Wang, W. C.; Oct. 08, 1998; 16p; In English
Report No.(s): DE2001-765963; DOE/ER/61073-1; No Copyright; Avail: Department of Energy Information Bridge

The objectives of our participation in the Atmospheric Radiation Measurement (ARM) program were: (1) to improve general circulation model (GCM) treatment of subgrid-scale variability of cloud-radiation interaction, and (2) to study the effect of variability on GCM climate simulations. Specifically, the studies focused on the development of a 'mosaic' approach to parameterize the variability associated with cloud vertical 'geometric association' and horizontal 'inhomogeneity' and the evaluation and improvement of radiative effects of aerosols and layer clouds. These studies were conducted using the shortwave and longwave radiation and cloud parameterizations employed in the SUNY-Albany regional climate model and the NCAR-CCM3 global climate model. The measurements at the ARM Southern Great Plains were used to evaluate and improve these GCM parameterizations. In addition, we also used the cloud resolving model simulations to supplement the cloud statistics, in particular the cloud geometric association and vertical water/ice distribution.
NTIS
Atmospheric General Circulation Models; Atmospheric Radiation; Climate Models; Climatology; Parameterization

20020001243 State Univ. of New York, Albany, NY USA
Atmospheric Ozone as a Climate Gas ***Final Report***
Wang, W. C.; Nov. 12, 1998; 7p; In English
Report No.(s): DE2001-765952; DOE/ER/61868-3; No Copyright; Avail: Department of Energy Information Bridge

This report summarizes the major research accomplishments of the project 'Atmospheric Ozone as a Climate Gas' for the period July 1, 1994 - March 31, 1998. The report is divided into three sections: research summary, publications, and participation of graduate students. The objectives of the research program were: (1) to improve understanding of the physical, chemical and dynamical processes that control mid-latitude O3 in the lower stratosphere and free troposphere; and (2) to develop improved

predictions of future O3 changes in these regions and their influence on (and response to) future climate changes. The research term includes a subcontractor, Professor Ivar Isaksen of the University of Oslo.
NTIS
Atmospheric Composition; Ozone; Stratosphere; Troposphere

20020001244 Massachusetts Univ., Amherst, MA USA
Climate System Studies ***Final Report***
Bradley, R. S.; Diaz, H. F.; Mar. 01, 2000; 12p; In English
Report No.(s): DE2001-765947; DOE/ER/69017-9; No Copyright; Avail: Department of Energy Information Bridge

In this final report, we summarize research on climate variability and forcing mechanisms responsible for these changes. We report on research related to high elevation climate change, changes in the hydrological cycle and the seasonality of precipitation, and on changes in climatic extremes. A comprehensive bibliography of research articles and books arising from this grant is included as an appendix.
NTIS
Climate Change; Climatology; Hydrological Cycle; Variability

20020001247 Meteorological Satellite Center, Kiyose, Japan
Monthly Report of the Meteorological Satellite Center: June 2001
June 2001; 2p; In English; CD-ROM conforms to the ISO 9660 standard for volume and file structure
Report No.(s): NONP-NASA-CD-2001150025; Copyright; Avail: Issuing Activity

The CD-ROM concerning the June 2001 Monthly Report of the Meteorological Satellite Center (MSC) contains the observation data derived from the Geostationary Meteorological Satellite (GMS) of Japan and the Polar Orbital Meteorological Satellites operated by NOAA. The CD-ROM contains the following observation data: Full Disk Earth's Cloud Image; Cloud Image of Japan and its vicinity; Cloud Amount; Sea Surface Temperature; Cloud Motion Wind; Water Vapor Motion Wind; Equivalent Blackbody Temperature; OLR (Out-going Longwave Radiation), Solar Radiation; Snow and Ice Index; Orbit Data; Attitude Data; VISSR Image Data Catalog (Cartridge Magnetic Tape (CMT), Micro Film); TOVS (TIROS Operational Vertical Sounder) Vertical Profile of Temperature and Precipitable Water; and TOVS Total Ozone Amount.
Derived from text
Satellite Observation; Satellite Sounding; Atmospheric Sounding; Meteorological Parameters; Satellite Imagery; Japan

20020001349 NASA Goddard Space Flight Center, Greenbelt, MD USA
Scanning Raman Lidar Measurements During the WVIOP2000 and AFWEX Field Experiments
Whiteman, David N., NASA Goddard Space Flight Center, USA; Evans, K. D., Maryland Univ. Baltimore County, USA; Berkoff, T. B., Maryland Univ. Baltimore County, USA; Demoz, B. D., Maryland Univ. Baltimore County, USA; DiGirolamo, P., Universita degli Studi della Basilicata, Italy; [2001]; 1p; In English; 2001 Atmospheric Radiation Measurement (ARM) Science Team Meeting, 19-23 Mar. 2001, Atlanta, GA, USA; No Copyright; Avail: Issuing Activity; Abstract Only

The NASA/Goddard Space Flight Center Scanning Raman Lidar (SRL) participated in the Water Vapor IOP 2000 (WVIOP2000) and ARM FIRE Water Vapor Experiment (AFWEX) at the DOE SGP CART site in northern Oklahoma. These experiments occurred during the period of September and December, 2000. The goals of both the WVIOP2000 and AFWEX were to better characterize the water vapor measurement capability of numerous sensors in the lower atmosphere and upper troposphere, respectively. The SRL received several hardware upgrades in anticipation of these experiments that permitted improved measurements of water vapor during the daytime and in the upper troposphere (UT). The daytime SRL water vapor error statistics were demonstrated a factor of 2-3 improvement compared to the permanently stationed CART Raman lidar (CARL). The performance of the SRL in the UT showed improvements as well. The technological upgrades that permitted these improved SRL measurements could also be implemented in the CARL system. Data examples demonstrating the new daytime and upper tropospheric measurement capability of the SRL will be shown at the meeting. In addition, preliminary analysis will be presented on several topics: 1) inter comparison of the water vapor measurements for several water vapor sensors including SRL, CARL, the NASA/Langley Lidar Atmospheric Sensing Experiment (LASE) flown onboard the NASA DC-8, in-situ sensors flown on the DC-8, and the Max Planck Institute Differential Absorption Lidar 2) comparison of cirrus cloud measurements using SRL and CARL and 3) case studies of meteorological events that occurred during the IOPs such as a cold frontal passage on the night of September 23.
Author
Optical Radar; Water Vapor; Radar Measurement; Gas Detectors; Clouds (Meteorology); Raman Spectroscopy

20020001516 Lawrence Livermore National Lab., Livermore, CA USA

Mean Evolution and Variability of the Asian Summer Monsoon: Comparison of ECMWF and NCEP/NCAR Reanalyses

Annamalai, H.; Hodges, K.; Slingo, J. M.; Sperber, K. R.; Apr. 21, 1999; 5p; In English

Report No.(s): DE2001-8801; UCRL-JC-129744-REV-2; No Copyright; Avail: Department of Energy Information Bridge, Microfiche

The behavior of the Asian Summer Monsoon is compared using the European Centre for Medium Range Weather Forecasts Reanalysis (ERA) and the National Centers for Environmental Prediction/National Center for Atmospheric Research (NCEP/NCAR) reanalysis. The goals of this paper are to identify common features between the reanalyses, to assess their robustness for model validation, and especially to use reanalyses to develop their understanding of the mean evolution of the Asian Summer Monsoon and the characteristics of its interannual and intraseasonal variability.

NTIS

Monsoons; Mathematical Models; Comparison; Prediction Analysis Techniques

20020001560 National Climatic Data Center, Asheville, NC USA

Data Preparation and Analysis for Annex III, USA/PRC Cooperation in the Field of Atmospheric Trace Gases

Easterling, D. R.; Karl, T. R.; Apr. 13, 1999; 13p; In English

Report No.(s): DE2001-6610; No Copyright; Avail: Department of Energy Information Bridge

The National Climatic Data Center (NCDC) has been a long-time and very active participant in the joint research program on the greenhouse effect created by the bilateral agreement Annex III to the Protocol on Fossil Energy Research and Development on Cooperation in the Field of Atmospheric Trace Gases. This agreement between the US Department of Energy (DOE) and the People's Republic of China, Chinese Academy of Sciences (CAS) has fostered a large amount of data set development and research, as well as science exchange between the two countries. Within the agreement there have been four basic tasks: (1) to analyze general circulation models, (2) to prepare, validate, and analyze data, (3) analyze the relationship between large scale and local climate, and (4) atmospheric trace gas measurements, particularly methane. Within this framework the NCDC has had two basic tasks in this program: to develop, validate, analyze and exchange long-term climate data sets suitable for analyzing past climate change, and to perform research into past climate change and linking large-scale and regional climates. Following is a brief review of NCDC's accomplishments in the project.

NTIS

Climate Change; Atmospheric Composition; Greenhouse Effect; International Cooperation

20020001578 Argonne National Lab., IL USA

Atmospheric Radiation Measurement Program Facilities Newsletter

Holdridge, D. J.; Sisterson, D. L.; June 1999; 5p; In English

Report No.(s): DE2001-12041; ANL/ER/RP-99516; No Copyright; Avail: Department of Energy Information Bridge

The Mesoscale Convective Systems (MCSs) Campaign is underway at the SGL CART site and will continue through September 1999. This field study is investigating the small-scale physics of precipitation and the convective dynamics of MCSs in the middle latitudes. An MCS is defined as a precipitation system that is 10-300 miles wide and contains deep convection at some time in its life span. MCSs occur in the midlatitudes of the US and can include large, isolated thunderstorms, squall lines, and mesoscale convective complexes.

NTIS

Precipitation (Meteorology); Convection; Mesoscale Phenomena; Atmospheric Radiation

20020001827 NASA Goddard Space Flight Center, Greenbelt, MD USA

Weather Prediction Improvement Using Advanced Satellite Technology

Einaudi, Franco, NASA Goddard Space Flight Center, USA; Uccellini, L., National Centers for Environmental Prediction, USA; Purdom, J., National Oceanic and Atmospheric Administration, USA; Rogers, D., National Oceanic and Atmospheric Administration, USA; Gelaro, R., NASA Goddard Space Flight Center, USA; Dodge, J., NASA, USA; Atlas, R., NASA Goddard Space Flight Center, USA; Lord, S., National Centers for Environmental Prediction, USA; [2001]; 4p; In English; IGARSS 2001, 9-13 Jul. 2001, Sydney, Australia; No Copyright; Avail: CASI; A01, Hardcopy; A01, Microfiche

We discuss in this paper some of the problems that exist today in the fall utilization of satellite data to improve weather forecasts and we propose specific recommendations to solve them. This discussion can be viewed as an aspect of the general debate on how best to organize the transition from research to operational satellites and how to evaluate the impact of a research instrument on numerical weather predictions. A method for providing this transition is offered by the National Polar-Orbiting Operational Environmental Satellite System (NPOESS) Preparatory Project (NPP). This mission will bridge the time between

the present NOAA and Department of Defense (DOD) polar orbiting missions and the initiation of the converged NPOESS series and will evaluate some of the Earth Observing System (EOS) instruments as appropriate for operational missions. Thus, this mission can be viewed as an effort to meet the operational requirements of NOAA and DOD and the research requirements of NASA. More generally, however, it can be said that the process of going from the conception of new, more advanced instruments to their operational implementation and full utilization by the weather forecast communities is not optimal. Instruments developed for research purposes may have insufficient funding to explore their potential operational capabilities. Furthermore, instrument development programs designed for operational satellites typically have insufficient funding for assimilation algorithms needed to transform the satellite observations into data that can be used by sophisticated global weather forecast models. As a result, years often go by before satellite data are efficiently used for operational forecasts. NASA and NOAA each have unique expertise in the design of satellite instruments, their use for basic and applied research and their utilization in weather and climate research. At a time of limited resources, the two agencies must combine their efforts to work toward common goals of full utilization of satellite data. This is a challenge that requires the assimilation of myriad new data into increasingly sophisticated numerical forecast models that run on increasingly sophisticated computer systems. In section II, we briefly outline the impact of satellite data on the quality of the National Centers for Environmental Prediction (NCEP) forecasts. In section III, we describe the present status of the utilization of satellite data in NCEP models and the challenges that lie ahead. In section IV, we propose solutions whose goals are summarized in section V.
Author
Weather Forecasting; Meteorological Satellites; Noess; Satellite Instruments

20020001835 Argonne National Lab., IL USA
CASES-97: Diurnal variation of the fair-weather PBL
Coulter, R. L.; Grossman, R. L.; Hicks, B.; Horst, T.; Klazura, G.; Nov. 18, 1997; 9p; In English
Report No.(s): DE2001-8888; ANL/ER/CP-94944; No Copyright; Avail: Department of Energy Information Bridge, Microfiche
The CASES-97 dataset, supplemented by data from the surrounding area and from satellite, will enable us to isolate the effects of soil moisture on boundary layer evolution. Our initial approach will be to use the integrated dataset to determine (a) the factors that contribute to PBL (planetary boundary layer) growth, and (b) the factors that determine the wind, temperature, and wind profiles in the growing PBL. This process will help us to consolidate the dataset and tease out remaining inconsistencies. As soon as reasonable, we want to use the dataset in mesoscale numerical models to test and refine our conclusions. Further detail on the CASES-97 field program can be found at the World Wide Web site at: http://www.mmm.ucar.edu/cases/cases.html.
NTIS
Soil Moisture; Boundary Layers; Earth Observations (From Space); Diurnal Variations

20020001843 Los Alamos National Lab., NM USA
Modeling the effects of land surface forcing on the North American Monsoon System
Gutzler, D. S.; Stalker, J. R.; Oct. 01, 2000; 5p; In English
Report No.(s): DE2001-765637; LA-UR-00-5080; No Copyright; Avail: Department of Energy Information Bridge, Microfiche
We describe a set of high-resolution model simulations of warm season precipitation using the RAMS (Regional Atmospheric Modeling System) nested grid model. We have three principal goals. First, we seek to ascertain whether RAMS produces a reasonable control simulation of summer rainfall across the southwestern USA, at the northern fringe of the North American Monsoon System (NAMS). Coarse resolution models have great difficulty producing precipitation across this inland, high-elevation region. Previous investigators have hypothesized that very high horizontal resolution may be required to property allow sufficient near-surface moisture to be advected as for inland as the Colorado Plateau.
NTIS
Monsoons; Atmospheric Models; Rain

20020001850 California Univ., San Diego, CA USA
ARESE (arm enhanced shortwave experiment) science plan (atmospheric radiation program)
Valero, F. P. J.; Schwartz, S. E.; Cess, R. D.; Ramanathan, V.; Collins, W. D.; Sep. 27, 1995; 35p; In English
Report No.(s): DE2001-765362; No Copyright; Avail: Department of Energy Information Bridge, Microfiche
Several recent studies have indicated that cloudy atmospheres may absorb significantly more solar radiation than currently predicted by models. The magnitude of this excess atmospheric absorption, is about 50% more than currently predicted and would have major impact on our understanding of atmospheric heating. Incorporation of this excess heating into existing general circulation models also appears to ameliorate some significant shortcomings of these models, most notably a tendency to overpredict the amount of radiant energy going into the oceans and to underpredict the tropopause temperature. However, some

earlier studies do not show this excess absorption and an underlying physical mechanism that would give rise to such absorption has yet to be defined. Given the importance of this issue, the Department of Energy's (DOE) Atmospheric Radiation Measurement (ARM) program is sponsoring the ARM Enhanced Shortwave Experiment (ARESE) to study the absorption of solar radiation by clear and cloudy atmospheres. The experimental results will be compared with model calculations. Measurements will be conducted using three aircraft platforms (ARM-UAV Egrett, NASA ER-2, and an instrumented Twin Otter), as well as satellites and the ARM central and extended facilities in North Central Oklahoma. The project will occur over a four week period beginning in late September, 1995. Spectral broadband, partial bandpass, and narrow bandpass (10nm) solar radiative fluxes will be measured at different altitudes and at the surface with the objective to determine directly the magnitude and spectral characteristics of the absorption of shortwave radiation by the atmosphere (clear and cloudy). Narrow spectral channels selected to coincide with absorption by liquid water and ice will help in identifying the process of absorption of radiation. Additionally, information such as water vapor profiles, aerosol optical depths, cloud structure and ozone profiles, needed to use as input in radiative transfer calculations, will be acquired using the aircraft and surface facilities available to ARESE. This document outlines the scientific approach and measurement requirements of the project.
NTIS
Solar Radiation; Clouds (Meteorology); Atmospheric Radiation; Atmospheric Heating

20020001852 Lamont-Doherty Geological Observatory, Palisades, NY USA
Recent changes of weather patterns in North America ***Progress Report, Aug. 15, 1985 - Feb. 28, 1998***
Kukla, G. J.; Dec. 31, 1998; 12p; In English
Report No.(s): DE2001-764707; DOE/ER/60372; No Copyright; Avail: Department of Energy Information Bridge
Several unique, quality adjusted data bases containing maximum and minimum surface air temperatures, the diurnal range, precipitation and cloud observations as well as upper air observations have been compiled over the course of this research. They have been made available through the National Climate Data Center (NCDC) as well as CDIAC of the Oak Ridge National Laboratory.
NTIS
North America; Diurnal Variations; Weather; Climate Change; Meteorology

20020001853 Pennsylvania State Univ., University Park, PA USA
Improvement in moist processes in atmospheric general circulation models: Validation and development through the CHAMMP Program ***Final Report***
Feb. 24, 2000; 5p; In English
Report No.(s): DE2001-764704; No Copyright; Avail: Department of Energy Information Bridge
The research supported by this grant consisted of two closely related studies. One of these involved further evolution and testing of a convective wake model designed to improve the parameterizatism of deep convection in climatic models. The second area consisted of a statistical analysis of two tropical data sets designed to examine the predictability of the moisture field in the atmosphere with the goal of determining the limits of predictability and to develop better methods of preventing slow drift of the moisture field in climate models.
NTIS
Moisture; Atmospherics; Climatology; Atmospheric General Circulation Models

20020002013 Mission Research Corp., Santa Barbara, CA USA
Sensitivity Assessment of Ozone Models
Shorter, J. A.; Rabitz, H. A.; Armstrong, R. A.; Jan. 24, 2000; 20p; In English
Report No.(s): DE2001-765534; No Copyright; Avail: Department of Energy Information Bridge, Microfiche
The activities under this contract effort were aimed at developing sensitivity analysis techniques and fully equivalent operational models (FEOMs) for applications in the DOE Atmospheric Chemistry Program (ACP). MRC developed a new model representation algorithm that uses a hierarchical, correlated function expansion containing a finite number of terms. A full expansion of this type is an exact representation of the original model and each of the expansion functions is explicitly calculated using the original model. After calculating the expansion functions, they are assembled into a fully equivalent operational model (FEOM) that can directly replace the original mode.
NTIS
Ozone; Sensitivity Analysis; Atmospheric Chemistry; Mathematical Models

20020002245 Arizona Univ., Tucson, AZ USA

Statistical analysis and interpretation of stratospheric ozone and temperature trends ***Final Report***

Hood, L. L.; Mar. 01, 2000; 7p; In English

Report No.(s): DE2001-765658; No Copyright; Avail: Department of Energy Information Bridge, Microfiche

The overall objective of the research conducted under this contract was to reduce uncertainties concerning anthropogenic changes to the ozone distribution, their causes, and possible climatic interactions.

NTIS

Statistical Analysis; Stratosphere; Ozone; Climate Change; Atmospheric Temperature

20020002372 NASA Goddard Space Flight Center, Greenbelt, MD USA

Microphysical Interpretation of Cirrus Measurements With Lidar

Reichardt, Jens, NASA Goddard Space Flight Center, USA; Lin, Ruei-Fong, NASA Goddard Space Flight Center, USA; Reichardt, Susanne, NASA Goddard Space Flight Center, USA; McGee, Thomas J., NASA Goddard Space Flight Center, USA; Starr, David OC., NASA Goddard Space Flight Center, USA; [2001]; 2p; In English; AGU Spring Meeting, 29 May - 2 Jun. 2001, Boston, MA, USA; Sponsored by American Geophysical Union, USA; No Copyright; Avail: Issuing Activity; Abstract Only

Cirrus measurements obtained with a ground-based polarization Raman lidar at 67.9 N in January 1997 reveal a strong correlation between the particle optical properties, specifically depolarization ratio delta and extinct ion-to-backscatter ratio S, for ambient cloud temperatures above approximately -45 C (delta less than approximately 40%), and an anti-correlation for colder temperatures (delta greater than approximately 40%). Over the length of the measurements (4-7.5 hours) the particle properties vary systematically: Initially, delta approximately equal to 60% and S approximately equal to 10sr are observed. Then, with decreasing delta, S first increases to approximately 27 sr(delta approximately equal to 40%) before decreasing to values around 10 sr again (delta approximately equal to 20%). The particle optical properties distinctly depend on the ambient temperature. For the microphysical analysis of the lidar observations. ray-tracing computations of particle scattering properties and a size-distribution resolving cirrus model with explicit microphysics have been used. The theoretical studies show that the optical properties and their temporal evolution can be interpreted in terms of size, shape, and growth of the cirrus particles: Near the cloud top in the early stage of the cirrus development, light scattering by small hexagonal columns with aspect ratios close to one is dominant. Over time the cloud base height extends to lower altitudes with warmer temperatures, the ice particles grow and get morphologically diverse (the scattering contributions of hexagonal columns and plates are roughly the same for large S and depolarization values of approximately 40%). In the lower ranges of the cirrus clouds, light scattering is predominantly by plate-like or complex ice particles. Mid-latitude cirrus data measured with the same instrument at 53.4 N between 1994 and 1996 follow closely the correlation between delta and S found in the warmer regions of the Arctic cirrus clouds (delta less than approximately 40%). Cirrus clouds with higher depolarization ratios are rarely observed, even for very cold ambient temperatures. Atmospheric parameters other than temperature, e.g., the availability of water vapor, are also important for the growth and the morphology of cirrus particles.

Author

Cirrus Clouds; Optical Radar; Optical Properties; Arctic Regions; Meteorological Parameters

20020002373 NASA Goddard Space Flight Center, Greenbelt, MD USA

Are US Great Plains Droughts Predictable on Seasonal and Longer Time Scales?

Schubert, Siegfried, NASA Goddard Space Flight Center, USA; [2001]; 1p; In English, 2 May 2001, Stony Brook, NY, USA; No Copyright; Avail: Issuing Activity; Abstract Only

The USA has experienced numerous episodes of unusually dry conditions lasting anywhere from months to several years. In this talk, I will examine the predictability of such episodes and the physical mechanisms controlling the variability of the summer climate of the continental United States. The analysis is based on ensembles of multi-year simulations and seasonal hindcasts generated with the NASA Seasonal-to-Interannual Prediction Project (NSIPP-1) General Circulation Model.

Author

Atmospheric General Circulation Models; Climate; Drought; Great Plains Corridor (North America); USA

20020002374 NASA Goddard Space Flight Center, Greenbelt, MD USA

Methods for Discerning Cloud Reflectivity Changes due to the Indirect Effect of Aerosol: A Pilot-study for Triana

Kinne, S., NASA Goddard Space Flight Center, USA; Wiscombe, Warren, NASA Goddard Space Flight Center, USA; [2001]; 1p; In English; AGU Meeting, 29 May - 2 Jun. 2001, Boston, MA, USA; Sponsored by American Geophysical Union, USA; No Copyright; Avail: Issuing Activity; Abstract Only

Understanding the effect of aerosol on cloud systems is one of the major challenges in atmospheric and climate research. Local studies suggest a multitude of influences on cloud properties. Yet the overall effect on cloud albedo, a critical parameter in climate simulations, remains uncertain. NASA's Triana mission will provide, from its EPIC multi-spectral imager, simultaneous data on aerosol properties and cloud reflectivity. With Triana's unique position in space these data will be available not only globally but also over the entire daytime, well suited to accommodate the often short lifetimes of aerosol and investigations around diurnal cycles. This pilot study explores the ability to detect relationships between aerosol properties and cloud reflectivity with sophisticated statistical methods. Sample results using data from the EOS Terra platform to simulate Triana are presented.
Author
Reflectance; Aerosols; NASA Space Programs; Cloud Physics; Climatology

20020002724 California Univ., Santa Barbara, CA USA
Climate Variability, Stochasticity and Learning in Integrated Assessment Models ***Final Report, 15 Sep. 1996 - 14 Sep. 1999***
Kolstad, C. D.; Sep. 14, 1999; 7p; In English
Report No.(s): DE2001-765627; No Copyright; Avail: Department of Energy Information Bridge, Microfiche
The focus of the work has been on climate variability and learning within computational climate-economy models (integrated assessment models - IAM's). The primary objective of the research is to improve the representation of learning in IAM's. This include's both endogenous and exogenous learning. A particular focus is on Bayesian learning about climate damage. A secondary objective is to improve the representation of climate variability within IAM's.
NTIS
Climate Models; Bayes Theorem; Climate; Variability

20020002732 Desert Research Inst., Reno, NV USA
Forest Response to CO2: Publications on or Related to Greenhouse Studies at the Desert Research Institute and Field Studies at Placerville
Johnson, D. W.; Oct. 14, 1998; 6p; In English
Report No.(s): DE2001-762870; No Copyright; Avail: Department of Energy Information Bridge
No abstract available.
NTIS
Deserts; Forests; Greenhouse Effect

20020002734 Aerodyne Research, Inc., Billerica, MA USA
Optical Water Vapor Sensor for Unmanned Aerial Vehicles
Berkoff, T. A.; Kebabian, P. L.; McClatchy, R. A.; Kolb, C. E.; Freedman, A.; Dec. 01, 1998; 70p; In English
Report No.(s): DE2001-762245; DOE/ER/81915; No Copyright; Avail: Department of Energy Information Bridge
The water vapor sensor developed by Aerodyne Research, based on the optical absorption of light at approximately 935 nm, has been successfully demonstrated on board the Pacific Northwest National Laboratory's Gulfstream-1 research aircraft during the Department of Energy's ARM Intensive Operations Period in August 1998. Data taken during this field campaign show excellent agreement with a chilled mirror and Lyman-alpha hygrometers and measurements confirm the ability to measure rapid, absolute water vapor fluctuations with a high degree of instrument stability and accuracy, with a noise level as low 10 ppmv (1 Hz measurement bandwidth). The construction of this small, lightweight sensor contains several unique elements which result in several significant advantages when compared to other techniques. First, the low power consumption Argon discharge lamp provides an optical beam at a fixed wavelength without a need for temperature or precision current control. The multi-pass absorption cell developed for this instrument provides a compact, low cost method that can survive deployment in the field. Fiber-optic cables, which are used to convey to light between the absorption cell, light source, and detection modules enable remote placement of the absorption cell from the opto-electronics module. Finally, the sensor does not use any moving parts which removes a significant source of potential malfunction. The result is an instrument which maintained its calibration throughout the field measurement campaign, and was not affected by high vibration and large uncontrolled temperature excursions. We believe that the development of an accurate, fast response water vapor monitor described in this report will open up new avenues of aerial-vehicle-based atmospheric research which have been relatively unexplored due to the lack of suitable low-cost, light-weight instrumentation.
NTIS
Optical Measuring Instruments; Water Vapor; Performance Tests

20020002749 Lawrence Livermore National Lab., Livermore, CA USA

Objective analysis of the ARM IOP data: Method and sensitivity

Cedarwall, R.; Lin, J. L.; Xie, S. C.; Yio, J. J.; Zhang, M. H.; Apr. 01, 1999; 51p; In English

Report No.(s): DE2001-12556; UCRL-JC-134096; No Copyright; Avail: Department of Energy Information Bridge

Motivated by the need of to obtain accurate objective analysis of field experimental data to force physical parameterizations in numerical models, this paper -first reviews the existing objective analysis methods and interpolation schemes that are used to derive atmospheric wind divergence, vertical velocity, and advective tendencies. Advantages and disadvantages of each method are discussed. It is shown that considerable uncertainties in the analyzed products can result from the use of different analysis schemes and even more from different implementations of a particular scheme. The paper then describes a hybrid approach to combine the strengths of the regular grid method and the line-integral method, together with a variational constraining procedure for the analysis of field experimental data. In addition to the use of upper air data, measurements at the surface and at the top-of-the-atmosphere are used to constrain the upper air analysis to conserve column-integrated mass, water, energy, and momentum. Analyses are shown for measurements taken in the Atmospheric Radiation Measurement Programs (ARM) July 1995 Intensive Observational Period (IOP). Sensitivity experiments are carried out to test the robustness of the analyzed data and to reveal the uncertainties in the analysis. It is shown that the variational constraining process significantly reduces the sensitivity of the final data products.

NTIS

Mathematical Models; Data Acquisition; Wind (Meteorology); Atmospheric Circulation; Radiation Measurement

20020002791 Argonne National Lab., IL USA

Comparing Modeled Isoprene with Aircraft-Based Measurements in the Atmospheric Boundary Layer

Doskey, P.; Gao, W.; Dec. 12, 1997; 7p; In English

Report No.(s): DE2001-8912; ANL/ER/CP-95090; No Copyright; Avail: Department of Energy Information Bridge, Microfiche

Nonmethane hydrocarbons (NMHCs) are involved in a complex series of reactions that regulate the levels of oxidants in the troposphere. Isoprene (C5H8), the primary NMHC emitted from deciduous trees, is one of the most important reactive hydrocarbons in the troposphere. The amount of isoprene entering the free troposphere is regulated by the compound's rate of emission from leaves and by chemical and physical processes in the forest canopy and the atmospheric boundary layer (ABL). This study uses a coupled canopy-ABL model to simulate these complex processes and compares calculated isoprene concentration profiles with those measured during aircraft flights above a forested region in the northeastern US. Land use information is coupled with satellite remote sensing data to describe spatial changes in canopy density during the field measurements. The high-resolution transport-chemistry model of Gao et al. for the ABL and the forest canopy layer is used to simulate vertical changes in isoprene concentration due to turbulent mixing and chemical reactions. The one-dimensional ABL model includes detailed radiation transfer, turbulent diffusion, biogenic emissions, dry deposition, and chemical processes within the forest canopy and the ABL. The measured profiles are compared with the model simulations to investigate the biological, physical, and chemical processes that regulate the levels of isoprene within the ABL.

NTIS

Atmospheric Boundary Layer; Canopies (Vegetation); Forests; Hydrocarbons; Turbulent Diffusion

20020002843 Los Alamos National Lab., NM USA

Shortwave transport in the cloudy atmosphere by anomalous/levy diffusion: New diagnostics using Forte Data

Davis, A. B.; Suszcynski, D. M.; Marshak, A.; Oct. 01, 2000; 21p; In English

Report No.(s): DE2001-766065; LA-UR-00-5193; No Copyright; Avail: Department of Energy Information Bridge, Microfiche

Anomalous photon diffusion can be described as an ad hoc modification of the popular 2-stream approximation, specifically the Eddington/diffusion version, for monochromatic radiative transfer in a scattering plane-parallel atmosphere. In the physical picture that describes the standard diffusion (hence the 2-stream) model, photons wander through horizontally infinite dense cloudy layers along convoluted random walks made of many short (theoretically Gaussian) steps.

NTIS

Clouds; Short Wave Radiation; Radiative Transfer; Photons

20020003574 Argonne National Lab., IL USA

Natural latitudinal distribution of atmospheric CO2

Taylor, J. A.; Orr, J. C.; May 30, 2000; 27p; In English

Report No.(s): DE2001-768563; ANL/CGC-002-0400; No Copyright; Avail: Department of Energy Information Bridge, Microfiche

Although poorly understood, the north-south distribution of the natural component of atmospheric CO2 offers information essential to improving our understanding of the exchange of CO2 between the atmosphere, oceans, and biosphere. The natural or unperturbed component is equivalent to that part of the atmospheric CO2 distribution, which is controlled by non-anthropogenic CO2 fluxes from the ocean and terrestrial biosphere. Models should be able to reproduce the true north-south gradient in CO2 due to the natural component before they can reliably estimate present-day CO2 sources and sinks and predict future atmospheric CO2. We have estimated the natural latitudinal distribution of atmospheric CO2, relative to the South Pole, using measurements of atmospheric CO2 during 1959-1991 and corresponding estimates of anthropogenic CO2 emissions to the atmosphere. Key features of the natural latitudinal distribution include (1) CO2 concentrations in the Northern Hemisphere that were lower than those in the Southern Hemisphere, (2) CO2 concentration differences that are higher in the tropics (associated with outgassing of the oceans) than those currently measured, and (3) CO2 concentrations over the Southern Ocean that are relatively uniform. This natural latitudinal distribution and its sensitivity to increasing fossil fuel emissions indicate that near-surface concentrations of atmospheric CO2 in the Northern Hemisphere are naturally lower than those in the southern hemisphere. Models that find the contrary will also mismatch present-day CO2 in the northern hemisphere and incorrectly ascribe that region as a large sink of anthropogenic CO2.

NTIS

Carbon Dioxide; Atmospheric Composition; Carbon Dioxide Concentration; Atmospheric Models

20020004024 NASA Ames Research Center, Moffett Field, CA USA

High Velocity Clouds

Wolfire, M. G., NASA Ames Research Center, USA; McKee, C. F., California Univ., USA; Hollenbach, D. J., NASA Ames Research Center, USA; Tielens, A. G. G. M., NASA Ames Research Center, USA; [1994]; 1p; In English; The Physics of the Interstellar Medium, 20-25 Jun. 1994, Elba, Italy; No Copyright; Avail: Issuing Activity; Abstract Only

We calculate the thermal equilibrium gas temperature of high velocity clouds (HVCs) in the Galactic Halo. Our method accounts for the photoelectric heating from small grains and PAHs, and includes a detailed treatment of the ionization rates and heating due to the soft X-ray background and due to cosmic rays. Phase diagrams (thermal pressure P versus gas density n) are presented for gas with a range of dust/gas ratios (D/G) and a range of metallicities (Z). Variations in D/G affect mainly the photoelectric heating rate, while variations in Z affect both the photoelectric heating and gas cooling. Curves are shown for D/G = 1 (local value) to D/G less than approx. equal to 0.005 and for Z=1 (local value) to Z= 0.005. We find that a two phase medium (CNM + WNM) can be in pressure equilibrium with a hot (T approximately 1-2 x 10(exp 6) K) halo within a range of permitted pressures, P(sup min) to P(sup max). We take halo parameters consistent with observed properties of the soft X-ray background. In general, both P(sup min) and P(sup max) decrease with lower D/G due to a drop in photoelectric heating from grains, while. P(sup min) and P(sup max) increase with lower Z due to a drop in gas coolants. We demonstrate that successful two phase models can be constructed with pressure in the range 10(exp 3) less than approximately equal to P/k less than approximately equal to 10(exp 4) K cm(exp -3) consistent with the thermal pressure in the Galactic disk. In addition, using the observed relation between CNM density and distance in HVCs, (n = 75/fDkpc cm(exp -3); Wakker & Schwarz 1991, AA, 250, 484) we show that our pressure curves constrain the allowed range of HVC heights to be between 0.3 - 16 kpc.

Author

Galactic Halos; Molecular Clouds; Photoelectricity; Thermodynamic Equilibrium; Gas Temperature; Velocity

20020004186 Pennsylvania State Univ., Dept. of Meteorology, University Park, PA USA

Numerical Study of the Role of Shallow Convection in Moisture Transport and Climate ***Final Report, 1 Jun. 1998 - 31 May 2001***

Seaman, Nelson L., Pennsylvania State Univ., USA; Stauffer, David R., Pennsylvania State Univ., USA; Munoz, Ricardo C., Pennsylvania State Univ., USA; Dec. 10, 2001; 205p; In English

Contract(s)/Grant(s): NAG8-1530; No Copyright; Avail: CASI; A10, Hardcopy; A03, Microfiche

The objective of this investigation was to study the role of shallow convection on the regional water cycle of the Mississippi and Little Washita Basins of the Southern Great Plains (SGP) using a 3-D mesoscale model, the PSU/NCAR MM5. The underlying premise of the project was that current modeling of regional-scale climate and moisture cycles over the continents is deficient without adequate treatment of shallow convection. At the beginning of the study, it was hypothesized that an improved treatment of the regional water cycle can be achieved by using a 3-D mesoscale numerical model having high-quality parameterizations for the key physical processes controlling the water cycle. These included a detailed land-surface parameterization (the Parameterization for Land-Atmosphere-Cloud Exchange (PLACE) sub-model of Wetzel and Boone), an advanced boundary-layer parameterization (the 1.5-order turbulent kinetic energy (TKE) predictive scheme of Shafran et al.), and a more complete shallow convection parameterization (the hybrid-closure scheme of Deng et al.) than are available in most current

models. PLACE is a product of researchers working at NASA's Goddard Space Flight Center in Greenbelt, MD. The TKE and shallow-convection schemes are the result of model development at Penn State. The long-range goal is to develop an integrated suite of physical sub-models that can be used for regional and perhaps global climate studies of the water budget. Therefore, the work plan focused on integrating, improving, and testing these parameterizations in the MM5 and applying them to study water-cycle processes over the SGP. These schemes have been tested extensively through the course of this study and the latter two have been improved significantly as a consequence.
Derived from text
Three Dimensional Models; Hydrological Cycle; Climatology; Convection; Computerized Simulation; Parameterization

20020004191 Maryland Univ. Baltimore County, Joint Center for Earth Systems and Technology, Catonsville, MD USA
Influence of 3D Radiative Effects on Satellite Retrievals of Cloud Properties
Varnai, Tamas, Maryland Univ. Baltimore County, USA; Marshak, Alexander, Maryland Univ. Baltimore County, USA; [2001]; 1p; In English; IAMAS Meeting, 10-18 Jul. 2001, Innsbruck, Austria; Sponsored by International Association of Meteorology and Atmospheric Sciences, Unknown; No Copyright; Avail: Issuing Activity; Abstract Only

When cloud properties are retrieved from satellite observations, the calculations apply 1D theory to the 3D world: they only consider vertical structures and ignore horizontal cloud variability. This presentation discusses how big the resulting errors can be in the operational retrievals of cloud optical thickness. A new technique was developed to estimate the magnitude of potential errors by analyzing the spatial patterns of visible and infrared images. The proposed technique was used to set error bars for optical depths retrieved from new MODIS measurements. Initial results indicate that the 1 km resolution retrievals are subject to abundant uncertainties. Averaging over 50 by 50 km areas reduces the errors, but does not remove them completely; even in the relatively simple case of high sun (30 degree zenith angle), about a fifth of the examined areas had biases larger than ten percent. As expected, errors increase substantially for more oblique illumination.
Author
Cloud Physics; Imaging Spectrometers; Satellite Observation; Infrared Imagery; Three Dimensional Models; Light (Visible Radiation)

20020004193 NASA Goddard Space Flight Center, Greenbelt, MD USA
Remote Sensing of Cloud, Aerosol, and Water Vapor Properties from MODIS
King, Michael D., NASA Goddard Space Flight Center, USA; Platnick, Steven, Maryland Univ. Baltimore County, USA; Menzel, W. Paul, National Environmental Satellite Service, USA; Kaufman, Yoram J., NASA Goddard Space Flight Center, USA; Ackerman, Steven A., Wisconsin Univ., USA; Tanre, Didier, Universite des Sciences et Techniques de Lille Flandres Artois, France; Gao, Bo-Cai, Naval Research Lab., USA; [2001]; 2p; In English; IGARSS 2001, 9-13 Jul. 2001, Sydney, Australia; No Copyright; Avail: Issuing Activity; Abstract Only

MODIS is an earth-viewing cross-track scanning spectroradiometer launched on the Terra satellite in December 1999. MODIS scans a swath width sufficient to provide nearly complete global coverage every two days from a polar orbiting, sun-synchronous, platform at an altitude of 705 kilometers, and provides images in 36 spectral bands between 0.415 and 14.235 micrometers with spatial resolutions of 250 meters (2 bands), 500 meters (5 bands) and 1000 meters (29 bands). These bands have been carefully selected to enable advanced studies of land, ocean, and atmospheric processes. In this presentation we review the comprehensive set of remote sensing algorithms that have been developed for the remote sensing of atmospheric properties using MODIS data, placing primary emphasis on the principal atmospheric applications of (i) developing a cloud mask for distinguishing clear sky from clouds, (ii) retrieving global cloud radiative and microphysical properties, including cloud top pressure and temperature, effective emissivity, cloud optical thickness, thermodynamic phase, and effective radius, (iii) monitoring tropospheric aerosol optical thickness over the land and ocean and aerosol size distribution over the ocean, (iv) determining atmospheric profiles of moisture and temperature, and (v) estimating column water amount. The physical principles behind the determination of each of these atmospheric products will be described, together with an example of their application using MODIS observations. All products are archived into two categories: pixel-level retrievals (referred to as Level-2 products) and global gridded products at a latitude and longitude resolution of 1 degree (Level-3 products). An overview of the MODIS atmosphere algorithms and products, status, validation activities, and early level-2 and -3 results will be presented.
Author
Aerosols; Atmospheric Chemistry; Remote Sensing; Troposphere; Cloud Physics; Scanners; Water Vapor; Imaging Spectrometers

20020004194 NASA Goddard Space Flight Center, Greenbelt, MD USA

A New "Cloud Mode" for the AERONET

Marshak, Alexander, Maryland Univ. Baltimore County, USA; Barker, H., Meteorological Service of Canada, Canada; Knyazikhin, Y., Boston Univ., USA; Wiscombe, W., NASA Goddard Space Flight Center, USA; [2001]; 1p; In English; IAMAS Meeting, 10-18 Jul. 2001, Innsbruck, Austria; Sponsored by International Association of Meteorology and Atmospheric Sciences, Unknown; No Copyright; Avail: Issuing Activity; Abstract Only

A key to predicting climate change is to observe an understand the global distribution of clouds and their physical properties such as optical thickness and droplet size. Since clouds change rapidly over short time and space intervals, they are difficult to simulate in computer models. But it is essential that global climate models predict realistic spatial and temporal distribution of cloud optical depth. The best way to verify these distributions is to infer optical depth from global coverage satellite data. However, satellite methods have many sources of uncertainty; thus, independent and reliable ground-based estimates are essential for validation. For aerosol, there is the AERONET - a ground based monitoring network that consists of identical multi-channel radiometers for assessing aerosol optical properties and validating their satellite retrievals. In addition to AEROSOL, we want the network monitoring CLOUD optical properties. It will use AERONET "time" (inappropriate for aerosol studies) to make basic new measurements related to cloud physics. In the presentation we will report on a new technique that retrieves cloud optical thickness for even broken clouds above green vegetation from surface measurements of zenith radiance in the visible (VIS) and near-IR (NIR) spectral regions. The idea of the method is simple: since green vegetation reflects 40-50% of incoming radiation in the NIR and only 5-10% in the VIS region, ground measurements under thin clouds have little spectral contrast between VIS and NIR, while thick clouds reflect much more of the surface-reflected radiation in the NIR than in VIS. Based on this idea, we use a combination of measurements (spectral indices) in VIS and NIR to estimate cloud optical thickness. by analogy with NDVI, the simplest index that can be defined is the Normalized Difference Cloud Index (NDCI) which is a ratio between the difference and the sum of two radiances measured for two narrow spectral bands in VIS and NIR.

Author

Climatology; Cloud Physics; Radiometers; Climate Models; Radiance; Optical Properties

20020005056 Los Alamos National Lab., NM USA

Balloon-Based High-Time Resolution Measurements of X-Ray Emissions from Lightning ***Final Report***

Eack, K.; Suszcynsky, D.; Aug. 01, 2000; 12p; In English

Report No.(s): DE2001-768729; LA-UR-00-3855; No Copyright; Avail: Department of Energy Information Bridge

This is the final report of a three-year, Laboratory-Directed Research and Development (LDRD) project at the Los Alamos National Laboratory (LANL). The project consisted of a series of balloon flights to collect high-time-resolution x-ray and electric-field-change measurements in thunderstorms in order to validate the existence of the runaway air-breakdown mechanism during lightning and/or sprite production. The runaway air-breakdown mechanism is currently the leading theory to account for unexplained balloon and aircraft-based measurements of x-ray enhancements associated with sprites. Balloon-borne gamma-ray and electric-field-change instruments were launched into a daytime summer thunderstorm. A greater than three-fold increase in the gamma-ray flux was observed as the balloon descended through a thunderstorm anvil where a strong electric field was present. These observations suggest that gamma-ray production in thunderstorms may not be as uncommon as previously believed.

NTIS

Balloon Sounding; Electrical Measurement; Gamma Rays; Lightning; X Rays

20020005096 NASA Goddard Space Flight Center, Greenbelt, MD USA

Interferometric Characterization of the Earth's Atmosphere from Lagrange Point 2

Herman, J. R., NASA Goddard Space Flight Center, USA; [2001]; 3p; In English; IGARSS 2001, July 2001, Sydney, Australia; No Copyright; Avail: CASI; A01, Hardcopy; A01, Microfiche

Part of the NASA plans for future Earth-Science missions calls for observations using novel vantage points that can produce science products otherwise unobtainable. Observations of the Earth from the Lagrange-2 point, L-2, (1.5 million kilometers behind the Earth on the Earth-Sun line) affords a unique vantage point for atmospheric science. Special observation of the Earth's atmosphere using solar occultation techniques in the near infrared (1 to 4 microns) provides one of the most accurate method of passively sensing altitude profiles of the major species (CO2, O3, O2, CH4, H2O, N2O). In addition to observation of the Earth's atmosphere, it will be possible to observe a portion of the solar disk at moderate spatial resolution without interference from the Earth.

Derived from text

Atmospheric Chemistry; Atmospheric Physics; Earth Atmosphere; Near Infrared Radiation; Earth Sciences

20020005193 Los Alamos National Lab., NM USA

Marine boundary-layer cloud structure from CM- to KM-scales

Davis, A.; Apr. 01, 2000; 10p; In English

Report No.(s): DE2001-768975; LA-UR-00-2067; No Copyright; Avail: Department of Energy Information Bridge

The authors analysis of small-scale LWC fluctuations in PVM-100A data from SOCEX-1 supports the still controversial claim that droplet concentration is not everywhere Poissonian. This does not exclude a slow (spectral exponent (beta) = 5/3) low-amplitude component in the variability of droplet number and size distribution. We believe the cause of the excess small-scale LWC variance causing the scale-break at 2-5 m lies in entrainment- and/or-mixing events; such processes may be related to the intermittency (occasional bursts of variability at the inner-scale) associated with the large-scale multifractality. Comparing exponents obtained for large-scale behavior with those previously obtained from two other field programs, we uncover remarkable similarities between the basic multifractal (i.e., arbitrary-order structure function) properties of LWC in SOCEX, FIRE and ASTEX clouds and those of passively advected scalars in turbulent flows. However, we also find interesting differences between the three kinds of marine cloud cover and with passive scalars but these are in the details of the various multifractal characterizations (inner and outer scales, high-order scaling). to reproduce these statistical behaviors defines a quantitatively-precise challenge for the cloud-modeling community.

NTIS

Marine Meteorology; Clouds (Meteorology); Boundary Layers; Cloud Cover

20020005208 Dalhousie Univ., Halifax, Nova Scotia Canada

Development and Testing of a Short-Wave Radiation Model for Interpreting ARM Data ***Final Report, 15 Jan. 1997 - 15 Mar. 2000***

Fu, Q.; Oct. 15, 2000; 10p; In English

Report No.(s): DE2001-769167; No Copyright; Avail: Department of Energy Information Bridge, Microfiche

A research program devoted to improving the understanding of atmospheric radiation processes has been supported by DOE ARM grants with Prof. Qiang Fu as the Principal Investigator. This final report summarizes our research efforts, which emphasizes the findings and their significance to the solar radiative transfer in clear atmospheres, the effects of 3-D cloud fields on the solar radiative energy budget, a better understanding of radiative properties of nonspherical ice crystals, and parameterization of radiation processes for use in the GCMs and satellite remote sensing.

NTIS

Atmospheric Radiation; Short Wave Radiation; Models; Clouds (Meteorology); Computational Chemistry

20020005410 NASA Goddard Space Flight Center, Greenbelt, MD USA

Cloud Structure and Cloud-Radiation Interaction: From Smallest Observable Scales (Less than 10 m) to GCM Grid Scales (More than 100 km)

Marshak, Alexander, Maryland Univ. Baltimore County, USA; Davis, A. B., Los Alamos National Lab., USA; Wiscombe, W. J., NASA Goddard Space Flight Center, USA; [2001]; 1p; In English; AGU Spring Meeting, 29 May - 2 Jun. 2001, Boston, MA, USA; Sponsored by American Geophysical Union, USA; No Copyright; Avail: Issuing Activity; Abstract Only

In this presentation we review the fractal nature of internal cloud structure from cm- to km-scales as captured by in-situ probes during long horizontal penetrations by aircraft. We uncover the non-Poissonian spatial distribution of cloud droplets at submeter scales and confirm scale-invariant behavior for large scales. Based on these structural characteristics, we generate simple fractal cloud models that reproduce statistical scaling properties of real clouds. These stochastic models represent a link between nonlinear science, in general, and cloud-radiation interaction, in particular. Next we run three-dimensional radiative transfer computations on these synthetic fractal clouds and compare the structure of the resulting radiation fields with the known structure of the cloud model and with satellite images of real clouds. The different behaviors observed for small and large-scale variabilities will be discussed in detail. We find that while the large-scale fluctuations of the resulting radiation fields resemble those in the original scale-invariant cloud structure, the radiation at small scales is much smoother than its cloud liquid water counterpart. This violates scale-invariance and produces a scale-break at 0.2-0.5 km that is clearly observed in high-resolution satellite data such as from LANDSAT. Finally, we show how radiative transfer Green function theory in the photon diffusion limit explains (and predicts) the above phenomena of ”radiative smoothing.”

Author

Cloud Physics; Clouds (Meteorology); Fractals; Atmospheric Models; Radiation Distribution

20020005413 NASA Goddard Space Flight Center, Greenbelt, MD USA

Polar Cirrus Cloud Properties Through Long-Term Lidar and Radiometer Observations

Spinhirne, James, NASA Goddard Space Flight Center, USA; Campbell, James, Maryland Univ. Baltimore County, USA; Mahesh, Ashwin, Science Systems and Applications, Inc., USA; Welton, Judd, Maryland Univ. Baltimore County, USA; [2001]; 1p; In English; IEEE IGARSS 2001 Meeting, 9-13 Jul. 2001, Sydney, Austria; Sponsored by Institute of Electrical and Electronics Engineers, USA; No Copyright; Avail: Issuing Activity; Abstract Only

In comparison to mid latitude cloud cover, knowledge of polar cirrus and other cloud cover is limited. The interpretations of satellite-based cloud imaging and retrievals in polar regions have major problems due to factors such as darkness and extreme low temperatures. Beginning in 2002 a NASA orbiting lidar instrument, GLAS, (Geoscience Laser Altimeter System) will unambiguously define cloud type and fraction with good coverage of polar regions. Active laser sensing gives the spatial and temporal distribution of clouds and diamond dust. In preparation for, and supplementing the GLAS measurements are ground based MP (micro pulse) lidar experiments providing continuous profiling. MP lidar installations have been operating at the South Pole since December 1999 and at the Atmospheric Radiation Measurement (ARM) program arctic site since 1996. Both at the ARM Barrow, Alaska site and at the South Pole station, Fourier-transform interferometers also observe clouds in the wavelength intervals between approximately 5 and 18 microns. Spectral instruments can yield cloud microphysical properties with additional information from lidar about the vertical extent of clouds being modeled. We examine the simultaneous lidar and spectral data from both Barrow and South Pole, to obtain cloud properties (optical depth, particle size) by the use of both instruments. The results have applications to interpretation of current satellite data, and GLAS measurements when available.
Author

Remote Sensing; Cirrus Clouds; Cloud Cover; Polar Regions; Cloud Physics

20020005414 NASA Goddard Space Flight Center, Greenbelt, MD USA

Optimizing Orbit-Instrument Configuration for Global Precipitation Mission (GPM) Satellite Fleet

Smith, Eric A., NASA Goddard Space Flight Center, USA; Adams, James, NASA Goddard Space Flight Center, USA; Baptista, Pedro, European Space Agency. European Space Research and Technology Center, ESTEC, Netherlands; Haddad, Ziad, Jet Propulsion Lab., California Inst. of Tech., USA; Iguchi, Toshio, Communications Research Lab., Japan; Im, Eastwood, Jet Propulsion Lab., California Inst. of Tech., USA; Kummerow, Christian, Colorado State Univ., USA; [2001]; 2p; In English; IEEE IGARSS 2001 Meeting, 9-13 Jul. 2001, Sydney, Australia; Sponsored by Institute of Electrical and Electronics Engineers, USA; No Copyright; Avail: Issuing Activity; Abstract Only

Following the scientific success of the Tropical Rainfall Measuring Mission (TRMM) spearheaded by a group of NASA and NASDA scientists, their external scientific collaborators, and additional investigators within the European Union's TRMM Research Program (EUROTRMM), there has been substantial progress towards the development of a new internationally organized, global scale, and satellite-based precipitation measuring mission. The highlights of this newly developing mission are a greatly expanded scope of measuring capability and a more diversified set of science objectives. The mission is called the Global Precipitation Mission (GPM). Notionally, GPM will be a constellation-type mission involving a fleet of nine satellites. In this fleet, one member is referred to as the "core" spacecraft flown in an approximately 70 degree inclined non-sun-synchronous orbit, somewhat similar to TRMM in that it carries both a multi-channel polarized passive microwave radiometer (PMW) and a radar system, but in this case it will be a dual frequency Ku-Ka band radar system enabling explicit measurements of microphysical DSD properties. The remainder of fleet members are eight orbit-synchronized, sun-synchronous "constellation" spacecraft each carrying some type of multi-channel PMW radiometer, enabling no worse than 3-hour diurnal sampling over the entire globe. In this configuration the "core" spacecraft serves as a high quality reference platform for training and calibrating the PMW rain retrieval algorithms used with the "constellation" radiometers. Within NASA, GPM has advanced to the pre-formulation phase which has enabled the initiation of a set of science and technology studies which will help lead to the final mission design some time in the 2003 period. This presentation first provides an overview of the notional GPM program and mission design, including its organizational and programmatic concepts, scientific agenda, expected instrument package, and basic flight architecture. Following this introduction, we focus specifically on the last topic, that being an analysis which leads to an optimal flight architecture dictated in part by science requirements but constrained by allowable orbital mechanics, instrument scan patterns, and antenna aperture properties. Because the optimal architecture involves an interplay between orbit mechanics and instrument specifications, it is important to recognize that in attempting to serve various scientific themes, the final optimal architecture will represent a compromise concerning dynamic range, spatial resolution, sampling interval, pointing, beam coincidence, and measurement uncertainty. Moreover, cost becomes a major factor in seeking the optimal architecture through the pathways of antenna and instrument scan designs, as well as propulsion requirements associated with the orbit heights of various

”constellation” members. Although the results presented at the IGARSS-2001 meeting will likely not be the fully refined flight architecture specifications, they are expected to be nearly complete.
Author
Precipitation (Meteorology); Satellite Constellations; Microwave Radiometers; Radar Measurement

20020005867 Naval Postgraduate School, Dept. of Meteorology, Monterey, CA USA
Verification and Validation of the Satellite Marine-Layer/Elevated Duct Height (SMDH) Technique ***Final Report, May-Dec. 2000***
Jordan, Mary S.; Durkee, Philip A.; Dec. 2000; 32p; In English; Original contains color images
Report No.(s): AD-A395269; NPS-MR-01-001; No Copyright; Avail: CASI; A03, Hardcopy; A01, Microfiche

This report is the verification and validation of the Satellite Marine-layer/Evaporation Duct Height (SMDH) technique under development by NAWC Point Mugu California. The technique provides an estimate of the cloud-top height of stratocumulus clouds in the marine boundary layer for the area viewed by a polar orbiting weather satellite. The top of the marine boundary layer is the optimum coupling height for elevated ducts. Knowledge of the elevated duct height over the tactical battlespace is quite important. The SMDH technique is one component of a potential shipboard operational system to provide estimates of elevated duct height. The SMDH technique is verified using NOAA AVHRR satellite data and coincident rawinsonde or aircraft measurements from the 1987 FIRE and 1994 MAST data sets The SMDH technique which uses an empirical relationship to relate the satellite cloud-top temperature sea-surface temperature and cloud-top height is quite useful. There are advantages to using a physically-based model rather than an empirical equation, to estimate cloud-top height. Some of these advantages are demonstrated using the Naval Postgraduate School’s physically-based model with the FIRE and MAST data sets. Conclusions/recommendations include (1) the automation of a cloud-top estimation technique is achievable and development should continue, (2) use a physically-based model, rather than an empirical equation, as the core component of the cloud-top height estimation process.
DTIC
Marine Meteorology; Clouds (Meteorology); Meteorological Satellites; Cloud Height Indicators; Data Acquisition; Advanced Very High Resolution Radiometer

48
OCEANOGRAPHY

Includes the physical, chemical and biological aspects of oceans and seas; ocean dynamics, and marine resources. For related information see also 43 Earth Resources and Remote Sensing.

20020000921 Smithsonian Institution, Edgewater, MD USA
Effects of long term elevated CO2 exposure on a Chesapeake Bay wetland. Final report
Drake, B. G.; Dec. 01, 1995; 8p; In English
Report No.(s): DE2001-764439; DOE/ER/60374-1-VOL-1; No Copyright; Avail: Department of Energy Information Bridge

Since 1987, a field project to determine the effects of elevated CO2 on an ecosystem’s processes has been in progress on a Chesapeake Bay wetland. Open top chambers are used to create a test atmosphere of present ambient CO2 and twice ambient (Drake, et al.,1989). Chambers were placed on the marsh from April as shoots emerge until late November. There were 45 sites in three plant communities. In each community, one third of the sites were exposed to normal ambient CO2, one third to elevated CO2 and the remaining sites have no chambers. CO2 was provided to increase the midday CO2 concentration 350 ppm above normal ambient and was continuously provided each growing season beginning in April, 1987. There were three plant communities: a monoculture of the C4 grass, Spartina patans, a monoculture of the C3 sedge, Scirpus olneyi,and the third a mixture of the other two with a third species, the C4 grass, Distichlis spicata. The site included a building to house monitoring equipment and personnel as well as a large screened porch where field experiments are assembled and other work is carried out. The goals of this project were to determine the impact of elevated CO2 on ecosystem processes, to do this, we studied biomass production, nutrient and water balance, net ecosystem CO2 and H2O exchange (measured by converting open top chambers to open gas exchange chambers with addition of a top and stack and monitoring change in CO2 and I-IZO concentrations of air passing through chamber), single leaf gas exchange, dark respiration, and competition among the three perennial species.
NTIS
Chesapeake Bay (US); Ecosystems; Exposure; Marshlands; Carbon Dioxide Concentration

20020001079 Lawrence Livermore National Lab., Livermore, CA USA

Initial statistical evaluation of ARAC COAMPS forecasts

Pace, J. C.; Jun. 30, 1999; 6p; In English

Report No.(s): DE2001-12119; UCRL-JC-134777; No Copyright; Avail: Department of Energy Information Bridge, Microfiche

This informal workshop was organized to bring together scientists and engineers from St0 and LLNL with a common interest in using and developing new in-situ measurement techniques for studying the coastal ocean, particularly near-surface waters in the biologically active photic layer. Much of the discussion focused on the current and potential capabilities of the LLNL "IMEEDS" ocean observation capability (Integrated Marine Environmental Element Detection System), and ways to complement and process the data that can be obtained from the system. Two important goals of the workshop were to identify the range of current activities that could be usefully integrated with the capabilities of the LLNL system, and to explore additional scientific problems of the coastal ocean that could be addressed through collaborative LLNL - SIO efforts. A short summary of the issues addressed follows, with lead discussants identified. A series of action items developed during the course of the workshop, a list of participants, and a conference agenda conclude this report.

NTIS

Weather Forecasting; Coastal Water; In Situ Measurement

20020001355 NASA Goddard Space Flight Center, Greenbelt, MD USA

A Multiyear Dataset of SSM/I-Derived Global Ocean Surface Turbulent Fluxes

Chou, Shu-Hsien, NASA Goddard Space Flight Center, USA; Shie, Chung-Lin, NASA Goddard Space Flight Center, USA; Atlas, Robert M., NASA Goddard Space Flight Center, USA; Ardizzone, Joe, NASA Goddard Space Flight Center, USA; Nelkin, Eric, NASA Goddard Space Flight Center, USA; [2001]; 1p; In English; 11th Conference on Interactions of Sea and Atmosphere, 14-18 May 2001, San Diego, CA, USA; No Copyright; Avail: Issuing Activity; Abstract Only

The surface turbulent fluxes of momentum, latent heat, and sensible heat over global oceans are essential to weather, climate and ocean problems. Evaporation is a key component of the hydrological cycle and the surface heat budget, while the wind stress is the major forcing for driving the oceanic circulation. The global air-sea fluxes of momentum, latent and sensible heat, radiation, and freshwater (precipitation-evaporation) are the forcing for driving oceanic circulation and, hence, are essential for understanding the general circulation of global oceans. The global air-sea fluxes are required for driving ocean models and validating coupled ocean-atmosphere global models. We have produced a 7.5-year (July 1987-December 1994) dataset of daily surface turbulent fluxes over the global oceans from the Special Sensor microwave/Imager (SSM/I) data. Daily turbulent fluxes were derived from daily data of SSM/I surface winds and specific humidity, National Centers for Environmental Prediction (NCEP) sea surface temperatures, and European Centre for Medium-Range Weather Forecasts (ECMWF) air-sea temperature differences, using a stability-dependent bulk scheme. The retrieved instantaneous surface air humidity (with a 25-km resolution) validated well with that of the collocated radiosonde observations over the global oceans. Furthermore, the retrieved daily wind stresses and latent heat fluxes were found to agree well with that of the in situ measurements (IMET buoy, RV Moana Wave, and RV Wecoma) in the western Pacific warm pool during the TOGA COARE intensive observing period (November 1992-February 1993). The global distributions of 1988-94 seasonal-mean turbulent fluxes will be presented. In addition, the global distributions of 1990-93 annual-means turbulent fluxes and input variables will be compared with those of UWM/COADS covering the same period. The latter is based on the COADS (comprehensive ocean-atmosphere data set) and is recognized to be one of the best climatological analyses of fluxes derived from ship observations.

Author

Atmospheric Models; Latent Heat; Ocean Surface; Remote Sensing; Turbulence; Climatology; Annual Variations; Microwave Imagery

20020001769 Coast Guard, Washington, DC USA

Report of the International Ice Patrol in the North Atlantic. 1992 Season

1992; 54p; In English

Report No.(s): PB2002-100029; USCG-188-47; USCG-BULL-78; No Copyright; Avail: CASI; A04, Hardcopy; A01, Microfiche

This is the 78th annual report on the International Ice Patrol (IIP). It contains information on Ice patrol operations, environmental conditions, and ice conditions for the 1992 IIP season. The U.S. Coast Guard conducts the International Ice Patrol Service in the North Atlantic under the provisions of U.S. Code, Title 46, Sections 738, 738a through 738d, and the International Convention for the Safety of Life at Sea (SOLAS), 1974, regulations 5-8. This service was initiated shortly after the sinking of the RMS TITANIC on April 15, 1912 and has been provided seasonally since that time.

NTIS

Sea Ice; Icebergs; Oceanography

20020001770 Coast Guard, Washington, DC USA

Report of the International Ice Patrol in the North Atlantic. 1995 Season

1995; 86p; In English

Report No.(s): PB2002-100023; USCG-BULL-81; USCG-188-50; No Copyright; Avail: CASI; A05, Hardcopy; A01, Microfiche

This is the 81st annual report of the International Ice Patrol (IIP). It contains information on Ice Patrol operations, environmental conditions, and ice conditions for the 1995 IIP season. The U.S. Coast Guard conducts the Ice Patrol in the North Atlantic under the provisions of U.S. Code, Title 46, Sections 738, 738a through 738d, and the International Convention for the Safety of Life at Sea (SOLAS), 1974. The IIP is supported by 17 member nations (Appendix A). It was initiated shortly after the sinking of the RMS TITANTIC on April 15, 1912 and has been conducted seasonally since that time.

NTIS

Ice; Weather Reconnaissance Aircraft; Atlantic Ocean; Coasts; Safety

20020001856 Rutgers - The State Univ., New Brunswick, NJ USA

Variability of carbon system parameters in coastal waters of the Mid-Atlantic Bight off New Jersey: A link to the Ocean Margins Program *Final Report*

Reimers, C. E.; Dec. 31, 1997; 4p; In English

Report No.(s): DE2001-764618; No Copyright; Avail: Department of Energy Information Bridge

The overall objective of this one year project was to maintain a program of inorganic carbon system parameters for waters from a region of the shelf off New Jersey as a temporal record of chemical and physical conditions 'upstream' of DOE's Ocean Margin Program experimental site off Cape Hatteras, NC.

NTIS

Carbon; Coastal Water; Oceans; Bays (Topographic Features)

20020001882 Princeton Univ., Plasma Physics Lab., NJ USA

Final report for 'Global survey of carbon dioxide in the ocean'

Sarmiento, J. L.; Key, R. M.; Sabine, C. L.; Jul. 01, 1998; 7p; In English

Report No.(s): DE2001-764607; No Copyright; Avail: Department of Energy Information Bridge

In the five years covered by this grant we have built a state-of-the-art, high precision, sea-going CO2 lab from scratch. We started off small, helping T. Takahashi's group make measurements as we built our instruments and trained personnel. Our first cruise with total responsibility for carbon measurements was near the end of the first year. Since then we have improved the precision of our measurements and more than doubled the number of samples we can process at sea. We have been an active part of the DOE science team and have contributed to several related DOE projects like the development of the DOE Methods Handbook (DOE, 1994) and instrument intercomparison exercises and training workshops. The underway pC02 instrument developed in our lab was selected by the science team to make measurements on every leg of the Indian Ocean survey. It ran nearly continuously during the 14 months of back-to-back-cruises and generated approximately 200,000 surface seawater and 50,000 marine air pC02 measurements. Princeton's portion of the field program was completed in September of 1997 with the completion of two meridional sections in the western North Atlantic. All data have been reported to the Carbon Dioxide Information Analysis Center (CDIAC) and are either published or in preparation.

NTIS

Carbon Dioxide; Seas; Oceans; Ecosystems

20020002246 North Carolina State Univ., Raleigh, NC USA

Benthic carbon budget for the Continental Slope off Cape Hatteras, NC

Blair, N.; Dec. 01, 1999; 103p; In English

Report No.(s): DE2001-765626; No Copyright; Avail: Department of Energy Information Bridge, Microfiche

The continental slope off Cape Hatteras, N,C. from approximately 36 deg. 00'N to 35 deg. 20'N is a region of relatively rapid sediment accumulation, organic matter deposition and subsequent remineralization. The measured fluxes are the highest reported for the slope off the eastern U.S. Sediment accumulation rates range from 40 to 140 cm ky(supi). Organic carbon deposition rates range from 3.5 to 7.4 moles C square m/yr. The areal coverage of this "depocenter" is probably controlled by interactions between physical oceanographic processes and the rugged topography of the seafloor.

NTIS

Carbon; Ocean Bottom; Continental Shelves; Cape Hatteras (Nc)

20020002295 North Carolina State Univ., Raleigh, NC USA

Biogeochemistry of carbon in continental slope sediments: The North Carolina margin

Blair, N.; Levin, L.; DeMaster, D.; Plaia, G.; Martin, C.; Dec. 01, 1999; 46p; In English

Report No.(s): DE2001-765318; No Copyright; Avail: Department of Energy Information Bridge

The responses of the continental slope benthos to organic detritus deposition were studied with a multiple trace approach. Study sites were offshore of Cape Fear (I) and Cape Hatteras (III), N.C. (both 850 m water depth) and were characterized by different organic C deposition rates, macrofaunal densities and taxa. Natural abundances of (sup 13)C and (sup 12)C in particulate organic carbon (POC), dissolved inorganic carbon (DIC) and macrofauna indicate that the reactive organic detritus is marine in origin. Natural abundance levels of (sup 14)C and uptake of (sup 13)C-labeled diatoms by benthic animals indicate that they incorporate a relatively young component of carbon into their biomass. (sup 13)C-labeled diatoms (Thalassiorsira pseudonana) tagged with (sup 210)Pb, slope sediment tagged with (sup 113)Sn and (sup 228)Th-labeled glass beads were emplaced in plots on the seafloor at both locations and the plots were sampled after 30 min., 1-1.5 d and 14 mo. At Site I, tracer diatom was intercepted at the surface primarily by protozoans and surface-feeding annelids. Little of the diatom C penetrated below 2 cm even after 14 months. Oxidation of organic carbon appeared to be largely aerobic. At Site III, annelids were primarily responsible for the initial uptake of tracer. On the time scale of days, diatom C was transported to a depth of 12 cm and was found in animals collected between 5-10 cm. The hoeing of tracer from the surface by the maldanid Praxillela sp. may have been responsible for some of the rapid nonlocal transport. Oxidation of the diatom organic carbon was evident to at least 10 cm depth. Anaerobic breakdown of organic matter is more important at Site III. Horizontal transport, which was probably biologically mediated, was an order of magnitude more rapid than vertical displacement over a year time scale. If the horizontal transport was associated with biochemical transformations of the organic matter, it may represent an important but nearly invisible diagenetic process.

NTIS

Biogeochemistry; Carbon; Ocean Bottom; Continental Shelves; Sediments

20020002299 North Carolina Univ., Chapel Hill, NC USA

Deposition and fate of modern organic carbon in shelf/upper slope sediments near Cape Hatteras, North Carolina ***Final Report***

Martens, C.; Alperin, M.; Albert, D.; Dec. 31, 1998; 17p; In English

Report No.(s): DE2001-765243; No Copyright; Avail: Department of Energy Information Bridge

Sulfate reduction rates (SRR) measured in North Carolina continental shelf and upper slope sediments using shipboard techniques appeared to be anomolously high relative to estimates or organic carbon input and remineralization. The SRR have also appeared to be incompatible with the relative lack of sulfate depletion seen in sediment porewaters below 30 cm depth unless relatively deep (but slow) bioirrigation is invoked. of the possible reason the rates could be too high, the most probable reason seemed to be the pressure shock associated with bringing deep samples to the surface, possibly releasing intracellular organic substrates usable by sulfate reducers.

NTIS

Sediments; Sulfates; Continental Shelves; North Carolina

20020002361 California State Univ., San Diego, CA USA

Measurements of Surface Ocean Carbon Dioxide Partial Pressure During WOCE ***Final Report, 1 Jun. 1990 - 31 May 1998***

Weiss, R. F.; May 31, 1998; 58p; In English

Report No.(s): DE2001-765744; No Copyright; Avail: Department of Energy Information Bridge, Microfiche

No abstract prepared.

NTIS

Ocean Surface; Carbon Dioxide; Partial Pressure

20020002860 Colorado Univ., Center for Astrodynamics Research, Boulder, CO USA

Comparison of QuikSCAT and GPS-Derived Ocean Surface Winds ***Final Report, 1 Aug. 2000 - 31 Jul. 2001***

Axelrad, Penina, Colorado Univ., USA; Dec. 05, 2001; 15p; In English

Contract(s)/Grant(s): NAG5-9727

Report No.(s): PA-01-235; No Copyright; Avail: CASI; A03, Hardcopy; A01, Microfiche

The Colorado Center for Astrodynamics has completed a study comparing ocean surface winds derived from GPS bistatic measurements with QuikSCAT wind fields. We have also compiled an extensive database of the bistatic GPS flight data collected

by NASA Langley Research Center over the last several years. The GPS data are augmented with coincident data from QuikSCAT, buoys, TOPEX, and ERS.
Author
Wind Velocity; Ocean Surface; Velocity Distribution

20020003349 NASA Goddard Space Flight Center, Greenbelt, MD USA
A Modeling Study of Oceanic Response to Daily and Monthly Surface Forcing
Sui, Chung-Hsiung, NASA Goddard Space Flight Center, USA; Li, Xiao-Fan, NASA Goddard Space Flight Center, USA; Rienecker, Michele M., NASA Goddard Space Flight Center, USA; Lau, William K.-M., NASA Goddard Space Flight Center, USA; [2001]; 1p; In English; AMS Conference, 14-18 May 2001, San Diego, CA, USA; Sponsored by American Meteorological Society, USA; No Copyright; Avail: Issuing Activity; Abstract Only

The goal of this study is to investigate the effect of high-frequency surface forcing (wind stresses and heat fluxes) on upper-ocean response. We use the reduced-gravity quasi-isopycnal ocean model by Schopf and Loughe (1995) for this study. Two experiments are performed: one with daily and the other with monthly surface forcing. The two experiments are referred to as DD and MM, respectively. The daily surface wind stress is produced from the SSM/I wind data (Atlas et al. 1991) using the drag coefficient of Large and Pond (1982). The surface latent and sensible heat fluxes are estimated using the atmospheric mixed layer model by Seager et al. (1995) with the time-varying air temperature and specific humidity from the NCEP-NCAR reanalysis (Kalnay et al. 1996). The radiation is based on climatological shortwave radiation from the Earth Radiation Budget Experiment (ERBE) [Harrison et al. 1993] and the daily GEWEX SRB data. The ocean model domain is restricted to the Pacific Ocean with realistic land boundaries. At the southern boundary the model temperature and salinity are relaxed to the Levitus (1994) climatology. The time-mean SST distribution from MM is close to the observed SST climatology while the mean SST field from DD is about 1.5 C cooler. to identify the responsible processes, we examined the mean heat budgets and the heat balance during the first year (when the difference developed) in the two experiments. The analysis reveals that this is contributed by two factors. One is the difference in latent heat flux. The other is the difference in mixing processes. to further evaluate the responsible processes, we repeated the DD experiment by reducing the based vertical diffusion from 1e-4 to 0.5e-5. The resultant SST field becomes quite closer to the observed SST field. SST variability from the two experiments is generally similar, but the equatorial SST differences between the two experiments show interannual variations. We are investigating the possible mechanisms responsible for the different responses.
Author
Heat Flux; Ocean Models; Remote Sensing; Climatology; Earth Radiation Budget Experiment; Heat Balance; Sea Surface Temperature

20020003734 Lawrence Livermore National Lab., Livermore, CA USA
Comparison of the 200 hPa circulation in CSM and CCM3 simulations and NCEP and ERA reanalysis: Seasonal cycle and interannual variation
Boyle, J. S.; Oct. 08, 1998; 57p; In English
Report No.(s): DE2001-2876; UCRL-ID-132138; No Copyright; Avail: Department of Energy Information Bridge

In this paper the monthly mean vorticity and divergence at 200 hPa are compared from four data sources: The NCEP/NCAR reanalyses 1958 through 1994, the ECMWF (ERA) reanalyses, 1979 through 1994, a NCAR CCM3 integration using prescribed SSTs from 1979 through 1993, and the NCAR CSM 300 year integration. The NCEP, ERA and CCM3 all provide data for the period 1979 through 1993. The timescales examined are the annual cycle and interannual variations. The annual mean vorticity of the ERA and NCEP match very closely. The annual cycle is likewise close except in the eastern equatorial Pacific and Indian Ocean. Compared to the reanalyses, the models have adequate annual means but suffer in the depiction of the annual cycle in the regions of the jet maxima and in some regions of the Tropics. The CSM appears to inherit errors from the CCM3 and apparently add some new ones. The annual mean divergence shows a much larger difference between the reanalyses. This is most pronounced in the Tropics especially over the African and South American land masses. The models also show large differences, with the CSM being an outlier in the tropical Pacific. For many tropical and extratropical locations even the annual cycle is not well defined between the NCEP and ERA reanalysis. The NCEP, ERA, CCM3 and CSM agree with respect to the variance of the monthly mean vorticity. The variance for low pass filtered data is too large in the ENSO regions for the CCM3, but too small for the CSM. Both models tend to underestimate the low frequency variance in midlatitudes. The ERA has substantially more monthly variance in the divergence than the NCEP data, especially over the tropical South America and Africa and the dateline. Both models have variance more on the order of the ERA, and have an anomalous maximum in the eastern Indian Ocean, the CSM much more so. The CSM shifts the maxima in the equatorial Pacific from 180 seen in the reanalyses to 150E. If anything the CCM 3 appears to

be too sensitive to SST anomalies, which exacerbates the poor ocean simulation in the tropical Pacific. There are errors in the CCM3 integration which foreshadow, deficiencies in the CSM integration, so the ocean is not solely at fault.
NTIS
Atmospheric Circulation; Annual Variations; Atmospheric Models

51
LIFE SCIENCES (GENERAL)

Includes general research topics related to plant and animal biology (non-human); ecology; microbiology; and also the origin, development, structure, and maintenance, of animals and plants in space and related environmental conditions. For specific topics in life sciences see categories 52 through 55.

20020000943 NASA Kennedy Space Center, Cocoa Beach, FL USA
Thermal Performance of Biological Substance Systems in Vitro Under Static and Dynamic Conditions at the Cryogenic Test Laboratory, NASA Kennedy Space Center, USA
Augustynowicz, S. D., DYNACS Engineering Co., Inc., USA; Fesmire, James E., NASA Kennedy Space Center, USA; [2001]; 10p; In English; International and European Congress of Cryosurgery, 5-7 Oct. 2001, Lisbon, Portugal
Contract(s)/Grant(s): NAS10-98001; No Copyright; Avail: CASI; A02, Hardcopy; A01, Microfiche

A unique research program, including a comprehensive study of thermal performance at cryogenic vacuum insulation systems, was performed at the NASA Kennedy Space Center. The main goal was to develop a new soft vacuum system (from 1 torr to 10 torr) that provides an intermediate level of performance (k-value below 4.8 mW/m-K). Liquid nitrogen boil-off methods were used to test conventional materials, novel materials, and certain combinations. The test articles included combinations of aluminum foil, fiberglass paper, polyester fabric, silica aerogel composite blanket, fumed silica, silica aerogel powder, and syntactic foam. A new LCI system was developed at the Cryogenics Test Laboratory. This system performs exceptionally well at soft vacuum levels and nearly as good as an MLI at high vacuum levels. Apparent thermal conductivities for the LCI range from 2 mW/m-K at soft vacuum to 0.1 mW/m-K at high vacuum. Several cryostats were designed, constructed, and calibrated by the Cryogenics Test Laboratory at KSC NASA as part of this research program. The cryostat test apparatus is a liquid nitrogen boil-off calorimeter system for direct measurement of the apparent thermal conductivity at a fixed vacuum level between 5 x 10(exp -5) and 760 torr. The apparatus is also used for transient measurements of temperature profiles. The development of efficient, robust cryogenic insulation systems has been a targeted area of research for a number of years. Improved methods of characterization, testing, and evaluation of complex biological substance systems for cryosurgery and cryobiology are the focus of this paper.
Author
Cryogenics; Thermal Insulation; In Vitro Methods and Tests; Cryostats

20020002756 National Inst. of Allergy and Infectious Diseases, Bethesda, MD USA
National Institute of Allergy and Infectious Diseases Profile: Fiscal Year 2000
Jun. 2001; 160p; In English
Report No.(s): PB2002-100476; No Copyright; Avail: CASI; A08, Hardcopy; A02, Microfiche

The National Institute of Allergy and Infectious Diseases (NIAID) conducts and supports scientific research on infectious and immunologic diseases. The goals of this research are to delineate pathogenesis, improve diagnosis and treatment, and develop vaccines to prevent these diseases, many of which significantly affect public health. to accomplish its goals, NIAID carries out a wide range of basic, applied, and clinical investigations within its own laboratories and provides research grant, contract, and cooperative agreement support to scientists at universities and other research institutions throughout the country and the world. The NIAID research program is predicated on the view that we live in an interconnected global community. Because of the enormous volume of international travel and trade, we cannot separate the health problems of the USA from those of the rest of the world. Clearly, it is naive to think that we are somehow isolated from diseases that are public health challenges elsewhere. As a nation, our interest in global health stems from both humanitarian concerns and what has been called enlightened self-interest. In addition to our obligation to ameliorate human suffering wherever possible, history tells us that healthy, stable countries make strong allies and trading partners. Conversely, poor health status can have a profound negative impact on social and economic development, and can contribute to political instability.
NTIS
Public Health; Allergic Diseases; Infectious Diseases

20020004359 NASA Ames Research Center, Moffett Field, CA USA

Space Flight Effects on Intracellular Ions in Sublingual Cells of Non-Human Primates

Arnaud, Sara B.; Dotsenko, R.; Fung, P.; Navidi, M.; Silver, B.; [1994]; 1p; In English; 65th Annual Scientific Meeting, 8-12 May 1994, San Antonio, TX, USA

Contract(s)/Grant(s): RTOP 199-26-12-02; No Copyright; Avail: Issuing Activity; Abstract Only

We have used a novel technique that quantifies minerals and electrolytes from smears of sublingual cells by x-ray microanalysis to monitor metabolic changes in bed rest subjects. Increases in intracellular calcium (CA), phosphorus (P), and potassium (K) were characteristic of subjects whose exercise regimen was inadequate to maintain calcium metabolism. to test the effects of space flight on intracellular ions, we analyzed cells from 2-4 kg Rhesus monkeys before and after 2 weeks in space or chair restraint (CR). There were increases in sublingual cell Ca, P and K after space flight which paralleled the clinical estimates of metabolic status of the animals and exceeded the levels found during CR on R+11. Increases after 2 weeks CR were 26% in Ca, 6% in P and 29% in K. Species similarity ill responses of intracellular ions to inactivity imposed by bed rest, restraint or microgravity suggest that this innovative non-invasive technique would be a useful in-flight monitor of exercise countermeasures directed toward maintaining calcium balance.

Author

Ions; Microanalysis; Primates; Space Flight; Cells (Biology); Aerospace Medicine

20020005133 NASA Ames Research Center, Moffett Field, CA USA

Determinants of Long Bone Structural Properties

Cleek, T. M., NASA Ames Research Center, USA; Katz, B., NASA Ames Research Center, USA; Whalen, R. T., NASA Ames Research Center, USA; [1994]; 2p; In English; University of California Biomedical Engineering Symposium, 13 May 1994, Davis, CA, USA

Contract(s)/Grant(s): RTOP 199-26-12-34; No Copyright; Avail: Issuing Activity; Abstract Only

The objective of our research is to determine whether a non-invasive determination of long bone cross-sectional areal properties using only the mineral component of bone accurately predicts the true structural properties. In this study section properties of a whole long bone were compared using two methods: (1) special analysis of bone densitometry data, and (2) experimental determination of flexural rigidities from bone surface strain measurements during controlled loading.

Derived from text

Bones; Density Measurement; Cross Sections

20020005214 International Association for Radiation Research, Bordeaux, France

11th International Conference of Radiation Research

Jul. 18, 1999; 19p; In English

Report No.(s): DE2001-770635; No Copyright; Avail: Department of Energy Information Bridge

Topics discussed in the conference included the following: Radiation Physics, Radiation Chemistry and modelling--Radiation physics and dosimetry; Electron transfer in biological media; Radiation chemistry; Biophysical and biochemical modelling; Mechanisms of DNA damage; Assays of DNA damage; Energy deposition in micro volumes; Photo-effects; Special techniques and technologies; Oxidative damage. Molecular and cellular effects-- Photobiology; Cell cycle effects; DNA damage: Strand breaks; DNA damage: Bases; DNA damage Non-targeted; DNA damage: other; Chromosome aberrations: clonal; Chromosomal aberrations: non-clonal; Interactions: Heat/Radiation/Drugs; Biochemical effects; Protein expression; Gene induction; Co-operative effects; 'Bystander' effects; Oxidative stress effects; Recovery from radiation damage. DNA damage and repair -- DNA repair genes; DNA repair deficient diseases; DNA repair enzymology; Epigenetic effects on repair; and Ataxia and ATM.

NTIS

Research; Conferences; Energy Transfer; Radiation Chemistry; Radiation Damage

20020005883 Wyoming Univ., Laramie, WY USA

Sequence Requirements of Spider Silk Elastic Proteins ***Final Report, 1 Jul. 1998-30 Jun. 2001***

Lewis, Randolph V.; Sep. 19, 2001; 6p; In English

Contract(s)/Grant(s): DAAG55-98-1-0262

Report No.(s): AD-A395379; ARO-37811.1-65-DPS; No Copyright; Avail: CASI; A02, Hardcopy; A01, Microfiche

Sequence for flagelliform silk proteins from Nephila, Argiope, and Araneus species have been obtained. These sequences show significant sequence differences although the changes are not predicted to affect the secondary structure of the protein and therefore its function will be the same. Araneus shows the presence of two proteins, one a flagelliform protein and the other a major

ampullate silk protein. In addition we have cloned and sequenced a number of silk proteins from glands of undetermined evolutionary origin in new spider species. We have also cloned and substantially sequenced a new protein cDNA from aciniform glands whose silk is used for prey wrapping.
DTIC
Proteins; Silk; Genetic Engineering; Elastic Properties

52
AEROSPACE MEDICINE

Includes the biological and physiological effects of atmospheric and space flight (weightlessness, space radiation, acceleration, and altitude stress) on the human being; and the prevention of adverse effects on those environments. For psychological and behavioral effects of aerospace environments see 53 Behavioral Science. For the effects of space on animals and plants see 51 Life Sciences.

20020001548 Sandia National Labs., Albuquerque, NM USA
Proposed Information Architecture for Telehealth System Interoperability
Warren, S.; Craft, R. L.; Parks, R. C.; Gallagher, L. K.; Garcia, R. J.; Apr. 07, 1999; 10p; In English
Report No.(s): DE2001-5692; SAND99-0864C; No Copyright; Avail: Department of Energy Information Bridge

Telemedicine technology is rapidly evolving. Whereas early telemedicine consultations relied primarily on video conferencing, consultations today may utilize video conferencing, medical peripherals, store-and-forward capabilities, electronic patient record management software, and/or a host of other emerging technologies. These remote care systems rely increasingly on distributed, collaborative information technology during the care delivery process, in its many forms. While these leading-edge systems are bellwethers for highly advanced telemedicine, the remote care market today is still immature. Most telemedicine systems are custom-designed and do not interoperate with other commercial offerings. Users are limited to a set of functionality that a single vendor provides and must often pay high prices to obtain this functionality, since vendors in this marketplace must deliver entire systems in order to compete. Besides increasing corporate research and development costs, this inhibits the ability of the user to make intelligent purchasing decisions regarding best-of-breed technologies. We propose a secure, object-oriented information architecture for telemedicine systems that promotes plug-and-play interaction between system components through standardized interfaces, communication protocols, messaging formats, and data definitions. In this architecture, each component functions as a black box, and components plug together in a lego-like fashion to achieve the desired device or system functionality. The architecture will support various ongoing standards work in the medical device arena.
NTIS
Telecommunication; Health; Clinical Medicine; Computer Systems Programs; Video Communication

20020002388 NASA Ames Research Center, Moffett Field, CA USA
Direction of Moving Plaids is Biased by Asymmetric Viewing Windows
Beutter, Brent Robert, NASA Ames Research Center, USA; Mulligan, J. B., NASA Ames Research Center, USA; Stone, L. S., NASA Ames Research Center, USA; [1994]; 1p; In English; Society for Neuroscience Meeting, 13-18 Nov. 1994, Miami Beach, FL, USA; Sponsored by Society for Neuroscience, USA
Contract(s)/Grant(s): NCC2-307; RTOP 199-16-12-37; No Copyright; Avail: Issuing Activity; Abstract Only

Directionally selective V1 neurons are tuned to particular spatiotemporal frequencies and respond to local 1-D edge motion. At least some MT neurons however appear to respond to the actual velocity of moving 2D patterns (Movshon et al., EBR, 11:117, 1986). to better understand how the 1D local motion information available from V1 is integrated to derive a 2D velocity signal we investigated human perception of moving plaids, 2-D patterns composed of the sum of two 1-D sinusoidal gratings of different orientations. We measured the effect of the shape of the viewing window on the perceived direction of plaid motion. The plaids were spatially windowed by 2-D Gaussians with unequal standard deviations (sigma l, sigma 2). Four observers indicated perceived direction by adjusting a pointer. Direction errors were measured as a function of the difference between window orientation and true plaid direction (delta theta) for several grating spatial frequencies (SF = 0.3, 0.6, 1.2 c/d) and window aspect ratios (AR = sigma 1/sigma 2 = 1, 1.4, 2,4). Observers showed systematic errors in perceived direction (approx. 15 degrees for R = 4 and SF = 0.6 c/d) that peaked at delta theta approximately 40 degrees. The errors increased for increasing aspect ratio and decreased for increasing spatial frequencies (or number of cycles). These results show that despite the unambiguous motion of the plaids, within asymmetric windows, human can systematically misperceive plaid direction. These data constrain models of

motion integration within extrastriate cortex and, in particular, are inconsistent with algorithms that use either the Intersection of Constraints rule or cross correlation to compute velocity.
Author
Algorithms; Asymmetry; Neurons; Standard Deviation

20020005094 NASA Ames Research Center, Moffett Field, CA USA
Cutaneous Microvascular Flow In the Foot During Simulated Variable Gravities
Chang, David S., NASA Ames Research Center, USA; Breit, Greg A., NASA Ames Research Center, USA; Styf, Jorma R., NASA Ames Research Center, USA; Hargens, Alan R., NASA Ames Research Center, USA; [2001]; 3p; In English
Contract(s)/Grant(s): RTOP 199-14-12-04; No Copyright; Avail: Issuing Activity; Abstract Only

Our objective was to elucidate how varying gravitational fields affect blood perfusion in the sole of the foot. Human subjects underwent whole-body tilting at four angles: upright (1 G(sub z), 22 deg (.38 G(sub z)), 10 deg (.17 G(sub z)), and supine (0 G(sub z)), simulating the gravitational fields of Earth, Mars, Moon, and microgravity, respectively. Cutaneous capillary blood flow was monitored on the plantar surface of the heel by laser Doppler flowmetry while weight bearing load was measured beneath the same foot with a calibrated scale. Foot mean arterial pressures (MAP) were calculated by adding estimated hydrostatic pressures to continuously recorded heart-level blood pressures for each subject. At each tilt angle, subjects increased weight bearing on one foot in graded load increments of one kilogram beginning with zero. The weight bearing at which null flow first occurred was determined as the closing load (CL). Subsequently, the weight bearing was reduced in reverse steps until blood flow returned (opening load, OL). CL and OL were normalized to each subject's body weight and expressed as percent of body weight. Mean CLs (SD in parentheses) for simulated Earth, Mars, Moon, and micro-gravities were 14 (5), 8 (2), 6 (2), and 5 (2) percent of body weight, respectively. OLs were 12 (3), 6 (1), 5 (2), and 4 (1), respectively. Calculated foot MAPs for each simulated gravitational field were 192 (19), 127 (12), 106 (10), and 87 (9) mm Hg, respectively. CL and OL were significantly correlated with foot MAP (r = 0.70, 0.72, respectively). Overall, CL and OL were significantly different (p is less than 0.001). The data suggest that decreased local arterial pressure in the foot lowers tolerance to external compression. Consequently, the human foot sole may be more prone to cutaneous ischernia during loading in microgravity than on Earth.
Author
Feet (Anatomy); Gravitational Fields; Blood Flow; Loads (Forces); Simulation

20020005884 Naval Air Warfare Center, Aircraft Div., Patuxent River, MD USA
Determination of Head and Neck Loads and Moments During Tactical and Rotary Wing Maneuvering Acceleration
Shender, Barry S.; Paskoff, Glenn; Askew, Gregory; Coughlan, Richard; Isdahl, Wayne; Sep. 17, 2001; 63p; In English
Report No.(s): AD-A395380; NAWCADPAX/TR-2001/97; No Copyright; Avail: CASI; A04, Hardcopy; A01, Microfiche

Neck injury risk can increase when aircrew wear head mounted equipment while exposed to +Gz loads. The effects of added weight and change in center of gravity (CG) were determined during a centrifuge study using an instrumented manikin at Brooks Air Force Base, Texas. Data included centrifuge Gz, head acceleration (three axes), head and C7-T1 pitch moment, and compressive and shear forces. Helicopter (0.5 G/sec at +1.75 and +4 Gz) and tactical aircraft (2 and 6 G/sec from +4 to 12 Gz) accelerations were simulated (5 sec plateau at each level). Effect of added weights (up to overall 2.7 kg) was measured in the forward pitch and lateral planes and tested using ANOVA. Seven real helmet systems were also tested. Head Gx and Gy increased with increasing +Gz load, head weight, as CG shifted in the forward pitch plane, and onset rate. Head Ox was greatest when weight was distributed laterally. The resultant head and neck force and moment increased with increasing weight, pitch angle, and +Gz load. Neck forces and moments were significantly larger than those measured in the head.
DTIC
Stress (Physiology); Injuries; Neck (Anatomy); Pitch (Inclination); Helmets

53
BEHAVIORAL SCIENCES

Includes psychological factors; individual and group behavior; crew training and evaluation; and psychiatric research.

20020005134 NASA Ames Research Center, Moffett Field, CA USA
Situational Variables in Expert Pilot Decision Making
Fischer, Ute, San Jose State Univ., USA; Orasanu, Judith, NASA Ames Research Center, USA; Wich, Mike, San Jose State Univ., USA; [1994]; 1p; In English; Society for Judgment and Decision Making Conference, 13-14 Nov. 1994, Saint Louis, MO, USA
Contract(s)/Grant(s): RTOP 199-06-12-23; No Copyright; Avail: Issuing Activity; Abstract Only

In traditional laboratory studies of decision making, the experimenter structures the problem, defines the goal and specifies available information. In contrast, when people make decisions in non-laboratory environments characterized as complex, dynamic and consequential, they must first identify the problem and determine what information and responses are relevant. The present research was designed to investigate which situational aspects are important to experienced pilots making aviation decisions. Twenty-eight professional pilots were asked to sort descriptions of 22 aircraft incidents into piles involving similar types of major decisions. Preliminary analyses suggest four underlying variables: time pressure, risk level, available resources, and certainty of goal attainment.
Author
Aircraft Pilots; Decision Making; Situational Awareness

20020005894 NASA Ames Research Center, Moffett Field, CA USA
Using EEG to Detect and Monitor Mental Fatigue
Montgomery, Leslie, NASA Ames Research Center, USA; Luna, Bernadette, NASA Ames Research Center, USA; Trejo, Leonard J., NASA Ames Research Center, USA; Montgomery, Richard, NASA Ames Research Center, USA; March 2001; 22p; In English; Human Systems 2001: The Conference on Technologies for Human Factors and Psycho-Social Adaptation, 20-22 Jun. 2001, Houston, TX, USA; No Copyright; Avail: CASI; A03, Hardcopy; A01, Microfiche

This project aims to develop EEG-based methods for detecting and monitoring mental fatigue. Mental fatigue poses a serious risk, even when performance is not apparently degraded. When such fatigue is associated with sustained performance of a single type of cognitive task it may be related to the metabolic energy required for sustained activation of cortical areas specialized for that task. The objective of this study was to adapt EEG to monitor cortical energy over a long period of performance of a cognitive task. Multielectrode event related potentials (ERPs) were collected every 15 minutes in nine subjects who performed a mental arithmetic task (algebraic sum of four randomly generated negative or positive digits). A new problem was presented on a computer screen 0.5 seconds after each response; some subjects endured for as long as three hours. ERPs were transformed to a quantitative measure of scalp electrical field energy. The average energy level at electrode P3 (near the left angular gyrus), 100-300 msec latency, was compared over the series of ERPs. For most subjects, scalp energy density at P3 gradually fell over the period of task performance and dramatically increased just before the subject was unable to continue the task. This neural response can be simulated for individual subjects using, a differential equation model in which it is assumed that the mental arithmetic task requires a commitment of metabolic energy that would otherwise be used for brain activities that are temporarily neglected. Their cumulative neglect eventually requires a reallocation of energy away from the mental arithmetic task.
Author
Electroencephalography; Mental Performance; Fatigue (Biology)

54
MAN/SYSTEM TECHNOLOGY AND LIFE SUPPORT

Includes human factors engineering; bionics, man-machine, life support, space suits and protective clothing. For related information see also 16 Space Transportation and 52 Aerospace Medicine..

20020000776 NASA Langley Research Center, Hampton, VA USA
Astronaut-Induced Disturbances to the Microgravity Environment of the Mir Space Station
Newman, Dava J., Massachusetts Inst. of Tech., USA; Amir, Amir R., Massachusetts Inst. of Tech., USA; Beck, Sherwin M., NASA Langley Research Center, USA; Journal of Spacecraft and Rockets; July - August 2001; Volume 38, No. 4, pp. 578-583; In English
Contract(s)/Grant(s): NAS1-18690; Copyright Waived; Avail: CASI; A02, Hardcopy; A01, Microfiche

In preparation for the International Space Station, the Enhanced Dynamic Load Sensors Space Flight Experiment measured the forces and moments astronauts exerted on the Mir Space Station during their daily on-orbit activities to quantify the astronaut-induced disturbances to the microgravity environment during a long-duration space mission. An examination of video recordings of the astronauts moving in the modules and using the instrumented crew restraint and mobility load sensors led to the identification of several typical astronaut motions and the quantification or the associated forces and moments exerted on the spacecraft. For 2806 disturbances recorded by the foot restraints and hand-hold sensor, the highest force magnitude was 137 N. For about 96% of the time, the maximum force magnitude was below 60 N, and for about 99% of the time the maximum force magnitude was below 90 N. For 95% of the astronaut motions, the rms force level was below 9.0 N. It can be concluded that

expected astronaut-induced loads from usual intravehicular activity are considerably less than previously thought and will not significantly disturb the microgravity environment.
Author
Astronauts; Mir Space Station; Long Duration Space Flight; Dynamic Loads; Microgravity; Intravehicular Activity

20020000897 Argonne National Lab., IL USA
Behavior Model for Performance Assessment
Borwn-VanHoozer, S. A.; Jul. 23, 1999; 7p; In English
Report No.(s): DE2001-11907; ANL/ED/CP-99665; No Copyright; Avail: Department of Energy Information Bridge, Microfiche

Every individual channels information differently based on their preference of the sensory modality or representational system (visual auditory or kinesthetic) we tend to favor most (our primary representational system (PRS)). Therefore, some of us access and store our information primarily visually first, some auditorily, and others kinesthetically (through feel and touch); which in turn establishes our information processing patterns and strategies and external to internal (and subsequently vice versa) experiential language representation. Because of the different ways we channel our information, each of us will respond differently to a task - the way we gather and process the external information (input), our response time (process), and the outcome (behavior). Traditional human models of decision making and response time focus on perception, cognitive and motor systems stimulated and influenced by the three sensory modalities, visual, auditory and kinesthetic. For us, these are the building blocks to knowing how someone is thinking. Being aware of what is taking place and how to ask questions is essential in assessing performance toward reducing human errors. Existing models give predications based on time values or response times for a particular event, and may be summed and averaged for a generalization of behavior(s). However, by our not establishing a basic understanding of the foundation of how the behavior was predicated through a decision making strategy process, predicative models are overall inefficient in their analysis of the means by which behavior was generated. What is seen is the end result.
NTIS
Data Processing; Decision Making; Touch; Auditory Perception; Visual Perception

20020001879 Sandia National Labs., Albuquerque, NM USA
Architecture for Teraflop Visualization
Breckenridge, A. R.; Haynes, R. A.; Apr. 09, 1999; 10p; In English
Report No.(s): DE2001-5694; SAND99-0890C; No Copyright; Avail: Department of Energy Information Bridge

Sandia Laboratories' computational scientists are addressing a very important question: How do we get insight from the human combined with the computer-generated information. The answer inevitably leads to using scientific visualization. Going one technology leap further is teraflop visualization, where the computing model and interactive graphics are an integral whole to provide computing for insight. In order to implement our teraflop visualization architecture, all hardware installed or software coded will be based on open modules and dynamic extensibility principles. We will illustrate these concepts with examples in our three main research areas: (1) authoring content (the computer), (2) enhancing precision and resolution (the human), and (3) adding behaviors (the physics).
NTIS
Architecture (Computers); Display Devices; Scientific Visualization

20020002223 NASA Ames Research Center, Moffett Field, CA USA
CELSS Antarctic Analog Project (CAAP): A New Paradigm for Polar Life Support and CELSS Research
Bubenheim, David L., NASA Ames Research Center, USA; Straight, Christian, NASA Ames Research Center, USA; Flynn, Michael, NASA Ames Research Center, USA; Bates, Maynard, NASA Ames Research Center, USA; [1994]; 1p; In English; 30th COSPAR Scientific Assembly, 11-21 Jul. 1994, Hamburg, Germany; Sponsored by Committee on Space Research, Unknown
Contract(s)/Grant(s): RTOP 199-61-12; No Copyright; Avail: Issuing Activity; Abstract Only

The CELSS Antarctic Analog Project (CAAP) is a joint National Science Foundation (NSF) and National Aeronautics and Space Administration (NASA) project for the development, deployment and operation of CELSS technologies at the Amundsen-Scott South Pole Station. CAAP is implemented through the joint NSF/NASA Antarctic Space Analog Program (ASAP), initiated to support the pursuit of future NASA missions and to promote the transfer of space technologies to the NSF. Under a Memorandum of Agreement, the CAAP represents an example of a working dual agency cooperative project. NASA goals are operational testing of CELSS technologies and the conduct of scientific study to facilitate . technology selection, system design and methods development, including human dynamics as required for the operation of a CELSS. Although not fully closed, food production, water purification, and waste recycle and reduction provided by CAAP will improve the quality of life for the South Pole inhabitants, reduce logistics dependence, and minimize environmental impacts associated with human presence on

the polar plateau. The CAAP facility will be highly integrated with the new South Pole Station infrastructure and will be composed of a deployed hardware facility and a research activity. This paper will include a description of CAAP and its functionality, conceptual designs, component selection and sizing for the crop growth chamber, crop production expectations, and a brief report on an initial on-site visit. This paper will also provide a discussion of issues associated with power and energy use and the applicability of CAAP to direct technology transfer to society in general and remote communities in particular.
Author
Antarctic Regions; Closed Ecological Systems; Aerospace Engineering; Systems Engineering; NASA Space Programs

20020002852 Federal Aviation Administration, Atlantic City, NJ USA
Human Factors Contract Management Handbook ***Final Report***
Barrientos, M. J.; Dixon, M.; Klock, B. A.; Morgan, S.; Neiderman, E. C.; May 15, 2001; 50p; In English
Report No.(s): PB2002-100251; No Copyright; Avail: CASI; A03, Hardcopy; A01, Microfiche
The Federal Aviation Administration's (FAA's) Acquisition Management System (AMS) was established to dramatically improve the agency's acquisition process by creating a framework and innovative decision-making. The AMS provides extensive guidance regarding the FAA's procurement system. The stated goal of the procurement system is 'to obtain high quality products, services, and real property in a timely, cost effective manner, at prices that are fair and reasonable'. The Aviation Security Research and Development Division (AAR-500) recognized the need to supplement the policy and guidance provided by the AMS by identifying internal processes. This Handbook meets that need by clearly defining AAR-500 personnel roles, responsibilities, and process activities that uphold the procurement policy of the agency.
NTIS
Human Factors Engineering; Contract Management; Cost Effectiveness; Decision Making; Management Systems

20020005878 Army Research Inst. for the Behavioral and Social Sciences, Alexandria, VA USA
Human Factors Evaluation of the SINCGARS ICOM Radio
Palmer, Richard L.; Apr. 1987; 35p; In English
Report No.(s): AD-A395353; ARI-WP-FH-8701; No Copyright; Avail: CASI; A03, Hardcopy; A01, Microfiche
The Human Factors Evaluation of the surface features and operating characteristics of SINCGARS ICOM radio is presented.
CASI
Human Factors Engineering; Radio Equipment; Communication Equipment

55
EXOBIOLOGY

Includes astrobiology; planetary biology; and extraterrestrial life. For the biological effects of aerospace environments on humans see 52 Aerospace medicine; on animals and plants see 51 Life Sciences. For psychological and behavioral effects of aerospace environments see 53 Behavioral Science.

20020002018 NASA Ames Research Center, Moffett Field, CA USA
General Meeting of the NASA Astrobiology Institute
April 2001; 362p; In English; General Meeting of the NASA Astrobiology Insititute, 10-12 April 2001, Washington, DC, USA; See also 20020002019 through 20020002208; No Copyright; Avail: Issuing Activity
This publication presents the extended abstracts submitted for presentation at the Annual Meeting of the NASA Astrobiology Institute held in Washington, DC, April 10-12, 2001.
CASI
Conferences; Exobiology; Aerospace Environments

20020002019 Carnegie Institution of Washington, Geophysical Lab., Washington, DC USA
Could Biochemistry Have Hydrothermal Origins?
Cody, George D., Carnegie Institution of Washington, USA; Boctor, Nabil, Carnegie Institution of Washington, USA; Hazen, Robert M., Carnegie Institution of Washington, USA; Scott, James, Carnegie Institution of Washington, USA; Sharma, Anurag, Carnegie Institution of Washington, USA; Yoder, Hatten S., Jr., Carnegie Institution of Washington, USA; General Meeting of the NASA Astrobiology Insititute; April 2001, pp. 3-4; In English; See also 20020002018; No Copyright; Avail: Issuing Activity; Abstract Only

The proposal that deep-sea hydrothermal vent systems might be an ideal environment for the emergence of Earth's first life is particularly compelling in that it greatly expands the possibility for life beyond the narrow band of solar luminosity that supports surface liquid water; thus, this theory accommodates the possibility of biochemistry, similar to that of terrestrial life, emerging within other planetary bodies in this and other solar systems. However, the theory is poorly constrained due to a lack of experimental data. In order to remedy this deficiency we have run high pressure hydrothermal reactions using sealed gold tube reactors and an internally heated high pressure apparatus. First, we studied the hydrothermal reactions of pure pyruvic acid and citric acid systems (sans catalysts), respectively, in CO2 - H2 bearing aqueous fluids in the temperature range of 150-350 C and 0.5 to 5.0 Kbar. At this stage our principal focus is in identifying the effect of pressure on reaction selectivity in systems that exhibit multi-channel reactions. Additional information is contained in the original extended abstract.
Author
Biochemistry; Hydrothermal Systems; Exobiology; Ocean Bottom

20020002020 Scripps Research Inst., Dept. of Chemistry, La Jolla, CA USA
A Chiroselective Peptide Replicator and its Relevance to Issues Concerning the Origin of Homochirality on Earth
Ghadiri, M. Reza, Scripps Research Inst., USA; Saghatelian, Alan, Scripps Research Inst., USA; Yokobayashi, Yohei, Scripps Research Inst., USA; Soltani, Kathy, Scripps Research Inst., USA; General Meeting of the NASA Astrobiology Insititute; April 2001, pp. 5-6; In English; See also 20020002018; No Copyright; Avail: Issuing Activity; Abstract Only

The origin of homochirality in living systems is often attributed to the generation of enantiomeric differences in a pool of chiral prebiotic molecules, but none of the possible physiochemical processes considered can produce the significant imbalance required if homochiral biopolymers are to result from simple coupling of suitable precursor molecules. This implies a central role either for additional processes that can selectively amplify an initially minute enantiomeric difference in the starting material, or for a nonenzymatic process by which biopolymers undergo chiroselective molecular replication. Given that molecular self-replication and the capacity for selection are necessary conditions for the emergence of life, chiroselective replication of biopolymers seems a particularly attractive process for explaining homochirality in nature. Here we report that a 32-residue peptide replicator, designed according to our earlier principles, is capable of efficiently amplifying homochiral products from a racemic mixture of peptide fragments through a chiroselective autocatalytic cycle. The chiroselective amplification process discriminates between structures possessing even single stereochemical mutations within otherwise homochiral sequences. Moreover, the system exhibits a dynamic stereochemical editing function making use of heterochiral sequences that arise through uncatalysed background reactions to catalyze the production of the 5 homochiral product. These results support the idea that self-replicating polypeptides could have played a key role in the origin of homochirality on Earth.
Author
Earth (Planet); Peptides; Physiochemistry; Planetary Evolution; Biopolymers; Chirality

20020002021 NASA Ames Research Center, Moffett Field, CA USA
Organic Synthesis in Simulated Interstellar Ice Analogs
Dworkin, Jason P., NASA Ames Research Center, USA; Bernstein, Max P., NASA Ames Research Center, USA; Sandford, Scott A., NASA Ames Research Center, USA; Allamandola, Louis J., NASA Ames Research Center, USA; Deamer, David W., California Univ., USA; Elsila, Jamie, Stanford Univ., USA; Zare, Richard N., Stanford Univ., USA; General Meeting of the NASA Astrobiology Insititute; April 2001, pp. 7-8; In English; See also 20020002018; No Copyright; Avail: Issuing Activity; Abstract Only

Comets and carbonaceous micrometeorites may have been significant sources of organic compounds on the early Earth. Ices on grains in interstellar dense molecular clouds contain a variety of simple molecules as well as aromatic molecules of various sizes. While in these clouds the icy grains are processed by ultraviolet light and cosmic radiation which produces more complex organic molecules. We have run laboratory simulations to identify the types of molecules which could have been generated photolytically in pre-cometary ices. Experiments were conducted by forming various realistic interstellar mixed-molecular ices with and without polycyclic aromatic hydrocarbons (PAHs) at approx. 10 K under high vacuum irradiated with UV light from a hydrogen plasma lamp. The residue that remained after warming to room temperature was analyzed by HPLC, and by laser desorption mass spectrometry. The residue contains several classes of compounds which may be of prebiotic significance.
Author
Comets; Interstellar Matter; Synthesis (Chemistry); Organic Compounds; Computerized Simulation; Ice

20020002022 NASA Johnson Space Center, Houston, TX USA

The Origin of Organic Matter in the Solar System: Evidence from Interplanetary Dust Particles

Flynn, G. J., State Univ. of New York, USA; Keller, L. P., NASA Johnson Space Center, USA; Jacobsen, C., State Univ. of New York, USA; Wirick, S., State Univ. of New York, USA; General Meeting of the NASA Astrobiology Insititute; April 2001, pp. 9-11; In English; See also 20020002018; No Copyright; Avail: Issuing Activity; Abstract Only

The origin of the organic matter in interplanetary materials has not been established. A variety of mechanisms have been proposed, with two extreme cases being a Fisher-Tropsch type process operating in the gas phase of the solar nebula or a Miller-Urey type process, which requires interaction with an aqueous fluid, presumably occurring on an asteroid. In the Fisher-Tropsch case, we might expect similar organic matter in hydrated and anhydrous interplanetary materials. However, aqueous alteration is required in the case of the Miller-Urey process, and we would expect to see organic matter preferentially in interplanetary materials that exhibit evidence of aqueous activity, such as the presence of hydrated silicates. The types and abundance of organic matter in meteorites have been used as an indicator of the origin of organic matter in the Solar System. Indigenous complex organic matter, including amino acids, has been found in hydrated carbonaceous chondrite meteorites, such as Murchison. Much lower amounts of complex organic matter, possibly only terrestrial contamination, have been found in anhydrous carbonaceous chondrite meteorites, such as Allende, that contain most of their carbon in elemental form. These results seem to favor production of the bulk of the organic matter in the Solar System by aqueous processing on parent bodies such as asteroids, a Miller-Urey process. However, the hydrated carbonaceous chondrite meteorites have approximately solar abundances of the moderately volatile elements, while all anhydrous carbonaceous chondrite meteorites have significantly lower contents of these moderately volatile elements. Two mechanisms, incomplete condensation or evaporation, both of which involve processing at approx. 1200 C, have been suggested to explain the lower content of the moderately volatile elements in all anhydrous meteorites. Additional information is contained in the original extended abstract.

Author

Interplanetary Dust; Organic Materials; Solar System; Carbonaceous Chondrites; Exobiology

20020002023 Carnegie Institution of Washington, Geophysical Lab., Washington, DC USA

Selective Adsorption of L- and D-Amino Acids on Calcite: Implications for the Origin of Biochemical Homochirality

Hazen, Robert M., Carnegie Institution of Washington, USA; Filley, Timothy R., Purdue Univ., USA; Goodfriend, Glenn A., George Washington Univ., USA; General Meeting of the NASA Astrobiology Insititute; April 2001, pp. 12; In English; See also 20020002018; No Copyright; Avail: Issuing Activity; Abstract Only

One of life's most distinctive biochemical signatures is its strong selectivity for chiral molecular species, notably L-amino acids and D-sugars. Prebiotic synthesis reactions, with the possible exception of some interstellar processes, yield essentially equal amounts of L- and D-enantiomers. A significant challenge in origin-of-life research, therefore, is to identify natural mechanisms for the homochiral selection, concentration and polymerization of molecules from an initially racemic mixture. Symmetry breaking on a chirally-selective mineral surface offers a viable scenario for the origin of life; according to Lahav (Biogenesis. NY: Oxford University Press, 1999, p.259), 'if a selective adsorption of chiral amino acids on certain crystal faces were observed, then the problem of biological homochirality would be possible to comprehend.' We demonstrate that crystals of the common rock-forming mineral calcite (CaCO3), when immersed in a racemic aspartic acid solution, display significant adsorption and chiral selectivity of D- and L-enantiomers on pairs of mirror-related crystal growth surfaces. This selective adsorption is greater on crystals with terraced surface textures, which suggests that D- and L-aspartic acid concentrate along step-like, linear growth features. Selective adsorption of D-and L-amino acids on calcite is thus a plausible geochemical mechanism for the chiral selection and subsequent homochiral polymerization of amino acids on the prebiotic Earth.

Author

Adsorption; Amino Acids; Biochemistry; Calcite; Enantiomers; Biological Evolution

20020002024 State Univ. of New York, Dept. of Geosciences, Stony Brook, NY USA

Effectiveness of Hydrogen Sulfide as a Reductant in Hydrothermal Systems: Implication for Prebiotic Synthesis of C-H-O-N Compounds

Schoonen, Martin, State Univ. of New York, USA; General Meeting of the NASA Astrobiology Insititute; April 2001, pp. 13-15; In English; See also 20020002018; No Copyright; Avail: Issuing Activity; Abstract Only

Equilibrium thermodynamic calculations indicate that the chemical disequilibrium in vent solutions discharging from submarine hydrothermal systems could have provided the necessary driving force to synthesize metastable C-H-O-N compounds. Carbon in vent solutions discharging from modern systems has an oxidation state of IV (i.e., CO2- carbon). Unless the overall oxidation state of the Earth's crust was significantly lower, the carbon discharging from ancient vent system would also have been in the IV-state. Barring a very reducing Earth's crust, nitrogen would have discharged as zerovalent N2 in ancient systems as it

does in modern vent systems. Because the redox state of C and N in C-H-O-N compounds is less than IV and 0, respectively, a reductant is needed to make the synthesis possible. While solution composition in primordial vent systems may have been different, there are only a few reductants available in any significant abundance. These are ferrous iron, hydrogen, and hydrogen sulfide. Dissolved ferrous iron is a relatively weak reductant. Furthermore, it is readily sequestered in Fe-S phases. This leaves hydrogen and hydrogen sulfide as possible reductants. The abundance of each of these reductants is governed by the mineral assemblage that effectively controls the redox state of the vent solution as it makes its way toward the point of discharge. Depending on these constraints, either hydrogen or hydrogen sulfide may be the more abundant reductant. Abundance is, however, less important than reactivity. A survey of the catalysis literature indicates that hydrogen is very reactive if it is present as atomic hydrogen, but largely unreactive as molecular hydrogen. In fact, dissociating molecular hydrogen on a suitable surface is a key step in hydrogenation reactions. Additional information is contained in the original extended abstract.
Author
Hydrogen Sulfide; Hydrothermal Systems; Synthesis (Chemistry); Reduction (Chemistry); Nitrogen; Carbon

20020002025 Massachusetts General Hospital, Dept. of Molecular Biology, Boston, MA USA
The Origins of Evolution
Szostak, Jack W., Massachusetts General Hospital, USA; Bartel, David P., Whitehead Inst. for Biomedical Research, USA; Luisi, P. Luigi, Eidgenoessische Technische Hochschule, Switzerland; General Meeting of the NASA Astrobiology Insititute; April 2001, pp. 16-17; In English; See also 20020002018; No Copyright; Avail: Issuing Activity; Abstract Only

The evolution of modern biochemistry is most easily explained by positioning a stage in the early evolution of life in which biochemical functions such as information transfer and replication were largely carried out by RNA molecules. The recently determined structure of the ribosome makes this point most dramatically, since it is RNA that is responsible for the synthesis of proteins. The importance of a membrane in providing a compartment boundary has also been stressed by many authors from varying points of view, including the establishment of cellular identity as distinct from the environment, as a locus for metabolism, and as a requisite for energy generation. Here we discuss the role of the membrane compartment in enabling the Darwinian evolution of its enclosed genetic material. Additional information is contained in the original extended abstract.
Author
Biochemistry; Biological Evolution; Genetics; Proteins

20020002026 National Oceanic and Atmospheric Administration, Aeronomy Lab., Boulder, CO USA
Atmospheric Aerosols in Prebiotic Chemistry
Tuck, Adrian F., National Oceanic and Atmospheric Administration, USA; Vaida, Veronica, Colorado Univ., USA; General Meeting of the NASA Astrobiology Insititute; April 2001, pp. 18; In English; See also 20020002018; No Copyright; Avail: Issuing Activity; Abstract Only

It is argued that atmospheric aerosols would have had many advantages as a reaction medium in prebiotic chemistry. This theme, published last October 24 in PNAS, will be reviewed and developed further as regards the generation of amphiphilic molecules, and the chemistry which could have occurred near the tropopause as stratospheric aerosols containing meteoric material coagulated with tropospheric aerosols containing marine material.
Author
Aerosols; Atmospheric Chemistry; Stratosphere; Exobiology

20020002027 Texas Univ., Dept. of Marine Sciences, Austin, TX USA
Stability and Transformations of Nitrogenous Compounds Under Hydrothermal Conditions
Brandes, Jay A., Texas Univ., USA; Cody, George D., Carnegie Institution of Washington, USA; Hazen, Robert M., Carnegie Institution of Washington, USA; Yoder, Hatten S., Jr., Carnegie Institution of Washington, USA; General Meeting of the NASA Astrobiology Insititute; April 2001, pp. 19; In English; See also 20020002018; No Copyright; Avail: Issuing Activity; Abstract Only

Hydrothermal systems have been hypothesized as locations for the genesis of life. However, few experiments have been conducted that examine the interplay of biologically important compounds with minerals associated with these systems. One element generally neglected in studies of prebiotic chemistry is nitrogen. Several key questions in the study of the early Earth's nitrogen cycle are: How and under what conditions was reduced nitrogen formed? How was this reduced nitrogen incorporated into organic compounds, and what were the important parameters controlling the stability of these nitrogen containing organic compounds? A series of high pressure-hydrothermal reactions were undertaken to investigate these questions. Oxidized forms of inorganic nitrogen, thought to be the predominant non-gaseous form reaching the hadean sea, are rapidly reduced to NH3 when in contact with a variety of common metal sulfides at elevated temperature. The reaction efficiency is a function of temperature

and mineral type, but reaction kinetics are extremely rapid, reaching steady state values within 1 hour. It has always been assumed and demonstrated in the literature that organic nitrogen forms, especially amino acids, are extremely labile under high pressure, high temperature conditions. Our data indicates that while marked decreases in stability are found with increased temperature (greater than 150 C) at any pressure, the deleterious effects of pressure upon amino acids may be in fact an artifact of the gold containers in which such studies are conducted. If such containers and their internal solutions are buffered with metal sulfides, no decrease in stability with pressure is noted going from 500 Atm. to 5000 Atm. Although not conducive to the long term stability of amino acids, HT-HP systems may not be the sites of nearly instantaneous destruction as presently thought.
Author
Hydrothermal Systems; Nitrogen; Organic Compounds; Stability; Phase Transformations

20020002028 Colorado Univ., Dept. of Philosophy, Boulder, CO USA
What is Life?
Cleland, Carol E., Colorado Univ., USA; General Meeting of the NASA Astrobiology Insititute; April 2001, pp. 20; In English; See also 20020002018; No Copyright; Avail: Issuing Activity; Abstract Only

One of the central issues facing astrobiologists is the question ”what is life?” Some researchers approach this question by trying to define ”life”. Yet all the popular definitions face counter-examples. This is not an accident. It reflects a fundamental confusion between two types of identity statements, definitions (e.g., bachelors are unmarried human males) and theoretical identities (e.g., water is H2O). This confusion is revealed in the nature of the definitions that have been proposed for the term ”life”. They invariably cite high-level properties that are used to recognize terrestrial life (e.g., complex hierarchical structure, self-regulation). This is analogous to defining water as a cooling, tasteless, odorless, wet liquid that quenches thirst. The later does not, however, provide a satisfactory answer to the question ”what is water?” it merely describes water in terms of the properties by which it is recognized by humans. Similarly, definitions of life don’t provide satisfactory answers to the question ”what is life?” Considerations such as this suggest that attempts to answer the question ”what is life?” ought to focus on formulating plausible theoretical identities rather than definitions. Other cases of successful theoretical identity statements (e.g., water is H2O, heat is the motion of molecules) provide hints about how we might go about this.
Author
Hydrogen Compounds; Life Sciences; Exobiology

20020002029 Arizona State Univ., Dept. of Geological Sciences, Tempe, AZ USA
Equilibrium Modeling of Hydrothermal Vent Fluid Cooling and its Application in a Lab-Scaled Reactor
Dalla-Betta, Peter J., Arizona State Univ., USA; Vogelsonger, Ken, Arizona State Univ., USA; ODay, Peggy, Arizona State Univ., USA; Holloway, John R., Arizona State Univ., USA; General Meeting of the NASA Astrobiology Insititute; April 2001, pp. 21-22; In English; See also 20020002018; No Copyright; Avail: Issuing Activity; Abstract Only

A catalytic reactor system was developed to operate at pressures and temperature ranges encountered at deep-sea hydrothermal vents. This system will be used to test the hypothesis that during the cooling of hydrothermal fluid, by conduction or mixing, simple organic compounds are formed metastably via catalysis by transition-metal sulfides. Hydrothermal fluid will be cooled as it passes through inert (quartz) or sulfide mineral catalysts (pyrite, chalcopyrite, sphalerite, pyrrhotite). to test the affects of precipitation and dissolution of the catalyst, sulfide mineral will either be synthesized in situ from fluid cooling or placed in the reactor beforehand. In our thermodynamic model, a simplified composition (550mM NaCl, 1mM Fe(2+), 10 mM HS(-), 5 mM HCO3(-), pH 4.3, initial fO2 = PPM) was used to mimic a 350 C vent fluid end-member solution as it cools. A 250 bar database was created for use in the equilibrium modeling program EQ3/6. This database was composed of C4 or smaller CH/O compounds (n-alkanes, alcohols, aldehydes, ketones, carboxylic and hydroxy acids). Additionally, pyruvic acid and several TCA cycle intermediates were also included in the model system along with CHS/O compounds (COS, CS2, n-thiols, sulfides, and disulfides). Additional information is contained in the original extended abstract.
Author
Cooling; Hydrothermal Systems; Vents; Organic Compounds; Equilibrium; Minerals

20020002030 Colorado Univ., Dept. of Molecular, Cellular and Developmental Biology, Boulder, CO USA
BASIC: A New Method for the Isolation of RNA Catalysts
deZwart, Ico, Colorado Univ., USA; Yarus, Mike, Colorado Univ., USA; General Meeting of the NASA Astrobiology Insititute; April 2001, pp. 23; In English; See also 20020002018; No Copyright; Avail: Issuing Activity; Abstract Only

We propose a new screening method for the isolation of catalytic RNAs from a randomized RNA pool without the need for selection or the need for catalyst selfmodification. In order to find catalytic RNAs, catalytic reaction products must be related to the RNA that produced them. This will be possible if both the product and the catalytic RNA can be spatially localized in the same

vicinity. BASIC (Bead Attached Substrates for the Identification of Catalysts) is a method that meets these requirements: a substrate that yields a fluorescent product and the DNA template used to produce RNA are confined to a bead. A fluorescent bead indicates that the desired reaction has taken place, and in addition, the fluorescent bead contains template information for the catalytic RNA.
Author
Catalysts; Ribonucleic Acids; Computer Programs; Substrates

20020002031 Massachusetts Inst. of Tech., Dept. of Chemistry, Cambridge, MA USA
Crystallization of a Ni and FeS Protein that Fixes CO2 into Cell Carbon
Doukov, Tzanko I., Massachusetts Inst. of Tech., USA; Ragsdale, Stephen W., Nebraska Univ., USA; Drennan, Catherine L., Massachusetts Inst. of Tech., USA; General Meeting of the NASA Astrobiology Insititute; April 2001, pp. 24; In English; See also 20020002018; No Copyright; Avail: Issuing Activity; Abstract Only

Clostridium thermoaceticum is an anaerobic thermoacetogenic bacteria whose reductive acetyl-CoA pathway for CO2 fixation is a remnant from the very early stages of life. In a pivotal work Wachtershauser and Huber found that a NiS and FeS converts CH3-SH and CO into acetic acid. In the acetyl-CoA pathway methyltetrahydrofolate:corrinoid/iron-sulfur protein methyltransferase (MeTr) transfers the N5-methyl group of (6S)- methyltetrahydrofolate to the cobalt(I) of a corrinoid/iron sulfur protein (CP). The methyl group then combines with a CO and coenzyme A to form acetyl-CoA at a Ni-FeS center of the acetyl-CoA synthase activity of the bifunctional carbon monoxide dehydrogenase/acetyl-CoA synthase (ctCODH/ACS) enzyme. MeTr from Clostridium thermoaceticum has been crystallized, and its structure determined by X-ray crystallography. In our laboratory we are trying to obtain diffracting crystals of the other two enzymes of the pathway -CP and CODH/ACS. The latest results from the crystallization experiments will be reported.
Author
Carbon Dioxide; Crystallization; Enzymes; Nickel; Bacteria; Iron Compounds

20020002032 Florida Univ., Dept. of Molecular Cell Biology, Gainesville, FL USA
Higher Order Models for Detecting Functional Divergence When Analyzing the Evolutionary Past
Gaucher, Eric A., Florida Univ., USA; Miyamoto, Michael M., Florida Univ., USA; Benner, Steven A., Florida Univ., USA; General Meeting of the NASA Astrobiology Insititute; April 2001, pp. 25-26; In English; See also 20020002018; Original contains color illustrations; No Copyright; Avail: Issuing Activity; Abstract Only

The divergent evolution of protein sequences from genomic databases can be analyzed using different mathematical models. The most common treat all sites in a protein sequence as equally variable. More sophisticated models acknowledge the fact that purifying selection generally tolerates variable amounts of amino acid replacement at different positions in a protein sequence. In their ”stationary” versions, such models assume that the replacement rate at individual positions remains constant throughout evolutionary history. Non-stationary covarion versions, however, allow the replacement rate at a position to vary in different branches of the evolutionary tree. Recently, statistical methods have been developed that highlight this type of variation in replacement rates. Here, we show how positions that have variable rates of divergence in different regions of a tree (”covarion behavior”), coupled with analyses of experimental three-dimensional structures, can provide experimentally testable hypotheses that relate individual amino acid residues to specific functional differences in those branches. We illustrate this in the elongation factor family of proteins using Bayesian inference. In addition, based on previous work in this laboratory, we show that incorporating higher order models of sequence evolution lead to predictions of ancestral reconstruction character states that are different than those predicted by the less sophisticated parsimony method. Thus, we advocate the use of higher order models in comparative evolutionary analyses especially as the community attempts to predict protein function from the large amount of genomic data currently being produced by sequencing projects. Additional information is contained in the original extended abstract.
Author
Mathematical Models; Statistical Analysis; Bayes Theorem; Biological Evolution

20020002033 Florida Univ., Dept. of Chemistry, Gainesville, FL USA
The Genetics of Extraterrestrial Life?
Geyer, C. Ronald, Florida Univ., USA; Battersby, Thomas R., Florida Univ., USA; Benner, Steven A., Florida Univ., USA; General Meeting of the NASA Astrobiology Insititute; April 2001, pp. 27-28; In English; See also 20020002018; Original contains color illustrations; No Copyright; Avail: Issuing Activity; Abstract Only

One of the central questions of Astrobiology as it relates to the ongoing work of NASA to search for life through missions to other planets and their moons asks: ”How would we recognize life if we were to find it?” The Watson-Crick model for DNA

provides, through its elegant simplicity, the illusion of universality, especially to terrean biochemists and molecular biologists who know of no other molecule that can support Darwinian evolution. Ultimately, organic chemists must be recruited to ask the question: ”What might life, having a genesis independent from life on Earth, look like?” For more than a decade now, the Benner laboratory has asked this question, and developed a range of new organic molecules that explore possible alternative biopolymeric structures, both genetic and catalytic. From this has emerged a ”second generation” model for nucleic acid structures, which places chemical constraints on the universal genetic molecule. This talk will focus on an artificially expanded genetic information system (AEGIS), a DNA-like biomolecular system that has 12 ”letters” instead of the four found in naturally occurring DNA. We have developed general rules, using the language of organic chemistry, that guides and predicts the behavior of non-standard genetic systems. These rules were developed by studying genetic behavior in a large range of DNA analogs. The results from these studies show that hydrogen bonding must be considered in any ”second generation” model to predict, explain, and manipulate the behavior of nucleic acid-like artificial genetics systems. Further, we provide guidelines for designing artificial genetic systems. Additional information is contained in the original extended abstract.
Author
Exobiology; Extraterrestrial Life; Genetics; Biopolymers

20020002034 Carnegie Institution of Washington, Geophysical Lab., Washington, DC USA
Emergence and the Origin of Life
Hazen, Robert M., Carnegie Institution of Washington, USA; General Meeting of the NASA Astrobiology Insititute; April 2001, pp. 29-30; In English; See also 20020002018; No Copyright; Avail: Issuing Activity; Abstract Only

The geochemical origin of life may be modeled as a sequence of emergent events, each of which adds to molecular complexity and order. Each of these steps, if properly formulated, should be amenable to experimental study. Each emergent step, furthermore, may result in characteristic isotopic, molecular, and structural fossils that might be measured in extraterrestrial environments that have not been subjected to reworking by biological activity. Natural systems with many interacting components, such as atoms, molecules, cells or stars, often display complex, emergent behavior not associated with their individual components. In some instances, as in the emergence of turbulent flow in fluids, the solid state properties of crystals, or the periodic spacing of sand dunes, such complex behavior can be modeled a posteriori when appropriate interaction parameters have been determined. Other phenomena, such as the emergence of consciousness from collections of neurons or the emergence of social behavior from collections of humans, are, at least for the present, less amenable to quantitative analysis. Additional information is contained in the original extended abstract.
Author
Biological Evolution; Extraterrestrial Environments; Geochemistry; Activity (Biology)

20020002035 Carnegie Institution of Washington, Geophysical Lab., Washington, DC USA
Hydrothermal Reactions of Pyruvate: Production of Amphiphilic Molecules and Vesicle Formation
Hazen, Robert M., Carnegie Institution of Washington, USA; Cody, George D., Carnegie Institution of Washington, USA; Yoder, Hatten S., Jr., Carnegie Institution of Washington, USA; Deamer, David W., California Univ., USA; General Meeting of the NASA Astrobiology Insititute; April 2001, pp. 31; In English; See also 20020002018; No Copyright; Avail: Issuing Activity; Abstract Only

The synthesis of amphiphilic molecules capable of aqueous self-assembly into membrane-like structures, including bilayers and micelles, is an essential step in the emergence of a protocell. Mechanisms for the prebiotic synthesis and assembly of amphiphiles are thus of considerable interest. We observe amphiphile synthesis from pyruvate in a CO2-water fluid subjected to temperatures from 250 C to 350 C and pressures from 0.05 to 0.2 GPa (500 to 2000 atmospheres) for 2 hours. Principal run products include acetic acid and CO2 (from decarbonation of pyruvate) and methyl succinate (from dimerization of pyruvate and subsequent decarboxylation). We also observe up to 50% conversion of pyruvate to a water-insoluble, yellow-brown, strongly aromatic oily residue. Analysis by GCMS reveals this material to be a complex suite, including cyclic aromatic compounds, presumably formed by polymerization and subsequent cycloaddition reactions. Additional information is contained in the original extended abstract.
Author
Pyruvates; Protobiology; Polymerization; Aqueous Solutions

20020002036 Harvard Medical School, Dept. of Genetics, Boston, MA USA
Functional Proteins from a Random-Sequence Library
Keefe, Anthony D., Harvard Medical School, USA; Szostak, Jack W., Harvard Medical School, USA; General Meeting of the NASA Astrobiology Insititute; April 2001, pp. 32; In English; See also 20020002018; No Copyright; Avail: Issuing Activity; Abstract Only

Functional primordial proteins presumably originated from random sequences, but it is not known how frequently functional, or even folded, proteins occur in collections of random sequences. to address these issues we used in vitro selection of mRNA displayed proteins to allow sampling of a large number of distinct random sequences. Starting from a library of 6x10(exp 12) proteins each containing eighty contiguous random amino acids, we selected functional proteins by enriching for those that bind to ATP. This selection yielded four novel ATP-binding proteins that appear to be unrelated to each other or to anything found in the current databases of biological proteins. The frequency of occurrence of functional proteins in random-sequence libraries appears to be similar to that observed for equivalent RNA libraries.
Author
Proteins; Ribonucleic Acids; Genetics; Molecular Biology

20020002037 Massachusetts General Hospital, Dept. of Molecular Biology, Boston, MA USA
Evolutionary Accretion of Small Motifs Modulates RNA Activity
Larralde, Rosa, Massachusetts General Hospital, USA; Szostak, Jack W., Massachusetts General Hospital, USA; General Meeting of the NASA Astrobiology Insititute; April 2001, pp. 33; In English; See also 20020002018; No Copyright; Avail: Issuing Activity; Abstract Only

During in vitro selection experiments, it has become apparent that the simplest (i.e. shortest) solutions, not necessarily the best performing ones, tend to dominate and take over the surviving populations. This can be understood in the light that simple motifs are usually much more frequent than complex ones in starting populations and they will remain so in successive generations as long as they are fit enough to satisfy the selective pressure. It is not so clear what happens to simple solutions in the context of a changing environment, scenarios in which the selective pressure, for example, sets a new, more stringent functional cut-off for survival. If a simple, dominant solution is challenged to the limit of its fitness, can it be somewhat improved upon, or would it have to be abandoned and transformed into a different and more apt design? to address this question, the simplest ATP-aptamer known (the SASsanfar motif) was placed in a context of extra random sequence, and taken through an in vitro selection aiming for tighter ATP-binding. The change of selective pressure upon pre-existing functionalities has lead, in this instance, not to the establishment of a totally new solution, but to the recruitment of very small motifs that seem to modestly modulate the activity of the pre-existing aptamer. This observation seems to indicate that very large and complex functional RNAs need not have been established all at once in answer to particular chemical needs, but they may have slowly increased in size and varied their activity through the addition of small modules.
Author
Ribonucleic Acids; Biological Evolution; Molecular Biology; Adenosine Triphosphate

20020002038 Stanford Univ., Dept. of Geological and Environmental Sciences, Stanford, CA USA
Synthesis of Alpha-Amino Acids in Hydrothermal Media from Selected Primitive Starting Compounds
Lemke, Kono H., Stanford Univ., USA; Ross, David S., Geological Survey, USA; Bischoff, James L., Geological Survey, USA; Bird, Dennis K., Stanford Univ., USA; General Meeting of the NASA Astrobiology Insititute; April 2001, pp. 34-35; In English; See also 20020002018; No Copyright; Avail: Issuing Activity; Abstract Only

The source of amino acids from primitive starting substances remains a matter of conjecture, and the commonly employed starting mix in laboratory studies of prebiotic synthesis includes formaldehyde and HCN. Thermodynamic calculations for a CO2/N2/liquid water system with iron oxide/silicate or iron oxide/sulfide redox buffers show, however, that suitable levels of formaldehyde and cyanide cannot be present. Our calculations show, rather, that NH4(+), HCO2(-) and higher carboxylic acids are strongly preferred. Thus either formaldehyde and HCN were externally supplied at sufficient rates, or early amino acids were derived from NH4(+) and HCO2(-). Formate is an attractive candidate for the starting mixture since it is the basis of Fischer-Tropsch synthesis, and therefore carbon-carbon bond formation. The study described here employs various combinations of formaldehyde, HCN, ammonium, and formate in liquid water at 210 C. The goal is to ascertain the minimum set of starting materials for amino acid synthesis. Additional information is contained in the original extended abstract.
Author
Amino Acids; Synthesis (Chemistry); Carboxylic Acids; Formaldehyde; Thermodynamics

20020002039 Texas Univ., Inst. for Cellular and Molecular Biology, Austin, TX USA
Molecular Recognition, Catalysis and the Origin of Life
Levy, Matthew, Texas Univ., USA; Ellington, Andrew D., Texas Univ., USA; General Meeting of the NASA Astrobiology Insititute; April 2001, pp. 36-37; In English; See also 20020002018; No Copyright; Avail: Issuing Activity; Abstract Only

In an effort to better understand how the principles of molecular recognition may have affected the origin of biocatalysis on Earth, we have been using two different systems to investigate the ability of peptides and small molecules to facilitate the ligation

of oligonucleotides. In the first of theses two systems, we have been attempting to reassemble fragmented RNA aptamers in the presence of their cognate peptide ligands. We have found using the activating agent cyanogen bromide that ligation of two RNA aptamer fragments is specifically enhanced up to approx. 10 fold in the presence of the aptamers cognate peptide. However the overall yields for these ligation reactions are low (approx. 1-5%), and the reactions are plagued by the formation of side products. Additional information is contained in the original extended abstract.
Author
Biological Evolution; Peptides; Catalysis; Ligands

20020002040 Marine Biological Lab., Josephine Bay Paul Center for Evolution and Comparative Molecular Biology, Woods Hole, MA USA
Gene Fusion: A Genome Wide Survey
Liang, Ping, Marine Biological Lab., USA; Riley, Monica, Marine Biological Lab., USA; General Meeting of the NASA Astrobiology Insititute; April 2001, pp. 38-39; In English; See also 20020002018
Contract(s)/Grant(s): NCC2-1054; No Copyright; Avail: Issuing Activity; Abstract Only

As a well known fact, organisms form larger and complex multimodular (composite or chimeric) and mostly multi-functional proteins through gene fusion of two or more individual genes which have independent evolution histories and functions. We call each of these components a module. The existence of multimodular proteins may improves the efficiency in gene regulation and in cellular functions, and thus may give the host organism advantages in adaptation to environments. Analysis of all gene fusions in present-day organisms should allow us to examine the patterns of gene fusion in context with cellular functions, to trace back the evolution processes from the ancient smaller and uni-functional proteins to the present-day larger and complex multi-functional proteins, and to estimate the minimal number of ancestor proteins that existed in the last common ancestor for all life on earth. Although many multimodular proteins have been experimentally known, identification of gene fusion events systematically at genome scale had not been possible until recently when large number of completed genome sequences have been becoming available. In addition, technical difficulties for such analysis also exist due to the complexity of this biological and evolutionary process. We report from this study a new strategy to computationally identify multimodular proteins using completed genome sequences and the results surveyed from 22 organisms with the data from over 40 organisms to be presented during the meeting. Additional information is contained in the original extended abstract.
Author
Genome; Proteins; Molecular Biology; Microorganisms; Cytology

20020002041 Tokyo Univ., Dept. of Complexity Science and Engineering, Hongo, Japan
In-Situ Spectroscopic Observation of Abiotic Chemical Reactions Producing Organic Matter
Matsui, Takafumi, Tokyo Univ., Japan; Sugita, Seiji, Tokyo Univ., Japan; Imanaka, Hiroshi, Tokyo Univ., Japan; Fuyuki, Masanori, Tokyo Univ., Japan; Kobayashi, Kensei, Yokohama National Univ., Japan; General Meeting of the NASA Astrobiology Insititute; April 2001, pp. 40-41; In English; See also 20020002018; No Copyright; Avail: Issuing Activity; Abstract Only

One of the most important issues in the origin of life is how organic matter was supplied to the surface of the Earth. Proposed mechanisms so far can be categorized generally to two types: endogenous and exogenous. The former is organic synthesis from inorganic components of either the atmosphere or the ocean with high-energy processes, such as lightening, impact-induced shock waves, and cosmic ray radiation. The latter is delivery of organic matter from the space through infall of asteroids, comets, meteors, and other bodies to the Earth. Although most attention is paid to the surviving organic matter through the exogenous mechanisms, most of organic matter reached the atmosphere or the surface of the Earth is expected to be destroyed upon its arrival because of the extremely high temperature (i.e., high thermal energy). Consequently, no matter which types of mechanism is dominant, high-energy chemical reactions play a crucial role in supply of organic matter on the prebiotic Earth. However, little direct observation has been made for such high-energy chemical reactions in laboratory experiments in the context of the origin of life. Since the physical conditions for high-energy chemical reaction is usually very dangerous and transient, most measurement methods cannot be 40 used. Thus, the high-energy chemical reactions have been treated as black boxes. Nevertheless, optical spectroscopy may provide a peep hole to the black boxes. Because of the high level of energy, these chemical reactions are often associated with intense light emission. The spectrum of the light emission reflects the physical and chemical conditions of the reaction field, and it has practically no time delay between change in the physical/chemical conditions and that in emission spectra. The purpose of our study is to understand the high-energy chemical reactions through in-situ spectroscopic observations. Additional information is contained in the original extended abstract.
Author
Chemical Reactions; Organic Materials; Spectroscopy; Abiogenesis

20020002042 Marine Biological Lab., Josephine Bay Paul Center for Comparative Molecular Biology and Evolution, Woods Hole, MA USA

Multiple Catalytic Functions of the Escherichia coli Fad B Protein Terminal Region: Anatomy of a Promiscuous Active Site

McCormack, Tom, Marine Biological Lab., USA; Riley, Monica, Marine Biological Lab., USA; General Meeting of the NASA Astrobiology Insititute; April 2001, pp. 42; In English; See also 20020002018; No Copyright; Avail: Issuing Activity; Abstract Only

In Escherichia coli, the fadBA operon encodes the fatty acid oxidation multienzyme complex. While the C-terminus of the FadB protein carries out a single reaction, NADH-dependent dehydrogenation, the N-terminal region, which shares homology with a wide range of CoA-binding enzymes, performs three separate catalytic functions, namely isomerization, hydration and epimerization. At least two of these reactions, epimerization and hydration, appear to occur at a single active site defined by two catalytic glutamate residues, while the third reaction, isomerization appears to possess an active site with elements both common to and separate from the active site of the other two reactions. The three-dimensional structures of several proteins from the hydratase/isomerase superfamily have been solved, providing much information about the active site residues and catalytic mechanisms of enzymes within a superfamily which shows considerable variability in both substrate specificity and reaction chemistry. Structural alignments reveal a strikingly similar active site fold in spite of a diverse combination of catalytic residues for different enzymes within the hydratase/isomerase superfamily. Among the proteins within this superfamily whose structures have been determined, the E. coli FadB N-terminal domain shares greatest sequence similarity to rat liver enoyl CoA hydratase, allowing us to construct a three-dimensional model of the FadB N-terminus. FadB illustrates the diversity of mechanisms by which proteins can perform multiple functions, even within a common active site motif.

Author

Escherichia; Proteins; Chemical Reactions; Isomerization; Catalysts

20020002043 Pennsylvania State Univ., Astrobiology Research Center, University Park, PA USA

MALDI-MS, HPLC-APCI-MS and Solids NMR Analysis of Hydrogen Cyanide Polymers

Minard, R. D., Pennsylvania State Univ., USA; Fiddler, M. N., Pennsylvania State Univ., USA; Shields, E. P., Pennsylvania State Univ., USA; Mueller, K. T., Pennsylvania State Univ., USA; Jones, A. D., Pennsylvania State Univ., USA; Eastwood, A. L., Virginia Univ., USA; Schendel, J., Puget Sound Univ., USA; General Meeting of the NASA Astrobiology Insititute; April 2001, pp. 43; In English; See also 20020002018; No Copyright; Avail: Issuing Activity; Abstract Only

The role of hydrogen cyanide polymer chemistry in the origin of life has provoked much speculation. In spite of extensive efforts by many groups, a satisfactory understanding of this polymer's structure and mechanism of formation still eludes us. Our studies involve the application of modern powerful instrumental methods to this problem. Using MALDI-MS we have found that hydrogen cyanide polymers, (HCN)n, formed from HCN monomer, showed MH+ peaks for n = 8 to 25 with the maximum occurring at n = 15 to 17. HCN polymer formed from diaminomaleonitrile (HCN tetramer) showed a similar MALDI spectra with no enhancement for peaks at n = 4, 8, 12, 16, etc. implying the breakdown of the tetramer to monomer followed by monomer repolymerization. The MALDI-MS spectra of polymer formed from aminomalononitrile (HCN trimer) showed oligomers from m/z 200 to 800, but these did not match an (HCN)n series. In other studies, the water soluble products derived from stirring HCN polymer with water at room temperature for 1 to 3 days consisted primarily of two compounds, urea and a compound with formula C6H8N6 as determined by APCI-exact mass MS whose structure we are determining. We are also carrying out the synthesis of (H13C15N)n. Solids C-13/N-15 NMR analysis of this labeled polymer should provide considerable structural detail of HCN polymer.

Author

Hydrocyanic Acid; Nuclear Magnetic Resonance; Polymer Chemistry; Solids; Liquid Chromatography; Biological Evolution

20020002044 Los Alamos National Lab., NM USA

Molecular Dynamics (MD) Lattice Gas for Modeling Molecular Self-Assembly and Self-Organization Processes

Nilsson, Martin, Los Alamos National Lab., USA; Rasmussen, Steen, Los Alamos National Lab., USA; General Meeting of the NASA Astrobiology Insititute; April 2001, pp. 44-46; In English; See also 20020002018; No Copyright; Avail: Issuing Activity; Abstract Only

This new simulation method fills a gap between traditional molecular dynamics (MD) simulations on the one hand and lattice gas automata (LGA) and lattice Boltzmann equations (LBE) on the other. MD simulations generally address molecular processes studied on length scales of angstroms to nanometers and over times scales of pico- to nanoseconds. LGA and LBE simulate complex fluids and fluid flow phenomena on length scales of submicrometers to meters and over time scales of microseconds to minutes. Our MD lattice gas simulations address molecular interactions on nanometer to micrometer length scales and over time

scales up to milliseconds on workstations and seconds on supercomputers. This intermediate range suits them to modeling molecular self-organization and self-assembly processes involving ions, monomers, complex polymers, polymer aggregates (supermolecular structures), complex surfaces with charge, and chemical reactions. With our MD lattice gas, we have simulated molecular interactions spanning three levels of complexity. At the first level, we begin with water molecules, ions, and both hydrophilic and hydrophobic monomers as our basic ingredients. At the second level in a aqueous environment, monomers can form amphiphilic chains (i.e., polymers with a hydrophilic head and hydrophobic tail). At the third level, these polymers can self assemble into amphiphilic aggregates such as micelles or vesicle membranes, which under certain conditions can self-reproduce. At each level, we observe how local interactions generate higher-order structures with new functionalities not exhibited at the level of their constituents. Additional information is contained in the original extended abstract.
Author
Molecular Dynamics; Mathematical Models; Crystal Lattices; Molecular Chains; Abiogenesis; Computerized Simulation

20020002045 NASA Ames Research Center, Moffett Field, CA USA
Models of Protocellular Structure, Function and Evolution
New, Michael H., NASA Ames Research Center, USA; Pohorille, Andrew, NASA Ames Research Center, USA; Szostak, Jack W., Massachusetts General Hospital, USA; Keefe, Tony, Massachusetts General Hospital, USA; Lanyi, Janos K., California Univ., USA; General Meeting of the NASA Astrobiology Insititute; April 2001, pp. 47-48; In English; See also 20020002018; No Copyright; Avail: Issuing Activity; Abstract Only

In the absence of any record of protocells, the most direct way to test our understanding of the origin of cellular life is to construct laboratory models that capture important features of protocellular systems. Such efforts are currently underway in a collaborative project between NASA-Ames, Harvard Medical School and University of California. They are accompanied by computational studies aimed at explaining self-organization of simple molecules into ordered structures. The centerpiece of this project is a method for the in vitro evolution of protein enzymes toward arbitrary catalytic targets. A similar approach has already been developed for nucleic acids in which a small number of functional molecules are selected from a large, random population of candidates. The selected molecules are next vastly multiplied using the polymerase chain reaction. A mutagenic approach, in which the sequences of selected molecules are randomly altered, can yield further improvements in performance or alterations of specificities. Unfortunately, the catalytic potential of nucleic acids is rather limited. Proteins are more catalytically capable but cannot be directly amplified. In the new technique, this problem is circumvented by covalently linking each protein of the initial, diverse, pool to the RNA sequence that codes for it. Then, selection is performed on the proteins, but the nucleic acids are replicated. Additional information is contained in the original extended abstract.
Author
Protobiology; Proteins; Mutagens; Cells (Biology)

20020002046 State Univ. of New York, Dept. of Geosciences, Stony Brook, NY USA
Fate of CO Hydration Products in Anoxic Solution: The Photochemical and Thermal Decomposition of Na-Formate
Penfield, Robin, State Univ. of New York, USA; Schoonen, Martin A. A., State Univ. of New York, USA; Kasting, James F., Pennsylvania State Univ., USA; Minard, Robert D., Pennsylvania State Univ., USA; General Meeting of the NASA Astrobiology Insititute; April 2001, pp. 49-50; In English; See also 20020002018; No Copyright; Avail: Issuing Activity; Abstract Only

The thermal and photochemical decomposition of sodium formate has been measured for dilute aqueous solutions over a range of temperatures (4-75 C), pH (5.4 - 9.0), and radiation sources (253.7 nm, 800-2500 nm, and darkness). Formaldehyde abundance was determined through spectrophotometry, and both sodium formate and acetate were measured through ion chromatography. This rate data will be used to evaluate carbon cycling between the early atmosphere and hydrosphere, and the potential accumulation of simple organics such as formate and formaldehyde in an early ocean. The secondary reactions of formate in the ocean may have been relevant to prebiotic synthesis. For instance, sodium formate disproportionates to formaldehyde and sodium bicarbonate in the absence of oxygen, and could potentially lead to formose polymerization if formaldehyde concentrations approached 10mmol/L. Additional information is contained in the original extended abstract.
Author
Anoxia; Photochemical Reactions; Sodium; Thermal Decomposition; Carbon Monoxide; Formates

20020002047 Los Alamos National Lab., NM USA

Creating a Proto-Organism Through Lowest Entropy Departure Path

Rasmussen, Steen, Los Alamos National Lab., USA; Chen, Liao-Hai, Los Alamos National Lab., USA; Colgate, Stirling, Los Alamos National Lab., USA; Lackner, Klaus, Los Alamos National Lab., USA; Nilsson, Martin, Los Alamos National Lab., USA;
General Meeting of the NASA Astrobiology Insititute; April 2001, pp. 51-52; In English; See also 20020002018; No Copyright; Avail: Issuing Activity; Abstract Only

We seek to construct a biochemical system that can derive energy from a coupled redox complex-a simple form of metabolism-and use information carried in proto-genes where both complexes are integrated in a lipid aggregate. This proto-organism can self replicate, use energy and nutrients available from its environment, undergo evolutionary change over time, and ultimately die. All the molecular species used are either simulated readily in prebiotic chemical reactions, or are present as organic components of carbonaceous chondrites and can thus be assumed to have existed on Earth some 4 billion years ago. Although we use such simple building blocks, we do not seek to reconstruct the origin of life on Earth. Indeed, our focus is on fundamental processes that could lead to the self-organization of matter into functional units and, thereby, helps describe the formation of life anywhere in the universe. Two experimental systems have to be integrated in the laboratory and in simulation combining the three critical physico-chemical structures. A templating polymer (proto-gene) with a hydrophobic backbone performs template directed replication at a lipid interface (compartment). by using the slight energy advantage from the lipid template complex compared to them being separated, more interface can form. A following hybridization reaction between the original template and two complementary oligomers is also thermodynamically down hill. As this new three component complex sinks into the hydrophobic environment, ligation (polymerization) becomes thermodynamically favorable as a means for generating more templates. Thus, a weak energetic coupling exists between templating and interface generation. Additional information is contained in the original extended abstract.
Author

Biochemistry; Entropy; Organisms; Physical Chemistry; Biological Evolution

20020002048 Marine Biological Lab., Woods Hole, MA USA

Evolution of Proteins

Riley, Monica, Marine Biological Lab., USA; McCormack, Tom, Marine Biological Lab., USA; Nahum, Laila, Marine Biological Lab., USA; Kerr, Alastair, Cereon Corp., USA; Liang, Ping, Marine Biological Lab., USA; General Meeting of the NASA Astrobiology Insititute; April 2001, pp. 53-54; In English; See also 20020002018; No Copyright; Avail: Issuing Activity; Abstract Only

The history of the evolution of proteins on planet earth can be reconstructed in important ways by the study of contemporary proteins. The expansion from simple beginnings of kinds and capabilities of proteins is a history of gene duplication and divergence. Families of contemporary proteins that seem likely to have shared ancestors have been assembled using information on protein sequences derived from fully sequenced microbial genomes. Clustering of related proteins based on sequence comparisons both within and between organisms has produced large classes of evolutionarily related enzymes, regulators and transporters. Using recursive sequence analysis, boundaries of groups of like proteins have been extended such that one can visualize the mechanisms by which ancestral proteins have diverged to yield progeny proteins with differences in function. We have examined relationships among evolutionarily related enzymes of intermediary metabolism and have found that the chemistry of the reaction is conserved in most cases, specificity for ligands in some cases, and both attributes in many cases. Going beyond sequence analysis, one can connect the amino acid sequence information with structural information, to see familial relationships based on structure that can no longer be detected on the basis of sequence alone. In these ways it is becoming possible to group classes of proteins together that plausibly came from one or a few ancestral proteins. Examples will be given. Additional information is contained in the original extended abstract.
Author

Genome; Proteins; Biological Evolution; Amino Acids

20020002049 Texas Univ., Inst. for Cellular and Molecular Biology, Austin, TX USA

Expanding the Limits of RNA Catalysis

Robertson, Michael P., Texas Univ., USA; Ellington, Andrew D., Texas Univ., USA; General Meeting of the NASA Astrobiology Insititute; April 2001, pp. 55-56; In English; See also 20020002018; No Copyright; Avail: Issuing Activity; Abstract Only

The RNA World hypothesis proposes that at some period during the evolution of life, RNA molecules performed the dual functions of genetic storage and enzymatic catalysis. The possibility that RNA can function in both these capacities was demonstrated with the discovery of catalytic RNA in the early 1980s. Since then the types of chemical reactions that RNA has been shown to catalyze has steadily increased and with it the feasibility of an all-RNA metabolism. However, a key aspect of

modern biocatalysis is the ability of enzymes to attenuate their level of activity in response to changing environmental conditions. Presumably, a similar regulation strategy would also be necessary to sustain a reasonably complex RNA-based metabolism. We have isolated and designed several RNA ligase ribozymes whose activity are regulated by the presence of a variety of different effectors. An oligonucleotidedependent ligase (L1) was isolated from a randomized pool of RNA using in vitro selection. We have isolated and designed several RNA ligase ribozymes whose activity are regulated by the presence of a variety of different effectors. An oligonucleotidedependent ligase (L1) was isolated from a randomized pool of RNA using in vitro selection. This ribozyme's activity in the presence of a specific oligonucleotide effector is 10,000-fold greater than when the effector is absent. Other allosterically regulated ribozymes were engineered by replacing a non-essential stem loop of L1 with various small molecule binding RNA aptamers to create aptamer-ribozyme hybrids (aptazymes). Ligand binding induces a conformational change in the aptamer domain which is propagated to the ribozyme domain through a short linking stem which allows the ribozyme domain to adopt an active conformation. The aptazyme's level of response to ligand can be adjusted by altering the basal stability of the stem linking the aptamer and ribozyme domains. This approach has resulted in aptazymes that are regulated by ATP, theophylline, and FMN with activations of 800, 1600, and 250 respectively. Additional information is contained in the original extended abstract.

Author

Biological Evolution; Chemical Reactions; Enzyme Activity; Ribonucleic Acids; Catalysis

20020002050 Geological Survey, Menlo Park, CA USA

Peptide Formation in Hydrothermal Environments

Ross, David S., Geological Survey, USA; Lemke, Kono, Geological Survey, USA; Matsuno, Koichiro, Nagaoka Univ. of Technology, Japan; General Meeting of the NASA Astrobiology Insititute; April 2001, pp. 57; In English; See also 20020002018; No Copyright; Avail: Issuing Activity; Abstract Only

The formation of prebiologically significant oligomers, including peptides and polynucleotides, is challenged by both thermodynamic and chemical kinetics factors, and the nature of their initial genesis is still not clear after more than 3 decades of study. For peptides it has been recognized that amide formation in aqueous solution is uphill by roughly 2 kcal/mol (25 C), and successive condensation will quickly lead to peptide concentrations well below meaningful values after just a few steps. Amide formation is estimated to be very slow, moreover, and even if there were there some means of eliminating reverse hydrolysis the estimated characteristic times of homogeneous condensation to dipeptides at 25 C and around pH 7 are about 5 x 10(exp 11) yr. The times fall to about 5 x 10(exp 7) yr only at temperatures above 100 C, but growth to larger oligomers would obviously be an unacceptably lengthy process even in astrobiological terms. We present here our consideration of recent data in experiments simulating the oceanic circulation of water through hydrothermal zones (Imai, et al., 1999), where glycine was converted to a range of polyglycines at 225 C. The analysis shows that prebiotic peptide formation may not be as difficult as has been projected. While the equilibrium levels of diglycine observed were about a factor of 2 greater than predicted thermochemically, a deviation perhaps within error limits, we estimate that the equilibrium quantities of triglycine exceeded prediction by factor a factor of about 200. The larger peptides observed were present at even greater divergences from prediction. The rates of peptide formation were similarly surprising: di- and triglycine attained equilibrium values over periods 30-40 times more rapidly than predictions based on known hydrolysis rate constants and the pertinent thermochemistry. Their rates of growth, moreover, were exponential, apparently reflecting the circulation of the reactant stream through temperature zones. Autocatalysis is known in some aqueous oxidation processes involving highly reactive free radical intermediates, but it has not been recognized in simple condensations such as these. These results suggest a means for peptide formation involving self-assisted condensation, a process which could develop through a kinetic and thermodynamic sequence stimulated by the thermal cycling of the reactant stream. Such a path could be vital to the ultimate formation of functional proteins in the prebiotic oceans.

Author

Aqueous Solutions; Hydrolysis; Peptides; Polynucleotides; Reaction Kinetics; Hydrothermal Systems

20020002051 Scripps Research Inst., Dept. of Chemistry and Molecular Biology, La Jolla, CA USA

A Chiroselective Peptide Replicator

Saghatelian, Alan, Scripps Research Inst., USA; Yokobayashi, Yohei, Scripps Research Inst., USA; Soltani, Kathy, Scripps Research Inst., USA; Ghadiri, M. Reza, Scripps Research Inst., USA; General Meeting of the NASA Astrobiology Insititute; April 2001, pp. 58-59; In English; See also 20020002018; No Copyright; Avail: Issuing Activity; Abstract Only

The origin of homochirality is often addressed from the perspective of enantioselection that seeks to evoke various scenarios for the production of enantiomeric differences within the prebiotic chiral pool. Although several plausible physicochemical processes have been suggested to be capable of producing minute enantiomeric differences, none can produce significant imbalances required for the production of homochiral biopolymers without some selectable chiral amplification process(es).

Therefore, it is believed that the origins of homochirality in living systems must have been based on selection and chiroselective amplification processes. Yet despite its central importance, the feasibility of nonenzymatic template-directed chiroselective amplification in biopolymers had not been previously demonstrated. Here we report that a 32-residue peptide replicator is capable of amplifying homochiral products efficiently and specifically through a chiroselective autocatalytic cycle. The chiroselective amplification is highly robust and can discriminate amongst structures possessing even single stereochemical mutations within otherwise homochiral sequences. Remarkably, the system also exhibits a hitherto unknown dynamic stereochemical editing function. The editing function is manifested through certain heterochiral sequences- mutants arising through uncatalyzed background fragment coupling reactions- that possess potent cross-catalytic activities for promoting the production of the homochiral product. This study thus lends support to the postulate that self-replicating polypeptides could have played a role in the origin of homochirality on Earth.
Author
Amplification; Biopolymers; Catalytic Activity; Polypeptides

20020002052 Australian Geological Survey Organisation, Canberra, Australian Capital Territory, Australia
When Can You Attribute Biological Origins to Small Organic Molecules?
Summons, Roger E., Australian Geological Survey Organisation, Canberra, Australia; General Meeting of the NASA Astrobiology Insititute; April 2001, pp. 60; In English; See also 20020002018; No Copyright; Avail: Issuing Activity; Abstract Only

The carbon chemistry of living systems is one of the most exactly known branches of all science and this chemistry provides precise tools for identifying and characterizing extant and extinct life on Earth and, potentially, throughout the universe. Lipids are especially ubiquitous and recalcitrant small organic compounds that are common to all living things and which carry structural and isotopic information pertaining to their mode of synthesis. Hydrocarbons, which encode diagnostic structural and isotopic information, are the most readily preserved lipid end-product and are widely distributed in terrestrial sediments of all ages. Hydrocarbons are also abundant components of carbonaceous meteorites. This paper summarizes deliberations of a group from the NASA Task Force on Biosignatures for Mars Exploration and presents some criteria that assist in distinguishing between biogenic and abiogenic hydrocarbons. Characteristics of biogenic hydrocarbons include: (1) Enantiomeric excess; (2) Preference for certain diasteromers; (3) Constitutional isomer preference; (4) Repeating constitutional sub-units or atomic ratios; (5) Clusters or patterns in carbon number, concentration for related compounds; and (6) Systematic isotopic ordering at molecular level. Their utility can be tested through comparisons of hydrocarbon distributions for ancient terrestrial sediments with those reported for meteorites.
Author
Carbonaceous Meteorites; Hydrocarbons; Life Sciences; Lipids; Organic Compounds

20020002053 California Univ., Chemistry Dept., Riverside, CA USA
Alternative Nucleic Acids
Switzer, Christopher, California Univ., USA; Chaput, John C., California Univ., USA; Haque, Azizul, California Univ., USA; Lee, Dong-Kye, California Univ., USA; Kim, Paul H., California Univ., USA; Sinha, Surajit, California Univ., USA; General Meeting of the NASA Astrobiology Insititute; April 2001, pp. 61; In English; See also 20020002018; No Copyright; Avail: Issuing Activity; Abstract Only

Our goal is to synthesize Alternative Nucleic Acids (ANAs) to attempt the optimization of polymer structure subject to the constraints of prebiotic availability, template-directed reproduction, replication conservative mutation, and fitness. We have identified ANAs by taking small steps in ”structure-space” away from RNA (the best model for a molecule bearing features both universal and unique to life) that may avoid some of the problems inherent in fulfillment of the aforementioned constraints. ANAs are under investigation with novel perturbations to (i) base-pairing domains (ii) formal charges, and (iii) the phosphodiester backbone. These studies help to define chemical parameters for molecular evolution. The work also addresses whether nucleic acid-like molecules are sufficient to enable the origin of life and what limitations exist for life elsewhere in the universe based on a single biopolymer (eg. RNA) rather than multiple biopolymers (DNA, RNA, proteins, carbohydrates). Recent accomplishments in these areas will be presented.
Author
Biological Evolution; Chemical Evolution; Deoxyribonucleic Acid; Molecules; Synthesis (Chemistry); Nucleic Acids

20020002054 Instituto Nacional de Tecnica Aeroespacial, Centro de Astrobiologia, Torrejon de Ardoz, Spain
Evolution of Gene Order in Prokaryotes
Tamames, Javier, Instituto Nacional de Tecnica Aeroespacial, Spain; Gonzalez, Maria, Instituto Nacional de Tecnica

Aeroespacial, Spain; Valencia, Alfonso, Instituto Nacional de Tecnica Aeroespacial, Spain; General Meeting of the NASA Astrobiology Insititute; April 2001, pp. 62-63; In English; See also 20020002018; No Copyright; Avail: Issuing Activity; Abstract Only

Gene order conservation (GOC) has been proposed as a very useful tool for predicting interactions between the proteins encoded in these genes. Also it has been proposed as a tool for studying the evolution of genomes and organisms (Lathe et al, 2000). We have performed an extensive study of GOC between 32 bacterial and 7 archaeal genomes. Our procedure runs alignments between all ORFS for every pair of genomes, and identifies orthologues and clusters with gene order conservation. For studying the relation between GOC and evolution, distances between organisms are estimated using both classical phylogenies using SSU rRNA sequences and genomic methods such as common gene content between species. The results show that GOC is a labile characteristic of genomes, that are considerably rearranged during evolution. Nevertheless, GOC is still detectable at medium phylogenetic distances (those between E.coli and B.subtilis, for instance), and therefore can be valuable information for studying evolution. GOC is a better measure of relationships between organisms than common gene content, and can help to uncover and solve inconsistencies in classical phylogenies. It can be used also for studying important evolutionary traits such as lateral gene transfer between organisms. Even if GOC tends to be lost during evolution, some specially conserved clusters are apparent. The cluster of ribosomal proteins is the best known example. This conservation implies an active selection process maintaining the structure of the clusters. Recently we have published new hypothesis for this selection. At least in one case (cluster dcw taking part in cell wall byosynthesis and cell division), it is likely the existence of a link between the organization of the cluster and phenotipic properties, cellular morphology in this case (Tamames et al, 2001). This is in accordance with previous hypothesis relating morphology of the bacterial cells with evolution (Seifert and Fox, 1998).

Author

Bacteria; Genome; Proteins; Gene Expression; Evolution (Development)

20020002055 Florida Univ., Dept. of Anatomy and Cell Biology, Gainesville, FL USA

Experimental Paleobiochemistry: Understanding Major Transitions in Life on Earth

Thomson, J. Michael, Florida Univ., USA; Aris, John P., Florida Univ., USA; Benner, Steven A., Florida Univ., USA; General Meeting of the NASA Astrobiology Insititute; April 2001, pp. 64-65; In English; See also 20020002018; Original contains color illustrations; No Copyright; Avail: Issuing Activity; Abstract Only

Astrobiology requires integrating concepts from natural history with concepts from the physical sciences. The former includes geology, paleontology, and paleoecology; the latter includes chemistry, physics, and molecular biology. In the past, this integration has required collaborations between individuals and laboratories in different disciplines. In the future, a single individual working in a single laboratory will be trained at this level of ”comprehensivity”, and to design insightful research projects. Following this strategy, we have explored the interaction between fungi and their environment over the past 100 million years, a period over which the planet has undergone dramatic upheavals in the climate that it carries and the life that it supports. We have reconstructed elements of the molecular biology of the yeasts that invaded the fruit, and gave rise to the modern process known as ”fermentation”. These fungi emerged to exploit the new resource made available by angiosperms (fruiting plants), that began to provide the dominant floral genera over much of the planet towards the end of the Cretaceous. Resurrection of these ancestral proteins in a ”paleobiochemistry” experiment, and data collected on their physical chemical behavior in the laboratory, provide insight into how this metabolic process arose through the interaction between the fungus and a host in the paleoecosystem. Further, experimental paleobiochemistry permits us to understand features of the ”downstream” paleoecology, including the interaction of fruit flies and other frugivorous animals with fruit in the ecology that emerged following the extinction of the dinosaurs. What follows is a remarkably complete understanding of ”function”, extending from the molecules to the planet. We have also focused on the reliability of ancestral reconstructions inferred by the analysis of DNA and protein sequences from contemporary organisms. Enhanced reliability comes, of course, from larger collections of descendent sequences, and we 64 have collected 15 of these from a collection of closely related yeasts. The robustness of the reconstructions with respect to different methods for their creation has also been explored. We have also developed tools for dating molecular changes with respect to altered developmental function. These changes accompany those of the surrounding environmental constraints placed on the interactions between fungi, fruit, and fruit flies, and extend a better understanding of the evolution of early life on earth. Additional information is contained in the original extended abstract.

Author

Chemical Reactions; Paleobiology; Paleontology; Fungi

20020002056 Scripps Research Inst., Dept. of Chemistry, La Jolla, CA USA

De Novo Catalysts of Biopolymer Synthesis

Wilcoxen, Keith M., Scripps Research Inst., USA; Weinberg, Dana, Scripps Research Inst., USA; Ghadiri, M. Reza, Scripps Research Inst., USA; General Meeting of the NASA Astrobiology Insititute; April 2001, pp. 66; In English; See also 20020002018; No Copyright; Avail: Issuing Activity; Abstract Only

Nucleophilic catalysis of acyl transfer reactions is a fundamental theme in the biological synthesis of many naturally occurring biopolymers and natural products. The ability of enzymes to carry out selective acyl transfer reactions has given the cellular organism a vast array of molecules needed for sustained life. Simple carbonyl reactions have provided a biological basis for carbon-carbon bond formation necessary for the production of peptides, fatty acids, polyesters, polynucleic acids, polysaccharides and most secondary metabolites, many of which are formed by the catalytic properties of another biopolymer. The formation of many of these biopolymers is achieved by the repetitive and controlled living polymerization of thioester monomers covalently bound to condensing enzymes through a thioester bond. Among these, catalytic amide bond formation has proven to be a versatile and ubiquitous method for the biosynthesis of proteins and non-ribosomal peptides. It is under this context that we have selected the sequence of a 33-residue -helical peptide, GCN4-LI, which is known to assemble into a stable, homomeric 4-helix bundle, as the basis scaffold for our acyl transfer catalysts, with catalytic residues located near the interface of the helices in the helical bundle. We wish to report initial results toward the development of de novo scaffold and active site engineering of an amino acid condensing enzyme, mimicking the properties of nonribosomal peptide synthase, in an effort to achieve elementary catalytic function in a versatile and programmable system. Additional information is contained in the original extended abstract.

Author

Catalysis; Biopolymers; Polymerization; Biosynthesis

20020002057 Connecticut Univ., Dept. of Molecular and Cell Biology, Storrs, CT USA

Mosaicism in 16S rRNA Genes

Zhaxbayeva, Olga A., Connecticut Univ., USA; Olendzenski, Lorraine, Connecticut Univ., USA; Gogarten, J. Peter, Connecticut Univ., USA; General Meeting of the NASA Astrobiology Insititute; April 2001, pp. 67-68; In English; See also 20020002018; No Copyright; Avail: Issuing Activity; Abstract Only

The observation that genome content trees and traditional small subunit ribosomal RNA phylogenies agree with each other has been used to discount the importance of horizontal gene transfer (HGT). However, this congruence is also in perfect agreement with the theory that prokaryotic taxonomic units might exclusively reflect HGT frequency and not vertical inheritance: If two organisms appear related because they more frequently exchange genes with each other; their genome content becomes more similar, and at the same time each individual gene tree becomes more likely to group the two particular organisms together, the more frequently the organisms exchanged genes. Nevertheless, other gene trees often show strong well supported conflicts with 16S and with genome content trees, thus the congruence between genome content and 16S rRNA trees remains somewhat surprising. Additional information is contained in the original extended abstract.

Author

Ribonucleic Acids; Prokaryotes; Genome; Genes

20020002058 NASA Ames Research Center, Moffett Field, CA USA

Biogeochemical Processes in Microbial Ecosystems

DesMarais, David J., NASA Ames Research Center, USA; General Meeting of the NASA Astrobiology Insititute; April 2001, pp. 73-74; In English; See also 20020002018; No Copyright; Avail: Issuing Activity; Abstract Only

The hierarchical organization of microbial ecosystems determines process rates that shape Earth's environment, create the biomarker sedimentary and atmospheric signatures of life, and define the stage upon which major evolutionary events occurred. In order to understand how microorganisms have shaped the global environment of Earth and, potentially, other worlds, we must develop an experimental paradigm that links biogeochemical processes with ever-changing temporal and spatial distributions of microbial populations and their metabolic properties. Additional information is contained in the original extended abstract.

Author

Biogeochemistry; Ecosystems; Microorganisms

20020002059 NASA Ames Research Center, Moffett Field, CA USA

Ecogenomics: Ensemble Analysis of Gene Expression in Microbial Communities

Sogin, Mitchell, Marine Biological Lab., USA; DesMarais, David J., NASA Ames Research Center, USA; Stahl, D. A., Manitoba Univ., Canada; Pace, Norman R., Colorado Univ., USA; General Meeting of the NASA Astrobiology Insititute; April 2001, pp. 75-76; In English; See also 20020002018; No Copyright; Avail: Issuing Activity; Abstract Only

The hierarchical organization of microbial ecosystems determines process rates that shape Earth's environment, create the biomarker sedimentary and atmospheric signatures of life, and define the stage upon which major evolutionary events occurred. In order to understand how microorganisms have shaped the global environment of Earth and, potentially, other worlds, we must develop an experimental paradigm that links biogeochemical processes with ever-changing temporal and spatial distributions of microbial populations and their metabolic properties. Additional information is contained in the original extended abstract. Author

Ecosystems; Gene Expression; Microorganisms; Temporal Distribution

20020002060 NASA Johnson Space Center, Houston, TX USA

Sulfur/Carbonate Springs and Life in Glacial Ice

Allen, Carlton, NASA Johnson Space Center, USA; Grasby, Stephen, Geological Survey of Canada, Canada; Longazo, Teresa, Hernandez Engineering, Inc., USA; General Meeting of the NASA Astrobiology Insititute; April 2001, pp. 77-79; In English; See also 20020002018; No Copyright; Avail: Issuing Activity; Abstract Only

Ice in the near subsurface of Mars apparently discharges liquid water on occasion. Cold-tolerant microorganisms are known to exist within terrestrial glacial ice, and may be brought to the surface as a result of melting events. We are investigating a set of springs that deposit sulfur and carbonate minerals, as well as evidence of microbial life, on the surface of a glacier in the Canadian arctic. Additional information is contained in the original extended abstract. Author

Carbonates; Deposits; Glaciers; Ice; Microorganisms; Sulfur

20020002061 Florida Univ., Gainesville, FL USA

Bioinformatics, Organic Chemistry, and Paleontology: Building a Comprehensive Model for Recent Life on Earth

Benner, Steven A., Florida Univ., USA; General Meeting of the NASA Astrobiology Insititute; April 2001, pp. 80-81; In English; See also 20020002018; No Copyright; Avail: Issuing Activity; Abstract Only

One of the great challenges of Astrobiology is to seamlessly integrate concepts from Natural History with those from Physical Science, using technology from both, as well as concepts and technology from information sciences and engineering. Disciplines from Natural History include inter alia geology, paleontology, and ecology; disciplines from Physical Science include chemistry, physics, and molecular biology.This talk/poster will focus on two bioinformatics tools developed in our laboratories that make it easier to exploit genomic sequence data to build a broadly comprehensive model for the history of life on Earth, "Darwin" and "The Master Catalog". Additional information is contained in the original extended abstract. Author

Ecology; Exobiology; Organic Chemistry; Molecular Biology

20020002062 Pennsylvania State Univ., Astrobiology Research Center, University Park, PA USA

Methane-Consuming Microbial Consortia Identified and Studied Using a Novel Combination of Fluorescent in-situ Hybridization and Ion Microprobe Delta C-13 Analysis

House, Christopher H., Pennsylvania State Univ., USA; Orphan, Victoria J., Monterey Bay Aquarium Research Inst., USA; McKeegan, Kevin D., California Univ., USA; Hinrichs, Kai-Uwe, Woods Hole Oceanographic Inst., USA; DeLong, Edward F., Monterey Bay Aquarium Research Inst., USA; General Meeting of the NASA Astrobiology Insititute; April 2001, pp. 82-83; In English; See also 20020002018; No Copyright; Avail: Issuing Activity; Abstract Only

Despite geochemical and experimental evidence that methane is oxidized under anaerobic conditions, the precise means by which methane is oxidized anaerobically is unknown, and the responsible organism or consortium of organisms has yet to be isolated and grown in culture. Recently, Hinrichs et al. (1999) found archaeal lipids that were highly depleted in C-13 in sediments from the Eel River Methane Seep off the coast of California, suggesting an archaeal prokaryote was consuming methane under anoxic conditions. In this investigation, Hinrichs et al. also conducted parallel studies of rRNA genes from the location, revealing several groups of previously unknown archaeal lineages. Hinrichs et al. suggested that these novel archaeal groups are responsible for anaerobic oxidation of methane. Additional circumstantial evidence, linking these novel microbial groups to the process of anaerobic methane oxidation, was subsequently provided by fluorescent in-situ hybridization (FISH) studies of methane seep environments by Boetius et al. (2000) and Orphan et al. (in press). The FISH technique revealed microbial aggregates consisting

of an archaeal core surrounded by a shell of sulfate-reducing bacteria (SRB). Boetius et al. (2000) and Orphan et al. (in press) have suggested that these aggregates containing Archaea and SRB are responsible for anaerobic methane oxidation (producing CO2 and H2) driven by the scavenging of hydrogen by the SRB. However, no direct evidence has linked the process of methane oxidation to these aggregates. Additional information is contained in the original extended abstract.
Author
Anoxia; Bacteria; Carbon Dioxide; Geochemistry; Microorganisms

20020002063 NASA Ames Research Center, Moffett Field, CA USA
Composition of Hydrothermal Vent Microbial Communities as Revealed by Analyses of Signature Lipids, Stable Carbon Isotopes and Aquificales Cultures
Jahnke, Linda L., NASA Ames Research Center, USA; Eder, Wolfgang, Regensburg Univ., Germany; Huber, Robert, Regensburg Univ., Germany; Hinrichs, Kai-Uwe, Woods Hole Oceanographic Inst., USA; Hayes, John M., Woods Hole Oceanographic Inst., USA; Cady, Sherry L., Portland State Univ., USA; DesMarais, David J., NASA Ames Research Center, USA; Hope, Janet M., Australian Geological Survey Organisation, Canberra, Australia; Summons, Roger E., Australian Geological Survey Organisation, Canberra, Australia; General Meeting of the NASA Astrobiology Insititute; April 2001, pp. 84-85; In English; See also 20020002018; No Copyright; Avail: Issuing Activity; Abstract Only

Extremely thermophilic microbial communities associated with the siliceous vent walls and outflow channel of Octopus Spring, Yellowstone National Park, have been examined for lipid biomarker and carbon isotopic signatures. These data were compared with that obtained from representatives of three Aquificales genera. Thermocrinis ruber, Thermocrinis sp. HI, Hydrogenobacter thermophilus, Aquifex pyrophilus and Aquifex aeolicus all contained phospholipids composed not only of the usual ester-linked fatty acids, but also ether-linked alkyl moieties. The fatty acids of all cultured organisms were dominated by very distinct pattern of n-C-20:1 and cy-C-21 compounds. The alkyl glycerol ethers were present primarily as C-18:0 monoethers with the exception of the Aquifex spp. in which dialkyl glycerol ethers with a boarder carbon-number distribution were also present. These Aquificales biomarker lipids were the major constituents in the lipid extracts of the Octopus Spring microbial samples. Two natural samples, a microbial biofilm growing in association with deposition of amorphous silica on the vent walls at 92 C, and the well-known ”pink-streamer community” (PSC), siliceous filaments of a microbial consortia growing in the outflow channel at 87 C were analyzed. Both the biofilm and PSC samples contained mono- and dialkyl glycerol ethers with a prevalence of C-18 and C-20 alkyls. Phospholipid fatty acids were comprised of both the characteristic. Additional information is contained in the original extended abstract.
Author
Hydrothermal Systems; Lipids; Carbon Isotopes; Thermophiles; Microorganisms

20020002064 Jet Propulsion Lab., California Inst. of Tech., Pasadena, CA USA
Application of Fe Isotopes to the Search for Life and Habitable Planets
Johnson, Clark M., Wisconsin Univ., USA; Beard, Brian L., Wisconsin Univ., USA; Nealson, Kenneth L., Jet Propulsion Lab., California Inst. of Tech., USA; General Meeting of the NASA Astrobiology Insititute; April 2001, pp. 86-88; In English; See also 20020002018; No Copyright; Avail: Issuing Activity; Abstract Only

The relatively new field of Fe isotope geochemistry can make important contributions to tracing the geochemical cycling of Fe, which bears on issues such as metabolic processing of Fe, surface redox conditions, and development of planetary atmospheres and biospheres. It appears that Fe isotope fractionation in nature and the lab spans about 4 per mil (%) in Fe-56/Fe-54, and although this range is small, our new analytical methods produce a precision of +/- 0.05% on sample sizes as small as 100 ng (10(exp -7) g); this now provides us with a sufficient ”signal-to-noise” ratio to make this isotope system useful. We review our work in three areas: 1) the terrestrial and lunar rock record, 2) experiments on inorganic fractionation, and 3) experiments involving biological processing of Fe. Additional information is contained in the original extended abstract.
Author
Iron Isotopes; Geochemistry; Planetary Atmospheres; Lunar Rocks; Bioprocessing

20020002065 British Antarctic Survey, Cambridge, UK
Pigments and Other Biomolecules in Extreme Antarctic Microbial Habitats: Analogues for Evaluating Raman Spectroscopic Evidence of Preserved or Relict Life on Mars?
Wynn-Williams, D. D., British Antarctic Survey, UK; Edwards, H. G. M., Bradford Univ., UK; Newton, E. M., Bradford Univ., UK; General Meeting of the NASA Astrobiology Insititute; April 2001, pp. 89-90; In English; See also 20020002018; No Copyright; Avail: Issuing Activity; Abstract Only

The unequivocal detection of biomolecules amongst extraneous organic materials on or near the surface of Mars is a primary goal for astrobiology. The characteristics of any biomolecules on Mars cannot be assumed to be identical to those on Earth, despite the common carbon-based nature of organic compounds in the Solar System as evidenced by carbonaceous chondrites and spectra of interplanetary dust. However, the evolutionary pressure of environmental constraints on early Mars such as UVB and UVC radiation, high and low temperatures, desiccation and hypersalinity would have required protective strategies to promote the origin, survival and evolution of any microbial life. Chemo-lithotrophic growth may have originated near the surface of early Mars, and heterotrophic microbial growth on organic compounds derived from meteorites, may have evolved on the surface. However, the most efficient known source for metabolism available in the Solar System is light from the Sun which drives photosynthesis. If it evolved this would have required pigments to capture photons and screen UV radiation. Pigmentation would also be advantageous for exposed heterotrophs. Additional information is contained in the original extended abstract.
Author
Analogs; Biochemistry; Carbonaceous Chondrites; Extraterrestrial Life; Interplanetary Dust; Pigments; Raman Spectroscopy

20020002066 Universidad Autonoma de Madrid, Centro de Biologia Molecular, Spain
Iron Geomicrobiology of the Tinto River
Amils, R., Universidad Autonoma de Madrid, Spain; Gomez, F., Instituto Nacional de Tecnica Aeroespacial, Spain; Rodriguez, N., Instituto Nacional de Tecnica Aeroespacial, Spain; Fernandez-Remolar, D., Instituto Nacional de Tecnica Aeroespacial, Spain; Zettler, L. A. Amaral, Marine Biological Lab., USA; Gonzalez-Toril, E., Universidad Autonoma de Madrid, Spain; General Meeting of the NASA Astrobiology Insititute; April 2001, pp. 91; In English; See also 20020002018; No Copyright; Avail: Issuing Activity; Abstract Only

Sulfur metabolism has been considered a key element on geomicrobiology probably as a consequence of its redox potential. Although iron is considered and extremely important element for life, its role has been mainly associated to structural enzymatic activities. From the geomicrobiological characterization of the Tinto River (Iberian Pyritic Belt), a 90 km acidic river (mean pH 2.3) holding a high level of prokaryotic and eukaryotic diversity, an earth living system under the iron control is emerging. Iron, in addition of its important structural role in biochemistry, can be used not only as an energy source, but also as an electron acceptor for anaerobic respiration, is responsible for the maintenance of a constant pH in the water table (probably needed to sustain the high level of microbial diversity), and can protect cell systems from ultraviolet radiation. A geomicrobiological model of this habitat considering most of the geological, physical, chemical and biological variables will be presented and its astrobiological implications discussed. Additional information is contained in the original extended abstract.
Author
Iron; Microorganisms; Geology; Water Tables; Sulfur; Metabolism

20020002067 Arizona State Univ., Dept. of Geological Sciences, Tempe, AZ USA
Imaging and Geochemistry of Black Smoker Chimneys Using Three-Dimensional Synchrotron X-Ray Computed Tomography
Ashbridge, Dawn A., Arizona State Univ., USA; ODay, Peggy A., Arizona State Univ., USA; Holloway, John R., Arizona State Univ., USA; Muccino, Julia C., Arizona State Univ., USA; General Meeting of the NASA Astrobiology Insititute; April 2001, pp. 92-93; In English; See also 20020002018; No Copyright; Avail: Issuing Activity; Abstract Only

Hydrothermal system black smoker chimney structures are critical to geologists, biologists, and fluid flow engineers for understanding where biology could occur due to mineralogy, geochemistry, and fluid flow dynamics. Studies of this extreme environment must be conducted at microscales (on the order of 10(exp -4) to 10(exp -9) m) on structurally preserved samples because chemical, thermal, mineral, and biological gradients occur at these scales. Understanding of microorganism ecology in hydrothermal systems is important for evaluating this setting as a possible origin of life environment. Three-dimensional data sets that combine physical structure and chemical composition are needed to reconstruct the microenvironments that support microbial colonies in black smoker chimneys. Additional information is contained in the original extended abstract.
Author
Chemical Composition; Chimneys; Geochemistry; Hydrothermal Systems; Imaging Techniques; Microorganisms; Smoke

20020002068 California Univ., Dept. of Integrative Biology, Berkeley, CA USA
Hyperthermophilic Microbial Communities in Silica-Depositing Yellowstone Hot Springs Exhibit More Morphological and Sequence Diversity than Previously Detected
Blank, Carrine E., California Univ., USA; Pace, Norman R., Colorado Univ., USA; Cady, Sherry L., Portland State Univ., USA; General Meeting of the NASA Astrobiology Insititute; April 2001, pp. 94-95; In English; See also 20020002018; No Copyright; Avail: Issuing Activity; Abstract Only

A picture of the kinds of hyperthermophilic microorganisms that inhabit slightly alkaline near-boiling silica depositing hot springs is beginning to emerge. We have reported previously that the microbial diversity as measured by small subunit ribosomal DNA (SSU rDNA) techniques in various springs in Yellowstone National Park is rather variable: some contain only one or two taxa whereas others contain up to six taxa. All taxa in these springs branch deeply in the bacterial domain of life near the last common ancestor, as do all hyperthermophilic bacteria. No archaeal taxa were found in these springs using PCR, despite repeated attempts to find them. All springs studied contain the lineage corresponding to EM17, now designated as Thermocrinis ruber, a hydrogen oxidizer belonging to the Aquificales isolated from the pink filaments of Octopus Spring (White Creek Area, Lower Geyser Basin). Communities associated with spicular geyserite at the air-water interface of Octopus Spring and Queen#s Laundry Pool (Sentinel Meadows, Lower Geyser Basin) contain a slightly higher number of taxa than communities in the subaqueous environment in both springs. This is attributed to a slightly lower temperature in the splash zone where spicular geyserite forms. In addition, several of the taxa seen on the spicular geyserite are many of the same taxa found in the cooler subaqueous regime. Additional information is contained in the original extended abstract.
Author
Microorganisms; Thermophiles; Silicon Dioxide; Deposition; Deoxyribonucleic Acid

20020002069 Woods Hole Oceanographic Inst., Astrobiology Inst., MA USA
Flagellate Growth and Survival Under Conditions Potentially Encountered at Deep Sea Hydrothermal Vents
Atkins, Michael S., Woods Hole Oceanographic Inst., USA; Teske, Andreas P., Woods Hole Oceanographic Inst., USA; Taylor, Craig D., Woods Hole Oceanographic Inst., USA; Wirsen, Carl O., Woods Hole Oceanographic Inst., USA; Anderson, O. Roger, Lamont-Doherty Geological Observatory, USA; General Meeting of the NASA Astrobiology Insititute; April 2001, pp. 96-97; In English; See also 20020002018; No Copyright; Avail: Issuing Activity; Abstract Only

Eighteen strains of flagellated protists, representing 9 species from 6 taxonomic orders, were isolated and cultured from four deep-sea hydrothermal vents. Many of the vent isolates are ubiquitous members of marine, freshwater, and terrestrial ecosystems worldwide, suggesting a global distribution of these flagellate species. This discovery advanced the hypothesis that ubiquity in distribution patterns among heterotrophic flagellates implies high tolerance and/or adaptability to a wide range of environmental conditions. Experiments under vent conditions of high pressure and high concentrations of metals and sulfide showed that some of these species are very tolerant to extreme environmental conditions. Additional information is contained in the original extended abstract.
Author
Flagellata; Fresh Water; Marine Environments; Survival

20020002070 NASA Johnson Space Center, Houston, TX USA
Carbonate Biogenic Structures in Storrs Lake, Bahamas
Byrne, Monica, Wellesley Coll., USA; Morris, Penny A., Houston Univ., USA; Wentworth, Susan J., Lockheed Martin Space Operations, USA; Brigmon, Robin L., Savannah River Co., USA; McKay, David S., NASA Johnson Space Center, USA; General Meeting of the NASA Astrobiology Insititute; April 2001, pp. 98-100; In English; See also 20020002018; No Copyright; Avail: Issuing Activity; Abstract Only

Storr's Lake, an inland hypersaline lake on San Salvador Island, Bahamas, contains calcium carbonate-rich lithified mats of filamentous microorganisms, diatoms, associated photosynthetic and chemotrophic bacteria, and trapped sediment. In addition, 16S rRNA analysis indicates the presence of five sulfur-reducing genera of bacteria. These microbes are potential modern-day analogs to some ancient stromatolitic structures. The goals of this study are to identify unique compositional and biogenic features, possibly correlating some of these with some of the sulfate-reducing bacteria. Additional information is contained in the original extended abstract.
Author
Bacteria; Sulfates; Carbonates; Biological Evolution

20020002071 Instituto Nacional de Tecnica Aeroespacial, Centro de Astrobiologia, Torrejon de Ardoz, Spain
Protection Ways Against Extreme Solar Ultraviolet Radiation: A Preliminary Study
Cordoba-Jabonero, C., Instituto Nacional de Tecnica Aeroespacial, Spain; Mancho, A.-M., Instituto Nacional de Tecnica Aeroespacial, Spain; Vazquez, L., Instituto Nacional de Tecnica Aeroespacial, Spain; General Meeting of the NASA Astrobiology Insititute; April 2001, pp. 101; In English; See also 20020002018; No Copyright; Avail: Issuing Activity; Abstract Only

Solar UV-B radiation is the more harmful radiation affecting the biological processes occurring in the Earth's ecosystems, and especially it is responsible for the increase of DNA damage in the living organisms. In this sense, UV levels on the Earth's surface can extremely change depending on atmospheric conditions. A preliminary study of possible protection ways, natural as

well as anthropogenic, in order to scream this radiation, or part of this radiation, is performed. Several forms of protection ways are considered: 1) a water layer, 2) a dense particulate layer of natural or anthropogenic origin, and 3) the mixed case of a aquatic media where are dissolved particles (possibly metal ions). Solar UV radiation reaching the surface, as well as its later propagation through the aquatic media is simulated with a ”two-stream” radiative transfer model. Input parameters as ozone content, solar zenith angle, aerosol concentration, etc., are varied for modeling the extreme UV radiation conditions, and the description of aquatic conditions is also simulated. Additional information is contained in the original extended abstract.
Author
Activity (Biology); Organisms; Protection; Radiative Transfer; Solar Radiation; Ultraviolet Radiation

20020002072 Marine Biological Lab., Josephine Bay Paul Center for Comparative Molecular Biology and Evolution, Woods Hole, MA USA
Molecular Basis of Spectral Tuning in Opsins
Cummings, Michael P., Marine Biological Lab., USA; McInerney, Laura A., Marine Biological Lab., USA; General Meeting of the NASA Astrobiology Insititute; April 2001, pp. 102-103; In English; See also 20020002018; No Copyright; Avail: Issuing Activity; Abstract Only

One of the most common organism-environment interactions is light perception. The visual system of animals is a well studied light perception example. Animal vision exhibits a range of sensitivities to different wavelengths of light, and visual sensitivity in different colors is due principally to differences in the amino acid sequences of opsins, which are the G-protein coupled receptors. We are using opsins as a model system to study organism-environment interactions and genotype-phenotype relationships. Our work consists of several parts, including laboratory work on odonate (dragonflies and damselflies) opsins, and computer analyses of opsins from a wide range of organisms. It is this later aspect we describe here. The specific research questions include the following: (1) How much of the variance in the wavelength of light absorbed by opsins can be explained by primary amino acid sequence alone? (2) What amino acid positions are important in determining differences in the spectrum of light absorbed by opsins? and (3) What biochemical characteristics of amino acids have the best relationship to light absorbing properties of opsins? Additional information is contained in the original extended abstract.
Author
Molecular Biology; Biochemistry; Organisms; Spectra; Visual Discrimination

20020002073 Marine Biological Lab., Josephine Bay Paul Center for Comparative Molecular Biology and Evolution, Woods Hole, MA USA
Evidence of Novel Eukaryotes in Guaymas Basin Hydrothermal Vent Sediments: Life at the Extremes
Edgcomb, Virginia, Marine Biological Lab., USA; Kysela, David, Marine Biological Lab., USA; Sogin, Mitchell L., Marine Biological Lab., USA; Gomez, Alvin, Woods Hole Oceanographic Inst., USA; Teske, Andreas, Woods Hole Oceanographic Inst., USA; General Meeting of the NASA Astrobiology Insititute; April 2001, pp. 104-105; In English; See also 20020002018; No Copyright; Avail: Issuing Activity; Abstract Only

The phylogenetic composition of eukaryotic communities in hydrothermal sediments of the Guaymas Basin (Gulf of California, Mexico) was surveyed by cloning and sequencing of PCR-amplified, partial 18S rRNA genes from environmental DNA. Cores with a clear and reproducible temperature profile were sliced and subsampled. We analyzed 18S rRNA genes from the top 3 cm of cores and from the sediment-seawater interface, with temperature profiles ranging from 4 - 65 C. Many sequences fall into a wide range of known eukaryotic taxa, including fungi, animals, diatoms, stramenopiles, alveolates, dinoflagellates, apicomplexa, and ciliates. of particular interest are several groups of deep-branching eukaryotic sequences with no known close relatives in available SSU rRNA databases. This suggests that the Guaymas Basin hydrothermal sediments provide a habitat for novel eukaryotic microorganisms that may provide important clues to early eukaryotic evolution. Additional information is contained in the original extended abstract.
Author
Eukaryotes; Genes; Hydrothermal Systems; Cloning (Biology); Microorganisms

20020002074 American Type Culture Collection, Manassas, VA USA
Morphological and Metabolic Aspects of Neutrophilic, Lithotrophic Fe-Oxidizing from Deep-Ocean Hydrothermal Vents in the Pacific Ocean
Emerson, David, American Type Culture Collection, USA; Bradburne, Chris, American Type Culture Collection, USA; General Meeting of the NASA Astrobiology Insititute; April 2001, pp. 106; In English; See also 20020002018; No Copyright; Avail: Issuing Activity; Abstract Only

Ferrous iron is a common and often abundant substituent of hydrothermal vent fluids; however there has been limited research on the microbes involved in oxidation of iron at deep-sea hydrothermal vents. We have investigated several hydrothermal vent sites at the summit of the Loihi Seamount (depth, 1100 m), which is part of the Hawaiian archipelago. Hydrothermal vent fluid at Loihi ranges in temperature from 10 C to 165 C and contains up to 50 micro M Fe(II); however there is very little H2S present. As a result, most of the vents have abundant microbial mats that are heavily encrusted with Fe-oxides. Observation by light microscopy revealed the mats were composed of three morphotypes of hydrous ferric oxides (HFOs). These were: 1) "Leptothrix ochracea"-type, hollow tubular sheaths with diameters of 1 - 3 microns; 2) twisted or irregular thin filaments, diameter 1 -2 microns, and 3) amorphous particulate oxides. Forms 1 and 2 can be directly attributed to the action of Fe-oxidizing bacteria; form 3 oxides may be formed biologically or abiologically. We quantified the morphotypes of oxides present at different vents at Loihi and found that at least 60% of the oxides at some sites were of form 1 or 2, indicating that the bulk of iron deposition was biologically mediated. Using cultural techniques we demonstrated that Fe-oxidizing bacteria were present at all the vent sites we tested, and were often abundant with numbers of up to 10(exp 7) cell/cc of mat. All the enrichments for lithotrophic, microaerophilic Fe-oxidizers done at 12 C or 25 C were successful; enrichments at 60 C or above did not yield microaerobic Fe-oxidizers. Additional information is contained in the original extended abstract.
Author
Morphology; Metabolism; Iron Oxides; Ferrous Metals; Vents; Oxidizers; Hydrogen Sulfide; Free Convection

20020002075 Arizona State Univ., Microbiology Dept., Tempe, AZ USA
Microbes That Follow the Water
Garcia-Pichel, Ferran, Arizona State Univ., USA; Pringault, Olivier, Bordeaux 1 Univ., France; General Meeting of the NASA Astrobiology Insititute; April 2001, pp. 107-108; In English; See also 20020002018; No Copyright; Avail: Issuing Activity; Abstract Only

Water is arguably Nature's most central molecule, and the most indispensable ingredient for active life. While some organisms can tolerate periods of severe desiccation (anhydrobiosis), the presence of liquid water is always required, at least temporarily, in order to guarantee metabolic activity and survival. This is the simple, compelling sine qua non of astrobiology: to search for life, follow the water. Additional information is contained in the original extended abstract.
Author
Microorganisms; Metabolism; Life Sciences

20020002076 Pennsylvania State Univ., Dept. of Geosciences, University Park, PA USA
GEOPULSE: Gene Expression Observations for Planetary Life Study
House, Chris H., Pennsylvania State Univ., USA; Lugo, Samantha Kaj, Pennsylvania State Univ., USA; Moran, James Joseph, Pennsylvania State Univ., USA; Freeman, Kate, Pennsylvania State Univ., USA; Brantley, Susan, Pennsylvania State Univ., USA; General Meeting of the NASA Astrobiology Insititute; April 2001, pp. 109-110; In English; See also 20020002018; No Copyright; Avail: Issuing Activity; Abstract Only

The Biogeochemistry at a Hydrothermal Vent Setting: A further understanding of hyperthermophiles is pertinent to astrobiology because the origin of life may have occurred in a hydrothermal setting, hyperthermophiles may be similar to the last common ancestor, and chemolithoautotrophic communities may reside in the subsurface of Mars or under the ice of Europa. In order to detect life in these planetary environments, the biogeochemistry of hydrothermal systems must be understood in greater detail. In order to understand the biogeochemistry of hydrothermal vent systems, a number of geochemical conditions will be investigated during growth of Pyrobaculum aerophilum and Pyrobaculum islandicum. Interactions of these microbes with minerals, metals, and various organic substrates under various growth conditions will be evaluated, coupled with gene expression studies to pinpoint specific genes involved in the biogeochemical processes. Additional information is contained in the original extended abstract.
Author
Biological Evolution; Gene Expression; Hydrothermal Systems; Microorganisms

20020002077 Geological Survey, Astrogeology Team, Flagstaff, AZ USA
Visible/Near-Infrared and Thermal Infrared Field Spectroscopy of Modern and Ancient Calcareous Tufa Deposits
Johnson, Jeffrey R., Geological Survey, USA; Plescia, Jeffrey B., Geological Survey, USA; General Meeting of the NASA Astrobiology Insititute; April 2001, pp. 111-113; In English; See also 20020002018; Original contains color illustrations; No Copyright; Avail: Issuing Activity; Abstract Only

Calcareous tufa deposits on Earth form through precipitation of CaCO3 when calcium-bearing spring waters come in contact with carbonate in saline or alkaline lake waters. Modern to Pleistocene-age deposits are observed at Mono Lake, CA whereas tufa

deposits near Searles Lake, CA are 104-105 years old. Field observations of tufas from both regions using visible/near-infrared (VNIR) and thermal infrared (TIR) spectrometers were undertaken to determine if tufa spectral signatures varied with age. Understanding such temporal variability in carbonate mineralogy will be relevant to the spectral search for carbonates on Mars. Additional information is contained in the original extended abstract.
Author
Deposits; Infrared Spectroscopy; Mineralogy; Near Infrared Radiation; Spectral Signatures

20020002078 NASA Ames Research Center, Moffett Field, CA USA
The Purification and Characterization of Superoxide Dismutase from Chloroflexus aurantiacus and the Effects of UV Radiation on the Activity of SOD and Catalase in Hydrothermal Mats of Yellowstone National Park
Lancaster, Vanessa, Arizona State Univ., USA; Blankenship, Robert E., Arizona State Univ., USA; Rothschild, Lynn, NASA Ames Research Center, USA; General Meeting of the NASA Astrobiology Insititute; April 2001, pp. 114; In English; See also 20020002018; No Copyright; Avail: Issuing Activity; Abstract Only

Chloroflexus aurantiacus is a thermotolerant anoxygenic green phototrophic bacterium that is prominent in alkaline hot springs at temperatures between 52 and 60 C. This species often grows in the hyperoxic environment beneath cyanobacterial mats at higher temperatures up to 70 - 72 C. Cf. aurantiacus is an evolutionarily important organism since it is in the earliest branch of the eubacteria that are capable of photosynthesis and many of its characteristics can be found in other diverse groups of phototrophic bacteria. Additional information is contained in the original extended abstract.
Author
Purification; Bacteria; Inorganic Peroxides; Photosynthesis

20020002079 Lockheed Martin Corp., Houston, TX USA
Detection and Enumeration of Microbial Life in the Perennially Ice Covered Lake of the McMurdo DryValleys
Lisle, John T., Lockheed Martin Corp., USA; Priscu, John C., Montana State Univ., USA; General Meeting of the NASA Astrobiology Insititute; April 2001, pp. 115; In English; See also 20020002018; No Copyright; Avail: Issuing Activity; Abstract Only

The McMurdo Dry Valleys of Antarctica (160 degrees - 164 degrees E, 76 degrees 20 minutes - 78 degrees 20 minutes S) represent the most Martian-like analogs on Earth. The extreme cold and arid conditions in this region have influenced the evolution of terrestrial, aquatic and ice ecosystems that may provide models of past Martian ecosystems. A unique feature of the Dry Valleys is the perennially ice covered lakes. These lakes can be generally characterized as having no vertical mixing and being highly stratified in regard to supersaturation of gases (O2, NO2, H2S), strong salinity gradients (-5 to 300 %), temperature (-5 to 25 C), organic and inorganic constituents and nutrients. Also, sunlight penetration to the water column is reduced by greater than 98% by the overlying ice cover. In spite of these harsh conditions, the lakes in the Dry Valleys support very active microbial ecosystems. We investigated the prevalence of and interaction between bacteria and viruses at several depths within Lake Bonney (east and west lobes), Lake Fryxell, Lake Hoare and Lake Vanda. Samples were collected from depths within, above and below a region of elevated microbial activity based on chlorophyll-a concentrations. Collected samples were processed to determine the number of bacteria and viruses and the percentage of the bacterial population that was lysogenic (i.e., was host to a dormant virus). All samples were labeled with the nucleic acid stain SYBR Gold and counted using epifluorescent microscopy. Our data indicate that the bacterial, viral and lysogen concentrations are similar to those found in open oceanic waters in more temperate climates. Bacteria, viruses and lysogens were recovered from waters with very high salinities (greater than 200 %), low temperatures (-5 C) and supersaturated gas concentrations. We have demonstrated that bacteria and viruses can survive and persist in aquatic environments that may model pockets of liquid water in the areas of the Martian ice caps and below the cryosphere. The use of fluorescent labeled molecular probes and detection methods provides an easy, dependable and rapid method to detect microbial life in samples collected from extreme environments.
Author
Bacteria; Ecosystems; Mars (Planet); Mars Surface; Microorganisms; Viruses; Antarctic Regions; Arid Lands; Fluorescence; Remote Sensing

20020002080 California Univ., Dept. of Earth and Space Sciences, Los Angeles, CA USA
Mass-Independent Fractionation of Oxygen Isotopes in Earth's Atmosphere
Lyons, James R., California Univ., USA; General Meeting of the NASA Astrobiology Insititute; April 2001, pp. 116; In English; See also 20020002018; No Copyright; Avail: Issuing Activity; Abstract Only

Nearly all oxygen-bearing geological materials exhibit normal, mass-dependent fractionation of oxygen isotopes, such that the fractionation of O(18) is approximately twice the fractionation of O(17). Recent measurements of mass-independently

fractionated (MIF) oxygen isotopes in Miocene sulfate deposits demonstrate the capability of sediments to record the presence of MIF in the atmosphere. In Earth's present atmosphere MIF derives almost entirely from the photochemical production of ozone. Oxidation of SO2 to sulfate occurs in the lower atmosphere by reaction with O3 and O3 products in aerosols. Thus, observation of MIF of oxygen isotopes in barites (for example) might serve as a marker for ozone chemistry throughout Earth history. Our understanding of MIF in Earth's modern atmosphere is far from complete. Because O3 is a photochemically active molecule, its MIF signature can be imparted to other atmospheric molecules. Using a photochemical equilibrium model I have computed the MIF expected for various molecules of interest due solely to interactions with ozone. The model predicts substantial MIF in HNO3 and smaller MIF in H2O2. Evidence for the latter has been obtained recently for hydrogen peroxide extracted from rainwater samples. Additionally, the model predicts that H2O produced photochemically in the stratosphere will exhibit MIF, in contrast to tropospheric water, which is mass-dependently fractionated during evaporation and condensation. The photochemical model presented here represents a first step towards understanding oxygen isotope chemistry in the atmosphere. The model suffers from many poorly known rate coefficients, and most likely from missing oxygen exchange reactions. Once these reaction rates have been better determined, such models may be applied to Earth's atmosphere during earlier epochs and to the atmosphere of Mars.
Author
Atmospheric Chemistry; Earth Atmosphere; Fractionation; Oxygen Isotopes; Photochemical Reactions

20020002081 New Mexico Inst. of Mining and Technology, Biology Dept., Socorro, NM USA
Archaeal and Bacterial Diversity in a Moderately Acidic Thermal Spring
McHale, Mary L., New Mexico Inst. of Mining and Technology, USA; Kieft, Thomas L., New Mexico Inst. of Mining and Technology, USA; Hinman, Nancy W., Montana Univ., USA; Wilson, Cindy L., Montana Univ., USA; General Meeting of the NASA Astrobiology Insititute; April 2001, pp. 117; In English; See also 20020002018; No Copyright; Avail: Issuing Activity; Abstract Only

We have characterized microbial communities in a thermal spring (approximately 70 C, pH 4) in Yellowstone National Park in order to relate the dominant microbial metabolic potentials (inferred from phylogenetic data) to the changing geochemistry of the spring in August 1999 and June 2000. The high temperature and chemolithotrophic energy sources within this spring may be analogous to the conditions during early life on Earth and possibly Mars, making it an excellent environment to discern interactions between evolving biological and geological parameters. Sediment and water samples taken from the collecting pool and run off channels were subject to chemical analysis, direct DNA extraction, PCR (polymerase chain reaction) amplification with universal Archaeal and Bacterial primers, cloning, RFLP (restriction fragment length polymorphism) screening, and sequencing of the 16S rRNA genes. During the first sampling event the spring had more reducing conditions, while the spring had more oxidizing conditions during the second sampling event. There were also significant differences in the concentrations of minor ions between the sampling events. Phylogenetic analysis has revealed a diverse community mainly belonging to the sulfur-dependent thermoacidophilic Crenarchaeota branch of Archaea, which are apparently responding to the geochemical changes. A majority of the 16S rRNA genes we analyzed are clustering in two distinct groups within Crenarchaeota with no close relatives. Several clones containing Bacterial inserts were collected; these mainly consisted of close phylogenetic relatives of Hydrogenobacter and Bacillus subtilis. Cluster analysis of RFLP ribotype frequencies grouped by sampling events, suggesting a correlation between the microbial community and the changing geochemistry. The phylogenetic positions of these ribotypes suggest that the biogeochemical reactions mediated by the microorganisms from which they are derived remain consistent with the geochemistry of the spring environment.
Author
Acidity; Bacteria; High Temperature; Biological Evolution; Planetary Evolution; Springs (Water); Archaebacteria; Mars (Planet)

20020002082 Marine Biological Lab., Woods Hole, MA USA
Cytosolic pH Maintenance in Eukaryotic Acidophiles
Messerli, Mark A., Marine Biological Lab., USA; Zettler, Linda A. Amaral, Marine Biological Lab., USA; Smith, Peter J. S., Marine Biological Lab., USA; Sogin, Mitchell L., Marine Biological Lab., USA; General Meeting of the NASA Astrobiology Insititute; April 2001, pp. 118-119; In English; See also 20020002018; No Copyright; Avail: Issuing Activity; Abstract Only

The waters of the Rio Tinto in Southwestern Spain are kept between pH 1.7 - 2.5 by chemolithotrophic bacteria and an ambient iron buffer content around 0.5 mg/ml and as high as 20 mg/ml. The acidic conditions dissolve large amounts of heavy metals like Cu, As, Zn, Ni, and Ag that are nearly insoluble at neutral pH. These harsh conditions are not suitable for multicellular life forms but the Tinto does support an abundant unicellular, eukaryotic population. We are currently studying a euglenid and chlamydomonad species from the Tinto that have been successfully cultured at pH equals approximately 2. With the fluorescent pH indicator BCECF we have found that both species maintain a neutral pH cytosol above 6.5. Along with a slightly negative

membrane potential there is a near 10(exp 5)-fold electrochemical transmembrane H(+) gradient. Neither species is an obligate acidophile; both grow at similar rates at pH 7 as at pH 2. Using weak acids to lower the cytosolic pH we find that the chlamydomonad can quickly neutralize the cytosolic pH after a brief cytosolic acidification. However, if the cytosolic pH drops to around 6.2, cells cannot recover cytosolic neutrality. From these data we suggest that cytosolic neutrality is necessary in order to maintain the transmembrane H(+) gradient. Presumably cytosolic acidification damages proteins necessary to maintain cellular function and yet the extracellular portions of membrane proteins do not appear to be affected by the extremely low extracellular pH. We are characterizing the active mechanisms by which these cells maintain the cytosolic neutrality by screening a battery of H(+) transporter inhibitors. Preliminary work shows that low concentrations of Diethylstilbestrol, a H(+)-ATPase inhibitor, lead to cytosolic acidification. Our working hypothesis is that these species protect their cytoplasm by maintaining a neutral pH environment, minimally, by actively transporting H(+) out of the cell via H(+) transporters. Additionally barriers to H(+) influx, at the level of the plasma membrane, may help to maintain cytosolic neutrality. However, we postulate that the surface proteins, exposed to the low extracellular pH, have been modified in order to function under these harsh conditions.
Author
Bacteria; Cytoplasm; Eukaryotes; Membranes; pH Factor; Hydrogen Ions; Acidity; Marine Environments

20020002083 Washington Univ., Dept. of Earth and Planetary Sciences, Saint Louis, MO USA
Hydrothermal Habitats in Astrobiology
Meyer, DArcy Renee, Washington Univ., USA; Shock, Everett L., Washington Univ., USA; Amend, Jan P., Washington Univ., USA; General Meeting of the NASA Astrobiology Insititute; April 2001, pp. 120-121; In English; See also 20020002018; No Copyright; Avail: Issuing Activity; Abstract Only

The search for life beyond Earth depends on accurate predictions about the environments and organisms that we can expect to find, using Earth ecosystems as templates. Hydrothermal systems on Mars and Europa are possible havens for life because they can supply the requisite water, energy and sources of carbon. The geologic history of Mars indicates that the planet, like early Earth, may have been wet and warm. Extensive volcanic activity and water on and below the surface would have inevitably led to the presence of hydrothermal systems. The inhospitable nature of the surface of Mars and the possibility of more amenable habitats in the subsurface require serious consideration of ecosystems and energy sources which are not dependent on sunlight as potential oases for life. Hydrothermal systems driven by tidal heating on Europa could also result in potential habitable zones of liquid water in the subsurface environments far beneath the frozen crust, and well beyond the reach of sunlight. Organisms living independent of sunlight require the availability of other energy sources to survive. The chemotrophic organisms in hydrothermal systems on Earth are an excellent example of the intricate relationship between biological and geochemical processes. These thermophilic organisms thrive on the chemical energy and mineral precipitates created by water/rock reactions and the cooling or mixing of hydrothermal fluids, processes that often result in chemical systems out of equilibrium. A model ecosystem for Mars or Europa, one necessitating operation independent of sunlight, would require the consideration of chemosynthetic life as candidate occupants. It is logical to look first to the hydrothermal environments on Earth as working templates for astrobiological models. One ideal place to study chemotrophic thermophiles is Yellowstone National Park, U.S.A. The hot springs, mudpots, and geysers in Yellowstone have yielded a host of cultured thermophilic organisms from both the Bacterial and Archaeal domains. However, these organisms are seldom considered in the context of their geochemical environments. Extreme ecosystems on Earth can only be useful as templates for astrobiological ecosystems if the environments are characterized along with the organisms that inhabit them. In an effort to characterize thermophilic organisms in the context of their geochemical environments, we have chosen the Greater Obsidian Pool Area (GOPA), Yellowstone National Park, as our study area. One major hydrothermal feature at GOPA, Obsidian Pool, is already well-known for its great diversity of thermophilic organisms determined by culture independent studies. These studies revealed 86 separate 16S rRNA signatures, few of which are represented by pure cultures. GOPA is a thermal area covering 1 sq km that is composed of seven 'major' hot spring features and a great number of equally interesting 'minor' features and channels. We have completed extensive analyses of geochemical samples taken in the field in 1999 and 2000 from hydrothermal environments in this area. These springs vary widely in fluid chemistry and physical characteristics, providing a plethora of microbial habitats in one small study area. For example, within the thermophilic environments, pH ranges from 2.1 - 7.9, and temperature ranges from 70 - 89 C. In conjunction with defining the geochemistry at GOPA, we are also culturing thermophiles from these environments so that organisms representative of these thermophilic communities can be studied in the laboratory. Unlike most traditional growth studies, we used aqueous growth media based on our geochemical data, so culturing conditions realistically represent the natural environment. Using this method, it is possible to design growth media for specific sample locations. Also, the most energetically favorable chemotrophic reactions were calculated for many sample areas, and nutrients were added to the media to target specific metabolic pathways. to date, we have obtained 38 mixed cultures from GOPA using our location-specific media, and two thermophilic Bacteria have been isolated from these cultures using a serial dilution method. We are currently characterizing these Bacteria for publication, and efforts are

underway to isolate more organisms from our mixed cultures. Our success with culturing thermophiles from these environments reflects the importance of accurately representing the geochemical environment in culturing studies. Because these isolates were obtained in the context of their natural environment, we are able to link them directly to the geochemical processes which govern these hydrothermal ecosystems.
Author
Activity (Biology); Exobiology; Geochemistry; Microorganisms; Organisms; Thermophiles; Yellowstone National Park (ID-MT-WY); Extraterrestrial Life; Habitats; Springs (Water); Hydrothermal Systems

20020002084 NASA Johnson Space Center, Houston, TX USA
Potential Evaporite Biomarkers from the Dead Sea
Morris, Penny A., Houston Univ., USA; Wentworth, Susan J., Lockheed Martin Corp., USA; Thomas-Keprta, Kathie, Lockheed Martin Corp., USA; Allen, Carlton C., NASA Johnson Space Center, USA; McKay, David S., NASA Johnson Space Center, USA; General Meeting of the NASA Astrobiology Insititute; April 2001, pp. 122-124; In English; See also 20020002018; No Copyright; Avail: Issuing Activity; Abstract Only

The Dead Sea is located on the northern branch of the African-Levant Rift systems. The rift system, according to one model, was formed by a series of strike slip faults, initially forming approximately two million years ago. The Dead Sea is an evaporite basin that receives freshwater from springs and from the Jordan River. The Dead Sea is different from other evaporite basins, such as the Great Salt Lake, in that it possesses high concentrations of magnesium and has an average pH of 6.1. The dominant cation in the Great Salt Lake is sodium, and the pH is 7.7. Calcium concentrations are also higher in the Dead Sea than in the Great Salt Lake. Both basins are similar in that the dominant anion is chlorine and the salinity levels are approximately 20 %. Other common cations that have been identified from the waters of the Dead Sea and the Great Salt Lake include sodium and potassium. A variety of Archea, Bacteria, and a single genus of a green algal, Dunaliella, has been described from the Dead Sea. Earlier studies concentrated on microbial identification and analysis of their unique physiology that allows them to survive in this type of extreme environment. Potential microbial fossilization processes, microbial fossils, and the metallic ions associated with fossilization have not been studied thoroughly. The present study is restricted to identifying probable microbial morphologies and associated metallic ions. XRD (X Ray Diffraction) analysis indicates the presence of halite, quartz, and orthoclase feldspar. In addition to these minerals, other workers have reported potassium chloride, magnesium bromide, magnesium chloride, calcium chloride, and calcium sulfate. Halite, calcium sulfate, and orthoclase were examined in this report for the presence of microbes, microbially induced deposits or microbial alteration. Neither the gypsum nor the orthoclase surfaces possesses any obvious indications of microbial life or fossilization. The sand-sized orthoclase particles are weathered with 122 extensive fan-shaped mineral deposits. The gypsum deposits are associated with halite minerals and also exhibit extensive weathering. Halite minerals represent the only substrates that have probable rod-shaped microbial structures with long, filamentous, apical extensions. EDS (energy dispersive x-ray) analysis of the putative microbes indicates elevated calcium levels that are enriched with magnesium. The rod-shaped structures exhibit possible fossilization stages. Rhombohedralshaped minerals of magnesium-enriched calcium carbonate are deposited on the microbial surfaces, and eventually coat the entire microbial surface. The sodium chloride continues to crystallize on nearby halite surface and even crystallizes on the fossilized microbial remains. The putative fossils are found exclusively on halite surfaces, and all contained elevated levels of calcium magnesium cations. Both of these metallic cations are associated with microbial activity and fossilization. Their morphological diversity is low in comparison with the reported living Dead Sea microbial population. If we examine the fossil record for multicellular organisms, fossilization rates are lower for soft-bodied organisms than for those possessing hard parts, i.e. shells, bones. For example, smaller, single celled organisms would have a smaller chance of fossilization; their fossilized shapes could be mistaken for abiotic products. Another consideration is that dead organisms in the water column are probably utilized as a food source by other microbes before fossilization processes are completed. This may be an important consideration as we attempt to model and interpret ancient microbial environments either on Earth or on Mars.
Author
Microorganisms; Salinity; Seas; Chlorine; Halites; Metal Ions; Quartz; Feldspars; Fossils; Extraterrestrial Life; Exobiology

20020002085 NASA Ames Research Center, Moffett Field, CA USA
Amino Acid Analyses of Acid Hydrolysates in Desert Varnish
Perry, Randall S., Washington Univ., USA; Staley, James T., Washington Univ., USA; Dworkin, Jason P., NASA Ames Research Center, USA; Engel, Mike, Oklahoma Univ., USA; General Meeting of the NASA Astrobiology Insititute; April 2001, pp. 125; In English; See also 20020002018; No Copyright; Avail: Issuing Activity; Abstract Only

There has long been a debate as to whether rock varnish deposits are microbially mediated or are deposited by inorganic processes. Varnished rocks are found throughout the world primarily in arid and semi-arid regions. The varnish coats are typically

up to 200 microns thick and are composed of clays and alternating layers enriched in manganese and iron oxides. The individual layers range in thickness from 1 micron to greater than 10 microns and may continue laterally for more than a 100 microns. Overlapping botryoidal structures are visible in thin section and scanning electron micrographs. The coatings also include small amounts of organic mater and detrital grains. Amino-acid hydrolysates offer a means of assessing the organic composition of rock varnish collected from the Sonoran Desert, near Phoenix, AZ. Chromatographic analyses of hydrolysates from powdered samples of rock varnish suggest that the interior of rock varnish is relatively enriched in amino acids and specifically in d-alanine and glutamic acid. Peptidoglycan (murein) is the main structural component of gram-positive bacterial cell walls. The d-enantiomer of alanine and glutamic acid are specific to peptidoglycan and are consequently an indicator for the presence of bacteria. D-alanine is also found in teichoic acid which is only found in gram-positive bacteria. Several researchers have cultured bacteria from the surface of rock varnish and most have been gram-positive, suggesting that gram-positive bacteria are intimately associated with varnish coatings and may play a role in the formation of varnish coatings.
Author
Phoenix (Az); Rocks; Varnishes; Amino Acids; Chromatography; Bacteria; Coatings

20020002086 Geological Survey, Flagstaff, AZ USA
Visible-Near Infrared Spectroscopy of Siliceous Sinter, Yellowstone National Park: Search for Organic Signatures
Plescia, J. B., Geological Survey, USA; Johnson, J. R., Geological Survey, USA; General Meeting of the NASA Astrobiology Insititute; April 2001, pp. 126-128; In English; See also 20020002018; Original contains color illustrations; No Copyright; Avail: Issuing Activity; Abstract Only

Widespread volcanism and fluvial activity during the Noachian and Hesperian periods of Mars suggest that volcanic hydrothermal systems, having surface expressions similar to those in Yellowstone National Park, Iceland or New Zealand may have occurred. The apparent absence of widespread carbonates on Mars suggests such martian hydrothermal systems would be dominated by silica. Given that hyperthermophiles are among the most primitive terrestrial organisms, it has been suggested that hyperthermophiles might have developed on Mars as well. Therefore, an examination of terrestrial hydrothermal silica deposits, to determine the extent to which they preserve detectable evidence of the associated hyperthermophile organisms, is relevant to Mars exploration. Several studies have examined siliceous and carbonate sinter for biologic indicators. Macroscopic fossils are rare, but SEM (scanning electron microscopy) images reveal a diversity of features due to biologic activity. Since spectral data (visible to near infrared reflectance (VNIR) and thermal emission) will be key to site selection and analysis, we have examined siliceous sinter in Yellowstone National Park to determine the extent to which biotic signatures are preserved. We have also collected VNIR data of the hyperthermophile organisms to characterize their spectral properties (see accompanying abstract). VNIR data of sinter at Octopus Spring, Mushroom Spring, and several geysers in the Old Faithful area were collected using an ASD Field SpecFr spectrometer under both natural and artificial illumination. Octopus and Mushroom Springs are alkaline with extensive hyperthermophile mats dominated by Thermocrinis ruber at high temperature, Synechococcus lividus-Chloroflexus aurantiacus at T is less than 73-74 C and Mastigocladus laminosus at T is less than 63-64 C. Visible hyperthermophile populations are absent at Spa, Spiteful and Bulger Geysers and these therefore serve as a control of the sinter spectra. Spectra for Spa, Spiteful and Bulger geyserite is typical of amorphous silica (e.g., opal and chalcedony); reflectance rises from the visible into the near-infrared with the steepest slopes at less than 600 nm. Maximum reflectance occurs at 1000-1250 nm beyond which reflectance decreases. Major absorptions at 1415, 1910 and 2275 nm and minor absorptions at approximately 970 and 1160 nm are due to bound water. Other significant absorptions are not noted. Spectra for sinter deposits at Mushroom and Octopus Springs, however, display several minor, but significant visible wavelength absorptions that are unrelated to silica. Fig. 2 illustrates spectra in the 350-1000 nm range for sinter from Mushroom and Octopus Springs. The prominent absorption at 680 nm is due to chlorophyll alpha. Additional minor absorptions occur at approximately 590, 610, 620 (all may be phycobiliproteins) and at approximately 760 nm. These absorptions may reflect organics and occur at positions similar to absorptions of the hyperthermophile organisms. These data suggest that signatures of biotic processes can be detected in siliceous sinter deposited in association with hyperthermophile organisms.
Author
Hydrothermal Systems; Spectroscopy; Exobiology; Thermophiles; Volcanoes; Silicon Dioxide; Yellowstone National Park (ID-MT-WY)

20020002087 Geological Survey, Flagstaff, AZ USA
Visible-Near Infrared Spectroscopy of Hyperthermophile Organisms, Yellowstone National Park
Plescia, J. B., Geological Survey, USA; Johnson, J. R., Geological Survey, USA; Ferris, M., Montana State Univ., USA; General Meeting of the NASA Astrobiology Insititute; April 2001, pp. 129-130; In English; See also 20020002018; Original contains color illustrations; No Copyright; Avail: Issuing Activity; Abstract Only

Hyperthermophile organisms have been suggested to lie at the base of the tree of life and may represent the earliest organisms on the Earth. by analogy, hyperthermophilic organisms may have developed on Mars. From an exploration standpoint, the question is whether such organisms (living or dead and entombed in sinter) could be detected in spectral data. We collected Visible-Near Infrared Reflectance (VNIR) data at springs in Yellowstone National Park to characterize the reflectance spectra of living hyperthermophile organisms. Data for Octopus Spring and Nymph Creek are presented here. In situ (350-2500 nm) data were collected using an ASD Field SpecFr spectrometer under both natural and artificial illumination. Octopus Spring is alkaline (pH 8.0, T 88 C) with temperature-dependent biotic mats lining the effluent channels. Pink filamentous Thermocrinis ruber occurs at high temperature, green Synechococcus lividus-Chloroflexus aurantiacus at T is less than 73-74 C and greenish-orange Mastigocladus laminosus at T is less than 63-64 C. Nymph Creek is acidic (pH 2.9, T 60 C) and the primary organism is Cyanidium caldarium. Despite being acquired through several cm of water, the data indicate the algae and bacteria exhibit unique spectral features. Figure 1a shows spectra for Cyanidium caldarium from Nymph Creek. It has a green peak at 542 nm, an otherwise flat visible spectra, a 'red edge' at 710 nm and an absorption at 878 nm. Mastigocladus laminosus, from Octopus Spring, has maxima at 590 and 648 nm, chlorophyll alpha absorption (675 nm), and absorptions at 740 (bacteriochlorophyll c), 798, and 874 nm. Spectra of extracted Synechococcus and Chloroflexus are in Fig. 2a and in situ spectra of the mat in Fig. 2b. Synechococcus lividus has a chlorophyll alpha absorption, red edge at 765 nm and absorptions at 716, 798 and 877 nm. For the in situ observations, the red color of the Chloroflexus is subdued as it lies below the Synechococcus. The general character of the spectra are similar to that obtained from in vivo studies, although those data were collected with lower spectral resolution. These data indicate that each hyperthermophile organism has unique spectral characteristics and these can be used to separate the organism in the field with in situ data. This provides a basis for quick evaluation of such environments in Yellowstone (and elsewhere) and a basis for understanding how such organisms (most likely in fossil form) might be recognized on Mars. The next step will be the analysis of sinter deposits to assess the extent that incorporated biota retain their spectral signature. Additional information is contained in the original extended abstract.

Author

Near Infrared Radiation; Light (Visible Radiation); Thermophiles; Spectroscopy; Algae; Bacteria; Line Spectra; Characterization

20020002088 NASA Ames Research Center, Moffett Field, CA USA

How Cyanobacterial Distributions Reveal Flow and Irradiance Conditions of Photosynthetic Biofilm Formation

Prufert-Bebout, Lee, NASA Ames Research Center, USA; General Meeting of the NASA Astrobiology Insititute; April 2001, pp. 131; In English; See also 20020002018; No Copyright; Avail: Issuing Activity; Abstract Only

Microbial life on Earth is enormously abundant at sediment-water interfaces. The fossil record in fact contains abundant evidence of the preservation of life on such surfaces. It is therefore critical to our interpretation of early Earth history, and potentially to history of life on other planets, to be able to recognize life forms at these interfaces. On Earth this life often occurs as organized structures of microbes and their extracellular exudates known as biofilms. When such biofilms occur in areas receiving sunlight photosynthetic biofilms are the dominant form in natural ecosystems due to selective advantage inherent in their ability to utilize solar energy. Cyanobacteria are the dominant phototrophic microbes in most modern and ancient photosynthetic biofilms, microbial mats and stromatolites. Due to their long (3.5 billion year) evolutionary history, this group has extensively diversified resulting in an enormous array of morphologies and physiological abilities. This enormous diversity and specialization results in very specific selection for a particular cyanobacterium in each available photosynthetic niche. Furthermore these organisms can alter their spatial orientation, cell morphology, pigmentation and associations with heterotrophic organisms in order to fine tune their optimization to a given micro-niche. These adaptations can be detected, and if adequate knowledge of the interaction between environmental conditions and organism response is available, the detectable organism response can be used to infer the environmental conditions causing that response. This presentation will detail two specific examples which illustrate this point. Light and water are essential to photosynthesis in cyanobacteria and these organisms have specific detectable behavioral responses to these parameters. We will present cyanobacterial responses to quantified flow and irradiance to demonstrate the interpretative power of distribution and orientation information. This study presents new results, but many such examples are already found in the literature. However this information exists in such a wide variety of journals, spanning decades of research that the utility of the vast storehouse of information is limited, not by the ability of cyanobacteria to respond in recognizable ways to environmental stimuli, but by our ability to compile and use this information. Recent advances in information technology will soon allow us to overcome these difficulties and utilize the detailed responses of cyanobacteria to environmental microniches as powerful records of the interaction between the biosphere and lithosphere.

Author

Bacteria; Biofilms; Biological Evolution; Biological Diversity

20020002089 Carnegie Institution of Washington, Geophysical Lab., Washington, DC USA

Use of the delta(C-13) Associated with Amino Acid Biosynthesis as a Proxy for Examining the Flow of Carbon Through Biological Systems

Scott, James H., Carnegie Institution of Washington, USA; Fogel, Marilyn L., Carnegie Institution of Washington, USA; Emerson, David, American Type Culture Collection, USA; General Meeting of the NASA Astrobiology Insititute; April 2001, pp. 132-133; In English; See also 20020002018; No Copyright; Avail: Issuing Activity; Abstract Only

By examining the delta(C-13) associated with specific amino acids it is possible to follow the flow of carbon through the intermediary metabolism of various microbes. We have examined how the pathways associated with methanogenesis, methylotrophy, and heterotrophy effect the delta(C-13) of specific amino acids. Furthermore our work indicates that key amino acids are proxies for essential intermediates in the central metabolism of microorganisms. By using aspartic acid, glutamic acid and alanine as proxies for essential central metabolic intermediates (oxaloacetate, 2-oxoglutarate and pyruvate) we are able to examine the flow of carbon through various metabolic pathways. For example, every cell must have a pool of oxaloacetate and pyruvate to grow. Our work indicates that Delta(delta(C-13)(sub ASP) - delta(C-13)(sub ALA) provides a powerful indicator of how these two pools are replenished. The action of PEP carboxylase in Escherichia coli grown anaerobically on pyruvate, Shewanella oneidensis MR1 grown with nitrate and fumurate as electron acceptors led to an average Delta = -2.39 +/- 0.20 ppm. This clearly indicates that in these bacteria during anaerobiosis oxaloacetate is formed by the carboxylation of pyruvate (or PEP). In contrast, methylotrophs and E. coli growing on acetate yields a Delta = 2.67 +/- 1.04 ppm. In methanogens the difference in Delta is even more dramatic. In the case of methylotrophy, methanogenesis and E. coli growing on acetate, pyruvate is formed from oxaloacetate (or malate) through a wide range of enzymes. The next step will be to use our observations on pure microbial cultures to examine the flow of carbon in complex biological communities. Additional information is contained in the original extended abstract.

Author

Amino Acids; Biosynthesis; Carbon; Metabolism; Microorganisms

20020002090 Carnegie Institution of Washington, Geophysical Lab., Washington, DC USA

Observations on Microbial Metabolism at Extreme Pressures!

Sharma, Anurag, Carnegie Institution of Washington, USA; Scott, James H., Carnegie Institution of Washington, USA; General Meeting of the NASA Astrobiology Insititute; April 2001, pp. 134; In English; See also 20020002018; No Copyright; Avail: Issuing Activity; Abstract Only

One of the largest hurdles in the area of microbial ecology is the inability to study a wide range of physical and chemical gradients that have an impact on the growth and viability of living organisms. For example, little is known about the effect that the phase changes associated with hydrothermal conditions has on metabolic processes. We are developing techniques for monitoring metabolic responses at extreme conditions. Here we present some of the preliminary results towards the quantification of in-situ interrogation of metabolism of microbes at high pressures and temperatures. These results show that metabolic activity remains viable under surprisingly extreme physical and chemical conditions. These techniques and instrumentation are aimed at developing a collaborative facility for testing the viability of life in various terrestrial and non-terrestrial environments.

Author

High Pressure; Metabolism; Microbiology; Microorganisms; Hydrothermal Systems

20020002091 Colorado Univ., Dept. of Molecular, Cellular and Developmental Biology, Boulder, CO USA

Molecular Survey of Microbial Diversity in Hypersaline Ecosystems

Spear, John R., Colorado Univ., USA; Pace, Norman R., Colorado Univ., USA; General Meeting of the NASA Astrobiology Insititute; April 2001, pp. 135; In English; See also 20020002018; No Copyright; Avail: Issuing Activity; Abstract Only

The hypersaline microbial mats of Guerrero Negro, Baja California Sur, are unique ecosystems that have long been studied for their unique chemistry. Correlations of biological and chemical information are significantly restricted, however, because there is not a comprehensive survey of the specific kinds of organisms that comprise these hypersaline mats. The overarching goal of this work is to describe and understand the organismal composition, structure and physiology of a selected hypersaline microbial ecosystem using ribosomal 16S RNA gene sequences. The traditional reliance on pure culture techniques to describe microbiota is circumvented by this molecular approach. It is estimated that greater than 99% of naturally occurring microorganisms are not cultured using standard techniques. As participants in the Ecogenomics focus group within NASA's Astrobiology Institute we are conducting a comprehensive survey to determine the phylotypes and relative abundance of organisms present in these hypersaline microbial mats. A description of the microbiota that occurs in this environment through their molecular phylotypes will provide us with an understanding of microbial complexity and put in place a biological context in which to understand the chemical processes of these ecosystems. Organisms of these kinds might be expected to be found in other hypersaline

environments. Representatives of all three domains of life, Bacteria, Archaea, and Eucarya will be characterized in several layers of the mats, based upon determined chemistry. We are currently studying representative samples obtained from ex situ Guerrero Negro microbial mats maintained at NASA Ames in a greenhouse, as well as samples recently obtained on site. We intend to explore several selected sites at relatively high resolution, approximately 1000 cloned rRNA genes per site, to gain a comprehensive view of the communities. Information from this molecular analysis will be crucial for further definition and delineation of the chemistries that occur within the mats. This work will advance substantially our understanding of the kinds and activities or organisms that comprise hypersaline microbial mats, and open new avenues for future investigations.
Author
Microorganisms; Surveys; Composition (Property); Salinity; Characterization; Exobiology; Chemical Analysis; Bioassay; Colonies

20020002092 Jet Propulsion Lab., California Inst. of Tech., Pasadena, CA USA
Determining Biosignatures by Complexity Analysis in Antarctic Cryptoendolithic Communities
Storrie-Lombardi, M. C., Jet Propulsion Lab., California Inst. of Tech., USA; Bhartia, R., Jet Propulsion Lab., California Inst. of Tech., USA; Nealson, K. H., Jet Propulsion Lab., California Inst. of Tech., USA; General Meeting of the NASA Astrobiology Insititute; April 2001, pp. 136; In English; See also 20020002018; No Copyright; Avail: Issuing Activity; Abstract Only

One of the most difficult problems of life detection is that of identifying biosignatures across a wide range of scales using multiple co-registered probes. The technique should be of equal utility across a wide range of search spaces from remote sensors probing volumes of space or planetary surfaces, visual eye or camera searches across the surface of a rock in Antarctica, low resolution microscopic scanning of a rock or a space craft in situ, or high resolution electron microscope and computerized tomography scanning of geobiological samples. We describe here an approach to this problem which derives in large part from past work done in the area of astrophysics - namely the analysis of complexity in galactic signals by data compression methods. This approach is a radically new one for geobiology and astrobiology, and allows us to assess the complexity (and thus potential biogenicity) of an object being examined. This is done by considering the information within pixels of an image (regardless the sensor used to gather the information) as an energetic system capable of description in terms of classical thermodynamics. The image data space is searched by an algorithm that judges complexity via data compression (e.g., the more compressible it is, the less complex, and vice versa) and maximum entropy as originally outlined by Shannon. At present we are implementing methods to utilize images from multiple sensors gathering different kinds of information (e.g., visible gray-scale data, color analyses, UV fluorescence, chemical information, etc). We present here preliminary data from deep UV fluorescence and ESEM (Environmental Scanning Electron Microscope) images from a layered cryptoendolithic community of an Antarctic rock.
Author
Remote Sensors; Life Detectors; Signature Analysis; Data Compression; Imaging Techniques

20020002093 Jet Propulsion Lab., California Inst. of Tech., Pasadena, CA USA
Deep UV Native Fluorescence Imaging of Antarctic Cryptoendolithic Communities
Storrie-Lombardi, M. C., Jet Propulsion Lab., California Inst. of Tech., USA; Douglas, S., Jet Propulsion Lab., California Inst. of Tech., USA; Sun, H., Jet Propulsion Lab., California Inst. of Tech., USA; McDonald, G. D., Jet Propulsion Lab., California Inst. of Tech., USA; Bhartia, R., Jet Propulsion Lab., California Inst. of Tech., USA; Nealson, K. H., Jet Propulsion Lab., California Inst. of Tech., USA; Hug, W. F., Photon Systems, USA; General Meeting of the NASA Astrobiology Insititute; April 2001, pp. 138; In English; See also 20020002018; No Copyright; Avail: Issuing Activity; Abstract Only

An interdisciplinary team at the Jet Propulsion Laboratory Center for Life Detection has embarked on a project to provide in situ chemical and morphological characterization of Antarctic cryptoendolithic microbial communities. We present here in situ deep ultraviolet (UV) native fluorescence and environmental scanning electron microscopy images transiting 8.5 mm into a sandstone sample from the Antarctic Dry Valleys. The deep ultraviolet imaging system employs 224.3, 248.6, and 325 nm lasers to elicit differential fluorescence and resonance Raman responses from biomolecules and minerals. The 224.3 and 248.6 nm lasers elicit a fluorescence response from the aromatic amino and nucleic acids. Excitation at 325 nm may elicit activity from a variety of biomolecules, but is more likely to elicit mineral fluorescence. The resultant fluorescence images provide in situ chemical and morphological maps of microorganisms and the associated organic matrix. Visible broadband reflectance images provide orientation against the mineral background. Environmental scanning electron micrographs provided detailed morphological information. The technique has made possible the construction of detailed fluorescent maps extending from the surface of an Antarctic sandstone sample to a depth of 8.5 mm. The images detect no evidence of microbial life in the superficial 0.2 mm crustal layer. The black lichen component between 0.3 and 0.5 mm deep absorbs all wavelengths of both laser and broadband illumination. Filamentous deep ultraviolet native fluorescent activity dominates in the white layer between 0.6 mm and 5.0 mm from the surface. These filamentous forms are fungi that continue into the red (iron-rich) region of the sample extending from 5.0 to 8.5 mm. Using

differential image subtraction techniques it is possible to identify fungal nuclei. The ultraviolet response is markedly attenuated in this region, apparently from the absorption of ultraviolet light by iron-rich particles coating the filaments. Below 8.5 mm the filamentous morphology of the upper layers gives way to punctate 1-2 micron particles evidencing fluorescent activity following excitation at both deep ultraviolet wavelengths.
Author
Antarctic Regions; Fluorescence; Microorganisms; Morphology; Scanning Electron Microscopy; Ultraviolet Radiation; Life Sciences

20020002094 Woods Hole Oceanographic Inst., Geology and Geophysics Dept., MA USA
Novel Archaea in Guaymas Basin Hydrothermal Vent Sediments: Evidence for Anaerobic Methanotrophy
Teske, Andreas P., Woods Hole Oceanographic Inst., USA; Hinrichs, Kai-Uwe, Woods Hole Oceanographic Inst., USA; Edgcomb, Virginia, Marine Biological Lab., USA; Kysela, David, Marine Biological Lab., USA; Sogin, Mitchell L., Marine Biological Lab., USA; General Meeting of the NASA Astrobiology Insititute; April 2001, pp. 138-139; In English; See also 20020002018; No Copyright; Avail: Issuing Activity; Abstract Only

Microbial communities in hydrothermal sediments of the Guaymas Basin (Gulf of California, Mexico) were analyzed by cloning and sequencing of PCR (polymerase chain reaction)-amplified 16S rRNA genes from environmental DNA, and by stable carbon isotope analysis of archaeal and bacterial lipids extracted from the same samples. In this way, the phylogenetic composition of the microbial community can be correlated to carbon assimilation pathways that are reflected in the isotopic composition of diagnostic lipids. The Guaymas sediments contained a major lineage of methanogen-related, uncultured archaea (ANME-1 and 1b cluster), and of uncultured members of the Methanosarcinales, the acetoclastic and methyl-disproportionating methanogens (ANME-2 cluster). Sequences of the euryarchaeotal ANME-1, ANME-1b and ANME-2 clusters dominated the archaeal 16S rDNA clone libraries of the Guaymas Basin; crenarchaeotal sequences were rarely found. The sequence profiles were congruent with lipid profiles. Predominant archaeal lipids in the Guaymas Basin sediments included archaeol, diagnostic for non-thermophilic euryarchaota, and sn-2-hydroxyarchaeol, diagnostic for members of the Methanosarcinales. These lipids were extremely C-13 depleted (delta C-13 = -80 to -60 %), indicating that they originated from anaerobic methanotrophic archaea that presumably oxidized and assimilated C-13-depleted methane, which is abundant in Guaymas Basin vent fluids. Archaeal populations with this lipid and sequence signature are widespread in cold methane seeps and anoxic marine sediments (for example Eel River Basin, Santa Barbara Basin), indicating that they are of general biogeochemical relevance. The Guaymas Basin sediments harbored highly diverse bacterial populations, including gamma, delta, and epsilon-Proteobacteria, green non-sulfur bacteria, and members of the uncultured candidate subdivision OP11. Bacteria can consume hydrogen and acetate, the reaction products of archaeal methane oxidation, and thus make this process thermodynamically feasible; delta-Proteobacterial sulfate reducers are good candidates. With the exception of sulfur-oxidizing gamma and epsilon Proteobacteria, the bacterial community in the Guaymas sediments is anaerobic. Related bacterial species were found at other vent sites, terrestrial hot springs such as Obsidian Pool in Yellowstone, in anoxic marine sediments, hydrocarbon seeps and contaminated oil spill sites. Most likely, bacteria and archaea together constitute an anaerobic, methane-cycling microbial consortium in the Guaymas Basin sediments, and provide a model system for microbial carbon cycling in anoxic extraterrestrial habitats and subsurface environments. Additional information is contained in the original extended abstract.
Author
Sediments; Anaerobes; Hydrothermal Systems; Archaebacteria; Colonies; Vents

20020002095 Tokyo Univ., Dept. of Earth & Planetary Science, Hongo, Japan
Archaean Park: A Research Project on Interaction Between Sub-Vent Biosphere and Geo-Environment
Urabe, Tetsuro, Tokyo Univ., Japan; Maruyama, Akihiko, National Inst. of Advanced Industrial Science and Technology, Japan; Marumo, Katsumi, National Inst. of Advanced Industrial Science and Technology, Japan; Ishibashi, Jun-ichiro, Kyushu Univ., Japan; Seama, Nobukazu, Kobe Univ., Japan; General Meeting of the NASA Astrobiology Insititute; April 2001, pp. 140-141; In English; See also 20020002018; No Copyright; Avail: Issuing Activity; Abstract Only

A multi-disciplinary research project on sub-vent biosphere Archaean Park started in 2000 as a five-year program of the Special Coordination Fund of the Ministry of Education, Culture, Sports, Science and Technology (MEXT), Japan. The key research gear of the project is BMS (Benthic Multicoring System), a tethered submarine drilling rig of the Metal Mining Agency of Japan to do direct sampling of micro-organisms, rock cores and fluids from seafloor hydrothermal sites. The drilled holes will be approached by ROV (remote operated vehicle) and manned submersible to install various long-term monitoring and in-situ measurement instruments to delineate the system response to the geo-environmental change in temperature, fluid flow, and chemistry of the fluid. Extensive acoustic, seismic and electromagnetic surveys will be conducted to map and explore the lateral extent and the structure of the biosphere beneath the vents. Two target sites are located at western and eastern Pacific; that is, Suiyo

Seamount caldera (D= 1380 m, Tmax= 317 C) in Izu-Bonin Arc and the NOAA's (National Oceanic and Atmospheric Administration) NeMO Observatory site at Axial Seamount Caldera (D= 1590 m, Tmax= 330 C) in the Juan de Fuca (JdF) Ridge. This is because the generation, evolution, and dispersion of the subvent biosphere will be best described if we compare long-lived mid-ocean ridge system with short-lived (less than 1 Ma), sporadic hydrothermal system developed in independent edifices of volcanic arc. A hydrothermal system is the 'window' of the mostly unknown fluid flow system within the oceanic crust and mantle. The deeper portion of the system is likely to be hot and strongly-reducing due to hydrogen, methane and hydrogen sulfide gases dissolved in the fluid. Such environment is analogous to the site for the origin and early evolution of life in Archaean age, since most of Domain Bacteria and Domain Archaea near the root of the Universal Tree are hyper-thermophilic. Direct drilling may lead us to find Our Common Ancestor which may have survived in least evolved form in such an environment Archaean Park. This is also a site to explore the temperature limit for the survival of micro-organisms. We can approach such environment within the depth limit (20 m) of the BMS from seafloor in high-temperature vent areas. The upper part of the circulation system will become oxidizing due to invasion of oxygenated seawater. Supply of free oxygen to the metabolic cycle of micro-organisms such as sulfur-oxidizing and methane-oxidizing bacteria will greatly enhance their growth rate. Therefore, exploration of the oxidation/reduction front is essential to estimate the total biomass which is produced by chemo-synthesis of endogenic energy and nutrients from the solid earth. We noticed through long-term seafloor monitoring at southern East Pacific Rise (EPR) that the earth and/or ocean tides act as a pump to move fluid back and forth which will consequently modify the redox front from a plane to a wide zone within the oceanic crust. The tide-induced fluctuation, together with more critical influence from geologic perturbation such as change in magmatic degassing and local stress shift will significantly affect the nature and life span of the sub-vent biosphere. On the other hand, most significant influence from sub-vent biosphere to the earth is the supply of chemo-synthetic biomass to the ocean through hydrothermal plumes. Dominance of Archaea in Juan de Fuca Ridge shows clear contrast to its absence (and dominance of Bacteria) in vent fluids and hydrothermal plumes at southern East Pacific Rise system. This may be due to the difference in the mode of fluid discharge in these two areas; that is frequent event plumes at JdF vs. chronic venting at EPR. Such hypotheses should be tested through direct drilling into active vent sites of different settings.
Author

Biosphere; Drilling; Habitats; Microorganisms; Ocean Bottom; Precambrian Period; Vents; Thermal Environments

20020002096 NASA Johnson Space Center, Houston, TX USA

A Structural and Molecular Approach for the Study Biomarkers

Thomas-Keprta, Kathie, NASA Johnson Space Center, USA; Vali, Hojatollah, McGill Univ., Canada; Sears, S. Kelly, McGill Univ., Canada; Roh, Yul, Oak Ridge National Lab., USA; General Meeting of the NASA Astrobiology Insititute; April 2001, pp. 142-143; In English; See also 20020002018; No Copyright; Avail: Issuing Activity; Abstract Only

Investigation of the nucleation and growth of crystals in both abiotic and biotic systems is critical to seemingly diverse disciplines of geology, biology, environmental science, and astrobiology. While there are abundant studies devoted to the determination of the structure and composition of inorganic crystals, as well as to the development of thermodynamic and kinetic models, it is only recently that research efforts have been directed towards understanding mineralization in biological systems (i.e., biomineralization). Biomineralization refers to the processes by which living organisms form inorganic solids. Studies of the processes of biomineralization under low temperature aqueous conditions have focused primarily on magnetite forming bacteria and shell forming marine organisms. Many of the biological building materials consist of inorganic minerals (calcium carbonate, calcium phosphate, silica or iron oxide) intricately combined with organic polymers (like proteins). More recently, efforts have been undertaken to explore the nature of biological activities in ancient rocks. In the absence of well-preserved microorganisms or genetic material required for the polmerase chain reaction (PCR) method in molecular phylogenetic studies, using biominerals as biomarkers offers an alternative approach for the recognition of biogenic activity in both terrestrial and extraterrestrial environments. The primary driving force in biomineralization is the interaction between organic and inorganic phases. Thus, the investigation of the ultrastructure and the nature of reactions at the molecular level occurring at the interface between inorganic and organic phases is essential to understanding the processes leading to the nucleation and growth of crystals. It is recognized that crystal surfaces can serve as the substrate for the organization of organic molecules that lead to the formation of polymers and other complex organic molecules, and in discussions of the origins of life, is referred to as organic synthesis on mineral surfaces. Furthermore, it is suggested that the interaction between mineral surfaces and simple organic molecules resulted in the formation of amino acids, RNA, and perhaps other more complex molecules such as proteins. On the other hand, in natural systems, it is recognized that functional groups on cell walls or membranes of microorganisms serve as sites of nucleation and crystallization. The precise replication of biominerals with controlled structure, morphology, size and texture is not confined to higher organisms as it also occurs in primitive prokaryotic cells such as magnetotactic bacteria and cyanobacteria. This suggests that the principal strategies of biomineralization were established early on in the evolutionary history of organisms. It is critical, therefore, to search for common mechanisms within diverse biological systems. One such common factor is the capability for

organization and self-assembly. Organic macromolecules such as proteins and lipids can aggregate and polymerize forming membranes or extracellular matrix. At the organic-inorganic interface, several factors such as lattice geometry, polarity, stereochemistry and topography may act in concert to control nucleation and growth of crystals. Although several models have been proposed that discuss the significance of these factors for biomineralization, no comprehensive experimental data are available. In contrast to crystallization in exclusively inorganic systems, the kinetics of reaction and structural relationships between organic and inorganic phases in biominerals or biomimetic material is poorly understood. For example, it is not clear if the concept of epitactic growth (geometrical matching of unit cells at the interface of a secondary crystal growing on a primary crystal) applies to organic-inorganic systems. In contrast to inorganic templates that often have a smooth and rigid surface that promotes epitactic growth, biological substrates are usually rough and result in a large degree of mismatch. It is apparent that factors controlling the reaction at the crystal-matrix interface are strongly dependent upon the nature of the substrate. Therefore, characterization of the assembled organic surface and surface structure of the inorganic phase is crucial to understanding the processes of biomineralization. The focus of our research is the investigation of the processes leading to the nucleation and growth of crystals on both natural and synthetic systems through an interdisciplinary approach that integrates molecular biology, morphology and mineralogy using advanced preparation and analytical techniques. We have studied run-products, particularly magnetite, siderite and other carbonates, that resulted from extracellular biomineralization by extremophiles isolated from a variety of extreme environments ranging from permafrost to hydrothermal vent systems. The results of this study are critical to recognizing biomarkers in terrestrial and extraterrestrial environments.
Author
Calcification; Cells (Biology); Crystal Growth; Crystallization; Crystals; Marking; Microorganisms; Mineralogy; Minerals; Activity (Biology)

20020002097 Colorado Univ., Molecular, Cellular, & Developmental Biology, Boulder, CO USA
Photoendolithic Ecosystems: Molecular Diversity and Structure
Walker, Jeffrey J., Colorado Univ., USA; Pace, Norman R., Colorado Univ., USA; General Meeting of the NASA Astrobiology Insititute; April 2001, pp. 144; In English; See also 20020002018; No Copyright; Avail: Issuing Activity; Abstract Only

The endolithic environment, comprised of the pore-spaces in rock, is a ubiquitous microbial habitat on Earth, and may harbor life elsewhere in the universe. Endolithic environments are a haven for life in some of the most severe hot and cold deserts on Earth, including the Mojave Desert of North America and the Ross Desert in Antarctica. Analogous endolithic environments must occur on Mars today, and may contain evidence of past or present life. Understanding the biological and physical dynamics of endolithic ecosystems on Earth informs the search for life on other bodies in the solar system. Photosynthetically driven microbial communities form biofilm-like photoendolithic ecosystems in the upper millimeters of rock, wherever it is exposed to sunlight and even trace amounts of water. Despite a global distribution, little is known about these ecosystems on Earth. This study examines the microbial composition and community structure of photoendolithic ecosystems inhabiting a variety of rock-types in the central Rocky Mountains of North America. A specific aim of this research is to test the hypothesis that rock-type plays a significant role in determining the microbial composition and community structure of photoendolithic ecosystems. A general principle in microbial ecology, that communities are driven by the chemical and physical characteristics of their environment, is predicted to influence photoendolithic community composition by determining the availability of nutrients along with other physico-chemical variables. Among the rock types examined in this study are sandstone, limestone, basalt, and granite. 16S and 18S ribosomal RNA sequence-based phylogenetic analysis of sandstone and limestone communities reveals a pattern in which phylogenetically related, but unique microbial constituents form similar kinds of communities in different types of rock. Attempts have been made to control for other physical characteristics thought to influence photoendolithic communities, including aspect, elevation, water availability, photosynthetically active radiation, and temperature. Preliminary results of this study support the hypothesis that rock-types significantly influence the microbial composition of photoendolithic communities.
Author
Ecosystems; Microorganisms; Rocks; Exobiology; Biofilms

20020002098 Montana Univ., Dept. of Geology, Missoula, MT USA
The Changing Geochemical Environment of a Thermal Spring May Provide Clues to Environmental Conditions and Microbial Evolution on Mars
Wilson, Cindy L., Montana Univ., USA; Hinman, Nancy W., Montana Univ., USA; General Meeting of the NASA Astrobiology Insititute; April 2001, pp. 145-146; In English; See also 20020002018; No Copyright; Avail: Issuing Activity; Abstract Only

The chemistry of a thermal spring in Yellowstone National Park has been monitored since June 1996. This spring was one of four springs examined in a previous study. Thermal springs were selected for these studies because they are modern analogs to environmental conditions on early Earth when life evolved. Any life that evolved on other planetary bodies may have developed

under similar conditions. Therefore, understanding how the geochemistry in a thermal system changes and how those changes affect the microbial populations is vital to understanding how life evolved on Earth and perhaps on other planetary bodies. Herein, we present data on the changing geochemical environment of a thermal spring in Yellowstone National Park. McHale and Kieft present data on the microbial populations for the different geochemical environments in the pool. The Roadside Springs in Yellowstone National Park were first studied in 1996 as part of a study on hydrogen peroxide cycling in thermal waters. Subsequent observations indicated that the spring geochemistry was changing in the iron-rich spring. In June 1996, the pool floor was covered with a thick layer of white sediments. Subsequent analysis of these sediments indicated high concentrations of arsenic, barium, chromium, strontium, and silica. Iron and sulfur were also present. The white sediments continued to dominate the system until late-1999 or early-2000. When the spring was revisited in June 2000, a thin layer of red sediments covered much of the pool floor. by October 2000, the red sediments covered the pool floor except around the vent where outgassing occurred. These red sediments contain lower concentrations of aluminum, barium, chromium, and strontium but higher concentrations of arsenic and iron than the white sediments. These observed changes in pool sediments are the result of changing oxidation conditions within the pool (i.e. the pool changed from a reducing environment to an oxidizing environment). The changing oxidation conditions may reflect changes in the source water for the spring. An increase in the amount of shallow groundwater mixing with the deeper, thermal water may produce more oxidizing conditions. Alternatively, less shallow groundwater mixing with the deeper, thermal water may produce more reducing conditions. These changes in the amount of shallow groundwater mixing with the deeper, thermal water could be due to wetter or drier climatic periods, respectively. Changing water chemistry supports the theory of an increased amount of shallow groundwater mixing with deeper, thermal water. From June 1996 to June 2000, the average mid-day temperature dropped from 78.3 C to 68.5 C. This drop in temperature is suggestive of more cooler water mixing with the thermal water. Additionally, an increase in water pH (3.37 to 4.00) during this time is indicative of an increase in the amount of shallow groundwater mixing with the deeper water. Finally, the concentrations of most metal ions decreased during the four year period reaching minimum concentrations in October 2000. The primary source for dissolved metals is leaching from the rock by the hot, acidic thermal waters. Therefore, an increase in shallow groundwater in the source water would result in decreased concentrations of dissolved metals. The changing geochemistry of this thermal spring suggests that thermal springs are dynamic environments. It is likely that thermal springs on Mars would also be dynamic environments where the spring geochemistry is influenced by changing groundwater levels and chemistry. Therefore, it is possible that cycling between oxidizing and reducing conditions may have occurred in thermal springs on Mars. Large outflow channels on Mars suggest that Mars once supported water on its surface. Furthermore, the chaotic terrain at the head of the outflow channels suggests that water discharge in these channels would have been episodic. These discharges would have been similar to the floods from Lake Missoula in Eastern Washington. However, the water for the Martian floods probably came from an underground aquifer rather than a surface lake. The massive discharge from these channels would have drained the regional subsurface aquifer. This would have resulted in less shallow water to mix with the deeper, thermal waters that formed springs in the area. Therefore, the regional thermal springs would have been a reducing environment. As the aquifer recharged, these thermal springs would become more oxidizing as the influence from the subsurface aquifer increased. The time scale for this cycling would have been several thousands of years rather than several years as seen on Earth. Therefore, each event horizon would have been considerably thicker than the horizons seen in this thermal spring.

Author

Geochemistry; Mars Environment; Microorganisms; Oxidation; Sediments; Hydrothermal Systems; Springs (Water)

20020002099 Marine Biological Lab., The Josephine Bay Paul Center for Comparative Molecular Biology and Evolution, Woods Hole, MA USA

Eukaryotic Diversity in an Acidic, Metal-Rich Environment: Spain's Tinto River

Zettler, Linda A. Amaral, Marine Biological Lab., USA; Amils, Ricardo, Universidad Autonoma de Madrid, Spain; Gomez, Felipe, Centro de Astrobiologia, Spain; Keenan, Brendan G., Connecticut Univ., USA; Sogin, Mitchell L., Marine Biological Lab., USA; General Meeting of the NASA Astrobiology Insititute; April 2001, pp. 147-148; In English; See also 20020002018; No Copyright; Avail: Issuing Activity; Abstract Only

With the discovery that life can thrive under extreme conditions have come microbial studies devoted to the exploration of the diversity of life present in different extreme environments. Such studies rarely focus on eukaryotic microbes. As a result, the list of prokaryotic organisms capable of growing at extreme temperatures, pH, or ionic strengths has expanded enormously, giving the impression that only prokaryotes are capable of adapting to harsh conditions. Spain's Tinto River, a high metal, acidic environment with a pH range of 1.7 - 2.5, exhibits an impressive level of biodiversity, which spans not only the prokaryotic domains (Bacteria and Archaea), but also the Eukaryotic domain of life. The Tinto River gets its name from the red color of its waters made so by the high concentrations of ferric iron dissolved in the water. Equally impressive are the shades of brown, green and ochre along the river's edge which result from algal blooms contributing as much as 60% of the biomass in some cases. The

Tinto River is a unique extreme system in that, at least in some regions, it is an environment dominated by eukaryotes. We present the results of a full-length, small-subunit ribosomal RNA based molecular characterization of several sampling stations along the Tinto River, including samples taken at the source of the river. Many of our clones showed high similarity to taxa reported in previous studies employing light-microscopical techniques. These included the highly conspicuous members of the Euglenozoa (euglenids), Chlorophyta (chlamydomonad and chlorella-like relatives), as well as the Bacillariophyta (diatoms). However, our results also revealed a diversity of other protists not previously identified with conventional technologies. These included several members of the stramenopiles (chrysophytes, bicosoecids) and the alveolates (ciliates, dinoflagellate-relatives). In addition there were several representative cercomonad relatives, one representative heterolobosean amoeba-relative, and a few clones that did not reveal high similarities with any known taxa. Other members of the Viridiplantae were represented by streptophyte and charophyte relatives. Our study also revealed a diversity of fungi somewhat different than those previously identified in the river using traditional methods. The majority of our clones belonged to the Ascomycota but there were a few representatives from the Zygomycota. We summarize our results in a phylogenetic analysis. The high level of eukaryotic diversity found associated with the low pH and high metal concentrations proves that adaptation to extreme conditions is much more widespread than originally expected.
Author
Eukaryotes; Microorganisms; Prokaryotes; Ecosystems; Tolerances (Physiology)

20020002100 Marine Biological Lab., The Josephine Bay Paul Center for Comparative Molecular Biology and Evolution, Woods Hole, MA USA
Eukaryotic Diversity in Alkaline Lakes of the Sandhills Region of Nebraska
Zettler, Linda A. Amaral, Marine Biological Lab., USA; Sogin, Mitchell L., Marine Biological Lab., USA; Keenan, Brendan G., Connecticut Univ., USA; General Meeting of the NASA Astrobiology Insititute; April 2001, pp. 149; In English; See also 20020002018; No Copyright; Avail: Issuing Activity; Abstract Only

Extreme alkaline areas are less frequently encountered in nature than extremely acidic ones. by definition, environments having pH values greater than 10.0 are considered extremely alkaline. In the USA, the lakes of the Sandhills Region of western Nebraska represent some of the most alkaline features available for investigation. Such alkaline areas are often characterized by poor drainage and high mineralization (sodium is greater than potassium is greater than magnesium is greater than calcium) created by leaching and evaporation. Given the rarity of alkaline environments, one might expect to find unique assemblages of organisms inhabiting such locations. Studies focusing on microbial diversity of these environments, certainly eukaryotic microbial diversity, are lacking. In order to assess the eukaryotic diversity at alkaline extremes, we collected sediment samples in several alkaline lakes in the Alkali Lakes region (the Sheridan and Garden Counties) of western Nebraska. These lakes are compositionally diverse and range in salinity from fresh to brine. Several of the lakes sampled were unnamed- most were located in the Crescent Lake National Wildlife Refuge. We used a rDNA-based approach and screened rDNA clone libraries to assess diversity. Perhaps the most surprising aspect of the eukaryotic diversity in the lakes we examined was that a large part of this diversity was not microbial. Our preliminary rDNA data analyses show a large metazoan component to many of the alkaline communities. These included such groups as the annelids, platyhelminths, nematodes, gastrotrichs, insects, ostracods, copepods, priapulids, rotifers, and sponges. Members of the Viridiplantae and Fungi were also present. Chlorophytes, streptophytes, and embryophytes were represented in BLAST hits for the Viridiplantae while fungi included chytrids, ascomycetes, and basidiomycetes. A diverse array of protists was also found. These included members or relatives of the alveolates (such as ciliates, dinoflagellates, apicomplexans), as well as representatives of the stramenopiles - diatoms, oomycetes, chysophytes, and labyrinthulids. Others groups detected included euglenids, amoeboid protists, glaucocystophytes, choanoflagellates, and cercomonads. Additional sequencing and phylogenetic analyses will determine the novelty of these clones.
Author
Eukaryotes; Lakes; Microorganisms; Ecosystems; Alkalinity; Tolerances (Physiology)

20020002101 Arizona State Univ., Dept. of Geological Sciences, Tempe, AZ USA
Exploring for Martian Life: Recent Results and Future Opportunities
Farmer, Jack D., Arizona State Univ., USA; General Meeting of the NASA Astrobiology Insititute; April 2001, pp. 153-154; In English; See also 20020002018; No Copyright; Avail: Issuing Activity; Abstract Only

The exploration for past or present Martian life and/or prebiotic chemistry are primary goals of the Mars exploration program. In implementing these goals, the Astrobiology community has consistently recommended an approach that will create the proper environmental context for exploration through the synergistic use of orbital reconnaissance and landed in situ science. These broadly-based investigations are regarded to be an essential prelude to the targeting of sites for in situ life detection experiments and sample return(s). In exploring for Martian life, two independent investigation pathways have been identified by the

Astrobiology community as co-priorities for missions preceding the 2007 opportunity. These include: 1) determining the locations of sedimentary deposits formed by past surface and subsurface hydrological processes (this will enable the exploration for a record of past life) and 2) mapping the three-dimensional distribution of water in all it forms (as a prelude to exploring potential habitats of subsurface liquid water that could sustain extant life). The mantra, 'follow the water', has been a guiding theme in constructing the new Mars exploration program architecture. It appears that over the next few opportunities (through 2007) implementation of this goal will be achieved through a combination of orbital mapping (infrared spectral mapping of mineralogy to identify ancient surface and subsurface water systems and radar sounding from orbit to locate reservoirs of modern subsurface water) and landed rover missions. Orbital missions in 2001 and 2005 will be interleaved with surface investigations in 2003 that will place twin 'Mars Exploration Rovers' (MER A and B) at two high priority sites to gather information about surface mineralogy and petrology. This data will provide the basis for assessing the nature of ancient depositional environments at each site, while providing ground truth mineralogy that will assist in the interpretation of previously acquired orbital data. Additional information is contained in the original extended abstract.
Author
Exobiology; Mars Exploration; Mineralogy; Water; Extraterrestrial Life

20020002102 Arizona State Univ., Dept. of Geological Sciences, Tempe, AZ USA
Europa: Views from the Galileo Mission
Greeley, Ronald, Arizona State Univ., USA; General Meeting of the NASA Astrobiology Insititute; April 2001, pp. 155-156; In English; See also 20020002018; No Copyright; Avail: Issuing Activity

Europa has the possibility of harboring a sub-surface liquid ocean, organic compounds, and a heat source from friction generated from tidal action. These potential conditions make Europa a high-priority for exobiological exploration. First viewed up-close during the Voyager 1 and 2 flybys in 1979, the Galileo mission has provided a wealth of high-resolution data which have provided new insight into this Jovian satellite. Models for the interior derived from values of the moment of inertia suggest that Europa is a rocky object with a central core and an outer shell of water composition some 150 km thick, the surface of which is frozen. Galileo magnetometer data suggest that a sub-ice zone of salt water could exist, although this interpretation is model-dependent. Remote sensing data includes spectra from the Near Infrared Mapping Spectrometer (NIMS), which show the presence of salts and sulfur compounds mixed with the ice, and images from the Solid State Imaging (SSI) system. From 23 near and distant flybys of Europa, more than 525 images were taken, with resolutions ranging from 11 m/pixel to 20 km/pixel. Europa is seen to have a geologically young surface dominated by tectonic and possible cryovolcanic (e.i., generation of 'magmas' consisting of volatiles such as water) activity which form complex ridge sets, zones of ice-crust separation, and areas in which the crust is disrupted and reformed. These areas suggest that materials from beneath the ice crust have been emplaced on the surface and have NIMS signatures showing the presence of non-ice compositions. The few large impact structures on Europa show excavation of similar compositions from the subsurface. Non-ice materials are also inferred to be implanted on the surface from exogenic sources, such as the volcanically-active moon, Io. Under the sponsorship of the NASA Astrobiology Institute, an informal Europa Focus Group was organized to provide a forum for discussion and to promote interdisciplinary research. The first workshop was held at NASA-Ames Research Center in February, 2001, during which key questions were posed for future work. Additional information is contained in the original extended abstract.
Author
Europa; Exobiology; Galileo Project; Jupiter Satellites; Water; Space Exploration

20020002103 Carnegie Institution of Washington, Geophysical Lab., Washington, DC USA
The Source of Extraterrestrial Water in Martian Meteorites
Boctor, N. Z., Carnegie Institution of Washington, USA; Alexander, C. M. O. D., Carnegie Institution of Washington, USA; Wang, J., Carnegie Institution of Washington, USA; Hauri, E., Carnegie Institution of Washington, USA; General Meeting of the NASA Astrobiology Insititute; April 2001, pp. 157-158; In English; See also 20020002018; No Copyright; Avail: Issuing Activity; Abstract Only

Polycyclic aromatic hydrocarbons were reported in Martian meteorite ALH 84001, and were interpreted as one of several lines of evidence for ancient life on Mars. For life to exist on any planet, water must be present. Geomorphological features on the surface of Mars suggest that water was abundant in its early history. Hydrogen isotopes measured on Martian meteorites provide important clues on the history and source of water on Mars. The Martian atmosphere is 5.2 times enriched in D/H relative to terrestrial values. Interaction of Martian meteorites with a water reservoir that equilibrated with the Martian atmosphere was invoked to explain the D enrichment in minerals from Martian meteorites. So, in principle the H isotope signatures of Martian meteorites of different ages may provide clues on the H isotope compositions of the water reservoirs on Mars and on the evolution of the Martian atmosphere through time. There have been recent reports of D enrichment in impact glasses and in post-stishovite

high pressure polymorph of silica in Martian meteorites. This finding calls for a reassessment of the role of shock metamorphism in hydrogen isotope fractionation. Additional information is contained in the original extended abstract.
Author
Mars (Planet); Water; Composition (Property); Extraterrestrial Life; Exobiology

20020002104 Raytheon Information Technology and Scientific Services, Greenbelt, MD USA
Radiolytic Chemistry at Europa's Doorstep - The First Meter
Cooper, John F., Raytheon Information Technology and Scientific Services, USA; General Meeting of the NASA Astrobiology Insititute; April 2001, pp. 159; In English; See also 20020002018; No Copyright; Avail: Issuing Activity; Abstract Only

Galileo Orbiter observations have revealed a relatively young (107 - 108 year old) icy surface with a molecular composition in the sensible top millimeter layer largely driven by radiolytic energy inputs and sputtering from magnetospheric particle irradiation. The observed sulfate hydrates (e.g., MgSO4 or H2SO4), surface (H2O2) and atmospheric (O2, O) oxidants, and sodium neutral cloud are characteristic of a heavily irradiated ice surface with access to endogenic and exogenic sources of sulfur and other non-ice materials. Leading/trailing asymmetries suggest magnetospheric plasma and energy inputs, while concentrations along tidal cracks are more indicative of salt water evaporites from the putative sub-surface ocean. Sputtering by magnetospheric ions produces vertical escape to space of lighter chemical species such as hydrogen and sodium. The ease of hydrogen escape from the irradiated surface and atmosphere allows buildup of oxidants on the surface. Horizontal dispersion of endogenic sulfur by sputtering on the trailing hemisphere, and larger energy inputs there from magnetospheric irradiation, could account for higher abundance of sulfates in that hemisphere. Although the magnetospheric particles irradiate the ice mainly at depths of microns to millimeters, the residual irradiation products can be buried to meter depths in the ice regolith by meteoritic gardening over the apparent surface lifetime of millions of years. Large reservoirs of such products may reside below the visible surface and eventually be transported to the sub-surface ocean as the result of crustal instabilities driven by tidal forces and thermal gradients. Measurements of vertical profiles for irradiation products could be a prime focus for meter-depth probe experiments on a Europa lander spacecraft. Cooper et al have reported, as upper limits derived from the incident energy fluxes of magnetospheric particles, that the radiolytic production rates of H2O2 and O2 are sufficient to fully saturate the 100-km deep ocean with dissolved oxygen in 107 years. Since reduced gases may be released from the ocean bottom at hydrothermal vents, the chemical disequilibrium required for evolution of life within Europa may present even without substantial inputs from photosynthetically active radiation (PAR) at the surface. Europa may therefore represent a new class of habitable objects in the universe - large icy satellites or planets orbiting in intense irradiation environments. Due to the fragility of life often exposed to catastrophic events on the surfaces of planets in the classical 'habitable zone', life forms evolving in protected sub-surface oceans of Europa-like objects might actually be more common in the universe than terrestrial life forms. Interplanetary transfer of astrobiological material in escaping ejecta from cometary impacts on such objects could then continually reseed terrestrial environments.
Author
Europa; Remote Sensing; Satellite Surfaces; Extraterrestrial Oceans; Chemical Analysis; Planetary Structure; Chemical Composition

20020002105 NASA Johnson Space Center, Houston, TX USA
Beagle 2: The Next Exobiology Mission to Mars
Gibson, Everett K., Jr., NASA Johnson Space Center, USA; Pillinger, Colin T., Open Univ., UK; Wright, Ian P., Open Univ., UK; Morse, Andy, Open Univ., UK; Stewart, Jenny, Open Univ., UK; Morgan, G., Open Univ., UK; Praine, Ian, Open Univ., UK; Leigh, Dennis, Open Univ., UK; Sims, Mark R., Leicester Univ., UK; General Meeting of the NASA Astrobiology Insititute; April 2001, pp. 160-162; In English; See also 20020002018; No Copyright; Avail: Issuing Activity; Abstract Only

Beagle 2 is a 60 kg probe (with a 30 kg lander) developed in the United Kingdom for inclusion on the European Space Agency's 2003 Mars Express. Beagle 2 will deliver to the Martian surface a payload which consists of a high percentage of science instruments to landed spacecraft mass. Beagle 2 will be launched in June, 2003 with Mars Express on a Soyuz-Fregat rocket from the Baikonur Cosmodrome in Kazakhstan. Beagle 2 will land on Mars on December 26, 2003 in the Isidis Planitia basin (approximately 10 degrees N and 275 degrees W), a large sedimentary basin that overlies the boundary between ancient highlands and northern plains. Isidis Planitia, the third largest basin on Mars, which is possibly filled with sediment deposited at the bottom of long-standing lakes or seas, offers an ideal environment for preserving traces of life. Beagle 2 was developed to search for organic material and other volatiles on and below the surface of Mars in addition to the study of the inorganic chemistry and mineralogy. Beagle 2 will utilize a mechanical mole and grinder to obtain samples from below the surface, under rocks and inside rocks. A pair of stereo cameras will image the landing site along with a microscope for examination of surface and rock samples. Analyses will include both rock and soil samples at various wavelengths, X-ray spectrometer and Mossbauer spectrometer as well

as a search for organics and other light element species (e.g. carbonates and water) and measurement of their isotopic compositions. Beagle 2 has as its focus the goal of establishing whether evidence for life existed in the past on Mars at the Isidis Planitia site or at least establishing if the conditions were ever suitable. Carbonates and organic components were first recognized as existing on Mars when they were found in the Martian meteorite Nakhla. Romanek et al showed the carbonates in ALH84001 were formed at low temperatures. McKay et al noted possible evidence of early life on Mars within the ALH84001 meteorite. Thomas-Keprta et al showed the magnetite biomarkers in ALH84001's carbonates are indistinguishable from those formed by magnetotactic bacteria found on Earth. Gibson et al showed there was significant evidence for liquid water and biogenic products present on Mars across a 3.9 billion year period. A mechanical arm (PAW) operates from the lander and is used for science operations along with sample acquisition. Instruments attached to the PAW include: stereo cameras, Mossbauer instrument, X-ray fluorescence instrument, microscope, environmental sensors, rock corer/grinder, a spoon, mirror, brushes, a mole attachment for acquisition of subsurface to depths of 1 to 2 meters and an illumination device. Each camera has 14 filters which have been optimized for mineralogy composition, dust and water vapor detection. The microscope's camera is designed for viewing the size and shape of dust particles, rock surfaces, microfossils, and characteristics of the samples prior to introduction into the gas analysis package (GAP). The camera has a resolution of 4 microns/pixel, features four color capability (red, green, blue and UV (ultraviolet) fluoresence), a depth of focus of 40 micrometers and translation stage of +3 millimeters. The heart of the Beagle 2's life detection package is the gas analysis package (GAP), which consists of a mass spectrometer with collectors at fixed masses for precise isotopic ratio measurements and voltage scanning for spectral analysis. Primary aim of the GAP is to search for the presence of bulk constituents, individual species, and isotopic fractionations for both extinct and extent life along with studying the low-temperature geochemistry of the hydrogen, carbon, nitrogen and oxygen components on Mars from both the surface and atmosphere. GAP is a magnetic sector mass spectrometer with the range of 1 to 140 amu which can be operated in both the static and dynamic modes. A triple Faraday collector array will be used for C, N and O ratios along with a double Faraday array for H/D. Pulse counting electron multiplier will be utilized for noble gases and selected organics. Anticipated detection limits are at the picomole level for operation in the static mode of operation and high precision isotopic measurements will be made in the dynamic mode. Sample processing and preparation system consists of reaction vessels along with references. Sample ovens capable of being heated are attached to the manifold for sample combustion. Surface, subsurface materials and interior rock specimens will be combusted in pure oxygen gas at various temperature intervals to release organic matter and volatiles. Combustion process will permit detection of all forms and all atoms of carbon present in the samples. A chemical processing system is capable of a variety of conversion reactions. Gases are manipulated either by cryogenic or chemical reactions and passed through the gas handling portion of the vacuum system. There are two modes of operation: quantitative analysis and precise isotopic measurements. Additional information is contained in the original extended abstract.

Author

Exobiology; Mars Missions; Spacecraft Instruments; European Space Programs; Space Probes

20020002106 California Univ., Dept. of Earth and Space Sciences, Los Angeles, CA USA

Europa: Crunchy or Chewy Inside?

Moore, William B., California Univ., USA; General Meeting of the NASA Astrobiology Insititute; April 2001, pp. 163; In English; See also 20020002018; No Copyright; Avail: Issuing Activity; Abstract Only

The presence of molten rock within a few kilometers of the water-rock interface in Europa is far more important for life than the presence of a liquid ocean. Hydrothermal vent communities on Earth depend on a flux of melt from the mantle into the lithosphere to drive the high-temperature chemistry that liberates nutrients from the rock. Europa's major internal energy sources at the present time are radioactive decay and tidal heating. In a body smaller than the Moon, consisting partly of ice and having a significant iron core, radiogenic heat production is quite small, probably not exceeding a few times 10 (exp 11) W. Tidal dissipation is capable of much greater heating rates and occurs both in the silicate and icy portions of the body. The maximum temperature reached within Europa's mantle depends on the balance between dissipation and heat transfer. Due to the sensitivity of both tidal heating and convective heat transfer on viscosity, there exist two stable equilibrium states for Europa's mantle: crunchy (Moon-like), in which weak subsolidus convection balances radiogenic heat production, and chewy (Io-like), in which the mantle is extensively molten and undergoes vigorous convection. Understanding the current state of Europa's interior is critical for assessing the potential for life. The current state of Europa's interior, though not accessible to our cameras or the limited geophysical observations of Galileo, may be probed by investigating its affect on the evolution of Europa's orbit. Tidal dissipation in a chewy Europa drives the evolution of its orbit more rapidly than the crunchy Europa would. The question can then be asked: if Europa is highly dissipative, what are the chances that we are observing it in its current orbital state? Europa's present large eccentricity may not survive very long if a chewy center is dissipating Io-like amounts of energy. If the lifetime of the current

eccentricity is found to be short (less than 105 years) then we may conclude that it is unlikely that we have stumbled upon Europa in a very special era of its history and that the interior is cold and crunchy: not the kind of place to look for life.
Author
Europa; Internal Energy; Space Exploration; Cores

20020002107 NASA Johnson Space Center, Houston, TX USA
Magnetofossils in Terrestrial Samples and Martian Meteorite ALH84001
ThomasKeptra, Kathie L., Lockheed Martin Corp., USA; Clemett, Simon J., Lockheed Martin Corp., USA; Bazylinski, Dennis A., Iowa State Univ. of Science and Technology, USA; Kirschvink, Joseph L., California Inst. of Tech., USA; General Meeting of the NASA Astrobiology Insititute; April 2001, pp. 164-166; In English; See also 20020002018; Original contains color illustrations; No Copyright; Avail: Issuing Activity; Abstract Only

Here we compare magnetite crystals produced by terrestrial magnetotactic bacteria strain MV-1 with a subpopulation of magnetites from ALH84001. We find both to be chemically and physically identical-specifically, both are single-domain, chemically pure, and exhibit an unusual crystal habit we describe as truncated hexa-octahedral. On Earth such truncated hexa-octahedral magnetites are only known to be produced by magnetotactic bacteria. We suggest that the observation of truncated hexa-octahedral magnetites in ALH84001 are both consistent with, and in the absence of terrestrial inorganic analogs, likely formed by biogenic processes. Additional information is contained in the original extended abstract.
Author
Crystals; Magnetite; SNC Meteorites

20020002108 NASA Johnson Space Center, Houston, TX USA
Astrobiology Investigations at a Martian Hematite Site
Allen, Carlton, C., NASA Johnson Space Center, USA; Westall, Frances, Lunar and Planetary Inst., USA; Schelble, Rachel T., New Mexico Univ., USA; General Meeting of the NASA Astrobiology Insititute; April 2001, pp. 167-169; In English; See also 20020002018; No Copyright; Avail: Issuing Activity; Abstract Only

Christensen et al, using data from the Mars Global Surveyor Thermal Emission Spectrometer (TES), have identified gray crystalline hematite in a 350 km by 750 km region near Sinus Meridiani. The deposit corresponds closely to the low-albedo highlands unit 'sm', mapped as a wind-eroded, ancient, subaqueous sedimentary deposit. Christensen et al interpreted the Sinus Meridiani deposit to be 'an in-place, rock-stratigraphic sedimentary unit characterized by smooth, friable layers composed primarily of basaltic sediments with approximately 10 to 15 % crystalline gray hematite.' Christensen et al discussed five possible mechanisms for the formation of this deposit: direct precipitation from standing, oxygenated, Fe-rich water; precipitation from Fe-rich hydrothermal fluids; low-temperature dissolution and precipitation through mobile groundwater leaching; surface weathering and coatings; thermal oxidation of magnetite-rich lavas. Four of these mechanisms involve the interactions of rock with water, and thus have implications in the search for evidence of microbial life.
Author
Exobiology; Hematite; Mars Surface

20020002109 Arizona State Univ., Dept. of Geological Sciences, Tempe, AZ USA
Confirmation of Spectrally Interpreted Mineralogy of Badwater Basin, Death Valley, CA: Applications to Identification of Evaporite Minerals on the Martian Surface
Baldridge, Alice M., Arizona State Univ., USA; Farmer, Jack D., Arizona State Univ., USA; Moersch, Jeffrey E., Tennessee Univ., USA; General Meeting of the NASA Astrobiology Insititute; April 2001, pp. 170-171; In English; See also 20020002018; No Copyright; Avail: Issuing Activity; Abstract Only

The exploration for past or present Martian life is a high priority goal of NASA's Mars Program. The present plan is to identify sites of ancient aqueous sedimentary environments on Mars by orbital reconnaissance, then conduct in situ robotic exploration at key sites (e.g. those that show evidence of past or present liquid water). Surface exploration will eventually lead to targeted selection and return of samples to Earth. Sites of particular importance for Astrobiology include sites of hydrothermal mineralization and evaporite deposition, among others. The Thermal Emission Spectrometer (TES), currently in orbit at Mars has so far only identified concentrations of specular hematite (an aqueous mineral) at a limited number of sites. This is perhaps not surprising, given the spatial resolution of TES (3km/pixel). This year the Mars Odyssey orbiter will deliver a much higher spatial resolution infrared instrument, the Thermal Emission Imaging Spectrometer (THEMIS), to Mars orbit which will map a substantial part of the Martian surface at a spatial resolution of 100m/pixel. This should greatly improve our ability to find aqueous minerals that may be present at abundances below the detection limits of TES. The Badwater Basin of Death Valley, CA provides an excellent analogue for evaporite basins that may have existed on Mars earlier in the planet's history. Moersch and Farmer

recently conducted a study of evaporite deposits in the Badwater Basin using MODIS/ASTER (MASTER) Airborne Simulator data. MASTER contains 50 channels (spectral bands), 10 of which fall within overlap the range of THEMIS. To simulate the data from TES and THEMIS, Death Valley MASTER data was de-resolved to match the respective spatial resolutions of those two instruments. The spectra were then cross-referenced to Arizona State University's TES library and analyzed for evaporite spectral signatures. At TES spatial resolution, ENVI (remote sensing analytical, software tool) identified only a few of the minerals detected at full resolution. However, when the data was de-resolved to simulate THEMIS resolution, evaporites were easily detected. to evaluate the validity of the spectral mapping by Moersch and Farmer, we have conducted detailed field and laboratory analyses of surface samples collected from 16 sites in the Badwater Basin during May and October 2000. Sites were selected to cover the range of spectral end-members identified by Moersch and Farmer. The surface morphology of each site was photo documented and surface samples collected, taking care to avoid mixing with subsurface materials. In the lab, samples were thin sectioned for petrographic analysis and analyzed by X-ray diffraction. In addition, thermal emission lab spectra were also acquired using a laboratory version of the TES instrument. Preliminary results show that the interpretation of spectral data in our study area can be confounded by a variety of factors, including overlaps of the spectral absorption features of different minerals. For example, areas interpreted spectrally to be sulfates have spectral features that overlap with clays. X-ray diffraction data and thin section analysis confirm that many of the samples indeed contain complex mixtures of evaporites and silicate minerals. In other cases, X-ray diffraction data confirms the presence of minerals identified spectrally, but those same minerals do not show up in laboratory spectra. Evaporite spectral signatures, especially those of chlorides, tend to be obscured by the silica and water present in playa minerals. to get an accurate picture of ground truth, thin sections will be analyzed to quantify the relative abundances of minerals in each sample. A spectral library of common evaporite minerals will also be compiled. When completed, MASTER and laboratory spectra will be re-analyzed to determine the precise resolution needed to for detect these minerals. Further sample analysis will be needed to confirm the prediction that THEMIS resolution (100 m/pixel) is sufficient to detect and identify evaporates from Mars orbit. In addition, we plan to incorporate near-IR spectral information for the Badwater Basin using Airborne Visible Infrared Imaging Spectrometer (AVIRIS) to simulate a hyperspectral near-IR spectrometer that is planned for the 2005 Mars orbiter. This will help us refine the analytical tools that will be used to detect minerals using data sets to be obtained by THEMIS.
Author
River Basins; Death Valley (CA); Mars Surface; Exobiology; Analogs; Spectrum Analysis; Sedimentary Rocks; Mineral Deposits

20020002110 Jet Propulsion Lab., California Inst. of Tech., Pasadena, CA USA
High Resolution Chemical Study of ALH84001
Conrad, Pamela G., Jet Propulsion Lab., California Inst. of Tech., USA; Douglas, Susanne, Jet Propulsion Lab., California Inst. of Tech., USA; Kuhlman, Kimberly R., Jet Propulsion Lab., California Inst. of Tech., USA; General Meeting of the NASA Astrobiology Insititute; April 2001, pp. 172; In English; See also 20020002018; No Copyright; Avail: Issuing Activity; Abstract Only

We have studied the chemistry of a sample of the SNC meteorite ALH84001 using an environmental scanning electron microscope (ESEM) with an energy dispersive chemical analytical detector and a focused ion beam secondary ion mass spectrometer (FIB-SIMS). Here we present the chemical data, both spectra and images, from two techniques that do not require sample preparation with a conductive coating, thus eliminating the possibility of preparation-induced textural artifacts. The FIB-SIMS instrument includes a column optimized for SEM with a quadrupole type mass spectrometer. Its spatial and spectral resolution are 20 nm and 0.4 AMU, respectively. The spatial resolution of the ESEM for chemical analysis is about 100 nm. Limits of detection for both instruments are mass dependent. Both the ESEM and the FIB-SIMS instrument revealed contrasting surficial features; crumbled, weathered appearance of the matrix in some regions as well as a rather ubiquitous presence of euhedral halite crystals, often associated with cracks or holes in the surface of the rock. Other halogen elements present in the vicinity of the NaCl crystals include K and Br. In this report, elemental inventories are shown as mass spectra and as X-ray maps.
Author
Chemical Analysis; SNC Meteorites; Halites; X Rays; Mass Spectra

20020002111 Jet Propulsion Lab., California Inst. of Tech., Pasadena, CA USA
Organization of P, S, and Fe Inclusions in a Freshwater Magnetococcus
Cox, Lea, Jet Propulsion Lab., California Inst. of Tech., USA; Popa Radu, Jet Propulsion Lab., California Inst. of Tech., USA; Douglas, Susanne, Jet Propulsion Lab., California Inst. of Tech., USA; Belz, Andrea, Jet Propulsion Lab., California Inst. of Tech., USA; Nealson, Kenneth H., Jet Propulsion Lab., California Inst. of Tech., USA; General Meeting of the NASA Astrobiology Insititute; April 2001, pp. 173-174; In English; See also 20020002018; No Copyright; Avail: Issuing Activity; Abstract Only

Magnetotactic bacteria are a heterogeneous group of motile, mainly aquatic procaryotes that align and swim along geomagnetic field lines. They are of interest to astrobiologists because of the magnetite crystals found in the Mars meteorite ALH84001 which share many characteristics with the magnetite produced intracellularly by magnetotactic bacteria. These bacteria are diverse morphologically, physiologically and phylogenetically, sharing a few key characteristics: 1) the presence of intracellular membrane-bound magnetic crystals (magnetosomes), usually but not always arranged in chains; 2) motility by means of flagella; and 3) microaerophillic or anaerobic physiology. The bilophotrichous (having two flagella bundles) magnetotactic cocci (MC) are ubiquitous in aquatic habitats but have proven extremely difficult to cultivate. Because only several marine strains have been isolated and grown in axenic culture, little is known about the physiology and the biogeochemical roles of the MC. We studied the composition and distribution of intracellular structures in an uncultured MC, designated ARB-1. to do this, a combination of light microscopy, environmental scanning electron microscopy (ESEM), transmission electron microscopy (TEM) and energy dispersive X-ray spectroscopy (EDS) were used. Cells of ARB-1 were separated from sediments collected from Baldwin Lake (Los Angeles Arboretum, Arcadia, CA). They are large spherical to oblate spheroidal Gram-negative cells, ranging from 1 to 4 micrometers along the maximum dimension, which is perpendicular to the direction of swimming. Cells have two large phosphorus-containing inclusions that comprise a large percentage of the cell volume. Many smaller sulfur inclusions are located at the convex end of the cell. Most of the cellular Fe is present in the magnetosomes. These may be arranged as a clump at the concave end of the cell, near the two flagella bundles, or as chains, or as both a clump and chains. The magnetosomes were identified as magnetite (Fe3O4) by selected area electron diffraction (SAED) and high resolution TEM. We saw a trend between cell size and organization of the magnetosomes. Smaller, more spherical cells were more likely to have chains than were larger, more oblate cells. This may indicate different populations of cells, or it may be attributed to variations in cell growth cycle. The size distribution (length) of magnetosomes in chains was similar to that of magnetosomes in clusters, except that there was a larger size range for clustered magnetosomes. Magnetosomes from ARB-1 cells average 82 nm in length. If plotted on a graph of length as a function of aspect ratio, they fall within the single domain region of the plot. If compared with the size distributions of magnetite from ALH84001 and magnetosomes from the cultured magnetotactic vibrio MV-1, the magnetites produced by ARB-1 cells are, on average, larger and have a wider range of aspect ratio. ARB-1 cells have a specific organization of the P, S, and Fe inclusions. The P inclusions always occupy the majority of the cell volume and separate the S inclusions from the disorganized clumps of magnetosomes and the flagella bundles. The P inclusions may contain polyphosphate, which could play several roles in motility, adaptation to stress, growth and division, buoyancy, and energy. The S inclusions might be a way to store S, a potential energy source, when the cells move from sulfide to oxygen zones. The consistency of P, S, and Fe organization in ARB-1 cells suggests that these inclusions have some specific and interactive functions.

Author

Bacteria; Magnetite; Sulfur; Phosphorus; Iron; Exobiology; Biogeochemistry; Fresh Water; Geomagnetism

20020002112 NASA Ames Research Center, Moffett Field, CA USA

Laboratory Studies of Hydrocarbon Nucleation on Tholin Particles and Thin Organic Films: Application to Titan's Atmosphere

Curtis, Daniel B., Colorado Univ., USA; Glandorf, David L., Colorado Univ., USA; Toon, Owen B., Colorado Univ., USA; Tolbert, Margaret A., Colorado Univ., USA; McKay, Christopher P., NASA Ames Research Center, USA; Khare, Bishun N., NASA Ames Research Center, USA; General Meeting of the NASA Astrobiology Insititute; April 2001, pp. 175; In English; See also 20020002018; No Copyright; Avail: Issuing Activity; Abstract Only

Titan, Saturn's largest satellite, has a thick nitrogen/methane atmosphere. In Titan's lower atmosphere, methane is saturated or supersaturated with respect to nucleation and may form clouds. to better characterize the properties of Titan's methane clouds we have measured the saturation ratio required to obtain butane nucleation, S (sub crit), on Titan tholin material and organic films. We find a critical saturation ratio for butane on tholin particles of S (sub crit) = 1.40, suggesting high supersaturations are required for nucleation. If methane is similar to butane, we expect high supersaturations of methane as well. This could favor the formation of a small number of large particles, consistent with recent measurements of methane rain on Titan.

Author

Titan; Satellite Atmospheres; Hydrocarbons; Nucleation; Thin Films

20020002113 Carnegie Institution of Washington, Geophysical Lab., Washington, DC USA

A New Molecular Recognition Instrument for Astrobiological Applications

Fogel, Marilyn L., Carnegie Institution of Washington, USA; Scott, James H., Carnegie Institution of Washington, USA; General Meeting of the NASA Astrobiology Insititute; April 2001, pp. 176-177; In English; See also 20020002018; No Copyright; Avail: Issuing Activity; Abstract Only

Protein Chip-based molecular recognition technology is being developed as a method for detecting life in environments here on Earth and on the surfaces of planets and other solar system bodies. The Ciphergen Biosystems ProteinChip Reader (PBSII) is dependent on the surface chemistry of small chips to selectively capture femtomole amounts of complex mixtures of organic molecules for molecular weight determination by time of flight mass spectrometry. The surfaced-enhanced chips spatially orient molecules that are bound to them, such that they are more efficiently uncoupled and ionized for mass spectral analysis. Nanograms of organic matter dissolved in 1-2 microliters of buffer solution are placed on the chip and allowed to interact and bind. by using different chips, experiments can be designed to recognize a complex combination of molecular markers by selecting a series of chip surface chemistries to pull apart complex mixtures. It is also possible to determine the chemical nature of molecules with unknown chemical composition or structure by combining molecular weight determination, chemical binding information, and further chemical testing on the surface of the chip. Additional information is contained in the original extended abstract.
Author
Exobiology; Mass Spectroscopy; Organic Materials; Chemical Composition; Proteins; Time of Flight Spectrometers

20020002114 European Space Agency. European Space Research and Technology Center, ESTEC, ESA Space Science Dept., Noordwijk, Netherlands
Astrobiology with ESA Science Missions
Foing, Bernard H., European Space Agency. European Space Research and Technology Center, ESTEC, Netherlands; General Meeting of the NASA Astrobiology Insititute; April 2001, pp. 178; In English; See also 20020002018; No Copyright; Avail: Issuing Activity; Abstract Only

Key questions of astrobiology can be addressed by several space missions from the ESA Science Horizons 2000 Programme, such as: (1) How do solar and stellar systems form? (with ISO, FIRST, SMART-1, Rosetta, Colombo, Gaia); (2) Geological evolution of terrestrial planets (with Living planet, Mars-express, SMART-1, Bepi-Colombo to Mercury); (3) Interstellar Complex organic chemistry (with ISO, ISS/EXPOSE, FIRST, Rosetta); (4) Co-evolution of Earth-Moon, impacts life frustration (with SMART-1, Bepi-Colombo); (5) How to detect other solar systems and habitable zones (with space photometry, COROT, Eddington, Gaia, Darwin); (6) Early Earth and alternative environments (Huygens/Cassini and Mars-express); (7) Signature of biosphere and photosynthesis evolution (living Planet missions, Darwin); (8) Water on Mars (with orbiter instruments on Mars Express); (9) Exobiology lander experiments (with Beagle-2 lander on Mars-Express); (10) Study of biomarkers and delivery of organics (with Mars-express and future missions). We shall review how the results from these ESA missions can be exploited in synergy to contribute to progress in astrobiology, and the perspectives for the next phases of solar system exploration, and life expansion beyond Earth.
Author
Exobiology; European Space Agency; Space Missions

20020002115 Los Alamos National Lab., Bioscience Div., NM USA
AFM and XPS Analysis of Fossilized Microorganisms
Forsythe, Jennifer, Los Alamos National Lab., USA; Fulghum, Julia, Kent State Univ., USA; Ferryman, Amy, Kent State Univ., USA; Maurice, Patricia, Notre Dame Univ., USA; Burde, Stefan, Bayer Pharmaceuticals, USA; Hersman, Larry, Los Alamos National Lab., USA; General Meeting of the NASA Astrobiology Insititute; April 2001, pp. 179-180; In English; See also 20020002018; No Copyright; Avail: Issuing Activity; Abstract Only

Identification of potential fossilized microorganisms from Mars will require an interdisciplinary approach combining a variety of methods. The hypothesis of our research is that x-ray photoelectron spectroscopy (XPS) and atomic force microscopy (AFM), used in combination, can increase significantly our ability to image and recognize microbial fossils, and in particular to understand the phylogeny and physiology of microorganisms of primitive environments. to this end, our primary objective is developing microfossil-specific applications of AFM and XPS. AFM is a nondestructive, high-resolution surface imaging technique that relies upon several surface/tip interactions (e.g., electrostatic, Pauli exclusion forces, Van der Waals interactions, frictional forces). Although AFM is most commonly used to map surface microtopography, advances in AFM technologies such as Phase Imaging, Force Modulation, and force-curve measurements using different tip materials, are allowing some degree of compositional sensitivity. XPS is a surface analysis technique with an analysis depth of approximately 10 nm. This technique involves bombarding a solid sample with x-rays and resulting in the emission of electrons (photoelectrons). The energy of the photoelectrons can be used to identify not only the elements present, but the chemical state of the elements. The particular XPS we are using is capable not only of point analysis, but of surface composition mapping. AFM and XPS have unique capabilities that compliment each other (resolution, surface sensitive, chemical signatures, etc.). Neither technology has been used previously in microfossil studies. Therefore, we are comparing XPS and AFM to more commonly used technologies (optical microscopy, scanning and transmission electron microscopy), using fossils of increasing age. A second objective is to gain greater

understanding of the fossilization process itself, with respect to the fossilization of individual cell components and macromolecules (membranes, DNA, ribosomes, etc.). We have chosen the cyanobacterium Calothrix as a model system. Additional information is contained in the original extended abstract.
Author
Fossils; Microorganisms; Atomic Force Microscopy; Photoelectron Spectroscopy; Mars (Planet); Exobiology; Spectrum Analysis

20020002116 Colorado Univ., Dept. of Geological Sciences, Boulder, CO USA
Mars Volatile and Climate History: Relevance to Life
Jakosky, Bruce M., Colorado Univ., USA; Phillips, Roger J., Washington Univ., USA; General Meeting of the NASA Astrobiology Insititute; April 2001, pp. 181-182; In English; See also 20020002018; No Copyright; Avail: Issuing Activity; Abstract Only

The possibility that life might exist at present or have existed in the past on Mars depends strongly on the abundance, distribution, and availability of water. In turn, the history and distribution of water is strongly coupled to the martian climate. These issues are inherently interdisciplinary, and couple measurements and processes related to the deep interior, the crust, the surface, the bulk atmosphere, the upper atmosphere, and interactions with the solar wind and escape to space. We have integrated observations from this wide variety of relevant disciplines that relate to martian climate and water, emphasizing recent Mars Global Surveyor and martian meteorite analyses, in order to construct a self-consistent view of the history of volatiles, climate, and water. While the result is not entirely unique, we are able to provide strong circumstantial evidence as to the nature of the martian environment through time. The major relevant observations are: (1) Nature of the early climate and connections to geology and geophysics; (2) Processes and timing in evolution of the atmosphere; (3) Geological evidence for crustal liquid water. Self-consistent scenarios for the history of martian climate and volatile abundance can be constructed from these observations: During some period of the Noachian the climate was sufficiently clement to allow significant fluvial erosion. This warm period, which terminated abruptly at the end of the Noachian, likely involved outgassing by volcanism associated with ancient highlands and Tharsis, subsequent turn-on of solar-wind stripping of atmosphere associated with the turn-off of the intrinsic magnetic field and ”erasure” of some local magnetic anomalies, and loss of volatiles to space by solar-wind stripping and by impact erosion. There is clear evidence that loss of the early atmosphere involved each of impact erosion, solar-wind stripping, and formation of subsurface carbonates, although the relative importance of these processes is not known. Additional information is contained in the original extended abstract.
Author
Mars (Planet); Exobiology; Mars Environment; Water; Planetary Evolution

20020002117 Carnegie Institution of Washington, Dept. of Terrestrial Magnetism, Washington, DC USA
Iron Isotope Measurements in Meteorites and Terrestrial Rocks
Kehm, Karl, Carnegie Institution of Washington, USA; O’DAlexander, Conel M., Carnegie Institution of Washington, USA; Hauri, Erik H., Carnegie Institution of Washington, USA; General Meeting of the NASA Astrobiology Insititute; April 2001, pp. 183-184; In English; See also 20020002018; No Copyright; Avail: Issuing Activity; Abstract Only

The geochemistry of iron is the subject of increasing interest within the astrobiology community because metabolic reactions in microorganisms may change the isotopic composition of iron to a greater extent than abiotic processes. If correct, iron isotopes provide a way to distinguish biological from abiological mass fractionation, potentially permitting identification of fossilized evidence of microbial activity in natural samples. to date, most iron isotope analyses have been performed on terrestrial rocks. Meteorites from asteroids provide a useful alternative setting in which to study abiological mass fractionation because they are devoid of biological processing. Variations in the isotopic composition of iron in meteorites can plausibly arise from the presence of unequilibrated presolar materials, temperature sensitive isotope exchange reactions, and kinetic processes. Such effects are interesting in their own right because they reflect physical and chemical conditions existing at the time the meteorite parent bodies formed. We have developed a technique for precisely measuring the isotopes of iron using multi-collector inductively coupled plasma mass spectrometry (ICP-MS). Our initial emphasis is on the analyses of meteoritic material where we hope to address a number of problems relating to the origin and evolution of planetary bodies as well as the geochemical behavior of iron itself. The analytical procedure includes acid dissolution of rock samples, followed by iron separation on an anion column. Purified samples are run on a multi-collector ICP-MS. The argon source plasma is operated at reduced power (so-called cold plasma mode) to eliminate ArN+ and ArO+, which otherwise would interfere with measurements of Fe-54 and Fe-56. Sample analyses are alternated with measurements of a pre-purified standard (Puratronic iron), dubbed ’P1’. Repeat analyses of isotopically spiked

standards suggest that the external reproducibility of the technique is comparable to the typical in-run precision. Additional information is contained in the original extended abstract.
Author
Iron Isotopes; Meteorites; Rocks; Meteoritic Composition; Exobiology

20020002118 Arizona State Univ., Dept. of Geological Sciences, Tempe, AZ USA
Isotopic Biosignature in Calcite Formed During Weathering of Basalt: Implications for Past Life on Mars, Early Life on Land, and ALH 84001
Knauth, L. Paul, Arizona State Univ., USA; General Meeting of the NASA Astrobiology Insititute; April 2001, pp. 185-186; In English; See also 20020002018; No Copyright; Avail: Issuing Activity; Abstract Only

Enormous variations in oxygen and carbon isotopes have been observed in carbonate developed as a weathering product (caliche) on less than 1 Ma basalts in 3 volcanic fields in Arizona. These variations are larger than those found in all terrestrial limestones and dolostones, everything taken together. Within each volcanic field, delta-O-18 is broadly co-variant with delta-C-13 and increases as delta-C-13 increases. In all cases, the most O-18 and C-13 enriched samples are for calcite developed on pinnacles, knobs, and flow lobes that protrude above tephra, rubble, and soil. These have apparently stood in the air since eruption and have never been exposed to the soil atmosphere environment. All of the O-18 and C-13 depleted samples are currently covered by soil or tephra and have been long exposed to soil atmospheres. Carbonate development is extensive for the covered samples and is sparsely developed on and within the subaerial samples. Calcite in isotopic equilibrium with Flagstaff meteoric waters has delta- O-18 values of +19% to +23%. The pedogenic, lower left end of the Flagstaff array is clearly soil calcite which formed in local meteoric waters and has low delta-C-13 characteristic of microbial soil CO2. Calcite at the upper right end of the Flagstaff array has clearly formed from O-18-rich evapoconcentrated meteoric waters that dried out on surfaces after local rains. The enormous C-13 enrichment is due either to removal of C-12 by photosynthesizers in the evaporating drops or to kinetic isotope effects associated with evaporation. The elongated data array is thus a mixing curve for calcite that forms in the atmosphere with that formed in soil rich in microbes. The same pattern is observed in the 2 other volcanic fields and is interpreted similarly. Individual vugs and amygdules filled with calcite display the same elongated data array on a smaller scale. Calcite thus initially forms with the isotopic signature of evaporation and is subsequently overlayered during burial by calcite carrying the isotopic signature of the soil environment. The enormous change in carbon isotope composition as calcite growth occurs is a unique signature of biology.
Author
Calcite; Basalt; Exobiology; Carbon Isotopes; Oxygen Isotopes; Weathering

20020002119 Arizona State Univ., Dept. of Geological Sciences, Tempe, AZ USA
Follow the Water, Beware the Brine: Astrobiological Implications of Aqueous Seeps on Mars
Knauth, L. Paul, Arizona State Univ., USA; Burt, Donald M., Arizona State Univ., USA; General Meeting of the NASA Astrobiology Insititute; April 2001, pp. 187-188; In English; See also 20020002018; No Copyright; Avail: Issuing Activity; Abstract Only

Photodissociation of water vapor in the upper atmosphere of Mars produces hydrogen that is able to escape from the planet much more easily than it does from the more massive Earth. Based on the high D/H ratio of water vapor in the current atmosphere, 50- 95% of the original martian hydrosphere was lost by this mechanism. Loss of water to space leaves the residual hydrosphere enriched in its dissolved constituents. The early martian hydrosphere therefore necessarily evolved into a NaCl brine. This brine became pore fluid in a megaregolith composed of high surface area particles (fractured and fragmented glasses, impact breccia, pyroclastic debris, ash sheets, melt sheets, and small rock fragments) of basaltic or komatiitic composition. Chemical interaction with these particles was inevitable and would have converted the NaCl brine into a concentrated Ca- Mg-Na-Cl brine with numerous other dissolved constituents. Mars subsequently froze, and the subsurface brines underwent eutectic freezing to produce a mixture of H2O ice, salts (mostly NaCl (center dot) 2H2O and CaCl (center dot) 6H2O), and highly concentrated brine. Such brines could still be seeping out of escarpments and readily account for the remarkable and otherwise perplexing outflow gullies. Eutectic brines therefore logically follow from current ideas regarding initial outgassing of volatiles, atmospheric water loss, and later freeze-down. If the scenario above is correct, past and any present surface and ground waters on Mars should have been primarily brines with concentrations greater than that of modern terrestrial sea water. During the ”warm, wet” early history of Mars, fresh water could have occurred locally as rain, runoff, and groundwater reservoirs. Such precipitation-derived water would have been very limited because erosional channels attributed to runoff (as opposed to catastrophic outflow) are not developed planet-wide. However, freeze-down of the planet should have generated widespread and extensive amounts of subsurface H2O ice cements as a consequence of eutectic freezing. Later melting of this ice by igneous activity could have produced liquid H2O in convecting cells and possible hydrothermal springs. On the other hand, such geothermal heating would also mobilize eutectic

brines and re-melt ice-brine-salt eutectic mixtures where they were still physically associated. Mixing of these diverse fluids during hydrothermal circulation combined with dissolution of megaregolith salts would probably prevent sustained hydrothermal reservoirs of dilute H2O for any significant length of time. In view of the above, we submit that ideas regarding the possible origin and early evolution of life on Mars must confront the issue of whether such life is enhanced or retarded by solutions with salinities greater than that of modern terrestrial sea water. Are there any halophilic bacteria deeply rooted in the rRNA tree? Is the formation of prebiotic molecules, membranes, and primitive cellular structures facilitated or inhibited by highly saline solutions? If salinity lower than that of modern terrestrial sea water is more optimal, where on Mars might such limited amounts of fluids have accumulated and become sequestered for early evolution of life? These question also apply to the origin and evolution of life on Earth or on any planetary object with similar initial Cl/H2O ratios. Additional information is contained in the original extended abstract.

Author

Exobiology; Brines; Water; Salinity; Mars (Planet); Mars Atmosphere

20020002120 Marburg Univ., Dept. of Nuclear Chemistry, Germany

Consequences and Artifacts: Terrestrial Findings and Martian Analogues of an Air-Water Interface

Lerman, Louis, Marburg Univ., Germany; General Meeting of the NASA Astrobiology Insititute; April 2001, pp. 189-190; In English; See also 20020002018; No Copyright; Avail: Issuing Activity; Abstract Only

Natural consequences of the terrestrial bubble-aerosol (bubblesol) cycle are objects with properties fascinatingly akin to those of ”nanobacteria”: in particular the basic morphology (spheres and sausages), gross chemistry (suites of organics along with metals), and size distributions (nanometers to microns). Whether of biological or bubblesol origin, these striking similarities reflect the universality of the chemical physics involved in the interactions of charge-polarized organic amphiphiles at an air-water interface. The contemporary terrestrial bubblesol cycle can include bubble formation, the adsorption of surface-active materials, bubble dissolution, and bubble bursting. The nonequilibrium energetics of bubble bursting is coupled to the formation of aerosols and their subsequent roles in atmospheric condensation. The bubblesol cycle provides an infrastructure for the concentration and transport of organic compounds, metal ions, and mineral catalysts through a rapid sequencing of hydration-dehydration reactions. Additionally the bubblesol cycle creates and seeds the principle nodes of heterogeneous organometallic chemistry in both the atmosphere and the ocean. On the contemporary Earth, in both particle number and total mass, bubble-generated aerosols and their atmospheric progeny are the largest transporters of organic matter between the atmosphere and ocean. Hence on an early Earth this geophysical-chemical cycle seems likely to have played a critical role in prebiotic chemical self-organization. More generally, whether we are considering Earth, Mars, Titan, or Europa...in the search for life and its origins the bubblesol cycle, its processes, and its resulting mass objects must be taken into account. With respect to current Mars mission planning: (1) The finding of bubblesol-generated objects (of Martian origin) in Martian meteorites or on Mars itself is prima facie evidence for the existence of a complex Martian hydrology cycle capable of gathering, concentrating, and transporting organics; (2) The presence of such bubblesol objects in (or from) an extraterrestrial location implies substantial environmental opportunities have existed for the support of prebiotic chemical evolution; (3) On a tectonically simple early Mars (with only intermittent surface liquid water), the bubblesol cycle may have been the only initiator and supporter of the rapid cycles of concentration, hydration, and dehydration necessary for organic polymerization in ”bulk” quantities; (4) Any life-searching Mars missions (or interpretations of Martian objects having come to Earth) must discriminate between the fossils of living systems at the nanobacterial scale and potential artifacts of the bubble-aerosol cycle necessarily created on any planet, planetoid, or satellite having both liquid water and amphiphiles; (5) Additionally, IF bacteria (with surface active membrane elements) have existed on Mars, and were coupled to a surface liquid water environment, then these same bubblesol processes could have been the principle mode of bacterial concentration and aerial transport. In analogy to current terrestrial processes the larger of these bubblesol-generated objects (in their hydrated state) could easily have transported such bacteria across a mostly arid planetary surface. This may have been critical for ”colonization”, and could also explain the deposition and subsequent fossilization of ”micro-clumps” of such bacteria in micro-environments much removed from their origin.

Author

Air Water Interactions; Bubbles; Aerosols; Evolution (Development); Exobiology; Mars (Planet); Mars Surface

20020002121 Arizona State Univ., Dept. of Geological Sciences, Tempe, AZ USA

Isotopic Analysis of High and Low Temperature Components of Tagish Lake: Anatomy of a New, Very Primitive Carbonaceous Chondrite

Leshin, Laurie A., Arizona State Univ., USA; Guan, Yunbin, Arizona State Univ., USA; Pizzarello, Sandra, Arizona State Univ., USA; Farquhar, James, California Univ., San Diego, USA; Jackson, Teresa L., California Univ., San Diego, USA; Thiemens, Mark H., California Univ., San Diego, USA; General Meeting of the NASA Astrobiology Insititute; April 2001, pp. 191-193; In English; See also 20020002018; No Copyright; Avail: Issuing Activity; Abstract Only

The Tagish Lake meteorite has properties intermediate between CI and CM meteorites, and may represent a new type of carbonaceous chondrite [1]. In order to explore its origin, history, and possible astrobiological relevance, we present oxygen isotope analyses of relatively high-temperature (olivine) and low-temperature (carbonate) components of Tagish Lake. Both conventional and ion microprobe oxygen isotope analyses are presented. About 600 mg of a ”degraded” Tagish Lake sample (i.e., a piece of a fragment collected after approximately 3 months on the frozen Tagish Lake bed;) was gently crushed and mixed. A 100 mg aliquot of this homogenized sample was disaggregated via ultrasonication, filtered, and transparent grains less than approximately 50 micrometers in size were hand-picked, mounted and polished with ion probe standards. We determined oxygen isotopic compositions of 5 forsterites, and 2 intermediate composition olivines using the Cameca IMS 6f ion microprobe at ASU. One of the forsterite grains has a thin (approximately 10 micrometers) rim of intermediate composition olivine. In this case, both core and rim were analyzed. Findings of this work can be summarized as follows: (1) Although the data are limited, Tagish Lake forsterites appear to be consistently more O-16-enriched (by a few %) than typical chondrule and isolated olivine from other carbonaceous chondrites. The comparison to CI and CM data is presented, but the observation holds for olivine from CV and CR chondrites as well; (2) although carbonate is more abundant in Tagish Lake than in CI and CM chondrites, the carbonates must be almost entirely less than approximately 50 micrometers in size, or they would have been found along with the olivine in the hand-picking of the sample. In this way, Tagish Lake more closely resembles CM than CI chondrites. (3) The Delta-O-17 values for Tagish Lake carbonates are significantly higher than O-18 values are higher than all but a few CM analyses. The delta-O-17 values are the highest ever measured in chondrite carbonate; (4) Because the carbonate delta-O-17 tracks that of the altering water, the data require that the water that interacted with Tagish Lake had a delta-O-17 value of at least + 1.9%. This value is lower than (and therefore consistent with) the ”High Water” value proposed in the two-reservoir (static) water-rock interaction model of Clayton and Mayeda, but higher than the ”Low Water” value from a previous model and the altering water composition discussed by Young et al. in their flow model; (5) Within the context of the two-component interaction model, the higher delta-O-17 of both the whole rock and carbonate in Tagish Lake compared to CM chondrite compositions is consistent with higher water:rock ratios in the Tagish Lake alteration relative to the alteration of CM chondrites. In summary, although Tagish Lake shows some isotopic similarities to both CI and CM meteorites, it is not clearly affiliated with either group. This may support the idea that Tagish Lake represents a new, unique C2 chondrite. Additional information is contained in the original extended abstract.
Author

Carbonaceous Chondrites; Oxygen Isotopes; Meteoritic Composition; Olivine; Carbonates; Exobiology

20020002122 NASA Johnson Space Center, Houston, TX USA

Abiotic Versus Biotic Weathering of Olivine As Possible Biosignatures

Longazo, Teresa G., Hernandez Engineering, Inc., USA; Wentworth, Susan J., Lockheed Martin Space Operations, USA; Clemett, Simon J., Lockheed Martin Space Operations, USA; Southam, Gordon, University of Northern Arizona, USA; McKay, David S., NASA Johnson Space Center, USA; General Meeting of the NASA Astrobiology Insititute; April 2001, pp. 194-196; In English; See also 20020002018; No Copyright; Avail: Issuing Activity; Abstract Only

We are investigating the weathering of silicate minerals by both purely inorganic, and biologically mediated processes using field-emission scanning electron microscopy (FESEM) and energy dispersive x-ray spectroscopy (EDS). By resolving surface textures and chemical compositions of weathered surfaces at the sub-micron scale we hope to be able to distinguish abiotic from biotic weathering processes and so establish a new biosignature applicable to the study of astromaterials including but not limited to the Martian meteorites. Sterilized olivine grains (San Carlos, Arizona) no more than 1-2 mm in their longest dimension were optically assayed to be uniform in color and free of inclusions were selected as weathering subjects. Prior to all experiments surface morphologies and Fe/Mg ratios were determined for each grain using FE-SEM and EDS. Experiments were divided into two categories abiotic and biotic and were compared with ”naturally” weathered samples. For the preliminary experiments, two trials (open and closed to the ambient laboratory environment) were performed under abiotic conditions, and three trials under biotic conditions (control, day 1 and day 2). The open system abiotic trials used sterile grains heated at 98 C and 200 C for both 24 and 48 hours in 1L double distilled de-ionized water. The closed system abiotic trials were conducted under the same conditions but in a sealed two layer steel/Teflon ”bomb” apparatus. The biotic trials used sterile grains mounted in a flow-through device attached to a wellhead on the Columbia River aquifer. Several discolored, altered, grains were selected to document ”natural” weathering

surface textures for comparison with the experimental samples. Preliminary results indicate there are qualitative differences in weathered surface textures among all the designed experiments. The olivine grains in abiotic trials displayed etching, pitting, denticulate margins, dissolution and clay formation. The scale of the features ranged from tens to a few microns with textures that remained relatively sharp and were crystallographically controlled. These results were comparable to that observed in the ”naturally” weathered comparison/reference grains. Chemical analysis by EDS indicates these textures correlated with the relative loss of Mg and Fe cations by diffusional processes. In contrast the biotic results indicated changes in the etching patterns on the scale of hundreds of nm, which are neither sharp nor crystallographically controlled (nanoetching). Organisms, organic debris and/or extracellular polymeric substances (biofilm) were often in close proximity or direct contact with the nanoetching. While there are many poorly constrained variables in natural weathering experiments to contend with, such as the time scale, the chemistry of the fluids and degree of biologic participation, some preliminary observations can be made: (1) certain distinct surface textures appear correlated with the specific processes giving rise to these textures; (2) the process of diffusing cations can produce many similar styles of surface textural changes; and (3) the main difference between abiotic and biotically produced weathering is the scale (microns versus nanometers) and the style (crystallographically versus noncrystallographically controlled) of the textural features. Further investigation into nanosize scale surface textures should attempt to quantify both textures and chemical changes of the role of microorganisms in the weathering of silicates. Additional experiments addressing nanoscale textures of shock features for comparison with the current data set.
Author
Weathering; Olivine; Textures; Chemical Composition; Exobiology

20020002123 Jet Propulsion Lab., California Inst. of Tech., Pasadena, CA USA
Thermal Desorption/GCMS Analysis of Astrobiologically Relevant Organic Materials
McDonald, Gene D., Jet Propulsion Lab., California Inst. of Tech., USA; General Meeting of the NASA Astrobiology Insititute; April 2001, pp. 197; In English; See also 20020002018; No Copyright; Avail: Issuing Activity; Abstract Only

Several macromolecular organic materials, both biologically-derived (type II kerogen and humic acid) and abiotic in origin (Murchison insoluble organic material, cyanide polymer, and Titan tholin) were subjected to thermal desorption using a Chromatoprobe attachment on a Varian Saturn 2000 GCMS system. Each sample was heated sequentially at 100, 200, and 300 C to release volatile components. The evolved compounds were then separated on a Supelco EC-1 dimethylsilica GC column and detected by the Saturn 2000 ion trap mass spectrometer. The various types of macromolecular organic material subjected to thermal desorption produced distinctly different GCMS chromatograms at each temperature, containing fractions of both low and high chromatographic mobility. The relative amounts of detectable volatiles released at each temperature also differed, with type II kerogen and cyanide polymer containing the highest percentage of low-temperature components. In all the samples, the highest yield of released compounds occurred at 300 C. Only cyanide polymer evolved a homologous hydrocarbon series, suggesting that it is the only material among those examined that contains a truly polymeric structure. Pyrolysis/gas chromatography/mass spectrometry has been used extensively for analysis of terrestrial organic macromolecular materials, and was also part of the instrument package on the Viking landers. Thorough analysis by pyrolysis usually employs temperatures of 500 C or higher, which for in situ analyses can be problematic given spacecraft power and materials constraints. This study demonstrates that heating of organic materials of astrobiological relevance to temperatures as low as 200-300 C for short periods releases volatile components that can be analyzed by gas chromatography and mass spectrometry. Even in the absence of full pyrolysis, useful chemical information on samples can be obtained, and materials from different biological and abiological sources can be distinguished. The research described in this paper was carried out at the Jet Propulsion Laboratory, California Institute of Technology, under a contract with the National Aeronautics and Space Administration.
Author
Organic Materials; Exobiology; Thermal Analysis; Desorption; Temperature Dependence

20020002124 NASA Johnson Space Center, Houston, TX USA
Possible Biologic Features in Martian Meteorite Nakhla
McKay, David S., NASA Johnson Space Center, USA; Wentworth, Sue, NASA Johnson Space Center, USA; Gibson, Everett, NASA Johnson Space Center, USA; Thomas-Keprta, Kathie, NASA Johnson Space Center, USA; General Meeting of the NASA Astrobiology Insititute; April 2001, pp. 198-200; In English; See also 20020002018; Original contains color illustrations; No Copyright; Avail: Issuing Activity; Abstract Only

We have been studying the martian meteorite, Nakhla. This meteorite was an observed fall in June, 1911 near the village of El Nakhla, Egypt, and was collected soon thereafter. We have been studying subsamples from a British Museum specimen that had a nearly complete fusion crust before it was broken up recently in a clean bench at Johnson Space Center for allocation. We have surveyed some of these chips with Field- Emission Scanning Electron Microscope (FESEM) and petrographic microscopy.

Nakhla is an igneous rock, a clinopyroxenite containing augite, olivine, and a mesotasis with feldspar, phosphates, magnetite, and other minerals. The rock also contains secondary minerals and phases, including carbonates, iron oxides, clay minerals, sulfates, chlorides, and amorphous or glassy material, which fill cracks and cavities and also appear to replace parts of the mesotasis. Textural evidence is presented in these papers supporting the hypothesis that most, if not all of these secondary minerals were formed on Mars. Nakhla also contains significant organic material which C-14 analysis indicates is at least 80% indigenous. In some of the cracks filled with secondary minerals, small (approximately 0.5 micrometers) specks are visible in optical microscope images. These specks are patchy in distribution, have a narrow size distribution, and are usually associated with carbonate, clay, or silica crack fillings. We propose that these specks may be fossilized bacteria from Mars. Lacking definitive evidence that they are truly fossilized bacteria, we term them bacteriamorphs. SEM examination of a number of small chips of Nakhla from both samples near the fusion crust and samples in the interior reveals a set of features which are the same size and shape as those observed in the petrographic microscope. These bacteriamorphs are of several types. Subspherical or coccoid forms are the most common, but elongated or rod-shaped bacteriamorphs are also present. Preliminary compositional data from energy dispersive x-ray analysis suggests that some of these features are richer in Fe and O compared to the surrounding matrix. In addition, some of the patchy material may be fossilized polymeric material originally generated by the bacteria. EDX analyses indicate it is considerably enriched in Si compared to the matrix, and could conceivably be SiO2. Many of the forms are partly embedded in a matrix, and some are mostly covered. The chips contain a number of small features which resemble fossilized bacteria from terrestrial samples. The morphologies of most of the biomorphic features in Nakhla are similar to known fossilized bacteria and associated features formed in Columbia River Basalt, using microbe-bearing water from subsurface aquifers. Additional work is underway to examine the Nakhla bacteriamorph features in the transmission electron microscope (TEM). These features could alternatively be mineral precipitates produced by inorganic processes. Close comparison of these features with known fossilized bacteria using both SEM and TEM will help determine whether these features are bacteria or inorganic precipitates. Search for chemical biomarkers such as hopanes or lipids is another approach. Even if shown that the Nakhla features are derived from bacteria, they could be formed from bacteria which entered the meteorite during its stay on Earth. While these features are apparently sandwiched between and wrapped in secondary minerals thought to have formed on Mars, detailed isotopic analysis is necessary to positively determine whether the bacteriamorphs and their associated features originated on Mars. Clearly more detailed work is necessary, but the possibility that these features are actually martian bacteria is clearly exciting. Additional information is contained in the original extended abstract.

Author

SNC Meteorites; Exobiology; Bacteria; Fossils; Meteoritic Composition

20020002125 Arizona State Univ., Dept. of Geological Sciences, Tempe, AZ USA

Volcano-Ice Interactions and the Exploration for Extant Martian Life

Payne, Meredith C., Arizona State Univ., USA; Farmer, Jack D., Arizona State Univ., USA; General Meeting of the NASA Astrobiology Insititute; April 2001, pp. 201-203; In English; See also 20020002018; No Copyright; Avail: Issuing Activity; Abstract Only

Recent discoveries have revealed terrestrial colonies of microbes both in 349 K geothermal groundwater located at a depth of 2800 m, beneath glaciers in the Canadian Arctic and subglacial lakes in Antarctica at a depth greater than 3 km. The existence of extremophiles in these subsurface environments has opened up important new directions in the exploration for Martian life. In keeping with NASA's programmatic initiative to "follow the water", exploration for extant life has been focused on the search for zones of subsurface water. to further explore glacial and periglacial environments of Mars for sites of recent hydrothermal activity, we conducted a survey of Viking orbiter images for the region north of 70 deg N. This poster reports preliminary results from that search. Further analysis of recently released Mars Orbiter Camera (MOC) images for several promising sites provided evidence for localized volcano-ice interactions along the margin of the North Polar cap. A detailed morphological comparison of these features with terrestrial analogs is presently underway. Additional information is contained in the original extended abstract.

Author

Volcanoes; Ice; Mars (Planet); Exobiology; Mars Photographs; Microorganisms; Geothermal Resources

20020002126 Arizona State Univ., Dept. of Chemistry and Biochemistry, Tempe, AZ USA

The Organic Content of the Tagish Lake Meteorite

Pizzarello, S., Arizona State Univ., USA; Huang, Y., Brown Univ., USA; Nieman, R. A., Arizona State Univ., USA; Williams, M. D., Arizona State Univ., USA; General Meeting of the NASA Astrobiology Insititute; April 2001, pp. 204; In English; See also 20020002018; No Copyright; Avail: Issuing Activity; Abstract Only

Carbonaceous chondrites offer a unique record of chemical evolution, the product of presolar and planetary abiotic processes. The Tagish Lake meteorite fell into an icy lake in the Yukon Territory in January 2000 and has an unusual post-impact history in that portions of it were recovered within hours of infall and immediately frozen. With such a collection history, samples from the meteorite may be the most pristine materials of their kind. The organic content of the meteorite has been investigated, and both its insoluble material and extractable compounds were analyzed. C-13 NMR spectroscopy shows that the Tagish Lake macromolecular material is dominated by aromatic features and differs from those isolated from both CM (Murchison) and CI (Orgueil) chondrites. Water soluble organics (as amines, carboxylic acids, amino- and hydroxy acids) are present in this meteorite in far lower abundance then in most carbonaceous meteorites studied so far. The only exception, so far, is presented by the suite of dicarboxylic acids, which is quantitatively, if not qualitatively, comparable to those of CM and CI chondrites. Solvent extracts also revealed an unique content dominated by straight chain hydrocarbons and a distinct isotopic composition. Although studies are still in progress, the results of these analyses show the Tagish Lake meteorite has an unusual and surprising organic content, with a distribution that only in part resembles that of CI and CM carbonaceous chondrites.
Author
Carbonaceous Chondrites; Chemical Evolution; Organic Materials; Meteoritic Composition; Exobiology

20020002127 Florida Univ., Dept. of Chemistry, Gainesville, FL USA
Detecting Organic Molecules on Mars
Ricardo, Alonso, Florida Univ., USA; Benner, Steven A., Florida Univ., USA; General Meeting of the NASA Astrobiology Insititute; April 2001, pp. 205; In English; See also 20020002018; No Copyright; Avail: Issuing Activity; Abstract Only

We recently pointed out that substantial amounts of benzenecarboxylic acids should be present on the accessible surface of Mars. This hypothesis was based on an analysis of the intrinsic chemical reactivity of organic molecules that would be delivered to the surface of Mars via meteor. These compounds would not have been detected by the Viking 1976 experiments. Further, if the hypothesis is true, it would greatly alter our view of the ”oxidizing” nature of the Martian surface. If these organic compounds are present in abundance, they would serve as a resource on Mars, including as a resource for human habitation. Almost immediately after the proposal was made, Luanne Becker and her collaborators noted a peak at 288 mass units in the mass spectrum of SNC meteorite. This would correspond to the anhydride of benzenehexacarboxylic acid, predicted to be the principal organic molecule on the surface of Mars. We have developed a novel approach that converts benzenecarboxylic acids to fluorescent compounds suitable for detection at very low concentrations. This approach is suitable for both Earth-bound research on SNC meteorites (and, in the future, on samples returned from Mars via human effort), and for in situ studies on Mars using the Martian lander.
Author
Detection; Organic Compounds; Mars (Planet); Mars Surface; Fluorescence

20020002128 NASA Johnson Space Center, Houston, TX USA
Biotechnology Approaches to Life Detection
Steele, Andrew, NASA Johnson Space Center, USA; McKay, David, NASA Johnson Space Center, USA; Schweitzer, Mary, Montana State Univ., USA; General Meeting of the NASA Astrobiology Insititute; April 2001, pp. 206-208; In English; See also 20020002018; No Copyright; Avail: Issuing Activity; Abstract Only

The direct detection of organic biomarkers for living or fossil microbes on Mars by an in situ instrument is a worthy goal for future lander missions. Several new and innovative biotechnology approaches are being explored. Firstly we have proposed an instrument based on immunological reactions to specific antibodies to cause activation of fluorescent stains. Antibodies are raised or acquired to a variety of general and specific substances that might be in Mars soil. These antibodies are then combined with various fluorescent stains and applied to micron sized numbered spots on a small (2-3 cm) test plate where they become firmly attached after freeze drying. Using technology that has been developed for gene mining in DNA technology up to 10,000 tests per square inch can now be applied to a test plate. On Mars or the planet/moon of interest, a sample of soil from a trench or drill core is extracted with water and/or an organic solvent and ultrasonication and then applied to the test plate. Any substance, which has an antibody on the test plate, will react with its antibody and activate its fluorescent stain. At the moment a small UV light source will illuminate the test plate, which is observed with a small CCD camera, although other detection systems will be applied. The numbered spots that fluoresce indicate the presence of the tested-for substance, and the intensity indicates relative amounts. Furthermore with up to a thousand test plates available false positives and several variations of antibody can also be screened for. The entire instrument can be quite small and light, on the order of 10 cm in each dimension. A possible choice for light source may be small UV lasers at several wavelengths. Some of the wells or spots can contain simply standard fluorescent stains used to detect live cells, dead cells, DNA, etc. The stains in these spots may be directly activated, with no antibodies being necessary. The proposed system will look for three classes of biomarkers: those from extant life, such as DNA, those from extinct life such

as hopanes, and those from organic compounds not necessarily associated with life such as PAHs, rocket exhaust contamination and other a/pre-biotic chemicals. Both monoclonal and polyclonal antibodies can be used. Monoclonal antibodies react with a very specific compound, but polyclonal antibodies may react to any of a whole family of compounds. Furthermore the technique of phage display to raise antibodies against classically non-antigenic molecules is also being considered. Additional information is contained in the original extended abstract.
Author
Biotechnology; Detection; Exobiology; Antibodies; Fluorescence; Microorganisms

20020002129 Jet Propulsion Lab., California Inst. of Tech., Pasadena, CA USA
Application of Computer Tomography for Life Detection
Tsapin, A., Jet Propulsion Lab., California Inst. of Tech., USA; Nealson, K., Jet Propulsion Lab., California Inst. of Tech., USA; General Meeting of the NASA Astrobiology Insititute; April 2001, pp. 209; In English; See also 20020002018; No Copyright; Avail: Issuing Activity; Abstract Only

Perhaps one of the most fundamentally difficult challenges facing those who would search for life is that of scale determination. Spatial scales of life on Earth range over more than 15 orders of magnitude in mass and volume, and more than 8 orders of magnitude in 2 dimensional space. If the distribution of life is sparse in comparison to the background on which it is found, then the choice of the right scale is critical to finding that life. But how does one identify the proper scale? to put this in other words, how does one recognize the ”haystacks” in which the needles (biosignatures and evidence of life) might be most profitably searched for? The problem is further exacerbated when conditions get extreme because much of the life moves from the clement surface environment into the pores and more clement environments inside of rocks, minerals and soils. Once encased in their lithic homes, these microbes become nearly impossible to study by standard techniques because of the opacity of the rocks. It is this problem that we propose to address in the work proposed here. Computer Tomography (CT) has been a very valuable tool in medicine, where the best resolution available has typically been of the order of about 0.5 mm. However, to adapt the approach for life detection of microbial endoliths, the resolution needs to be moved to the micrometer and even submicrometer levels. Thus for the studies proposed here, we begin with a commercially available instrument that can yield resolution of approximately 10 micrometers. The rational for this is twofold: first, this is the ”state of the art” in laboratory instruments; and second, that while the usual size of a microbial cell is about 1 micron, microorganisms tend to live in communities that usually exceed the 10 micrometer size range. The resolution also depends on the sample size itself, so having a small lab instrument into which small samples can be placed will be beneficial to the resolution. We have now used several different CT systems, beginning with the medical scanners (Arcadia CT group) for the detection of layered communities in sandstone rocks from Antarctica. Even this crude instrument was able to point to the areas of the rock that were dominated by microbial populations - this provides the critical first information that says, ”Go back and look at these sites with other methods.” We showed that without sample preparation or destruction it was possible to gain knowledge as to the presence of density differences suggestive of life.
Author
Computer Aided Tomography; Exobiology; Microorganisms

20020002130 Lunar and Planetary Inst., Houston, TX USA
Dry Mars: Parched Rocks and Fallen Dust
Treiman, Allan H., Lunar and Planetary Inst., USA; General Meeting of the NASA Astrobiology Insititute; April 2001, pp. 210-211; In English; See also 20020002018
Contract(s)/Grant(s): NAG5-8270; No Copyright; Avail: Issuing Activity; Abstract Only

While ”following the water” to find life on Mars, it is easy to overlook evidence that Mars is harshly dry, and to neglect ideas that do not invoke water. Direct evidence for a dry Mars comes from the ALH 84001 meteorite, which has seen little or no liquid water during its last 3.9 billion years on Mars. Its aridity is difficult to reconcile with a Mars of abundant near-surface surface water or with episodes of warm wet climate. Alternative scenarios are also possible, even likely, for the martian gullies and debris flows that have been cited as evidence of liquid water. It is reasonable that the gullies flows are the remnants of massive dust avalanches, comparable to large climax snow avalanches seen on Earth. Mars’ surface is now desiccated, and at least part of it has been equally desiccated for the past 3.9 billion years. With this background, and the wealth of atmospheric, imaging, and chemical data available from Mars, one must be very cautious in evaluating claims for liquid water recently at or near Mars’ surface. Additional information is contained in the original extended abstract.
Author
Mars (Planet); SNC Meteorites; Water; Extraterrestrial Life

20020002131 University of South Florida, Dept. of Geology, Tampa, FL USA

Concomitant Microbial Carbonate Precipitation and Maskelynite Alteration by Archaeoglobus fulgidus

VanCleave, K. A., University of South Florida, USA; Robbins, L. L., Geological Survey, USA; General Meeting of the NASA Astrobiology Insititute; April 2001, pp. 212-213; In English; See also 20020002018; Original contains color illustrations; No Copyright; Avail: Issuing Activity; Abstract Only

It has been suggested that carbonates in ALH 84001 may have formed approximately 3.95 Ga. The proposed age of the carbonates corresponds to the time period in which microorganisms first appeared and developed on the Earth and conditions on Mars were characterized by abundant water and warm temperatures. delta-O-18 isotope values indicate that some of the carbonates in ALH 84001 may have formed at temperatures between 70 and 90 C. Textural observations imply that carbonates in ALH 84001 selectively replaced maskelynite during their formation. These carbonates appear to have an intimate association with maskelynite that is distinct from carbonates associated with orthopyroxene (opx). We attempted to produce alteration features in opx and maskelynite chips and concomitant carbonate precipitation using the microbe Archaeoglobus fulgidus, an archaeon species of ancient origin. Archaeons are believed to be the first types of living organisms to have appeared on the Earth. A. fulgidus is a hyperthermophillic, chemolithoheterotrophic archaeon that gains energy through dissimilatory sulfate-reduction and the complete oxidation of lactate to CO2. This vent-dwelling, obligate anaerobe grows at an optimum temperature of 83 C, indicating that it could have potentially thrived under the thermal regime of early Mars. Two 50 mg chips of maskelynite obtained from the Manicouagan impact crater (Quebec, Canada) and two 50 mg chips of opx obtained from the Frank ultramafic body (Avery County, NC) were placed in sealed serum bottles containing 50 ml of microbial media (6.5 pH) highly concentrated in Mg2+ and Ca2+ ions. Bottles were gassed to 2 bars overpressure with a mixture of 20% CO2 and 80% N2 in order to create an anaerobic environment. Fifty mL of an A. fulgidus culture with a cell concentration of 8.7 x 10(exp 7) cells/mL were added to two bottles and centrifuged. The supernatant was discarded from the bottles and the remaining microbial pellets were re-suspended in the microbial media present in two of the serum bottles, one containing opx and one containing maskelynite. The two remaining bottles served as sterile controls. All four bottles were incubated at 83 C for a period of 4 days. Approximately 1 mL of solution was then extracted from each bottle, stained with sybergold and then used to make wet-mount slides, which were analyzed by light microscopy and epiflourescent microscopy. An additional 5 mL of solution were extracted from each bottle and filtered using a 0.022 micrometer filter. The filters were sputter-coated with carbon and the maskelynite and opx chips from each bottle were sputter-coated with gold. The filters were analyzed using energy dispersive X-ray (EDX) and the maskelynite and opx pieces were photographed using a Hitachi S-3500N scanning electron microscope (SEM). Carbonate minerals with ovoid and globular morphologies similar to carbonates associated with maskelynite in ALH 84001 were present on wet mount slides made from bottles containing A. fulgidus cells. Cells were located within the interiors of the carbonate minerals. SEM photographs of the maskelynite exposed to A. fulgidus cells show extensive rounded and pitted dissolution features, carbonates with ovoid morphologies extending out from these alteration features and clumps of A. fulgidus encased in biofilm covered with precipitated carbonate. None of these features were present in the control samples. EDX data on these minerals indicated the presence of Ca, Mg and SR. In contrast to the maskelynite samples, opx chips showed no evidence of microbial alteration with simultaneous carbonate precipitation.

Author

Carbonates; Biological Evolution; Exobiology; Microorganisms; SNC Meteorites; Mars (Planet)

20020002132 NASA Johnson Space Center, Houston, TX USA

Visualization of Microbial Biomarkers by Scanning Electron Microscopy

Wainwright, Norman R., Marine Biological Lab., USA; Allen, Carlton C., NASA Johnson Space Center, USA; Child, Alice, Marine Biological Lab., USA; General Meeting of the NASA Astrobiology Insititute; April 2001, pp. 214; In English; See also 20020002018; No Copyright; Avail: Issuing Activity; Abstract Only

We are developing tools to link the biochemical structure of selected biomarkers with putative biogenic structures observed in mineralized samples. The detection of evidence of life on Mars and other planets will rely on methods that can discriminate compounds formed exclusively by living organisms. While biogenic compounds, such as amino acids and nucleotides have been discovered in extraterrestrial sources, such as meteorites and comets, their formation can be explained by abiotic means. The formation of cellular structures, or more elaborate organic molecules, such as complex lipids, proteins or nucleic acids, however, is strongly correlated to the presence of even the most primitive life processes. Recent evidence lends support to the hypothesis that life may have once existed on Mars. Carbonate globules and ppm concentrations of polycyclic aromatic hydrocarbons (PAHs) have been described in ALH84001, a meteorite originating from Mars ejecta captured by Earth over 13,000 years ago. The localized high concentration of PAHs that follow an increasing gradient from the intact fusion crust towards the interior corresponds to microgram quantities of hydrocarbon. Even though ALH84001 and other similar meteorites have withstood the forces capable of ejecting rock through Mars' escape velocity, upon entering Earth's atmosphere, their core temperatures are likely

not to have been raised significantly, as evidenced by the survival of remanent magnetic signatures. Ideal biomarkers of ancient or modern biological life would include molecules that are (or were) pervasive and highly resistant to degradation. Also, requisite methods of detection should be simple, extremely sensitive and broadly inclusive (NASA SP-530). Lipopolysaccharide (LPS), peptidoglycan or pseudopeptidoglycan and beta-glucan are microbial cell wall components which together cover the entire microbial spectrum of eubacteria, archea and fungi. They are all remarkably resistant to thermal degradation. Fortunately, many antimicrobial defense systems of higher organisms require sensitive detection to combat microbial pathogens. We employ here the primitive immune system of the evolutionarily ancient horseshoe crab, Limulus polyphemus. This species relies on multi-enzyme signal amplification detection of cell wall molecules and they can be applied to the development of useful detectors of life. An extension of this work includes the visualization of microbial signatures by labeling LAL components with chromogenic or electron dense markers. The protein Limulus Anti-LPS Factor (LALF) has an extremely high affinity for LPS. by coupling LALF binding with colloidal gold labels we demonstrate a correlation of the structures visible by electron microscopy with biochemical evidence of microbial cell wall materials. Pure silica particles were mixed with cultures of E. coli (10(exp 6) cfu/mL). Samples were washed sequentially with buffered saline, LALF, antibody to LALF and finally colloidal gold-labeled Protein A. Negative controls were not exposed to E. coli but received identical treatment otherwise. Samples were coated with carbon and imaged on a JEOL JSM-840 scanning electron microscope with LaB6 source in the back scatter mode with the JEOL annular back scatter detector. 20 nm-scale black spots in this contrast-reversed image originate from electrons back-scattered by gold atoms. Negative controls did not give any signal. Future work will expand application of this technique to soil simulants and mineralized rock samples.

Author

Scanning Electron Microscopy; Exobiology; Biochemistry; Biological Evolution; Cells (Biology); Extraterrestrial Life

20020002133 NASA Johnson Space Center, Houston, TX USA

SNC Meteorites, Organic Matter and a New Look at Viking

Warmflash, David M., NASA Johnson Space Center, USA; Clemett, Simon J., Lockheed Martin Space Operations, USA; McKay, David S., NASA Johnson Space Center, USA; General Meeting of the NASA Astrobiology Insititute; April 2001, pp. 216-218; In English; See also 20020002018; No Copyright; Avail: Issuing Activity; Abstract Only

Recently, evidence has begun to grow supporting the possibility that the Viking GC-MS would not have detected certain carboxylate salts that could have been present as metastable oxidation products of high molecular weight organic species. Additionally, despite the instrument's high sensitivity, the possibility had remained that very low levels of organic matter, below the instrument's detection limit, could have been present. In fact, a recent study indicates that the degradation products of several million microorganisms per gram of soil on Mars would not have been detected by the Viking GC-MS. Since the strength of the GC-MS findings was considered enough to dismiss the biology packet, particularly the LR results, any subsequent evidence suggesting that organic molecules may in fact be present on the Martian surface necessitates a re-evaluation of the Viking LR data. In addition to an advanced mass spectrometer to look for isotopic signatures of biogenic processes, future lander missions will include the ability to detect methane produced by methanogenic bacteria, as well as techniques based on biotechnology. Meanwhile, the identification of Mars samples already present on Earth in the form of the SNC meteorites has provided us with the ability to study samples of the Martian upper crust a decade or more in advance of any planned sample return missions. While contamination issues are of serious concern, the presence of indigenous organic matter in the form of polycyclic aromatic hydrocarbons has been detected in the Martian meteorites ALH84001 and Nakhla, while there is circumstantial evidence for carbonaceous material in Chassigny. The radiochronological ages of these meteorites are 4.5 Ga, 1.3 Ga, and 165 Ma respectively representing a span of time in Earth history from the earliest single-celled organisms to the present day. Given this perspective on organic material, a biological interpretation to the Viking LR results can no longer be ruled out. In the LR experiment, a solution containing C-14 labeled organic compounds was injected into soil samples. The detection of radioactivity in the overhead space would indicate that one or more of the substrates had been chemically converted into a carbon-containing gas. to serve as a control, some samples were heated enough to destroy most known terrestrial microbes so that an indication for life would be a positive response from unheated samples and a negative response from heated samples. On Mars, the LR results had met minimum criteria for a biological interpretation but due to the GC-MS results, the LR responses were later attributed to putative soil inorganic oxidants. Since the time of Viking, studies have been carried out with the objective of determining an oxidant or combination of oxidants that might exist on Mars and have produced the observed kinetics of the LR response. to date, no such agent has been found that produces all aspects of the LR results on Mars. While the above considerations in no way imply the existence of life forms at the two Viking landing sites, inorganic and biological explanations for the Viking LR data should now be considered equally plausible until more complete studies of the Martian surface are carried out. Therefore, in light of the SNC meteorites data and their implications for the possibility of organic matter near or on the Martian surface the Viking biology experiments should

thus be seen, not as failures for their inability to provide unambiguous evidence for or against Martian life, but as a foundation for the development of future life-detection instruments. Additional information is contained in the original extended abstract.
Author
Organic Materials; SNC Meteorites; Viking Mars Program; Mars Surface Samples; Exobiology

20020002134 Lockheed Martin Space Operations, Houston, TX USA
Salts in Martian Meteorites: A Complex Martian History
Velbel, Michael A., Michigan State Univ., USA; Wentworth, Susan J., Lockheed Martin Space Operations, USA; McKay, David S., Lockheed Martin Space Operations, USA; Thomas-Keptra, Kathie L., Lockheed Martin Space Operations, USA; Longazo, Teresa G., Hernandez Engineering, Inc., USA; General Meeting of the NASA Astrobiology Insititute; April 2001, pp. 219-221; In English; See also 20020002018; Original contains color illustrations; No Copyright; Avail: Issuing Activity; Abstract Only

Rock samples from Mars (i.e., Martian meteorites) contain evidence of low-temperature aqueous weathering that occurred on Mars. Weathering features in the Martian meteorites will be of key importance in understanding both the near-surface history of Mars and any possible life (past or present) on Mars. Known Martian weathering features include dissolution textures on primary igneous mineral surfaces, secondary phyllosilicates and oxides, and evaporite minerals (sulfates, halite, and carbonates). Established petrographic criteria which identify a secondary phase as Martian include the following: (1) phase present in interior of meteorite but not on exterior (fusion crust); (2) phase included within another, unambiguously Martian, phase (e.g., impact-produced glass); (3) phase partly volatilized; (4) phase terminated by fusion crust; or (5) microfaulting present within phase. We have determined that Martian secondary minerals can also be identified by finding similar weathering features in different Martian meteorites with dissimilar terrestrial histories. For example, the Martian meteorites Nakhla and Shergotty (observed falls in Egypt and India, respectively) contain very similar weathering features and evaporite assemblages, implying that their Martian history is similar. A characteristic that seems common to Martian meteorite evaporites is that they themselves contain a wide range of alteration features. The following figures are presented and compared: (1) Ca-sulfate with little evidence of dessication or weathering; (2) Dessicated Ca-sulfate partly coated by halite; (3) Weathered silicate substrate overlain by partly eroded Ca-sulfate, in turn coated with thin layer of secondary silicate; (4) Detrital Ca-sulfate included in cluster of Ca-carbonate grains; (5) Halite on px substrate; (6) Halite spherule with beveled and pitted surface. In summary, the history of the Martian near-surface environment is long and very complex, and factors such as shock or other heating events must be considered in understanding any low-temperature processes, including biological ones, that might have occurred. Additional information is contained in the original extended abstract.
Author
SNC Meteorites; Exobiology; Meteoritic Composition; Mineral Deposits

20020002135 Pennsylvania State Univ., Dept. of Biology, University Park, PA USA
Evolutionary Genomics Focus Group
Hedges, S. Blair, Pennsylvania State Univ., USA; Lake, James A., California Univ., USA; General Meeting of the NASA Astrobiology Insititute; April 2001, pp. 225; In English; See also 20020002018; No Copyright; Avail: Issuing Activity; Abstract Only

Evolutionary analysis of the genomes of organisms will help to build a clearer picture of how life originated, adapted to diverse environments, and increased in complexity on this planet. In turn, it will lead to a better understanding of life elsewhere in the Universe. This focus group includes astrobiologists from seven NAI Lead Institutions and several other institutions, combining expertise in molecular evolutionary analysis, organic chemistry and biochemistry, earth history, and paleontology. The unifying goal is to compare the early evolutionary history of life, as revealed through analyses of genomic sequence data, with changes in Earth's environment through time. A web site (www.evogenomics.org) has been established for the focus group, providing contact information, publications, research activities, databases, and position announcements. Inter-team collaborations are underway in three research areas and are facilitated by monthly or bimonthly videoconferences and periodic workshops: (1) Phylogeny and Timescale. This is a research initiative (Animal Origins Project) that involves use of genomic tools to obtain large numbers of DNA sequences from representative animal phyla. These data will be used to estimate the phylogeny and timing of animal evolution to examine the influence of geologic and planetary-scale climatic events in the Neoproterozoic; (2) Gene Function. Research here includes documentation of recruitment in prokaryotic and eukaryotic proteins and development of computational tools to extract signals of form and function; (3) Horizontal Transfer. Analysis of complete genomes is made to understand the role of horizontal gene transfer in the evolution of life on Earth.
Author
Biological Evolution; Genome; Organisms; Exobiology; Research Management

20020002136 Harvard Univ., Botanical Museum, Cambridge, MA USA

Protistan Microfossils in Early Mesoproterozoic Rocks

Javaux, Emmanuelle J. J. M., Harvard Univ., USA; Knoll, Andrew H., Harvard Univ., USA; Walter, Malcolm R., MacQuarie Univ., Australia; General Meeting of the NASA Astrobiology Insititute; April 2001, pp. 226-227; In English; See also 20020002018; No Copyright; Avail: Issuing Activity; Abstract Only

The Roper Group, Northern Australia, comprises a thick (greater than 1000 m), ramp-like succession of siliciclastic rocks deposited 1400-1500 million years ago in a rapidly subsiding intracratonic basin. The group can be divided into six principal depositional sequences bounded by conformable surfaces in the basin interior. Sequences are highly asymmetric, consisting mostly of highstand systems tracts dominated by deep basinal to distal shelf mudstones that shallow upward to coastal sandstones and intercalated shales. Poorly developed transgressive systems tracts consist of fluviatile to coastal marine redbeds overlain by shelf mudstones and thin, intercalated sand beds. Fossils were first discovered in Roper rocks by Peat and others, who reported leiosphaerid acritarchs, small unicells, and filamentous microfossils in shales near the top of the succession. Our new study shows that microfossils are both abundant and unusually well preserved throughout the group. Thus, Roper rocks provide an unparalleled opportunity to study the distribution of Mesoproterozoic organisms in time and space. The most abundant and diverse Roper assemblages come from estuarine to tidedominated shoreline facies. Shales in lower shoreface to storm-dominated inner shelf facies preserve a lower abundance and diversity of acritarchs, as well as large striated tubes of uncertain, but probably eukaryotic, affinities. More distal shelf facies contain still fewer fossils; basinal mudstones contain much organic debris but few well-preserved microfossils. The observed onshore-offshore pattern of decreasing abundance, declining diversity, and changing dominance among fossils of probable eukaryotic origin is consistent with the hypothesis that trace elements critical to the biological N-cycle were sharply limited in Mesoproterozoic oceans. Under the hypothesized conditions, eukaryotic algae might well have been most abundant and diverse in estuarine settings, where Mo was most available. The sole, but important exception to this distribution comes from shales deposited within the maximum flooding interval at the top of a deepening upward, transgressive systems tract. These samples contain distinctive acritarchs that bear one to twenty or more processes distributed asymmetrically about the vesicle surface. The processes vary in length within and among individuals, and some branch dichotomously. The irregular morphology and asymmetric distribution of these processes stand in marked contrast to the regular size and distribution of processes in most younger acanthomorphic acritarchs and suggest that the Roper fossils may have been actively growing cells or germinating cysts rather than metabolically inert vesicles. Bulbous protrusions on some specimens further suggest vegetative reproduction by budding. The kind of morphological remodeling necessary to form the morphologies represented in the Roper population requires a dynamic cytoskeleton, as well as sophisticated molecular signaling pathways for its regulation. Thus, by life's middle age, eukaryotes had evolved the cytoskeletal architecture and regulatory networks that characterize living protists. Roper paleontology indicates that 1500 million years ago, marine protists were cytologically sophisticated but environmentally limited. Roper fossils thus contribute to an emerging picture of Mesoproterozoic biology as transitional between an older world dominated by bacteria and archaea and a new world in which eukaryotes are also diverse and ecologically important.

Author

Microorganisms; Fossils; Australia; Biological Evolution

20020002137 Colorado Univ., Dept. of Geological Sciences, Boulder, CO USA

Lithosphere-Hydrosphere Interactions on the Hadean (greater than 4.0 Ga) Earth

Mojzsis, Stephen J., Colorado Univ., USA; General Meeting of the NASA Astrobiology Insititute; April 2001, pp. 228-229; In English; See also 20020002018; No Copyright; Avail: Issuing Activity; Abstract Only

Sources of information about environments for emergent life are provided by rare and scattered exposures of the oldest known granitoid gneisses and supracrustal enclaves, which are only between 3.8 - 4.0 Ga. The time period after primary accretion of the planets and the first appearance of a rock record has long been considered off-limits to geologists. Studies of the isotopic record of planetary evolution on Earth, the Moon and meteorites point to rapid planetary accretion, core formation and the differentiation of some incompatible-element rich crust at an early stage. to investigate conditions existing at the Earth's surface prior to 4 Ga requires discovery of yet older materials. Indeed, such ancient materials appear to have survived to the present. Early Archean (approximately 3 Ga) quartzites of the Narryer Gneiss Complex in Western Australia host detrital zircon populations with ages greater than 4 Ga and new work has identified some of these as between 4.3 and 4.4 Ga, thereby establishing them as the oldest known terrestrial materials. Trace element distributions as well as oxygen isotope compositions in zircon reflect the evolution and bulk geochemical characteristics of the parent melt. Recently reported in situ U-Pb and oxygen isotope results for the greater than 4 Ga zircons from Western Australia have revealed details on the age and composition of their source magmas and represent the first steps toward directly exploring the nature of the Hadean crust. Measurements of oxygen isotopes in rocks and minerals provide a means for understanding the magmatic, fluid and thermal history of the crust. Furthermore, oxygen isotopes are used

to discriminate among possible granitoid sources (mantle, metasedimentary, hybrid) in accessory phases e.g., igneous zircons. Crustal contamination can strongly affect oxygen isotope compositions in igneous rocks so that this signal becomes incorporated into crystallizing zircons. Zircon provides reliable U-Pb crystallization ages and can survive both high-grade metamorphism and sedimentary transport processes. Exchange rates for oxygen in zircon are very slow, thereby potentially permitting preservation of the protolith oxygen isotope composition even through high-grade metamorphism. Granitoids derived largely from orthogneiss protoliths (so-called ”I-types”) tend to have delta-O-18 values below 9% whereas those derived by melting of clay-rich sedimentary rocks (”S-types”) have delta-O-18 values that are higher. In general, granitoids considered as ”S-type” form by melting of metasedimentary rocks enriched in O-18; this is in contrast to ”I-types” that form from melting of igneous rocks derived from arc processes. Since the average delta-O-18 values of Archean sedimentary rocks is greater than 9%, it requires only small inputs of this component to a primitive source magma to measurably raise its delta-O-18 from the canonical mantle value of +5.5%. This mechanism can create ”S-type” zircons in the rock record. Multi-collector ion microprobe measurements yield delta-O(sub SMOW)-18 values of Hadean zircons ranging from +5.4 +/- 0.6% to +15.4 +/- 0.4%. The oxygen isotope fractionation between zircon and melt at magmatic temperatures is about -2% allowing an estimate of the delta-O-18 value of the whole rock from which the zircon crystallized. Source delta-O-18 values calculated in this fashion for all zircon cores analyzed range from ca. 7.4 to 10.2%. Based on these results, it is postulated that the ca. 4.3 Ga zircons formed from magmas containing a significant component of re-worked continental crust that formed in the presence of water near the Earth#s surface. Mineral assemblages including muscovite and monazite suggestive of derivation from a peraluminous melt were found as inclusions in 4.2 Ga zircons from the Narryer Gneiss Complex . Since the dominant mechanism to create peraluminous granitoids is melting of a graywacke protolith, this observation is also consistent with the presence of a hydrosphere on Earth prior to 4.2 Ga, that apparently was liquid and supported weathering and clay formation perhaps from emergent (continental?) landmasses. The formation of continental crust appears to be a feature unique to the geology of Earth. A sequence of events, beginning with water introduced to the shallow mantle by deep emplacement of hydrated oceanic crust and sediments, seems necessary for the production of granitoid melts in an arc environment. This process ultimately leads to the formation of continental crust. Additional information is contained in the original extended abstract.

Author

Earth Hydrosphere; Biological Evolution; Earth Crust

20020002138 Pennsylvania State Univ., Astrobiology Research Center, University Park, PA USA

The Evolution of O2 and CO2 in the Atmosphere

Ohmoto, Hiroshi, Pennsylvania State Univ., USA; General Meeting of the NASA Astrobiology Insititute; April 2001, pp. 231-232; In English; See also 20020002018; No Copyright; Avail: Issuing Activity; Abstract Only

The geochemical data on Precambrian rocks that have been used to support the first and second models of atmospheric O2 evolution include the following: (1) occurrences of banded iron formations (BIFs) in some greater than 1.8 Ga marine sedimentary sequences; (2) occurrences of detrital grains of ”unstable minerals” (uraninite, pyrite, and siderite) in some greater than 2.4 Ga fluvial sediments; (3) occurrences of ”Fe-depleted” rocks in some greater than 2.0 Ga paleosols; (4) occurrences of less than 2.0 Ga redbeds; (5) large positive delta-C-13 values for some approximately 2.0 Ga carbonates; (6) small delta-S-34 variations among pyrite crystals in some greater than 2.2 Ga marine sediments; (7) possible presence of mass-independent fractionation of S-33 and S-36 among sulfide and sulfates greater than 2.0 Ga in age. The controversy on the atmospheric O2 evolution exists primarily because all the above geochemical data can also be explained by the third model. The third model presents the following additional lines of (bio)geochemical evidence: (1) occurrences of BIFs in modern oceans; (2a) occurrences of the ”unstable” detrital minerals in some modern sediments; (2b) absence of ”unstable” detrital minerals in ”normal” sedimentary rocks of all ages; (3a) occurrences of ”Fe-depleted” rocks in soils of all ages; (3b) occurrences of Fe3+ -enriched rocks in paleosols of all ages; (3c) higher Fe3+/Fe2+ ratios in sedimentary rocks, compared to igneous rocks, of all ages; (4) occurrence of some greater than 2.2 Ga redbeds; (5) occurrences of carbonates with large delta-C-13 values in other geologic age; (6) large delta-S-34 variations for pyrite and barite in some greater than 2.2 Ga sedimentary rocks; (7) possible presence of mass independent fractionation of S-36 among sulfide and sulfates of less than 2.0 Ga in age; (8) presence of Ce anomalies in BIFs of all ages; (i) biomarkers of eukaryotes in 2.7 Ga marine shales; (9) spatial (regional) and temporal (less than 100 Ma) variations in delta-C-13 of organic matter in some greater than 2.0 Ga marine sequences; (10) correlations between delta-C-13 of organic matter and delta-S-34 of pyrite in some Archean marine sequences; (11) similar contents of Mo, U, and V in shales of all ages; (12) similar contents of organic carbon and pyrite in shales of all ages; and (13) kerogen of cyanobacterial origin in 2.6 Ga paleosols. Another approach to understand the evolution of atmospheric O2 and CO2 is from modeling of geochemical cycles. The atmospheric O2 level has been controlled by the balance between the production flux, F(sub prod.O2) (equal to the burial flux of organic matter in marine sediments, F(sub b.org), and the consumption flux, F(sub sink.O2), which is composed of the consumption flux by reduced volcanic gas (e.g., H2, CO, CH4, H2S), F(sub v.O2), and that by weathering of reduced compounds in rocks (organic carbon, sulfides, and FeO) during

soil formation, F(sub s.O2). Presently, F(sub b.org) = F(sub v.O2) + F(sub s.O2). The first and second models of atmospheric O2 evolution suggest very high fluxes of reduced volcanic gases prior to approximately 2.0 Ga, resulting in the relationships of F(sub b.org) is less than F(sub v.O2), pO2 = approximately 0, and F(sub s.O2) = approximately 0. Our computer simulation of the coupled carbon-oxygen geochemical cycles, however, suggests that such a scenario would have resulted in nearly a complete conversion of CO2 in the atmosphere and carbonates in the crust to organic carbon in less than 1 Ga since the emergence of cyanobacteria; this was an unlikely scenario. Under moderate fluxes of reduced volcanic gases, the pO2 would have risen to approximately 1 PAL in less than 30 Ma since the emergence of cyanobacteria and the pO2 level would have stayed at approximately 1 PAL over 3 Ga period while the atmospheric pCO2 gradually decreased from approximately 1000 PAL to 1 PAL. Because this scenario also explains the present sizes of the carbonate and organic carbon reservoirs, it is a favorable one. Additional information is contained in the original extended abstract.
Author
Carbon Dioxide; Oxygen; Evolution (Development); Earth Atmosphere

20020002139 Massachusetts Inst. of Tech., Earth Atmospheric and Planetary Sciences, Cambridge, MA USA
Geochronological Constraints on Early Animal Evolution and the Significance of the Precambrian-Cambrian Boundary
Bowring, Samuel A., Massachusetts Inst. of Tech., USA; Grotzinger, John P., Massachusetts Inst. of Tech., USA; Amthor, J. E., PDO, Oman; Schroder, S., Massachusetts Inst. of Tech., USA; Martin, Mark W., Massachusetts Inst. of Tech., USA; General Meeting of the NASA Astrobiology Insititute; April 2001, pp. 233-234; In English; See also 20020002018; No Copyright; Avail: Issuing Activity; Abstract Only

The past five years have seen intensive efforts by paleontologists, evolutionary and developmental biologists, and geologists to better understand the first appearance and subsequent explosive diversification of animals. A high-precision U-Pb geochronological framework may be combined with paleontological, chemostratigraphic, and geological data to allow evaluation of models that invoke both intrinsic and extrinsic triggers for the Cambrian radiation. Geochronological data from late Neoproterozoic rocks indicate Ediacaran fossils range from at least 575 Ma (Newfoundland) to 543 Ma (Namibia) and perhaps into the Cambrian. Complex trace-fossils occur at least as far back as 555 Ma (White Sea, Russia). The number and complexity of trace fossils increases dramatically to the Cambrian explosion which occurs over approximately a 10 Ma interval (530-520 Ma). Critical to understanding the role of extrinsic factors in animal evolution is high-precision calibration of the global chemostratigraphic data. This will allow detailed evaluation of whether sudden isotopic excursions reflect globally synchronous events at the 100-300 ka level. Outstanding questions are: (1) What is the duration and number of late Neoproterozoic glacial events and their relationship to diversity in the fossil record? (2) Is the negative delta-13 excursion at the Cambrian-Precambrian boundary globally synchronous and does it signal a major extinction and the creation of ecological niches for the ensuing Cambrian explosion? Continued integration of high-precision geochronology with biological and paleontological studies will allow new insights into the history of early animal evolution. We believe that this approach should allow discussion of the late Neoproterozoic-Cambrian record at the 100-300 ka level. Additional information is contained in the original extended abstract.
Author
Fossils; Geochronology; Paleontology; Biological Evolution; Cambrian Period

20020002140 Marine Biological Lab., Woods Hole, MA USA
Pelobionts: Ancient Eukaryotes or Degenerate Protists?
Edgcomb, V. P., Marine Biological Lab., USA; Zettler, L. Amaral, Marine Biological Lab., USA; Sogin, M. L., Marine Biological Lab., USA; Simpson, A. G. B., Sydney Univ., Australia; Patterson, D., Sydney Univ., Australia; Nerad, T. A., American Type Culture Collection, USA; General Meeting of the NASA Astrobiology Insititute; April 2001, pp. 235-236; In English; See also 20020002018; No Copyright; Avail: Issuing Activity; Abstract Only

Phylogenetic analysis of small subunit ribosomal RNA (SSU rRNA) genes, including new pelobiont sequences from Mastigella commutans, Mastigamoeba sp., and Mastigamoeba simplex, forces us to re-evaluate some of our preconceived ideas about the early evolution of eukaryotes; namely the notion of ultrastructural simplicity as an ancestral trait. Based on cytoskeletal features, models of evolution in the early 1990's placed these free-living amoeboid flagellated protists close to the origins of the eukaryotic cell, in agreement with some early molecular phylogenies. Because of their potential significance to the understanding of the origins of early eukaryotes, sequences of the small subunit ribosomal RNA gene (SSU rRNA) were obtained from three additional pelobionts and subjected to a rigorous phylogenetic analysis. Despite the absence of typical eukaryotic organelles, e.g., mitochondria, dictyosomes, chloroplasts, coated vesicles, and peroxisomes, pelobionts are not basal to other eukaryotes in our molecular analyses nor are they specifically related to a previously described pelobiont-like organism, Mastigamoeba invertens. Many analyses suggest the pelobionts share common ancestry with the Entamoebidae, with Endolimax nana sharing an unique common evolutionary history with Mastigamoeba simplex. The reduction in cytoskeletal complexity may have occurred in a

common ancestor of pelobionts and entamoebae, forcing us to re-evaluate our assumptions about what constitutes an ancestral eukaryotic trait. Additional information is contained in the original extended abstract.
Author
Eukaryotes; Biological Evolution; Cytology; Ribonucleic Acids

20020002141 California Univ., Dept. of Chemistry and Biochemistry, San Diego, CA USA
Considerations for Evaluation of Isotopic Evidence for Biological Activity
Farquhar, James, California Univ., USA; Airieau, Sabine, California Univ., USA; Thiemens, Mark H., California Univ., USA; Canfield, Don, Odense Univ., Denmark; Habicht, Kirsten, Odense Univ., Denmark; General Meeting of the NASA Astrobiology Insititute; April 2001, pp. 237-239; In English; See also 20020002018; No Copyright; Avail: Issuing Activity; Abstract Only

Large isotopic fractionations have traditionally been earmarked as one of the hallmarks of biological activity. This is because biological processes can generate large magnitude isotopic fractionations in comparison to other geologically relevant fractionation processes. Atmospheric reactions have been known to be an exception to this rule and can generate some of the largest isotopic fractionations observed in nature, but they have generally been dismissed because they have not been thought capable of imprinting their character on minerals (and other phases) in rocks. Recent observation of mass-independent fractionations for sulfur and oxygen isotopes in samples of terrestrial rocks and also of secondary minerals from SNC meteorites presents several interesting considerations for the use of stable isotopes as probes for biological activity early in Earth history and on other planets. Here we discuss some of the considerations to be observed when using isotopes as probes of biological activity in environments where there is the potential for atmospheric imprints onto the isotope systematics observed in the rock record. Additional information is contained in the original extended abstract.
Author
Activity (Biology); Chemical Fractionation; Atmospheric Effects; Sulfur Isotopes; Oxygen Isotopes

20020002142 University of South Florida, Dept. of Biology, Tampa, FL USA
Deep Bilaterian Phylogeny: The Evolution of Adaptation to Extreme Environments
Garey, James R., University of South Florida, USA; General Meeting of the NASA Astrobiology Insititute; April 2001, pp. 240-241; In English; See also 20020002018; No Copyright; Avail: Issuing Activity; Abstract Only

Current studies of animal evolution based on a combination of molecular and morphological evidence and have shown that the bilateral animals are composed of three major groups: (1) Deuterostomes such as echinoderms and vertebrates; (2) Ecdysozoa, the molting protostomes, such as arthropods and nematodes; and (3) Lophotrochozoa, the nonmolting protostomes such as annelids, molluscs and flatworms. Adaptation to extreme environments has evolved in a number of ecdysozoan and lophotrochozoan phyla in a number of different ways. Some animals survive to extreme environments through symbiotic bacteria and other adaptations. The most well-known example are the animals associated with hydrothermal vents and cold seeps, such as vestimentiferan annelid and certain bivalve molluscs. These animals have adapted to hypersaline water rich in sulfide, methane, and ammonia. Adult vestimentiferan worms have no mouth or gut and survive by symbiotic relationships with sulfur reducing and methanogenic bacteria contained within a large organ known as the trophosome. Additional information is contained in the original extended abstract.
Author
Adaptation; Animals; Biological Evolution

20020002143 Arizona State Univ., Dept. of Geological Sciences, Tempe, AZ USA
Environmental Conditions of the Early Earth at the Time of the Earliest Microfossil Record
Knauth, L. Paul, Arizona State Univ., USA; Lowe, Donald R., Stanford Univ., USA; General Meeting of the NASA Astrobiology Insititute; April 2001, pp. 242-243; In English; See also 20020002018; No Copyright; Avail: Issuing Activity; Abstract Only

The 3.5 Ga Swaziland Supergroup, South Africa, contains some of the oldest known, and least metamorphosed, sedimentary rocks on Earth. These rocks represent a preserved archive of early life, surficial processes, and environmental conditions on the early Earth. Chert is the most abundant sedimentary rock type in the volcanic part of this succession, the Onverwacht Group, and is widespread in the overlying Fig Tree Group. The cherts are enormously depleted in the heavy isotope of oxygen relative to younger cherts, and this has been interpreted as indicating very warm climatic temperatures, early oceans enormously depleted in heavy oxygen, or complete 'resetting' of oxygen isotopes during later alteration. It now appears that the oxygen isotopic composition of the ocean is strongly controlled by circulation through hot mid-ocean ridges and could not have been significantly different in the past. Later resetting of the oxygen isotopes in cherts is an issue that cannot be settled by isotope geochemistry alone. We have therefore examined the isotopic variations in cherts within the context of their geologic setting to test all suggested alteration scenarios. We conclude below that altered cherts are readily recognizable and that the depletions in heavy oxygen

relative to more recent cherts cannot be reasonably explained in terms of later resetting. The isotopic data strongly indicate that climatic temperatures of the early Earth were on the order of 55-85 C and that the early evolution of life was a high temperature affair. Additional information is contained in the original extended abstract.
Author
Geochemistry; Oxygen Isotopes; Sedimentary Rocks

20020002144 Pennsylvania State Univ., Dept. of Geosciences and Astrobiology Research, University Park, PA USA
Glacial Eustasy and the Flux of Iron from Midocean Ridge Hydrothermal Systems
Kump, Lee R., Pennsylvania State Univ., USA; Seyfried, William E., Minnesota Univ., USA; General Meeting of the NASA Astrobiology Insititute; April 2001, pp. 244-245; In English; See also 20020002018; No Copyright; Avail: Issuing Activity; Abstract Only

Midocean ridge hydrothermal systems support a diverse ecosystem on Earth, and perhaps on other planets or moons as well. A considerable body of experimental and observational evidence indicates, however, that the chemistry of these seawater-derived fluids is highly sensitive to the temperature and pressure at which they interact with the basalts of the seafloor, in part because the fluids tend to be close to the critical point of seawater. Thus, the particular fluid compositions that support life in the deep sea on Earth today may not have always been present on Earth or may not be present on other planetary bodies. In experimental simulations of seafloor hydrothermal systems, pH falls and both Fe2+ and H2S concentrations increase with increasing temperature, but the ratio Fe2+/H2S increases as well. This fact has fueled speculation that higher temperatures of water-rock interaction in the Archean may have promoted the establishment of Fe2+-rich oceans that supported widespread banded iron formation. Less discussed is the pressure dependence of the Fe2+ concentration. Additional information is contained in the original extended abstract.
Author
Hydrothermal Systems; Iron 58; Ocean Bottom; Concentration (Composition)

20020002145 Australian Geological Survey Organisation, Canberra, Australian Capital Territory, Australia
Biogeochemistry of the 1640 Ma McArthur River (HYC) Lead-Zinc Ore and Host Sediments, Northern Territory, Australia
Logan, Graham A., Australian Geological Survey Organisation, Canberra, Australia; Hinman, Mark C., Hinman GeoSolutions, Australia; Walter, Malcolm R., MacQuarie Univ., Australia; Chen, Junhong, MacQuarie Univ., Australia; Summons, Roger E., Australian Geological Survey Organisation, Canberra, Australia; General Meeting of the NASA Astrobiology Insititute; April 2001, pp. 246-247; In English; See also 20020002018; No Copyright; Avail: Issuing Activity; Abstract Only

The 1640 Ma McArthur River (HYC) lead-zinc-silver deposit of northern Australia is the largest known stratiform base-metal deposit. It formed in a hydrothermal system. It is extraordinarily well preserved, with all indicators of thermal maturity suggesting that the country rocks have not been heated beyond the 'oil window'. Oil bleeds from drill cores from nearby indicate petroleum source rocks have generated oil close to HYC. The deposit has been intersected by more than 100 drill holes, and is exposed in an underground mine. It represents a superb opportunity to examine this class of ore deposits, and consequently has been intensively studied. It also represents an extraordinary opportunity to study the paleobiology of an ancient hydrothermal system. Interpretations of the genesis of the ore vary widely, with there being three end-member models: syngenetic (exhalative) in a deep marine setting; early diagenetic in the mud and silt of an ephemeral lake or sabkha; and early diagenetic in a marine environment below wave-base. Our work supports the last of these, as do recent sedimentological studies. Additional information is contained in the original extended abstract.
Author
Biogeochemistry; Mineral Deposits; Sediments; Hydrocarbons

20020002146 NASA Ames Research Center, Moffett Field, CA USA
Carbon Dioxide Cycling and the Climate of Ancient Earth
Zahnle, Kevin, NASA Ames Research Center, USA; Sleep, Norman H., Stanford Univ., USA; General Meeting of the NASA Astrobiology Insititute; April 2001, pp. 248; In English; See also 20020002018; No Copyright; Avail: Issuing Activity; Abstract Only

The continental cycle of silicate weathering and metamorphism dynamically buffers atmospheric CO2 and climate. Feedback is provided by the strong temperature dependence of silicate weathering. Here we argue that hydrothermal alteration of oceanic basalts also dynamically buffers CO2. The oceanic cycle links with the mantle via subduction and the midocean ridges. Feedback is provided by the dependence of carbonatization on dissolved carbonates in seawater. Unlike the continental cycle, the oceanic cycle has no thermostat. Currently the continental cycle is more important, but earlier in Earth's history, especially if heat flow

were higher than it is now, more vigorous plate tectonics would have made the oceanic cycle dominant. We find that CO2 greenhouses thick enough to defeat the faint early Sun are implausible and that, if no other greenhouse gases are invoked, very cold climates are expected for much of the Proterozoic and the Archean. We echo current fashion and favor biogenic methane as the chief supplement to CO2. Fast weathering and probable subduction of abundant impact ejecta would have reduced CO2 levels still further in the Hadean. Despite its name, the Hadean would have been the coldest era in the history of the Earth.
Author
Carbon Dioxide; Paleoclimatology; Carbon Cycle; Oceanography

20020002147 Pennsylvania State Univ., Dept. of Geosciences, University Park, PA USA
A Model for Evolution of the Seawater Oxygen Isotope Composition
Arthur, Michael A., Pennsylvania State Univ., USA; Kump, Lee R., Pennsylvania State Univ., USA; General Meeting of the NASA Astrobiology Insititute; April 2001, pp. 249-250; In English; See also 20020002018; No Copyright; Avail: Issuing Activity; Abstract Only

Several well-argued interpretations of oxygen isotope data from apparently well-preserved marine carbonate components, as well as interpretations of the delta-18-O of chert, require substantial changes in the oxygen-isotopic composition of seawater (delta-w) through time. However, most workers have concluded that such changes are unlikely because delta-w is so strongly buffered by high-temperature alteration of basalts at the mid-ocean ridge. In light of the fundamental disagreement between the data and models we have constructed a steady-state, time-dependent model for seawater delta-w using the latest analyses of fluxes and isotopic fractionations that influence seawater delta-w. We have conducted sensitivity tests of the steady-state model, and have driven the preferred forward model with a combination of parameters that are judged to be most important in forcing system changes. In particular, we vary the seafloor basalt production rate and the global silicate weathering rate in accordance with values derived from independent geochemical cycle models for the Phanerozoic and with fewer constraints from the Precambrian. We also explore the early evolution of delta-w in response to the growth of continents and the sedimentary shell. Additional information is contained in the original extended abstract.
Author
Ocean Bottom; Oxygen Isotopes; Sea Water; Concentration (Composition)

20020002148 NASA Ames Research Center, Moffett Field, CA USA
Ecophysiological Changes in Microbial Mats Incubated in a Greenhouse Collaboratory
Bebout, Brad, NASA Ames Research Center, USA; DesMarais, David J., NASA Ames Research Center, USA; GarciaPichel, Ferran, Arizona State Univ., USA; Hogan, Mary, NASA Ames Research Center, USA; Jahnke, Linda, NASA Ames Research Center, USA; Keller, Richard M., NASA Ames Research Center, USA; Miller, Scott R., NASA Ames Research Center, USA; General Meeting of the NASA Astrobiology Insititute; April 2001, pp. 251-252; In English; See also 20020002018; No Copyright; Avail: Issuing Activity; Abstract Only

Microbial mats are modern examples of the earliest microbial communities known. Among the best studied are microbial mats growing in hypersaline ponds managed for the production of salt by Exportadora de Sal, S.A. de C.V., Guerrero Negro, Baja California Sur, Mexico. In May, 2001, we collected mats from Ponds 4 and 5 in this system and returned them to Ames Research Center, where they have been maintained for a period of over nine months. We report here on both the ecophysiological changes occurring in the mats over that period of time as well as the facility in which they were incubated. Mats (approximately 1 sq. meter total area) were incubated in a greenhouse facility modified to provide the mats with natural levels of visible and ultraviolet radiation as well as constantly flowing, temperature-controlled water. Two replicated treatments were maintained, a 'high salinity' treatment (about 120 ppt) and a 'low salinity' treatment (about 90 ppt). Rates of net biological activity (e.g., photosynthesis, respiration, trace gas production) in the mats were relatively constant over the several months, and were similar to rates of activity measured in the field. However, over the course of the incubation, mats in both treatments changed in physical appearance. The most obvious change was that mats in the higher salinity treatments developed a higher proportion of carotenoid pigments (relative to chlorophyll), resulting in a noticeably orange color in the high salinity mats. This trend is also seen in the natural salinity gradient present at the field site. Changes in the community composition of the mats, as assayed by denaturing gradient gel electrophoresis (DGGE), as well as biomarker compounds produced in the mats were also monitored. The degree to which the mats kept in the greenhouse changed from the originally collected mats, as well as differences between high and low salinity mats will be discussed. Additional information is contained in the original extended abstract.
Author
Microorganisms; Salinity; Color

20020002149 Pennsylvania State Univ., Dept. of Biology, University Park, PA USA

The Evolutionary Position of Nematodes

Blair, Jaime E., Pennsylvania State Univ., USA; Hedges, S. Blair, Pennsylvania State Univ., USA; General Meeting of the NASA Astrobiology Insititute; April 2001, pp. 253; In English; See also 20020002018; No Copyright; Avail: Issuing Activity; Abstract Only

The complete genomes of three animals (metazoans) have been sequenced by global research efforts: a nematode (Caenorhabditis elegans; Phylum Nematoda), an insect (Drosophila melanogaster; Arthropoda), and a vertebrate (Homo sapiens; Vertebrata). Remarkably, the relationships of these three species have yet to be clarified, primarily because of confusion surrounding the position of nematodes. Traditional morphology-based phylogenies place the pseudocoelomate nematodes and the acoelomate platyhelminthes basal to other bilateral animals. Those phylogenies also place arthropods and annelids together in the clade Articulata, based on the shared characteristic of segmentation. A new arrangement for metazoans was recently proposed based on 18S rDNA sequence data. In this molecular-based phylogeny, nematodes occupy a higher position in the tree, grouping with arthropods and other molting animals in a clade termed Ecdysozoa (based on the shared characteristic of ecdysis). However, only a slowly evolving nematode (Trichinella, Trichocephalida) generated this clade; inclusion of faster evolving species (e.g., Caenorhabditis, Rhabditida) pulled the nematodes back into a basal position. Further analysis of 18S sequence data has both supported and failed to support the Ecdysozoa clade. Also, a recent analysis of 50 nuclear proteins failed to support Ecdysozoa. Resolving this question will facilitate more efficient use of genomic data for animal evolution and genetics. Additional information is contained in the original extended abstract.

Author

Genetics; Genome; Sequencing; Insects; Vertebrates; Worms

20020002150 Portland State Univ., Dept. of Geology, OR USA

Detection of Morphological Fossils of Microbial Communities at Life's Upper Temperature Limit: An Astrobiological Search Strategy for Evidence of Biofilms

Cady, Sherry L., Portland State Univ., USA; General Meeting of the NASA Astrobiology Insititute; April 2001, pp. 254-255; In English; See also 20020002018; No Copyright; Avail: Issuing Activity; Abstract Only

Biogeochemical interactions in high-temperature (>80 C) ecosystems produce microbial biosignatures, any number of which could become preserved in the rock record. Geomicrobiological studies in modern silica-depositing hydrothermal ecosystems (e.g., hot springs) demonstrate the variety of microbial biosignatures that can form. These include microbial fossils, microbially influenced accretionary growth structures (e.g., biogenic stromatolites), organic biomarker compounds, biologically fractionated isotopic signatures of organic compounds and minerals, and minerals whose microstructure or morphology were influenced by microbes. Paleobiological studies of hydrothermally precipitated chert deposits and hydrothermally silicified sediments have shown that relicts of these microbial biosignatures, albeit highly altered, are preserved even in Archean rocks. Since ancient hyperthermophilic biosignatures are significantly altered, deciphering paleobiological and paleoenvironmental information from them requires an understanding of how such biosignatures formed and were altered by taphonomic processes and diagenetic mineral transformations. An iterative approach to the problem, the one taken here, involves comparing siliceous sinters formed in modern ecosystems occupied by hyperthermophilic communities, hydrothermal sinters produced abiotically, and hydrothermal cherts preserved in older analog deposits. Additional information is contained in the original extended abstract.

Author

Microorganisms; Biofilms; Paleobiology; Biogeochemistry

20020002151 NASA Ames Research Center, Moffett Field, CA USA

Biogenic Methane and the Rise of Oxygen

Catling, David, Search for Extraterrestrial Intelligence Inst., USA; McKay, Christopher, NASA Ames Research Center, USA; General Meeting of the NASA Astrobiology Insititute; April 2001, pp. 256-257; In English; See also 20020002018; No Copyright; Avail: Issuing Activity; Abstract Only

Oxygenic photosynthesis does not make the rise of oxygen inevitable. What is required is that reductant and oxygen be separated and permanently segregated. The usual picture for Earth is that oxygenic photosynthesis split CO2 into carbon and oxygen, with the carbon buried in sediments and the oxygen mostly taken up by oxides of iron and sulfur. The relatively small atmospheric reservoir of O2 is regulated by the carbon burial rate, reaction with volcanic and metamorphic gases, and oxidation of reduced carbon released as old sediments weather. Absent from this picture is a distinction between the Archean and modern times: on average, carbon burial fluxes would have been matched by oxygen losses then as now. Separation of reductant from oxidant is only provisional. No net oxidation of the continents occurs, and so no change of diagenetic, metamorphic, or volcanic gases is expected. Nor would any change in oxidative weathering be expected. Something more than carbon burial is required

to make the Archean different. The escape of hydrogen to space permanently separates the reductant from the oxidant. Hydrogen escape is widely believed to have led to the present highly oxidized states of Mars and Venus. Hydrogen escape has usually been thought small for Archaean Earth, because water vapor is cold-trapped at the troposphere and thus held to levels of a few ppmv in the stratosphere. This cold trapping renders hydrogen escape negligible. However, methane is not cold trapped, and its expected abundance in the Archaean, given low oxygen levels and a biogenic source, would have been high, probably more than 100 times present. At such levels methane would have driven geologically significant levels of hydrogen escape. Additional information is contained in the original extended abstract.
Author
Hydrogen; Oxygen; Precambrian Period; Trapping; Atmospheric Chemistry

20020002152 Pennsylvania State Univ., Dept. of Geosciences, University Park, PA USA
Constraints on Early Mantle Redox State
Churchill, Deneyse J., Pennsylvania State Univ., USA; Kasting, James F., Pennsylvania State Univ., USA; General Meeting of the NASA Astrobiology Insititute; April 2001, pp. 258; In English; See also 20020002018; No Copyright; Avail: Issuing Activity; Abstract Only

Recent work by Delano and Canil indicates that Earth's mantle was at or near its present oxidation state, the fayalite-magnetite-quartz (FMQ) buffer, since the Archean and possibly as far back as 3.9 Ga. A FQM mantle with an oxygen fugacity of 10(exp -7) to 10(exp -8) would produce volcanic gases dominated by water (H2O) and carbon dioxide (CO2), with trace amounts (approximately 1-3%) reduced gases such as hydrogen (H2) and carbon monoxide (CO). This presents problems for origin of life theories that rely on reduced gases and lightning to produce the first prebiotic molecules for life. A mantle at or near the iron-wustite (IW) buffer with oxygen fugacities around 10(exp -12) would volcanically outgas more H2, CO, and CH4 (methane), producing a more reduced atmosphere that would have been more conducive to the formation of life in situ. In addition, it has been shown that the Moon has a redox state near IW. If the Moon was formed from a Mars-sized impactor that hit Earth and retained Earth-mantle material, this is an indicator that the early mantle was more reduced, possibly near IW. In this work, we investigate this possibility, suggested earlier by Kasting, et al., and discuss how Earth's mantle may have evolved in redox state from IW to FMQ through hydration, followed by outgassing of H2.
Author
Earth Mantle; Oxidation; Outgassing; Hydration; Paleontology

20020002153 NASA Ames Research Center, Moffett Field, CA USA
How Does C. elegans Respond to Altered Gravity?
Conley, Catharine A., NASA Ames Research Center, USA; Udranszky, Ingrid, NASA Ames Research Center, USA; Hoffman, David, NASA Ames Research Center, USA; Kim, Stuart K., Stanford Univ., USA; General Meeting of the NASA Astrobiology Insititute; April 2001, pp. 259-260; In English; See also 20020002018; No Copyright; Avail: Issuing Activity; Abstract Only

All organisms on Earth have evolved at unit gravity (1xG), and thus are probably adapted to function optimally at 1xG. However, with the advent of space exploration, it has been shown that organisms are capable of surviving at much less than 1xG, as well as at greater than 1xG. Organisms subjected to increased G levels exhibit alterations in physiological processes that compensate for novel environmental stresses, such as increased weight and density-driven sedimentation. These physiological adaptations illustrate the plasticity of organisms when presented with environmental conditions in which they could not possibly have evolved. Investigating the mechanism(s) behind these adaptations may uncover biological pathways that have not previously been identified. An easily-cultured and well-studied organism, such as C. elegans, would be a desirable model system for these studies. Additional information is contained in the original extended abstract.
Author
Organisms; Gravitational Effects; Physiological Responses

20020002154 Pennsylvania State Univ., Dept. of Geosciences, University Park, PA USA
Late Archean Biomarkers in Carbonates from the Hamersley Basin, Pilbara Craton, Western Australia
Eigenbrode, Jennifer L., Pennsylvania State Univ., USA; Freeman, Katherine H., Pennsylvania State Univ., USA; Summons, Roger E., Australian Geological Survey Organisation, Canberra, Australia; Logan, Graham A., Australian Geological Survey Organisation, Canberra, Australia; Brocks, Jochen J., Sydney Univ., Australia; General Meeting of the NASA Astrobiology Insititute; April 2001, pp. 261-262; In English; See also 20020002018; No Copyright; Avail: Issuing Activity; Abstract Only

Little is known about the extent of microbial metabolic diversity in the Archean. Detection of indigenous molecular fossils and the assessment of the isotopic expression of carbon and sulfur in sediment give us the potential to reach an improved understanding of microbial evolution and its role in biogeochemical cycles. Here we report the distribution of hydrocarbon

biomarkers detected in diamond drill core carbonate samples of a late Archean (2.8-2.5 Ga) rock succession from the Hamersley Basin on the Pilbara Craton, Western Australia. Our data suggest the preservation of molecular fossils from metabolically diverse ancient ecosystems of carbonate environments. Additional information is contained in the original extended abstract.
Author
Microorganisms; Precambrian Period; Biological Diversity; Hydrocarbons

20020002155 National Museum of Natural History, Dept. of Paleobiology, Washington, DC USA
Biotic Recoveries from Mass Extinctions: Insights into Evolutionary Innovation
Erwin, Douglas H., National Museum of Natural History, USA; General Meeting of the NASA Astrobiology Insititute; April 2001, pp. 263-264; In English; See also 20020002018; No Copyright; Avail: Issuing Activity; Abstract Only

Biotic recoveries following mass extinctions involve the rebuilding of ecological communities following massive perturbations, and often display significant biological innovations. Consequently they serve as important systems to examine the interplay between genetics/development, environment and ecology in evolutionary innovation. Significant apparent evolutionary innovations include the spread of angiosperms and placental mammals following the end-Cretaceous mass extinction, ammonoids after the end-Devonian, end-Permian and end-Triassic mass extinctions, echinoids following the end-Permian and end-Triassic mass extinctions and caenogastropods after the end-Permian mass extinction. Yet the spread of placental mammals and angiosperms does not mark the origin of either clade, and may not mark the origin of any significant subclades. In each case, molecular evidence suggests the clades may pre-date the extinction, with their diversification being an ecological response to the mass extinction. Ammonoids considerably predate each biotic crisis they suffered, and although some significant innovations do occur during their history, the pattern of biotic overturn appears to also follow an ecological model. Caenogastropods and echinoids, in contrast, exhibit patterns of morphological innovation more closely linked to the post-extinction biotic recovery. Thus there is no close correlation between developmental and morphological inventions (to use an analogy from the study of technological innovation) and their ecological spread as innovations. Additional information is contained in the original extended abstract.
Author
Extinction; Biological Evolution; Molecular Biology

20020002156 Woods Hole Oceanographic Inst., Biology Dept., MA USA
Genes Involved in Photosymbiotic Interactions
Gast, Rebecca J., Woods Hole Oceanographic Inst., USA; Beaudoin, David J., Marine Biological Lab., USA; Caron, David A., University of Southern California, USA; General Meeting of the NASA Astrobiology Insititute; April 2001, pp. 265-266; In English; See also 20020002018; No Copyright; Avail: Issuing Activity; Abstract Only

We are interested in understanding how photosymbiotic relationships are controlled through the genetic communication of two cells, and perhaps, how this may relate to the evolution of organelles. The presence of an algal symbiont represents the acquisition of novel functions by the host cell. There is an increasing body of evidence for the eukaryotic origin of chloroplasts in cryptophytes, chlorarachniophytes, euglenophytes, heterokonts, haptophytes, and dinoflagellates. In these different hosts, the endosymbiotic algae are in various states of genetic and physical reduction. In all cases it is impossible to remove the alga from its host and culture it independently. Additional information is contained in the original extended abstract.
Author
Symbiosis; Genetics; Algae; Communication

20020002157 Arizona State Univ., Dept. of Biology, Tempe, AZ USA
Modeling the Evolution of Food Webs Under Biogeochemical Constraints
Fagan, William F., Arizona State Univ., USA; Odell, Garrett M., Washington Univ., USA; Meir, Eli, Washington Univ., USA; General Meeting of the NASA Astrobiology Insititute; April 2001, pp. 267; In English; See also 20020002018; No Copyright; Avail: Issuing Activity; Abstract Only

Biological stoichiometry is the study of the balance of energy and multiple chemical elements (e.g., C, N, P) in living systems. Over the last decade, biologists have shown that stoichiometric relationships - in particular disparities in the relative availability of chemical elements in autotrophic resource species in comparison with the relative demand for those elements in the body tissues of consumer species - can affect the behavior, population stability, and evolution of species, the structure and dynamics of ecological communities, and biogeochemical cycling in food webs. However, such stoichiometric principles are not present in traditional models for exploring the complexity of ecological systems. Under the auspices of NASA's Astrobiology program, we are developing a new conceptual framework for exploring species evolution and the development of speciose ecological communities under stoichiometric constraints. Specifically, we aim to understand how species evolution and community

development depend upon ecosystem-level factors (e.g., chemical nutrients, photosynthetically active radiation) that restrict species' life strategies. In our model, evolution and community assembly occur within a model ecosystem, where the stoichiometry of resources constrains both the exploration of adaptive landscapes and food-web complexity. Eventually, we hope that these theoretical efforts will provide insight into the development of living systems on Earth (and elsewhere?) by connecting evolving, interacting lineages to the chemical properties of living systems. In particular, stoichiometric considerations may prove relevant to diversification-extinction dynamics during key periods in earth's history such as the Precambrian-Cambrian boundary, the colonization of terrestrial habitats, and mass extinction events.
Author
Biogeochemistry; Ecosystems; Biological Evolution; Stoichiometry; Food Chain

20020002158 Pennsylvania State Univ., Dept. of Biology, University Park, PA USA
A Genomic Timescale for the Origin of Eukaryotes
Hedges, S. Blair, Pennsylvania State Univ., USA; Chen, Hsiong, Pennsylvania State Univ., USA; Wang, Daniel Y.-C., Pennsylvania State Univ., USA; Thompson, Amanda S., Pennsylvania State Univ., USA; Kumar, Sudhir, Arizona State Univ., USA; Watanabe, Hidemi, Institute of Physical and Chemical Research, Japan; General Meeting of the NASA Astrobiology Insititute; April 2001, pp. 268; In English; See also 20020002018; No Copyright; Avail: Issuing Activity; Abstract Only

Genomic analyses have shown that horizontal gene transfer occurred during the origin of eukaryotes following symbiosis. However, the number of symbiotic events and their relationship with changes in Earth's environment are unclear. Our protein sequence analyses support two symbiotic events: one pre-mitochondrial and a later mitochondrial event. Molecular time estimates of these events, and of the origin of cyanobacteria, suggest that the innovation of oxygenic photosynthesis had a relatively rapid impact on the environment and evolution of eukaryotes.
Author
Eukaryotes; Proteins; Genome; Bioassay; Sequencing

20020002159 Pennsylvania State Univ., Dept. of Geosciences, University Park, PA USA
Microbial Mats as Self-Regulating Systems
Herman, Ellen K., Pennsylvania State Univ., USA; Kump, Lee R., Pennsylvania State Univ., USA; General Meeting of the NASA Astrobiology Insititute; April 2001, pp. 269; In English; See also 20020002018; No Copyright; Avail: Issuing Activity; Abstract Only

We have adopted a numerical model of microbial mat biogeochemistry to investigate the properties of this important ecosystem. Specifically we are interested in the ability of the microbial mat ecosystem to regulate nutrient and light availability, and to damp the effects of external and internal stresses. The persistence of these ecosystems for billions of years on Earth, and the likelihood of their existence elsewhere, depends in part on their resilience to environmental perturbation. A number of scenarios are being investigated, including the response of mats to diurnal and seasonal variations in light availability, and changes in specified heterotrophic activity (aerobic respiration and anaerobic sulfate reduction). of relevance to studies of the Archean Earth are simulations where the mat is subjected to reduced (and elevated) surface O2 concentrations and ultraviolet light intensity. Various stabilizing feedback loops exist; their sensitivity to various parameters is investigated quantitatively.
Author
Biogeochemistry; Ecosystems; Computerized Simulation; Microorganisms; Regulatory Mechanisms (Biology)

20020002160 Pennsylvania State Univ., Dept. of Geosciences, University Park, PA USA
Using Homolog Groups to Create a Whole-Genomic Tree of Free-Living Organisms: An Update
House, Christopher H., Pennsylvania State Univ., USA; FitzGibbon, Sorel T., California Univ., USA; General Meeting of the NASA Astrobiology Insititute; April 2001, pp. 270-271; In English; See also 20020002018; No Copyright; Avail: Issuing Activity; Abstract Only

Evolutionary relationships and significant evolutionary events can be studied using whole genome sequences in many different ways, including the building of genomic trees using methods based on the presence and absence of genes in each genome. Several different methods for the generation of trees using gene content have been proposed. These different processes for building genome trees can be divided into two broad categories: those based on the presence and absence of suspected ortholog pairs or the 'Ortholog method' and those based on the presence and absence of gene families or 'the Homolog method'. Additional information is contained in the original extended abstract.
Author
Genes; Genome; Sequencing; Biological Evolution

20020002161 Pennsylvania State Univ., Dept. of Geosciences, University Park, PA USA

Towards an Understanding of the Late Archean Sulfur Cycle

Hurtgen, Matthew T., Pennsylvania State Univ., USA; Arthur, Michael A., Pennsylvania State Univ., USA; General Meeting of the NASA Astrobiology Insititute; April 2001, pp. 272-273; In English; See also 20020002018; No Copyright; Avail: Issuing Activity; Abstract Only

The isotope records of sedimentary sulfides and sulfates have been used to interpret the biogeochemical cycling of sulfur and constrain global redox levels. The sulfur isotopic composition of sedimentary pyrite is influenced by a significant kinetic isotope effect that occurs during bacterial sulfate reduction as obligate anaerobes preferentially dissimilate the lighter S-32 in the production of H2S and pyrite. A negative delta(sup 34, sub Spyrite) excursion occurs at circa 2.3 Ga. The sulfur isotopic composition of sedimentary sulfates and sulfides deposited before 2.3 Ga cluster around the mantle value of 0 +/- 5%. One interpretation of the minimal fractionation between sulfates and sulfides (Delta(sup 34)S(sub sulfate-pyrite)) is that pyrite formed from magmatic sulfide rather than biogenically produced sulfide. The assumption is that the pre-2.3 Ga ocean was sulfate-poor, and that with essentially no dissolved sulfate there would be no bacterial sulfate reduction and, therefore, minimal isotopic fractionation. A contrasting interpretation is that the minimal fractionation is a result of very rapid rates of sulfate reduction in a relatively sulfate-rich ocean. Experimental evidence suggests that increased rates of sulfate reduction diminish the discriminating effects of bacterial isotope fractionation. Additional information is contained in the original extended abstract.
Author

Biogeochemistry; Precambrian Period; Sulfates; Pyrites; Chemical Fractionation

20020002162 Pennsylvania State Univ., Dept. of Geosciences, University Park, PA USA

The Sulfur Isotopic Composition of Neoproterozoic Seawater Sulfate: Implications for a Snowball Earth

Hurtgen, Matthew T., Pennsylvania State Univ., USA; Arthur, Michael A., Pennsylvania State Univ., USA; Suits, Neil S., Colorado State Univ., USA; Kaufman, Alan J., Maryland Univ., USA; General Meeting of the NASA Astrobiology Insititute; April 2001, pp. 274-275; In English; See also 20020002018; No Copyright; Avail: Issuing Activity; Abstract Only

Biogeochemical processes impose significant and predictable isotopic fractionations on sulfur species as they are cycled between oxidized (i.e., sulfate) and reduced (i.e., sulfide) forms. Consequently, the isotope records of sedimentary sulfides and sulfates are sensitive indicators of environmental change. Sedimentary pyrite most commonly forms as a result of bacterial sulfate reduction and its common occurrence in sedimentary rocks has enabled researchers to partially reconstruct the evolution of delta(sup 34)S(sub pyrite) through the Neoproterozoic. In order to assess the true extent of fractionation and interpret variations in delta(sup 34)S(sub pyrite), the contemporaneous delta(sup 34)S(sub sulfate) must be evaluated. Previous secular delta(sup 34)S(sub sulfate) trends for the Neoproterozoic have been developed using rarely occurring evaporitic gypsum and barite deposits that provide only a low temporal resolution of sulfate evolution. However, trace amounts of sulfate incorporated into marine carbonates can be analyzed for its S-isotopic composition as an indicator of seawater delta(sup 34)S history. Carbonates are significantly more abundant and relatively continuously deposited in the Neoproterozoic than sedimentary sulfate deposits and therefore can provide a relatively continuous marine sulfate sulfur isotopic signal that may be utilized to assess environmental change. Additional information is contained in the original extended abstract.
Author

Chemical Fractionation; Sulfur Isotopes; Sulfates; Sedimentary Rocks; Biogeochemistry

20020002163 Pennsylvania State Univ., Dept. of Geosciences, University Park, PA USA

Photochemical Modeling of Mass-Independent Sulfur Isotope Fractionation in Low-O2 Atmospheres

Kasting, James F., Pennsylvania State Univ., USA; Pavlov, Alex A., Pennsylvania State Univ., USA; General Meeting of the NASA Astrobiology Insititute; April 2001, pp. 276-277; In English; See also 20020002018; No Copyright; Avail: Issuing Activity; Abstract Only

Farquhar et al. have presented evidence for mass-independent sulfur isotope fractionation in rocks of Archean and early Proterozoic age. Such fractionation is not observed in younger rocks. The most likely mechanism for producing mass-independent fractionation involves photochemical reactions initiated by photolysis of either SO2 or H2S. Farquhar et al. suggested that atmospheric O2 and O3 levels must have been low during the Archean to allow these sulfur gases to be photolyzed. We agree with Farquhar et al. regarding the general requirement for low O2 in the Archean. However, the actual upper limit on O2 should be set, not by photolysis considerations, but by the requirement that sulfur species can leave the atmosphere in different chemical forms. Additional information is contained in the original extended abstract.
Author

Chemical Fractionation; Oxygen; Precambrian Period; Concentration (Composition); Atmospheric Chemistry

20020002164 Maryland Univ., Dept. of Geology, College Park, MD USA

Proterozoic CO2 Levels Estimated from In-situ Carbon-Isotopic Compositions of Organic-Walled Microfossils

Kaufman, Alan Jay, Maryland Univ., USA; Xiao, Shuhai, Tulane Univ., USA; General Meeting of the NASA Astrobiology Insititute; April 2001, pp. 278-279; In English; See also 20020002018; No Copyright; Avail: Issuing Activity; Abstract Only

Ion microprobe analyses of robust, organic-walled microfossils - macerated from billion-year-old shales - indicate magnitudes of carbon-isotopic fractionation consistent with elevated levels of CO2 in the ancient atmosphere, assuming Calvin cycle metabolism. The acritarchs (considered to be an encystment phase of the protist life cycle) used in this study consisted of a single species (Shuiyousphaeridium macroreticulatum) of is greater than 150 micron diameter microfossils from the Ruyang Group in Shanxi Province. Granites that intrude overlying sediments are dated at 999 Ma. Microscopic and SEM investigations reveal a complex of interlocking polygonal plates on the acritarch surface as well as an irregular distribution of 5-10 micron long tubular spines. Additional information is contained in the original extended abstract.

Author

Carbon Dioxide; Fossils; Chemical Fractionation; Precambrian Period

20020002165 Arizona State Univ., Dept. of Biology, USA

NAI Evolutionary Genomics Focus Group Plans for Investigating the Metazoan Radiation (Cambrian Explosion) in the Context of the Snowball Earth

Kumar, Sudhir, Arizona State Univ., USA; Kirschvink, Joseph L., California Inst. of Tech., USA; Marshall, Charles R., Harvard Univ., USA; Hedges, S. Blair, Pennsylvania State Univ., USA; Jacobs, David K., California Univ., USA; Lake, James A., California Univ., USA; Runnegar, Bruce N., California Univ., USA; Benner, Steven A., Florida Univ., USA; Garey, James R., University of South Florida, USA; General Meeting of the NASA Astrobiology Insititute; April 2001, pp. 280-281; In English; See also 20020002018; No Copyright; Avail: Issuing Activity; Abstract Only

The goal of this research initiative is to examine the influence of geologic and planetary-scale climatic events during the Neoproterozoic, 1000-545 million years (Ma) ago, on the early evolution of metazoans (animals). The first undisputed evidence of animals in the fossil record is in the latest Neoproterozoic (approx. 570 Ma) and most major groups appear shortly thereafter in the ”Cambrian Explosion” which accelerated dramatically about 545 Ma ago. However, virtually all molecular estimates of divergence times made over the last three decades have indicated a much earlier period of animal evolution which is unrecorded in the fossil record and perhaps began as early as 1,600 Ma ago. It has been 280 suggested that early animals were small and soft-bodied, which would explain their absence from the fossil record. If true, animals would have had to survive planetary-scale climatic events (”Snowball Earth” events) of the Neoproterozoic that occurred between about 750 and 600 Ma ago. The environmental conditions that existed during Snowball Earth periods have been debated, but even under the mildest of scenarios, they would have been challenging for any complex organism. Understanding how Earth#s life was affected by these major environmental perturbations will help us understand how life might have evolved and adapted elsewhere in the Solar System and beyond. However, the single greatest limit to progress at present is our incomplete knowledge of the relationships and timing of animal evolution. Therefore, we plan to obtain DNA sequences of large numbers of genes from representatives of most of the major groups of animals. A robust evolutionary framework that is well tied to the fossil record will permit hypotheses about rates, relationships, and divergence times to be tested and, at the same time, guide future studies on all aspects of animal evolution, including development, gene function, and adaptation.

Author

Animals; Biogeny; Climatology; Genes; Planetary Environments; Abiogenesis; Genome; Radiation Effects; Snow; Genetics

20020002166 Missouri Univ., Dept. of Geological Sciences, Columbia, MO USA

Constraining Sulfate and Oxygen Availability in the Mesoproterozoic Ocean

Lyons, Timothy W., Missouri Univ., USA; Kah, Linda C., Tennessee Univ., USA; Gellatly, Anne M., Missouri Univ., USA; Formolo, Michael J., Missouri Univ., USA; General Meeting of the NASA Astrobiology Insititute; April 2001, pp. 282-283; In English; See also 20020002018; No Copyright; Avail: Issuing Activity; Abstract Only

Unambiguous constraints on seawater compositions are among the more vexing challenges in Precambrian biogeochemistry. We discuss here two methods, one proven and one in the developmental phase, that speak to two of the more important dissolved species in the Precambrian ocean: oxygen and sulfate. Both methods, Fe/Al (Mo/Al) ratios in shales and trace sulfate in carbonates, are relatively simple in theory and in application but have strength in the broad availability of suitable samples and in the potential for preserving primary signals over complex burial histories. Canfield proposed that the ocean was anoxic until the Neoproterozoic when a global-scale event triggered the onset of oxygenation throughout the water column. Despite this assertion, constraints on the depositional redox chemistry of the Proterozoic ocean remain elusive. Traditional proxies for water-column oxygen concentrations commonly fail when applied to Proterozoic sediments, including the simple use of presence or absence

of lamination to indicate benthic macrofaunal activity, as is widely applied in the Phanerozoic. As a result, models for Precambrian oxygenation commonly rely on terrestrial records (e.g., paleosol redox relationships) or indirect marine geochemical indicators, such as sulfate availability as inferred from the distribution of gypsum through time. Beyond inherent ambiguities, these methods are weakest when used to address local-scale patterns in marine oxygen availability. Given the lack of Proterozoic bioturbating organisms and the failure of the other traditional approaches, laminated Proterozoic black shales are less clearly products of anoxic deposition than their Phanerozoic equivalents. Recent work in modern anoxic settings (e.g., Black Sea and Cariaco Basin) has shown that Fe/Al ratios in fine-grained siliciclastic sediments are controlled by the presence or absence of hydrogen sulfide in the water column. In anoxic-sulfidic environments, the Fe/Al ratio is elevated relative to oxic sediments due to the scavenging of dissolved iron during water-column (syngenetic) pyrite formation. Delivery of this scavenged Fe is decoupled from the local terrigenous influx and therefore can drive up the Fe/Al ratio in anoxic basins during periods of low sediment accumulation. The basic hypothesis asserts that Fe/Al ratios in Proterozoic deep-water black shales will record the availability of oxygen during deposition and in doing so test basic models for the distribution of anoxia in the Proterozoic ocean. More specifically than addressing the absence of oxygen in the ocean, this method is intrinsically linked to the presence of hydrogen sulfide in the water column. Unfortunately, few data exist for coeval, shallow-shelf red shales of known oxic origin. These red shales, the focus of our ongoing study, provide the essential Fe/Al baseline for the continental influx, against which anoxic Fe enrichment and corresponding distributions of Proterozoic marine anoxia can be measured. It is our assertion that these red shales represent the oxic shallow waters of an ocean that may have otherwise been largely anoxic and sulfidic at depth. In this presentation, we will discuss the theory behind this method, results from modern and ancient Phanerozoic settings (e.g., Devonian and Pennsylvanian) and our preliminary results from Precambrian shales. Throughout, we will emphasize the importance of comparing data from temporally and spatially proximal red shales to the results for laminated black shales of uncertain paleoredox origin. We will also highlight analogous relationships for Mo/Al, wherein Mo is effectively scavenged (enriched) in the sulfidic water column so that, as for iron, the magnitude of enrichment relative to oxic crustal end members reflects the presence of sulfide in the water column in combination with the extent of dilution from the detrital influx. The balance between oxidation and reduction of sulfur at the earth's surface is intimately linked to the availability of oxygen in the coupled ocean-atmosphere system. This balance manifests as broad temporal shifts in the sulfur isotope composition of seawater sulfate and is well recorded in gypsum deposits throughout the Phanerozoic. In the near absence of gypsum in pre-Phanerozoic sediments, trace amounts of sulfate trapped within abiotic limestones and dolostones of Precambrian successions can be used to constrain the amount and isotopic composition of sulfate in ancient seawater. Our results to date for this carbonate-associated sulfate (CAS) in Mesoproterozoic samples show up to 10 permil sulfur isotope variation over relatively thin stratigraphic intervals. At one locality, this isotopic variability in CAS is corroborated by trends within coexisting gypsum. When compared to the temporally broader shifts of the Phanerozoic, this rapid Mesoproterozoic sulfur isotope response suggests an appreciably smaller oceanic sulfate reservoir. Such limitations in sulfate availability, presumably constrained by lower levels of ocean-atmosphere oxygen in the Proterozoic, may also be reflected in the global scarcity of gypsum prior to approximately 1.3 Ga and the abundance of isotopically heavy bacteriogenic iron sulfides. Model results will be presented linking inferred seawater sulfate concentrations to rates and magnitudes of sulfate-S isotope variability in the global ocean. CAS results will be discussed from the approx. 1.4 Ga Belt Supergroup of the northwestern USA, the approx. 1.2 Ga Apache Group of central Arizona, the approx. 1.2 Ga Bylot Group and approx. 1.3 Ga Dismal Lakes Group of arctic Canada, as well as the approx. 1.7 Ga McNamara Group of northwestern Queensland. Ultimately, our ability to integrate Fe- Mo-CAS records will allow construction of a comprehensive model for Mesoproterozic oceanic oxygen availability on both local and global scales.

Author

Precambrian Period; Sea Water; Sulfur; Oxygen; Oceans; Geochemistry; Marine Chemistry; Sediments

20020002167 California Univ., Dept. of Earth and Space Sciences, Los Angeles, CA USA

Geology and Age of Supracrustal Rocks, Akilia Island, Greenland: New Evidence for a greater than 3.83 Ga Origin of Life

Manning, Craig E., California Univ., USA; Mojzsis, Stephen J., Colorado Univ., USA; Harrison, T. Mark, California Univ., USA; Caciagli, Natalie, California Univ., USA; General Meeting of the NASA Astrobiology Insititute; April 2001, pp. 284-285; In English; See also 20020002018; No Copyright; Avail: Issuing Activity; Abstract Only

Supracrustal rocks on and near Akilia Island, southwest Greenland, have been proposed to contain both the oldest marine sediments in the geologic record, and the oldest evidence for active biological processes. These interpretations rely on three strongly contested geologic observations, including (1) the nature of crosscutting relations that constrain the age of sediments that host biosignatures; (2) the sedimentary origin of some lithologies; and (3) the interpretation of zircon ages. Despite heated debate about this locality and its geologic significance, the exposure has never been mapped or sampled on a scale appropriate to address the contested issues. In July 2000, we mapped the supracrustal outcrop at a scale of 1:250. This work substantially improves constraints on geologic and geochemical models of these rocks, and supports a is greater than 3.83 Ga origin of life. Supracrustal

rocks of Akilia Island are part of the early Archean Itsaq Gneiss Complex of west Greenland, in which bodies of deformed and metamorphosed sediments and lavas occur as meter to > 10 km blocks in highly deformed, heterogeneous tonalitic gneisses. The regionally extensive Itsaq Gneiss Complex is assigned an early Archean age based on numerous is greater than 3.5 Ga ages of igneous zircons in the tonalitic gneisses. The complex is intruded by younger Archean mafic dikes (Ameralik dikes, approx. 3.0 Ga) and Proterozoic granitic pegmatites, and experienced at least two middle to late Archean episodes of highgrade metamorphism and deformation. On Akilia Island, the main supracrustal sequence is exposed on the southwestern peninsula. The outcrop is approx. 150 x 200m. Supracrustal lithologies comprise compositionally distinct, mappable layers that are interpreted to correspond to original stratigraphy. Units include mafic amphibolites, ultramafic rocks, and Fe-rich clinopyroxene-quartz rocks, interpreted as metasedimentary banded iron formation. Map relations reveal that Fe-rich metasediment is part of the stratigraphy, rather than a later vein or intrusion. Found within the supracrustals, but not part of the stratigraphy, are from oldest to youngest: tonalitic orthogneiss of the Itsaq Gneiss Complex, Ameralik dikes and late leucocratic pegmatites. Structural relations of the supracrustals are complex. Three early ductile deformation (D1-D3) events were followed by one brittle deformation (D4). The earliest structures are foliations (S1) parallel to lithologic contacts, with locally preserved upright fold hinges. S1 foliations are isoclinally folded (D2) about a steep axial surface (S2). D3 refolded S2 about a steep NS axial plane (S3). Later brittle deformation is recorded as pegmatitic veins and dikes of presumed Proterozoic age. A key question about the age of the Akilia supracrustal lithologies centers on the nature of contacts between tonalitic gneisses and the supracrustal rocks. Tonalitic orthogneisses host the supracrustal block, but are also found within it. If the contacts are igneous, then the age of the tonalitic gneisses is a minimum for the supracrustals; if the contacts are structural, then the tonalite age is only a maximum supracrustal age. Ignoring exposures at the margins of the supracrustals, which are ambiguous as to origin, we identified two crosscutting tonalite bodies. When retrodeformed, both require dike-like geometric relations with the host supracrustals. The larger exposure is a 1-10 m wide tonalitic orthogneiss that is deformed by D1-D3 and crosscuts an ultramafic-amphibolite contact in the supracrustal stratigraphy. The second is a small (approx. 15 cm wide) tonalitic orthogneiss vein at a high angle to layering in a mixed amphibolite + ultramafic unit. Ion microprobe U-Pb geochronology has been carried out on zircons separated from the crosscutting tonalitic orthogneisses. The larger body yielded zircons of 3.85 Ga. High-resolution U-Pb ion microprobe measurements of 21 zircons from the smaller tonalite yielded ages of 3.6 to 3.83 Ga. of these zircons, a significant number (8/21) have ages that exceed 3.8 Ga and have a tight clustering of ages at 3.83 0.005 Ga. The oldest grains generally have higher Th/U and are interpreted to be the original magmatic population. In summary, the Fe-rich rocks, in which C isotopic evidence for biologic activity is preserved, define a mappable, laterally continuous lithology that is part of a coherent supracrustal stratigraphy. When the complex geometric relations in the supracrustals are retrodeformed, two tonalitic orthogneisses preserve clear crosscutting relations. Measurement of Th/U vs. U-Pb age by depth-profiling reveal that the only possible igneous components of these zircons are the 3.83 Ga cores. All other components are the result of later zircon growth associated with documented high-grade metamorphic events in the early to mid Archean. Thus, our new geologic and geochronologic constraints provide the strongest evidence yet for a sedimentary component to, and a is greater than 3.83 Ga age of, the Akilia supracrustals.
Author

Biological Evolution; Geochronology; Greenland; Earth Crust; Sediments; Precambrian Period; Minerals; Lithology; Geochemistry; Abiogenesis

20020002168 Harvard Univ., Botanical Museum, Cambridge, MA USA

Sedimentary Parameters Controlling Occurrence and Preservation of Microbial Mats in Siliciclastic Depositional Systems

Noffke, Nora, Harvard Univ., USA; Knoll, Andrew H., Harvard Univ., USA; General Meeting of the NASA Astrobiology Insititute; April 2001, pp. 286; In English; See also 20020002018

Contract(s)/Grant(s): NCC2-1053; DFG Proj. 380/1-1; DFG Proj. 380/1-2; BMFT LDP-9901/8-2; No Copyright; Avail: Issuing Activity; Abstract Only

Shallow-marine, siliciclastic depositional systems are governed by physical sedimentary processes. Mineral precipitation or penecontemporaneous cementation play minor roles. Today, coastal siliciclastic environments may be colonized by a variety of epibenthic, mat-forming cyanobacteria. Studies on microbial mats showed that they are not randomly distributed in modern tidal environments. Distribution and abundancy is mainly function of a particular sedimentary facies. Fine-grained sands composed of ”clear” (translucent) quartz particles constitute preferred substrates for cyanobacteria. Mat-builders also favor sites characterized by moderate hydrodynamic flow regimes, which permit biomass enrichment and construction of mat fabrics without lethal burial of mat populations by fine sediments. A comparable facies relationship can be observed in ancient siliciclastic shelf successions from the terminal Neoproterozoic Nama Group, Namibia. Wrinkle structures that record microbial mats are present but sparsely distributed in mid- to inner shelf sandstones of the Nudaus Formation. The sporadic distribution of these structures reflects both the narrow ecological window that governs mat development and the distinctive taphonomic conditions needed to

preserve the structures. These observations caution that statements about changing mat abundance across the Proterozoic-Cambrian boundary must be firmly rooted in paleoenvironmental and taphonomic analysis. Understanding the factors that influence the formation and preservation of microbial structures in siliciclastic regimes can facilitate exploration for biological signatures in Earth's oldest rocks. Moreover, insofar as these structures can be preserved on bedding surfaces and are not easily mimicked by physical processes, they constitute a set of biological markers that can be searched for on Mars by remotely controlled rovers.

Author

Bacteria; Mars Surface; Microorganisms; Rocks; Sediments; Petrology; Extraterrestrial Life

20020002169 Connecticut Univ., Dept. of Molecular and Cell Biology, USA

How Much Did Horizontal Gene Transfer Contribute to Early Evolution? Quantifying Archaeal Genes in Two Bacterial Lineages

Olendzenski, Lorraine, Connecticut Univ., USA; Zhaxybayeva, Olga, Connecticut Univ., USA; Gogarten, J. Peter, Connecticut Univ., USA; General Meeting of the NASA Astrobiology Insititute; April 2001, pp. 287-288; In English; See also 20020002018; No Copyright; Avail: Issuing Activity; Abstract Only

The occurrence of horizontal gene transfer (HGT) among microbes is well accepted, but the extent to which the transfer of genes has impacted microbial evolution is unclear. Transfers most often occur between closely related organisms, however instances of transfer across domains can be inferred from the analysis of gene sequences. In the case of proton pumping ATPases, the bacterial lineages Deinococcaceae and Spirochaetaceae do not have an F-ATPase like other bacteria, but possess a complete A/V-ATPase typically found in Archaea and Eukaryotes. Members of these lineages also possess archaeal type prolyl tRNA synthetases and malate dehydrogenases (Gogarten et al., 1999). to understand the extent to which these Bacteria have acquired genes from the Archaea, we have used a bioinformatics approach employing whole genome analysis to assess the occurrence of interdomain transfer into these lineages. Putative open reading frames (ORFs) from the prerelease version of the Deinococcus radiodurans genome and ORFs from the available completed genomes of Borrelia burgdorferi and Treponema pallidum were screened for genes more closely related to archaeal or eukaryotic genes. ORFs were searched against representative reference genomes from each of the three domains using a local version of automated BLAST. Gapped BLAST was run for each ORF against amino acid sequences of ORFs from a single reference genome, using BLASTP with the BLOSUM62 matrix with filtering for low complexity regions. Sequence manipulations using the SEALS package of programs (Walker and Koonin, 1997) greatly facilitated the analysis of the Treponema and Borrelia genomes. For each BLAST run, only the top hit was reported and the High Score Pair (HSP) or Bit Score was retained in a file. These data were then loaded into an Oracle database or into a Microsoft Excel spreadsheet and ranked according to the difference: MAX SCORE(Archaea, Eukaryotes) - MAX SCORE(Bacteria) where SCORE represents HSP values or Bit Score values depending on the version of BLAST used. Each potential D. radiodurans ORF was compared against each of five individual reference genomes: Saccharomyces cerevisiae, Methanococcus jannaschii, Escherichia coli, Bacillus subtilis, and Aquifex aeolicus. Reference genomes for the Treponema and Borrelia analyses were the same as those used for D. radiodurans, plus Drosophila melanogaster and Archeoglobus fulgidus. ORFs showing highest matches against archaeal and eukaryotic genes were collected and ranked. For Deinococcus, the top ranked hits were the A/VATPase catalytic and non-catalytic subunits and the prolyl RS genes. For each top ranking hit, datasets of orthologous amino acid sequences were assembled from the nonredundant protein database of Genbank and analyzed using neighbor joining as implemented in Clustal W and quartet puzzling methods found in PUZZLE. All trees were assessed for evidence of horizontal gene transfer. Trees scored as positive for HGT were of two varieties-- those that showed typical three domain structure with few bacterial species (including Borrelia, Treponema or Deinococcus) grouping with Archaea or Eukaryotes, and those that showed disjunct distribution among species represented in the non-redundant database. Disjunct distribution (i.e. with most representatives found among Archaea or Eukaryotes and few homologs among the Bacteria) are interpreted to represent genes that have been transferred among the representatives (as opposed to being inherited vertically and lost multiple times). Negative topologies were found among those hits that were not represented in the reference genomes, or among those genes which were highly conserved and showed relatively high bit scores for two or more domains. of the 45 top ranked genes for Deinococcus, 20 showed topologies in which D. radiodurans homologs clearly group with eukaryotic or archaeal homologs, and seventeen additional trees were found to show probable evidence of horizontal gene transfer. Top ranked hits for Borrelia were the isoleucyl-tRNA synthetase, the V-type ATPase, prolyl-tRNA synthetase, methionyl-tRNA synthetase and lysyl-tRNA synthetase. of 37 top ranked Borrelia ORFs analyzed with phylogenetic methods, 27 showed evidence or potential evidence for horizontal gene transfer between domains. Compared to the total number of ORFs in the Deinococcus and Borrelia genomes, those that can be identified as having been acquired from Archaea or Eukaryotes are relatively few (approximately 1-1.5%), suggesting that interdomain transfer is rare. Similar methods need to be employed to assess the potential contribution of intradomain transfer from other Bacterial lineages into these genomes. Additionally, many of the phylogenies showing presence of archaeal genes in the

Deinococcaceae or Spirochetes, also include Chlamydia, Chlamydophila, Rickettsia, Mycobacterium, and Streptomyces. These Bacteria could be candidates for higher occurrence of interdomain gene transfer in comparison to other Bacterial lineages. Author

Bacteria; Enzymes; Genes; Genome; Microorganisms; Biological Evolution

20020002170 Pennsylvania State Univ., Astrobiology Research Center, University Park, PA USA

Dissolution Kinetics of Natural Uraninite and the Evolution of Atmospheric Oxygen

Ono, Shuhei, Pennsylvania State Univ., USA; Ohmoto, Hiroshi, Pennsylvania State Univ., USA; General Meeting of the NASA Astrobiology Insititute; April 2001, pp. 289-290; In English; See also 20020002018; No Copyright; Avail: Issuing Activity; Abstract Only

The evolution of the early Earth's atmosphere is a key to understand how the terrestrial biosphere has co-evolved with the Earth's environment. Oxygenic photosynthesis emerged on the Earth sometime before 2.7 Ga and set the stage for the establishment of abundant atmospheric oxygen. However, the current dominant model of atmospheric evolution suggests that the atmospheric oxygen level remained very low until about 2.2 Ga (e.g. Holland, 1984). The occurrence of detrital uraninite (UO2) in some 2.9 to 2.2 Ga quartz-pebble conglomerates is the most important evidence of oxygen-poor atmosphere prior to 2.2 Ga. Since uraninite is thermodynamically unstable under an oxygenated environment, the survival of detrital uraninite in river sediments would imply oxygen-poor atmosphere. A quantitative estimate of the pre-2.2 Ga atmospheric oxygen level relies on the dissolution kinetics of uraninite. Based on the kinetic data obtained by Grandstaff (1976), Holland (1984) estimated the pO2 level of the Archean atmosphere to be less than 0.1% of the present atmospheric level (PAL). No systematic study on the dissolution rates of natural uraninite has been reported since Grandstaff (1976) but the dissolution rate of synthetic UO2 glass was recently reported to be about 2 orders of magnitude slower than that obtained by Grandstaff for natural uraninite (e.g. de Pablo et al., 1999). We constructed a flow-through system to study dissolution rates of natural uraninite under various pH (4 to 8), pCO2 (1 PAL and 100 PAL) and pO2 (1 PAL and 0.1 PAL) conditions, in order to better constrain the dissolution kinetics of natural uraninite. The system is similar to the one used by de Pablo et al. (1999) for the dissolution experiments of synthetic UO2 glass. Natural uraninite samples taken from three localities were powdered to a particle size of 80 to 120 microns, washed, weighed to approx. 0.5 g, and introduced into the reactors. The ionic strength of the leaching solution is set to 0.01 M by NaClO4 and pH is controlled by HClO4 and NaOH. A mixture of N2, CO2, and O2 gas was bubbled through the leaching solution to simulate the Archean atmosphere. Our data suggest uraninite dissolution rates are slower and less dependent on pH, pO2 and pCO2 than those reported by Grandstaff (1976). Dissolution rates of natural uraninite under high pCO2 (100 PAL) and low pH (4 to 5) solution, a likely condition for the Archean rainwater, are much slower than that computed from Grandstaff's rate law, indicating detrital uraninite may survive under high pCO2 Archean atmosphere regardless of pO2 level. We suggest the occurrence of pre-2.2 Ga placer uraninite deposits may reflect the abundant uraninite-rich source rocks in the area rather than the atmospheric evolution of the early Earth.

Author

Dissolving; Earth Atmosphere; Uranium Oxides; Earth Environment; Biological Evolution; Planetary Evolution; Oxygen; Precambrian Period

20020002171 Pennsylvania State Univ., Dept. of Geosciences, University Park, PA USA

Hydrocarbon Haze as a Source of Low C-13 Late Archean Kerogens

Pavlov, Alexander, Pennsylvania State Univ., USA; Kasting, James F., Pennsylvania State Univ., USA; General Meeting of the NASA Astrobiology Insititute; April 2001, pp. 291-292; In English; See also 20020002018; No Copyright; Avail: Issuing Activity; Abstract Only

High concentrations of greenhouse gases are required to offset low solar luminosity early in Earth's history. Previous studies suggested high CO2 concentrations as a solution to the faint young sun paradox. However, the late Archean atmosphere should have been rich in biologically-generated CH4 which would have provided additional warming. Calculations based on the thermodynamic energy yield from microbial metabolism predict that methanogens should have converted most of the available H2 into CH4, producing an atmospheric CH4 concentration of about 1000 ppm. An independent line of evidence for high methane abundances comes from the photochemical modeling of methane destruction. If the Archean biota were manufacturing CH4 at a rate comparable to the modern biota, atmospheric CH4 mixing ratios of the order of 10(exp -3) are predicted. Such a high atmospheric CH4 abundance should have led to CO2 drawdown by way of a negative feedback loop involving the carbonate-silicate geochemical cycle. High CH4 levels would have raised surface temperature, Ts, by increasing the atmospheric greenhouse effect, stimulating biological production of CH4 and facilitating silicate weathering on the continents, causing atmospheric CO2 concentrations to decrease. We suggest here that the atmospheric CH4/CO2 ratio approached the value of approx. 1 needed to trigger formation of Titan-like organic haze. Previous studies predicted CH4 polymerization and formation

of organic haze in the Archean atmosphere. However, there was no constraint on how thick this haze layer could have been and at what rate the haze should have been generated. Our calculations show that the optical thickness of the layer could not have been more than 0.6 otherwise, a strong ”antigreenhouse effect” would have cooled the surface and killed the methanogens. Assuming that the Archean surface temperature was not too different from its present value, we have calculated the abundance of hydrocarbon particles in the Archean atmosphere and the rate of their production. The total deposition flux of organic haze particles under those conditions would have been comparable to the modern rate of organic carbon burial. This haze should have been strongly depleted in C-13 relative to C-12 because it was formed from isotopically ”light” biological methane and was fractionated further during the polymerization process. Hence, it could provide an alternative explanation for the presence of extremely low C-13 kerogens in Late Archean sediments.

Author

Geochemistry; Kerogen; Carbon 13; Solar Radiation; Microorganisms; Hydrocarbons; Atmospheric Effects; Atmospheric Composition; Carbon Dioxide Concentration; Gas Composition; Methane; Photochemical Reactions

20020002172 Puget Sound Univ., Dept. of Biology, Tacoma, WA USA

The Anoxygenic Filamentous Phototrophs: (1) Recent Advances in Diversity and Phylogeny (2) The Place of Chloroflexus in High Iron Hot Springs

Pierson, Beverly K., Puget Sound Univ., USA; Scapa, Victor, Puget Sound Univ., USA; Klappenbach, Joel, Michigan State Univ., USA; General Meeting of the NASA Astrobiology Insititute; April 2001, pp. 293-294; In English; See also 20020002018; No Copyright; Avail: Issuing Activity; Abstract Only

The anoxygenic filamentous phototrophs are the deepest branching phototrophs on the Bacterial branch of the tree of life. Until recently, phylogenetic data as complete 16S rDNA sequences were available only for species of the genus Chloroflexus. Other uncultured organisms that were thought to be related to Chloroflexus were known only from their similar ultrastructural and physiological characteristics. All filamentous phototrophs were lumped into this group with Chloroflexus with little or no sequence data to support that association. In the past year sequence data have been obtained in different laboratories for several different filamentous phototrophs. New species descriptions have appeared, new cultures have been isolated, and new physiological data have been produced. We now know that this group of phototrophs is surprisingly large and diverse. All the filamentous phototrophs indeed appear to belong together. Because of their diversity, these organisms may hold as a group important information about the evolution of photosynthesis. Among the recently obtained phylogenetic data are sequences for Chloronema, Oscillochloris, the hypersaline marine Chloroflexus-like organism (MCLO), and the red filamentous ”Roseiflexus castenholzii.” New physiological data are also available for all of these organisms as well as for the red filamentous RCR organisms. We present a phylogenetic tree showing that substantial differences exist among these organisms but that all the filamentous phototrophs form a cohesive cluster distinct from the chemotrophs in this branch of the tree. There may be a ”green line” of descent that includes Chloroflexus, Oscillochloris, Chloronema, and the MCLO, all of which have chlorosomes and bacteriochlorophyll c. A ”red line” of descent may include Roseiflexus, Heliothrix, and the RCR, all of which lack chlorosomes and bacteriochlorophyll c but do have bacteriochlorophyll a. The incomplete sequence data for Heliothrix and the absence of sequence data for the RCR make this conclusion speculative. All of these organisms except Chloronema, are mat-formers. Chloronema is planktonic and found in anoxic zones in lakes containing sulfide and reduced iron. Chloronema, Oscillochloris and the MCLO are mesophiles. The others are moderate thermophiles. Among the interesting features of the diversity of this group are distinctive absorption spectra of the bacteriochlorophylls and diversity in the carbon dioxide fixation pathways. Chloroflexus has the unique 3-hydroxypropionate pathway and Oscillochloris uses the Calvin Cycle. Chloroflexus sp. are universal inhabitants of microbial mats in neutral to alkaline hot springs around the world. We have found and cultured a strain from a high iron hot spring mat at 50-54 C. In situ, it forms a mat in association with the unicellular cyanobacteria Synechococcus lividus and Cyanothece minnervae. The mats are very thin and form near the sources of the springs which are anoxic and high in ferrous iron (0.1 mM). Studies of the mats in situ have shown that oxygenic photosynthesis occurs in the light. The mats are substantially lower in oxygen levels and pH, however, than typical Synechococcus/Chloroflexus mats observed in low iron springs. We are attempting to determine the relationship, if any, between the iron in the springs and the photosynthetic activity in both the cyanobacteria and Chloroflexus.

Author

Bacteria; Microorganisms; Photosynthesis; Plankton; Biological Evolution; Photochemical Reactions

20020002173 Pennsylvania State Univ., Dept. of Biology, University Park, PA USA

Independent Land Colonization Events by Myriapods and Hexapods During the Neoproterozoic

Poling, Laura L., Pennsylvania State Univ., USA; Lyons-Weiler, Maureen, Pennsylvania State Univ., USA; Hedges, S. Blair, Pennsylvania State Univ., USA; General Meeting of the NASA Astrobiology Insititute; April 2001, pp. 295; In English; See also 20020002018; No Copyright; Avail: Issuing Activity; Abstract Only

The fossil record suggests the macroevolutionary events that led to increased diversity of Metazoan (animal) body plans occurred within a short geological time span known as the Cambrian 'Explosion'. However, recent molecular studies have suggested that animal diversification occurred much earlier. The arthropods figure prominently in the Cambrian Explosion and therefore we chose this group to examine these questions in more detail with new molecular data. Arthropoda is a diverse animal phylum composed of four living classes whose evolutionary relationships have been controversial. These are Myriapoda (centipedes and millipedes), Hexapoda (insects), Crustacea (crabs, brine shrimp, and water fleas), and Chelicerata (spiders, scorpions, and horseshoe crabs). Traditionally Myriapoda and Hexapoda were considered sister taxa based on characteristics associated with terrestrialization and were placed together in the taxon "Atelocerata". However, new sequence data from two genes, enolase and glyceraldehyde 3-phosphate dehydrogenase, combined with two genes from a previous study, RNA polymerase II (large subunit) and elongation factor 1 alpha, significantly support a Myriapoda-Chelicerata grouping to the exclusion of Hexapoda and suggest a placement of Hexapoda with Crustacea. This indicates that the two separate lineages, Myriapoda and Hexapoda, colonized land independently and that the terrestrial characteristics used to group them are due to convergence. Additionally, these four genes and several others were used for divergence time estimation. The times indicate that these colonizing events took place at about the same time as the Neoproterozoic 'Snowball Earth' episodes, much earlier than the Cambrian Explosion.

Author

Organisms; Biological Evolution; Biological Diversity; Biochemistry; Precambrian Period

20020002174 Pennsylvania State Univ., Dept. of Biochemistry and Molecular Biology, University Park, PA USA

Characterization of a Carbonic Anhydrase from an Obligately Chemolithoautotrophic Thermophilic Archaeon

Smith, Kerry S., Pennsylvania State Univ., USA; Ferry, James G., Pennsylvania State Univ., USA; General Meeting of the NASA Astrobiology Insititute; April 2001, pp. 296; In English; See also 20020002018; No Copyright; Avail: Issuing Activity; Abstract Only

The atmosphere of earth at the origin of life is thought to be a weakly reduced mixture of CO2 and N2 combined with lesser amounts of CO, H2, and reduced S gases. Experiments by Wachtershauser suggest a chemoautotrophic origin of life in which early organisms could fix CO2 and CO enzymatically. Carbonic anhydrase, a zinc-containing enzyme catalyzing the reversible hydration of CO2 (CO2 + H2O <#0106>> HCO3(-) + H(+)), plays a key role in CO2 fixation in extant organisms. Based on amino acid sequence comparisons, carbonic anhydrases belong to three genetically distinct classes (alpha, beta, and gamma) suggesting this enzyme has been invented independently at least three times. Molecular clock analysis indicates that both the beta and gamma classes have ancient origins suggesting a role for this enzyme in the CO2 fixation of early organisms. To better understand the role of this enzyme in early organisms, we have both biochemically and structurally characterized bata class carbonic anhydrase (Cab) from the deeply branching obligately chemolithoautotrophic archaeon Methanobacterium thermoautotrophicum. This microbe has a high demand for CO2 in that not only does all of its cellular energy derive from the reduction of CO2 to methane but also all of its cellular carbon derives from CO2. Therefore, Cab is expected to play an important role in the growth of M. thermoautotrophicum and may have several functions. of the three known classes of carbonic anhydrase, the beta class is the most diverse at the amino acid sequence level. The results of my work confirm that the beta class is in fact composed of two subclasses and both biochemical and structural experiments indicate that Cab is the prototype for one of these subclasses. In addition, only five amino acid residues are completely conserved in all class sequences. Three of these conserved residues serve as ligands for the active site zinc and we have identified potential roles for other two conserved amino acid residues in the catalytic mechanism of beta class enzymes.

Author

Biochemistry; Biological Evolution; Carbonic Anhydrase; Carbon; Earth Atmosphere; Microorganisms; Archaebacteria; Thermophiles

20020002175 Arizona State Univ., Astrobiology Program, Tempe, AZ USA

Molecular Evolution Analysis of Photosynthesis

Raymond, Jason R., Arizona State Univ., USA; Lince, Michael T., Arizona State Univ., USA; Blankenship, Robert E., Arizona State Univ., USA; General Meeting of the NASA Astrobiology Insititute; April 2001, pp. 297; In English; See also 20020002018; No Copyright; Avail: Issuing Activity; Abstract Only

Recent initiatives in whole genome sequencing and the collection and successful culturing of new organisms have greatly facilitated the study of the evolution of photosynthesis at the molecular level. The first of these two fronts has resulted in the completion of representative genomes from four of the five known prokaryotic photosynthetic lineages. The second front has lead to the discovery of Acaryochloris marina, a cyanobacterial-type marine endosymbiont singular in its use of chlorophyll d as a major photopigment. Chlorophyll d is structurally and energetically intermediate between chlorophyll a and bacteriochlorophyll a, a characteristic consistent with a pigment which might have been utilized in the evolutionary transition from anoxygenic to oxygenic photosynthesis. Our current work is focused on addressing the biochemical and evolutionary aspects of the novel pigment complement in A. marina through the sequencing of photosystem and chlorophyll biosynthesis genes. Concurrently, phylogenetic analyses are being carried out using these and newly completed sequences from representative anoxygenic and primitive oxygenic phototrophs with the goal of refining our understanding of early evolutionary events in photosynthesis.
Author
Biosynthesis; Chlorophylls; Genes; Genome; Organisms; Photosynthesis; Biological Evolution; Molecular Biology

20020002176 Pittsburgh Univ., Dept. fo Geology and Planetary Science, Pittsburgh, PA USA
Geochemical and Isotopic Investigation of Paleozoic Paleosols Formed Under Varying Redox Conditions
Reynolds, Amanda C., Pittsburgh Univ., USA; Capo, Rosemary C., Pittsburgh Univ., USA; Stewart, Brian W., Pittsburgh Univ., USA; General Meeting of the NASA Astrobiology Insititute; April 2001, pp. 298-300; In English; See also 20020002018; No Copyright; Avail: Issuing Activity; Abstract Only

The Permo-Pennsylvanian Monongahela Group consists of cyclic freshwater bay, deltaic, and alluvial fan sediments deposited approximately 290 million years ago in the Dunkard basin (SW Pennsylvania, W. Virginia and Ohio). The lacustrine Benwood limestone dominates the deeper parts of the basin. Toward the basin edges, the deposits grade into thin interbedded marly limestones, claystones and shales indicative of a shallower water regime and fluctuating lake levels. These lake-edge deposits can be divided into two end members: the green (northern) and red (southern) facies. In the northern part of the basin, massive limestones are interbedded with green shale and thin (cm-scale) claystones. to the southeast, the limestone beds thin and grade into shales and redbeds. Thick (1-4 m) redbeds, interbedded with clay-shales and limestones, are ubiquitous along the southern rim. to better understand the geochemistry of ancient freshwater lacustrine sequences and sediments affected by variable redox conditions, we are studying outcrops of red and green units formed along the lake edge, and deeper water lacustrine limestones and claystones from a 50 m core. Units from both facies display evidence of soil-forming processes and/or subaerial exposure. Limestone layers with mudcracks, microkarst, and dolomite suggest cyclic wet and dry periods. Both red and green facies paleosols are characterized by root casts, a diffuse lower contact with the calcareous clay-shale parent material, and a sharp erosional contact with the overlying limestone. Some redbed paleosols also contain calcareous nodules, blocky to columnar ped-like structures, mottling (5R 4/4 and Gley 2 4/5pb), and gilgai, indicative of arid, oxidizing conditions. Green paleosols contain evidence of reducing conditions (such as gley textures, color and mineralogy) Geochemistry of two redbed paleosol units (Middle Island Creek and England's Run) indicate the net loss of base cations (Ca, P, Mg, K and Na) from the profile and the displacement of more immobile cations (Mn, Fe, and Si) to lower parts of the weathering profile. Preliminary Nd isotope data indicate a narrow range of e(Nd) values (-8 to -10) for the silicate fraction of lacustrine calcareous shales and paleosol silicates, suggesting derivation from a common, constant sediment source. Nd-143/Nd-144 vs. Sm-147/Nd-144 and Rb-87/SR-86 vs. SR-87/SR-86 display linear correlations consistent with the derivation of both lake detritus and paleosols from isotopically homogeneous Permo-Pennsylvanian sediments that were fractionated with respect to REE and Rb/SR during sedimentary or pedogenic processes.
Author
Geochemistry; Oxidation-Reduction Reactions; Isotope Ratios; Mineralogy; Paleozoic Era; Paleontology; Biological Evolution

20020002177 California Univ., Dept. of Earth and Space Sciences, Los Angeles, CA USA
Archean Sulfates from Western Australia: Implications for Earth's Early Atmosphere and Ocean
Runnegar, Bruce, California Univ., USA; General Meeting of the NASA Astrobiology Insititute; April 2001, pp. 301-302; In English; See also 20020002018; No Copyright; Avail: Issuing Activity; Abstract Only

Early Archean sedimentary sulfates (barites) from Africa, Australia, and India are only slightly enriched in the heavy isotope of sulfur in comparison with contemporaneous sulfides. This small separation of oxidized and reduced reservoirs has long been used as evidence for and against the activity of sulfate-reducing bacteria prior to about 2.5-2.7 Ga ago. However, it is now clear that the accelerated rates of bacterial sulfate reduction together with higher ambient temperatures and closed-system settings advocated by Ohmoto and others cannot easily explain the limited isotopic variability and slight 34S enrichment of Archean sulfates. The recent discovery of sizeable, mass-independent fractionations of all four stable isotopes of sulfur in early Archean sulfates from Africa and Australia, confirming earlier evidence from India, provides a new opportunity for understanding the

Archean sulfur cycle. Pioneering work on bedded barites from the North Pole area of Western Australia indicated that they are diagenetic replacements of evaporitic gypsum crystals that had grown on or just below the Archean sea floor. This interpretation was based on interfacial angles measured with a universal stage on relatively few crystals. In order to improve the crystallographic database, X-ray computerized tomography (CT) was used to image in situ barite crystals. At the operating energy levels, barite attenuates X-rays significantly more than metallic iron, so the contrast between the barite crystals and the quartz matrix is profound. Analysis of the processed images, casts of natural external molds of barite crystals, and large thin sections using polarized light, conclusively demonstrates that the original mineralogy was barite, not gypsum. A close genetic link between the bedded barites and syndepositional barite dikes is provided by plots of all four stable isotopes of sulfur which form arrays that parallel terrestrial mass fraction lines but have y-axis intercepts significantly far from zero. This is excellent evidence that the hydrothermal fluids involved in dike production were cycling sulfates from the same source as the bedded barites. The non-zero intercepts are indicative of sizeable mass-independent fractionations of the sulfate. As these effects are only known to be produced by atmospheric (gas-phase) processes in terrestrial materials, it is likely that the barites were formed from sulfate sulfur that had participated in atmospheric reactions. A corollary is that the Archean oceans may not have contained much sulfate.
Author

Atmospheric Chemistry; Atmospheric Composition; Sulfides; Earth Atmosphere; Australia; Geochemistry; Mineralogy; Oceans; Precambrian Period; Sediments; Planetary Evolution

20020002178 Pittsburgh Univ., Dept. of Geology and Planetary Science, Pittsburgh, PA USA

Neodymium Isotope Investigation of a Precambrian Weathering Profile: Hokkalampi Paleosol, North Karelia, Eastern Finland

Stafford, Sherry L., Pittsburgh Univ., USA; Capo, Rosemary C., Pittsburgh Univ., USA; Stewart, Brian W., Pittsburgh Univ., USA; Marmo, Jukka, Geological Survey of Finland, Finland; Ohmoto, Hiroshi, Pennsylvania State Univ., USA; General Meeting of the NASA Astrobiology Insititute; April 2001, pp. 303-304; In English; See also 20020002018; No Copyright; Avail: Issuing Activity; Abstract Only

Paleosols, preserved ancient soils, are significant to the study of past life, climate, and landscapes on Earth and serve as the primary analogues for the development of life on other planets. by preserving chemical products of atmospheric-mineral interaction, Precambrian paleosols are also key to understanding the past chemistry and evolution of the Earth#s atmosphere. However, many challenges inhibit the interpretation of the Precambrian soil record including difficulty constraining ages, overprinting by thermal events, and deformation of soil textures and structures. to better understand the diagenetic and metamorphic processes that have obscured the ancient soil record, we have begun a neodymium (Nd) isotope study of the Hokkalampi paleosol in eastern Finland. Nd isotopes have proven useful in previous study of the 3.0 Ga Steep Rock paleosol, which was overprinted by a 2.7 Ga greenschist metamorphic event. The thermal event did not mask the geochemical signature of the Nd isotopic system. The measurements formed an apparent isochron that could date the age of soil formation. The Hokkalampi paleosol is of particular interest because it formed between 2.5 Ga and 2.1 Ga during the proposed rise of atmospheric oxygen. Previous work by Marmo established geochemical evidence that the Hokkalampi area contains a widespread paleosol. The weathering profile formed on Archean basement and glacioigenic material and is unconformably overlain by aluminum, quartz, and/or hematite rich metasedimentary rocks The age of the paleosol is constrained between the Archean basement (3.1-2.5 Ga) and the 2.1 Ga mafic rock which intrudes the overlying metasediments. The profile grades upward from granitoid parent to carbonate bearing, quartz-feldspar sericite (partially altered parent) to quartz-sericite schist (weathering profile). The paleosol, produced by intense chemical weathering, ranges in thickness from 15 meters at the paleotopographic high to 80 meters at the paleotopographic low. The weathering profile ranges from oxidized, iron-enriched areas to reduced, iron-poor areas. The paleosol was altered by a greenschist metamorphic event 1.9 Ga during the Svecofennian Orogeny. Outcrop and drill core samples were collected from two localities: Nuutilanvaara and Paukkayanvaara. Both paleosol locations formed over Archean basement. However, Nuutilanvaara contains oxidized paleosol with iron enrichment and is interpreted to be above the paleo-water table; Paukkayanvaara contains reduced paleosol with iron depletion and is interpreted to be below the paleo-water table. Whole rock Sm-Nd measurements were carried out on representative zones from each locality, including parent rock, quartz-feldspar sericite (partially altered parent), and quartz-sericite schist (weathering profile). When Nd-143/Nd-144 and Sm-147/Nd-144 data from both localities are plotted together, they form a linear array corresponding to an apparent age of 2.4 +/- 0.4 Ga. If the correlation indeed represents a crude isochron, two possible explanations are suggested: (1) The age corresponds to timing of basement formation, and the whole rock samples represent reworked, fractionated basement material; or (2) pedogenic processes fractionated Sm/Nd, the age represents the time of pedogenesis. In either case, the Nd isotope systematics indicate that the parent

material for both profiles is derived from the same, relatively uniform source. This makes the Hokkalampi profile an excellent candidate to compare early Proterozoic weathering processes under locally varying redox conditions.
Author
Isotope Ratios; Precambrian Period; Neodymium Isotopes; Geochemistry; Weathering; Metamorphism (Geology); Mineralogy; Sediments; Soils; Planetary Evolution

20020002179 Stanford Univ., Dept. of Geological and Environmental Sciences, Palo Alto, CA USA
Shallow to Deep Water Transitions on Early Archean Subsiding Platforms, Barberton Greenstone Belt, South Africa
Tice, Michael M., Stanford Univ., USA; Lowe, Donald R., Stanford Univ., USA; General Meeting of the NASA Astrobiology Insititute; April 2001, pp. 305; In English; See also 20020002018; No Copyright; Avail: Issuing Activity; Abstract Only

Sediments from the early Archean were commonly extensively and syndepositionally silicified. In areas of high organic burial and low clastic input, typical resultant carbonaceous facies are massive black cherts, black and white banded cherts, and banded ferruginous cherts. While these chert types are recognized in many early Archean units, their significance for environmental interpretation is unclear. Two sections were measured through carbonaceous cherts in the uppermost Mendon and Kromberg formations. The detrital content of each section was extremely low; this is interpreted to indicate deposition on platforms. The first section (MBC1), in the uppermost Mendon, progresses from an erosional contact with the underlying Msauli Chert to banded ferruginous cherts and flat-laminated ash at the top. The second section (BRC1), in the uppermost Kromberg, progresses from silicified evaporites at the base to banded ferruginous cherts at the top. Both sections show characteristic progressions from massive or current/wave structured black cherts, through black and white banded cherts showing progressively thinner and more laterally continuous bands, to banded ferruginous cherts. It is possible that this progression generally characterizes shallow to deep water transitions in clastic-poor, organic-rich, silicified sediments from the early Archean, and that these sections record changing environments on subsiding platforms. Ongoing work on these sections includes a petrographic classification of carbonaceous grain types, measurement of bulk elemental compositions, and measurement of carbon isotopic compositions of bulk kerogen, carbonate, and individual carbonaceous grains. These analyses should allow description of changing microbial communities and redox conditions accompanying changing water depth on these platforms.
Author
Shallow Water; Sediments; Precambrian Period; Mineral Deposits; Microorganisms; Isotopic Labeling; Chemical Composition; Carbonates; Planetary Evolution; Petrology; Geochemistry

20020002180 Portsmouth Univ., School of Earth and Environmental Sciences, Portsmouth, UK
The Combined Detection of Morphological and Molecular Biomarkers: Implications for Astrobiology
Toporski, J., Portsmouth Univ., UK; Steele, A., Montana State Univ., USA; Westall, F., Lunar and Planetary Inst., USA; McKay, D. S., NASA Johnson Space Center, USA; General Meeting of the NASA Astrobiology Insititute; April 2001, pp. 306-307; In English; See also 20020002018; No Copyright; Avail: Issuing Activity; Abstract Only

Experience gathered by previous researchers during their hunt for evidence of early Earth life has shown the complexity in interpreting observations of possible microfossils and to establish the evidence to be positive. Similarly, the stillsimmering controversy on the nature of the nano-structures in Martian meteorite ALH84001 described by McKay et al. (1996) emphasizes the difficulties of conclusively identifying those structures as (a) fossilized bacterial cells and (b) establish their indigeneity. A better understanding of biological signatures in rocks is needed in order to identify traces of microbial life, which include morphological, mineralogical and chemical traces. It is thus considered crucial to tackle the problems emerging in the search for evidence of early life on Earth and in exopaleontological research with a multidisciplinary approach. With this is mind we applied surface sensitive Time of Flight-Secondary Ion Mass Spectroscopy (ToF-SIMS) to a previously described 25 m.y. old fossil bacterial biofilm. This technique allows in situ analysis with high mass resolution as well as molecular imaging of micron sized structures. As no extraction or derivatisation of the sample is required for ToF-SIMS analysis, electron microscopical investigation of the same samples subsequent to analysis is possible, thus allowing the combination of molecular and morphological biomarkers. The analysed fossil bacterial biofilms were associated with macrofossils from volcanoclastic lacustrine sediments from the Upper Oligocene Enspel formation (Germany). Preliminary scanning electron microscopy (SEM) studies have shown that a fossil structure interpreted as a coprolite purely consisted of fossilized bacterial biofilm. For ToF-SIMS investigation small particles were taken from the fossil biofilm and mounted onto Au-coated In-foil and analysed in a Phi Evans T-2000 TRIFT system. The ToF-SIMS analysed samples were Au/Pd-sputter coated and imaged using a Philips XL40 Field Emission Gun SEM (FEG-SEM). ToF-SIMS analysis of the organic rich fossil biofilm (TOC 29%) in the 0-100 Dalton (Da) range showed significant amounts of inorganic species, confirming the results obtained previously by EDX analysis, clearly showing the bacterial fossils to be mineralised. ToF-SIMS furthermore revealed the presence of a variety of low- and high-mass organic molecules and fragments thereof. These include peaks indicative of alkenes and alkanes, aromatic organic species and the

polycyclic aromatic hydrocarbon naphthalene. More tentatively, peaks indicative of alkyl pyrroles and pyridyl-CH2 were identified. Other peaks of interest include peaks indicative of C(n)H(2n)O2 and C(n)H(2n-2)O2, which according to their general formula would suggest the presence of both saturated and unsaturated fatty acids although further in situ derivatisation experiments and GC-MS (Gas Chromatography MS) need to be applied to verify this beyond doubt. Furthermore, peaks at m/z 370, 384, 398, 412, 426, 440, 454 and 468 were identified, which indicate the potential presence of bacterial hopanes, a class of biomarkers indicative of bacteria. The main diagnostic peak for this group of chemicals is the fragment at m/z 191.18. Our studies conducted on purified hopane standards have shown that in the high-mass resolution mode differentiation of this diagnostic hopane peak and polyethylene at m/z 191.05 is possible. However, the spectra discussed here were collected in the lower resolution mapping mode, therefore this differentiation was not possible. The centroids of the possible hopane peaks obtained on the fossil biofilms are well within the range associated with bacterial hopanes. There is a strong possibility therefore that hopanoids may be associated with the fossil bacterial cells. Due to the non-destructive nature of ToF-SIMS, analysed samples can be studied using SEM, thus allowing the combination of morphological and molecular biomarkers. Subsequent SEM analysis of the ToF-SIMS analysed samples confirmed that the analysed material purely consists of fossil bacterial cells. This is thus the first successful effort to demonstrate the combination of spectral and morphological biomarkers. The advantages of highly sensitive non-destructive in situ analysis techniques for biomarker detection are invaluable, particularly with respect to envisaged Mars sample return missions, as it may allow us to identify remains and traces of former microbial life in both ancient terrestrial and extraterrestrial materials. This technique may prove particularly useful in the quest for extraterrestrial life with respect to precious extraterrestrial materials, as minute quantities are sufficient to conduct analysis.

Author

Bacteria; Exobiology; Extraterrestrial Life; Microorganisms; Mineralogy; Alkyl Compounds; Molecules; Morphology; Sediments; Biological Evolution

20020002181 California Univ., Inst. of Geophysics and Planetary Physics, Los Angeles, CA USA

Earth's Orbital History Revisited

Varadi, Ferenc, California Univ., USA; Runnegar, Bruce, California Univ., USA; Ghil, Michael, California Univ., USA; General Meeting of the NASA Astrobiology Insititute; April 2001, pp. 308; In English; See also 20020002018; No Copyright; Avail: Issuing Activity; Abstract Only

Orbital calculations are increasingly being used, in conjunction with sedimentary and geochemical data, to analyze environmental evolution on planetary scales. In order to better understand the history of the inner Solar System over timescales of hundreds of millions of years, we have carried out a number of accurate, long-term, numerical simulations of the orbits of the nine major planets using physical models with increasing complexity. In this work, equations of motions are directly integrated by a Stormer-Cowell multi-step scheme which is optimized for reduced round-off errors. We gradually refine the physical models to include corrections required by general relativity, the finite size of the lunar orbit, and the solar gravitational quadrupole moment. In one case, the Earth-Moon system was resolved as two separate bodies and the results were compared to those based on analytically averaging the lunar orbit. A better analytical averaging model is obtained by means of these comparisons. The computed orbits are in good agreement with those of previous studies for the past five million years but not for earlier times. Chaos in the motion of the inner planets limits the validity of the computations beyond 50 million years. Nevertheless, we detect a number of significant transitions at earlier times that involve changes in the precession of the orbits of Earth and Mars. One in particular, about 65 million years ago, is associated with clearly discernible, macroscopic changes in the evolution of Mercury#s orbit, suggesting the possibility of a dramatic shift in the dynamics of the Solar System at that time. This dynamical transition could have been responsible for significant perturbations within the asteroid belt and that it corresponds, approximately, to the Cretaceous-Tertiary boundary.

Author

Earth-Moon System; Planetary Evolution; Planetary Environments; Solar System; Earth Orbits; Equations of Motion; Lunar Orbits

20020002182 Pennsylvania State Univ., Astrobiology Research Center, University Park, PA USA

Development of Cyanobacterial Mats on Soil Surface Under an Oxygenated Atmosphere 2.6 Gya Ago at Schagen, Eastern Transvaal, South Africa

Watanabe, Yumiko, Pennsylvania State Univ., USA; Ohmoto, Hiroshi, Pennsylvania State Univ., USA; General Meeting of the NASA Astrobiology Insititute; April 2001, pp. 309-310; In English; See also 20020002018; No Copyright; Avail: Issuing Activity; Abstract Only

The 2.6 Ga Schagen paleosol developed on a is greater than 2.7 Ga ultramafic rock (serpentinized dunite) and was overlain by a 2.56 Ga marine-quartzite unit. They were subjected to the green-schist facies metamorphism 2.06 Ga. The present thickness

of the paleosol is about 17 m. This paleosol, characterized by high contents of organic carbon (up to 1.2 wt%) as well as of calcite and dolomite, is similar to modern ”calcretes” and ”dolocretes” that developed under (semi) arid climate. Another noteworthy characteristic of the paleosol is an association of organic matter and ferric-bearing silicates (ferri-stilpnomelane), especially at the top. Aluminous minerals (e.g., sericite) are generally rare because the parental rock is poor in Al. Based on the mineralogical characteristics, the Schagen paleosol is divisible into six zones. From top to bottom, they are: (I) quartz-rich zone, (II) calcite-rich zone, (III) talcrich zone, (IV) dolomite-rich zone, (V) calcite-rich zone, and (VI) carbonated-rich serpentinized zone. Organic C is mostly accumulated with fine-grained clay minerals, forming seams in the upper 5 m of this section (i.e., zones I - III). In the quartz-rich zone I, organic-rich seams occur on fine-grained layers of detrital grains of quartz; the organicrich seams are sometimes traceable over a few centimeters in thin sections. Organic matter also occurs along grain boundaries of quartz, carbonate and talc. Such occurrences of organic matter suggest that it is a remnant of microbial mats developed on soil surface. This suggestion is supported by the finding that the organic C contents, ranging from 0.2 to 1.2 wt%, positively correlate with the contents of bio-essential elements, such as P and N. The delta C-13 values of the organic C range from -17.4 to -14.3 perthusand These values are significantly different from those of organic matter in the overlain marine sediment (i.e., approx. -33 prethousand), but are similar to those of modern, cyanobacteria-dominated microbial mats developed on land. The carbon isotopic fractionation between the organic matter and the contemporaneous atmospheric CO2 is estimated to be about -12 perthousand. This value is consistent with the fractionation during CO2-fixation by oxygenic cyanobacteria via the Calvin cycle. The possibility of other types of photoautotrophs (e.g., purple sulfur bacteria that use H2S as an electron donor instead of H2O) as candidates for the microbial mats can be ruled out because of the virtual absence of sulfur in this soil profile. The organic matter at Schagen is closely associated with Fe-bearing minerals, particularly ferric-bearing mineral, such as ferri-stilpnomelane, in the upper part of the paleosol. The precursor minerals of ferri-stilpnomalane were probably goethite, as the Fe(3+) source, and kaolinite as the Al source. The presence of goethite suggests that the soil developed under an oxic atmosphere. Significant losses of Fe from the lower paleosol section, especially from zones II and III, by organic acids generated from the decay of bacterial mats are suggested from the following observations: (a) significant decreases in Fe(3+)/Ti and Sigma-Fe/Ti ratios compared to the parental rock; (b) decreasing contents of organic carbon downward; (c) occurrences of organic carbon: primarily as fine-grained dissemination along grain boundaries; (d) lower C-13 values (by approx. 2 perthousand) of carbonates in zones II - IV, compared to those in organic-C poor carbonates of zones V - VI. A loss of Fe from paleosol has been considered by previous researchers as an important line of evidence for a reducing atmosphere prior to 2.2 Ga (e.g., Holland, 1994). However, our observations of the 2.6 Ga Schagen paleosols suggest that the mechanism of Fe loss during soil formation has been the same since at least 2.6 Ga, i.e., by organic acids produced by the decay of soil organisms, rather than by organic-free, H2-rich soil water. A loss of Fe from a paleosol, regardless of whether it is pre- or post-2.2 Ga in age, may be an excellent indicator of biological activity on the land surface.
Author
Bacteria; Atmospheric Composition; Carbon 13; Carbon Dioxide Concentration; Carbonates; Earth Surface; Microorganisms; Minerals; Organic Materials; Oxygenation; Rocks; Sediments; Biological Evolution

20020002183 Pennsylvania State Univ., Astrobiology Research Center, University Park, PA USA
Organic Carbon, S, Mo, U, and V in the Archean and Paleoproterozoic Black Shales
Yamaguchi, Kosei E., Pennsylvania State Univ., USA; Ohmoto, Hiroshi, Pennsylvania State Univ., USA; General Meeting of the NASA Astrobiology Insititute; April 2001, pp. 311-312; In English; See also 20020002018; No Copyright; Avail: Issuing Activity; Abstract Only

Holland (1984) suggests that concentration relationships between organic carbon (OC) and some redox-sensitive elements (Mo, U, V, etc.) in marine shales are useful indicators of the atmospheric oxygen level. According to his theory, an oxic atmosphere promotes the dissolution of some redox-sensitive elements from rocks during weathering, increasing the concentrations of these elements in the ocean water. Consequently, the marine shales deposited under an oxic atmosphere are expected to have higher contents of these elements and positive correlations with the OC contents compared to those deposited under an anoxic atmosphere. However, the Mo-U-V-C-S relationships in modern marine sediments do not fit into such a simple prediction. We have also found that the Mo-U-V-C-S relationships in shales of Archean and Proterozoic age are essentially the same as those in the Phanerozoic shales. We have analyzed more than 100 samples of black shale from South Africa and Australia that are Archean and Paleoproterozoic in age. They are all from deep drill cores, thus free of the modern weathering effects. They include black shale from the approx. 3.4 Ga Fig Tree, the approx. 2.9 Ga West Rand, the approx. 2.7 Ga Fortescue, the approx. 2.6 Ga Platberg, the approx. 2.5 Ga Wolkberg, the approx. 2.5 Ga Chuniespoort, the approx. 2.5 Ga Hamersley, and the approx. 2.4 Ga Pretoria Groups. For comparison, similar data sets from more than 100 samples are collected from literature on OC-rich shales and sediments of many different ages. The compositions of most Archean-Paleoproterozoic black shales are essentially identical to those of the PAAS (post-Archean Australian average shale) and of some Cretaceous black shales: OC = 0 - 1 wt.%, S = 0 - 1 wt.%, Mo = 0 - 5 ppm, U = 0 - 3 ppm (some as high as 7 ppm) and V = 10 - 200 ppm. The molybdenum and OC content of most of the

Archean-Paleoproterozoic shales are also comparable to those of some modern marine sediments in the Sannich Inlet and the Oslo Fjord. High Mo content are typically associated with high sulfide-S content (e.g., is greater than 4 wt.%) in the approx. 2.5 Ga Hamersley Group samples, as well as in the Phanerozoic, and modern sediments. These data suggest that the geochemical cycles of the redox-sensitive elements have been essentially the same since the Archean, specifically the Mo content of seawater has been essentially the same and the concentration mechanisms have been the same. This suggestion is substantiated from a theoretical consideration (below). Most of molybdenum in sedimentary, metamorphic and igneous rocks occurs as a trace constituent of pyrite and minor molybdenite. Therefore, the weathering flux of Mo during soil formation can be quantitatively evaluated using the theoretical model of oxidation of kerogen in soil (Lasaga and Ohmoto, in review) and experimental data on the kinetics of pyrite oxidation (e.g., Kamei and Ohmoto, 2000). Our calculations suggest that all pyrite grains less than 1 cu cm in size will be completely oxidized and all Mo will be leached out from a soil zone in less than 10,000 years, if the atmospheric pO2 level is higher than 10(exp -6) atm (= 0.0005 % PAL). This pO2 value will be lowered if the grain size of pyrite is smaller and/or the residence time of pyrite in a soil zone is longer. Therefore, in contrast to a popular view, the riverine flux of Mo into ocean has most likely been constant since Archean. The enhanced Mo enrichments in shales have occurred only in local or regional basins with an euxinic (and sulfidic) bottom water body. Our study suggests that the Phanerozoic-style redox structure of the ocean, i.e., generally oxic ocean with localized anoxic/euxinic basins where bacterial sulfate reduction is active, may have already developed in the Archean.

Author

Carbon; Organic Materials; Molybdenum; Uranium; Sediments; Geochemistry; Minerals; Vanadium; Paleontology; Oxidation-Reduction Reactions; Precambrian Period; Planetary Atmospheres

20020002184 Connecticut Univ., Dept. of Molecular and Cell Biology, Storrs, CT USA

Maximum Likelihood Mapping as Tool for Comparative Genome Analyses

Zhaxybayeva, Olga, Connecticut Univ., USA; Gogarten, J. Peter, Connecticut Univ., USA; General Meeting of the NASA Astrobiology Insititute; April 2001, pp. 313-314; In English; See also 20020002018; No Copyright; Avail: Issuing Activity; Abstract Only

Comparative genome analyses confirm that horizontal gene transfer (HGT) played an important role in shaping microbial genomes. In addition to genes under sporadic selection, HGT also affects housekeeping genes (e.g., archaeal-type ATPsynthase transferred to Deinococcaceae and Spirochetes) and functions involved in information processing (e.g., archaeal lysyl-tRNA synthase in Rickettsia and Spirochetes), and even ribosomal RNA encoding genes. However, the association of tree-like diagrams and evolution is so strongly engrained in evolutionary theory that few alternatives have been explored. Here we describe a tool that provides an assessment and graphic illustration of the mosaic nature of microbial genomes. The focus on tree-like behavior has been a limitation of previous methods to analyze the phylogenetic information contained in molecular data. Split trees and maximum likelihood mapping are two of the few methods developed to assess the non-tree like nature of molecular data. Focusing on the analyses of quartets of molecular sequences, maximum likelihood mapping transforms the threedi- mensional data for each sequence quartet into an easily visualized diagram depicting the phylogenetic content. This approach was designed to gauge the phylogenetic information contained in a multiple sequence alignment; however, it can be easily adapted to the analyses of all quartets of orthologous genes found in four genomes. We have automated the assembly and analyses of these quartets of orthologues given the selection of four genomes, and have analyzed several genome quartets using this maximum likelihood mapping approach. The possible phylogenetic relationships between four homologous sequences are three unrooted trees. If L1, L2, L3 are the three maximum likelihoods for the data under the three possible tree topologies, and if one assumes an equal prior probability for each of the topologies, then the posterior probability pi for topology i (i=1,2,3) is pi = Li /(L1 + L2 + L3). The probabilities for the three tree topologies add up to one; therefore, the three dimensional data for each sequence quartet can be depicted in a two dimensional simplex. Given a quartet of genomes, we used blast searches of every ORF against the other three genomes to define quartets of putative orthologues. Our appr oach to define orthologues is similar to the NCBI's definition of COGs; however, Tatusov et al. require reciprocal matches for only 3 genomes, whereas our analyses requires reciprocal matches between the four genomes analyzed. In many instances we find nearly equal numbers of quartets supporting the three possible topologies. Furthermore, the strength of support of individual quartets for the different topologies is surprisingly strong. For the largest part these data do not appear to reflect ill resolved phylogenies, rather, each of the three possible topologies has surprising strong aupport by a large fraction of the analyzed quartets. We will present data comparing the ML-mapping approach to a similar approach using bootstrap probabilities, and analyses using mitochondrial genomes, which presumably were inherited as a single linkage group, as test cases. Our analyses of the genome of the cyanobacterium Synechocystis sp. indicate that a large part of the cyanobacterial genome is related to that of low GC Gram positives, confirming an analysis of the evolution of the chlorophyll biosynthetic pathway. Our analyses suggest that the interkingdom relationships among prokaryotes cannot be depicted by the tree

like evolution of a core of conserved and little transferred genes, rather the prokaryotic genomes are mosaic where different parts have different evolutionary histories.
Author
Maximum Likelihood Estimates; Genome; Biological Evolution; Genes; Biosynthesis; Microorganisms; Probability Theory

20020002185 Carnegie Institution of Washington, Dept. of Terrestrial Magnetism, Washington, DC USA
Extrasolar Planets
Butler, R. Paul, Carnegie Institution of Washington, USA; Marcy, Geoffrey W., California Univ., USA; General Meeting of the NASA Astrobiology Insititute; April 2001, pp. 319; In English; See also 20020002018; No Copyright; Avail: Issuing Activity; Abstract Only

All sixty of the planets found to date have been discovered from precision Doppler surveys. The substellar companion mass function derived from these surveys is strongly peaked at less than 5 Jupiter-masses. About 6% of late F and G dwarf stars have easily detectable Jupiter-mass companions within 3 AU, while fewer than 0.5% of these stars have brown dwarf companions. About 0.75% of late F and G dwarfs harbor planets in ”51 Peg-like” circular orbits with periods of 3 to 5 days. With one exception, all planets orbiting beyond 0.1 AU are in eccentric orbits (e is greater than 0.1). The planet bearing stars are metal rich relative to both the field stars and the Sun. Our group is surveying 1,100 of the nearest and brightest Sun-like stars in the sky using the Lick 3-m (California), Keck 10-m (Hawaii), and the 3.9-m Anglo-Australian Telescopes. Next year we will add the remaining nearby stars (out to 50 parsecs) with the 6.5-m Magellan Telescope in Chile. With measurement precision of 3 m/s, these are the only active surveys capable of detecting ”Solar System” analogs. Recent discoveries from our group include all three known systems of multiple planets, the only known transit planet, and the only known resonance planets. Solar System analogs, Jupiter and Saturn-like planets orbiting beyond 4 AU, have not yet been discovered. Detecting these elusive planets will require precision of 3 m/s maintained for more than a decade. by 2010 our surveys will provide a first planetary census of nearby stars, allowing us to estimate the ubiquity of planetary systems and of ”Solar System” analogs. The central question is whether Jupiters at 5 AU will be found in circular or eccentric orbits.
Author
Extrasolar Planets; Planetary Systems; Galactic Evolution; Solar System; Planets

20020002186 NASA Ames Research Center, Moffett Field, CA USA
Stratospheric Observatory for Infrared Astronomy
Becklin, Eric E., NASA Ames Research Center, USA; General Meeting of the NASA Astrobiology Insititute; April 2001, pp. 320; In English; See also 20020002018; Original contains color illustrations; No Copyright; Avail: Issuing Activity; Abstract Only

The joint U.S. and German SOFIA project to develop and operate a 2.5-meter infrared airborne telescope in a Boeing 747-SP is now well into development. First science flights will begin in 2004 with 20% of the observing time assigned to German investigators. The observatory is expected to operate for over 20 years. The sensitivity, characteristics and science instrument complement are discussed. Present and future instrumentation will allow unique astrobiology experiments to be carried out. Several experiments related to organic molecules in space will be discussed.
Author
Sofia (Airborne Observatory); Spaceborne Astronomy; Infrared Astronomy; Exobiology

20020002187 NASA Ames Research Center, Moffett Field, CA USA
Prospects for the Detection of Earths Orbiting Other Stars
Borucki, William J., NASA Ames Research Center, USA; Koch, David G., NASA Ames Research Center, USA; Jenkins, Jon M., Search for Extraterrestrial Intelligence Inst., USA; Lissauer, Jack J., NASA Ames Research Center, USA; Dunham, Edward W., Lowell Observatory, USA; General Meeting of the NASA Astrobiology Insititute; April 2001, pp. 321; In English; See also 20020002018; No Copyright; Avail: Issuing Activity; Abstract Only

Extrasolar planets have been detected by timing the radio signals from millisecond pulsars, from Doppler velocity changes in the spectra of main sequence stars, and most recently by the white-light transit of HD209458. Detection of Earth-sized planets in and near the habitable zone of main-sequence stars appears to be extremely difficult, if not impossible, from ground-based observatories because of noise introduced by scintillation and transparency changes in the Earth#s atmosphere. to overcome these difficulties, several spaceborne photometric missions have been proposed. The COROT mission is a CNES/ESA mission with a 30 cm aperture telescope that will monitor each of several star fields for five months to find short period planets. The Kepler project is a USA effort designed to monitor 100,000 solar-like stars in a single field of view for a period of four years. The long duration enables the reliable detection of planets with orbital periods from a few days to as long as two years. Thus it should be able to determine the frequency of planets in and near the habitable zone and associate them with stellar spectral types. Canadian

and Scandinavian missions are also being developed. This paper compares these missions and discusses their expected contribution to our understanding of the frequency of terrestrial-sized planets around other stars.
Author
Extrasolar Planets; Planetary Systems; Astronomical Photometry; Telescopes; Terrestrial Planets; Astronomical Observatories

20020002188 European Space Agency. European Space Research and Technology Center, ESTEC, ESA Space Sciences Dept., Noordwijk, Netherlands
Large and Complex Organics in Space
Foing, Bernard H., European Space Agency. European Space Research and Technology Center, ESTEC, Netherlands; Ehrenfreund, Pascale, Leiden Univ., Netherlands; General Meeting of the NASA Astrobiology Insititute; April 2001, pp. 322; In English; See also 20020002018; No Copyright; Avail: Issuing Activity; Abstract Only

There are signatures of large organic molecules in the interstellar medium, from the ultraviolet to the infrared. Some infrared emission bands, which have been ascribed to families of large aromatic compounds are not specific for individual identification (and for discriminating free floating PAH molecules from loosely bound aromatics in amorphous carbon compounds). Red fluorescence and FUV absorption have also been ascribed to these aromatic compounds. Electronic transitions in the visible are a key to identify free gas phase molecules. The origin of Diffuse Interstellar Bands, more than 300 in recent surveys is still a mystery. However the measurements of sub-structures rotational contours in DIBs indicate large molecules such as chains (12-18C), rings, 50 C PAHs or fullerenes. The distribution of DIB widths permit to estimate a distribution of size of molecular carriers. The environment properties of DIB carriers also indicate ionisation potentials similar to those of cations of large carbonaceous molecules, such as large PAHs or fullerenes. The correlation studies of DIBS also indicate different carriers for the strong DIBs observed in the visible. Recent simulations show that medium-size PAHs (below 40 C atoms) are partially dehydrogenated in the diffuse interstellar medium. Finally the detection of NIR bands at 9577 and 9632 A coinciding with laboratory transitions of C60(+) suggest that significant interstellar carbon could reside in complex fullerene type compounds. These results indicate that many different large and complex organic molecules can form and survive in the very harsh interstellar environments. The survival of these large and complex organics will be measured in space on the SEBA-EXPOSE experiment on ISS, and in a simulation of Mars surface conditions. A follow up interdisciplinary work is required between astronomical observations, laboratory matrix and gas phase spectroscopy, theoretical work and modelling, and active experiments in space to study the formation, evolution, survival and transport of these complex organics.
Author
Carbon Compounds; Molecules; Organic Materials; Interstellar Matter; Electron Transitions; Detection; Astronomical Observatories

20020002189 Instituto Nacional de Tecnica Aeroespacial, Centro de Astrobiologia, Madrid, Spain
Eddington: A European Mission to Search for Earth-Like Habitable Planets
Gimenez, Alvaro, Instituto Nacional de Tecnica Aeroespacial, Spain; Favata, Fabio, European Space Agency, Netherlands; General Meeting of the NASA Astrobiology Insititute; April 2001, pp. 323; In English; See also 20020002018; No Copyright; Avail: Issuing Activity; Abstract Only

Eddington is an F-type mission within the package recently selected by the European Space Agency, ESA, for the period 2006-2012. It has two scientific goals: 1) the study of stellar interiors by means of asteroseismology in a large number of stars, all along the HR diagram, and 2) the search for transits of Earth-like planets in front of solar-type stars. The satellite will be in an L2 orbit with a 1-m class three-reflection telescope and a camera of tiled CCDs. It is expected that the planet searching part of the mission will monitor around 500,000 stars. During a period of 3 years, the same field of view will be monitored with a high duty cycle, around 95%, and an excellent photometric precision leading to the detection of planet transits in solar-type stars between 11 and 17 V magnitudes using 30 s exposures. The relatively small defocusing of the CCD camera, and its capability to observe faint objects, will allow Eddington to monitor many candidate stars despite a field of view of only 3 degrees in diameter. Transits of Earthlike planets will be detected in stars up to V around 14, while thousands of giant planets will be found in the full range. Eddington will contribute to our knowledge of extra-solar planetary systems with an unbiased statistics. Radial velocity and astrometric methods are more efficient in the discovery of massive close companions, but the photometric transit method opens the way to the discovery of terrestrial planets in the habitable zone, with long enough orbital periods. The expected results will no doubt have a profound impact on the study of Astrobiology and will set the scene for an in-depth study of the discovered systems using other space missions like TPF or Darwin.
Author
Asteroseismology; Astrometry; Astronomical Photometry; Planetary Systems; Terrestrial Planets; Space Missions; Stars; Celestial Bodies

20020002190 Southwest Research Inst., Boulder, CO USA

Planetary Formation: Fast or Rare?

Throop, Henry, Southwest Research Inst., USA; Bally, John, Colorado Univ., USA; Esposito, Larry, Colorado Univ., USA; Mccaughrean, Mark, Astrophysikalisches Inst., Germany; General Meeting of the NASA Astrobiology Insititute; April 2001, pp. 324-326; In English; See also 20020002018; No Copyright; Avail: Issuing Activity; Abstract Only

Planet formation is generally believed to start with the coagulation of sub-micron-sized interstellar dust into planetesimals and eventually planets. The earliest stages of grain growth from interstellar dust into cm-sized pebbles has been described theoretically but not previously observed: a direct observation would complete a causal link between young circumstellar disks and evolved planetary systems. Here we present three lines of evidence for grain growth in young proto-planetary disks in the Orion nebula: 1) We find large, translucent regions of the disks to be achromatic as observed by the the Hubble Space Telescope implying grains larger than 4 micro-m; 2) We propose that the non-detection of the disks in the 1.3 mm continuum can be most easily explained by grains larger than 1 cm; and 3) New numerical evolutionary modeling of grain growth within the photo-evaporative environment of the Orion nebula indicates that grains can grow to cm-sizes or larger in 10(exp 5) yr. Observations indicate that most stars form in high-mass clusters where photo-evaporation rapidly destroys young circumstellar disks and may frustrate planetary formation. While terrestrial planet formation may be largely unaffected by external illumination, Jovian planets and icy bodies must form quickly to capture sufficient mass before the volatiles in the proto-planetary nebula are lost to photo-evaporation.

Author

Interstellar Matter; Planetary Evolution; Planetary Systems; Cosmic Dust; Protoplanets; Solar System Evolution

20020002191 Carnegie Institution of Washington, Dept. of Terrestrial Magnetism, Washington, DC USA

Gas Giant Protoplanet Formation: Rapid or Slow?

Boss, Alan P., Carnegie Institution of Washington, USA; General Meeting of the NASA Astrobiology Insititute; April 2001, pp. 327-328; In English; See also 20020002018; No Copyright; Avail: Issuing Activity; Abstract Only

Two very different mechanisms exist for the formation of gas giant planets like Jupiter, core accretion and disk instability. Core accretion is the generally favored means for explaining the formation of Jupiter and Saturn, and detailed models typically require several million years for an ice/rock core to grow to Jupiter's mass by accreting nebular gas. Disk instability, on the other hand, is rapid, as a gravitationally unstable disk can form a self-gravitating clump with Jupiter's mass in thousand years. In the latter case, collisional accumulation of solids to form habitable, terrestrial planets in the inner planetary system will have considerably less time to occur before long range gravitational perturbations from Jupiter will become important. While these perturbations will not necessarily prevent the growth of terrestrial planets (Kortenkamp & Wetherill 2000), certainly the timing of gas giant planet formation is of fundamental importance for the formation of habitable planets. This work is directed toward a better understanding of the disk instability mechanism for rapid gas giant planet formation. A protoplanetary disk with sufficient mass to form gas giant planets by the core accretion mechanism (Pollack et al. 1996) is likely to be marginally unstable to the formation of self-gravitating clumps that could become gas giant protoplanets (Boss 1997, 1998). Such a disk instability can only occur if the disk is massive enough and cold enough to become gravitationally unstable. Recent disk instability models (Boss 2000) have shown that the instability can form clumps containing several Jupiter masses even in disks with surface densities within the range inferred for the minimum mass solar nebula (Weidenschilling 1977) and seemingly required for core accretion (Pollack et al. 1996). However, this work (Boss 2000) as well as much of the previous work on disk instability has assumed simplified disk thermodynamics, such as locally isothermal'' behavior (Boss 1997, 1998, 2000; Nelson et al. 1998; Pickett et al. 1998), which is the most permissive assumption for clump formation. With less permissive thermodynamical assumptions, such as locally isentropic'', adiabatic, or adiabatic with heating by artificial viscosity (but no cooling), the growth of density waves was suppressed compared to the case of locally isothermal'' disks (Pickett et al. 2000a, 2000b). Disk instability calculations which included both heating by artificial viscosity as well as cooling by a simple radiative prescription have also found that the resulting disk heating was sufficient to suppress the growth of self-gravitating clumps (Nelson et al. 2000; Nelson 2000). "Additional information is contained in the original extended abstract."

Author

Gas Giant Planets; Planetary Evolution; Protoplanetary Disks; Accretion Disks; Saturn (Planet); Jupiter (Planet); Clumps

20020002192 Lockheed Martin Space Systems Co., Astronautics, Denver, CO USA

On the Threshold of Inorganic Life

Clark, Benton C., Lockheed Martin Space Systems Co., USA; General Meeting of the NASA Astrobiology Insititute; April 2001, pp. 329-330; In English; See also 20020002018; No Copyright; Avail: Issuing Activity; Abstract Only

Terrestrial life as we know it is organically based, with key roles played by organic molecules incorporating numerous elements other than C and H, especially the key elements N, O, P and S. Although evolutionary diversity has branched through staggeringly diverse biological forms, employing different and sometimes novel molecular compounds, commonality is conserved in critical molecules such as the nucleic acids, proteins, energy-rich compounds, and many other constituents. While inorganic structures are sometimes synthesized by bioorganisms, most notably involving Ca, P, Si or Fe, the key components of informational macromolecules and enzymatic facilitators of controlled metabolism are invariably organic, or metalloorganic. I suggest here that a primarily inorganic form of life is not only possible, but currently in the process of formation. Specifically, in this life form, information storage is carried by digital circuits of inorganic makeup (Si, SiOx, Cu, Au, etc.), and analysis and control functions are orchestrated by computer program software. Energy transduction into electrical power is achieved from solar insolation (solar cells of Si, GaAs, etc.), nuclear radiation (radioisotope thermoelectric conversion from Pu or SR, or fission reactor sources of U or Pu), or inorganic electrochemical energy sources (fuel cells and batteries of various, often inorganic, forms). Mutation occurs via software modifications, using self-altering program codes and an influx of new programming material from human sources. All this resides in an artificial machine intelligence entity or network of entities that comprise a single, but possibly distributed lifeform. ”Additional information is contained in the original extended abstract.”
Author
Organometallic Compounds; Silicon; Copper; Silver; Silicon Oxides; Thermoelectric Power Generation; Macromolecules

20020002193 Carnegie Institution of Washington, Dept. of Terrestrial Magnetism, Washington, DC USA
Shock Chemistry in the Inner Solar Nebula
Desch, S. J., Carnegie Institution of Washington, USA; Kress, M. E., Washington Univ., USA; General Meeting of the NASA Astrobiology Insititute; April 2001, pp. 331-332; In English; See also 20020002018; No Copyright; Avail: Issuing Activity; Abstract Only

Chondritic meteorites are among the most primitive remnants of the birth of our solar system. Notably, many chondrites contain complex organics such as amino acids, despite the prediction by chemical equilibrium models that nitrogen in the inner solar nebula should have been locked up in N2. Chondrites also contain chondrules, millimeter-sized spheres of melted silicate rock, processed by hours-long energetic events before being incorporated into parent bodies. Here we describe work in progress that shows that shock waves, one proposed source of energetic processing of chondrules, might have altered, or initiated the formation of, meteoritic organics. The chemistry driven by chondrule-forming shocks in the solar nebula is treated as a nonequilibrium reacting flow, and solved using the the SHOCK Module of the ChemKin-III software package. We assume a shock speed 7.5 km/s, about that needed to melt chondrules and consistent with shock speeds found in numerical simulations of the solar nebula. We set the (pre-shock) gas pressure P = 10(exp -6) atm, gas temperature T = 300K, and use solar (cosmic) abundances of C, H, O and N, in the forms CO, H2, H2O, and N2. Our results (Figure) show that a fraction of the nitrogen is liberated from N2 into the forms N, NH, NH3 and NO, and that even some of the CO is converted into atomic and hydrogenated forms. From cooling rates of chondrules, we expect the entire system to be quenched on timescales less than hours, and possibly less. These chemically reactive radicals will thus find their way into cooler gas, potentially making these C- and N-bearing radicals available for a ”nebular generation” of organic compounds. These nebula organics would be isotopically closer to solar than their interstellar counterparts, possibly explaining the identification of an organic component isotopically light in N found in chondrites. The gas-phase radical NO produced in the shock is not stable, but it may be detectable by future generations of radio telescopes (such as ALMA, the Atacama Large Millimeter Array), if shocks are frequent enough. Such detections may confirm the role of the energetic events that melted chondrules in the chemical processing of the solar nebula.
Author
Chondrites; Solar Nebula; Meteoritic Composition; Shock Waves; Meteorites; Chondrule; Chemical Equilibrium; Nonequilibrium Flow; Amino Acids

20020002194 Southwest Research Inst., Dept. of Space Sciences, Boulder, CO USA
Volcanically Induced Climate Change on CO2-Dominated Terrestrial Planets
Grinspoon, David H., Southwest Research Inst., USA; Bullock, Mark A., Southwest Research Inst., USA; General Meeting of the NASA Astrobiology Insititute; April 2001, pp. 333-334; In English; See also 20020002018; Original contains color illustrations; No Copyright; Avail: Issuing Activity; Abstract Only

Judging from the small statistical sample presently available to us, terrestrial planets with CO2-dominated atmospheres are likely to be common in the universe. Several recent results suggest that geological and atmospheric evolution are closely coupled on such worlds. Thus, understanding the limits of the continuously habitable zone around main sequence stars, and the kinds of planetary environments likely to evolve, will require a deep understanding of surface/atmosphere/interior interactions on such worlds. We have begun a program of study in which we seek to identify and quantify the processes responsible for geological

forcing of climate change on CO2-dominated terrestrial planets. The ultimate goal is to determine the most likely evolutionary paths followed by terrestrial planets as a function of size, composition and stellarcentric distance. The first step is to understand and successfully simulate climate evolution over the age of the observed surfaces of Venus and Mars. We are exploring the role that volcanism may have played in inducing climate change on recent Venus and on early Mars through the use of climate models that couple the effects of radiation, convection, cloud formation, heterogeneous surface chemistry, atmospheric escape and volcanic outgassing. As on the Earth, processes that affect climate on Mars and Venus include the distribution of absorbed solar radiation, geochemical cycles, and the role of mantle outgassing via volcanism. Until recently the volcanic source functions for Mars and Venus were poorly constrained. With the Magellan spacecraft mission to Venus and the Mars Global Surveyor mission to Mars, however, more reliable records of the volcanic histories of these planets have become available. On Venus, small changes in atmospheric water or sulfur gases are sufficient to significantly perturb both cloud structure and the greenhouse effect. Large volcanic edifices on the order of several hundred My old and the vast, volcanic plains attest to significant volcanic fluxes in the past 1 billion years. Venus, like Earth and unlike any other planet within several light years, has a dynamic climate system which is maintained by complex feedbacks and a geologically active surface. ”Additional information is contained in the original extended abstract.”
Author
Climate Change; Volcanoes; Terrestrial Planets; Carbon Dioxide; Surface Reactions; Planetary Environments

20020002195 Carnegie Institution of Washington, Dept. of Terrestrial Magnetism, Washington, DC USA
Searches for Planets and Brown Dwarfs
McCarthy, Chris, Carnegie Institution of Washington, USA; Zuckerman, B., California Univ., USA; Becklin, E. E., California Univ., USA; General Meeting of the NASA Astrobiology Insititute; April 2001, pp. 335; In English; See also 20020002018; No Copyright; Avail: Issuing Activity; Abstract Only

The results of an infrared coronographic search for extrasolar planets and brown dwarfs orbiting nearby young stars are presented. Infrared coronography was used to detect brown dwarfs (with masses between 12 and 80 times the mass of jupiter) and giant planets with masses between 5 and 12 times the mass of Jupiter, at orbital separations between 50 and 2000 Astronomical Units. Approximately 1% of stars are found to have brown dwarfs in this range. No giant planets were found implying a frequency of such distant planets of is less than 2%. These results are compared to the results of an ongoing precise radial velocity survey being conducted at the Carnegie Institute (DTM) and elsewhere, and with other results. The implications on the theories of star and planet formation as well as for the survivability of terrestrial planets are discussed.
Author
Infrared Radiation; Planetary Evolution; Terrestrial Planets; Brown Dwarf Stars; Extrasolar Planets

20020002196 Pennsylvania State Univ., Dept. of Astronomy and Astrophysics, University Park, PA USA
Numerical Modeling of Solar System Dust Environments
Olsson, Bertil, Pennsylvania State Univ., USA; General Meeting of the NASA Astrobiology Insititute; April 2001, pp. 336; In English; See also 20020002018; No Copyright; Avail: Issuing Activity; Abstract Only

A numerical model for integration of dust orbits in stellar systems has been developed. The model is efficient enough to give useful results, in a reasonable execution time, when running on a single personal computer. The terrestrial and martian accretion of dust produced in various parts of the asteroid belt has been modeled, with a resulting flux into the atmosphere that in the terrestrial case seems to correlate with late Pleistocene glaciations.
Author
Mathematical Models; Stellar Systems; Dust; Solar System

20020002197 NASA Ames Research Center, Moffett Field, CA USA
The Runaway Greenhouse Effect on Earth and other Planets
Rabbette, Maura, NASA Ames Research Center, USA; Pilewskie, Peter, NASA Ames Research Center, USA; McKay, Christopher, NASA Ames Research Center, USA; Young, Robert, NASA Ames Research Center, USA; General Meeting of the NASA Astrobiology Insititute; April 2001, pp. 337-338; In English; See also 20020002018; Original contains color illustrations; No Copyright; Avail: Issuing Activity; Abstract Only

Water vapor is an efficient absorber of outgoing longwave infrared radiation on Earth and is the primary greenhouse gas. Since evaporation increases with increasing sea surface temperature, and the increase in water vapor further increases greenhouse warming, there is a positive feedback. The runaway greenhouse effect occurs if this feedback continues unchecked until all the water has left the surface and enters the atmosphere. For Mars and the Earth the runaway greenhouse was halted when water vapor became saturated with respect to ice or liquid water respectively. However, Venus is considered to be an example of a planet where

the runaway greenhouse effect did occur, and it has been speculated that if the solar luminosity were to increase above a certain limit, it would also occur on the Earth. Satellite data acquired during the Earth Radiation Budget Experiment (ERBE) under clear sky conditions shows that as the sea surface temperature (SST) increases, the rate of outgoing infrared radiation at the top of the atmosphere also increases, as expected. Over the pacific warm pool where the SST exceeds 300 K the outgoing radiation emitted to space actually decreases with increasing SST, leading to a potentially unstable system. This behavior is a signature of the runaway greenhouse effect on Earth. However, the SST never exceeds 303K, thus the system has a natural cap which stops the runaway. According to Stefan-Boltzmann's law the amount of heat energy radiated by the Earth's surface is proportional to (T(sup 4)). However, if the planet has a substantial atmosphere, it can absorb all infrared radiation from the lower surface before the radiation penetrates into outer space. Thus, an instrument in space looking at the planet does not detect radiation from the surface. The radiation it sees comes from some level higher up. For the earth#s atmosphere the effective temperature (T(sub e)) has a value of 255 K corresponding to the middle troposphere, above most of the water vapor and clouds. "Additional information is contained in the original extended abstract."

Author

Greenhouse Effect; Water Vapor; Infrared Radiation; Long Wave Radiation; Atmospheric Temperature; Earth (Planet); Venus (Planet)

20020002198 NASA Ames Research Center, Astrophysics Branch, Moffett Field, CA USA

Detecting and Identifying Organic Molecules in Space - The AstroBiology Explorer (ABE) MIDEX Mission Concept

Sandford, Scott A., NASA Ames Research Center, USA; General Meeting of the NASA Astrobiology Insititute; April 2001, pp. 339; In English; See also 20020002018; No Copyright; Avail: Issuing Activity; Abstract Only

Infrared spectroscopy in the 2.5-16 micron (4000-625/cm) range is a principle means by which organic compounds are detected and identified in space. Ground-based, airborne, and spaceborne IR spectral studies have already demonstrated that a significant fraction of the carbon in the interstellar medium (ISM) resides in the form of complex organic molecular species. Unfortunately, neither the distribution of these materials nor their genetic and evolutionary relationships with each other or their environments are well understood. The Astrobiology Explorer (ABE) is a MIDEX (Medium-class Explorer) mission concept currently under study at NASA's Ames Research Center in collaboration with Ball Aerospace and Technologies Corporation. ABE will conduct IR spectroscopic observations to address outstanding important problems in astrobiology, astrochemistry, and astrophysics. The core observational program would make fundamental scientific progress in understanding (1) the evolution of ices and organic matter in dense molecular clouds and young forming stellar systems, (2) the chemical evolution of organic molecules in the ISM as they transition from AGB outflows to planetary nebulae to the general diffuse ISM to H II regions and dense clouds, (3) the distribution of organics in the diffuse ISM, (4) the nature of organics in the Solar System (in comets, asteroids, satellites), and (5) the nature and distribution of organics in local galaxies. Both the scientific goals of the mission and how they would be achieved will be discussed.

Author

Organic Materials; Infrared Spectroscopy; Interstellar Matter; Stellar Systems; Carbon; Molecular Gases; Organic Compounds; Planetary Nebulae; Chemical Evolution

20020002199 NASA Ames Research Center, Moffett Field, CA USA

Identifying Young, Nearby Stars

Webb, Rich, NASA Ames Research Center, USA; Song, Inseok, California Univ., USA; Zuckerman, Ben, California Univ., USA; Bessell, Mike, Australian National Univ., Australia; General Meeting of the NASA Astrobiology Insititute; April 2001, pp. 340; In English; See also 20020002018; No Copyright; Avail: Issuing Activity; Abstract Only

Young stars have certain characteristics, e.g., high atmospheric abundance of lithium and chromospheric activity, fast rotation, distinctive space motion and strong X-ray flux compared to that of older main sequence stars. We have selected a list of candidate young (is less than 100Myr) and nearby (is less than 60pc) stars based on their space motion and/or strong X-ray flux. to determine space motion of a star, one needs to know its coordinates (RA, DEC), proper motion, distance, and radial velocity. The Hipparcos and Tycho catalogues provide all this information except radial velocities. We anticipate eventually searching approx. 1000 nearby stars for signs of extreme youth. Future studies of the young stars so identified will help clarify the formation of planetary systems for times between 10 and 100 million years. Certainly, the final output of this study will be a very useful resource, especially for adaptive optics and space based searches for Jupiter-mass planets and dusty proto-planetary disks. We have begun spectroscopic observations in January, 2001 with the 2.3 m telescope at Siding Spring Observatory (SSO) in New South Wales, Australia. These spectra will be used to determine radial velocities and other youth indicators such as Li 6708A absorption strength and Hydrogen Balmer line intensity. Additional observations of southern hemisphere stars from SSO are scheduled in April and northern hemisphere observations will take place in May and July at the Lick Observatory of the University

of California. AT SSO, to date, we have observed about 100 stars with a high resolution spectrometer (echelle) and about 50 stars with a medium spectral resolution spectrometer (the ”DBS”). About 20% of these stars turn out to be young stars. Among these, two especially noteworthy stars appear to be the closest T-Tauri stars ever identified. Interestingly, these stars share the same space motions as that of a very famous star with a dusty circumstellar disk--beta Pictoris. This new finding better constrains the age of beta Pictoris to be approx. 10 Myr.
Author
Lithium; B Stars; Stellar Envelopes; T Tauri Stars; Adaptive Optics; Coordinates; High Resolution; Identifying; Radial Velocity

20020002200 Carnegie Institution of Washington, Dept. of Terrestrial Magnetism, Washington, DC USA
A New Approach to Planet and Asteroid Formation
Wetherill, George, Carnegie Institution of Washington, USA; Kortenkamp, Stephen, Carnegie Institution of Washington, USA; Inaba, Satoshi, Carnegie Institution of Washington, USA; General Meeting of the NASA Astrobiology Insititute; April 2001, pp. 341-342; In English; See also 20020002018; No Copyright; Avail: Issuing Activity; Abstract Only

Primarily as an outcome of the work of Safronov (1969) a ”standard model” of planet formation has been developed (reviewed by Kortenkamp et al., 2000, Canup and Agnor, 2000). The general features of this model are described in paragraph (A) below. More recently, discovery of giant planets of other stars (Marcy et al, 2000), together with advances in the understanding of dynamical processes in circumstellar disks (Boss, 2000), have identified what appear to be serious problems with the standard model, as described in paragraph (B). A: According to the standard model, in the terrestrial planet region, planetesimals grow from approx. 10(exp 14)g bodies to approx. 10(exp 26)g bodies (”planetary embryos”) on a time scale of approx.10(exp 5) years by a characteristic size distribution instability termed ”runaway growth”. After further accumulation of small bodies and merger with one another, the present planets form in approx. 10(exp 8) years. In the asteroid belt the planetary embryos require approx. 10(exp 6) years to form bodies more similar to the mass of Mars than to the present asteroids. Jupiter and Saturn form by a two-stage process whereby Jupiter ”cores” of about 10 Earth masses grow in about approx. 10(exp 6) years. These cores then accumulate gas from the disk on a time scale of approx. 10(exp 7) years to form the present gas giant planets. Following the formation of the giant planets, perturbations by these planets remove most of the mass from the asteroid region on a time scale of approx. 10(exp 8) years, leaving behind a greatly depleted asteroid region. The formation of Uranus and Neptune has not been firmly established within the framework of the standard model. On the whole, until lately, this model seemed very promising. B: As mentioned earlier, there are difficulties with the standard model. For example, it seems likely that the giant planets, Jupiter and Saturn, must have formed far more quickly than the traditional approx. 10(exp 7) year growth interval in order to avoid drifting into the Sun as a result of gravitational interactions between the very massive circumsolar gas disk and the growing giant planets (Turquem et al 2000). These differences require major modifications of the dynamical concepts and algorithms of the standard model. Because of the early presence of the giant planets, the Earth and other terrestrial planets do not grow by gravitational perturbations between planetesimals alone. Instead, at first, they will be nearly totally influenced by the giant planets and gas drag. Despite these differences, at approx. 1 AU, a different type of runaway growth produces an end product not too dissimilar to that of the standard model and on a similar approx. 10(exp 5) year time scale. On the other hand, these calculations indicate that the role of the asteroid region in the formation of habitable planets is likely to be much different from that found for the standard model.
Author
Planetary Evolution; Asteroids; Gravitational Effects; Size Distribution; Stellar Envelopes; Asteroid Belts; Gas Giant Planets

20020002201 California Inst. of Tech., Geological and Planetary Sciences, Pasadena, CA USA
Supergreenhouse Molecules and the Limits of the Habitable Zone
Yung, Yuk, California Inst. of Tech., USA; General Meeting of the NASA Astrobiology Insititute; April 2001, pp. 343; In English; See also 20020002018; No Copyright; Avail: Issuing Activity; Abstract Only

Supergreenhouse molecules have been shown to exist in a quantum mechanical code. They are more powerful than any such molecules known in nature or in the laboratory. They are made from carbon, fluorine and sulfur, and they have the following properties: 1. very intense absorption in the infrared, 2. very inert, with lifetimes in thousands of years 3. can be made from cheap and abundant raw material. There are applications to: 1. terraforming of Mars and satellites in the outer solar system, 2. artificial greenhouse in space or extreme environments (e.g. Antarctica), and 3. detection of advanced civilization by identifying these molecules and the limits of the habitable zone of their planetary systems.
Author
Greenhouse Effect; Habitability; Fluorine; Carbon; Sulfur; Planetary Systems; Molecules

20020002202 Pennsylvania State Univ., Penn State Astrobiology Research Center and PA Space Grant Consortium, University Park, PA USA

Astrobiology Education and Outreach at Penn State

Brown, Lisa L., Pennsylvania State Univ., USA; Phelps, Angela M., Pennsylvania State Univ., USA; General Meeting of the NASA Astrobiology Insititute; April 2001, pp. 349-350; In English; See also 20020002018; No Copyright; Avail: Issuing Activity; Abstract Only

This poster presentation will outline several of the education and outreach activities being carried out by the Penn State Astrobiology Research Center (PSARC). Program activities target undergraduate students, K-12 educators and students, and the general public. Undergraduate students at Penn State can now earn a Minor in Astrobiology. The program includes courses from the departments of Geosciences, Astronomy & Astrophysics, Biology, Microbiology, and Biochemistry & Molecular Biology. First-year undergraduate students gain invaluable experience and mentoring from PSARC scientists who participate in this research internship program which is designed to retain women students in the science and engineering fields. First-year undergraduate students gain invaluable experience and mentoring from PSARC scientists who participate in this research internship program which is designed to retain women students in the science and engineering fields. An annual five-day residential workshop for in-service teachers in life science, chemistry or earth science, grades 7-12. The workshop is designed to provide teachers with astrobiology content knowledge as well as inquiry-based activities for use in the classroom. The teachers interact directly with several of the PSARC coinvestigators through research presentations, laboratory tours, and field trips. an annual one-week residential program for young women in the 11th grade. PSARC investigators participate by involving the students in two-hour hands-on workshops or week-long projects. PSARC scientists work with Penn State Public Broadcasting to introduce the exciting field of astrobiology through this multimedia children#s current events program. Aimed primarily at grades 4-7, the weekly programs reach more than 5 million children in 32 states across the country. Along with the broadcasts, WITN provides printed support materials, a newspaper column, instructional kits, and webbased information and activities that offer a range of resources for both teachers and students. The first astrobiology episode aired March 3, 2000. The on-line component of that program is archived at the WITN website (http://witn.psu.edu/2223/). "Additional information is contained in the original extended abstract."

Author

Astrophysics; Biochemistry; Education; Exobiology; Microbiology; Students; Broadcasting; Earth Sciences; Geophysics

20020002203 Arizona State Univ., Astrobiology Program, Tempe, AZ USA

Astrobiology at Arizona State University: Program Overview and Research/Outreach Highlights

Davis, Rebecca, Arizona State Univ., USA; Unser, Leslee, Arizona State Univ., USA; Farmer, Jack, Arizona State Univ., USA; General Meeting of the NASA Astrobiology Insititute; April 2001, pp. 351-352; In English; See also 20020002018; No Copyright; Avail: Issuing Activity; Abstract Only

ASU's Astrobiology Program is an interdisciplinary program of study and research that offers exciting opportunities for both undergraduate and graduate students who seek a high-level academic experience at a Research One University. The current program includes faculty researchers and students at all levels from the Departments of Geological Sciences, Chemistry and Biochemistry, Biology, Plant Biology, and Microbiology. We also are supported by affiliated programs in Astronomy, Aerospace Engineering, and Biotechnology. The current program supports 15 funded ASU Co-Investigators across these disciplines with collaborative ties to the College of William & Mary, University of Alaska, University of Arizona, University of Connecticut, University of Puget Sound, University of Tennessee, Indiana University, and the National University of Mexico (UNAM), Mexico City. At last count, ongoing research projects are providing training opportunities for 19 graduate and 7 undergraduate students. Active research areas include the 1) cosmochemistry of carbonaceous meteorites, 2) organosynthesis in seafloor hydrothermal systems, 3) the origins and evolution of photosynthesis, 4) studies of the microbial fossil record, 5) environmental conditions on Archean Earth, 6) the structure, function and persistence of complex ecosystems in extreme environments, 7) the effects of impact processes on planetary habitability and evolution, and 8) the exploration for habitable environments and life on Mars and Europa. In this presentation we will review the present current research highlights and review recent Education and Public Outreach activities from the past year. Some research highlights from the past year include the analysis of 1) a pristine carbonaceous meteorite which recently fell in Canada, 2) the synthesis of methanol under simulated seafloor hydrothermal conditions, 3) the discovery of novel photosynthetic organisms and molecular phylogenies which trace the origins of photosynthetic genes, 4) a robust model for the Archean oceans which suggests it was hypersaline, 5) discoveries of probable microbial biosignatures in subsurface hydrothermal deposits, and 6) the first detection of aqueous mineral deposits (specular hematite) on the surface of Mars by midinfrared remote sensing methods. For more detailed information about these research projects and results, please see poster presentations by individual ASU investigators at this meeting. Education and public outreach highlights for the year include a public lecture by Dr. Baruch Blumberg, Director of the NASA Astrobiology Institute and an NAI-supported workshop and poster

session for local K-12 science teachers. High attendance at both of these events illustrates the high level of enthusiasm and excitement that Astrobiology generates within our local community. Other highlights include our participation in ASU's Earth Sciences Day activities and SEE ASU, a day-long K-12 outreach program that provides students from Arizona schools with an opportunity to explore the many exciting degree programs offered at ASU. We will also present highlights from the ASU Astrobiology Program website as an effective education and outreach tool and as a means to recruit top graduate students into the program. A list of the most recent publications from the ASU research team will be available.
Author
Aerospace Engineering; Education; Biotechnology; Students; Universities; Extraterrestrial Life; Exobiology; Earth Sciences; Microbiology

20020002204 Uniformed Services Univ. of the Health Sciences, SPACELINE Office, Bethesda, MD USA
SPACELINE, a Bibliographic Database for Astrobiology: Capabilities and Issues
Dutcher, F. Ronald, Uniformed Services Univ. of the Health Sciences, USA; Powers, Janet V., Uniformed Services Univ. of the Health Sciences, USA; Babski, Dianne P., Uniformed Services Univ. of the Health Sciences, USA; General Meeting of the NASA Astrobiology Insititute; April 2001, pp. 353-354; In English; See also 20020002018; No Copyright; Avail: Issuing Activity; Abstract Only

SPACELINE (http://spaceline.usuhs.mil) contains bibliographic references to publications in astrobiology and the space life sciences. It is a collaborative effort between NASA and the National Library of Medicine of the National Institutes of Health. The purposes of this poster are to demonstrate the database#s capabilities, discuss some of the issues and challenges that accompany a bibliographic approach to astrobiology, and obtain feedback from the astrobiology community. SPACELINE is undergoing significant changes in its search interface and how it is searched during the first half of 2001, changes that will result in greater integration with National Library of Medicine databases. Online demonstrations will be given during the meeting. A distinguishing characteristic of astrobiology is its interdisciplinary nature. It is a continuing challenge to balance the integration of different disciplines that a bibliographic database like SPACELINE can achieve against the effort necessary to provide comprehensive bibliographic coverage in individual disciplines. An interdisciplinary database best meets the needs of individuals in the field seeking interdisciplinary updates or scientists new to this field seeking to find out what is known, and in this way SPACELINE contributes to solving the interdisciplinary hurdles faced by astrobiology. to what extent such a database can, or should, also meet the more detailed needs of researchers within their own disciplines is an open question. Other challenges include the evolving role of scientific publication and bibliographic databases in a web-linked world and SPACELINE/National Library of Medicine plans for keeping up with these changes; and the possibility and value of creating a distinct astrobiology entity within SPACELINE.
Author
Bibliographies; Data Bases; Exobiology; Aerospace Engineering

20020002205 NASA Johnson Space Center, Houston, TX USA
An Astrobiology Microbes Exhibit and Education Module
Lindstrom, Marilyn M., NASA Johnson Space Center, USA; Allen, Jaclyn S., Lockheed Martin Corp., USA; Stocco, Karen, Pasadena Independent School District, USA; Tobola, Kay, Clear Creek Independent School District, USA; Olendzenski, Lorraine, Marine Biological Lab., USA; General Meeting of the NASA Astrobiology Insititute; April 2001, pp. 355-356; In English; See also 20020002018; No Copyright; Avail: Issuing Activity; Abstract Only

Telling the story of NASA-sponsored scientific research to the public in exhibits is best done by partnerships of scientists and museum professionals. Likewise, preparing classroom activities and training teachers to use them should be done by teams of teachers and scientists. Here we describe how we used such partnerships to develop a new astrobiology augmentation to the Microbes! traveling exhibit and a companion education module. "Additional information is contained in the original extended abstract."
Author
Exobiology; Microorganisms; Education

20020002206 Pennsylvania State Univ., Dept. of Astronomy and Astrophysics, University Park, PA USA
Fly Me to the Moon: A System for Technologically Enhanced Outreach
Olsson, Bertil, Pennsylvania State Univ., USA; Jangren, Anna, Pennsylvania State Univ., USA; Schindler, Trent, The Chedd-Angier Production Co., USA; General Meeting of the NASA Astrobiology Insititute; April 2001, pp. 357; In English; See also 20020002018; No Copyright; Avail: Issuing Activity; Abstract Only

The NASA Astrobiology Institute is a ”virtual organization”, and as such makes it possible to perform outreach in remote areas, which have until recently been excluded from such activities by preventive travel costs. We show how new technology available for internal administration within NAI can be used for the creation of a simulated space mission, in which children in remote regions of the USA and elsewhere are sent on educational trips to other planets, under the supervision of a ”mission base” in the form of one or two scientists located in a NAI center. Since the required equipment and personnel are already available within the NAI IT infrastructure the project cost can be held modest, while the result is still ”slick” enough to excite teenagers with years of experience from highly advanced game and movie computer graphic.
Author
Education; Exobiology; Remote Regions; Computer Graphics

20020002207 Sydney Univ., Australia
micro*scope and Biose-IT - Web Based Resources for Promoting Awareness of Microbial Biodiversity
Patterson, David J., Sydney Univ., Australia; AmaralZettler, Linda A., Marine Biological Lab., USA; Edgcomb, Virginia P., Marine Biological Lab., USA; McArthur, Andrew G., Marine Biological Lab., USA; Sogin, Mitchell L., Marine Biological Lab., USA; General Meeting of the NASA Astrobiology Insititute; April 2001, pp. 358-359; In English; See also 20020002018; No Copyright; Avail: Issuing Activity; Abstract Only

Although Bacteria, Archaea, and protists are major players in all natural ecosystems, a lack of adequate traditional taxonomic resources hinders progress in many areas of microbial ecology. The resources that are currently available for microbiota do not compare favorably with those available for the macrobiota and there is a particular gap in availability of materials for educational purposes. micro*scope is a new internet initiative which aims to provide such resources. ”Additional information is contained in the original extended abstract.”
Author
Biological Diversity; Bacteria; Ecosystems; Microorganisms; Taxonomy; Microbiology; Ecology

20020002208 Academy of Sciences (USSR), Paleontological Inst., Moscow, USSR
Bacterial Paleontology as a Course of the Lectures for the Students- Geologist and Paleontologist of Moscow University
Rozanov, A. Yu., Academy of Sciences (USSR), USSR; General Meeting of the NASA Astrobiology Insititute; April 2001, pp. 360; In English; See also 20020002018; No Copyright; Avail: Issuing Activity; Abstract Only

The materials, obtained per last decade, on fossil bacteria and products of their vital function from Phanerozoic and Pre-Cambrian deposits of the Earth were a stimulus to isolation of a new branch bacterial paleontology. The data of bacterial paleontology are extremely important for the studying of sedimentology, including elucidation of genesis of a series of important sedimentary mineral resources such as phosphorites, bauxites, manganese ores, oil, for discussion of problems of evolution of Biosphere, specially in a Pre-Cambrian and early Paleozoic, and for paleogeographic researches. At last, bacterial paleontology is one of key aspects for studying of astromaterials. For acquainting the paleontology and sedimentology students with achievements of bacterial paleontology A.Yu. Rozanov during two years was giving a course of lectures for geologists in Moscow State University. Additional information is contained in the original extended abstract.
Author
Paleontology; Bacteria; Sedimentary Rocks; Fossils; Mineral Deposits; Geological Surveys

59
MATHEMATICAL AND COMPUTER SCIENCES (GENERAL)

Includes general topics and overviews related to mathematics and computer science. For specific topics in these areas see categories 60 through 67.

20020000781 NASA Marshall Space Flight Center, Huntsville, AL USA
System Simulation by Recursive Feedback: Coupling a Set of Stand-Alone Subsystem Simulations
Nixon, D. D., NASA Marshall Space Flight Center, USA; October 2001; 198p; In English
Report No.(s): NASA/TP-2001-211331; M-1032; NAS 1.60:211331; No Copyright; Avail: CASI; A09, Hardcopy; A03, Microfiche

Conventional construction of digital dynamic system simulations often involves collecting differential equations that model each subsystem, arran g them to a standard form, and obtaining their numerical gin solution as a single coupled, total-system simultaneous set. Simulation by numerical coupling of independent stand-alone subsimulations is a fundamentally different approach that is attractive because, among other things, the architecture naturally facilitates high fidelity, broad scope, and

discipline independence. Recursive feedback is defined and discussed as a candidate approach to multidiscipline dynamic system simulation by numerical coupling of self-contained, single-discipline subsystem simulations. A satellite motion example containing three subsystems (orbit dynamics, attitude dynamics, and aerodynamics) has been defined and constructed using this approach. Conventional solution methods are used in the subsystem simulations. Distributed and centralized implementations of coupling have been considered. Numerical results are evaluated by direct comparison with a standard total-system, simultaneous-solution approach.
Author
Digital Systems; Simulation; Dynamical Systems; Feedback; Coupling

20020000864 Los Alamos National Lab., NM USA
Construction of Difference Equations Using Lie Groups
Axford, R. A.; Aug. 01, 1998; 78p; In English
Report No.(s): DE2001-1172; LA-13499; No Copyright; Avail: Department of Energy Information Bridge, Microfiche

The theory of prolongations of the generators of groups of point transformations to the grid point values of dependent variables and grid spacings is developed and applied to the construction of group invariant numerical algorithms. The concepts of invariant difference operators and generalized discrete sources are introduced for the discretization of systems of inhomogeneous differential equations and shown to produce exact difference equations. Invariant numerical flux functions are constructed from the general solutions of first order partial differential equations that come out of the evaluation of the Lie derivatives of conservation forms of difference schemes. It is demonstrated that invariant numerical flux functions with invariant flux or slope limiters can be determined to yield high resolution difference schemes. The introduction of an invariant flux or slope limiter can be done so as not to break the symmetry properties of a numerical flux-function.
NTIS
Difference Equations; Lie Groups; Transformations (Mathematics)

20020000884 Argonne National Lab., IL USA
High-performance spectral element algorithms and implementations
Fischer, P. F.; Tufo, H. M.; Aug. 28, 1999; 10p; In English
Report No.(s): DE2001-11952; ANL/MCS/CP-99926; No Copyright; Avail: Department of Energy Information Bridge, Microfiche

We describe the development and implementation of a spectral element code for multimillion gridpoint simulations of incompressible flows in general two- and three-dimensional domains. Parallel performance is present on up to 2048 nodes of the Intel ASCI-Red machine at Sandia.
NTIS
Algorithms; Performance Prediction; Spectra; Parallel Processing (Computers)

20020001779 Center for Mathematics and Computer Science, Amsterdam Netherlands
Computer Verification of the Ankeny-Artin-Chowla Conjecture for all Primes less than 100 000 000 000. Modelling, Analysis and Simulation
van der Poorten, A. J.; te Riele, H. J. J.; Williams, H. C.; Mar. 1999; 28p; In English
Report No.(s): PB2001-108625; MAS-R9905; Copyright; Avail: National Technical Information Service (NTIS), Microfiche

No abstract available.
NTIS
Simulation; Proving

20020001839 Argonne National Lab., IL USA
Scalable libraries for solving systems of nonlinear equations and unconstrained minimization problems
Gropp, W. D.; McInnes, L. C.; Smith, B. F.; Oct. 27, 1997; 10p; In English
Report No.(s): DE2001-8878; ANL/MCS/CP-94757; No Copyright; Avail: Department of Energy Information Bridge, Microfiche

Developing portable and scalable software for the solution of large-scale optimization problems presents many challenges that traditional libraries do not adequately meet. Using object-oriented design in conjunction with other innovative techniques, they address these issues within the SNES (Scalable Nonlinear Equation Solvers) and SUMS (Scalable Unconstrained Minimization Solvers) packages, which are part of the multilevel PETSCs (Portable, Extensible Tools for Scientific Computation) library. This paper focuses on the authors' design philosophy and its benefits in providing a uniform and versatile framework for

developing optimization software and solving large-scale nonlinear problems. They also consider a three-dimensional anisotropic Ginzburg-Landau model as a representative application that exploits the packages' flexible interface with user-specified data structures and customized routines for function evaluation and preconditioning.
NTIS
Computer Programs; Nonlinear Programming; Nonlinear Systems; Object-Oriented Programming; Nonlinear Equations

20020002341 Booz-Allen and Hamilton, Inc., McLean, VA USA
Security Requirements for Cryptographic Modules
Daley, W. M.; Shavers, C.; Kammer, R.; May 25, 2001; 59p; In English
Report No.(s): PB2001-106755; FIPS-PUB-140-2; No Copyright; Avail: CASI; A04, Hardcopy; A01, Microfiche
The selective application of technological and related procedural safeguards is an important responsibility of every Federal organization in providing adequate security in its Computer and telecommunication systems. This publication provides a standard to be used by Federal organizations when these organizations specify that cryptographic-based security systems are to be used to provide protection for sensitive or valuable data. Protection of a cryptographic module within a security system is necessary to maintain the confidentiality and integrity of the information protected by the module.
NTIS
Cryptography; Standards; Modules

20020003935 Los Alamos National Lab., NM USA
New Approach for Fingerprint Image Compression
Mazieres, B.; Dec. 01, 1997; 57p; In English
Report No.(s): DE2001-763151; LA-UR-98-4298; LA-UR-99-4298; No Copyright; Avail: Department of Energy Information Bridge, Microfiche
The FBI has been collecting fingerprint cards since 1924 and now has over 200 million of them. Digitized with 8 bits of grayscale resolution at 500 dots per inch, it means 2000 terabytes of information. Also, without any compression, transmitting a 10 Mb card over a 9600 baud connection will need 3 hours. Hence we need a compression and a compression as close to lossless as possible : all fingerprint details must be kept. A lossless compression usually do not give a better compression ratio than 2:1, which is not sufficient. Compressing these images with the JPEG standard leads to artefacts which appear even at low compression rates. Therefore the FBI has chosen in 1993 a scheme of compression based on a wavelet transform, followed by a scalar quantization and an entropy coding : the so-called WSQ. This scheme allows to achieve compression ratios of 20:1 without any perceptible loss of quality.
NTIS
Fingers; Printing; Technology Assessment; Compression Ratio; Coding

20020005063 Los Alamos National Lab., NM USA
GENIE: A Hybrid Genetic Algorithm for Feature Classification in Multi-Spectral Images
Perkins, S.; Dec. 01, 2000; 12p; In English
Report No.(s): DE2001-769263; LA-UR-00-5892; No Copyright; Avail: Department of Energy Information Bridge, Microfiche
We consider the problem of pixel-by-pixel classification of a multi-spectral image using supervised learning. Conventional supervised classification techniques such as maximum likelihood classification and less conventional ones such as neural networks, typically base such classifications solely on the spectral components of each pixel. It is easy to see why the color of a pixel provides a nice, bounded, fixed dimensional space in which these classifiers work well. It is often the case however, that spectral information alone is not sufficient to correctly classify a pixel. Maybe spatial neighborhood information is required as well. Or may be the raw spectral components do not themselves make for easy classification, but some arithmetic combination of them would. In either of these cases we have the problem of selecting suitable spatial, spectral or spatio-spectral features that allow the classifier to do its job well. The number of all possible such features is extremely large. How can we select a suitable subset. We have developed GENIE, a hybrid learning system that combines a genetic algorithm that searches a space of image processing operations for a set that can produce suitable feature planes, and a more conventional classifier which uses those feature planes to output a final classification. In this paper we show that the use of a hybrid GA provides significant advantages over using either a GA alone or more conventional classification methods alone. We present results using high-resolution IKONOS data, looking for regions of burned forest and for roads.
NTIS
Genetic Algorithms; Image Classification; Pixels

20020005239 Argonne National Lab., IL USA

Second Argonne theory institute on differentiation of computational approximations of functions

Bischof, C. H.; Eberhard, P.; Hovland, P. D.; Oct. 09, 1998; 41p; In English

Report No.(s): DE2001-774051; ANL/MCS-TM-236; No Copyright; Avail: Department of Energy Information Bridge, Microfiche

A Theory Institute on ”Differentiation of Computational Approximations to Functions” was held at Argonne National Laboratory on May 18-20, 1998. The institute was organized by Christian Bischof and Paul Hovland of the Mathematics and Computer Science Division at Argonne National Laboratory. The Theory Institute brought together 38 researchers from the US, Great Britain, France, and Germany. Mathematicians, computer scientists, physicists, and engineers from diverse disciplines discussed advances in automatic differentiation (AD) theory and software and described benefits from applying AD methods in application areas. These areas include fluid mechanics, structural engineering, optimization, meteorology, and computational mathematics for the solution of ordinary differential equations (ODEs) or differential algebraic equations (DAEs). This meeting was the fourth workshop dedicated to automatic differentiation. Earlier meetings were the 1991 SIAM conference in Breckenridge, Colorado; the first Argonne Theory Institute on computational differentiation in 1993; and the 1996 SIAM conference in Santa Fe, New Mexico. AD methods can be used whenever gradient information or higher-order derivative information must be computed. The problem is defined by a computer program (without gradient information) that is able to compute numerical values of some output variables for a given set of input variables. As a result of applying AD methods to this computer program, a new computer program is generated automatically to compute the derivatives of the output variables with respect to the input variables. This at first glance, astonishing fact can be easily understood by viewing the program from a compiler angle. A complicated computational sequence is split into a sequence of simple operations. Then, to compute the gradients, the chain rule of differentiation is applied successively to this sequence completely automatically. The resultant gradients are accurate up to roundoff errors (which are always present in numerical evaluations).

NTIS

Conferences; Approximation; Differential Equations; Computer Programs

60
COMPUTER OPERATIONS AND HARDWARE

Includes hardware for computer graphics, firmware and data processing. For components see 33 Electronics and Electrical Engineering. For computer vision see 63 Cybernetics, Artificial Intelligence and Robotics.

20020002800 Los Alamos National Lab., NM USA

Design issues for hardware implementation of an algorithm for segmenting hyperspectral imagery

Theiler, J.; Leeser, M.; Oct. 01, 2000; 11p; In English

Report No.(s): DE2001-766208; LA-UR-00-3003; No Copyright; Avail: Department of Energy Information Bridge, Microfiche

Modern hyperspectral imagers can produce data cubes with hundreds of spectral channels and millions of pixels. One way to cope with this massive volume is to organize the data so that pixels with similar spectral content are clustered together in the same category. This provides both a compression of the data and a segmentation of the image that can be useful for other image processing tasks downstream. The classic approach for segmentation of multidimensional data is the k-means algorithm; this is an iterative method that produces successively better segmentations. It is a simple algorithm, but the computational expense can be considerable, particularly for clustering large hyperspectral images into many categories. The ASAPP (Accelerating Segmentation And Pixel Purity) project aims to relieve this processing bottleneck by putting the k-means algorithm into field-programmable gate array (FPGA) hardware. The standard software implementation of k-means uses floating-point arithmetic and Euclidean distances. by fixing the precision of the computation and by employing alternative distance metrics (we consider the ’Manhattan’ and the ’Max’ metrics as well as a linear combination of the two), we can fit more distance-computation nodes on the chip, obtain a higher degree of fine-grain parallelism, and therefore faster performance, but at the price of slightly less optimal clusters. We investigate the effects of different distance metrics from both a theoretical using random ical viewpoint (using 224-channel AVIRIS images and 10-channel multispectral images that are derived from the AVIRIS data to simulate MTI data).

NTIS

Image Processing; Algorithms; Cubes (Mathematics); Euclidean Geometry

20020005082 Argonne National Lab., IL USA

Grid-enabled MPI: message passing in heterogeneous distributed computing systems

Foster, I.; Karonis, N. T.; Nov. 30, 2000; 11p; In English

Report No.(s): DE2001-772114; ANL/MCS/CP-103558; No Copyright; Avail: Department of Energy Information Bridge, Microfiche

Application development for high-performance distributed computing systems, or computational grids as they are sometimes called, requires grid-enabled tools that hide mundate aspects of the heterogeneous grid environment without compromising performance. As part of an investigation of these issues, they have developed MPICH-G, a grid-enabled implementation of the Message Passing Interface (MPI) that allows a user to run MPI programs across multiple computers at different sites using the same commands that would be used on a parallel computer. This library extends the Argonne MPICH implementation of MPI to use services provided by the globus grid toolkit. In this paper, they describe the MPICH-G implementation and present preliminary performance results.

NTIS

Computer Networks; Computational Grids; Systems Engineering; Parallel Computers

20020005187 California Univ., Lawrence Berkeley Lab., Berkeley, CA USA

Effective I/O bandwidth benchmark (b-eff-io)

Koniges, A. E.; Rabehseifner, R.; Feb. 17, 2000; 10p; In English

Report No.(s): DE2001-757N55; UCRL-JC-137704; DP0101038; No Copyright; Avail: Department of Energy Information Bridge

The effective I/O bandwidth benchmark (b-eff-io) covers two goals: (1) to achieve a characteristic average number for the I/O bandwidth achievable with parallel MPI-I/O applications, and (2) to get detailed information about several access patterns and buffer lengths. The benchmark examines 'first write' 'rewrite'; and 'read' access, strided (individual and shared pointers) and segmented collective patterns on one file per application and non-collective access to one file per process. The number of parallel accessing processes is also varied and wellformed I/O is compared with non-wellformed. On systems, meeting the rule that the total memory can be written to disk in 10 minutes, the benchmark should not need more than 15 minutes for a first pass of all patterns. The benchmark is designed analogously to the effective bandwidth benchmark for message passing (b(-)eff) that characterizes the message passing capabilities of a system in a few minutes. First results of the b-elf-io benchmark are given for IBM SP and Cray T3E systems and compared with existing benchmarks based on parallel Posix-I/O.

NTIS

Cray Computers; Parallel Processing (Computers); Computer Programming

20020005213 Quantum Research Services, Inc., Durham, NC USA

Development of fibre channel disk clusters ***Final Report, 2 Sep. 1998 - 17 Mar. 1999***

Dunn, W. L.; Justice, J. R.; Stockert, T. D.; Barker, A. R.; Yacout, A. M.; Aug. 01, 1999; 13p; In English

Report No.(s): DE2001-770613; DOE/ER/82648; No Copyright; Avail: Department of Energy Information Bridge, Microfiche

This report documents the accomplishments of a Phase I project whose purpose was to demonstrate feasibility of developing inexpensive and fast data storage using multi-host Fibre Channel disk clusters. In Phase I, a working file system called ZFS was developed and tested. The ZFS approach was designed to be suited for high energy physics applications, but is general and flexible enough to be useful for other high-volume applications. The ZFS approach, which borrows from the networking concept of cut-through routing, uses Linux boxes and disk clusters in a Fibre Channel--Arbitrated Loop architecture. In ZFS, file locking and other meta-data level operations are carried out over the primary data network, after which all data are sent directly over a Fibre Channel between the workstation and the disk cluster. No intermediate server is required. Substantially higher throughputs than in traditional networked disk architectures have been demonstrated. The ZFS architecture is described and tests of the first implementation of ZFS at Fermilab are discussed. The current system is implemented for Linux and is being optimized for Fermilab's needs, but extensions to other operating systems and other data-intensive applications are clearly foreseen.

NTIS

Data Storage; Feasibility Analysis; Product Development

61
COMPUTER PROGRAMMING AND SOFTWARE

Includes software engineering, computer programs, routines, algorithms, and specific applications, e.g., CAD/CAM. For computer software applied to specific applications, see also the associated category.

20020000755 Sandia National Labs., Albuquerque, NM USA
DGTOEXO2: A Distorted Grid Output File to Exodus II Finite Element Database Conversion Utility
Moffat, H. K.; Dec. 01, 1998; 30p; In English
Report No.(s): DE2001-3191; SAND98-2717; No Copyright; Avail: Department of Energy Information Bridge

This report describes how to obtain publication-quality graphics from distorted grid electronic structure codes using the combination of the conversion utility, dgtoexo2, and mustafa, an AVS (Advanced Visual Systems) Express application. Dgtoexo2 converts scalar function results from a format applicable to distorted grid codes into the Exodus II unstructured finite element data representation. Mustafa can read Exodus II files and use the AVS Express engine to visualize data on UNIX and Windows NT platforms. Though not designed for the purpose, the dgtoexo2/EXOdUS II/mustafa combination is sufficiently versatile to provide for the specialized graphics needs of electronic structure codes. The combination also scales well, producing robust performance for problems involving millions of grid points.
NTIS
Computer Graphics; Computational Grids; Computer Programs; Data Conversion Routines

20020001032 NASA Kennedy Space Center, Cocoa Beach, FL USA
Collaboration Between NASA Centers of Excellence on Autonomous System Software Development
Goodrich, Charles H., DYNACS Engineering Co., Inc., USA; Larson, William E., NASA Kennedy Space Center, USA; [2001]; 8p; In English; 51st International Astronautical Federation, 1-5 Oct. 2001, Toulouse, France; No Copyright; Avail: CASI; A02, Hardcopy; A01, Microfiche

Software for space systems flight operations has its roots in the early days of the space program when computer systems were incapable of supporting highly complex and flexible control logic. Control systems relied on fast data acquisition and supervisory control from a roomful of systems engineers on the ground. Even though computer hardware and software has become many orders of magnitude more capable, space systems have largely adhered to this original paradigm In an effort to break this mold, Kennedy Space Center (KSC) has invested in the development of model-based diagnosis and control applications for ten years having broad experience in both ground and spacecraft systems and software. KSC has now partnered with Ames Research Center (ARC), NASA's Center of Excellence in Information Technology, to create a new paradigm for the control of dynamic space systems. ARC has developed model-based diagnosis and intelligent planning software that enables spacecraft to handle most routine problems automatically and allocate resources in a flexible way to realize mission objectives. ARC demonstrated the utility of onboard diagnosis and planning with an experiment aboard Deep Space I in 1999. This paper highlights the software control system collaboration between KSC and ARC. KSC has developed a Mars In-situ Resource Utilization testbed based on the Reverse Water Gas Shift (RWGS) reaction. This plant, built in KSC's Applied Chemistry Laboratory, is capable of producing the large amount of Oxygen that would be needed to support a Human Mars Mission. KSC and ARC are cooperating to develop an autonomous, fault-tolerant control system for RWGS to meet the need for autonomy on deep space missions. The paper will also describe how the new system software paradigm will be applied to Vehicle Health Monitoring, tested on the new X vehicles and integrated into future launch processing systems.
Author
Autonomy; Software Engineering; Systems Engineering; Aerospace Systems; Control Systems Design; Model Reference Adaptive Control

20020001222 Sandia National Labs., Albuquerque, NM USA
Multimedia Feedback Systems for Engineering
Gladwell, S.; Gottlieb, E. J.; McDonald, M. J.; Slutter, C. L.; Dec. 15, 1998; 9p; In English
Report No.(s): DE2001-2828; SAND98-2664C; No Copyright; Avail: Department of Energy Information Bridge, Microfiche

The World Wide Web (WWW) has become a key tool for information sharing. Engineers and scientists are finding that the web is especially suited to publishing the graphical, multi-layered information that is typical of their work. Web pages are easier to distribute than hardcopy. Web movies have become more accessible, in many offices, than videos. Good VRML (Virtual Reality Modeling Language) viewing software, bundled with most new PCs (personal computer), has sufficient power to support many engineering needs. In addition to publishing information, science and engineering have an important tradition of peer and customer review. Reports, drawings and graphs are typically printed, distributed, reviewed, marked up, and returned to the author.

Adding review comments to paper is easy. When, however, the information is in electronic form, this ease of review goes away. It's hard to write on videos. It's even harder to write comments on animated 3D (three dimensional) models. These feedback limitations reduce the value of the information overall. Fortunately, the web can also be a useful tool for collecting peer and customer review information. When properly formed, web reports, movies, and 3D animations can be readily linked to review notes. This paper describes three multimedia feed-back systems that Sandia National Laboratories has developed to tap that potential. Each system allows people to make context-sensitive comments about specific web content and then electronically ties the comments back to the web content being referenced. The first system ties comments to specific web pages, the second system ties the comments to specific frames of digital movies, and the third ties the comments to specific times and viewpoints within 3D animations. In addition to the technologies, this paper describes how they are being used to support intelligent machine systems design at Sandia.
NTIS
Information Dissemination; World Wide Web; Multimedia; Electronic Publishing; Websites; Engineers; Scientists

20020001245 Scientific Digital Visions, Inc., San Jose, CA USA
Interactive Web Technologies for Dissemination of Scientific Graphics, September 2, 1998-March 17, 1999 ***Final Report***
Stone, C.; Feb. 28, 1999; 13p; In English
Report No.(s): DE2001-765174; No Copyright; Avail: Department of Energy Information Bridge
An interactive software tool was developed to support the dissemination of scientific graphics. The technologies were developed both as a Java applet and stand-alone application and allow images to be disseminated as a data collection and an appearance script. Phase I efforts defined the model for the grahics tools. Software prototypes were constructed to test the utility of the graphics tool and refine the model.
NTIS
Prototypes; Computer Graphics; Software Development Tools; Mathematical Models

20020001447 Lawrence Livermore National Lab., Livermore, CA USA
Optimizations for Parallel Object Oriented Frameworks
Basetti, F.; Davis, K.; Quinlan, D.; Sep. 22, 1998; 12p; In English
Report No.(s): DE2001-8791; UCRL-JC-132005; KJ0101010; No Copyright; Avail: Department of Energy Information Bridge, Microfiche
Application codes reliably under perform the advertised performance of existing architectures, compilers have only limited mechanisms with which to effect sophisticated transformations to arrest this trend. Compilers are forced to work within the broad semantics of the complete language specification and thus can not guarantee correctness of more sophisticated transformations. Object-oriented frameworks provide a level of tailoring of the C++ language to specific, albeit often restricted contexts. But such frameworks traditionally rely upon the compiler for most performance level optimization, often with disappointing results since the compiler must work within the context of the full language rather than the restricted semantics of abstractions introduced within the class library. No mechanism exists to express the restricted semantics of a class library to the compiler and effect correspondingly more sophisticated optimizations. In this paper, the authors explore both a family of transformations/optimizations appropriate to object-oriented frameworks for scientific computing and present a preprocessor mechanism, ROSE, which delivers the more sophisticated transformations automatically from the use of abstractions represented within high level object-oriented frameworks. They have found that these optimizations permit improved performance over FORTRAN 77 by factors of three to four, sufficiently interesting to suggest that higher level abstractions can contain greater semantics and that the greater semantics can be used to drive more sophisticated optimizations than are possible within lower level languages.
NTIS
Compilers; Object-Oriented Programming; Optimization; Semantics

20020001452 Argonne National Lab., IL USA
Infrastructure and Interfaces for Large-Scale Numerical Software
Freitag, L.; Gropp, W. D.; Hovland, P. D.; McInnes, L. C.; Smith, B. F.; Jun. 10, 1999; 9p; In English
Report No.(s): DE2001-11844; ANL/MCS/CP-99213; No Copyright; Avail: Department of Energy Information Bridge
The complexity of large-scale scientific simulations often necessitates the combined use of multiple software packages developed by different groups in areas such as adaptive mesh manipulations, scalable algebraic solvers, and optimization. Historically, these packages have been combined by using custom code. This practice inhibits experimentation with and comparison of multiple tools that provide similar functionality through different implementations. The ALICE project, a

collaborative effort among researchers at Argonne National Laboratory, is exploring the use of component-based software engineering to provide better interoperability among numerical toolkits. They discuss some initial experiences in developing an infrastructure and interfaces for high-performance numerical computing.
NTIS
Applications Programs (Computers); Computer Programming; Interoperability

20020001456 Argonne National Lab., IL USA
3D Visualization of Port Simulation
Horsthemke, W. H.; Macal, C. M.; Nevins, M. R.; Jun. 14, 1999; 16p; In English
Report No.(s): DE2001-11850; ANL/DIS/CP-99225; No Copyright; Avail: Department of Energy Information Bridge

Affordable and realistic three dimensional visualization technology can be applied to large scale constructive simulations such as the port simulation model, PORTSIM. These visualization tools enhance the experienced planner's ability to form mental models of how seaport operations will unfold when the simulation model is implemented and executed. They also offer unique opportunities to train new planners not only in the use of the simulation model but on the layout and design of seaports. Simulation visualization capabilities are enhanced by borrowing from work on interface design, camera control, and data presentation. Using selective fidelity, the designers of these visualization systems can reduce their time and efforts by concentrating on those features which yield the most value for their simulation. Offering the user various observational tools allows the freedom to simply watch or engage in the simulation without getting lost. Identifying the underlying infrastructure or cargo items with labels can provide useful information at the risk of some visual clutter. The PortVis visualization expands the PORTSIM user base which can benefit from the results provided by this capability, especially in strategic planning, mission rehearsal, and training. Strategic planners will immediately reap the benefits of seeing the impact of increased throughput visually without keeping track of statistical data. Mission rehearsal and training users will have an effective training tool to supplement their operational training exercises which are limited in number because of their high costs. Having another effective training modality in this visualization system allows more training to take place and more personnel to gain an understanding of seaport operations. This simulation and visualization training can be accomplished at lower cost than would be possible for the operational training exercises alone. The application of PORTSIM and PortVis will lead to more efficient planning overall and ultimately increase port utilization and throughput, decreasing the amount of time required to transport cargo from its origin to its final destination.
NTIS
Education; Computerized Simulation; Scientific Visualization

20020001464 Argonne National Lab., IL USA
Software for the parallel adaptive solution of conservation laws by discontinuous Galerkin methods
Flaherty, J. E.; Loy, R. M.; Shephard, M. S.; Teresco, J. D.; Aug. 17, 1999; 13p; In English
Report No.(s): DE2001-11936; ANL/MCS/CP-99808; No Copyright; Avail: Department of Energy Information Bridge, Microfiche

The authors develop software tools for the solution of conservation laws using parallel adaptive discontinuous Galerkin methods. In particular, the Rensselaer Partition Model (RPM) provides parallel mesh structures within an adaptive framework to solve the Euler equations of compressible flow by a discontinuous Galerkin method (LOCO). Results are presented for a Rayleigh-Taylor flow instability for computations performed on 128 processors of an IBM SP computer. In addition to managing the distributed data and maintaining a load balance, RPM provides information about the parallel environment that can be used to tailor partitions to a specific computational environment.
NTIS
Conservation Laws; Galerkin Method; Flow Equations; Differential Equations

20020001550 Sandia National Labs., Albuquerque, NM USA
Transformation as a Design Process and Runtime Architecture for High Integrity Software
Bespalko, S. J.; Winter, V. L.; Apr. 05, 1999; 15p; In English
Report No.(s): DE2001-5687; SAND99-0808C; No Copyright; Avail: Department of Energy Information Bridge

We have discussed two aspects of creating high integrity software that greatly benefit from the availability of transformation technology, which in this case is manifest by the requirement for a sophisticated backtracking parser. First, because of the potential for correctly manipulating programs via small changes, an automated non-procedural transformation system can be a valuable tool for constructing high assurance software. Second, modeling the processing of translating data into information as a, perhaps, context-dependent grammar leads to an efficient, compact implementation. From a practical perspective, the transformation process should begin in the domain language in which a problem is initially expressed. Thus in order for a transformation system

to be practical it must be flexible with respect to domain-specific languages. We have argued that transformation applied to specification results in a highly reliable system. We also attempted to briefly demonstrate that transformation technology applied to the runtime environment will result in a safe and secure system. We thus believe that the sophisticated multi-lookahead backtracking parsing technology is central to the task of being in a position to demonstrate the existence of HIS.
NTIS
Software Engineering; Design Analysis; Computer Programming; Parsing Algorithms

20020001558 Los Alamos National Lab., NM USA
Amrita: a computational facility
Shepherd, J. E.; Quirk, J. J.; Feb. 23, 1998; 155p; In English
Report No.(s): DE2001-758791; LA-SUB-99-64; No Copyright; Avail: Department of Energy Information Bridge

Amrita is a software system for automating numerical investigations. The system is driven using its own powerful scripting language, Amrita, which facilitates both the composition and archiving of complete numerical investigations, as distinct from isolated computations. Once archived, an Amrita investigation can later be reproduced by any interested party, and not just the original investigator, for no cost other than the raw CPU time needed to parse the archived script. In fact, this entire lecture can be reconstructed in such a fashion. to do this, the script: constructs a number of shock-capturing schemes; runs a series of test problems, generates the plots shown; outputs the LATEX to typeset the notes; performs a myriad of behind-the-scenes tasks to glue everything together. Thus Amrita has all the characteristics of an operating system and should not be mistaken for a common-or-garden code.
NTIS
Programming Languages; Computer Programs; Computer Programming

20020001593 Fermi National Accelerator Lab., Batavia, IL USA
Software system for measurement of accelerator magnets using a relational database
Sim, J. W.; Oct. 08, 1999; 6p; In English
Report No.(s): DE2001-12605; FERMILAB-CONF-99-275; No Copyright; Avail: Department of Energy Information Bridge, Microfiche

Two major upgrades to the Fermilab accelerator complex required the measurement of magnetic field strength and shape for a large number of electromagnets and permanent magnets. This paper describes the software system developed at Fermilab to measure these magnets. The data produced by this system was used to feed back information to the magnet design and fabrication process, as well as to help in determining magnet placement within the accelerator. The central framework of the measurement software is a relational database management system (RDBMS). Tables within the RDBMS are designed to store magnet design and identification information, measurement prescriptions, magnetic field strength and shape data, comment text entered by measurement technicians, lists of instrumentation used during measurements, calibration constants used to convert data to appropriate engineering units, and quality control limits for measurement data. The system employs a client-server architecture in which measurement computers, distributed at each of the magnet test stands, retrieved measurement prescriptions from the RDBMS server, controlled the data acquisition hardware used to run the measurement, and communicated measurement data back to the RDBMS. Additional client software was developed to apply analysis algorithms to the measurement data. These clients run either at the test stand, or from analysts' workstations. Standard tools provided by the RDBMS vendor facilitated report generation, ad-hoc queries, and manual data entry.
NTIS
Magnets; Electromagnets; Computer Programs

20020001781 Center for Mathematics and Computer Science, Amsterdam Netherlands
Specification of PSIDE. Modelling, Analysis and Simulation
de Swart, J. J. B.; Lioen, W. M.; van der Veen, W. A.; Dec. 1998; 22p; In English
Report No.(s): PB2001-108611; MAS-R9833; Copyright; Avail: National Technical Information Service (NTIS), Microfiche

PSIDE is a code for solving implicit differential equations on parallel computers. It is an implementation of the four-stage Radau IIA method. The nonlinear systems are solved by a modified Newton process, in which every Newton iterate itself is computed by an iteration process. This process is constructed such that the four stage values can be computed simultaneously. We describe here how PSIDE is set up as a modular system and what control strategies have been chosen.
NTIS
Numerical Analysis; Computer Programs; Parallel Processing (Computers)

20020001964 Lawrence Livermore National Lab., Livermore, CA USA

Evolutionary software for autonomous path planning

Couture, S.; Hage, M.; Feb. 10, 1999; 11p; In English

Report No.(s): DE2001-12570; UCRL-JC-133191; No Copyright; Avail: Department of Energy Information Bridge, Microfiche

This research project demonstrated the effectiveness of using evolutionary software techniques in the development of path-planning algorithms and control programs for mobile vehicles in radioactive environments. The goal was to take maximum advantage of the programmer's intelligence by tasking the programmer with encoding the measures of success for a path-planning algorithm, rather than developing the path-planning algorithms themselves. Evolutionary software development techniques could then be used to develop algorithms most suitable to the particular environments of interest. The measures of path-planning success were encoded in the form of a fitness function for an evolutionary software development engine. The task for the evolutionary software development engine was to evaluate the performance of individual algorithms, select the best performers for the population based on the fitness function, and breed them to evolve the next generation of algorithms. The process continued for a set number of generations or until the algorithm converged to an optimal solution. The task environment was the navigation of a rover from an initial location to a goal, then to a processing point, in an environment containing physical and radioactive obstacles. Genetic algorithms were developed for a variety of environmental configurations. Algorithms were simple and non-robust strings of behaviors, but they could be evolved to be nearly optimal for a given environment. In addition, a genetic program was evolved in the form of a control algorithm that operates at every motion of the robot. Programs were more complex than algorithms and less optimal in a given environment. However, after training in a variety of different environments, they were more robust and could perform acceptably in environments they were not trained in. This paper describes the evolutionary software development engine and the performance of algorithms and programs evolved by it for the chosen task.

NTIS

Software Engineering; Navigation; Autonomy; Coding

20020001999 California Univ., Lawrence Berkeley Lab., Berkeley, CA USA

Trlan user guide

Wu, K.; Simon, H.; Mar. 09, 1999; 35p; In English

Report No.(s): DE2001-6539; LBNL-42953; No Copyright; Avail: Department of Energy Information Bridge

TRLAN is a program designed to find a small number of extreme eigenvalues and their corresponding eigenvectors of a real symmetric matrix. Denote the matrix as A, the eigenvalue as (lambda), and the corresponding eigenvector as x, they are defined by the following equation, Ax = (lambda)x. There are a number of different implementations of the Lanczos algorithm available. Why another one? Our main motivation is to develop a specialized version that only target the case where one wants both eigenvalues and eigenvectors of a large real symmetric eigenvalue problems that cannot use the shift-and-invert scheme. In this case the standard non-restarted Lanczos algorithm requires one to store a large number of Lanczos vectors which can cause storage problems and make each iteration of the method very expensive. The underlying algorithm of TRLAN is a dynamic thick-restart Lanczos algorithm. Like all restarted methods, the user can choose how many vectors can be generated at once. Typically, the user chooses a moderate size so that all Lanczos vectors can be stored in core. This allows the restarted methods to execute efficiently. This implementation of the thick-restart Lanczos method also uses the latest restarting technique, it is very effective in reducing the time required to compute a desired solution compared to similar restarted Lanczos schemes, e.g., ARPACK.

NTIS

Eigenvalues; Eigenvectors; User Manuals (Computer Programs); Computer Programs

20020002001 Sandia National Labs., Albuquerque, NM USA

Ultra-Precise Assembly of Micro-Electromechanical Systems (MEMS) Components

Feddema, J. T.; Simon, R.; Polosky, M.; Christenson, T.; Apr. 01, 1999; 79p; In English

Report No.(s): DE2001-5833; SAND99-0746; No Copyright; Avail: Department of Energy Information Bridge

This report summarizes a three year effort to develop an automated microassembly workcell for the assembly of LIGA (Lithography Galvonoforming Abforming) parts. Over the last several years, Sandia has developed processes for producing surface machined silicon and LIGA parts for use in weapons surety devices. Some of these parts have outside dimensions as small as 100 micron, and most all have submicron tolerances. Parts this small and precise are extremely difficult to assembly by hand. Therefore, in this project, we investigated the technologies required to develop a robotic workcell to assembly these parts. In particular, we concentrated on micro-grippers, visual servoing, micro-assembly planning, and parallel assembly. Three different micro-grippers were tested: a pneumatic probe, a thermally actuated polysilicon tweezer, and a LIGA fabricated tweezer. Visual servoing was used to accuracy position two parts relative to one another. Fourier optics methods were used to generate synthetic microscope images from CAD drawings. These synthetic images are used off-line to test image processing routines under varying

magnifications and depths of field. They also provide reference image features which are used to visually servo the part to the desired position. We also investigated a new aspect of fine motion planning for the micro-domain. As parts approach 1-10 (micro)m or less in outside dimensions, interactive forces such as van der Waals and electrostatic forces become major factors which greatly change the assembly sequence and path plans. We developed the mathematics required to determine the goal regions for pick up, holding, and release of a micro-sphere being handled by a rectangular tool. Finally, we implemented and tested the ability to assemble an array of LIGA parts attached to two 3 inch diameter wafers. In this way, hundreds of parts can be assembled in parallel rather than assembling each part individually.
NTIS
Miniaturization; Robots; Microelectromechanical Systems; Computer Aided Manufacturing; Fabrication

20020002247 Army Research Lab., White Sands Missile Range, NM USA
Weather Effects on Target Acquisition, Part 1, Sensor Performance Model Infrared Algorithms ***Final Report***
Shirkey, Richard C.; Sauter, Barbara J.; Cormier, Rene V.; Jul. 2001; 55p; In English
Report No.(s): AD-A392763; ARL-TR-821-Pt-1; No Copyright; Avail: Defense Technical Information Center (DTIC)
The U.S. Air Force, Navy, and Army are in the process of upgrading the Electro-Optical Tactical Decision Aid (EOTDA). The EOTDA has been used to predict the impact of weather and time of day on target acquisition. The upgraded program is called the Target Acquisition Weather Software (TAWS). New features of the TAWS will include: automated data access; upgraded path radiance routines; replacement of separate infrared (IR); television (TV) and night vision (NV) sensor performance models with Acquire; and a U.S. Army standard sensor performance model, which has become a standard in Department of Defense for IR, TV, and NV systems. to quantify the effects on predicted target acquisition range of upgrading the sensor performance model, a comparison of the TAWS Version 2 with Acquire has been undertaken. Weather effects on target acquisition are examined also in some detail.
DTIC
Decision Support Systems; Computer Techniques; Weather; Target Acquisition

20020002263 Texas Univ., Center for Transportation Research, Austin, TX USA
CRCP-9: Improved Computer Program for Mechanistic Analysis of Continuously Reinforced Concrete Pavements ***Topical Report, Sep. 1999 - Aug. 00***
Kim, S. M.; Won, M. C.; McCullough, B. F.; Feb. 2001; 120p; In English
Report No.(s): PB2002-100099; No Copyright; Avail: CASI; A06, Hardcopy; A02, Microfiche
A new version of the CRCP computer program CRCP-9, has been developed in this study. The numerical model of the CRC pavements was developed using finite element theories, the crack spacing prediction model was developed using the Monte Carlo method, and the failure prediction model was developed using probability theories. CRCP-9 uses two-dimensional numerical methods to calculate stresses and strains, which is a totally different approach compared with the previous computer program CRCP-8 that uses one-dimensional analytical methods to calculate them. The major characteristics of CRCP-9 that differ from CRCP-8 include consideration of nonlinear variations in temperature and drying shrinkage through the depth of the concrete slab, nonlinear bond-slip relationship between concrete and steel bars, viscoelastic effect of concrete, curling and warping effects, and the ability of changing location of the longitudinal steel bars. Detail of the theoretical background of mechanistic modeling have been presented in this report. The descriptions of the computer program and input and output procedures have also been explained. Sample analysis results from CRCP-9 have been shown and comparisons of the results between CRCP-9 and CRCP-8 have been made.
NTIS
Composite Materials; Pavements; Concretes

20020002322 Society for Industrial and Applied Mathematics, Philadelphia, PA USA
SIAM report on Uncertainty Assessment and Management: A report on the Workshop on Uncertainty in Modeling and Simulation
Jun. 01, 1998; 30p; In English; Workshop on Uncertainty in Modeling and Simulation, June 1998, USA
Report No.(s): DE2001-764711; DOE/ER/25362-1; No Copyright; Avail: Department of Energy Information Bridge
Uncertainty has become a critically important issue in modeling and simulation of complex systems. We urgently need research leading to new tools to enable us to quantify and manage uncertainty in our simulations. Simulation by computer modeling has become fundamental to design, control, and prediction throughout science and engineering, especially in large, complex systems. Simulation, though still a relatively young specialty, is already indispensable in many fields, from designing aircraft to modeling the brain and understanding climatic change. Computation is also central, along with theory and experiment

to the conduct of science itself. Researchers will need to use simulation to address the kinds of questions that are presently intractable, such as predicting global climate in the year 2050, preventing electrical outages in the newly complex world of deregulated utilities, and anticipating the effect on California water supplies of a 10 percent increase in municipal usage.
NTIS
Computerized Simulation; Mathematical Models; Predictions

20020002810 Kansas City Plant, Kansas City, MO USA
Integration of FBTol into CADKEY
Brown, C. W.; May 04, 2000; 6p; In English
Report No.(s): DE2001-754578; KCP-613-6334; CRADA-97KCP1051; No Copyright; Avail: Department of Energy Information Bridge

A well-known but unsolved issue among CAD (Computer-Aided Design) modelers is their inability to advance the representation of non-shape information beyond the confines of decorative annotations. Experts recognized that this issue is the missing piece toward achieving both true product modeling and toward satisfying advanced solid-based applications' requirement for an enhanced representation of meaningful non-shape attributes--particularly product tolerances. Feature-Based Tolerancing (FBTol) is an enabling component technology that augments solid-based systems with a complete and unambiguous representation of tolerances. No commercial CAD system on the market contains the capabilities that FM and T's (Federal Manufacturing and Technologies) FBTol technology provides. This project was needed to infuse additional quality into the design of manufacturable products. Ensuring the quality of tolerance designs before delivery of designs will avoid significant costs encountered if errors were to be found later in the product life cycle. The union of CADKEY and FBTol will aid in product design defect detection and provide downstream applications with explicit non-shape information.
NTIS
Computer Aided Design; Manufacturing; Systems Integration; Design Analysis

20020002813 Kansas City Plant, Kansas City, MO USA
Advanced CAN (Controller Area Network) Tool
Terry, D. J.; Mar. 17, 2000; 9p; In English
Report No.(s): DE2001-752339; KCP-613-6313; CRADA96KCP1029; No Copyright; Avail: Department of Energy Information Bridge

The CAN interface cards that are currently in use are PCMCIA based and use a microprocessor and CAN chip that are no longer in production. The long-term support of the SGT CAN interface is of concern due to this issue along with performance inadequacies and technical support. The CAN bus is at the heart of the SGT trailer. If the CAN bus in the SGT trailer cannot be maintained adequately, then the trailer itself cannot be maintained adequately. These concerns led to the need for a CRADA to help develop a new product that would be called the 'Gryphon' CAN tool. FM and T provided manufacturing expertise along with design criteria to ensure SGT compatibility and long-term support. FM and T also provided resources for software support. Dearborn provided software and hardware design expertise to implement the necessary requirements. Both partners worked around heavy internal workloads to support completion of the project. This CRADA establishes a US source for an item that is very critical to support the SGT project. The Dearborn Group had the same goal to provide a US alternative to German suppliers. The Dearborn Group was also interested in developing a CAN product that has performance characteristics that place the Gryphon in a class by itself. This enhanced product not only meets and exceeds SGT requirements; it has opened up options that were not even considered before the project began. The cost of the product is also less than the European options.
NTIS
Controllers; Microprocessors; Computer Aided Manufacturing; Software Development Tools

20020002857 Computer Sciences Corp., Moffett Field, CA USA
Approaches to the Successful Design and Implementation of VR Applications
Bryson, Steve, Computer Sciences Corp., USA; [1994]; 1p; In English; Virtual Reality Applications International Conference, 7-8 Jun. 1994, Leeds, UK
Contract(s)/Grant(s): RTOP 536-01-11; No Copyright; Avail: Issuing Activity; Abstract Only

The successful design of virtual reality applications involves both "top-down" and "bottom-up" strategies. This talk will broadly outline these strategies: how bottom-up strategies are driven primarily by performance considerations; and how top-down strategies are driven primarily by the application task, the interaction metaphors, and the integration of the virtual environment. How to ensure these two approaches "meet in the middle" through Iterative design processes will be stressed. The discussion will be motivated by examples of both success and failure. The talk contains information bryson presented at SIGGRAPH '93 and

Visualization ’93, and is a high-level discussion of design principles for virtual reality. There will be essentially no discussion of virtual wind tunnel specific issues or any other matters relating to aerospace, the tutorial is a repeat of the tutorial Bryson and Steve Feiner presented at Visualization ’93 In October 1993 in San Jose, CA, and will cite the virtual windtunnel only as an example. Author

Design Analysis; Virtual Reality; Systems Integration; Applications Programs (Computers)

20020003970 Lawrence Livermore National Lab., Livermore, CA USA

Visualization of Scalar topology for structural enhancement

Bajaj, C. L.; Pascucci, V.; Schikore, D. R.; Sep. 22, 1998; 10p; In English

Report No.(s): DE2001-2866; UCRL-JC-132016; DP0101031; No Copyright; Avail: Department of Energy Information Bridge

Scalar fields arise in every scientific application. Existing scalar visualization techniques require that the user infer the global scalar structure from what is frequently an insufficient display of information. We present a visualization technique which numerically detects the structure at all scales, removing from the user the responsibility of extracting information implicit in the data, and presenting the structure explicitly for analysis. We further demonstrate how scalar topology detection proves useful for correct visualization and image processing applications such as image co-registration, isocontouring, and mesh compression. NTIS

Topology; Scalars

20020003971 Lawrence Livermore National Lab., Livermore, CA USA

Hypervolume visualization: A challenge in simplicity

Bajaj, C. L.; Pascucci, V.; Rabbiolo, G.; Schikore, D. R.; Sep. 22, 1998; 10p; In English

Report No.(s): DE2001-2865; UCRL-JC-132015; DP0101031; No Copyright; Avail: Department of Energy Information Bridge

Hyper-volume visualization is designed to provide simple and fully explanatory images that give comprehensive insights into the global structure of scalar fields of any dimension. The basic idea is to have a dimension independent viewing system that scales nicely with the geometric dimension of the dataset and that can be combined with classical approaches like isocontouring and animation of slices of data. We completely abandon (for core simplicity) rendering techniques, such as hidden surface removal or lighting or radiosity, that enhance three dimensional realism and concentrate on the real-time display of images that highlight structural (topological) features of the dataset (holes, tunnels, cavities, depressions, extrema, etc). Hyper-volume visualization on the one hand is a generalization of direct parallel projection methods in volume rendering. to achieve efficiency (and real-time performance on a graphics workstation) we combine the advantages of (1) a hierarchical representations of the hyper-volume data for multiresolution display and (2) generalized object space splatting combined with texture-mapped graphics hardware acceleration. The development of a system that implements display techniques for multidimensional datasets requires careful design of both algorithms and user interfaces that scale linearly with the dimension n of the input geometric space. This is a major challenge since straightforward generalizations of standard techniques that are suitable for display of 3D data yield exceedingly intricate interfaces. For example, a view manipulation graphical user interface is usually based on a rotation of the object about Cartesian rotation axes, with possibly unit quaternions internal representations for the rotation group. Unfortunately the number of independent rotation axes grows quadratically with dimension(three in 3D to six in 4D to ten in 5D to fifteen in 6D space). Going back to the basics of parallel projections, we develop an alternative scheme that is very simple to implement and immediately gives a view manipulation graphical user interface that scales linearly with the dimension. One can still utilize matrix or quaternion or higher dimensional rotational group representations, internally for calculations.The main results of our paper are thus both a multi-resolution direct rendering algorithm and scalable graphical user interface that provides insightful global views of scalar fields in any dimension. NTIS

Scalars; Computer Graphics

20020004017 Los Alamos National Lab., NM USA

Analysis and databasing software for integrated tomographic gamma scanner (TGS) and passive-active neutron (PAN) assay systems

Estep, R.; Melton, S.; Buenafe, C.; Aug. 01, 2000; 11p; In English

Report No.(s): DE2001-768891; LA-UR-00-3347; No Copyright; Avail: Department of Energy Information Bridge, Microfiche

The CTEN FIT program, written for Windows 9x/NT in C++, performs databasing and analysis of combined thermal/epithermal neutron (CTEN) passive and active neutron assay data and integrates that with isotopics results and gamma-ray data from methods such as tomographic gamma scanning (TGS). The binary database is reflected in a companion Excel database that allows extensive customization via Visual Basic for Applications macros. Automated analysis options make

the analysis of the data transparent to the assay system operator. Various record browsers and information displays simplify record keeping tasks.
NTIS
Tomography; Gamma Rays; Scanners; Computer Programs; Assaying

20020004353 Institute for Computer Applications in Science and Engineering, Hampton, VA USA
An Analysis Mechanism for Automation in Terminal Area *Final Report*
Parikh, Stavan M., Institute for Computer Applications in Science and Engineering, USA; October 2001; 15p; In English
Contract(s)/Grant(s): NAS1-97046; RTOP 505-90-52-01
Report No.(s): NASA/CR-2001-211235; ICASE-2001-32; NAS 1.26:211235; No Copyright; Avail: CASI; A03, Hardcopy; A01, Microfiche

This paper describes an Air Traffic Simulator (ATS) that provides a simulation capability for terminal area automation. The ATS is capable of realistic terminal area modeling, automation performance and feasibility studies, and system wide fault-tolerance analysis. The ATS is evaluated through modeling of self-spacing and self-merging of aircraft following Standard Terminal Arrival (STARs). These algorithms are described in detail and preliminary analysis results are provided. The analysis exposes the limitations of the algorithms due to their integration. Possible modifications to overcome these limitations are suggested. Future work planned for the ATS is described. Overall the ATS is an easily extensible and powerful tool for preliminary analysis of new technologies.
Author
Air Traffic Control; Simulators; Algorithms; Terminal Facilities; Computerized Simulation; Airfield Surface Movements

20020004354 Institute for Computer Applications in Science and Engineering, Hampton, VA USA
A Parallel Multigrid Solver for Viscous Flows on Anisotropic Structured Grids *Final Report*
Prieto, Manuel, Universidad Complutense, Spain; Montero, Ruben S., Universidad Complutense, Spain; Llorente, Ignacio M., Universidad Complutense, Spain; October 2001; 24p; In English
Contract(s)/Grant(s): NAS1-97046; RTOP 505-90-52-01
Report No.(s): NASA/CR-2001-211238; ICASE-2001-34; NAS 1.26:211238; No Copyright; Avail: CASI; A03, Hardcopy; A01, Microfiche

This paper presents an efficient parallel multigrid solver for speeding up the computation of a 3-D model that treats the flow of a viscous fluid over a flat plate. The main interest of this simulation lies in exhibiting some basic difficulties that prevent optimal multigrid efficiencies from being achieved. As the computing platform, we have used Coral, a Beowulf-class system based on Intel Pentium processors and equipped with GigaNet cLAN and switched Fast Ethernet networks. Our study not only examines the scalability of the solver but also includes a performance evaluation of Coral where the investigated solver has been used to compare several of its design choices, namely, the interconnection network (GigaNet versus switched Fast-Ethernet) and the node configuration (dual nodes versus single nodes). As a reference, the performance results have been compared with those obtained with the NAS-MG benchmark.
Author
Computer Systems Performance; Anisotropy; Parallel Processing (Computers); Multigrid Methods; Smoothing

20020004355 Raytheon Technical Services Co., Hampton, VA USA
Parallelization of Program to Optimize Simulated Trajectories (POST3D)
Hammond, Dana P., Raytheon Technical Services Co., USA; November 2001; 34p; In English
Contract(s)/Grant(s): NASA Order L-70750-D; RTOP 725-10-31-03
Report No.(s): NASA/CR-2001-211250; NAS 1.26:211250; RAE001-CR-0701.00; No Copyright; Avail: CASI; A03, Hardcopy; A01, Microfiche

This paper describes the parallelization of the Program to Optimize Simulated Trajectories (POST3D). POST3D uses a gradient-based optimization algorithm that reaches an optimum design point by moving from one design point to the next. The gradient calculations required to complete the optimization process, dominate the computational time and have been parallelized using a Single Program Multiple Data (SPMD) on a distributed memory NUMA (non-uniform memory access) architecture. The Origin2000 was used for the tests presented.
Author
Computer Programs; Trajectory Optimization; Finite Difference Theory; Parallel Processing (Computers); Optimization

20020005090 Argonne National Lab., IL USA

Agent-based tool for infrastructure interdependency policy analysis

North, M. J.; Dec. 14, 2000; 9p; In English

Report No.(s): DE2001-772132; ANL/DIS/CP-103636; No Copyright; Avail: Department of Energy Information Bridge, Microfiche

Complex Adaptive Systems (CAS) can be applied to investigate complex infrastructure interdependencies such as those between the electric power and natural gas markets. These markets are undergoing fundamental transformations including major changes in electric generator fuel sources. Electric generators that use natural gas as a fuel source are rapidly gaining market share. These generators introduce direct interdependency between the electric power and natural gas markets. These interdependencies have been investigated using the emergent behavior of CAS model agents within the Spot Market Agent Research Tool Version 2.0 Plus Natural Gas (SMART II+).

NTIS

Software Engineering; Electric Power; Natural Gas

20020005162 Colorado Univ., Dept. of Computer Science, Boulder, CO USA

Software Environments in Support of Wide-Area Development ***Final Report, 28 Aug. 1994 - 26 Jul. 2000***

Heimbigner, Dennis; King, Roger; Wolf, Alexander; Dziegiel, Roger J.; Apr. 2001; 89p; In English

Contract(s)/Grant(s): F30602-94-C-0253; AF Proj. B126

Report No.(s): AD-A390919; AFRL-IF-RS-TR-2001-46; No Copyright; Avail: Defense Technical Information Center (DTIC)

The goal of the University of Colorado Arcadia project was to explore the problems of wide-area software engineering. Historically, the project was the second phase in a long-term Arcadia consortium of universities and companies whose goal was to advance the state of the art in software engineering environments. The Univ of Colorado Arcadia project has been successful in achieving its objective: producing innovative, useful and interesting research results in the areas of software process, software architecture, configuration management, deployment data management, distributed computing and web-data management. These research results were embodied in a number of prototype systems: Q(distributed computing), Process Wall (software process execution) Balboa (software process capture), Sybil (databased integration), NUCM (distributed configuration Management), SRM (software release), DVS (distributed development), Software Dock (distributed wide-area deployment), Siena (Internet-scale event notification), Aladdin (software architecture analysis), Menage (configurable software architecture), and WIT (Federating web-data). The results from this project have been widely disseminated in the form of publications software distribution to over 600 sites, technical transfers to commercial practice, and through the conferring of degrees upon quality Ph.D. and M.S. students.

DTIC

Software Engineering; Wide Area Networks; Computer Programs; Architecture (Computers); Computer Programming; Programming Environments

20020005180 Lawrence Livermore National Lab., Livermore, CA USA

Using Python to Develop Graphical Interfaces to Scientific Data

MacFarland, L.; Streletz, G. J.; Sep. 24, 1999; 10p; In English

Report No.(s): DE2001-756952; UCRL-JC-135877; DP0101031; No Copyright; Avail: Department of Energy Information Bridge

At Lawrence Livermore National Laboratory (LLNL), Python has proven to be a convenient language for the development of graphical user interfaces (GUIs) which allow scientists to view, plot, and analyze scientific data. Two such applications are described in this paper. The first, EOSView, is a browser application for an equation of state data library at LLNL. EOSView is used by scientists throughout the laboratory who use simulation codes that access the data library, or who need equation of state data for other purposes. EOSView provides graphical visualization capabilities, as well as the capability to analyze the data in many different ways. The second application, Zimp, is a GUI that allows interactive use of the Stark Line Shape Database. It is used to access and plot data. The quick construction of Zimp from elements of the EOSView code provides a useful lesson in code reuse, and illustrates how the object-oriented nature of Python facilitates this goal. In general, Python has proven to be an appropriate choice of language for applications of this type for several reasons, including the easy access to GUI functionality provided by Tkinter, the ease with which C functions can be called from Python, and the convenient handling of strings in Python. Moreover, the features of the Python language, combined with the fact that it is interpreted rather than compiled, have allowed for extremely quick prototyping.

NTIS

Computer Graphics; Equations of State; Display Devices; Graphical User Interface; Object-Oriented Programming

20020005181 Lawrence Livermore National Lab., Livermore, CA USA

Improving the Extension Facilities in C+

Dubois, P. F.; Scott, B. A.; Sep. 24, 1999; 9p; In English

Report No.(s): DE2001-756953; UCRL-JC-135886; No Copyright; Avail: Department of Energy Information Bridge

CXX is a facility for extending Python using C++. Recently, the authors have substantially revised and improved the way in which you create extension objects and extension modules in C++. The method is now much more natural and has much less overhead, both in the code generated and in the effort needed to create the objects and extensions.

NTIS

C++ (Programming Language); Programming Languages; Computer Programming

20020005238 Argonne National Lab., IL USA

Scientific data management system for irregular applications

No, J.; Thakur, R.; Kaushik, D.; Freitag, L.; Choudhary, A.; Jan. 15, 2001; 8p; In English

Report No.(s): DE2001-774048; ANL/MCS/CP-103840; No Copyright; Avail: Department of Energy Information Bridge, Microfiche

Many scientific applications are I/O intensive and generate or access large data sets, spanning hundreds or thousands of ”files”. Management, storage, efficient access, and analysis of this data present an extremely challenging task. We have developed a software system, called Scientic Data Manager (SDM), that uses a combination of parallel file I/O and database support for high-performance scientic data management. SDM provides a high-level API to the user and, internally, uses a parallel file system to store real data and a database to store application-related metadata. In this paper, we describe how we designed and implemented SDM to support irregular applications. SDM can efficiently handle the reading and writing of data in an irregular mesh as well as the distribution of index values. We describe the SDM user interface and how we implemented it to achieve high performance. SDM makes extensive use of MPI-IO’s noncontiguous collective I/O functions. SDM also uses the concept of a ”history file” to optimize the cost of the index distribution using the metadata stored in the database. We present performance results with two irregular applications, a CFD code called FUN3D and a Rayleigh-Taylor instability code, on the SGI Origin2000 at Argonne National Laboratory.

NTIS

Data Management; Systems Management; Data Bases

20020005262 Sandia National Labs., Albuquerque, NM USA

Implementation of the Berlekamp-Massey Linear Feedback Shift-Register Synthesis Algorithm in the C Programming Language

Campbell, P. L.; Aug. 01, 1999; 18p; In English

Report No.(s): DE2001-12658; SAND99-2033; No Copyright; Avail: Department of Energy Information Bridge, Microfiche

This report presents an implementation of the Berlekamp-Massey linear feedback shift-register (LFSR) synthesis algorithm in the C programming language. Two pseudo-code versions of the code are given, the operation of LFSRs is explained, C-version of the pseudo-code versions is presented, and the output of the code, when run on two input samples, is shown.

NTIS

C (Programming Language); Feedback; Shift Registers

20020005396 California Univ., Lawrence Berkeley Lab., Berkeley, CA USA

Survey of packages for large linear systems

Wu, K.; Milne, B.; Feb. 11, 2000; 41p; In English

Report No.(s): DE2001-775109; LBNL-45446; No Copyright; Avail: Department of Energy Information Bridge, Microfiche

This paper evaluates portable software packages for the iterative solution of very large sparse linear systems on parallel architectures. While we cannot hope to tell individual users which package will best suit their needs, we do hope that our systematic evaluation provides essential unbiased information about the packages and the evaluation process may serve as an example on how to evaluate these packages. The information contained here include feature comparisons, usability evaluations and performance characterizations. This review is primarily focused on self-contained packages that can be easily integrated into an existing program and are capable of computing solutions to very large sparse linear systems of equations. More specifically, it concentrates on portable parallel linear system solution packages that provide iterative solution schemes and related preconditioning schemes because iterative methods are more frequently used than competing schemes such as direct methods. The eight packages evaluated are: Aztec, BlockSolve,ISIS++, LINSOL, P-SPARSLIB, PARASOL, PETSc, and PINEAPL. Among the eight portable parallel iterative linear system solvers reviewed, we recommend PETSc and Aztec for most application

programmers because they have well designed user interface, extensive documentation and very responsive user support. Both PETSc and Aztec are written in the C language and are callable from FORTRAN. For those users interested in using FORTRAN 90, PARASOL is a good alternative. ISIS++is a good alternative for those who prefer the C++ language. Both PARASOL and ISIS++ are relatively new and are continuously evolving. Thus their user interface may change. In general, those packages written in FORTRAN 77 are more cumbersome to use because the user may need to directly deal with a number of arrays of varying sizes. Languages like C++ and FORTRAN 90 offer more convenient data encapsulation mechanisms which make it easier to implement a clean and intuitive user interface. In addition to reviewing these portable parallel iterative solver packages, we also provide a more cursory assessment of a range of related packages, from specialized parallel preconditioners to direct methods for sparse linear systems.
NTIS
Computer Programs; Iterative Solution; Linear Systems

20020005417 Computer Sciences Corp., USA
The NAS Trace Visualizer (NTV)
Lopez, Louis, Computer Sciences Corp., USA; [1994]; 1p; In English
Contract(s)/Grant(s): RTOP 536-01-11; No Copyright; Avail: Issuing Activity; Abstract Only

NTV is a tool used to visualize execution traces from message passing systems. It is designed to be ported easily to different trace formats. The first version of NTV uses trace files produced using AIMS Version 2.2. Versions for the native traces from the IBM SP2 and Intel Paragon are nearing completion. A distinctive characteristic of NTV is that it uses static displays rather then time varying displays. This, in combination with mouse controlled zooming, gives the user the ability to get a global view of the execution and a focused view of details. The principal display is a time line display that shows a color coded time line for each processor. The color coding shows the processor status. Messages between processors are indicated by lines connecting the processors involved in the communications. Controls for these message edges let the user show all messages, no messages, or only message between specified sets of processors. Summary (profiling) displays are also produced. These are of two types. One allocates information by processor, e.g., the time the processor was blocked sending, and the other allocates information by function, e.g., the time a function was blocked sending.
Author
Messages; Message Processing

20020005865 RECOM Technologies, Inc., Moffett Field, CA USA
Practical Planning in COLLAGE
Lansky, Amy L., RECOM Technologies, Inc., USA; Getoor, Lise C., RECOM Technologies, Inc., USA; [1994]; 1p; In English; AAAI Fall Symposium on Planning and Learning, 4-6 Nov. 1994, New Orleans, LA, USA; Sponsored by American Association for Artificial Intelligence, USA
Contract(s)/Grant(s): RTOP 233-01-02; No Copyright; Avail: Issuing Activity; Abstract Only

COLLAGE is a domain-independent planner that differs from traditional planners in two key ways: (1) it uses a diverse and extendible set of (it action-based) plan constructions methods; and (2) it utilizes a technique called (it localization) to partition the planning problem into smaller (and potentially interacting) sub problems. In this paper, we describe these features and how they are exploited in two different real-world planning domains. The first domain, building construction planning, has served as a framework for us to investigate how localization can improve scalability. The second domain, data analysis planning, benefits from COLLAGE's unique plan construction and representation methods. In addition, we describe extensions that were necessary to tackle these real-world problems.
Author
Construction; Layouts

20020005869 North Carolina State Univ., Raleigh, NC USA
Abstraction-Based Approaches to Correct Reactive Software ***Final Report, 1 Jul. 1998-30 Jun. 2001***
Iyer, S. P.; Sep. 17, 2001; 5p; In English
Contract(s)/Grant(s): DAAG55-98-1-0309
Report No.(s): AD-A395324; ARO-38682.1-CI; No Copyright; Avail: CASI; A01, Hardcopy; A01, Microfiche

This final reports on our efforts to make abstraction-based reasoning of reactive software possible. Concurrency Workbench, a tool for designs of reactive concurrent systems was enriched to handle programs. The enrichment depends upon notions of

abstractions, a technique used in compilers. Furthermore, work was also done on enriching the Concurrency Workbench to deal with probabilistic information regarding errors during a systems execution.
DTIC
Concurrent Engineering; Compilers; Software Engineering; Applications Programs (Computers)

20020005870 Naval Postgraduate School, Monterey, CA USA
Enhancements and Extensions of Formal Models for Risk Assessment in Software Projects
Murrah, Michael R.; Luqi,; Johnson, Craig S.; Jan. 2001; 8p; In English
Report No.(s): AD-A395325; ARO-40473.32-MA-SP; No Copyright; Avail: CASI; A02, Hardcopy; A01, Microfiche

Over the past 40 years limited progress has been made to help practitioners estimate the risk and the required effort necessary to deliver software solutions. Recent developments improve this outlook, one in particular, the research conducted by Juan Carlos Nogueira. Dr. Nogueira developed a formal model for risk assessment that can be used to estimate a software project's risk when examined against a desired development time-line. This model is based on easily obtainable software metrics. These metrics are quantifiable early in the software development process.
DTIC
Software Engineering; Mathematical Models; Risk; Technology Assessment

20020005876 Naval Postgraduate School, Dept. of Computer Science, Monterey, CA USA
JAVA Wrappers for Automated Interoperability
Cheng, Ngom; Berzins, Valdis; Luqi,; Bhattacharya, Swapan; Dec. 2000; 22p; In English; Publ. in proceedings of Databases in Networked Information Systems International Workshop, Aizu, Japan, Dec 2000, Lecture Notes in Computer Science, n1966 p45-64, 2000
Report No.(s): AD-A395337; ARO-40473.30-MA-SP; No Copyright; Avail: CASI; A03, Hardcopy; A01, Microfiche

This paper concentrates on the issues related to implementation of interoperability between distributed subsystems, particularly in the context of re engineering and integration of several centralized legacy systems. Currently most interoperability techniques require the data or services to be tightly coupled to a particular server. Furthermore, as most programmers are trained in designing stand-alone application, developing distributed system proves to be time-consuming and difficult. Here, we addressed those concerns by creating an interface wrapper model that allows developers to treat distributed objects as local objects. A tool that automatically generates the features of Java interface wrapper from a specification language called the Prototyping System Description Language has been developed based on the model.
DTIC
Interoperability; Java (Programming Language); Automation; Software Engineering; Applications Programs (Computers)

20020005881 Sytronics, Inc., Dayton, OH USA
Integrate 1.28: A Software Tool for Visualizing, Analyzing, and Manipulating Three-Dimensional Data ***Interim Report, Jan. 1996-Mar. 1997***
Burnsides, Dennis; Files, Patrick; Whitestone, Jennifer; Jan. 1998; 175p; In English
Contract(s)/Grant(s): F41624-93-C-6001; Proj-7184
Report No.(s): AD-A395374; AFRL-HE-WP-TR-2000-0100; No Copyright; Avail: CASI; A08, Hardcopy; A02, Microfiche

This report documents the functionality available using Integrate 1.28, a Silicon Graphics-based software package, to visualize, analyze, and manipulate three-dimensional topographic data. The analysis capability represented by this software is robust, flexible, and instrumental in applying 3-D anthropometry toward the improved fit of protective equipment, clothing, commercial head gear, and medical devices. Tutorials are available to guide the user through representative applications.
DTIC
Anthropometry; Software Development Tools; Three Dimensional Models

62
COMPUTER SYSTEMS

Includes computer networks and distributed processing systems. For information systems see 82 Documentation and Information Science. For computer systems applied to specific applications, see the associated category.

20020001840 Argonne National Lab., IL USA
Dynamic information architecture system: an advanced simulation framework for military and civilian applications
Campbell, A. P.; Hummel, J. R.; Jan. 08, 1998; 8p; In English
Report No.(s): DE2001-8876; ANL/DIS/CP-94722; No Copyright; Avail: Department of Energy Information Bridge, Microfiche

DIAS, the Dynamic Information Architecture System, is an object-oriented simulation system that was designed to provide an integrating framework in which new or legacy software applications can operate in a context driven frame of reference. DIAS provides a flexible and extensible mechanism to allow disparate, and mixed language, software applications to interoperate. DIAS captures the dynamic interplay between different processes or phenomena in the same frame of reference. Finally, DIAS accommodates a broad range of analysis contexts, with widely varying spatial and temporal resolutions and fidelity.
NTIS
Object-Oriented Programming; Information Systems; Architecture (Computers)

20020002017 National Computer Security Center, Fort Meade, MD USA
A Guide to Procurement of Trusted Systems: Computer Security Contract Data Requirements List and Data Item Description Tutorial, Volumes 3-4, 1 ***Final Report***
Feb. 28, 1994; 159p; In English
Report No.(s): AD-A393184; NCSC-TG-024-Vols-3-4; No Copyright; Avail: Defense Technical Information Center (DTIC)

A Guide to Procurement of Trusted Systems: Computer Security Contract Data Requirements List and Data Item Description Tutorial, Volume 3 of 4 in the Procurement Guideline Series, is written to be used by Federal Agencies to help facilitate the definition of computer security deliverables required in the acquisition of trusted products in accordance with DoD 5200.28-STD, Department of Defense Trusted Computer System Evaluation Criteria. It is designed for new or experienced automated information system developers, purchasers, or program managers who must identify and satisfy requirements associated with security-relevant acquisitions. The emphasis of this guideline is on the data requirements for products. Volume 3 specifies the data deliverables to meet security assurance needs by providing guidance on Contract Data Requirements Lists (CDRLs) and their associated Data Item Descriptions (DIDs).
DTIC
Computer Information Security; Defense Program; Information Systems; Procurement

20020002249 Sandia National Labs., Albuquerque, NM USA
Dynamic Isosurface Extraction and Level-of-Detail in Voxel Space
Lamphere, P. B.; Linebarger, J. M.; Mar. 01, 1999; 25p; In English
Report No.(s): DE2001-5649; SAND98-1224-REV; No Copyright; Avail: Department of Energy Information Bridge, Microfiche

A new visualization representation is described, which dramatically improves interactivity for scientific visualizations of structured grid data sets by creating isosurfaces at interactive speeds and with dynamically changeable levels-of-detail (LOD). This representation enables greater interactivity by allowing an analyst to dynamically specify both the desired isosurface threshold and required level-of-detail to be used while rendering the image. A scientist can therefore view very large isosurfaces at interactive speeds (with a low level-of-detail), but has the full data set always available for analysis. The key idea is that various levels-of-detail are represented as differently sized hexahedral virtual voxels, which are stored in a three-dimensional binary tree, or kd-tree; thus the level-of-detail representation is done in voxel space instead of the traditional approach which relies on surface or geometry space decimations. Utilizing the voxel space is an essential step to moving from a post-processing visualization paradigm to a quantitative, real-time paradigm. This algorithm has been implemented as an integral component of the EIGEN/VR project at Sandia National Laboratories, which provides a rich environment for scientists to interactively explore and visualize the results of very large-scale simulations performed on massively parallel supercomputers.
NTIS
Structured Grids (Mathematics); Scientific Visualization; Parallel Processing (Computers)

20020002285 Los Alamos National Lab., NM USA

Performance evaluation of the quadrics interconnection network

Petrini, F.; Hoisie, A.; Oct. 01, 2000; 44p; In English

Report No.(s): DE2001-766063; LA-UR-00-5205; No Copyright; Avail: Department of Energy Information Bridge, Microfiche

We present an initial performance evaluation of the Quadrics interconnection network (QNET). We describe the main hardware and software features of QNET of relevance to the system designer and to the end user. A benchmark methodology is proposed in which important performance and scalability parameters are included. Actual benchmarks are performed on an experimental cluster. Based on these benchmarks, a thorough performance analysis of the QNET is presented in the paper. The preliminary analysis indicates a remarkably good performance of the interconnect, such as user-level latency of 2.1 ps, a communication bandwidth of 200 MB/s with lV1j2 of 512 bytes, efficient support to collective communication patterns and good contention resolution under heavy traffic.

NTIS

Computer Networks; Performance Prediction; Computers; Computer Programs

20020002785 Sandia National Labs., Albuquerque, NM USA

Software Systems: Consequence versus Functionality

Berg, R.; Winter, V. L.; Aug. 05, 1999; 4p; In English

Report No.(s): DE2001-9694; SAND99-2046C; No Copyright; Avail: Department of Energy Information Bridge, Microfiche

The purpose of this panel is to present different perspectives and opinions regarding the issues surrounding why software should or shouldn't be entrusted with critical (high consequence) functionality.

NTIS

Computer Programs; Functional Analysis

20020004348 Computer Sciences Corp., Moffett Field, CA USA

A Parallel Implementation of Multilevel Recursive Spectral Bisection for Application to Adaptive Unstructured Meshes, Chapter 1

Barnard, Stephen T., Cray Research, Inc., USA; Simon, Horst, Computer Sciences Corp., USA; [1994]; 6p; In English; 7th SIAM Conference on Parallel Processing for Scientific Computing, 15-17 Feb. 1994, San Francisco, CA, USA; Sponsored by Society for Industrial and Applied Mathematics, USA

Contract(s)/Grant(s): RTOP 536-01-11; No Copyright; Avail: CASI; A02, Hardcopy; A01, Microfiche

The design of a parallel implementation of multilevel recursive spectral bisection is described. The goal is to implement a code that is fast enough to enable dynamic repartitioning of adaptive meshes.

Author

Computational Grids; Algorithms; Parallel Processing (Computers)

20020005866 Sandia National Labs., Albuquerque, NM USA

A Brief Overview of Sandia National Laboratories IO/IA Modeling Research & Development

Pollock, Bob; Sep. 2001; 56p; In English; Original contains color images

Report No.(s): AD-A395165; No Copyright; Avail: CASI; A04, Hardcopy; A01, Microfiche

An overview of Sandia National Laboratories contribution to IO/IA Modeling and Research.

DTIC

Research and Development; Mathematical Models; Computer Information Security; Communication Networks

63
CYBERNETICS, ARTIFICIAL INTELLIGENCE AND ROBOTICS

Includes feedback and control theory, information theory, machine learning, and expert systems. For related information see also 54 Man/System Technology and Life Support.

20020001551 Sandia National Labs., Albuquerque, NM USA

Adaptive Remote-Sensing Techniques Implementing Swarms of Mobile Agents

Cameron, S. M.; Loubriel, G. M.; Rbinett, R. D.; Stantz, K. M.; Trahan, M. W.; Apr. 01, 1999; 20p; In English

Report No.(s): DE2001-5682; SAND99-0770C; No Copyright; Avail: Department of Energy Information Bridge

This paper focuses on our recent work at Sandia National Laboratories toward engineering a physics-based swarm of mobile vehicles for distributed sensing applications. Our goal is to coordinate a sensor array that optimizes sensor coverage and multivariate signal analysis by implementing artificial intelligence and evolutionary computational techniques. These intelligent control systems integrate both globally operating decision-making systems and locally cooperative information-sharing modes using genetically-trained neural networks. Once trained, neural networks have the ability to enhance real-time operational responses to dynamical environments, such as obstacle avoidance, responding to prevailing wind patterns, and overcoming other natural obscurants or interferences (jammers). The swarm realizes a collective set of sensor neurons with simple properties incorporating interactions based on basic community rules (potential fields) and complex interconnecting functions based on various neural network architectures, Therefore, the swarm is capable of redundant heterogeneous measurements which furnishes an additional degree of robustness and fault tolerance not afforded by conventional systems, while accomplishing such cognitive tasks as generalization, error correction, pattern recognition, and sensor fission. The robotic platforms could be equipped with specialized sensor devices including transmit/receive dipole antennas, chemical or biological sniffers in combination with recognition analysis tools, communication modulators, and laser diodes. Our group has been studying the collective behavior of an autonomous, multi-agent system applied to emerging threat applications. to accomplish such tasks, research in the fields of robotics, sensor technology, and swarms are being conducted within an integrated program. Mission scenarios under consideration include ground penetrating impulse radar (GPR) for detection of under-ground structures, airborne systems, and plume detection/remediation. We will describe our research in these areas and give a status report on our progress, including simulations and laboratory-based sensor experiments.

NTIS

Radar; Robots; Remote Sensing; Mobility; Error Analysis

20020001773 National Aerospace Lab., Amsterdam, Netherlands

Divide and Control: Making Distributed Real-Time Simulations Work

Kesseler, E.; ten Dam, A. A.; van Sterkenburg, R. P.; van de Sluis, E.; Aug. 2000; 24p; In English; Color illustrations reproduced in black and white. Also pub. in Proceedings of the International Workshop on Simulation for European Space Programmes (6th), SESP 2000, Noordwijk, The Netherlands, Octo; Original contains color illustrations

Report No.(s): PB2001-108825; NLR-TP-2000-412; No Copyright; Avail: CASI; A03, Hardcopy; A01, Microfiche

Traditionally real-time simulators are single-site facilities. Nowadays, the use of simulators for engineering and training requires increased capabilities to simulate total system behaviour by including accurate rendering of the constituent subsystems. For complex systems, like those encountered in the space domain, various organisations have good simulators for their own subsystems. to save costs and reduce time-to-market it is advantageous to combine these proprietary simulators of the various companies into a single facility, a federation. For these situations NLR has developed a tool, SmartFED (Scenario MAnager for Real-Time FEderation Directing), which facilitates that proprietary simulators at various geographic locations participate in a joint simulation. The result is a single simulation operating a shared scenario. The High Level Architecture (HLA) based SmartFED accomplishes this by performing three main tasks: control, monitor and scenario definition and execution. Each task is implemented in an independent software component. This approach to distributed simulation allows the human experiment leader to control the execution of the simulation federation while each organisation retains full control over its proprietary simulator.

NTIS

Real Time Operation; Computerized Simulation; Complex Systems; Computer Programs; Guidance (Motion)

20020002003 Sandia National Labs., Albuquerque, NM USA

Dynamical Behavior of Multi-Robot Systems Using Lattice Gas Automata

Cameron, S. M.; Robinett, R.; Stantz, K. M.; Trahan, M. W.; Wagner, J. S.; Mar. 11, 1999; 13p; In English

Report No.(s): DE2001-4280; SAND99-0598C; No Copyright; Avail: Department of Energy Information Bridge, Microfiche

Recent attention has been given to the deployment of an adaptable sensor array realized by multi-robotic systems. Our group has been studying the collective behavior of autonomous, multi-agent systems and their applications in the area of remote-sensing and emerging threats. to accomplish such tasks, an interdisciplinary research effort at Sandia National Laboratories are conducting tests in the fields of sensor technology, robotics, and multi-robotic and multi-agents architectures. Our goal is to coordinate a constellation of point sensors that optimizes spatial coverage and multivariate signal analysis using unmanned robotic vehicles (e.g., RATLERs, Robotic All-ten-sin Lunar Exploration Rover-class vehicles). Overall design methodology is to evolve complex collective behaviors realized through simple interaction (kinetic) physics and artificial intelligence to enable real-time operational responses to emerging threats. This paper focuses on our recent work understanding the dynamics of many-body systems using the physics-based hydrodynamic model of lattice gas automata. Three design features are investigated. One, for single-speed

robots, a hexagonal nearest-neighbor interaction topology is necessary to preserve standard hydrodynamic flow. Two, adaptability, defined by the swarm's deformation rate, can be controlled through the hydrodynamic viscosity term, which, in turn, is defined by the local robotic interaction rules. Three, due to the inherent non-linearity of the dynamical equations describing large ensembles, development of stability criteria ensuring convergence to equilibrium states is developed by scaling information flow rates relative to a swarm's hydrodynamic flow rate. An initial test case simulates a swarm of twenty-five robots that maneuvers past an obstacle while following a moving target. A genetic algorithm optimizes applied nearest-neighbor forces in each of five spatial regions distributed over the simulation domain. Armed with knowledge, the swarm adapts by changing state in order to avoid the obstacle. Simulation results are qualitatively similar to lattice gas.
NTIS
Automata Theory; Genetic Algorithms; Remote Sensing; Computerized Simulation; Robotics

20020002262 Forest Service, Pacific Northwest Research Station, Portland, OR USA
Fuzzy Logic Knowledge Bases in Integrated Landscape Assessment: Examples and Possibilities
Reynolds, K. M.; Sep. 2001; 36p; In English
Report No.(s): PB2002-100128; FSGTR-PNW-521; No Copyright; Avail: CASI; A03, Hardcopy; A01, Microfiche

The literature on ecosystem management has articulated the need for integration across disciplines and spatial scales, but convincing demonstrations of integrated analysis to support ecosystem management are lacking. This paper focuses on integrated ecological assessment because ecosystem management fundamentally is concerned with integrated management, which presupposes integrated analysis. Knowledge-based solutions are particularly relevant to ecosystem management because the topic is conceptually broad and complex and involves many abstract concepts whose assessment depends on many interdependent states and processes. Logic constructs are useful in this context because the problem can be evaluated as long as the entities and their logical relations are understood in a general way and can be expressed by subject matter authorities. As an example, ecosystem management decision-support system provides a formal logic framework for integrated analysis across multiple problem domains, has the ability to reason with incomplete information, and assists with optimizing the conduct of assessments by setting priorities on missing data. Most significant, however, is the possibility that knowledge-based reasoning could readily be extended to networks of knowledge bases that provide logical specifications for integrated analysis across spatial scales.
NTIS
Fuzzy Systems; Management Systems; Information Theory; Domains

20020003397 Los Alamos National Lab., NM USA
Optimizing through co-evolutionary avalanches
Boettcher, S.; Percus, A.; Aug. 01, 2000; 13p; In English
Report No.(s): DE2001-768248; LA-UR-00-3652; No Copyright; Avail: Department of Energy Information Bridge, Microfiche

We explore a new general-purpose heuristic for finding high-quality solutions to hard optimization problems. The method, called extremal optimization, is inspired by "self-organized critically," a concept introduced to describe emergent complexity in many physical systems. In contrast to Genetic Algorithms which operate on an entire "gene-pool" of possible solutions, extremal optimization successively replaces extremely undesirable elements of a sub-optimal solution with new, random ones. Large fluctuations, called "avalanches," ensue that efficiently explore many local optima. Drawing upon models used to simulate far-from-equilibrium dynamics, extremal optimization complements approximation methods inspired by equilibrium statistical physics, such as simulated annealing. With only one adjustable parameter, its performance has proved competitive with more elaborate methods, especially near phase transitions. Those phase transitions are found in the parameter space of most optimization problems, and have recently been conjectured to be the origin of some of the hardest instances in computational complexity. We will demonstrate how extremal optimization can be implemented for a variety of combinatorial optimization problems. We believe that extremal optimization will be a useful tool in the investigation of phase transitions in combinatorial optimization problems, hence valuable in elucidating the origin of computational complexity.
NTIS
Heuristic Methods; Optimization; Theoretical Physics

20020004007 Los Alamos National Lab., NM USA
Combining local search with co-evolution in a remarkably simple way
Boettcher, S.; Percus, A.; May 01, 2000; 10p; In English
Report No.(s): DE2001-768990; LA-UR-00-2318; No Copyright; Avail: Department of Energy Information Bridge

The authors explore a new general-purpose heuristic for finding high-quality solutions to hard optimization problem. The method, called extremal optimization, is inspired by self-organized criticality, a concept introduced to describe emergent

complexity in physical systems. In contrast to genetic algorithms, which operate on an entire gene-pool of possible solutions, extremal optimization successively replaces extremely undesirable elements of a single sub-optimal solution with new, random ones. Large fluctuations, or avalanches, ensue that efficiently explore many local optima. Drawing upon models used to simulate far-from-equilibrium dynamics, extremal optimization complements heuristics inspired by equilibrium statistical physics, such as simulated annealing. With only one adjustable parameter, its performance has proved competitive with more elaborate methods, especially near phase transitions. Phase transitions are found in many combinatorial optimization problems, and have been conjectured to occur in the region of parameter space containing the hardest instances. We demonstrate how extremal optimization can be implemented for a variety of hard optimization problems. We believe that this will be a useful tool in the investigation of phase transitions in combinatorial optimization, thereby helping to elucidate the origin of computational complexity.
NTIS
Genetic Algorithms; Combinatorial Analysis; Heuristic Methods; Phase Transformations; Simulated Annealing; Statistical Mechanics

20020004016 Los Alamos National Lab., NM USA
Towards measures of intelligence based on semiotic control
Joslyn, C.; Aug. 01, 2000; 9p; In English
Report No.(s): DE2001-768903; LA-UR-00-3576; No Copyright; Avail: Department of Energy Information Bridge, Microfiche
We address the question of how to identify and measure the degree of intelligence in systems. We define the presence of intelligence as equivalent to the presence of a control relation. We contrast the distinct atomic semiotic definitions of models and controls, and discuss hierarchical and anticipatory control. We conclude with a suggestion about moving towards quantitative measures of the degree of such control in systems.
NTIS
Control Theory; Computer Techniques; Artificial Intelligence

20020004189 NASA Ames Research Center, Moffett Field, CA USA
A Framework for Distributed Rover Control and Three Sample Applications
McGuire, Steve, NASA Ames Research Center, USA; [2001]; 4p; In English; No Copyright; Avail: CASI; A01, Hardcopy; A01, Microfiche
In order to develop quality control software for multiple robots, a common interface is required. by developing components in a modular fashion with well-defined boundaries, roboticists can write code to program a generic rover, and only require very simple modifications to run on any robot with a properly implemented framework. The proposed framework advances a Generic Rover that could be any rover, from Real World Interface's All Terrain Robot Vehicle Jr. series to the Fido-class rovers from the Jet Propulsion Laboratory to any other research robot. Using these generic hardware interfaces, software designers and engineers can concentrate on the actual code, and not have to worry about hardware details. In addition to the hardware support framework, three sample applications have been developed to demonstrate the flexibility and extensibility of the framework.
Author
Distributed Parameter Systems; Roving Vehicles; Software Development Tools; Human-Computer Interface

20020005877 North Carolina Agricultural and Technical State Univ., Dept. of Mechanical Engineering, Greensboro, NC USA
Artificial Nerves for Structural Condition Monitoring
Martin, William N., Jr.; Ghoshal, Anindya; Lebby, Gary; Sundaresan, Mannur J.; Schulz, Mark J.; Sep. 14, 2001; 11p; In English; Presented at the Workshop on Structural Health Monitoring (3d), Held in Stanford, CA on September 12-14, 2001. Prepared in cooperation with the Dept. of Mechanical Engineering, Univ. of Cincinnati, Cincinnati, OH
Contract(s)/Grant(s): F49620-00-1-0232
Report No.(s): AD-A395341; No Copyright; Avail: CASI; A03, Hardcopy; A01, Microfiche
Structural condition monitoring refers to using in-situ sensors to monitor the internal loads and the health of a structure in real-time. This will allow a structure to be operated at its maximum performance and efficiency while minimizing the fatigue damage. to achieve this on a large structure, new highly distributed sensor concepts are investigated in which piezoceramic sensors are used to mimic biological nerves. A simulation model and a corresponding experiment show how these artificial nerves can measure large dynamic strains and simulated acoustic emissions that represent damage in structures.
DTIC
Nerves; Artificial Intelligence; Computerized Simulation; Fatigue (Materials)

64
NUMERICAL ANALYSIS

Includes iteration, differential and difference equations, and numerical approximation.

20020000918 Los Alamos National Lab., NM USA
Maximum-Path Leaves Relative to Vertices and the Vertex One Center of a Spanning Tree: An Enumeration and Analysis of Configurations
Dowell, L. J.; Oct. 01, 1998; 19p; In English
Report No.(s): DE2001-1179; LA-13521-MS; No Copyright; Avail: Department of Energy Information Bridge, Microfiche

This paper enumerates the configurations of a pair of vertices (one of which is a leaf) relative to the unique vertex one center and the leaf of greatest path length from this center in a spanning tree of a graph. From this enumeration, it demonstrates that the vertex one center is between the vertex and the leaf of greatest path length from the vertex for every such pair of vertices. Using this result this paper develops an algorithm for the optimal reconfiguration of a tree infrastructure required to recover from the failure of a network element.

NTIS
Algorithms; Network Analysis; Fault Trees; Apexes

20020001885 Lawrence Livermore National Lab., Livermore, CA USA
Fourier mode analysis of slab-geometry transport iterations in spatially periodic media
Larsen, E. W.; Zika, M. R.; May 07, 1999; 12p; In English
Report No.(s): DE2001-14570; UCRL-JC-133713-REV-1; No Copyright; Avail: Department of Energy Information Bridge, Microfiche

We describe a Fourier analysis of the diffusion-synthetic acceleration (DSA) and transport-synthetic acceleration (TSA) iteration schemes for a spatially periodic, but otherwise arbitrarily heterogeneous, medium. Both DSA and TSA converge more slowly in a heterogeneous medium than in a homogeneous medium composed of the volume-averaged scattering ratio. In the limit of a homogeneous medium, our heterogeneous analysis contains eigenvalues of multiplicity two at ”resonant” wave numbers. In the presence of material heterogeneities, error modes corresponding to these resonant wave numbers are ”excited” more than other error modes. For DSA and TSA, the iteration spectral radius may occur at these resonant wave numbers, in which case the material heterogeneities most strongly affect iterative performance.

NTIS
Eigenvalues; Fourier Analysis; Iteration

20020001960 Lawrence Livermore National Lab., Livermore, CA USA
Fourier mode analysis of slab-geometry transport iterations in spatially periodic media
Larsen, E.; Zika, M.; Apr. 01, 1999; 12p; In English
Report No.(s): DE2001-14572; UCRL-JC-133713; No Copyright; Avail: Department of Energy Information Bridge, Microfiche

We describe a Fourier analysis of the diffusion-synthetic acceleration (DSA) and transport-synthetic acceleration (TSA) iteration schemes for a spatially periodic, but otherwise arbitrarily heterogeneous, medium. Both DSA and TSA converge more slowly in a heterogeneous medium than in a homogeneous medium composed of the volume-averaged scattering ratio. In the limit of a homogeneous medium, our heterogeneous analysis contains eigenvalues of multiplicity two at ”resonant” wave numbers. In the presence of material heterogeneities, error modes corresponding to these resonant wave numbers are ”excited” more than other error modes. For DSA and TSA, the iteration spectral radius may occur at these resonant wave numbers, in which case the material heterogeneities most strongly affect iterative performance.

NTIS
Fourier Analysis; Iteration; Eigenvalues

20020001963 Lawrence Livermore National Lab., Livermore, CA USA
Least-squares streamline diffusion finite element approximations to singularly perturbed convection-diffusion problems
Lazarov, R. D.; Vassilevski, P. S.; May 06, 1999; 14p; In English
Report No.(s): DE2001-12571; UCRL-JC-134161; REPT-97-ERD-114; No Copyright; Avail: Department of Energy Information Bridge, Microfiche

In this paper we introduce and study a least-squares finite element approximation for singularly perturbed convection-diffusion equations of second order. by introducing the flux (diffusive plus convective) as a new unknown, the problem is written in a mixed form as a first order system. Further, the flux is augmented by adding the lower order terms with

a small parameter. The new first order system is approximated by the least-squares finite element method using the minus one norm approach of Bramble, Lazarov, and Pasciak (2). Further, we estimate the error of the method and discuss its implementation and the numerical solution of some test problems.
NTIS
Finite Element Method; Convection-Diffusion Equation; Diffusivity; Approximation

20020002256 Sandia National Labs., Albuquerque, NM USA
Seacas Theory Manuals, Part 3, Finite Element Analysis in Nonlinear Solid Mechanics
Laursen, T. A.; Attaway, S. W.; Zadoks, R. I.; Mar. 01, 1999; 119p; In English
Report No.(s): DE2001-4711; SAND98-1760/3; No Copyright; Avail: Department of Energy Information Bridge, Microfiche

This report outlines the application of finite element methodology to large deformation solid mechanics problems, detailing also some of the key technological issues that effective finite element formulations must address. The presentation is organized into three major portions: first, a discussion of finite element discretization from the global point of view, emphasizing the relationship between a virtual work principle and the associated fully discrete system, second, a discussion of finite element technology, emphasizing the important theoretical and practical features associated with an individual finite element; and third, detailed description of specific elements that enjoy widespread use, providing some examples of the theoretical ideas already described. Descriptions of problem formulation in nonlinear solid mechanics, nonlinear continuum mechanics, and constitutive modeling are given in three companion reports.
NTIS
Finite Element Method; Manuals; Solid Mechanics

20020002333 Institute for Computer Applications in Science and Engineering, Hampton, VA USA
Random Field Solutions Including Boundary Condition Uncertainty for the Steady-state Generalized Burgers Equation ***Final Report***
Huyse, Luc, Institute for Computer Applications in Science and Engineering, USA; Walters, Robert W., Virginia Polytechnic Inst. and State Univ., USA; October 2001; 30p; In English
Contract(s)/Grant(s): NAS1-97046; RTOP 505-90-52-01
Report No.(s): NASA/CR-2001-211239; NAS 1.26:211239; ICASE-2001-35; No Copyright; Avail: CASI; A03, Hardcopy; A01, Microfiche

CFD results are subject to considerable uncertainty associated with the operating conditions. Even when the operational uncertainty is omitted under very controlled circumstances during wind tunnel experiments, substantial disagreement between experimental and CFD results persists. This discrepancy must be attributed to model uncertainty. This report discusses the various sources of uncertainty. The need for advanced uncertainty modeling is illustrated by means of a computationally inexpensive 1-D Burgers equation model. We specifically address the uncertainty due to missing variables (inexact or incomplete differential equations). to this extent a random field model is used for the viscosity and the fundamental differences between the solutions of the stochastic differential equations and a simple random variable model is highlighted. The Burgers equation theoretically needs to be integrated over an infinite domain. In a deterministic approach, the integration domain is cut off at some far field boundary. This truncation effectively ignores all variability outside this far field boundary. We present a practical treatment for the uncertainty on the boundary conditions. The results indicate that ignoring the boundary condition uncertainty dramatically underestimates the variance of the velocity in the interior of the domain.
Author
Boundary Conditions; Burger Equation; Mathematical Models; Uncertain Systems; Error Analysis

20020004022 Old Dominion Univ., Research Foundation, Norfolk, VA USA
Development of Numerical Models for Performance Predictions of Single-Photon Avalanche Photodetectors (SPAP) for the 2-Micron Regime ***Final Report***
Joshi, Ravindra P., Old Dominion Univ., USA; [2001]; 43p; In English
Contract(s)/Grant(s): NAG1-01077; No Copyright; Avail: CASI; A03, Hardcopy; A01, Microfiche

Field dependent drift velocity results are presented for electron transport in bulk Indium Arsenide (InAs) material based on a Monte Carlo model, which includes an analytical treatment of band-to-band impact ionization. Avalanche multiplication and related excess noise factor (F) are computed as a function of device length and applied voltage. A decrease in F with increases in device length is obtained. The results suggest an inherent utility for InAs-based single-photon avalanche detectors, particularly around the 2 microns region of interest for atmospheric remote sensing applications. The dark current response was also evaluated.

The role of the various components has been analyzed. For shorter devices, the tunneling component is shown to dominate at low temperatures. Finally, possible structures for enhanced photodetection are proposed for future research.
Author
Numerical Analysis; Photons; Avalanches; Photometers; Indium Arsenides; Drift Rate

20020005868 Brown Univ., Div. of Applied Mathematics, Providence, RI USA
High Order Numerical Methods for Long Time Solutions with Discontinuities ***Final Report, 1 Jun. 1997-31 May 2001***
Shu, Chi Wang; May 2001; 12p; In English
Contract(s)/Grant(s): DAAG55-97-1-0318
Report No.(s): AD-A395323; ARO-36620.5-MA; No Copyright; Avail: CASI; A03, Hardcopy; A01, Microfiche

This project is about the design, analysis and application of high order accurate and nonlinearly stable finite difference (including finite volume) WENO schemes, finite element discontinuous Galerkin methods, and spectral algorithms for computing solutions of partial differential equations which are either discontinuous or with sharp gradients. Algorithm development, theoretical study about stability and convergence of the algorithms, investigation about efficient implementation including parallel implementations, and applications in compressible and incompressible gas dynamics and in semiconductor device simulations, are performed. The achievement strengthens our objective to obtain powerful and reliable high order numerical algorithms and use them to solve problems containing discontinuous solutions, especially those of Army interest.
DTIC
Algorithms; Discontinuity; Finite Element Method; Numerical Analysis; Nonlinearity

65
STATISTICS AND PROBABILITY

Includes data sampling and smoothing; Monte Carlo method; time series and analysis; and stochastic processes.

20020002224 Research Inst. for Advanced Computer Science, Moffett Field, CA USA
Operations on Graphical Models with Plates
Buntine, Wray L., Research Inst. for Advanced Computer Science, USA; [1994]; 1p; In English
Contract(s)/Grant(s): RTOP 233-01-02; No Copyright; Avail: Issuing Activity; Abstract Only

This paper explains how graphical models, for instance Bayesian or Markov networks, can be extended to model problems in data analysis and learning. This provides a unified framework that combines lessons learned from the artificial intelligence, statistical and connectionist communities. This also offers a set of principles for developing a software generator for data analysis, whereby a learning or discovery system can be compiled from specifications. Many of the popular learning algorithms can be compiled in this way from graphical specifications. While in a sense this paper is a multidisciplinary review of learning, the main contribution here is the presentation of the material within the unifying framework of graphical models, and the observation that, as a result, the process of developing learning algorithms can be partly automated.
Author
Algorithms; Artificial Intelligence; Bayes Theorem; Computer Graphics; Mathematical Models

20020002252 Sandia National Labs., Albuquerque, NM USA
Numerical Techniques to Evaluate Moments of Dynamic System Response
Field, R. V.; Paez, T. L.; Red-Horse, J. R.; Mar. 24, 1999; 6p; In English
Report No.(s): DE2001-5043; SAND99-0700C; No Copyright; Avail: Department of Energy Information Bridge, Microfiche

Probabilistic uncertainty is a phenomenon that occurs to a certain degree in many engineering applications. The effects that this uncertainty has upon a given system response are a matter of some concern. Techniques which provide insight to these effects will be required as modeling and prediction becomes a more vital tool in the engineering design process. The purpose of this paper is to outline a procedure to evaluate uncertainty in dynamic system response exploiting various numerical methods. Specifically, the goal is to attain the statistics of the response with minimal computational effort. Numerical interpolation and integration techniques are utilized in conjunction with the iterative form of the Advanced Mean Value (AMV+) method to efficiently and accurately estimate statistical moments of the response random process. A numerical example illustrating the use of this analytical tool in a practical framework is presented.
NTIS
Dynamic Response; Numerical Integration; Probability Density Functions

20020002747 Lawrence Livermore National Lab., Livermore, CA USA

Clinical implementation of the Peregrine Monte Carlo dose calculations system for photon beam therapy

Albright, N.; Bergstrom, P. M.; Daly, T. P.; Descalle, M.; Garrett, D.; Jul. 01, 1999; 6p; In English

Report No.(s): DE2001-12558; UCRL-JC-133076; Rept-99-ERD-046; No Copyright; Avail: Department of Energy Information Bridge

PEREGRINE is a 3D Monte Carlo dose calculation system designed to serve as a dose calculation engine for clinical radiation therapy treatment planning systems. Taking advantage of recent advances in low-cost computer hardware, modern multiprocessor architectures and optimized Monte Carlo transport algorithms, PEREGRINE performs mm-resolution Monte Carlo calculations in times that are reasonable for clinical use. PEREGRINE has been developed to simulate radiation therapy for several source types, including photons, electrons, neutrons and protons, for both teletherapy and brachytherapy. However the work described in this paper is limited to linear accelerator-based megavoltage photon therapy. Here we assess the accuracy, reliability, and added value of 3D Monte Carlo transport for photon therapy treatment planning. Comparisons with clinical measurements in homogeneous and heterogeneous phantoms demonstrate PEREGRINE's accuracy. Studies with variable tissue composition demonstrate the importance of material assignment on the overall dose distribution. Detailed analysis of Monte Carlo results provides new information for radiation research by expanding the set of observables.

NTIS

Photon Beams; Monte Carlo Method; Dosage; Clinical Medicine; Radiation Therapy

20020002846 California Univ., Lawrence Berkeley Lab., Berkeley, CA USA

Uncertainty and sensitivity analyses of ballast life-cycle cost and payback period

McMahon, J. E.; Liu, X.; Turiel, I.; Hakim, S.; Fisher, D.; Jun. 01, 2000; 68p; In English

Report No.(s): DE2001-767554; LBNL-44450; No Copyright; Avail: Department of Energy Information Bridge

The paper introduces an innovative methodology for evaluating the relative significance of energy-efficient technologies applied to fluorescent lamp ballasts. The method involves replacing the point estimates of life cycle cost of the ballasts with uncertainty distributions reflecting the whole spectrum of possible costs, and the assessed probability associated with each value. The results of uncertainty and sensitivity analyses will help analysts reduce effort in data collection and carry on analysis more efficiently. These methods also enable policy makers to gain an insightful understanding of which efficient technology alternatives benefit or cost what fraction of consumers, given the explicit assumptions of the analysis.

NTIS

Life Cycle Costs; Sensitivity Analysis; Ballasts (Impedances); Fluorescence; Luminaires

20020004358 NASA Ames Research Center, Moffett Field, CA USA

Smoothing DCT Compression Artifacts

Ahumada, A. J., Jr., NASA Ames Research Center, USA; Horng, R., Stanford Univ., USA; [1994]; 1p; In English; Society for Information Display Symposium, 12-17 Jun. 1994, San Jose, CA, USA; Sponsored by Society for Information Display, USA

Contract(s)/Grant(s): NCA2-307; RTOP 199-06-31; RTOP 505-64-53; No Copyright; Avail: Issuing Activity; Abstract Only

Image compression based on quantizing the image in the discrete cosine transform (DCT) domain can generate blocky artifacts in the output image. It is possible to reduce these artifacts and RMS error by adjusting measures of block edginess and image roughness, while restricting the DCT coefficient values to values that would have been quantized to those of the compressed image. We also introduce a DCT coefficient amplitude adjustment that reduces RMS error.

Author

Discrete Cosine Transform; Data Smoothing; Statistical Analysis

20020005135 Research Inst. for Advanced Computer Science, Moffett Field, CA USA

A Guide to the Literature on Learning Graphical Models

Buntine, Wray L., Research Inst. for Advanced Computer Science, USA; [1994]; 1p; In English

Contract(s)/Grant(s): RTOP 233-01-02; No Copyright; Avail: Issuing Activity; Abstract Only

This literature review discusses different methods under the general rubric of learning Bayesian networks from data, and more generally, learning probabilistic graphical models. Because many problems in artificial intelligence, statistics and neural networks can be represented as a probabilistic graphical model, this area provides a unifying perspective on learning. This paper organizes the research in this area along methodological lines of increasing complexity.

Author

Bayes Theorem; Machine Learning

66
SYSTEMS ANALYSIS AND OPERATIONS RESEARCH

Includes mathematical modeling of systems; network analysis; mathematical programming; decision theory; and game theory.

20020005055 Los Alamos National Lab., NM USA
Example of a Monte Carlo Code Applied to the Modeling of Complex Systems
Waters, L.; Aug. 01, 2000; 22p; In English
Report No.(s): DE2001-768724; LA-UR-00-3910; No Copyright; Avail: Department of Energy Information Bridge
No abstract available.
NTIS
Complex Systems; Monte Carlo Method

67
THEORETICAL MATHEMATICS

Includes algebra, functional analysis, geometry, topology set theory, group theory and and number theory.

20020001778 Center for Mathematics and Computer Science, Amsterdam Netherlands
Factorization in Block-Triangularly Implicit Methods for Shallow Water Applications. Modelling, Analysis and Simulation
van der Houwen, P. J.; Sommeijer, B. P.; Mar. 1999; 24p; In English
Report No.(s): PB2001-108626; MAS-R9906; Copyright; Avail: National Technical Information Service (NTIS), Microfiche
In this paper the authors analyzed the convergence of iterative solution methods. In particular, the authors focused on the integration of ODE's originating from shallow water applications, where the ODE system contains a highly stiff part corresponding with the horizontal derivative terms. The authors considered iteration methods based on the approximate factorizations of the system matrix associated with the application of modified Newton.
NTIS
Shallow Water; Boundary Value Problems; Numerical Analysis; Convergence; Approximation

20020004178 NASA Ames Research Center, Moffett Field, CA USA
On the Dynamics of TVD Schemes
Yee, H. C., NASA Ames Research Center, USA; Sweby, P. K., Reading Univ., UK; [1994]; 1p; In English; SIAM National Conference, 25-29 Jul. 1994, San Diego, CA, USA; Sponsored by Society for Industrial and Applied Mathematics, USA
Contract(s)/Grant(s): RTOP 505-59-00; No Copyright; Avail: Issuing Activity; Abstract Only
The dynamics of a class of TVD schemes for model hyperbolic and parabolic equations is studied numerically using a highly parallel supercomputer (CM-5). The objective is to utilize the highly parallel property of the CM-5 to reveal the reliable time step and entropy parameter ranges, and the degree of compressible flux limiters to avoid slow convergence and the production of nonphysical numerical solutions. We choose to study the nonlinear stability property of TVD schemes numerically since it is otherwise not amenable analytically.
Author
Supercomputers; TVD Schemes; Numerical Analysis; Hyperbolic Differential Equations; Mathematical Models

70
PHYSICS (GENERAL)

Includes general research topics related to mechanics, kinetics, magnetism, and electrodynamics. For specific areas of physics see categories 71 through 77. For related instrumentation see 35 Instrumentation and Photography; for geophysics, astrophysics or solar physics see 46 Geophysics, 90 Astrophysics, or 92 Solar Physics.

20020000738 Los Alamos National Lab., NM USA
Assessment of Alternative RF Linac Structures for APT
Mar. 26, 1997; 375p; In English
Report No.(s): DE2001-763025; LA-SUB-99-31; D59700016-8Y; No Copyright; Avail: Department of Energy Information Bridge, Microfiche

The APT program has been examining both normal and superconducting variants of the APT linac for the past two years. A decision on which of the two will be the selected technology will depend upon several considerations including the results of ongoing feasibility experiments,the performance and overall attractiveness of each of the design concepts, and an assessment of the system-level features of both alternatives. The primary objective of the Assessment of Alternative RF Linac Structures for APT study reported herein was to assess and compare, at the system-level, the performance, capital and life cycle costs, reliability/availability/ maintainability (RAM) and manufacturing schedules of APT RF linear accelerators based upon both superconducting and normal conducting technologies. A secondary objective was to perform studies to explore opportunities for system optimization, technology substitution and alternative growth pathways and to identify sensitivities to design uncertainties. NTIS

Linear Accelerators; Radio Frequencies; Superconductors (Materials)

20020000745 FAS Engineering, Inc., Glendale, CA USA
Two-Phase Reaction Turbine
Fabris, G.; Apr. 01, 2000; 85p; In English
Report No.(s): DE2001-764445; No Copyright; Avail: Department of Energy Information Bridge

In the prior semi-annual report, for the period of July-December 1999, we have covered extensively the details on how our turbine, housing, and other key components of the heat engine are going to be built. We have also discussed the issue of stresses in the rotor and how we have managed to strengthen it. We have also spent a great effort in looking for a generator and sprocket/chain transmission system that would reduce RPMs from the high-speed turbine rotating at 20,000 rpm to about 6,000 rpm at the electric generator. In this report, we are going to cover additional details by discussing two more issues of importance: 1) sprocket/chain transmission, and 2) used of 10% steam quality brine delivered to the energy conversion part of a geothermal power plant. We will also include, in the attachment section, additional technical details of the assembly parts. NTIS

Electric Generators; Turbine Engines; Two Phase Flow; Heat Engines

20020000763 Lawrence Livermore National Lab., Livermore, CA USA
TOPAZ3D validation report
Kang, E.; Jul. 01, 1999; 42p; In English
Report No.(s): DE2001-8428; UCRL-ID-131877; No Copyright; Avail: Department of Energy Information Bridge, Microfiche

This document presents thirteen verification problems for the TOPAZ3D three-dimensional finite-element heat transfer code. Code verification is performed by comparing TOPAZ3D-generated solutions to analytical solutions for a variety of problems, including those involving slide lines and internal elements. This verification examines linear, one-dimensional problems of both steady and transient nature. In all thirteen comparisons conducted, TOPAZ3D performs well. The results and input files are listed so as to make the verifications easily reproducible. NTIS

Computer Programs; Heat Transfer

20020000877 Argonne National Lab., IL USA
Impedance Considerations for the Intense Pulse Neutron Source (IPNS) Rapid Cycling Synchrotron (RCS)
Brumwell, F. R.; Dooling, J. C.; McMichael, G. E.; Sep. 08, 1999; 12p; In English; Workshop on Instabilities of High Intensity Hadron Beams in Rings, 28 Jun. - 1 Jul. 1999, Long Island, NY, USA
Contract(s)/Grant(s): W-31109-ENG-38
Report No.(s): DE2001-11963; ANL/IPNS/CP-100007; No Copyright; Avail: Department of Energy Information Bridge, Microfiche

The use of Second Harmonic (SH) rf is being investigated to increase the Rapid Cycling Synchrotron (RCS) current limit. Hofmann-Pedersen distributions are employed to provide analytical guidance. The SH phase (theta), is optimized using a numerical analysis to maximize transmission and minimize instabilities. The effect of the RCS stainless steel liner on the impedance of the machine is also discussed.
NTIS
Neutron Sources; Radio Frequencies; Synchrotrons

20020000879 Argonne National Lab., IL USA
Gamma-Ray Spectroscopy of N = Z Nuclei
Lister, C. J.; Sep. 10, 1999; 8p; In English; Experimental Nuclear Physics in Europe Facing the Next Millennium, 21-26 Jun. 1999, Seville, Spain
Report No.(s): DE2001-11960; ANL/PHY/CP-99995; No Copyright; Avail: Department of Energy Information Bridge, Microfiche
The use of (gamma)-ray spectroscopy to probe the properties of marginally bound nuclear states has evolved from being a curiosity a decade ago to being the mainstream use for these devices. The key to this success has been the development of ultra-sensitive channel selection techniques which allow the parentage of each emitted y-ray to be established. With these techniques, and the enhanced efficiency of the arrays themselves, the level of sensitivity for nuclear spectroscopy has increased by several orders of magnitude, in some special cases reaching the 10's nanobarns level, 1000 times more sensitive than was possible a decade ago. In this paper the author discusses some recent developments in light nuclear spectroscopy, on nuclei with N = Z, below mass 100. These examples have been chosen to compliment other presentations at this conference which have covered similar experiments in heavier nuclei.
NTIS
Gamma Ray Spectrometers; Nuclei (Nuclear Physics); Spectroscopy

20020000882 Argonne National Lab., IL USA
Bunch stabilization using rf phase modulation in the Intense Pulse Neutron Source (IPNS) Rapid Cycling Synchrotron (RCS)
Brumwell, F. R.; Dooling, J. C.; McMichael, G. E.; Sep. 01, 1999; 12p; In English
Report No.(s): DE2001-11954; ANL/IPNS/CP-99951; No Copyright; Avail: Department of Energy Information Bridge, Microfiche
Phase modulation (PM) is used to increase the current limit in the IPNS RCS. A device referred to as a scrambler introduces a small oscillating phase between the two RCS rf cavities at approximately twice the synchrotrons frequency, f(sub s). The modulation introduced by the scrambler generates longitudinal oscillations in the bunch at 2f(sub s). Modulations in the bunch are also observed transversely indicating a coupling between longitudinal and transverse motion. Comparing PM with amplitude modulation (AM), coupling to the beam is roughly equivalent at 2f(sub s).
NTIS
Stabilization; Scrambling (Communication); Beamforming

20020000892 Argonne National Lab., IL USA
Results from experiment E917 for Au + Au collisions at the AGS
Back, B. B.; Betts, R. R.; Chang, J.; Chang, W. C.; Gillitzer, A.; Aug. 04, 1999; 9p; In English
Report No.(s): DE2001-11921; ANL/PHY/CP-99724; No Copyright; Avail: Department of Energy Information Bridge, Microfiche
The effects of baryon stopping and its resulting energy deposition on the dynamics of Au + Au collisions at 6, 8 and 10.8 GeV/nucleon are explored with recent results from the AGS (Alternating Gradient Synchrotrons) experiment E917. Current analyses of stopping, collective flow signals and HBT(Heterojunction Bipolar Transistors) parameters are presented. Strangeness and anti-baryon production is examined using the yields of anti-lambdas and anti-protons.
NTIS
Particle Production; Synchrotrons; Gold; Particle Collisions

20020000893 Argonne National Lab., IL USA
Preliminary flow analysis in experiment E917 at the AGS
Back, B. B.; Betts, R. R.; Chang, J.; Chang, W. C.; Chi, C. Y.; Aug. 04, 1999; 7p; In English
Report No.(s): DE2001-11920; ANL/PHY/CP-99723; No Copyright; Avail: Department of Energy Information Bridge, Microfiche

The study of directed flow in heavy ion collisions as a probe of collision dynamics has been of heightened interest to the physics community in recent years. The E917 collaboration is addressing this interest by investigating signatures of flow as a function of rapidity and centrality for fixed target gold on gold collisions at 11.7A GeV/c. The purpose of this report is to demonstrate E917's capability to establish the reaction plane on an event-by-event basis and present preliminary results of the proton data collected at Brookhaven National Laboratory's Alternating Gradient Synchrotrons (AGS) facility.
NTIS
Heavy Ions; Ionic Collisions

20020000894 Argonne National Lab., IL USA
Magnetism in single-crystalline CePtSn
Bordallo, H. N.; Chang, S.; Lacerda, A. H.; Nakotte, H.; Takabatake, T.; Aug. 04, 1999; 8p; In English
Report No.(s): DE2001-11919; ANL/IPNS/CP-99722; No Copyright; Avail: Department of Energy Information Bridge, Microfiche

CePtSn exhibits two antiferromagnetic transitions at low temperatures. We report on magnetoresistance and in magnetization studies of single-crystalline CePtSn in magnetic fields up to 18 T. The data were taken to establish the magnetic phase diagrams for CePtSn in fields applied along the principal directions.
NTIS
Magnetization; Magnetoresistivity

20020000903 Argonne National Lab., IL USA
Neutrino induced muons in Soudan 2
DeMuth, D. M.; Jun. 23, 1999; 5p; In English
Report No.(s): DE2001-11874; ANL-HEP-CP-99-57; No Copyright; Avail: Department of Energy Information Bridge, Microfiche

The neutrino-induced muon rate underground has been measured at Soudan 2. To discriminate from the intense background of atmospheric muons we consider only the through-going muons which originate from horizontal direction ((minus)0.14 < cos(theta) < 0.14). We calculate the horizontal, neutrino-induced muon rate at Soudan 2 from an exposure of 1.23 x 10(exp 8) s as (Phi)(sub (nu)(mu)) = (3.45 (+/-) 0.52 (+/-) 0.61) x 10(exp -13) sq cm sr s)(sup (minus)1).
NTIS
Exposure; Muons; Neutrinos

20020000908 Argonne National Lab., IL USA
Absorbed dose from 7-GeV bremsstrahlung in a PMMA phantom
Job, P. K.; Pisharody, M.; Semones, E.; Aug. 04, 1999; 7p; In English
Report No.(s): DE2001-11923; ANL/XFD/CP-99726; No Copyright; Avail: Department of Energy Information Bridge, Microfiche

Electron storage rings generate energetic bremsstrahlung photons through radiative interaction of the particle beam with the residual gas molecules and other components inside the storage ring. At the Advanced Photon Source (APS), where the stored beam energy is 7 GeV, bremsstrahlung generated in the straight sections of the insertion devices comes down through the beamlines. The resulting absorbed dose distributions by, this radiation in a 300 mm x 300 mm x 300 mm tissue substitute phantom were measured with LiF:Mg,Ti (TLD-700) thermoluminescent dosimeters. The average normalized absorbed dose, in a cross sectional area of 100 mm(sup 2) at a depth of 150 mm of the PMMA (polymethyl methacrylate) phantom, was measured as 3.3 x 10(sup 6) mGy h(sup (minus)1)W(sup (minus)1) for a 7-GeV bremsstrahhmg spectrum.
NTIS
Polymethyl Methacrylate; Bremsstrahlung; Storage Rings (Particle Accelerators)

20020000922 Lawrence Livermore National Lab., Livermore, CA USA
TART98 a coupled neutron-photon 3-D, combinatorial geometry time dependent Monte Carlo Transport code
Cullen, D. E.; Nov. 22, 1998; 117p; In English
Report No.(s): DE2001-8435; UCRL-ID-126455-REV-2; DP0102052; No Copyright; Avail: Department of Energy Information Bridge, Microfiche

TART98 is a coupled neutron-photon, 3 Dimensional, combinatorial geometry, time dependent Monte Carlo radiation transport code. This code can run on any modern computer. It is a complete system to assist you with input preparation, running Monte Carlo calculations, and analysis of output results. TART98 is also incredibly FAST; if you have used similar codes, you

will be amazed at how fast this code is compared to other similar codes. Use of the entire system can save you a great deal of time and energy. TART98 is distributed on CD. This CD contains on-line documentation for all codes included in the system, the codes configured to run on a variety of computers, and many example problems that you can use to familiarize yourself with the system. TART98 completely supersedes all older versions of TART, and it is strongly recommended that users only use the most recent version of TART98 and its data files.
NTIS
Computer Programs; Monte Carlo Method; Photons; Neutrons; Radiation Transport

20020001026 Argonne National Lab., IL USA
Low mass lepton pair production in hadron collisions
Berger, E. L.; Klasen, M.; Jun. 29, 1999; 8p; In English
Report No.(s): DE2001-11885; ANL-HEP-CP-99-72; No Copyright; Avail: Department of Energy Information Bridge, Microfiche

The hadroproduction of lepton pairs with mass Q and transverse momentum Q(sub T) can be described in perturbative QCD by the same partonic sub-processes as prompt photon production. They demonstrate that, like prompt photon production, lepton pair production is dominated by quark-gluon scattering in the region Q(sub T) greater than Q/2. This leads to sensitivity to the gluon density in kinematical regimes that are accessible both at collider and fixed target experiments while eliminating the theoretical and experimental uncertainties present in prompt photon production.
NTIS
Gluons; Leptons; Mass; Pair Production; Elementary Particle Interactions; Hadrons

20020001044 Lawrence Livermore National Lab., Livermore, CA USA
Simulation of an EBPVD Titanium Vapor Plume and Comparison to Experiment
Anklam, T. M.; Balakrishnan, J.; Berzins, L. V.; Blackfield, D. T.; Boyd, I.; Oct. 01, 1998; 20p; In English
Report No.(s): DE2001-8543; UCRL-JC-131782; No Copyright; Avail: Department of Energy Information Bridge, Microfiche

A two-dimensional vapor code has been used to simulate the electron-beam vaporization of titanium and its subsequent deposition on a horizontal substrate in experiments performed at Lawrence Livermore National Laboratory (LLNL). Previous work has modeled the Titanium melt. Using those results, the present work models the expansion of the atomic vapor from the melt surface to the substrate. The flow speed of the vapor expansion and its kinetic and internal temperatures were measured in the LLNL experiment as a function of the vaporization rate and the electron-beam footprint. The deposition profile on the substrate was also measured post-run. This work describes the experimental configuration and compares the measured quantities to those of the computer simulation.
NTIS
Computerized Simulation; Deposition; Electron Beams; Titanium; Vaporizing

20020001048 Lawrence Livermore National Lab., Livermore, CA USA
Advantages of Evaporation of Hafnium in a Reactive Environment to Manufacture High Damage Threshold Multilayer Coatings by Electron-Beam Deposition
Bevis, R. P.; Sheehan, L. M.; Smith, D. J.; Stolz, C. J.; Von Gunten, M. K.; Apr. 22, 1999; 9p; In English
Report No.(s): DE2001-8557; UCRL-JC-132251; DP0213000; No Copyright; Avail: Department of Energy Information Bridge, Microfiche

Electron-beam deposition is the current method to produce large-aperture high laser-induced damage threshold coatings for the National Ignition Facility, a 1.8 MJ fusion laser. The e-beam process is scalable to large optics up to 0.25 sq m and with laser conditioning has relatively benign coating defect ejections resulting in high damage threshold thin films. The latest technological breakthrough in manufacturing high damage threshold coatings is e-beam deposition of hafnia by evaporation from a metallic instead of an oxide source in a reactive environment. Although the damage threshold is not significantly increased, a 3-10x defect reduction occurs resulting in significantly less coating modification during laser conditioning. Additional benefits of this technology include improved interfaces for the elimination of flat-bottom pits and up to 3x reduction in plume instability for improved layer thickness control and spectral performance.
NTIS
Deposition; Electron Beams; Evaporation; Hafnium; Yield Point

20020001061 Fermi National Accelerator Lab., Batavia, IL USA
Jet Calorimetric Trigger
Green, D.; Sep. 27, 1999; 14p
Contract(s)/Grant(s): AC02-76CH03000
Report No.(s): DE2001-11974; FERMILAB-TM-2088; No Copyright; Avail: Department of Energy Information Bridge, Microfiche

The problem in triggering on jets in hadron colliders is that the largest background in the trigger is also a jet. Therefore, we must strive to trigger as incisively as possible. Since the basic physics resides in the transverse momentum, Pt, of the jet, this means to trigger with as sharp a Pt discriminant as possible. The basic problem is different for electrons or photons, where the backgrounds are typically jets. For heavy quarks, like b, the backgrounds are mismeasured secondary vertices. The situation is similar to that for muons, where the largest background is due to real muons from pion decays in particle cascades or from heavy flavor semi-leptonic decays arising from gluon splitting in ordinary QCD jets. As with jets, the issue for the muon trigger is to make as sharp a Pt cut as possible since the background muons dominate at low Pt.
NTIS
Elementary Particle Interactions; Gluons; Hadrons; Muons

20020001064 Lawrence Livermore National Lab., Livermore, CA USA
Laser programs highlights 1996
Jacobs, R. R.; Sep. 01, 1997; 23p; In English
Report No.(s): DE2001-11982; UCRL-ID-109089-96; No Copyright; Avail: Department of Energy Information Bridge, Microfiche

No abstract prepared.
NTIS
Lasers; Research Projects

20020001065 Lawrence Livermore National Lab., Livermore, CA USA
Harnessing the power of the new SMP cluster architecture
Anderson, S. E.; Cohen, R. H.; Curtis, B. C.; Dannevik, W. P.; Dimits, A. M.; Jun. 16, 1999; 20p; In English
Report No.(s): DE2001-11985; UCRL-JC-134547; No Copyright; Avail: Department of Energy Information Bridge, Microfiche

In 1993, members of our team collaborated with Silicon Graphics to perform the first full-scale demonstration of the computational power of the SMP cluster supercomputer architecture. That demonstration involved the simulation of homogeneous, compressible turbulence on a uniform grid of a billion cells, using our PPM gas dynamics code. This computation was embarrassingly parallel, the ideal test case, and it achieved only 4.9 Gflop/s performance, slightly over half that achievable by this application on the most expensive supercomputers of that day. After four to five solid days of computation, when the prototype machine had to be dismantled, the simulation was only about 20% completed. Nevertheless, this computation gave us important new insights into compressible turbulence and also into a powerful new mode of cost-effective, commercially sustainable supercomputing (S). In the intervening 6 years, the SMP cluster architecture has become a fundamental strategy for several large supercomputer centers in the US, including the DOE's ASCI centers at Los Alamos National Laboratory and at the Lawrence Livermore National Laboratory and the NSF's center NCSA at the University of Illinois. This SMP cluster architecture now underlies product offerings at the high-end of performance from SGI, IBM, and HP, among others. Nevertheless, despite many successes, it is our opinion that the computational science community is only now beginning to exploit the full promise of these new computing platforms. In this paper, we will briefly discuss two key architectural issues, vector computing and the flat multiprocessor architecture, which continue to drive spirited discussions among computational scientists, and then we will describe the hierarchical shared memory programming paradigm that we feel is best suited to the creative use of SMP cluster systems. Finally, we will give examples of recent large-scale simulations carried out by our team on these kinds of systems and point toward the still more challenging work which we foresee in the near future.
NTIS
Multiprocessing (Computers); Prototypes; Supercomputers; Architecture (Computers); Applications Programs (Computers)

20020001066 Lawrence Livermore National Lab., Livermore, CA USA
Prototype dipole septum magnet for fast high current kicker systems
Brown, T. F.; Caporaso, G. J.; Chen, Y. J.; Lund, S. M.; Poole, B. R.; Mar. 01, 1999; 5p; In English
Report No.(s): DE2001-11986; UCRL-JC-132313; REPT-39DP01000; No Copyright; Avail: Department of Energy Information Bridge, Microfiche

A dipole septum magnet without a material septum has been designed and tested as part of a fast beam kicker system for use in intense, electron-beam induction accelerators. This septum magnet is a simple, iron-based electromagnet with two static, oppositely oriented dipole field regions used to provide further separation of beam centroids given a small angle kick by a fast beam kicker. The magnet geometry includes removable pole pieces to allow experimental flexibility. Field errors experienced by the beam depend crucially on the magnitude of the initial kick that provides displacement of the beam centroids from the transition region between the two dipole field regions. Results of simulations are reported.
NTIS
Electromagnets; Prototypes; Septum; Simulation; High Current; Magnetic Dipoles

20020001073 Argonne National Lab., IL USA
Longitudinal instability studies at the SURF II storage ring at NIST
Harkay, K. C.; Sereno, N. S.; Aug. 27, 1998; 19p; In English
Report No.(s): DE2001-12093; No Copyright; Avail: Department of Energy Information Bridge, Microfiche

Measurements of the longitudinal instability observed in the storage ring at the Synchrotrons Ultraviolet Radiation Facility (SURF II) at the National Institute of Standards and Technology (NET) were performed to understand the mechanism driving the instability. The instability, studied in depth by Ralcowsky and others, manifests itself in broad resonance features in the horizontal and vertical motion spectrum of the synchrotrons light from DC to a few kHz. Also observed are multiple synchrotrons harmonics that modulate the revolution harmonics; these are characteristic of longitudinal phase oscillations. These spectral features of the motion are found to be correlated with the periodic lengthening and shortening of the bunch length on time scales from approximately 0.1 ms to 20 ms, depending on machine and radio-frequency (rf) system parameters. In this report, the growth rate of the instability is determined from measurements using an rf pickup electrode. The measured growth rates are compared to computed growth rates from an analytical model. Recommendations are made regarding options to control or mitigate the instability. In light of upgrade plans for SURF III, a few comments are presented about the beam lifetime.
NTIS
Storage Rings (Particle Accelerators); Stability

20020001074 Argonne National Lab., IL USA
Four-button BPM coefficients in cylindrical and elliptic beam chambers
Kim, S. H.; Apr. 08, 1999; 16p; In English
Report No.(s): DE2001-12095; No Copyright; Avail: Department of Energy Information Bridge, Microfiche

Beam position monitor (BPM) coefficients are calculated from induced charges on four-button BPMs in circular and elliptic beam chambers for (gamma) 1. Since the beam chamber cross-section for the APS storage ring is different from an exact elliptic geometry, numerical values of the BPM coefficients and their inversions are computed from two-dimensional electrostatic field distributions inside an exact geometry of the beam chamber. Utilizing Green's reciprocation theorem, a potential value is applied to the buttons rather than changing the beam position, and potential distributions corresponding to the beam positions are then computed.
NTIS
Beams (Radiation); Cylindrical Chambers; Storage Rings (Particle Accelerators)

20020001075 Argonne National Lab., IL USA
Benchmark and comparisons of FEL simulation programs TDA3D and GENESIS
Chae, Y. C.; Milton, S. V.; Sep. 11, 1999; 22p; In English
Report No.(s): DE2001-12098; No Copyright; Avail: Department of Energy Information Bridge, Microfiche

A low-energy undulator test line (LEUTL) is under construction at the Advanced Photon Source (APS). This line will initially be used to demonstrate a free-electron laser (FEL) based on the self-amplified spontaneous-emission (SASE) process. The FEL simulation programs, TDA3D and GENESIS, together with several other codes have been used for the LEUTL project. In order to increase the confidence on the simulation results, we attempted to benchmark two programs TDA3D and GENESIS. The results are reported here.
NTIS
Computerized Simulation; Free Electron Lasers

20020001160 Lawrence Livermore National Lab., Livermore, CA USA

Role of Starting Material Composition in Interfacial Damage Morphology of Hafnia Silica Multilayer Coatings

Bevis, R. P.; Stolz, C. J.; Von Gunten, M. K.; Weakley, S. C.; Wu, Z. L.; Dec. 23, 1999; 9p; In English

Report No.(s): DE2001-8580; UCRL-JC-131214; DP0212000; No Copyright; Avail: Department of Energy Information Bridge, Microfiche

Flat bottom pits, previously shown to be unstable above a critical fluence, may be impacted by interfacial characteristics of the multilayer. Transmission electron microscopic (TEM) cross-sections reveal multilayer coatings deposited from hafnium have fewer interfacial voids than those deposited from hafnia. to correlate this reduction with the occurrence of flat bottom pits, multilayer high reflectors deposited by reactive electron-beam evaporation from both metallic and oxide sources were damage tested with 3-ns, 1064-nm pulses. to shift the electric-field peaks to the adjacent interface, half of the samples included an additional buried half-wave of silica in their all quarter-wave design. All quarter-wave reflectors deposited from hafnia had flat bottom pit damage in the outer six layers at fluences of 20 J/sq cm. Interfacial damage also occurred in hafnium deposited coatings at fluences as low as 20 J/sq cm, but at significantly different depths. The only interfacial damage observed on the all quarter-wave coatings was at the substrate multilayer interface. Flat bottom pits were observed in the buried half-wave coatings with a correlation to electric-field position and preference to interface type.

NTIS

Damage; Hafnium; Morphology; Pitting

20020001196 Argonne National Lab., IL USA

Forward-backward asymmetries of atomic photoelectrons

Biheux, J. C.; Dunford, R. W.; Gemmell, D. S.; Hasegawa, S.; Kanter, E. P.; Jan. 19, 1999; 12p; In English; International Workshop on Atomic and Molecular Physics at High Brilliance Synchrotron Radiation Facilities, 4-6 Apr. 1998, Hyogo, Japan

Contract(s)/Grant(s): W-31109-ENG-38

Report No.(s): DE2001-12390; ANL/CHM/CP-98229; No Copyright; Avail: Department of Energy Information Bridge, Microfiche

When atomic photoionization is treated beyond the dipole approximation, photoelectron angular distributions are asymmetric forward and backward with respect to the direction of the photon beam. We have measured forward-backward asymmetries of Ar 1s and Kr 1s and 2s photoelectrons using 2-19 keV x-rays. The measured asymmetries compare well with calculations which include interference between electric-dipole and electric-quadrupole amplitudes within the nonrelativistic, independent-particle approximations.

NTIS

Asymmetry; Argon; Krypton; Photoionization

20020001198 Argonne National Lab., IL USA

Development of Solid Methane Neutron Moderators at the Intense Pulsed Neutron Source Facility of Argonne National Laboratory

Carpenter, J. M.; Miller, M. E.; Scott, T. L.; Mar. 10, 1999; 8p; In English; International Workshop on Cold Moderators for Pulsed Neutron Sources, 29 Sep. - 2 Oct. 1997, Argonne, IL, USA

Report No.(s): DE2001-12385; ANL/IPNS/CP-98533; No Copyright; Avail: Department of Energy Information Bridge, Microfiche

The Intense Pulsed Neutron Source (IPNS) started using solid methane moderators in 1985 because of their efficient conversion (about 3.5 times greater than was achieved with a liquid hydrogen moderator) of fast neutrons to long wavelength neutrons. However, the solid methane moderators experienced numerous failures due to pressure surges caused by a combination of (1) the release of stored energy, which occurred when methane radiolytic products recombined, and (2) the expansion of hydrogen, which built up in the solid methane during irradiation. During the ensuing years studies were made to determine how to operate the solid methane moderators without causing failure. The rate at which stored energy built up during irradiation and the temperature at which hydrogen was released during annealing were determined. Since 1993 IPNS has successfully operated the solid methane moderators (at about 30 K) by periodically annealing to the liquid state around 90 K after every roughly three days of irradiation.

NTIS

Methane; Moderators; Neutron Sources; Solidified Gases

20020001210 Argonne National Lab., IL USA

Susy production cross sections

Berger, E. L.; Harris, B.; Klasen, M.; Tait, T.; Mar. 19, 1999; 10p; In English

Report No.(s): DE2001-12347; ANL-HEP-CP-98-93; No Copyright; Avail: Department of Energy Information Bridge, Microfiche

We summarize the status of next-to-leading order perturbative quantum chromodynamics (pQCD) calculations of the cross sections for the production of squarks, gluinos, neutralinos, charginos, and sleptons as a function of the produced particle masses in proton-antiproton collisions at the hadronic center-of-mass energy 2 TeV.

NTIS

Quantum Chromodynamics; Elementary Particles; Particle Collisions

20020001239 Texas Univ., Houston, TX USA

Medium Energy Measurements of N-N Parameter ***Final Report, 1 Apr. 1994 - 30 Sep. 1996***

Ambrose, D.; Betts, W.; Coffey, P.; Glass, G.; McDonough, J.; Aug. 20, 1998; 26p; In English

Report No.(s): DE2001-766164; No Copyright; Avail: Department of Energy Information Bridge

Our research program had four main thrusts, only one of which can be considered as measurements of N-N parameters: (1) Finishing the data analyses associated with recent LAMPF and TRIUMPF N-N experiments, whose overall purpose has been the determination of the nucleon-nucleon amplitudes, both for isospin 0 and 1 at medium energies; (2) continuing work on BNL E871, a search for rare decay modes of the KL; (3) work on the RHIC-STAR project, an experiment to create and study a quark gluon plasma and nuclear matter at high energy density; (4) beginning a new AGS experiment (E896) which will search for the lowest mass state of the predicted strange di-baryons, the Ho, and other exotic states of nuclear matter through nucleus-nucleus collisions.

NTIS

Data Processing; Plasmas (Physics); Nucleon-Nucleon Interactions

20020001241 Physical Sciences, Inc., Andover, MA USA

Testing of a 3 MW Coaxial Gyrotron ***Final Report***

Read, M. E.; Sep. 25, 1998; 9p; In English

Report No.(s): DE2001-766041; DOE/ER/54324-1; PSI 1235; TR-1238; No Copyright; Avail: Department of Energy Information Bridge

The primary goal of the program was to assist MIT in the testing of a 140 GHz, 3 MW coaxial gyrotron. This gyrotron was designed and fabricated under a Department of Energy-sponsored SBIR program at PSI. The program commenced shortly after the gyrotron was delivered to MIT. However, due to many factors, MIT did not complete the installation until almost a year following delivery. Subsequent testing was intermittent, with a full time graduate student being assigned to the program only after about two years. Thus, the PSI contract was extended born one to three years. Testing is not complete, but enough information regarding the gyrotron has been transferred to MIT personnel to allow them to complete the tests without significant further assistance.

NTIS

Cyclotron Resonance Devices; Fabrication; Performance Tests

20020001282 Lawrence Livermore National Lab., Livermore, CA USA

X-ray diffraction studies using diamond coated rhenium gasket to megabar pressures

Akella, J.; Catledge, S. A.; Chesnut, G. N.; Prokop, H.; Vohra, Y. K.; Sep. 30, 1999; 6p; In English

Report No.(s): DE2001-12222; UCRL-JC-133812; No Copyright; Avail: Department of Energy Information Bridge, Microfiche

X-ray diffraction studies at megabar pressures are limited by the sample thickness between the diamond anvils. High strength gaskets are desirable to improve the quality of x-ray diffraction data. We present a technique which employs a microwave plasma chemical vapor deposited diamond layer on one side of a rhenium gasket. As a test case, we show energy dispersive x-ray diffraction data on rare earth metal neodymium to 153 GPa using a synchrotron source. The increased sample thickness results in an unambiguous crystal structure determination of a monoclinic phase in neodymium above 75 GPa.

NTIS

X Ray Diffraction; Rhenium; Diamonds; High Pressure; Vapor Deposition

20020001288 Lawrence Livermore National Lab., Livermore, CA USA

Toward a common component architecture for high-performance scientific computing

Armstrong, R.; Gannon, D.; Geist, A.; Katarzyna, K.; Kohn, S.; Jun. 09, 1999; 12p; In English

Report No.(s): DE2001-12179; UCRL-JC-134475; REPT-99-ERD-078; No Copyright; Avail: Department of Energy Information Bridge, Microfiche

This paper describes work in progress to develop a standard for interoperability among high-performance scientific components. This research stems from growing recognition that the scientific community must better manage the complexity of multidisciplinary simulations and better address scalable performance issues on parallel and distributed architectures. Driving forces are the need for fast connections among components that perform numerically intensive work and parallel collective interactions among components that use multiple processes or threads. This paper focuses on the areas we believe are most crucial for such interactions, namely an interface definition language that supports scientific abstractions for specifying component interfaces and a ports connection model for specifying component interactions.

NTIS

Interoperability; Simulation

20020001289 Fermi National Accelerator Lab., Batavia, IL USA

Subjet multiplicity in quark and gluon jets at D-Zero

Abbott, B.; Sep. 29, 1999; 11p; In English

Report No.(s): DE2001-12176; FERMILAB-CONF-99/208-E; No Copyright; Avail: Department of Energy Information Bridge, Microfiche

The authors measure the subjet multiplicity M in jets reconstructed with a successive combination type of jet algorithm (K(sub T)). They select jets with 55 less than E(sub T) less than 100 GeV and (vert-bar)(eta)(vert-bar) less than 0.5. They compare similar samples of jets at (radical)s = 1800 and 630 GeV. The HERWIG Monte Carlo simulation predicts that 59% of the jets are gluon jets at (radical)s = 1800 GeV, and 33% at (radical)s = 630 GeV. Using this information, they extract the subjet multiplicity in quark (M(sub q)) and gluon (M(sub g)) jets. They also measure the ratio R (equivalent-to) (M(sub g))(minus)1/(M(sub g))(minus)1 = 1.91 (+-) 0.04(stat)(sub (minus)0.19)(sup +0.23) (sys).

NTIS

Algorithms; Gluons; Monte Carlo Method; Quarks

20020001290 Lawrence Livermore National Lab., Livermore, CA USA

Equation of state of HF under shock compression

Fried, L. E.; Howard, W. M.; Jun. 01, 1999; 6p; In English

Report No.(s): DE2001-12173; UCRL-JC-134486; No Copyright; Avail: Department of Energy Information Bridge, Microfiche

We develop a model of chemical equilibrium mixtures containing the elements H, C, F. We show that the shock response of a wide variety of molecular and polymeric fluorocarbons can be modeled as a chemical equilibrium mixture of a small number of dissociation product molecules. HF is known to strongly associate in the supercritical fluid phase. We predict that such an association also occurs under shock conditions.

NTIS

Chemical Equilibrium; Equations of State; Shock Loads; Hydrofluoric Acid; Fluorocarbons; Polymers

20020001292 Lawrence Livermore National Lab., Livermore, CA USA

Sub-nanometer interferometry and precision turning for large optical fabrication

Klingmann, J. L.; Sommargren, G. E.; Apr. 01, 1999; 10p; In English

Report No.(s): DE2001-12168; UCRL-JC-134052; No Copyright; Avail: Department of Energy Information Bridge, Microfiche

At Lawrence Livermore National Laboratory (LLNL), we have the unique combination of precision turning and metrology capabilities critical to the fabrication of large optical elements. We have developed a self-referenced interferometer to measure errors in aspheric optics to sub-nanometer accuracy over 200-millimeter apertures, a dynamic range of 5(approximately)10. We have utilized diamond turning to figure optics for X-ray to IR wavelengths and, with fast-tool-servo technology, can move optical segments from off-axis to on-axis. With part capacities to 2.3-meters diameter and the metrology described above, segments of very large, ultra-lightweight mirrors can potentially be figured to final requirements. precision of diamond-turning will carryover although the surface finish may be degraded. Finally, the most critical component of a fabrication process is the metrology that enables an accurate part. Well characterized machines are very repeatable and part accuracy must come from proper metrology. A self-referencing interferometer has been developed that can measure accurately to sub-nanometer values. As with traditional

interferometers, measurements are fast and post-processed data provides useful feedback to the user. The simplicity of the device allows it to be used on large optics and systems.
NTIS
Fabrication; Interferometry; Metrology; Precision; Aspheric Optics

20020001298 Argonne National Lab., IL USA
POW3-workhorse powder diffractometer-reference instrument WBS 1.7.3
Crawford, R. K.; Jan. 20, 1999; 27p; In English
Report No.(s): DE2001-12073; ANL/SNS/98-1; No Copyright; Avail: Department of Energy Information Bridge, Microfiche
POW3 provides rapid data collection while maintaining reasonably good resolution. THe figure provides a schematic representation of POW3, and Table gives the parameters for this instrument. This is a workhorse refinement instrument for structures of modest complexity. In addition, this instrument views a cold moderator to enable long-wavelength neutrons to be used to measure long d-spacings.
NTIS
Data Acquisition; Diffractometers; Neutrons; Wavelengths

20020001300 Argonne National Lab., IL USA
Elemental ABAREX: A user's manual
Smith, A. B.; May 26, 1999; 36p; In English
Report No.(s): DE2001-12068; ANL/NDM-147; No Copyright; Avail: Department of Energy Information Bridge, Microfiche
ELEMENTAL ABAREX is an extended version of the spherical optical-statistical model code ABAREX, designed for the interpretation of neutron interactions with elemental targets consisting of up to ten isotopes. The contributions from each of the isotopes of the element are explicitly dealt with, and combined for comparison with the elemental observables. Calculations and statistical fitting of experimental data are considered. The code is written in FORTRAN-77 and arranged for use on the IBM-compatible personal computer (PC), but it should operate effectively on a number of other systems, particularly VAX/VMS and IBM work stations. Effort is taken to make the code user friendly. With this document a reasonably skilled individual should become fluent with the use of the code in a brief period of time.
NTIS
User Manuals (Computer Programs); Mathematical Models; Neutrons; Isotopes

20020001301 Argonne National Lab., IL USA
Neutron scattering and models: molybdenum
Smith, A. B.; May 26, 1999; 85p; In English
Report No.(s): DE2001-12066; ANL/NDM-142; No Copyright; Avail: Department of Energy Information Bridge, Microfiche
A comprehensive interpretation of the fast-neutron interaction with elemental and isotopic molybdenum at energies of (le) 30 MeV is given. New experimental elemental-scattering information over the incident energy range 4.5 (r arrow) 10 MeV is presented. Spherical, vibrational and dispersive models are deduced and discussed, including isospin, energy-dependent and mass effects. The vibrational models are consistent with the 'Lane potential'. The importance of dispersion effects is noted. Dichotomies that exist in the literature are removed. The models are vehicles for fundamental physical investigations and for the provision of data for applied purposes. A 'regional' molybdenum model is proposed. Finally, recommendations for future work are made.
NTIS
Neutron Diffraction; Neutron Scattering; Molybdenum; Mathematical Models

20020001302 Argonne National Lab., IL USA
Hydrocarbon rate coefficients for proton and electron impact ionization, dissociation, and recombination in a hydrogen plasma
Alman, D. A.; Brooks, J. N.; Ruzic, D. N.; Wang, Z.; Jul. 21, 1999; 40p; In English
Report No.(s): DE2001-12063; ANL/FPP/TM-297-REV; No Copyright; Avail: Department of Energy Information Bridge, Microfiche

We estimate cross sections and rate coefficients for proton and electron impact ionization, dissociation, and recombination of neutral and ionized hydrocarbon molecules and fragments of the form C(sub x)H(sub y)(sup k), x = 1-3, y = 1-6, k = 0,1 in a thermalized hydrogen-electron plasma.
NTIS
Ionization; Hydrocarbons; Electrons; Hydrogen Plasma; Proton Impact

20020001444 Argonne National Lab., IL USA
Atlas 10 ghz ecr ions source upgrade project
Moehs, D. P.; Pardo, R. C.; Vondrasek, R.; Xie, D.; Aug. 10, 1999; 14p; In English
Report No.(s): DE2001-11932; ANL/PHY/CP-99800; No Copyright; Avail: Department of Energy Information Bridge, Microfiche

A major upgrade of the first ATLAS (Argonne Tandem Linac Accelerator System) 10 GHz ECR (Electron Cyclotron Resonance) ion source, which began operations in 1987, is in the planning and procurement phase. The new design will convert the old two-stage source into a single-stage source with an electron donor disk and high gradient magnetic field that preserves radial access for solid material feeds and pumping of the plasma chamber. The new magnetic field profile allows for the possibility of a second ECR zone at a frequency of 14 GHz. An open hexapole configuration, using a high energy-product Nd-Fe-B magnet material, having an inner diameter of 8.8 cm and pole gaps of 2.4 cm has been adopted. Models indicate that the field strengths at the chamber wall, 4 cm in radius, will be 9.3 kG along the magnet poles and 5.6 kG along the pole gaps. The individual magnet bars will be housed in austenitic stainless steel allowing the magnet housing within the aluminum plasma chamber to be used as a water channel for direct cooling of the magnets. Eight solenoid coils from the existing ECR will be enclosed in an iron yoke to produce the axial mirror. Based on a current of 500 A, the final model predicts a minimum B field of 3 kG with injection and extraction mirror ratios of 4.4 and 2.9 respectively.
NTIS
Linear Accelerators; Ion Sources; Plasmas (Physics)

20020001453 Argonne National Lab., IL USA
Uncertainty Assessment for Accelerator-Driven Systems
Finck, P. J.; Gomes, I.; Micklich, B.; Palmiotti, G.; Jun. 10, 1999; 11p; In English
Report No.(s): DE2001-11846; ANL/RA/CP-99217; No Copyright; Avail: Department of Energy Information Bridge

The concept of a subcritical system driven by an external source of neutrons provided by an accelerator ADS (Accelerator Driver System) has been recently revived and is becoming more popular in the world technical community with active programs in Europe, Russia, Japan, and the US. A general consensus has been reached in adopting for the subcritical component a fast spectrum liquid metal cooled configuration. Both a lead-bismuth eutectic, sodium and gas are being considered as a coolant; each has advantages and disadvantages. The major expected advantage is that subcriticality avoids reactivity induced transients. The potentially large subcriticality margin also should allow for the introduction of very significant quantities of waste products (minor Actinides and Fission Products) which negatively impact the safety characteristics of standard cores. In the US these arguments are the basis for the development of the Accelerator Transmutation of Waste (ATW), which has significant potential in reducing nuclear waste levels. Up to now, neutronic calculations have not attached uncertainties on the values of the main nuclear integral parameters that characterize the system. Many of these parameters (e.g., degree of subcriticality) are crucial to demonstrate the validity and feasibility of this concept. In this paper we will consider uncertainties related to nuclear data only. The present knowledge of the cross sections of many isotopes that are not usually utilized in existing reactors (like Bi, Pb-207, Pb-208, and also Minor Actinides and Fission Products) suggests that uncertainties in the integral parameters will be significantly larger than for conventional reactor systems, and this raises concerns on the neutronic performance of those systems.
NTIS
Particle Accelerators; Liquid Metals; Coolants

20020001459 Argonne National Lab., IL USA
Measurement of the mass of the W boson from the Tevatron
Thurman-Keup, R.; Aug. 10, 1999; 14p; In English
Report No.(s): DE2001-11930; ANL-HEP-CP-99-87; No Copyright; Avail: Department of Energy Information Bridge, Microfiche

This paper presents measurements of the mass of the W vector boson from the CDF (cumulative distribution function) and D0 experiments using data collected at (radical)s = 1.8 TeV during the 1994-1995 data taking run. CDF finds a preliminary mass of M(sub W) = 80.43 (+-) 0.16 GeV and D0 measures a mass of M(sub W) = 80.44 +/- 0.12 GeV.
NTIS
Particle Accelerators; Bosons

20020001461 Argonne National Lab., IL USA
Circular polarization with crossed-planar undulators in high gain FELs
Kim, K. J.; Aug. 31, 1999; 10p; In English
Report No.(s): DE2001-11933; ANL/ASD/CP-99801; No Copyright; Avail: Department of Energy Information Bridge, Microfiche

We propose a crossed undulator configuration for a high-gain free-electron laser (FEL) to allow versatile polarization control. This configuration consists of a long (saturation length) planar undulator, a dispersive section, and a short (a few gain lengths) planar undulator oriented perpendicular to the first one. In the first undulator, a radiation component linearly polarized in the x-direction is amplified to saturation. In the second undulator, the x-polarized component propagates freely, while a new component, polarized in the y-direction, is generated and reaches saturation in a few gain lengths. by adjusting the strength of the dispersive section, the relative phase of two radiation components can be adjusted to obtain a suitable polarization for the total radiation field, including the circular polarization. The operating principle of the high-gain crossed undulator, which is quite different from that of the crossed undulator for spontaneous radiation, is illustrated in terms of 1-D (one dimensional) FEL theory.
NTIS
Free Electron Lasers; High Gain; Linear Polarization

20020001462 Argonne National Lab., IL USA
Kick and phase errors in spontaneous and amplified radiation
Kim, K. J.; Aug. 31, 1999; 10p; In English
Report No.(s): DE2001-11934; ANL/ASD/CP-99802; No Copyright; Avail: Department of Energy Information Bridge, Microfiche

Two types of magnet errors are considered: the random phase error (RPE), in which the phase errors are evenly distributed along the magnet, and the random kick error (RKE), in which the errors in the derivative of the phase are evenly distributed. We compute the reduction in performance of both spontaneous radiation and high-gain free-electron lasers (FEL) for both types of errors within the framework of 1-D (one dimensional) free-electron laser theory.
NTIS
Free Electron Lasers; Magnets

20020001463 Argonne National Lab., IL USA
Production of (phi) mesons in Au-Au collisions at the AGS
Back, B. B.; Betts, R. R.; Chang, J.; Gillitzer, A.; Henning, W. F.; Aug. 10, 1999; 6p; In English
Report No.(s): DE2001-11935; ANL/PHY/CP-99803; No Copyright; Avail: Department of Energy Information Bridge, Microfiche

The first measurements of (phi) meson production in Au-Au collisions at AGS (Alternating Gradient Synchrotron) energies are presented via the decay to K(sup +) K(sup (minus)). A measurement of the centrality dependence of the yield shows an increase similar to that seen for the K(sup (minus)) with a spectral shape consistent with a relativistic Breit-Wigner distribution within the statistical errors of the present data set. Future analysis using the full data set with 4 times the statistics will allow a more accurate determination of the yields, slopes and spectral shapes.
NTIS
Mesons; Atomic Collisions; Gold; Synchrotrons

20020001534 Stanford Univ., Stanford, CA USA
Final Report on the Construction of the HERS Endstation ***Final Report, 1 Sep. 1996 - 31 Oct. 1998***
Kellar, S. A.; Shen, Z. X.; Apr. 03, 2000; 13p; In English
Report No.(s): DE2001-765525; No Copyright; Avail: Department of Energy Information Bridge, Microfiche

The construction of the HERS endstation was successfully completed. The resolution of the photoemission apparatus is better than 7meV. The angular resolution is +0.15 degrees. The system has a high precision sample manipulator w/five-degrees of

freedom and a temperature range from 10 - 450 degrees K. The sample transfer system allows transfer of a sample from atmosphere onto the crystal at 5x10 in less than 2 hrs.
NTIS
Manipulators; Photoelectric Emission; Measuring Instruments; Architecture

20020001535 Lawrence Livermore National Lab., Livermore, CA USA
Constraints on target chamber first wall and target designs that will enable NIF debris shields to survive
Hibbard,; Burnham, A. K.; Curran, D. R.; Genin, F. Y.; Gerassimenko, M.; Jul. 09, 1998; 12p; In English
Report No.(s): DE2001-2769; UCRL-JC-129707; No Copyright; Avail: Department of Energy Information Bridge, Microfiche

The National Ignition Facility target chamber interior materials and target designs themselves have to be compatible with survival of the final-optics debris shields. to meet the planned maintenance and refinishing rate, the contamination of the debris shields cannot exceed about 1 nm equivalent thickness per shot of total material. This implies that the target mass must be limited to no more than 1 gram and the ablated mass released to the chamber from all other components must not exceed 3 grams. In addition, the targets themselves must either completely vaporize or send any minor amounts of shrapnel towards the chamber waist to prevent excessive cratering of the debris shields. The constraints on the first-wall ablation require that it be louvered to provide passive collection of remobilized contamination, because the expected target debris will remobilize at a rate fast enough to require cleaning every 3 weeks, about three times more frequent than possible with planned robotics. Furthermore, a comparison of ablatants from B4C and stainless-steel louvers suggests that remobilization of target debris by x rays will be greater than of the base material in both cases, thereby reducing the performance advantage of clean B4C over much-cheaper stainless steel. Neutronics calculations indicate that activation of thin Ni-free stainless steel is not a significant source of maintenance personnel radiation dose. Consequently, the most attractive first wall design consists of stainless-steel louvers. Evaluation of various unconverted-light beam dump designs indicates that stainless steel louvers generate no more debris than other materials, so one single design can serve as both first wall and beam dumps, eliminating beam steering restrictions caused by size and location of the beam dumps. One reservation is that the allowable contamination rate of the debris shield is not yet completely understood.
NTIS
Targets; Debris; Shielding; Louvers; Contamination

20020001564 Argonne National Lab., IL USA
Luminosity monitor topics for RHIC spin and AA, and pA interactions
Underwood, D.; Feb. 17, 1998; 41p; In English
Report No.(s): DE2001-12015; ANL-HEP-TR-97-100; No Copyright; Avail: Department of Energy Information Bridge

This is a note to define topics to be studied in more depth for the Luminosity monitoring for Spin Asymmetries. My numerical examples here are to stimulate discussion and should be taken with a grain of salt. The RHIC Spin experiments will require a very high degree of coordination between the experiments and the accelerator. For example see AGS/RHIC/SN 035. In this note we list some of the issues to be considered in monitoring the relative luminosity between various beam-beam spin combinations and beam-gas combinations. We give simplified numerical examples of the problems encountered in doing the luminosity monitoring to the 10(exp -4) level. It is hoped that this will provide a framework for serious study of these problems with simulations and other means. Many of the issues may also be relevant to pA and AA running where there may be sizable beam-gas backgrounds.
NTIS
Electron Beams; Numerical Analysis; Spin; Luminosity

20020001579 Argonne National Lab., IL USA
Laterally graded multilayer double-monochromator
AlsNielsen, J.; Erdmann, J.; Gaarde, P.; Krasnicki, S.; Liu, C.; Sep. 01, 1999; 9p; In English
Report No.(s): DE2001-12436; ANL/XFD/CP-98505; No Copyright; Avail: Department of Energy Information Bridge, Microfiche

The authors describe a tunable multilayer monochromator with an adjustable bandpass to be used for reflectivity and grazing incidence diffraction studies on surfaces at energies near 10 keV. Multilayers have a bandpass typically 100 times larger than the Si(111) reflection, and by using multilayers an experimenter can significantly increase data collection rates over those available with a Si monochromator. The transmission through 1 and 2 laterally graded multilayer (LGML) reflections was recorded versus photon energy. The identical LGMLs were comprised of 60 bilayers of W and C on 100 x 25 x 3 mm float glass with a bilayer spacing varying from 35 to 60 (angstrom). The average gradient was 0.27 (angstrom)/mm along the long dimension. The rms deviation of the data for the bilayer spacing from a linear fit was 0.36 (angstrom). Data were obtained for a nondispersive ((+-)) double-multilayer arrangement. The relative bandpass width (FWHM) when the two multilayers exposed the same bilayer

spacing was measured to be 2.2% with a transmission of 78.7 (+-) 1.6%. This value is consistent with the transmission of 88.9% that they also measured for a single LGML at HASYLAB beamline D4. The bandpass was tunable in the range 1.1% to 2.2%.
NTIS
Diffraction; Grazing Incidence; Monochromators; Laminates; Lateral Control

20020001580 Argonne National Lab., IL USA
Development of Sn-Li coolant/breeding material for APEX/ALPS applications
Sze, D. K.; Jul. 08, 1999; 15p; In English
Report No.(s): DE2001-12429; ANL/TD/CP-98298; No Copyright; Avail: Department of Energy Information Bridge, Microfiche

A Sn-Li alloy has been identified to be a coolant/breeding material for D-T fusion applications. The key feature of this material is its very low vapor pressure, which will be very useful for free surface concepts employed in APEX, ALPS and inertial confinement fission. The vapor is dominated by lithium, which has very low Z. Initial assessment of the material indicates acceptable tritium breeding capability, high thermal conductivity, expected low tritium volubility, and expected low chemical reactivities with water and air. Some key concerns are the high activation and material compatibility issues. The initial assessment of this material, for fission applications, is presented in this paper.
NTIS
Lithium; Blankets (Fission Reactors); Reaction Kinetics; Thermal Conductivity; Tritium; Tin Alloys

20020001582 Argonne National Lab., IL USA
High power density self-cooled lithium-vanadium blanket
Gohar, Y.; Majumdar, S.; Smith, D.; Jul. 01, 1999; 21p; In English
Report No.(s): DE2001-12426; ANL/TD/CP-98294; No Copyright; Avail: Department of Energy Information Bridge, Microfiche

A self-cooled lithium-vanadium blanket concept capable of operating with 2 MW/m(sup 2) surface heat flux and 10 MW/m(sup 2) neutron wall loading has been developed. The blanket has liquid lithium as the tritium breeder and the coolant to alleviate issues of coolant breeder compatibility and reactivity. Vanadium alloy (V-4Cr-4Ti) is used as the structural material because it can accommodate high heat loads. Also, it has good mechanical properties at high temperatures, high neutron fluence capability, low degradation under neutron irradiation, good compatibility with the blanket materials, low decay heat, low waste disposal rating, and adequate strength to accommodate the electromagnetic loads during plasma disruption events. Self-healing electrical insulator (CaO) is utilized to reduce the MHD pressure drop. A poloidal coolant flow with high velocity at the first wall is used to reduce the peak temperature of the vanadium structure and to accommodate high surface heat flux. The blanket has a simple blanket configuration and low coolant pressure to reduce the fabrication cost, to improve the blanket reliability, and to increase confidence in the blanket performance. Spectral shifter, moderator, and reflector are utilized to improve the blanket shielding capability and energy multiplication, and to reduce the radial blanket thickness. Natural lithium is used to avoid extra cost related to the lithium enrichment process.
NTIS
Liquid Lithium; Magnetohydrodynamics; Mechanical Properties; Vanadium Alloys; Fabrication; Neutron Irradiation

20020001660 Argonne National Lab., IL USA
High Energy Physics Division Research Activities ***Semiannual Report, 1 Jul. - 31 Dec. 1997***
Norem, J.; Rezmer, R.; Schuur, C.; Wagner, R.; Aug. 11, 1998; 92p; In English
Report No.(s): DE2001-12018; ANL-HEP-TR-98-30; No Copyright; Avail: Department of Energy Information Bridge, Microfiche

This report describes the research conducted in the High Energy Physics Division of Argonne National Laboratory during the period July 1, 1997--December 31, 1997. Topics covered here include experimental and theoretical particle physics, advanced accelerator physics, detector development, and experimental facilities research. Lists of Division publications and colloquia are included.
NTIS
High Energy Interactions; Research Facilities; Numerical Analysis; Experimentation; Research

20020001831 Argonne National Lab., IL USA

Gamma-Ray Array Physics

Lister, C. J.; May 25, 1999; 13p; In English

Report No.(s): DE2001-11825; ANL/PHY/CP-99103; No Copyright; Avail: Department of Energy Information Bridge

In this contribution I am going to discuss the development of large arrays of Compton Suppressed, High Purity Germanium (HpGe) detectors and the physics that has been, that is being, and that will be done with them. These arrays and their science have dominated low-energy nuclear structure research for the last twenty years and will continue to do so in the foreseeable future. John Sharpey Schafer played a visionary role in convincing a skeptical world that the development of these arrays would lead to a path of enlightenment. The extent to which he succeeded can be seen both through the world-wide propagation of ever more sophisticated devices, and through the world-wide propagation of his students. I, personally, would not be working in research if it were not for John's inspirational leadership. I am eternally grateful to him. Many excellent reviews of array physics have been made in the past which can provide detailed background reading. The review by Paul Nolan, another ex-Sharpey Schafer student, is particularly comprehensive and clear.

NTIS

Gamma Rays; Nuclear Structure; Arrays

20020001974 Argonne National Lab., IL USA

Diffraction at HERA: inclusive measurements

Derrick, M.; Jan. 19, 1999; 15p; In English

Report No.(s): DE2001-12367; ANL-HEP-CP-98-141; No Copyright; Avail: Department of Energy Information Bridge, Microfiche

In this, the second of two reports on diffractive studies at HERA, the inclusive measurements made by the two collaborations, H1 and ZEUS, are summarized.

NTIS

Diffraction; Storage Rings (Particle Accelerators)

20020001982 Argonne National Lab., IL USA

Synchrotron Environmental Science-I Workshop Report

Jul. 08, 1999; 34p; In English

Report No.(s): DE2001-12024; ANL/APS/TM-17; No Copyright; Avail: Department of Energy Information Bridge

Attendees of the Synchrotrons Environmental Science 1 (SES-1) workshop represented a broad spectrum of environmental science research areas and expertise in all of the current synchrotrons techniques (X-ray scattering and diffraction, X-ray absorption spectroscopy, and two- and three-dimensional X-ray imaging). These individuals came together to discuss current measurement obstacles in environmental research and, more specifically, ways to overcome such obstacles by applying synchrotrons radiation techniques. Significant obstacles in measurement affect virtually all of the research issues described. Attendees identified synchrotrons approaches of potential value in their research. A number of the environmental research studies discussed are currently being addressed with some success by synchrotron-based approaches. Nevertheless, improvements in low-Z measurement capabilities are needed to facilitate the use of synchrotrons radiation methodologies in environmental research.

NTIS

Absorption Spectroscopy; Synchrotron Radiation; Environment Effects; Atomic Physics

20020001985 Argonne National Lab., IL USA

High Energy Physics Division Research Activities ***Semiannual Report, 1 Jul. - 31 Dec. 1998***

Berger, E. L.; Bodwin, G.; Drake, G.; Goodman, M. C.; Guarino, V.; Aug. 20, 1999; 78p; In English

Report No.(s): DE2001-12020; ANL-HEP-TR-99-32; No Copyright; Avail: Department of Energy Information Bridge

This report describes the research conducted in the High Energy Physics Division of Argonne National Laboratory during the period July 1, 1998--December 31, 1998.

NTIS

Energy Technology; High Energy Interactions

20020001986 Argonne National Lab., IL USA

High Energy Physics Division Research Activities ***Semiannual Report, 1 Jan. - 30 Jun. 1998***

Ayres, D. S.; Berger, E. L.; Blair, R.; Bodwin, G. T.; Drake, G.; Mar. 09, 1999; 94p; In English

Report No.(s): DE2001-12017; ANL-HEP-TR-98-134; No Copyright; Avail: Department of Energy Information Bridge

This report describes the research conducted in the High Energy Physics Division of Argonne National Laboratory during the period of January 1, 1998 through June 30, 1998. Topics covered here include experimental and theoretical particle physics, advanced accelerator physics, detector development, and experimental facilities research. Lists of Division publications and colloquia are included.

NTIS

Theoretical Physics; Energy Technology; High Energy Interactions

20020001989 Virginia Polytechnic Inst. and State Univ., Blacksburg, VA USA

Partial wave analysis of scattering below 2 GeV

Arndt, R. A.; Workman, R. L.; Sep. 01, 1999; 15p; In English

Report No.(s): DE2001-764189; No Copyright; Avail: Department of Energy Information Bridge

In 1988, our group was maintaining and updating analyses of the elastic TN, NN, and KN databases. to these we have added databases and analyses of pion photoproduction, elastic Td scattering, and the reaction Td -/+ pp. In addition to this, a database for pion electroproduction has been assembled for future analysis, Our results were initially made available through Telnet connections to a VAX computer at Virginia Tech and through the distribution of tapes to sites around the world. Since 1988, we have moved our analyses to UNIX workstations and have started a website, in order to make our results available to a wider range of users.

NTIS

Elastic Scattering; Wave Scattering; Photoproduction; Pions

20020001994 Oklahoma State Univ., Stillwater, OK USA

Theoretical studies in weak, electromagnetic and strong interactions. Attachments

Nandi, S.; Sep. 01, 1999; 11p; In English

Report No.(s): DE2001-763329; No Copyright; Avail: Department of Energy Information Bridge

The project covered a wide area of current research in theoretical high-energy physics. This included Standard Model (SM) as well as physics beyond the Standard Model. Specific topics included supersymmetry (SUSY), perturbative quantum chromodynamics (QCD), a new weak interaction for the third family (called topflavor), neutrino masses and mixings, topcolor model, Pade approximation, and its application to perturbative QCD and other physical processes.

NTIS

Quantum Chromodynamics; Supersymmetry; Theoretical Physics; Neutrinos; Standard Model (Particle Physics); Pade Approximation; Weak Interactions (Field Theory); Strong Interactions (Field Theory)

20020001998 Georgia State Univ., Atlanta, GA USA

Research in Heavy Ion Nuclear Reactions

Petitt, G. A.; Nelson, W. H.; He, X.; Lee, W.; Apr. 14, 1999; 16p; In English

Report No.(s): DE2001-6559; No Copyright; Avail: Department of Energy Information Bridge

This is the final progress report for the experimental nuclear physics program at Georgia State University (GSU) under the leadership of Gus Petitt. In June, 1996, Professor Petitt retired for health reasons and the DOE (Department of Energy) contract was extended for another year to enable the group to continue it's work. This year has been a productive one. The group has been heavily involved in the E866 experiment at Fermilab where we have taken on the responsibility of developing a new level-3 trigger for the experiment. Bill Lee, the graduate student in our group expects to obtain his thesis data from the run extension currently in progress, which focuses on the A dependence of J/(psi)'s and (Upsilon)'s from beryllium, tungsten, and iron targets. In the past year and a half the GSU group has led the development of a new level-3 software trigger system for E866. Our work on this project is described.

NTIS

Heavy Ions; Nuclear Reactions; Ionic Reactions

20020002012 Lawrence Livermore National Lab., Livermore, CA USA

Management of unconverted light for the National Ignition Facility target chamber

Anderson, A. T.; Bletzer, K.; Burnham, A. K.; Dixit, S.; Genin, F. Y.; Jul. 08, 1998; 14p; In English

Report No.(s): DE2001-2770; UCRL-JC-129706; No Copyright; Avail: Department of Energy Information Bridge, Microfiche

The NIF target chamber beam dumps must survive high x-ray, laser, ion, and shrapnel exposures without excessive generation of vapors or particulate that will contaminate the final optics debris shields, thereby making the debris shields susceptible to subsequent laser damage. The beam dumps also must be compatible with attaining and maintaining the required target chamber vacuum and must not activate significantly under high neutron fluxes. Finally, they must be developed, fabricated, and maintained for a reasonable cost. The primary challenge for the beam dump is to survive up to 20 J/square cm of lpm light and 1 - 2 J/square cm of nominally 200 - 350 eV blackbody temperature x rays. Additional threats include target shrapnel, and other contamination issues. Designs which have been evaluated include louvered hot-pressed boron carbide (B4C) or stainless steel (SS) panels, in some cases covered with transparent Teflon film, and various combinations of inexpensive low thermal expansion glasses backed by inexpensive absorbing glass. Louvered designs can recondense a significant amount of ablated material that would otherwise escape into the target chamber. Transparent Teflon was evaluated as an alternative way to capture ablated material. The thin Teflon sheet would need to be replaced after each shot since it exhibits both laser damage and considerable x- ray ablation with each shot. Uncontaminated B4C, SS, and low thermal expansion glasses have reasonably small x-ray and laser ablation rates, although the glasses begin to fail catastrophically after 100 high fluence shots. Commercially available absorbing glasses require a pre-shield of either Teflon or low thermal expansion glass to prevent serious degradation by the x-ray fluence. Advantages of the hot-pressed B4C and SS over glass are their performance against microshrapnel, their relative indifference to contamination, and their ability to be refurbished by aggressive cleaning using CO2 pellets, glass beads, high pressure water or ultrasonic tanks. In addition the expected replacement rate to avoid catastrophic failure makes the glass option more costly. SS is less expensive, more easily formed into a louver design with high capture efficiency, and otherwise equivalent to B4C. Hence, it would be preferred as long as debris shield damage is not substantially greater for SS as compared to damage from an equivalent mass of contamination of B4C. If debris shield damage is problematic, the escape of SS could be mitigated by use of a transparent Teflon film. The Teflon film would require increased target chamber pumping and cleaning capability to accommodate the x-ray decomposition products. NTIS

Targets; Laser Damage; Debris; Shielding; Louvers

20020002015 Texas A&M Univ., College Station, TX USA

Collider Physics ***Final Report, 1 Apr. 1995 - 31 Mar. 1999***

White, J. T.; Dec. 10, 1999; 12p; In English

Report No.(s): DE2001-765420; DOE/ER/40916; No Copyright; Avail: Department of Energy Information Bridge, Microfiche

This report summarizes the work done over the period April 1, 1995 through March 31, 1999. Detailed progress have been submitted for the years through March 31, 1999. The primary project during this period was the D0 experiment at Fermilab and is discussed first. The last year of the period was an extension to complete the study of laser induced fluorescence in neon. This work is discussed in the section Detector R and D. NTIS

Mesons; Neon; Particle Theory; Laser Induced Fluorescence

20020002241 Massachusetts Inst. of Tech., Cambridge, MA USA

Measurements of Core Conditions, Implosion Symmetry, and Anomaloes Acceleration Mechanisms on Omega through Charged Particle Spectroscopy ***Final Report, 1 Nov. 1997 - 31 Dec. 1998***

Petrasso, R.; Li, C. K.; Oct. 19, 1999; 13p; In English

Report No.(s): DE2001-765739; No Copyright; Avail: Department of Energy Information Bridge, Microfiche

This work concerns the first spectroscopic measurements of energetic charged particles on Omega. Individual line profiles include D-3He protons (14.7 MeV) and alphas (3.6 MeV), D-T alphas (3.5 MeV), D-D protons (3.0 MeV), and D-D tutons (1.0 MeV). NTIS

Charged Particles; Spectroscopy; Acceleration (Physics)

20020002242 Alameda Applied Science Corp., San Leandro, CA USA

High voltage, fast turn-on and turn-off switch ***Final Report, 2 Sep. 1998 - 17 Mar. 1999***

Schein, J.; Xu, X.; Qi, N.; Gensler, S.; Prasad, R.; Apr. 10, 1999; 28p; In English

Report No.(s): DE2001-765665; AASC99TM-59; No Copyright; Avail: Department of Energy Information Bridge, Microfiche

The aspect to be investigated during this contract was an electron-beam triggered diamond switch to be used in high power modulators. Today's high power modulators require higher voltage switches than those developed to date. Specifically, the proposed 1 TeV linear collider, the NLC/ILC at the Stanford Linear Accelerator Center (SLAC), consists of two linacs with 6600 X-Band klystrons powered by 3300 high power modulators. These modulators require switches capable of handling 80 kV, switching 8 kA with pulse durations ranging from 2 ps (linac) to 6 (micro)s (pre-linac) with switching times greater than 50 ns at pulse repetition frequencies up to 180 Hz. In addition the large number of switches and other components dictate a pulse to pulse jitter of greater than 10 ns and a mean time between failures of at least 50,000 hours. The present approach is to use hydrogen filled thyratrons. While these switches meet the voltage and conduction current requirements they lack the required reliability (pulse to pulse jitter) and lifetime. Research to improve these aspects is in progress. A solid state switch inherently offers the required reliability and lifetime. However, Si-based switches developed to date are limited to about 5 kV and several must be stacked in series to deliver the required voltage. This further increases the already large parts count and compromises reliability and lifetime. A monolithic, solid state switch capable of meeting all the requirements for X-Band modulators would be ideal. DOE selected this proposal for a Phase 1 SBIR award and this final report describes the progress made during the contract.
NTIS
Linear Accelerators; Switches; Modulators

20020002273 Lawrence Livermore National Lab., Livermore, CA USA
Scrounge-atron: a proton radiography demonstration accelerator
Alford, O. J.; Barnes, P. D.; Chargin, A. K.; Hartouni, E. F.; Hockman, J. N.; December 1998; 46p; In English
Report No.(s): DE2001-12467; UCRL-LR-134107; REPT-98-ERD-088; No Copyright; Avail: Department of Energy Information Bridge, Microfiche

The Scrounge-atron is a concept that could provide a demonstration accelerator for proton radiography. As discussed here, the Scrounge-atron would be capable of providing a 20 GeV beam of ten pulses, 10(sup 11) protons each, spaced 250 ns apart. This beam could be delivered once every minute to a single-axis radiographic station centered at the BEEF facility of the Nevada Test Site. These parameters would be sufficient to demonstrate, in five years, the capabilities of a proton-based Advanced Hydrotest Facility, and could return valuable information to the stockpile program, information that could not be obtained in any other way. The Scrounge-atron could be built in two to three years for $50-100 million. to meet this schedule and cost, the Scrounge-atron would rely heavily on the availability of components from the decommissioned Fermilab Main Ring.
NTIS
Particle Accelerators; Radiography; Protons

20020002302 Lawrence Livermore National Lab., Livermore, CA USA
Precision SUSY Measurements at LHC: Point 3
Hinchliffe, I.; Paige, F. E.; Nagy, E.; Shapiro, M. D.; Soderqvist, J.; Nov. 01, 1998; 18p; In English
Report No.(s): DE2001-6388; LBNL-40954; ATLAS-NOTE-PHYS-109; No Copyright; Avail: Department of Energy Information Bridge, Microfiche

This paper, which is one of a series, presents detailed studies of mass reconstructions and other measurements in a case study illustrating the power of the ATLAS detector to perform measurements of supersymmetric particle production. A particular point in the parameter space of the Minimal Supergravity inspired model is used. Reconstruction of gluino, sbottom, and light squarks and the measurement of neutral ion mass differences is shown.
NTIS
Elementary Particles; Particle Production; Supersymmetry

20020002317 North Carolina Agricultural and Technical State Univ., Greensboro, NC USA
2H(n,p)2n experiment to measure accurately the neutron-neutron scattering length ***Final Report, 1 May 1995 - 31 Oct. 1998***
Jackson, C. R.; Feb. 26, 1999; 34p; In English
Report No.(s): DE2001-765646; No Copyright; Avail: Department of Energy Information Bridge, Microfiche

The neutron-neutron (n-n) scattering length a(sub nn) is a parameter that represents the strength of the n-n interaction at low energies. It can be compared with the proton-proton (p-p) scattering length a(sub pp) to investigate the charge-symmetry breaking in nuclear forces. The difference a(sub pp)-a(sub nn) is a measure of the mass difference of the up and down quarks and therefore it is of fundamental interest. Experiments to determine a(sub nn) use mainly one of two deuteron reactions: Pi -d capture or Pi -d breakup. For both of these deuteron reactions, a (sub nn) is extracted by analysis of the cross-section data. However, the experimental values of a(sub nn) from the two reactions disagree. What is more confusing than this discrepancy is that

significantly different values for a(sub nn) are reported from similar (sup 2)H(n,p) 2n experiments. This problem must be resolved before the differences between Pi -d and n-d reactions can be addressed further.
NTIS
Particle Interactions; Neutron Scattering; Broken Symmetry

20020002348 Brookhaven National Lab., Upton, NY USA
Muon Dynamics and Ionization Cooling at Muon Collider
Parsa, Z.; Nov. 01, 1998; 7p; In English
Report No.(s): DE2001-6266; BNL-66077; No Copyright; Avail: Department of Energy Information Bridge, Microfiche

Muon dynamics and beam cooling methods for muon colliders are presented. Formulations and effects of ionization cooling as the preferred method used to compress the phase space to reduce the emittance and to obtain high luminosity muon beams are also included.
NTIS
Cooling; Ionization; Muons; Linear Accelerators

20020002750 Argonne National Lab., IL USA
Aqueous complexation of trivalent lanthanide and actinide cations by N,N,N(sup 1),N(sup 1)-tetrakis (2-pyridylmethyl)ethylenediamine
Beitz, J. V.; Ensor, D. D.; Jensen, M. P.; Morss, L. R.; Jun. 16, 1999; 18p; In English
Report No.(s): DE2001-12423; ANL/CHM/CP-98344; No Copyright; Avail: Department of Energy Information Bridge, Microfiche

The aqueous complexation reactions of trivalent lanthanide and actinide cations with the hexadentate ligand N,N,N(prime),N(prime) -tetrakis(2-pyridylmethyl) ethylenediamine (TPEN), have been characterized using potentiometric and spectroscopic techniques in 0.1 M NaClO(sub 4). At 25 C, the stability constant of Am(TPEN)(sup 3+) is two orders of magnitude larger than that of Sm(TPEN)(sup 3+), reflecting the stronger interactions of the trivalent actinide cations with softer ligands as compared to lanthanide cations.
NTIS
Cations; Ligands; Actinide Series Compounds

20020002767 Argonne National Lab., IL USA
Weak interaction studies with an on-line Penning trap mass spectrometer
Barber, R. C.; Buchinger, F.; Crawford, J. E.; Feng, X.; Gulick, S.; Mar. 10, 1999; 8p; In English
Report No.(s): DE2001-12418; ANL/PHY/CP-98560; No Copyright; Avail: Department of Energy Information Bridge, Microfiche

Superallowed (beta)-decays are a sensitive probe of the fundamental aspects of the weak interaction. Such decays are used to stringently test the CVC (conserved vector current) hypothesis, deduce a precise value of the weak vector coupling constant, test the unitarity of the CKM (Cabibbo-Kobayashi-Maskawa) matrix and look for deviation from the V-A structure for the weak interaction. The ability to efficiently capture and store short-lived superallowed beta-emitters in ion traps will help to elucidate discrepancies in the most precise unitarity test of the CKM matrix and tighten the present limits on interactions outside the standard V-A form.
NTIS
Mass Spectrometers; Particle Interactions

20020002774 Argonne National Lab., IL USA
Extension of the Application of the generalized pole representation to the treatment of resonance cross sections
Hwang, R. N.; Jammes, C.; Mar. 12, 1999; 13p; In English
Report No.(s): DE2001-12409; ANL/RA/CP-98582; No Copyright; Avail: Department of Energy Information Bridge, Microfiche

One reliable and convenient way of processing the cross sections in the resolved energy region is by use of the generalized pole representation, whereby the Doppler-broadening calculation can be carried out rigorously using the analytical approach. So far, its applications have been limited to cases with resonance parameters specified by the Reich-Moore formalism. Although such an approach, in principle, can be extended to all three remaining representations of resolved resonance parameters specified by the ENDF (Evaluated Nuclear Data File) data format, there is no computational tool for handling such a task at present. Given that Breit-Wigner formalisms are probably the most widely used by any evaluated nuclear data library to represent cross sections,

a special effort has to be made to convert the single level and multilevel Breit-Wigner resonance parameters to pole parameters. A FORTRAN computer code BW2PR has been developed for this purpose. Extensive calculations have been performed to demonstrate that the proposed method ensures the conservation of the information contained originally in Breit-Wigner resonance parameters. This will make it possible to apply the exact Doppler-broadening method to a larger collection of nuclides.
NTIS
Doppler Effect; Resonance; Scattering Cross Sections

20020002780 Argonne National Lab., IL USA
Precise tests of x-ray scattering theories in the Compton regime
Dunford, R. W.; Gemmell, D. S.; Kanter, E. P.; Krassig, B.; Southworth, S. H.; Jan. 15, 1999; 13p; In English
Report No.(s): DE2001-12394; ANL/CHM/CP-98214; No Copyright; Avail: Department of Energy Information Bridge, Microfiche

The authors report two experiments intended to test the accuracy of state-of-the-art theoretical predictions for x-ray scattering from low-Z atoms. The first one deals with the differential x-ray scattering cross sections in Ne and He from 11-22 keV and the Ne Compton-to-Rayleigh scattering ratio in this energy range. It was found that, in order to be consistent with the experimental results, an accurate description at low Z must include nonlocal exchange, electron correlation, and dynamic effects. The second experiment concerns the ratio of helium double-to-single ionization for Compton scattering in the 8-28 keV energy range where published experimental and theoretical results so far fail to give a consistent picture. The progress of the experiment and the data analysis is reported.
NTIS
Compton Effect; X Ray Scattering

20020002796 California Univ., Lawrence Berkeley Lab., Berkeley, CA USA
Beam Simulations for IRE and Driver-Status and Strategy
Friedman, A.; Grote, D. P.; Lee, E. P.; Sonnendrucker, E.; Mar. 01, 2000; 20p; In English
Report No.(s): DE2001-767593; LBNL-45682; HIFAN 1036; No Copyright; Avail: Department of Energy Information Bridge, Microfiche

The methods and codes employed in the U.S. Heavy Ion Fusion program to simulate the beams in an Integrated Research Experiments (IRE) facility and a fusion driver are presented in overview. A new family of models incorporating accelerating module impedance, multi-beam, and self-magnetic effects is described, and initial WARP3d particle simulations of beams using these models are presented. Finally, plans for streamlining the machine-design simulation sequence, and for simulating beam dynamics from the source to the target in a consistent and comprehensive manner, are described.
NTIS
Heavy Ions; Magnetic Effects; Particle Beams

20020002848 Argonne National Lab., IL USA
Deformed proton emitters
Carpenter, M. P.; Cizewski, J. A.; Davids, C. N.; Davinson, T.; Fotiades, N.; Feb. 17, 1999; 13p; In English
Report No.(s): DE2001-12406; ANL/PHY/CP-98432; No Copyright; Avail: Department of Energy Information Bridge, Microfiche

The mechanisms of proton radioactivity from deformed rare earth nuclei are discussed and preliminary results on the fine structure decay of (sup 131)Eu are presented.
NTIS
Europium Isotopes; Protons; Nuclei (Nuclear Physics); Particle Decay

20020003403 Lawrence Livermore National Lab., Livermore, CA USA
Quantum suppression of beamstrahlung for future e + e- linear colliders
Xie, M.; May 01, 1998; 19p; In English
Report No.(s): DE2001-6480; LBNL-41808; CBP-NOTE-252; No Copyright; Avail: Department of Energy Information Bridge

Beamstrahlung at interaction point may present severe limitations on linear collider performance. The approach to reduce this effect adopted for all current designs at a center-of-mass energy of 0.5 TeV will become more difficult and less effective at

higher energy. We discuss the feasibility of an alternative approach, based on an effect known as quantum suppression of beamstrahlung, for future linear colliders at multi-TeV energy.
NTIS
Linear Accelerators; Bremsstrahlung; Beams (Radiation)

20020003404 Lawrence Livermore National Lab., Livermore, CA USA
Photon-Electron Interaction and Condense Beams
Chattopadhyay, S.; Nov. 01, 1998; 24p; In English
Report No.(s): DE2001-6492; LBNL-42334; No Copyright; Avail: Department of Energy Information Bridge
We discuss beams of charged particles and radiation from multiple perspectives. These include fundamental acceleration and radiation mechanisms, underlying electron-photon interaction, various classical and quantum phase-space concepts and fluctuational interpretations.
NTIS
Charged Particles; Photon-Electron Interaction; Photons

20020003405 Lawrence Livermore National Lab., Livermore, CA USA
Preliminary Ionization Efficiencies of C-11 and O-14 with the LBNL ECR Ion Sources
Xie, Z. Q.; Cerny, J.; Guo, F. Q.; Joosten, R.; Larimer, R. M.; Oct. 05, 1998; 12p; In English
Report No.(s): DE2001-6493; LBNL-42444; No Copyright; Avail: Department of Energy Information Bridge
High charge states, up to fully stripped C-11 and O-14 ion, beams have been produced with the electron cyclotron resonance ion sources (LBNL, ECR and AECR-U) at Lawrence Berkeley National Laboratory. The radioactive atoms of C-11 and O-14 were collected in batch mode with an LN(sub 2) trap and then bled into the ECR ion sources. Ionization efficiency as high as 11% for C-11(4+) was achieved.
NTIS
Carbon Isotopes; Ion Beams; Ionization; Oxygen Isotopes; Ion Sources

20020003406 California Univ., Lawrence Berkeley Lab., Berkeley, CA USA
NA49 Results on Single Particle and Correlation Measurements in Central PB+PB Collisions
Wang, F.; Appelshauser, H.; Bachler, J.; Bailey, S. J.; Barna, D.; Dec. 01, 1998; 16p; In English
Report No.(s): DE2001-6498; LBNL-42591; No Copyright; Avail: Department of Energy Information Bridge
Single-particle spectra and two-particle correlation functions measured by the NA49 collaboration in central Pb+Pb collisions at 158 GeV/nucleon are presented. These measurements are used to study the kinetic and chemical freeze-out conditions in heavy ion collisions. We conclude that large baryon stopping, high baryon density and strong transverse radial flow are achieved in central Pb+Pb collisions at the SPS.
NTIS
Ionic Collisions; Heavy Ions; Baryons; Correlation; Radial Flow

20020003407 Lawrence Livermore National Lab., Livermore, CA USA
Colliding Crystalline Beams
Wei, J.; Sessler, A. M.; Jun. 01, 1998; 7p; In English
Report No.(s): DE2001-6515; LBNL-42091; No Copyright; Avail: Department of Energy Information Bridge
The understanding of crystalline beams has advanced to the point where one can now, with reasonable confidence, undertake an analysis of the luminosity of colliding crystalline beams. Such a study is reported here. It is necessary to observe the criteria, previously stated, for the creation and stability of crystalline beams. This requires, firstly, the proper design of a lattice. Secondly, a crystal must be formed, and this can usually be done at various densities. Thirdly, the crystals in a colliding-beam machine are brought into collision. We study all of these processes using the molecular dynamics (MD) method. The work parallels what was done previously, but the new part is to study the crystal-crystal interaction in collision. We initially study the zero-temperature situation. If the beam-beam force (or equivalent tune shift) is too large then over-lapping crystals can not be created (rather two spatially separated crystals are formed). However, if the beam-beam force is less than but comparable to that of the space-charge forces between the particles, we find that overlapping crystals can be formed and the beam-beam tune shift can be of the order of unity. Operating at low but non-zero temperature can increase the luminosity by several orders of magnitude over that of a usual

collider. The construction of an appropriate lattice, and the development of adequately strong coding, although theoretically achievable, is a challenge in practice.
NTIS
Collisions; Crystallinity; Crystals; Molecular Dynamics

20020003409 Lawrence Livermore National Lab., Livermore, CA USA
Quantum Suppression of beamstrahlung for future e+e- linear collider: an evaluation of QED backgrounds
Xie, M.; Oct. 13, 1998; 14p; In English
Report No.(s): DE2001-6523; LBNL-42286; No Copyright; Avail: Department of Energy Information Bridge
Beamstrahlung at interaction point may present severe limitations on linear collider performance. The approach to reduce this effect adopted for all current designs at 0.5 TeV range in center-of-mass energy will become more difficult and less effective at higher energy. We discuss the feasibility of an alternative approach, based on an effect known as quantum suppression of beamstrahlung, for future linear colliders at multi-TeV energy.
NTIS
Quantum Electrodynamics; Linear Accelerators; Bremsstrahlung

20020003410 California Univ., Lawrence Berkeley Lab., Berkeley, CA USA
Momentum Aperture of the Advanced Light Source
Decking, W.; Robin, D.; Aug. 01, 1998; 14p; In English
Report No.(s): DE2001-6530; LBNL-42462; No Copyright; Avail: Department of Energy Information Bridge
This paper shows measurements of the momentum aperture of the Advanced Light Source (ALS) based on Touschek lifetime measurements. The measured data is compared with tracking simulations and a simple model for the apertures will help to explain the observed effects.
NTIS
Apertures; Light Sources; Simulation; Angular Momentum

20020003412 California Univ., Lawrence Berkeley Lab., Berkeley, CA USA
Two-photon physics in nucleus-nucleus collisions at RHIC
Nystrand, J.; Klein, S.; Sep. 01, 1998; 19p; In English
Report No.(s): DE2001-6533; LBNL-42524; No Copyright; Avail: Department of Energy Information Bridge
Ultra-relativistic heavy-ions carry strong electromagnetic and nuclear fields. Interactions between these fields in peripheral nucleus-nucleus collisions can probe many interesting physics topics. This presentation will focus on coherent two-photon and photonuclear processes at RHIC. The rates for these interactions will be high. The coherent coupling of all the protons in the nucleus enhances the equivalent photon flux by a factor Z(sup 2) up to an energy of approximately 3 GeV. The plans for studying coherent interactions with the STAR experiment will be discussed. Experimental techniques for separating signal from background will be presented.
NTIS
Heavy Ions; Photons; Protons; Photonuclear Reactions

20020003424 Los Alamos National Lab., NM USA
Investigation of halo formation in continuous beams using weighted polynomial expansions and perturbational analysis
Allen, C.; Aug. 01, 2000; 6p; In English
Report No.(s): DE2001-768810; LA-UR-00-3810; No Copyright; Avail: Department of Energy Information Bridge
We consider halo formation in continuous beams oscillating at natural modes by inspecting particle trajectories. Trajectory equations containing field nonlinearities are derived from a weighted polynomial expansion. We then use perturbational techniques to further analyze particle motion.
NTIS
Polynomials; Particle Beams; Halos; Perturbation Theory

20020003425 Los Alamos National Lab., NM USA
Relativistic foundations of pseudospin symmetry in nuclear structure and scattering
Ginnocchio, J.; Aug. 01, 2000; 9p; In English
Report No.(s): DE2001-768815; LA-UR-00-3646; No Copyright; Avail: Department of Energy Information Bridge

Pseudospin doublets were discovered about thirty years ago but their origins had been a mystery. We show that pseudospin doublets originate from an SU(2) symmetry of the Dirac Hamiltonian which occurs when the scalar and vector potentials c f are opposite in sign but equal in magnitude. Furthermore, we survey the evidence that pseudospin symmetry is approximately conserved for realistic nuclear scalar and vector potentials. We demonstrate that pseudospin symmetry is partially conserved in medium energy nucleon-nucleus scattering as well. We briefly discuss the relationship of pseudospin symmetry with chiral symmetry.
NTIS
Particle Spin; Symmetry; Relativistic Theory; Nuclear Structure; Nucleon-Nucleon Scattering

20020003427 Los Alamos National Lab., NM USA
Progress on the 140 KV, 10 megawatt peak, 1 metawatt average polyphase quasi-resonant boost converter for the Spallation Neutron Source (SNS) Klystron power System
Reass, W.; Aug. 01, 2000; 6p; In English
Report No.(s): DE2001-768817; LA-UR-00-3748; No Copyright; Avail: Department of Energy Information Bridge
This paper describes electrical design and operational characteristics of a zero-voltage-switching 20 kHz polyphase bridge, boost converter/modulator for klystron pulse application. The DC-DC (direct current) converter derives the buss voltages from a standard 13.8 kV to 2300 Y substation cast-core transformer. Energy storage and filtering is provided by self-clearing metallized hazy polypropylene traction capacitors. Three H-Bridge IGBT (insulated gate bipolar transistor) switching networks are used to generate the polyphase 20 kHz transformer's primary drive waveforms. The 20 kHz drive waveforms are chirped the appropriate duration to generate the desired klystron pulse width. PWM (pulse width modulation) of the individual 20 kHz pulses is utilized to provide regulated output waveforms with adaptive feedforward and feedback techniques. The boost transformer design utilizes amorphous nanocrystalline material that provides the required low core loss at design flux levels and switching frequencies. Resonant shut peaking is used on the transformer secondary to boost output voltage and resonate transformer leakage inductance. With the appropriate transformer leakage inductance and peaking capacitance, zero-voltage-switching of the IGBTs is attained, minimizing switching losses. A review of these design parameters and a comparison of computer calculations, scale model, and first article results will be performed.
NTIS
Klystrons; Neutron Sources; Spallation; Voltage Converters (DC to DC)

20020003428 Los Alamos National Lab., NM USA
Beam emittance measurements for the Low-Energy Demonstration Accelerator (LEDA) Radio-Frequency Quadrupole (RFQ)
Schulze, M.; Aug. 01, 2000; 6p; In English
Report No.(s): DE2001-768820; LA-UR-00-3749; No Copyright; Avail: Department of Energy Information Bridge
The Low-Energy Demonstration Accelerator (LEDA) radio-frequency quadrupole (RFQ) is a 100% duty factor (CW) linac that delivers greater than 100 mA of H(+) beam at 6.7 MeV. The 8-m-long, 350 MHz RFQ structure accelerates a dc (direct current), 75-ekV, 110-mA H(+) beam from the LEDA injector with greater than 90% transmission. LEDA consists of a 75-keV proton injector, 6.7-MeV, 350 MHz CW RFQ with associated high-power and low-level rf (radio frequency) systems, a short high-energy beam transport (HEBT) and high-power (670-kW CW) beam stop. The beam emittance is inferred from wire scanner measurements of the beam profile at a single location in the HEBT. The beam profile is measured as a function of the magnetic field gradient in one of the HEBT quadrupoles. As the gradient is changed the spot size passes through a transverse waist. Measurements are presented for peak currents between 25 and 100 mA.
NTIS
Linear Accelerators; Hydrogen Ions; Quadrupoles; Beams (Radiation)

20020003431 Los Alamos National Lab., NM USA
Design and high-heat flux testing of an interceptive-diagnostic device for a proton beam
Valdiviez, R.; Dec. 01, 2000; 8p; In English
Report No.(s): DE2001-768858; LA-UR-00-5785; No Copyright; Avail: Department of Energy Information Bridge
The design and high-heat flux testing of an interceptive-diagnostic device that will be used to probe an intense-proton beam is described in this paper. An intense-proton beam is produced in a Radio Frequency Quadrupole (RFQ) accelerator and injected into a magnetically Focusing-Defocusing (FODO) lattice in order to study the formation of beam halo. Due to the nature of making beam halo formation measurements in a proton beam it becomes necessary to insert an interceptive device near the center of the

beam. The interceptive device used to probe the beam is referred to here as a scraper. The peak heat flux experienced by the scraper is on the order of 610 kW/sq cm. The scraper consists of a copper base that is water cooled, with a piece of graphite joined to it.
NTIS
Systems Engineering; Proton Beams; Heat Flux; Measuring Instruments

20020003573 Los Alamos National Lab., NM USA
Beam positions-phase monitors for SNS Linac
Kurennoy, S.; Aug. 01, 2000; 6p; In English
Report No.(s): DE2001-768811; LA-UR-00-3825; No Copyright; Avail: Department of Energy Information Bridge

Electromagnetic modeling with MAFIA of the combined beam position-phase monitors (BPPMs) for the Spallation Neutron Source (SNS) linac has been performed. Time-domain 3-D (three dimensional) simulations are used to compute signal amplitudes and phases on the BPPM electrodes provides a good way to measure accurately the beam phase. While for an off-axis beam the signal phases on the individual electrodes can differ from those for a centered beam by a few degrees, the phase of the summed signal is found to be independent of the beam transverse position inside the device. Based on the analysis results, an optimal BPPM design with four one-end-shorted 60-degree electrodes has been chosen. It provides a good linearity and sufficient signal power for both position and phase measurements, while satisfying the linac geometrical constraints and mechanical requirements.
NTIS
Linear Accelerators; Monitors; Beams (Radiation); Neutron Sources

20020003730 Lawrence Livermore National Lab., Livermore, CA USA
Moment Equation Approach to a Muon Collider Cooling Lattice
Celata, C. M.; Sessler, A. M.; Lee, P. B.; Shadwick, B. A.; Wurtele, J. S.; Jun. 01, 1998; 7p; In English
Report No.(s): DE2001-6421; LBNL-42088; No Copyright; Avail: Department of Energy Information Bridge

Equations are derived which describe the evolution of the second order moments of the beam distribution function in the ionization cooling section of a muon collider. Ionization energy loss, multiple scattering, and magnetic fields have been included, but forces are linearized. A computer code using the equations agrees well with tracking calculations. The code is extremely fast, and can be used for preliminary design, where such issues as beam halo, which must be explored using a tracking code, are not the focus.
NTIS
Method of Moments; Muons; Linear Accelerators; Computer Aided Design; Cooling; Computer Programs

20020003735 Lawrence Livermore National Lab., Livermore, CA USA
Elastic wave propagation and attenuation in a double-porosity dual-permeability medium
Berryman, J. G.; Wang, H. F.; Oct. 12, 1998; 27p; In English
Report No.(s): DE2001-2875; UCRL-JC-132136; KC0403010; No Copyright; Avail: Department of Energy Information Bridge

To account for large-volume low-permeability storage porosity and low-volume high-permeability fracture/crack porosity in oil and gas reservoirs, phenomenological equations for the poroelastic behavior of a double porosity medium have been formulated and the coefficients in these linear equations identified. The generalization from a single porosity model increases the number of independent inertial coefficients from three to six, the number of independent drag coefficients from three to six, and the number of independent stress-strain coefficients from three to six for an isotropic applied stress and assumed isotropy of the medium. The analysis leading to physical interpretations of the inertial and drag coefficients is relatively straightforward, whereas that for the stress-strain coefficients is more tedious. In a quasistatic analysis, the physical interpretations are based upon considerations of extremes in both spatial and temporal scales. The limit of very short times is the one most relevant for wave propagation, and in this case both matrix porosity and fractures are expected to behave in an undrained fashion, although our analysis makes no assumptions in this regard. For the very long times more relevant for reservoir drawdown, the double porosity medium behaves as an equivalent single porosity medium. At the macroscopic spatial level, the pertinent parameters (such as the total compressibility) may be determined by appropriate field tests. At the mesoscopic scale pertinent parameters of the rock matrix can be determined directly through laboratory measurements on core, and the compressibility can be measured for a single fracture. We show explicitly how to generalize the quasistatic results to incorporate wave propagation effects and how effects that are usually attributed to squirt flow under partially saturated conditions can be explained alternatively in terms of the double-porosity model.
NTIS
Wave Propagation; Elastic Waves; Wave Attenuation

20020003936 Los Alamos National Lab., NM USA

Determining phase-space properties of the leda rfq output beam

Lysenko, W.; Aug. 01, 2000; 6p; In English

Report No.(s): DE2001-768770; LA-UR-00-3882; No Copyright; Avail: Department of Energy Information Bridge, Microfiche

Quadruple scans were used to characterize the LEDA RFQ beam. Experimental data were fit to computer simulation models for the rms beam size. The codes were found to be inadequate in accurately reproducing details of the wire scanner data. When this discrepancy is resolved, we plan to fit using all the data in wire scanner profiles, not just the rms value.

NTIS

Accelerators; Proton Beams; Quadrupoles; Mean Square Values; Root-Mean-Square Errors

20020003989 Abilene Christian Univ., TX USA

Measurements of observables in the pion-nucleon system, nuclear A-dependence of heavy quark production and rare decays of D and B mesons ***Progress Report, 15 Feb. - 30 Dec. 1993***

Sadler, M. E.; Isenhower, L. D.; Dec. 30, 1993; 82p; In English

Report No.(s): DE2001-763080; DE-FG05-88ER40451-NOS-1-6; No Copyright; Avail: Department of Energy Information Bridge, Microfiche

This report summarizes the progress by the ACU particle physics research group under grant number DE-FG05-88ER40451 from the U.S. Department of Energy. The period covered is from the date of renewal (15 May 1991) to 20 December 1993 with emphasis on the progress since the last report on 15 February 1993. Laboratories where experiments (or their preparation) have been conducted during this period are the Clinton P. Anderson Meson Physics Facility at Los Alamos (LAMPF), Fermilab, the Petersburg Nuclear Physics Institute (PNPI), the Brookhaven AGS and CEBAF.

NTIS

Pions; Nucleons; Measure and Integration; Quarks; Particle Production

20020003993 Brookhaven National Lab., Upton, NY USA

QCDOC: A 10-teraflops scale computer for lattice QCD

Chen, D.; Christ, N. H.; Cristian, C.; Dong, Z.; Gara, A.; Aug. 17, 2000; 8p; In English

Report No.(s): DE2001-773954; BNL-67856; KB0201; No Copyright; Avail: Department of Energy Information Bridge, Microfiche

The numerical evaluation of Euclidean-space Feynman path integrals provides a unique and powerful tool to study non-perturbative phenomena in quantum field theory. These techniques permit both qualitative and quantitative study of low-energy hadronic physics through first-principles, Quantum Chromodynamics calculations. These methods also hold the promise of revealing new non-perturbative phenomena that may be present in other quantum field theories that are potential candidates for the theory beyond the standard model.

NTIS

Quantum Chromodynamics; Computers

20020003996 Federal Energy Technology Center, Morgantown, WV USA

Fiber optic/cone penetrometer system for subsurface heavy metal detection

Saggese, S.; Sep. 30, 1999; 214p; In English

Contract(s)/Grant(s): AC21-95MC32089

Report No.(s): DE2001-773809; DE-AC21-95MC32089-01; No Copyright; Avail: Department of Energy Information Bridge, Microfiche

Science and Engineering Associates (SEA) developed a prototype subsurface soil characterization tool for the evaluation of heavy metals. The system, based on Laser-Induced Breakdown Spectroscopy (LIBS), is deployed using a cone penetrometer. The LIBS system consists of a laser source to produce the plasma, a novel hollow waveguide method of delivering the laser source to the subsurface, a small penetrometer probe for focusing the laser light to create a spark and return the light emission for analysis, a spectrometer to spectrally resolve the emission spectrum, an array detector for simultaneous measurements of emission intensities over a range of wavelengths and a computer to conduct equipment control, data acquisition, and data analysis. Under this two phase effort, the system was designed, fabricated and tested, culminating in a successful field demonstration at the DOE Sandia Chemical Waste Landfill for the evaluation of chromium contamination. During this CPT/LIBS test, six penetrations were conducted and the data obtained with the system was used to generate graphs depicting the concentration of chromium as a function of depth to approximately 15 feet, with a range of concentrations from background (approx. 30 ppm) to about 1200 ppm. In addition, prototype LIBS instruments, developed by DOE LANL personnel, were successfully field deployed by SEA at a

Formerly Utilized Remedial Action Plan (FUSRAP) site for the detection of beryllium. This 6 week field effort generated a high density surface contour plot of the beryllium concentration over a 40 acre site. Utilizing both van-mounted and backpack systems, SEA evaluated 1664 samples at the site. This was the first full scale field deployment of the portable LIBS instruments and the beryllium concentration data was used successfully for real-time decision-making during the site characterization and for the development of additional plans for subsurface analysis.
NTIS
Heavy Metals; Laser-Induced Breakdown Spectroscopy; Penetrometers; Fiber Optics

20020004004 Los Alamos National Lab., NM USA
LEDA beam diagnostics instrumentation: Measurement comparisons and operational experience
Gilpatrick, J.; May 01, 2000; 11p; In English
Report No.(s): DE2001-768993; LA-UR-00-2316; No Copyright; Avail: Department of Energy Information Bridge

The Low Energy Demonstration Accelerator (LEDA) facility has been used to characterize the pulsed- and cw-beam performance of a 6.7-MeV, 100-mAradio frequency quadruple (RFQ). Diagnostic instrumentation, primarily located in a short beam transport downstream of the RFQ, allow facility commissioners and operators to measure and monitor the RFQ's accelerated and total beam transmission, beam loss, bunched beam current beam energy and output phase, and beam position. Transverse beam profile measurements are acquired under both low and high duty-factor pulsed beam conditions using a slow wire scanner and a camera that images beam-induced fluorescence. The wire scanner is also used to acquire transverse beam emittance information using a technique known as a 'quad scan'. This paper reviews the measurement performance and discusses the resulting data.
NTIS
Beams (Radiation); Accelerators; Continuous Radiation; Diagnosis

20020004008 Los Alamos National Lab., NM USA
Slow wire scanner beam profile measurement for LEDA
O'Hara, J.; May 01, 2000; 11p; In English
Report No.(s): DE2001-768989; LA-UR-00-2362; No Copyright; Avail: Department of Energy Information Bridge

The Low Energy Demonstration Accelerator (LEDA), located at Los Alamos National Laboratory, utilizes a slow wire scanner to measure beam profiles. The beam energy is 6.7 MeV and the peak current is 100 mA. This wire scanner profile measurement is located in the High Energy Beam Transport (HEBT) section of the LEDA beam line. This section of beam line is used to expand the proton beam coming out of the LEDA Radio Frequency Quadruple (RFQ) prior to impacting the beam-stop. The purpose of the scanner is to provide horizontal and vertical beam profiles. The wires or fibers are a Silicon Carbide (SiC) material, and are attached to an actuator driven by a stepping motor. The actuator drives the fibers through the beam in incremental steps. At each step, the amount of secondary electrons generated by the interactions of the proton beam and the wire are measured. From these incremental measurements the beam profile is constructed. This paper will discuss the operation of the scanner, two of the experiments conducted to understand the capability of the SiC wire to survive and some of the different uses of the beam profile data acquired during the ongoing commissioning of LEDA.
NTIS
Proton Beams; Accelerators; Scanners; Beams (Radiation)

20020004009 Los Alamos National Lab., NM USA
LEDA beam diagnostics instrumentation: Beam current measurement
Barr, D.; May 01, 2000; 11p; In English
Report No.(s): DE2001-768988; LA-UR-00-2360; No Copyright; Avail: Department of Energy Information Bridge

The Low Energy Demonstration Accelerator (LEDA) facility located at Los Alamos National Laboratory (LANL) accelerates protons to an energy of 6.7-MeV and current of 100- mA operating in either a pulsed or cw mode. Two types of current measurements are used. The first is an AC or pulsed-current measurement which uses three LANL built toroids. They are placed in the beamline in such a way as to measure important transmission parameters and act as a differential current-loss machine protection system. The second system is a DC current measurement used to measure cw beam characteristics and uses toroids from Bergoz Inc. There are two of these systems, so they can also be used for transmission measurements. The AC system uses custom processing electronics whereas the DC system uses a modified Bergoz electronics system. Both systems feature data acquisition via a series of custom TMS320C40 Digital Signal Processing (DSP) boards. of special interest to this paper is the operation of these systems, the calibration technique, the differential current loss measurements and fast-protection processing, current droop

characteristics for the AC system, and existing system noise levels. This paper will also cover the DSP system operations and their interaction with the main accelerator control system.
NTIS
Beam Currents; Continuous Radiation; Accelerators; Data Acquisition; Diagnosis; Signal Processing

20020004010 Los Alamos National Lab., NM USA
Physics models and nuclear data evaluations for enhanced monte-carlo transport
Chadwick, M.; Aug. 01, 2000; 9p; In English
Report No.(s): DE2001-768910; LA-UR-00-3601; No Copyright; Avail: Department of Energy Information Bridge, Microfiche
We describe recent evaluations of neutron and proton interaction cross sections up to 150 MeV in the LA150 Data Library, for use in MCNPX computer code simulations of accelerator-driven systems (ADS). An overview is provided of the nuclear theory used. A number of benchmark comparisons against experiments are described, for thin and thick-target neutron production, neutron transmission through macroscopic slabs, and neutron heating and damage. Future data needs for waste transmutation are also briefly described.
NTIS
Radiation Transport; Monte Carlo Method; Libraries; Particle Accelerators; Nuclear Physics

20020004011 Los Alamos National Lab., NM USA
Study of residual nuclide yields from 1.0, 2.0, and 2.6 GeV protons irradiated thin NAT Hg targets
Tiarenko, Y.; Aug. 01, 2000; 12p; In English
Report No.(s): DE2001-768909; LA-UR-00-3600; No Copyright; Avail: Department of Energy Information Bridge, Microfiche
The direct y-spectrometry method is used to measure more than 350 residual product nuclide yields from 0.1, 0.2, 0.8, and 2.6 GeV proton irradiated (nat)HgO targets. The y-spectrometer resolution is 1.8 keV in 1332 keV y-line. The resultant y-spectra are processed by GENIE2000 code. The y-1ines are identified, and the cross-sections calculated, by the ITEP (Institute for Theoretical and Experimental Physics)-designed SIGMA code using the PCNUDAT radioactive database. The 27-Al(p,x)22-Na reaction is used as monitor. The experimental results are compared with the yields simulated by the I-IETC, LAHET, INUCL, CEM95, CASCADE, and YIELDX codes that simulate hadron-nucleus interactions.
NTIS
Irradiation; Targets; Nuclides; Protons

20020004012 Los Alamos National Lab., NM USA
Threshold reaction rates inside and on the surface of thick W-NA target irradiated with 0.8 GeV protons
Tiarenko, Y.; Aug. 01, 2000; 9p; In English
Report No.(s): DE2001-768908; LA-UR-00-3599; No Copyright; Avail: Department of Energy Information Bridge, Microfiche
The preliminary results are presented of the experimental determination of threshold reaction rates in experimental samples made of Al, Co, Bi, In, Au et al. placed both inside and on the surface of extended thick W-Na target irradiated with 0.8 GeV protons. The target consists of 26 alternating discs each 150 mm in diameter: six tungsten discs are 20 mm thick, seven tungsten discs are 40 mm thick, and 13 sodium discs are 40 mm thick. The relative position of discs is matched with the aim of flattening the neutron field along the target surface. The comparison is made of the measured rates with results of their simulation using LAHET and KASKAD-S codes, and ENDF/B6, MENDL2, MENDL2P, SADKO-2, and ABBN-93 databases. The results are of interest both in terms of integral data collection and demonstrating the up-to-the-date predictive power of codes applied in designing hybrid (ADS) (Accelerator-Driven System) systems that use tungsten targets cooled with sodium.
NTIS
Irradiation; Protons; Reaction Kinetics; Tungsten; Sodium

20020004013 Los Alamos National Lab., NM USA
Spectral measurements of Pb, W, and NA targets irradiated by 0.8 and 1.6 GeV protons
Tiarenko, Y.; Aug. 01, 2000; 11p; In English
Report No.(s): DE2001-768907; LA-UR-00-3598; No Copyright; Avail: Department of Energy Information Bridge, Microfiche
The preliminary results of the spectra measurements of neutrons generated in W and Na targets irradiated by 0.8 and 1.6 GeV protons are presented. Measurements have been carried out using the proton beam extracted from ITEP (Institute for Theoretical and Experimental Physics) synchrotrons and the TOF (time of flight) technique. Neutron registration has been carried out using BICRON MAB511 liquid scintillation counters. Spectra measured at angles of 30DG, 60DG, 90DG, 120DG and 150DG have been correlated with the results of their simulation using the LAHET code system. The results are of interest both from data

gathering viewpoint and as a demonstration of up-to-the-date predictive power of codes applied in the design of hybrid Accelerator Driven Systems (ADS) using lead or lead-bismuth targets, and sodium-cooled targets.
NTIS
Irradiation; Neutrons; Spectrum Analysis

20020004195 Los Alamos National Lab., NM USA
Hydrogen and helium gas formation and their release kinetics in tungsten rods after irradiation with 800 MeV protons
Oliver, B.; May 01, 2000; 14p; In English
Report No.(s): DE2001-768995; LA-UR-00-2314; No Copyright; Avail: Department of Energy Information Bridge

en the Accelerator Production of Tritium Program, thermalized neutrons produced from multiplication and moderation of spallation neutrons will be absorbed in He gas to produce tritium. The spallation neutrons will be generated by the interaction of high energy (1 GeV) protons with solid tungsten rods. An unavoidable byproduct of the spallation reactions will be large amounts of helium and hydrogen gas generated in the rods. The release kinetics of these gases during various proposed off-normal scenarios involving loss of coolant and after-heat induced rises in temperature is of particular interest. In addition, the magnitude of the gas generation cross sections and the fractional retention of these gases is necessary for extrapolation to higher exposures. Tungsten rod specimens irradiated with 800 MeV protons in the Los Alamos Neutron Science Center to rather high exposures have been sectioned to produce small specimens suitable for measurement of both helium and hydrogen. Hydrogen evolution was measured both by dropping the specimen into a small ceramic crucible at 1200C and also by subjecting the specimen to a simulated temperature ramp from -200 to 1200C. The latter technique showed four distinct hydrogen release peaks at temperatures of approximately 500, 800, 1000 and 1200C, indicating a variety of trapping sites with different binding energies. Helium release and total content were measured by subjecting the specimens to a similar temperature excursion, followed later by melting to release the remaining helium. Approximately 99% of the helium was retained until melting occurred. For both gases, release measurements were conducted using mass spectrometric techniques.
NTIS
Irradiation; Helium; Hydrogen; Gas Evolution; Tungsten; Protons; Ceramics; Rods

20020004914 Thomas Jefferson National Accelerator Facility, Newport News, VA USA
Nuclear Structure in the Resonance Region
Burkert, V.; Jul. 01, 2001; 13p; In English
Report No.(s): DE2001-785456; JLAB-PHY-01-21; DOE/ER/40150-1899; No Copyright; Avail: Department of Energy Information Bridge, Microfiche

I discuss recent results from Jefferson Lab of inclusive and exclusive electroproduction experiments at Jefferson Lab. They include measurements of the spin response for protons and neutrons in the resonance region, exclusive single pion and multiple pion production to measure resonance transition multipoles, and searches for missing quark model states. A brief outlook to the new domain of Generalized Parton Distribution is given as well.
NTIS
Nuclear Physics; Neutrons; Nuclear Structure; Protons; Spin Resonance

20020005089 Argonne National Lab., IL USA
Water-cooled x-ray monochromator for using off-axis undulator beam
Khounsary, A.; Maser, J.; Dec. 11, 2000; 19p; In English
Report No.(s): DE2001-772129; ANL/UPD/CP-103623; No Copyright; Avail: Department of Energy Information Bridge, Microfiche

Undulator beamlines at third-generation synchrotrons x-ray sources are designed to use the high-brilliance radiation that is contained in the central cone of the generated x-ray beams. The rest of the x-ray beam is often unused. Moreover, in some cases, such as in the zone-plate-based microfocusing beamlines, only a small part of the central radiation cone around the optical axis is used. In this paper, a side-station branch line at the Advanced Photon Source that takes advantage of some of the unused off-axis photons in a microfocusing x-ray beamline is described. Detailed information on the design and analysis of a high-heat-load water-cooled monochromator developed for this beamline is provided.
NTIS
Monochromators; Loads (Forces); Synchrotrons; X Ray Sources; Liquid Cooling

20020005098 Brookhaven National Lab., Upton, NY USA

Muon polarization in a front-end channel of a neutrino factory

Fukui,; Fernow,; Gallardo,; Jun. 18, 2001; 6p; In English

Report No.(s): DE2001-785371; BNL-68564; No Copyright; Avail: Department of Energy Information Bridge, Microfiche

As one of the figures of merit, muon polarization and its correlation to the particle arrival time was studied for the high intensity muon beam source of a Neutrino Factory. Muon polarization, 100% polarized in the parent pion rest system, was tracked down the pion capture, phase rotation, and ionization cooling channels, using the BMT equation. A study was done of the dependence of the muon polarization and its correlation on the configuration of induction linac channels in the phase rotation channel. Depolarization effects of the muon polarization through absorbers in the ionization cooling channel was simulated.

NTIS

Muons; Polarization; Neutrinos; Linear Accelerators; Cooling

20020005099 Brookhaven National Lab., Upton, NY USA

Analytic properties of the longitudinal beam transfer function

Towne,; Jun. 18, 2001; 5p; In English

Report No.(s): DE2001-785374; BNL-68589; No Copyright; Avail: Department of Energy Information Bridge, Microfiche

The frequency dependence of the longitudinal beam transfer function (BTF) in a storage ring, when expressed in a basis of azimuthal harmonics of the line density, is the Fourier transform of a causal function that depends on the radio-frequency potential well in which the bunch moves. The effect of all synchrotron harmonics are included in this function, which is derived from Krinsky and Wang's expression for the BTF expressed in the same basis (S. Krinsky and J.-M. Wang, Part. Accel. 17, 109-139 (1985)). Analytic properties of the terms of the TF expressed in a series of synchrotron harmonics, which are approximately Shaposhnikova's BTF matrix elements (E. Shaposhnikova, CERN Report No. SL-94-19-RF (1994)), are studied through the large-argument asymptotics of corresponding causal functions.

NTIS

Storage Rings (Particle Accelerators); Radio Frequencies; Azimuth; Transfer Functions

20020005100 Argonne National Lab., IL USA

Argonne Wakefield Accelerator facility upgrade

Conde, M. E.; Gai, W.; Konecny, R.; Power, J. G.; Schoessow, P.; Jul. 11, 2001; 3p; In English

Report No.(s): DE2001-785375; ANL-HEP-CP-01-58; No Copyright; Avail: Department of Energy Information Bridge, Microfiche

The Argonne Wakefield Accelerator has been successfully used for conducting wakefield experiments were successful, higher drive beam quality would substantially improve the wakefield accelerating gradients. For this reason we have built a new 1-1/2 cell L-band photocathode RF gun. This gun is expected to produce 10-100 nC bunches with 2-5 ps rms pulse length and normalized emittance less than 100 mm mrad. The gun will initially have a copper photocathode, which will soon be replaced by a high quantum efficiency cesium telluride one, allowing the generation of a train of high charge bunches. The beam energy at the exit of the gun cavity will be in the range 7.5-10 MeV. A standing-wave linac structure operating at the same frequency (1.3 GHz) will increase the beam energy to about 15 MeV. This beam will be used in high-gradient wakefield acceleration experiments and other high intensity electron beam applications. Travelling-wave dielectric loaded structures, operating at 7.8 and 15.6 GHz, will be excited by the propagation of single bunches or by trains of up to 32 electron bunches, reaching gradients in excess of 100 MV/m over distances of the order of 1 meter.

NTIS

Linear Accelerators; Electron Beams; High Acceleration; Traveling Waves

20020005101 Argonne National Lab., IL USA

Thermoelastic response of suddenly heated liquid targets in high-power colliders

Hassanein, A.; Konkashbaev, I.; Norem, J.; Aug. 08, 2001; 3p; In English

Report No.(s): DE2001-785376; ANL-HEP-CP-01-70; No Copyright; Avail: Department of Energy Information Bridge, Microfiche

Thermoelastic response of liquid metal targets exposed to high-volumetric-energy deposition in times shorter than the target hydrodynamic response time (i.e., sound travel time) is of interest to several research areas, including targets for high-power accelerators such as the Spallation Neutron Source, muon collider targets, etc. Sudden energy deposition causes shock and rarefaction waves of magnitude + or - (delta)P that corresponds to an initial thermal pressure of tens of katm. Nevertheless a liquid

subjected to a negative pressure is metastable. The problem of liquid target oscillations in the presence of large negative pressure, and the mechanism of fragmentation and its consequences, are considered in this paper.
NTIS
Thermoelasticity; Metastable State; Shock Waves; Neutron Sources

20020005102 Argonne National Lab., IL USA
Analysis of low energy AGS polarimeter data and potential consequences for RHIC spin physics
Cadman, R.; Krueger, K.; Spinka, H.; Underwood, D.; Yokosawa, A.; Jun. 22, 2001; 24p; In English
Report No.(s): DE2001-785377; ANL-HEP-TR-01-36; No Copyright; Avail: Department of Energy Information Bridge, Microfiche

The small asymmetries measured at G (gamma)=7.5 during the RHIC spin commissioning were a serious concern. In earlier runs, asymmetries double those from the spin commissioning time (September 2000) had sometimes been observed, and there had been few changes to the AGS polarimeter hardware or operating conditions. Recently, the observed changes in the asymmetries measured at G (gamma)=7.5 have been ascribed to contamination of the carbon target asymmetry with that from the fishline target and vice-versa, because of the sizeable beam spot size compared to the separation of the targets. This note addresses this hypothesis using the observed asymmetries. This problem could directly impact the spin physics of RHIC.
NTIS
Asymmetry; Polarimeters; Contamination

20020005108 Brookhaven National Lab., Upton, NY USA
Ultrashort electron bunch length measurements at duvfel
Graves,; Carr,; Dimauro,; Doyuran,; Heese,; Jun. 18, 2001; 5p; In English
Report No.(s): DE2001-786071; BNL-68552; No Copyright; Avail: Department of Energy Information Bridge, Microfiche

The DUVFEL electron linac is designed to produce sub-picosecond, high brightness electron bunches for driving a short wavelength FEL. Four experiments have been commissioned to address the challenge of accurately measuring bunch lengths on this timescale. In the frequency domain, a short 12 period undulator is used to produce both off-axis coherent emission and on-axis incoherent single-shot spectra. The total coherent infrared power scale inversely with bunch length and the spectral cutoff is an indication of bunch length. The density of power spikes in the single-shot visible spectrum may also be used to estimate bunch length. In the time domain, the linac accelerating sections and a bending magnet are used to implement the RF-zero phasing method, and a sub-picosecond streak camera is also installed. Beam measurements and comparisons of these methods are reported.
NTIS
Electron Beams; Linear Accelerators; Free Electron Lasers; Electron Bunching

20020005109 Brookhaven National Lab., Upton, NY USA
Measured properties of the duvfel high brightness, ultrashort electron beam
Graves,; Carr,; Dimauro,; Doyuran,; Heese,; Jun. 18, 2001; 5p; In English
Report No.(s): DE2001-786072; BNL-68553; No Copyright; Avail: Department of Energy Information Bridge, Microfiche

The DUVFEL electron linac is designed to produce sub-picosecond, high brightness electron bunches to drive an ultraviolet FEL. The accelerator consists of a 1.6 cell S-band photoinjector, variable pulse length Ti:Sapp laser, 4 SLAC-type S-band accelerating sections, and 4-dipole chicane bunch compressor. In preparation for FEL operation, the compressed electron beam has been fully characterized. Measurement of the beam parameters and simulation of the beam are presented.
NTIS
Electron Beams; Electron Bunching; Linear Accelerators; Compressors

20020005138 Los Alamos National Lab., NM USA
Hybrid baryon signatures
Page, P.; Apr. 01, 2000; 11p; In English
Report No.(s): DE2001-768976; LA-UR-00-2054; No Copyright; Avail: Department of Energy Information Bridge

The authors discuss whether a low-lying hybrid baryon should be defined as a three quark-gluon bound state or as three quarks moving on an excited adiabatic potential. We show that the latter definition becomes exact, not only for very heavy quarks, but also for specific dynamics. We review the literature on the signatures of hybrid baryons, with specific reference to strong hadronic decays, electromagnetic couplings, diffractive production and production in (psi) decay.
NTIS
Baryons; Quarks; Particle Decay

20020005189 Los Alamos National Lab., NM USA
Spallation Neutron Source (SNS) Linac RF System
Lynch, M.; Aug. 01, 2000; 7p; In English
Report No.(s): DE2001-768915; LA-UR-00-3575; No Copyright; Avail: Department of Energy Information Bridge
No abstract prepared.
NTIS
Linear Accelerators; Spallation

20020005190 Los Alamos National Lab., NM USA
Collector failures on 350 MHz, 1.2 MW CW klystrons at the Los Energy Demonstration Accelerator (LEDA)
Rees, D.; Roybal, W.; Bradley, J.; Aug. 01, 2000; 6p; In English
Report No.(s): DE2001-768916; LA-UR-00-3574; No Copyright; Avail: Department of Energy Information Bridge
We are currently operating the front end of the accelerator production of tritium (APT) accelerator, a 7 MeV radio frequency quadrupole (RFQ) using three, 1.2 MW CW klystrons. These klystrons are required and designed to dissipate the full beam power in the collector. The klystrons have less than 1500 operational hours. One collector has failed and all collectors are damaged. This paper will discuss the damage and the difficulties in diagnosing the cause. The collector did not critically fail. Tube operation was still possible and the klystron operated up to 70% of full beam power with excellent vacuum. The indication that finally led us to the collector failure was variable emission. This information will be discussed. A hydrophonic system was implemented to diagnose collector heating. The collectors are designed to allow for mixed-phase cooling and with the hydrophonic test equipment we are able to observe: normal, single-phase cooling, mixed-phase cooling, and a hard boil. These data will be presented. The worst case beam profile from a collector heating standpoint is presented. The paper will also discuss the steps taken to halt the collector damage on the remaining 350 MHz klystrons and design changes that are being implemented to correct the problem.
NTIS
Accumulators; Klystrons; Damage; Failure

20020005196 Los Alamos National Lab., NM USA
Experience with beam loss monitors in the low energy demonstration accelerator
Sellyey, W.; 2000; 11p; In English
Report No.(s): DE2001-768986; LA-UR-00-2355; No Copyright; Avail: Department of Energy Information Bridge
This paper will discuss the operational experience with the Ionization Chamber Beam Loss Monitors (ICBLM) in the Low Energy Demonstration Accelerator facility at LANL. LEDA is a test bed for a 6.7-MeV, CW, 100-mA proton radio frequency quadruple (RFQ). There are three ICBLM'S located in a short beam transport downstream of the RFQ. (This transport is called HEBT for High Energy Beam Transport.) Their function is to convey beam loss information to the operators and to protect the accelerator from being damaged by large beam spills. Signals from the ionization chambers are ten times less than expected. This results in a signal to drift ratio of 0.4 for a 1 ma beam loss and prevents protection of the machine below 2.5 ma loss. Since it is important to protect the machine down to 0.2 ma loss, improvements in and alternatives to the ICBLM are being investigated and will be implemented.
NTIS
Ionization Chambers; Beams (Radiation); Losses; Monitors

20020005220 California Univ., Lawrence Berkeley Lab., Berkeley, CA USA
Post-growth thermal treatment of the InAs/GaAs quantum dots
Jasinski, J.; Babinski, A.; Bozek, R.; Baranowski, J. M.; Nov. 22, 2000; 4p; In English
Report No.(s): DE2001-771942; LBNL-46982; No Copyright; Avail: Department of Energy Information Bridge
The effect of post-growth thermal treatment of the InAs/GaAs quantum dots is investigated in this work. The photoluminescence (PL) and transmission electron microscopy (TEM) studies of samples annealed at temperatures up to 950 degrees C are presented. A complete dissolution of QDs and substantial broadening of the wetting layer (WL) can be seen from TEM. We propose that the thermally induced modification of the WL rather than QDs can be responsible for a blue-shift and narrowing of PL peaks in structures containing InAs/GaAs QDs.
NTIS
Transmission Electron Microscopy; Temperature Effects; Indium Arsenides; Gallium Arsenides

20020005232 Brookhaven National Lab., Upton, NY USA

Intense muon beams and neutrino factories

Parsa, Z.; Oct. 05, 2000; 13p; In English

Report No.(s): DE2001-772450; BNL-67823; KA04; No Copyright; Avail: Department of Energy Information Bridge, Microfiche

High intensity muon sources are needed in exploring neutrino factories, lepton flavor violating muon processes, and lower energy experiments as the stepping phase towards building higher energy (mu)(sup +)(mu)(sup (minus)) colliders. We present a brief overview, sketch of a neutrino source, and an example of a muon storage ring at BNL (Brookhaven National Laboratory) with detector(s) at Fermilab, Sudan, etc. Physics with low energy neutrino beams based on muon storage rings ((mu)SR) and conventional Horn Facilities are described and compared. CP (charge parity) violation Asymmetries and a new Statistical Figure of Merit to be used for comparison is given. Improvements in the sensitivity of low energy experiments to study Flavor changing neutral currents are also included.

NTIS

Neutrinos; Muons; Neutrino Beams

20020005233 Brookhaven National Lab., Upton, NY USA

Energy recovery electron linac-on-ring collider

Merminga, L.; Krafft, G. A.; Lebedev, V. A.; Ben-Zvi, I.; Sep. 14, 2000; 27p; In English

Report No.(s): DE2001-772452; BNL-67849; KA0403000; No Copyright; Avail: Department of Energy Information Bridge, Microfiche

We present the design of high-luminosity electron-proton/ion colliders in which the electrons are produced by an Energy Recovering Linac (ERL). Electron-proton/ion colliders with center of mass energies between 14 GeV and 100 GeV (protons) or 63 GeV/A (ions) and luminosities at the 10(sup 33)(per nucleon) level have been proposed recently as a means for studying hadronic structure. The linac-on-ring option presents significant advantages with respect to: (1) spin manipulations (2) reduction of the synchrotron radiation load in the detectors (3) a wide range of continuous energy variability. Rf power and beam dump considerations require that the electron linac recover the beam energy. Based on extrapolations from actual measurements and calculations, energy recovery is expected to be feasible at currents of a few hundred mA and multi-GeV energies. Luminosity projections for the linac-ring scenario based on fundamental limitations are presented. The feasibility of an energy recovery electron linac-on-proton ring collider is investigated and four conceptual point designs are shown corresponding to electron to proton energies of: 3 GeV on 15 GeV, 5 GeV on 50 GeV and 10 GeV on 250 GeV, and for gold ions with 100 GeV/A. The last two designs assume that the protons or ions are stored in the existing RHIC (Relativistic Heavy Ion Collider) accelerator. Accelerator physics issues relevant to proton rings and energy recovery linacs are discussed and a list of required R (research) and D (development) for the realization of such a design is presented.

NTIS

Linear Accelerators; Electron Energy; Particle Collisions

20020005234 Oak Ridge National Lab., TN USA

Vacancy Clusters at Nanoparticle Surfaces

Xu, J.; Moxom, J.; Somieski, B.; White, C. W.; Mills, A. P.; Aug. 06, 2000; 3p; In English

Report No.(s): DE2001-772460; P00-108484; No Copyright; Avail: Department of Energy Information Bridge, Microfiche

The authors detect vacancy clusters at Au nanoparticle surfaces using a combination of positron lifetime spectroscopy, 1-detector, and 2-detector measurements of Doppler broadening of annihilation radiation. Gold nanoparticles are formed by MeV implantation of gold ions into MgO (100) followed by annealing. Clusters of two Mg and two O vacancies (v(sub 4)) are attached to the gold nanoparticle surfaces within the projected range (R(sub p)).

NTIS

Nanostructure (Characteristics); Positrons; Annihilation Reactions; Vacancies (Crystal Defects)

20020005246 Fermi National Accelerator Lab., Batavia, IL USA

D-Zero detector upgrade and physics program

Ellison, J.; Feb. 08, 2001; 11p; In English

Contract(s)/Grant(s): AC02-76CH03000

Report No.(s): DE2001-774354; FERMILAB-CONF-01/012-E; No Copyright; Avail: Department of Energy Information Bridge, Microfiche

The D-zero detector at Fermilab is in the final stages of an extensive upgrade. It is designed to meet the demands imposed by high luminosity Tevatron running planned to begin March 2001. The design and performance of the detector subsystems are described and a brief outline of the physics potential is presented.
NTIS
Particle Accelerators; Mesons; Detectors

20020005247 Fermi National Accelerator Lab., Batavia, IL USA
Higgs and B Physics in Run II
Kuznetsov, V. E.; Feb. 08, 2001; 7p; In English; International Conference on High Energy Physics, 27 Jul. - 2 Aug. 2000, Osaka, Japan
Contract(s)/Grant(s): AC02-76CH03000
Report No.(s): DE2001-774355; FERMILAB-CONF-01/013-E; No Copyright; Avail: Department of Energy Information Bridge, Microfiche
Various aspects of Higgs and B physics in Run II are discussed.
NTIS
Higgs Bosons; Nuclear Physics

20020005248 Oak Ridge National Lab., TN USA
Breakup and Recombination of Identical Bosons: He Dimer-Monomer Collisions
Macek, J. H.; Jan. 10, 2001; 3p; In English; 16th; 16th International Accelerator Conference, 1-4 Nov. 2000, Denton, TX, USA
Contract(s)/Grant(s): AC05-96OR22464
Report No.(s): DE2001-774467; P00-109197; No Copyright; Avail: Department of Energy Information Bridge, Microfiche
Three He atoms can react in vapor at temperatures of the order of a few degrees Kelvin to form a dimer and a free atom by three-body collisions. Conversely, the dimer may fragment by collisions with free He atoms. Cross sections and reaction rates for these processes have been computed at milliKelvin temperatures using the hyperspherical hidden crossing theory. At higher energies, of the order of 0.1 to 5 Kelvin, the impulse approximation has been used to estimate these processes. The computed fragmentation cross section is reported.
NTIS
Bosons; Particle Collisions; Scattering Cross Sections

20020005397 California Univ., Lawrence Berkeley Lab., Berkeley, CA USA
Results from the Scaled Final Focus Experiment
MacLaren, S. A.; de Hoon, M. J. L.; Falten, A.; Ghiorso, W.; Seidl, P.; Sep. 15, 2000; 16p; In English
Report No.(s): DE2001-775116; LBNL-45668; HIFAN 1065; No Copyright; Avail: Department of Energy Information Bridge, Microfiche
Vacuum ballistic focusing is the straightforward method to obtain a heavy ion beam spot size necessary to drive an inertial confinement fusion target. The beam is first expanded then focused to obtain the desired convergence angles at the exit of the last element. This is done in an attempt to achieve a focal spot size in which emittance is the limiting factor; however, aberrations and space charge will influence the spot radius. Proper scaling of particle energy, mass, beam current, beam emittance, and magnetic field replicates the dynamics of a full driver beam at the focus in a small laboratory experiment. by scaling the beam current to (approximately)100 (mu)A, 160 keV Cs+ has been used to study experimentally a proposed driver design at one-tenth scale. Once a nominal focal spot is achieved, the magnet strengths are deliberately de-tuned to simulate the effect of an off-momentum slice of the beam. Additionally, several methods will be used to inject electrons into beam following the last focusing element in order to study the neutralization of space charge and its effect on the focus. Transverse phase space and beam current density measurements at various stages of the focus will be presented as well as spot size measurements from the various trials. This data will be compared to the results of a PIC (particle-in-cell) model of the experiment.
NTIS
Ion Beams; Emittance; Inertial Confinement Fusion

20020005398 California Univ., Lawrence Berkeley Lab., Berkeley, CA USA
Intense ion beam propagation in a reactor sized chamber
Vay, J. L.; Deutsch, C.; Mar. 17, 2000; 14p; In English
Report No.(s): DE2001-775117; LBNL-45672; HIFAN 1028; No Copyright; Avail: Department of Energy Information Bridge, Microfiche

The authors consider the physics of the ballistic transport of intense ion beams in a heavy ion fusion reactor chamber filled with low pressure FLIBE (LiF-BeF2) gas. The authors consider first a single beam envelope model and show via a simple case that emittance growth is an issue in the chamber as well as in the accelerator. They develop a model for the neutralization of beam space-charge by the electrons produced by gas ionization by the beam and derive an expression for the evolution of the neutralization factor as the beam propagates into the chamber. They then extend the envelope model from a one species beam to a beam of ions of several charge states by considering the entire beam as a set of subbeams (one for each charge state) each described with coupled envelope equation. The fully electromagnetic PIC (particle-in-cell) code BPIC was used to investigate the behavior in greater detail. A parametric study of the sensitivity of the final spot radius at the target versus the ion beam stripping and gas ionization cross-sections (which are characterized by large uncertainties) shows that, in the studied regime (Hylife-II parameters), the accessible window of cross-sections for ballistic transport in the chamber through neutral FLIBE gas is eventually small. The temperature evolution for each species and the emittance growth for the entire ion beam was studied for a typical scenario and indicates that a fair amount of the initial electric potential energy carried by the beam as it enters the chamber is converted into temperature and transverse emittance. The high temperature of the ionization-produced electrons prevents a full charge neutralization of the ion beam as it approaches the target. It is shown that focusing a beam array or pre-ionizing a fraction of the background gas may help in reducing the focal spot.
NTIS
Ion Beams; Fusion Reactors; Thermonuclear Reactions; Heavy Ions

20020005399 California Univ., Lawrence Berkeley Lab., Berkeley, CA USA
Ion Sources and Injectors for HIF Induction Linacs
Kwan, J. W.; Ahle, L.; Beck, D. N.; Bieniosek, F. M.; Faltens, A.; Jul. 24, 2000; 19p; In English
Report No.(s): DE2001-775119; LBNL-45677; HIFAN-1031; No Copyright; Avail: Department of Energy Information Bridge, Microfiche

Ion source and injector development is one of the major parts of the HIF (Heavy Ion Fusion) program in the USA. Our challenge is to design a cost effective driver-scale injector and to build a multiple beam module within the next couple of years. In this paper, several current-voltage scaling laws are summarized for guiding the injector design. Following the traditional way of building injectors for HIF induction linac, we have produced a preliminary design for a multiple beam driver-scale injector. We also developed an alternate option for a high current density injector that is much smaller in size. One of the changes following this new option is the possibility of using other kinds of ion sources than the surface ionization sources. So far, we are still looking for an ideal ion source candidate that can readily meet all the essential requirements.
NTIS
Ion Sources; Linear Accelerators; Scaling Laws; Beam Injection

20020005400 California Univ., Lawrence Berkeley Lab., Berkeley, CA USA
Development of the 2-MV injector for HIF
Bieniosek, F. M.; Kwan, J. W.; Henestroza, E.; Kim, C.; Mar. 17, 2000; 17p; In English
Report No.(s): DE2001-775120; LBNL-45680; HIFAN 1034; No Copyright; Avail: Department of Energy Information Bridge, Microfiche

The 2-MV Injector consists of a 17-cm-diameter surface ionization source, an extraction diode, and an electrostatic quadrupole (ESQ) accelerator, with maximum current of 0.8 A of potassium beam at 2 MeV. Previous performance of the Injector produced a beam with adequate current and emittance but with a hollow profile at the end of the ESQ section. We have examined the profile of the beam as it leaves the diode. The measured nonuniform beam density distribution qualitatively agrees with EGUN (electron gun) simulation. Implications for emittance growth in the post acceleration and transport phase will be investigated.
NTIS
Particle Accelerators; Surface Ionization; Beam Injection; Emittance; Injectors

20020005406 Los Alamos National Lab., NM USA
Initial operation of the leda beam-induced fluorescence diagnostic
Kamperschroer, J.; Jun. 01, 2000; 9p; In English
Report No.(s): DE2001-769065; LA-UR-00-2361; No Copyright; Avail: Department of Energy Information Bridge, Microfiche

A diagnostic based on beam-induced fluorescence has been developed and used to examine the expanded beam in the High-Energy Beam Transport (HEBT) section of the Low Energy Demonstration Accelerator (LEDA). The system consists of a camera, a gas injector, a spectrometer, and a control system. Gas is injected to provide a medium for the beam to excite, the camera captures the resulting image of the fluorescing gas, and the spectrometer measures the spectrum of the emitted light. EPICS

was used to control the camera and acquire and store images. Data analysis is presently being performed offline. A Kodak DCS420m professional CCD camera is the primary component of the optical system. InterScience, Inc. modified the camera with the addition of a gain of 4000 image intensifier, thereby producing an intensified camera with a sensitivity of (approximately)0.5 milli-lux. Light is gathered with a 1 inch format, 16-160 mm, Computer zoom lens. This lens is attached to the camera via a Century Precision Optics relay lens. Images obtained using only hydrogen from the beam stop exhibited features not yet understood. Images with good signal-to-noise ratio were obtained with the injection of sufficient nitrogen to raise the HEBT pressure to 2-8x10(sup (minus)6) torr. Two strong nitrogen lines, believed to be of the first negative group of N(sub 2)(sup +), were identified at 391 and 428 nm.
NTIS
Fluorescence; Diagnosis; Beam Injection

20020005641 Los Alamos National Lab., NM USA
Resonance control for the coupled cavity linac and drift tube linac structures of the spallation neutron source linac using a closed-loop water cooling system
Bernardin, J. D.; Brown, R. L.; Jun. 01, 2001; 4p; In English
Report No.(s): DE2001-783309; LA-UR-01-3209; No Copyright; Avail: Department of Energy Information Bridge

The Spallation Neutron Source (SNS) is a facility being designed for scientific and industrial research and development. SNS will generate and use neutrons as a diagnostic tool for medical purposes, material science, etc. The neutrons will be produced by bombarding a heavy metal target with a high-energy beam of protons, generated and accelerated with a linear particle accelerator, or linac. The low energy end of the linac consists of two room temperature copper structures, the drift tube linac (DTL), and the coupled linac (CCL). Both of these accelerating structures use large amounts of electrical energy to accelerate the protons to an energy of 185 MeV. Approximately 60-80% of the electrical energy is dissipated in the copper structure and must be removed. This is done using specifically designed water cooling passages within the linac's copper structure. Cooling water is supplied to these cooling passages by specially designed resonance control and water cooling systems.
NTIS
Accelerators; Cooling Systems; Feedback Control; Linear Accelerators; Neutron Sources

20020005648 Oak Ridge National Lab., TN USA
Workshop Summary: Fundamental Neutron Physics in the USA: An Opportunity in Nuclear, Particle, and Astrophysics. for the Next Decade
Greene, G.; Aug. 24, 2001; 8p; In English
Report No.(s): DE2001-786480; P01-111696; No Copyright; Avail: Department of Energy Information Bridge, Microfiche

Conclusions based on the talks and discussions at the FPPNB2000 workshop are described. Low-energy neutrons are of great interest as experimental probes for the study of important questions in nuclear physics, particle physics, and astrophysics. Many precision experiments of the past were limited by systematic uncertainties. Compared to reactor sources, pulsed spallation neutron source offer significant advantages in improving signal-to-noise ratios and in characterizing energy-dependent systematic uncertainties. The proposed Spallation Neutron Source at Oak Ridge National Laboratory will provide the highest peak flux neutron source in the world, and offers the USA scientific community an unmatched opportunity in nuclear, particle, and astrophysics for the next decade.
NTIS
Neutron Physics; Signal to Noise Ratios; Nuclear Physics

20020005812 Brookhaven National Lab., Upton, NY USA
Intensification of Harmonic Spontaneous Radiation with a Novel Undulator
Marshall, T. C.; Shao, Y.; Parsa, Z.; Nov. 01, 1998; 9p; In English
Report No.(s): DE2001-6236; BNL-66096; No Copyright; Avail: Department of Energy Information Bridge, Microfiche

We have calculated the on-axis spectrum of spontaneous radiation emitted by an electron moving along a planar undulator that has a magnetic profile along the axis that approximates a square wave. (This could be obtained in practice by driving a ferromagnetic undulator into saturation by excessive current in the windings.) We find considerable enhancement of the harmonic radiation spectrum. We compare the harmonic power emitted by an electron moving through an undulator having a sine-wave field profile with the radiation emitted from an undulator having a square-wave profile; the latter is approximated by the first three Fourier components of the undulator magnetic field profile along the axial direction. Examples are computed for 40MeV electrons taking K < 1, for spontaneous radiation emitted along the axis of the system. The emission at harmonics f > 1 is greatly enhanced for the approximate square-wave magnetic profile: the ratio of the power emitted at f=5 by the square-wave

undulator to that of the sine-wave undulator is about 15 (whereas the corresponding ratio at f=1 is only 1.5). While this enhancement might be expected because of the appreciable n=1 and n=5 Fourier components of the undulator field, higher odd harmonics are enhanced even more (e.g., x1000 at f=11). FEL gain at the harmonics should be enhanced by similar factors.
NTIS
Harmonic Radiation; Computation; Spectra; Emittance; Electrons

20020005823 Los Alamos National Lab., NM USA
Beam diagnostics instrumentation for a 6.7-MeV proton beam halo experiment
Gilpatrick, J.; Aug. 01, 2000; 6p; In English
Report No.(s): DE2001-768807; LA-UR-00-3796; No Copyright; Avail: Department of Energy Information Bridge

A 52-magnet lattice is presently being installed in the Low Energy Demonstration Accelerator (LEDA) facility between the radio frequency Quadrupole (RFQ) and the simple LEDA high-energy beam transport (HEBT) (1,2). The purpose of this FODO-lattice beam transport is to provide a beam line apparatus to measure the formation of beam halo and compare the measured data with halo simulations. to attain this measurement goal, several types of beam diagnostics instrumentation are being installed in the magnet lattice. The instrumentation suite include nine beam profile measurement stations capable of detecting the beam distribution charge past 0.01% of the distribution peak. These profile measurement stations each use a slow wire scanner to detect the distribution core, a graphite/copper scraper that detects the 'tails' of the distribution, and a separate prompt gamma loss measurement that detects that the 'tail' particles are protons with energies greater than approximately 4-MeV. Included also in the instrumentation suite are five pairs of beam position monitors (BPM), five scintillator/photomultiplier tube loss monitors (BLM), three-pulsed-current measurements, and a time-of-flight energy measurement. This paper describes each instrument, initial test data, and how they are expected to perform.
NTIS
Proton Beams; Quadrupoles; Measuring Instruments; Radio Frequencies; Halos

20020005839 Los Alamos National Lab., NM USA
Testing Metglas for use in DARHT accelerator cells
Rose, E. A.; Dalmas, D. A.; Downing, J. N.; Temple, R. D.; Jun. 01, 2001; 4p; In English
Report No.(s): DE2001-783302; LA-UR-01-3211; No Copyright; Avail: Department of Energy Information Bridge

The Dual Axis Radiographic Hydrotest Facility (DARHT) at Los Alamos will use two induction linacs to produce high-energy electron beams. The electron beams will be used to generate x-rays from bremsstrahlung targets. The x-rays will be used to produce radiographs. The first accelerator is operational now, producing a 60-nanosecond electron beam. The second accelerator is under construction. It will produce a 2-microsecond electron beam.
NTIS
Electron Beams; Radiography

20020005847 Thomas Jefferson National Accelerator Facility, Newport News, VA USA
New Tool for Correlation Studies in Hall A JLAB
Wojtsekhowski, B.; Degtyarenko, P.; Lindgren, R.; Jun. 01, 2001; 10p; In English
Report No.(s): DE2001-786410; JLAB-PHY-01-22; DOE/ER/40150-1905; No Copyright; Avail: Department of Energy Information Bridge, Microfiche

The study of short-range nucleon-nucleon correlations has a long history. The idea was first invoke in order to explain the large photo-induced proton yield on nuclei. Such studies have become more feasible in recent years due to the availability of CW photon and electron beams at LEGS, NIKHEF, Mainz and J-Lab. Several dedicated two nucleon 2N, knock-out experiments in photo-and electro-production have been completed recently, for a review, see reference. In order to emphasize various aspects of the physics, kinematics must be chosen to permit measurements in the Q2 range up to several (GeV/c)2. Such difficult measurements are only possible with beam energies and intensities available at J-Lab. In Hall A at J-Lab luminosities up to 5.1038 cm-2/s are available, required for the measurement of low cross sections at high Q2. However, the usable luminosity depends on the target thickness, background, detector parameters, and other details of the proposed experiment. In Hall B at J-Lab, where the CLAS detector subtends a large phase space, the available luminosity is 1.1034 cm-2/s. The data with CLAS have already been taken, but must be summed over several kinematics parameters including Q2 in order to provide sufficient statistics.
NTIS
Nucleon-Nucleon Interactions; Continuous Radiation; Photon Beams; Correlation; Kinematics

20020005848 Brookhaven National Lab., Upton, NY USA

Five-watts g-m/j-t refrigerator for lhe target at BNL

Jia,; Wang,; Addessi,; Miglionico,; Martin,; Jul. 2001; 6p; In English

Report No.(s): DE2001-786431; BNL-68082; No Copyright; Avail: Department of Energy Information Bridge, Microfiche

A five-watts G-M/J-T refrigerator was built and installed for the high-energy physics research at Brookhaven National Laboratory in 2001. A liquid helium target of 8.25 liters was required for an experiment in the proton beam line at the Alternating Gradient Synchrotron (AGS) of BNL. The large radiation heat load towards the target requires a five-watts refrigerator at 4.2 K to support a liquid helium flask of 0.2 meter in diameter and 0.3 meter in length, which is made of Mylar film of 0.35 mm in thickness. The liquid helium flask is thermally exposed to the vacuum windows that are also made of 0.35 mm thickness Mylar film at room temperature. The refrigerator uses a two-stage Gifford-McMahon cryocooler for precooling the Joule-Thomson circuit that consists of five Linde-type heat exchangers. A mass flow rate of 0.8-1.0 grams per second at 17.7 atm is applied to the refrigerator cold box. The two-phase helium flows between the liquid target and liquid/gas separator by means of thermosyphon. The paper presents the system design as well as the test results including the control of thermal oscillation.

NTIS

Refrigerators; Cryogenic Cooling; Mass Flow Rate; Two Phase Flow

20020005849 Brookhaven National Lab., Upton, NY USA

Thermal oscillations in liquid helium targets

Wang,; Jia,; Jul. 16, 2001; 6p; In English

Report No.(s): DE2001-786432; BNL-68081; No Copyright; Avail: Department of Energy Information Bridge, Microfiche

A liquid helium target for the high-energy physics was built and installed in the proton beam line at the Alternate Gradient Synchrotron of Brookhaven National Laboratory in 2001. The target flask has a liquid volume of 8.25 liters and is made of thin Mylar film. A G-M/J-T cryocooler of five-watts at 4.2K was used to produce liquid helium and refrigerate the target. A thermosyphon circuit for the target was connected to the J-T circuit by a liquid/gas separator. Because of the large heat load to the target and its long transfer lines, thermal oscillations were observed during the system tests. To eliminate the oscillation, a series of tests and analyses were carried out. This paper describes the phenomena and provides the understanding of the thermal oscillations in the target system.

NTIS

Liquid Helium; Cryogenic Cooling; Mylar (Trademark)

20020005850 Thomas Jefferson National Accelerator Facility, Newport News, VA USA

Cebaf at 12 and 25 gev

Harwood, L.; Reece, C.; Sep. 01, 2001; 5p; In English

Report No.(s): DE2001-786470; JLAB-ACC-01-18; DOE/ER/40150-1907; No Copyright; Avail: Department of Energy Information Bridge, Microfiche

The US nuclear physics community has identified an upgrade of CEBAF to 12 GeV as one of its top priorities. The principal motivation is to enable meson spectroscopy with 9 GeV polarized, quasi-monochromatic photons. A plan for implementing the 12 GeV upgrade has been prepared. Subsystem designs are being tested. Additional opportunities to reduce total project costs have been identified and will be pursued. The plan now calls for the addition to CEBAF of 10 new high-performance cryomodules and a new recirculation arc, yielding 12 GeV after 5.5 passes through the accelerator. Formal construction start could be in 2006. The same cryomodule design would subsequently be the building block for an eventual upgrade to 25 GeV.

NTIS

Electron Beams; Photons; Mesons

71
ACOUSTICS

Includes sound generation, transmission, and attenuation. For noise pollution see 45 Environment Pollution. For aircraft noise see also 02 Aerodynamics and 07 Aircraft Propulsion Propulsion and Power.

20020000764 Lawrence Livermore National Lab., Livermore, CA USA
In-situ identification of anti-personnel mines using acoustic resonant spectroscopy
Perry, R. L.; Roberts, R. S.; Feb. 01, 1999; 18p; In English
Report No.(s): DE2001-8430; UCRL-ID-133165; DP0401283; No Copyright; Avail: Department of Energy Information Bridge, Microfiche

A new technique for identifying buried Anti-Personnel Mines is described, and a set of preliminary experiments designed to assess the feasibility of this technique is presented. Analysis of the experimental results indicates that the technique has potential, but additional work is required to bring the technique to fruition. In addition to the experimental results presented here, a technique used to characterize the sensor employed in the experiments is detailed.
NTIS
Acoustic Resonance; Spectroscopy; Identifying; Mines (Ordnance)

20020001458 Argonne National Lab., IL USA
Formalizing the concept of sound
Kaper, H. G.; Tipei, S.; Aug. 03, 1999; 6p; In English
Report No.(s): DE2001-11918; ANL/MCS/CP-99711; No Copyright; Avail: Department of Energy Information Bridge, Microfiche

The notion of formalized music implies that a musical composition can be described in mathematical terms. In this article we explore some formal aspects of music and propose a framework for an abstract approach.
NTIS
Algorithms; Harmonics; Music

20020001531 Los Alamos National Lab., NM USA
Stochastic Articulatory-to-Acoustic Mapping as a Basis for Speech Recognition
Hogden, J. E.; Valdez, P. F.; Oct. 01, 2000; 12p; In English
Report No.(s): DE2001-765228; LA-UR-00-4807; No Copyright; Avail: Department of Energy Information Bridge, Microfiche

Hidden Markov models (HMMs) of speech acoustics are the current state-of-the-art in speech recognition, but these models bear little resemblance to the processes underlying speech production (Lee, 1989). In this respect, using an HMM to model speech acoustics is like using a Gaussian distribution to model data generated by a Poisson process-to the extent that the model is not an accurate representation of generating process, the accuracy of the model, and the meaning of the inferred parameters, is limited. of this model mismatch likely contributes to the fact that state-of-the-art recognition performance (word accuracy) on recorded telephone conversations is only around 60-65%. There have been recent attempts to create stochastic models of speech acoustics make more realistic assumptions about the mechanisms underlying speech production (Bakis, 1991; Deng, 1998; Hogden, 1998; Picone et al., 1999). In this paper we describe two stochastic models of speech 'Production Conditional Observable Maximum Likelihood Mapping (CO-MALCOM) and its predecessor, Maximum Likelihood Continuity Mapping (MALCOM)'. The main component of both of these models is a stochastic mapping between speech acoustics and speech articulation.
NTIS
Poisson Density Functions; Speech Recognition; Stochastic Processes; Mathematical Models; Articulation (Speech); Acoustics

20020002765 Argonne National Lab., IL USA
Ultrasonic techniques for process monitoring and control
Chien, H. T.; Mar. 24, 1999; 13p; In English
Report No.(s): DE2001-12420; ANL/ET/CP-98639; No Copyright; Avail: Department of Energy Information Bridge, Microfiche

Ultrasonic techniques have been applied successfully to process monitoring and control for many industries, such as energy, medical, textile, oil, and material. It helps those industries in quality control, energy efficiency improving, waste reducing, and cost saving. This paper presents four ultrasonic systems, ultrasonic viscometer, on-loom, real-time ultrasonic imaging system,

ultrasonic leak detection system, and ultrasonic solid concentration monitoring system, developed at Argonne National Laboratory in the past five years for various applications.
NTIS
Quality Control; Ultrasonic Flaw Detection; Nondestructive Tests; Ultrasonic Scanners

20020003570 Los Alamos National Lab., NM USA
Separation of gas mixtures by thermoacoustic waves
Swift, G. W.; Geller, D. A.; Spoor, P. S.; Jun. 01, 2001; 3p; In English
Report No.(s): DE2001-783159; LA-UR-01-3040; No Copyright; Avail: Department of Energy Information Bridge, Microfiche

Imposing sound on a binary gas mixture in a duct that separates the two gases along the acoustic-propagation axis. Mole-fraction differences as large as 10% and separation fluxes as high as 0.001 M-squared c, where M is Mach number and c is sound speed, are easily observed. We describe the accidental discovery of this phenomenon in a helium-xenon mixture, subsequent experiment with a helium-argon mixture, and theoretical developments. The phenomenon occurs because a thin layer of the gas adjacent to the wall is immobilized by viscosity while the rest of the gas moves back and forth with the wave, and the heat capacity of the wall holds this thin layer of the gas at constant temperature while the rest of the gas experiences temperature oscillations due to the wave's oscillating pressure. The oscillating temperature gradient causes the light and heavy atoms in the gas to take turns diffusing into and out of the immobilized layer, so that the oscillating motion of the wave outside the immobilized layer tends to carry light-enriched gas in one direction and heavy-enriched gas in the opposite direction. Experiment and theory are in very good agreement for the initial separation fluxes and the saturation mole-fraction differences.
NTIS
Acoustic Propagation; Gas Mixtures; Acoustic Velocity

72
ATOMIC AND MOLECULAR PHYSICS

Includes atomic and molecular structure, electron properties, and atomic and molecular spectra. For elementary particle physics see 73 Nuclear Physics.

20020000862 Los Alamos National Lab., NM USA
Three-Body Collision Contributions to Recombination and Collision-Induced Dissociation, 2, Kinetics
Kendrick, B.; Pack, R. T.; Walker, R. B.; Apr. 10, 1998; 44p; In English
Report No.(s): DE2001-1311; LA-UR-98-1677; No Copyright; Avail: Department of Energy Information Bridge, Microfiche

Detailed rate constants for the reaction Ne + Ne + H (r equilibrium) Ne(sub 2) + H are generated, and the master equations governing collision-induced dissociation (CID) and recombination are accurately solved numerically. The temperature and pressure dependence are explored. At all pressures, three-body (3B) collisions dominate. The sequential two-body energy-transfer (ET) mechanism gives a rate that is more than a factor of two too small at low pressures and orders of magnitude too small at high pressures. Simpler models are explored; to describe the kinetics they must include direct 3B rates connecting the continuum to the bound states and to the quasibound states. The relevance of the present reaction to more general CID/recombination reactions is discussed. For atomic fragments, the 3B mechanism usually dominates. For diatomic fragments, the 3B and ET mechanism are competitive, and for polyatomic fragments the ET mechanism usually dominates.
NTIS
Dissociation; Reaction Kinetics; Recombination Reactions; Molecular Interactions; Energy Transfer

20020000866 Brookhaven National Lab., Upton, NY USA
Centrality Definition using Mid-Rapidity at Distributions from P+Be to Au+Au at AGS Energies
Tannenbaum,; May 10, 1999; 5p; In English; 14th; 14th International Conference on Ultra-Relativistic Nucleus-Nucleus Collisions, Quark Matter, 10-15 May 1999, Turin, Italy
Contract(s)/Grant(s): AC02-98CH10886
Report No.(s): DE2001-11463; BNL-66739; KB020201; No Copyright; Avail: Department of Energy Information Bridge, Microfiche

Measurements by the E802 Collaboration of the A-dependence and pseudorapidity interval ((delta)(eta)) dependence of mid-rapidity ET distributions in a half-azimuth electromagnetic calorimeter are presented for p+Be, p+Au, O+Cu, Si+Au and Au+Au collisions at the BNL-AGS. The issues addressed are (1) whether the shapes of the upper edges of the ET distributions vary with (delta)(eta) similarly to the variation in shapes of mid-rapidity charged particle distributions and (2) how small a

(delta)(eta) interval would still give a meaningful characterization of the 'nuclear geometry' of a reaction. A new way of plotting ET distributions was found from which the reaction dynamics could be read directly.
NTIS
Calorimeters; Charged Particles

20020000868 Brookhaven National Lab., Upton, NY USA
Story of Sigma Hypernuclei: A Modern Fable
Chrien, R. E.; Feb. 19, 1999; 9p; In English; International Workshop on Strangeness Nuclear Physics, 19-22 Feb. 1999, Seoul, Korea, Republic of
Contract(s)/Grant(s): AC02-98CH10886
Report No.(s): DE2001-11451; BNL-66476; KB0101; No Copyright; Avail: Department of Energy Information Bridge, Microfiche

The reality of (Sigma) hypernuclei has been the subject of intense concern among experimenters and theoreticians for more than 20 years. The possible existence of (Sigma) hypernuclei was first suggested by a pioneering experiment on a (sup 9)Be target at the CERN PS. There were reported to be two narrow ((Gamma) < 8 MeV) peaks in the continuum region. This finding was quite unexpected since the widths of (Sigma) states were believed to be large due to the strong conversion process. It is obvious that if such relatively long-lived systems were confirmed unambiguously by experiment, their masses and widths provide important constraints on the (Sigma)N effective interaction and its relation to the (Lambda)N and NN interactions. Since the (Sigma) carries isospin, the role of isospin and isospin conservation in hadronic reactions could be explored. This report stimulated a number of subsequent experiments at the BNL-AGS and KEK, along with further experiments with a specially created short kaon beam at the CERN PS. Experimental data were reported for different targets at different momenta and at different conditions. Various tagging techniques were employed to suppress backgrounds, but always at the expense of a reduction in statistical quality. Because of problems with resolution and statistics, contradictions among the different sets of data resulted more often in clouding the issues than clarifying them. Thus, up until a few years ago, there was no statistically clear confirmation of this surprising finding. In the last few years, however, a series of definitive experiments has been performed at the BNL-AGS in an effort to resolve the discrepancies and settle the controversy. Besides repeating the initial experiment on Be, a target of (sup 6)Li was run. The earlier stopped kaon data on (sup 4)He was repeated in an in-flight experiment, and the suggestion of a (Sigma) bound state, with virtually pure isospin, confirmed. We now have a better understanding of the role of isospin in the nucleon-hyperon interaction and the importance of three body forces in hyper-nuclei. According to that understanding, it is unlikely that (Sigma) states for A > 5 will ever be seen. In this review, a critique of the past BNL experiments is presented and conclusions on the status of the (Sigma) database drawn.
NTIS
Hypernuclei; Baryons; Nuclear Interactions

20020000928 Los Alamos National Lab., NM USA
Workshop on Probing Frontiers in Matter with Neutron Scattering, Wrap-up Session Chaired by John C. Browne
Mezei, F.; Thompson, J.; Dec. 01, 1998; 34p; In English, 14 Dec. 1997, Los Alamos, NM, USA
Report No.(s): DE2001-2634; LA-13545-C; No Copyright; Avail: Department of Energy Information Bridge, Microfiche

The Workshop on Probing Frontiers in Matter with Neutron Scattering consisted of a series of lectures and discussions about recent highlights in neutron scattering. In this report, we present the transcript of the concluding discussion session (wrap-up session) chaired by John C. Browne, Director of Los Alamos National Laboratory. The workshop had covered a spectrum of topics ranging from high T(sub c) superconductivity to polymer science, from glasses to molecular biology, a broad review aimed at identifying trends and future needs in condensed matter research. The focus of the wrap-up session was to summarize the workshop participants' views on developments to come. Most of the highlights presented during the workshop were the result of experiments performed at the leading reactor-based neutron scattering facilities. However, recent advances with very high power accelerators open up opportunities to develop new approaches to spallation technique that could decisively advance neutron scattering research in areas for which reactor sources are today by far the best choice. The powerful combination of neutron scattering and increasingly accurate computer modeling emerged as another area of opportunity for research in the coming decades.
NTIS
Computerized Simulation; Condensed Matter Physics; Neutron Scattering; Spallation

20020000933 Oak Ridge National Lab., TN USA

Preliminary Pulsing Experiments to Measure Delayed Neutron Emission Parameters

Charlton, W. S.; Parish, T. A.; Raman, S.; Oct. 05, 1998; 10p; In English

Report No.(s): DE2001-1754; ORNL/CP-100047; No Copyright; Avail: Department of Energy Information Bridge, Microfiche

Recent interest in delayed neutron parameters including comparisons between macroscopic (experimental) and microscopic (calculated) results have prompted a set of experiments using the 1MW Triga Reactor at the Texas A and M University (TAMU) Nuclear Science Center (NSC) designed to measure the complete set of seven-group delayed neutron parameters for several higher actinides. Operating the Nuclear Science Center Reactor (NSCR) in a pulsed mode, a complete set of delayed neutron parameters were measured for Np-237 and Am-243. The total delayed neutron yield per 100 fissions for Np-237 and Am-243 was found to be 1.14 +/- 0.07 and 0.85 +/- 0.05, respectively. Comparisons to previous measurements are made where such measurements are available.

NTIS

Neutrons; Neutron Emission; Parameter Identification

20020000935 Los Alamos National Lab., NM USA

Sources 4a: a code for calculating (alpha,n), spontaneous fission, and delayed neutron sources and spectra

Madland, D. G.; Arthur, E. D.; Estes, G. P.; Stewart, J. E.; Bozoian, M.; Sep. 01, 1999; 159p; In English

Report No.(s): DE2001-15215; LA-13639-MS; No Copyright; Avail: Department of Energy Information Bridge, Microfiche

SOURCES 4A is a computer code that determines neutron production rates and spectra from ((alpha),n) reactions, spontaneous fission, and delayed neutron emission due to the decay of radionuclides. The code is capable of calculating ((alpha),n) source rates and spectra in four types of problems: homogeneous media (i.e., a mixture of (alpha)-emitting source material and low-Z target material), two-region interface problems (i.e., a slab of (alpha)-emitting source material in contact with a slab of low-Z target material), three-region interface problems (i.e., a thin slab of low-Z target material sandwiched between (alpha)-emitting source material and low-Z target material), and ((alpha),n) reactions induced by a monoenergetic beam of (alpha)-particles incident on a slab of target material. Spontaneous fission spectra are calculated with evaluated half-life, spontaneous fission branching, and Watt spectrum parameters for 43 actinides. The ((alpha),n) spectra are calculated using an assumed isotropic angular distribution in the center-of-mass system with a library of 89 nuclide decay (alpha)-particle spectra, 24 sets of measured and/or evaluated ((alpha),n) cross sections and product nuclide level branching fractions, and functional (alpha)-particle stopping cross sections for Z 106. The delayed neutron spectra are taken from an evaluated library of 105 precursors. The code outputs the magnitude and spectra of the resultant neutron source. It also provides an analysis of the contributions to that source by each nuclide in the problem.

NTIS

Neutron Sources; Computer Programs; Neutron Emission

20020001218 Lawrence Livermore National Lab., Livermore, CA USA

Highly charged ion trapping and cooling

Beck, B. R.; Church, D. A.; Gruber, L.; Holder, J. P.; Schneider, D.; Oct. 22, 1998; 8p; In English

Report No.(s): DE2001-2836; UCRL-JC-132208; DP0102012; No Copyright; Avail: Department of Energy Information Bridge, Microfiche

In the past few years a cryogenic Penning trap (RETRAP) has been operational at the Electron Beam Ion Trap (EBIT) facility at Lawrence Livermore National Laboratory. The combination of RETRAP and EBIT provides a unique possibility of producing and re-trapping highly charged ions and cooling them to very low temperatures. Due to the high Coulomb potentials in such an ensemble of cold highly charged ions the Coulomb coupling parameter (the ratio of Coulomb potential to the thermal energy) can easily reach values of 172 and more. To study such systems is not only of interest in astrophysics to simulate White Dwarf star interiors but opens up new possibilities in a variety of areas (e.g. laser spectroscopy), cold highly charged ion beams.

NTIS

Ion Beams; Ion Traps (Instrumentation); Quenching (Atomic Physics)

20020001219 Lawrence Livermore National Lab., Livermore, CA USA

Coulomb clusters in RETRAP

Beck, B. R.; Church, D. A.; Gruber, L.; Holder, J. P.; Schneider, D.; Oct. 22, 1998; 8p; In English

Report No.(s): DE2001-2835; UCRL-JC-132209; DP0102012; No Copyright; Avail: Department of Energy Information Bridge, Microfiche

Storage rings and Penning traps are being used to study ions in their highest charge states. Both devices must have the capability for ion cooling in order to perform high precision measurements such as mass spectrometry and laser spectroscopy. This is accomplished in storage rings in a merged beam arrangement where a cold electron beam moves at the speed of the ions. In RETRAP, a Penning trap located at Lawrence Livermore National Laboratory, a sympathetic laser/ion cooling scheme has been implemented. In a first step, singly charged beryllium ions are cooled electronically by a tuned circuit and optically by a laser. Then hot, highly charged ions are merged into the cold Be plasma. by collisions, their kinetic energy is reduced to the temperature of the Be plasma. First experiments indicate that the highly charged ions form a strongly coupled plasma with a Coulomb coupling parameter.
NTIS
Kinetic Energy; Laser Spectroscopy; Ions

20020001221 Lawrence Livermore National Lab., Livermore, CA USA
Experimental observation of resonance effects in intensely irradiated atomic clusters
Ditmire, T.; Komashko, A.; Perry, M. D.; Rubenchik, A. M.; Zweiback, J.; Jul. 10, 1998; 5p; In English
Report No.(s): DE2001-2830; UCRL-JC-129764; DP0210000; No Copyright; Avail: Department of Energy Information Bridge, Microfiche

We have resolved the expansion of intensely irradiated atomic clusters on a femtosecond time scale. These data show evidence for resonant heating, similar to resonance absorption, in spherical cluster plasmas.
NTIS
Atomic Clusters; Radiant Heating; Spherical Plasmas

20020001227 Argonne National Lab., IL USA
Supercritical pomeron in QCD
White, A. R.; Jun. 29, 1998; 14p; In English
Report No.(s): DE2001-10864; ANL-HEP-CP-98-31; No Copyright; Avail: Department of Energy Information Bridge

Deep-inelastic diffractive scaling violations have provided fundamental insight into the QCD (quantum chromodynamics) pomeron, suggesting a single gluon inner structure rather than that of a perturbative two-gluon bound state. This talk outlines a derivation of a high-energy, transverse momentum cut-off, confining solution of QCD. The pomeron, in first approximation, is a single reggeized gluon plus a 'wee parton' component that compensates for the color and particle properties of the gluon. This solution corresponds to a super-critical phase of Reggeon Field Theory.
NTIS
Quantum Chromodynamics; Particle Theory; Pomerons

20020001450 Argonne National Lab., IL USA
Direct flow in 10.8 GeV/nucleon Au+Au collisions measured in experiment E917 at the AGS
Back, B. B.; Betts, R. R.; Britt, H. C.; Chang, J.; Chang, W. C.; May 19, 1999; 7p; In English
Report No.(s): DE2001-11818; ANL/PHY/CP-99065; No Copyright; Avail: Department of Energy Information Bridge, Microfiche

Analysis of directed flow observable for protons and pions from Au+Au collisions at 10.8 GeV/nucleon from experiment E917 at the AGS (Alternating Gradient Synchrotron) is presented. Using a Fourier series expansion, the first Fourier component, (nu)(sub 1) was extracted as a function of rapidity for mid-central collisions (17-24%). Clear evidence for positive directed flow is found in the proton data, and a weak, possibly negative directed flow signal is observed for (pi)(sup +) and (pi)(sup (minus)).
NTIS
Synchrotrons; Atomic Collisions; Protons

20020001537 Lawrence Livermore National Lab., Livermore, CA USA
Use of diffusion synthetic acceleration in parallel 3D neutral particle transport calculations
Brown, P.; Chang, B.; May 14, 1998; 8p; In English
Report No.(s): DE2001-2775; UCRL-JC-130877; No Copyright; Avail: Department of Energy Information Bridge, Microfiche

The linear Boltzmann transport equation (BTE) is an integro-differential equation arising in deterministic models of neutral and charged particle transport. In slab (one-dimensional Cartesian) geometry and certain higher-dimensional cases, Diffusion Synthetic Acceleration (DSA) is known to be an effective algorithm for the iterative solution of the discretized BTE. Fourier and asymptotic analyses have been applied to various idealizations (e.g., problems on infinite domains with constant coefficients) to obtain sharp bounds on the convergence rate of DSA in such cases. While DSA has been shown to be a highly effective acceleration

(or preconditioning) technique in one-dimensional problems, it has been observed to be less effective in higher dimensions. This is due in part to the expense of solving the related diffusion linear system. We investigate here the effectiveness of a parallel semicoarsening multigrid (SMG) solution approach to DSA preconditioning in several three dimensional problems. In particular, we consider the algorithmic and implementation scalability of a parallel SMG-DSA preconditioner on several types of test problems.
NTIS
Boltzmann Transport Equation; Transport Theory; Particle Diffusion; Neutral Particles; Charged Particles

20020001586 Argonne National Lab., IL USA
How far from stability can we go using gammasphere and the FMA
Lister, C. J.; Jan. 27, 1999; 7p; In English
Report No.(s): DE2001-12372; ANL/PHY/CP-98279; No Copyright; Avail: Department of Energy Information Bridge, Microfiche

GammaSphere has been successfully moved from LBNL to ANL for a cycle of research. Most importantly, the direction of research with the device has changed and is presently directed at far-from-stability issues. This new direction matches initiatives for producing radioactive beams for far-from-stability research. We have lowered the cross-section for effective 'in-beam' experiments into the sub-100 nb regime, more than an order-of-magnitude improvement. In many cases this allows us to move one or two isotopes further from stability than was previously possible. With stable beams, and with very sensitive instrumentation, we can reach the proton dripline for most mass regions and we can study some of the heaviest nuclei. These projects have revealed interesting new structural effects. However, their full significance will lie in the future, when radioactive beams allow us to probe the entire nuclear landscape. Only then can we move to a more general understanding of nuclear structure and nucleosynthesis.
NTIS
Spectroscopy; Gamma Ray Spectra

20020001845 Los Alamos National Lab., NM USA
Implications of results of neutrino mass experiments
McKellar, B. H.; Garbutt, M.; Oct. 01, 2000; 9p; In English
Report No.(s): DE2001-765633; LA-UR-00-5038; No Copyright; Avail: Department of Energy Information Bridge, Microfiche

The long standing negative (mass)(sup 2) anomaly encountered in attempts to measure the mass of the electron neutrino may be an indication of physics beyond the standard model. It is demonstrated that an additional charged current interaction which is not of V-A form, and which is at least an order of magnitude weaker than the standard model charged current interaction, will produce a spectrum, which, if fitted by the standard model, may give a negative value for m(sub (nu))(sup 2). A possible physical explanation of the time dependent effects seen by the Troitsk experiment is also provided.
NTIS
Neutrinos; Standard Model (Particle Physics); Mass

20020001849 Los Alamos National Lab., NM USA
Hypernuclear physics: A brief past and bright future
Gibson, B. F.; Oct. 01, 2000; 13p; In English
Report No.(s): DE2001-765579; LA-UR-00-5026; No Copyright; Avail: Department of Energy Information Bridge, Microfiche

A primary reason for investigating the structure and reactions of baryon systems is to achieve an understanding of the fundamental baryon-baryon force in the realm of non-perturbative QCD (quantum chromodynamics). Few baryon systems play an essential role, because one can calculate complete solutions to test a particular baryon-baryon interaction ansatz. Hypernuclei, exotic nuclei containing one or more hyperons (Y = (Lambda), (Sigma), or (Xi)) are crucial to this investigation, because they permit one to probe models based upon our experience in the nonstrange sector; they lie outside of the conventional world where our models were developed. That is, we can test whether our sophisticated models of the nucleon-nucleon (NN) interaction extrapolate successfully beyond the zero strangeness region in which the parameters were determined, or whether the models merely interpolate. The presence of the strangeness degree of freedom (flavor) adds a new dimension to our evolving picture of nuclear physics. We shall see that the physics of hypernuclei is both novel and puzzling, stretching our intuition and analysis capability beyond that developed during the more than half century that we have explored conventional nuclear physics. The hypernuclear sector of hadronic physics is not just a simple extension of zero-strangeness phenomena.
NTIS
Nuclear Physics; Theoretical Physics; Baryons; Hypernuclei; Strangeness

20020001983 Argonne National Lab., IL USA
Experimental Facilities Division ***Progress Report, 1997-1998***
Oct. 22, 1998; 194p; In English
Report No.(s): DE2001-12022; ANL/APS/TB-34; No Copyright; Avail: Department of Energy Information Bridge

This Progress Report summarizes the activities of the APS Experimental Facilities Division (XFD) over the period 1997-98. The XFD personnel focused on supporting the Advanced Photon Source (APS) users from day-to-day operations support to long-term research and development (R&D) needs. The XFD personnel would like to proudly share their major accomplishments with the readers of this report.

NTIS
Photons; Sources; Research Facilities; Particle Accelerators

20020002287 Kansas State Univ., Manhattan, KS USA
Atomic Physics of Strongly Correlated Systems ***Final Report, 1 Aug. 1986 - 31 Jul. 1999***
Lin, C. D.; Oct. 01, 1999; 10p; In English
Report No.(s): DE2001-766045; No Copyright; Avail: Department of Energy Information Bridge, Microfiche

The goal of this research is to develop new novel methods for studying correlated motion of atomic systems. This involves new formulations of the theoretical approaches, the performance of numerical calculations, and the detailed comparison with available experiment. Different theoretical methods have been developed for different classes of problems. The basis of our theoretical method is the hyperspherical approach. We have studied in general three-body systems and restricted four-body systems, and examined the qualitative properties such as the visualization of the wavefunctions which then allows us to do classifications, and then develop accurate theoretical methods for performing calculations to predict results that can be compared to experiments.

NTIS
Atomic Physics; Correlation Detection; Numerical Analysis

20020002298 Florida State Univ., Tallahassee, FL USA
Heavy fermions and other highly correlated electron systems ***Final Report***
Schlottmann, P.; Oct. 12, 1998; 26p; In English
Report No.(s): DE2001-765245; No Copyright; Avail: Department of Energy Information Bridge

Properties of highly correlated electrons, such as heavy fermion compounds, metal-insulator transitions, one-dimensional conductors and systems of restricted dimensionality are studied theoretically. The main focus is on Kondo insulators and impurity bands due to Kondo holes, the low-temperature magnetoresistivity of heavy fermion alloys, the n-channel Kondo problem, mesoscopic systems and one-dimensional conductors.

NTIS
Electrons; Fermions; Kondo Effect; Heavy Fermion Systems

20020002301 Pittsburgh Univ., Pittsburgh, PA USA
Studies of relativistic heavy ion collisions at the AGS: Experiments 814/877 ***Final Report***
Cleland, W. E.; Apr. 30, 1997; 39p; In English
Report No.(s): DE2001-764718; DOE/ER/40363-10; No Copyright; Avail: Department of Energy Information Bridge

The University of Pittsburgh effort in the area of relativistic heavy ion physics has continued its analysis efforts of the data taken in Experiments E814 and E877. The last run of E877 was carried out in Oct-Dec 1995, and the University of Pittsburgh contributed to this effort primarily through an improvement of the data acquisition system and an expansion of the trigger to include track information, including particle identification. These tasks were successful, with the result that the final run of E877 resulted in a much richer sample of data than has been collected in all of the previous runs added together.

NTIS
Ionic Collisions; Heavy Ions

20020002351 Brookhaven National Lab., Upton, NY USA
Polarization and Luminosity Requirements for the First Muon Collider
Parsa, Z.; Nov. 01, 1998; 12p; In English
Report No.(s): DE2001-6250; BNL-66097; No Copyright; Avail: Department of Energy Information Bridge, Microfiche

Muon Polarization and Luminosity requirement for physics studies at a muon collider are discussed. An overview of a muon collider concepts and design parameters for 0.1, 0.5, and 4 Tev muon colliders are also presented.
NTIS
Design Analysis; Muons; Linear Accelerators

20020002353 Brookhaven National Lab., Upton, NY USA
Polarization Effects at a Muon Collider
Parsa, Z.; Nov. 01, 1998; 7p; In English
Report No.(s): DE2001-6240; BNL-66078; No Copyright; Avail: Department of Energy Information Bridge, Microfiche
For Muon Colliders, Polarization will be a useful tool if high polarization is achievable with little luminosity loss. Formulation and effects of beam polarization and luminosity including polarization effects in Higgs resonance studies are discussed for improving precision measurements and Higgs resonance 'discovery' capability, e.g., at the First Muon Collider (FMC).
NTIS
Muons; Polarization; Linear Accelerators

20020002737 New Mexico Univ., Albuquerque, NM USA
Final Report to the U.S. DOE Grant DE-FG03-93-ER14326 Covering Period from June 1977 to March 1999 ***Final Report, Jun. 1977 - Mar. 1999***
Bryant, H. C.; Jun. 30, 1999; 30p; In English
Report No.(s): DE2001-762077; No Copyright; Avail: Department of Energy Information Bridge, Microfiche
This document presents an overview of the results of the Department of Energy's (DOE's) support of experimental research into the structure and interactions of the negative ion of hydrogen conducted by the Department of Physics and Astronomy of the University of New Mexico at the Los Alamos National Laboratory. The work involves many collaborations with scientists from both institutions, as well as others. Although official DOE support for this work began in 1977, the experiment that led to it was done in 1971, near the time the 800 MeV linear accelerator at Los Alamos (LAMPF) first came on line. Until the mid nineties, the work was performed using the relativistic beam at LAMPF. The most recent results were obtained using the 35 keV injector beam for the Ground Test Accelerator at Los Alamos. A list of all published results from this work is presented.
NTIS
Hydrogen; Negative Ions; Atomic Structure

20020002798 Brookhaven National Lab., Upton, NY USA
Some Physical and Engineering Aspects of High Current EBIS
Pikin, A.; Prelec, K.; May 21, 1999; 15p; In English
Report No.(s): DE2001-7664; BNL-66446; No Copyright; Avail: Department of Energy Information Bridge, Microfiche
Some applications of an Electron Beam Ion Source (EBIS) require intensities of highly charged ions significantly greater than those which have been achieved in present EBIS sources. For example, the ion source for the Relativistic Heavy Ion Collider (RHIC) at Brookhaven National Laboratory (BNL) must be capable of generating 3 x 10(sup 9) ions of Au(sup 35+) or 2 x 10(sup 9) ions of U(sup 45+) per pulse. In this case, if the fraction of ions of interest is 20% of the total ion space charge, the total extracted charge is (approximately) 5 x 10(sup 11). It is also desirable to extract these ions in a 10 (micro)s pulse to allow single turn injection into the first synchrotrons. Requirements for an EBIS which could meet the needs of the LHC at CERN are similar ((approximately) 1.5 x 10(sup 9) ions of Pb(sup 54+) in 5.5 (micro)s). This charge yield is about an order of magnitude greater than that achieved in existing EBIS sources, and is what is meant here by high current. This also implies, then, an EBIS with a high electron beam current.
NTIS
Ion Sources; High Current; Ion Charge; Ion Beams; Electron Beams

20020003358 Los Alamos National Lab., NM USA
Neutrino masses or new interactions
McKellar, B. H.; Garbutt, M.; Jun. 01, 2001; 13p; In English
Report No.(s): DE2001-782783; LA-UR-01-3522; No Copyright; Avail: Department of Energy Information Bridge, Microfiche

Recent proposals to study the mass of the 'electron' neutrino at a sensitivity of 0.3. eV can be used to place limits on the right handed and scalar charged currents at a level which improves on the present experimental limits. Indeed the neglect of the possibility of such interactions can lead to the inference of an incorrect value for the mass, as we illustrate.
NTIS
Inference; Neutrinos; Scalars

20020003359 Los Alamos National Lab., NM USA
Multi-GeV Gluonic Mesons
Page, P. R.; Jun. 01, 2001; 10p; In English
Report No.(s): DE2001-782785; LA-UR-01-3521; No Copyright; Avail: Department of Energy Information Bridge, Microfiche
Lattice QCD gives reliable predictions for hybrid charmonium and multi-GeV glueball masses. Proton-antiproton annihilation may offer an excellent opportunity for the first observation of these states. There are two distinct possible programs: The search for J-PC-exotic and non-J-PC exotic states. The latter program represents substantially higher cross sections and does not absolutely require partial wave analysis, two very attractive features. The program can be performed with a varying p energy is less than GeV and a fixed target.
NTIS
Proton-Antiproton Interactions; Annihilation Reactions; Charm (Particle Physics); Gluons; Quantum Chromodynamics

20020003362 Los Alamos National Lab., NM USA
Excess rf power required for rf control of the spallation neutron source (sns) linac, a pulsed high-intensity superconducting proton accelerator
Lynch, M.; Kwon, S.; Jun. 01, 2001; 4p; In English
Report No.(s): DE2001-783156; LA-UR-01-3046; No Copyright; Avail: Department of Energy Information Bridge, Microfiche
A high-intensity proton linac, such as that being planned for the SNS, requires accurate RF control of cavity fields for the entire pulse in order to avoid beam spill. The current design requirement for the SNS is RF field stability within +0.5deg (1). This RF control capability is achieved by the control electronics using the excess RF power to correct disturbances. To minimize the initial capital costs, the RF system is designed with 'just enough' RF power. All the usual disturbances exist, such as beam noise, klystron/HVPS noise, coupler imperfections, transport losses, turn-on and turn-off transients, etc. As a superconducting linac, there are added disturbances of large magnitude, including Lorentz detoning and microphonics. The effects of these disturbances and the power required to correct them are estimated, and the results shows that the highest power systems in the SNS have just enough margin, with little or no excess margin.
NTIS
Linear Accelerators; Radio Frequencies; Neutron Sources; Superconducting Magnets

20020003803 Los Alamos National Lab., NM USA
Perturbation theory in the one-phase region of an electron-ion system
Baker, G.; Johnson, J.; Sep. 01, 2000; 13p; In English
Report No.(s): DE2001-768782; LA-UR-00-3922; No Copyright; Avail: Department of Energy Information Bridge, Microfiche
The region of validity of our previously derived series expansion for the pressure of an electron-ion system in powers of the electron charge is investigated. For the case of Hydrogen, we both assess the radius of convergence of the series, as a function of the de Broglie density, and cross-compare the results with those from the spherical cellular model. These methods more or less agree in an understandable way, and indicate that the region of validity lies well inside the one-phase region. We are then in a position to combine the series results with our experiential knowledge and thus extend our assessment to general values of Z. Also, as is well known, there is a region of high density and low temperature where the pressure and the internal energy are almost independent of temperature. For this region we may, for each density, use the highest temperature for which that independence holds (to the desired accuracy) and thus extend the series results.
NTIS
Perturbation Theory; Hydrogen; Convergence; Mathematical Models; Electrons; Ions

20020003821 Argonne National Lab., IL USA
Molecular dynamics simulation of lattice structure, radiation damage, and vibrational spectra of zircon (ZrSiO4)
Liu, G. K.; Zhuang, H. Z.; Beitz, J. V.; Nov. 03, 2000; 4p; In English
Report No.(s): DE2001-768604; ANL/CHM/CP-103228; No Copyright; Avail: Department of Energy Information Bridge

The lattice structure, phonon density of states, and infrared spectrum for crystalline zircon, ZrSiO(sub 4), have been studied using a molecular dynamics (MD) simulation method that utilizes the Born-Mayer-Huggins and Coulomb pair potentials and the Stillinger-Weber three-body potential. A lattice block of ZrSiO(sub 4), which contains 343 unit cells with dimensions of 4.6249 x 4.6249 x 4.1874 nm(sub 3) and containing 8232 ions, was considered in our calculations. The simulated lattice structure agreed with that determined from x-ray and neutron diffraction experiments. The vibrational modes and absorption spectrum were calculated based on the simulated lattice and compared with infrared absorption spectra. Characteristic lines in infrared spectra obtained from previous experiments on natural and synthetic zircon were assigned to specific bond structures by interactive MD simulations with variation of selected potential parameters. It is shown that the O-Si-O three-body correlations in the SiO(sub 4) tetrahedron significantly influence the spectrum. It is demonstrated that the oxygen ions that are parallel and perpendicular to the c-axis in the SiO(sub 4) tetrahedron are inequivalent and make different contributions to the vibration spectrum. The energy distribution among 24 atoms in a unit cell in the 1011-cm(sup (minus)1) vibrational mode is shown in Fig. 1. Comparison between the simulated infrared absorption spectrum and that from experiments on synthetic zircon is shown in Fig. 2. The interactive method of fitting simulated results to those determined from experiments may be used as a tool for studying nanostructure and thermodynamics properties of materials. The model potentials for the ZrSiO(sub 4) lattice are refined and further applied to MD simulation of lattice disordering and line broadening that are induced by radiation damage processes and amorphization. We have further simulated alpha-decay-induced damage and dynamical recovery in the lattice of ZrSiO(sub 4). The simulated lattice with structure damage is used for reproducing infrared spectra that were obtained from radiation-damaged samples. The mechanisms and microscopic behavior of lattice disordering and dynamical recovery will be discussed.
NTIS
Crystal Lattices; Molecular Dynamics; Radiation Effects; Zirconium Oxides; Silicon Oxides

20020003826 Argonne National Lab., IL USA
Masses and proton separation energies obtained from Q(sub a) and Q(sub p) measurements
Davids, C. N.; Woods, P. J.; Batchelder, J. C.; Bingham, C. R.; Blumenthal, D. J.; Oct. 20, 2000; 9p; In English
Report No.(s): DE2001-768579; ANL/PHY/CP-102174; No Copyright; Avail: Department of Energy Information Bridge, Microfiche

For many nuclei beyond the proton drip line in the Z greater than 72, N greater than 82 region, both proton and a emission are energetically allowed. In the case of some proton emitters, there are alpha-decay chains emanating from both parent and daughter nuclei. This means that if the mass excess of one member of an (alpha)-decay chain is known, then the mass excesses for all members of both chains can be obtained. In addition, proton separation energies may be derived for nuclei in the (alpha)-decay chain of the proton emitter. The method of time- and space-correlations also allows the identification of isomeric states in these nuclei. As an example, a large number of mass excesses and proton separation energies for ground and metastable states have been derived from Q(sub a) and Q(sub p) values obtained from the proton emitters (sup 165,166,167)Ir, Au-171, Tl-177, and their daughters.
NTIS
Atomic Physics; Alpha Decay; Proton Energy

20020003931 Los Alamos National Lab., NM USA
Nonlinear atom optics
Milonni, T.; Csanak, G.; Jul. 01, 1999; 10p; In English
Report No.(s): DE2001-768234; LA-UR-99-2325; No Copyright; Avail: Department of Energy Information Bridge, Microfiche

This is the final report of a three-year, Laboratory Directed Research and Development (LDRD) project at Los Alamos National Laboratory (LANL). The project objectives were to explore theoretically various aspects of nonlinear atom optics effects in cold-atom waves and traps. During the project a major development occurred the observation, by as many as a dozen experimental groups, of Bose-Einstein condensation (BEC) in cold-atom traps. This stimulated us to focus our attention on those aspects of nonlinear atom optics relating to BEC, in addition to continuing our work on a nonequilibrium formalism for dealing with the interaction of an electromagnetic field with multi-level atomic systems, allowing for macroscopic coherence effects such as BEC. Studies of several problems in BEC physics have been completed or are near completion, including the suggested use of external electric fields to modify the nature of the interatomic interaction in cold-atom traps; properties of two-phase condensates; and molecular loss processes associated with BEC experiments involving a so-called Feshbach resonance.
NTIS
Atoms; Nonlinear Optics; Electromagnetic Fields

20020004014 Los Alamos National Lab., NM USA

Study of residual nuclide yields in 1.0 GeV proton irradiated (208)Pb and 2.6 GeV proton irradiated (NAT)W thin targets

Tiarenko, Y.; Aug. 01, 2000; 16p; In English

Report No.(s): DE2001-768906; LA-UR-00-3597; No Copyright; Avail: Department of Energy Information Bridge, Microfiche

Some 113 residual product nuclide yields in a 1.0 GeV proton-irradiated thin monoisotopic 208-Pb sample and some 107 residual product nuclide yields in a 2.6 GeV proton-irradiated (nat)W sample have been measured and simulated by different codes. The irradiations were made using proton beams extracted from the ITEP (Institute for Theoretical and Experimental Physics) synchrotrons. The nuclide yields were y-spectrometered directly using a high-resolution Ge-detector. The y-spectra were processed by the GENIE2000 code. The ITEP-developed SIGMA code was used together with the PCNUDAT nuclear decay database to identify the y-lines and to determine the cross-sections. The 27Al(p,x)22Na reaction was used to monitor the proton flux. The measured yields are compared with their values simulated by the LAHET, CEM95, HETC, CASCADE, IN-JCL, YIELDX, and other codes. Estimates of the mean deviation factor are used to demonstrate the predictive power of the codes. The results obtained may be of interest in studying the hybrid Accelerator-Driven System (ADS) facilities.

NTIS

Nuclear Reactions; Protons; Nuclides; Synchrotrons

20020005112 Thomas Jefferson National Accelerator Facility, Newport News, VA USA

DC Field Emission Studies on Nb

Wang, T.; Reece, C.; Sundelin, R.; Sep. 01, 2001; 4p; In English

Report No.(s): DE2001-786147; JLAB-OTP-01-02; DOE/ER/40150-1901; No Copyright; Avail: Department of Energy Information Bridge, Microfiche

The DC field emission studies in TJNAF aim to further explore the causes of field emission from Niobium surfaces and enhance our understanding of various preparation techniques for the purpose of improving field emission suppression. Field emitters on Nb samples are located by a DC field emission scanning apparatus in ultra high vacuum, then individually studied under SEM with EDS for characterization. Results at above 100 MV/m from samples prepared by BCP, and by electropolishing are presented and compared.

NTIS

Niobium; Field Emission; Electric Fields; Electropolishing

20020005215 Wayne State Univ., Detroit, MI USA

Microdosimetry for Boron Neutron Capture Therapy

Maughan, R. L.; Kota, C.; Sep. 05, 2000; 8p; In English

Report No.(s): DE2001-770637; No Copyright; Avail: Department of Energy Information Bridge

The specific aims of the research proposal were as follows: (1) to design and construct small volume tissue equivalent proportional counters for the dosimetry and microdosimetry of high intensity thermal and epithermal neutron beams used in BNCT, and of modified fast neutron beams designed for boron neutron capture enhanced fast neutron therapy (BNCEFNT). (2) to develop analytical methods for estimating the biological effectiveness of the absorbed dose in BNCT and BNCEFNT based on the measured microdosimetric spectra. (3) To develop an analytical framework for comparing the biological effectiveness of different epithermal neutron beams used in BNCT and BNCEFNT, based on correlated sets of measured microdosimetric spectra and radiobiological data. Specific aims (1) and (2) were achieved in their entirety and are comprehensively documented in Jay Burmeister's Ph.D. dissertation entitled 'Specification of physical and biologically effective absorbed dose in radiation therapies utilizing the boron neutron capture reaction' (Wayne State University, 1999). Specific aim (3) proved difficult to accomplish because of a lack of sufficient radiobiological data.

NTIS

Therapy; Boron; Neutrons; Dosimeters

20020005813 Louisiana State Univ., Baton Rouge, LA USA

Structure of Nuclei Far from Stability

Zganjar, E. F.; Feb. 25, 1999; 76p; In English

Report No.(s): DE2001-6238; DOE/ER/40159-228; No Copyright; Avail: Department of Energy Information Bridge, Microfiche

From among a number of important nuclear structure results that have emerged from our research program during the past few years, two stand out as being of extra significance. These are: (a) the identification of a diabatic coexisting structure in Au-187 which arises solely from differences in proton occupation of adjacent oscillator shells, and (b) the realization of a method for

estimating EO strength in nuclei and the resulting prediction that the de-excitation of superdeformed bands may proceed, in some cases, by strong EO transitions.
NTIS
Nuclear Structure; Stability; Creep Rupture Strength

20020005821 Los Alamos National Lab., NM USA
Second-order stochastic leap-frog algorithm for Langevin simulation
Qiant, J.; Habib, S.; Aug. 01, 2000; 6p; In English
Report No.(s): DE2001-768728; LA-UR-00-3861; No Copyright; Avail: Department of Energy Information Bridge

Langevin simulation provides an effective way to study collisional effects in beams by reducing the six-dimensional Fokker-Planck equation to a group of stochastic ordinary differential equations. These resulting equations usually have multiplicative noise since the diffusion coefficients in these equations are functions of position and time. Conventional algorithms, e.g. Euler and Heun, give only first order convergence of moments in a finite time interval. In this paper, a stochastic leap-frog algorithm for the numerical integration of Langevin stochastic differential equations with multiplicative noise is proposed and tested. The algorithm has a second-order convergence of moments in a finite time interval and requires the sampling of only one uniformly distributed random variable per time step. As an example, we apply the new algorithm to the study of a mechanic oscillator with multiplicative noise.
NTIS
Algorithms; Langevin Formula; Stochastic Processes; Numerical Integration; Computerized Simulation

73
NUCLEAR PHYSICS

Includes nuclear particles; and reactor theory. For space radiation see 93 Space Radiation. For atomic and molecular physics see 72 Atomic and Molecular Physics. For elementary particle physics see 77 Physics of Elementary Particles and Fields. For nuclear astrophysics see 90 Astrophysics.

20020000945 Argonne National Lab., IL USA
Plutonium and surrogate fission products in a composite ceramic waste form
Esh, D. W.; Frank, S. M.; Goff, K. M.; Johnson, S. G.; Moschetti, T. L.; May 19, 1999; 11p; In English
Report No.(s): DE2001-11819; ANL/NT/CP-99068; No Copyright; Avail: Department of Energy Information Bridge, Microfiche

Argonne National Laboratory is developing a ceramic waste form to immobilize salt containing fission products and transuranic elements. Preliminary results have been presented for ceramic waste forms containing surrogate fission products such as cesium and the lanthanides. In this work results from scanning electron microscopy/energy dispersive spectroscopy and x-ray diffraction are presented in greater detail for ceramic waste forms containing surrogate fission products. Additionally, results for waste forms containing plutonium and surrogate fission products are presented. Most of the surrogate fission products appear to be silicates or aluminosilicates whereas the plutonium is usually found in an oxide form. There is also evidence for the presence of plutonium within the sodalite phase although the chemical speciation of the plutonium is not known.
NTIS
Fission Products; Ceramics; Plutonium

20020001058 Argonne National Lab., IL USA
Fracture toughness measurements on a glass bonded sodalite high-level waste form
DiSanto, T.; Goff, K. M.; Johnson, S. G.; O'Holleran, T. P.; May 19, 1999; 10p; In English
Report No.(s): DE2001-11820; ANL/NT/CP-99069; No Copyright; Avail: Department of Energy Information Bridge, Microfiche

The electrometallurgical treatment of metallic spent nuclear fuel produces two high-level waste streams; cladding hulls and chloride salt. Argonne National Laboratory is developing a glass bonded sodalite waste form to immobilize the salt waste stream. The waste form consists of 75 Vol.% crystalline sodalite (containing the salt) with 25 Vol.% of an 'intergranular' glassy phase. Microindentation fracture toughness measurements were performed on representative samples of this material using a Vickers indenter. Palmqvist cracking was confirmed by post-indentation polishing of a test sample. Young's modulus was measured by an acoustic technique. Fracture toughness, microhardness, and Young's modulus values are reported, along with results from scanning electron microscopy studies.
NTIS
Glass; Fracture Strength; Metal Fuels; Waste Treatment

20020001202 Argonne National Lab., IL USA

Progress in developing very-high-density low-enriched-uranium fuels

Hayes, S. L.; Hofman, G. L.; Meyer, M. K.; Snelgrove, J. L.; Strain, R. V.; Feb. 19, 1999; 9p; In English

Report No.(s): DE2001-12359; ANL/TD/CP-98451; No Copyright; Avail: Department of Energy Information Bridge, Microfiche

Preliminary results from the postirradiation examinations of microplates irradiated in the RERTR-1 and -2 experiments in the ATR have shown several binary and ternary U-MO alloys to be promising candidates for use in aluminum-based dispersion fuels with uranium densities up to 8 to 9 g/cubic cm. Ternary alloys of uranium, niobium, and zirconium performed poorly, however, both in terms of fuel/matrix reaction and fission-gas-bubble behavior, and have been dropped from further study. Since irradiation temperatures achieved in the present experiments (approximately 70 C) are considerably lower than might be experienced in a high-performance reactor, a new experiment is being planned with beginning-of-cycle temperatures greater than 200 C in 8-g U/cubic cm fuel.

NTIS

Uranium Alloys; Nuclear Fuels; Irradiation

20020001299 Argonne National Lab., IL USA

Nuclear Data and Measurement Series: a method to construct covariance files in ENDF/B format for criticality safety applications

Naberejnev, D. G.; Smith, D. L.; Jul. 30, 1999; 56p; In English

Report No.(s): DE2001-12069; ANL/NDM-148; No Copyright; Avail: Department of Energy Information Bridge, Microfiche

Argonne National Laboratory is providing support for a criticality safety analysis project that is being performed at Oak Ridge National Laboratory. The ANL role is to provide the covariance information needed by ORNL for this project. The ENDF/B-V evaluation is being used for this particular criticality analysis. In this evaluation, covariance information for several isotopes or elements of interest to this analysis is either not given or needs to be reconsidered. For some required materials, covariance information does not exist in ENDF/B-V: U-233, U-236, Zr, Mg, Gd, and Hf. For others, existing covariance information may need to be re-examined in light of the newer ENDF/B-V evaluation and recent experimental data. In this category are the following materials: U-235, U-238, Pu-239, Pu-240, Pu-241, Fe, H, C, N, O, Al, Si, and B. A reasonable estimation of the fractional errors for various evaluated neutron cross sections from ENDF/B-V can be based on the comparisons between the major more recent evaluations including ENDF/B-VI, JENDL3.2, BROND2.2, and JEF2.2, as well as a careful examination of experimental data. A reasonable method to construct correlation matrices is proposed here. Coupling both of these considerations suggests a method to construct covariances files in ENDF/B format that can be used to express uncertainties for specific ENDF/B-V cross sections.

NTIS

Nuclear Structure; Data Acquisition; Error Analysis; Safety

20020001546 Lawrence Livermore National Lab., Livermore, CA USA

High intensity positron program at LLNL

Asoka-Kumar, P.; Howell, R. H.; Stoeffl, W.; Sep. 23, 1998; 6p; In English

Report No.(s): DE2001-2788; UCRL-JC-132024; DP0401281; No Copyright; Avail: Department of Energy Information Bridge, Microfiche

Lawrence Livermore National Laboratory (LLNL) is the home of the world's highest current beam of keV positrons. The potential for establishing a national center for materials analysis using positron annihilation techniques around this capability is being actively pursued. The high LLNL beam current will enable investigations in several new areas. We are developing a positron microprobe that will produce a pulsed, focused positron beam for 3-dimensional scans of defect size and concentration with submicron resolution. Below we summarize the important design features of this microprobe. Several experimental end stations will be available that can utilize the high current beam with a time distribution determined by the electron linac pulse structure, quasi-continuous, or bunched at 20 MHz, and can operate in an electrostatic or (and) magnetostatic environment. Some of the planned early experiments are: two-dimensional angular correlation of annihilation radiation of thin films and buried interfaces, positron diffraction holography, positron induced desorption, and positron induced Auger spectra.

NTIS

Positrons; Positron Annihilation; Linear Accelerators

20020001854 Virginia Univ., Charlottesville, VA USA

UVA experimental and high energy physics *Final Report*

Cox, B.; Oct. 07, 1999; 8p; In English

Report No.(s): DE2001-764702; No Copyright; Avail: Department of Energy Information Bridge

The period 1992--1997 was a mixture of frustrations and of accomplishments for the UVa HEP group. The experimental HEP group began this period with the completion of a truncated run of Experiment E771 at Fermilab in 1992. This experiment was designed to measure the cross section for beauty production in 800 GeV/c pN interactions. It succeeded in this goal as well as in obtaining one of the best limits on FCNC in charm decays by setting an upper limit on D(0) yields mu(+) mu(-). In addition, they were able to measure Psi, Psi, chi(1), chi(2) and upsilon production. Three UVa PhD theses have resulted from this experiment (as well as 12 other PhD's at other institutions). At the same time, the UVa experimental group was vigorously pursuing the goal of studying CP violation in B production. This took the form of a proposal to the SSC for a super fixed target facility, the SFT, which would focus on studies of B mesons. B. Cox was the spokesman of this experiment that had over thirty institutions. This proposal EOI-14 had a good reception by the SSC PAC. A R and D activity to prove the technique of crystal channeling was undertaken to prove the accelerator aspects of this proposal. This activity, known as E853 or CEX at Fermilab, resulted in proof of the crystal channeling technique as viable for the extraction of 20 TeV beam at the SSC. In addition to this activity, the UVa group investigated many other aspects of B physics at the SSC. They were among the leaders of the 1993 Snowmass meeting on B Physics at Hadronic Accelerators. The UVa HEP group worked vigorously on developing the ideas for B physics at the SSC, as evidenced by the many different studies listed in the publication list given, up to the very day the SSC was terminated by an act of Congress.
NTIS
Research and Development; High Energy Interactions; Theoretical Physics

20020001855 Michigan Univ., Ann Arbor, MI USA
Accelerator physics R&D ***Final Report, Dec. 15, 1993 - Dec. 14, 1997***
Krisch, A. D.; May 01, 1998; 15p; In English
Report No.(s): DE2001-764620; DOE/ER/40822; No Copyright; Avail: Department of Energy Information Bridge
During the 1990's, we focused our Accelerator Physics program on research and development of TeV polarized proton beams using Siberian snakes (a Siberian snake is a device which forces an accelerator ring's depolarizing fields to cancel themselves by rotating each proton's spin by 180(degree) on each turn around the ring): (1) Siberian snake experiments at the IUCF Cooler ring; (2) Design of polarized beam capability for the SSC; (3) Design of polarized beam capability for the Main Injector and Tevatron (funded by Fermilab); and (4) Design of polarized beam capability for HERA (funded by DESY). During FY 1994 to 1997, our Siberian snake experiments at IUCF continued to be unexpectedly successful. Their data have helped us to design polarized proton beam capability for Fermilab's Tevatron and Main Injector and now for DESY's HERA.
NTIS
Particle Accelerators; Research Facilities

20020002314 Bettis Atomic Power Lab., West Mifflin, PA USA
Cooperative Learning of Neutron Diffusion and Transport Theories
Robinson, M. A.; Apr. 30, 1999; 13p; In English
Report No.(s): DE2001-6271; B-T-3236; No Copyright; Avail: Department of Energy Information Bridge, Microfiche
A cooperative group instructional strategy is being used to teach a unit on neutron transport and diffusion theory in a first-year-graduate level, Reactor Theory course that was formerly presented in the traditional lecture/discussion style. Students are divided into groups of two or three for the duration of the unit. Class meetings are divided into traditional lecture/discussion segments punctuated by cooperative group exercises. The group exercises were designed to require the students to elaborate, summarize, or practice the material presented in the lecture/discussion segments. Both positive interdependence and individual accountability are fostered by adjusting individual grades on the unit exam by a factor dependent upon group achievement. Group collaboration was also encouraged on homework assignments by assigning each group a single grade on each assignment. The results of the unit exam have been above average in the two classes in which the cooperative group method was employed. In particular, the problem solving ability of the students has shown particular improvement. Further,the students felt that the cooperative group format was both more educationally effective and more enjoyable than the lecture/discussion format.
NTIS
Problem Solving; Students; Transport Theory; Education

20020002362 Vrije Univ., Amsterdam, Netherlands
Coherent Pi(0) Electroproduction on (4)He in the Delta Region
Botto, T. E. G.; Nov. 23, 1999; 152p; In English
Report No.(s): PB2002-100088; No Copyright; Avail: CASI; A08, Hardcopy; A02, Microfiche

Nuclear physics deals with the strong interaction, a fundamental force of nature, active at the extremely small scales found inside the atomic nucleus. Its ultimate goal is to give a consistent description and understanding of the properties of nuclear systems in terms of the interactions among their constituents or nucleons, i.e., the proton and the neutron. This is an extremely challenging many-body problem in quantum mechanics. Furthermore, the choice of considering nucleons as the appropriate degrees of freedom is inevitably questioned, since the nucleon radius is so close to the average intra-nucleon distance in a nucleus that the strongly interacting nucleons will mostly overlap with each other. At the nucleon level, the strong interaction is mediated via the exchange of mesons. Such a view, should bridge with the regime of perturbative Quantum Chromo Dynamics (QCD), which at high energy provides a valid description of the phenomena observed so far. In the QCD regime, the strong interaction is described at the level of point-like nucleon constituents, the quarks, via the exchange of gluons.
NTIS
Quantum Chromodynamics; Nuclear Physics; Helium Isotopes

20020002703 Los Alamos National Lab., NM USA
Direct Energy Conversion (DEC) Fission Reactors: A US NERI Project
Beller, D.; Polansky, G.; Nov. 01, 2000; 12p; In English
Report No.(s): DE2001-768171; LA-UR-00-4076; No Copyright; Avail: Department of Energy Information Bridge

The direct conversion of the electrical energy of charged fission fragments was examined early in the nuclear reactor era, and the first theoretical treatment appeared in the literature in 1957. Most of the experiments conducted during the next ten years to investigate fission fragment direct energy conversion (DEC) were for understanding the nature and control of the charged particles. These experiments verified fundamental physics and identified a number of specific problem areas, but also demonstrated a number of technical challenges that limited DEC performance. Because DEC was insufficient for practical applications, by the late 1960s most R&D ceased in the US. Sporadic interest in the concept appears in the literature until this day, but there have been no recent programs to develop the technology. This has changed with the Nuclear Energy Research Initiative that was funded by the U.S. Congress in 1999. Most of the previous concepts were based on a fission electric cell known as a triode, where a central cathode is coated with a thin layer of nuclear fuel. A fission fragment that leaves the cathode with high kinetic energy and a large positive charge is decelerated as it approaches the anode by a charge differential of several million volts, it then deposits its charge in the anode after its kinetic energy is exhausted. Large numbers of low energy electrons leave the cathode with each fission fragment; they are suppressed by negatively biased on grid wires or by magnetic fields. Other concepts include magnetic collimators and quasi-direct magnetohydrodynamic generation (steady flow or pulsed). We present the basic principles of DEC fission reactors, review the previous research, discuss problem areas in detail and identify technological developments of the last 30 years relevant to overcoming these obstacles. A prognosis for future development of direct energy conversion fission reactors will be presented.
NTIS
Energy Conversion; Fission Electric Cells; Energy Technology; Magnetic Fields

20020002740 California Univ., Berkeley, CA USA
STAR: The Secure Transportable Autonomous Reactor System, Encapsulated Fission Heat Source *Progress Report, Period ending 31 Mar. 2000*
Greenspan, E.; Apr. 24, 2000; 54p; In English
Report No.(s): DE2001-761826; No Copyright; Avail: Department of Energy Information Bridge, Microfiche

Significant progress has been made since the beginning of this project, in September 1999. So far we have found no 'show-stopper'. In fact, based on the findings accumulated so far it appears to us that the Encapsulated Nuclear Heat Source (ENHS) is technologically feasible and looks even more attractive than initially conceived.
NTIS
Heat Sources; Nuclear Heat; Fission

20020002768 Argonne National Lab., IL USA
Comparisons of steady-state and transient thermal hydraulic results from SAS-DIF3DK and RELAP5 mod 3.2 for an RBMK reactor
Dunn, F. E.; Mar. 10, 1999; 16p; In English
Report No.(s): DE2001-12417; ANL/RA/CP-98562; No Copyright; Avail: Department of Energy Information Bridge, Microfiche

The SAS-DIF3DK code couples a detailed 3-D neutron kinetics treatment with a detailed thermal hydraulics treatment. One goal of the work on SAS (shared address space)-DIF3DK is to produce a detailed code that will run a wide range of transients

in real time. Achieving this goal will require efficient numerical methods and efficient coding, and it will probably require the use of multiple processors for larger problems. In order to obtain clean code-to-code thermal hydraulics comparisons with a recognized and established code, a detailed thermal hydraulic model was set up for an RBMK (Channelized Large Power Reactor) assembly and its associated piping, The same identical input model was implemented in both SAS-DIF3DK and RELAP5 mod 3.2. Both steady-state and transient thermal hydraulics calculations were made with this model. Except for cladding temperatures in one transient, the SAS-DIF3DK results were similar to or almost identical to the RELAP5 results, and SAS-DIF3DK ran an order of magnitude or more faster than RELAP5. The cladding temperature differences can be explained in terms of different post-DNB models and heat transfer coefficients.
NTIS
Numerical Analysis; Thermohydraulics; Power Reactors; Kinetics; Steady State

20020003353 Argonne National Lab., IL USA
Observations of bunch lengthening effects in the APS 7-GeV storage ring
Lumpkin, A. H.; Yang, B. X.; Chae, Y. C.; Dec. 31, 1996; 22p; In English
Report No.(s): DE2001-432947; ANL/ASD/CP-90147; CONF-9608133-15; No Copyright; Avail: Department of Energy Information Bridge, Microfiche

Measurements of the bunch length and horizontal beam size at a dispersive point in the lattice versus single-bunch current have been done on the Advanced Photo Source (APS) 7-GeV storage ring. These data are relevant to issues (limits) of obtaining high peak currents for storage-ring-based FELs. Bunch lengths from (sigma)(sub (tau)) (approximately) 25 to 70 ps were measured using a Hamamatsu C5680 dual-sweep streak camera. Additional complementary data on energy spread deduced from horizontal beam size at a dispersive point in the lattice were also tracked versus single-bunch current. Both optical synchrotron radiation (OSR) and x-ray synchrotron radiation (XSR) techniques were used. For the set of data taken at a synchrotron frequency of 1.2 kHz (indicating rf gap voltage (le) 6 MV), the significant bunch lengthening without a comparable horizontal size change ((Delta)E growth) is consistent with the potential well distortion model rather than the predictions of a microwave instability calculation. With higher rf gap voltage, peak currents up to 400 A were observed. A bunch-lengthening effect in multibunch mode was also observed as the stored-beam current approached the available rf power limit.
NTIS
Storage Rings (Particle Accelerators); Radiation Spectra; Microwaves; Electric Potential; Beam Currents

20020003361 Los Alamos National Lab., NM USA
Beam emittance diagnostic for the DARHT second axis injector
Bartsch, R.; Ekdahl, C.; Jun. 01, 2001; 5p; In English
Report No.(s): DE2001-783155; LA-UR-01-3050; No Copyright; Avail: Department of Energy Information Bridge, Microfiche

Low beam emittance is key to achieving the required spot size at the output focus of the DARHT Second Axis. The nominal electron beam parameters at the output of the injector are 2 kA, 4.6 MeV, 2-microsecond pulse width and an rms radius less than 1 cm. Emittance is measured by bringing the beam to a focus in which the emittance is a dominant influence in determining the spot size. The spot size is measured from Cerenkov or optical transition radiation (OTR) generated from a target intercepted by the beam. The current density in the focused DARHT beam would melt this target in less than 1/2 microsec. to prevent this we have designed a DC magnetic transport system that defocuses the beam on the emittance target to prevent overheating, and uses a 125-ns half period pulsed solenoid to selectively focus the beam for short times during the beam pulse.
NTIS
Emittance; Electron Beams; Optical Transition; Pulse Duration

20020003363 Los Alamos National Lab., NM USA
Availability model for the sns linac rf system
Tallerico, P.; Rees, D.; Anderson, D.; Jun. 01, 2001; 5p; In English
Report No.(s): DE2001-783157; LA-UR-01-3045; No Copyright; Avail: Department of Energy Information Bridge, Microfiche

The Linac RF system is broken down into eight major components for this model. These components are: the klystrons, the waveguide, the water loads, the circulators, the converter/modulator, the transmitter, the window, and the low level RF (LLRF) controls. The mean time between failures (MTBF) for several of the components vary with voltage or klystron power level, and the variation is discussed below. In general, these MTBF's are design requirements supplied to the vendors of the subsystems, and verified at design reviews and by the experience at other accelerators. We assume that the scheduled operational time for the SNS is 6000 hours per year, and use this number to calculate the availability. We have to calculate the total down time during the 6000 hours of operation, and the availability is defined as one minus the unexpected down time for the year, divided by the number

of operating hours in the year. Ideally, we would use distributions of MTBF's and MTTR's, since each failure will be different, but the equipment is not yet built, so the distributions are not available, and we make the assumption of constant MTBF and MTTR.
NTIS
Neutron Sources; Linear Accelerators; Transmitters; Electric Potential

20020003364 Los Alamos National Lab., NM USA
Tuning section 2 of the leda ccdtl
Rybarcyk, L.; Wood, R.; Jun. 01, 2001; 4p; In English
Report No.(s): DE2001-783163; LA-UR-01-3032; No Copyright; Avail: Department of Energy Information Bridge, Microfiche
As part of the Low-Energy Demonstration Accelerator (LEDA) portion of the Advanced Accelerator Applications (AAA) project we have fabricated and will perform high-power RF tests on Section 2 of the 700-MHz Coupled-Cavity Drift-Tube Linac (CCDTL). This CCDTL section contains six, two-gap accelerating cells. This portion of the CCDTL was designed to accelerate the 100-mA, LEDA RFQ proton beam to 7.3 MeV. This paper reports on the process and results of tuning Section 2 leading up to high-power RF testing.
NTIS
Linear Accelerators; Cavities; Fabrication

20020003365 Los Alamos National Lab., NM USA
Transverse electron-proton two-stream instability in a bunched beam
Wang, T. F.; Channell, P. J.; Macek, R. J.; Davidson, R. C.; Jun. 01, 2001; 4p; In English
Report No.(s): DE2001-783189; LA-UR-01-3024; No Copyright; Avail: Department of Energy Information Bridge, Microfiche
This paper is an analytical investigation of the transverse electron-proton (e-p) two-stream instability in a proton bunch propagating through a stationary electron background. The equations of motion, including the effect of damping, are derived for the centroids of the proton beam and the electron cloud. An approach is developed to solve the coupled linear centroid equations in the time domain describing the e-p instability in proton bunches with non-uniform line densities. Examples are presented for proton line densities corresponding to uniform and parabolic profiles.
NTIS
Proton Beams; Electron Clouds; Centroids

20020003366 Los Alamos National Lab., NM USA
Water purity development for the coupled cavity linac (ccl) and drift tube linac (dtl) structures of the spallation neutron source (sns) linac
Katonak, D.; Bernardin, J.; Hopkins, S.; Jun. 01, 2001; 4p; In English
Report No.(s): DE2001-783200; LA-UR-01-3066; No Copyright; Avail: Department of Energy Information Bridge, Microfiche
The Spallation Neutron Source (SNS) is a facility being designed for scientific and industrial research and development. SNS will generated and use neutrons as a diagnostic tool for medical purposes, material science, etc. The neutrons will be produced by bombarding a heavy metal target with a high-energy beam of protons, generated and accelerated with a linear particle accelerator or linac. The low energy end of the linac consists of two room temperature copper structures use large amounts of electrical energy to accelerate the proton beam. Approximately 60-80% of the electrical energy is dissipated in the copper structure and must be removed. This is done using specifically designed water cooling passages within the linac's copper structure. Cooling water is supplied to these cooling passages by specially designed resonance control and water cooling systems.
NTIS
Spallation; Linear Accelerators; Cooling Systems; Neutron Sources

20020003367 Los Alamos National Lab., NM USA
Parameters for quantifying beam halo
Allen, C. K.; Wangler, T. P.; Jun. 01, 2001; 4p; In English
Report No.(s): DE2001-783203; LA-UR-01-3093; No Copyright; Avail: Department of Energy Information Bridge, Microfiche
Two different parameters for the quantitative description of beam halo are introduced, both based on moments of the particle distribution. One parameter is a measure of spatial halo formation and has been defined previously by Wangler and Crandall, termed the profile parameter. The second parameter relies on kinematic invariants to quantify halo formation in phase space; we

call it the halo parameter. The profile parameter can be computed from experimental beam profile data. The halo parameter provides a theoretically more complete description of halo in phase space, but is difficult to obtain experimentally.
NTIS
Halos; Kinematics

20020003379 Sandia National Labs., Albuquerque, NM USA
Self-Adjoint Angular Flux Equation for Coupled Electron-Photon Transport
Liscum-Powell, J. L.; Lorence, L. J.; Morel, J. E.; Prinja, A. K.; Jul. 08, 1999; 7p; In English
Report No.(s): DE2001-8948; SAND99-1698C; No Copyright; Avail: Department of Energy Information Bridge, Microfiche

Recently, Morel and McGhee described an alternate second-order form of the transport equation called the self adjoint angular flux (SAAF) equation that has the angular flux as its unknown. The SAAF formulation has all the advantages of the traditional even- and odd-parity self-adjoint equations, with the added advantages that it yields the full angular flux when it is numerically solved, it is significantly easier to implement reflective and reflective-like boundary conditions, and in the appropriate form it can be solved in void regions. The SAAF equation has the disadvantage that the angular domain is the full unit sphere and, like the even- and odd- parity form, S(sub n) source iteration cannot be implemented using the standard sweeping algorithm. Also, problems arise in pure scattering media. Morel and McGhee demonstrated the efficacy of the SAAF formulation for neutral particle transport. Here we apply the SAAF formulation to coupled electron-photon transport problems using multigroup cross-sections from the CEPXS code and S(sub n) discretization.
NTIS
Electron Transfer; Protons; Numerical Analysis

20020003380 Sandia National Labs., Albuquerque, NM USA
Unattended Monitoring System Design Methodology
Drayer, D. D.; DeLand, S. M.; Harmon, C. D.; Matter, J. C.; Martinez, R. L.; Jul. 08, 1999; 10p; In English
Report No.(s): DE2001-8949; SAND99-1699; No Copyright; Avail: Department of Energy Information Bridge, Microfiche

A methodology for designing Unattended Monitoring Systems starting at a systems level has been developed at Sandia National Laboratories. This proven methodology provides a template that describes the process for selecting and applying appropriate technologies to meet unattended system requirements, as well as providing a framework for development of both training courses and workshops associated with unattended monitoring. The design and implementation of unattended monitoring systems is generally intended to respond to some form of policy based requirements resulting from international agreements or domestic regulations. Once the monitoring requirements are established, a review of the associated process and its related facilities enables identification of strategic monitoring locations and development of a conceptual system design. The detailed design effort results in the definition of detection components as well as the supporting communications network and data management scheme. The data analyses then enables a coherent display of the knowledge generated during the monitoring effort. The resultant knowledge is then compared to the original system objectives to ensure that the design adequately addresses the fundamental principles stated in the policy agreements. Implementation of this design methodology will ensure that comprehensive unattended monitoring system designs provide appropriate answers to those critical questions imposed by specific agreements or regulations. This paper describes the main features of the methodology and discusses how it can be applied in real world situations.
NTIS
Data Processing; Monitors

20020003384 Argonne National Lab., IL USA
Figaro: detecting nuclear materials using high-energy gamma rays for oxygen
Michlich, B. J.; Smith, D. L.; Massey, T. N.; Ingram, D.; Fessler, A.; Oct. 10, 2000; 6p; In English
Report No.(s): DE2001-766332; ANL/TD/CP-103050; No Copyright; Avail: Department of Energy Information Bridge, Microfiche

Potential diversion of nuclear materials is a major international concern. Fissile (e.g., U, Pu) and other nuclear materials (e.g., D, Be) can be detected using 6-7 MeV gamma rays produced in the (sup 19)F(p,(alpha)(gamma))(sup 16)O reaction. These gamma rays will induce neutron emission via the photoneutron and photofission processes in nuclear materials. However, they are not energetic enough to generate significant numbers of neutrons from most common benign materials, thereby reducing the false alarm rate. Neutrons are counted using an array of BF3 counters in a polyethylene moderator. Experiments have shown a strong increase in neutron count rates for depleted uranium, Be, D(sub 2)O, and (sup 6)Li, and little or no increase for other materials (e.g., H(sub 2)O, SS, Cu, Al, C, (sup 7)Li). Gamma source measurements using solid targets of CaF(sub 2) and MgF(sub 2) and

a SF(sub 6) gas target show that proton accelerator of 3 MeV and 10-100 microampere average current could lead to acceptable detection sensitivity.
NTIS
Neutron Emission; Fissionable Materials; Detection; Nuclear Particles

20020003386 Argonne National Lab., IL USA
Development of probabilistic RESRAD computer codes for NRC decommissioning and license termination applications
Chen, S. Y.; Yu, C.; Trottier, C.; Oct. 17, 2000; 15p; In English
Report No.(s): DE2001-766347; ANL/EA/CP-103154; No Copyright; Avail: Department of Energy Information Bridge, Microfiche

In 1999, the US Nuclear Regulatory Commission (NRC) tasked Argonne National Laboratory to modify the existing RESRAD and RESRAD-BUILD codes to perform probabilistic, site-specific dose analysis for use with the NRC's Standard Review Plan for demonstrating compliance with the license termination rule. The RESRAD codes have been developed by Argonne to support the US Department of Energy's (DOEs) cleanup efforts. Through more than a decade of application, the codes already have established a large user base in the nation and a rigorous QA support. The primary objectives of the NRC task are to: (1) extend the codes' capabilities to include probabilistic analysis, and (2) develop parameter distribution functions and perform probabilistic analysis with the codes. The new codes also contain user-friendly features specially designed with graphic-user interface. In October 2000, the revised RESRAD (version 6.0) and RESRAD-BUILD (version 3.0), together with the user's guide and relevant parameter information, have been developed and are made available to the general public via the Internet for use.
NTIS
Reactor Safety; Computer Programs; Decommissioning; Revisions

20020003392 Los Alamos National Lab., NM USA
Thermal hydraulic analysis of a liquid-metal-cooled neutron spallation target
Gregory, W.; Martin, R.; Valachovic, T.; Jul. 01, 2000; 9p; In English
Report No.(s): DE2001-768229; LA-UR-99-2340; No Copyright; Avail: Department of Energy Information Bridge, Microfiche

We have carried out numerical simulations of the thermal hydraulic behavior of a neutron spallation target where liquid metal lead-bismuth serves as both coolant and as a neutron spallation source. The target is one of three designs provided by the Institute of Physics and Power Engineering (IPPE) in Russia. This type of target is proposed for Accelerator-driven Transmutation of Waste (ATW) to eliminate plutonium from hazardous fission products. The thermal hydraulic behavior was simulated by use of a commercial CFD computer code called CFX. Maximum temperatures in the diaphragm window and in the liquid lead were determined. In addition the total pressure drop through the target was predicted. The results of the CFX analysis were close to those results predicted by IPPE in their preliminary analysis.
NTIS
Thermal Analysis; Neutron Sources; Spallation; Thermohydraulics

20020003396 Los Alamos National Lab., NM USA
Americium separations from nitric acid process effluent streams
Barr, M.; Jarvinen, G.; Aug. 01, 2000; 20p; In English
Report No.(s): DE2001-768246; LA-UR-00-3549; No Copyright; Avail: Department of Energy Information Bridge, Microfiche

The aging of the US nuclear stockpile presents a number of challenges, including the ever-increasing radioactivity of plutonium residues from Am-241. Minimization of this weak gamma-emitter in process and waste solutions is desirable to reduce both worker exposure and the effects of radiolysis on the final waste product. Removal of americium from plutonium nitric acid processing effluents, however, is complicated by the presence of large.quantities of competing metals, particularly Fe and Al, and-strongly oxidizing acidic solutions. The reprocessing operation offers several points at which americium removal maybe attempted, and we are evaluating two classes of materials targeted at different steps in the process. Extraction chromatography resin materials loaded with three different alkylcarbamoyl phosphinates and phosphine oxides were accessed for Am removal efficiency and Am/Fe selectivity from 1-7 molar nitric acid solutions. Commercial and experimental mono- and bifunctional anion-exchange resins were evaluated for total alpha-activity removal from post-evaporator solutions whose composition, relative to the original nitric acid effluent, is reduced in acid and greatly increased in total salt content. With both classes of

materials, americium/total alpha emission removal is sufficient to meet regulatory requirements even under sub-optimal conditions. Batch distribution coefficients, column performance data, and the effects of Fe-masking agents will be presented.
NTIS
Americium 241; Radioactive Wastes; Waste Disposal; Chromatography

20020003568 Los Alamos National Lab., NM USA
Fundamental-mode sources in approach-to-critical experiments
Goda, J.; Busch, R.; May 01, 2000; 16p; In English
Report No.(s): DE2001-769001; LA-UR-00-2423; No Copyright; Avail: Department of Energy Information Bridge

The 1/M method is commonly used in approach-to-critical experiments to ensure criticality safety. Ideally, a plot of 1/M versus amount of nuclear material or separation distance will be linear. However, the result is usually a curve. If the curve is concave up it is said to be conservative, since the critical mass is underestimated. However, it is possible for the curve to be non-conservative and overestimate the critical mass. This paper discusses one of the factors contributing to the shape of the 1/M curve and how it can be predicted and measured. Two source distributions, producing the same number of spontaneous fission neutrons, will not necessarily contribute equally towards the multiplication of a given system. For this reason equally sized units added during an approach-to-critical will have different effects on the multiplication of the system. A method of denoting the relative importance of source distributions is needed. One method is to compare any given source distribution to its equivalent fundamental-mode source distribution. An equivalent fundamental-mode source is an imaginary source distributed identically in space, energy, and angle to the fundamental-mode fission source that would produce the same neutron multiplication as the given source distribution. A factor, denoted as g* and defined as the ratio of the fixed-source multiplication to the fundamental-mode multiplication, is used to relate a given source strength to its equivalent fundamental-mode source strength.
NTIS
Critical Experiments; Mathematical Models; Critical Mass

20020003569 Argonne National Lab., IL USA
Molecular dynamics simulation of local structure and vibrational spectrum of uranyl UO2(2+) in vitreous B2O3
Zhuang, Z. H.; Liu, G. K.; Beitz, J. V.; Nov. 03, 2000; 4p; In English
Report No.(s): DE2001-768603; ANL/CHM/CP-103227; No Copyright; Avail: Department of Energy Information Bridge

Laser spectroscopic and extended X-ray absorption fine structure (EXAFS) spectra have shown that uranium in B(sub 2)O(sub 3) glass matrix forms uranyl in the electronic configuration of (UO(sub 2))(sup 2+),but its surrounding structure is not well known. Understanding of uranyl local structure, ion-ligand interaction, and chemical stability on the nanometer scale in glasses is essential in management of long-term performance of high-level nuclear wastes after disposal in a geologic repository. In the present work, the structure, phonon density of states, and vibrational spectrum of vitreous B(sub 2)O(sub 3) and the surrounding environment that contains a uranyl ion have been studied using a molecular dynamics (MD) simulation method that utilizes the Born-Mayer-Huggins and Coulomb pair potentials and the Stillinger-Weber three-body potential. A system of 406 ions was considered in our calculation. Simulation of a thermal quenching from 3000 K to 300 K was performed to generate a uniform and equilibrium model glass matrix before structure configuration and vibrational frequencies were obtained from the system. The structure of the simulated glass is in agreement with that reported by Krogh-Moe and Mozzi et al. The characteristic network of planar boroxol (B(sub 3)O(sub 6)) rings is evident in the simulated system. A configuration of a U(sup 6+) cation in the vitreous B(sub 2)O(sub 3) matrix is shown in Fig. 1. It is shown that a nearly linear (UO(sub 2))(sup 2+) uranyl ion is coordinated by four equatorial oxygen anions in an approximately planar arrangement. The U-O bond length is approximately 0.178 nm for the axial oxygen and 0.254 nm for the equatorial oxygen, which is in good agreement with the U-O distances obtained from fitting EXAFS spectra. Based on the simulated model structure, the uranyl vibrational spectrum is simulated and compared with experimental results obtained using site-selective fluorescence line narrowing (FLN) techniques.
NTIS
Laser Spectroscopy; Uranium Compounds; Molecular Dynamics

20020003806 Los Alamos National Lab., NM USA
3He Magnetometry for a Neutron EDM Measurement
Bangert, P.; Aug. 01, 2000; 11p; In English
Report No.(s): DE2001-768778; LA-UR-00-3993; No Copyright; Avail: Department of Energy Information Bridge, Microfiche

The behavior of small amounts of polarized (sup 3)He in a bath of superfluid (sup 4)He at temperatures below 1 K is critical to a new technique for measuring the EDM of the neutron. We report on studies to enhance the number of ultracold neutrons

produced in such a bath, on the development of neutron tomography in gaseous mixtures, on magnet properties associated with the precession of (sup 3)He, and on preparations for tests of the distribution and diffusion coefficients of (sup 3)He in the bath. NTIS

Polarization; Diffusion; Magnetic Properties; Diffusion Coefficient; Gas Mixtures

20020003811 Atomic Energy Commission, Idaho Falls, ID USA

Corrosion Evaluation of INTEC Waste Storage Tank WM-182

Dirk, W. J.; Anderson, P. A.; Nov. 01, 1999; 23p; In English

Report No.(s): DE2001-768740; INEEL/EXT-99-01109; No Copyright; Avail: Department of Energy Information Bridge, Microfiche

Irradiated nuclear fuel has been stored and reprocessed at the Idaho National Engineering and Environmental Laboratory since 1953 using facilities located at the Idaho Nuclear Technology and Engineering Center (INTEC). This reprocessing produced radioactive liquid waste which was stored in the Tank Farm. The INTEC Tank Farm consists of eleven vaulted 300,000-gallon underground tanks including Tank WM-182. Tank WM-182 was put into service in 1955, has been filled four times, and has contained aluminum and zirconium fuel reprocessing wastes as well as sodium bearing waste. A program to monitor corrosion in the waste tanks was initiated in 1953 when the first of the eleven Tank Farm tanks was placed in service. Austenitic stainless steel coupons representative of the materials of construction of the tanks are used to monitor internal tank corrosion. This report documents the final inspection of the WM-182 corrosion coupons. Physical examination of the welded corrosion test coupons exposed to the tank bottom conditions of Tank WM-182 revealed very light uniform corrosion. Examination of the external surfaces of the extruded pipe samples showed very light uniform corrosion with slight indications of preferential attack parallel to extrusion marks and start of end grain attack of the cut edges. These indications were only evident when examined under stereo microscope at magnifications of 20X and above. There were no definite indications of localized corrosion, such as cracking, pitting, preferential weld attack, or weld heat affected zone attack on either the welded or extruded coupons. Visual examination of the coupon support cables, where they were not encased in plastic, failed to reveal any indication of liquid-liquid interface attack of any crevice corrosion. Based on the WM-182 coupon evaluations, which have occurred throughout the life of the tank, the metal loss from the tank wall due to uniform corrosion is not expected to exceed 5.5 x 10-1 mil (0.00 055 inch). For purposes of waste storage, this is a negligible amount of metal loss. Localized corrosion such as cracking, pitting, preferential weld attack, or weld heat affected zone attack is not expected to be a materials problem in the tank.
NTIS

Liquid Wastes; Corrosion; Radioactive Wastes; Corrosion Tests

20020003816 Argonne National Lab., IL USA

Characterization of uranium corrosion product colloids by dynamic light scattering

Mertz, C.; Bowers, D.; Goldberg, M.; Shelton-Davis, C.; Nov. 16, 2000; 12p; In English

Report No.(s): DE2001-768626; ANL/CMT/CP-103433; No Copyright; Avail: Department of Energy Information Bridge

The Department of Energy (DOE) plans to dispose of approximately 2100 metric tons of spent metallic uranium fuel in the mined repository at Yucca Mountain. Laboratory studies at Argonne National Laboratory have shown that corrosion of metallic uranium fuel with groundwater generates significant quantities of stable colloids. This finding is considered very important in light of the recent report (1) of rapid subsurface transport of radionuclides at the Nevada Test Site via colloids. Thus, sparingly soluble radionuclides can be transported with the colloids through the subsurface aqueous environment to much greater distances than is predicted based on the aqueous volubility of the radionuclides alone. Accordingly, characterization of colloids generated by fuel corrosion is necessary for assessing the long-term fate and transport of radionuclides in the repository environment.
NTIS

Colloids; Uranium; Spent Fuels; Waste Disposal; Radioactive Wastes; Transport Properties

20020003818 Argonne National Lab., IL USA

Thermal fatigue due to beam interruptions in a Lead-Bismuth cooled ATW blanket

Dunn, F.; Nov. 15, 2000; 11p; In English

Report No.(s): DE2001-768624; ANL/RA/CP-103424; No Copyright; Avail: Department of Energy Information Bridge

Thermal fatigue consequences of frequent accelerator beam interruptions are quantified for both sodium and lead-bismuth cooled blankets in current designs for accelerator transmutation of waste devices. Temperature response was calculated using the SASSYS-1 systems analysis code for an immediate drop in beam current from full power to zero. Coolant temperatures from SASSYS-1 were fed into a multi-node structure temperature calculation to obtain thermal strains for various structural components. Fatigue curves from the American Society of Mechanical Engineers Boiler and Pressure Vessel Code were used to

determine the number of cycles that these components could endure, based on these thermal strains. Beam interruption frequency data from a current accelerator were used to estimate design lifetimes for components. Mitigation options for reducing thermal fatigue are discussed.
NTIS
Particle Acceleration; Beam Currents; Thermal Fatigue; Radioactive Wastes; Transmutation

20020003822 Argonne National Lab., IL USA
Measurement and analysis of quadruple alpha gamma gamma angular correlations for high spin states of Mg-24
Wiedenhover, I.; Wuosmaa, A. H.; Lister, C. J.; Carpenter, M. P.; Janssens, R. V. F.; Oct. 30, 2000; 8p; In English
Report No.(s): DE2001-768601; ANL/PHY/CP-103223; No Copyright; Avail: Department of Energy Information Bridge
The high-lying, (alpha)-decaying states in (sup 24)Mg have been studied by measuring the complete decay path of (alpha) and (gamma) emissions using five segmented Silicon detectors in conjunction with GAMMASPHERE. The authors analyzed the ((alpha)(gamma)) triple angular correlations and, for the first time, ((alpha)(gamma)(gamma)) quadruple correlations. The data analysis is based on a new Fourier transformation technique. The power of the technique is demonstrated.
NTIS
Fourier Transformation; Radioactive Decay; Magnesium Isotopes; Isotopic Spin

20020003932 Argonne National Lab., IL USA
Preliminary assessment of the BREST reactor design and fuel cycle concept
Khalil, H.; Lineberry, J. E.; Cahalan, J. E.; Willit, J. L.; Spencer, B. W.; Sep. 19, 2000; 46p; In English
Report No.(s): DE2001-768560; ANL-00/22; No Copyright; Avail: Department of Energy Information Bridge, Microfiche
A preliminary assessment has been performed of the BREST reactor design and fuel cycle concept being developed by Russian Federation nuclear-power design organizations and research institutes. BREST is an advanced nuclear power concept employing a fast-spectrum reactor, liquid lead coolant, uranium-plutonium nitride fuel, and a pool type plant configuration featuring design simplification and passive 'deterministic' safety as targeted means of achieving cost reduction. A closed fuel cycle that avoids separation of fissile materials, retains a fraction of the fission products in recycled fuel, and minimizes discharge of long-lived radio-toxic nuclides is proposed for eventual large-scale deployment.
NTIS
Fast Nuclear Reactors; Closed Cycles; Fission Products; Fissionable Materials

20020003939 Los Alamos National Lab., NM USA
LEDA beam operations milestone and observed beam transmission characteristics
Rybarcyk, L.; Sep. 01, 2000; 6p; In English
Report No.(s): DE2001-768253; LA-UR-00-3742; No Copyright; Avail: Department of Energy Information Bridge, Microfiche
Recently, the Low-Energy Demonstration Accelerator (LEDA) portion of the Accelerator Production of Tritium (APT) project reached its 100-mA, 8-hr CW beam operation milestone. LEDA consists of a 75-keV proton injector, 6.7-MeV, 350-MHz CW radio-frequency quadruple (RFQ) with associated high-power and low-level rf systems, a short high-energy beam transport (HEBT) and high-power (670-kW CW) beam dump. During the commissioning phase it was discovered that the RFQ field level needs to be approximately 5-10% higher than design in order to accelerate the full 100-mA beam with low losses. Upon further investigation, we have observed that the beam transmission for the 100-mA low-duty-factor beam is unexpectedly low for RFQ field levels between 90 and 105% of design. This paper will describe some aspects of LEDA operations critical to achieving the above milestone. Measurement and simulation results focused on understanding this reduced beam transmission for the RFQ operating at design conditions are also presented.
NTIS
Continuous Radiation; Protons; Injectors

20020004345 Los Alamos National Lab., NM USA
Reducing beam coupling impedances in sns ring extraction kickers
Kurennoy, S. S.; Davino, D.; Lee, Y.; Jun. 01, 2001; 4p; In English
Report No.(s): DE2001-783205; LA-UR-01-3092; No Copyright; Avail: Department of Energy Information Bridge, Microfiche
The Spallation Neutron Source (SNS) Accumulator ring extraction system includes 14 modules of window-frame ferrite pulsing kicker magnets with the rise time of about 200 ns. Their contribution to the beam coupling impedances is a serious concern. The kicker impedances, as well as its deflecting magnetic field versus time, are studied using detailed 3-D MAFIA modeling. Various design options, external circuit resistances, and a range of ferrite permeabilities are explored. A kicker module with wide

conductor windings around the ferrite behind the kicker current sheet suggests a significant reduction of the kicker transverse and longitudinal coupling impedances. This design provides a good extraction field performance, as demonstrated by electromagnetic simulations. Results of measurements for a small model are also presented.
NTIS
Proton Beams; Spallation; Neutron Sources; Magnetic Fields

20020004346 Los Alamos National Lab., NM USA
Testing pulse forming networks with darht accelerator cells
Rose, E. A.; Dalmas, D. A.; Downing, J. N.; Temple, R. D.; Jun. 01, 2001; 5p; In English
Report No.(s): DE2001-783206; LA-UR-01-3112; No Copyright; Avail: Department of Energy Information Bridge, Microfiche
The Dual Axis Radiographic Hydrotest Facility (DARHT) at Los Alamos will use two induction linacs to produce high-energy electron beams. The electron beams will be used to generate x-rays from bremsstrahlung targets. The x-rays will be used to produce radiographs. The first accelerator is operational now, generating a 60-nanosecond electron beam. The second accelerator is under construction. It will generate a 2-microsecond electron beam.
NTIS
Pulses; Electron Beams; Radiography

20020005054 Argonne National Lab., IL USA
Isotopic Germanium Targets for High Beam Current Applications at GAMMASPHERE
Greene, J. P.; Lauritsen, T.; Nov. 29, 2000; 5p; In English
Report No.(s): DE2001-768637; ANL/PHY/CP-103548; No Copyright; Avail: Department of Energy Information Bridge
The creation of a specific heavy ion residue via heavy ion fusion can usually be achieved through a number of beam and target combinations. Sometimes it is necessary to choose combinations with rare beams and/or difficult targets in order to achieve the physics goals of an experiment. A case in point was a recent experiment to produce Dy-152 at very high spins and low excitation energy with detection of the residue in a recoil mass analyzer. Both to create the nucleus cold and with a small recoil-cone so that the efficiency of the mass analyzer would be high, it was necessary to use the Se-80 on Ge-76 reaction rather than the standard Ca-48 on Pd-108 reaction. Because the recoil velocity of the Dy-152 residues was very high using this symmetric reaction (5% v/c), it was furthermore necessary to use a stack of two thin targets to reduce the Doppler broadening. Germanium targets are fragile and do not withstand high beam currents, therefore the Ge-76 target stacks were mounted on a rotating target wheel. A description of the Ge-76 target stack preparation will be presented and the target performance described.
NTIS
Dysprosium Isotopes; Germanium Isotopes; Residues; Targets

20020005079 Sandia National Labs., Albuquerque, NM USA
Study of Phosphors Efficiency and Homogeneity using a Nuclear Microprobe
Yang,; Doyle,; Nigam,; ElBouanani,; Duggan,; Dec. 08, 2000; 10p; In English
Report No.(s): DE2001-771525; SAND2000-3054C; No Copyright; Avail: Department of Energy Information Bridge
Ion Beam Induced Luminescence (IBIL) and Ion Beam Induced Charge Collection (IBICC) have been applied in the study of the luminescence emission efficiency and investigation of the homogeneity of the luminescence emission in phosphors. The IBIL imaging was performed by using sharply focused ion beams or broad/partially-focused ion beams. The luminescence emission homogeneity in samples was examined to reveal possible distributed crystal-defects that may lead to the inhomogeneity of the luminescence emission in samples.The purpose of the study is to search for suitable luminescent thin films that have high homogeneity of luminescence emission, large IBIL efficiency under heavy ion excitation, and can be placed as a thin layer on the top of microelectronic devices to be analyzed with Ion Photon Emission Microscopy (IPEM). The emission yield was found to be low for organic materials, due to saturation of the light output dependence on the energy deposition of heavy ions. The emission yield of a typical Bicron plastic scintillator is about 70 photons/ion/micron. Inorganic materials may have higher IBIL yield under high-energy and heavy-ion excitation, but the challenging problem is the inhomogeneity of the IBIL emission. The IBIL image techniques are applied in the investigation of the homogeneity of a GaN epitaxial thin film, a zircon single crystal and a thin layer coated by Thiogallate(EuII) ceramic.
NTIS
Ion Beams; Phosphors; Homogeneity; Photons; Luminescence; Imaging Techniques; Microelectronics

20020005088 Argonne National Lab., IL USA

Some highlights in few-body nuclear physics

Holt, R. J.; Dec. 07, 2000; 20p; In English

Report No.(s): DE2001-772126; ANL/PHY/CP-103613; No Copyright; Avail: Department of Energy Information Bridge, Microfiche

During the past five years, there have been tremendous advances in both experiments and theoretical calculations in few-body nuclear systems. Advances in technology have permitted experiments of unprecedented accuracy. Jefferson Laboratory has begun operation and the first round of experimental results have become available. New polarization techniques have been exploited at a number of laboratories, in particular, at Jefferson Lab, IUCF, RIKEN, NIKHEF, Mainz, MIT-Bates and HERMES. Some of these results will be shown here. In addition, there have been tremendous advances in few-body theory. Five modern two-nucleon potentials have which describe the nucleon-nucleon data extremely well have become available. A standard model of nuclear physics based on these two nucleon potentials as well as modern three-nucleon forces has emerged. This standard model has enjoyed tremendous success in the few body systems. Exact three-body calculations have been extended into the continuum in order to take full advantage of scattering data in advancing our understanding of the the few-nucleon system. In addition, the application of chiral symmetry has become an important constraint on nucleon-nucleon as well as three-nucleon forces. As a result of all these efforts, we have seen rapid developments in the three-body force. Despite these advances, there remain some extremely important open issues: (1) What is the role of quarks and gluons in nuclear structure; (2) Can we distinguish meson exchange from quark interchange; (3) Is few-body theory sufficient to describe simultaneously the mass 2, 3 and 4 form factors; (4) What is the isospin and spin dependence of the three-body force; (5) Are there medium modifications for nucleons and mesons in nuclei; (6) Is there an enhancement of antiquarks or pions in nuclei related to the binding; and (7) Are short range correlations observable in nuclei. In this paper the author summarizes the status of our understanding of these issues.

NTIS

Nuclear Physics; Quarks; Scattering; Nucleon-Nucleon Interactions

20020005221 Argonne National Lab., IL USA

Fast-neutrons incident on holmium

Smith, A. B.; Dec. 07, 2000; 40p; In English

Report No.(s): DE2001-772141; ANL/NDM-151; No Copyright; Avail: Department of Energy Information Bridge

Reports in the Argonne National Laboratory Nuclear Data and Measurement Series present results of studies in the field of microscopic nuclear data. The primary objective of the series is the dissemination of information in the comprehensive form required for nuclear technology applications. This Series is devoted to: (1) measured microscopic nuclear parameters, (2) experimental techniques and facilities employed in measurements, (3) the analysis, correlation and interpretation of nuclear data, and (4) the compilation and evaluation of nuclear data. Contributions to this Series are reviewed to assure technical competence and, unless otherwise stated, the contents can be formally referenced. This Series does not supplant formal journal publication, but it does provide the more extensive information required for technological applications (e.g., tabulated numerical data) in a timely manner.

NTIS

Fast Neutrons; Holmium; Technology Utilization

20020005237 Atomic Energy Commission, Idaho Falls, ID USA

Design of an Actinide Burning, Lead or Lead-Bismuth Cooled Reactor that Produces Low Cost Electricity

MacDonald, P. E.; Todreas, N.; Jul. 01, 2000; 173p; In English

Report No.(s): DE2001-773994; INEEL/EXT-2000-00994; MIT-ANP-PR-071; No Copyright; Avail: Department of Energy Information Bridge, Microfiche

The purpose of this Idaho National Engineering and Environmental Laboratory (INEEL) and Massachusetts Institute of Technology (MIT) University Research Consortium (URC) project is to investigate the suitability of lead or lead-bismuth cooled fast reactors for producing low-cost electricity as well as for actinide burning. The goal is to identify and analyze the key technical issues in core neutronics, materials, thermal-hydraulics, fuels, and economics associated with the development of this reactor concept. Work has been accomplished in four major areas of research: core neutronic design, material compatibility, plant engineering, and coolant activation. In the area of core neutronic design, the reactivity vs. burnup and discharge isotopics of both non-fertile and fertile fuels were evaluated. An innovative core for pure actinide burning that uses streaming, fertile-free fuel assemblies was studied in depth. This particular core exhibits excellent reactivity performance upon coolant voiding, even for voids that occur in the core center, and has a transuranic (TRU) destruction rate that is comparable to the proposed accelerator transmutation of waste (ATW) facility. These studies suggest that a core can be designed to achieve a long life while maintaining

safety and minimizing waste. In the area of material compatibility studies, an experimental apparatus for the investigation of the flow-assisted dissolution and precipitation (corrosion) of potential fuel cladding and structural materials has been designed and built at the INEEL. The INEEL forced-convection corrosion cell consists of a small heated vessel with a shroud and gas flow system. The corrosion cell is being used to test steel that is commercially available in the US to temperatures above 650 C. Progress in plant engineering was made for two reactor concepts, one utilizing an indirect cycle with heat exchangers and the other utilizing a direct-contact steam cycle. The evaluation of the indirect cycle designs has investigated the effects of various parameters to increase electric production at full power. For the direct-contact reactor, major issues related to the direct-contact heat transfer rate and entrainment and carryover of liquid lead-bismuth to the turbine have been identified and analyzed. An economic analysis approach was also developed to determine the cost of electricity production in the lead-bismuth reactor. The approach will be formulated into a model and applied to develop scientific cost estimates for the different reactor designs and thus aid in the selection of the most economic option. In the area of lead-bismuth coolant activation, the radiological hazard was evaluated with particular emphasis on the direct-contact reactor. In this system, the lack of a physical barrier between the primary and secondary coolant favors the release of the alpha-emitter Po-210 and its transport throughout the plant. Modeling undertaken on the basis of the scarce information available in the literature confirmed the importance of this issue, as well as the need for experimental work to reduce the uncertainties on the basic characteristics of volatile polonium chemical forms.
NTIS
Electric Power Supplies; Fast Nuclear Reactors; Bismuth; Lead (Metal); Reactor Design

20020005402 Los Alamos National Lab., NM USA
Theory of proton emitters
Talou, P.; Aug. 01, 2000; 14p; In English
Report No.(s): DE2001-768889; LA-UR-00-3478; No Copyright; Avail: Department of Energy Information Bridge, Microfiche
Modern theoretical methods used to interpret recent experimental data on ground-state proton emission near the proton drip line are reviewed. Most of them are stationary and are aimed to compute proton decay widths (Gamma)(sub p) only. Comparison is made between these approaches before being compared to experimental data. Our time-dependent approach based on the numerical solution of the time-dependent Schroedinger equation (TDSE) for initial quasi-stationary single-proton states is then introduced. It is shown that much deeper insights into the physics of this clean multidimensional quantum tunneling effect can be accessed, and that in addition to (Gamma)(sub p), other physical quantities could be tested experimentally, offering new stringent tests on nuclear physics models away from the valley of (beta)-stability. Finally, the necessity of using the TDSE approach in more complex, dynamical, problems is demonstrated.
NTIS
Nuclear Physics; Protons; Particle Decay; Emitters

20020005409 Los Alamos National Lab., NM USA
Subpicosecond electron bunch diagnostic
Russell, S.; Jun. 01, 2000; 18p; In English
Report No.(s): DE2001-769084; LA-UR-00-2135; No Copyright; Avail: Department of Energy Information Bridge, Microfiche
This is the final report of a three-year, Laboratory-Directed Research and Development (LDRD) project at the Los Alamos National Laboratory (LANL). The purpose of this LDRD project was to develop new, inexpensive, simple electron beam bunch-length diagnostics with resolutions below 1/4 picosecond (ps). Our approach to this problem was three pronged. First, it was our intent to build a streak camera with 1/2 ps resolution. This conventional diagnostic was to be used to verify the results of two novel measurement techniques. Second, we wished to investigate the utility of off-axis coherent Smith-Purcell radiation as a bunch-length diagnostic. Finally, we planned to demonstrate a measurement of the electron bunch-length using a transversely deflecting RF field and a beam position monitor (BPM).
NTIS
Beams (Radiation); Coherent Radiation; Diagnosis; Electron Bunching

20020005815 Los Alamos National Lab., NM USA
High-power circulator test results at 350 and 700 MHz
Roybal, W.; Aug. 01, 2000; 13p; In English
Report No.(s): DE2001-768261; LA-UR-00-3726; No Copyright; Avail: Department of Energy Information Bridge
The high-power RF systems for the Accelerator Production of Tritium (APT) program require high-power circulators at 350 MHz and 700 MHz to protect 1 MW Continuous Wave (CW) klystrons from reflected power. The 350 MHz circulator is based on the CERN, EXF, and APS designs and has performed very well. The 700 MHz circulator is a new design. Prototype 700 MHz

circulators have been high-power tested at Los Alamos National Laboratory (LANL). The first of these circulators has satisfied performance requirements. The circulator requirements, results from the testing, and lessons learned from this development are presented and discussed.
NTIS
Continuous Radiation; Radio Frequencies; Klystrons; Accelerators

20020005838 Los Alamos National Lab., NM USA
Effects of transverse beam size in beam positions monitors
Kurennoy, S. S.; Jun. 01, 2001; 4p; In English
Report No.(s): DE2001-783300; LA-UR-01-3180; No Copyright; Avail: Department of Energy Information Bridge

The fields produced by a long beam with a given transverse charge distribution in a homogeneous vacuum chamber are studied. Signals induced by the displaced finite-size beam on electrodes of a beam position monitor (BPM) are calculated and compared to those from a pencil beam. The non-linearities and corrections to BPM signals due to a finite transverse beam size are calculated for an arbitrary chamber cross section. Simple analytical expressions are given for a few particular transverse distributions of the beam current in a circular or rectangular chamber. of particular interest is a general proof that in an arbitrary homogeneous chamber the beam-size corrections vanish for any axisymmetric bean current distribution.
NTIS
Beams (Radiation); Beam Currents; Charge Distribution; Current Distribution

20020005840 Los Alamos National Lab., NM USA
Analysis of the slot heating of the coupled cavity linac cavity
Konecni, S.; Bultman, N. K.; Jun. 01, 2001; 4p; In English
Report No.(s): DE2001-783311; LA-UR-01-3208; No Copyright; Avail: Department of Energy Information Bridge

A series of four linear implosions experiments, denoted the Near Term Linear Experiments (NTLX) was recently conducted on the Shiva Star capacitor bank at the Air Force Research Laboratory (AFRL). Measurement of the driving currents in these experiments is required for post-shot analysis of the liner implosion and experiments conducted in the target cylinder. A Faraday rotation measurement was fielded on Shiva Star to measure the current and compare with the current measured by a Rogowski coil technique. The Faraday rotation technique measured the 16 MA currents in these experiments with better than 1% precision.
NTIS
Faraday Effect; Capacitors; Heating

20020005846 Brookhaven National Lab., Upton, NY USA
Coherent synchrotron radiation analysis for the photoinjected energy recovery linac and UVFEL projects at the NSLS
Wu,; Murphy,; Yakimenko,; Ben-Zvi,; Graves,; Aug. 16, 2001; 5p; In English
Report No.(s): DE2001-785360; BNL-68543; No Copyright; Avail: Department of Energy Information Bridge

When an electron bunch is compressed either in a chicane or a bending arc, the CSR will induce an energy redistribution along the bunch. Such energy redistribution will affect the longitudinal emittance as a direct consequence. It will also excite betatron oscillation due to the chromatic transfer functions, and hence a transverse emittance change. For the proposed Photoinjected Energy Recovery Linac (PERL) at the NSLS, bending arcs will be used for bunch compression, while for the UV Free Electron Laser (UVFEL), chicane compressors are used. Since it is normally thought to be deleterious, the CSR effects are analyzed carefully for both projects. It turns out that the CSR effect could be serious, hence schemes to reduce the effect are investigated. Such schemes are incorporated into the PERL arc design. For the UVFEL, chicane parameters are carefully chosen to minimize the CSR effects.
NTIS
Electron Bunching; Ultraviolet Lasers; Transfer Functions; Coherent Radiation

20020005852 Oak Ridge National Lab., TN USA
Materials Selection for the HFIR Cold Neutron Source
Farrell, K.; Aug. 24, 2001; 58p; In English
Report No.(s): DE2001-786477; ORNL/TM-1999/208; No Copyright; Avail: Department of Energy Information Bridge, Microfiche

In year 2002 the high Flux Isotope Reactor (HFIR) will be fitted with a source of cold neutrons to upgrade and expand its existing neutron scattering facilities. The in-reactor components of the new source consist of a moderator vessel containing supercritical hydrogen gas moderator at a temperature of 20K and pressure of 15 bar, and a surrounding vacuum vessel. They will

be installed in an enlarged beam tube located at the site of the present horizontal beam tube, HB-4, which terminates within the reactor's beryllium reflector. These components must withstand exceptional service conditions. This report describes the reasons and factors underlying the choice of 6061-T6 aluminium alloy for construction of the in-reactor components. The overwhelming considerations are the need to minimize generation of nuclear heat and to remove that heat through the flowing moderator, and to achieve a minimum service life of about 8 years coincident with the replacement schedule for the beryllium reflector. 6061-T6 aluminum alloy offers the best combination of low nuclear heating, high thermal conductivity, good fabricability, compatibility with hydrogen, superior cryogenic properties, and a well-established history of satisfactory performance in nuclear environments. These features are documented herein. An assessment is given of the expected performance of each component of the cold source.
NTIS
Cold Neutrons; High Flux Isotope Reactors; Neutron Scattering; Thermal Conductivity

20020005885 Sandia Corp., Albuquerque, NM USA
Preliminary Evaluation of Earth Targets for Use in Impact Effects Studies
Thompson, Louis J.; Colp, John L.; Mar. 1964; 66p; In English
Report No.(s): AD-A395386; SC-DR-316-63; TID-4500; No Copyright; Avail: CASI; A04, Hardcopy; A01, Microfiche

The Aerospace Nuclear Safety Program at Sandia Corporation requires an independent assessment of the safety of all nuclear power supplies used in aerospace under all conditions from factory shipment through re-entry from space. The effects of impact against any point on the earth by a nuclear power supply or its components must he evaluated as part of this assessment. This report: (1) evaluates the fundamental mechanisms involved in soil impacts by cylindrical projectiles with velocities of 500-700 feet per second; (2) defines the problem of specifying impact targets which closely simulate various portions of the earth's surface; and (3) describes an analytical and experimental program intended to obtain the information needed to properly specify a simulated earth target for use in Aerospace Nuclear Safety impact tests.
DTIC
Targets; Nuclear Electric Power Generation; Spacecraft Power Supplies; Evaluation

20020005891 Atomic Energy Commission, Idaho Falls, ID USA
Critical Parameters of Complex Geometries of Intersecting Cylinders Containing Uranyl Nitrate Solution
Briggs, J. B.; Rothe, R. E.; Jun. 14, 1999; 187p
Report No.(s): DE2001-769012; INEEL/EXT-99-00425; No Copyright; Avail: Department of Energy Information Bridge, Microfiche

About three dozen previously unreported critical configurations are presented for very complex geometries filled with high concentration enriched uranyl nitrate solution. These geometries resemble a tall, thin Central Column (or trunk of a 'tree') having long, thin arms (or 'branches') extending up to four directions off the column. Arms are equally spaced from one another in vertical planes, and that spacing ranges from arms in contact to quite wide spacings. Both the Central Column and the many different arms are critically safe by themselves with each, alone, is filled with fissile solution; but, in combination, criticality occurs due to the interactions between arms and the column. Such neutronic interactions formed the principal focus of this study. While these results are fresh to the nuclear criticality safety industry and to those seeking novel experiments against which to validate computer codes, the experiments, themselves, are not recent. Over 100 experiments were performed at the Rocky Flats Critical Mass Laboratory between September, 1967, and February of the following year.
NTIS
Critical Mass; Cylindrical Shells; Uranium Compounds

74
OPTICS

Includes light phenomena and the theory of optical devices. For lasers see 36 Lasers and Masers.

20020000747 Lawrence Livermore National Lab., Livermore, CA USA
Development of continuous glass melting for production of Nd-doped phosphate glasses for the NIF and LMJ laser system
Campbell, J. H.; Ficini-Dorn, G.; Hawley-Fedder, R.; McLean, M. J.; Suratwala, T.; Aug. 14, 1998; 11p; In English
Report No.(s): DE2001-2761; UCRL-JC-129804; DP0212000; No Copyright; Avail: Department of Energy Information Bridge, Microfiche

The NIF and LMJ laser systems require about 3380 and 4752 Nd-doped laser glass slabs, respectively. Continuous laser glass melting and forming will be used for the first time to manufacture these slabs. Two vendors have been chosen to produce the glass:

Hoya Corporation and Schott Glass Technologies. The laser glass melting systems that each of these two vendors have designed, built and tested are arguably the most advanced in the world. Production of the laser glass will begin on a pilot scale in the fall of 1999.
NTIS
Glass; Laser Materials; Melting; Doped Crystals; Phosphates; Neodymium

20020000748 Lawrence Livermore National Lab., Livermore, CA USA
Fail-safe design for square vacuum-barrier windows
Campbell, J. H.; Steele, R. A.; Steele, W. A.; Suratwala, T. I.; Jul. 30, 1998; 12p; In English
Report No.(s): DE2001-2762; UCRL-JC-129805; No Copyright; Avail: Department of Energy Information Bridge, Microfiche

Laser-induced damage on the tensile side of vacuum-barrier fused silica optics can result in catastrophic fracture. This fracture can lead to two possible modes of failure: a benign failure resulting in a slow air leak into the vacuum chamber or an implosion. In previous work, they measured fracture in round vacuum windows and lenses and proposed a fail-safe design that would insure the benign failure mode by fracturing into only two parts, thus eliminating the possibility of implosion. In this paper, they extend the previous work to include square vacuum-barrier windows and lenses.
NTIS
Fail-Safe Systems; Fracturing; Vacuum Chambers; Solid State Lasers; Silica Glass

20020000752 Oak Ridge National Lab., TN USA
Advanced Micro Optics Characterization Using Computer Generated Holograms
Arnold, S.; Maxey, L. C.; Moreshead, W.; Nogues, J. L.; Nov. 01, 1998; 28p; In English
Report No.(s): DE2001-3146; ORNL/M-6622; C/ORNL96-0424; No Copyright; Avail: Department of Energy Information Bridge

This CRADA (Cooperative Research and Development Agreement) has enabled the validation of Computer Generated Holograms (CGH) testing for certain classes of micro optics. It has also identified certain issues that are significant when considering the use of CGHs in this application. Both contributions are advantageous in the pursuit of better manufacturing and testing technologies for these important optical components.
NTIS
Holography; Computer Graphics; Optical Equipment

20020000867 Brookhaven National Lab., Upton, NY USA
Nanometer Precision in Large Surface Profilometry
Takacs,; Aug. 30, 1999; 11p; In English; 9th; 9th International Conference on Production Engineering, 30 Aug. - 1 Sep. 1999, Osaka, Japan
Contract(s)/Grant(s): AC02-98CH10886
Report No.(s): DE2001-11454; BNL-66587; KC0204011; No Copyright; Avail: Department of Energy Information Bridge, Microfiche

The Long Trace Profiler (LTP) is in use at many synchrotron radiation (SR) laboratories throughout the world and by a number of manufacturers who specialize in fabricating grazing incidence mirrors for SR and x-ray telescope applications. Recent improvements in the design and operation of the LTP system have reduced the statistical error in slope profile measurement to the 1 standard deviation level of 0.3 microradian for 0.5 meter long mirrors. This corresponds to a height error on the order of 10-20 nanometers. This level of performance allows one to measure with confidence the absolute shape of large cylindrical aspheres and spheres that have kilometer radii of curvature in the axial direction. The LTP is versatile enough to make measurements of a mirror in the face up, sideways, and face down configurations. We will illustrate the versatility of the current version of the instrument, the LTP II, and present results from two new versions of the instrument: the in situ LTP (ISLTP) and the Vertical Scan LTP (VSLTP). Both of them are based on the penta prism LTP (ppLTP) principle that utilizes a stationary optical head and moving penta prism. The ISLTP is designed to measure the distortion of high heat load mirrors during actual operation in SR beam lines. The VSLTP is designed to measure the complete 3-dimensional shape of x-ray telescope cylinder mirrors and mandrels in a vertical configuration. Scans are done both in the axial direction and in the azimuthal direction.
NTIS
Profilometers; Mirrors

20020000914 Argonne National Lab., IL USA

Retuning the APS storage ring for better chromaticity correction

Chae, Y. C.; Crosbie, E. A.; Sep. 11, 1999; 13p; In English

Report No.(s): DE2001-12097; No Copyright; Avail: Department of Energy Information Bridge, Microfiche

When the APS storage ring was retuned to provide smaller (beta)(sub y) values in the insertion straight sections, it was necessary to increase the vertical tune by at least two units. Since the design values for the horizontal and vertical tunes are 35.22 and 16.30, respectively, this put the tunes dangerously close to the sextupole 2v(sub y)-v(sub x) coupling resonance. The large injection horizontal oscillations could couple to the vertical plane and exceed the 5-mm vertical apertures that exist in some of the insertion straight sections. to avoid this resonance, the vertical tune was raised beyond the resonance to 19.30. The result was a reduction in the ability of the chromaticity sextuples to correct the chromaticity. Recent investigation has shown that the chromaticity correction capability of the sextuples can be greatly increased by a modest increase in the horizontal tune. Increasing the horizontal tune by one unit and reducing the vertical tune by three units produces a lattice with better chromaticity control while maintaining an acceptable dynamic aperture.

NTIS

Storage Rings (Particle Accelerators); Aberration; Color

20020000926 Lawrence Livermore National Lab., Livermore, CA USA

Vendor-based laser damage metrology equipment supporting the National Ignition Facility

Campbell, J. H.; Jennings, R. T.; Kimmons, J. F.; Kozlowski, M. R.; Mouser, R. P.; Jul. 27, 1998; 8p; In English

Report No.(s): DE2001-2760; UCRL-JC-129719; DP0212000; No Copyright; Avail: Department of Energy Information Bridge, Microfiche

A sizable laser damage metrology effort is required as part of optics production and installation for the 192 beam National Ignition Facility (NIF) laser. The large quantities, high damage thresholds, and large apertures of polished and coated optics necessitates vendor-based metrology equipment to assure component quality during production. This equipment must be optimized to provide the required information as rapidly as possible with limited operator experience. The damage metrology tools include: (1) platinum inclusion damage test systems for laser amplifier slabs, (2) laser conditioning stations for mirrors and polarizers, and (3) mapping and damage testing stations for UV transmissive optics. Each system includes a commercial Nd:YAG laser, a translation stage for the optics, and diagnostics to evaluate damage. The scanning parameters, optical layout, and diagnostics vary with the test fluences required and the damage morphologies expected. This paper describes the technical objectives and milestones involved in fulfilling these metrology requirements.

NTIS

Ignition; Laser Damage; Metrology; Neodymium Lasers; YAG Lasers; Light Amplifiers

20020000927 Lawrence Livermore National Lab., Livermore, CA USA

Up-conversion time microscope demonstrates 103x magnification of an ultrafast waveforms with 300 fs resolution

Bennett, C. V.; Kolner, B. H.; Oct. 17, 1998; 5p; In English

Report No.(s): DE2001-2693; UCRL-JC-132458; REPT-98-ERD-027; No Copyright; Avail: Department of Energy Information Bridge, Microfiche

We have demonstrated a system for the temporal expansion of arbitrarily shaped ultrafast optical waveforms based on the principle of temporal imaging. This system has demonstrated 103x magnification of an input signal with 300 fs resolution, thus allowing ultrafast phenomena to be recorded with slower conventional technology. The physics of temporal imaging work on a single shot basis, thus it is expected that this technology will lead to a new class of single transient recorders with ultrafast resolution.

NTIS

Imaging Techniques; Magnification; Waveforms; Optical Properties; Lasers

20020000947 Argonne National Lab., IL USA

Three-dimensional analysis of harmonic generation in self-amplified spontaneous emission

Huang, Z.; Kim, K. J.; Sep. 01, 1999; 12p

Report No.(s): DE2001-11814; ANL/ASD/CP-99050; No Copyright; Avail: Department of Energy Information Bridge, Microfiche

In a high-gain free-electron laser, strong bunching at the fundamental wavelength can drive substantial harmonic bunching and sizable power levels at the harmonic frequencies. In this paper, we investigate the three-dimensional evolution of the harmonic fields based on the coupled Maxwell-Vlasov equations that take into account the nonlinear harmonic interaction. Each harmonic

field is the sum of a self-amplified term and a term driven by the nonlinear harmonic interaction. In the exponential gain regime, the growth rate of the dominant nonlinear term is much faster than that of the self-amplified harmonic field. As a result, the gain length and the transverse profile of the first few harmonics are completely determined by those of the fundamental. A percentage of the fundamental power level is found at the third harmonic frequency right before saturation for the current self-amplified spontaneous emission projects.
NTIS
Free Electron Lasers; Harmonic Generations; Spontaneous Emission; Bunching; High Gain

20020000948 Argonne National Lab., IL USA
Observation of the structural phase transition in manganite films by magneto-optical imaging
Crabtree, G. W.; Lin, Y.; Miller, D. J.; Nikitenko, V. I.; Vlasko-Vlasov, V. K.; Aug. 31, 1999; 13p; In English
Report No.(s): DE2001-11955; ANL/MSD/CP-99963; No Copyright; Avail: Department of Energy Information Bridge, Microfiche

A high-resolution magneto-optical imaging technique is used to reveal the formation of twins occurring during a martensitic phase transition at (approximately)105K in LCMO films grown on STO substrates. The magnetic contrast arises due to the magneto-elastic tilts of the Mn - magnetic moments in the twins. Different magnetic structures are found in LCMO films grown on MgO, NGO, and LAO substrates showing the importance of the substrate material for the manganite film properties.
NTIS
Magnetic Materials; Twinning; Manganese Oxides; Substrates; Imaging Techniques; Magnetic Field Configurations; Magneto-Optics

20020001039 Lawrence Livermore National Lab., Livermore, CA USA
Installation of line replaceable units into the National Ignition Facility
Bahowick, S.; Mcmahon, D.; Rowe, A.; Tiszauer, D.; Yakuma, S.; Mar. 08, 1999; 10p; In English
Report No.(s): DE2001-8515; UCRL-JC-133204; No Copyright; Avail: Department of Energy Information Bridge, Microfiche

In the National Ignition Facility (NIF), currently under design and construction at Lawrence Livermore National Laboratory (LLNL), 192 high-power laser beamlines incorporating over 8,000 large optics, are focused onto a target smaller than a dime. The actual laser path will be contained within the Laser Target Area Building (LTAB), but the smaller adjacent building, the Optics Assembly Building, is where the optic modules are assembled and aligned. After the optics are finished in the OAB they must be transported and installed into the LTAB. While this is done strict cleanliness and handling conditions must be maintained. to maximize the efficiency of this process the optics are assembled into Line Replaceable Units (LRUs), which typically consist of a mechanical housing, laser optics, utilities, actuators and kinematic mounts. In this paper the Optical Transport and Material Handling designs that will be used to deliver the LRUs into the NIF laser bays are presented. Five types of delivery systems have been developed to deliver the LRUs to their locations in the LTAB. They are top loading, bottom loading, side loading, switchyard loading and target area loading. The first three operate in the laser bay of the LTAB and are transported between the OAB and the LTAB by the Laser Bay Transport System (LBTS). All delivery systems must maintain each optical LRU assemblies and specified shock, vibration, cleanliness, and environmental requirements. The design for each delivery system must take into consideration the cleanliness, functionality and alignment of the LRUs while maximizing commonality in order to meet the beamline installation schedule. This paper focuses on the design challenges of the bottom, side and top loading delivery systems and especially on how commonality among these varied systems is achieved.
NTIS
Optical Materials; Materials Handling; Loading Operations

20020001049 Lawrence Livermore National Lab., Livermore, CA USA
Brewster's Angle Thin Film Plate Polarizer Design Study from an Electric Field Perspective
Stolz, C. J.; Apr. 27, 1999; 9p; In English
Report No.(s): DE2001-8561; UCRL-JC-132199; DP0213000; No Copyright; Avail: Department of Energy Information Bridge, Microfiche

The electric field magnitude and profile influence the laser-induced damage threshold the morphology of a multilayer coating. Through the use of non-quarter-wave layer pairs in high reflector designs, the electric field peaks are shifted into the low index layers thus reducing the electric fields in the high index layers and interfaces. Similarly the electric field profile in a polarizer can be optimized for low electric fields within the high index layers and film interfaces by proper design selection.
NTIS
Electric Fields; Polarizers; Thin Films

20020001052 Lawrence Livermore National Lab., Livermore, CA USA

Laser-Induced Damage of Absorbing and Diffusing Glass Surfaces Under IR and UV Irradiation

Bletzer, K.; Genin, F. Y.; Hendrix, J. L.; Hester, M.; Whitman, P. K.; Dec. 22, 1998; 12p; In English

Report No.(s): DE2001-8569; UCRL-JC-131213; DP0212000; No Copyright; Avail: Department of Energy Information Bridge, Microfiche

In high peak power lasers used for inertial confinement fusion experiments, scattered and reflected light can carry sufficient energy to ablate metal structures or even damage other optics. Absorbing and diffuse scattering materials are required to manage the 'ghosts', stimulated Raman scattering (SRS) and unconverted light in the laser chain and target chamber. Absorbing and diffuse scattering glasses were evaluated for use at 1053-nm and 351-nm to dissipate stray light and to absorb stimulated Raman scattering from the conversion crystals. Glass samples with surfaces ranging from specular to highly scattering (etched, sandblasted) were evaluated. The morphologies of laser damage at 1064 nm and 355 nm were characterized by Nomarski optical microscopy. Laser damage was quantified by measuring mass loss. Surface treatment and bulk absorption coefficient were the two material properties most strongly correlated to laser damage. Etched and sandblasted surfaces always had lower damage threshold than their specular counterparts. Reducing rear surface fluence either by bulk absorption or scattering at the input surface delayed the onset of catastrophic failure under extreme (60 J/sq cm) conditions.

NTIS

Radiation Damage; Glass; Irradiation; Laser Damage; Raman Spectra; Scattering

20020001053 Lawrence Livermore National Lab., Livermore, CA USA

Crack Propagation in Fused Silica During UV and IR ns-Laser Illumination

Chinsio, R.; Genin, F.; Salleo, A.; Jan. 06, 1999; 16p; In English

Report No.(s): DE2001-8570; UCRL-JC-131218; No Copyright; Avail: Department of Energy Information Bridge, Microfiche

The functional lifetime of large-aperture optical components used on a laser such as the National Ignition Facility is an important engineering parameter. to predict the lifetime of fused silica transmissive optics, it is necessary to measure the rate of damage propagation as a function of fluence and understand the effects of the laser parameters (e.g., wavelength and pulse width). In order to begin such predictions without a large-area flat-top laser beam, damage growth experiments were conducted using a small (1 mm diameter) Gaussian beam. Damage was initiated by producing mechanical flaws on the surface of the optic. Since output surface damage in transmissive optics can propagate at least two orders of magnitude faster than input surface damage, the experiments were focused on damage initiated at the output surface.

NTIS

Crack Propagation; Damage; Laser Beams; Silica Glass

20020001054 Argonne National Lab., IL USA

Drive laser for the APS LEUTL FEL RF photoinjector

Arnold, N.; Koldenhoven, R.; Travish, G.; Sep. 01, 1999; 4p; In English

Report No.(s): DE2001-11813; ANL/ASD/CP-99049; No Copyright; Avail: Department of Energy Information Bridge, Microfiche

The APS LEUTL free-electron laser (FEL) is a high-gain, short-wavelength device requiring a high-current, low-emittance beam. An rf photoinjector driven by a laser is used to provide the requisite beam. The drive laser consists of a diode-pumped Nd:Glass oscillator and a chirped pulse amplification (CPA) system consisting of a grating stretcher, a flashlamp-pumped Nd:Glass regenerative amplifier, and a grating compressor. The system generates 4-mj pulses in the R with a pulse length as short as 2 ps FWHM and a repetition rate of 6 Hz. Nonlinear doubling crystals are used to generate fourth-harmonic output of (approx)500 (micro)J in the UV (263 nm), which is required to exceed the work function of the copper cathode in the gun. This paper describes the drive laser as well as the extensive controls implemented to allow for remote operation and monitoring. Performance measurements as well as the operating experience are presented.

NTIS

Beam Injection; Free Electron Lasers; High Current

20020001060 Lawrence Livermore National Lab., Livermore, CA USA

Novel Condenser for EUV Lithography Ring-field Projection Optics

Chapman, H.; Nugent, K. A.; Jul. 15, 1999; 14p; In English; 44th; 44th Annual Meeting of the International Symposium on Optical Science, Engineering, and Instrumentation, 19-23 July 1999, Denver, CO, USA; Sponsored by Society of Photographic Scientists and Engineers, USA

Contract(s)/Grant(s): W-7405-ENG-48

Report No.(s): DE2001-11971; UCRL-JC-133281; No Copyright; Avail: Department of Energy Information Bridge, Microfiche

A condenser for a ring-field extreme ultra-violet (EUV) projection lithography camera is presented. The condenser consists of a gently undulating mirror, that we refer to as a ripple plate, and which is illuminated by a collimated beam at grazing incidence. The light is incident along the ripples rather than across them, so that the incident beam is reflected onto a cone and subsequently focused on to the arc of the ring field. A quasistationary illumination is achieved, since any one field point receives light from points on the ripples, which are distributed throughout the condenser pupil. The design concept can easily be applied to illuminate projection cameras with various ring-field and numerical aperture specifications. Ray-tracing results are presented of a condenser for a 0.25 NA EUV projection camera.
NTIS
Extreme Ultraviolet Radiation; Lithography; Photographic Rectifiers; Cameras; Grazing Incidence

20020001080 Lawrence Livermore National Lab., Livermore, CA USA
Performance and production requirements for the optical components in a high-average-power laser system
Chow, R.; Doss, F. W.; Taylor, J. R.; Wong, J. N.; Jul. 02, 1999; 11p; In English
Report No.(s): DE2001-12121; UCRL-JC-132682; No Copyright; Avail: Department of Energy Information Bridge, Microfiche
Optical components needed for high-average-power lasers, such as those developed for Atomic Vapor Laser Isotope Separation (AVLIS), require high levels of performance and reliability. Over the past two decades, optical component requirements for this purpose have been optimized and performance and reliability have been demonstrated. Many of the optical components that are exposed to the high power laser light affect the quality of the beam as it is transported through the system. The specifications for these optics are described including a few parameters not previously reported and some component manufacturing and testing experience. Key words: High-average-power laser, coating efficiency, absorption, optical components
NTIS
Optical Equipment; High Power Lasers; Laser Outputs; Power Efficiency

20020001083 Lawrence Livermore National Lab., Livermore, CA USA
Analysis of Shane telescope aberration before and after collimation
Gavel, D. T.; Jan. 26, 1999; 7p; In English
Report No.(s): DE2001-12126; UCRL-ID-133548; REPT-97-ERD-037; No Copyright; Avail: Department of Energy Information Bridge, Microfiche
The Shane 3 meter telescope was recollimated in August 1998 to remove aberrations that were perceived to affect image quality in good seeing conditions. The Lick Adaptive Optics system is capable, indirectly, of measuring the static aberrations introduced by the telescope primary and secondary mirror pair. Since A0 runs were scheduled both before and after the collimation, this allowed a comparison of the pre and post collimation telescope aberrations. The absolute calibration of the wavefront measurement is complicated by the indirect measurement technique, which uses the shape of the deformable mirror in its closed-loop corrected position as an indicator of telescope wavefront. The shape of the deformable mirror is not measured directly, but is inferred from the voltages applied to its piezoelectric actuators. The actuators are known to have temperature-dependent hysteresis and is thus a source of error in this technique. In November, an interferometer was added to the A0 system which will allow more direct measurements of corrected wavefront in future tests. Data from six measurements in July (pre-collimation) and nine measurements in September and November (post-collimation) were analyzed. The resulting phase maps show a slight difference in the wavefront with some improvement in the coma and spherical zernike terms but essentially no change (except for rotation) in astigmatism and some degradation in tricoma.
NTIS
Calibrating; Telescopes; Adaptive Optics; Piezoelectricity; Temperature Dependence; Wave Fronts

20020001167 Lawrence Livermore National Lab., Livermore, CA USA
Medical Applications of Ultrashort Pulse Lasers
DaSilva, L. B.; Feit, M. D.; Kim, B. M.; Rubenchil, A. M.; Mar. 16, 1999; 5p; In English
Report No.(s): DE2001-8702; UCRL-JC-133470; REPT-97-LW-074; No Copyright; Avail: Department of Energy Information Bridge, Microfiche
The characteristics of the ultrashort pulse laser (USPL, and 1 ps) ablation of biological tissues are investigated both theoretically and experimentally. Effective USPL parameters for minimal damage and high ablation rates are discussed.
NTIS
Ablation; Laser Applications; Pulsed Lasers; Tissues (Biology)

20020001204 Argonne National Lab., IL USA

Performance of an optimally contact-cooled high-heat-load mirror at the APS

Cai, Z.; Khounsary, A.; Lai, B.; McNulty, I.; Yun, W.; Nov. 18, 1998; 14p; In English

Report No.(s): DE2001-12356; ANL/XFD/CP-97686; No Copyright; Avail: Department of Energy Information Bridge, Microfiche

X-ray undulator beamlines at third-generation synchrotrons facilities use either a monochromator or a mirror as the first optical element. In this paper, the thermal and optical performance of an optimally designed contact-cooled high-heat-load x-ray mirror used as the first optical element on the 2ID undulator beamline at the Advanced Photon Source (APS) is reported. It is shown that this simple and economical mirror design can comfortably handle the high heat load of undulator beamlines and provide good performance with long-term reliability and ease of operation. Availability and advantages of such mirrors can make the mirror-first approach to high-heat-load beamline design an attractive alternative to monochromator-first beamlines in many circumstances.

NTIS

Photons; Mirrors; X Rays

20020001216 Lawrence Livermore National Lab., Livermore, CA USA

Laser Conditioning Methods of Hafnia Silica Multilayer Mirrors

Hue, J.; Maricle, S. M.; Schwartz, S.; Sheehan, L. M.; Stolz, C. J.; Dec. 23, 1999; 11p; In English

Report No.(s): DE2001-8579; UCRL-JC-131215; DP0212000; No Copyright; Avail: Department of Energy Information Bridge, Microfiche

A variety of 1064-nm laser conditioning methods were investigated to find the optimum method for production of large aperture (0.25 sq m) multilayer coatings for the National Ignition Facility and Laser MegaJoule. Two conditioning methods were explored, multi-step and single-step on two different laser systems. Off-line conditioning was done on PLATO, a small beam (diameter-1 mm) raster scanning system. On-line conditioning was done on Beamlet, a single beam prototype of the National Ignition Facility with a large rectangular beam (35 cm x 35 cm). Concurrent with this work, coating process development for low-defect density high damage threshold coatings was realized by switching from hafnia to hafnium starting materials. The results of this study suggest that single-step raster-scan off-line laser conditioning is an effective method to raise the damage threshold of multilayer mirrors deposited from hafnium and silica by reactive electron beam deposition.

NTIS

Lasers; Mirrors; Laser Beams

20020001223 Sandia National Labs., Albuquerque, NM USA

Photoluminescence Studies of Lateral Composition Modulated Short-Period AlAs/InAs Superlattices

Ahrenkiel, S. P.; Follstaedt, D. M.; Jones, E. D.; Lee, S. R.; Mascarenhas, A.; Jan. 04, 1999; 8p; In English

Report No.(s): DE2001-2827; SAND98-1478C; No Copyright; Avail: Department of Energy Information Bridge, Microfiche

We present low temperature photoluminescence data for a series of spontaneous lateral composition modulation in (AlAs)(sub m)/(InAs)(sub n) short period superlattices on InP with differing average lattice constants, i.e., varying global strain. The low temperature photoluminescence peak energies were found to be much lower than the corresponding energy expected for the equivalent In(sub x)Al(sub 1(minus)x)As alloy. The bandgap energy reductions are found to approach 500 meV and this reduction is found to correlate with the strength of the composition modulation wave amplitude.

NTIS

Photoluminescence; Superlattices; Indium Arsenides; Aluminum Arsenides

20020001296 Lawrence Livermore National Lab., Livermore, CA USA

Medical applications of ultra-short pulse lasers

Kim, B. M.; Marion, J. E.; Jun. 08, 1999; 11p; In English

Report No.(s): DE2001-12151; UCRL-JC-133470-REV-1; No Copyright; Avail: Department of Energy Information Bridge, Microfiche

The medical applications for ultra short pulse lasers (USPLs) and their associated commercial potential are reviewed. Short pulse lasers offer the surgeon the possibility of precision cutting or disruption of tissue with virtually no thermal or mechanical damage to the surrounding areas. Therefore the USPL offers potential improvement to numerous existing medical procedures. Secondly, when USPLs are combined with advanced tissue diagnostics, there are possibilities for tissue-selective precision ablation that may allow for new surgeries that cannot at present be performed. Here we briefly review the advantages of short pulse lasers, examine the potential markets both from an investment community perspective, and from the view. of the technology

provider. Finally nominal performance and cost requirements for the lasers, delivery systems and diagnostics and the present state of development will be addressed.
NTIS
Medical Science; Ultrashort Pulsed Lasers; Tissues (Biology); Commerce

20020001513 Argonne National Lab., IL USA
Overview of bunch length measurements
Lumpkin, A. H.; Feb. 19, 1999; 12p; In English
Report No.(s): DE2001-12343; ANL/ASD/CP-98442; No Copyright; Avail: Department of Energy Information Bridge, Microfiche

An overview of particle and photon beam bunch length measurements is presented in the context of free-electron laser (FEL) challenges. Particle-beam peak current is a critical factor in obtaining adequate FEL gain for both oscillators and self-amplified spontaneous emission (SASE) devices. Since measurement of charge is a standard measurement, the bunch length becomes the key issue for ultrashort bunches. Both time-domain and frequency-domain techniques are presented in the context of using electromagnetic radiation over eight orders of magnitude in wavelength. In addition, the measurement of microbunching in a micropulse is addressed.
NTIS
Particle Beams; Photon Beams; Free Electron Lasers

20020001518 Lawrence Livermore National Lab., Livermore, CA USA
Optical interferometry diagnostics in laser-driven equation of state experiments
Cauble, R. C.; Celliers, P. M.; Collins, G. W.; Da Silva, L. B.; Gold, D. M.; Jun. 18, 1999; 6p; In English
Report No.(s): DE2001-12155; UCRL-JC-134798; No Copyright; Avail: Department of Energy Information Bridge, Microfiche

We have developed and tested several optical interferometric diagnostics to measure preheat and shock velocity in high-pressure equation of state experiments on the Nova laser. Theory and practical application of interferometric measurement techniques with illustrative experimental results are presented.
NTIS
Diagnosis; Equations of State; Interferometry; Lasers; Optical Properties

20020001544 Lawrence Livermore National Lab., Livermore, CA USA
IODC98 optical design problem: method of progressing from an ahromatic to an apochromatic design
Seppala, L. G.; Jul. 20, 1998; 11p; In English
Report No.(s): DE2001-2804; UCRL-JC-131432; No Copyright; Avail: Department of Energy Information Bridge, Microfiche

A general method of designing an apochromatic lens by using a triplet of special glasses, in which the buried surfaces concept is used, can be outlined. First, one initially chooses a starting point which is already achromatic. Second, a thick plate or shell is added to the design, where the plate or shell has an index of refraction 1.62, which is similar to the special glass triplet average index of refraction (for example: PSK53A, KZFS1 and TIF6). Third, the lens is then reoptimized to an achromatic design. Fourth, the single element is replaced by the special glass triplet. Fifth, only the internal surfaces of the triplet are varied to correct all three wavelengths. Although this step will produce little improvement, it does serve to stabilize further optimization. Sixth and finally, all potential variables are used to fully optimize the apochromatic lens. Microscope objectives, for example, could be designed using this technique. The important concept to apply is the use of multiple buried surfaces in which each interface involves a special glass, after an achromatic design has been achieved. This extension relieves the restriction that all special glasses have a common index of refraction and allows a wider variety of special glasses to be used. However, it is still desirable to use glasses which form a large triangle on the P versus V diagram.
NTIS
Lenses; Glass; Optical Properties

20020001554 Oak Ridge National Lab., TN USA
Production of Testing of Laser Crystals
Schmidt, T.; Jan. 21, 1999; 19p; In English
Report No.(s): DE2001-4283; Y/AMT-621; CRADA-Y-1295-0354; No Copyright; Avail: Department of Energy Information Bridge, Microfiche

Lasers and nonlinear optical system are being developed to allow the construction of all solid state lasers with tunable output in the mid-infrared (3-5(micro)m). In these systems potassium titanyl phosphate (KTP) and its analogs (KTA, RTA and CTA) are

used to construct Optical Parametric Oscillators (OPOs). In the past, large (5 mm x 5 mm x 15 mm) crystals of KTA, RTA and CTA have been difficult to obtain, and were costly as well. Also, the arsenate materials were limited in spectral range due to an AsO(sub 4) overtone in the 3.5 to 5.0 (micro)m region. There has also been interest in materials which self-OPO. This process is done by doping nonlinear materials with lasing ions. This effort investigated the development of mixed metal analogs of KTA, which would last and also suppress the AsO(sub 4) absorption overtones to allow more efficient mid-infrared OPO operation.
NTIS
Crystals; Nonlinearity; Solid State Lasers; Parametric Amplifiers; Optical Properties

20020001583 Argonne National Lab., IL USA
Vibratory response modeling and verification of a high precision optical positioning system
Barraza, J.; Kuzay, T.; Royston, T. J.; Shu, D.; Jun. 18, 1999; 14p; In English
Report No.(s): DE2001-12425; ANL/XFD/CP-98207; No Copyright; Avail: Department of Energy Information Bridge, Microfiche

A generic vibratory-response modeling program has been developed as a tool for designing high-precision optical positioning systems. Based on multibody dynamics theory, the system is modeled as rigid-body structures connected by linear elastic elements, such as complex actuators and bearings. The full dynamic properties of each element are determined experimentally or theoretically, then integrated into the program as inertial and stiffness matrices. Utilizing this program, the theoretical and experimental verification of the vibratory behavior of a double-multilayer monochromator support and positioning system is presented. Results of parametric design studies that investigate the influence of support floor dynamics and highlight important design issues are also presented. Overall, good matches between theory and experiment demonstrate the effectiveness of the program as a dynamic modeling tool.
NTIS
Monochromators; Vibration; Mathematical Models; Dynamic Characteristics; Program Verification (Computers); Responses

20020001592 Lawrence Livermore National Lab., Livermore, CA USA
NIF small optics laser damage test specifications
Sheehan, L.; Apr. 01, 1999; 6p; In English
Report No.(s): DE2001-12626; UCRL-ID-133979-REV-1; No Copyright; Avail: Department of Energy Information Bridge, Microfiche

The Laser Damage Group is currently conducting tests on small optics samples supplied for initial evaluation of potential NIF suppliers. This document is meant to define the specification of laser-induced damage for small optics and the test methods used to collect the data. A rating system which will be applied for vendor selection is presented. Presented here is the plan for qualification of NIF small optics vendors based on laser damage performance. The raster scan test method was chosen in order to provide for testing of significant areas of the samples. The vendor performance at a given fluence is categorized as either 'qualified', 'probable', or 'fail', depending on the level of damage observed. This binning system allows a conservative stance for qualification, while providing some insight into lever of risk associated with a lowering on the specifications. The R: 1 mapping technique is reserved in cases where comparisons, not qualifications are needed. Once suppliers are selected, an less intensive pass/fail test will be instituted for production optics.
NTIS
Lasers; Optics; Laser Damage

20020002227 Lawrence Livermore National Lab., Livermore, CA USA
Inner-shell photoionized x-ray lasers
Moon, S. J.; Jun. 01, 1998; 85p; In English
Report No.(s): DE2001-12527; UCRL-LR-131000; No Copyright; Avail: Department of Energy Information Bridge, Microfiche

The inner-shell photoionized x-ray lasing scheme is an attractive method for achieving x-ray lasing at short wavelengths, via population inversion following inner-shell photoionization (ISPI). This scheme promises both a short wavelength and a short pulse source of coherent x rays with high average power. In this dissertation a very complete study of the ISPI x-ray laser scheme is done concerning target structure, filter design and lasant medium. An investigation of the rapid rise time of x-ray emission from targets heated by an ultra-short pulse high-intensity optical laser was conducted for use as the x-ray source for ISPI x-ray lasing. Lasing by this approach in C at a wavelength of 45 (angstrom) requires a short pulse (about 50 fsec) driving optical laser with an energy of 1-5 J and traveling wave optics with an accuracy of (approximately) 15 (micro)m. The optical laser is incident on a high-Z target creating a high-density plasma which emits a broadband spectrum of x rays. This x-ray source is passed through a filter to eliminate the low-energy x rays. The remaining high-energy x rays preferentially photoionize inner-shell electrons

resulting in a population inversion. Inner-shell photoionized x-ray lasing relies on the large energy of a K-(alpha) transition in the initially neutral lasant. The photo energy required to pump this scheme is only slightly greater than the photon energy of the lasing transition yielding a lasing scheme with high quantum efficiency. However, the overall efficiency is reduced due to low x-ray conversion efficiency and the large probability of Auger decay yielding an overall efficiency of (approximately) 10(sup (minus)7) resulting in an output energy of (micro)'s. They calculate that a driving laser with a pulse duration of 40 fs, a 10(micro)m x 1 cm line focus, and an energy of 1 J gives an effective gain length product (gl) of 10 in C at 45 (angstrom). At saturation (gl (approximately) 18) they expect an output of (approximately) 0.1 (micro)J per pulse. The short duration of x-ray lasing (>100 fs) combined with a 10-Hz repetition rate (P(sub avg) = 1(micro)W) makes this source of coherent x rays ideal for pump-probe experiments to study fast dynamical processes in chemistry and material science.
NTIS
Quantum Efficiency; Pulse Duration; X Ray Lasers; Broadband

20020002306 Pacific Northwest National Lab., Richland, WA USA
Fiber-Optic Neutron Detector for a Drive-By Scenario
Miley, H. S.; Mar. 30, 1999; 10p; In English
Report No.(s): DE2001-5036; PNNL-12148; GC-04-02-000; No Copyright; Avail: Department of Energy Information Bridge, Microfiche

The measurement scenario of a neutron source driving by a detector has been evaluated. It is possible to use PNNL lithium-loaded fiber optics to measure the source, even at reasonably high speeds. A detector sufficient to detect the neutrons from the source at a high confidence level can be produced in a compact and robust configuration for a reasonable cost. In addition, the PNNL solution measures gamma-ray signals and will effectively add the function of a proximity sensor, lower the false-alarm rate, and allow discrimination between certain neutron source scenarios. Finally, the need for definition of confidence levels (both the method of computation and the required false alarm probability), emplacement form-factor, and electronic interface is required of a potential user to revise or customize the design outlined in this paper.
NTIS
Fiber Optics; Neutron Counters

20020002312 Sandia National Labs., Albuquerque, NM USA
Optical Readout of Micro-Accelerometer Code Features
Dickey, F. M.; Holswade, S. C.; Polosky, M. A.; Shagam, R. N.; Sullivan, C. T.; Jul. 08, 1999; 10p; In English
Report No.(s): DE2001-8855; SAND98-2583C; No Copyright; Avail: Department of Energy Information Bridge, Microfiche

Micromachine accelerometers offer a way to enable critical functions only when a system encounters a particular acceleration environment. This paper describes the optical readout of a surface micromachine accelerometer containing a unique 24-bit code. The readout uses waveguide-based optics, which are implemented as a photonic integrated circuit (PIC). The PIC is flip-chip bonded over the micromachine, for a compact package. The shuttle moves 500 micrometers during readout, and each code element is 17 micrometers wide. The particular readout scheme makes use of backscattered radiation from etched features in the accelerometer shuttle. The features are etched to create corner reflectors that return radiation back toward the source for a one bit. For a zero bit, the shuttle is not etched, and the radiation scatters forward, away from the detector. This arrangement provides a large signal difference between a one and zero signal, since the zero signal returns virtually no signal to the detector. It is thus superior to schemes that interrogate the code vertically, which have a limited contrast between a one and a zero. Experimental results are presented for mock shuttle features etched into a silicon substrate. to simulate the shuttle moving under a fixed PIC, a commercially available waveguide source was scanned over the mock code.
NTIS
Accelerometers; Waveguides; Microelectromechanical Systems

20020002327 NASA Langley Research Center, Hampton, VA USA
Ultra Narrowband Optical Filters for Water Vapor Differential Absorption Lidar (DIAL) Atmospheric Measurements
Stenholm, Ingrid, Lund Univ., Sweden; DeYoung, Russell J., NASA Langley Research Center, USA; December 2001; 34p; In English; Original contains color illustrations
Contract(s)/Grant(s): RTOP 622-63-13-70
Report No.(s): NASA/TM-2001-211261; L-18108; NAS 1.15:211261; No Copyright; Avail: CASI; A03, Hardcopy; A01, Microfiche

Differential absorption lidar (DIAL) systems are being deployed to make vertical profile measurements of atmospheric water vapor from ground and airborne platforms. One goal of this work is to improve the technology of such DIAL systems that they could be deployed on space-based platforms. Since background radiation reduces system performance, it is important to reduce

it. One way to reduce it is to narrow the bandwidth of the optical receiver system. However, since the DIAL technique uses two or more wavelengths, in this case separated by 0.1 nm, a fixed-wavelength narrowband filter that would encompass both wavelengths would be broader than required for each line, approximately 0.02 nm. The approach employed in this project is to use a pair of tunable narrowband reflective fiber Bragg gratings. The Bragg gratings are germanium-doped silica core fiber that is exposed to ultraviolet radiation to produce index-of-refraction changes along the length of the fiber. The gratings can be tuned by stretching. The backscattered laser radiation is transmitted through an optical circulator to the gratings, reflected back to the optical circulator by one of the gratings, and then sent to a photodiode. The filter reflectivities were is greater than 90 percent, and the overall system efficiency was 30 percent.
Author
Bragg Gratings; Differential Absorption Lidar; Narrowband; Optical Filters; Reflectance; Atmospheric Moisture

20020002350 Brookhaven National Lab., Upton, NY USA
Advanced Diagnostics for Developing High-Brightness Electron Beams
Ben-Zvi, I.; Babzien, M.; Malone, R.; Wang, X. J.; Yakimenko, V.; Nov. 24, 1998; 12p; In English
Report No.(s): DE2001-6255; BNL-66228; KA0403000; No Copyright; Avail: Department of Energy Information Bridge, Microfiche

The production of high-brightness particle beams calls for the development of advanced beam diagnostics. High brightness beams, meaning beams with a high density in phase space, are important for many applications, such as short-wavelength Free-Electron Lasers and advanced accelerator systems. A diagnostic that provides detailed information on the density distribution of the electron bunch in multi-dimensional phase-space is an essential tool for obtaining small emittance at a high charge. This diagnostic system has been developed at Brookhaven National Laboratory. One component of the system is the measurement of a slice emittance which provides a measurement of transverse beam properties (such as emittance) as a function of the longitudinal position. Changing the laser pulse profile of a photocathode radio frequency gun has been suggested as one way to achieve non-linear emittance compensation and improve the brightness and that can be diagnosed by the slice emittance system. The other element of the diagnostic is the tomographic reconstruction of the transverse phase. In our work we give special attention to the accuracy of the phase space reconstruction and present an analysis using a transport line with nine focusing magnets and techniques to control the optical functions and phases. This high precision phase space tomography together with the ability to modify the radial charge distribution of the electron beam presents an opportunity to improve the emittance and apply non-linear radial emittance corrections. Combining the slice emittance and tomography diagnostics leads to an unprecedented visualization of phase space distributions in five-dimensional phase-space and an opportunity to perform high-order emittance corrections. This should lead to great improvements in the beam brightness.
NTIS
Brightness; Density Distribution; Electron Beams; Emittance; Charge Distribution

20020002702 Los Alamos National Lab., NM USA
Optical wavepackets (optical bullets): A new diffraction free form of light travel
Funk, D.; Nicholson, J.; Sep. 01, 1999; 13p; In English
Report No.(s): DE2001-768225; LA-UR-99-2338; No Copyright; Avail: Department of Energy Information Bridge

This is the final report of a three-year, Laboratory-Directed Research and Development (LDRD) project at the Los Alamos National Laboratory (LANL). We conducted studies of the propagation of self-confined packets of light or 'Optical Bullets' through air. These packets are self-forming and require no active optics. At the present time, theoretical explanations provide an incomplete description of this process. Generation of these pulses requires a light source of sufficient energy and with a short enough pulse-width that the intensity exceeds a critical wavelength dependent value. We used a Ti:Sapphire based system to generate the pulses and we observed pulse-splitting and chirp-dependent control of the formation of these filaments. In addition, we developed a novel algorithm for extracting the phase and electric field of these pulses using Frequency Resolved Optical Gating coupled to genetic algorithms for pulse retrieval.
NTIS
Air; Electric Fields; Wavelengths; Light Sources; Wave Packets

20020002715 Federal Energy Technology Center, Morgantown, WV USA
Coherent Laser Vision System (CLVS) option phase
Clark, R.; Nov. 18, 1999; 66p; In English
Report No.(s): DE2001-767402; DE-AR21-94MC31190-02; No Copyright; Avail: Department of Energy Information Bridge

The purpose of this research project was to develop a prototype fiber-optic based Coherent Laser Vision System (CLVS) suitable for DOE's EM Robotic program. The system provides three-dimensional (3D) vision for monitoring situations in which it is necessary to update the dimensional spatial data on the order of once per second. The system has total immunity to ambient lighting conditions.
NTIS
Fiber Optics; Robotics; Light (Visible Radiation); Coherent Radiation; Systems Engineering

20020002783 Sandia National Labs., Albuquerque, NM USA
High Peak Power Gain Switched Flared Waveguide Lasers
Chow, W. W.; Indik, R.; Koch, S. W.; Mar, A.; Vawter, G. A.; Aug. 05, 1999; 7p; In English
Report No.(s): DE2001-9697; SAND99-2050C; No Copyright; Avail: Department of Energy Information Bridge, Microfiche
We gain-switch flared waveguide lasers to obtain 14.5 W peak powers and 0.5 nJ pulse energies with laser structures compatible with the generation of diffraction-limited beams. The results are in excellent agreement with a microscopic laser model.
NTIS
Waveguide Lasers; Power Gain; Switching

20020002797 Los Alamos National Lab., NM USA
Femtosecond pulse delivery through single-mode optical fiber with adaptive pulse shaping
Omenetto, F.; Taylor, A.; Nov. 01, 2000; 6p; In English
Report No.(s): DE2001-767464; LA-UR-00-5489; No Copyright; Avail: Department of Energy Information Bridge, Microfiche
Adaptive control is used to defeat nonlinear effects that severely distort ultrafast pulses during propagation through optical fibers.
NTIS
Optical Fibers; Pulses; Fiber Optics; Distortion

20020002802 Kansas City Plant, Kansas City, MO USA
Develop Solid State Laser Sources for High Resolution Video Projection Systems
Brickeen, B. K.; Oct. 24, 2000; 9p; In English
Report No.(s): DE2001-766163; KCP-613-6371; No Copyright; Avail: Department of Energy Information Bridge, Microfiche
Magic Lantern and Honeywell FM and T worked together to develop lower-cost, visible light solid-state laser sources to use in laser projector products. Work included a new family of video displays that use lasers as light sources. The displays would project electronic images up to 15 meters across and provide better resolution and clarity than movie film, up to five times the resolution of the best available computer monitors, up to 20 times the resolution of television, and up to six times the resolution of HDTV displays. The products that could be developed as a result of this CRADA could benefit the economy in many ways, such as: (1) Direct economic impact in the local manufacture and marketing of the units. (2) Direct economic impact in exports and foreign distribution. (3) Influencing the development of other elements of display technology that take advantage of the signals that these elements allow. (4) Increased productivity for engineers, FAA controllers, medical practitioners, and military operatives.
NTIS
Solid State Lasers; Video Tapes; Display Devices

20020003343 Argonne National Lab., IL USA
First use of a laser-driven polarized H/D target at the IUCF cooler
Bailey, K.; Brack, J.; Cadman, R. V.; Cummings, W. J.; Fedchak, J.; Dec. 05, 1997; 10p; In English
Report No.(s): DE2001-8900; ANL/PHY/CP-95025; No Copyright; Avail: Department of Energy Information Bridge, Microfiche
The HERMES Laser-Driven Target Task Force (Argonne, Erlangen and Illinois) is charged with developing a polarized H/D target for use in the HERA ring at DESY. Rapid progress was made in the beginning of 1996, leading us to the decision to test the target in a realistic experimental environment. In particular, polarizations of 0.6 and flows above 10(sup 18) atoms(center dot)s(sup (minus)1) have been achieved on the bench. The laser-driven target and a simple detector system are currently installed in Cooler storage ring at the Indiana University Cyclotron Facility in order to test its applicability to nuclear physics experiments.

Target polarizations are being measured using the (rvec H)(p, p) and (rvec D)(p, p) reactions. Initial tests were reasonably successful and the target is well along toward becoming viable for nuclear physics.
NTIS
Coolers; Cyclotrons; Nuclear Physics; Laser Targets; Deuterium; Hydrogen; Polarization

20020003976 Lawrence Livermore National Lab., Livermore, CA USA
3(omega) damage threshold evaluation of final optics components using Beamlet mule and off-line testing
Kozlowski, M. F.; Maricle, S.; Mouser, R.; Schwartz, S.; Wegner, P.; Jul. 27, 1998; 20p; In English
Report No.(s): DE2001-2852; UCRL-JC-129721; DP0212000; No Copyright; Avail: Department of Energy Information Bridge

A statistics-based model is being developed to predict the laser-damage-limited lifetime of UV optical components on the NIF laser. In order to provide data for the model, laser damage experiments were performed on the Beamlet laser system at LLNL. An early prototype NIF focus lens was exposed to twenty 35 1 nm pulses at an average fluence of 5 J/sq cm, 3ns. Using a high resolution optic inspection system a total of 353 damage sites was detected within the 1160 sq cm beam aperture. Through inspections of the lens before, after and, in some cases, during the campaign, pulse to pulse damage growth rates were measured for damage initiating both on the surface and at bulk inclusions. Growth rates as high as 79 micro-m/pulse (surface diameter) were observed for damage initiating at pre-existing scratches in the surface. For most damage sites on the optic, both surface and bulk, the damage growth rate was approximately l0 micro-m/pulse. The lens was also used in Beamlet for a subsequent 1053 micro-m/526 micro-m campaign. The 352 micro-m-initiated damage continued to grow during that campaign although at generally lower growth rate.
NTIS
Optical Equipment; Inertial Confinement Fusion; Solid State Lasers; Laser Damage; Yield Point

20020003981 Lawrence Livermore National Lab., Livermore, CA USA
Application of adaptive optics for controlling the NIF laser performance and spot size
Auerbach, J.; Bliss, E.; Henesian, M.; Lawson, J.; Manes, K.; Aug. 17, 1998; 13p; In English
Report No.(s): DE2001-2841; UCRL-JC-130028; No Copyright; Avail: Department of Energy Information Bridge

The National Ignition Facility (NIF) laser will use a 192-beam multi-pass architecture capable of delivering several MJ of UV energy in temporal pulse formats varying from sub-ns square to 20 ns precisely-defined high-contrast shapes. Each beam wavefront will be subjected to effects of optics inhomogeneities, figuring errors, mounting distortions, prompt and slow thermal effects from flashlamps, driven and passive air-path turbulence, and gravity-driven deformations. A 39-actuator intra-cavity deformable mirror, controlled by data from a 77-lenslet Hartman sensor will be used to correct these wavefront aberrations and thus to assure that stringent farfield spot requirements are met. We have developed numerical models for the expected distortions, the operation of the adaptive optic system, and the anticipated effects on beam propagation, component damage, frequency conversion, and target-plane energy distribution. These models have been extensively validated against data from LLNL's Beamlet, and Amplab lasers. We review the expected beam wavefront aberrations and their potential for adverse effects on the laser performance, describe our model of the corrective system operation, and display our predictions for corrected-beam operation of the NI.
NTIS
Deformable Mirrors; Solid State Lasers; Inertial Confinement Fusion; Laser Outputs; Adaptive Optics; Laser Beams

20020003994 Brookhaven National Lab., Upton, NY USA
Report of the terawatt laser pressure vessel committee
Woodle, M. H.; Beauman, R.; Czajkowski, C.; Dickinson, T.; Lynch, D.; Sep. 25, 2000; 95p; In English
Contract(s)/Grant(s): AC02-98CH10886
Report No.(s): DE2001-773949; BNL-52602; KC0204011; No Copyright; Avail: Department of Energy Information Bridge, Microfiche

In 1995 the ATF project sent out an RFP for a CO2 Laser System having a TeraWatt output. Eight foreign and US firms responded. The Proposal Evaluation Panel on the second round selected Optoel, a Russian firm based in St. Petersburg, on the basis of the technical criteria and cost. Prior to the award, BNL representatives including the principal scientist, cognizant engineer and a QA representative visited the Optoel facilities to assess the company's capability to do the job. The contract required Optoel to provide a x-ray preionized high pressure amplifier that included: a high pressure cell, x-ray tube, internal optics and a HV pulse forming network for the main discharge and preionizer. The high-pressure cell consists of a stainless steel pressure vessel with various ports and windows that is filled with a gas mixture operating at 10 atmospheres. In accordance with BNL Standard ESH 1.4.1 'Pressurized Systems For Experimental Use', the pressure vessel design criteria is required to comply with the ASME Boiler

and Pressure Vessel Code In 1996 a Preliminary Design Review was held at BNL. The vendor was requested to furnish drawings so that we could confirm that the design met the above criteria. The vendor furnished drawings did not have all dimensions necessary to completely analyze the cell. Never the less, we performed an analysis on as much of the vessel as we could with the available information. The calculations concluded that there were twelve areas of concern that had to be addressed to assure that the pressure vessel complied with the requirements of the ASME code. This information was forwarded to the vendor with the understanding that they would resolve these concerns as they continued with the vessel design and fabrication. The assembled amplifier pressure vessel was later hydro tested to 220 psi (15 Atm) as well as pneumatically to 181 psi (12.5 Atm) at the fabricator's Russian facility and was witnessed by a BNL engineer. The unit was shipped to the US and installed at the ATF. As part of the commissioning of the device the amplifier pressure vessel was disassembled several times at which time it became apparent that the vendor had not addressed 7 of the 12 issues previously identified. Closer examination of the vessel revealed some additional concerns including quality of workmanship. Although not required by the contract, the vendor furnished radiographs of a number of pressure vessel welds. A review of the Russian X-rays revealed radiographs of both poor and unreadable quality. However, a number of internal weld imperfections could be observed. All welds in question were excavated and then visually and dye penetrant inspected. These additional inspections confirmed that the weld techniques used to make some of these original welds were substandard. The applicable BNL standard, ESH 1.4.1, addresses the problem of pressure vessel non-compliance by having a committee appointed by the Department Chairman review the design and provide engineering solutions to assure equivalent safety. On January 24, 2000 Dr. M. Hart, the NSLS Chairman, appointed this committee with this charge. This report details the engineering investigations, deliberations, solutions and calculations which were developed by members of this committee to determine that with repairs, new components, appropriate NDE, and lowering the design pressure, the vessel can be considered safe to use.
NTIS
Lasers; Pressure Vessels

20020004671 Thomas Jefferson National Accelerator Facility, Newport News, VA USA
New Dynamics Facility Combining a Storage Ring with a Synchronized FEL
Dylla, H. F.; Hutton, A.; Neil, G.; Williams, G. P.; Aug. 01, 2001; 12p; In English
Report No.(s): DE2001-786150; JLAB-ACC-01-17; DOE/ER/40150-1904; No Copyright; Avail: Department of Energy Information Bridge, Microfiche

Jefferson Laboratory currently operates a kilowatt average power, sub-picosecond mid-IR Free Electron Laser as a user facility. We present plans to add an electron storage ring to this facility. Pulses of light from both sources will be synchronized at repetition rates up to 125 MHz to allow pump-probe dynamics experiments to be performed. We will present an outline of the new facility together with the operational parameters of the 2 sources. The new facility could be on line as a user facility in 2004.
NTIS
Free Electron Lasers; Infrared Radiation; Storage Rings (Particle Accelerators)

20020005091 NASA Goddard Space Flight Center, Greenbelt, MD USA
Fiber Grating Coupled Light Source Capable of Tunable, Single Frequency Operation
Krainak, Michael A., Inventor, NASA Goddard Space Flight Center, USA; Duerksen, Gary L., Inventor, NASA Goddard Space Flight Center, USA; Feb. 13, 2001; 36p; In English; Provisional US-Patent-Appl-SN-044378, filed 16 May 1997
Patent Info.: Filed 15 May 1998; US-Patent-6,188,705; US-Patent-Appl-SN-079383; US-Patent-Appl-SN-044378; No Copyright; Avail: CASI; A03, Hardcopy; A01, Microfiche

Fiber Bragg grating coupled light sources can achieve tunable single-frequency (single axial and lateral spatial mode) operation by correcting for a quadratic phase variation in the lateral dimension using an aperture stop. The output of a quasi-monochromatic light source such as a Fabry Perot laser diode is astigmatic. As a consequence of the astigmatism, coupling geometries that accommodate the transverse numerical aperture of the laser are defocused in the lateral dimension, even for apsherical optics. The mismatch produces the quadratic phase variation in the feedback along the lateral axis at the facet of the laser that excites lateral modes of higher order than the TM(sub 00). Because the instability entails excitation of higher order lateral submodes, single frequency operation also is accomplished by using fiber Bragg gratings whose bandwidth is narrower than the submode spacing. This technique is particularly pertinent to the use of lensed fiber gratings in lieu of discrete coupling optics. Stable device operation requires overall phase match between the fed-back signal and the laser output. The fiber Bragg grating acts as a phase-preserving mirror when the Bragg condition is met precisely. The phase-match condition is maintained throughout the fiber tuning range by matching the Fabry-Perot axial mode wavelength to the passband center wavelength of the Bragg grating.
Official Gazette of the U.S. Patent and Trademark Office
Bragg Gratings; Light Sources; Frequencies; Tunable Lasers; Semiconductor Lasers

20020005107 Brookhaven National Lab., Upton, NY USA

Duvfel photoinjector dynamics: measurement and simulation

Graves,; Dimauro,; Heese,; Johnson,; Rose,; Jun. 18, 2001; 5p; In English

Report No.(s): DE2001-786070; BNL-68551; No Copyright; Avail: Department of Energy Information Bridge, Microfiche

The DUVFEL photoinjector consists of a 1.6 cell BNL gun IV with copper cathode, variable pulse length Ti:Sapp laser, and solenoid magnet. The beam dynamics and the electromagnetic fields in the photoinjector have been characterized by producing a short electron beam with very low charge that is used as a field probe. Transverse beam size and divergence are measured as a function of initial RF phase and initial spot size and compared with simulations using the code HOMDYN. The electromagnetic fields used in the simulations are produced by SUPERFISH, and have been verified with RF measurements. The simulations and measurements of beam dynamics are presented.

NTIS

Free Electron Lasers; Radio Frequencies; Copper; Divergence

20020005114 Thomas Jefferson National Accelerator Facility, Newport News, VA USA

Second Harmonic FEL Oscillation

Neil, G. R.; Benson, S. V.; Biallas, G.; Freund, H. P.; Gubeli, J.; Sep. 01, 2001; 15p; In English

Report No.(s): DE2001-786149; JLAB-ACC-01-16; DOE/ER/40150-1903; No Copyright; Avail: Department of Energy Information Bridge, Microfiche

We have produced and measured for the first time second harmonic oscillation in the infrared region by the high average power Jefferson Lab Infrared Free Electron Laser. Although such lasing is ideally forbidden, since gain is zero on axis for a perfect electron beam in an infinite wiggler, the finite geometry and beam emittance allows sufficient gain for lasing to occur. We were able to lase at pulse rates up to 74.85 MHz and could produce over 4.5 watts average and 40 kW peak of IR power in a 40 nm FWHM bandwidth at 2925 nm. In agreement with predictions, the source preferentially lased in a TEM01 mode. We present results of initial source performance measurements and comparisons of gain as calculated by different approaches.

NTIS

Harmonic Oscillation; Free Electron Lasers; Electron Beams

20020005170 Sandia National Labs., Albuquerque, NM USA

Surface Micromachined Components for a Safety Subsystem Application

Garcia, E. J.; Holswade, S.; Plummer, D. W.; Polosky, M. A.; Shul, R. J.; Mar. 04, 1999; 12p; In English

Report No.(s): DE2001-4238; SAND99-0534C; No Copyright; Avail: Department of Energy Information Bridge, Microfiche

We have designed and fabricated a system using micromachining technologies that represents the first phase of an effort to develop a miniaturized or micro trajectory safety subsystem. Two Surface Micromachined (SMM) devices have been fabricated. The first is a device, denoted the Shuttle Mechanism, that contains a suspended shuttle that has a unique code imbedded in its surface. The second is a mechanical locking mechanism, denoted a Stronglink, that uses the code imbedded in the Shuttle Mechanism for unlocking. The Stronglink is designed to block a beam of optical energy until unlocked. A Photonic Integrated Circuit (PIC) fabricated in Gallium Arsenide (GaAs) and an ASIC have been designed to read the code contained in the Shuttle Mechanism. The ASIC interprets the data read by the PIC and outputs low-level drive signals for the actuators used by the Stronglink. An off-chip circuit amplifies the drive signals. Once the Stronglink is unlocked, a laser array that is assembled beneath the device is energized and light is transmitted through an aperture.

NTIS

Fabrication; Micromachining; Miniaturization; Photonics; Application Specific Integrated Circuits

20020005172 Sandia National Labs., Albuquerque, NM USA

Photoluminescence Investigations of InGaAsN Alloys Lattice-Matched to GaAs

Jones, E. D.; Modine, N. R.; Allerman, A. A.; Fritz, I. J.; Kurtz, S. R.; Jun. 01, 1999; 10p; In English

Report No.(s): DE2001-7126; SAND99-0203C; No Copyright; Avail: Department of Energy Information Bridge

InGaAsN is a semiconductor alloy system with the property that the inclusion of only 2% nitrogen reduces the bandgap by more than 30%. In this paper, we have measured the conduction-band mass measurements by three different techniques for 2% nitrogen in InGaAsN lattice matched to GaAs. Additionally, we also report pressure dependent measurements of the conduction-band mass between ambient and 40 kbar. Based on our results, we suggest that the observed changes in masses are a result of Lambda-X mixing.

NTIS

Gallium Arsenides; Nitrogen; Photoluminescence; Semiconductors (Materials); Indium Gallium Arsenides

20020005240 Fermi National Accelerator Lab., Batavia, IL USA

C0 low-(beta) optics

Johnstone, J. A.; Feb. 02, 2001; 5p; In English

Report No.(s): DE2001-774151; FERMILAB-TM-2139; No Copyright; Avail: Department of Energy Information Bridge, Microfiche

A low-(beta) insertion has been designed for the BTeV experiment at C0. With +/- 12 m for detector space, a (beta) of 0.5 m can be achieved using 170 T/m magnets in the final focus triplets. A total half-crossing angle of 240 (micro)r is necessary to keep the beams separated by 5(sigma) at the 2nd parasitic crossing. There are 2 possible Tevatron collision scenarios: B0 and D0, but not C0, and; C0, but not B0 or D0.

NTIS

Beams (Radiation); Particle Accelerators

20020005261 Sandia National Labs., Albuquerque, NM USA

Photonic Band Gap Structures as a Gateway to Nano-Photonics

Fritz, I. J.; Gourley, P. L.; Hammons, G.; Hietala, V. M.; Jones, E. D.; Aug. 01, 1999; 15p; In English

Report No.(s): DE2001-12654; SAND99-0926; No Copyright; Avail: Department of Energy Information Bridge, Microfiche

This Laboratory-Directed Research and Development (LDRD) project explored the fundamental physics of a new class of photonic materials, photonic bandgap structures (PBG), and examine its unique properties for the design and implementation of photonic devices on a nanometer length scale for the control and confinement of light. The low loss, highly reflective and quantum interference nature of a PBG material makes it one of the most promising candidates for realizing an extremely high-Q resonant cavity, 10,000, for optoelectronic applications and for the exploration of novel photonic physics, such as photonic localization, tunneling and modification of spontaneous emission rate. Moreover, the photonic bandgap concept affords us with a new opportunity to design and tailor photonic properties in very much the same way we manipulate, or bandgap engineer, electronic properties through modern epitaxy.

NTIS

Energy Gaps (Solid State); Photonics; Nanotechnology

20020005401 Los Alamos National Lab., NM USA

Rapidly-tunable acousto-optic spectrometer for a space environment

Thompson, D.; Hewitt, C.; Wilson, C.; Aug. 01, 2000; 15p; In English

Report No.(s): DE2001-768886; LA-UR-00-3403; No Copyright; Avail: Department of Energy Information Bridge, Microfiche

As a complement to our work developing rapidly-tunable ((approximately)10-100 kHz) CO2 lasers for differential absorption lidar (DIAL) applications,l we have developed a rapidly-tunable spectrometer. A rapid spectral diagnostic is critical for a high speed DIAL system, since analysis of the return signals depends on knowing the spectral purity of the transmitted beam. The spectrometer developed for our lidar system is based on a double-passed large- (75 mm) aperture acousto-optic deflector, a grating, and a fast single-element room temperature mercury-cadmium-telluride detector. The spectrometer has a resolution of (approximately)0.5 cm(sup (minus)1), a tuning range of 9.0-11.4 pm, a random-access tuning speed of greater than 80 kHz and a S/N ratio of greater than 100:1. We describe the design and performance of this device, as well as of future devices featuring improved resolution, higher speed and easier and more robust alignment. We will also briefly discuss the applications and limitations of the technique in a space environment.

NTIS

Alignment; Design Analysis; Carbon Dioxide Lasers; Optical Radar

20020005643 Northland Scientific, Inc., Olmstead Falls, OH USA

Solar Collector With Image-Forming Mirror Cavity to Irradiate Small Central Volume

Buchele, Don, Northland Scientific, Inc., USA; Castle, Charles, Northland Scientific, Inc., USA; Bonoetti, Joseph A., Alabama Univ., USA; September 2001; 36p; In English

Contract(s)/Grant(s): NASA Order C-71734-K; RTOP 274-00-00

Report No.(s): NASA/CR-2001-211072; E-12911; NAS 1.26:211072; No Copyright; Avail: CASI; A03, Hardcopy; A01, Microfiche

A unique solar thermal chamber has been designed and fabricated to produce the maximum concentration of solar energy and higher temperature possible. Its primary purpose was for solar plasma propulsion experiments and related material specimen testing above 3000 K. The design not only maximized solar concentration, but also, minimized infrared heat loss. This paper provides the underlying theory and operation of the chamber and initial optical correlation to the actual fabricated hardware. The

chamber is placed at the focal point of an existing primary concentrator with a 2.74 m (9 ft) focal length. A quartz lens focuses a small sun image at the inlet hole of the mirrored cavity. The lens focuses two image planes at prescribed positions; the sun at the cavity's entrance hole and the primary concentrator at the junction plane of two surfaces that form the cavity chamber. The back half is an ellipsoid reflector that produces a 1.27 cm diameter final sun image. The image is "suspended in space," 7.1 cm away from the nearest cavity surface, to minimize thermal and contaminate damage to the mirror surfaces. A hemisphere mirror makes up the front chamber and has its center of curvature at the target image, where rays leaving the target are reflected back upon themselves, minimizing radiation losses.
Author
Concentrators; Solar Collectors; Optics

20020005649 Thomas Jefferson National Accelerator Facility, Newport News, VA USA
Trends Opportunities in Light Source Development
Neil, G. R.; Aug. 01, 2001; 14p; In English
Report No.(s): DE2001-786471; JLAB-ACC-01-19; DOE/ER/40150-1908; No Copyright; Avail: Department of Energy Information Bridge, Microfiche

After a decade of rather quiet growth for FELs there is now a lot of activity in the light source community. This is the result of a combination of factors including successful operation of the third generation light sources, the establishment of a very productive user community at both synchrotrons and FELs, and the continuing technical improvements of accelerators and related technology which allow ever more challenging machines to be considered. There are a number of themes that carry this development including pushing wavelengths shorter, brightnesses higher, pulses shorter, increasing average power, and providing for multiple synchronized photon beams with multiple wavelengths. This talk will discuss some of the plans and proposals currently circulating and attempt to provide a glimpse into the near future of our field by illustrating the technologies that drive source development.
NTIS
Light Sources; Brightness; Circulation; Photon Beams

20020005844 California Univ., Lawrence Berkeley Lab., Berkeley, CA USA
Monitoring performance of the Advanced Light Source
Byrne, W. E.; Lampo, E. J.; Samuelson, B. C.; Jun. 13, 2001; 3p; In English
Report No.(s): DE2001-785306; LBNL-48279; No Copyright; Avail: Department of Energy Information Bridge

Providing high quality light to users in a consistent and reliable manner is one of the main goals of the accelerator physics group at the Advanced Light source (ALS). to meet this goal considerable time is spent monitoring the performance of the machine. At the Group's weekly meeting the performance of the accelerator over the previous week's run is reviewed. This paper describes the parameters that are monitored to optimize the performance of the ALS.
NTIS
Light Sources; Light (Visible Radiation)

20020005851 Thomas Jefferson National Accelerator Facility, Newport News, VA USA
Overview of SRF-related Activities at Jefferson Lab
Reece, C.; Sep. 01, 2001; 9p; In English
Report No.(s): DE2001-786472; JLAB-ACC-01-20; DOE/ER/40150-1909; No Copyright; Avail: Department of Energy Information Bridge, Microfiche

SRF-related activities at JLab are varied and increasing. Operation of CEBAF at 5.7 GeV for nuclear physics is now routine. There has been significant progress in the development and testing of components and subsystems for a new cryomodule design for coming upgraldes of the JLab CEBAF and FEL. Construction of the first such module has begun, and further optimization studies continue. Jefferson Lab joined the collaboration to build the Spallation Neutron Source (SNS). JLab will contribute 81 cavities in 23 SNS cryomodules. Prototyping of the beta. 0.61 and 0.81 cavities is nearing completion. Development and testing of the high-power coaxial input coupler for SNS is underway. Fresh efforts have been initiated to pursue improved understanding and control of SRF surfaces. JLab has led discussions and development of modern low-level rf controls tailored for power-efficient operation of high-gradient SRF cavities in lightly-beamloaded, cw applications. to support these efforts, major upgrades and renovations to the JLab SRF facilities and information infrastructures are underway. The lab has recognized the importance of SRF to future developments in the accelerator community by the creation of the new Institute for SRF Science and Technology.
NTIS
Nuclear Physics; Continuous Radiation; Neutron Sources; Radio Frequencies

75
PLASMA PHYSICS

Includes magnetohydrodynamics and plasma fusion. For ionospheric plasmas see 46 Geophysics. For space plasmas see 90 Astrophysics.

20020000749 Lawrence Livermore National Lab., Livermore, CA USA
Drifts, boundary conditions and plasma convection on open magnetic field lines
Cohen, R. H.; Nov. 20, 1998; 24p; In English
Report No.(s): DE2001-2763; UCRL-JC-132451; AT5020100; No Copyright; Avail: Department of Energy Information Bridge, Microfiche

In a number of plasmas of practical interest, including the scrape-off layer of a tokamak with a divertor or toroidal limiter, some gas discharge devices, and in the vicinity of spacecraft, magnetic field lines intersect bounding surfaces at shallow angles. Under these circumstances a number of interesting and important effects arise. Drifts can compete with parallel flows in establishing the boundary conditions for plasma mass-flow and current (sheath current-voltage characteristics). We derive the mass-flow constraints including both poloidal and radial drifts, review the current boundary conditions, and survey the consequences, including along-field density and heat-flux asymmetries, convection created by a wavy surface, generation of electric fields and surface currents associated with shadows from surface structures, and modification of instability growth.
NTIS
Asymmetry; Boundary Conditions; Magnetic Fields; Plasmas (Physics); Magnetohydrodynamic Flow; Diverters

20020000758 Princeton Univ., Plasma Physics Lab., NJ USA
Energetic Particle Transport in Compact Quasi-axisymmetric Stellarators
Redi, M. H.; Mynick, H. E.; Suewattana, M.; White, R. B.; Zarnstorff, M. C.; Mar. 01, 1999; 55p; In English
Report No.(s): DE2001-3589; PPPL-3341; No Copyright; Avail: Department of Energy Information Bridge

Hamiltonian coordinate, guiding-center code calculations of the confinement of suprathermal ions in quasi-axisymmetric stellarator (QAS) designs have been carried out to evaluate the attractiveness of compact configurations which are optimized for ballooning stability. A new stellarator particle-following code is used to predict ion loss rates and particle confinement for thermal and neutral beam ions in a small experiment with R = 145 cm, B = 1-2 T and for alpha particles in a reactor-size device. In contrast to tokamaks, it is found that high edge poloidal flux has limited value in improving ion confinement in QAS, since collisional pitch-angle scattering drives ions into ripple wells and stochastic field regions, where they are quickly lost. The necessity for reduced stellarator ripple fields is emphasized. The high neutral beam ion loss predicted for these configurations suggests that more interesting physics could be explored with an experiment of less constrained size and magnetic field geometry.
NTIS
Stellarators; Charged Particles; Particle Beams; Ions

20020000885 Argonne National Lab., IL USA
Simulation of intense heating and shock hydrodynamics in free-moving liquid targets
Hassanein, A.; Aug. 27, 1999; 14p; In English
Report No.(s): DE2001-11951; ANL/ET/CP-99911; No Copyright; Avail: Department of Energy Information Bridge, Microfiche

Recently, significant interest has focused on the use of free or open liquid-metal targets flowing with high velocities in various nuclear and high-energy physics applications such as the ISOLDE and muon collider projects. This is because the heat generated in solid targets due to beam bombardment cannot be removed easily and the resulting thermal shock damage is a serious problem. The behavior of a free-moving liquid mercury or gallium jet due to a proton beam deposition in a strong magnetic field has been modeled and analyzed for the muon collider project. Free liquid-metal jets offer significant advantages over conventional solid targets, particularly for the more demanding and challenging high-power applications.
NTIS
Nuclear Physics; Linear Accelerators; Computerized Simulation; Heating; Hydrodynamics; Thermal Shock

20020000929 Department of Energy, Nevada Operations Office, Las Vegas, NV USA
Screening Resonances In Plasmas
Winkler, P.; Dec. 01, 1998; 6p; In English
Report No.(s): DE2001-2576; UNR 1330-112-1652; No Copyright; Avail: Department of Energy Information Bridge, Microfiche

When it was suggested that a new recombination mechanism (Resonant Radiative Recombination (RRR)) which, based on very general physical arguments, should happen in dense plasmas and promises to provide useful information for the local

temperature and density diagnostics of plasmas, they assumed the existence of screening resonances. For model potentials the existence of screening resonances has been demonstrated beyond reasonable doubt in a number of calculations. The key question, how well those potentials describe the dominant effects of a real plasma remains open. The relation of theoretical predictions to experimentally measurable effects is an important issue at the present stage of their research. In particular, RRR is expected to account for enhanced recombination rates of low energetic electrons with their ions, since the first stage is the resonant capture of a slow electron by an atom or ion. The mechanism that traps an electron is a combination of complicated many-body interactions of the ions and electrons. For clarity they start here, however, with a discussion in terms of local potential traps the shapes of which are determined predominantly and in an average way by two factors: the degree of screening present at the ionic site and the degree of short-range order in the immediate neighborhood of this ion.
NTIS
Plasma Diagnostics; Dense Plasmas; Radiative Recombination; Plasma Resonance; Predictions

20020001047 Lawrence Livermore National Lab., Livermore, CA USA
Current Status of the Recirculator Project at LLNL
Ahle, L.; Autrey, D.; Barnard, J.; Craig, G.; Debeling, A.; Mar. 23, 1999; 5p; In English
Report No.(s): DE2001-8554; UCRL-JC-132273; AT5015031; No Copyright; Avail: Department of Energy Information Bridge, Microfiche

The Heavy Ion Fusion Group at Lawrence Livermore National Laboratory has for several years been developing the world's first circular ion induction accelerator designed to transport space charge dominated beams. Currently, the machine extends to 90 degrees, or 10 half-lattice periods (HLP) with induction cores for acceleration placed on every other HLP. Full current transport with acceptable emittance growth without acceleration has been achieved. Recently, a time stability measurement revealed a 2% energy change with time due to a source heating effect. Correcting for this and conducting steering experiments has ascertained the energy to an accuracy of 0.2%. In addition, the charge centroid is maintained to within 0.6-mm throughout the bend section. Initial studies of matches dependencies on beam quality indicate significant effects.
NTIS
Ion Accelerators; Heavy Ions; Space Charge

20020001169 Lawrence Livermore National Lab., Livermore, CA USA
Radiographic Simulations and Analysis for ASCI
Aufderheide, M.; Stone, D.; VonWittenau, A.; Dec. 18, 1998; 10p; In English
Report No.(s): DE2001-8734; UCRL-JC-132806; DP0101031; No Copyright; Avail: Department of Energy Information Bridge, Microfiche

In this paper, the authors describe their work on developing quantitatively accurate radiographic simulation and analysis tools for ASCI hydro codes. They have extended the ability of HADES, the code which simulates radiography through a mesh, to treat the complex meshes used in ASCI calculations. The ultimate goal is to allow direct comparison between experimental radiographs and full physics simulated radiographs of ASCI calculations. They describe the ray-tracing algorithm they have developed for fast, accurate simulation of dynamic radiographs with the meshes used in ALE3D, an LLNL ASCI code. Spectral effects and material compositions are included. In addition to the newness of the mesh types, the distributed nature of domain decomposed problems requires special treatment by the radiographic code. Because of the size of such problems, they have parallelized the radiographic simulation, in order to have quick turnaround time. presently, this is done using the domain decomposition from the hydro code. They demonstrate good parallel scaling as the size of the problem is increased. They show a comparison between an experimental radiograph of a high explosive detonation and a simulated radiograph of an ALE3D calculation. They conclude with a discussion of future work.
NTIS
Radiography; Computerized Simulation; Computer Programs; Hydrodynamics

20020001224 Sandia National Labs., Albuquerque, NM USA
Wire Array Z-Pinch Insights for Enhanced X-Ray Production
Apruzese, J. P.; Chittenden, J. P.; Greenly, J. B.; Haines, M. G.; Mock, R. C.; Jan. 04, 1999; 42p; In English
Report No.(s): DE2001-2826; SAND98-1659C; No Copyright; Avail: Department of Energy Information Bridge, Microfiche

Comparisons of measured total radiated x-ray power from annular wire-array z-pinches with a variety of models as a function of wire number, array mass, and load radius are reviewed. The data, which are comprehensive, have provided important insights into the features of wire-array dynamics that are critical for high x-ray power generation. Collectively, the comparisons of the data with the model calculations suggest that a number of underlying dynamical mechanisms involving cylindrical asymmetries and

plasma instabilities contribute to the measured characteristics. For example, under the general assumption that the measured risetime of the total-radiated-power pulse is related to the thickness of the plasma shell formed on axis, the Heuristic Model agrees with the measured risetime under a number of specific assumptions about the way the breakdown of the wires, the wire-plasma expansion, and the Rayleigh-Taylor instability in the r-z plane, interact. Likewise, in the high wire-number regime (where the wires are calculated to form a plasma shell prior to significant radial motion of the shell) the comparisons show that the variation in the power of the radiation generated as a function of load mass and array radius can be simulated by the 2-D (two dimensional) Eulerian radiation magnetohydrodynamics code (E-RMHC), using a single random-density perturbation that seeds the Rayleigh-Taylor instability in the r-z plane. For a given pulse-power generator, the comparisons suggest that (1) the smallest interwire gaps compatible with practical load construction and (2) the minimum implosion time consistent with the optimum required energy coupling of the generator to the load should produce the highest total-radiated-power levels.
NTIS
Zeta Pinch; X Rays; Magnetohydrodynamic Stability; Plasmas (Physics)

20020001291 Princeton Univ., Plasma Physics Lab., NJ USA
MHD Stability Calculations of High-Beta Quasi-Axisymmetric Stellarators
Kessel, C.; Fu, G. Y.; Ku, L. P.; Redi, M. H.; Pomphrey, N.; Sep. 01, 1999; 4p; In English
Report No.(s): DE2001-12170; PPPL-3357; No Copyright; Avail: Department of Energy Information Bridge, Microfiche

The MHD stability of quasi-axisymmetric compact stellarators is investigated. It is shown that bootstrap current driven external kink modes can be stabilized by a combination of edge magnetic shear and appropriate 3D plasma boundary shaping while maintaining good quasi-axisymmetry. The results demonstrate that there exists a new class of stellarators with quasi-axisymmetry, large bootstrap current, high MHD beta limit, and compact size.
NTIS
Magnetohydrodynamic Stability; Stellarators; Symmetry; Three Dimensional Flow

20020001543 Lawrence Livermore National Lab., Livermore, CA USA
Integrated simulation and modeling capability for alternate magnetic fusion concepts
Cohen, B. I.; Hooper, E. B.; Jarboe, T. R.; LoDestro, L. L.; Pearlstein, L. D.; Nov. 03, 1998; 44p; In English
Report No.(s): DE2001-2810; UCRL-ID-132327; AT5020100; No Copyright; Avail: Department of Energy Information Bridge, Microfiche

This document summarizes a strategic study addressing the development of a comprehensive modeling and simulation capability for magnetic fusion experiments with particular emphasis on devices that are alternatives to the mainline tokamak device. A code development project in this area supports two defined strategic thrust areas in the Magnetic Fusion Energy Program: (1) comprehensive simulation and modeling of magnetic fusion experiments and (2) development, operation, and modeling of magnetic fusion alternate- concept experiment
NTIS
Nuclear Fusion; Tokamak Devices

20020001588 Lawrence Livermore National Lab., Livermore, CA USA
Theory of the equation of state of hot dense matter
Barbee, T. W.; Surh, M.; Yang, L. H.; Jul. 23, 1999; 7p; In English
Report No.(s): DE2001-12730; UCRL-JC-133454; No Copyright; Avail: Department of Energy Information Bridge, Microfiche

Ab initio molecular dynamics calculations are adapted to treat dense plasmas for temperatures exceeding the electronic Fermi temperature. Extended electronic states are obtained in a plane wave basis by using pseudopotentials for the ion cores in the local density approximation to density functional theory. The method reduces to conventional first principles molecular dynamics at low temperatures with the expected high level of accuracy. The occurrence of thermally excited ion cores at high temperatures is treated by means of final state pseudopotentials. The method is applied to the shock compression Hugoniot equation of state for aluminum. Good agreement with experiment is found for temperatures ranging from zero through 105 K.
NTIS
Equations of State; Molecular Dynamics; Dense Plasmas

20020001663 Lawrence Livermore National Lab., Livermore, CA USA

2-D electric fields and drifts near the magnetic separatrix in divertor tokamaks

Mattor, N.; Porter, G. D.; Rognlien, T. D.; Ryutov, D. D.; Nov. 15, 1998; 22p; In English

Report No.(s): DE2001-2808; UCRL-JC-132425; AT5020100; No Copyright; Avail: Department of Energy Information Bridge, Microfiche

A 2-D calculation is presented for the transport of plasma in the edge region of a divertor tokamak solving continuity, momentum, and energy balance fluid equations. The model uses anomalous radial diffusion, including perpendicular ion momentum, and classical cross-field drifts transport. Parallel and perpendicular currents yield a self-consistent electrostatic potential on both sides of the magnetic separatrix. Outside the separatrix, the simulation extends to material divertor plates where the incident plasma is recycled as neutral gas and where the plate sheath and parallel currents dominate the potential structure. Inside the separatrix, various radial current terms - from viscosity, charge-exchange and poloidal damping, inertia, and (triangledown)B - contribute to the determining the potential. The model rigorously enforces cancellation of gyro-viscous and magnetization terms from the transport equations. The results emphasize the importance of E x B particle flow under the X-point which depends on the sign of the toroidal magnetic field. Radial electric field (E(sub y)) profiles at the outer midplane are small with weak shear when high L-mode diffusion coefficients are used and are large with strong shear when smaller H-mode diffusion coefficients are used. The magnitude and shear of the electric field (E(sub y)) is larger both when the core toroidal rotation is co-moving with the inductive plasma current and when the ion (triangledown)B-drift is towards the single-null X-point.

NTIS

Diverters; Tokamak Devices; Plasma Drift; Plasmas (Physics); Two Dimensional Models

20020001962 Lawrence Livermore National Lab., Livermore, CA USA

Recent laser-plasma interaction studies at LLNL

Berger, R. L.; Decker, C.; Divol, L.; Geddes, C.; Glenzer, S. H.; Sep. 01, 1999; 8p; In English

Report No.(s): DE2001-12732; UCRL-JC-133633; No Copyright; Avail: Department of Energy Information Bridge, Microfiche

Recent analysis and modeling of Nova experiments which address our understanding of stimulated Brillouin scattering (SBS) and stimulated Raman scattering (SRS) will be presented. Forward and backward SBS levels have been investigated with SSD of varying bandwidth and with polarization smoothing using an f/8 focusing geometry to emulate NIF conditions. The interpretation of the experiments is aided using F3D, a fluid code which includes modeling of SBS and SRS; a parallel version of F3D is being developed which will allow the modeling of a plasma approaching the size of an entire NIF laser beam. Cryogenic targets have recently been employed to investigate the dependence of SRS saturation levels on ion wave damping via the Langmuir decay instability.

NTIS

Laser Plasma Interactions; Brillouin Effect; Raman Spectra

20020001970 Argonne National Lab., IL USA

ALPS: advanced limiter-divertor plasma-facing systems

Allain, J. P.; Bastasz, R.; Brooks, J. N.; Evans, T.; Hassanein, A.; Sep. 15, 1999; 28p; In English

Report No.(s): DE2001-12437; ANL/TD/CP-98438; No Copyright; Avail: Department of Energy Information Bridge, Microfiche

The Advanced Limiter-divertor Plasma-facing Systems (ALPS) program was initiated in order to evaluate the potential for improved performance and lifetime for plasma-facing systems. The main goal of the program is to demonstrate the advantages of advanced limiter/divertor systems over conventional systems in terms of power density capability, component lifetime, and power conversion efficiency, while providing for safe operation and minimizing impurity concerns for the plasma. Most of the work to date has been applied to free surface liquids. A multi-disciplinary team from several institutions has been organized to address the key issues associated with these systems. The main performance goals for advanced limiters and diverters are a peak heat flux of & amp;gt;50 MW/m(sup 2),elimination of a lifetime limit for erosion, and the ability to extract useful heat at high power conversion efficiency ((approximately)40%). The evaluation of various options is being conducted through a combination of laboratory experiments, modeling of key processes, and conceptual design studies. The current emphasis for the work is on the effects of free surface liquids on plasma edge performance.

NTIS

Limiters (Fusion Reactors); Plasmas (Physics); Power Efficiency; Systems Engineering

20020002008 Sandia National Labs., Albuquerque, NM USA

High Temperature Dynamic Hohlraums on the Pulsed Power Driver Z

Armijo, J.; Chandler, G. A.; Cooper, G.; Derzon, M. S.; Fehl, D.; Jan. 04, 1999; 39p; In English

Report No.(s): DE2001-2824; SAND98-1660C; No Copyright; Avail: Department of Energy Information Bridge, Microfiche

In the concept of the dynamic hohlraum an imploding z-pinch is optically thick to its own radiation. Radiation may be trapped inside the pinch to give a radiation temperature inside the pinch greater than that outside the pinch. The radiation is typically produced by colliding an outer Z-pinch liner onto an inner liner. The collision generates a strongly radiating shock, and the radiation is trapped by the outer liner. As the implosion continues after the collision the radiation temperature may continue to increase due to ongoing PdV (pressure times change in volume) work done by the implosion. In principal the radiation temperature may increase to the point at which the outer liner burns through, becomes optically thin, and no longer traps the radiation. One application of the dynamic hohlraum is to drive an ICF (inertial confinement fusion) pellet with the trapped radiation field. Members of the dynamic hohlraum team at Sandia National Labs have used the pulsed power driver Z (20 LMA, 100 ns) to create a dynamic hohlraum with temperature linearly ramping from 100 to 180 eV over 5 ns. On this shot zp214 a nested tungsten wire array of 4 and 2 cm diameters with masses of 2 and 1 mg imploded onto a 2.5 mg plastic annulus at 5 mm diameter. The current return can on this shot was slotted. It is likely the radiation temperature may be increased to over 200 CV by stabilizing the pinch with a solid current return can. A current return can with 9 slots imprints 9 filaments onto the imploding pinch. This degrades the optical trapping and the quality of the liner collision. A 1.6 mm diameter capsule situated inside this dynamic hohlraum of zp214 would see 15 kJ of radiation impinging on its surface before the pinch itself collapses to a 1.6 mm diameter. Dynamic hohlraum shots including pellets are scheduled to take place on Z in September of 1998.

NTIS

Zeta Pinch; Inertial Confinement Fusion; Hohlraums; Radiation Trapping

20020002276 Lawrence Livermore National Lab., Livermore, CA USA

Inertial fusion science and technology for the next century

Campbell, E. M.; Hogan, W. J.; Landes, S.; Sep. 10, 1999; 13p; In English

Report No.(s): DE2001-12445; UCRL-JC-135589; No Copyright; Avail: Department of Energy Information Bridge, Microfiche

This paper reviews the leading edge of the basic and applied science and technology that use high-intensity facilities and looks at what opportunities lie ahead. The more than 15,000 experiments on the Nova laser since 1985 and many thousands more on other laser, particle beam, and pulsed power facilities around the world have established the new laboratory field of high-energy-density plasma physics and have furthered development of inertial fusion. New capabilities such as those provided by high-brightness femtosecond lasers have enabled the study of matter in conditions previously unachievable on earth. These experiments, along with advanced calculations now practical because of the progress in computing capability, have established the specifications for the National Ignition Facility and Laser MegaJoule and have enhanced new scientific fields such as laboratory astrophysics. Science and technology developed in inertial fusion have found near-term commercial use, have enabled steady progress toward the goal of fusion ignition and gain in the laboratory, and have opened up new fields of study for the 21st century.

NTIS

Plasma Physics; Confinement; Lasers; Inertial Fusion (Reactor); Laser Beams; Progress; Technologies

20020002280 Princeton Univ., Plasma Physics Lab., NJ USA

Collisional Delta-f Scheme with Evolving Background for Transport Time Scale Simulations

Valeo, E.; Krommes, J.; Brunner, S.; Jul. 01, 1999; 52p; In English

Report No.(s): DE2001-8844; PPPL-3350; DE-AC02-CHO03073; No Copyright; Avail: Department of Energy Information Bridge, Microfiche

The delta-f approach is extended for simulating the transport time-scale evolution of near-Maxwellian distributions in collisional plasmas. This involves simultaneously advancing weighted marker particles for representing the intrinsically kinetic component delta-f, and fluid equations for the parameters of the shifted Maxwellian background f(subSM). The issue of increasing numerical noise in a collisional delta-f algorithm, due to marker particle weight spreading, is addressed in detail, and a solution to this problem is proposed. To obtain higher resolution in critical regions of phase space, a practical procedure for implementing sources and sinks of marker particles is developed. As a proof of principal, this set of methods are applied for computing electrical Spitzer conductivity as well as collisional absorption in a homogeneous plasma.

NTIS

Collisional Plasmas; Simulation

20020002289 California Univ., Los Angeles, CA USA
Experimental Investigation of Nonlinear Plasma Wake-Fields
Rosenzweig, J.; Oct. 31, 1997; 27p; In English
Report No.(s): DE2001-765808; No Copyright; Avail: Department of Energy Information Bridge, Microfiche

We discuss the exploration of the newly proposed blowout regime of the plasma wakefield accelerator and advanced photoinjector technology for linear collider applications. The plasma wakefield experiment at ANL produced several ground-breaking results in the physics of the blowout regime. The photoinjector R and D effort produced breakthroughs in theoretical, computational, and experimental methods in high brightness beam physics. Results have been published.
NTIS
Nonlinearity; Experimentation; Wakes; Plasma Accelerators; Injectors

20020002293 Texas Univ., Austin, TX USA
Plasma Colloquium Travel Grant Program ***Final Report, 15 Sep. 1997 - 14 Sep. 1998***
Hazeltine, R. D.; Sep. 14, 1998; 7p; In English
Report No.(s): DE2001-765654; No Copyright; Avail: Department of Energy Information Bridge, Microfiche

The purpose of the Travel Grant Program is to increase the awareness of plasma research. The new results and techniques of plasma research in fusion plasmas, plasma processing space plasmas, basic plasma science, etc, have broad applicability throughout science. The benefits of these results are limited by the relatively low awareness and appreciation of plasma research in the larger scientific community. Whereas spontaneous interactions between plasma scientists and other scientists are useful, a focused effort in education and outreach to other scientists is efficient and is needed. The academic scientific community is the initial focus of this effort, since that permits access to a broad cross-section of scientists and future scientists including undergraduates, graduate students, faculty, and research staff.
NTIS
Plasmas (Physics); Controlled Fusion; Research

20020002297 Wisconsin Univ., Madison, WI USA
TFTR ICRF (Ion Cyclotron Range of Frequencies) modeling
Scharer, J. E.; Sund, R.; Oct. 01, 1998; 22p; In English
Report No.(s): DE2001-765304; No Copyright; Avail: Department of Energy Information Bridge

The report presents results and analysis of computer modeling of ICRF (ion cyclotron resonant frequency) shots performed over several days during the final TFTR (Tokamak Fusion Test Reactor) run period. These include shot numbers 103575, 103577, 104911, 104913, 104920, 104921, and 104925. In particular we have examined mode-conversion shots in DT plasmas including supershots with tritium beams and a fast alpha component. In such shots a fraction of the fast wave (FW) energy launched by antennas on the low-field side of the device is converted to ion-Bernstein waves (IBW) near the tow-ion hybrid resonance.
NTIS
Cyclotrons; Cyclotron Frequency; Computerized Simulation; Ion Cyclotron Radiation

20020003355 Maryland Univ., College Park, MD USA
Soft X-Ray Spectroscopic Measurements of Plasma Conditions at Early Times in ICF Experiments on OMEGA.
Griem, H. R.; Elton, R. C.; Feb. 28, 2000; 34p; In English
Report No.(s): DE2001-761595; DOE/SF/21783-2; No Copyright; Avail: Department of Energy Information Bridge, Microfiche

The preheating of laser-heated microballoon targets has been measured by time-resolved x-ray and extreme ultraviolet (euv) spectroscopy on the 30 kJ, 351 nm, 60-beam laser-fusion system at the University of Rochester Laboratory for Laser Energetics. Thin coating of aluminum overcoated with magnesium served as indicators. Both the sequence of the x-ray line emission and the intensity of euv radiation were used to determine a preheating peaking at 10 ns prior to onset of the main laser pulse, with a power density 1% of the main pulse. The measurements are supported by numerical modeling. Further information is provided by absorption spectra from the aluminum coating, backlighted by continuum from the heated surface. The exact source of the preheating energy remains unknown at present, but most likely arrives from early laser leakage through the system. The present target diagnostic is particularly useful when all beams cannot be monitored directly at all laser wavelengths.
NTIS
Extreme Ultraviolet Radiation; Absorption Spectra; Aluminum Coatings; X Rays

20020003417 California Univ., Lawrence Berkeley Lab., Berkeley, CA USA

New 500-kV Ion Source Test Stand for HIF

Sangster, T. C.; Ahle, L. E.; Halaxa, E. F.; Karpenko, V. P.; Oldaker, M. E.; Oct. 05, 2000; 10p; In English

Report No.(s): DE2001-767595; LBNL-45684; HIFAN 1038; No Copyright; Avail: Department of Energy Information Bridge, Microfiche

One of the most challenging aspects of ion beam driven inertial fusion energy is the reliable and efficient generation of low emittance, high current ion beams. The primary ion source requirements include a rise time of order 1-msec, a pulse width of at least 20-msec, a flattop ripple of less than 0.1% and a repetition rate of at least 5-Hz. Naturally, at such a repetition rate, the duty cycle of the source must be greater than 108 pulses. Although these specifications do not appear to exceed the state-of-the-art for pulsed power, considerable effort remains to develop a suitable high current ion source. Therefore, we are constructing a 500-kV test stand specifically for studying various ion source concepts including surface, plasma and metal vapor arc. This paper will describe the test stand design specifications as well as the details of the various subsystems and components.

NTIS

Ion Sources; Pulse Duration; Low Currents; Emittance

20020003422 Los Alamos National Lab., NM USA

Production of a raleigh-taylor instability target

Day, R.; Aug. 01, 2000; 6p; In English

Report No.(s): DE2001-768255; LA-UR-00-3739; No Copyright; Avail: Department of Energy Information Bridge, Microfiche

Raleigh-Taylor (RT) instabilities occur when a low-density fluid attempts to accelerate a high-density fluid. The instability manifests itself by forming bubbles of the low-density that percolate through the high-density fluid. Concurrently, spikes of the high-density fluid jet into the low-density fluid. This instability is seen in familiar occurrences such as the growth of icicles and the draining of sinks. If the interface between the two fluids remains perfectly smooth the instability will not occur; that is, it must be 'seeded' by a wave-like perturbation. For the two cases mentioned above, a vibration can be sufficient to perform the 'seeding.'

NTIS

Targets; Taylor Instability; Perturbation; Stability

20020003731 Lawrence Livermore National Lab., Livermore, CA USA

Capillary waveguide for laser acceleration in vacuum, gases and plasmas

Xie, M.; Jun. 01, 1998; 7p; In English

Report No.(s): DE2001-6420; LBNL-42055; No Copyright; Avail: Department of Energy Information Bridge

The authors propose a new method for laser acceleration of relativistic electrons using the leaky modes of a hollow dielectric waveguide. The hollow core of the waveguide can be either in vacuum or filled with uniform gases or plasmas. In of vacuum and gases, TM(sub 01) mode is used for direct acceleration. In case of plasmas, EH(sub 11) mode is used to drive longitudinal plasma wave for acceleration. Structure damage by high power laser is avoided by choosing a core radius much larger than laser wavelength.

NTIS

Dielectric Waveguides; High Energy Electrons; High Power Lasers; Acceleration (Physics); Plasma Waves; Vacuum Systems; Accelerators

20020003933 Argonne National Lab., IL USA

Summary report: working group 5 on 'electron beam-driven plasma and structure based acceleration concepts'

Conde, M. E.; Katsouleas, T.; Oct. 19, 2000; 5p; In English

Report No.(s): DE2001-766351; ANL-HEP-CP-00-111; No Copyright; Avail: Department of Energy Information Bridge, Microfiche

The talks presented and the work performed on electron beam-driven accelerators in plasmas and structures are summarized. Highlights of the working group include new experimental results from the E-157 Plasma Wakefield Experiment, the E-150 Plasma Lens Experiment and the Argonne Dielectric Structure Wakefield experiments. The presentations inspired discussion and analysis of three working topics: electron hose instability, ion channel lasers and the plasma afterburner.

NTIS

Electron Beams; Dielectrics; Lasers

20020003940 California Univ., Lawrence Berkeley Lab., Berkeley, CA USA

3.3 MJ, Rb(sup +1) Driver Design Based on an Integrated Systems Analysis

Meier, W. R.; Barnard, J. J.; Bangerter, R. O.; Sep. 15, 2000; 14p; In English

Report No.(s): DE2001-767629; LBNL-46787; HIFAN 1060; No Copyright; Avail: Department of Energy Information Bridge, Microfiche

A computer model for systems analysis of heavy ion drivers has been developed and used to evaluate driver designs for inertial fusion energy (IFE). The present work examines a driver for a close-coupled target design that requires less total beam energy but also smaller beam spots sizes than previous target designs. Design parameters and a cost estimate for a 160 beam, 3.3 MJ driver using rubidium ions (A = 85) are reported, and the sensitivity of the results to variations in selected design parameters is given. NTIS

Heavy Ions; Sensitivity; Systems Analysis; Design Analysis

20020003941 Princeton Univ., Plasma Physics Lab., NJ USA

Magnetic Reconnection with Sweet-Parker Characteristics in Two-dimensional Laboratory Plasmas

Carter, T.; Hsu, S.; Ji, H.; Kulsrud, R.; Yamada, M.; Jan. 01, 1999; 22p; In English

Report No.(s): DE2001-3001; PPPL-3336; No Copyright; Avail: Department of Energy Information Bridge

Magnetic reconnection has been experimentally studied in a well-controlled, two-dimensional laboratory magnetohydrodynamic plasma. The observations are found to be both qualitatively and quantitatively consistent with a generalized Sweet-Parker model which incorporates compressibility, downstream pressure, and the effective resistivity. The latter is significantly enhanced over its classical values in the collisionless limit. This generalized Sweet-Parker model also applies to the case in which an unidirectional, sizable third magnetic component is present. NTIS

Magnetic Field Reconnection; Plasmas (Physics); Magnetohydrodynamics

20020003974 Lawrence Livermore National Lab., Livermore, CA USA

High yield ICF target design for a Z-pinch driven hohlraum

Bailey, D. S.; Hammer, J. H.; Lindl, J. D.; Rambo, P. W.; Tabak, M.; Nov. 13, 1998; 24p; In English

Report No.(s): DE2001-2856; UCRL-JC-131389; DP0210000; No Copyright; Avail: Department of Energy Information Bridge

We describe calculations for a high yield inertial fusion design, employing indirect drive with a double-ended z-pinch-driven hohlraum radiation source. A high current (approximately 60 MA) accelerator implodes z-pinches within an enclosing hohlraum. Radial spoke arrays and shine shields isolate the capsule from the pinch plasma, magnetic field and direct x-ray shine. Our approach places minimal requirements on z-pinch uniformity and stability, usually problematic due to magneto-Rayleigh Taylor (MRT) instability. Large inhomogeneities of the pinch and spoke array may be present, but the hohlraum adequately smooths the radiation field at the capsule. Simultaneity and reproducibility of the pinch x-ray output to better than 7% are required, however, for good symmetry. Recent experiments suggest a pulse shaping technique, through implosion of a multishell z-pinch. X-ray bursts are calculated and observed to occur at each shell collision. A capsule absorbing 1 MJ of x-rays at a peak drive temperature of 210 eV is found to have adequate stability and to produce 400 MJ of yield. NTIS

Inertial Confinement Fusion; Radiation Distribution; Zeta Pinch; Magnetohydrodynamic Stability

20020003977 Lawrence Livermore National Lab., Livermore, CA USA

Anomalous resistivity of high-Z plasma with hydrogen admixture

Ryutov, D. D.; Toor, A.; Nov. 06, 1998; 16p; In English

Report No.(s): DE2001-2849; UCRL-JC-132401; DP0102012; No Copyright; Avail: Department of Energy Information Bridge

Among microinstabilities that may affect the resistance of a Z is greater than > 1 plasma in fast Z pinches, are the ion acoustic and the lower hybrid instabilities. We discuss effects of hydrogen ions on these instabilities and find that, by properly adjusting the hydrogen concentration, one can considerably increase the threshold current density for the onset of the instability. In addition to a strong Landau damping on hydrogen ions; there is a collisional stabilizing mechanism related to a collisional friction between the two ion species. Another interesting aspect of the stability analysis is related to the fact that the magnetization (a product of the gyrofrequency and the collisional frequency) of the heavy ions and the hydrogen ions is very different. We discuss possible ways of adding the hydrogen to high-Z material. This is simple in case of gas-puff pinches, where the hydrogen could be added

to the main gas before the puffing. For the wire arrays, one might try to saturate th e assembled array by hydrogen prior to the main discharge. One more possibility is using interwoven thin wires of a main component (say, tungsten) and polymer.
NTIS
Ion Acoustic Waves; Plasma Pinch; Magnetohydrodynamic Stability; Heavy Ions; Hydrogen Ions; Landau Damping

20020003980 Lawrence Livermore National Lab., Livermore, CA USA
Antiproton Fast Ignition for Inertial Confinement Fusion
Perkins, L. J.; Oct. 24, 1997; 21p; In English
Report No.(s): DE2001-2846; UCRL-ID-128923; AT5015033; No Copyright; Avail: Department of Energy Information Bridge
With 180MJ/micro-g, antiprotons offer the highest stored energy per unit mass of any known entity. We investigate the use of antiprotons to promote fast ignition in an ICF capsule and seek high gains with only modest compression of the main fuel. Unlike standard fast ignition where the ignition energy is supplied by an energetic, short pulse laser, the energy here is supplied through the ionization energy deposited when antiprotons annihilate at the center of a compressed fuel capsule. In the first of two candidate fast ignition schemes, the antiproton package is delivered by a low energy external ion beam. In the second, 'autocatalytic' scheme, the antiprotons are pre-emplaced at the center of the capsule prior to compression. In both schemes, we estimate that approximately 3 x 10(exp 13) antiprotons are required to initiate fast ignition in a typical ICF capsule and show that incorporation of a thin, heavy metal shell is desirable to enhance energy deposition in the igniter zone. In addition to obviating the need for a second energetic fast laser and vulnerable final optics, this scheme would achieve central without reliance on laser channeling through halo plasma or houlrahm debris. However, in addition to the unknowns involved in the storage and manipulation of antiprotons at low energy, the other large uncertainty for the practicality of such a scheme is the ultimate efficiency of antiproton production in, an external, optimized facility.
NTIS
Ignition; Inertial Confinement Fusion; Antiprotons; Ion Beams; Annihilation Reactions; Plasmas (Physics); Pulsed Lasers

20020004015 Los Alamos National Lab., NM USA
Observation of the Josephson Plasma Resonance in Tl(2)Ba(2)CaCu(2)O(8) Using THz spectroscopy
Thorsmolle, V.; Aug. 01, 2000; 6p; In English
Report No.(s): DE2001-768904; LA-UR-00-3612; No Copyright; Avail: Department of Energy Information Bridge, Microfiche
Employing terahertz time-domain spectroscopy in transmission, we have unambiguously observed the Josephson Plasma Resonance in Tl2Ba2CaCu2,08 high-T(c) thin films in zero magnetic field as a function of temperature.
NTIS
Spectroscopy; Josephson Effect; Plasma Resonance; Superconducting Films

20020005209 Wisconsin Univ., Madison, WI USA
Investigation of the Spherical Stellarator Concept *Final Report*
Moroz, P. E.; Oct. 15, 2000; 13p; In English
Report No.(s): DE2001-769258; No Copyright; Avail: Department of Energy Information Bridge, Microfiche
This document is a final report of the U.S. DOE grant entitled 'Investigation of the Spherical Stellarator Concept' which supported theoretical and numerical investigation of a novel fusion concept, the ultra-low-aspect-ratio stellarator system called Spherical Stellarator (SS). The research was concentrated on (a) search for principally different types of SS configurations, (b) optimization of SS configurations by varying the parameters of the coil systems, (c) finite beta and finite plasma current (including bootstrap current) equilibria in the SS, and (d) Monte Carlo particle transport simulations for the SS.
NTIS
Stellarators; Plasma Currents; Spherical Shells

20020005218 California Univ., Lawrence Berkeley Lab., Berkeley, CA USA
Heavy Ion Fusion Program in the USA
Bangerter, R. O.; Davidson, R. C.; Herrmannsfeldt, W. B.; Lindl, J. D.; Logan, B. G.; Oct. 03, 2000; 13p; In English
Report No.(s): DE2001-771937; LBNL-46933; HIFAN-1073; No Copyright; Avail: Department of Energy Information Bridge
Inertial fusion energy research has enjoyed increased interest and funding. This has allowed expanded programs in target design, target fabrication, fusion chamber research, target injection and tracking, and accelerator research. The target design effort examines ways to minimize the beam power and energy and increase the allowable focal spot size while preserving target gain. Chamber research for heavy ion fusion emphasizes the use of thick liquid walls to serve as the coolant, breed tritium, and protect the structural wall from neutrons, photons, and other target products. Several small facilities are now operating to model fluid

chamber dynamics. A facility to study target injection and tracking has been built and a second facility is being designed. Improved economics is an important goal of the accelerator research. The accelerator research is also directed toward the design of an Integrated Research Experiment (IRE). The IRE is being designed to accelerate ions to greater than MeV, enabling experiments in beam dynamics, focusing, and target physics. Activities leading to the IRE include ion source development and a High Current Experiment (HCX) designed to transport and accelerate a single beam of ions with a beam current of approximately 1 A, the initial current required for each beam of a fusion driver. In terms of theory, the program is developing a source-to-target numerical simulation capability. The goal of the entire program is to enable an informed decision about the promise of heavy ion fusion in about a decade.
NTIS
Heavy Ions; Fusion Reactors; Energy Technology; Design Analysis

20020005254 Princeton Univ., Plasma Physics Lab., NJ USA
Small-action Resonance in Hamiltonian Systems and Redistribution of Energetic Ions in Tokamaks
White, R. B.; Lutsenko, V. V.; Kolesnichenko, Y. I.; Yakovenko, Y. V.; Jul. 01, 1999; 10p; In English
Report No.(s): DE2001-8976; PPPL-3349; DE-AC02-CHO-3073; No Copyright; Avail: Department of Energy Information Bridge, Microfiche

It has been found that an arbitrary small perturbation in an integrable Hamiltonian system typically leads to driven resonance in the regions of the phase space where at least one of the action variables is sufficiently small. In particular, such a small-action resonance is shown to play a dominant role in the sawtooth-crash-induced disappearance of a strongly localized gamma-ray and neutron emitting region in a tokamak plasma, which was observed experimentally.
NTIS
Hamiltonian Functions; Ions; Perturbation; Tokamak Devices; Energetic Particles

20020005265 Sandia National Labs., Albuquerque, NM USA
Prospects for High-Yield ICF with a Z-Pinch Driven Dynamic Hohlraum
Chandler, G. A.; Chrien, R.; Cooper, G. W.; Derzon, M. S.; Douglas, M. R.; Sep. 07, 1999; 10p; In English
Report No.(s): DE2001-12721; SAND99-0832C; No Copyright; Avail: Department of Energy Information Bridge, Microfiche

Recent success with the Sandia Z machine has renewed interest in utilizing fast z-pinenes for Inertial Confinement Fusion (ICF). One promising concept places the ICF capsule internal to the imploding z-pinch. At machine parameters relevant to achieving high yield, the imploding z-pinch mass has sufficient opacity to trap radiation giving rise to a dynamic hohlraum. The concept utilizes a 12 MJ, 54 MA z-pinch driver producing a capsule drive temperature exceeding 300 eV to realize a 550 MJ thermonuclear yield. They present the current high-yield design and its development that supports high-yield ICF with a z-pinch driven dynamic hohlraum.
NTIS
Hohlraums; Zeta Pinch; Inertial Confinement Fusion

20020005266 Sandia National Labs., Albuquerque, NM USA
Z, ZX, and X-1: A Realistic Path to High Fusion Yield
Cook, D. L.; Oct. 07, 1999; 7p; In English
Report No.(s): DE2001-12722; SAND99-0983C; No Copyright; Avail: Department of Energy Information Bridge, Microfiche

Z-pinches now constitute the most energetic and powerful sources of x-rays available by a large margin. The Z accelerator at Sandia National Laboratories has produced 1.8 MJ of x-ray energy, 280 TW of power, and hohlraum temperatures of 200 eV. These advances are being applied to inertial confinement fusion (ICF) experiments on Z. The requirements for high fusion yield are exemplified in the target to be driven by the X-1 accelerator. X-1 will drive two z-pinches, each producing 7 MJ of x-ray energy and about 1000 TW of x-ray power. Together, these radiation sources will heat a hohlraum containing the 4-mm diameter ICF capsule to a temperature exceeding 225 eV for about 10 ns, with the pulse shape required to drive the capsule to high fusion yield, in the range of 200-1000 MJ. Since X-1 consists of two identical accelerators, it is possible to mitigate the technical risk of high yield by constructing one accelerator. This accelerator, ZX, will bridge the gap from Z to X-1 by driving an integrated target experiment with a very efficient energy source, ZX will also provide experimental condition that the full specifications of the X-1 accelerator for high yield are achievable, and that a realistic path to high fission yield exists.
NTIS
Inertial Confinement Fusion; Radiation Sources; X Rays; Zeta Pinch

20020005647 Princeton Univ., Plasma Physics Lab., NJ USA

Turbulence Scattering of High Harmonic Fast Waves

Ono, M.; Hosea, J.; LeBlanc, B.; Menard, J.; Phillips, C. K.; May 31, 2001; 8p; In English

Report No.(s): DE2001-786532; PPPL-3571; No Copyright; Avail: Department of Energy Information Bridge, Microfiche

Effect of scattering of high-harmonic fast-magnetosonic waves (HHFW) by low-frequency plasma turbulence is investigated. Due to the similarity of the wavelength of HHFW to that of the expected low-frequency turbulence in the plasma edge region, the scattering of HHFW can become significant under some conditions. The scattering probability increases with the launched wave parallel-phase-velocity as the location of the wave cut-off layer shifts toward the lower density edge. The scattering probability can be reduced significantly with higher edge plasma temperature, steeper edge density gradient, and magnetic field. The theoretical model could explain some of the HHFW heating observations on the National Spherical Torus Experiment (NSTX).

NTIS

Scattering; Plasma Turbulence; Magnetoacoustic Waves; Magnetic Fields; Plasmas (Physics)

20020005860 Princeton Univ., Plasma Physics Lab., NJ USA

Ion Heating by Fast Particle Induced Alfven Turbulence

Gates, D.; Gorelenkov, N.; White, R. B.; May 31, 2001; 19p; In English

Report No.(s): DE2001-786534; PPPL-3572; No Copyright; Avail: Department of Energy Information Bridge

A novel mechanism that directly transfers energy from Super-Alfvenic energetic ions to thermal ions in high-beta plasmas is described. The mechanism involves the excitation of compressional Alfven eigenmodes (CAEs) in the frequency range with omega less than or approximately equal to omega(subscript ci). The broadband turbulence resulting from the large number of excited modes causes stochastic diffusion in velocity space, which transfers wave energy to thermal ions. This effect may be important on the National Spherical Torus Experiment (NSTX), and may scale up to reactor scenarios. This has important implications for low aspect ratio reactor concepts, since it potentially allows for the modification of the ignition criterion.

NTIS

Plasma Heating; Plasmas (Physics)

20020005861 Princeton Univ., Plasma Physics Lab., NJ USA

Transient Transport Experiments in the CDX-U Spherical Torus

Munsat, T.; Efthimion, P. C.; Jones, B.; Kaita, R.; Majeski, R.; Jun. 12, 2001; 25p; In English

Report No.(s): DE2001-786537; PPPL-3574; No Copyright; Avail: Department of Energy Information Bridge

Electron transport has been measured in CDX-U using two separate perturbative techniques. Gas modulation at the plasma edge was used to introduce cold-pulses which propagate towards the plasma center, providing time-of-light information leading to a determination of Xe as a function of radius. Sawteeth at the q=1 radius (r/a approx. 0.15) induced heat-pulses which propagated outward towards the plasma edge, providing a complementary time-of- light based Xe profile measurement. This work represents the first localized measurement of Xe in a spherical torus. It is found that Xe = 1 - 2 m 2 =s in the plasma core (r/a is less than 1/3), increasing by an order of magnitude or more outside of this region. Furthermore, the Xe profile exhibits a sharp transition near r/a=1/3. Spectral and profile analyses of the soft x-rays, scanning interferometer, and edge probe data show no evidence of a significant magnetic island causing the high Xe region.

NTIS

Electron Transfer; Plasmas (Physics); Spectrum Analysis

76
SOLID-STATE PHYSICS

Includes condensed matter physics, crystallography, and superconductivity. For related information see also 33 Electronics and Electrical Engineering and 36 Lasers and Masers.

20020000739 Los Alamos National Lab., NM USA

Comparison between Radiation Damage Accumulation in Oxides with Pyrochlore and Fluorite Structures

Sickafus, K. E.; Minnervini, L.; Sep. 21, 2000; 11p; In English

Report No.(s): DE2001-763039; LA-UR-00-4469; No Copyright; Avail: Department of Energy Information Bridge, Microfiche

Ion irradiation damage experiments were performed on single crystals of the pyrochlore compound Er2Ti2O7 and the fluorite compound Er2Zr2O7. Results indicate that the pyrochlore compound is far more susceptible to defect accumulation and

amorphization than the fluorite compound. In particular, Er2Ti2O7 irradiated with 350 keV Xe(sup plus plus) ions succumbs to a amorphization transformation by a fluence of lx 10(exp 15) Xe/sq cm, while Er2Zr2O7 remains crystalline with no change in crysta1 structure to at least 5x10(exp 16)Xe/sq cm. Atomistic computer simulations were used to explain this difference in radiation damage behavior between compounds with similar structures. Simulations of defect formation energies reveal that point defects induced by irradiation, such as cation antisite and anion Frenkel pairs, are far more stable in the fluorite compound than in the pyrochlore compound.
NTIS
Oxides; Radiation Damage; Ion Irradiation; Single Crystals; Amorphous Materials

20020000881 Argonne National Lab., IL USA
Direct imaging of the first order spin flop transition in the layered manganite La1.4SR1.6Mn2O7
Berger, A.; Gray, K. E.; Miller, D. J.; Mitchell, J. F.; Vlasko-Vlasov, V. K.; Aug. 31, 1999; 15p; In English
Report No.(s): DE2001-11956; ANL/MSD/CP-99964; No Copyright; Avail: Department of Energy Information Bridge, Microfiche

The spin-flop transition in the antiferromagnetic layered manganite La(1.4)SR(1.6)Mn2O7 was studied using magnetization measurements and a high-resolution magneto-optical imaging technique. We report the direct observation of the formation of ferromagnetic domains appearing at the first order spin-flop transition. The magnetization process proceeds through nucleation of polarized domains at crystal defect sites and not through the expansion of polarized domains due to domain wall motion. A small magnetic hysteresis is caused by the difference between the mechanisms of nucleation and annihilation of domains in the mixed state. These results establish a direct link between the magnetic structure on the atomic scale as seen in neutron scattering and the macroscopic properties of the sample as seen in magnetization and conductivity measurements.
NTIS
Spin; Antiferromagnetism; Phase Transformations; Ferromagnetic Materials; Magnetic Field Configurations

20020000883 Argonne National Lab., IL USA
Studies of ferroelectric heterostructure thin films and interfaces via in situ analytical techniques
Auciello, O.; Dhote, A.; Gao, Y.; Gruen, D. M.; Im, J.; Aug. 30, 1999; 15p; In English
Report No.(s): DE2001-11953; ANL/MSD/CP-99947; No Copyright; Avail: Department of Energy Information Bridge, Microfiche

The science and technology of ferroelectric thin films has experienced an explosive development during the last ten years. Low-density non-volatile ferroelectric random access memories (NVFRAMs) are now incorporated in commercial products such as 'smart cards', while high permittivity capacitors are incorporated in cellular phones. However, substantial work is still needed to develop materials integration strategies for high-density memories. We have demonstrated that the implementation of complementary in situ characterization techniques is critical to understand film growth and interface processes, which play critical roles in film microstructure and properties. We are using uniquely integrated time of flight ion scattering and recoil spectroscopy (TOF-ISARS) and spectroscopic ellipsometry (SE) techniques to perform in situ, real-time studies of film growth processes in the high background gas pressure required to growth ferroelectric thin films. TOF-ISARS provides information on surface processes, while SE permits the investigation of buried interfaces as they are being formed. Recent studies on SRBi2Ta2O9 (SBT) and Ba(sub x)SR(1-x)TiO3 (BST) film growth and interface processes are discussed.
NTIS
Thin Films; Technologies; Real Time Operation; Ion Scattering; Gas Pressure; Ferroelectricity; Memory (Computers)

20020000898 Argonne National Lab., IL USA
Studies of ferroelectric heterostructure thin films, interfaces, and device-related processes via in situ analytical techniques
Aggarwal, S.; Auciello, O.; Dhote, A. M.; Gao, Y.; Gruen, D. M.; Jun. 29, 1999; 19p; In English
Report No.(s): DE2001-11884; ANL/MSD/CP-99433; No Copyright; Avail: Department of Energy Information Bridge, Microfiche

The science and technology of ferroelectric thin films has experienced an explosive development during the last ten years. Low-density non-volatile ferroelectric random access memories (NVFRAMS) are now incorporated in commercial products such as 'smart cards', while high permittivity capacitors are incorporated in cellular phones. However, substantial work is still needed to develop materials integration strategies for high-density memories. We have demonstrated that the implementation of complementary in situ characterization techniques is critical to understand film growth and device processes relevant to device development. We are using uniquely integrated time of flight ion scattering and recoil spectroscopy (TOF-ISARS) and spectroscopic ellipsometry (SE) techniques to perform in situ, real-time studies of film growth processes in the high background

gas pressure required to growth ferroelectric thin films. TOF-ISARS provides information on surface processes, while SE permits the investigation of buried interfaces as they are being formed. Recent studies on SRBi(sub 2)Ta(sub 2)O(sub 9) (SBT) and Ba(sub x)SR(sub 1(minus)x)TiO(sub 3) (BST) film growth and interface processes are discussed. Direct imaging of ferroelectric domains under applied electric fields can provide valuable information to understand domain dynamics in ferroelectric films. We discuss results of piezoresponse scanning force microscopy (SFM) imaging for nanoscale studies of polarization reversal and retention loss in Pb(Zr(sub x)Ti(sub 1(minus)x))O(sub 3) (PZT)-based capacitors. Another powerful technique suitable for in situ, real-time characterization of film growth processes and ferroelectric film-based device operation is based on synchrotrons X-ray scattering, which is currently being implemented at Argonne National Laboratory.
NTIS
Ferroelectric Materials; Thin Films; Numerical Analysis; Imaging Techniques; Real Time Operation

20020000909 Argonne National Lab., IL USA
Jahn-Teller Splitting and Zeeman Effect of Acceptors in Diamond
Anthony, T. R.; Grimsditch, M.; Kim, H.; Ramdas, A. K.; Rodriguez, S.; Sep. 11, 1999; 15p; In English; 20th; 20th International Conference on Defects in Semiconductors, 26-30 Jul. 1999, Berkeley, CA, USA
Report No.(s): DE2001-11964; ANL/MSD/CP-100009; No Copyright; Avail: Department of Energy Information Bridge, Microfiche

Employing the high resolution of a 5+4 tandem Fabry-Perot interferometer, we discovered that (Delta)(prime), the Raman active electronic transition between the spin-orbit split 1s(p(sub 3/2)): (Lambda)(sub 8) and 1s(P(sub 1/2)) (Lambda)(sub 7) acceptor ground states, is a doublet for a boron impurity in diamond with a clearly resolved spacing of 0.81 (+-) 0.15 cm(sup (minus)1). The direct observation of a Stokes/anti-Stokes pair with 0.80 (+-) 0.04 cm(sup (minus)1) shift provides a striking confirmation that the lower 1s(p(sub3/2)): (Lambda)(sub 8) ground state has experienced a splitting due to astatic Jahn-Teller distortion. The Zeeman effect of (Delta)(prime) has been investigated with a magnetic field along several crystallographic directions. Theory of the Zeeman effect, formulated in terms of the symmetry of the substitutional acceptor and the Luttinger parameters of the valence band, allows quantitative predictions of the relative intensities of the Zeeman components in full agreement with experiments.The observation of transitions within the (Lambda)(sub 8) Zeeman multiplet, i.e., the Raman-electron-paramagnetic-resonances, is yet another novel feature to emerge from the present study. The investigation has also yielded g-factors characterizing the Zeeman multiplets.
NTIS
Acceptor Materials; Jahn-Teller Effect; Zeeman Effect; Diamonds

20020000920 Argonne National Lab., IL USA
Vibrational analysis of the elpasolites Cs2NaAlF6 and Cs2NaGaF6 doped with Cr(3+) ions by fluorescence spectroscopy
Bordallo, H. N.; Sosman, L. P.; Tavares, A. D.; da Fonseca, R. J. M.; Sep. 07, 1999; 27p; In English
Report No.(s): DE2001-11957; ANL/IPNS/CP-99974; No Copyright; Avail: Department of Energy Information Bridge, Microfiche

Interest in 3d transition metal impurities in ionic crystals has increased due to their important role in the laser activity of these materials. Moreover, recent advances in tunable solid-state lasers and high-power semiconductor laser diode arrays have generated a strong interest in investigating new compounds that emit in the visible and near-infrared spectral regions. In particular, many optical studies have been devoted to Cr(sup 3+)-doped fluoride crystals as a consequence of the high quality of some Cr(sup 3+)-based laser materials. In the present investigation, the low temperature emission spectra of Cr(sup 3+) ions in the hexagonal elpasolites Cs2NaAlF6 and Cs2NaGaF6 have been measured. Each compound has two crystallographically inequivalent octahedral sites for the Al(sup 3+) and Ga(sup 3+) ions that can be occupied by Cr(sup 3+) ions. For both materials, the luminescence spectrum presents two zero-phonon lines accompanied by a well-defined vibrational structure. The different peaks of the emission broadband are described in terms of phonons of the lattice and normal modes of the octahedral complex (CrF6)(sup 3(minus)). A detailed analysis of the vibrational structure observed leads to the conclusion that the (sup 2)E and (sup 4)T2 excited states of the (CrF6)(sup 3(minus)) ions are displaced along the e(sub g), a(sub 1g) and probably the t(sub 2g) coordinates.
NTIS
Vibration; Ionic Crystals; Spectroscopy; Fluorescence; Spectral Bands

20020000931 Lawrence Livermore National Lab., Livermore, CA USA
Atomistic simulations for multiscale modeling in bcc metal
Belak, J.; Moriarty, J. A.; Soderlind, P.; Xu, W.; Yang, L. H.; Sep. 25, 1998; 1p; In English
Report No.(s): DE2001-2539; UCRL-JC-132068; DP0101031; No Copyright; Avail: Department of Energy Information Bridge, Microfiche

Quantum-based atomistic simulations are being used to study fundamental deformation and defect properties relevant to the multiscale modeling of plasticity in bcc (body centered cube) metals at both ambient and extreme conditions. Ab initio electronic structure calculations on the elastic and ideal strength properties of Ta and Mo help constrain and validate many-body interatomic potentials used to study grain boundaries and dislocations. The predicted C(capital Sigma)5 (310)(100) grain boundary structure for Mo has recently been confirmed in HREM (high resolution electron microscopy) measurements. The core structure, (small gamma) surfaces, Peierls stress, and kink-pair formation energies associated with the motion of a/2(111) screw dislocations in Ta and Mo have also been calculated. Dislocation mobility and dislocation junction formation and breaking are currently under investigation.
NTIS
Crystal Defects; Metals; Body Centered Cubic Lattices; Deformation; Mathematical Models

20020001059 Argonne National Lab., IL USA
MAD Data Collection: Current Trends
Dementieva, I.; Evans, G.; Joachimiak, A.; Sanishvili, R.; Walsh, M. A.; Sep. 20, 1999; 23p; In English; CCP4 Annual Meeting, 5-10 Jan. 1999, Sheffield, UK
Contract(s)/Grant(s): W-31109-ENG-38
Report No.(s): DE2001-11966; ANL/BIO/CP-100053; No Copyright; Avail: Department of Energy Information Bridge, Microfiche

The multi-wavelength anomalous diffraction, or MAD, method of determining protein structure is becoming routine in protein crystallography. An increase in the number of tuneable synchrotrons beamlines coupled with the widespread availability position-sensitive X-ray detectors based on charged-coupled devices and having fast readout raised MAD structure determination to a new and exciting level. Ultra-fast MAD data collection is now possible. Recognition of the value of selenium for phasing protein structures and improvement of methods for incorporating selenium into proteins in the form of selenomethionine have attracted greater interest in the MAD method. Recent developments in crystallographic software are complimenting the above advances, paving the way for rapid protein structure determination. An overview of a typical MAD experiment is described here, with emphasis on the rates and quality of data acquisition now achievable at beamlines developed at third-generation synchrotrons sources.
NTIS
Proteins; Crystallography; Diffraction; X Ray Detectors

20020001070 Argonne National Lab., IL USA
Practical superconductor development for electrical power applications annual report for FY 1998
Askew, T. R.; Balachandran, U.; Cha, Y. S.; Dorris, S. E.; Dusek, J. T.; Jan. 27, 1999; 26p; In English
Report No.(s): DE2001-12004; ANL-98/32; No Copyright; Avail: Department of Energy Information Bridge, Microfiche

Development of useful high-T(sub c) superconductors requires synthesis of superconducting compounds; fabrication of wires, tapes, and films from these compounds; production of composite structures that incorporate stabilizers or insulators; and design and testing of efficient components. This report describes FY 1998 technical progress of research and development efforts aimed at producing superconducting components in the Bi-(Pb)-SR-Ca-Cu and Y-Ba-Cu oxide systems. Topics discussed are synthesis and heat treatment of high-T(sub c) superconductors, formation of monolithic and composite conductors, characterization of structures and superconducting and mechanical properties, and fabrication and testing of prototype components. Collaborations with industry and academia are documented.
NTIS
Mechanical Properties; Electric Power; Prototypes; Fabrication; High Temperature Superconductors; Synthesis (Chemistry)

20020001174 Argonne National Lab., IL USA
Modeling crystal-field interaction for f-elements in LaCl3
Liu, G. K.; Zhorin, V. V.; Jul. 14, 1997; 14p; In English
Report No.(s): DE2001-12353; ANL/CHM/CP-93629; No Copyright; Avail: Department of Energy Information Bridge, Microfiche

The results of crystal field calculations in the framework of exchange charge model (ECM) are reported for trivalent lanthanide and actinide ions doped into LaCl(sub 3). Whereas the scalar strength of the model crystal field parameters are consistent with that previously determined by fitting the experimental data, the sign of the second-order parameter is found to be negative, in contrast to previous reports. The contribution from long-range electrostatic interactions exceeds that from the nearest neighboring ligands and leads to the negative sign of the second-order crystal field parameter. Other interaction mechanisms

including overlap, covalence, and charge exchange are less important to the second order parameter, but dominate the fourth- and sixth-order parameters. This work provides a consistent interpretation of the previously controversial experimental results for both lanthanide and actinide ions in this classical host.
NTIS
Crystal Field Theory; Lanthanum Chlorides; Charge Exchange

20020001193 Argonne National Lab., IL USA
New experiments elucidating the current limiting mechanisms of Ag-sheathed (Bi,Pb)(sub 2)SR(sub 2)Ca(sub 2)Cu(sub 3)O(sub x) tapes
Anderson, J. W.; Babcock, S. E.; Cai, X. Y.; Dorris, S. E.; Feldmann, M.; Jan. 15, 1999; 8p; In English; 11th; 11th International Symposium on Superconductivity, 11-19 Nov. 1998, Fukuoka, USA
Contract(s)/Grant(s): W-31109-ENG-38
Report No.(s): DE2001-12393; ANL/ET/CP-98209; No Copyright; Avail: Department of Energy Information Bridge, Microfiche

Multiple current limiting mechanisms exist from the nanometer to millimeter scale in Ag-sheathed (Bi,Pb)-2223 tapes. Recent studies of the zero-field critical current density (J(sub c) (0T, 77K)), the irreversibility field (H*) and the crack microstructure elucidate these properties. We show that H*(77K) can vary significantly over the range (approximately)120-260 mT, independently of J(sub c) (0T, 77K). Cracks, actual or incipient, exist on the sub to several hundred micron scale. Surface magneto optical imaging of whole tapes, correlated to subsequent ultrasonic fracture analysis of. the bare 2223 filaments extracted by dissolving away the Ag shows that even composites having J(sub c) (0T, 77K) values of 60 kA/cm(sup 2) exhibit strong signs of unhealed rolling damage. These combined studies show that today's very best 2223 tapes are still far from full optimization.
NTIS
High Temperature Superconductors; Calcium Oxides; Copper Oxides; Microstructure

20020001194 Argonne National Lab., IL USA
Role of intergrowths in the properties of the naturally layered manganites
Bader, S. D.; Berger, A.; Jiang, J. S.; Miller, D. J.; Mitchell, J. F.; Oct. 27, 1998; 28p; In English; 7th; 7th NEC Symposium on Fundamental Approaches to New Material Phases, 11-15 Oct. 1998, Nasu, Japan
Report No.(s): DE2001-12392; ANL/MSD/CP-97231; No Copyright; Avail: Department of Energy Information Bridge, Microfiche

The structural and magnetic properties of the two-layered Ruddlesden-Popper phase SRO(La(sub 1(minus)x)SR(sub x)MnO(sub 3))(sub 2) with x = 0.3 and x = 0.4 are investigated. These naturally layered manganites exhibit a colossal magnetoresistance, a magnetic anisotropy which is strongly composition-dependent, almost no remanence, and a non-vanishing magnetization in an extended temperature range above the Curie temperature (T(sub c)). The magnetization in this temperature range is not intrinsic to the crystal, but is attributed to intergrowths. These two-dimensional lattice imperfections consist of additional or missing SRO layers and have been observed in transmission electron micrographs. The magnetic properties of the intergrowths differ from the bulk crystal which results in unusual magnetic behavior.
NTIS
Crystal Defects; Manganese Compounds

20020001201 Argonne National Lab., IL USA
Current Transport and Microstructural Evolution in BSCCO Tapes Fabricated by Groove Rolling
Balachandran, U.; Iyer, A. N.; Mironova, M.; Salama, K.; Stolbov, S.; Jan. 27, 1999; 15p; In English; 1998 Applied Superconductivity Conference, 13-18 Sep. 1998, Palm Desert, CA, USA
Contract(s)/Grant(s): W-31109-ENG-38
Report No.(s): DE2001-12376; ANL/ET/CP-98288; No Copyright; Avail: Department of Energy Information Bridge, Microfiche

The powder-in-tube technique, consisting of wire drawing and rolling, has been widely used to fabricate superconducting tapes for possible electric power applications. In this study, instead of wire drawing, the starting billet was reduced in size by groove rolling. to optimize the deformation and thermomechanical treatment process, wires of varying dimensions were fabricated. The wires were flat-rolled to a final thickness of 250 mm. Short-length tapes were subjected to a series of thermal and deformation steps. Phase development and microstructural evolution during the process were monitored by XRD, SEM, and TEM. The BSCCO-2223 tapes, which were subjected to thermomechanical treatment, had average critical current densities of 18,000 A cm(sup (minus)2). Colony boundaries, examined by TEM, near the superconductor-silver interface were found to form

in certain preferred orientations. Polytypoids of 2212 phase were also observed at the colony boundary. The effects of grain boundary on superconducting order parameter and critical current density have also been examined.
NTIS
BSCCO Superconductors; Critical Current; Current Density; Microstructure

20020001208 Argonne National Lab., IL USA
ATLAS level 2 trigger supervisor
Abolins, M.; Blair, R. E.; Dawson, J. W.; Owen, D.; Pope, B. G.; Apr. 03, 1997; 5p; In English
Report No.(s): DE2001-12350; ANL-HEP-CP-96-82; No Copyright; Avail: Department of Energy Information Bridge, Microfiche

This paper presents an overview of the hardware and software proposed for the ATLAS level 2 Trigger ROI Builder/Supervisor. The essential requirements of this system are that it operate at the design Level 1 Trigger rate of 100kHz and that it support the technical requirements of the architectures suggested for the ATLAS Level 2 Trigger. Commercial equipment and software support are used to the maximum extent possible, with support from dedicated hardware. Timing requirements and latencies are discussed and simulation results are presented.
NTIS
Linear Accelerators; Architecture (Computers); Computer Programs

20020001209 Argonne National Lab., IL USA
Magnetic circular x-ray dichroisms of Fe-Ni alloys at K edge
Freeman, A. J.; Gofron, K. J.; Kimball, C. W.; Lee, P. L.; Montano, P. A.; Apr. 03, 1997; 9p; In English
Report No.(s): DE2001-12349; ANL/MSD/CP-92755; No Copyright; Avail: Department of Energy Information Bridge, Microfiche

Magnetic Circular X-ray Dichroism (MCXD) studies at K edges of Fe-Ni alloys reveal changes of the MCXD signal with composition and crystal structure. We observe that the signal at the invar composition is of comparable strength as other compositions. Moreover, the edge position is strongly dependent on lattice constant. First principles calculations demonstrate that the shape and strength of the signal strongly depends on the crystal orientation, composition, and lattice constant. We find direct relation between the MCXD signal and the p DOS. We find that the MCXD at K edge probes the magnetism due to itinerant electrons.
NTIS
Nickel Alloys; Iron Alloys; Dichroism; X Rays

20020001214 Argonne National Lab., IL USA
Probing excited states in nuclei at and beyond the proton dripline
Carpenter, M. P.; Mar. 15, 1999; 14p; In English
Report No.(s): DE2001-12341; ANL/PHY/CP-98590; No Copyright; Avail: Department of Energy Information Bridge, Microfiche

The coupling of a Compton-suppressed Ge (CSGe) detector array to a recoil separator has seen limited use in the past due to the low efficiency for measuring recoil - (gamma) ray coincidences (< 0.1%). With the building of new generation recoil separators and gamma-ray arrays, a substantial increase in detection efficiency has been achieved. This allows for the opportunity to measure excited states in nuclei with cross-sections below 100 nb. In this paper, results from the coupling of a modest array of CSGe detectors (AYE-Ball) and a current generation Ge array (Gammasphere) with a recoil separator (FMA) will be presented.
NTIS
Nuclei (Nuclear Physics); Excitation; Protons

20020001215 Argonne National Lab., IL USA
HREM of general and twist grain boundaries
Merkle, K. L.; Thompson, L. J.; Mar. 10, 1999; 5p; In English
Report No.(s): DE2001-12340; ANL/MSD/CP-98513; No Copyright; Avail: Department of Energy Information Bridge, Microfiche

The observation of atomic-scale structures of grain boundaries (GBs) via axial illumination HREM has been largely restricted to tilt GBs, due to the requirement that the electron beam be parallel to a low-index zone axis on both sides of the interface. This condition can be fulfilled for all tilt GBs with disorientation about a low-index direction. The information obtained through HREM studies in many materials has brought important insights concerning the atomic-scale structure of such boundaries. However, it

is well known that tilt GBs occupy only an infinitesimally small fraction of the 5-dimensional phase space which describes the macroscopic geometry of all GBs. Therefore, although tilt GBs are very important due to their low energy, it would be useful to also study twist GBs and general GBs that contain twist and tilt components.
NTIS
Grain Boundaries; Atomic Structure; Electron Beams

20020001250 Argonne National Lab., IL USA
BSCCO superconductors: hole-like fermi surface and doping dependence of the gap function
Campuzano, J. C.; Ding, H.; Fretwell, H. M.; Kadowaki, K.; Kaminski, A.; Aug. 18, 1999; 8p; In English
Report No.(s): DE2001-11940; ANL/MSD/CP-99834; No Copyright; Avail: Department of Energy Information Bridge, Microfiche

We use the gradient of the energy-integrated angle resolved photoemission (ARPES) intensity in order to define precisely the Fermi surface (FS) in BSCCO superconductors. We show that, independent of the photon energy, the FS is a hole barrel centered at ((pi),(pi)), Then, the superconducting gap along the FS is precisely determined from ARPES measurements on over-doped and underdoped samples of Bi2212. As the doping decreases, the maximum gap increases, but the slope of the gap near the nodes decreases. Though consistent with d-wave symmetry, the gap with underdoping cannot be fit by the simple cos(k(sub x))-cos(k(sub y)) form. A comparison of our ARPES results with available penetration depth data indicates that the renormalization of the linear T suppression of the superfluid density at low temperatures due to quasiparticle excitations around the d-wave nodes is large and doping dependent.
NTIS
Superconductivity; BSCCO Superconductors; Fermi Surfaces; Energy Gaps (Solid State)

20020001303 Argonne National Lab., IL USA
Energy Technology Division research summary, 1999
Mar. 31, 1999; 189p; In English
Report No.(s): DE2001-12060; ANL/ET/RP-98730; No Copyright; Avail: Department of Energy Information Bridge, Microfiche

The Energy Technology Division provides materials and engineering technology support to a wide range of programs important to the US Department of Energy. As shown on the preceding page, the Division is organized into ten sections, five with concentrations in the materials area and five in engineering technology. Materials expertise includes fabrication, mechanical properties, corrosion, friction and lubrication, and irradiation effects. Our major engineering strengths are in heat and mass flow, sensors and instrumentation, nondestructive testing, transportation, and electromechanics and superconductivity applications. The Division Safety Coordinator, Environmental Compliance Officers, Quality Assurance Representative, Financial Administrator, and Communication Coordinator report directly to the Division Director. The Division Director is personally responsible for cultural diversity and is a member of the Laboratory-wide Cultural Diversity Advisory Committee. The Division's capabilities are generally applied to issues associated with energy production, transportation, utilization, or conservation, or with environmental issues linked to energy. As shown in the organization chart on the next page, the Division reports administratively to the Associate Laboratory Director (ALD) for Energy and Environmental Science and Technology (EEST) through the General Manager for Environmental and Industrial Technologies. While most of our programs are under the purview of the EEST ALD, we also have had programs funded under every one of the ALDs. Some of our research in superconductivity is funded through the Physical Research Program ALD. We also continue to work on a number of nuclear-energy-related programs under the ALD for Engineering Research. Detailed descriptions of our programs on a section-by-section basis are provided in the remainder of this book.
NTIS
Superconductivity; Research and Development; Nondestructive Tests; Energy Conservation; Environmental Quality

20020001304 Argonne National Lab., IL USA
Practical superconductor development for electrical power applications ***Quarterly Report, Period ending 31 Dec. 1998***
Jan. 29, 1999; 22p; In English
Report No.(s): DE2001-12059; ANL/ET/RP-98335; No Copyright; Avail: Department of Energy Information Bridge, Microfiche

This is a multiyear experimental research program focused on improving relevant material properties of high-T(sub c) superconductors and on development of fabrication methods that can be transferred to industry for production of commercial conductors. The development of teaming relationships through agreements with industrial partners is a key element of this

program. Recent results on Y-123 bicrystals and grain boundaries, flux dissipation, novel sheathed Bi-2223 tapes, AC losses in multifilament Bi-2223 conductors, and oxygen diffusion in Bi-2223 are discussed.
NTIS
Bicrystals; High Temperature Superconductors; Fabrication

20020001305 Argonne National Lab., IL USA
Practical superconductor development for electrical power applications ***Quarterly Report, Period ending 31 Mar. 1998***
May 18, 1998; 23p; In English
Report No.(s): DE2001-12058; ANL/ET/RP-96422; No Copyright; Avail: Department of Energy Information Bridge, Microfiche
This is a multiyear experimental research program focused on improving relevant material properties of high-T(sub c) superconductors and on development of fabrication methods that can be transferred to industry for production of commercial conductors. The development of teaming relationships through agreements with industrial partners is a key element of this program. Recent work on microstructural development and current distribution in Bi-2223 powder-in-tube (PIT) tapes, grain-boundary studies, and a novel application for high-temperature (high-T(sub c)) superconductors are discussed.
NTIS
Fabrication; Research; High Temperature Superconductors; Grain Boundaries

20020001306 Argonne National Lab., IL USA
Practical superconductor development for electrical power applications ***Quarterly Report, Period ending 31 Dec. 1997***
Feb. 12, 1998; 25p; In English
Report No.(s): DE2001-12057; ANL/ET/RP-95637; No Copyright; Avail: Department of Energy Information Bridge, Microfiche
This is a multiyear experimental research program focused on improving relevant material properties of high-T(sub c) superconductors and on development of fabrication methods that can be transferred to industry for production of commercial conductors. The development of teaming relationships through agreements with industrial partners is a key element of this program. Recent work on microstructural development and current distribution in Bi-2223 powder-in-tube tapes and a novel application for high-temperature superconductors are discussed.
NTIS
Fabrication; Research; High Temperature Superconductors

20020001307 Argonne National Lab., IL USA
Calorimetric study of the transitions between the different vortex states in YBa2Cu3O7
Bouquet, F.; Calemczuk, R.; Crabtree, G. W.; Erb, A.; Fisher, R. A.; Aug. 17, 1999; 19p; In English
Report No.(s): DE2001-11941; ANL/MSD/CP-99839; No Copyright; Avail: Department of Energy Information Bridge, Microfiche
We have studied the vortex phase diagram of YBa(sub 2)Cu(sub 3)O(sub 7(minus)(delta)) (YBCO) in very strong magnetic field (0-26 Tesla) by a.c. calorimetry. We describe the anomalies associated with the transitions between the different vortex states (solid, liquid, and glass), with special emphasis on the first order flux lattice melting.
NTIS
YBCO Superconductors; Yttrium Oxides; Barium Oxides; Copper Oxides; Heat Measurement; Vortices

20020001308 Argonne National Lab., IL USA
Theory of high-T(sub c) cuprates based on experimental evidence
Abrikosov, A. A.; Aug. 17, 1999; 33p; In English
Report No.(s): DE2001-11938; ANL/MSD/CP-99815; No Copyright; Avail: Department of Energy Information Bridge, Microfiche
A model of superconductivity in layered high-temperature superconducting cuprates is proposed, based on the extended saddle point singularities in the electron spectrum, weak screening of the Coulomb interaction and phonon-mediated interaction between electrons plus a small short-range repulsion of Hund's, or spin-fluctuation, origin. This permits to explain the large values of T(sub c), features of the isotope effect on oxygen and copper, the existence of two types of the order parameter, the peak in the inelastic neutron scattering, the positive curvature of the upper critical field, as function of temperature, etc.
NTIS
Cuprates; Superconductivity; High Temperature Superconductors

20020001454 Argonne National Lab., IL USA

Training Effects and the Microscopic Magnetic Structure of Exchange Biased Co/CoO Bilayers

Berger, A.; Dahlberg, E. D.; Felcher, G. P.; Hill, B. K.; teVelthius, S. G. E.; Sep. 01, 1999; 13p; In English

Report No.(s): DE2001-11848; ANL/IPNS/CP-99222; No Copyright; Avail: Department of Energy Information Bridge

Exchange bias of a partially oxidized thin film of ferromagnetic Co was studied by magnetization measurements and polarized neutron reflectivity (PNR). The magnetization curve shows strong effects of training with cycling of the magnetic field. Reflectivity measurements with the field parallel to the cooling field showed the onset of spin-dependent diffuse scattering--off the specular reflection--after a training cycle. Such scattering, of the Yoneda type, is due to misaligned Co domains possibly close to the Co/CoO interface. Subjecting the field cooled Co/CoO pair to a field perpendicular to the cooling field causes a rotation of the magnetization. PNR measurements confirmed earlier susceptibility studies by indicating that the rotation of the magnetization is reversible in fields up to 400 ohms. The rotation of the magnetization of Co is uniform across the film thickness. NTIS

Ferromagnetic Materials; Magnetization; Microstructure; Cobalt; Neutron Diffraction

20020001507 Lawrence Livermore National Lab., Livermore, CA USA

Finite difference micromagnetic simulation with self-consistent currents and smooth surfaces

Cerjan, C.; Gibbons, M. R.; Hewett, D. W.; Parker, G.; May 27, 1999; 14p; In English

Report No.(s): DE2001-12217; UCRL-JC-134517; No Copyright; Avail: Department of Energy Information Bridge, Microfiche

A micromagnetic algorithm has been developed using the finite difference method (FDM). Elliptic field equations are solved on the mesh using the efficient Dynamic Alternating Direction Implicit method. Smooth surfaces have been included in the FDM formulation so structures of irregular shape can be modeled. The current distribution and temperature of devices are also calculated.

NTIS

Algorithms; Finite Difference Theory; Elliptic Differential Equations; Alternating Direction Implicit Methods

20020001542 Lawrence Livermore National Lab., Livermore, CA USA

Superconducting tunnel junction array development for high-resolution energy-dispersive x-ray spectroscopy

Barfknecht, A. T.; Cramer, S. P.; Frank, M.; Friedrich, S.; Hiller, L. J.; Jul. 01, 1998; 14p; In English

Report No.(s): DE2001-2815; UCRL-JC-132104; No Copyright; Avail: Department of Energy Information Bridge, Microfiche

Cryogenic energy-dispersive x-ray detectors are being developed because of their superior energy resolution ((less than or equal to) 10 eV FWHM for keV x rays) compared to semiconductor EDS systems. So far, their range of application is limited due to their comparably small size and low count rate. We present data on the development of superconducting tunnel junction (STJ) detector arrays to address both of these issues. A single STJ detector has a resolution around 10 eV below 1 keV and can be operated at count rates of order 10,000 counts/s. We show that the simultaneous operation of several STJ detectors does not diminish their energy resolution significantly, while increasing the detector area and the maximum count rate by a factor given by the total number of independent channels.

NTIS

Superconductivity; Tunnel Junctions; X Ray Detectors; Cryogenics

20020001556 Alabama Univ., Birmingham, AL USA

Mechanism of constitution liquid film migration

Jun. 01, 1999; 138p; In English

Report No.(s): DE2001-761948; DOE/ER/45449-3; No Copyright; Avail: Department of Energy Information Bridge

Liquid film migration (LFM) in liquid phase sintering classically involves a large metastable liquid volume adjacent to solid, and migration occurs at an isolated solid-liquid (S-L) interface. Constitutional liquid film migration (CLFM), discovered in alloy 718, has major characteristics similar to those of LFM, except that the metastable liquid is from the constitutional liquation of precipitates on the grain boundary. The similarity between LFM and CLFM has led to the theory that coherency lattice strain responsible for LFM is also responsible for CLFM. The coherency strain hypothesis was tested in this study by evaluating whether the Hillert model of LFM would also apply for CLFM. Experimental results of CLFM in alloy 718 showed that migration velocity followed the trend predicted by the Hillert model. This indicates that the coherency strain hypothesis of LFM also applies for CLFM and that the coherency lattice strain responsible for LFM is also the driving force for CLFM.

NTIS

Fluid Films; Liquid Phase Sintering; Nickel Alloys; Metastable State; Heat Resistant Alloys; Liquid Phases

20020001563 Argonne National Lab., IL USA

Neutrons and the crystal ball experiments

Alyer, J.; Grosnick, D.; Koetke, D.; Manweiler, R.; Spinka, H.; Nov. 07, 1997; 41p; In English

Report No.(s): DE2001-12016; ANL-HEP-TR-97-87; No Copyright; Avail: Department of Energy Information Bridge

The Crystal Ball detector, as originally constructed, consisted of a set of 672 optically-isolated NaI crystals, forming an approximately spherical shell and each crystal viewed by a photomultiplier, a charged-particle tracker within the NaI shell, and two endcaps to cover angles close to two colliding beams. The detector geometry subtends a solid angle of about 93% of 4(pi) st (20(degree) (le) (theta) (le) 160(degree) and 0(degree) (le) (phi) (le) 360(degree)) from the center. The Crystal Ball detector was used for two long series of experiments at the e(sup +)e(sup (minus)) colliding beam accelerators SPEAR (1, 2, 3, 4) at SLAC and DORIS (5, 6, 7, 8) at DESY. A new set of measurements using the Crystal Ball detector is planned at the Brookhaven National Laboratory Alternating Gradient Synchrotrons (BNL AGS). These new experiments will use the 672 NaI crystals from the original detector, but neither the tracker nor endcaps. The 'Crystal Ball' in this note will refer only to the set of NaI crystals. Initially, the reactions to be studied will include (pi)(sup (minus))p(r arrow) neutrals with pion beam momenta (approximately)400-750 MeV/c and K(sup (minus)) p(r arrow) neutrals with kaon beam momenta (approximately)600-750 MeV/c. Each of these reactions will include a neutron in the final state. whereas the fraction of e(sup +)e(sup (minus)) interactions with neutrons at SLAC or DESY was quite small. Consequently, there is relatively little experience understanding the behavior of neutrons in the Crystal Ball.

NTIS

Detectors; Neutrons; Charged Particles; Crystals; Radiation Detectors

20020001568 Argonne National Lab., IL USA

X-Ray and Neutron Scattering Studies of Complex Confined Fluids

Sinha, S. K.; Aug. 04, 1999; 29p; In English

Report No.(s): DE2001-11835; ANL/XFD/CP-99157; No Copyright; Avail: Department of Energy Information Bridge

We review recent X-ray and neutron scattering studies of the structure and dynamics of confined complex fluids. This includes the study of polymer conformations and binary fluid phase transitions in porous media using Small Angle Neutron scattering, and the use of synchrotrons radiation to study ordering and fluctuation phenomena at solid/liquid and liquid/air interfaces. Ordering of liquids near a solid surface or in confinement will be discussed, and the study, via specular and off-specular X-ray reflectivity, of capillary wave fluctuations on liquid polymer films. Finally, we shall discuss the use of high-brilliance beams from X-ray synchrotrons to study via photon correlation spectroscopy the slow dynamics of soft condensed matter systems.

NTIS

Fluid Films; Phase Transformations; Neutron Scattering; X Ray Diffraction

20020001584 Argonne National Lab., IL USA

High angular resolution measurements of K shell x-ray emission created by electron channeling in the analytical electron microscope

Zaluzec, N. J.; Mar. 10, 1999; 5p; In English

Report No.(s): DE2001-12375; ANL/MSD/CP-98514; No Copyright; Avail: Department of Energy Information Bridge, Microfiche

Since the original observations by Duncumb in 1962, a number of studies have been conducted on the effects of electron channel on characteristic x-ray emission and microanalysis. Most of the recent studies have concentrated upon using the phenomenon to perform site specific distributions of impurity elements in ordered compounds using the ALCHEMI methodology. Very few studies have attempted to accurately measure the effect as a function of orientation and compare these results to theories. In this study, two dimensional high angular resolution studies of channeling enhance x-ray emission were performed and herein the results are compared to theoretical calculations of Allen et al. All experimental measurements presented here were conducted on a Philips EM 420T analytical electron microscope. The instrument was operated in the TEM mode, at 120 kV using an LaB6 electron source. The characteristic x-ray emission was measured using an EDAX ultra thin window Si(Li) detector having a FWHM of (approximately)145 eV at Mn Km Nominal probe sizes used during the study were 200-500 nm with beam convergence half angle defined by the Condenser apertures. Control of the relative orientation of the incident probe was accomplished via direct computer control of the beam tilt coils, after the specimen was first manually oriented to an appropriate zone axis using the specimen tilt stage. Two dimensional measurements were carried out using a 128 x 100 pixel scan corresponding to an angular range of (approximately)100 by 80 mR using customized computer program running on a EDAX 9900 microanalyzer system. Careful alignment and manual optimization/adjustments of beam tilt pivot coils, minimized probe wobble during data acquisition. The effects of this were additionally mitigated due to the relative uniformity of the specimen thickness in the analyzed zone. Typical acquisition times for a complete two dimensional scan were 18-24 hours. Essential to the success of these measurements

was the stability of the probe current, minimal specimen drift, and absence of hydrocarbon contamination. The latter being accomplished using argon plasma processing of the specimen (MgAl(sub 2)O(sub 4)) which was initially prepared by mechanical tripod polishing.
NTIS
Transmission Electron Microscopy; Electron Sources; X Rays; Emission; Dimensional Measurement

20020001786 NASA Goddard Space Flight Center, Greenbelt, MD USA
A Magnetoresistive Heat Switch for the Continuous ADR
Canavan, E. R., NASA Goddard Space Flight Center, USA; Dipirro, M. J., NASA Goddard Space Flight Center, USA; Jackson, M., NASA Goddard Space Flight Center, USA; Panek, J., NASA Goddard Space Flight Center, USA; Shirron, P. J., NASA Goddard Space Flight Center, USA; Tuttle, J. G., NASA Goddard Space Flight Center, USA; Jul. 16, 2001; 8p; In English; Advances in Cryogenics, Melville, NY, USA; No Copyright; Avail: CASI; A02, Hardcopy; A01, Microfiche

In compensated elemental metals at low temperature, a several Tesla field can suppress electronic heat conduction so thoroughly that heat is effectively carried by phonons alone. In approximately one mm diameter single crystal samples with impurity concentrations low enough that electron conduction is limited by surface scattering, the ratio of zerofield to high-field thermal conductivity can exceed ten thousand. We have used this phenomenon to build a compact, solid-state heat switch with no moving parts and no enclosed fluids. The time scale for switching states is limited by time scale for charging the magnet that supplies the controlling field. Our design and fabrication techniques overcome the difficulties associated with manufacturing and assembling parts from single crystal tungsten. A clear disadvantage of the magnetoresistive switch is the mass and complexity of the magnet system for the controlling field. We have discovered a technique of minimizing this mass and complexity, applicable to the continuous adiabatic demagnetization refrigerator.
Author
Magnetoresistivity; Solid State; Switches; Tungsten; Adiabatic Demagnetization Cooling

20020001830 Argonne National Lab., IL USA
Tunneling Spectra and Superconducting Gap in Bi2SR2CaCu2O(8+delta) and Tl2Ba2CuO(6+delta)
Miyakawa, N.; Qzyuzer, L.; Zasadzinski, J. F.; Jul. 21, 1999; 7p; In English
Report No.(s): DE2001-11826; ANL/MSD/CP-99106; No Copyright; Avail: Department of Energy Information Bridge

Tunneling spectra are reported for Bi2SR2CaCu2O(8+delta) (Bi-2212) over a wide doping range using superconductor-insulator-superconductor (SIS) break junctions. The energy gap inferred from the tunneling data displays a remarkable monotonic dependence on doping, increasing to very large values in the underdoped region even as T(sub c) decreases. This leads to unphysically large values of the strong coupling ratio (approximately 20). The tunneling spectra are qualitatively similar over the entire doping range even though the gap parameter, Delta, changes from 12 meV to 80 meV. Each spectrum exhibits dip and hump features at high bias with characteristic energies that scale with the superconducting gap. Tunneling spectra of near optimally-doped Tl2Ba2CuO(6+delta) (Tl-2201) also display a weak dip feature in superconductor-insulator-normal metal (SIN) junctions. Generated SIS spectra of Tl-2201 are compared with measured spectra on Bi-2212 and it is concluded that the dip and hump features are generic to high temperature superconductors.
NTIS
Additives; Doped Crystals; SIS (Superconductors); High Temperature Superconductors

20020001841 Sandia National Labs., Albuquerque, NM USA
MOCVD growth of algainn for UV emitters
Crawford, M.; Han, J.; Jul. 07, 1999; 10p; In English
Report No.(s): DE2001-8866; SAND98-1520C; No Copyright; Avail: Department of Energy Information Bridge, Microfiche

Issues related to the growth of nitride-based UV (ultraviolet) emitters are investigated in this work. More than 100 times of improvement in the optical efficiency of the GaN active region can be attained with a combination of raising the growth pressure and introducing a small amount of indium. The unique issue in the UV emitter concerning the use of AlGaN for confinement and the associated tensile cracking is also investigated. They showed that the quaternary AlGaInN is potentially capable of providing confinement to GaN and GaN:In active regions while maintaining lattice matching to GaN, unlike the AlGaN ternary system.
NTIS
Emission; Metalorganic Chemical Vapor Deposition; Emitters; Semiconductors (Materials)

20020001858 California Univ., Lawrence Berkeley Lab., Berkeley, CA USA

Selective excitation of the yellow luminescence of GaN

Colton, J. S.; Yu, P. Y.; Teo, K. L.; Weber, E. R.; Grzegory, I.; Jul. 01, 1999; 12p; In English

Report No.(s): DE2001-764349; LBNL-44298; No Copyright; Avail: Department of Energy Information Bridge

The yellow luminescence of n-type GaN has been studied with selective excitation using a combination of Ar ion and dye lasers. Narrower structures whose peak energies follow the excitation photon energy over the width of the yellow luminescence have been observed. Unlike the yellow luminescence excited by above band gap excitations, these fine structures exhibits thermal activated quenching behavior. We propose that these fine structures are due to emission occurring at complexes of shallow donors and deep acceptors which can be resonantly excited by photons with energies below the band gap. The activation energy deduced from their intensity is that for delocalization of electrons out of the complexes. Our results therefore suggest that there is more than one recombination channel (usually assumed to be due to distant donor-acceptor pairs) to the yellow luminescence in GaN. NTIS

Excitation; Luminescence; Dye Lasers; Electrons; Fine Structure; Temperature Effects

20020001975 Argonne National Lab., IL USA

Observation of an elementary cuboctahedron of Xe nanocrystal in an Al matrix

Allen, C. W.; Birtcher, R. C.; Donnelly, S. E.; Furuya, K.; Ryan, E. A.; Mar. 10, 1999; 5p; In English

Report No.(s): DE2001-12365; ANL/MSD/CP-98511; No Copyright; Avail: Department of Energy Information Bridge, Microfiche

When a noble gas element such as Xe is implanted in an fcc metal matrix such as Al at room temperature, a fine dispersion of precipitates forms. The precipitates are elementary fcc crystals up to diameters of several nanometers (for Xe in Al, 8-10 rim), above which they are non-crystalline. The precipitates exhibit a cube-on-cube orientation relation with the matrices and have lattice parameters which are much larger than those of the matrices (a(sub Xe) = 1.5a(sub Al)). Thus the interphase interfaces are incommensurate though the lattices are isotactic. The precipitates assume the shape of matrix cavities; for an Al matrix, at equilibrium this is a cuboctahedron, a (r-brace)111(l-brace) octahedron truncated at the corners on (l-brace)100(r-brace). Fig. 1 is a sketch of a dispersion of such cuboctahedra, viewed approximately along a (l-angle)110(r-angle). For this study specimens were prepared in the HVEM-Tandem Facility at Argonne National Laboratory by implanting 35 keV Xe to a dose of 4x10(sup 19) m(sup (minus)2) into well-annealed 5N Al discs which had been thinned by jet electropolishing. The range of the implant is approximately 25 nm. Specimens were examined at high resolution in the JEOL ARM-1000 high voltage electron microscope (HVEM) at the High Resolution Beam Station of the National Research Institute for Metals (NRIM), Tsukuba, Japan. The HVEM was operated at 1 MeV with a LaB(sub 6) electron source. A series of studies of electron irradiation effects in this material have been conducted, which have revealed a number of irradiation-induced phenomena including migration within the matrix, changes in shape, faulting, melting, crystallization and coalescence of Xe precipitates. In this presentation, the structure of the smallest possible cuboctahedral Xe nanocrystal will be discussed and its apparently random migration under the influence of the electron irradiation will be demonstrated.

NTIS

Crystallization; Xenon; Nanocrystals; Aluminum; Matrix Materials

20020001976 Argonne National Lab., IL USA

Periodic arrays of pinning centers in thin vanadium films

Brueck, S. R. J.; Chung, K.; Crabtree, G.; DeLong, L. E.; Hesketh, P. J.; Jul. 13, 1997; 14p; In English

Report No.(s): DE2001-12361; ANL/MSD/CP-96785; No Copyright; Avail: Department of Energy Information Bridge, Microfiche

Commensurability effects between the superconducting flux line lattice and a square lattice (period d=1(micro)m and diameter D=0.4(micro)m) of submicron holes in 1500 (angstrom) vanadium films were studied by atomic force microscopy, DC magnetization, AC susceptibility, magnetoresistivity and I-V measurements. Peaks in the magnetization and critical current at matching fields are found to depend nonlinearly upon the value of external AC field or current, as well as the inferred symmetry of the flux line lattice.

NTIS

Atomic Force Microscopy; Vanadium; Thin Films; Pinning; Arrays

20020001978 Argonne National Lab., IL USA

Practical superconductor development for electrical power applications ***Quarterly Report, Period ending 30 Sep. 1997***

Oct. 30, 1997; 17p; In English

Report No.(s): DE2001-12056; ANL/ET/RP-94811; No Copyright; Avail: Department of Energy Information Bridge

This is a multiyear experimental research program focused on improving relevant material properties of high-T(sub c) superconductors and on development of fabrication methods that can be transferred to industry for production of commercial conductors. The development of teaming relationships through agreements with industrial partners is a key element of this program. Recent work on strain tolerance of Bi-2223 tapes, AC downlink construction, fundamental studies of flux pinning, and application of coils from powder-in-tube tapes to particle detectors is discussed.

NTIS

High Temperature Superconductors; Fabrication

20020001987 Argonne National Lab., IL USA

X-ray Reflectivity Study of Formation of Multilayer Porous Anodic Oxides of Silicon

Chu, Y.; Fenollosa, R.; Parkhutik, V.; You, H.; Jul. 21, 1999; 9p; In English

Report No.(s): DE2001-11831; ANL/MSD/CP-99136; No Copyright; Avail: Department of Energy Information Bridge

The paper reports data on the kinetics of anodic oxide films growth on silicon in aqueous solutions of phosphoric acids as well as a study of the morphology of the oxides grown in a special regime of the oscillating anodic potential. X-ray reflectivity measurements were performed on the samples of anodic oxides using an intense synchrotron radiation source. They have a multilayer structure as revealed by theoretical fitting of the reflectivity data. The oscillations of the anodic potential are explained in terms of synchronized oxidation/dissolution reactions at the silicon surface and accumulation of mechanic stress in the oxide film.

NTIS

Anodes; Morphology; Oxide Films; Reflectance; Silicon Oxides

20020002011 Lawrence Livermore National Lab., Livermore, CA USA

Magnetic and thermodynamic properties of the 3-D periodic anderson lattice hamiltonian

Huscrot, C.; McMahan, A. K.; Pollock, E. I.; Scalettar, R. T.; Sep. 10, 1998; 27p; In English

Report No.(s): DE2001-2782; UCRL-JC-131838; No Copyright; Avail: Department of Energy Information Bridge, Microfiche

Tight-binding models capture many of the qualitative features of interaction-induced effects in solids. For example, the simplest such model, the single-band Hubbard Hamiltonian, describes the Mott insulating phase which occurs in correlated systems, despite the fact that the one electron band is nominally only half-filled, as well as the tendency towards magnetic order. Both phenomena occur in the transition metal oxides. The Periodic Anderson Model (PAM) is a step towards incorporating more complex orbital structure. It contains a pair of orbitals on each site--a delocalized conduction band and a set of highly correlated, localized states. The PAM successfully describes conditions for transitions between antiferromagnetic order of the local moments and phases in which these moments are quenched into singlets paired with conduction electrons. These phenomena are central to heavy fermion systems. The pressure-induced volume collapse in Ce has also been attributed to Kondo-like quenching of the local f moments in this metal, as has been discussed in the context of the impurity Anderson Model. The authors describe Quantum Monte Carlo (QMC) calculations of the magnetic and thermodynamic properties of the PAM in three dimensions. Previous QMC studies have been reported in one and two dimensions. A focus of our attention will be on the density of states and the specific heat. The organization of this paper is as follows. They first introduce the PAM and outline some of its properties. Next, a brief presentation of the Quantum Monte Carlo, Maximum Entropy, and Hartree-Fock methods is given. They then show the equilibrium magnetic properties of the PAM, including the spin correlations between conduction and localized orbitals, and antiferromagnetic correlations in the localized band, before turning to the thermodynamics and the density of states. A concluding section describes connections of this work to the problem of the rare earth volume collapse transitions.

NTIS

Magnetic Properties; Thermodynamic Properties; Hamiltonian Functions; Orbitals; Specific Heat

20020002346 Lawrence Livermore National Lab., Livermore, CA USA

Two-Dimensional Nuclear Magnetic Resonance of Quadrupolar Systems

Wang, S.; Sep. 17, 1997; 204p; In English

Report No.(s): DE2001-6387; LBNL-40841; No Copyright; Avail: Department of Energy Information Bridge, Microfiche

This dissertation describes two-dimensional nuclear magnetic resonance theory and experiments which have been developed to study quadruples in the solid state. The technique of multiple-quantum magic-angle spinning (MQMAS) is extensively

reviewed and expanded upon in this thesis. Specifically, MQMAS is first compared with another technique, dynamic-angle spinning (DAS). The similarity between the two techniques allows us to extend much of the DAS work to the MQMAS case. Application of MQMAS to a series of aluminum containing materials is then presented. The superior resolution enhancement through MQMAS is exploited to detect the five- and six-coordinated aluminum in many aluminosilicate glasses. Combining the MQMAS method with other experiments, such x HETCOR, greatly expands the possibility of the use of MQMAS to study a large range of problems and is demonstrated in Chapter 5. Finally, the technique switching-angle spinning (SAS) is applied to quadrupolar nuclei to fully characterize a quadrupolar spin system in which all of the eight NMR parameters are accurately determined. This dissertation is meant to demonstrate that with the combination of two-dimensional NMR concepts and new advanced spinning technologies, a series of multiple-dimensional NMR techniques can be designed to allow a detailed study of quadrupolar nuclei in the solid state.
NTIS
Nuclear Magnetic Resonance; Quadrupoles

20020002347 Lawrence Livermore National Lab., Livermore, CA USA
High-Resolution NMR of Quadrupolar Nuclei in the Solid State
Gann, S. L.; Nov. 30, 1995; 130p; In English
Report No.(s): DE2001-6371; LBL-38346; No Copyright; Avail: Department of Energy Information Bridge, Microfiche

This dissertation describes recent developments in solid state nuclear magnetic resonance (NMR), for the most part involving the use of dynamic-angle spinning (DAS) NMR to study quadrupolar nuclei. Chapter 1 introduces some of the basic concepts and theory that will be referred to in later chapters, such as the density operator, product operators, rotations, coherence transfer pathways, phase cycling, and the various nuclear spin interactions, including the quadrupolar interaction. Chapter 2 describes the theory behind motional averaging experiments, including DAS, which is a technique where a sample is spun sequentially about two axis oriented at different angles with respect to the external magnetic field such that the chemical shift and quadrupolar anisotropy are averaged to zero. Work done on various rubidium-87 salts is presented as a demonstration of DAS. Chapter 3 explains how to remove sidebands from DAS and magic-angle spinning (MAS) experiments, which result from the time-dependence of the Hamiltonian under sample spinning conditions, using rotor-synchronized x-pulses. Data from these experiments, known as DAH-180 and are presented for both rubidium and lead salts. In addition, the applicability of this technique to double rotation (DOR) experiments is discussed. Chapter 4 concerns the addition of cross-polarization to DAS (CPDAS). The theory behind spin locking and cross polarizing quadrupolar nuclei is explained and a method of avoiding the resulting problems by performing cross polarization at 0 deg (parallel) with respect to the magnetic field is presented. Experimental results are shown for a sodium-23 compound, sodium pyruvate, and for oxygen-17 labeled L-alanine. In Chapter 5, a method for broadening the Hartmann-Hahn matching condition under MAS, called variable effective field cross-polarization (VEFCI), is presented, along with experimental work on adamantane and polycarbonate.
NTIS
Cross Polarization; Nuclear Magnetic Resonance; Solid State Physics

20020002349 Brookhaven National Lab., Upton, NY USA
Enhanced Harmonic Spontaneous Radiation using a Novel Undulator
Marshall, T. C.; Shao, Y.; Parsa, Z.; Oct. 01, 1998; 5p; In English
Report No.(s): DE2001-6261; BNL-66034; No Copyright; Avail: Department of Energy Information Bridge, Microfiche

In a typical free electron laser (FEL), the electron beam interacts with a dipole undulator that has a sinusoidal magnetic field variation; the electron motion is sinusoidal in the plane transverse to this field and emits odd-numbered harmonic radiations along the axis. However, one need not limit the choice of undulator field profile to the sinusoid, providing other profiles result in significant advantages. In connection with the IFEL accelerator, in the past we have pointed out that the use of an undulator profile that approximates a square wave will result in an enhanced acceleration gradient, by as much as a factor of two (equivalent in effect to an increase of laser drive intensity by a factor of four). This improvement (essentially at the fundamental FEL resonance) results largely from the fact that, for a given peak undulator field amplitude, the rms electron acceleration obtained from the square wave undulator is larger than that from the sinusoid; furthermore, the electron orbit is stable as well. In this paper, we find additional advantages that should result particularly at harmonic numbers f1 if the undulator field profile is nearly 'square wave' namely, a large enhancement of the harmonic spontaneous power radiated, together with enhanced FEL gain. The modification of undulatory to enhance FEL gain has been examined in the past, usually with a particular design in mind, but with similar conclusions.
NTIS
Free Electron Lasers; Harmonic Radiation; Particle Motion

20020002725 Edtek, Kent, WA USA

Bandgap-Engineered Thermophotovoltaic Devices for Hi Efficiency Radioisotope Power, July 9, 1996-July 8, 1999 ***Final Report, 9 Jul. 1996 - 8 Jul. 1999***

Sundaram, V.; Morgan, M. D.; Horne, W. E.; Mar. 15, 2000; 32p; In English

Report No.(s): DE2001-765625; No Copyright; Avail: Department of Energy Information Bridge, Microfiche

During Phase I the feasibility of fabricating high-performance, low bandgap (0.58ev)PV cells by thermally diffusing p-n junctions in GaSb based quaternary materials was established. During phase II, bandgap engineered thermophotovoltaic (TPV) cells were optimized, development of a low-cost build source material for quaternary devices was investigated, and a diesel-fueled, TPV test-bed was built and tested allowing its performance to be characterized.

NTIS

Photovoltaic Cells; Radioisotope Batteries

20020002744 Department of Energy, Aiken, SC USA

Application of High Transition Temperature Superconductors at the Savannah River Site

Payne, J. E.; Apr. 01, 1995; 11p; In English

Report No.(s): DE2001-759184; DOE/DE-FG09-92SR18273-3; No Copyright; Avail: Department of Energy Information Bridge, Microfiche

A study of the properties of single crystals of high transition temperature superconductors and the applications of these materials in devices that could be used at SRS. The research concentrates on superconducting quantum interference devices (SQUIDs) and BiSCCO materials.

NTIS

High Temperature Superconductors; Single Crystals; Squid (Detectors); Bismuth Compounds

20020002776 Argonne National Lab., IL USA

Behavior of nanocrystalline Xe precipitates in Al under 1 MeV electron irradiation

Allen, C. W.; Birtcher, R. C.; Donnelly, S. E.; Furuya, K.; Mitsuishi, K.; Mar. 10, 1999; 19p; In English

Report No.(s): DE2001-12407; ANL/MSD/CP-98512; No Copyright; Avail: Department of Energy Information Bridge, Microfiche

Crystalline nanoprecipitates of Xe have been produced by ion implantation into high purity Al at 300 K. With an off-zone axis TEM (transmission electron microscopy) imaging technique, the nanocrystals may be clearly structure imaged against a nearly featureless background. Under the 1 MeV electron irradiation employed for the HREM (high resolution electron microscopy) observation, Xe nanocrystals exhibit a number of readily observed physical phenomena including migration within the matrix, changes in shape, faulting, melting, crystallization and coalescence. The various phenomena observed as changes in the Xe nanocrystals reflect changes of matrix cavity-surface structure. The Xe nanocrystal thus allows investigation indirectly into changes in interface morphology at the atomic level, resulting in this instance from electron irradiation damage. Such changes have heretofore been inaccessible to observation.

NTIS

Electron Irradiation; Precipitates; Nanocrystals; Electron Microscopy; Xenon

20020002778 Argonne National Lab., IL USA

c-axis twist Bi(sub 2)SR(sub 2)CaCu(sub 2)O(sub 8+(delta)) josephson junctions: a new phase-sensitive test of order parameter symmetry

Klemm, R. A.; Rieck, C. T.; Scharnberg, K.; Jan. 22, 1999; 9p; In English

Report No.(s): DE2001-12398; ANL/MSD/CP-98254; No Copyright; Avail: Department of Energy Information Bridge, Microfiche

Li et al. found that the critical current density J(sub c)(sup J) across atomically clean c-axis twist junctions of Bi(sub 2)SR(sub 2)Ca Cu(sub 2)O(sub 8+(delta)) is the same as that of the constituent single crystal, J(sub c)(sup S), independent of the twist angle (phi)(sub 0), even at T(sub c). They investigated theoretically if a d(sub x(sup 2)-y(sup 2))-wave order parameter might twist by mixing in d(sub xy) components, but find that such twisting cannot possibly explain the data near to T(sub c). Hence, the order parameter contains an s-wave component, but not any d(sub x(sup 2)-y(sup 2))-wave component. In addition, the c-axis Josephson tunneling is completely incoherent. They also propose a c-axis junction tricrystal experiment which does not rely upon expensive substrates.

NTIS

Josephson Junctions; High Temperature Superconductors; Twisting

20020002781 Sandia National Labs., Albuquerque, NM USA
Ultrathin Alumina Film Al-Sublattice Structure, Metal Island Nucleation at Terrace Point Defects, and How Hydroxylation Affects Wetting
Bogicevic, A.; Jennison, D. R.; Aug. 09, 1999; 18p; In English
Report No.(s): DE2001-9701; SAND99-2069C; No Copyright; Avail: Department of Energy Information Bridge, Microfiche
In this paper, we include for discussion three topics of current interest in metal oxide surface science. Using first principles density functional theory (DFT) (1) calculations, we have investigated: (1) the atomic-scale structure of experimentally-relevant ultrathin alumina films, (2) the role of common point defects in metal island nucleation on oxide terraces, and (3) the growth and morphology of metals on oxide surfaces which have high concentrations of a common impurity.
NTIS
Nucleation; Thin Films; Aluminum Oxides

20020002787 Sandia National Labs., Albuquerque, NM USA
Review of Issues for Development of Self-Doping Metallizations
Smith, D. D.; Aug. 04, 1999; 7p; In English
Report No.(s): DE2001-9691; SAND99-2024C; No Copyright; Avail: Department of Energy Information Bridge, Microfiche
This paper will focus on the required growth conditions for self-doping metals and the various lifetime issues. Recent results for a novel self-doping metal system will be discussed briefly.
NTIS
Additives; Metallizing

20020002794 Argonne National Lab., IL USA
What is the Symmetry of the High Tc Order Parameter
Klemm, R. A.; Apr. 16, 1998; 14p; In English
Report No.(s): DE2001-8904; ANL/MSD/CP-95045; No Copyright; Avail: Department of Energy Information Bridge, Microfiche
In recent years, there has been a raging controversy regarding the orbital symmetry of the superconducting order parameter (OP) in the high temperature superconductors. Many experiments were interpreted in terms of a d(sub x(sup 2)-y(sup 2))-wave OP, but many others were interpreted in terms of a more conventional s-wave OP. We review the problems of both intrinsic and extrinsic natures with the phase-sensitive experiments on YBCO. The authors further show that the photoemission experiments of the purported superconducting gap in Bi2SR2CaCu2O(g+delta) are entirely consistent with charge- and/or spin-density wave formation in that material. The presence of such density waves greatly complicates the analysis of most experiments. Hence, we conclude that the orbital symmetry of the superconducting OP is still unknown in any of the high temperature superconductors.
NTIS
YBCO Superconductors; Superconductivity; Symmetry

20020002795 Argonne National Lab., IL USA
Development of Ag-Clad Bi-2223 Superconductors for Electric Power Applications
Balachandran, U.; Eror, N. G.; Haldar, P.; Lelovic, M.; Selvamanickam, V.; Feb. 17, 1998; 17p; In English
Report No.(s): DE2001-8903; ANL/ET/CP-95041; No Copyright; Avail: Department of Energy Information Bridge, Microfiche
Development of high-temperature superconductor technology will make possible the design and fabrication of smaller, lighter, and more efficient power devices such as motors, generators, transformers, transmission cables, and fault-current limiters. A prototype fault-current limiter, a 200-hp motor, and a 50-m-long transmission cable have already been demonstrated using Ag-clad Bi-2223 superconductor tapes. We have recently enhanced the transport current properties of long lengths of multifilament Ag-clad Bi-2223 tapes through increased packing density of precursor powder, improved mechanical deformation, optimization of conductor design, and adjusted cooling rate. These improved processing parameters had a pronounced effect on the transport critical current of the superconducting tapes. Our improvements are briefly discussed and their implications are assessed in this paper.
NTIS
High Temperature Superconductors; Prototypes; Transport Properties

20020002809 Sandia National Labs., Albuquerque, NM USA
Microstructure and Texture Development of Compressed 421 Single Crystals and 421/13 4 -3 bicrystals
Hughes, D. A.; Godfrey, A.; Jan. 05, 1999; 6p; In English
Report No.(s): DE2001-755828; No Copyright; Avail: Department of Energy Information Bridge

Grain boundaries and grain-grain interactions may change the slip pattern of deforming crystals. The extent of this change is investigated by comparing the behavior of a random-like orientation in a single crystal compared to a bicrystal. Following deformation, a range of microscopy techniques are used to characterize the effect of the bicrystal boundary on the evolution of the dislocation structure, grain subdivision and slip pattern. It is observed that slip differences required for compatibility at the bicrystal boundary are spread across half the sample rather than being concentrated at the boundary, although some subtle effects also occur within 1m of the boundary. Microstructural subdivision occurs at three size scales with wide macroscopic bands of secondary slip forming at the largest level in both the single crystals and bicrystals as a result of the compression. These bands form in part to accommodate the deformation constraint imposed by the compression platens. In the bicrystals, the distribution of these macroscopic bands is additionally influenced by the grain boundary.
NTIS
Bicrystals; Microstructure; Textures; Crystal Structure

20020003356 Argonne National Lab., IL USA
Practical superconductor development for electric power applications
Balachandran, U.; Nov. 15, 2000; 39p; In English
Report No.(s): DE2001-768566; ANL/ET/RP-103400; No Copyright; Avail: Department of Energy Information Bridge, Microfiche

This is a multiyear experimental research program focused on improving relevant material properties of high-Tc superconductor (HTSs) and on development of fabrication methods that can be transferred to industry for production of commercial conductors. The development of teaming relationships through agreements with industrial partners is a key element of the Argonne (ANL) program.
NTIS
Superconductors (Materials); High Temperature Superconductors

20020003369 Argonne National Lab., IL USA
Electron self-energy of high temperature superconductors as revealed by angle-resolved photoemission
Ding, H.; Norman, M. R.; Randeria, M.; Dec. 05, 1997; 8p; In English
Report No.(s): DE2001-8896; ANL/MSD/CP-94990; No Copyright; Avail: Department of Energy Information Bridge, Microfiche

In this paper, we review some of the work our group has done in the past few years to obtain the electron self-energy of high temperature superconductors by analysis of angle-resolved photoemission data. We focus on three examples which have revealed: (1) a d-wave superconducting gap, (2) a collective mode in the superconducting state, and (3) pairing correlations in the pseudogap phase. In each case, although a novel result is obtained which captures the essence of the data, the conventional physics used leads to an incomplete picture. This indicates that new physics needs to be developed to obtain a proper understanding of these materials.
NTIS
Electron Energy; High Temperature Superconductors; Photoelectric Emission; Energy Gaps (Solid State)

20020003370 Argonne National Lab., IL USA
Exchange-spring behavior in epitaxial hard/soft magnetic bilayer films
Bader, S. D.; Fullerton, E. E.; Grimsditch, M.; Jiang, J. S.; Sowers, C. H.; Dec. 05, 1997; 17p; In English
Report No.(s): DE2001-8897; ANL/MSD/CP-94997; No Copyright; Avail: Department of Energy Information Bridge, Microfiche

We present results on the magnetic reversal process in epitaxial Sm-Co (1(bar 1)00)/TM (TM = Fe, Co) bilayer films prepared via magnetron sputtering onto Cr-buffered single-crystal MgO substrates. The magnetically hard Sm-Co films have 20-T uniaxial anisotropy and coercivities >3 T at room temperature. The magnetization of the soft layer is pinned at the interface to the hard-magnet layer and switches reversibly as expected for an exchange-spring magnet. With increasing soft layer thickness, the coercive field of the hard layer becomes significantly less than that of a single layer. We also present numerical solutions of a one-dimensional model that provide the spin configuration for each atomic layer. Comparison of the experimental results with the model simulations indicates that the exchange-spring behavior of our bilayer films can be understood from the intrinsic parameters of the hard and soft layers.
NTIS
Epitaxy; Magnetization; Numerical Analysis; Magnetic Films; Laminates; Magnetron Sputtering

20020003372 Argonne National Lab., IL USA

Converting films for x-ray detectors, applied to amorphous silicon arrays

Ross, S.; Zentai, G.; Dec. 05, 1997; 8p; In English

Report No.(s): DE2001-8902; ANL/ECT/CP-95038; No Copyright; Avail: Department of Energy Information Bridge, Microfiche

This paper presents results from our on-going efforts to characterize semiconductor thin films for direct x-ray conversion. We deposit these thin films onto an amorphous silicon (a-Si:H) readout array with the overall goal of developing a large area x-ray detector for protein crystallography, and for other x-ray imaging fields.

NTIS

Amorphous Silicon; Crystallography; Thin Films; X Ray Detectors; Semiconductors (Materials)

20020003376 Federal Energy Technology Center, Morgantown, WV USA

Life Cycle Cost Study for Coated Conductor Manufacture by Electron Beam and Pulsed Laser Deposition Systems

Chapman, J. N.; Apr. 14, 1999; 51p; In English

Report No.(s): DE2001-8939; DE-AC22-95PC95231-21; No Copyright; Avail: Department of Energy Information Bridge, Microfiche

The results of this study establish a framework for evaluation of the cost impact of many performance parameters in coated conductor manufacturing systems. Since the cost and concepts are based on early developmental results and engineering judgment, the study should be updated periodically based on latest data to enhance its usefulness. The study should be expanded to include other promising processes under consideration or development for manufacture of coated conductors. Review of this study by as wide a group of experts from industry, national laboratories and universities as possible is desirable to facilitate improving accuracy of the estimates and communication on the issues involved. The results for the case of achieving the $10/kA-m goal at a J(sub c) of 10(exp 5) a/sq cm applicable to applications requiring a magnetic field perpendicular to the direction of current flow may be viewed as somewhat discouraging. However, there is ample margin for improvement due to continued development and engineering that could enable meeting the goal of $10/kA-m.

NTIS

Coatings; Life Cycle Costs; Cost Analysis; Manufacturing

20020003377 Federal Energy Technology Center, Morgantown, WV USA

Characterization of High-Temperature Superconductor Film Layers Using Raman Spectroscopy

Cunningham, J. M.; Apr. 08, 1999; 56p; In English

Report No.(s): DE2001-8941; DE-AC22-95PC95231-20; No Copyright; Avail: Department of Energy Information Bridge, Microfiche

High-temperature superconductor films can be characterized using Raman spectroscopy to obtain the crystal orientation, oxygen concentration, and layer thickness for the film layers. This information is essential in determining characteristics of the films, such as transition temperature and current density. Good quality films need high transition temperature and current density. Previously published work shows that the theory and background work on Raman spectroscopy on high-temperature superconductor films gives this information. Earlier research on high-temperature superconductor films shows how the films can be characterized. by applying these different methods Raman data can be used as an effective analytical technique. An experimental setup is designed to evaluate the feasibility of acquiring the data quickly in an industrial environment using alternate technology than that used by previous researchers. Previous work in this area has been constricted to microprobe techniques that study single crystals of the superconductor. A technique is used which could give overall Raman data from a large area of the film, as opposed to single crystals or grains. Background and experimental work described in this thesis describes a method for determining layer thickness in buffer and superconducting film layers. Data is collected from a single film sample and a proposed buffer layer sample. This data is used to identify necessary improvements to the basic experimental setup to create a real-time, in situ, Raman diagnostic setup for use in industrial, high-temperature superconductor film processes.

NTIS

High Temperature Superconductors; Raman Spectroscopy; Spectroscopic Analysis; Superconducting Films

20020003401 Oak Ridge Y-12 Plant, TN USA

Solid state nuclear magnetic resonance studies of prion peptides and proteins

Heller, J.; Aug. 28, 1997; 222p; In English

Report No.(s): DE2001-6428; LBNL-42161; No Copyright; Avail: Department of Energy Information Bridge

High-resolution structural studies using x-ray diffraction and solution nuclear magnetic resonance (NMR) are not feasible for proteins of low volubility and high tendency to aggregate. Solid state NMR (SSNMR) is in principle capable of providing structural information in such systems, however to do this efficiently and accurately, further SSNMR tools must be developed This dissertation describes the development of three new methods and their application to a biological system of interest, the priori protein (PrP).
NTIS
Nuclear Magnetic Resonance; Peptides; Proteins; X Ray Diffraction

20020003421 Los Alamos National Lab., NM USA
Analysis of the sns superconducting rf control system
Wang, Y.; Kwon, S.; Regan, A.; Sep. 01, 2000; 6p; In English
Report No.(s): DE2001-768252; LA-UR-00-3743; No Copyright; Avail: Department of Energy Information Bridge, Microfiche
The RF system for the RF system for the SNS superconducting linac consists of a superconducting cavity, a klystron, and a low-level RF (LLRF) control system. For a proton linac like SNS, the field in each individual cavity needs to be controlled to meet an overall system requirement. The purpose of the LLRF control system is to maintain the RF cavity field to a desired magnitude and phase by controlling the klystron driver signal. The Lorentz force detuning causes the shift of the resonant frequency during the normal operation in the order of a few hundreds hertz. In order to compensate the Lorentz force detuning effects, the cavity is pretuned into the middle of the expected frequency shift caused by the Lorentz force detuning. Meanwhile to reduce the overshoot in the transient response, an error feedforward algorithm is proposed to get away a repetitive noise caused by the pulsed operation.
NTIS
Superconducting Devices; Electromagnetic Fields; Linear Accelerators; Superconducting Magnets

20020003973 Lawrence Livermore National Lab., Livermore, CA USA
Laboratory measurements of materials in extreme conditions; The use of high energy radiation sources for high pressure studies
Cauble, R.; Remington, B. A.; Jun. 01, 1998; 38p; In English
Report No.(s): DE2001-2857; UCRL-JC-131079; DP0102012; No Copyright; Avail: Department of Energy Information Bridge
High energy lasers can be used to study material conditions that are appropriate fort inertial confinement fusion: that is, materials at high densities, temperatures, and pressures. Pulsed power devices can offer similar opportunities. The National Ignition Facility (NIF) will be a high energy multi-beam laser designed to achieve the thermonuclear ignition of a mm-scale DT-filled target in the laboratory. At the same time, NE will provide the physics community with a unique tool for the study of high energy density matter at states unreachable by any other laboratory technique. Here we describe how these lasers and pulsed power tools can contribute to investigations of high energy density matter in the areas of material properties and equations of state, extend present laboratory shock techniques such as high-speed jets to new regimes, and allow study of extreme conditions found in astrophysical phenomena.
NTIS
Equations of State; High Power Lasers; Inertial Confinement Fusion; Lasers; Ignition; Radiation Sources; Radiation Effects

20020003975 Lawrence Livermore National Lab., Livermore, CA USA
Toward a predictive atomistic model of ion implantation and dopant diffusion in silicon
Caturla, M.; Johnson, M. D.; Zhu, J.; Sep. 18, 1998; 40p; In English
Report No.(s): DE2001-2853; UCRL-ID-130457; No Copyright; Avail: Department of Energy Information Bridge
We review the development and application of kinetic Monte Carlo simulations to investigate defect and dopant diffusion in ion implanted silicon. In these type of Monte Carlo models, defects and dopants are treated at the atomic scale, and move according to reaction rates given as input principles. These input parameters can be obtained from first principles calculations and/or empirical molecular dynamics simulations, or can be extracted from fits to experimental data. Time and length scales differing several orders of magnitude can be followed with this method, allowing for direct comparison with experiments. The different approaches are explained and some results presented.
NTIS
Reaction Kinetics; Ion Implantation; Diffusion; Monte Carlo Method; Atoms; Silicon

20020003983 Dartmouth Coll., Hanover, NH USA

Excitons and Plasmas in Semiconducting Microstructures and Ternary Alloys

Sturge, M. D.; Jun. 27, 2000; 17p; In English

Report No.(s): DE2001-763159; No Copyright; Avail: Department of Energy Information Bridge, Microfiche

This report summarizes the work supported by this grant over a period of more than twelve years, and is necessarily rather brief in its coverage of the early years. For a fuller account of the early work, the annual progress reports submitted to DOE should be consulted. The work deals primarily with semiconducting superlattices (SLS), in which two semiconductors with different band gaps are interleaved, with layer thicknesses defined to one monolayer. The electronic and optical properties of the SL are quite different from those of the constituents and offer interesting new possibilities both in device design and in basic physics. This research aims to improve our understanding of optically excited states in SLS. We studied these structures by time-and space-resolved tunable laser spectroscopy, with and without external perturbations such as magnetic field, electric field, and uniaxial stress.

NTIS

Semiconductor Devices; Superlattices; Excitons; Plasmas (Physics); Ternary Alloys; Crystal Lattices

20020003984 State Univ. of New York, Research Foundation, Buffalo, NY USA

Tl2Ba2CuO(6+delta) As a Model System for Fundamental Studies of High Temperature Superconductivity

Ren, Z. F.; Wang, J. H.; May 22, 2000; 5p; In English

Report No.(s): DE2001-763150; No Copyright; Avail: Department of Energy Information Bridge, Microfiche

During the past year, the Principal Investigator (PI) (Z. F. Ren) moved from SUNY-Buffalo to Boston College as an Associate Professor in the Department of Physics to further enhance the future success of this program. Due to the moving and set up of the new laboratory at Boston College, the project was slowed down in some extent. Nevertheless, the PI and his associates have been able to accomplish the following: (1) The upper critical field study has been carried out on the early samples (made when the PI was still with SUNY-Buffalo). Those samples have either high (Tc) (20K) with single transition or low TC but with double transitions. Therefore, there has no definitive conclusion been drawn yet. (2) X-ray photoemission has been used to study the Tl-2201 thin films. (3) In addition, J. Y. Lao has synthesized the epitaxial thallium-containing 1212 films with critical current density up to 10(exp 6)/sq cm at 77 K and zero magnetic field as part of his Ph.D thesis. The success of this research has enabled us to consider using this material as an alternative for YBa2Cu3O7 (YBCO) or TlBa2Ca2Cu3O9 (Tl-1223) for long length wire development for applications such as transmission cables, motors, generators, etc.

NTIS

Barium Oxides; Copper Oxides; High Temperature Superconductors; Thallium Compounds

20020003990 Argonne National Lab., IL USA

Spin-flop tendencies in exchange-biased Co/CoO thin films

Felcher, G. P.; Borchers, J. A.; Ijiri, Y.; Lee, S. H.; Majkrzak, C. F.; Dec. 02, 1997; 16p; In English

Report No.(s): DE2001-8894; ANL/MSD/CP-94979; No Copyright; Avail: Department of Energy Information Bridge, Microfiche

In order to study the antiferromagnetic (AFM) spin structure near the interface of exchange-biased bilayers, polarized neutron diffraction measurements were performed on a series of (111) Co(7.5 nm)/CoO(X nm) and CoO(X nm) thin films where X = 20, 40 and 100 nm. In these samples, field cooling through the Neel temperature of the AFM increases the component of the CoO moment perpendicular to the applied field, relative to the parallel component. The subsequent application of a 500 Oe field perpendicular to the cooling direction rotates both the Co and CoO moments. Experiments on CoO films without Co showed a smaller difference between the parallel and perpendicular CoO moments in response to cooling and applied fields. Exchange coupling between the Co and CoO layers is apparently responsible for the increased projection of the AFM moments perpendicular to the cooling field.

NTIS

Antiferromagnetism; Thin Films; Cobalt Oxides; Cobalt; Electron Spin

20020003991 Argonne National Lab., IL USA

Depth-dependent magnetism of layered superconductors: Nb/Si

Felcher, G. P.; Fullerton, E. E.; Osgood, R. M.; Yusuf, S. M.; Dec. 02, 1997; 13p; In English

Report No.(s): DE2001-8893; ANL/MSD/CP-94973; No Copyright; Avail: Department of Energy Information Bridge, Microfiche

We have studied magnetic field penetration and vortex line formation in a (Nb(100 (angstrom))/Si(15 (angstrom)))x20 multilayer by magnetization and polarized neutron reflection. With the magnetic field applied parallel to the surface, the magnetization revealed the presence of a kink above H(sub cl) indicative of transitions between one row of fluxoids and two rows of fluxoids parallel to the surface. The spin-dependence of neutron reflectivity below H(sub cl) was consistent with a penetration depth of 1200 (angstrom), substantially larger than that of bulk Nb. In the mixed phase (H(sub ext) > H(sub cl)) the field was found to penetrate the surface, with a slope as found in the case of H(sub ext) H(sub cl). At H(sub ext) H(sub cl) vortex forms in addition to surface penetration. A modulation of the vortex fields was found with the periodicity of the Nb/Si bilayers as evidenced by the spin dependence of the reflectivity at the first Bragg peak of the multilayer.
NTIS
Silicides; Niobium; Laminates; Superconductors (Materials); Neutrons; Magnetization; Depth

20020003995 Oak Ridge National Lab., TN USA
Ion-Irradiation-Induced Amorphization of Cadmium Niobate Pyrochlore
Meldrum, A.; Jan. 04, 2001; 8p; In English; Fall 2000 Materials Research Society Meeting, 27 November 2000, Boston, MA, USA
Contract(s)/Grant(s): AC05-96OR22464
Report No.(s): DE2001-773927; P00-109294; No Copyright; Avail: Department of Energy Information Bridge, Microfiche

Pyrochlores represent a large class of compounds with the general chemical formula A(sub 2)B(sub 2)O(sub 7). The pyrochlore structure consists of interconnected AO(sub 8) and BO(sub 6) cation polyhedra where the BO(sub 6) octahedra are slightly distorted and form a continuous corner-sharing network. The large, 8-fold coordinated A-site cations and the seventh oxygen occupy channels in the (B(sub 2)O(sub 6)) network of octahedra. The structure is an anion-deficient MX(sub 2) flourite structure in which the A and B cations are ordered on the M sites. One eighth of the X anions are absent in the pyrochlore structure, and the resulting oxygen vacancies are ordered on the anion sublattice.
NTIS
Amorphous Materials; Niobates; Cadmium Compounds; Polyhedrons; Cations

20020004006 Los Alamos National Lab., NM USA
Improvements in the modelling of the recrystallization textures of Al-alloys
Engler, O.; May 01, 2000; 11p; In English
Report No.(s): DE2001-768991; LA-UR-00-2322; No Copyright; Avail: Department of Energy Information Bridge

During the thermomechanical processing of Al-alloys control of the microstructure the final sheet product is a vital step. The crystallographic texture is of importance of in controlling mechanical anisotropy - e.g. the earing behavior - which affects the forming properties of the sheet. Thus, modelling of the evolution of microstructure and texture during thermomechanical processing is of great interest to predict the properties and so to maintain the quality of the final sheet products.
NTIS
Aluminum Alloys; Crystallography; Microstructure; Recrystallization; Textures; Mathematical Models

20020004363 NASA Ames Research Center, Moffett Field, CA USA
Carbon Nanotubes in Water: MD Simulations of Internal and External Flow, Self Organization
Jaffe, Richard L., NASA Ames Research Center, USA; Halicioglu, Timur, Eloret Corp., USA; Werder, Thomas, Eidgenoessische Technische Hochschule, Switzerland; Walther, Jens, Eidgenoessische Technische Hochschule, Switzerland; Koumoutsakos, Petros, Eidgenoessische Technische Hochschule, Switzerland; [2001]; 1p; In English; 9th Conference on Molecular Nanotechnology, 9-11 Nov. 2001, Santa Clara, CA, USA
Contract(s)/Grant(s): RTOP 519-40-12; No Copyright; Avail: Issuing Activity; Abstract Only

We have developed computational tools, based on particle codes, for molecular dynamics (MD) simulation of carbon nanotubes (CNT) in aqueous environments. The interaction of CNTs with water is envisioned as a prototype for the design of engineering nano-devices, such as artificial sterocillia and molecular biosensors. Large scale simulations involving thousands of water molecules are possible due to our efficient parallel MD code that takes long range electrostatic interactions into account. Since CNTs can be considered as rolled up sheets of graphite, we expect the CNT-water interaction to be similar to the interaction of graphite with water. However, there are fundamental differences between considering graphite and CNTs, since the curvature of CNTs affects their chemical activity and also since capillary effects play an important role for both dynamic and static behaviour of materials inside CNTs. In recent studies Gordillo and Marti described the hydrogen bond structure as well as time dependent properties of water confined in CNTs. We are presenting results from the development of force fields describing the interaction of CNTs and water based on ab-initio quantum mechanical calculations. Furthermore, our results include both water flows external to CNTs and the behaviour of water nanodroplets inside heated CNTs. In the first case (external flows) the hydrophobic behaviour

of CNTs is quantified and we analyze structural properties of water in the vicinity of CNTs with diagnostics such as hydrogen bond distribution, water dipole orientation and radial distribution functions. The presence of water leads to attractive forces between CNTs as a result of their hydrophobicity. Through extensive simulations we quantify these attractive forces in terms of the number and separation of the CNT. Results of our simulations involving arrays of CNTs indicate that these exhibit a hydrophobic behaviour that leads to self-organising structures capable of trapping water clusters. In the second case (internal flows) we study the behaviour of water droplets confined inside CNTs. Constant temperature simulations allow us to capture structural properties such as the contact angles and density profiles of the equilibrated drops. by heating and subsequently cooling of the CNT, we are able to measure the evaporation and the condensation rate of the entrapped water.
Author
Carbon Nanotubes; Water; Molecular Dynamics; Water Flow; Computerized Simulation

20020004668 Radiation Science, Inc., Belmont, MA USA
Development of a High Resolution Imaging Spectrometer ***Final Report, 4 Sep. 1999 - 4 Mar. 2000***
Krieger, A. S.; Parsignault, D. R.; Oct. 01, 2000; 28p; In English
Report No.(s): DE2001-769203; No Copyright; Avail: Department of Energy Information Bridge, Microfiche

In this program we demonstrated that a quartz crystal could be bent to a spherical shape around a convex form, thereby eliminating the problems of deviations in the flatness of the crystal, non-uniformities in crystal thickness, and variations in the thickness of the epoxy bonding the crystal to its support form. Optical testing showed that the front surface of the crystal was spherical with an RMS deviation of 1/20 of a wave. X-ray testing showed that the resolving power of this crystal was on the order of 10(exp 4). We developed a design concept for a spherical crystal spectrometer for use at NSTX and established that it could be built at a cost within the parameters of phase II.
NTIS
Crystal Structure; Images; Manufacturing; High Resolution; Imaging Spectrometers

20020004910 California Univ., Lawrence Berkeley Lab., Berkeley, CA USA
Influence of Mg and In on defect formation in GaN: Bulk and MOCVD grown samples
Liliental-Weber, Z.; Benamara, M.; Jasinski, J.; Swider, W.; Washburn, J.; Nov. 22, 2000; 8p; In English
Report No.(s): DE2001-771943; LBNL-46983; No Copyright; Avail: Department of Energy Information Bridge

Transmission electron microscopy studies were applied to study GaN crystals doped with Mg. Both: bulk GaN:Mg crystals grown by a high pressure and high temperature process and those grown by metal-organic chemical-vapor deposition (MOCVD) have been studied. Structural dependence on growth polarity was observed in the bulk crystals. Spontaneous ordering (formation of polytypoids) was observed for growth in the N to Ga polar direction (N polarity). On the opposite site of the crystal (growth in the Ga to N polar direction) Mg-rich pyramidal defects with base on the basal planes and with walls inclined about 45O to these planes, empty inside (pinholes) were observed. A high concentration of these pyramidal defects was also observed in the MOCVD grown crystals. For samples grown with Mg delta doping planar defects were also observed especially at the early stages of growth followed by formation of pyramidal defects. TEM and x-ray studies of InxGa(sub 1(minus)x)N crystals for the range of 28-45% nominal In concentration shows formation of two sub-layers: strained and relaxed, with a much lower In concentration in the strained layer. Layers with the highest In concentration were fully relaxed.
NTIS
Crystal Defects; Magnesium; Indium; Gallium Nitrides

20020005188 Los Alamos National Lab., NM USA
Solid-State NMR ***Progress Report***
Stephens, T.; Labouriau, A.; Aug. 01, 2000; 12p; In English
Report No.(s): DE2001-768913; LA-UR-00-3591; No Copyright; Avail: Department of Energy Information Bridge

It is well established that the zero shear bulk viscosity of all amorphous polymers is directly proportional to the molecular weight below a critical low molecular weight and above this molecular weight increases as the 3.5 power of M. This effect manifests itself on the NMR proton spin-spin relaxation time (T2). For polydimethyl siloxane the break in the proton T2-molecular weight curve occurs at about M=50000 g/mol and is about 30000 g/mol from viscosity measurements. Thus, there is a direct connection between the critical molecular weight representing the influence of entanglements on the bulk viscosity and other properties and the spin-spin relaxation time of amorphous polymers. Therefore, the entanglements must modulate the segmental motions so that even in amorphous state they area major reason for the incomplete motional narrowing. This effect would then be further accentuated with cross-links, filler, etc. For high molecular weights in the amorphous state polymer chains exhibit both liquid-like and solid-like properties from the point of view of NMR measurements. The liquid-like properties are manifested in

the high frequency segmental motions. The solid-like properties are a result of residual dipolar couplings caused by incomplete motional narrowing.
NTIS
Nuclear Magnetic Resonance; Viscosity; Molecular Weight; Solid State

20020005222 California Univ., Lawrence Berkeley Lab., Berkeley, CA USA
Formation of ohmic contacts to MOCVD grown p-GaN by controlled activation of Mg
Kaminska, E.; Piotrowska, A.; Barcz, A.; Bour, D.; Zielinski, M.; Nov. 27, 2000; 4p; In English
Report No.(s): DE2001-772145; LBNL-46981; No Copyright; Avail: Department of Energy Information Bridge

We report on the formation of low resistivity ohmic contacts to p-GaN, r(sub c) 10(sup (minus)4)(Omega)cm(sup 2), by increasing the concentration of the active Mg in the subcontact zone, via Zr-mediated release of hydrogen. We have investigated the process of evolution of hydrogen from MOCVD (metalorganic chemical vapor deposition) grown p-GaN via Zr-based metallization, and determined the optimum processing conditions (temperature and gas ambient) for fabrication of low resistance ohmic contacts. When the process is conducted in N(sub 2) flow, the metallization remains stable at temperatures required to achieve the ohmic behavior, and the morphology of the metal/semiconductor interface is unaltered by such a heat treatment. The processing in O(sub 2), on the contrary, causes the interdiffusion of metallization constituents and the incorporation of oxygen into the semiconductor subcontact region, which could be responsible for increased resistivity of these contacts.
NTIS
Hydrogen; Magnesium; Metalorganic Chemical Vapor Deposition; Metallizing; Semiconductors (Materials)

20020005245 Fermi National Accelerator Lab., Batavia, IL USA
Higgs searches at the Tevatron, run 1 results and run 2 prospects
Roco, M. T.; Feb. 08, 2001; 4p; In English; International Conference on High Energy Physics, 27 Jul. - 2 Aug. 2000, Osaka, Japan
Contract(s)/Grant(s): AC02-76CH03000
Report No.(s): DE2001-774341; FERMILAB-CONF-00/203-E; No Copyright; Avail: Department of Energy Information Bridge, Microfiche

Recent results from searches for the SM and SUSY Higgs bosons in Run 1 at the Tevatron have been shown. The sensitivity of the present SM Higgs searches at the Tevatron is limited by statistics leading to a reach in p(bar p) (r arrow) VH production more than an order of magnitude higher than the SM prediction. The search for the neutral SUSY Higgs via p(bar p) (r arrow) b(bar b)(psi) (r arrow) b(bar b)b(bar b) excludes regions in the tan (beta) vs M(sub A) space which extend significantly those previously probed by LEP. They have presented results from studies of the discovery and sensitivity reach for the Higgs bosons in Run 2. Combining all search channels and the data from both experiments a SM Higgs can be excluded at 95% CL over the full mass range M(sub H) 190 GeV with 15 fb(sup (minus)1). The sensitivity to neutral SUSY Higgs production with b(bar b) has been shown. The p(bar p) (r arrow) b(bar b)(psi) (r arrow) b(bar b)b(bar b) channel serves as the most important mode for discovering or ruling out the MSSM Higgs at large tan (beta).
NTIS
Higgs Bosons; Particle Theory; Quantum Statistics

20020005250 Oak Ridge National Lab., TN USA
Method to Improve Activation of Implanted Dopants in SiC
Holland, O. W.; Jan. 16, 2001; 9p; In English; Materials Research Society Fall 2000 Meeting, 27 Nov. - 1 Dec. 2000, Boston, MA, USA
Contract(s)/Grant(s): AC05-96OR22464
Report No.(s): DE2001-774474; P01-109558; No Copyright; Avail: Department of Energy Information Bridge, Microfiche

Implantation of dopant ions in SiC has evolved according to the assumption that the best electrical results (i.e., carrier concentrations and mobility) is achieved by using the highest possible processing temperature. This includes implantation at > 600 C followed by furnace annealing at temperatures as high as 1,750 C. Despite such aggressive and extreme processing, implantation suffers because of poor dopant activation, typically ranging between < 2%--50% with p-type dopants represented in the lower portion of this range and n-types in the upper. Additionally, high-temperature processing can led to several problems including changes in the stoichiometry and topography of the surface, as well as degradation of the electrical properties of devices. A novel approach for increasing activation of implanted dopants in SiC and lowering the activation temperature will be discussed. This approach utilizes the manipulation of the ion-induced damage to enhance activation of implanted dopants. It will be shown that nearly amorphous layers containing a small amount of residual crystallinity can be

recrystallized at temperatures below 900 C with little residual damage. It will be shown that recrystallization traps a high fraction of the implanted dopant residing within the amorphous phase (prior to annealing) onto substitutional sites within the SiC lattice.
NTIS
Implantation; Ion Implantation; Silicon Carbides; Additives

20020005268 Argonne National Lab., IL USA
Raman and Infrared Studies of the Sharp 890 cm(-1) Mode in Organic Superconductors
Eldridge, J. E.; Lin, Y.; Schlueter, J. A.; Wang, H. H.; Kini, A. M.; Nov. 28, 2000; 13p; In English
Report No.(s): DE2001-768631; ANL/MSD/CP-103486; No Copyright; Avail: Department of Energy Information Bridge

Raman and infrared spectra of several organic superconductors are presented, showing some unusual behaviors of a sharp line at 890/cm in both spectra. These include a frequency shift below T(sub c), a positive deuterium isotope shift, frequency softening at low temperatures, and sensitivity to lattice superstructure. It is proposed that either the ion or the neutral molecule has a distortion with a strong v(sub 60)(B(sub 3g)) mode component.
NTIS
Infrared Radiation; Organic Superconductors; Raman Spectra

20020005395 Federal Energy Technology Center, Morgantown, WV USA
Life cycle cost study for coated conductor manufacture by metal organic chemical vapor deposition
Chapman, J. N.; Jul. 13, 1999; 22p; In English
Report No.(s): DE2001-775041; DE-AC22-95PC95231-25; No Copyright; Avail: Department of Energy Information Bridge, Microfiche

The purpose of this report is to calculate the cost of producing high temperature superconducting wire by the Metal Organic Chemical Vapor Deposition (MOCVD) process. The technology status is reviewed from the literature and a plant conceptual design is assumed for the cost calculation. The critical issues discussed are the high cost of the metal organic precursors, the material utilization efficiency and the capability of the final product as measured by the critical current density achieved. Capital, operating and material costs are estimated and summed as the basis for calculating the cost per unit length of wire. Sensitivity analyses of key assumptions are examined to determine their effects on the final wire cost. Additionally, the cost of wire on the basis of cost per kiloampere per meter is calculated for operation at lower temperatures than the liquid nitrogen boiling temperature. It is concluded that this process should not be ruled out on the basis of high cost of precursors alone.
NTIS
Electric Wire; Metalorganic Chemical Vapor Deposition; Superconducting Films; High Temperature Superconductors

20020005804 Sandia National Labs., Albuquerque, NM USA
Wide-Bandgap Compound Semiconductors to Enable Novel Semiconductor Devices
Crawford, M. H.; Chow, W. W.; Wright, A. F.; Lee, S. R.; Jones, E. D.; Apr. 01, 1999; 27p; In English
Report No.(s): DE2001-5901; SAND99-0817; No Copyright; Avail: Department of Energy Information Bridge, Microfiche

This report represents the completion of a three-year Laboratory-Directed Research and Development (LDRD) program that focused on research and development of GaN-based wide bandgap semiconductor materials (referred to as III-N materials). Our theoretical investigations include the determination of fundamental materials parameters from first-principles calculations, the study of gain properties of III-N heterostructures using a microscopic laser theory and density-functional-theory, charge-state calculations to determine the core structure and energy levels of dislocations in III-N materials. Our experimental investigations include time-resolved photoluminescence and magneto-luminescence studies of GaN epilayers and multiquantum well samples as well as x-ray diffraction studies of AlGaN ternary alloys. In addition, we performed a number of experiments to determine how various materials processing steps affect both the optical and electrical properties of GaN-based materials. These studies include photoluminescence studies of GaN epilayers after post-growth rapid thermal annealing, ion implantation to produce n- and p-type material and electrical and optical studies of plasma-etched structures.
NTIS
Research and Development; Gallium Nitrides; Semiconductors (Materials); Energy Gaps (Solid State); Optical Properties; Charged Particles

20020005808 Sandia National Labs., Albuquerque, NM USA
Random and Uniform Reactive Ion Etching Texturing of Si
Zaidi, S. H.; Apr. 01, 1999; 24p; In English
Report No.(s): DE2001-5938; SAND99-0748; No Copyright; Avail: Department of Energy Information Bridge, Microfiche

The performance of a solar cell is critically dependent on absorption of incident photons and their conversion into electrical current. This report describes research efforts that have been directed toward the use of nanoscale surface texturing techniques to enhance light absorption in Si. This effort has been divided into two approaches. The first is to use plasma-etching to produce random texturization on multicrystalline Si cells for terrestrial use, since multicrystalline Si cannot be economically textured in any other way. The second approach is to use interference lithography and plasma-etching to produce gettering structures on Si cells for use in space, so that long-wavelength light can be absorbed close to the junction and make the cells more resistant to cosmic radiation damage.
NTIS
Photons; Solar Cells; Silicon; Radiation Damage; Plasma Etching; Electromagnetic Absorption

20020005814 Los Alamos National Lab., NM USA
SNS superconducting cavity modeling: Iterative Learning Control (ILC)
Kwon, S.; Aug. 01, 2000; 6p; In English
Report No.(s): DE2001-768260; LA-UR-00-3727; No Copyright; Avail: Department of Energy Information Bridge
Raleigh-Taylor (RT) instabilities occur when a low-density fluid attempts to accelerate a high-density fluid. The instability manifests itself by forming bubbles of the low-density that percolate through the high-density fluid. Concurrently, spikes of the high-density fluid 'let' into the low-density fluid. This instability is seen in familiar occurrences such as the growth of icicles and the draining of sinks. If the interface between the two fluids remains perfectly smooth the instability will not occur that is, it must be 'seeded' by a wave-like perturbation. For the two cases mentioned above, a vibration can be sufficient to perform the 'seeding'.
NTIS
Superconductivity; Taylor Instability; Mathematical Models; Iteration; Learning

20020005816 Sandia National Labs., Albuquerque, NM USA
Microstructural characterization of catalyzed NaAlH4
Thomas, G. J.; Gross, K. J.; Yang, N. Y. C.; Jensen, C.; Oct. 01, 2000; 15p; In English
Report No.(s): DE2001-768282; SAND2000-8905C; No Copyright; Avail: Department of Energy Information Bridge
A number of laboratories have now demonstrated that catalyst-assisted NaAlH4 can reversibly absorb and desorb hydrogen in the solid state at moderate temperatures. An understanding of the mechanisms by which bulk decomposition and reformation of the compound can occur in the presence of a surface catalyst is important to improving the kinetic and thermodynamic properties of alanates for use in hydrogen storage applications. Using scanning electron microscopy (SEM) and energy dispersive spectroscopy (EDS), the authors have examined the microstructure and elemental composition of Na alanate samples, doped using a liquid Ti/Zr catalyst precursor, for a number of conditions. First, microscopy and compositional analyses were performed at different stages of the decomposition process within the first desorption cycle. Second, the material was characterized after multiple absorption/desorption cycles (5 cycles). Finally, the effects of the catalyst doping procedure on particle size, surface morphology and surface composition were examined. Significant changes in particle morphology and in elemental distribution were found to be induced by the desorption and cycling processes. Importantly, the measurements indicate that the initial dehydriding reactions were accompanied by significant enhancement of Al concentration toward the surface of particles and that elemental segregation occurred with repeated absorption/desorption cycles.
NTIS
Sodium; Thermodynamic Properties; Morphology; Microstructure; Aluminum Hydrides; Surface Properties; Catalysis

20020005817 Sandia National Labs., Albuquerque, NM USA
Evaluation of NH4F/H2O2 Effectiveness as a Surface Passivation Agent for Cd(1-x)Zn(x)Te Crystals
Wright, G. W.; James, R. B.; Chinn, D.; Brunett, B. A.; Olsen, R. W.; Jul. 01, 2000; 14p; In English
Report No.(s): DE2001-768287; SAND2001-8022C; No Copyright; Avail: Department of Energy Information Bridge
Various passivating agents that reduced the surface leakage current of CZT crystals have been previously reported. In one of the studies, NH4F/H202 was identified as a promising passivation agent for CZT. We now present a study that includes the effect of N&F/H202 treatment on the surface properties and detector performance. An elemental depth profile was obtained via Auger Electron Spectroscopy. Furthermore, X-ray Photoelectron Spectroscopy acquired at different processing times to identify the chemical states of the elemental species that composed the dielectric layer. It was found that the NH4F/H202 surface passivation significantly improved the sensitivity and energy resolution of CZT detectors. Furthermore, the NH4F/H202 treatment did not attack the Au electrodes, which eliminated the need to protect the contacts in the detector fabrication process.
NTIS
Crystals; Hydrogen Peroxide; Cadmium Tellurides; Fabrication; Ammonium Compounds; Surface Properties; Zinc; Fluorides

20020005896 Federal Energy Technology Center, Morgantown, WV USA

Development of in-situ control diagnostics for application of epitaxial superconductor and buffer layers

Winkleman, B. C.; Giel, T. V.; Cunningham, J.; Jun. 30, 1999; 32p; In English

Report No.(s): DE2001-775040; DE-AC22-95PC95231-24; No Copyright; Avail: Department of Energy Information Bridge, Microfiche

The recent achievements of critical currents in excess of 1x10(sup 6)amp/cm(sup 2) at 77K in YBCO (Yttrium Barium Copper Oxides) deposited over suitably textured buffer/substrate composites have stimulated interest in the potential fabrication of these coated conductors as wire. Numerous approaches and manufacturing schemes for producing coated conductor wire are currently being developed. Recently, under the U.S. Department of Energy (DOE's) sponsorship, the University of Tennessee Space Institute (UTSI) performed an extensive evaluation of leading coated conductor processing options. In general, it is our feeling that the science and chemistry that are being developed in the coated conductor wire program now need proper engineering evaluation to define the most viable options for a commercial fabrication process. All fabrication processes will need process control measurements. This report provides a specific review of the needs and available technologies for process control for many of the coated conductor processing options. This report also addresses generic process monitoring areas in which additional research and development is needed. The concentration is on the two different approaches for obtaining the textured substrates that have been identified as viable candidates. These are the Los Alamos National Laboratory's (LANL) ion-beam assisted deposition, called IBAD, to obtain a highly textured yttria-stabilized zirconia (YSZ) buffer on nickel alloy strips, and Oak Ridge National Laboratory's (ORNL) rolling assisted, bi-axially textured substrate option called RABiTS(trademark).

NTIS

Superconducting Films; YBCO Superconductors; Electric Wire; Fabrication

77
PHYSICS OF ELEMENTARY PARTICLES AND FIELDS

Includes quantum mechanics; theoretical physics; and statistical mechanics. For related information see also 72 Atomic and Molecular Physics, 73 Nuclear Physics, and 25 Inorganic, Organic and Physical Chemistry.

20020000869 Brookhaven National Lab., Upton, NY USA

QCD Phase Transitions, Volume 15

Schafer,; Nov. 04, 1998; 213p; RIKEN Research Center Proceedings Workshop on QCD Phase Transitions, 4-7 Nov. 1998, Upton, NY, USA

Contract(s)/Grant(s): AC02-98CH10886

Report No.(s): DE2001-11450; BNL-52561; KB0201; No Copyright; Avail: Department of Energy Information Bridge, Microfiche

The title of the workshop, 'The QCD Phase Transitions' in fact happened to be too narrow for its real contents. It would be more accurate to say that it was devoted to different phases of QCD and QCD-related gauge theories, with strong emphasis on discussion of the underlying non-perturbative mechanisms which manifest themselves as all those phases. Before we go to specifics, let us emphasize one important aspect of the present status of non-perturbative Quantum Field Theory in general. It remains true that its studies do not get attention proportional to the intellectual challenge they deserve, and that the theorists working on it remain very fragmented. The efforts to create Theory of Everything including Quantum Gravity have attracted the lion share of attention and young talent. Nevertheless, in the last few years there was also a tremendous progress and even some shift of attention toward emphasis on the unity of non-perturbative phenomena. For example, we have seen some efforts to connect the lessons from recent progress in Supersymmetric theories with that in QCD, as derived from phenomenology and lattice. Another example is Maldacena conjecture and related development, which connect three things together, string theory, super-gravity and the (N=4) supersymmetric gauge theory. Although the progress mentioned is remarkable by itself, if we would listen to each other more we may have chance to strengthen the field and reach better understanding of the spectacular non-perturbative physics.

NTIS

Quantum Chromodynamics; Quantum Theory; Unified Field Theory

20020001200 Argonne National Lab., IL USA

Dyson-Schwinger Equations: Connecting Small and Large Length-scales

Roberts, C.; Feb. 08, 1999; 10p; In English; International Conference on Nuclear and Particle Physics, 3-8 Nov. 1998, Dubrovnik (HR)

Contract(s)/Grant(s): W-31109-ENG-38
Report No.(s): DE2001-12378; ANL/PHY/CP-98390; No Copyright; Avail: Department of Energy Information Bridge, Microfiche

The phenomenological application of Dyson-Schwinger equations to the calculation of meson properties observable at TJNAF is illustrated. Particular emphasis is given to the ability of this framework to unify long-range effects constrained by chiral symmetry with short-range effects prescribed by perturbation theory, and interpolate between them.
NTIS
Mesons; Perturbation Theory; Chirality

20020001205 Argonne National Lab., IL USA
Four-point correlation functions in the AdS/CFT correspondence
Chalmers, G.; Schalm, K.; Feb. 09, 1999; 18p; In English
Report No.(s): DE2001-12355; ANL-HEP-CP-98-142; No Copyright; Avail: Department of Energy Information Bridge, Microfiche

We examine correlation functions within the correspondence between gauged supergravity on anti-de Sitter space and N = 4 super Yang-Mills theory in Minkowski space. The imaginary parts of four-point functions in momentum space are computed, in addition to particular examples of three-point functions. Exchange diagrams for gravitons are included. The results indicate additional structure in N = 4 super Yang-Mills theory at strong ’t Hooft coupling and in the large N limit.
NTIS
Correlation; Minkowski Space; Supergravity

20020001455 Argonne National Lab., IL USA
Hybrid Collimation for Industrial Gamma-Ray Imaging
He, Z.; Knoll, G. F.; Smith, L. E.; Wehe, D. K.; Jun. 22, 1999; 6p; In English
Report No.(s): DE2001-11849; ANL/NT/CP-99223; No Copyright; Avail: Department of Energy Information Bridge

Portable photon imaging devices with a broad energy range of sensitivity, adequate angular resolution, and high efficiency are useful in applications such as environmental remediation and industrial surveys. The vast majority of past systems built for these applications have relied on mechanical collimation although a few have used electronic collimation. to our knowledge, no devices have been built that exploit the benefits of both mechanical and electronic collimation in the same system. The combination of a mechanically-collimated camera with an electronically-collimated camera offers both the high efficiency and good angular resolution typical in a mechanically-collimated camera for lower energies and the uncoupling of spatial resolution and efficiency provided by an electronically-collimated camera at higher energies.
NTIS
Cameras; Collimation; Gamma Rays

20020001457 Argonne National Lab., IL USA
Bd(0) Mixing and CP Violation Measurements at the Tevatron
Byrum, K. L.; Jun. 10, 1999; 6p; In English
Report No.(s): DE2001-11851; ANL-HEP-CP-99-64; No Copyright; Avail: Department of Energy Information Bridge

The authors present six time-dependent B(sub d,sup 0) mixing measurements of Delta-m(sub d) from the CDF Run I data. The CDF average is Delta-m(sub d) = .494(sub +/- 0.26)(sup +/- 0.26)/ps. They also present a measurement of the CP-violating asymmetry sin(2(beta)) using a sample of B(sup 0)/(bar B)(sup 0) to J/(psi)K(sub s,sup 0) decays and report sin(2(beta)) = .79(sub -.44,sup +.41).
NTIS
Particle Accelerators; Time Dependence

20020001566 Argonne National Lab., IL USA
Detailed Comparison of Next-to-Leading Order Predictions for Jet Photoproduction at HERA
Harris, B. W.; Klassen, M.; Vossebeld, J.; Jun. 02, 1999; 12p; In English
Report No.(s): DE2001-11838; ANL-HEP-CP-99-43; No Copyright; Avail: Department of Energy Information Bridge

The precision of new HERA data on jet photoproduction opens up the possibility to discriminate between different models of the photon structure. This requires equally precise theoretical predictions from perturbative QCD calculations. In the past years, next-to-leading order calculations for the photoproduction of jets at HERA have become available. Using the kinematic cuts of recent ZEUS analyses, we compare the predictions of three calculations for different dijet and three-jet distributions. We find that

in general all three calculations agree within the statistical accuracy of the Monte Carlo integration yielding reliable theoretical predictions. In certain restricted regions of phase space, the calculations differ by up to 5%.
NTIS
Photons; Photoproduction; Quantum Chromodynamics

20020001567 Argonne National Lab., IL USA
Heavy Quark Production in Deep-Inelastic Scattering at HERA
Harris, B. W.; Laenen, E.; Moch, S.; Smith, J.; Jun. 02, 1999; 12p; In English
Report No.(s): DE2001-11837; ANL-HEP-CP-99-35; No Copyright; Avail: Department of Energy Information Bridge

We discuss two topics in the production of heavy quarks in deep-inelastic scattering: the next-to-leading order Monte-Carlo HVQDIS and the next-to-leading logarithmic resummation of soft gluon effects, including estimates of next-to-next-to-leading order corrections therefrom.
NTIS
Gluons; Inelastic Scattering; Monte Carlo Method; Quarks; Particle Production

20020001727 Argonne National Lab., IL USA
SLAB Symmetric Dielectric Micron Scale Structures for High Gradient Electron Acceleration
Rosenzweig, J. B.; Schoessow, P. V.; Jun. 12, 1999; 5p; In English
Report No.(s): DE2001-11852; ANL-HEP-CP-99-65; No Copyright; Avail: Department of Energy Information Bridge

A class of planar microstructure is proposed which provide high accelerating gradients when excited by an infrared laser pulse. These structures consist of parallel dielectric slabs separated by a vacuum gap; the dielectric or the outer surface coating are spatially modulated at the laser wavelength along the beam direction so as to support a standing wave accelerating field. We have developed numerical and analytic models of the accelerating mode fields in the structure. We show an optimized coupling scheme such that this mode is excited resonantly with a large quality factor. The status of planned experiments on fabricating and measuring these planar structures will be described.
NTIS
Dielectrics; Electron Acceleration; Mathematical Models; Microstructure

20020001833 Argonne National Lab., IL USA
Differences between heavy and light quarks
Maris, P.; Roberts, C. D.; Nov. 10, 1997; 6p; In English
Report No.(s): DE2001-8890; ANL/PHY/CP-94961; No Copyright; Avail: Department of Energy Information Bridge, Microfiche

The quark Dyson-Schwinger equation shows that there are distinct differences between light and heavy quarks. The dynamical mass function of the light quarks is characterized by a sharp increase below 1 GeV, whereas the mass function of the heavy quarks is approximately constant in this infrared region. As a consequence, the heavy meson masses increase linearly with the current quark masses, whereas the light pseudoscalar meson masses are proportional to the square root of the current quark masses.
NTIS
Quarks; Mesons

20020001834 Argonne National Lab., IL USA
Architecture of the APS real-time orbit feedback system
Carwardine, J. A.; Lenkszus, F. R.; Nov. 21, 1997; 6p; In English
Report No.(s): DE2001-8889; ANL/ASD/CP-94960; No Copyright; Avail: Department of Energy Information Bridge, Microfiche

The APS (Advanced Photon Source) Real-Time Orbit Feedback System is designed to stabilize the orbit of the stored positron beam against low-frequency sources such as mechanical vibration and power supply ripple. A distributed array of digital signal processors is used to measure the orbit and compute corrections at a 1kHz rate. The system also provides extensive beam diagnostic tools. This paper describes the architectural aspects of the system and describes how the orbit correction algorithms are implemented.
NTIS
Photons; Feedback; Positrons; Particle Beams

20020001836 Argonne National Lab., IL USA

Leptonic and semileptonic decays of heavy mesons

Ivanov, M. A.; Kalinovsky, Y. L.; Maris, P.; Roberts, C. D.; Nov. 18, 1997; 6p; In English

Report No.(s): DE2001-8883; ANL/PHY/CP-94878; No Copyright; Avail: Department of Energy Information Bridge, Microfiche

No abstract available.

NTIS

Mesons; Particle Decay

20020001838 Argonne National Lab., IL USA

Deuteron photodisintegration: new results from TJNAF

Abbott, D. J.; Ahmidouch, A.; Armstrong, C. S.; Arrington, J.; Cummings, W. J.; Nov. 18, 1997; 11p; In English

Report No.(s): DE2001-8880; ANL/PHY/CP-94845; No Copyright; Avail: Department of Energy Information Bridge, Microfiche

The first measurements of the differential cross section from d((gamma),p)n up to 4.0 GeV were performed at the Thomas Jefferson National Accelerator Facility (TJNAF, formerly CEBAF). Bremsstrahlung photons from electron beam impinging on a copper radiator and a liquid deuterium target were employed for this experiment. The experiment was performed in Hall C where the photoprotons at forward angles in the center-of-mass were detected in the High Momentum Spectrometer (HMS) and photoprotons at backward angles were detected in the Short Orbit Spectrometer (SOS). The bremsstrahlung photon energy was reconstructed from the measured proton momentum and angle using the two-body kinematics. We report the cross section results at the proton center-of-mass angles of 37(degree) and 90(degree). These results are in good agreement with previous lower energy measurements. The 90(degree) data continue to show the constituent-counting-rule behavior up to 4 GeV. The results will be compared with models based on QCD (Quantum Chromodynamics) as well as those based on meson-exchange theory.

NTIS

Deuterons; Bremsstrahlung; Photons; Linear Accelerators; Photonuclear Reactions

20020001967 Fermi National Accelerator Lab., Batavia, IL USA

Physical effects of infrared quark eigenmodes in LQCD

Eichten, E.; Thacker, H.; Duncan, A.; Oct. 07, 1999; 5p; In English

Report No.(s): DE2001-12563; FERMILAB-CONF-99/253-T; No Copyright; Avail: Department of Energy Information Bridge, Microfiche

A truncated determinant algorithm is used to study the physical effects of the quark eigenmodes associated with eigenvalues below 300 MeV. This initial study focuses on coarse lattices (with O(a(sup 2)) improved gauge action), light internal quark masses and large physical volumes. Four bellweather full QCD processes are discussed: topological charge distributions, the eta prime propagator, string breaking as observed in the static energy and the rho decay into two pions.

NTIS

Algorithms; Measuring Instruments; Determinants; Infrared Radiation; Strings; Pions

20020001971 Argonne National Lab., IL USA

Equation of motion of an electron: a debate in classical and quantum physics

Kim, K. J.; Jan. 27, 1999; 15p; In English

Report No.(s): DE2001-12371; ANL/ASD/CP-98283; No Copyright; Avail: Department of Energy Information Bridge, Microfiche

The current status of understanding of the equation of motion of an electron is summarized. Classically, a consistent, linearized theory exists for an electron of finite extent, as long as the size of the electron is larger than the classical electron radius. Nonrelativistic quantum mechanics seems to offer a tine theory even in the point-particle limit.

NTIS

Equations of Motion; Electrons

20020002225 Lawrence Livermore National Lab., Livermore, CA USA

Two wire wakefield measurements of the DARHT accelerator cell

Nelson, S. D.; Vella, M.; May 01, 1998; 7p; In English

Report No.(s): DE2001-12530; UCRL-ID-134164; Rept-39DP01000; No Copyright; Avail: Department of Energy Information Bridge

One of the characteristics specifying the performance of an accelerator cell as it relates to the electron beam, is the Wakefield impedance. The real part of the transverse wakefield impedance relates to offsets of the beam as it travels through the accelerator cell. to verify that the cell operates as expected, and that simulations and design predictions of the cell are within acceptable parameters (before building more cells) it is desirable to measure the wakefield impedance using the traditional two-wire technique. This technique benefits from its reproducibility and physical simplicity but is complicated by the need to fabricate a test fixture. But once the fixture is fabricated, it is simple to measure any number of accelerator cells. The following is a description of the two-wire measurement technique as performed at Lawrence Berkeley Lab (LBL) on a prototype DARHT accelerator cell.
NTIS
Design Analysis; Electron Beams; Impedance; Simulation

20020002226 Lawrence Livermore National Lab., Livermore, CA USA
Precision fast kickers for kiloampere electron beams
Caporaso, G. J.; Chen, Y. J.; Weir, J. T.; Oct. 06, 1999; 5p; In English
Report No.(s): DE2001-12529; UCRL-JC-131945; REPT-39DP01000; No Copyright; Avail: Department of Energy Information Bridge, Microfiche

These kickers will be used to make fast dipoles and quadrupoles which are driven by sharp risetime pulsers to provide precision beam manipulations for high current kA electron beams. This technology will be used on the 2nd axis of the DARHT linac at LANL. It will be used to provide 4 micropulses of pulse width 20 to 120 nsec. selected from a 2 (micro)sec., 2kA, 20MeV macropulse. The fast pulsers will have amplitude modulation capability to compensate for beam-induced steering effects and other slow beam centroid motion to within the bandwidth of the kicker system. Scaling laws derived from theory will be presented along with extensive experimental data obtained on the test bed ETA-II.
NTIS
Magnets; Electron Beams; Linear Accelerators; Magnetic Poles

20020002727 California Univ., Inst. for Theoretical Physics, Santa Barbara, CA USA
Institute for Theoretical Physics
Giddings, S. B.; Ooguri, H.; Peet, A. W.; Schwarz, J. H.; Jun. 01, 1998; 20p; In English
Report No.(s): DE2001-765571; No Copyright; Avail: Department of Energy Information Bridge, Microfiche

String theory is the only serious candidate for a unified description of all known fundamental particles and interactions, including gravity, in a single theoretical framework. Over the past two years, activity in this subject has grown rapidly, thanks to dramatic advances in understanding the dynamics of supersymmetric field theories and string theories. The cornerstone of these new developments is the discovery of duality which relates apparently different string theories and transforms difficult strongly coupled problems of one theory into weakly coupled problems of another theory.
NTIS
String Theory; Supersymmetry; Duality Theorem; Theoretical Physics

20020002728 Lawrence Livermore National Lab., Livermore, CA USA
Studies of Beam Dynamics in Relativistic Klystron Two-Beam Accelerators
Lidia, S. M.; Nov. 01, 1999; 229p; In English
Report No.(s): DE2001-765200; LBNL-45254; CBP-331; No Copyright; Avail: Department of Energy Information Bridge

Two-beam accelerators (TBAs) based upon free-electron lasers (FELs) or relativistic klystrons (RK-TBAs) have been proposed as efficient power sources for next generation high-energy linear colliders. Studies have demonstrated the possibility of building TBAs from X-band (approximately 8-12 GHz) through Ka band (approximately 30-35 GHz) frequency regions. Provided that further prototyping shows stable beam propagation with minimal current loss and production of good quality, high-power radio frequency (rf) fields, this technology is compatible with current schemes for electron-positron colliders in the multi-TeV center-of-mass scale. A new method of simulating the beam dynamics in accelerators of this type has been developed in this dissertation. There are three main components to this simulation. The first is a tracking algorithm to generate nonlinear transfer maps for pushing noninteracting particles through the external fields. The second component is a 3D Particle-In-Cell (PIC) algorithm that solves a set of Helmholtz equations for the self-fields, including the conducting boundary condition, and generates impulses that are interleaved with the nonlinear maps by means of a split-operation algorithm. The Helmholtz equations are solved by a multi-grid algorithm. The third component is an equivalent circuit equation solver that advances the modal rf cavity fields in time due to excitation by the modulated beam. The RTA project is described, and the simulation code is used to design the latter portions of the experiment. Detailed calculations of the beam dynamics and of the rf cavity output are presented and discussed. A beamline design is presented that will generate nearly 1.2 GW of power from 40 input, gain, and output rv cavities

over a 10 m distance. The simulations show that beam current losses are acceptable, and that longitudinal and transverse focusing techniques are sufficient capable of maintaining a high degree of beam quality along the entire beamline. Additional experimental efforts are also described.
NTIS
Algorithms; Cavities; Radio Frequencies; Linear Accelerators

20020002730 Argonne National Lab., IL USA
Utilization of CTR to Measure the Evolution of Electron-Beam Microbunching in a SASE FEL
Lumpkin, A. H.; Yang, B. X.; Berg, W. J.; Chae, Y. C.; Sereno, N. S.; Sep. 20, 2000; 24p; In English
Report No.(s): DE2001-764234; ANL/AOD/CP-101983; No Copyright; Avail: Department of Energy Information Bridge
The authors report the first measurements of the z-dependent evolution of electron-beam microbunching as revealed through coherent transition radiation (CTR) measurements in a visible self-amplified spontaneous emission (SASE) free-electron laser (FEL) experiment. The increase in microbunching was detected by tracking the growth of the visible CTR signals as generated from insertable metal mirrors/foils after each of the last three undulators. The same optical imaging diagnostics that were used to track the z-dependent intensity of the undulator radiation (UR) were also used to track the electron beam/CTR information. Angular distribution, beam size, and intensity data were obtained after each of the last three undulators in the five-undulator series, and spectral information was obtained after the last undulator. The exponential growth rate of the CTR was found to be very similar to that of the UR and consistent with simulations using the code GENESIS.
NTIS
Electron Beams; Free Electron Lasers; Electron Bunching; Coherent Radiation

20020002741 OMEGA-P, Inc., New Haven, CT USA
Microwave Inverse Cerenkov Accelerator
Hirshfield, J. L.; Jul. 01, 1999; 94p; In English
Report No.(s): DE2001-761738; DOE/ER/82047; No Copyright; Avail: Department of Energy Information Bridge, Microfiche
The objective of this Phase 2 SBIR research program was to complete the final design originated during Phase 1 for a prototype Microwave Inverse Cerenkov Accelerator (MICA), to fabricate the prototype MICA, and to test its performance as an electron accelerator. This report contains details of the design, predictions of accelerator performance, results of cold tests on the MICA structure, and details of the installation of MICA on the Yale Beam Physics Laboratory 6-MeV beamline. Discussion of future work is also included.
NTIS
Electron Accelerators; Prototypes

20020002746 Fermi National Accelerator Lab., Batavia, IL USA
Top quark physics at the Tevatron
Kim, S.; Oct. 07, 1999; 8p; In English
Report No.(s): DE2001-12559; FERMILAB-CONF-99/262-E; No Copyright; Avail: Department of Energy Information Bridge
The authors present the recent results and future prospects on top quark physics at the Tevatron. They describe the measurements of the top quark mass and the search for single top quark production in 1.8-TeV p(bar p) collisions. The CDF and D0 combined results yield a top quark mass of 174.3 (+/-) 5.1 GeV/c(sup 2). The upper limit at 95% C.L. of the single top production cross section is found to be 16.0 pb and 15.6 pb for the W-gluon fusion process and s-channel W* process, respectively.
NTIS
Particle Production; Collision Parameters; Particle Accelerators; Quarks

20020002748 Lawrence Livermore National Lab., Livermore, CA USA
Development of high-energy neutron imaging for use in NDE applications
Dietrich, F.; Hall, J.; Logan, C.; Schmid, G.; Jun. 01, 1999; 14p; In English
Report No.(s): DE2001-12557; UCRL-JC-134562; No Copyright; Avail: Department of Energy Information Bridge
We are currently developing a high-energy (10 - 15 MeV) neutron imaging system for use in NDE applications. Our goal is to develop an imaging system capable of detecting cubic-mm-scale voids or other structural defects in heavily-shielded low-Z materials within thick sealed objects. The system will be relatively compact (suitable for use in a small laboratory) and capable of acquiring tomographic image data sets. The design of a prototype imaging detector and multi-axis staging system will be discussed and selected results from recent imaging experiments will be presented. The development of an intense,

accelerator-driven neutron source suitable for use with the imaging system will also be discussed. Keywords: neutron imaging, neutron radiography, computed tomography, non-destructive inspection, neutron sources
NTIS
Imaging Techniques; Neutron Radiography; Nondestructive Tests; Computerized Simulation

20020002788 Argonne National Lab., IL USA
Problems at the Interface Between Heavy Flavor Physics, QCD and Hadron Spectroscopy
Lipkin, H. J.; Dec. 12, 1997; 6p; In English
Report No.(s): DE2001-8916; ANL-HEP-CP-97-91; No Copyright; Avail: Department of Energy Information Bridge, Microfiche

The following subjects are discussed in this report: (1) Pentaquark--why it is important and how new technologies (vertex detectors) suggest drastically different approaches form the search used by Ashery et al.; (2) problems in B decays with implications for heavy quark decays to excited light quark states like the Al; (3) problems in B and D decays to final states including eta and eta(prime) indicating that standard quark mixing might not hold; (4) possible contributions of hybrid quarkonium states to B decays; (5) heavy flavor decays to omega(tau) which disagree with conventional expectations; and (6) possible new spin effects in lambda(sub b) decay and the effect on the lifetime difference between the lambda(sub b) and B mesons.
NTIS
Hadrons; Particle Decay; Quantum Chromodynamics; Quarks

20020002789 Argonne National Lab., IL USA
Problems in Communication Between Heavy Flavor Experiment and Hadron Spectroscopy
Lipkin, H. J.; Dec. 12, 1997; 6p; In English
Report No.(s): DE2001-8915; ANL-HEP-CP-97-92; No Copyright; Avail: Department of Energy Information Bridge, Microfiche

The implications of hadron spectroscopy are generally overlooked both by experimenters presenting results and theorists making predictions. Two examples are: (1) possible effects of nodes in wave functions of final state mesons produced in beta decay; and (2) dependence of predictions for beta decays into final states containing eta or eta(prime) on models and mixing angles for these states.
NTIS
Beta Particles; Hadrons; Spectroscopy

20020003340 Los Alamos National Lab., NM USA
Improvement and renormalization constants in o(a) improved lattice qcd
Bhattacharya, T.; Dec. 01, 2000; 7p; In English
Report No.(s): DE2001-768855; LA-UR-00-5683; No Copyright; Avail: Department of Energy Information Bridge, Microfiche

We present results at (beta) = 6.0 and 6.2 for the O(a) improvement and renormalization constants for bilinear operators using axial and vector Ward identities. We discuss the extraction of the mass dependence of the renormalization constants and the coefficients of the equation of motion operators.
NTIS
Coefficients; Quantum Chromodynamics; Vectors (Mathematics); Renormalization Group Methods

20020003368 Argonne National Lab., IL USA
Experimental results on the design for the APS PID global orbit control system
Chung, Y.; Kirchman, J. A.; Dec. 05, 1997; 13p; In English
Report No.(s): DE2001-8895; ANL/ASD/CP-94983; No Copyright; Avail: Department of Energy Information Bridge, Microfiche

The Advanced Photon Source third generation synchrotrons light source needs a stabilized particle beam position to produce high brightness and low emittance radiation. Global orbit correction control is introduced and is utilized to satisfy the demanding needs of the accelerator. This paper presents the experimental results for determining an effective and optimal controller to meet the global orbit correction requirements. These requirements include frequency/time domain demands consisting of vibrational noise attenuation, limiting of controller gains for stability and improving the system time response. Experiments were conducted

with a digital signal processor implementing various PID sets to make comparisons between simulations and experiments. Measurements at these PID sets supported the results of software simulation.
NTIS
Computerized Simulation; Particle Beams; Photons; Synchrotrons; Controllers

20020003382 Argonne National Lab., IL USA
First results from the PHOBOS experiment at RHIC
Wuosmaa, A. H.; Back, B. B.; Baker, M. D.; Barton, D. S.; Basilev, S.; Oct. 02, 2000; 6p; In English
Report No.(s): DE2001-766298; ANL/PHY/CP-102364; No Copyright; Avail: Department of Energy Information Bridge, Microfiche

The PHOBOS experiment at RHIC has measured the charged-particle density dN/d(eta) at mid-rapidity for central Au+Au collisions at center of mass energies of (radical)s(sub NN) = 56, and 130 GeV. We deduce that dN/d(eta) = 408 (+/-) 12(stat) (+/-)30(syst) and 555 (+/-) 12(stat) (+/-) 35(syst) for collision energies of 56, and 130, GeV, respectively. These numbers suggest energy densities that are some 70% higher than have been achieved in any heavy-ion collisions previously studied, and also 25-40% higher than nucleon-nucleon collisions at comparable center of mass energies.
NTIS
Charged Particles; Ionic Collisions; Nucleon-Nucleon Interactions

20020003394 Los Alamos National Lab., NM USA
Transient quantum mechanical processes
Collins, L.; Kress, J.; Walker, R.; Jul. 01, 1999; 10p; In English
Report No.(s): DE2001-768235; LA-UR-99-2324; No Copyright; Avail: Department of Energy Information Bridge, Microfiche

Our principal objective has centered on the development of sophisticated computational techniques to solve the time-dependent Schroedinger equation that governs the evolution of quantum mechanical systems. We have perfected two complementary methods, discrete variable representation and real space product formula, that show great promise in solving these complicated temporal problems. We have applied these methods to the interaction of laser light with molecules with the intent of not only investigating the basic mechanisms but also devising schemes for actually controlling the outcome of microscopic processes. Lasers now exist that produce pulses of such short duration as to probe a molecular process many times within its characteristic period--allowing the actual observation of an evolving quantum mechanical system. We have studied the potassium dimer as an example and found agreement with experimental changes in the intermediate state populations as a function of laser frequency - a simple control prescription. We have also employed elaborate quantum chemistry programs to improve the accuracy of basic input such as bound-bound and bound-free coupling moments. These techniques have far-ranging applicability; for example, to trapped quantum systems at very low temperatures such as Bose-Einstein condensates.
NTIS
Schroedinger Equation; Quantum Mechanics

20020003398 Los Alamos National Lab., NM USA
Lessons from hadron phenomenology
Brisudova, M.; Buakovsky, L.; Goldman, T.; Aug. 01, 2000; 7p; In English
Report No.(s): DE2001-768249; LA-UR-00-3678; No Copyright; Avail: Department of Energy Information Bridge, Microfiche

Meson spectra can be well approximated by a specific form of a nonlinear Regge trajectory which is consistent with a finite number of bound states. This may have important consequences for experiment, and may be a hint for the theory.
NTIS
Hadrons; Mesons; Trajectories

20020003400 Lawrence Livermore National Lab., Livermore, CA USA
Whiteheadian process and quantum theory
Stapp, H.; Aug. 01, 1998; 16p; In English
Report No.(s): DE2001-6426; LBNL-42143; No Copyright; Avail: Department of Energy Information Bridge

There are deep similarities between Whitehead's idea of the process by which nature unfolds and the ideas of quantum theory. Whitehead says that the world is made of 'actual occasions' each of which arises from potentialities created by prior actual occasions. These actual occasions are happenings modeled on experiential events, each of which comes into being and then perishes, only to be replaced by a successor. It is these experience-like happenings that are the basic realities of nature, according to Whitehead, not the persisting physical particles that Newtonian physics to be the basic entities. Similarly, Heisenberg says that

what is really happening in a quantum process is the emergence of an actual from potentialities created by prior actualities. In the orthodox Copenhagen interpretation of quantum theory the actual things to which the theory refer are increments in 'our knowledge'. These increments are experiential events. The particles of classical physics lose their fundamental status: they dissolve into diffuse clouds of possibilities. At each stage of the unfolding of nature the complete cloud of possibilities acts like the potentiality for the occurrence of a next increment in knowledge, whose occurrence can radically change the cloud of possibilities/potentialities for the still-later increments in knowledge. The fundamental difference between these ideas about nature and the classical ideas that reigned from the time of Newton until this century concerns the status of the experiential aspects of nature. These are things such as thoughts, ideas, feelings, and sensations. They are distinguished from the physical aspects of nature, which are described in terms of quantities explicitly located in tiny regions of space and time. According to the ideas of classical physics the physical world is made up exclusively of things of this latter type, and the unfolding of the physical world is determined by causal connections involving only these things. Thus experiential-type things could be considered to influence the flow of physical events only insofar as they themselves were completely determined by physical things. In other words, experiential-type qualities, insofar as they could affect the flow of physical events, could--within the framework of classical physics--not be free: they must be completely determined by the physical aspects of nature that are, by themselves sufficient to determine the flow of physical events.
NTIS
Classical Mechanics; Quantum Theory

20020003560 Los Alamos National Lab., NM USA
Beam halo in proton linac beams
Wangler, T.; Crandall, K.; Aug. 01, 2000; 9p; In English
Report No.(s): DE2001-768783; LA-UR-00-3792; No Copyright; Avail: Department of Energy Information Bridge, Microfiche
In this paper we review the present picture of km halo in proton linacs. Space-charge forces acting in mismatched beams have been identified as a major cause of beam-halo. We present a definition of halo based on a ratio of moments of the distribution of the beam coordinates. We find from our initial studies that for halo detined in this way, a beam can have rms emittance growth without halo growth, but halo growth is always accompanied by rms emittance growth. We describe the beam-halo experiment that is in preparation at Los Alamos, which will address questions about the beam profiles, maximum particle amplitudes, and rms emittance growth associated with the halo.
NTIS
Emittance; Halos; Linear Accelerators; Proton Beams

20020003572 Argonne National Lab., IL USA
Drabkin energy filter for experiments at a spallation neutron source
Parizzi, A. A.; Felcher, G. P.; Klose, F.; Nov. 21, 2000; 12p; In English
Report No.(s): DE2001-768630; ANL/MSD/CP-103464; No Copyright; Avail: Department of Energy Information Bridge
We present a new approach for dynamic monochromatization of neutrons suitable for time-of-flight experiments at spallation neutron sources. The method requires polarized neutrons and is based on the Drabkin energy filter. In its initial application, this magnetic resonator device, consisting of a polarizer/analyzer system and a wavelength-dependent spin flipper, was proposed for extracting a narrow bandwidth from a broad bandwidth polarized neutron beam. At a spallation neutron source, wavelength is determined by time-of-flight (TOF) from the source to the detector. However, at each instant a spread of wavelengths is recorded due to the non-zero emission time of the source/moderator system. Particularly, high-intensity moderators for cold neutrons produce long 'tails' in the intensity/time distribution for all wavelengths, degrading the resolution of the experiments. The Drabkin energy filter can be used to cut the neutron tails for all wavelengths, by drifting the resonance condition in synchronization with the TOF. Calculations show that the method is viable, and that substantial resolution gains are obtained by application to a TOF neutron reflectometer.
NTIS
Neutron Sources; Spallation; Time of Flight Spectrometers

20020003800 Los Alamos National Lab., NM USA
Light quark masses: a status report at dpf 2000
Gupta, R.; Maltman, K.; Dec. 01, 2000; 12p; In English
Report No.(s): DE2001-768854; LA-UR-00-5684; No Copyright; Avail: Department of Energy Information Bridge, Microfiche

A summary of the extraction of light quark masses from both QCD sumrules and lattice QCD simulations is presented. The focus is on providing a careful statement of the potential weaknesses in each calculation, and on integrating the work of different collaborations to provide a coherent picture.
NTIS
Quantum Chromodynamics; Quarks; Computerized Simulation; Lattices (Mathematics)

20020003804 Los Alamos National Lab., NM USA
Large-Scale Simulation of Beam Dynamics in High Intensity Ion Linacs Using Parallel Supercomputers
Ryne, R.; Qiang, J.; Aug. 01, 2000; 6p; In English
Report No.(s): DE2001-768781; LA-UR-00-3971; No Copyright; Avail: Department of Energy Information Bridge, Microfiche
In this paper we present results of using parallel supercomputers to simulate beam dynamics in next-generation high intensity ion linacs. Our approach uses a three-dimensional space charge calculation with six types of boundary conditions. The simulations use a hybrid approach involving transfer maps to treat externally applied fields (including rf cavities) and parallel particle-in-cell techniques to treat the space-charge fields. The large-scale simulation results presented here represent a three order of magnitude improvement in simulation capability, in terms of problem size and speed of execution, compared with typical two-dimensional serial simulations. Specific examples will be presented, including simulation of the spallation neutron source (SNS) linac and the Low Energy Demonstrator Accelerator (LEDA) beam halo experiment.
NTIS
Linear Accelerators; Neutron Sources; Supercomputers; Two Dimensional Models; Parallel Computers; Computerized Simulation

20020003805 Los Alamos National Lab., NM USA
GaAs Detector for Dark Matter and Solar Neutrino Research
Bowles, T.; Aug. 01, 2000; 10p; In English
Report No.(s): DE2001-768779; LA-UR-00-3994; No Copyright; Avail: Department of Energy Information Bridge, Microfiche
The ability to produce large GaAs crystals with the requisite electronic properties to be fabricated into charged particle and photon detectors would provide a detector medium that would find numerous applications in both applied and fundamental research. Various applications would likely include x-ray detectors on satellites, environmental monitoring, medical imaging, bore hole mining spectroscopy, searches for dark matter, and solar neutrino research. We have carried out the development of GaAs detectors using two commercial crystal growing techniques. We have shown it should be able to grow detectors with 20 cm(sup 2) area and a depletion depth of 1 mm. Detectors of this size would find immediate applications in high-resolution, room temperature, low energy gamma ray measurements. We have also arrived at an understanding of the limitations of the common techniques used to grow GaAs and have determined that it should be possible to produce larger detectors using proprietary methods.
NTIS
Dark Matter; Gallium Arsenides; Photons; X Ray Detectors; Fabrication; Solar Neutrinos

20020003809 Los Alamos National Lab., NM USA
LEDA: A High-Power Test Bed of Innovation and Opportunity
Schneider, J.; Sheffield, R.; Aug. 01, 2000; 6p; In English
Report No.(s): DE2001-768769; LA-UR-00-3820; No Copyright; Avail: Department of Energy Information Bridge, Microfiche
The low-energy demonstration accelerator (LEDA) is an operational 6.7-MeV. 100-mA proton accelerator consisting of an injector, radio-frequency quadrupole (RFQ), and all associated integration equipment. In order to achieve this unprecedented level of performance (670-kW of beam power) from an RFQ, a number of design innovations were required. They will highlight a number of those more significant technical advances, including those in the proton injector, the RFQ configuration, the RF klystrons, the beam stop, and the challenges of beam measurements. In addition to identifying the importance of these innovations to LEDA performance, they will summarize the plans for further testing, and the possibilities for addition of more accelerating structures, including the planned use of very-low-beta super-conducting structures. LEDA's current and upgradable configuration is appropriate for several future high-power accelerators, including those for the transmutation of radioactive waste.
NTIS
Accelerators; Klystrons; Proton Beams; Radioactive Wastes

20020003817 Argonne National Lab., IL USA

Two-colour QCD at finite fundamental quark-number density and related theories

Hands, S. J.; Kogut, J. B.; Morrison, S. E.; Sinclair, D. K.; Nov. 15, 2000; 6p; In English

Report No.(s): DE2001-768625; ANL-HEP-CP-00-110; No Copyright; Avail: Department of Energy Information Bridge

We are simulating SU(2) Yang-Mills theory with four flavors of dynamical quarks in the fundamental representation of SU(2) color at finite chemical potential, p for quark number, as a model for QCD (quantum chromodynamics) at finite baryon number density. In particular we observe that for p large enough this theory undergoes a phase transition to a state with a diquark condensate which breaks quark-number symmetry. In this phase we examine the spectrum of light scalar and pseudoscalar bosons and see evidence for the Goldstone boson associated with this spontaneous symmetry breaking. This theory is closely related to QCD at finite chemical potential for isospin, a theory which we are now studying for SU(3) color.

NTIS

Quantum Chromodynamics; Quarks; Yang-Mills Theory; Flavor (Particle Physics)

20020003820 Argonne National Lab., IL USA

Fully differential QCD corrections to single top quark final states

Harris, B. W.; Laenen, E.; Phaf, L.; Sullivan, Z.; Weinzierl, S.; Nov. 14, 2000; 5p; In English

Report No.(s): DE2001-768618; ANL-HEP-CP-00-094; No Copyright; Avail: Department of Energy Information Bridge

The authors have performed a fully differential calculation of QCD (quantum chromodynamics) corrections to electroweak production of single top quarks. The method used allows for jet definitions and experimental cuts. The corresponding computer code passes the necessary check of reproducing the previously known total rate. First examination of the rapidity and transverse momentum of the top quark shows the corrections to be flat relative to leading order. Additional phenomenological studies are in order. Further work is in progress on the corrections to t-b-jet final states which will give a comprehensive set of tools for studying single-top-quark production at future hadron-hadron colliders.

NTIS

Quantum Chromodynamics; Quarks

20020003830 Los Alamos National Lab., NM USA

Design of the sns normal conducting linac rf control system

Regan, A.; Aug. 01, 2000; 6p; In English

Report No.(s): DE2001-768259; LA-UR-00-3728; No Copyright; Avail: Department of Energy Information Bridge, Microfiche

The Spallation Neutron Source (SNS) is in the process of being, designed for operation in 2004. The SNS is a 1 GeV machine consisting of both a normal-conducting and super-conducting linac as well as a ring and target area The linac front end is a 402.5 MHz RFQ being developed by Lawrence Berkeley Lab. The DTL, being developed at Los Alamos National Laboratory, is also a copper structure operating at 402.5 MHz, with an 805 MHz CCL structure downstream of it. The expected output energy of the DTL is 87 MeV and that of the CCL is 185 MeV. The RF control system under development for the linac is based on the Low Energy Demonstration Accelerator's (LEDA) control system with some new features. This paper will discuss the new design approach and its benefits. Block diagrams and circuit specifics will be addressed. The normal conducting RF control system will be described in detail with reference to the super-conducting control system when appropriate.

NTIS

Linear Accelerators; Neutron Sources; Spallation

20020003937 Argonne National Lab., IL USA

APS intranet as a man-machine interface

Ciarlette, D.; Gerig, R.; McDowell, W.; Dec. 02, 1997; 6p; In English

Report No.(s): DE2001-8892; ANL/ASD/CP-94972; No Copyright; Avail: Department of Energy Information Bridge, Microfiche

The Advanced Photon Source at Argonne National Laboratory has implemented a number of methods for people to interact with the accelerator systems. The accelerator operators use Sun workstations running MEDM and WCL to interface interactively with the accelerator, however, many people need to view information rather than interact with the machine. One of the most common interfaces for viewing information at the Advanced Photon Source is the World Wide Web. Information such as operations logbook entries, machine status updates, and displays of archived and current data are easily available to APS personnel. This interface between people and the accelerator has proven to be quite useful. Because the Intranet is

operating-system independent and inherently unidirectional, ensuring the prevention of unauthorized or accidental control of the accelerators is straightforward.
NTIS
Photons; Internets; Computer Networks; Human-Computer Interface

20020004672 Los Alamos National Lab., NM USA
Pseudospin Symmetry in Nuclei, Spin Symmetry in Hadrons
Page, P.; Goldman, T.; Ginocchio, J.; Aug. 01, 2000; 6p; In English
Report No.(s): DE2001-768725; LA-UR-00-3914; No Copyright; Avail: Department of Energy Information Bridge

Ginocchio argued that chiral symmetry breaking in quantum chromodynamics (QCD) is responsible for the relativistic pseudospin symmetry in the Dirac equation, explaining the observed approximate pseudospin symmetry in sizable nuclei. On a much smaller scale, it is known that spin-orbit splittings in hadrons are small. Specifically, new experimental data from CLEO indicate small splittings in D-mesons. For heavy-light mesons we identify a cousin of pseudospin symmetry that suppresses these splittings in the Dirac equation, known as spin symmetry. We suggest an experimental test of the implications of spin symmetry for wave functions in electron-positron annihilation. We investigate how QCD can give rise to two different dynamical symmetries on nuclear and hadronic scales.
NTIS
Dirac Equation; Hadrons; Quantum Chromodynamics; Symmetry; Chirality

20020004912 Argonne National Lab., IL USA
Electroproduction of Kaons on light nuclei
Zeidman, B.; Abbott, D.; Ahmidouch, A.; Ambrozewicz, P.; Armstrong, C. S.; Dec. 07, 2000; 8p; In English
Report No.(s): DE2001-772127; ANL/PHY/CP-103614; No Copyright; Avail: Department of Energy Information Bridge, Microfiche

The A(e,e(prime)K(sup +))YX reaction on H, D, (sup 3)He, and (sup 4)He was investigated in Hall C at CEBAF. Data were obtained for Q(sup 2) (approx) 0.35 and 0.5 GeV(sup 2) at 3.245 GeV. The missing mass spectra for both H and D are fitted with Monte-Carlo simulations incorporating peaks corresponding to (Lambda) production on the proton and (Sigma) production on both the proton and neutron. For D, the cross section ratio (Sigma)(sup 0)/(Sigma)(sup (minus)) (approx) 2, and excess yield close to the thresholds for (Lambda) and (Sigma) production can be attributed to final-state interactions that are compared to the data. The analysis of the data for the He targets is in a more preliminary state with broader quasi-free peaks resulting from the higher Fermi momenta. Evidence for bound (Lambda)-hypernuclear states is seen and other structure may be present.
NTIS
Kaons; Linear Accelerators; Mass Spectra; Monte Carlo Method; Targets

20020005140 Los Alamos National Lab., NM USA
Field Symmetrization Selection Rules
Page, P.; Aug. 01, 2000; 13p; In English
Report No.(s): DE2001-768726; LA-UR-00-3915; No Copyright; Avail: Department of Energy Information Bridge

Quantum chromodynamics (QCD) and quantum electrodynamics (QED) exhibit an infinite set of three-point Green's functions that contain only OZI rule violating contributions, and (for QCD) are subleading in the large N(sub c) expansion. We prove that the QCD amplitude for a neutral hybrid (l brace)1,3,5.(r brace)(+-) exotic current to create eta(pi)(sup 0) only comes from OZI rule violating contributions under certain conditions, and is subleading in N(sub c).
NTIS
Quantum Chromodynamics; Quantum Electrodynamics

20020005253 Brookhaven National Lab., Upton, NY USA
QCD Phase Transitions, Volume 15
Schaefer, T.; Shuryak, E.; Mar. 20, 1999; 238p; In English
Report No.(s): DE2001-8960; BNL-52561; KB0201; No Copyright; Avail: Department of Energy Information Bridge, Microfiche

The title of the workshop, 'The QCD Phase Transitions' in fact happened to be too narrow for its real contents. It would be more accurate to say that it was devoted to different phases of quantum chromodynamics (QCD) and QCD-related gauge theories, with strong emphasis on discussion of the underlying non-perturbative mechanisms which manifest themselves as all those phases. Before we go to specifics, let us emphasize one important aspect of the present status of non-perturbative Quantum Field

Theory in general. It remains true that its studies do not get attention proportional to the intellectual challenge they deserve, and that the theorists working on it remain very fragmented. The efforts to create Theory of Everything including Quantum Gravity have attracted the lion's share of attention and young talent. Nevertheless, in the last few years there was also a tremendous progress and even some shift of attention toward emphasis on the unity of non-perturbative phenomena. For example, we have seen some efforts to connect the lessons from recent progress in supersymmetric theories with that in QCD, as derived from phenomenology and lattice. Another example is Maldacena conjecture and related development, which connect three things together, string theory, super-gravity and the (N=4) supersymmetric gauge theory. Although the progress mentioned is remarkable by itself, if we would listen to each other more we may have chance to strengthen the field and reach better understanding of the spectacular non-perturbative physics.
NTIS
Gauge Theory; Phase Transformations; Quantum Chromodynamics; Quantum Theory

20020005270 Argonne National Lab., IL USA
Design of a TOF-SANS Instrument for the Proposed Long Wavelength Target Station at the Spallation Neutron Source
Thiyagarajan, P.; Littrell, K.; Seeger, P. A.; Nov. 28, 2000; 14p; In English
Report No.(s): DE2001-768633; ANL/IPNS/CP-103505; No Copyright; Avail: Department of Energy Information Bridge

We have designed a versatile high-throughput SANS instrument (Broad Range Intense Multipurpose SANS (BRIMS)) for the proposed Long Wavelength Target Station at the SNS by using acceptance diagrams and the Los Alamos NISP Monte Carlo simulation package. This instrument has been fully optimized to take advantage of the 10 Hz source frequency (broad wavelength bandwidth) and the cold neutron spectrum from a tall coupled solid methane moderator (12 cm x 20 cm). BRIMS has been designed to produce data in a Q range spanning from 0.001 to 0.7/angstrom in a single measurement by simultaneously using neutrons with wavelengths ranging from 1 to 14.5 angstroms in a time of flight mode. A supermirror guide and bender assembly is employed to separate and redirect the useful portion of the neutron spectrum with lambda greater than 1 angstrom, by 2.3 deg away from the direct beam containing high energy neutrons and gamma rays. The effects of the supermirror coating of the guide, the location of the bender assembly with respect to the source, the bend angle, and various collimation choices on the flux, resolution and Q(sub min) have been characterized using spherical particle and delta function scatterers. The overall performance of BRIMS has been compared with that of the best existing reactor-based SANS instrument D22 at ILL.
NTIS
Monte Carlo Method; Neutron Sources; Design Analysis

81
ADMINISTRATION AND MANAGEMENT

Includes management planning and research.

20020000777 NASA, Washington, DC USA
ASK Magazine, Volume 4
Laufer, Alexander, Editor, Maryland Univ., USA; Collins, Michelle, Editor, NASA, USA; Post, Todd, Editor, EduTech Ltd., USA; July 2001; 45p; In English; Original contains color illustrations
Report No.(s): NASA/NP-2001-10-271-HQ; NAS 1.83:10-271-HQ; No Copyright; Avail: CASI; A03, Hardcopy; A01, Microfiche

Not everyone looks forward to reviews. Dog and pony shows I've heard them called. Exercises in putting together Power Point charts. Other less tasteful descriptions abound, but I won't bother to summarize these. This is a tasteful magazine after all. In this issue, we've assembled a number of articles on the subject of reviews, particularly as they occur in the NASA project world (although we cover the subject from other perspectives too). Veteran NASA Project Manager Marty Davis, in his article Tangled Up in Reviews, writes, "Many people regard reviews as something onerous, but if we can tailor them so that they're not as bad as they have to be, it can be a great benefit to a project manager." Great benefits to the project manager is what you'll find in Marty's story as he describes not only tailoring a single review but the entire lifecycle of reviews in his project. In Jo Gunderson's story, Calling Down the Fire on Yourself, she describes a young NASA Project Manager who does just that because, as he tells her, I needed to know if there was anything that I had overlooked." How he brings fire down on himself at his project review will inspire other young Project Managers, seasoned managers, and anyone else who reads this powerful story. Leave Your Ego at the Door, by Jenny Baer-Reidhart and Ray Morgan, uses reviews to highlight the creative collaboration that existed between NASA and one of its industry partners. The protagonist of this story is a company who took advantage of NASAs expert advice during reviews and accomplished amazing feats as a result. The story also examines how disasters might well have been avoided by two other

NASA partners had they been as open-minded as the first company during their reviews. In Roy Malone's story, Standing Offer, a NASA Project Manager describes how he used a crack review team to help him pass a critical certification inspection while he was a Combat Systems Officer in the Navy. Malone invited the reviewers to come back several times so that they would be able to focus in detail on the many areas of the program that would be scrutinized during the certification inspection. These are just a sampling of some of the articles you'll find in this issue of ASK. We believe this issue offers ample evidence that talented Project Managers know how to use reviews to the great benefit of their projects. A talented Project Manager will typically figure out a way to turn any onerous task into a useful learning exercise. These Project Managers demonstrate that the real value of reviews is that they provide a chance to learn something. No dog and pony shows here.
Author
Project Management; Decision Making

20020001027 Princeton Univ., Plasma Physics Lab., NJ USA
Audits that Make a Difference
Malsbury, J.; Feb. 01, 1999; 10p; In English
Report No.(s): DE2001-3445; CFPAPER-3970; DE-AC02-CHO-3073; No Copyright; Avail: Department of Energy Information Bridge

This paper presents guidance on how to perform internal audits that get management's attention and result in effective corrective action. It assumes that the reader is already familiar with the basic constructs of auditing and knows how to perform them. Instead, it focuses on additional techniques that have proven to be effective in our internal auditing program. Examples using a theoretical audit of a calibration program are included.
NTIS
Management; Management Planning; Management Methods; Operations Research

20020001028 DYNACS Engineering Co., Inc., Cocoa Beach, FL USA
Demonstrating and Evaluating an Action Learning Approach to Building Project Management Competence
Kotnour, Tim, University of Central Florida, USA; Starr, Stan, DYNACS Engineering Co., Inc., USA; [2001]; 5p; In English; ASEM Conference 2001, 11-13 Oct. 2001, Huntsville, AL, USA
Contract(s)/Grant(s): NAS10-98001; No Copyright; Avail: CASI; A01, Hardcopy; A01, Microfiche

This paper contributes a description of an action-learning approach to building project management competence. This approach was designed, implemented, and evaluated for use with the Dynacs Engineering Development Contract at the Kennedy Space Center. The aim of the approach was to improve three levels of competence within the organization: individual project management skills, project team performance. and organizational capabilities such as the project management process and tools. The overall steps to the approach, evaluation results, and lessons learned are presented. Managers can use this paper to design a specific action-learning approach for their organization.
Author
Project Management; Learning

20020001246 Bareiss Associates, New Port Richey, FL USA
Technology transfer for newly developed sensors *Final Report*
Bareiss, R. A.; Mar. 01, 1998; 59p; In English
Report No.(s): DE2001-763052; DOE/GO/10562-F; No Copyright; Avail: Department of Energy Information Bridge, Microfiche

The objective of this contract is to obtain better utilization for the pulp and paper industry. It was thought that a barrier to utilization of these technologies was the unfamiliarity with the industry on the part of the technology developers, and that this barrier might be lowered through the participation of someone intimately familiar with the industry who could arrange contacts and appropriate trials for selected technologies. The project design consisted of six tasks as described in Appendix D of the contract. Later in the contract period as the AGENDA 2020 compact between the DOE and the paper industry came into being other tasks were added to the contract. These included: (1) defining the industry's priority needs for sensors and controls; (2) providing consultation to the DOE labs as they began to work on selected projects; (3) arranging presentations at paper industry technical conferences of key technologies in sensors and controls developed under the Agenda 2020 program. A final task was added to prepare an overview of the Forest Products industry needs in sensors and controls for a meeting at the National Academy of Sciences sponsored by the DOE. At this meeting the Industries of the Future presented their needs with a view towards determining if there might be any commonality of needs that could be met by focused research.
NTIS
Sensors; Technology Transfer; Papers; Industries

20020001514 California Univ., Lawrence Berkeley Lab., Berkeley, CA USA

Laboratory Directed Research and Development Program FY98

Hansen, T.; Chartock, M.; Feb. 05, 1999; 152p; In English

Report No.(s): DE2001-8699; PUB-5444; No Copyright; Avail: Department of Energy Information Bridge, Microfiche

The Ernest Orlando Lawrence Berkeley National Laboratory (LBNL or Berkeley Lab) Laboratory Directed Research and Development Program FY 1998 report is compiled from annual reports submitted by principal investigators following the close of the fiscal year. This report describes the supported projects and summarizes their accomplishments. It constitutes a part of the Laboratory Directed Research and Development (LDRD) program planning and documentation process that includes an annual planning cycle, projection selection, implementation, and review. The LBNL LDRD program is a critical tool for directing the Laboratory's forefront scientific research capabilities toward vital, excellent, and emerging scientific challenges. The program provides the resources for LBNL scientists to make rapid and significant contributions to critical national science and technology problems. The LDRD program also advances LBNL's core competencies, foundations, and scientific capability, and permits exploration of exciting new opportunities. All projects are work in forefront areas of science and technology. Areas eligible for support include the following: Advanced study of hypotheses, concepts, or innovative approaches to scientific or technical problems; Experiments and analyses directed toward 'proof of principle' or early determination of the utility of new scientific ideas, technical concepts, or devices; and Conception and preliminary technical analyses of experimental facilities or devices.

NTIS

Project Planning; Research and Development; Documents

20020002243 Hampton Univ., VA USA

Hampton University Undergraduate Computational Science Education Program ***Final Report***

Socolovsky, E. A.; Sep. 01, 1999; 12p; In English

Report No.(s): DE2001-765664; No Copyright; Avail: Department of Energy Information Bridge, Microfiche

The achievements in the two and a half years of this project completely satisfy and exceed the goals and objectives established in the original proposal. The educational tasks have been performed, and its objectives have been satisfied and surpassed. Furthermore, with an efficient allocation of the funding provided by the Grant supplemented by additional University funds, we have established a sustainable infrastructure that provides access to the prevalent paradigms of high performance computation, and is the foundation for future access to distributed parallel computation. This access is extended beyond Hampton University through cooperation and support to regional institutions, in particular to researchers from DOE's Jefferson Lab in Newport News, Virginia.

NTIS

Computation; Education

20020002257 General Accounting Office, Washington, DC USA

Financial Management: FFMIS Implementation Critical for Federal Accountability

Oct. 2001; 80p; In English

Report No.(s): PB2002-100187; GAO/02-29; No Copyright; Avail: CASI; A05, Hardcopy; A01, Microfiche

The inability to produce the data needed to efficiently and effectively manage the day-to-day operations of the federal government and provide accountability to taxpayers and the Congress has been a long-standing weakness at most federal agencies. The central challenge to producing reliable, useful, and timely data throughout the year and at year-end is overhauling financial and related management information systems. One of the key legislative underpinnings for addressing this issue is the Chief Financial Officers (CFO) Act of 1990. The CFO Act calls for the modernization of financial management systems, including the systematic measurement of performance, the development of cost information, and the integration of program, budget, and financial information. The Federal Financial Management Improvement Act of 1996 builds on the CFO Act by emphasizing the need for agencies to have systems that can generate timely, accurate, and useful information which to make informed decisions and the ensure accountability on an ongoing basis. FFMIA requires the 24 major departments and agencies covered by the CFO Act to implement and maintain financial management system the comply substantially with federal financial management systems requirements, applicable federal accounting standards, and the 'U.S. Standard General Ledger' at the transaction level. FFMIA also requires auditors to report in their CFO Act financial statement audit reports whether the agencies' financial management systems comply with FFMIA's requirements. We are required to report annually on the implementation of the act. This, our fifth annual report, discusses the FFMIA determinations, our assessment of the auditors' bases for the determinations, and agencies' plans to bring their systems into compliance.

NTIS

Financial Management; Standards; Costs

20020002260 General Accounting Office, Washington, DC USA

Department of Agriculture: Status of Achieving Key Outcomes and Addressing Major Management Challenges

Aug. 2001; 42p; In English

Report No.(s): PB2002-100169; GAO/01-761; No Copyright; Avail: CASI; A03, Hardcopy; A01, Microfiche

This report reviewed the U. S. Department of Agriculture's (USDA) fiscal year 2000 performance report and fiscal year 2002 performance plan required by the Government Performance and Results Act of 1993 (GPRA) to assess the agency's progress in achieving selected key outcomes that you identified as important mission areas for the agency. USDA presented one performance report with agency-by-agency coverage and 1 departmental and 24 agency and office performance plans. We reviewed the same outcomes we addressed in our June 2000 review of the agency's fiscal year 1999 performance report and fiscal year 2001 performance plans to provide a baseline by which to measure the agencys performance from year-to-year. These selected key outcomes are ensuring an adequate and reasonably priced food supply; opening, expanding, and maintaining global market opportunities for agricultural producers; reducing hunger and ensuring food for the hungry; ensuring a safe and wholesome food supply; and reducing food stamp fraud and error.

NTIS

Reviewing; Errors; Progress

20020002689 Hawaii Univ., Honolulu, HI USA

Determination of Interrelationships between Organizational System Variables during Implementation of Change. Measurement of Motivation Factors among Technical Groups at HDOT, Oahu District, Using Maslow's Needs Hierarchy Theory. Report 8 of 17

Shoura, M. M.; Singh, A.; Jan. 1998; 52p; In English

Report No.(s): PB2002-100365; No Copyright; Avail: CASI; A04, Hardcopy; A01, Microfiche

This report emphasizes total self-development of the individual for improved motivation and organization management. It develops on Maslow's Hierarchy of Needs Theory to examine motivational levels for four levels of engineering staff at a public construction agency. The researchers studied these engineering groups qualitatively through interviews and quantitatively using a questionnaire. Using a holistic approach, this study focused on 15 parameters from Maslow's five basic need levels - physical, safety, social, esteem, and self-actualization. A considerable emphasis was placed on the development of Maslow's principles of self-actualization. According to Maslow, this difficult to grasp concept is as pre-requisite for enlightened management. The researchers analyzed engineers' perception regarding: (1) fulfillment of need parameters, and (2) measured the perception of the importance of those parameters. Among specific findings were that junior project engineers had higher scores on self-actualization than senior engineers. Improvements were desirable in the areas of meaningfulness of tasks, self-sufficiency in doing the job, and individuality and sense of mission. The application of Maslow's theory directly benefits the agency and other organizations in developing programs.

NTIS

Motivation; Organizations; Engineers

20020002690 Hawaii Univ., Honolulu, HI USA

Determination of Interrelationships between Organizational System Variables during Implementation of Change. Findings on Motivation among Technical Groups at HDOT, Oahu District: A Study in the Application of Herzberg's Motivation Theory. Report 7

Shoura, M. M.; Singh, A.; Aug. 1997; 54p; In English

Report No.(s): PB2002-100364; No Copyright; Avail: CASI; A04, Hardcopy; A01, Microfiche

This paper examines motivational measures of engineers at HDOT applying Herzberg's two-factor model of motivators and hygiene factors. The study measures the perception of individuals regarding satisfaction and dissatisfaction from various motivational elements; obtains an evaluation of the relative importance of these elements, and then combines these two measures to produce an indicator called development index for each motivational element. It was discovered from this study that, at HDOT, the relative importance of elements and the satisfaction experience are vastly different from Herzberg's study 40 years ago. The category of salary exhibited the greatest change in relative importance. The organization studied is analyzed for the motivation prevalent; the development index indicates that there are some serious issues that need to be confronted by the organization's leadership for job enrichment.

NTIS

Engineers; Motivation; Enrichment; Leadership

20020002691 Hawaii Univ., Honolulu, HI USA

Determination of Interrelationships between Organizational System Variables during Implementation of Change. Personality Assessment. Report 5 of 17

Johnson, H. M.; Singh, S.; Jul. 1997; 40p; In English

Report No.(s): PB2002-100362; No Copyright; Avail: CASI; A03, Hardcopy; A01, Microfiche

A short form of the MBTI questionnaire, developed by the researchers, was administered to HDOT design and construction engineers. The purpose was to determine whether personality differences exist between the two branches. Four personality preferences were measured-interaction preference, information gathering preference, decision making preference, and structure preference. Design and construction engineers were found to share many similar traits, but significant differences were also found. Design and construction engineers were found to be predominantly introverted, and prefer to use their sense faculties for gathering data, in contrast to using intuition. When making decisions, they prefer to forgo pure logic, relying instead on personal and organizational values. They show their maximum differences in their preference for decision making. Designers prefer to choose value-oriented responses more frequently than construction engineers do.

NTIS

Engineers; Decision Making

20020002692 Hawaii Univ., Honolulu, HI USA

Determination of Interrelationships between Organizational System Variables during Implementation of Change. Findings on Intuition and Concern for People among Engineers at OAHU District, HDOT. Report 4 of 17

Singh, A.; Jun. 1997; 40p; In English

Report No.(s): PB2002-100361; No Copyright; Avail: CASI; A03, Hardcopy; A01, Microfiche

This study seeks to determine how much intuition affects the decision making of construction engineer-managers, especially because decision making is fundamental to the organizational health and culture. It is also sought to determine how much concern for people the construction engineers have. The data received came from responses to a two-part questionnaire. It was found that a majority of engineers believe in the applicability of intuition. They also care deeply for self-esteem and respect. Intuition was related to the vision that managers may develop for their organization. Managers were categorized in five zones. There was reasonable balance found between intuitive capability and concern for people. The construction engineers feel a sense of loyalty to HDOT, so it is worth the effort to expend resource in human development and personal affairs to ensure that the engineers enjoy their work. The well-being of engineers should be given greater emphasis.

NTIS

Decision Making; Health

20020002693 Hawaii Univ., Honolulu, HI USA

Determination of Interrelationships between Organizational System Variables during Implementation of Change. Analysis of General Management Questionnaire at Oahu District, HDOT. Report 3 or 17

Singh, A.; May 18, 1997; 60p; In English

Report No.(s): PB2002-100360; No Copyright; Avail: CASI; A04, Hardcopy; A01, Microfiche

A questionnaire was circulated among all Oahu District engineers, with an aim at finding general behavior and management scores on parameters such as self-esteem, happiness and contentment, and management caliber. Some of the specific parameters studied were confidence, professionalism, satisfaction, cooperation, contractor skills, quality and talent. Among the conclusions, it was discovered that design-construction integration is a serious problem; there is dissatisfaction with salaries; there is interest in change; there is dissatisfaction with supervisors. The work at Oahu District was understood to be 'engineering management' in contrast to straight engineering; PE's display considerable confidence in themselves compared to RE/AE's; there is a perceived lack of engineering management talent at HDOT. Among the recommendations for intervention, a few techniques for improving design-construction integration and communication fare provided; personal and organizational grievances need to be addressed much more effectively; greater attention should be given to the authority of RE's/AE's in decision making and conflict handling.

NTIS

Behavior; Construction; Decision Making; Engineering Management

20020002694 Hawaii Univ., Honolulu, HI USA

Determination of Interrelationships between Organizational System Variables during Implementation of Change. Teamwork and Leadership Analysis among Engineers of Oahu District, HDOT. Report 2 of 17

Singh, A.; Mar. 18, 1997; 51p; In English

Report No.(s): PB2002-100359; No Copyright; Avail: CASI; A04, Hardcopy; A01, Microfiche

A questionnaire was distributed among engineers of Oahu District to evaluate teamwork and leadership skills. The model evaluates two basic parameters-the decision taking capability (D-scale) and information input by group during decision making (I-scale). These two scales are plotted on X and Y-axes respectively. Five types of leaders are evaluated-consultative autocrats, complete autocrats, consensus managers, impoverished managers (or shareholders), and active managers. The results showed overwhelmingly that 70% of RE's/AE's and 50% of PE's can be categorized as falling in the impoverished manager's zone. These percentage figures might be reduced slightly if certain gray areas are granted to the zones. However, any such impact is not significant. Demographic evaluations are made for age, years of experience, years of design experience, years with HDOT and Oahu District, religious mindedness, ethnic origin, religion, marital status, and family encouragement. The analysis for each is provided in detail in the text and illustrated in visual graphs of D-I plots. Among the recommendations are to provide intensive training, a nurturing and coaching environment, improve the quality of the work premises, provide significant work recognition awards, increase authority delegation, and reorganize.
NTIS
Leadership; Decision Making; Education

20020002695 Hawaii Univ., Honolulu, HI USA
Determination of Interrelationships between Organizational System Variables during Implementation of Change. Preliminary Findings of Qualitative Research for Construction Management Practice Undertaken at HDOT, Oahu District. Report 1 of 17
Singh, A.; Mar. 18, 1997; 46p; In English
Report No.(s): PB2002-100358; No Copyright; Avail: CASI; A03, Hardcopy; A01, Microfiche

Qualitative studies were undertaken by having group discussions and one-on-one interview sessions with all engineers working for the Oahu District. Among the positive finding are that there is adequate team work, engineers are motivated by the nature of work and challenges posed, engineers wish to enhance their knowledge, and job responsibilities were clear. Among the negative findings are that the change order procedure is unduly cumbersome, design-construction coordination and integration is inadequate, and engineers have insufficient knowledge and training in their construction management vocation. Oahu District engineers perceive a complete lack of trust, faith, or support from upper management. There is a lack of formal motivation by HDOT; organization structure is inadequate to respond to tasks; some field offices have serious management and morale problems; and janitorial work is disliked. Whereas the recent induction of computers is a positive change, quite a few engineers were not sure how to use them. Resident engineers reported difficulties with CE III's and inspectors alike. Inspectors reported inexperience and the unwillingness of engineers to do field work as a reason for poor engineering caliber.
NTIS
Morale; Motivation; Coordination

20020002755 General Accounting Office, Washington, DC USA
National Laboratories: Better Performance Reporting Could Aid Oversight of Laboratory-Directed R&D Program
Sep. 2001; 26p
Report No.(s): PB2002-100601; GAO-01-927; No Copyright; Avail: CASI; A03, Hardcopy; A01, Microfiche

In fiscal year 1992, the Department of Energy (DOE) created the Laboratory Directed Research and Development (LDRD) program, which formalized a long-standing policy of allowing its multi-program national laboratories discretion to conduct self-initiated, independent research and development (R&D). DOE requires that LDRD work must focus on the advanced study of scientific or technical problems, experiments directed toward proving a scientific principle, or early analysis of experimental facilities or devices. Concerned that some laboratories may have been funding LDRD projects that did not meet DOE's guidelines, you asked us to determine how much DOE's multi-program national laboratories have spent on LDRD projects since fiscal year 1992 (when the LDRD program was created), evaluate whether LDRD projects meet DOE's selection guidelines, and provide observations on how the program might be improved. to address these objectives, we reviewed program-related information and annual reports, budgets, and procedures for selecting LDRD projects at all nine of DOE's multi-program national laboratories. At five of those laboratories, representing 83 percent of all LDRD funding, we examined the selection and review processes that each used to select LDRD projects to determine if internal controls were in place that would reasonably ensure compliance with DOE's LDRD project-selection guidelines. In addition, we examined oversight practices used by DOE's headquarters and field offices for the LDRD program. We also randomly selected five projects from each laboratory for detailed analysis and evaluation. For each project selected, we interviewed researchers and managers to determine how their projects met the guidelines. Because of our coverage, we believe our findings reflect the condition of the review and selection processes for the vast majority of DOE's

LDRD program. Our examination of the randomly selected projects from the five laboratories provides additional confidence, at those laboratories, in the results of the internal control tests. Appendix I describes our scope and methodology in more detail.
NTIS
Research and Development; Laboratories

20020002757 Hawaii Univ., Honolulu, HI USA
Determination of Interrelationships between Organizational System Variables during Implementation of Change. Final Report. Report 17 of 17
Singh, A.; Aug. 15, 1997; 20p; In English
Report No.(s): PB2002-100374; No Copyright; Avail: CASI; A03, Hardcopy; A01, Microfiche

This final and seventeenth report represents a brief summary of the major findings and conclusions of the sixteen earlier reports submitted as part of this study. The entire study was completed over a period of four years. Studies were performed on topics of leadership, team-work, intuition, conflict management, personality, hemisphericity, change management, motivation, organization power and politics, trust, and scheduling. Three qualitative surveys were undertaken; one general management questionnaire was also analyzed. Considerable problems were discovered across a broad range of management and administration categories, for which immediate interventions were recommended. The capabilities and response of the sections studied stood to be compromised without adequate intervention. The process of change undertaken so far has appeared to benefit the primary organization that was the focus of this study - Oahu District. However, there is still considerable need for further and continuous intervention. Overall, engineers are still desirous of change at a faster pace.
NTIS
Engineers; Motivation; Leadership; Politics

20020002758 Hawaii Univ., Honolulu, HI USA
Determination of Interrelationships between Organizational System Variables during Implementation of Change. Evaluation of Change: A Third Year Survey. Report 16 of 17
Singh, A.; Jul. 2000; 34p; In English
Report No.(s): PB2002-100373; No Copyright; Avail: CASI; A03, Hardcopy; A01, Microfiche

This report is a study on change management. An earlier study on change (Report no. 9 of 17) sought to understand the science behind beginning change, while this study seeks to measure the effects and impacts the change program has had. The study was conducted by means of a questionnaire sent to the engineering staff of the Division in June 1999. Engineers welcome the changes and desire the pace of change to be increased. The engineers are encouraged by the changes implemented, but want more changes in procedural and technical areas. by the correlation tests carried out, commitment by upper leadership, responsiveness, and support are seen to directly affect staff participation and morale. It was discovered that leadership, commitment and responsiveness are significantly correlated. Correspondingly, morale is also better if the leaders are committed and responsive, else morale plummets. The average grade given by the engineers to the organization was a C+. There are major differences between the design and construction branches, with the Design branch scores being lower than those of Oahu District.
NTIS
Engineers; Leadership; Construction

20020002759 Hawaii Univ., Honolulu, HI USA
Determination of Interrelationships between Organizational System Variables during Implementation of Change. Third Qualitative Study of Design and Construction Branches at HDOT (Highways). Report 15 of 17
Singh, A.; Jun. 2000; 24p; In English
Report No.(s): PB2002-100372; No Copyright; Avail: CASI; A03, Hardcopy; A01, Microfiche

There are sensitive issues facing HDOT (Hwy). There have been positive developments in some areas, and negative in other. This report provides areas in detail where there have been positive developments, no change, and negative developments, compared to last year, when an earlier qualitative survey was conducted. It seemed obvious that engineers desire inspirational leadership, and seek planned change. They prefer to see the pace of change increased. It was observed that change and evolution must continue at a steady, perhaps fast pace to modernize the division. The division must make effort to maintain the positive achievements attained. All recommendations made in the report of October 1998 are recommended again, save for the factors satisfactorily fulfilled in the paragraph above.
NTIS
Engineers; Construction; Highways; Leadership

20020002760 Hawaii Univ., Honolulu, HI USA

Determination of Interrelationships between Organizational System Variables during Implementation of Change. Explaining Behavior of Civil Engineers through Hemisphericity. Report 14 of 17

Singh, A.; Aug. 1999; 38p; In English

Report No.(s): PB2002-100371; No Copyright; Avail: CASI; A03, Hardcopy; A01, Microfiche

A study was conducted to measure the hemisphericity orientation of construction and design engineers in a large public construction organization. It is known from literature that people of different hemisphericity orientations have unlike personalities and dissimilar perspectives of specific situations. The essential characteristics of hemisphericity as established in literature are presented and used in analyzing the organization (Design and Construction Branches only). From this study of engineers, it was seen that construction engineers in the organization are predominantly left-brained while design engineers are predominantly right-brained. This difference in orientation partially explains why the design and construction engineers are unable to see eye to eye on issues concerning implementation of drawings. Left hemisphere dominant engineers are also seen to desire more organizational changes than their right hemisphere dominant counterparts. Ideally, a 50-50 distribution of hemisphericities in an organization is considered desirable. Detail, analysis, and recommendations are presented in the paper.

NTIS

Eye (Anatomy); Structural Engineering

20020002761 Hawaii Univ., Honolulu, HI USA

Determination of Interrelationships between Organizational System Variables during Implementation of Change. Plan for Modifying the Scheduling System at Oahu District. Report 12 of 17

Singh, A.; May 1999; 8p; In English

Report No.(s): PB2002-100369; No Copyright; Avail: CASI; A02, Hardcopy; A01, Microfiche

A brief plan is submitted to enhance the scheduling system at Oahu District. The engineers at Oahu District are perceived to require substantial training in the use of modern scheduling systems using conventional software. A training program is proposed. The scheduling specifications are also perceived to be in need of revision. The scheduling specifications and requirements are proposed to be divided into three categories-low cost projects, medium cost projects, and high cost projects.

NTIS

Engineers; Scheduling; Low Cost

20020002762 Hawaii Univ., Honolulu, HI USA

Determination of Interrelationships between Organizational System Variables during Implementation Change. An Examination of Use of Power, Trust, and Politics at HDOT (Highways). Report 11 of 17

Singh, A.; Shoura, M. M.; Nov. 1998; 44p; In English

Report No.(s): PB2002-100368; No Copyright; Avail: CASI; A03, Hardcopy; A01, Microfiche

Survey data on topics related to power, politics, and trust was obtained from the engineering staff of the Construction District at Hawaii Department of Transportation (HDOT). The data was collected by the use of a questionnaire sent to Area Engineers (AEs), Resident Engineers (REs), and Project Engineers (PEs). The results provide insights to the application of the power styles-the formal, reward, coercive, expert, and referent powers. Resident engineers reflected the most effective use of power, and they exhibited highly correlated results between predominant use and acceptance in formal, coercive, and referent powers. Area engineers exhibited the least effective use of power while yet exhibiting the highest need for more power. Most predominant is the use of formal (legitimate or bureaucratic) power, and least frequent are the use of force, coercion, and threat. However, expert and referent powers are the forms that staff would be most responsive to. Generally, power is perceived positively, but politics is perceived negatively, and its organizational use is even misunderstood in team building.

NTIS

Coercivity; Transportation

20020002763 Hawaii Univ., Honolulu, HI USA

Determination of Interrelationships between Organizational System Variables during Implementation of Change. Qualitative Study of Design and Construction Branches at HDOT (Highways), Oahu. Report 10 of 17

Singh, A.; Oct. 1998; 34p; In English

Report No.(s): PB2002-100367; No Copyright; Avail: CASI; A03, Hardcopy; A01, Microfiche

Interviews were conducted of engineers at the design branch at the Punchbowl office and area engineers/resident engineers at Oahu District. The aim was to let the engineers speak of major issues confronting them, and air their concerns. Interviews were all voluntary and confidential. Some units and sections were more vocal and expressive than others were. The expressive units

also displayed great unity and candidness in their responses in group situations. For two design sections, openness and sharing of identical opinions was so high and unanimous that private group sessions were not indicated. In groups where there was not the same openness and unity, it was found necessary to go into individual interviews. High unanimity was also found in two areas of the Oahu District during group sessions. There was no need in such circumstances to conduct individual interviews. However, individual interviews were conducted on occasions when the regular resident engineers were absent and were filled in by acting RE's. Newly hired engineers, especially at the design branch, had very little to say and report.
NTIS
Coordination; Highways; Construction

20020002764 Hawaii Univ., Honolulu, HI USA
Determination of Interrelationships between Organizational System Variables during Implementation Change. Evaluation of Change Management Parameters among Engineers at HDOT, Oahu District. Report 9 of 17
Shoura, M. M.; Singh, A.; Feb. 1998; 48p; In English
Report No.(s): PB2002-100366; No Copyright; Avail: CASI; A03, Hardcopy; A01, Microfiche

This report studies change management for restructuring a public construction organization. The report presents a model for organizational change (OC) and studies 20 change management parameters for three engineering management levels - area managers, project managers, and project engineers. The researchers studied the perception of engineers and the change process from initiation through completion - starting with forces that destabilize, spreading to awareness and management of anxiety, then acceptance and management of tasks, and ending with integration and restart. These were studied quantitatively and qualitatively. The report concluded that engineers realize that changes are necessary but they perceive change management negatively. Though most engineers are aware and committed to change, they perceive communication of changes to be poor. Recommendations were made to adopt a participative style, improve the commitment of upper leadership, and apply incentives to implement changes. The OC model provides a simplified approach for any organization going through the process of change and re-engineering.
NTIS
Management; Engineering Management; Management Methods; Leadership

20020002851 Hawaii Univ., Honolulu, HI USA
Determination of Interrelationships between Organizational System Variables during Implementation of Change. Existing Capabilities and Potential Strategies for Computerized Scheduling at Oahu District. Report 13 of 17
Singh, A.; Jan. 1999; 24p; In English
Report No.(s): PB2002-100370; No Copyright; Avail: CASI; A03, Hardcopy; A01, Microfiche

There is an expressed need to change the existing scheduling system at Oahu District. Training in scheduling is desired to be imparted to the engineers. A modern computerized scheduling system is necessary to allow for proper decision-making on projects. This report evaluates the existing capabilities of the engineers and the prevailing system at Oahu District and then recommends alternate strategies for overcoming the shortcomings. The report describes the various skills and duties pertaining to scheduling, and provides an overview of tasks necessary in running a successful scheduling and reporting system. The study methodology included visiting field offices, having meetings with resident engineers and staff, and scrutinizing the existing scheduling systems. System implementation issues are discussed. Approximate costs of software installation are estimated. Four approaches to education and training are provided.
NTIS
Scheduling; Engineers; Estimating

20020002854 Hawaii Univ., Honolulu, HI USA
Determination of Interrelationships between Organizational System Variables during Implementation of Change. Conflict Management Diagnosis of HDOT. Report 6 of 17
Johnson, H. M.; Singh, A.; Jul. 1997; 56p; In English
Report No.(s): PB2002-100363; No Copyright; Avail: CASI; A04, Hardcopy; A01, Microfiche

This study presents one method which engineering managers can use to diagnose conflict at HDOT. A survey was distributed to design and construction branch engineers to diagnose conflict intensities and frequencies. The results indicate that HDOT engineers predominantly use a problem-solving style to find mutual win-win resolutions to conflict, showing that HDOT can thrive under conditions of conflict. The results also indicate, however, that HDOT may be suffering from a lack of conflict. The average intensity of conflict perceived by all engineers in 1.40 on a scale of 0-4, or only a slight impact. Intra-group conflict is low. Likewise, the frequency with which conflict occurs is low, at 1.59 on the same scale. The design department maximum

conflicts due to administrative procedures and technical opinions. The construction branch perceived maximum conflicts due to administrative procedures and schedules, followed by personality differences.
NTIS
Engineers; Diagnosis

20020003934 Los Alamos National Lab., NM USA
Accelerator Production of Tritium PPO Management Plan
Fultonberg, D. N.; Mar. 01, 1998; 113p; In English
Report No.(s): DE2001-763156; LA-UR-98-4608; APT-PPO-0001-REV-0; No Copyright; Avail: Department of Energy Information Bridge, Microfiche

The purpose of the Management Plan is to describe the scope and responsibilities of the Accelerator Production of Tritium (APT) Plant Project Office (PPO); the PPO organization; guiding vision and strategies; and PPO work processes and controls.
NTIS
Management Planning; Tritium

20020005110 Fermi National Accelerator Lab., Batavia, IL USA
Report of the Fermilab Committee for Site Studies
Kuchler, V.; Holmes, S.; Sep. 10, 2001; 94p; In English
Report No.(s): DE2001-786131; FERMILAB-TM-2142; No Copyright; Avail: Department of Energy Information Bridge, Microfiche

Fermilab is the flagship laboratory of the U.S. high-energy physics program. The Fermilab accelerator complex has occupied the energy frontier nearly contnuously since its construction in the early 1970s. it will remain at the frontier until the Large Hadron Collider at CERN begins operating in 2006-7. A healthy future for Fermilab will likely require construction of a new accelerator in the post-LHC era. The process of identifying, constructing and operating a future forefront facility will require the support of the world high-energy-physics community, the governments and funding agencies of many nations and the people of surrounding communities.
NTIS
Accelerators; High Energy Interactions; Hadrons

20020005806 Sandia National Labs., Albuquerque, NM USA
Readiness Reviews: Key to Successfully Implementing Enterprise Systems
Bendure, A. O.; Apr. 20, 1999; 8p; In English
Report No.(s): DE2001-5918; SAND99-0990C; No Copyright; Avail: Department of Energy Information Bridge, Microfiche

Sandia has implemented a formal process to verify that new or modified facilities and operations are ready to safely operate. The readiness review process focuses on the status of management systems, personnel, and systems, structures, and components to do work safely. The scope and depth of the review are tailored to match the potential consequences and the likelihood that the consequences could occur. The precepts and methodology of the process are applicable to verifying the readiness of enterprise systems, and should comprise the final element in developing and implementing an enterprise system. This paper describes the readiness review process, the key elements for success, lessons learned from Sandia's readiness assessment process, and outlines how the process can be applied to enterprise systems. Specific topics addressed include selecting the criteria, approach, and lines of inquiry to be used for the review; selecting members for the review team; team leader responsibilities; reporting and closing deficiencies; and, responsibilities of the facility/project owner and management.
NTIS
Research Facilities; Management Systems; Safety

82
DOCUMENTATION AND INFORMATION SCIENCE

Includes information management; information storage and retrieval technology; technical writing; graphic arts; and micrography. For computer documentation see 61 Computer Programming and Software.

20020000736 Research and Technology Organization, Neuilly-sur-Seine, France
RTO Technical Publications: A Quarterly Listing ***Quarterly Report, 1 Jul. - 30 Sep. 2001***
October 2001; 5p; In English
Report No.(s): RTO-01-03; No Copyright; Avail: CASI; A01, Hardcopy; A01, Microfiche

This is a listing of recent unclassified RTO technical publications processed by the NASA Center for AeroSpace Information. Reports may be downloaded for free from the RTO website at http:/www.rta.nato.int or they may be purchased from the NASA Center for AeroSpace Information, 7121 Standard Drive, Hanover, MID 21076-1320 USA, phone 301-621-0390, fax 301-621-0134. Prices and order forms are available from the NASA STI website at http://www.sti.nasa.gov. An automatic distribution of unclassified RTO technical publications in CD-ROM is also available within the U.S. through the NASA Standing Order Service from the NASA Center for AeroSpace Information.
CASI
Bibliographies; Indexes (Documentation); Military Technology

20020000769 Fermi National Accelerator Lab., Batavia, IL USA
Retrospective application of online catalog author authority control: A pilot project
Berkhout, T. A.; Tompson, S. R.; Jul. 07, 1999; 6p; In English
Report No.(s): DE2001-8494; FERMILAB-TM-2079; No Copyright; Avail: Department of Energy Information Bridge
A total of 56 author authority records were created or revised in the Fermilab online catalog. An example of a correct author authority record is given. Since the author authority records used 400 fields and thus pipe all the variant names to the one record, any additions of records with any of these variants will be handled by the online catalog. It is likely that we have included most of the common variants of key Fermilab authors' names, so the database should stay cleaner and more functional for years to come. This project was a success. Therefore an immediate future plan is to implement additional author authority records for the remainder of the authors in the database. Afterwards, authority maintenance should be built in to Library work processes as an ongoing task.
NTIS
Catalogs (Publications); Data Bases; Information Systems

20020000774 NASA Kennedy Space Center, Cocoa Beach, FL USA
Advanced Data Acquisition Systems with Self-Healing Circuitry
Larson, William E., NASA Kennedy Space Center, USA; Ihlefeld, Curtis M., NASA Kennedy Space Center, USA; Medelius, Pedro J., DYNACS Engineering Co., Inc., USA; [2001]; 10p; In English; 51st International Astronautical Federation, 1-5 Oct. 2001, Toulouse, France; No Copyright; Avail: CASI; A02, Hardcopy; A01, Microfiche
Kennedy Space Center's Spaceport Engineering & Technology Directorate has developed a data acquisition system that will help drive down the cost of ground launch operations. This system automates both the physical measurement set-up function as well as configuration management documentation. The key element of the system is a self-configuring, self-calibrating, signal-conditioning amplifier that automatically adapts to any sensor to which it is connected. This paper will describe the core technology behind this device and the automated data system in which it has been integrated. The paper will also describe the revolutionary enhancements that are planned for this innovative measurement technology. All measurement electronics devices contain circuitry that, if it fails or degrades, requires the unit to be replaced, adding to the cost of operations. Kennedy Space Center is now developing analog circuits that will be able to detect their own failure and dynamically reconfigure their circuitry to restore themselves to normal operation. This technology will have wide ranging application in all electronic devices used in space and ground systems.
Author
Data Acquisition; Data Systems; Ground Operational Support System

20020000910 Lawrence Livermore National Lab., Livermore, CA USA
Electronic weight- and dimensional-data entry in a computer database
Estill, J.; Jul. 02, 1996; 8p; In English
Report No.(s): DE2001-2765; UCRL-ID-132294; No Copyright; Avail: Department of Energy Information Bridge, Microfiche
The purpose of this technical implementing procedure (TIP) is to describe the procedure used to obtain dimensional and weight information for test specimens and enter that data into an electronic database. This TIP applies to Activity E-20-50, 'Long-Term Corrosion Studies', and it pertains to weighing and measuring of specimens, and the storage of that data in an electronic database. Data is stored in the electronic database 'Microsoft Access'. Data is entered by electronic data transfer from a digital caliper (Fowler Ultra-Cal Mark III) and an electronic analytical balance (Mettler AT200).
NTIS
Weight (Mass); Dimensions; Data Bases; Corrosion

20020000919 Lawrence Livermore National Lab., Livermore, CA USA

Design of the HYPRE preconditioner library

Chow, E.; Cleary, A.; Falgout, R.; Sep. 22, 1998; 13p; In English

Report No.(s): DE2001-8519; UCRL-JC-132025; No Copyright; Avail: Department of Energy Information Bridge, Microfiche

The authors discuss the design of hypre, an object-oriented library for the solution of extremely large sparse linear systems on parallel computers. The mathematical emphasis of hypre is on modern powerful and scalable preconditioners. The design of hypre allows it to be used as both a solver package and a framework for algorithm development. The object model used for hypre is more general and flexible than the current generation of solver libraries.

NTIS

Object-Oriented Programming; Linear Systems; Libraries

20020000934 Oak Ridge National Lab., TN USA

Nuclear Data Project Evaluation Activity Report

Akovali, Y. A.; Artna-Cohen, A.; Blackmon, J. C.; Radford, D.; Smith, M. S.; Dec. 14, 1998; 9p; In English

Report No.(s): DE2001-1744; ORNL/CP-100118; KB-04-03-00-0; No Copyright; Avail: Department of Energy Information Bridge, Microfiche

This report summarizes the activities of the ORNL (Oak Ridge National Laboratory) Nuclear Data Project since the IAEA (International Atomic Energy Association) Advisory Group meeting in October 1996. The group's future plans are also included.

NTIS

Data Management; Nuclear Electric Power Generation

20020001029 Computer Sciences Corp., USA

Spinning a Useful Weblet

Globus, Al, Computer Sciences Corp., USA; Beaumont, Chris, Computer Sciences Corp., USA; [1994]; 5p; In English; Second International World Wide Web Conference, 17-20 Oct. 1994, Chicago, IL, USA

Contract(s)/Grant(s): RTOP 536-01-50

Report No.(s): RNR-94-017; No Copyright; Avail: CASI; A01, Hardcopy; A01, Microfiche

Weblet is defined as a highly interconnected portion of the World Wide Web devoted to a particular end, usually maintained by a single individual or organization and located at a single site. The WWW is a marvelous medium, but in spite of rapid improvement, the content leaves something to be desired. Our research group has addressed three content related deficiencies: (1) lack of technical depth; (2) disorganization; and (3) few educational materials on traditional subjects. We briefly discuss each item, what we've done about it, and examine usage statistics gathered by our Web Server and custom software.

Author

World Wide Web; Education; Systems Analysis

20020004001 Thomas Jefferson National Accelerator Facility, Newport News, VA USA

Building the Mass Storage System at Jefferson Lab

Bird, I.; Hess, B.; Kowalski, A.; Jan. 01, 2001; 9p; In English; 18th; 9th; 18th IEEE Symposium on Mass Storage Systems, 17 April 2001, San Diego, CA, San Diego, CA, USA, USA

Report No.(s): DE2001-773368; JLAB-PHY-01-01; DOE/ER/40150-1800; No Copyright; Avail: Department of Energy Information Bridge, Microfiche

Thomas Jefferson National Accelerator Facility (Jefferson Lab) is a U.S. Department of Energy Facility (1) conducting Nuclear Physics experiments that currently have data collection rates of up to 20 MB/second. Future experiments, however, are expected to greatly exceed these rates. Post processing and data analysis produce similar amounts of data. Both the raw and processed data are stored on tape and need to be easily accessible. Between data collection and processing, the Mass Storage System at Jefferson Lab currently moves over 2 TB of data per day.

NTIS

Research Facilities; Data Management; Data Processing; Data Storage; Data Acquisition

20020004002 Los Alamos National Lab., NM USA

Adaptive system approach to the implementation and evaluation of digital library recommendation systems

Bollen, J.; Rocha, L.; May 01, 2000; 14p; In English

Report No.(s): DE2001-768999; LA-UR-00-2402; No Copyright; Avail: Department of Energy Information Bridge

The focus for information retrieval systems in digital libraries has shifted from passive repositories of information to recommendation systems that actively participate in retrieving useful information, and can furthermore learn from the retrieval behavior of users. The new approach to IR emphasizes the shortcomings of the traditional evaluation methodology of IR systems. In addition to describing our research on adaptive recommendation systems, we propose a novel evaluation methodology for such systems. Rather than relying on measures of precision and recall, interactive, adaptive systems can best be evaluated by how well they can capture the knowledge of specific user communities. Our proposed methodology, based on the concept of shared knowledge structures, allows a quantitative assessment of recommendation systems.
NTIS
Digital Systems; Information Systems; Libraries

20020005872 Ohio State Univ., Columbus, OH USA
Aiding the Intelligence Analyst in Situations of Data Overload: A simulation Study of Computer-Supported Inferential Analysis under Data Overload ***Interim Report, Mar. 1998-May 1999***
Patterson, Emily S.; Roth, Emilie M.; Woods, David D.; May 1999; 137p; In English; Original contains color images; --Original contains color plates: All DTIC reproductions will be in black and white. Prepared in cooperation with Roth Cognitive Engineering, Brookline, MA
Contract(s)/Grant(s): F41624-94-D-6000; Proj-7184
Report No.(s): AD-A395332; AFRL-HE-WP-TR-1999-0241; No Copyright; Avail: CASI; A07, Hardcopy; A02, Microfiche

A simulation study of inferential analysis was conducted with ten professional intelligence analysts. Using a process tracing methodology, patterns in vulnerabilities were identified when analysts were asked to analyze something outside their base of expertise, were tasked with a tight deadline, and had a large data set. Study participants were vulnerable to missing critical information. All the participants were observed to use relatively primitive search tactics, quickly narrowing in on a set of documents through the addition of keywords to an initial query. All of the participants missed some of the nine documents that were categorized as high quality. A group of four participants who found and relied upon some of the high quality documents took more time, read more documents, and made fewer inaccurate statements in their verbal briefings than a group of four participants who did not. In addition, three sources of inaccurate statements were identified. First, study participants sometimes relied upon assumptions that would normally be correct, but did not apply in this situation. Second, participants sometimes repeated information that was inaccurate in a document that they had read. Third, participants were observed to rely upon information that was considered accurate at one point in time, but then was later overturned in subsequent updates. The main contribution from this research was a model of potential vulnerabilities in inferential analysis under challenging conditions. These vulnerabilities are informative because they point to a set of challenging design criteria that human-centered solutions to data overload need to meet.
DTIC
Computer Techniques; Data Simulation; Data Processing; Artificial Intelligence

84
LAW, POLITICAL SCIENCE AND SPACE POLICY

Includes: aviation law; space law and policy; international law; international cooperation; and patent policy

20020002259 General Accounting Office, Washington, DC USA
Foreign Assistance: Lessons Learned from Donors' Experiences in the Pacific Region
Aug. 2001; 64p; In English
Report No.(s): PB2002-100170; GAO/01-808; No Copyright; Avail: CASI; A04, Hardcopy; A01, Microfiche

From fiscal years 1987 to 2001, the USA gave at least $2.6 billion in economic assistance to the Federated States of Micronesia and the Republic of the Marshall Islands. A major portion of this assistance, about $1.7 billion, was provided under an international agreement, the Compact of Free Association. The Compact provided for assistance to the two Pacific Island nations over a 15-year period, starting in 1986. Currently, the USA is negotiating with the two countries to extend the economic assistance provisions of the Compact, which are set to end in late 2001. to address concerns that (1) the countries remain highly dependent on U.S. assistance; (2) the assistance has not significantly improved conditions in the countries; and (3) the expenditures have received little oversight, the U.S. negotiator is considering the use of different assistance strategies than those in the current agreements. to assist the Congress in its review of the proposals for providing economic assistance that are under consideration in the negotiations, you asked us to identify useful lessons from the experiences of other donors in the Pacific. Specifically, we (1) identify the major donors of development assistance to the Pacific Island nations and their objectives, (2)

discuss the assistance provided to the Republic of the Marshall Islands. donors development assistance strategies and the factors or experiences that influence their choice of strategies, and (3) report lessons from the other donors assistance strategies that could be useful for U.S. consideration.
NTIS
International Cooperation; Pacific Islands

85
TECHNOLOGY UTILIZATION AND SURFACE TRANSPORTATION

Includes aerospace technology transfer; urban technology; surface and mass transportation. For related information see 03 Air Transportation and Safety, 16 Space Transportation and Safety, and 44 Energy Production and Conversion. For specific technology transfer applications see also the category where the subject is treated.

20020005115 Department of Energy, Aiken, SC USA
Letter Report on the Issue of Noble Metals in the DWPF Melter
Hutson, N. D.; Sep. 05, 2001; 53p; In English
Report No.(s): DE2001-786152; WSRC-TR-2001-00337-REV-0; No Copyright; Avail: Department of Energy Information Bridge, Microfiche

This report presents some historical data from the radioactive operation of the DWPF melter. Some of the data seem to indication that the melter is displaying symptoms that may be linked to accumulation of noble metal or other conductive material on the melter floor. The complex and often competing effects of waste composition, glass pool temperatures, and operating conditions must also be considered.
NTIS
Radioactivity; Noble Metals; Radioactive Wastes

88
SPACE SCIENCES (GENERAL)

Includes general research topics related to the natural space sciences. For specific topics in Space Sciences see categories 89 through 93.

20020003813 Los Alamos National Lab., NM USA
Ices on titan: laboratory measurements that complement the huygens probe
Robinson, J.; Aug. 01, 2000; 19p; In English
Report No.(s): DE2001-768737; LA-UR-00-3987; No Copyright; Avail: Department of Energy Information Bridge, Microfiche

This is the final report of a three-year, Laboratory-Directed Research and Development (LDRD) project at the Los Alamos National Laboratory (LANL). The composition of the cold bodies in the outer solar system may hold some of the key molecular clues concerning the composition of the prestellax molecular cloud that gave rise to the solar system. We studied the physical chemistry and heterogeneous (gas/surface) reactivity of extraterrestrial ice analogs of the surfaces of Saturn's moon Titan. This program coupled our surface spectroscopic techniques with physical adsorption measurements. We addressed several of the pressing questions regarding Titan such as: Is storage of hydrocarbons in Titan's water ice crust feasible. Do heterogeneous processes influence the atmospheric chemical composition of Titan. Are phase transitions to be expected. These data can be incorporated into photochemical models with the goal of improved modeling of the chemical composition and meteorology of Titan's atmosphere. Titan will be probed by the Cassini-Huygens Mission. Our results on Titan ice analogs can be used to help interpret the mission data.
NTIS
Chemical Composition; Moon; Physical Chemistry; Photochemical Reactions; Molecular Clouds

89
ASTRONOMY

Includes observations of celestial bodies, astronomical instruments and techniques; radio, gamma-ray, x-ray, ultraviolet, and infrared astronomy; and astrometry.

20020001031 Smithsonian Astrophysical Observatory, Cambridge, MA USA
Spectroscopic Determination of the Physical Conditions in Hot, Optically Thin Sources ***Annual Report, 1 Jan. - 31 Dec. 2001***
Brickhouse, N., Smithsonian Astrophysical Observatory, USA; November 2001; 8p; In English
Contract(s)/Grant(s): NAG5-3559; No Copyright; Avail: CASI; A02, Hardcopy; A01, Microfiche

This annual report covers the period from Oct 1, 2000 to Sep 30, 2001. The Astrophysics Plasma Emission Code and Database (APEC/APED), developed in part under this grant, have been upgraded to Version 1.1 and are now beginning to be used outside our research group in applications to X-ray spectral data from Chandra and XMM-Newton. These models represent the best theoretical data currently available and are reasonably complete below about 30 angstroms. Stellar coronae are being used to benchmark the atomic data in APED as part of the Emission Line Project. Initial results suggest that the models for most of the strongest lines are in good agreement with the observations, including the H-like and He-like emission from dominant elements and the Fe L shell emission, both near 1 keV and in the extreme ultraviolet near 100 eV. At this point in time, we define 'good agreement' at the level of accuracy expected from the atomic physics, approximately 20-30%. In order to benchmark the spectral models beyond the canonical theoretical accuracy, we are working closely with the Chandra gratings calibration group to ensure that we are using the optimal calibration, primarily effective areas and line response functions.
Derived from text
Data Bases; Spectroscopy; Computerized Simulation; Spectral Methods

20020001217 Lawrence Livermore National Lab., Livermore, CA USA
Variable stars in the MACHO bulge database
Quinn, P. J.; Alcock, C.; Allsman, R. A.; Alves, D. R.; Axelrod, T. S.; Oct. 01, 1998; 6p; In English
Report No.(s): DE2001-2837; UCRL-JC-132529; No Copyright; Avail: Department of Energy Information Bridge, Microfiche

The MACHO (Massive Compact Halo Object) Project has been monitoring large fields in the direction of the Galactic bulge, the LMC (Large Magellanic Cloud) and SMC (Small Magellanic Cloud) for over six years. The nightly observations of this microlensing survey provide very large databases for astronomers. The MACHO database contains (approximately) 5 Terabytes of data as of mid-1998. For comparison, the HST (Hubble Space Telescope) Archive contains about (approximately) 2 Tb, and the Sloan Digital Sky Survey will reach (approximately) 1.0 Tb. Our database can be used to attack a variety of astrophysical problems, and has produced results relevant to microlensing, galactic structure, and stellar evolution. of particular importance are the large numbers of variable stars (tens of thousands) found as byproducts of the microlensing search. In years to come, the microlensing databases will play a dominant role in variable star science. Important science can still be done with limited resources, even in places with no access to large telescopes (all you need is computer).
NTIS
Variable Stars; Data Bases; Massive Compact Halo Objects; Sky Surveys (Astronomy)

20020001249 NASA Ames Research Center, Moffett Field, CA USA
Stability Analysis of the Planetary System Orbiting Upsilon Andromedae, 2, Simulations Using New Lick Observatory Fits
Lissauer, Jack J., NASA Ames Research Center, USA; Rivera, Eugenio J., NASA Ames Research Center, USA; Astrophysical Journal; Jun. 20, 2001; Volume 554, pp. 1141-1150; In English
Contract(s)/Grant(s): NAG5-4640; NAG5-9680; RTOP 344-30-50-01; Copyright; Avail: Issuing Activity

We present results of long-term numerical orbital integrations designed to test the stability of the three-planet system orbiting upsilon Andromedae and short-term integrations to test whether mutual perturbations among the planets can be used to determine planetary masses. Our initial conditions are based on recent fits to the radial velocity data obtained by the planet search group at Lick Observatory. The new fits result in significantly more stable systems than did the initially announced planetary parameters. Our integrations using the 2000 February parameters show that if the system is nearly planar, then it is stable for at least 100 Myr for m(sub f) = 1/sin i less than or = 4. In some stable systems, the eccentricity of the inner planet experiences large oscillations. The relative periastra of the outer two planets' orbits librate about 0 deg. in most of the stable systems; if future observations imply

that the periastron longitudes of these planets are very closely aligned at the present epoch, dynamical simulations may provide precise estimates for the masses and orbital inclinations of these two planets.
Author
Stability; Stability Tests; Data Acquisition; Many Body Problem; Orbital Elements; Oscillations; Planetary Mass; Stellar Orbits

20020001825 NASA Goddard Space Flight Center, Greenbelt, MD USA
The Integration of COTS/GOTS within NASA's HST Command and Control System
Pfarr, Thomas, Computer Sciences Corp., USA; Reis, James E., NASA Goddard Space Flight Center, USA; [2001]; 11p; In English; International Conference on COTS/GOTS, 2-4 Feb. 2001, Orlando, FL, USA; No Copyright; Avail: CASI; A03, Hardcopy; A01, Microfiche

NASA's mission critical Hubble Space Telescope (HST) command and control system has been re-engineered with commercial-off-the-shelf (COTS/GOTS) and minimal custom code. This paper focuses on the design of this new HST Control Center System (CCS) and the lessons learned throughout its development. CCS currently utilizes more than 30 COTS/GOTS products with an additional 1/2 million lines of custom glueware code; the new CCS exceeds the capabilities of the original system while significantly reducing the lines of custom code by more than 50%. The lifecycle of COTS/GOTS products will be examined including the package selection process, evaluation process, and integration process. The advantages, disadvantages, issues, concerns, and lessons learned for integrating COTS/GOTS into the NASA's mission critical HST CCS will be examined in detail. This paper will reveal the many hidden costs of COTS/GOTS solutions when compared to traditional custom code development efforts; this paper will show the high cost of COTS/GOTS solutions including training expenses, consulting fees, and long-term maintenance expenses.
Author
Commercial Off-The-Shelf Products; Hubble Space Telescope; Command and Control

20020002239 Lawrence Livermore National Lab., Livermore, CA USA
Solar system events at high spatial resolution
Baines, K. H.; Gavel, D. T.; Getz, A. M.; Gibbartd, S. G.; MacIntosh, B.; Feb. 19, 1999; 57p; In English
Report No.(s): DE2001-12548; UCRL-ID-133267; ERI-002; No Copyright; Avail: Department of Energy Information Bridge

Until relatively recent advances in technology, astronomical observations from the ground were limited in image resolution by the blurring effects of earth's atmosphere. The blur extent, ranging typically from 0.5 to 2 seconds of arc at the best astronomical sights, precluded ground-based observations of the details of the solar system's moons, asteroids, and outermost planets. With the maturing of a high resolution image processing technique called speckle imaging the resolution limitation of the atmosphere can now be largely overcome. Over the past three years they have used speckle imaging to observe Titan, a moon of Saturn with an atmospheric density comparable to Earth's, Io, the volcanically active innermost moon of Jupiter, and Neptune, a gas giant outer planet which has continually changing planet-encircling storms. These observations were made at the world's largest telescope, the Keck telescope in Hawaii and represent the highest resolution infrared images of these objects ever taken.
NTIS
Solar System; Spatial Resolution; Image Resolution; Imaging Techniques; Atmospheric Effects

20020002844 Smithsonian Astrophysical Observatory, Cambridge, MA USA
Membership and Coronal Activity in the NGC 2232 and Cr 140 Open Clusters ***Final Report, 1 Mar. 2001 - 28 Feb. 2002***
Patten, Brian M., Smithsonian Astrophysical Observatory, USA; December 2001; 2p; In English
Contract(s)/Grant(s): NAG5-9131; No Copyright; Avail: CASI; A01, Hardcopy; A01, Microfiche

This is the second annual performance report for our grant "Membership and Coronal Activity in the NGC 2232 and Cr 140 Open Clusters." We propose to identify X-ray sources and extract net source counts in 8 archival ROSAT HRI images in the regions of the NGC 2232 and Cr 140 open clusters. These X-ray data will be combined with ground-based photometry and spectroscopy in order to identify G, K, and early-M type cluster members. At present, no members later than approximately F5 are currently known for either cluster. With ages of approximately 25 Myr and at a distance of just 320 - 360 pc, the combined late-type membership of the NGC 2232 and Cr 140 clusters will yield an almost unique sample of solar-type stars in the post-T Tauri/pre-main sequence phase of evolution. These stars will be used to assess the level and dispersion in coronal activity levels, as part of a probe of the importance of magnetic braking and the level of magnetic dynamo activity, for solar-type stars just before they reach the ZAMS. Over the past year we have successfully acquired all of the ground-based data necessary to support the analysis of the archival ROSAT X-ray data in the regions around both of these clusters. by the end of 2001 we expect to have completed the reduction and analysis of the ground-based photometry and spectroscopy and will begin the integration of these data with the ROSAT X-ray data. A certain amount of pressure to complete the work on NGC 2232 is coming from the SIRTF

project, as this cluster may be a key component to a circumstellar disk evolution GTO program. We are only too happy to try to help and have worked to speed the analysis as much as possible. The primary activity to be undertaken in the next few months is the integration of the groundbased photometry and spectroscopy with the archival ROSAT X-ray data and then writing the paper summarizing our results. The most time consuming portion of this next phase is, of course, seeing the paper through publication in a peer-reviewed journal. Therefore, we have requested a no-cost extension to the grant to allow us to bring this project to a conclusion.
Author
Stellar Coronas; Open Clusters; X Ray Sources

90
ASTROPHYSICS

Includes cosmology; celestial mechanics; space plasmas; and interstellar and interplanetary gases and dust.

20020001035 NASA Goddard Space Flight Center, Greenbelt, MD USA
Book Review: Encyclopedia of Astronomy and Astrophysics, Volumes 1-4
Maran, Stephen Paul, NASA Goddard Space Flight Center, USA; [2001]; 3p; In English; No Copyright; Avail: CASI; A01, Hardcopy; A01, Microfiche

This massive reference work (hereafter EAA) summarizes a great deal of what we knew in the astronomical sciences at the most recent Millennium. An associated website may keep much of it up-to-date for years to come. The contents are extensive indeed: the index alone consists of 76 pages, each with three columns of fine-type listings, and there are 'nearly 700 main articles'. The main articles are what make EAA worthwhile. They are generally by experts, who took much care in their preparation. The degree to which the articles are illustrated and referenced, however, seems to depend on the inclination of the individual author. On the other hand, articles on Saturn's rings and on its satellites are heavily illustrated, but with just two or three citations in each. The coverage of solar physics is especially thorough in EAA. There are numerous articles on major topics, notably in the physics and phenomena of the corona and the chromosphere, and some on more specialized areas, such as 'Polar Plumes' and 'Coronal Cavities.'
Derived from text
Astronomy; Astrophysics; Solar Physics; Documents

20020001063 Lawrence Livermore National Lab., Livermore, CA USA
Scaling supernova hydrodynamics to the laboratory
Kane, J. O.; Jun. 01, 1999; 152p; In English
Report No.(s): DE2001-11979; UCRL-LR-132438; REPT-98-ERD-022; No Copyright; Avail: Department of Energy Information Bridge, Microfiche

Supernova (SN) 1987A focused attention on the critical role of hydrodynamic instabilities in the evolution of supernovae. to test the modeling of these instabilities, we are developing laboratory experiments of hydrodynamic mixing under conditions relevant to supernovae. Initial results were reported in J. Kane et al., Astrophys. J.478, L75 (1997) The Nova laser is used to shock two-layer targets, producing Richtmyer-Meshkov (RM) and Rayleigh-Taylor (RT) instabilities at the interfaces between the layers, analogous to instabilities seen at the interfaces of SN 1987A. Because the hydrodynamics in the laser experiments at intermediate times (3-40 ns) and in SN 1987A at intermediate times (5 s-10(sup 4) s) are well described by the Euler equations, the hydrodynamics scale between the two regimes. The experiments are modeled using the hydrodynamics codes HYADES and CALE, and the supernova code PROMETHEUS, thus serving as a benchmark for PROMETHEUS. Results of the experiments and simulations are presented. Analysis of the spike and bubble velocities in the experiment using potential flow theory and a modified Ott thin shell theory is presented. A numerical study of 2D vs. 3D differences in instability growth at the O-He and He-H interface of SN 1987A, and the design for analogous laser experiments are presented. We discuss further work to incorporate more features of the SN in the experiments, including spherical geometry, multiple layers and density gradients. Past and ongoing work in laboratory and laser astrophysics is reviewed, including experimental work on supernova remnants (SNRs). A numerical study of RM instability in SNRs is presented.
NTIS
Astrophysics; Hydrodynamics; Supernova 1987A; Supernova Remnants; Mathematical Models; Scaling Laws

20020001197 Argonne National Lab., IL USA

Molybdenum Isotopic Composition of Single Silicon Carbides from Supernovae

Amari, S.; Clayton, R. N.; Davis, A. M.; Lewis, R. S.; Pellin, M. J.; Feb. 03, 1999; 5p; In English; 30th; 30th Lunar and Planetary Science Conference, 15-19 March 1999, Houston, TX, USA

Contract(s)/Grant(s): W-31109-ENG-38

Report No.(s): DE2001-12386; ANL/CHM/CP-98350; No Copyright; Avail: Department of Energy Information Bridge, Microfiche

Presolar silicon carbide grains form in a variety of types of stars, including asymptotic giant branch red giant stars and supernovae. The dominant mechanisms of heavy element nucleosynthesis, the s-process and r-process, are thought to occur in AGB stars and supernovae, respectively. We have previously reported that mainstream SiC grains have strong enrichments in the s-process isotopes of SR, Zr and Mo. We report here the first measurements of Mo isotopes in X-type SiC grains, which have previously been identified as having formed from supernova ejecta.

NTIS

Molybdenum Isotopes; Supernovae; Nuclear Fusion

20020001515 Lawrence Livermore National Lab., Livermore, CA USA

Macho rr lyrae in the inner halo and bulge

Drake, A.; Alcock, C.; Allsman, R. A.; Alves, D. R.; Axelrod, T. S.; Oct. 01, 1998; 8p; In English

Report No.(s): DE2001-2838; UCRL-JC-132528; No Copyright; Avail: Department of Energy Information Bridge, Microfiche

The RR (random-random) Lyrae in the bulge have been proposed to be the oldest populations in the Milky Way, tracers of how the galaxy formed. We study here the distribution of (approximately) 1600 bulge RR Lyrae stars found by the MACHO Project. The RR Lyrae with 0.4 less than R less than 3 kpc show a density law that is well fit by the extension of the metal-poor stellar halo present in the outer regions of the Milky Way.

NTIS

Lyra Constellation; Galactic Evolution; Milky Way Galaxy

20020001536 Lawrence Livermore National Lab., Livermore, CA USA

Four new BL Lac surveys: sampling new populations

Schmidt, G.; Becker, R. H.; Brinkmann, W.; Feigelson, E. D.; Kollgaard, R. I.; Jun. 01, 1998; 6p; In English

Report No.(s): DE2001-2773; UCRL-JC-132530; REPT-95-ERI-006; No Copyright; Avail: Department of Energy Information Bridge, Microfiche

The advent of large area deep radio and X-ray surveys is leading to the creation of many new BLLac samples. In particular, the ROSAT All-Sky, Green Bank and FIRST surveys are proving to be rich sources of new BLLacs. We will discuss the methods used in four in-dependent BLLac searches based on these surveys. Comparison of the broadband spectral energy distributions of these BLLac with those of previously known objects clearly points to the existence of a large previously unrecognized population of objects with characteristics intermediate between those exhibited by Low and High energy peaked BLLacs.

NTIS

BL Lacertae Objects; X Ray Spectra

20020001545 Lawrence Livermore National Lab., Livermore, CA USA

Elliptical galaxies in high-z clusters: how old are they

Stanford, S. A.; Jun. 01, 1998; 10p; In English

Report No.(s): DE2001-2800; UCRL-JC-132531; No Copyright; Avail: Department of Energy Information Bridge, Microfiche

I review recent research on the evolution of elliptical galaxies in high redshift galaxy clusters. Significant progress is being made on many fronts using the powerful tools of e.g. HST and 10 m class telescopes. But determining the actual age of composite stellar populations in distant galaxies is still beyond our capabilities.

NTIS

Galactic Clusters; Red Shift; Elliptical Galaxies

20020002325 Los Alamos National Lab., NM USA

Nuclear reaction rates and the nova outburst

Starrfield, S. G.; Iliadis, C.; Oct. 01, 2000; 10p; In English

Report No.(s): DE2001-765751; LA-UR-00-5082; No Copyright; Avail: Department of Energy Information Bridge, Microfiche

In this paper we examined the consequences of improving the nuclear reaction library on our simulations of TNRs on 1.25M, WD and 1.35M, WDS. We have found that the changes in the rates have affected the nucleosynthesis predictions of our calculations but not, to any great extent, the gross features. In addition, we have used a lower mass accretion rate than in our previous studies in order to accrete (and eject) more material. This has, as expected, caused the peak values of some important parameters to increase over our previous studies at the same WD mass. However, because some important reaction rates have declined in the new compilation this has not increased the abundances for nuclei above aluminum and, in fact, they have declined while the abundances of both (sup 26)Al and (sup 27)Al have increased at both WD masses. In contrast, the abundance of (sup 22)Na has declined at both WD masses over the values predicted in our earlier work. This has important implications with respect to predictions of the observability of novae with INTEGRAL.
NTIS
Novae; Nuclear Reactions; Reaction Kinetics

20020002719 California Univ., Berkeley, CA USA
High Energy Physics and Cosmology, June 1, 1984-May 31, 1999 ***Final Report, 1 Jun. 1884 - 31 May 1999***
Silk, J.; May 31, 1999; 12p; In English
Report No.(s): DE2001-765814; No Copyright; Avail: Department of Energy Information Bridge, Microfiche
The DOE grant supported the theoretical particle astrophysics group, and is coordinated by the Principal Investigator. Participants include faculty members Marc Davis, Lawrence Hall and Hitoshi Murayama, together with several postdoctoral fellows. During the previous and current funding period (1996-1998), several important results have been obtained that are briefly summarized in this report, including: dark matter; cosmic microwave background; and early universe and structure formation.
NTIS
Astrophysics; Cosmology

20020002805 Lawrence Livermore National Lab., Livermore, CA USA
Distance to the Large Magellanic Cloud
Popowski, P.; Jan. 31, 2000; 7p; In English
Report No.(s): DE2001-756808; UCRL-JC-137446; No Copyright; Avail: Department of Energy Information Bridge
The author demonstrates that the two unexpected results in the local Universe: anomalous intrinsic (V--I)(sub 0) colors of RR Lyrae stars and clump giants in the Galactic center, and very short distances to Magellanic Clouds inferred from clump giants, can be at least partially resolved with a modified coefficient of selective extinction A(sub V)/E(V--I). With this modification, the author found a new clump-giant distance modulus to the Large Magellanic Cloud, (mu)(sub LMC) = 18.27 (+-) 0.07, which is 0.09 larger than the Udalski (1998b) result. When distance estimates from the red clump, RR Lyrae stars and the eclipsing binary HV2274 are combined, one obtains (mu)(sub LMC) = 18.31 (+-) 0.04 (internal).
NTIS
Eclipsing Binary Stars; Magellanic Clouds; Distance; Astrophysics

20020003430 Los Alamos National Lab., NM USA
Core-collapse supernovae: Nature's laboratory for particle physics
Fryer, C.; Dec. 01, 2000; 12p; In English
Report No.(s): DE2001-768856; LA-UR-00-5685; No Copyright; Avail: Department of Energy Information Bridge
Astronomers have long relied upon particle physicists to understand the observable universe, from the Big Bang to stars such as our own Sun. In the past, the transfer of knowledge between astronomers and particle physicists has been in one direction with particle physicists providing astronomers the essential information to understand their observations. But observations of astronomical phenomena can be used to help our understanding of particle physics as well. Because of the extreme densities and temperatures which occur in neutron stars and the outbursts that make them (core-collapse supernovae), astronomers can use the objects to probe aspects of particle physics.
NTIS
Supernovae; Theoretical Physics; Collapse; Elementary Particles

20020003566 Colorado Univ., Boulder, CO USA
Stellar Evolution in Starburst Galaxies ***Interim Report***
Conti, Peter, Colorado Univ., USA; Dec. 06, 2001; 1p; In English
Contract(s)/Grant(s): NGT5-50194; No Copyright; Avail: Issuing Activity; Abstract Only

The main thrust of the program was to obtain UV spectroscopy of a number of massive and hot luminous (OB type) stars in the nearby galaxy called the Small Magellanic Cloud (SMC). The objective was to analyze their atmospheres and winds so as to determine the effect of the lower abundance of the SIVIC on these parameters. Furthermore, the differences in evolution could be investigated. Additionally, the UV spectra themselves would be suitably weighted and systematically combined to provide a template for comparison to very distant galaxies formed in the early history of the Universe which also have a low abundance of elements. The spectra have been obtained and the analysis is proceeding, primarily by the groups in Munich and at STScI who are the leads for this project. Given the important role of the nearby SMC galaxy as a template of low metal abundance, I have begun to investigate the YOUNGEST phases of massive star birth, before the most massive and hottest stars become optically visible. Typically these stars form in clusters, in some cases having tens to hundreds of OB type stars. In this phase, each star is still buried in its natal cloud and visible only in the infrared (IR) from its self-heated dust and/or from radio free-free emission of the surrounding hydrogen (HII) region. Efforts to find and identify these buried clusters were conducted using a large radio telescope. A number of these were found and further analysis of the data is underway. These clusters are not visible optically, but ought to be seen in the IR, and are a likely topic for HST photometry on NICMOS. A proposal to do this will be made next semester. These objects are the precursors of the optically visible clusters that contain massive and hot luminous stars.
Author
Stellar Evolution; Starburst Galaxies; O Stars; B Stars; Magellanic Clouds; Massive Stars

20020003810 Los Alamos National Lab., NM USA
Supermassive black holes and the strong field limit of general relativity
Zurek, W.; Aug. 01, 2000; 6p; In English
Report No.(s): DE2001-768768; LA-UR-00-3860; No Copyright; Avail: Department of Energy Information Bridge, Microfiche

The energy driving a quasar or active galactic nucleus (AGN) is thought to come from the accretion of gas on to a supermassive black hole at the center of the host galaxy. Evidence for this has been hard to find, but the extremely broad iron line observed in the X-ray spectrum of one particular AGN (the Seyfert galaxy known as MCG-6-30-15) may well be the calling card of a supermassive black hole. A new model-independent approach to analyzing these intriguing X-ray emissions extracts more information about the black hole within--including the position of the inner edge of the accretion disk and the rate at which the black hole is rotating.
NTIS
Quasars; Black Holes (Astronomy); Active Galactic Nuclei

20020003827 Argonne National Lab., IL USA
Toward complete isotopic analysis of individual presolar silicon carbide grains: C, N, Si, SR, Zr, Mo, and Ba in single grains of type X
Pellin, M. J.; Calaway, W. F.; Davis, A. M.; Lewis, R. S.; Amari, S.; Mar. 01, 2000; 5p; In English
Report No.(s): DE2001-768572; ANL/CHM/CP-101228; No Copyright; Avail: Department of Energy Information Bridge, Microfiche

Presolar silicon carbide grains form in a variety of types of stars, including asymptotic giant branch red giant stars and supernovae. The dominant mechanisms of heavy element nucleosynthesis, the s-process and r-process, are thought to occur mainly in AGB stars and supernovae, respectively. We have previously reported that mainstream SiC grains have strong enrichments in the s-process isotopes of SR, Zr and Mo and initial results for X-type SiC grains showing enrichments in the r-process isotopes of Mo. We report here the first measurements of Zr, SR, and Ba isotopes along with expanded studies of Mo in individual X-type SiC grains, which have previously been identified as having formed from supernova ejects.
NTIS
Asymptotic Giant Branch Stars; Supernovae; Silicon Carbides

20020003828 Argonne National Lab., IL USA
Zr and Mo isotopic constraints on the origins of unusual types of presolar SiC grains
Pellin, M. J.; Davis, A. M.; Calaway, W. F.; Lewis, R. S.; Clayton, R. N.; Mar. 01, 2000; 5p; In English
Report No.(s): DE2001-768571; ANL/CHM/CP-101227; No Copyright; Avail: Department of Energy Information Bridge, Microfiche

Although most presolar silicon carbide grains form in asymptotic giant branch red giant stars (the so-called mainstream grains) or supernovae (the X-grains), there are a number of other minor types of grains whose origin is less clear. The dominant mechanisms of heavy element nucleosynthesis, the s-process and r-process, are thought to occur mainly in AGB stars and supernovae, respectively, and the isotopic patterns in heavy elements in presolar grains can be used to constrain their origins. We

have previously reported that mainstream SiC grains have strong enrichments in the s-process isotopes of SR, Zr and Mo and that X-grains have an unusual Mo isotopic composition that differs from s- and r-process expectations. We report here the first measurements of Zr and Mo isotopes in several grains of other rare types that were found in the same mount as the mainstream and X-grains reported previously.
NTIS
Silicon Carbides; Supernovae; Asymptotic Giant Branch Stars

20020004362 Search for Extraterrestrial Intelligence Inst., Moffett Field, CA USA
Forecast for the Remainder of the Leonid Storm Season
Jenniskens, Peter, Search for Extraterrestrial Intelligence Inst., USA; [2001]; 18p; In English
Contract(s)/Grant(s): RTOP 344-50-25-01; No Copyright; Avail: CASI; A03, Hardcopy; A01, Microfiche
The dust trails of comet 55P/Tempel-Tuttle lead to Leonid storms on Earth, threatening satellites in orbit. We present a new model that accounts in detail for the observed properties of dust tails evolved by the comet at previous oppositions. The prediction model shows the 1767-dust trail closer to Earth's orbit in 2001 than originally thought; increasing expected peak rates for North America observers. Predictions for the 2002 storms are less affected. We demonstrate that the observed shower profiles can be understood as a projection of the comet lightcurve.
Author
Interplanetary Dust; Forecasting; Leonid Meteoroids; Light Curve

20020005057 Los Alamos National Lab., NM USA
Population synthesis and gamma ray burst progenitors
Freyer, C. L.; Dec. 11, 2000; 16p; In English
Report No.(s): DE2001-769157; LA-UR-00-5878; No Copyright; Avail: Department of Energy Information Bridge, Microfiche
Population synthesis studies of binaries are always limited by a myriad of uncertainties from the poorly understood effects of binary mass transfer and common envelope evolution to the many uncertainties that still remain in stellar evolution. But the importance of these uncertainties depends both upon the objects being studied and the questions asked about these objects. Here I review the most critical uncertainties in the population synthesis of gamma-ray burst progenitors. With a better understanding of these uncertainties, binary population synthesis can become a powerful tool in understanding, and constraining, gamma-ray burst models. In turn, as gamma-ray bursts become more important as cosmological probes, binary population synthesis of gamma-ray burst progenitors becomes an important tool in cosmology.
NTIS
Gamma Ray Bursts; Cosmology; Mass Transfer

20020005062 Los Alamos National Lab., NM USA
Rotational instabilities and centrifugal hangup
New, K.; Centrella, J.; Dec. 01, 2000; 14p; In English
Report No.(s): DE2001-769262; LA-UR-00-5924; No Copyright; Avail: Department of Energy Information Bridge, Microfiche
One interesting class of gravitational radiation sources includes rapidly rotating astrophysical objects that encounter dynamical instabilities. We have carried out a set of simulations of rotationally induced instabilities in differentially rotating polytropes. An n=1.5 polytrope with the Maclaurin rotation law will encounter the m=2 bar instability at T/(vert-bar)W(vert-bar) (ge) 0.27. Our results indicate that the remnant of this in-stability is a persistent bar-like structure that emits a long-lived gravitational radiation signal. Furthermore, dynamical instability is shown to occur in n=3.33 polytropes with the j-constant rotation law at T/(vert-bar)W(vert-bar) (ge) 0:14. In this case, the dominant mode of instability is m=1. Such instability may allow a centrifugally-hung core to begin collapsing to neutron star densities on a dynamical timescale. If it occurs in a supermassive star, it may produce gravitational radiation detectable by LISA.
NTIS
Gravitational Waves; Stability; Neutron Stars; Astrophysics

20020005185 Lawrence Livermore National Lab., Livermore, CA USA
Exposure History of Separated Phases from the Kapoeta Meteorite
Caffee, M. W.; Nishiizumi, K.; Mazarik, J.; Jan. 14, 2000; 4p; In English
Report No.(s): DE2001-757462; UCRL-JC-132357-REV-1; No Copyright; Avail: Department of Energy Information Bridge
The cosmogenic radionuclides, Be-10 (1.5 Ma), Al-26 (0.705 Ma), CL-36 (0.301 Ma), and Mn-53 (3.7 Ma) were measured in selected clasts and matrix samples from the howardite Kapoeta. This work is an extension of that based on Be-10 and Al-26.

Recent work based on measurements of cosmogenic Ne-21 suggest the possibility of a complex recent exposure history for Kapoeta. The measurement of these radionuclides, in conjunction with production rates based on Monte Carlo calculations, can constrain exposure conditions and durations. Taken together, the radionuclide data are entirely consistent with a single stage 4(pi) exposure lasting approximately 3 Ma.
NTIS
Kapoeta Achondrite; Meteorites; Meteoritic Composition; Radioactive Isotopes; Monte Carlo Method; Isotope Ratios; Geochronology

91
LUNAR AND PLANETARY SCIENCE AND EXPLORATION

Includes planetology; selenology; meteorites; comets; and manned and unmanned planetary and lunar flights. For spacecraft design or space stations see 18 Spacecraft Design, Testing and Performance.

20020000735 Malin Space Science Systems, San Diego, CA USA
Mars Data Analysis Program 4th Quarter Deliverable: Slides from the November 2000 Geological Society of America Presentation on Dark Wind Streaks
Edgett, Kenneth S., Malin Space Science Systems, USA; Jul. 16, 2001; In English; Summit 2000: Geological Society of America Annual Meeting and Exposition, 11-19 Nov. 2000, Reno, NV, USA; Sponsored by Geological Society of America, USA; CD-ROM contains j-peg images, HTML files, and Quick-Time motion pictures
Report No.(s): NONP-NASA-CD-2001152919; No Copyright; Avail: CASI; C01, CD-ROM

More than 27,000 pictures at aerial photograph scales (1.5-12 m/pixel) have been acquired by the Mars Global Surveyor (MGS) Mars Orbiter Camera (MOC) since September 1997. The pictures are valuable for testing hypotheses about geologic history and processes of Mars. of particular interest are eolian features connected to surface albedo patterns. This work is focused on low-albedo wind streaks, some over 100 km long, in western Arabia Terra. Each streak is widest where it originates at an impact crater (typically 25-150 km diameter). The streaks taper downwind. Within the associated craters there is a lower-albedo surface that, in nearly all observed cases, includes barchan dunes indicative of transport in the same direction as the wind streaks. Upwind of the dunes there is usually an outcrop of layered material that might have served as a source for dune sand. MOC images show that the west Arabia streaks consist of a smooth-surfaced, multiple-meters-thick, mantle (smooth at 1.5 m/pixel) that appears to be superposed on local surfaces. No dunes are present, indicating that down-streak transport of sediment via saltation and traction have not occurred. Two models might explain the observed properties: (1) the streaks consist of dark silt- and clay-sized grains deflated from the adjacent crater interiors and deposited from suspension or (2) they are remnants (protected in the lee of impact crater rims) of a formerly much larger, regional covering of low albedo, smooth-surfaced mantle. The latter hypothesis is based on observation of low albedo mantled surfaces occurring south of west Arabia in Terra Meridiani. For reasons yet unknown, a large fraction of the martian equatorial regions are covered by low albedo, mesa-forming material that lies unconformably atop eroded layered and cratered terrain. Both hypotheses are being explored via continued selective targeting of new MOC images as well as analyses of the new data.
Author
Albedo; Mars Surface; Sediment Transport; Wind Effects; Spaceborne Photography; Mars Photographs

20020000916 Malin Space Science Systems, San Diego, CA USA
Mars Data Analysis Program 3rd Quarter Deliverable: Small Eolian Landforms-Mars Orbiter Camera Images
Edgett, Kenneth S., Malin Space Science Systems, USA; Jul. 09, 2001; In English; CD-ROM contains several GIF images
Report No.(s): NONP-NASA-CD-2001152917; No Copyright; Avail: CASI; C01, CD-ROM

This CD-ROM is comprised of photographs taken by the Mars Orbital Camera from the Mars Global Surveyor spacecraft. The images are presented in GIF format.
CASI
Mars Photographs; Mars Surface; Landforms; Wind Effects

20020000924 California Univ., Inst. of Geophyics and Planetary Physics, Los Angeles, CA USA
Pick-Up Ion Instabilities at Planetary Magnetospheres ***Final Report, 1 Apr. 1998 - 31 Mar. 2001***
Strangeway, Robert J., California Univ., USA; [2001]; 4p; In English
Contract(s)/Grant(s): NAG5-6965; No Copyright; Avail: CASI; A01, Hardcopy; A01, Microfiche

This effort involved the analysis of low frequency waves as observed by the Galileo spacecraft near the Galilean moon, Io. Io is a significant source of material, especially SO2, and various products of dissociation, and further these atoms and molecules are readily ionized. The initial velocity of the ions is essentially that of the neutral species, i.e., the Keplerian velocity. The plasma, on the other hand is co-rotating, and there is a differential flow of the order 57 km/s between the plasma and the neutral particles. Thus pick-up ion instabilities are Rely to occur within the Jovian magnetosphere. Indeed, magnetometer observations from the Galileo spacecraft clearly show ion cyclotron waves that have been identified with a large variety of plasma species, such as O+, S++ (which has the same gyro-frequency as O+), S+, and SO2+. Typically, however, the dominant frequency is near the SO2+ gyro-frequency. The research effort was originally planned to be a team effort between Robert J. Strangeway as the Principal Investigator, and Debbie Huddleston, who was an Assistant Research Geophysicist at UCLA. Unfortunately, Dr. Huddleston took a position within Industry. The effort was therefore descoped, and Dr. Strangeway instead pursued a collaboration with Dr. Xochitl Blanco-Cano, of the Instituto de Geofisica, Universidad Nacional Autonoma de Mexico. This has proved to be a productive collaboration, with several papers and publications arising out of the effort. The magnetic field oscillations near lo generally fall into two types: ion cyclotron waves, with frequencies near an ion gyro-frequency, and lower frequency mirror-mode waves. The ion cyclotron waves are mainly transverse, and frequently propagate along the ambient magnetic field. The mirror-mode waves are compressional waves, and they have essentially zero frequency in the plasma rest frame. One of the purposes of our investigation is to understand what controls the types of wave modes that occur, since both wave modes can be drive unstable by the pressure anisotropy associated with the pick up ions. The pick ion velocity is perpendicular to the ambient magnetic field, and is generally much larger than the thermal velocity, at least initially. At its simplest, we found that the ion cyclotron waves are controlled by the parameters of the species in gyro-resonance with the wave. Thus, while the growth rates for the lower mass (higher gyro-frequency) pick-up ions are generally larger, we found that the heavier SO2+ ion cyclotron waves are generally preferred. This is because one of the effects of the wave instability is to diffuse the ions in pitch angle and energy. The lower mass ions therefore consist of both a ring of recently created pick-up ions, and a thermal background. This thermal background quenches the ion cyclotron instability. SO2+ is different, however. Being a molecule, the species can also dissociate. Our analysis suggests that the dissociation acts on a time scale comparable to or faster than the velocity space diffusion time scale. There are consequently no thermal SO2+ ions to quench the instability. We have also investigated the mirror-mode. This mode can at times grow more rapidly than the individual ion cyclotron waves. This is mainly because the mirror-mode can grow off the pressure anisotropy of the individual species with which the waves are in resonance. Lastly, as part of this effort we have begun to investigate the instability for obliquely propagating modes. Galileo observations show that at times the ion cyclotron waves are significantly elliptically polarized, and further the wave vector is at a large angle to the field, significant growth can occur for oblique propagation. Depending on the group velocity of the waves, it is possible that obliquely propagating modes have higher advective growth rate, but this has yet to be determined.

Author

Galileo Spacecraft; Io; Ion Cyclotron Radiation; Ionic Waves; Compression Waves

20020000946 NASA Kennedy Space Center, Cocoa Beach, FL USA

A Survey of Alternative Oxygen Production Technologies

Lueck, Dale E., NASA Kennedy Space Center, USA; Parrish, Clyde F., NASA Kennedy Space Center, USA; Buttner, William J., DYNACS Engineering Co., Inc., USA; Surma, Jan M., DYNACS Engineering Co., Inc., USA; [2001]; 7p; In English; Space Technology and International Forum 2001, 11-14 Feb. 2001, Albuquerque, NM, USA; No Copyright; Avail: CASI; A02, Hardcopy; A01, Microfiche

Utilization of the Martian atmosphere for the production of fuel and oxygen has been extensively studied. The baseline fuel production process is a Sabatier reactor, which produces methane and water from carbon dioxide and hydrogen. The oxygen produced from the electrolysis of the water is only half of that needed for methane-based rocket propellant, and additional oxygen is needed for breathing air, fuel cells and other energy sources. Zirconia electrolysis cells for the direct reduction of CO2 are being developed as an alternative means of producing oxygen, but present many challenges for a large-scale oxygen production system. The very high operating temperatures and fragile nature of the cells coupled with fairly high operating voltages leave room for improvement. This paper will survey alternative oxygen production technologies, present data on operating characteristics, materials of construction, and some preliminary laboratory results on attempts to implement each.

Author

Oxygen Production; Mars Atmosphere; Electrolysis

20020001262 Malin Space Science Systems, San Diego, CA USA

Observations Regarding Small Eolian Dunes and Large Ripples on Mars

Edgett, Kenneth S., Malin Space Science Systems, USA; Jul. 12, 2001; 1p; In English; Geological Society of America Annual Meeting, Nov. 2001, USA; No Copyright; Avail: Issuing Activity; Abstract Only

Eolian bedforms occur at the interface between a planetary surface and its atmosphere; they present a proxy record of the influence of climate, expressed in sediment transport, over that surface. High resolution images (1.5 - 12 m/pixel) from the Mars Global Surveyor (MGS) Mars Orbiter Camera provide glimpses of the most recent events shaping the martian landscape. Thousands of images exhibit small transverse dunes or large eolian ripples that have crest-to-crest spacings of 10 to 60 m, heights of a few to 10 m. Bedforms of the size and patterns seen in the Mars photographs are rarely described among Earth's eolian landforms; in terms of size and morphology, most of these fall between traditional definitions of "ripples" and "dunes". Dunes are composed chiefly of materials transported by saltation, ripples are smaller forms moved along by the impact of saltating grains (traction). The largest reported eolian ripples on Earth (granule ripples, megaripples) are typically smaller than the bedforms observed on Mars; likewise, most dunes are typically larger. The small dunes and large ripples on Mars come in a variety of relative albedos, despite an early MGS impression that they are all of high albedo. Some ripples occur on the surfaces of sand dunes; these are most likely true granule ripples. However, most of these bedforms occur in troughs, pits, craters, and on deflated plains. Despite impressions early in the MGS mission, they do not occur everywhere (e.g., they are rare on the northern plains) but they do occur at a range of elevations from the highest volcanoes to the deepest basins. Where they occur on a hard substrate among larger sand dunes, the big dunes have over-ridden the smaller bedforms, indicating that the smaller features are older and perhaps indurated or very coarse-grained. At other locales, the small bedforms have been mantled by material settled from suspension, in other cases they are being exhumed and may be lithified. Still other examples are peppered with small impact craters, implying considerable age. These bedforms present a complicated record of the geologically-recent past, one that has involved changes in climate, sediment transport capabilities, and sediment sources and sinks over time.
Author
Dunes; Sands; Mars Surface; Ripples; Wind Effects

20020001354 Minnesota Univ., Dept. of Geology and Geophysics, Minneapolis, MN USA
High-Temperature Deformation of Dry Diabase with Application to Tectonics on Venus
Mackwell, S. J., Pennsylvania State Univ., USA; Zimmerman, M. E., Minnesota Univ., USA; Kohlstedt, D. L., Minnesota Univ., USA; Journal of Geophysical Research; Jan. 10, 1998; ISSN 0148-0227; Volume 103, No. B1, pp. 975-984; In English
Report No.(s): Paper-97JB02671; Copyright; Avail: Issuing Activity

We have performed an experimental study to quantify the high-temperature creep behavior of natural diabase rocks under dry deformation conditions. Samples of both Maryland diabase and Columbia diabase were investigated to measure the effects of temperature, oxygen fugacity, and plagioclase-to-pyroxene ratio on creep strength. Flow laws determined for creep of these diabases were characterized by an activation energy of Q = 485 +/- 30 kJ/mol and a stress exponent of n = 4.7 +/- 0.6, indicative of deformation dominated by dislocation creep processes. Although n and Q are the same for the two rocks within experimental error, the Maryland diabase, which has the lower plagioclase content, is significantly stronger than the Columbia diabase. Thus the modal abundance of the various minerals plays an important role in defining rock strength. Within the s ample-to-sample variation, no clear influence of oxygen fugacity on creep strength could be discerned for either rock. The dry creep strengths of both rocks are significantly greater than values previously measured on diabase under "as-received" or wet conditions. Application of these results to the present conditions in the lithosphere on Venus predicts a high viscosity crust with strong dynamic coupling between mantle convection and crustal deformation, consistent with measurements of topography and gravity for that planet.
Author
High Temperature; Deformation; Drying; Tectonics; Venus (Planet); Creep Properties; Creep Strength; Lithosphere

20020001357 NASA Goddard Space Flight Center, Greenbelt, MD USA
The Mars Orbiter Altimeter (MOLA) Investigation of the Shape and Topography of Mars
Smith, David E., NASA Goddard Space Flight Center, USA; Zuber, Maria T., Massachusetts Inst. of Tech., USA; [2001]; 1p; In English; 3rd Topical Meeting on Optoelectric Distance/Displacement Measurements and Applications, 20-22 Sep. 2001, Pavia, Italy; No Copyright; Avail: Issuing Activity; Abstract Only

The Mars Orbiter Laser Altimeter (MOLA) is an instrument on the Mars Global Surveyor (MGS) spacecraft that has been orbiting Mars since September 1997. After some preliminary observations in Sept/Oct, 1997 and in the spring and summer of 1998, the MGS spacecraft entered its mapping orbit of 400 km above the surface of Mars in February 1999. MGS began a 2 year program of systematically mapping the planet with a camera (MOC), thermal emission spectrometer (TES), magnetometer (MAG), laser altimeter (MOLA), and a radio science investigation for gravity and radio occultations. MOLA has a 48mJ, 1064 nrn ND:YAG, diode pumped laser with a 8 nanosecond pulse width, a pulse rate of 10 Hz, and a range precision of less than 40 cm. MOLA has been operating almost continuously for over two years and obtained over 600 million measurements of the radius of Mars. Using very precise orbits for the MGS spacecraft derived from the Doppler and range tracking of MGS by the Deep Space

Network a topographical map of Mars has been developed with an average radial accuracy of a meter and a horizontal accuracy of 100 meters. This topographical map has revealed a new Mars, a planet with some of the flattest areas in the solar system and one of the largest impact basins. MOLA has revealed clear evidence of the effect of past fluid action on the surface and found icecaps that contain as much water ice today as the icecap of Greenland.
Author
Laser Altimeters; Mars (Planet); Mars Global Surveyor; Topography; Planetary Geology

20020001358 NASA Goddard Space Flight Center, Greenbelt, MD USA
Mapping Mars with a Laser Altimeter
Smith, David E., NASA Goddard Space Flight Center, USA; [2001]; 1p; In English; SPIE's International Symposium on Remote Sensing, 17-21 Sep. 2001, Toulouse, France; Sponsored by International Society for Optical Engineering, USA; No Copyright; Avail: Issuing Activity; Abstract Only

In November 1996 the Mars Global Surveyor (MGS) spacecraft was launched to Mars. One of the instruments on the spacecraft was a laser altimeter, MOLA, for measuring the shape and topography of the planet. The altimeter has a diode pumped Q-switched ND:YAG laser at 1064nm, operating at 10Hz with an 8 nsec pulse width. The pulse energy is 48mJ, and the instrument has a 37cm ranging precision. The laser illuminates a spot on the surface of Mars approximately 160 meters in diameter and the instrument has accumulated over 600 million range measurements of the surface since arrival at Mars in September 1997. MOLA has operated continuously for over 2 years and has mapped the planet at a horizontal resolution of about 1 km and a radial accuracy of about a meter. MOLA has measured the shape of the planet, the heights of the volcanoes, the depths of the canyons, and the volumes of the polar icecaps. It has detected carbon dioxide clouds and measured the accumulation of seasonal CO2 on the polar icecaps. This new remote sensing tool has helped transform our understanding of Mars and its geological history, and opened a new door to planetary exploration.
Author
Laser Altimeters; Mars Surface; Remote Sensing; Planetary Mapping; Mars (Planet)

20020002000 Sandia National Labs., Albuquerque, NM USA
Structural Analyses of the JPL Mars Pathfinder Impacts
Gwinn, K. W.; Apr. 01, 1999; 116p; In English
Report No.(s): DE2001-5898; SAND99-0752; No Copyright; Avail: Department of Energy Information Bridge

The purpose of this report is to detail the general design loadings determined from an analytical study of the Jet Propulsion Laboratory (JPL) Mars Pathfinder vehicle landing onto the Martian surface. The Pathfinder is a tetrahedral shaped structure that is protected by large airbags attached to the four faces of the lander. This lander system uses airbags to envelope the lander experiment package, protecting it with large deformation upon contact. The airbags protect the lander by deforming, thereby lengthening the impact duration in order to limit the accelerations into the Pathfinder structure. The loadings onto the Pathfinder during several impact scenarios have been predicted using explicit finite element analysis. This report details these results.
NTIS
Impact Strength; Structural Analysis; Numerical Analysis; Spacecraft

20020002274 Lawrence Livermore National Lab., Livermore, CA USA
Wet mars: plentiful, readily-available martian water and its implications
Hyde, R.; Ishikawa, M.; Nuckolls, J.; Whitehead, J.; Wood, L.; Aug. 12, 1999; 14p; In English
Report No.(s): DE2001-12466; UCRL-JC-135329; No Copyright; Avail: Department of Energy Information Bridge, Microfiche

Water and its major constituent, oxygen, in large specific quantities are essential for maintenance of human life. Providing them in adequate quantities is widely believed to be a major challenge for human Mars exploration and settlement. The Martian regolith isn't known to bear either water or hydrogen, the ice-rich Martian polar regions are thermally inhospitable, and the measured water content of Mars' thin atmosphere represents a layer of liquid water of average thickness only about 1% that of the Moon: (approximately)0.001 cm. Crucially, however, the atmospheric Martian water inventory is advected to every place on Mars by meteorological phenomena, so that the few cubic kilometers of liquid water-equivalent in the atmosphere are available most anywhere when, merely for the effort of condensing it. Well-engineered apparatus deployed essentially anywhere on Mars can condense water from the atmosphere in daily quantities not much smaller than its own mass, rejecting into space from radiators deployed over the local terrain the water's heat-of-condensation and the heat from non-ideality of the equipment's operation. Thus, an optimized, photovoltaically-powered 0.3 ton water-condensing system could strip 40 tons of water each year from (approximately)10(exp 4) times this mass of thin, dry Martian air. Given a 480 set I(sub sp) of H2-O2 propulsion systems exhausting into the 6 millibar Mars-surface atmosphere and the 5.0 km/s Martian gravity well, (ge)40 tons of water two-thirds

converted into 5:1 O2/H2 cryogenic fuel could support exploration and loft a crew-of-four and their 8-ton ascent vehicle into Earth-return trajectory. The remaining water and excess oxygen would suffice for half-open-cycle life support for a year's stay on Mars. A Mars Expedition thus needs to land only explorers, dehydrated food, habitation gear and unfueled exploration I Earth-return equipment - and a water/oxygen/fuel plant with embedded power supply which operates on Martian atmospheric water. All of the oxygen, water and propellants necessary for life-support, extensive exploration and Earth-return can be provided quite readily by the host planet. The most challenging technical problem with respect to human expeditions to Mars is that of escaping from Earth's deep, 11.2 km/s gravity well. Living on Mars, exploring it extensively and returning to Earth each are technically much less difficult, thanks in no small part to the effective 'wetness'of Mars.
NTIS
Oxygen; Water; Mars (Planet); Mars Atmosphere; Mars Surface; Meteorological Parameters; Moisture Content

20020005122 NASA Ames Research Center, Moffett Field, CA USA
Intensity Measurements of the 01(sup 1)21-00(sup 0)01 Perpendicular CO2 band at 5315 cm (sup -1) and 4 related hot bands
Giver, Lawrence P., NASA Ames Research Center, USA; Chackerian, Charles, Jr., NASA Ames Research Center, USA; Spencer, Mark N., NASA Ames Research Center, USA; Brown, Linda R., Jet Propulsion Lab., California Inst. of Tech., USA; Wattson, Richard B., Stuart Radiance Lab., USA; [1994]; 1p; In English; 26th Annual Meeting of the Division of Planetary Sciences of the American Astronomical Society, 31 Oct. - 4 Nov. 1994, Bethesda, MD, USA
Contract(s)/Grant(s): RTOP 154-50-80; No Copyright; Avail: Issuing Activity; Abstract Only

The near-infrared thermal emission windows in the spectrum of the night-side of Venus have stimulated new determinations of the intensities of weak CO2 bands which are prominent absorption features in Venus spectra. We have previously measured the 31(sup 1)04-00(sup 0)01 band at 4416 cm (sup -1), which dominates a portion of the 2.2 micrometer window, using the 25-meter White absorption cell at Ames. Parameters for many of the unmeasured bands have been recomputed for the HITRAN compilation using direct numerical diagonalization. This procedure has some uncertainties, particularly for higher overtone-combination perpendicular bands, and substantial differences were noted for these bands when comparing the 1986 HITRAN tabulation with the 1992 values. To clarify this situation, we decided to measure the intensities of several of these bands; L.R.B. obtained spectra using the McMath FTS and 6 meter White cell, covering the region 3800 to 7700 cm (sup -1). A table is provided in which we compare our measured intensities and Herman-Wallis al parameters for the 01(sup 1)21-00(sup 0)01 band and 4 associated hot bands with both Hitran tabulations. It is anticipated that these measured values will be useful in further DND calculations of many very weak unmeasurable bands.
Author
Venus (Planet); Carbon Dioxide; Absorption Spectra

20020005136 Malin Space Science Systems, San Diego, CA USA
Mars Global Surveyor Mars Orbiter Camera: Interplanetary Cruise through Primary Mission
Malin, Michael C., Malin Space Science Systems, USA; Edgett, Kenneth S., Malin Space Science Systems, USA; Journal of Geophysical Research; 2001; ISSN 0148-0277, pp. 1-146; In English
Contract(s)/Grant(s): JPL-959060; JPL-1200780
Report No.(s): Paper-2000JE001455; Copyright; Avail: Issuing Activity

More than three years of high-resolution (1.5-20 m/pixel) photographic observations of the surface of Mars have dramatically changed our view of that planet. Among the most important observations and interpretations derived therefrom are that much of Mars, at least to depths of several kilometers, is layered; that substantial portions of the planet have experienced burial and subsequent exhumation; that layered and massive units, many kilometers thick, appear to reflect an ancient period of large-scale erosion and deposition within what are now the ancient heavily cratered regions of Mars; and that processes previously unsuspected, including gully-forming fluid action and burial and exhumation of large tracts of land, have operated within near-contemporary times. These and many other attributes of the planet argue for a complex geology and complicated history.
Author
Planetary Geology; Mars Surface; Photographic Recording; Folds (Geology)

20020005141 NASA Ames Research Center, Moffett Field, CA USA
Planetary Rings
Cuzzi, Jeffrey N., NASA Ames Research Center, USA; [1994]; 1p; In English; 1994 American Geophysical Union (AGU) Meeting, 5-9 Dec. 1994, San Francisco, CA, USA; Sponsored by American Geophysical Union, USA; No Copyright; Avail: Issuing Activity; Abstract Only

Just over two decades ago, Jim Pollack made a critical contribution to our understanding of planetary ring particle properties, and resolved a major apparent paradox between radar reflection and radio emission observations. At the time, particle properties were about all there were to study about planetary rings, and the fundamental questions were, why is Saturn the only planet with rings, how big are the particles, and what are they made of? Since then, we have received an avalanche of observations of planetary ring systems, both from spacecraft and from Earth. Meanwhile, we have seen steady progress in our understanding of the myriad ways in which gravity, fluid and statistical mechanics, and electromagnetism can combine to shape the distribution of the submicron-to-several-meter size particles which comprise ring systems into the complex webs of structure that we now know them to display. Insights gained from studies of these giant dynamical analogs have carried over into improved understanding of the formation of the planets themselves from particle disks, a subject very close to Jim's heart. The now-complete reconnaissance of the gas giant planets by spacecraft has revealed that ring systems are invariably found in association with families of regular satellites, and there is ark emerging perspective that they are not only physically but causally linked. There is also mounting evidence that many features or aspects of all planetary ring systems, if not the ring systems themselves, are considerably younger than the solar system

Author

Planetary Rings; Planetary Evolution; Gas Giant Planets

20020005863 NASA Ames Research Center, Moffett Field, CA USA

The Greenhouse and Anti-Greenhouse Effects on Titan

McKay, C. P., NASA Ames Research Center, USA; [1994]; 1p; In English; 1994 American Geophysical Union Meeting, 5-9 Dec. 1994, San Francisco, CA, USA; No Copyright; Avail: Issuing Activity; Abstract Only

Titan is the largest moon of Saturn and is the only moon in the solar system with a substantial atmosphere. Its atmosphere is mostly made of nitrogen, with a few percent CH4, 0.1% H2 and an uncertain level of Ar (less than 10%). The surface pressure is 1.5 atms and the surface temperature is 95 K, decreasing to 71 at the tropopause before rising to stratospheric temperatures of 180 K. In pressure and composition Titan's atmosphere is the closest twin to Earth's. The surface of Titan remains unknown, hidden by the thick smog layer, but it may be an ocean of liquid methane and ethane. Titan's atmosphere has a greenhouse effect which is much stronger than the Earth's - 92% of the surface warming is due to greenhouse radiation. However an organic smog layer in the upper atmosphere produces an anti-greenhouse effect that cuts the greenhouse warming in half - removing 35% of the incoming solar radiation. Models suggest that during its formation Titan's atmosphere was heated to high temperatures due to accretional energy. This was followed by a cold Triton-like period which gradually warmed to the present conditions. The coupled greenhouse and haze anti-greenhouse may be relevant to recent suggestions for haze shielding of a CH4 - NH3 early atmosphere on Earth or Mars. When the NASA/ESA mission to the Saturn System, Cassini, launches in a few years it will carry a probe that will be sent to the surface of Titan and show us this world that is strange and yet in many ways similar to our own. Author

Greenhouse Effect; Titan; Satellite Atmospheres

92
SOLAR PHYSICS

Includes solar activity, solar flares, solar radiation and sunspots. For related information see 93 Space Radiation.

20020001264 Science Applications International Corp., San Diego, CA USA

Global Magnetohydrodynamic Modeling of the Solar Corona ***Final Report, 30 Sep. 1998 - 29 Sep. 2001***

Linker, Jon A., Science Applications International Corp., USA; 2001; 17p; In English; Original contains color illustrations

Contract(s)/Grant(s): NASW-98030

Report No.(s): SAIC-01/8020:APPAT-287; No Copyright; Avail: CASI; A03, Hardcopy; A01, Microfiche

The solar corona, the hot, tenuous outer atmosphere of the Sun, exhibits many fascinating phenomena on a wide range of scales. One of the ways that the Sun can affect us here at Earth is through the large-scale structure of the corona and the dynamical phenomena associated with it, as it is the corona that extends outward as the solar wind and encounters the Earth's magnetosphere. The goal of our research sponsored by NASA's Supporting Research and Technology Program in Solar Physics is to develop increasingly realistic models of the large-scale solar corona, so that we can understand the underlying properties of the coronal magnetic field that lead to the observed structure and evolution of the corona. We describe the work performed under this contract. Derived from text

Magnetohydrodynamics; Solar Corona; Solar Magnetic Field; Mathematical Models; Heliosphere; Solar Simulation

20020002221 NASA Ames Research Center, Moffett Field, CA USA

Structure, Shape and Movement of the Termination Shock

Barnes, Aaron, NASA Ames Research Center, USA; [1994]; 1p; In English, 31 May - 3 Jun. 1994, Durham, NH, USA
Contract(s)/Grant(s): RTOP 170-10-10-16; No Copyright; Avail: Issuing Activity; Abstract Only

In this paper we review current ideas concerning the morphology and dynamics of the heliospheric termination shock. The mean distance of the shock is expected to lie somewhere in the range 50-200 AU, and should vary with latitude, depending on mean latitude variation of the dynamical pressure of the solar wind. The shock is expected to move in response to variation in upstream solar wind conditions, so that at any particular instant the termination shock will resemble a distorted asymmetric balloon with some parts moving inward and others moving outward. The simplest model of the shock is that of an infinitely thin gasdynamic or magnetohydrodynamic shock wave, which moves inward or outward at speeds of approximately 100 kilometers per second. The structure and motion of the shock will be strongly modified if an appreciable fraction of the incident solar wind energy goes into acceleration of energetic particles, specifically the anomalous cosmic rays.
Author

Heliosphere; Magnetohydrodynamic Waves; Morphology; Shock Waves; Acceleration (Physics)

20020002330 NASA Goddard Space Flight Center, Greenbelt, MD USA

Model of Wave Driven Flow Oscillation for Solar Cycle

Mayr, Hans G., NASA Goddard Space Flight Center, USA; Wolff, Charles L., NASA Goddard Space Flight Center, USA; [2001]; 1p; In English; AGU Spring Meeting, 29 May - 2 Jun. 2001, Boston, MA, USA; Sponsored by American Geophysical Union, USA; No Copyright; Avail: Issuing Activity; Abstract Only

At low latitudes in the Earth's atmosphere, the observed zonal flow velocities are dominated by the semi-annual and quasi-biennial oscillations with periods of 6 months and 20 to 32 months respectively. These terrestrial oscillations, the SAO and QBO respectively, are driven by wave-mean flow interactions due to upward propagating planetary-scale waves (periods of days) and small-scale gravity waves (periods of hours). We are proposing (see also Mayr et al., GRL, 2001) that such a mechanism may drive long period oscillations (reversing flows) in stellar and planetary interiors, and we apply it to the Sun. The reversing flows would occur below the convective envelope where waves can propagate. We apply a simplified, one dimensional, analytical flow model that incorporates a gravity wave parameterization due to Hines (1997). Based on this analysis, our estimates show that relatively small wave amplitudes less than 10 m/s can produce zonal flow amplitudes of 20 m/s, which should be sufficient to generate the observed variations in the magnetic field. to produce the 22-year period of oscillation, a low buoyancy frequency must be chosen, and this places the proposed flow in a region that is close to (and below) the base of the convective envelope. Enhanced turbulence associated with this low stability should help to generate the dynamo currents. With larger stability at deeper levels in the solar interior, the model can readily produce also oscillations with much longer periods. to provide an understanding of the fluid dynamics involved, we present numerical results from a 2D model for the terrestrial atmosphere that exemplify the non-linear nature of the wave interaction for which a mechanical analog is the escapement mechanism of the clock.
Author

Oscillating Flow; Solar Cycles; Sun; Wave Propagation; Mathematical Models

20020002700 NASA Goddard Space Flight Center, Greenbelt, MD USA

Obliquity Modulation of the Incoming Solar Radiation

Liu, Han-Shou, NASA Goddard Space Flight Center, USA; Recent Research Development in Atmosphere Sciences; 2001; Volume 1, pp. 15-37; In English; ISBN 81-7736-059-0; No Copyright; Avail: CASI; A03, Hardcopy; A01, Microfiche

Based on a basic principle of orbital resonance, we have identified a huge deficit of solar radiation induced by the combined amplitude and frequency modulation of the Earth's obliquity as possibly the causal mechanism for ice age glaciation. Including this modulation effect on solar radiation, we have performed model simulations of climate change for the past 2 million years. Simulation results show that: (1) For the past 1 million years, temperature fluctuation cycles were dominated by a 100-Kyr period due to amplitude-frequency resonance effect of the obliquity; (2) From 2 to 1 million years ago, the amplitude-frequency interactions. of the obliquity were so weak that they were not able to stimulate a resonance effect on solar radiation; (3) Amplitude and frequency modulation analysis on solar radiation provides a series of resonance in the incoming solar radiation which may shift the glaciation cycles from 41-Kyr to 100-Kyr about 0.9 million years ago. These results are in good agreement with the marine and continental paleoclimate records. Thus, the proposed climate response to the combined amplitude and frequency modulation of the Earth's obliquity may be the key to understanding the glaciation puzzles in paleoclimatology.
Author

Amplitude Modulation; Paleoclimatology; Solar Radiation; Solar Terrestrial Interactions; Obliqueness; Orbital Resonances (Celestial Mechanics)

20020002855 California Univ., Lawrence Berkeley Lab., Berkeley, CA USA

Towards the resolution of the solar neutrino problem

Friedland, A.; Aug. 29, 2000; 190p; In English

Report No.(s): DE2001-767627; LBNL-46714; No Copyright; Avail: Department of Energy Information Bridge

A number of experiments have accumulated over the years a large amount of solar neutrino data. The data indicate that the observed solar neutrino flux is significantly smaller than expected and, furthermore, that the electron neutrino survival probability is energy dependent. This 'solar neutrino problem' is best solved by assuming that the electron neutrino oscillates into another neutrino species. Even though one can classify the solar neutrino deficit as strong evidence for neutrino oscillations, it is not yet considered a definitive proof. Traditional objections are that the evidence for solar neutrino oscillations relies on a combination of hard, different experiments, and that the Standard Solar Model (SSM) might not be accurate enough to precisely predict the fluxes of different solar neutrino components. Even though it seems unlikely that modifications to the SSM alone can explain the current solar neutrino data, one still cannot completely discount the possibility that a combination of unknown systematic errors in some of the experiments and certain modifications to the SSM could conspire to yield the observed data. to conclusively demonstrate that there is indeed new physics in solar neutrinos, new experiments are aiming at detecting 'smoking gun' signatures of neutrino oscillations, such as an anomalous seasonal variation in the observed neutrino flux or a day-night variation due to the regeneration of electron neutrinos in the Earth. In this dissertation we study the sensitivity reach of two upcoming neutrino experiments, Borexino and KamLAND, to both of these effects. Results of neutrino oscillation experiments for the case of two-flavor oscillations have always been presented on the (sin(sup 2) 2(theta), (Delta)m(sup 2)) parameter space. We point out, however, that this parameterization misses the half of the parameter space (pi)/4 < (theta) (le) (pi)/2, which is physically inequivalent to the region 0 (le) (theta) (le) (pi)/4 in the presence of matter effects. The MSW solutions to the solar neutrino problem can extend to the ((theta) greater than (pi)/4) side. Furthermore, even the 'vacuum oscillation' solutions are affected by solar matter effects and hence are different in the two sides.

NTIS

Solar Neutrinos; Solar Oscillations; Parameterization; Annual Variations

20020003562 Los Alamos National Lab., NM USA

Solar terrestrial coupling through space plasma processes

Birn, J.; Dec. 01, 2000; 33p; In English

Report No.(s): DE2001-768901; LA-UR-00-5748; No Copyright; Avail: Department of Energy Information Bridge, Microfiche

This is the final report of a three-year, Laboratory-Directed Research and Development (LDRD) project at the Los Alamos National Laboratory (LANL). The project investigates plasma processes that govern the interaction between the solar wind, charged particles ejected from the sun, and the earth's magnetosphere, the region above the ionosphere governed by the terrestrial magnetic field. Primary regions of interest are the regions where different plasma populations interact with each other. These are regions of particularly dynamic plasma behavior, associated with magnetic flux and energy transfer and dynamic energy release. The investigations concerned charged particle transport and energization, and microscopic and macroscopic instabilities in the magnetosphere and adjacent regions. The approaches combined space data analysis with theory and computer simulations.

NTIS

Earth Magnetosphere; Plasmas (Physics); Solar Activity

20020005095 NASA Ames Research Center, Moffett Field, CA USA

Meteoritic Constraints on Models of the Solar Nebula: The Abundances of Moderately Volatile Elements

Cassen, P., NASA Ames Research Center, USA; [1994]; 1p; In English; 26th Annual Meeting of the Division for Planetary Sciences, 29 Oct. - 9 Nov. 1994, Washington, DC, USA

Contract(s)/Grant(s): RTOP 452-21-93-99; No Copyright; Avail: Issuing Activity; Abstract Only

The "moderately volatile" elements are those which condense (or evaporate) in the temperature range 650 - 1350 K, as a mix of material with solar abundances is cooled (or heated) under equilibrium conditions. Their relative abundances in chondritic meteorites are solar (or "cosmic", as defined by tile composition of CI meteorites) to within a factor of several, but vary within that range in a way that correlates remarkably well with condensation temperature, independent of chemical affinity. It has been argued that this correlation reflects a systematically selective process which favored the accretion of refractory material over volatile material from a cooling nebula. Wasson and Chou suggested that condensation and settling of solids contemporaneously with the cooling and removal of nebular gas could produce tile observed abundance patterns, but a quantitative model has been lacking. We show that the abundance patterns of the moderately volatile elements in chondritic meteorites can be produced, in some degree of quantitative detail, by models of the solar nebula that are designed to conform to observations of T Tauri stars and the global conservation laws. For example, even if the local surface density of the nebula is not decreasing, condensation and

accretion of solids from radially inflowing gas in a cooling nebula can result in depletions of volatiles, relative to refractories, like those observed. The details of the calculated abundance patterns depend on (but are not especially sensitive to) model parameters, and can exhibit the variations that distinguish the meteorite classes. Thus it appears that nebula characteristics Such as cooling rates, radial flow velocities, and particle accumulation rates can be quantitatively constrained by demanding that they conform to meteoritic data; and the models, in turn, can produce testable hypotheses regarding the time and location of the formation of the chondrite parent bodies and the planets.
Author
Solar Nebula; Meteoritic Composition; Volatility

20020005191 Los Alamos National Lab., NM USA
Does the Sun still shine?
Karataglidis, S.; Jennings, B.; Jun. 01, 2000; 11p; In English
Report No.(s): DE2001-768967; LA-UR-00-2428; No Copyright; Avail: Department of Energy Information Bridge

The astrophysical S factor for the Be-7(p, (gamma))B-8 reaction at threshold is investigated using simple models to determine the model dependence in the extrapolation of the laboratory data to the region of astrophysical interest near 20 keV. We find that the energy dependence below 400 keV is largely well understood in terms of the Coulomb interaction and constrained by the data for the elastic scattering of low-energy neutrons from Li-7.
NTIS
Elastic Scattering; Astrophysics; Sun

93
SPACE RADIATION

Includes cosmic radiation; and inner and outer Earth radiation belts. For biological effects of radiation on plants and animals see 52 Aerospace Medicine. For theory see 73 Nuclear Physics.

20020000904 Argonne National Lab., IL USA
Seasonal variations in Soudan 2
Goodman, M. C.; Jun. 23, 1999; 6p; In English
Report No.(s): DE2001-11872; ANL-HEP-CP-99-62; No Copyright; Avail: Department of Energy Information Bridge, Microfiche

Seasonal Variations in an underground detector may be a signature for Dark Matter. The Soudan 2 detector searches for nucleon decay and atmospheric neutrinos. The trigger rate is about 0.5 Hertz. It is dominated by approximately equal numbers of atmospheric muons and low level radioactivityy. The muon rate has a seasonal variation of (+-)2%, which is consistent with a similar effect at MACRO. The MACRO effect has been correlated with temperature in the upper atmosphere. Our trigger rate has a seasonal variation of (+-)15% which we believe is due to radon in the mine, and variations in air flow with outside temperature.
NTIS
Radiation Detectors; Annual Variations; Dark Matter

20020000905 Argonne National Lab., IL USA
Cygnus X-3 revisited: 10 years of muon and radio observations
Allison, W. W. M.; Alner, G. J.; Ayres, D. S.; Barrett, W. L.; Bode, C.; Jun. 23, 1999; 6p; In English
Report No.(s): DE2001-11871; ANL-HEP-CP-99-61; No Copyright; Avail: Department of Energy Information Bridge, Microfiche

The Soudan 2 deep underground tracking calorimeter has recorded cosmic ray muon tracks from the direction of the galactic x-ray binary Cygnus X-3 on most transits during the interval 1989-1998. We analyze these events in the context of previous reports of Cygnus X-3-related muon flux during major radio flares of that source. We find some evidence for excess flux during a small number of transits coincident with major radio flares. We also find an indication that these events maybe distributed around the source with a Gaussian point spread function with (sigma) = 1.3(degree), larger than the instrumental angular spread of < 0.3(degree), verified by observation of the shadow of the moon.
NTIS
Calorimeters; Muons; Detection; Cosmic Rays

20020001356 NASA Goddard Space Flight Center, Greenbelt, MD USA

Are Soft Gamma-ray Repeaters (SGRs) 'Magnetars'?

Strohmayer, Tod E., NASA Goddard Space Flight Center, USA; [2001]; 1p; In English, 4 Apr. 2001, University Park, PA, USA; No Copyright; Avail: Issuing Activity; Abstract Only

Soft Gamma-ray repeaters (SGRs) are among the most powerful Galactic sources of high energy radiation. These objects are even powerful enough to influence processes occurring in the near Earth environment. In the last few years X-ray observations with the Rossi X-ray Timing Explorer (RXTE) have provided us with a new understanding of SGRs. RXTE was instrumental in the discovery that SGRs are rapidly slowing X-ray pulsars and is still providing continued monitoring of their pulse periods. SGR bursts have now been observed with unprecedented sensitivity. I will review the current status of our knowledge of SGRs based on these recent X-ray observations and discuss their implications for models of SGRs, including the now substantial evidence that these objects are highly magnetized neutron stars or 'magnetars'. I will also describe recent spectral studies of SGR bursts which have revealed several new phenomena, including a burst with strong spectral evolution and evidence for a 6.4 keV emission line. Author

X Ray Timing Explorer; Magnetars; Soft Gamma Repeaters; Astrophysics

20020001664 Lawrence Livermore National Lab., Livermore, CA USA

Batse observations of bl lac objects

Connaughton, V.; Laurent-Muehleisen, S.; McCollough, M. A.; Robinson, C. F.; Jun. 01, 1998; 6p; In English

Report No.(s): DE2001-2798; UCRL-JC-132532; REPT-95-ERI-006; No Copyright; Avail: Department of Energy Information Bridge, Microfiche

The Burst and Transient Source Experiment (BATSE) on the Compton Gamma-Ray Observatory has been shown to be sensitive to non-transient hard X-ray sources in our galaxy, down to flux levels of 100 mCrab for daily measurements, 3 mCrab for integrations over several years. We use the continuous BATSE database and the Earth Occultation technique to extract average flux values between 20 and 2OO keV from complete and radio- and X-ray- selected BL Lac samples over a 2 year period. NTIS

BL Lacertae Objects; X Ray Sources; Flux Quantization

99
GENERAL

Includes aeronautical, astronautical, and space science related histories, biographies, and pertinent reports too broad for categorization; histories or broad overviews of NASA programs such as Apollo, Gemini, and Mercury spacecraft, Earth Resources Technology Satellite (ERTS), and Skylab; NASA appropriations hearings.

20020000779 NASA Goddard Space Flight Center, Greenbelt, MD USA

A New Sputnik Surprise?

Lowman, Paul D., Jr., NASA Goddard Space Flight Center, USA; [2001]; 19p; In English; No Copyright; Avail: CASI; A03, Hardcopy; A01, Microfiche

This paper suggests that a new "Sputnik surprise" in the form of a joint Chinese-Russian lunar base program may emerge in this decade. The Moon as a whole has been shown to be territory of strategic value, with discovery of large amounts of hydrogen (probably water ice) at the lunar poles and helium 3 everywhere in the soil, in addition to the Moon's scientific value as an object of study and as a platform for astronomy. There is thus good reason for a return to the Moon, robotically or manned. Relations between China and Russia have thawed since the mid-1990s, and the two countries have a formal space cooperation pact. It is argued here that a manned lunar program would be feasible within 5 years, using modern technology and proven spacecraft and launch vehicles. The combination of Russian lunar hardware with Chinese space technology would permit the two countries together to take the lead in solar system exploration in the 21st century.
Author

Aerospace Engineering; Sputnik Satellites; Spacecraft Launching; Lunar Programs

Subject Term Index

A

ABERRATION, 445
ABIOGENESIS, 274, 276, 330, 332
ABLATION, 63, 448
ABLATIVE MATERIALS, 147, 148, 161
ABRASIVES, 228
ABSORBENTS, 65
ABSORPTION SPECTRA, 465, 532
ABSORPTION SPECTROSCOPY, 161, 163, 394
ACCELERATED LIFE TESTS, 37, 206
ACCELERATION (PHYSICS), 16, 396, 466, 534
ACCELERATORS, 205, 404, 405, 406, 414, 442, 466, 504, 516
ACCELEROMETERS, 452
ACCEPTOR MATERIALS, 472
ACCIDENTS, 4
ACCRETION DISKS, 345
ACCUMULATORS, 410
ACETYLENE, 107
ACIDITY, 216, 289, 290
ACIDS, 45
ACOUSTIC EXCITATION, 235
ACOUSTIC PROPAGATION, 418
ACOUSTIC RESONANCE, 417
ACOUSTIC VELOCITY, 235, 418
ACOUSTICS, 417
ACRYLATES, 96
ACTINIDE SERIES, 27
ACTINIDE SERIES COMPOUNDS, 213, 398
ACTIVATED CARBON, 215
ACTIVATION ENERGY, 43
ACTIVE GALACTIC NUCLEI, 526
ACTIVITY (BIOLOGY), 272, 286, 291, 298, 322
ACTUATORS, 157
ADAPTATION, 322
ADAPTIVE CONTROL, 23
ADAPTIVE OPTICS, 349, 448, 455
ADDITIVES, 480, 485, 493
ADENOSINE TRIPHOSPHATE, 273
ADHESIVES, 102
ADIABATIC DEMAGNETIZATION COOLING, 480
ADSORPTION, 71, 81, 268
ADVANCED VERY HIGH RESOLUTION RADIOMETER, 255
AERIAL EXPLOSIONS, 8
AEROBES, 220
AERODYNAMIC DRAG, 2
AERODYNAMIC INTERFERENCE, 15
AERODYNAMIC LOADS, 2
AERODYNAMICS, 1, 115
AEROGELS, 84
AEROSOLS, 187, 211, 215, 220, 224, 232, 248, 251, 269, 310
AEROSPACE ENGINEERING, 266, 351, 537
AEROSPACE ENVIRONMENTS, 266
AEROSPACE INDUSTRY, 116
AEROSPACE MEDICINE, 261
AEROSPACE SYSTEMS, 357
AEROSPACE VEHICLES, 16
AFRICA, 178
AGING (MATERIALS), 37, 88
AGING (METALLURGY), 121
AGRICULTURE, 108, 229
AIR, 146, 453
AIR CONDITIONING, 120
AIR CONDITIONING EQUIPMENT, 203
AIR FLOW, 144, 150, 152, 153
AIR INTAKES, 119
AIR LOCKS, 18
AIR NAVIGATION, 7
AIR POLLUTION, 32, 66, 67, 99, 192, 211, 214, 215, 216, 217, 218, 219, 223, 226, 227, 230, 233
AIR QUALITY, 108, 215, 216, 226, 228
AIR SAMPLING, 213, 219
AIR TRAFFIC CONTROL, 3, 8, 128, 365
AIR TRANSPORTATION, 3, 5
AIR WATER INTERACTIONS, 235, 310
AIRBORNE LASERS, 163
AIRCRAFT ACCIDENT INVESTIGATION, 8
AIRCRAFT ACCIDENTS, 4, 8
AIRCRAFT APPROACH SPACING, 3
AIRCRAFT COMMUNICATION, 9
AIRCRAFT CONTROL, 7, 145
AIRCRAFT INDUSTRY, 7
AIRCRAFT PILOTS, 264
AIRCRAFT STRUCTURES, 10
AIRCRAFT WAKES, 3
AIRFIELD SURFACE MOVEMENTS, 365
AIRFOILS, 11
AIRLINE OPERATIONS, 3, 5, 6, 9
AIRPORT SECURITY, 6
AIRPORTS, 4, 6, 7
AIRSHIPS, 14
ALASKA, 184
ALBEDO, 528
ALCOHOLS, 112
ALGAE, 293, 327
ALGORITHMS, 123, 130, 169, 187, 238, 263, 353, 355, 365, 371, 375, 377, 388, 417, 428, 478, 498, 500
ALIGNMENT, 458
ALIPHATIC HYDROCARBONS, 103, 225
ALKALINITY, 300
ALKANES, 104
ALKYL COMPOUNDS, 340
ALLERGIC DISEASES, 260
ALLOYS, 73, 76, 80, 118
ALPHA DECAY, 426
ALPHA PARTICLES, 27
ALTERNATING CURRENT, 208
ALTERNATING DIRECTION IMPLICIT METHODS, 478
ALTERNATIVES, 211
ALUMINUM, 10, 41, 58, 65, 79, 113, 481
ALUMINUM ALLOYS, 27, 74, 78, 490
ALUMINUM ARSENIDES, 449
ALUMINUM COATINGS, 465
ALUMINUM GALLIUM ARSENIDES, 73
ALUMINUM HYDRIDES, 494
ALUMINUM OXIDES, 35, 55, 61, 82, 83, 485
AMERICIUM, 46
AMERICIUM 241, 436
AMINO ACIDS, 268, 273, 277, 292, 294, 346
AMMONIA, 32, 218
AMMONIUM COMPOUNDS, 494
AMORPHOUS MATERIALS, 37, 92, 96, 471, 490
AMORPHOUS SILICON, 487
AMPLIFICATION, 279
AMPLITUDE MODULATION, 534
ANAEROBES, 296
ANALOGS, 284, 305
ANALYTICAL CHEMISTRY, 27, 32
ANGULAR DISTRIBUTION, 59
ANGULAR MOMENTUM, 401
ANGULAR VELOCITY, 16
ANIMALS, 322, 330
ANISOTROPY, 82, 365
ANNEALING, 47, 82, 129, 133

ANNIHILATION REACTIONS, 411, 425, 468
ANNUAL VARIATIONS, 226, 237, 238, 256, 260, 535, 536
ANODES, 195, 196, 482
ANOMALIES, 226
ANOXIA, 276, 283
ANTARCTIC REGIONS, 266, 288, 296
ANTENNA DESIGN, 138
ANTENNAS, 127
ANTHROPOMETRY, 369
ANTIBODIES, 315
ANTIFERROMAGNETISM, 140, 471, 489
ANTIPROTONS, 468
APERTURES, 130, 401
APEXES, 375
APPLICATION SPECIFIC INTEGRATED CIRCUITS, 457
APPLICATIONS PROGRAMS (COMPUTERS), 144, 359, 364, 369, 384
APPROXIMATION, 355, 376, 379
AQUEOUS SOLUTIONS, 218, 272, 278
AQUIFERS, 65, 181, 185
ARCHAEBACTERIA, 289, 296, 336
ARCHITECTURE, 392
ARCHITECTURE (COMPUTERS), 4, 124, 265, 366, 370, 384, 475
ARCTIC REGIONS, 247
ARGON, 386
ARID LANDS, 288
ARMATURES, 157
ARRAYS, 394, 481
ARTICULATION (SPEECH), 417
ARTIFICIAL INTELLIGENCE, 201, 374, 377, 519
ARTIFICIAL SATELLITES, 196
ASIA, 199
ASPHERIC OPTICS, 389
ASSAYING, 172, 365
ASSIMILATION, 225
ASTEROID BELTS, 349
ASTEROIDS, 349
ASTEROSEISMOLOGY, 344
ASTROMETRY, 344
ASTRONAUTS, 265
ASTRONOMICAL OBSERVATORIES, 344
ASTRONOMICAL PHOTOMETRY, 344
ASTRONOMY, 523
ASTROPHYSICS, 350, 523, 525, 527, 536, 537
ASYMMETRY, 132, 263, 386, 409, 460
ASYMPTOTIC GIANT BRANCH STARS, 526, 527
ATLANTIC OCEAN, 257
ATLANTIS (ORBITER), 20
ATMOSPHERIC ATTENUATION, 16
ATMOSPHERIC BOUNDARY LAYER, 234, 249
ATMOSPHERIC CHEMISTRY, 218, 224, 227, 238, 246, 251, 252, 269, 289, 326, 329, 338
ATMOSPHERIC CIRCULATION, 232, 249, 260
ATMOSPHERIC COMPOSITION, 206, 218, 240, 241, 243, 244, 250, 335, 338, 341
ATMOSPHERIC EFFECTS, 322, 335, 522
ATMOSPHERIC GENERAL CIRCULATION MODELS, 237, 242, 246, 247
ATMOSPHERIC HEATING, 246
ATMOSPHERIC MODELS, 210, 224, 226, 235, 245, 250, 253, 256, 260
ATMOSPHERIC MOISTURE, 453
ATMOSPHERIC PHYSICS, 252
ATMOSPHERIC RADIATION, 16, 242, 244, 246, 253
ATMOSPHERIC SOUNDING, 243
ATMOSPHERIC TEMPERATURE, 9, 238, 247, 348
ATMOSPHERICS, 246
ATOMIC CLUSTERS, 421
ATOMIC COLLISIONS, 391, 421
ATOMIC ENERGY LEVELS, 59
ATOMIC FORCE MICROSCOPY, 308, 481
ATOMIC INTERACTIONS, 47
ATOMIC PHYSICS, 394, 423, 426
ATOMIC STRUCTURE, 73, 424, 476
ATOMS, 426, 488
AUDITORY PERCEPTION, 265
AUSTENITIC STAINLESS STEELS, 69, 70, 72
AUSTRALIA, 319, 338
AUTOMATA THEORY, 373
AUTOMATIC CONTROL, 121, 132
AUTOMATION, 369
AUTOMOBILE ENGINES, 213
AUTOMOBILE FUELS, 213
AUTOMOBILES, 86, 102, 108, 223
AUTONOMY, 8, 201, 357, 361
AUXILIARY POWER SOURCES, 97, 210
AVALANCHES, 186, 377
AXISYMMETRIC FLOW, 154
AZIMUTH, 408

B

B STARS, 349, 526
BACTERIA, 271, 280, 283, 285, 288, 289, 290, 292, 293, 306, 313, 333, 334, 335, 340, 341, 352
BAGGAGE, 5, 6
BALANCING, 23
BALLASTS (IMPEDANCES), 378
BALLISTIC MISSILES, 239
BALLOON SOUNDING, 252
BALLS, 167
BARIUM OXIDES, 136, 477, 489
BARIUM TITANATES, 39
BARYONS, 400, 409, 419, 422
BASALT, 309
BATTERY CHARGERS, 135
BAYES THEOREM, 248, 271, 377, 378
BAYS (TOPOGRAPHIC FEATURES), 257
BEAM CURRENTS, 406, 432, 438, 442
BEAM INJECTION, 413, 414, 447
BEAMFORMING, 381
BEAMS (RADIATION), 385, 400, 402, 403, 405, 410, 441, 442, 458
BEHAVIOR, 511
BERYLLIUM, 68, 71
BETA PARTICLES, 501
BIBLIOGRAPHIES, 351, 517
BICRYSTALS, 477, 486
BILLETS, 95
BIOASSAY, 295, 328
BIOCHEMISTRY, 37, 267, 268, 269, 277, 284, 286, 317, 336, 350
BIOCONVERSION, 107, 110
BIODEGRADATION, 225
BIOFILMS, 293, 298, 325
BIOGENY, 330
BIOGEOCHEMISTRY, 258, 281, 306, 323, 325, 328, 329
BIOLOGICAL DIVERSITY, 293, 327, 336, 352
BIOLOGICAL EVOLUTION, 268, 269, 271, 272, 273, 274, 275, 277, 278, 279, 285, 287, 289, 293, 316, 317, 318, 319, 320, 321, 322, 327, 328, 332, 334, 335, 336, 337, 340, 341, 343
BIOMASS, 45, 106, 107, 108, 110, 111, 114, 115, 183, 192, 195, 231
BIOMASS BURNING, 192, 199, 210
BIOMASS ENERGY PRODUCTION, 107, 110, 111, 231
BIOPOLYMERS, 267, 272, 279, 281
BIOPROCESSING, 283
BIOREACTORS, 49
BIOSPHERE, 297
BIOSYNTHESIS, 281, 294, 337, 343
BIOTECHNOLOGY, 315, 351
BIREFRINGENCE, 159, 160
BISMUTH, 51, 441
BISMUTH ALLOYS, 132
BISMUTH COMPOUNDS, 484

BL LACERTAE OBJECTS, 524, 537
BLACK HOLES (ASTRONOMY), 526
BLADE TIPS, 2
BLANKETS (FISSION REACTORS), 393
BLANKETS (FUSION REACTORS), 32
BLOCK COPOLYMERS, 39
BLOOD FLOW, 263
BLOOD PLASMA, 142
BLOWING, 121
BLOWOUTS, 100
BODY CENTERED CUBIC LATTICES, 82, 473
BOILERS, 113, 114, 115, 167, 171, 231
BOILING, 24, 120
BOLTED JOINTS, 176
BOLTZMANN TRANSPORT EQUATION, 422
BONDING, 134, 168
BONES, 261
BOREHOLES, 100
BORIDES, 129
BORON, 427
BORON CARBIDES, 41
BORON ISOTOPES, 179
BOROSILICATE GLASS, 94
BOSONS, 391, 412
BOUNDARY CONDITIONS, 58, 376, 460
BOUNDARY LAYER CONTROL, 14
BOUNDARY LAYERS, 154, 245, 253
BOUNDARY VALUE PROBLEMS, 379
BRAGG GRATINGS, 453, 456
BRAIDED COMPOSITES, 39
BREMSSTRAHLUNG, 382, 400, 401, 498
BRIDGES (STRUCTURES), 58
BRIGHTNESS, 453, 459
BRILLOUIN EFFECT, 463
BRINES, 310
BRITTLE MATERIALS, 96
BRITTLENESS, 176
BROADBAND, 452
BROADCASTING, 123, 350
BROKEN SYMMETRY, 398
BROWN DWARF STARS, 347
BSCCO SUPERCONDUCTORS, 475, 476
BUBBLES, 152, 153, 310
BUILDINGS, 52, 95, 150, 172, 197, 210
BUNCHING, 446
BUOYANCY, 56
BURGER EQUATION, 376
BURNERS, 226
BURNETT EQUATIONS, 151

C

C (PROGRAMMING LANGUAGE), 367
C++ (PROGRAMMING LANGUAGE), 367
CADMIUM COMPOUNDS, 490
CADMIUM TELLURIDES, 494
CALCIFICATION, 298
CALCITE, 268, 309
CALCIUM OXIDES, 474
CALIBRATING, 40, 63, 65, 154, 155, 157, 169, 179, 216, 448
CALIFORNIA, 110, 188, 204, 208
CALIFORNIUM ISOTOPES, 172
CALORIMETERS, 172, 419, 536
CAMBRIAN PERIOD, 321
CAMERAS, 157, 448, 496
CANOPIES (VEGETATION), 249
CANTILEVER BEAMS, 138
CAPACITORS, 43, 86, 133, 442
CAPE HATTERAS (NC), 257
CARBENES, 33
CARBIDES, 95
CARBON, 30, 35, 92, 96, 196, 219, 257, 258, 269, 294, 336, 342, 348, 349
CARBON 13, 335, 341
CARBON 14, 179
CARBON COMPOUNDS, 344
CARBON CYCLE, 229, 324
CARBON DIOXIDE, 35, 104, 119, 206, 229, 232, 237, 250, 257, 258, 271, 283, 321, 324, 330, 347, 532
CARBON DIOXIDE CONCENTRATION, 250, 255, 335, 341
CARBON DIOXIDE LASERS, 458
CARBON FIBERS, 39
CARBON ISOTOPES, 283, 309, 400
CARBON MONOXIDE, 60, 210, 276
CARBON NANOTUBES, 491
CARBON STEELS, 73
CARBON TETRACHLORIDE, 65
CARBON-CARBON COMPOSITES, 63
CARBONACEOUS CHONDRITES, 268, 284, 311, 314
CARBONACEOUS METEORITES, 279
CARBONATES, 99, 204, 282, 285, 311, 316, 339, 341
CARBONIC ANHYDRASE, 336
CARBOXYLIC ACIDS, 273
CASE HISTORIES, 190
CAST ALLOYS, 70, 74
CASTINGS, 69, 70, 74
CATALOGS (PUBLICATIONS), 517
CATALYSIS, 36, 44, 53, 59, 274, 278, 281, 494
CATALYSTS, 51, 57, 61, 63, 64, 66, 95, 101, 105, 112, 113, 114, 119, 198, 212, 271, 275
CATALYTIC ACTIVITY, 109, 279
CATHODES, 137, 138
CATIONS, 398, 490
CAVITIES, 140, 167, 227, 433, 500
CAVITY FLOW, 147
CAVITY RESONATORS, 127, 132
CELESTIAL BODIES, 344
CELL CATHODES, 199
CELLS (BIOLOGY), 261, 276, 298, 317
CELLULOSE, 45
CENTRIFUGES, 144
CENTROIDS, 433
CERAMIC MATRIX COMPOSITES, 40, 41, 91, 92
CERAMICS, 28, 33, 35, 55, 81, 85, 86, 87, 90, 92, 94, 96, 134, 407, 428
CERIUM COMPOUNDS, 61
CERIUM OXIDES, 212
CESIUM IODIDES, 156
CHARACTERIZATION, 51, 122, 293, 295
CHARGE CARRIERS, 234
CHARGE DISTRIBUTION, 442, 453
CHARGE EXCHANGE, 474
CHARGE TRANSFER, 234
CHARGED PARTICLES, 396, 400, 419, 422, 460, 479, 493, 502
CHARM (PARTICLE PHYSICS), 425
CHEMICAL ANALYSIS, 26, 295, 302, 305
CHEMICAL BONDS, 44
CHEMICAL COMPOSITION, 29, 284, 302, 307, 312, 339, 520
CHEMICAL ENERGY, 202
CHEMICAL ENGINEERING, 115, 116
CHEMICAL EQUILIBRIUM, 346, 388
CHEMICAL EVOLUTION, 279, 314, 348
CHEMICAL EXPLOSIONS, 100
CHEMICAL FRACTIONATION, 103, 322, 329, 330
CHEMICAL INDICATORS, 23
CHEMICAL PROPERTIES, 227
CHEMICAL REACTIONS, 43, 45, 58, 60, 62, 63, 192, 203, 220, 274, 275, 278, 280
CHESAPEAKE BAY (US), 255
CHIMNEYS, 284
CHIRALITY, 267, 496, 506
CHLORIDES, 52
CHLORINE, 291
CHLOROCARBONS, 65, 225
CHLOROPHYLLS, 337
CHONDRITES, 346

CHONDRULE, 346
CHROMATES, 58
CHROMATOGRAPHY, 31, 292, 436
CHROMIUM OXIDES, 201
CHRONOLOGY, 203
CIRCULATION, 459
CIRRUS CLOUDS, 247, 254
CITIES, 226
CIVIL AVIATION, 7
CLASSICAL MECHANICS, 503
CLAYS, 28, 51, 105, 196
CLEAN FUELS, 99, 108
CLEAN ROOMS, 117, 179
CLEANING, 24, 35
CLIMATE, 211, 247, 248
CLIMATE CHANGE, 104, 179, 190, 218, 241, 243, 244, 246, 247, 347
CLIMATE MODELS, 232, 242, 248, 252
CLIMATOLOGY, 9, 180, 222, 225, 226, 237, 241, 242, 243, 246, 248, 251, 252, 256, 259, 330
CLINICAL MEDICINE, 204, 262, 378
CLONING (BIOLOGY), 286
CLOSED CYCLES, 438
CLOSED ECOLOGICAL SYSTEMS, 220, 266
CLOUD COVER, 253, 254
CLOUD HEIGHT INDICATORS, 255
CLOUD PHYSICS, 221, 241, 248, 251, 252, 253, 254
CLOUDS, 249
CLOUDS (METEOROLOGY), 155, 238, 243, 246, 253, 255
CLUMPS, 345
CLUTTER, 125
CMOS, 137
COAL, 56, 64, 66, 99, 113, 114, 167, 202, 210, 231
COAL DERIVED GASES, 101, 106, 112, 227
COASTAL WATER, 256, 257
COASTS, 257
COATING, 35, 139
COATINGS, 34, 37, 57, 69, 155, 292, 487
COBALT, 65, 66, 79, 114, 478, 489
COBALT OXIDES, 79, 489
CODE DIVISION MULTIPLE ACCESS, 124
CODING, 354, 361
COEFFICIENT OF FRICTION, 31, 33
COEFFICIENTS, 501
COERCIVITY, 68, 514
COGENERATION, 80
COHERENT RADIATION, 441, 442, 454, 500
COHESION, 176
COLD NEUTRONS, 443
COLLAPSE, 525
COLLIMATION, 496
COLLISION PARAMETERS, 500
COLLISIONAL PLASMAS, 464
COLLISIONS, 401
COLLOIDS, 141, 437
COLONIES, 295, 296
COLOR, 324, 445
COMBINATORIAL ANALYSIS, 374
COMBUSTION, 43, 56, 59, 60, 67, 213, 217
COMBUSTION CHAMBERS, 25, 26, 66, 165
COMBUSTION CONTROL, 216
COMBUSTION EFFICIENCY, 213
COMBUSTION PHYSICS, 8, 45
COMBUSTION PRODUCTS, 165, 226, 230, 233
COMETS, 267
COMMAND AND CONTROL, 125, 126, 128, 522
COMMERCE, 111, 198, 450
COMMERCIAL AIRCRAFT, 3
COMMERCIAL OFF-THE-SHELF PRODUCTS, 169, 522
COMMERCIALIZATION, 97
COMMUNICATION, 327
COMMUNICATION EQUIPMENT, 266
COMMUNICATION NETWORKS, 126, 128, 371
COMPACTING, 34
COMPARISON, 244
COMPATIBILITY, 29
COMPILERS, 358, 369
COMPLEX COMPOUNDS, 32
COMPLEX SYSTEMS, 141, 372, 379
COMPONENT RELIABILITY, 138, 169, 170, 174
COMPOSITE MATERIALS, 10, 38, 39, 41, 42, 94, 362
COMPOSITION (PROPERTY), 93, 295, 302
COMPRESSED GAS, 194
COMPRESSIBLE FLOW, 1
COMPRESSION LOADS, 41, 78
COMPRESSION RATIO, 354
COMPRESSION WAVES, 529
COMPRESSIVE STRENGTH, 163
COMPRESSORS, 409
COMPTON EFFECT, 399
COMPUTATION, 415, 509
COMPUTATIONAL CHEMISTRY, 253
COMPUTATIONAL FLUID DYNAMICS, 1, 11, 15, 44, 144, 147, 150, 151, 152, 153
COMPUTATIONAL GRIDS, 123, 356, 357, 371
COMPUTER AIDED DESIGN, 117, 170, 363, 403
COMPUTER AIDED MANUFACTURING, 362, 363
COMPUTER AIDED TOMOGRAPHY, 169, 315
COMPUTER GRAPHICS, 352, 357, 358, 364, 366, 377, 444
COMPUTER INFORMATION SECURITY, 123, 370, 371
COMPUTER NETWORKS, 123, 124, 155, 356, 371, 506
COMPUTER PROGRAMMING, 356, 359, 360, 366, 367
COMPUTER PROGRAMS, 44, 97, 108, 147, 153, 170, 217, 271, 354, 355, 357, 360, 361, 365, 366, 368, 371, 372, 380, 383, 403, 420, 435, 461, 475
COMPUTER SYSTEMS PERFORMANCE, 365
COMPUTER SYSTEMS PROGRAMS, 262
COMPUTER TECHNIQUES, 125, 182, 362, 374, 519
COMPUTERIZED SIMULATION, 31, 44, 95, 132, 141, 143, 145, 149, 150, 154, 159, 162, 227, 251, 267, 276, 328, 359, 363, 365, 372, 373, 374, 383, 385, 419, 428, 460, 461, 465, 491, 501, 502, 504, 521
COMPUTERS, 371, 404
CONCENTRATION (COMPOSITION), 217, 323, 324, 329
CONCENTRATORS, 459
CONCRETE STRUCTURES, 57
CONCRETES, 52, 58, 362
CONCURRENT ENGINEERING, 369
CONDENSATION, 42
CONDENSED MATTER PHYSICS, 419
CONDUCTING POLYMERS, 133
CONDUCTIVE HEAT TRANSFER, 39, 53
CONDUCTIVITY, 87
CONFERENCES, 36, 70, 168, 197, 219, 261, 266, 355
CONFIGURATION MANAGEMENT, 126, 128
CONFINEMENT, 464
CONSERVATION LAWS, 359
CONSTRUCTION, 58, 368, 511, 513, 515
CONSTRUCTION MATERIALS, 118
CONTACT RESISTANCE, 69
CONTAINMENT, 28, 43, 78
CONTAMINANTS, 101, 182, 183, 190, 215, 219, 225, 227

CONTAMINATION, 24, 186, 392, 409
CONTINENTAL SHELVES, 257, 258
CONTINUOUS RADIATION, 162, 405, 406, 415, 438, 442, 459
CONTINUUMS, 186
CONTRACT MANAGEMENT, 266
CONTRACTORS, 6
CONTROL, 136
CONTROL SIMULATION, 145
CONTROL SYSTEMS DESIGN, 22, 145, 357
CONTROL THEORY, 27, 39, 146, 374
CONTROLLABILITY, 7
CONTROLLED FUSION, 465
CONTROLLERS, 145, 157, 363, 502
CONVECTION, 236, 244, 251
CONVECTION-DIFFUSION EQUATION, 376
CONVERGENCE, 149, 379, 425
COOLANTS, 390
COOLERS, 23, 455
COOLING, 24, 95, 270, 398, 403, 408
COOLING SYSTEMS, 119, 152, 414, 433
COORDINATES, 349
COORDINATION, 512, 515
COPOLYMERS, 87, 89, 90
COPPER, 74, 163, 346, 457
COPPER ALLOYS, 49, 70
COPPER OXIDES, 474, 477, 489
COPPER SULFIDES, 47
CORES, 304
CORRELATION, 400, 415, 496
CORRELATION DETECTION, 423
CORROSION, 13, 52, 65, 78, 82, 85, 171, 437, 517
CORROSION PREVENTION, 35, 52
CORROSION RESISTANCE, 55, 74
CORROSION TESTS, 73, 437
COSMIC DUST, 345
COSMIC RAYS, 536
COSMOLOGY, 525, 527
COST ANALYSIS, 213, 487
COST EFFECTIVENESS, 126, 165, 266
COST REDUCTION, 198
COSTS, 509
COUPLING, 58, 104, 353
COUPLINGS, 236
CRACK INITIATION, 72
CRACK PROPAGATION, 75, 92, 96, 175, 447
CRACKING (CHEMICAL ENGINEERING), 82, 105
CRACKING (FRACTURING), 174
CRACKS, 42, 74, 96, 174, 175
CRASHES, 4
CRAY COMPUTERS, 356
CREEP PROPERTIES, 75, 103, 173, 233, 530
CREEP RUPTURE STRENGTH, 428
CREEP STRENGTH, 530
CREW PROCEDURES (INFLIGHT), 17, 18, 19, 20, 21
CREW PROCEDURES (PREFLIGHT), 19
CRITICAL CURRENT, 132, 475
CRITICAL EXPERIMENTS, 436
CRITICAL FLOW, 24
CRITICAL MASS, 436, 443
CRITICAL TEMPERATURE, 79
CROP GROWTH, 220
CROSS POLARIZATION, 483
CROSS SECTIONS, 261
CRUDE OIL, 43, 97, 101, 103, 109
CRUSTAL FRACTURES, 180, 233
CRYOGENIC COOLING, 416
CRYOGENIC FLUIDS, 115
CRYOGENIC ROCKET PROPELLANTS, 18
CRYOGENICS, 84, 115, 118, 156, 194, 260, 478
CRYOSTATS, 260
CRYPTOGRAPHY, 354
CRYSTAL DEFECTS, 473, 474, 491
CRYSTAL FIELD THEORY, 474
CRYSTAL GROWTH, 298
CRYSTAL LATTICES, 52, 135, 276, 426, 489
CRYSTAL STRUCTURE, 27, 486, 491
CRYSTALLINITY, 207, 401
CRYSTALLIZATION, 45, 85, 271, 298, 481
CRYSTALLOGRAPHY, 86, 473, 487, 490
CRYSTALS, 159, 161, 298, 304, 401, 451, 479, 494
CUBES (MATHEMATICS), 355
CULTURAL RESOURCES, 194
CUPRATES, 477
CURRENT CONVERTERS (AC TO DC), 137
CURRENT DENSITY, 58, 475
CURRENT DISTRIBUTION, 442
CYCLES, 106, 166, 237
CYCLIC HYDROCARBONS, 121
CYCLIC LOADS, 136
CYCLOTRON FREQUENCY, 465
CYCLOTRON RESONANCE DEVICES, 387
CYCLOTRONS, 455, 465
CYLINDRICAL BODIES, 67
CYLINDRICAL CHAMBERS, 385
CYLINDRICAL SHELLS, 443
CYTOLOGY, 274, 322
CYTOPLASM, 290

D

DAMAGE, 43, 171, 174, 386, 410, 447
DAMAGE ASSESSMENT, 96
DARK MATTER, 504, 536
DATA ACQUISITION, 171, 188, 236, 249, 255, 389, 406, 429, 517, 518, 522
DATA BASE MANAGEMENT SYSTEMS, 97, 183
DATA BASES, 80, 97, 351, 367, 517, 521
DATA COMPRESSION, 295
DATA CONVERSION ROUTINES, 357
DATA MANAGEMENT, 190, 224, 367, 518
DATA PROCESSING, 173, 216, 225, 231, 265, 387, 434, 518, 519
DATA REDUCTION, 231
DATA SIMULATION, 519
DATA SMOOTHING, 378
DATA STORAGE, 356, 518
DATA SYSTEMS, 225, 517
DATA TRANSMISSION, 124, 126, 127
DAYTIME, 95
DEACTIVATION, 101
DEATH VALLEY (CA), 305
DEBONDING (MATERIALS), 10
DEBRIS, 392, 396
DECISION MAKING, 8, 201, 264, 265, 266, 508, 511, 512
DECISION SUPPORT SYSTEMS, 362
DECOMMISSIONING, 435
DECOMPOSITION, 102
DEFECTS, 73, 91
DEFENSE PROGRAM, 11, 370
DEFORMABLE MIRRORS, 455
DEFORMATION, 10, 75, 92, 173, 473, 530
DEGREES OF FREEDOM, 117, 177
DEHYDROGENATION, 104, 105
DENITROGENATION, 181
DENSE PLASMAS, 461, 462
DENSITY DISTRIBUTION, 453
DENSITY MEASUREMENT, 261
DEOXYRIBONUCLEIC ACID, 50, 279, 285
DEPLOYMENT, 122, 124
DEPOSITION, 27, 51, 61, 138, 285, 383
DEPOSITS, 282, 288
DEPTH, 490
DESERTS, 248

DESIGN ANALYSIS, 24, 52, 131, 151, 159, 165, 193, 205, 360, 363, 364, 424, 458, 467, 469, 499, 507
DESIGN OPTIMIZATION, 138
DESORPTION, 312
DESULFURIZING, 59, 101, 106, 227
DETECTION, 13, 23, 27, 37, 314, 315, 344, 435, 536
DETECTORS, 412, 479
DETERMINANTS, 498
DETONATION, 50
DEUTERIUM, 43, 455
DEUTERONS, 498
DEVELOPING NATIONS, 209
DIAGNOSIS, 405, 406, 414, 441, 450, 516
DIAMONDS, 93, 387, 472
DICHROISM, 475
DIELECTRIC WAVEGUIDES, 466
DIELECTRICS, 39, 127, 139, 466, 497
DIESEL ENGINES, 165, 166, 210, 214
DIESEL FUELS, 99, 109, 208, 210
DIFFERENCE EQUATIONS, 353
DIFFERENTIAL ABSORPTION LIDAR, 453
DIFFERENTIAL EQUATIONS, 355, 359
DIFFRACTION, 207, 393, 394, 473
DIFFRACTOMETERS, 389
DIFFUSION, 437, 488
DIFFUSION COEFFICIENT, 437
DIFFUSIVITY, 376
DIGITAL ELECTRONICS, 135
DIGITAL SYSTEMS, 353, 519
DILUTION, 45
DIMENSIONAL MEASUREMENT, 480
DIMENSIONS, 517
DIMETHYL COMPOUNDS, 46
DIODES, 136, 163
DIRAC EQUATION, 506
DISCONTINUITY, 377
DISCRETE COSINE TRANSFORM, 378
DISKS (SHAPES), 167
DISPERSIONS, 39
DISPLAY DEVICES, 4, 88, 265, 366, 454
DISSOCIATION, 59, 418
DISSOLVING, 81, 85, 334
DISTANCE, 525
DISTORTION, 454
DISTRIBUTED PARAMETER SYSTEMS, 374
DISTRIBUTED PROCESSING, 170
DIURNAL VARIATIONS, 245, 246
DIVERGENCE, 457
DIVERTERS, 460, 463
DOCUMENTS, 141, 509, 523
DOMAINS, 373
DOPED CRYSTALS, 71, 148, 199, 444, 480
DOPPLER EFFECT, 399
DOSAGE, 378
DOSIMETERS, 155, 427
DRAG REDUCTION, 2
DRIFT RATE, 377
DRILLING, 201, 297
DROPS (LIQUIDS), 145
DROUGHT, 237, 247
DRUGS, 5
DRYING, 530
DUALITY THEOREM, 499
DUCTILITY, 178
DUNES, 530
DUST, 211, 347
DYE LASERS, 481
DYNAMIC CHARACTERISTICS, 33, 451
DYNAMIC LOADS, 78, 169, 174, 265
DYNAMIC RESPONSE, 176, 377
DYNAMIC STRUCTURAL ANALYSIS, 174, 193
DYNAMICAL SYSTEMS, 353
DYSPROSIUM ISOTOPES, 439

E

EARTH (PLANET), 267, 348
EARTH ATMOSPHERE, 206, 239, 242, 252, 289, 321, 334, 336, 338
EARTH CRUST, 184, 320, 332
EARTH ENVIRONMENT, 334
EARTH HYDROSPHERE, 320
EARTH MAGNETOSPHERE, 535
EARTH MANTLE, 326
EARTH OBSERVATIONS (FROM SPACE), 245
EARTH OBSERVING SYSTEM (EOS), 225
EARTH ORBITS, 340
EARTH PLANETARY STRUCTURE, 184
EARTH RADIATION BUDGET EXPERIMENT, 22, 259
EARTH SCIENCES, 180, 252, 350, 351
EARTH SURFACE, 341
EARTH-MOON SYSTEM, 340
EARTHQUAKES, 172, 184, 234
ECLIPSING BINARY STARS, 525
ECOLOGY, 282, 352
ECONOMIC ANALYSIS, 108
ECONOMICS, 101, 119, 228
ECOSYSTEMS, 255, 257, 281, 282, 288, 298, 300, 328, 352
EDGE DISLOCATIONS, 82
EDUCATION, 141, 168, 350, 351, 352, 359, 430, 509, 512, 518
EFFICIENCY, 97, 226
EFFLUENTS, 49
EIGENVALUES, 361, 375
EIGENVECTORS, 361
ELASTIC BODIES, 34
ELASTIC PROPERTIES, 39, 87, 175, 262
ELASTIC SCATTERING, 395, 536
ELASTIC WAVES, 184, 403
ELASTOMERS, 37, 172
ELECTRIC BATTERIES, 135, 195, 196, 207, 209
ELECTRIC CONNECTORS, 134
ELECTRIC FIELDS, 427, 446, 453
ELECTRIC GENERATORS, 83, 191, 380
ELECTRIC HYBRID VEHICLES, 103, 200, 223
ELECTRIC MOTOR VEHICLES, 136, 200, 206, 207
ELECTRIC POTENTIAL, 432, 433
ELECTRIC POWER, 366, 473
ELECTRIC POWER PLANTS, 12, 114, 208, 231
ELECTRIC POWER SUPPLIES, 208, 441
ELECTRIC WIRE, 493, 495
ELECTRICAL IMPEDANCE, 139
ELECTRICAL MEASUREMENT, 137, 252
ELECTRICAL PROPERTIES, 73, 133, 198, 201, 202
ELECTRICAL RESISTIVITY, 132, 141, 234
ELECTRICITY, 99, 104, 119, 197, 209
ELECTRIFICATION, 209
ELECTROCATALYSTS, 36
ELECTROCHEMICAL CELLS, 200, 207
ELECTROCHEMICAL CORROSION, 71
ELECTROCHEMISTRY, 193, 198
ELECTRODEPOSITION, 31
ELECTRODES, 71, 193, 195, 197, 201
ELECTRODYNAMICS, 127
ELECTROENCEPHALOGRAPHY, 264
ELECTROLYSIS, 529
ELECTROLYTES, 49, 193, 195, 197, 199, 200
ELECTROLYTIC CELLS, 191, 207
ELECTROMAGNETIC ABSORPTION, 494
ELECTROMAGNETIC FIELDS, 426, 488

ELECTROMAGNETIC INTERACTIONS, 126
ELECTROMAGNETIC PULSES, 134
ELECTROMAGNETIC WAVE TRANSMISSION, 156
ELECTROMAGNETS, 360, 385
ELECTROMETERS, 155
ELECTRON ACCELERATION, 497
ELECTRON ACCELERATORS, 500
ELECTRON AVALANCHE, 156
ELECTRON BEAMS, 137, 383, 392, 408, 409, 415, 416, 424, 432, 439, 453, 457, 466, 476, 499, 500
ELECTRON BUNCHING, 409, 441, 442, 500
ELECTRON CLOUDS, 433
ELECTRON ENERGY, 411, 486
ELECTRON GUNS, 159
ELECTRON IRRADIATION, 484
ELECTRON MICROSCOPY, 49, 90, 484
ELECTRON SOURCES, 480
ELECTRON SPIN, 489
ELECTRON TRANSFER, 48, 57, 160, 434, 470
ELECTRON TRANSITIONS, 344
ELECTRON TUNNELING, 60
ELECTRONIC PUBLISHING, 358
ELECTRONIC STRUCTURE, 46, 47, 73
ELECTRONS, 390, 415, 423, 425, 481, 498
ELECTROPHORESIS, 31
ELECTROPOLISHING, 427
ELECTROSTATICS, 131
ELEMENTARY PARTICLE INTERACTIONS, 383, 384
ELEMENTARY PARTICLES, 387, 397, 525
ELEVATION, 103
ELLIPTIC DIFFERENTIAL EQUATIONS, 478
ELLIPTICAL GALAXIES, 524
EMISSION, 480
EMISSION SPECTRA, 30
EMITTANCE, 412, 413, 415, 432, 453, 466, 503
EMITTERS, 441, 480
ENANTIOMERS, 268
END EFFECTORS, 117, 122
ENDEAVOUR (ORBITER), 17, 19, 21
ENERGETIC PARTICLES, 469
ENERGY CONSERVATION, 120, 476
ENERGY CONSUMPTION, 209, 223
ENERGY CONVERSION, 107, 431
ENERGY CONVERSION EFFICIENCY, 43, 102
ENERGY DISSIPATION, 145
ENERGY GAPS (SOLID STATE), 458, 476, 486, 493
ENERGY POLICY, 110, 111
ENERGY SOURCES, 204
ENERGY SPECTRA, 67
ENERGY TECHNOLOGY, 114, 185, 191, 208, 394, 395, 431, 469
ENERGY TRANSFER, 261, 418
ENGINE DESIGN, 165
ENGINE PARTS, 165
ENGINEERING MANAGEMENT, 511, 515
ENGINEERS, 358, 510, 511, 513, 514, 515, 516
ENRICHMENT, 510
ENTHALPY, 111, 112
ENTROPY, 151, 277
ENVIRONMENT EFFECTS, 99, 118, 237, 394
ENVIRONMENT MANAGEMENT, 194, 228
ENVIRONMENT MODELS, 22, 182, 183, 217, 227
ENVIRONMENT POLLUTION, 182
ENVIRONMENT PROTECTION, 119, 215, 226
ENVIRONMENTAL CONTROL, 119
ENVIRONMENTAL LABORATORIES, 211
ENVIRONMENTAL MONITORING, 125
ENVIRONMENTAL QUALITY, 476
ENVIRONMENTAL SURVEYS, 183, 194
ENVIRONMENTAL TESTS, 85
ENVIRONMENTS, 241
ENZYME ACTIVITY, 278
ENZYMES, 271, 334
EPITAXY, 61, 486
EPOXIDATION, 61
EPOXY RESINS, 25, 42, 57, 136, 175
EQUATIONS OF MOTION, 340, 498
EQUATIONS OF STATE, 36, 142, 366, 388, 450, 462, 488
EQUILIBRIUM, 32, 270
EQUIVALENT CIRCUITS, 139
EROSION, 26
ERROR ANALYSIS, 173, 372, 376, 429
ERRORS, 510
ESCHERICHIA, 275
ESTERS, 109
ESTIMATES, 189
ESTIMATING, 54, 111, 515
ETHANE, 48
ETHYL ALCOHOL, 110, 111, 195
ETHYL COMPOUNDS, 29
ETHYLENE, 45
EUCLIDEAN GEOMETRY, 355
EUKARYOTES, 286, 290, 300, 322, 328
EULER EQUATIONS OF MOTION, 1
EUROPA, 301, 302, 304
EUROPEAN SPACE AGENCY, 307
EUROPEAN SPACE PROGRAMS, 303
EUROPIUM ISOTOPES, 399
EUTECTIC ALLOYS, 85
EVALUATION, 108, 131, 443
EVAPORATION, 62, 91, 383
EVAPOTRANSPIRATION, 181
EVOLUTION (DEVELOPMENT), 280, 310, 321
EXCITATION, 157, 162, 176, 475, 481
EXCITONS, 489
EXERGY, 122
EXHAUST EMISSION, 67, 103, 165, 190, 199, 211, 213, 214, 215, 217, 231
EXHAUST GASES, 103, 190, 199
EXHAUST SYSTEMS, 219
EXOBIOLOGY, 266, 267, 268, 269, 270, 272, 282, 291, 292, 295, 298, 301, 302, 303, 304, 305, 306, 307, 308, 309, 310, 311, 312, 313, 314, 315, 316, 317, 318, 340, 343, 350, 351, 352
EXOTHERMIC REACTIONS, 104
EXPERIMENT DESIGN, 147
EXPERIMENTATION, 37, 143, 393, 465
EXPLOSIONS, 51, 140, 235
EXPLOSIVES, 34, 50, 99, 101, 102
EXPLOSIVES DETECTION, 6
EXPOSURE, 255, 382
EXTINCTION, 327
EXTRACTION, 113, 206
EXTRASOLAR PLANETS, 343, 344, 347
EXTRATERRESTRIAL ENVIRONMENTS, 272
EXTRATERRESTRIAL LIFE, 272, 284, 291, 301, 302, 315, 317, 333, 340, 351
EXTRATERRESTRIAL OCEANS, 302
EXTRAVEHICULAR ACTIVITY, 18, 20
EXTREME ULTRAVIOLET RADIATION, 155, 158, 448, 465
EYE (ANATOMY), 514

F

FABRICATION, 24, 26, 77, 83, 87, 90, 117, 132, 135, 137, 158, 159, 162, 163, 172, 207, 362, 387, 389, 393, 433, 457, 473, 477, 482, 494, 495, 504
FAIL-SAFE SYSTEMS, 444
FAILURE, 170, 410

FAILURE ANALYSIS, 8
FAILURE MODES, 10, 41
FAR INFRARED RADIATION, 137
FAR ULTRAVIOLET RADIATION, 48
FARADAY EFFECT, 442
FARM CROPS, 220
FAST NEUTRONS, 440
FAST NUCLEAR REACTORS, 438, 441
FASTENERS, 11
FATIGUE (BIOLOGY), 264
FATIGUE (MATERIALS), 69, 72, 175, 374
FATTY ACIDS, 49
FAULT DETECTION, 12, 170
FAULT TREES, 170, 375
FEASIBILITY ANALYSIS, 356
FEEDBACK, 136, 177, 353, 367, 497
FEEDBACK CONTROL, 8, 16, 145, 414
FEET (ANATOMY), 263
FELDSPARS, 291
FERMI SURFACES, 476
FERMIONS, 423
FERRITES, 69
FERRITIC STAINLESS STEELS, 81
FERROELECTRIC MATERIALS, 87, 472
FERROELECTRICITY, 471
FERROMAGNETIC MATERIALS, 70, 80, 140, 471, 478
FERROUS METALS, 287
FIBER COMPOSITES, 40, 41, 91
FIBER OPTICS, 172, 405, 452, 454
FIBER-MATRIX INTERFACES, 91
FICKS EQUATION, 149
FIELD EMISSION, 427
FIELD TESTS, 175
FIELD-PROGRAMMABLE GATE ARRAYS, 156
FIGHTER AIRCRAFT, 11
FILMS, 31
FINANCIAL MANAGEMENT, 5, 509
FINE STRUCTURE, 481
FINGERS, 354
FINITE DIFFERENCE THEORY, 365, 478
FINITE DIFFERENCE TIME DOMAIN METHOD, 126
FINITE ELEMENT METHOD, 33, 162, 175, 376, 377
FIRES, 157, 222
FISCHER-TROPSCH PROCESS, 57, 64, 66, 95, 113, 114
FISSION, 24, 431
FISSION ELECTRIC CELLS, 431
FISSION PRODUCTS, 65, 428, 438
FISSIONABLE MATERIALS, 435, 438
FLAGELLATA, 285
FLAME PROPAGATION, 56
FLAMES, 45
FLAMMABILITY, 54
FLAVOR (PARTICLE PHYSICS), 505
FLIGHT ENVELOPES, 14
FLIGHT OPERATIONS, 8
FLIGHT SAFETY, 7
FLIGHT SIMULATORS, 4, 14
FLIGHT VEHICLES, 12
FLOW CHARACTERISTICS, 14, 154
FLOW CHARTS, 171
FLOW DISTRIBUTION, 15, 210, 239
FLOW EQUATIONS, 359
FLOW GEOMETRY, 149
FLOW VISUALIZATION, 143
FLUE GASES, 53
FLUID BOUNDARIES, 143
FLUID DYNAMICS, 143
FLUID FILMS, 478, 479
FLUID FLOW, 146, 153, 182
FLUID MECHANICS, 141, 147, 149, 151, 152
FLUID-SOLID INTERACTIONS, 28, 227
FLUIDIZED BED PROCESSORS, 59, 106
FLUIDS, 32, 33
FLUORESCENCE, 63, 288, 296, 314, 315, 378, 414, 472
FLUORIDES, 494
FLUORINATION, 54
FLUORINE, 349
FLUOROCARBONS, 54, 388
FLUX DIFFERENCE SPLITTING, 146
FLUX QUANTIZATION, 537
FOAMS, 152
FOILS (MATERIALS), 96
FOLDS (GEOLOGY), 532
FOOD CHAIN, 328
FORECASTING, 527
FORESTS, 106, 184, 237, 248, 249
FORGING, 164
FORMALDEHYDE, 273
FORMALISM, 152
FORMATES, 276
FORMING TECHNIQUES, 121
FOSSIL FUELS, 104, 210
FOSSILS, 291, 308, 313, 319, 321, 330, 352
FOURIER ANALYSIS, 375
FOURIER TRANSFORMATION, 438
FRACTALS, 253
FRACTIONATION, 289
FRACTOGRAPHY, 37
FRACTURE MECHANICS, 96, 138, 175, 176, 177, 178
FRACTURE STRENGTH, 70, 72, 175, 428
FRACTURES (MATERIALS), 188
FRACTURING, 175, 444
FREE CONVECTION, 287
FREE ELECTRON LASERS, 137, 159, 161, 163, 385, 391, 409, 446, 447, 450, 456, 457, 483, 500
FREE ENERGY, 78
FREE RADICALS, 65
FREE-PISTON ENGINES, 210
FREQUENCIES, 4, 456
FREQUENCY DISTRIBUTION, 175
FREQUENCY RESPONSE, 136, 177
FRESH WATER, 285, 306
FRICTION, 92
FRICTION FACTOR, 33, 139, 176
FRICTION REDUCTION, 129
FUEL CELLS, 98, 191, 193, 198, 200, 202, 204, 208
FUEL CONSUMPTION, 102, 103, 223
FUEL INJECTION, 213
FUEL PRODUCTION, 107, 217
FUEL SYSTEMS, 26, 102, 211
FUEL TANKS, 8
FUELS, 102, 107, 108, 112, 195, 198
FULL SCALE TESTS, 10
FUNCTIONAL ANALYSIS, 371
FUNGI, 280
FURNACES, 98
FUSION REACTORS, 413, 469
FUSION WELDING, 80
FUZZY SYSTEMS, 130, 201, 373

G

GALACTIC CLUSTERS, 524
GALACTIC EVOLUTION, 343, 524
GALACTIC HALOS, 250
GALERKIN METHOD, 142, 359
GALILEO PROJECT, 301
GALILEO SPACECRAFT, 529
GALLIUM, 54
GALLIUM ARSENIDE LASERS, 162
GALLIUM ARSENIDES, 135, 161, 410, 457, 504
GALLIUM NITRIDES, 491, 493
GALLIUM PHOSPHIDES, 202
GAMMA RAY BURSTS, 527
GAMMA RAY SPECTRA, 422
GAMMA RAY SPECTROMETERS, 381
GAMMA RAYS, 67, 155, 252, 365, 394, 496
GAS COMPOSITION, 226, 335
GAS DETECTORS, 157, 243

GAS EVOLUTION, 407
GAS EXPLOSIONS, 170
GAS FLOW, 44
GAS GIANT PLANETS, 345, 349, 533
GAS HEATING, 64
GAS MIXTURES, 87, 156, 164, 418, 437
GAS PRESSURE, 471
GAS STREAMS, 53, 228
GAS TEMPERATURE, 250
GAS TUNGSTEN ARC WELDING, 80
GAS TURBINES, 12, 13, 64, 166, 168, 193, 205, 213
GAS-SOLID INTERACTIONS, 47
GASEOUS DIFFUSION, 54
GASES, 45, 56, 215, 220, 238
GASIFICATION, 106
GASKETS, 168
GASOLINE, 110
GAUGE THEORY, 507
GELATION, 28
GENE EXPRESSION, 280, 282, 287
GENES, 281, 286, 328, 330, 334, 337, 343
GENETIC ALGORITHMS, 138, 354, 373, 374
GENETIC ENGINEERING, 262
GENETICS, 269, 272, 273, 325, 327, 330
GENOME, 274, 277, 280, 281, 318, 325, 328, 330, 334, 337, 343
GEOCHEMISTRY, 272, 283, 284, 291, 299, 323, 331, 332, 335, 337, 338, 339, 342
GEOCHRONOLOGY, 188, 321, 332, 528
GEOLOGICAL SURVEYS, 182, 183, 185, 352
GEOLOGY, 178, 183, 284
GEOMAGNETISM, 235, 306
GEOPHYSICS, 178, 193, 350
GEOTEMPERATURE, 188
GEOTHERMAL ENERGY CONVERSION, 191
GEOTHERMAL ENERGY EXTRACTION, 191
GEOTHERMAL RESOURCES, 188, 191, 313
GERMANIUM ISOTOPES, 439
GIBBS FREE ENERGY, 111
GLACIERS, 234, 282
GLASS, 28, 76, 85, 91, 92, 93, 428, 444, 447, 450
GLASS FIBERS, 213
GLOBAL POSITIONING SYSTEM, 9, 129, 187, 189
GLOBAL WARMING, 199
GLOW DISCHARGES, 77
GLUONS, 383, 384, 388, 425, 497
GLYCEROLS, 45
GLYCOLS, 28
GOLD, 381, 391
GRADIENTS, 139
GRAIN BOUNDARIES, 83, 174, 476, 477
GRAIN SIZE, 173
GRANULAR MATERIALS, 36, 150
GRAPHICAL USER INTERFACE, 366
GRAPHITE, 25, 30, 34, 70, 95
GRAPHITE-EPOXY COMPOSITES, 42
GRASSES, 111
GRATINGS (SPECTRA), 207
GRAVITATIONAL EFFECTS, 326, 349
GRAVITATIONAL FIELDS, 263
GRAVITATIONAL WAVES, 527
GRAVITY ANOMALIES, 182
GRAZING INCIDENCE, 393, 448
GREAT PLAINS CORRIDOR (NORTH AMERICA), 237, 247
GREENHOUSE EFFECT, 195, 199, 217, 241, 244, 248, 348, 349, 533
GREENLAND, 234, 332
GRID GENERATION (MATHEMATICS), 173
GROUND OPERATIONAL SUPPORT SYSTEM, 517
GROUND PENETRATING RADAR, 130
GROUND TRUTH, 140
GROUND WATER, 149, 179, 181, 182, 183, 185, 212, 225
GROUND WIND, 189
GUIDANCE (MOTION), 372
GYRATION, 16

H

HABITABILITY, 349
HABITATS, 291, 297
HADRONS, 383, 384, 501, 502, 506, 516
HAFNIUM, 383, 386
HALITES, 291, 305
HALOGEN OCCULTATION EXPERIMENT, 238, 239
HALOGENATION, 65
HALOS, 401, 415, 434, 503
HAMILTONIAN FUNCTIONS, 469, 482
HARDNESS, 34
HARMONIC GENERATIONS, 446
HARMONIC OSCILLATION, 457
HARMONIC RADIATION, 415, 483
HARMONICS, 417
HAY, 118
HAZARDOUS MATERIALS, 172
HAZARDS, 184
HEALTH, 217, 262, 511
HEAT BALANCE, 259
HEAT BUDGET, 241
HEAT ENGINES, 380
HEAT EXCHANGERS, 122
HEAT FLUX, 24, 259, 403
HEAT MEASUREMENT, 112, 172, 477
HEAT PIPES, 24, 151, 200
HEAT RESISTANT ALLOYS, 12, 478
HEAT SOURCES, 431
HEAT TRANSFER, 24, 58, 59, 74, 145, 148, 150, 380
HEAT TRANSFER COEFFICIENTS, 74
HEATING, 160, 442, 460
HEATING EQUIPMENT, 203
HEAVY FERMION SYSTEMS, 423
HEAVY IONS, 382, 395, 399, 400, 401, 413, 423, 461, 467, 468, 469
HEAVY METALS, 405
HELIOSPHERE, 533, 534
HELIUM, 80, 407
HELIUM ISOTOPES, 431
HELMETS, 263
HEMATITE, 304
HETEROGENEITY, 63, 134
HEURISTIC METHODS, 373, 374
HIGGS BOSONS, 412, 492
HIGH ACCELERATION, 408
HIGH ALTITUDE, 239
HIGH CURRENT, 385, 424, 447
HIGH ENERGY ELECTRONS, 466
HIGH ENERGY INTERACTIONS, 393, 394, 395, 430, 516
HIGH FLUX ISOTOPE REACTORS, 443
HIGH GAIN, 135, 391, 446
HIGH POWER LASERS, 78, 162, 448, 466, 488
HIGH PRESSURE, 46, 56, 169, 294, 387
HIGH RESOLUTION, 124, 349, 491
HIGH TEMPERATURE, 83, 92, 289, 530
HIGH TEMPERATURE GASES, 101, 109, 227
HIGH TEMPERATURE PLASMAS, 160
HIGH TEMPERATURE SUPERCONDUCTORS, 89, 127, 128, 143, 203, 473, 474, 477, 480, 482, 484, 485, 486, 487, 489, 493
HIGH TEMPERATURE TESTS, 56, 111
HIGHWAYS, 513, 515
HOHLRAUMS, 147, 464, 469
HOLMIUM, 440
HOLOGRAPHY, 155, 444
HOMOGENEITY, 439
HUBBLE SPACE TELESCOPE, 522
HUGONIOT EQUATION OF STATE, 154
HUMAN FACTORS ENGINEERING, 168, 266

HUMAN-COMPUTER INTERFACE, 374, 506
HUMIDITY, 9
HYDRATION, 326
HYDRIDES, 27
HYDROCARBONS, 33, 44, 105, 108, 210, 249, 279, 306, 323, 327, 335, 390
HYDROCRACKING, 101
HYDROCYANIC ACID, 275
HYDRODYNAMICS, 119, 142, 143, 145, 146, 154, 460, 461, 523
HYDROFLUORIC ACID, 388
HYDROFORMING, 68
HYDROGEN, 65, 80, 82, 94, 191, 326, 407, 424, 425, 455, 492
HYDROGEN COMPOUNDS, 270
HYDROGEN IONS, 60, 290, 402, 468
HYDROGEN PEROXIDE, 494
HYDROGEN PLASMA, 92, 390
HYDROGEN PRODUCTION, 101, 105
HYDROGEN SULFIDE, 269, 287
HYDROGENATION, 59, 92
HYDROGENOLYSIS, 59
HYDROLOGICAL CYCLE, 188, 243, 251
HYDROLOGY, 149, 183, 185, 188, 214
HYDROLOGY MODELS, 181
HYDROLYSIS, 42, 45, 278
HYDROPHONES, 160
HYDROPONICS, 220
HYDROTHERMAL SYSTEMS, 267, 269, 270, 278, 283, 284, 286, 287, 291, 292, 294, 296, 299, 323
HYPERBOLIC DIFFERENTIAL EQUATIONS, 379
HYPERGEOMETRIC FUNCTIONS, 173
HYPERNUCLEI, 419, 422
HYPERSONICS, 239
HYPERVELOCITY IMPACT, 100

I

ICE, 173, 257, 267, 282, 313
ICEBERGS, 256
IDEAL GAS, 142
IDENTIFYING, 5, 349, 417
IGNEOUS ROCKS, 180
IGNITION, 24, 46, 68, 164, 445, 468, 488
ILLUMINANCE, 95
ILLUMINATING, 95
IMAGE ANALYSIS, 157
IMAGE CLASSIFICATION, 354
IMAGE PROCESSING, 4, 157, 355
IMAGE RESOLUTION, 522
IMAGES, 131, 491
IMAGING SPECTROMETERS, 187, 251, 491
IMAGING TECHNIQUES, 88, 124, 158, 169, 193, 236, 284, 295, 439, 445, 446, 472, 501, 522
IMPACT DAMAGE, 14
IMPACT LOADS, 174
IMPACT STRENGTH, 100, 531
IMPACT TESTS, 94
IMPEDANCE, 127, 499
IMPLANTATION, 493
IMPURITIES, 101
IN SITU MEASUREMENT, 169, 221, 232, 256
IN SITU RESOURCE UTILIZATION, 43
IN VITRO METHODS AND TESTS, 260
IN-FLIGHT MONITORING, 11
INCOMPRESSIBLE FLOW, 1, 146, 149, 151
INDEPENDENT VARIABLES, 88, 145
INDEXES (DOCUMENTATION), 517
INDIA, 110
INDIAN OCEAN, 222
INDIUM, 491
INDIUM ARSENIDES, 377, 410, 449
INDIUM COMPOUNDS, 50
INDIUM GALLIUM ARSENIDES, 162, 457
INDIUM PHOSPHIDES, 162
INDOOR AIR POLLUTION, 119, 228
INDUCTION, 205
INDUSTRIAL PLANTS, 61
INDUSTRIES, 110, 508
INELASTIC SCATTERING, 72, 497
INERTIAL CONFINEMENT FUSION, 412, 455, 464, 467, 468, 469, 488
INERTIAL FUSION (REACTOR), 464
INFECTIOUS DISEASES, 260
INFERENCE, 425
INFILTRATION, 150
INFORMATION DISSEMINATION, 358
INFORMATION RESOURCES MANAGEMENT, 224
INFORMATION SYSTEMS, 123, 126, 183, 190, 370, 517, 519
INFORMATION THEORY, 373
INFRARED ABSORPTION, 190
INFRARED ASTRONOMY, 343
INFRARED DETECTORS, 190
INFRARED IMAGERY, 91, 251
INFRARED RADIATION, 35, 190, 347, 348, 456, 493, 498
INFRARED SOURCES (ASTRONOMY), 35
INFRARED SPECTROMETERS, 215
INFRARED SPECTROSCOPY, 52, 71, 288, 348
INHOMOGENEITY, 152
INJECTORS, 413, 438, 465
INJURIES, 263
INORGANIC PEROXIDES, 288
INSECTS, 325
INSTRUMENT FLIGHT RULES, 9
INSULATION, 121
INTEGRATED CIRCUITS, 133
INTERFACE STABILITY, 154
INTERFACES, 96, 138, 140, 141
INTERFACIAL TENSION, 87
INTERFEROMETRY, 131, 389, 450
INTERMETALLICS, 75, 78
INTERNAL ENERGY, 304
INTERNATIONAL COOPERATION, 244, 520
INTERNATIONAL SPACE STATION, 17, 18, 19, 20, 21
INTERNETS, 4, 506
INTEROPERABILITY, 359, 369, 388
INTERPLANETARY DUST, 268, 284, 527
INTERPOLATION, 130, 142
INTERSTELLAR MATTER, 35, 267, 344, 345, 348
INTERSTITIALS, 82
INTRAVEHICULAR ACTIVITY, 265
INVENTORIES, 184
IO, 529
ION ACCELERATORS, 461
ION ACOUSTIC WAVES, 468
ION BEAMS, 118, 400, 412, 413, 420, 424, 439, 468
ION CHARGE, 424
ION CURRENTS, 26
ION CYCLOTRON RADIATION, 465, 529
ION ENGINES, 26
ION IMPLANTATION, 38, 73, 92, 133, 488, 493
ION IRRADIATION, 43, 82, 87, 91, 471
ION MOBILITY SPECTROSCOPY, 37
ION SCATTERING, 471
ION SOURCES, 390, 400, 413, 424, 466
ION TRAPS (INSTRUMENTATION), 420
IONIC COLLISIONS, 382, 400, 423, 502
IONIC CRYSTALS, 472
IONIC REACTIONS, 395
IONIC WAVES, 529
IONIZATION, 148, 390, 398, 400
IONIZATION CHAMBERS, 410
IONIZING RADIATION, 65
IONS, 133, 261, 421, 425, 460, 469

IRON, 57, 64, 66, 82, 114, 235, 284, 306
IRON 58, 323
IRON ALLOYS, 83, 201, 475
IRON COMPOUNDS, 271
IRON ISOTOPES, 283, 309
IRON OXIDES, 287
IRRADIANCE, 22
IRRADIATION, 79, 80, 406, 407, 429, 447
ISCCP PROJECT, 225
ISOMERIZATION, 59, 275
ISOMERS, 66
ISOTOPE EFFECT, 103
ISOTOPE RATIOS, 103, 188, 337, 339, 528
ISOTOPES, 88, 172, 389
ISOTOPIC LABELING, 339
ISOTOPIC SPIN, 438
ITERATION, 375, 494
ITERATIVE SOLUTION, 100, 368

J

JAHN-TELLER EFFECT, 472
JAPAN, 243
JAVA (PROGRAMMING LANGUAGE), 369
JET ENGINE FUELS, 8
JOINTS (JUNCTIONS), 167
JOSEPHSON EFFECT, 468
JOSEPHSON JUNCTIONS, 484
JUPITER (PLANET), 345
JUPITER SATELLITES, 301

K

KANSAS, 99, 181
KAONS, 506
KAPOETA ACHONDRITE, 528
KARHUNEN-LOEVE EXPANSION, 176
KENTUCKY, 225
KEROGEN, 335
KINEMATICS, 415, 434
KINETIC ENERGY, 421
KINETICS, 112, 432
KLYSTRONS, 402, 410, 442, 504
KONDO EFFECT, 423
KRYPTON, 386

L

LABORATORIES, 513
LAGRANGIAN FUNCTION, 142
LAKES, 300
LAMINAR FLOW, 11, 14
LAMINATES, 393, 486, 490
LAND ICE, 227
LAND SURFACE TEMPERATURE, 225
LANDAU DAMPING, 468
LANDFORMS, 528
LANGEVIN FORMULA, 428
LANTHANUM CHLORIDES, 474
LAPLACE EQUATION, 126
LARGE EDDY SIMULATION, 144, 151
LASER ALTIMETERS, 232, 531
LASER APPLICATIONS, 448
LASER BEAMS, 162, 447, 449, 455, 464
LASER CAVITIES, 162, 179
LASER DAMAGE, 161, 396, 445, 447, 451, 455
LASER DOPPLER VELOCIMETERS, 142
LASER FUSION, 179
LASER INDUCED FLUORESCENCE, 31, 396
LASER MATERIALS, 444
LASER OUTPUTS, 160, 448, 455
LASER PLASMA INTERACTIONS, 463
LASER PUMPING, 162
LASER SPECTROSCOPY, 421, 436
LASER TARGET INTERACTIONS, 30
LASER TARGETS, 455
LASER-INDUCED BREAKDOWN SPECTROSCOPY, 405
LASERS, 50, 75, 160, 162, 163, 384, 445, 449, 450, 451, 456, 464, 466, 488
LASING, 162
LATENT HEAT, 256
LATERAL CONTROL, 393
LATTICES (MATHEMATICS), 504
LAUNCHING, 16
LAUNCHING BASES, 15
LAYOUTS, 368
LEAD (METAL), 441
LEAD ACID BATTERIES, 206
LEAD ZIRCONATE TITANATES, 134
LEADERSHIP, 510, 512, 513, 515
LEAKAGE, 18, 150, 156
LEARNING, 494, 508
LEAST SQUARES METHOD, 142
LENSES, 450
LEONID METEOROIDS, 527
LEPTONS, 383
LETHALITY, 100
LEVITATION, 115
LIAPUNOV FUNCTIONS, 145
LIBRARIES, 406, 518, 519
LIE GROUPS, 142, 353
LIFE (DURABILITY), 89, 96
LIFE CYCLE COSTS, 203, 378, 487
LIFE DETECTORS, 295
LIFE SCIENCES, 270, 279, 287, 296
LIGANDS, 274, 398
LIGHT (VISIBLE RADIATION), 251, 293, 454, 459
LIGHT AMPLIFIERS, 445
LIGHT CURVE, 527
LIGHT EMISSION, 86, 234
LIGHT GAS GUNS, 53
LIGHT SOURCES, 52, 62, 161, 401, 453, 456, 459
LIGHT WATER REACTORS, 72
LIGHTNING, 16, 252
LIMITERS (FUSION REACTORS), 463
LINE SPECTRA, 293
LINEAR ACCELERATORS, 60, 137, 140, 152, 163, 380, 390, 397, 398, 400, 401, 402, 403, 408, 409, 410, 411, 413, 414, 424, 425, 429, 433, 460, 475, 488, 498, 499, 500, 503, 504, 505, 506
LINEAR ALTERNATORS, 210
LINEAR POLARIZATION, 391
LINEAR SYSTEMS, 368, 518
LIPIDS, 279, 283
LIQUID CHROMATOGRAPHY, 275
LIQUID COOLING, 120, 407
LIQUID FUELS, 98
LIQUID HELIUM, 416
LIQUID HYDROGEN, 118, 194
LIQUID LITHIUM, 393
LIQUID METALS, 32, 390
LIQUID NITROGEN, 120
LIQUID PHASE SINTERING, 478
LIQUID PHASES, 478
LIQUID SURFACES, 30
LIQUID WASTES, 219, 221, 437
LIQUID-LIQUID INTERFACES, 81, 154
LITHIUM, 200, 207, 349, 393
LITHIUM ALLOYS, 32
LITHIUM BATTERIES, 195, 198, 205
LITHIUM CHLORIDES, 145
LITHIUM COMPOUNDS, 49
LITHOGRAPHY, 75, 76, 155, 448
LITHOLOGY, 186, 332
LITHOSPHERE, 184, 530
LOAD DISTRIBUTION (FORCES), 207
LOADING OPERATIONS, 17, 18, 21, 446
LOADS (FORCES), 131, 167, 193, 263, 407
LOCAL THERMODYNAMIC EQUILIBRIUM, 150
LOGIC CIRCUITS, 135
LONG DURATION SPACE FLIGHT, 265

LONG WAVE RADIATION, 348
LONGITUDINAL CONTROL, 145
LORENTZ FORCE, 88
LOSSES, 5, 410
LOUVERS, 392, 396
LOW COST, 514
LOW CURRENTS, 466
LOW EARTH ORBITS, 187
LOW MOLECULAR WEIGHTS, 95
LOW TEMPERATURE, 65, 86
LUMINAIRES, 378
LUMINESCENCE, 439, 481
LUMINOSITY, 392
LUNAR ORBITS, 340
LUNAR PROGRAMS, 537
LUNAR ROCKS, 283
LYRA CONSTELLATION, 524

M

MACHINE LEARNING, 378
MACHINE TOOLS, 117
MACHINING, 118, 164
MACROMOLECULES, 57, 141, 346
MAGELLANIC CLOUDS, 525, 526
MAGNESIUM, 82, 491, 492
MAGNESIUM COMPOUNDS, 85
MAGNESIUM ISOTOPES, 438
MAGNETARS, 537
MAGNETIC DIPOLES, 385
MAGNETIC DISTURBANCES, 235
MAGNETIC EFFECTS, 399
MAGNETIC FIELD CONFIGURATIONS, 446, 471
MAGNETIC FIELD RECONNECTION, 467
MAGNETIC FIELDS, 136, 431, 439, 460, 470
MAGNETIC FILMS, 68, 77, 140, 486
MAGNETIC MATERIALS, 446
MAGNETIC POLES, 499
MAGNETIC PROPERTIES, 27, 437, 482
MAGNETIC RESONANCE, 193
MAGNETIC SURVEYS, 182
MAGNETITE, 304, 306
MAGNETIZATION, 79, 382, 478, 486, 490
MAGNETO-OPTICS, 446
MAGNETOACOUSTIC WAVES, 470
MAGNETOHYDRODYNAMIC FLOW, 460
MAGNETOHYDRODYNAMIC STABILITY, 462, 467, 468
MAGNETOHYDRODYNAMIC WAVES, 534
MAGNETOHYDRODYNAMICS, 32, 202, 203, 393, 467, 533
MAGNETOMETERS, 235
MAGNETORESISTIVITY, 382, 480
MAGNETRON SPUTTERING, 486
MAGNETS, 360, 391, 499
MAGNIFICATION, 445
MAGNITUDE, 210
MAN ENVIRONMENT INTERACTIONS, 241
MANAGEMENT, 97, 508, 515
MANAGEMENT METHODS, 508, 515
MANAGEMENT PLANNING, 216, 508, 516
MANAGEMENT SYSTEMS, 12, 15, 266, 373, 516
MANDRELS, 42
MANGANESE, 65
MANGANESE ALLOYS, 80
MANGANESE COMPOUNDS, 474
MANGANESE OXIDES, 446
MANGANIN (TRADEMARK), 169
MANIPULATORS, 392
MANUALS, 376
MANUFACTURING, 133, 171, 198, 204, 363, 487, 491
MANY BODY PROBLEM, 522
MAPPING, 242
MARINE CHEMISTRY, 331
MARINE ENVIRONMENTS, 285, 290
MARINE METEOROLOGY, 253, 255
MARKET RESEARCH, 122, 204
MARKETING, 97
MARKING, 298
MARS (PLANET), 288, 289, 302, 308, 310, 313, 314, 315, 316, 531, 532
MARS ATMOSPHERE, 310, 529, 532
MARS ENVIRONMENT, 299, 308
MARS EXPLORATION, 24, 301
MARS GLOBAL SURVEYOR, 531
MARS MISSIONS, 303
MARS PHOTOGRAPHS, 313, 528
MARS SURFACE, 288, 304, 305, 310, 314, 333, 528, 530, 531, 532
MARS SURFACE SAMPLES, 318
MARSHLANDS, 255
MARTENSITIC STAINLESS STEELS, 70
MARTENSITIC TRANSFORMATION, 78
MASS, 383, 422
MASS DISTRIBUTION, 221
MASS FLOW RATE, 416
MASS SPECTRA, 305, 506
MASS SPECTROMETERS, 20, 24, 77, 398
MASS SPECTROSCOPY, 18, 307
MASS TRANSFER, 527
MASSIVE COMPACT HALO OBJECTS, 521
MASSIVE STARS, 526
MATERIALS HANDLING, 121, 446
MATERIALS RECOVERY, 86, 101, 118
MATERIALS SELECTION, 40, 41, 165
MATERIALS TESTS, 163, 170
MATHEMATICAL MODELS, 9, 10, 16, 33, 47, 50, 63, 66, 83, 112, 125, 130, 145, 147, 149, 162, 172, 176, 178, 181, 192, 193, 207, 209, 221, 224, 236, 239, 244, 246, 249, 271, 276, 347, 358, 363, 369, 371, 376, 377, 379, 389, 417, 425, 436, 451, 473, 490, 494, 497, 523, 533, 534
MATRIX MATERIALS, 481
MATRIX METHODS, 150
MAXIMUM LIKELIHOOD ESTIMATES, 343
MAXWELL EQUATION, 126
MEAN SQUARE VALUES, 63, 404
MEASURE AND INTEGRATION, 160, 404
MEASUREMENT, 217
MEASURING INSTRUMENTS, 69, 83, 138, 392, 403, 415, 498
MECHANICAL ENGINEERING, 132, 168
MECHANICAL PROPERTIES, 34, 37, 41, 70, 80, 90, 93, 95, 121, 131, 164, 176, 178, 236, 393, 473
MECHANICAL SHOCK, 176
MEDICAL EQUIPMENT, 142
MEDICAL SCIENCE, 450
MEDICAL SERVICES, 204
MELTING, 444
MELTING POINTS, 92, 200
MEMBRANES, 87, 94, 104, 228, 290
MEMORY (COMPUTERS), 471
MENTAL PERFORMANCE, 264
MERCURY (METAL), 29, 53, 67, 186, 215, 216, 230, 231, 233
MERCURY COMPOUNDS, 230, 233
MERCURY VAPOR, 29
MESOMETEOROLOGY, 222
MESONS, 391, 396, 412, 416, 496, 497, 498, 502
MESOSCALE PHENOMENA, 222, 244
MESSAGE PROCESSING, 368
MESSAGES, 128, 368
METABOLISM, 284, 287, 294
METAL BONDING, 61
METAL CLUSTERS, 73
METAL COATINGS, 138
METAL FILMS, 36, 72

METAL FOILS, 74, 75, 113
METAL FUELS, 428
METAL IONS, 92, 205, 207, 291
METAL MATRIX COMPOSITES, 42
METAL OXIDES, 54, 59
METAL SHELLS, 26
METAL WORKING, 121
METALLIC GLASSES, 85
METALLIC HYDROGEN, 53
METALLIZING, 485, 492
METALLURGY, 81
METALORGANIC CHEMICAL VAPOR DEPOSITION, 50, 480, 492, 493
METALS, 71, 78, 86, 473
METAMORPHISM (GEOLOGY), 339
METASTABLE STATE, 409, 478
METEORITES, 309, 346, 528
METEORITIC COMPOSITION, 309, 311, 313, 314, 318, 346, 528, 536
METEOROLOGICAL INSTRUMENTS, 242
METEOROLOGICAL PARAMETERS, 196, 212, 218, 231, 243, 247, 532
METEOROLOGICAL SATELLITES, 245, 255
METEOROLOGY, 224, 246
METHANE, 32, 92, 104, 107, 226, 335, 386
METHOD OF MOMENTS, 403
METHOXY SYSTEMS, 29
METHYL ALCOHOL, 112
METHYL CHLORIDE, 62
METHYL COMPOUNDS, 60, 109
METROLOGY, 171, 389, 445
MICELLES, 45
MICROANALYSIS, 33, 197, 261
MICROBIOLOGY, 50, 294, 350, 351, 352
MICROCRACKS, 174
MICROELECTROMECHANICAL SYSTEMS, 37, 93, 117, 131, 132, 137, 138, 139, 170, 362, 452
MICROELECTRONICS, 86, 129, 439
MICROGRAVITY, 115, 265
MICROINSTRUMENTATION, 23, 139
MICROMACHINING, 50, 117, 137, 457
MICROMECHANICS, 137
MICROMINIATURIZATION, 138
MICROORGANISMS, 37, 49, 274, 281, 282, 283, 284, 285, 286, 287, 288, 291, 294, 295, 296, 297, 298, 299, 300, 308, 313, 315, 316, 319, 324, 325, 327, 328, 333, 334, 335, 336, 339, 340, 341, 343, 351, 352
MICROPARTICLES, 105
MICROPROCESSORS, 363
MICROSATELLITES, 22
MICROSTRUCTURE, 38, 47, 73, 76, 90, 474, 475, 478, 486, 490, 494, 497
MICROWAVE IMAGERY, 235, 256
MICROWAVE RADIOMETERS, 255
MICROWAVES, 166, 432
MIDDLE ATMOSPHERE, 240
MIDDLE EAST, 178
MILITARY AIRCRAFT, 4
MILITARY TECHNOLOGY, 89, 124, 517
MILKY WAY GALAXY, 524
MILLIMETER WAVES, 134
MINERAL DEPOSITS, 190, 305, 318, 323, 339, 352
MINERALOGY, 288, 298, 301, 337, 338, 339, 340
MINERALS, 39, 47, 85, 270, 298, 332, 341, 342
MINES, 130
MINES (ORDNANCE), 417
MINIATURIZATION, 138, 362, 457
MINKOWSKI SPACE, 496
MIR SPACE STATION, 265
MIRRORS, 201, 444, 449
MISSILE CONTROL, 25
MISSILE RANGES, 25
MISSILES, 25
MIXING RATIOS, 232
MIXTURES, 87
MOBILITY, 372
MODEL REFERENCE ADAPTIVE CONTROL, 357
MODELS, 58, 107, 108, 111, 112, 176, 253
MODERATORS, 386
MODULATORS, 397
MODULES, 155, 159, 354
MODULUS OF ELASTICITY, 34
MOISTURE, 156, 241, 246
MOISTURE CONTENT, 214, 532
MOLECULAR BIOLOGY, 273, 274, 282, 286, 327, 337
MOLECULAR CHAINS, 89, 176, 276
MOLECULAR CLOUDS, 35, 250, 520
MOLECULAR DYNAMICS, 276, 401, 426, 436, 462, 491
MOLECULAR GASES, 348
MOLECULAR INTERACTIONS, 48, 418
MOLECULAR STRUCTURE, 66
MOLECULAR WEIGHT, 90, 96, 492
MOLECULES, 279, 340, 344, 349
MOLTEN CARBONATE FUEL CELLS, 204
MOLTEN SALTS, 145
MOLYBDENUM, 342, 389
MOLYBDENUM ALLOYS, 77
MOLYBDENUM ISOTOPES, 524
MOMENTUM THEORY, 186
MONGOLIA, 195
MONITORS, 20, 140, 219, 235, 403, 410, 434
MONOCHROMATORS, 393, 407, 451
MONOMERS, 42
MONSOONS, 244, 245
MONTE CARLO METHOD, 162, 173, 224, 378, 379, 383, 388, 406, 488, 497, 506, 507, 528
MOON, 520
MORALE, 512
MORPHOLOGY, 96, 161, 287, 296, 340, 386, 482, 494, 534
MOTIVATION, 510, 512, 513
MULLITES, 35, 55
MULTIGRID METHODS, 100, 365
MULTILAYER INSULATION, 89
MULTIMEDIA, 358
MULTIPHASE FLOW, 147, 154, 236
MULTIPROCESSING (COMPUTERS), 384
MULTISPECTRAL PHOTOGRAPHY, 158
MUONS, 382, 384, 398, 403, 408, 411, 424, 536
MUSIC, 417
MUTAGENS, 276
MYLAR (TRADEMARK), 63, 416

N

NANOCOMPOSITES, 39
NANOCRYSTALS, 481, 484
NANOSTRUCTURE (CHARACTERISTICS), 39, 411
NANOSTRUCTURES (DEVICES), 133
NANOTECHNOLOGY, 458
NARCOTICS, 5
NARROWBAND, 453
NASA PROGRAMS, 180
NASA SPACE PROGRAMS, 14, 17, 248, 266
NATIONAL AIRSPACE SYSTEM, 7
NATURAL GAS, 108, 185, 366
NAVIER-STOKES EQUATION, 144, 149
NAVIGATION, 361
NAVIGATION INSTRUMENTS, 129
NEAR INFRARED RADIATION, 252, 288, 293
NECK (ANATOMY), 263
NEGATIVE IONS, 424
NEODYMIUM, 444
NEODYMIUM ISOTOPES, 339
NEODYMIUM LASERS, 445

NEON, 396
NERVES, 374
NETWORK ANALYSIS, 375
NEURONS, 263
NEUTRAL PARTICLES, 422
NEUTRINO BEAMS, 411
NEUTRINOS, 382, 395, 408, 411, 422, 425
NEUTRON COUNTERS, 173, 452
NEUTRON DIFFRACTION, 52, 53, 389, 478
NEUTRON EMISSION, 67, 420, 435
NEUTRON IRRADIATION, 43, 49, 70, 393
NEUTRON PHYSICS, 414
NEUTRON RADIOGRAPHY, 172, 501
NEUTRON SCATTERING, 53, 389, 398, 419, 443, 479
NEUTRON SOURCES, 152, 381, 386, 402, 403, 409, 414, 420, 425, 433, 435, 439, 459, 503, 504, 505, 507
NEUTRON STARS, 527
NEUTRONS, 67, 80, 96, 383, 389, 407, 420, 427, 479, 490
NEVADA, 188
NEW JERSEY, 191
NEW MEXICO, 198
NEW YORK, 191
NICKEL, 79, 271
NICKEL ALLOYS, 27, 83, 475, 478
NIOBATES, 490
NIOBIUM, 36, 427, 490
NITRATES, 181
NITRIC OXIDE, 105
NITRIDING, 166
NITROGEN, 134, 237, 269, 270, 457
NITROGEN OXIDES, 66, 113, 114, 115, 163, 192, 213, 217, 231, 240
NITROGENATION, 52
NOBLE METALS, 520
NOESS, 245
NONDESTRUCTIVE TESTS, 10, 69, 81, 91, 169, 172, 173, 418, 476, 501
NONEQUILIBRIUM FLOW, 346
NONLINEAR EQUATIONS, 354
NONLINEAR OPTICS, 38, 426
NONLINEAR PROGRAMMING, 354
NONLINEAR SYSTEMS, 145, 354
NONLINEARITY, 177, 377, 451, 465
NORTH AMERICA, 242, 246
NORTH CAROLINA, 258
NORTHERN HEMISPHERE, 239
NOVAE, 525
NOZZLE DESIGN, 2, 26
NOZZLE FLOW, 2
NOZZLE GEOMETRY, 2
NOZZLE THRUST COEFFICIENTS, 2
NUCLEAR ELECTRIC POWER GENERATION, 443, 518
NUCLEAR FUELS, 83, 429
NUCLEAR FUSION, 462, 524
NUCLEAR HEAT, 431
NUCLEAR INTERACTIONS, 419
NUCLEAR MAGNETIC RESONANCE, 195, 275, 483, 488, 492
NUCLEAR PARTICLES, 435
NUCLEAR PHYSICS, 406, 407, 412, 414, 422, 431, 440, 441, 455, 459, 460
NUCLEAR POWER PLANTS, 219, 221
NUCLEAR REACTIONS, 147, 395, 427, 525
NUCLEAR REACTORS, 81, 172
NUCLEAR RESEARCH, 70
NUCLEAR STRUCTURE, 394, 402, 407, 428, 429
NUCLEAR WEAPONS, 89
NUCLEATION, 161, 306, 485
NUCLEI (NUCLEAR PHYSICS), 381, 399, 475
NUCLEIC ACIDS, 279
NUCLEON-NUCLEON INTERACTIONS, 387, 415, 440, 502
NUCLEON-NUCLEON SCATTERING, 402
NUCLEONS, 404
NUCLIDES, 406, 427
NUMERICAL ANALYSIS, 68, 76, 100, 143, 151, 184, 360, 377, 379, 392, 393, 423, 432, 434, 472, 486, 531
NUMERICAL CONTROL, 170
NUMERICAL FLOW VISUALIZATION, 153
NUMERICAL INTEGRATION, 377, 428

O

O RING SEALS, 89
O STARS, 526
OBJECT-ORIENTED PROGRAMMING, 354, 358, 366, 370, 518
OBLIQUENESS, 534
OCEAN BOTTOM, 240, 257, 258, 267, 297, 323, 324
OCEAN MODELS, 235, 259
OCEAN SURFACE, 187, 234, 256, 258, 259
OCEANOGRAPHY, 256, 324
OCEANS, 257, 331, 338
OHMS LAW, 149
OIL FIELDS, 99
OIL RECOVERY, 43, 99
OILS, 61, 201
OLIVINE, 311, 312
ON-LINE SYSTEMS, 18, 130
OPACITY, 150
OPEN CLUSTERS, 523
OPERATIONS RESEARCH, 508
OPTICAL EQUIPMENT, 45, 444, 448, 455
OPTICAL FIBERS, 454
OPTICAL FILTERS, 453
OPTICAL MATERIALS, 446
OPTICAL MEASURING INSTRUMENTS, 248
OPTICAL PATHS, 128
OPTICAL PROPERTIES, 155, 202, 247, 252, 445, 450, 451, 493
OPTICAL RADAR, 221, 232, 243, 247, 458
OPTICAL SCANNERS, 192
OPTICAL THICKNESS, 211
OPTICAL TRANSITION, 432
OPTICS, 451, 459
OPTIMIZATION, 231, 358, 365, 373
ORBITAL ELEMENTS, 522
ORBITAL RENDEZVOUS, 19
ORBITAL RESONANCES (CELESTIAL MECHANICS), 534
ORBITALS, 482
ORGANIC CHEMISTRY, 282
ORGANIC COMPOUNDS, 24, 267, 270, 279, 314, 348
ORGANIC MATERIALS, 30, 38, 57, 160, 268, 274, 307, 312, 314, 318, 341, 342, 344, 348
ORGANIC SILICON COMPOUNDS, 30
ORGANIC SUPERCONDUCTORS, 493
ORGANISMS, 277, 286, 291, 318, 326, 336, 337
ORGANIZATIONS, 224, 510
ORGANOMETALLIC COMPOUNDS, 346
ORGANOMETALLIC POLYMERS, 118
ORTHOPHOTOGRAPHY, 183
OSCILLATING FLOW, 534
OSCILLATIONS, 522
OUTGASSING, 326
OVERPRESSURE, 24
OXIDATION, 33, 47, 53, 78, 104, 230, 233, 299, 326
OXIDATION-REDUCTION REACTIONS, 61, 62, 105, 337, 342
OXIDE FILMS, 482
OXIDES, 471
OXIDIZERS, 287
OXYGEN, 90, 321, 326, 329, 331, 334, 532
OXYGEN ISOTOPES, 289, 309, 311, 322, 323, 324, 400
OXYGEN PRODUCTION, 529

OXYGENATION, 341
OZONE, 212, 217, 218, 222, 229, 240, 243, 246, 247
OZONOMETRY, 229

P

PACIFIC ISLANDS, 520
PACKAGING, 117, 132
PADE APPROXIMATION, 395
PAIR PRODUCTION, 383
PALEOBIOLOGY, 280, 325
PALEOCLIMATOLOGY, 241, 324, 534
PALEONTOLOGY, 280, 321, 326, 337, 342, 352
PALEOZOIC ERA, 337
PALLADIUM ALLOYS, 80
PANELS, 121
PAPERS, 508
PARABOLIC REFLECTORS, 192
PARAFFINS, 54
PARALLEL COMPUTERS, 11, 356, 504
PARALLEL PROCESSING (COMPUTERS), 182, 353, 356, 360, 365, 370, 371
PARAMETER IDENTIFICATION, 420
PARAMETERIZATION, 242, 251, 535
PARAMETRIC AMPLIFIERS, 451
PARSING ALGORITHMS, 360
PARTIAL PRESSURE, 258
PARTICLE ACCELERATION, 438
PARTICLE ACCELERATORS, 390, 391, 397, 406, 412, 413, 423, 430, 458, 496, 500
PARTICLE BEAMS, 399, 401, 450, 460, 497, 502
PARTICLE COLLISIONS, 381, 387, 411, 412
PARTICLE DECAY, 399, 409, 441, 498, 501
PARTICLE DIFFUSION, 422
PARTICLE INTERACTIONS, 76, 398
PARTICLE MOTION, 483
PARTICLE PRODUCTION, 381, 397, 404, 497, 500
PARTICLE SPIN, 402
PARTICLE THEORY, 396, 421, 492
PARTICULATES, 215
PATTERN RECOGNITION, 157
PAVEMENTS, 362
PAYLOADS, 16, 158
PECLET NUMBER, 56
PENETRATION, 99
PENETROMETERS, 405
PEPTIDES, 267, 274, 278, 488
PERFORMANCE, 16
PERFORMANCE PREDICTION, 209, 353, 371
PERFORMANCE TESTS, 2, 6, 24, 87, 89, 127, 131, 149, 151, 157, 166, 172, 248, 387
PERMANENT MAGNETS, 68
PERMEABILITY, 40, 180, 188, 236
PERSONNEL DEVELOPMENT, 4
PERTURBATION, 235, 466, 469
PERTURBATION THEORY, 148, 401, 425, 496
PETROLOGY, 85, 333, 339
PH, 81
PH FACTOR, 290
PHASE CHANGE MATERIALS, 203
PHASE STABILITY (MATERIALS), 32
PHASE TRANSFORMATIONS, 46, 67, 87, 270, 374, 471, 479, 507
PHILIPPINES, 208
PHOENIX (AZ), 292
PHONONS, 72
PHOSPHATES, 444
PHOSPHORS, 439
PHOSPHORUS, 306
PHOSPHORUS COMPOUNDS, 65
PHOTOCHEMICAL REACTIONS, 276, 289, 335, 520
PHOTOCONDUCTIVITY, 134, 135
PHOTOELECTRIC EMISSION, 392, 486
PHOTOELECTRICITY, 250
PHOTOELECTROCHEMICAL DEVICES, 105
PHOTOELECTROCHEMISTRY, 57
PHOTOELECTRON SPECTROSCOPY, 308
PHOTOELECTRONS, 48
PHOTOGRAPHIC RECORDING, 532
PHOTOGRAPHIC RECTIFIERS, 448
PHOTOGRAPHY, 158
PHOTOIONIZATION, 48, 386
PHOTOLITHOGRAPHY, 129, 158, 197
PHOTOLUMINESCENCE, 449, 457
PHOTOLYSIS, 59, 105
PHOTOMETERS, 377
PHOTON BEAMS, 378, 415, 450, 459
PHOTON-ELECTRON INTERACTION, 400
PHOTONICS, 135, 160, 457, 458
PHOTONS, 60, 161, 249, 377, 383, 400, 401, 416, 423, 439, 449, 494, 497, 498, 502, 504, 506
PHOTONUCLEAR REACTIONS, 401, 498
PHOTOPRODUCTION, 395, 497
PHOTOSYNTHESIS, 108, 288, 335, 337
PHOTOVOLTAIC CELLS, 484
PHOTOVOLTAIC CONVERSION, 194, 196, 197, 198, 203, 209
PHYSICAL CHEMISTRY, 277, 520
PHYSIOCHEMISTRY, 267
PHYSIOLOGICAL RESPONSES, 326
PIEZOELECTRIC MOTORS, 134
PIEZOELECTRICITY, 448
PIGMENTS, 284
PILOT PLANTS, 64
PILOTLESS AIRCRAFT, 16, 155
PINNING, 481
PIONS, 395, 404, 498
PIPELINING (COMPUTERS), 123
PIPES (TUBES), 120
PISTONS, 174
PITCH (INCLINATION), 263
PITTING, 386
PIXELS, 354
PLANETARY ATMOSPHERES, 237, 283, 342
PLANETARY ENVIRONMENTS, 330, 340, 347
PLANETARY EVOLUTION, 267, 289, 308, 334, 338, 339, 340, 345, 347, 349, 533
PLANETARY GEOLOGY, 233, 531, 532
PLANETARY MAPPING, 531
PLANETARY MASS, 522
PLANETARY NEBULAE, 348
PLANETARY RINGS, 533
PLANETARY STRUCTURE, 302
PLANETARY SYSTEMS, 343, 344, 345, 349
PLANETS, 343
PLANKTON, 335
PLANTS (BOTANY), 62
PLASMA ACCELERATORS, 465
PLASMA CURRENTS, 468
PLASMA DIAGNOSTICS, 461
PLASMA DRIFT, 463
PLASMA ELECTRODES, 159
PLASMA ETCHING, 494
PLASMA HEATING, 470
PLASMA PHYSICS, 464
PLASMA PINCH, 468
PLASMA RESONANCE, 461, 468
PLASMA TURBULENCE, 470
PLASMA WAVES, 466
PLASMAS (PHYSICS), 36, 387, 390, 460, 462, 463, 465, 467, 468, 470, 489, 535
PLASTIC DEFORMATION, 73
PLASTIC FLOW, 175
PLASTIC PROPERTIES, 175
PLUMES, 30
PLUTONIUM, 77, 428

PLUTONIUM 238, 26
PLUTONIUM OXIDES, 26, 43, 62
POINT DEFECTS, 82
POISSON DENSITY FUNCTIONS, 417
POLAR METEOROLOGY, 239
POLAR REGIONS, 239, 254
POLARIMETERS, 409
POLARIZATION, 408, 424, 437, 455
POLARIZERS, 446
POLITICS, 513
POLLUTION CONTROL, 66, 182, 211, 214, 215, 223, 226, 230
POLLUTION TRANSPORT, 181
POLYCRYSTALS, 170
POLYCYCLIC AROMATIC HYDROCARBONS, 35
POLYETHYLENES, 28
POLYHEDRONS, 490
POLYIMIDES, 84, 132
POLYMER BLENDS, 87
POLYMER CHEMISTRY, 275
POLYMERIZATION, 39, 114, 272, 281
POLYMERS, 28, 39, 89, 94, 96, 191, 388
POLYMETHYL METHACRYLATE, 382
POLYNOMIALS, 401
POLYNUCLEOTIDES, 278
POLYPEPTIDES, 279
POLYURETHANE FOAM, 86, 121
POLYURETHANE RESINS, 88
POMERONS, 421
POROSITY, 2, 30, 33, 184
POROUS MATERIALS, 36, 56
POROUS SILICON, 50
POSITRON ANNIHILATION, 132, 429
POSITRONS, 411, 429, 497
POWDER METALLURGY, 33
POWER AMPLIFIERS, 159
POWER EFFICIENCY, 448, 463
POWER GAIN, 454
POWER LINES, 89
POWER PLANTS, 168, 205
POWER REACTORS, 432
PRECAMBRIAN PERIOD, 297, 326, 327, 329, 330, 331, 332, 334, 336, 338, 339, 342
PRECIPITATES, 484
PRECIPITATION (CHEMISTRY), 91
PRECIPITATION (METEOROLOGY), 226, 244, 255
PRECISION, 117, 389
PREDICTION ANALYSIS TECHNIQUES, 37, 244
PREDICTIONS, 181, 363, 461
PRESSURE, 9
PRESSURE DISTRIBUTION, 11
PRESSURE EFFECTS, 88
PRESSURE MEASUREMENT, 11
PRESSURE SENSORS, 131
PRESSURE VESSELS, 194, 456
PRESSURIZED WATER REACTORS, 171
PREVENTION, 223
PREVENTIVE MAINTENANCE, 202
PRIMARY BATTERIES, 202
PRIMATES, 261
PRINTED CIRCUITS, 158
PRINTING, 354
PRISMS, 128
PROBABILITY DENSITY FUNCTIONS, 377
PROBABILITY THEORY, 174, 176, 184, 343
PROBLEM SOLVING, 430
PROCEDURES, 226
PROCUREMENT, 4, 370
PRODUCT DEVELOPMENT, 11, 167, 203, 356
PRODUCTION ENGINEERING, 144
PROFILOMETERS, 444
PROGRAM VERIFICATION (COMPUTERS), 12, 451
PROGRAMMING ENVIRONMENTS, 366
PROGRAMMING LANGUAGES, 360, 367
PROGRESS, 464, 510
PROJECT MANAGEMENT, 508
PROJECT PLANNING, 509
PROJECTILES, 100
PROKARYOTES, 281, 300
PROPELLANT BINDERS, 88
PROPELLANT CONSUMPTION, 26
PROPELLANTS, 26
PROPIONIC ACID, 109
PROPULSION, 165
PROTECTION, 84, 286
PROTECTIVE COATINGS, 12, 32, 55, 156
PROTEIN CRYSTAL GROWTH, 45
PROTEINS, 60, 262, 269, 273, 274, 275, 276, 277, 280, 307, 328, 473, 488
PROTOBIOLOGY, 272, 276
PROTOCOL (COMPUTERS), 4, 29, 127
PROTON BEAMS, 403, 404, 405, 415, 433, 439, 503, 504
PROTON ENERGY, 426
PROTON IMPACT, 390
PROTON-ANTIPROTON INTERACTIONS, 425
PROTONS, 80, 397, 399, 401, 406, 407, 421, 427, 434, 438, 441, 475
PROTOPLANETARY DISKS, 345
PROTOPLANETS, 345
PROTOTYPES, 125, 358, 384, 385, 473, 485, 500
PROVING, 58, 353
PUBLIC HEALTH, 260
PULSE DURATION, 432, 452, 466
PULSE DURATION MODULATION, 138
PULSE GENERATORS, 205
PULSED LASERS, 74, 448, 468
PULSES, 439, 454
PURIFICATION, 288
PYRITES, 329
PYROTECHNICS, 50
PYRUVATES, 272

Q

QUADRUPOLES, 20, 402, 404, 415, 483
QUALIFICATIONS, 205
QUALITY CONTROL, 216, 418
QUANTITATIVE ANALYSIS, 20, 112
QUANTUM CHROMODYNAMICS, 387, 395, 404, 421, 425, 431, 495, 497, 501, 504, 505, 506, 507
QUANTUM EFFICIENCY, 452
QUANTUM ELECTRODYNAMICS, 401, 506
QUANTUM ELECTRONICS, 141
QUANTUM MECHANICS, 45, 60, 502
QUANTUM STATISTICS, 492
QUANTUM THEORY, 96, 495, 503, 507
QUARKS, 388, 404, 409, 440, 497, 500, 501, 504, 505
QUARTZ, 291
QUASARS, 526
QUASI-BIENNIAL OSCILLATION, 222
QUENCHING (ATOMIC PHYSICS), 420

R

RADAR, 131, 372
RADAR DETECTION, 125
RADAR IMAGERY, 129
RADAR MEASUREMENT, 243, 255
RADAR SIGNATURES, 125
RADIAL FLOW, 400
RADIAL VELOCITY, 349
RADIANCE, 155, 252
RADIANT HEATING, 78, 421
RADIATION, 14, 137, 239
RADIATION CHEMISTRY, 261
RADIATION COUNTERS, 156
RADIATION DAMAGE, 37, 91, 261, 447, 471, 494
RADIATION DETECTORS, 156, 479, 536

RADIATION DISTRIBUTION, 253, 467
RADIATION EFFECTS, 330, 426, 488
RADIATION MEASUREMENT, 16, 249
RADIATION SOURCES, 469, 488
RADIATION SPECTRA, 432
RADIATION THERAPY, 378
RADIATION TRANSPORT, 383, 406
RADIATION TRAPPING, 464
RADIATIVE HEAT TRANSFER, 16
RADIATIVE RECOMBINATION, 461
RADIATIVE TRANSFER, 249, 286
RADICALS, 33
RADIO EQUIPMENT, 266
RADIO FREQUENCIES, 16, 138, 159, 380, 381, 408, 415, 425, 442, 457, 459, 500
RADIOACTIVE CONTAMINANTS, 213
RADIOACTIVE DECAY, 438
RADIOACTIVE ISOTOPES, 190, 528
RADIOACTIVE MATERIALS, 63, 121
RADIOACTIVE WASTES, 28, 93, 122, 172, 180, 236, 436, 437, 438, 504, 520
RADIOACTIVITY, 172, 228, 520
RADIOCHEMISTRY, 185
RADIOGRAPHY, 397, 415, 439, 461
RADIOISOTOPE BATTERIES, 484
RADIOMETERS, 252
RADIOSONDES, 222
RAIN, 245
RAMAN SPECTRA, 447, 463, 493
RAMAN SPECTROSCOPY, 243, 284, 487
RANDOM ACCESS MEMORY, 155
RANDOM PROCESSES, 176
RARE EARTH ALLOYS, 27
RARE EARTH ELEMENTS, 53, 68
RATINGS, 3
REACTION KINETICS, 32, 45, 50, 51, 59, 60, 62, 104, 119, 192, 230, 233, 278, 393, 406, 418, 488, 525
REACTION TIME, 100
REACTOR DESIGN, 441
REACTOR MATERIALS, 32
REACTOR SAFETY, 435
REACTOR TECHNOLOGY, 93, 104
REAL TIME OPERATION, 18, 124, 372, 471, 472
RECOMBINATION REACTIONS, 418
RECOVERY, 150
RECRYSTALLIZATION, 78, 82, 490
RED SHIFT, 524
REDUCTION (CHEMISTRY), 105, 269
REFLECTANCE, 30, 75, 76, 181, 248, 453, 482
REFLECTOMETERS, 30
REFRACTIVITY, 9
REFRIGERANTS, 120
REFRIGERATORS, 121, 416
REGENERATION (ENGINEERING), 109
REGRESSION ANALYSIS, 216
REGULATIONS, 216, 223
REGULATORY MECHANISMS (BIOLOGY), 328
RELATIVISTIC THEORY, 402
RELIABILITY, 124, 126, 170, 206
RELIABILITY ANALYSIS, 174, 206
REMOTE CONTROL, 124
REMOTE MANIPULATOR SYSTEM, 17
REMOTE REGIONS, 352
REMOTE SENSING, 125, 155, 187, 189, 190, 232, 235, 238, 251, 254, 256, 259, 288, 302, 372, 373, 531
REMOTE SENSORS, 295
REMOVAL, 212
RENEWABLE ENERGY, 108, 110, 194, 204, 208
RENORMALIZATION GROUP METHODS, 501
RESEARCH, 261, 393, 465, 477
RESEARCH AND DEVELOPMENT, 36, 371, 430, 476, 493, 509, 513
RESEARCH FACILITIES, 393, 423, 430, 516, 518
RESEARCH MANAGEMENT, 219, 318
RESEARCH PROJECTS, 141, 384
RESERVOIRS, 188
RESIDUAL STRESS, 42, 47, 83, 177
RESIDUES, 62, 439
RESISTORS, 131, 141, 156
RESONANCE, 399
RESONATORS, 139, 162
RESOURCES MANAGEMENT, 190, 195
RESPONSES, 175, 451
RESTORATION, 158
REUSE, 101
REVIEWING, 510
REVISIONS, 435
REYNOLDS AVERAGING, 144
RHENIUM, 387
RHEOLOGY, 233, 234
RIBONUCLEIC ACIDS, 271, 273, 278, 281, 322
RIPPLES, 530
RISK, 4, 217, 369
RIVER BASINS, 185, 190, 305
RIVERS, 179, 185
ROBOTICS, 12, 117, 121, 373, 454
ROBOTS, 362, 372
ROBUSTNESS (MATHEMATICS), 146
ROCK MECHANICS, 236
ROCKET ENGINES, 25
ROCKET LAUNCHING, 24
ROCKET VEHICLES, 17
ROCKS, 233, 292, 298, 309, 333, 341
RODS, 407
ROLLER BEARINGS, 69
ROOT-MEAN-SQUARE ERRORS, 404
ROTARY WINGS, 2
ROTATION, 128, 237
ROTOR AERODYNAMICS, 2
ROVING VEHICLES, 12, 374
RUNGE-KUTTA METHOD, 142
RUTILE, 81

S

SAFETY, 5, 168, 179, 257, 429, 516
SAFETY MANAGEMENT, 8
SALINITY, 291, 295, 310, 324
SAMPLING, 185, 212, 225
SANDS, 240, 530
SANDWICH STRUCTURES, 201
SAPPHIRE, 86, 160
SATELLITE ATMOSPHERES, 306, 533
SATELLITE CONSTELLATIONS, 255
SATELLITE IMAGERY, 181, 243
SATELLITE INSTRUMENTS, 218, 245
SATELLITE OBSERVATION, 222, 243, 251
SATELLITE SOUNDING, 243
SATELLITE SURFACES, 302
SATELLITE TEMPERATURE, 22
SATURATION, 184
SATURN (PLANET), 345
SCALARS, 364, 425
SCALING LAWS, 413, 523
SCANNERS, 4, 251, 365, 405
SCANNING ELECTRON MICROSCOPY, 296, 317
SCATTERING, 132, 211, 440, 447, 470
SCATTERING CROSS SECTIONS, 399, 412
SCHEDULING, 514, 515
SCHROEDINGER EQUATION, 502
SCIENTIFIC VISUALIZATION, 265, 359, 370
SCIENTISTS, 17, 358
SCRAMBLING (COMMUNICATION), 381
SCRUBBERS, 29
SEA ICE, 256
SEA LEVEL, 9

SEA SURFACE TEMPERATURE, 238, 259
SEA WATER, 324, 331
SEALING, 168
SEAS, 238, 257, 291
SECURITY, 5, 7
SEDIMENT TRANSPORT, 528
SEDIMENTARY ROCKS, 305, 323, 329, 352
SEDIMENTS, 219, 221, 258, 296, 299, 323, 331, 332, 333, 338, 339, 340, 341, 342
SEISMIC WAVES, 234, 240
SEISMOLOGY, 140, 178, 179, 184, 193, 236
SELF ASSEMBLY, 87
SELF CONSISTENT FIELDS, 54
SEMANTICS, 358
SEMICONDUCTOR DEVICES, 31, 489
SEMICONDUCTOR LASERS, 136, 161, 162, 456
SEMICONDUCTORS (MATERIALS), 35, 132, 134, 135, 457, 480, 487, 492, 493
SEMISOLIDS, 121
SENSITIVITY, 131, 467
SENSITIVITY ANALYSIS, 148, 226, 246, 378
SENSORS, 23, 129, 158, 508
SEPARATED FLOW, 147
SEPARATORS, 142, 144
SEPTUM, 385
SEQUENCING, 325, 328
SERVICE LIFE, 37, 94
SHALLOW WATER, 339, 379
SHAPE MEMORY ALLOYS, 78
SHAPED CHARGES, 99
SHAPES, 174
SHEAR STRESS, 176
SHELLS (STRUCTURAL FORMS), 98
SHIELDING, 82, 392, 396
SHIFT REGISTERS, 367
SHOCK LAYERS, 14
SHOCK LOADS, 154, 388
SHOCK TUNNELS, 154
SHOCK WAVES, 50, 146, 235, 346, 409, 534
SHORT WAVE RADIATION, 249, 253
SHOT PEENING, 78
SIGNAL ANALYSIS, 130
SIGNAL PROCESSING, 158, 406
SIGNAL REFLECTION, 189
SIGNAL TO NOISE RATIOS, 414
SIGNATURE ANALYSIS, 125, 295
SILICA GLASS, 444, 447
SILICIDES, 490
SILICON, 38, 207, 346, 488, 494
SILICON CARBIDES, 35, 55, 493, 526, 527
SILICON DIOXIDE, 58, 89, 90, 91, 285, 292
SILICON NITRIDES, 88, 166
SILICON OXIDES, 346, 426, 482
SILICON POLYMERS, 138, 170
SILK, 262
SILOXANES, 42
SILVER, 346
SILVER COMPOUNDS, 47
SIMULATED ANNEALING, 374
SIMULATION, 32, 145, 226, 263, 353, 385, 388, 401, 464, 499
SIMULATORS, 100, 365
SINGLE CRYSTALS, 81, 82, 86, 210, 471, 484
SINTERING, 33
SIS (SUPERCONDUCTORS), 480
SITUATIONAL AWARENESS, 264
SIZE DISTRIBUTION, 349
SKY SURVEYS (ASTRONOMY), 521
SLOTS, 2
SMOKE, 211, 222, 284
SMOOTHING, 365
SNC METEORITES, 304, 305, 313, 315, 316, 318
SNOW, 330
SNOW COVER, 242
SODALITE, 28
SODAR, 242
SODIUM, 276, 406, 494
SODIUM CARBONATES, 200
SODIUM CHLORIDES, 240
SOFIA (AIRBORNE OBSERVATORY), 343
SOFT GAMMA REPEATERS, 537
SOFTWARE DEVELOPMENT TOOLS, 358, 363, 369, 374
SOFTWARE ENGINEERING, 357, 360, 361, 366, 369
SOFTWARE RELIABILITY, 153
SOI (SEMICONDUCTORS), 38
SOIL MOISTURE, 214, 245
SOILS, 186, 216, 339
SOL-GEL PROCESSES, 210
SOLAR ACTIVITY, 535
SOLAR CELLS, 202, 203, 207, 494
SOLAR COLLECTORS, 459
SOLAR CORONA, 533
SOLAR CYCLES, 534
SOLAR ELECTRIC PROPULSION, 26
SOLAR ENERGY, 196, 198, 203, 209
SOLAR ENERGY CONVERSION, 200, 201, 203, 209
SOLAR HEATING, 122, 203
SOLAR MAGNETIC FIELD, 533
SOLAR NEBULA, 346, 536
SOLAR NEUTRINOS, 504, 535
SOLAR OSCILLATIONS, 535
SOLAR PHYSICS, 523
SOLAR RADIATION, 22, 196, 246, 286, 335, 534
SOLAR SIMULATION, 533
SOLAR SYSTEM, 268, 340, 343, 347, 522
SOLAR SYSTEM EVOLUTION, 345
SOLAR TERRESTRIAL INTERACTIONS, 534
SOLAR WIND VELOCITY, 237
SOLDERING, 76
SOLDERS, 86
SOLID ELECTROLYTES, 198, 207
SOLID LUBRICANTS, 33
SOLID MECHANICS, 376
SOLID OXIDE FUEL CELLS, 197, 199, 201
SOLID PHASES, 29
SOLID STATE, 480, 492
SOLID STATE DEVICES, 133
SOLID STATE LASERS, 136, 444, 451, 454, 455
SOLID STATE PHYSICS, 81, 197, 483
SOLID WASTES, 109, 185, 231
SOLIDIFIED GASES, 386
SOLIDS, 34, 50, 56, 275
SOLUBILITY, 88, 91, 93
SOLUTIONS, 67
SOLVENT EXTRACTION, 27
SOLVENTS, 88, 89
SONAR, 160
SOOT, 45
SORBENTS, 212
SOUND DETECTING AND RANGING, 242
SOURCES, 423
SOUTHERN HEMISPHERE, 222
SOUTHERN OSCILLATION, 222
SPACE CHARGE, 461
SPACE EXPLORATION, 115, 116, 301, 304
SPACE FLIGHT, 261
SPACE HEATING (BUILDINGS), 120
SPACE MISSIONS, 307, 344
SPACE POWER REACTORS, 24
SPACE PROBES, 303
SPACE SHUTTLES, 14, 20
SPACE STATION MODULES, 21
SPACE TRANSPORTATION, 17
SPACEBORNE ASTRONOMY, 343
SPACEBORNE PHOTOGRAPHY, 528
SPACEBORNE TELESCOPES, 84

SPACECRAFT, 531
SPACECRAFT DESIGN, 22
SPACECRAFT DOCKING, 19, 20, 21
SPACECRAFT ENVIRONMENTS, 22
SPACECRAFT INSTRUMENTS, 303
SPACECRAFT LANDING, 20
SPACECRAFT LAUNCHING, 19, 537
SPACECRAFT POWER SUPPLIES, 443
SPACECRAFT PROPULSION, 26
SPACECREWS, 17, 18, 19, 21
SPALLATION, 80, 83, 152, 178, 402, 410, 419, 433, 435, 439, 503, 505
SPARKS, 164
SPATIAL RESOLUTION, 522
SPECIFIC HEAT, 482
SPECTRA, 177, 286, 353, 415
SPECTRAL BANDS, 472
SPECTRAL METHODS, 521
SPECTRAL SIGNATURES, 288
SPECTRORADIOMETERS, 242
SPECTROSCOPIC ANALYSIS, 14, 487
SPECTROSCOPY, 33, 38, 274, 292, 293, 381, 396, 417, 422, 468, 472, 501, 521
SPECTRUM ANALYSIS, 305, 308, 407, 470
SPEECH RECOGNITION, 417
SPENT FUELS, 437
SPHERICAL PLASMAS, 421
SPHERICAL SHELLS, 468
SPIN, 392, 471
SPIN RESONANCE, 407
SPONTANEOUS EMISSION, 446
SPRAYERS, 60
SPRINGS (WATER), 289, 291, 299
SPUTNIK SATELLITES, 537
SPUTTERING, 47, 71, 118, 138
SQUARE WAVES, 138
SQUID (DETECTORS), 128, 484
STABILITY, 270, 385, 428, 466, 522, 527
STABILITY TESTS, 163, 522
STABILIZATION, 381
STAINLESS STEELS, 67, 68, 79
STANDARD DEVIATION, 263
STANDARD MODEL (PARTICLE PHYSICS), 395, 422
STANDARDS, 141, 209, 354, 509
STANDING WAVES, 81
STARBURST GALAXIES, 526
STARS, 344
STATISTICAL ANALYSIS, 93, 176, 207, 247, 271, 378
STATISTICAL MECHANICS, 374
STATORS, 61
STEADY STATE, 432
STEELS, 69, 71, 77, 83
STELLAR CORONAS, 523
STELLAR ENVELOPES, 349
STELLAR EVOLUTION, 526
STELLAR ORBITS, 522
STELLAR SYSTEMS, 347, 348
STELLARATORS, 460, 462, 468
STIMULATION, 185
STIRLING ENGINES, 200
STOCHASTIC PROCESSES, 417, 428
STOICHIOMETRY, 328
STORAGE BATTERIES, 202
STORAGE RINGS (PARTICLE ACCELERATORS), 159, 382, 385, 394, 408, 432, 445, 456
STRAIN DISTRIBUTION, 175
STRANGENESS, 422
STRATOSPHERE, 218, 221, 222, 232, 236, 243, 247, 269
STREAMS, 186
STRESS (PHYSIOLOGY), 263
STRESS ANALYSIS, 188
STRESS CONCENTRATION, 75
STRESS CORROSION CRACKING, 171
STRESS DISTRIBUTION, 96
STRESS MEASUREMENT, 177
STRESS RELAXATION, 47
STRESS-STRAIN RELATIONSHIPS, 10
STRESSES, 69, 131
STRING THEORY, 499
STRINGS, 498
STRONG INTERACTIONS (FIELD THEORY), 395
STRONTIUM, 51
STRUCTURAL ANALYSIS, 140, 174, 531
STRUCTURAL BASINS, 182
STRUCTURAL DESIGN, 184
STRUCTURAL ENGINEERING, 514
STRUCTURAL FAILURE, 10
STRUCTURAL PROPERTIES (GEOLOGY), 184
STRUCTURAL VIBRATION, 176, 177
STRUCTURED GRIDS (MATHEMATICS), 370
STUDENTS, 350, 351, 430
SUBSIDENCE, 103
SUBSTRATES, 61, 76, 79, 271, 446
SUBSTRUCTURES, 73
SULFATES, 258, 285, 329
SULFIDES, 54, 338
SULFUR, 109, 282, 284, 306, 331, 349
SULFUR COMPOUNDS, 220
SULFUR DIOXIDES, 212
SULFUR ISOTOPES, 322, 329
SULFUR OXIDES, 46
SUN, 84, 534, 536
SUNLIGHT, 105
SUPERCOMPUTERS, 379, 384, 504
SUPERCONDUCTING DEVICES, 140, 488
SUPERCONDUCTING FILMS, 136, 468, 487, 493, 495
SUPERCONDUCTING MAGNETS, 425, 488
SUPERCONDUCTIVITY, 210, 476, 477, 478, 485, 494
SUPERCONDUCTORS (MATERIALS), 132, 380, 486, 490
SUPERCRITICAL FLUIDS, 35, 113
SUPERFLUIDITY, 80
SUPERGRAVITY, 496
SUPERLATTICES, 72, 77, 449, 489
SUPERNOVA 1987A, 523
SUPERNOVA REMNANTS, 523
SUPERNOVAE, 524, 525, 526, 527
SUPERSONIC DIFFUSERS, 14
SUPERSONIC FLOW, 11
SUPERSONIC NOZZLES, 2
SUPERSONIC WIND TUNNELS, 14
SUPERSYMMETRY, 395, 397, 499
SUPPORT SYSTEMS, 170
SURFACE EMITTING LASERS, 132
SURFACE IONIZATION, 413
SURFACE PROPERTIES, 30, 71, 81, 494
SURFACE REACTIONS, 347
SURFACE ROUGHNESS, 234
SURFACE WATER, 201
SURFACTANTS, 32
SURVEILLANCE, 160
SURVEYS, 183, 295
SURVIVAL, 285
SWEPT WINGS, 11
SWITCHES, 134, 135, 397, 480
SWITCHING, 454
SYMBIOSIS, 327
SYMMETRY, 402, 462, 485, 506
SYNCHRONISM, 128
SYNCHROTRON RADIATION, 137, 394
SYNCHROTRONS, 52, 71, 381, 391, 407, 421, 427, 502
SYNTHESIS (CHEMISTRY), 29, 38, 39, 68, 87, 92, 95, 109, 267, 269, 273, 279, 473
SYNTHETIC APERTURE RADAR, 124, 129, 130, 234
SYNTHETIC FUELS, 98, 110
SYSTEMS ANALYSIS, 467, 518

SYSTEMS ENGINEERING, 12, 44, 125, 158, 169, 170, 193, 194, 266, 356, 357, 403, 454, 463
SYSTEMS INTEGRATION, 4, 363, 364
SYSTEMS MANAGEMENT, 367

T

T TAURI STARS, 349
TANGENTS, 138
TANTALUM COMPOUNDS, 51
TARGET ACQUISITION, 362
TARGETS, 392, 396, 406, 439, 443, 466, 506
TAXONOMY, 352
TAYLOR INSTABILITY, 149, 466, 494
TECHNOLOGIES, 464, 471
TECHNOLOGY ASSESSMENT, 109, 136, 151, 166, 172, 197, 206, 241, 354, 369
TECHNOLOGY TRANSFER, 13, 205, 508
TECHNOLOGY UTILIZATION, 26, 132, 440
TECTONICS, 530
TELECOMMUNICATION, 124, 262
TELESCOPES, 344, 448
TEMPERATURE, 231
TEMPERATURE CONTROL, 22, 165, 203
TEMPERATURE DEPENDENCE, 75, 111, 312, 448
TEMPERATURE DISTRIBUTION, 238
TEMPERATURE EFFECTS, 121, 410, 481
TEMPERATURE MEASUREMENT, 77, 80
TEMPORAL DISTRIBUTION, 282
TENSILE STRENGTH, 41
TENSILE STRESS, 178
TERMINAL FACILITIES, 365
TERNARY ALLOYS, 52, 489
TERRA SPACECRAFT, 187
TERRESTRIAL PLANETS, 233, 344, 347
TEST FACILITIES, 150
TESTS, 4
TETRAHEDRONS, 173
TEXTURES, 312, 486, 490
THALLIUM COMPOUNDS, 489
THEORETICAL PHYSICS, 373, 395, 422, 430, 499, 525
THERAPY, 427
THERMAL ANALYSIS, 58, 148, 312, 435
THERMAL CONDUCTIVITY, 33, 146, 393, 443
THERMAL CONTROL COATINGS, 12
THERMAL DECOMPOSITION, 276
THERMAL DEGRADATION, 88
THERMAL DIFFUSIVITY, 91
THERMAL ENERGY, 84, 191
THERMAL ENVIRONMENTS, 22, 169, 297
THERMAL EXPANSION, 90
THERMAL FATIGUE, 438
THERMAL INSTABILITY, 207
THERMAL INSULATION, 12, 84, 89, 260
THERMAL PROTECTION, 14
THERMAL SHOCK, 460
THERMAL STABILITY, 76
THERMAL STRESSES, 180
THERMIONIC CATHODES, 137
THERMIONIC EMISSION, 137
THERMIONIC EMITTERS, 138
THERMOCHEMISTRY, 63
THERMODYNAMIC EQUILIBRIUM, 250
THERMODYNAMIC PROPERTIES, 39, 482, 494
THERMODYNAMICS, 90, 92, 111, 112, 122, 180, 234, 273
THERMOELASTICITY, 409
THERMOELECTRIC POWER GENERATION, 346
THERMOGRAVIMETRY, 56
THERMOHYDRAULICS, 432, 435
THERMONUCLEAR REACTIONS, 32, 161, 413
THERMOPHILES, 283, 285, 291, 292, 293, 336
THERMOSPHERE, 237
THICK FILMS, 86
THICK PLATES, 94
THIN FILMS, 31, 38, 39, 51, 71, 72, 76, 79, 84, 90, 92, 93, 129, 133, 137, 138, 197, 306, 446, 471, 472, 481, 485, 487, 489
THREE DIMENSIONAL FLOW, 147, 151, 210, 462
THREE DIMENSIONAL MODELS, 31, 44, 126, 144, 180, 232, 251, 369
THRESHOLD CURRENTS, 161
THRUST CHAMBERS, 25
TILTING ROTORS, 7
TIME DEPENDENCE, 125, 496
TIME OF FLIGHT SPECTROMETERS, 307, 503
TIME SERIES ANALYSIS, 161
TIN ALLOYS, 393
TISSUES (BIOLOGY), 162, 448, 450
TITAN, 306, 533
TITANIUM, 74, 160, 383
TITANIUM ALUMINIDES, 75
TOKAMAK DEVICES, 462, 463, 469
TOLERANCES (PHYSIOLOGY), 300
TOMOGRAPHY, 365
TOOLS, 122, 168
TOPOGRAPHY, 81, 158, 531
TOPOLOGY, 364
TOTAL OZONE MAPPING SPECTROMETER, 218, 222
TOTAL QUALITY MANAGEMENT, 3
TOUCH, 265
TOXICITY, 26, 29
TRACE CONTAMINANTS, 238
TRACE ELEMENTS, 220
TRAJECTORIES, 502
TRAJECTORY OPTIMIZATION, 365
TRANSFER FUNCTIONS, 408, 442
TRANSFORMATIONS (MATHEMATICS), 353
TRANSITION METALS, 34, 44, 54, 68
TRANSMISSION ELECTRON MICROSCOPY, 410, 480
TRANSMISSION LINES, 127
TRANSMITTERS, 433
TRANSMUTATION, 438
TRANSONIC WIND TUNNELS, 15
TRANSPORT PROPERTIES, 146, 182, 437, 485
TRANSPORT THEORY, 422, 430
TRANSPORTATION, 514
TRAPPING, 326
TRAVELING WAVES, 408
TREND ANALYSIS, 130
TRIBOLOGY, 31, 93
TRITIUM, 393, 516
TRMM SATELLITE, 226
TROPICAL REGIONS, 212, 218, 222, 226, 236, 241
TROPOPAUSE, 236
TROPOSPHERE, 155, 218, 229, 238, 243, 251
TRUCKS, 165, 223
TUBES, 27
TUNABLE LASERS, 163, 456
TUNGSTEN, 406, 407, 480
TUNGSTEN ISOTOPES, 77
TUNNEL JUNCTIONS, 478
TURBINE ENGINES, 380
TURBINE PUMPS, 149
TURBINES, 166, 167, 206
TURBOCOMPRESSORS, 118
TURBOGENERATORS, 97
TURBULENCE, 152, 235, 256
TURBULENT DIFFUSION, 249
TURBULENT FLAMES, 8, 164
TURBULENT FLOW, 147, 149, 151, 154

TURBULENT JETS, 149
TURBULENT MIXING, 154
TVD SCHEMES, 379
TWINNING, 446
TWISTING, 484
TWO DIMENSIONAL MODELS, 68, 142, 144, 463, 504
TWO PHASE FLOW, 120, 152, 153, 380, 416

U

ULTRASHORT PULSED LASERS, 450
ULTRASONIC FLAW DETECTION, 418
ULTRASONIC SCANNERS, 418
ULTRAVIOLET LASERS, 442
ULTRAVIOLET RADIATION, 37, 229, 286, 296
UNCERTAIN SYSTEMS, 376
UNDERGROUND COMMUNICATION, 128
UNDERGROUND EXPLOSIONS, 140
UNDERWATER ACOUSTICS, 240
UNDERWATER EXPLOSIONS, 113
UNDERWATER VEHICLES, 131
UNIFIED FIELD THEORY, 495
UNITED STATES, 110, 247
UNIVERSITIES, 351
UNSTEADY FLOW, 143, 149, 151, 153
UNSTRUCTURED GRIDS (MATHEMATICS), 142
URANIUM, 190, 342, 437
URANIUM ALLOYS, 27, 429
URANIUM COMPOUNDS, 436, 443
URANIUM OXIDES, 334
URBAN TRANSPORTATION, 191, 206
USER MANUALS (COMPUTER PROGRAMS), 22, 44, 97, 217, 361, 389

V

VACANCIES (CRYSTAL DEFECTS), 411
VACUUM CHAMBERS, 444
VACUUM DEPOSITION, 36
VACUUM SYSTEMS, 228, 466
VALLEYS, 188
VALVES, 20, 174
VANADIUM, 43, 129, 342, 481
VANADIUM ALLOYS, 32, 393
VAPOR DEPOSITION, 32, 90, 92, 197, 387
VAPOR PHASES, 119, 215
VAPORIZING, 383
VAPORS, 46
VARIABILITY, 212, 224, 243, 248
VARIABLE STARS, 521
VARIANCE (STATISTICS), 95
VARNISHES, 292
VECTORS (MATHEMATICS), 501
VEGETATION, 158, 183
VELOCITY, 250
VELOCITY DISTRIBUTION, 184, 259
VELOCITY MEASUREMENT, 186, 235
VENTILATION, 119, 120
VENTS, 270, 287, 296, 297
VENUS (PLANET), 348, 530, 532
VERTEBRATES, 325
VERTICAL DISTRIBUTION, 212, 232
VIBRATION, 451, 472
VIBRATION DAMPING, 23, 176
VIBRATION EFFECTS, 24
VIBRATIONAL SPECTRA, 66
VIDEO COMMUNICATION, 262
VIDEO DATA, 124
VIDEO TAPES, 454
VIKING MARS PROGRAM, 318
VINYL POLYMERS, 207
VINYLIDENE, 207
VIRTUAL REALITY, 364
VIRUSES, 125, 288
VISCOSITY, 146, 492
VISCOUS FLOW, 151
VISUAL DISCRIMINATION, 286
VISUAL PERCEPTION, 265
VISUAL SIGNALS, 128
VOICE COMMUNICATION, 128
VOLATILE ORGANIC COMPOUNDS, 65, 212, 228
VOLATILITY, 536
VOLCANOES, 180, 292, 313, 347
VOLCANOLOGY, 180
VOLTAGE CONVERTERS (DC TO DC), 402
VORTEX AVOIDANCE, 3
VORTICES, 143, 239, 477

W

WAFERS, 129
WAKES, 465
WALLS, 15
WASTE DISPOSAL, 180, 436, 437
WASTE ENERGY UTILIZATION, 122, 150
WASTE MANAGEMENT, 78, 86, 91, 170
WASTE TREATMENT, 49, 428
WASTE UTILIZATION, 110, 231
WASTE WATER, 179, 220
WASTES, 27, 85
WATER, 62, 81, 105, 301, 302, 308, 310, 315, 491, 532
WATER COOLED REACTORS, 41
WATER FLOW, 149, 152, 153, 227, 491
WATER HEATING, 122
WATER POLLUTION, 186, 212
WATER RESOURCES, 188, 190
WATER SAMPLING, 186
WATER SPLITTING, 105
WATER TABLES, 284
WATER VAPOR, 215, 229, 243, 248, 251, 348
WATER WAVES, 240
WATERSHEDS, 181
WAVE ATTENUATION, 403
WAVE FRONTS, 448
WAVE PACKETS, 453
WAVE PROPAGATION, 100, 234, 235, 403, 534
WAVE SCATTERING, 395
WAVEFORMS, 445
WAVEGUIDE LASERS, 454
WAVEGUIDES, 452
WAVELENGTHS, 389, 453
WAXES, 95, 113
WEAK INTERACTIONS (FIELD THEORY), 395
WEAR, 31, 94
WEAR TESTS, 26
WEATHER, 196, 226, 246, 362
WEATHER FORECASTING, 222, 245, 256
WEATHER RECONNAISSANCE AIRCRAFT, 257
WEATHERING, 47, 309, 312, 339
WEBSITES, 358
WEIGHT (MASS), 517
WELDED JOINTS, 79
WELLS, 100, 185, 201, 212, 236
WICKS, 200
WIDE AREA NETWORKS, 127, 366
WIND (METEOROLOGY), 208, 210, 212, 234, 237, 249
WIND EFFECTS, 528, 530
WIND MEASUREMENT, 208
WIND TUNNEL MODELS, 14
WIND TUNNEL TESTS, 2, 15
WIND TURBINES, 193, 207
WIND VARIATIONS, 234
WIND VELOCITY, 189, 259
WINDING, 157
WINDPOWER UTILIZATION, 191, 195, 204, 208
WINDPOWERED GENERATORS, 204
WIRE, 73, 128
WORKING FLUIDS, 39

WORLD WIDE WEB, 358, 518
WORMS, 325
WYOMING, 185

X

X RAY APPARATUS, 163
X RAY DETECTORS, 473, 478, 487, 504
X RAY DIFFRACTION, 67, 387, 479, 488
X RAY LASERS, 162, 163, 452
X RAY SCATTERING, 399
X RAY SOURCES, 407, 523, 537
X RAY SPECTRA, 524
X RAY SPECTROSCOPY, 147
X RAY TIMING EXPLORER, 537
X RAYS, 155, 161, 169, 252, 305, 449, 462, 465, 469, 475, 480
XENON, 82, 83, 481, 484
XEROGELS, 30

Y

YAG LASERS, 445
YAGI ANTENNAS, 138
YANG-MILLS THEORY, 505
YBCO SUPERCONDUCTORS, 61, 79, 477, 485, 495
YELLOWSTONE NATIONAL PARK (ID-MT-WY), 291, 292
YIELD POINT, 383, 455
YIELD STRENGTH, 175
YTTRIA-STABILIZED ZIRCONIA, 199
YTTRIUM OXIDES, 83, 477

Z

ZEEMAN EFFECT, 472
ZEOLITES, 54, 91, 104, 105, 141
ZETA PINCH, 462, 464, 467, 469
ZINC, 65, 494
ZIRCONIUM OXIDES, 53, 83, 426

Personal Author Index

A

Abbott, B., 388
Abbott, D., 506
Abbott, D. J., 498
Abeyounis, William K., 1
Abolins, M., 475
Abraham, D. P., 64, 78
Abrajano, T., 102
Abrams, M., 63
Abrikosov, A. A., 477
Aceves, S. M., 144, 194
Ackerman, Steven A., 251
Adams, D. P., 118
Adams, James, 254
Adams, Richard J., 8
Addessi,, 416
Adizzone, Joe, 234
Adkins, D. R., 88
Adler, Robert F., 225
Adriaans, M. J., 80
Afanasyev, I., 82
Agarwal, D., 126
Aggarwal, S., 471
Ahle, L., 413, 461
Ahle, L. E., 466
Ahluwalia, R., 191
Ahluwalia, R. K., 193
Ahmed, S., 98
Ahmidouch, A., 498, 506
Ahrenkiel, S. P., 449
Ahuja, S., 91
Ahumada, A. J., Jr., 378
Airieau, Sabine, 322
Akella, J., 387
Akovali, Y. A., 518
Akyurtlu, A., 212
Akyurtlu, J. F., 212
Albert, D., 258
Albright, N., 378
Alcock, C., 521, 524
Ale, B., 4
Alexander, C. M. O. D., 301
Alford, O. J., 397
Alger, T., 159
Alhorn, Dean C., 137, 157
Allain, J. P., 463
Allamandola, L. J., 35
Allamandola, Louis J., 267
Allderdice, A., 208
Allen, C., 401
Allen, C. K., 433
Allen, C. W., 481, 484
Allen, Carlton, 282
Allen, Carlton C., 291, 316
Allen, Carlton, C., 304
Allen, J., 132
Allen, J. J., 136
Allen, Jaclyn S., 351
Allen, T. H., 43
Allen, T. R., 90
Allerman, A. A., 50, 162, 201, 457
Allison, W. W. M., 536
Allsman, R. A., 521, 524
Alman, D. A., 389
Alme, H. J., 161
Alner, G. J., 536
Alonso, E., 43
Alp, E. E., 72
Alperin, M., 258
Alptekin, G., 104
AlsNielsen, J., 392
Althouse, P. E., 212
Alvares, N., 43
Alves, D. R., 521, 524
Alyer, J., 479
AmaralZettler, Linda A., 352
Amari, S., 524, 526
Ambrose, D., 387
Ambrozewicz, P., 506
Amend, Jan P., 290
Amils, R., 284
Amils, Ricardo, 299
Amine, K., 207
Amir, Amir R., 264
Amthor, J. E., 321
Amzajerdian, Farzin, 128
An, F., 223
Andersen, P., 61
Anderson, A. T., 396
Anderson, B. J., 21, 22
Anderson, D., 432
Anderson, J., 103
Anderson, J. W., 474
Anderson, O. Roger, 285
Anderson, P. A., 437
Anderson, R. P., 107
Anderson, S. E., 384
Andersson, A., 159
Andraka, C. E., 200
Andrews, Arlyn E., 232
Anklam, T. M., 383
Annamalai, H., 244
Anthony, T. R., 472
Appelshauser, H., 400
Apruzese, J. P., 461
Aranson, I. S., 150, 186
Arbogast, T., 183
Arcand, B., 177
Ardizzone, Joe, 256
Argueta, J., 206
Aris, John P., 280
Armatys, Michael, 189
Armendariz, M. G., 131
Armijo, J., 464
Armstrong, C. S., 498, 506
Armstrong, R., 388
Armstrong, R. A., 246
Arnaud, Sara B., 261
Arndt, R. A., 395
Arnold, N., 447
Arnold, N. D., 161
Arnold, S., 444
Arrington, J., 498
Arthur, E. D., 420
Arthur, Michael A., 324, 329
Artna-Cohen, A., 518
Aselage, T. L., 80
Ashbridge, Dawn A., 284
Ashby, C. I., 129
Askew, Gregory, 263
Askew, T. R., 473
Asoka-Kumar, P., 429
Assink, R. A., 88
Atkins, Michael S., 285
Atkinson, Christopher, 210
Atlas, R., 244
Atlas, Robert M., 234, 256
Attaway, S. W., 376
Attwood, D., 158
Atwood,, 58
Auciello, O., 93, 133, 471
Auerbach, J., 455
Aufderheide, M., 461
Aufderheide, M. B., 169
Augustynowicz, S. D., 84, 89, 260
Aumiller, D. L., 153
Autrey, D., 461
Auvray, L., 28
Axelrad, Penina, 189, 258
Axelrod, T. S., 521, 524
Axford, R. A., 142, 353
Ayres, D. S., 395, 536

B

Babcock, S. E., 474
Babinski, A., 410
Baboul, A. G., 49
Babski, Dianne P., 351
Babu, Sachi, 156
Babzien, M., 453
Baca, A. G., 134
Bachler, J., 400
Back, B. B., 381, 391, 421, 502
Bader, S. D., 77, 79, 474, 486
Baer, M. R., 7
Baer, T., 62
Bahowick, S., 446
Bailey, D. S., 467
Bailey, K., 454
Bailey, S. J., 400
Baines, K. H., 522
Bajaj, C. L., 364
Bajit, S., 76
Bajt, S., 74
Baker, G., 425
Baker, John W., 205
Baker, M. D., 502
Baker, R., 63
Baker, S. A., 157
Bakker, W. T., 201
Balachandran, U., 86, 94, 473, 474, 485, 486
Balakrishnan, J., 383
Balas, Gary J., 145
Baldridge, Alice M., 304
Baldridge, W., 184
Ballinger, M. Y., 211
Bally, John, 345
Bandey, H. L., 139
Bandopadhyay, S., 90
Bangert, P., 436
Bangerter, R. O., 467, 468
Baptista, Pedro, 254
Baranowski, J. M., 410
Barbee, T. W., 47, 462
Barben, C. L., 134
Barber, R. C., 398
Barcz, A., 492
Bareiss, R. A., 508
Barfknecht, A. T., 478
Barker, A. R., 356
Barker, H., 252
Barmore, Bryan E., 8
Barna, D., 400
Barnard, J., 461
Barnard, J. J., 467
Barnard, Stephen T., 371
Barnes, Aaron, 534
Barnes, L. M., 171
Barnes, P. D., 397
Barr, D., 405
Barr, M., 435
Barraza, J., 451
Barrett, W. L., 536
Barrientos, M. J., 266
Bartel, David P., 269
Bartholomay, R. C., 185
Barton, D. S., 502
Bartsch, R., 432
Basetti, F., 358
Basilev, S., 502
Bastasz, R., 463
Batchelder, J. C., 426
Bates, J. K., 84
Bates, Maynard, 265
Battersby, Thomas R., 271
Batts, G. W., 21, 22
Baucom, K. C., 50
Bauer, S. J., 103
Bauer, Steven X. S., 2
Bauer, T. H., 64
Baugher, B. M., 29
Bauschlicher, Charles W., Jt., 54
Bayliss, S., 172
Bazylinski, Dennis A., 304
Beard, Brian L., 283
Beauchamp, E. K., 95
Beaudoin, David J., 327
Beauman, R., 455
Beaumont, Chris, 518
Bebout, Brad, 324
Beck, B. R., 420
Beck, D. N., 413
Beck, Sherwin M., 264
Becker, G. K., 171
Becker, R. H., 524
Becklin, E. E., 347
Becklin, Eric E., 343
Bedrossian, P. J., 73
Bedzyk, M. J., 81
Begnaud, M., 139
Behymer, R. D., 76
Beitz, J. V., 398, 425, 436
Bel, 68
Belak, J., 472
Bell, Thomas L., 237
Beller, D., 431
Beltran,, 95
Belz, Andrea, 305
Ben-Naim, E., 176
Ben-Zvi,, 442
Ben-Zvi, I., 411, 453
Benamara, M., 491
Benavides, G. L., 118
Bender, S. C., 158
Bendure, A. O., 516
Benner, J., 197
Benner, Steven A., 271, 280, 282, 314, 330
Bennett, C. V., 445
Bennett, D. H., 227
Benson, C., 161
Benson, D. A., 32
Benson, S. V., 457
Berg, P. A., 184
Berg, R., 371
Berg, S., 161
Berg, W., 161
Berg, W. J., 500
Berge, P. A., 180, 186
Berger, A., 79, 471, 474, 478
Berger, E. L., 383, 387, 394, 395
Berger, R. L., 463
Bergman, W., 46
Bergstrom, P. M., 378
Berkhout, T. A., 517
Berkoff, T. A., 248
Berkoff, T. B., 243
Bernardin, J., 433
Bernardin, J. D., 414
Bernstein, Max P., 267
Berrah, N., 62
Berrier, Bobby L., 1
Berry, H. G., 60
Berryman, J. G., 184, 403
Bertete-Aguirre, H., 186
Berzins, L. V., 383
Berzins, Valdis, 369
Bespalko, S. J., 359
Bessell, Mike, 348
Betts, R. R., 381, 391, 421
Betts, W., 387
Beus, S. G., 152, 153
Beutter, Brent Robert, 262
Bevis, R. P., 383, 386
Bewley, R., 107
Beyerlein, S., 119
Bharathan, D., 103
Bhartia, P. K., 229
Bhartia, R., 295
Bhattacharya, Swapan, 369
Bhattacharya, T., 501
Biallas, G., 457
Biedron, S., 159
Biedron, S. G., 159, 161
Biefeld, R. M., 50
Bieniosek, F. M., 413

Bierkens, M. F. P., 181
Biheux, J. C., 386
Biltoft, P., 159
Bingert, S., 77
Bingham, C., 37
Bingham, C. R., 426
Bird, Dennis K., 273
Bird, E. L., 68
Bird, I., 518
Birn, J., 535
Birtcher, R. C., 481, 484
Bischof, C., 149
Bischof, C. H., 355
Bischoff, James L., 273
Bise, R. T., 58
Blackfield, D. T., 383
Blackmon, J. C., 518
Blackwell, B. F., 148
Blackwell, C. C., 150
Blair, Jaime E., 325
Blair, N., 257, 258
Blair, R., 395
Blair, R. E., 475
Blair, S. C., 180
Blake, T. A., 190
Blank, Carrine E., 284
Blankenship, Robert E., 288, 336
Bleakly, D. R., 183
Bletzer, K., 396, 447
Bliss, E., 455
Bloch, A. M., 146
Bloomquist, C. A. A., 51
Blum,, 161
Blume, B., 130
Blumenthal, D. J., 426
Boctor, N. Z., 301
Boctor, Nabil, 266
Bode, C., 536
Bodwin, G., 394
Bodwin, G. T., 395
Boer, D., 132
Boering, Kristie A., 232
Boettcher, S., 373
Bogicevic, A., 485
Boley, C. D., 159
Bollen, J., 518
Bolvin, David, 225
Bondarenko, S. V., 68
Bonner, B. P., 184
Bonoetti, Joseph A., 458
Bootz, B. L., 104
Boparai, A. S., 32
Borchers, J. A., 489
Bordallo, H. N., 27, 382, 472
Borucki, William J., 343
Borup, R. L., 198
Borwn-VanHoozer, S. A., 265
Bose, A. C., 94
Bosilovich, Michael G., 225
Boss, Alan P., 345
Botto, T. E. G., 430
Bouquet, F., 477
Bour, D., 492
Bowen, Brent D., 3
Bowers, D., 437
Bowers, D. L., 32
Bowker, L. M., 179
Bowles, T., 504
Bowmaker, G. A., 71
Bowman, L. E., 101
Bowring, Samuel A., 321
Boyd, I., 383
Boyd, N. K., 185
Boyd, R., 24
Boyle, B. R., 93
Boyle, J. S., 259
Boyle, T. J., 51
Bozek, R., 410
Bozoian, M., 420
Brack, J., 454
Bracken, D., 172
Bradburne, Chris, 286
Bradley, J., 410
Bradley, L., 155
Bradley, R. S., 243
Braginsky,, 33
Brandes, Jay A., 269
Brantley, Susan, 287
Bray, S., 135
Breckenridge, A. R., 265
Breit, Greg A., 263
Bresnahan, J., 123
Bretz, S., 204
Brewster, R. A., 147
Breznik, Greg S., 18
Brickeen, B. K., 454
Brickhouse, N., 521
Bridges, M. M., 129
Briggs, J. B., 443
Briggs, R. D., 131
Brigmon, Robin L., 285
Brimhall, G., 47
Brinker,, 89
Brinkmann, W., 524
Brisudova, M., 502
Britt, H. C., 421
Brock, B. C., 158
Brockmann, J. E., 143
Brocks, Jochen J., 326
Brooks, J. N., 389, 463
Brown, C. W., 363
Brown, D. J., 134
Brown, D. R., 202
Brown, H., 110
Brown, I. G., 92
Brown, Linda R., 532
Brown, Lisa L., 350
Brown, M. J., 210, 231
Brown, P., 421
Brown, Phillip W., 11
Brown, R. L., 414
Brown, T. F., 384
Browning, N. D., 90
Brueck, S. R. J., 481
Brumwell, F. R., 380, 381
Brunett, B. A., 494
Brunner, S., 464
Bryant, H. C., 424
Bryant, Melvin A., III, 168
Bryant, S., 183
Bryson, Steve, 363
Buakovsky, L., 502
Bubenheim, David L., 220, 265
Buchanan, C. R., 149
Buchele, Don, 458
Buchheit, T. E., 37, 170
Buchinger, F., 398
Buck, E. C., 84
Buenafe, C., 364
Bullen, T., 179
Bullington, D. M., 158
Bullock, Mark A., 346
Bultman, N. K., 442
Bundy, Mark L., 16
Buning, Pieter G., 14
Buntine, Wray L., 377, 378
Burde, Stefan, 307
Burkert, V., 407
Burnham, A. K., 392, 396
Burns, J. E., 126
Burnsides, Dennis, 369
Burt, Donald M., 309
Busch, R., 436
Bush, J., 172
Busnaina, A., 34
Butler, M. A., 23, 36, 88
Butler, R. Paul, 343
Butterfield, S., 207
Buttner, William J., 529
Byrd, D. A., 158
Byrne, Monica, 285
Byrne, W. E., 459
Byrum, K. L., 496

C

Caciagli, Natalie, 331
Cadieu, Fred J., 68
Cadman, R., 409
Cadman, R. V., 454
Cadogan, David P., 84
Cady, Sherry L., 283, 284, 325
Caffee, M. W., 527
Cahalan, J. E., 438
Cai, X. Y., 474
Cai, Z., 449
Caimi, Raoul, 24
Cairelli, James E., 23
Calaway, W. F., 526
Calemczuk, R., 477
Calhoun, R., 151
Call, Lance R., 4
Calo, J. M., 56
Cameron, S. M., 371, 372
Camobreco, V., 109
Campbell, A. P., 370
Campbell, E. M., 464
Campbell, J. H., 443, 444, 445
Campbell, James, 232, 254
Campbell, P. L., 367
Campuzano, J. C., 476
Canavan, E. R., 480
Canfield, Don, 322
Cap,, 175
Capo, Rosemary C., 337, 338
Caporaso, G. J., 384, 499
Cappuccio, Frank, 4
Carlson, L., 16
Caron, David A., 327
Carpenter, J. M., 386
Carpenter, M. P., 399, 438, 475
Carr,, 409
Carr, G. L., 52
Carr, T. R., 99
Carrado, K. A., 51
Carrasquillo, R. L., 57
Carter, J. D., 199
Carter, T., 467
Carter, V., 183
Carver, M., 217
Carwardine, J. A., 497
Cassen, P., 535
Castle, Charles, 458
Catledge, S. A., 387
Catling, David, 325
Catrakis, H. J., 149
Caturla, M., 488
Caturla, M. J., 43
Cauble, R., 488
Cauble, R. C., 450
Cedarwall, R., 249
Cederwall, R., 151
Celata, C. M., 403
Celia, M. A., 182
Celina,, 94
Celina, M., 88
Celliers, P. M., 450
Centeno, C. J., 200
Centrella, J., 527
Cerino, A. T., 5, 6
Cerjan, C., 478
Cernosek, R. W., 139
Cerny, J., 400
Cesario, M., 104
Cess, R. D., 245
Cha, Y. S., 473
Chackerian, Charles, Jr., 532
Chadraa, B., 195
Chadwick, M., 406
Chae, Y. C., 159, 385, 432, 445, 500
Chalmers, G., 496
Chambers, D. M., 29
Chamuel, Jacques R., 240
Chandler, E. A., 163
Chandler, G. A., 464, 469
Chandra, S., 229
Chang, B., 421
Chang, David S., 263
Chang, J., 381, 391, 421
Chang, J. J., 30
Chang, P. C., 201
Chang, R. P. H., 133
Chang, S., 382
Chang, W. C., 381, 421
Channell, P. J., 433
Chapman, Dean R., 151
Chapman, H., 447
Chapman, J. N., 209, 487, 493
Chaput, John C., 279
Chargin, A. K., 397
Charlton, W. S., 420
Chartock, M., 509
Chattopadhyay, S., 400
Chen, C. I., 48
Chen, D., 404
Chen, E. P., 175
Chen, Hsiong, 328
Chen, Junhong, 323
Chen, Liao-Hai, 277
Chen, S. Y., 435
Chen, Y. J., 384, 499
Cheng, L., 81
Cheng, Ngom, 369
Cheng, S., 60
Chesnut, G. N., 387
Cheung, Samson, 11
Chi, C. Y., 381
Chien, H. T., 417
Chien, Janet Y. L., 241
Child, Alice, 316
Chinn, D., 494
Chinsio, R., 447
Chitanvis, S. M., 87
Chittenden, J. P., 461
Cho, H. S., 156
Choi, G. N., 108
Choi, S. R., 96
Chopra, O. K., 70, 72
Choquette, K. D., 131, 162
Chou, C. J., 185
Chou, Ming-Dah, 237
Chou, Shu-Hsien, 234, 256
Choudhary, A., 367
Chow, E., 518
Chow, R., 448
Chow, W. W., 162, 454, 493
Chrien, R., 469
Chrien, R. E., 419
Christ, N. H., 404
Christenson, T., 361
Chu, A. S., 88
Chu, S., 238
Chu, Y., 482
Chung, K., 481
Chung, Y., 501
Church, D. A., 420
Churchill, Deneyse J., 326
Chuu, Y. J., 48
Chyu, M. C., 120
Ciarlette, D., 505
Cizewski, J. A., 399
Claassen, P. J., 158
Clancy, Dan, 12
Clapsaddle, C. A., 216
Clark, Benton C., 345
Clark, D. K., 150
Clark, Nigel, 210
Clark, R., 453
Clark, W. C., 241
Clarke, W. G., 153
Clayton, R. N., 524, 526
Cleary, A., 518
Cleek, T. M., 261
Cleland, Carol E., 270
Cleland, W. E., 423
Clements, G. R., 15
Clemett, Simon J., 304, 311, 317
Clemmons, M. A., 217
Clift, W. M., 74

Clough,, 37
Cloyd, Richard A., 167
Coan, B., 126
Coburn, M. D., 101
Cody, George D., 266, 269, 272
Coffey, P., 387
Cohen, B. I., 462
Cohen, D. H., 147, 148, 160
Cohen, R. H., 384, 460
Colberg, R. D., 108
Cole, R. L., 213
Coleman, J. J., 72
Coleman, R. G., 176
Colgate, Stirling, 277
Collins, G. W., 450
Collins, L., 502
Collins, Michelle, 507
Collins, W. D., 245
Colombano, Silvano P., 138
Colp, John L., 443
Colton, J. S., 481
Colvin, J. D., 75, 163
Comeaux, Keith A., 151
Conde, M. E., 139, 408, 466
Conley, Catharine A., 326
Connaughton, V., 537
Connolly, M. J., 171
Conrad, Pamela G., 305
Conti, Peter, 525
Cook, A. W., 149
Cook, D. L., 469
Cooper, G., 464
Cooper, G. W., 469
Cooper, Gene R., 16
Cooper, John F., 302
Copeland, R. J., 104
Cordoba-Jabonero, C., 285
Cormier, Rene V., 362
Cornelius, Charles S., 25
Costa, D., 62
Coughlan, Richard, 263
Coulter, R. L., 180, 242, 245
Counce, D., 187
Counts, Richard H., 25
Couture, S., 361
Coveney, V. A., 172
Cox, B., 429
Cox, B. N., 92
Cox, Lea, 305
Crabtree, G., 481
Crabtree, G. W., 143, 446, 477
Craft, R. L., 262
Craig, D. F., 81
Craig, G., 461
Cramer, S. P., 478
Crandall, K., 503
Crawford, C., 87
Crawford, J. E., 398
Crawford, M., 480
Crawford, M. H., 493
Crawford, R. K., 30, 389
Crawford, T., 234
Cristian, C., 404
Cromwell, J., 209
Crosbie, E. A., 445
Crouch, P. E., 146
Crowe, B. M., 179
Csanak, G., 426
Cullen, D. E., 382
Cummings, Michael P., 286
Cummings, W. J., 454, 498
Cunningham, B. J., 93
Cunningham, J., 495
Cunningham, J. M., 487
Curran,, 58
Curran, D. R., 392
Curtis, B. C., 384
Curtis, Daniel B., 306
Curtis, L. J., 60
Curtis, Scott, 225
Curtiss, L. A., 104
Cuzzi, Jeffrey N., 532
Czajkowski, C., 455

D

da Fonseca, R. J. M., 472
Da Silva, L. B., 450
Dadkhah, M. S., 92
Dahlberg, E. D., 478
Daley, T. M., 236
Daley, W. M., 354
Dalla-Betta, Peter J., 270
Dalmas, D. A., 415, 439
Daly, J., 78
Daly, M. J., 111
Daly, T. P., 378
Dane, C. B., 78
Daniels, E. J., 86
Daniels, R., 228
Dannevik, W. P., 384
Darren, C., 156
Darwin, D., 57
daSilva, Arlindo, 225
DaSilva, L. B., 448
Daube, Bruce C., Jr., 232
Davidovits, P., 218, 219
Davids, C. N., 399, 426
Davidson, R. C., 433, 468
Davino, D., 438
Davinson, T., 399
Davis, A., 253
Davis, A. B., 249, 253
Davis, A. M., 524, 526
Davis, B. H., 64, 66, 114
Davis, K., 358
Davis, K. A., 113, 114, 231
Davis, L. C., 185
Davis, P., 172
Davis, Rebecca, 350
Davisson, M. L., 179
Dawson, C. N., 183
Dawson, J. W., 475
Day, R., 466
de Boer, M. P., 138
de Hoon, M. J. L., 412
De La Torre Ugarte, D., 108
de Supinski, B. R., 123
de Swart, J. J. B., 360
Deamer, David W., 267, 272
Dearden, Richard, 12
Deb, S., 197
Debeling, A., 461
DeBlasio, R., 209
deBoer, M. P., 131
Decker, C., 463
Decker, William A., 7
Decking, W., 401
Dees, D. W., 199
Degtyarenko, P., 415
Deiwert, G. S., 153
Dejus, R. J., 159
DeLand, S. M., 434
DeLay, Thomas K., 41
DeLong, Edward F., 282
DeLong, L. E., 481
DeMaster, D., 258
Dementieva, I., 473
Demko, J. A., 89
Demoz, B. D., 243
DeMuth, D. M., 382
Denison, G. J., 133
Derrick, M., 394
Derzon, M. S., 464, 469
Descalle, M., 378
Desch, P., 77
Desch, S. J., 346
DesMarais, David J., 281, 282, 283, 324
Dessler, A. E., 236
Deutsch, C., 412
DeYoung, Russell J., 452
deZwart, Ico, 270
Dhote, A., 471
Dhote, A. M., 471

Diaz De La Rubia, T., 43
Diaz, H. F., 243
DiazdelaRubia, T., 82
Dickey, F. M., 452
Dickinson, T., 455
Diehl, R. C., 132
Dietrich, F., 500
Dietz, N., 78
DiGirolamo, P., 243
Dignon, J., 210
Dillon, J., 56
Dilts, G. A., 142
Dimauro,, 409, 457
Dimits, A. M., 384
Dimotakis, P. E., 149
Ding, H., 476, 486
Ding, Y., 51
Dipirro, M. J., 480
Dirk, W. J., 437
DiSanto, T., 428
Ditmire, T., 421
Diver, R. B., 201
Divol, L., 463
Dixit, S., 396
Dixon, A. G., 103
Dixon, B. G., 132
Dixon, M., 266
Djomehri, M. Jahed, 14
Do, M., 83
Doctor, R. D., 241
Dodge, J., 244
Doerry, A. W., 124
Domonkos, Matthew T., 26
Donaldson, R. D., 134
Dong, Z., 404
Donnelly, S. E., 481, 484
Dooley, K. M., 53
Dooling, J. C., 380, 381
Doran, N. E., 130
Dorris, S. E., 86, 473, 474
Doskey, P., 249
Doss, E. D., 191
Doss, F. W., 448
Dotsenko, R., 261
Douglas, Donya, 22
Douglas, M. R., 469
Douglas, S., 295
Douglas, Susanne, 305
Douglass, Anne R., 231
Doukov, Tzanko I., 271
Dowding, K. J., 148
Dowell, L., 125, 128
Dowell, L. J., 375
Downing, J. N., 415, 439
Doyle,, 439
Doyuran,, 409
Drake, A., 524
Drake, B. G., 255
Drake, G., 394, 395
Drayer, D. D., 434
Drennan, Catherine L., 271
Drulis, H., 27
Dubois, P. F., 367
Dubovik, Oleg, 211
Duerksen, Gary L., 456
Duffield, J., 109
Duggan,, 439
Dugger, M. T., 33
Duley, Jacqueline A., 8
Duncan, A., 498
Duncan, R. V., 80
Dunford, R. W., 60, 386, 399
Dunham, Edward W., 343
Dunham, T., 36
Dunlap, C., 187
Dunn, F., 437
Dunn, F. E., 431
Dunn, J., 162
Dunn, K., 79
Dunn, W. L., 356
Durkee, Philip A., 255
Dusek, J. T., 86, 473
Dutcher, F. Ronald, 351
Dworkin, Jason P., 267, 291
Dylla, H. F., 456
Dziegiel, Roger J., 366
Dziuba, R. F., 141

E

Eack, K., 252
Easterling, D. R., 244
Eastman, J. A., 39
Eastwood, A. L., 275
Eaton, W. P., 117
Ebadian, M. A., 228
Eberhard, P., 355
Eberhardt, J. J., 98, 223
Eberle, C. S., 145
Ebert, W. L., 84
Eddings, E. G., 113, 114, 231
Eder, Wolfgang, 283
Edgcomb, V. P., 321
Edgcomb, Virginia, 286, 296
Edgcomb, Virginia P., 352
Edgett, Kenneth S., 528, 529, 532
Edler, J., 166
Edwards, D. L., 211
Edwards, H. G. M., 283
Effinger, Michael R., 167
Efthimion, P. C., 470
Ehrenfreund, Pascale, 344
Eichten, E., 498
Eigenbrode, Jennifer L., 326
Einaudi, Franco, 244
Eisenberg,, 89
Ekdahl, C., 432
Ekerdt, J. G., 59
Ekin, J., 135
ElBouanani,, 439
Elder, M. G., 151
Eldridge, J. E., 493
Ellingson, W. A., 91
Ellington, Andrew D., 273, 277
Elliott, D., 195, 208
Elliott, S., 238
Ellison, J., 411
Elsila, Jamie, 267
Elton, R. C., 465
Emerson, David, 286, 294
Emery, K., 196
Emmerich, S. J., 119
Enderby, J., 115
Engel, Mike, 291
Englehart, D. A., 80
Engler, O., 490
English, B. C., 111
Ensor, D. D., 27, 398
Erb, A., 477
Erdemir, A., 31, 68, 92, 129
Erdmann, J., 392
Erickson, G. F., 91
Erickson, Larry L., 14
Erikson,, 58
Eriksson, M., 159
Eror, N. G., 485
Erwin, Douglas H., 327
Eryilmaz, O. L., 31, 92
Esh, D. W., 428
Eshelman, L., 183
Esposito, Larry, 345
Estep, R., 172, 364
Estes, G. P., 420
Estes, M. G., Jr., 189
Estill, J., 517
Estill, J. C., 73
Eudy, L., 107
Evans, G., 473
Evans, K. D., 243
Evans, T., 463

F

Faatz, B., 159
Fabris, G., 380
Fadley, C., 62
Fagan, William F., 327
Fagerstroem, J., 125
Falgout, R., 518
Falten, A., 412
Faltens, A., 205, 413
Famouri, Parviz, 210
Fan, Y., 177
Farmer, J. C., 73
Farmer, Jack, 350
Farmer, Jack D., 300, 304, 313
Farquhar, James, 311, 322
Farrell, K., 442
Fatigati, M. A., 217
Favata, Fabio, 344
Fearon, E., 98
Fedchak, J., 454
Feddema, J. T., 361
Fehl, D., 464
Feigelson, E. D., 524
Feinroth, H., 40
Feit, M. D., 448
Felcher, G. P., 478, 489, 503
Feldmann, M., 474
Feng, W., 47, 126
Feng, X., 398
Fenollosa, R., 482
Fenske, G. R., 31, 92, 129
Fenter, P., 81
Fernandez-Remolar, D., 284
Fernow,, 408
Ferraris, J. P., 29
Ferris, M., 292
Ferry, James G., 336
Ferryman, Amy, 307
Fesmire, J. E., 84
Fesmire, James E., 89, 119, 260
Fessler, A., 434
Ficini-Dorn, G., 443
Fiddler, M. N., 275
Field, R. V., 377
Files, Patrick, 369
Filley, Timothy R., 268
Finck, P. J., 390
Fincke, J. R., 107
Fink, J. K., 64
Finnegan, N., 78
Fischer, A. J., 162
Fischer, P. F., 143, 353
Fischer, Ute, 263
Fisher, D., 378
Fisher, R. A., 477
FitzGibbon, Sorel T., 328
Flack, A., 209
Flaherty, J. E., 359
Fleming, D. L., 70
Fleming, J. G., 135, 139
Fleshler, S., 132
Flynn, G. J., 268
Flynn, Michael, 265
Fochs, S., 159
Fogel, Marilyn L., 294, 306
Foing, Bernard H., 307, 344
Follstaedt, D. M., 449
Folta, J., 76
Folta, J. A., 74, 155
Foltz, M. F., 102
Forbes, J. W., 50, 169
Formolo, Michael J., 330
Forsythe, Jennifer, 307
Fortgang, C. M., 137
Fortuin, P., 222
Fosmire, C. J., 193
Foster, I., 123, 356
Foster, J., 130
Foster, John E., 26
Foster, P. A., 102
Fotiades, N., 399
Foulk, J. W., 175
Fournier, K. B., 150
Fox, B., 97
Fox, M. A., 57
France, D. M., 120
Francfort, J., 206
Frank, M., 478
Frank, S. M., 428
Freedman, A., 248
Freeman, A. J., 475
Freeman, Kate, 287
Freeman, Katherine H., 326
Freitag, L., 358, 367
Freitag, L. A., 173
Freitas, B. L., 162
Fretwell, H. M., 476
Freund, Friedemann, 233
Freund, H., 159
Freund, H. P., 159, 457
Freyer, C. L., 527
Fried, L. E., 51, 388
Friedland, A., 535
Friedman, A., 399
Friedrich, S., 478
Frink, L. J. D., 141
Fritz, I. J., 457, 458
Frolov, A. D., 218, 221
Frye, J. G., 101
Frye-Mason, G. C., 23, 32
Fryer, C., 525
Fu, G. Y., 462
Fu, Q., 253
Fujiwara, M., 221
Fukui,, 408
Fulghum, Julia, 307
Fullerton, E. E., 77, 486, 489
Fulton, J. L., 101
Fultonberg, D. N., 516
Fung, P., 261
Funk, D., 453
Funkhouser, B., 159
Furuya, K., 481, 484
Fuyuki, Masanori, 274

G

Gaarde, P., 392
Gabbard, W. A., 121
Gai, W., 139, 408
Galambos, P., 117
Gallagher, L. K., 262
Gallaher, J. R., 65
Gallardo,, 408
Gammon, P. T., 183
Gangwal, S. K., 56, 100, 109
Gann, S. L., 483
Gannon, D., 388
Gao, Bo-Cai, 251
Gao, H., 175
Gao, W., 249
Gao, Y., 471
Gara, A., 404
Garbutt, M., 422, 424
Garcia, E. J., 457
Garcia, F., 169
Garcia, Joseph A., 11
Garcia, M., 207
Garcia, R. J., 262
Garcia-Pichel, Ferran, 287
Garcia-Villazana, O., 194
GarciaPichel, Ferran, 324
Gardner, S. D., 157
Garey, James R., 322, 330
Garino,, 33
Garrett, D., 378
Gast, Rebecca J., 327
Gates, D., 470
Gaucher, Eric A., 271
Gautier, C., 15
Gavel, D. T., 448, 522
Gebhard, S., 104
Geddes, C., 463

Gee,, 206
Gee, J. M., 201
Gegueldre, C., 83
Geib, K. M., 131, 162
Geist, A., 388
Gelaro, R., 244
Gellatly, Anne M., 330
Geller, D. A., 418
Gemmell, D. S., 386, 399
Genin, F., 447
Genin, F. Y., 392, 396, 447
Gensler, S., 396
George, Douglas S., 205
Gerald, R. E., 193
Gerassimenko, M., 392
Gerig, R., 505
Gershanovich, Y., 104
Getoor, Lise C., 368
Getz, A. M., 522
Geyer, C. Ronald, 271
Geyer, H. K., 193
Geyer, U., 85
Ghadiri, M. Reza, 267, 278, 281
Gharavi, H., 124
Ghil, Michael, 340
Ghiorso, W., 412
Ghoshal, Anindya, 374
Gibbartd, S. G., 522
Gibbons, M. R., 478
Gibson, B. F., 422
Gibson, Everett, 312
Gibson, Everett K., Jr., 302
Giddings, S. B., 499
Giel, T. V., 495
Gillen,, 37, 94
Gillen, K. T., 88
Gillitzer, A., 381, 391
Gilpatrick, J., 405, 415
Gimenez, Alvaro, 344
Ginnocchio, J., 401
Ginocchio, J., 506
Girrens, S. P., 174
Giver, Lawrence P., 532
Gladwell, S., 357
Glandorf, David L., 306
Glass, G., 387
Glass, S. J., 37, 76, 95
Glenn, L. A., 99
Glenzer, S. H., 463
Glimm, James, 154
Glissmeyer, J. A., 218
Globus, Al, 518
Glorieux, B., 115
Gochberg, L. A., 153
Goda, J., 436
Godfrey, A., 485
Goff, F., 187
Goff, K. M., 428
Gofron, K. J., 475
Gogarten, J. Peter, 281, 333, 342
Gohar, Y., 393
Going, D. J., 67, 229, 230, 232
Gold, D. M., 75, 163, 450
Goldberg, M., 437
Goldman, A. S., 44
Goldman, T., 502, 506
Goldsby, D. L., 173
Goldsby, David L., 234
Gomes, I., 390
Gomez, Alvin, 286
Gomez, F., 284
Gomez, Felipe, 299
Gonzales, A., 82
Gonzalez, E., 28
Gonzalez, Maria, 279
Gonzalez-Toril, E., 284
Goodfriend, Glenn A., 268
Goodman, D. M., 169
Goodman, M. C., 394, 536
Goodman, S. J., 189
Goodman, T., 36
Goodrich, Charles H., 357
Goodwin, J. G., 56
Gordley, Larry L., 238
Gorelenkov, N., 470
Goretta, K. C., 85
Gorman, V. W., 184
Gornakov, V. S., 77
Gottlieb, E. J., 357
Gourley, P. L., 458
Graboski, M., 109
Graczyk, D. G., 32
Graff, R. T., 197
Gragon, E. P., 30
Graham, A. C., 88
Graham, R. L., 106, 108, 111
Grasby, Stephen, 282
Grasiani, F. R., 150
Grasser, T. W., 143
Graves,, 409, 442, 457
Gray, K. E., 471
Gray, S. K., 44
Greeley, Ronald, 301
Green, D., 384
Green, D. J., 95
Green, D. W., 32, 99
Greene, Catherine, 220
Greene, G., 414
Greene, J. P., 439
Greene, M. R., 185
Greenly, J. B., 461
Greenough, J. A., 143
Greenspan, E., 431
Gregory, D. L., 176
Gregory, W., 435
Griego, L., 129
Griem, H. R., 465
Griffin, Timothy P., 18, 20
Grimes, P., 206
Grimsditch, M., 472, 486
Grinspoon, David H., 346
Gritto, R., 236
Gropp, W. D., 353, 358
Grosnick, D., 479
Gross, K. J., 494
Gross, R. J., 7
Gross, T. S., 175
Grossman, J. W., 201
Grossman, R. L., 245
Grote, D. P., 399
Grotzinger, John P., 321
Gruber, E. E., 70
Gruber, L., 420
Gruen, D. M., 93, 133, 471
Grzegory, I., 481
Guan, J., 86, 94
Guan, Yunbin, 311
Guarino, V., 394
Gubeli, J., 457
Guess, T. R., 175
Gulick, S., 398
Gullett, B. K., 215
Gullikson, E. M., 74
Gulman, P. J., 208
Gunda, N., 32
Guo, F. Q., 400
Gupta, R., 503
Gupta, S. B., 45
Gutzler, D. S., 245
Gwinn, K. W., 531
Gyekenyesi, J. P., 96

H

Habib, S., 428
Habicht, Kirsten, 322
Hackel, L. A., 78
Hackney, S. A., 194
Haddad, Ziad, 254
Hage, M., 361
Haggag, F. M., 81
Hahn, F., 71
Haines, M. G., 461
Hakim, S., 378

Halaxa, E. F., 466
Haldar, P., 485
Hale, L. C., 116
Halicioglu, Timur, 490
Hall, Dorothy K., 241
Hall, J., 500
Halter, M., 129
Hammer, J. H., 467
Hammond, Dana P., 365
Hammons, B. E., 201
Hammons, G., 458
Han, J., 480
Hands, S. J., 505
Hansen, R., 209
Hansen, T., 509
Hantush, M. M., 181
Haque, Azizul, 279
Hare, D. E., 86
Hargens, Alan R., 263
Harkay, K. C., 385
Harmon, C. D., 434
Harper, Lynn D., 220
Harris, B., 387
Harris, B. W., 496, 497, 505
Harris, D. B., 32, 215
Harris, J. S., 141
Harrison, J., 78
Harrison, T. Mark, 331
Harte, J. A., 150
Hartle, Richard E., 237
Hartouni, E. F., 397
Harvey, D. W., 193
Harwood, L., 416
Haschke, J. M., 43
Hasegawa, S., 386
Hashmonay, R. A., 32, 215
Haskell, William D., 18
Hassanein, A., 408, 460, 463
Hatch, U., 189
Hatchett, S. P., 160
Hauer, A. A., 163
Hauri, E., 301
Hauri, Erik H., 308
Havela, L., 27
Havrilla, G., 62
Hawkins, J., 58
Hawley-Fedder, R., 443
Haworth, D. C., 144
Hayes, J. P., 197
Hayes, John M., 283
Hayes, S. L., 429
Haynes, R. A., 265
Haynes, T. E., 133
Hayter, S. J., 197
Hazeltine, R. D., 465
Hazen, Robert M., 266, 268, 269, 272
He, J., 103
He, X., 395
He, Z., 496
Headley, Dean E., 3
Hedges, S. Blair, 318, 325, 328, 330, 336
Heese,, 409, 457
Heimbigner, Dennis, 366
Hektor, B., 111
Helgeson, W. D., 133, 134
Heller, J., 487
Helms, William R., 18, 20
Henderson, H., 120
Hendricks, T. J., 190
Hendrix, J. L., 447
Henesian, M., 455
Henestroza, E., 413
Henning, W. F., 391
Henriksen, G. L., 207
Hensley, R. D., 125
Hensley, W. H., 124
Heraty, L. J., 102
Herman, Ellen K., 328
Herman, J. R., 221, 252
Hernandez, C. L., 76, 85
Herrmann, S. D., 145
Herrmannsfeldt, W. B., 468
Hersman, Larry, 307
Hertel, E. S., 100
Hervig, Mark E., 238
Herwig, S., 100
Herzenberg, S., 203
Hesketh, P. J., 481
Hess, B., 518
Hester, M., 447
Heuer, J., 75
Heuer, J. K., 91
Hewett, D. W., 478
Hewitt, C., 458
Hibbard,, 392
Hicks, B., 245
Hietala, V. M., 458
Hill, B. K., 478
Hill, R. R., 198
Hiller, L. J., 478
Hillman, A. R., 139
Hinchliffe, I., 397
Hinchman, R., 62
Hinman, Mark C., 323
Hinman, Nancy W., 289, 298
Hinrichs, Kai-Uwe, 282, 283, 296
Hirshfield, J. L., 500
Hjalmarson, H. P., 133, 134
Hockman, J. N., 397
Hodges, K., 244
Hoffman, David, 326
Hofman, G. L., 429
Hogan, Mary, 324
Hogan, W. J., 464
Hogden, J. E., 417
Hogeland, S. R., 112
Hoisie, A., 371
Hoitink, D. J., 193
Holben, Brent, 187
Holben, Brent N., 211
Holder, J. P., 420
Holdridge, D. J., 244
Holland, David M., 227
Holland, O. W., 37, 492
Hollenbach, D. J., 250
Holloway, John R., 270, 284
Hollowell, D. E., 74
Holmes, N. C., 86, 235
Holmes, S., 516
Holswade, S., 457
Holswade, S. C., 452
Holt, A. C., 93
Holt, B. D., 102
Holt, R. J., 440
Holtkamp, D. B., 137
Hong, W. S., 156
Hood, L. L., 247
Hooker, M. W., 133
Hooper, E. B., 462
Hooton, R. D., 52
Hope, Janet M., 283
Hopkins, S., 433
Hord, B. L., 93
Horne, W. E., 484
Horng, R., 378
Horst, T., 245
Horsthemke, W. H., 359
Hosea, J., 470
Hosking, F. M., 76
Hou, Arthur Y., 237
Hou, H. Q., 201
Hou, P. Y., 201
House, Chris H., 287
House, Christopher H., 282, 328
Houser, Paul R., 225
Hovland, P., 149
Hovland, P. D., 355, 358
Howard, David E., 137, 157
Howard, W. M., 51, 388
Howell, R. H., 429
Hoyt, J. J., 75
Hranisavljevic, J., 60
Hsia, A. H., 131
Hsiung, L. M., 75
Hsu, S., 467

Hu, M. Z. C., 67
Huang, K., 201
Huang, L., 102
Huang, Y., 313
Huang, Y. J., 120
Huang, Z., 445
Huber, Robert, 283
Hudson, H. G., 127
Hudson, R. D., 218, 221
Hue, J., 449
Huebner, M., 187
Huffman, G. P., 64
Huffman, George, 225
Hug, W. F., 295
Huggins, F. E., 64
Hughen, K. A., 179
Hughes, D. A., 485
Hughes, R. C., 23
Hummel, J. R., 370
Hunsche,, 236
Hunter,, 176
Hurd,, 89
Hurtgen, Matthew T., 329
Huscrot, C., 482
Hutchings, L., 192
Hutson, N. D., 520
Hutton, A., 456
Huyse, Luc, 376
Hwang, R. N., 398
Hyde, R., 531
Hyde, T., 107
Hyder, M. L., 65

I

Iguchi, Toshio, 254
Ihlefeld, Curtis M., 517
Ijiri, Y., 489
Iliadis, C., 524
Ilkaeva, L. A., 68
Im, Eastwood, 254
Im, J., 133, 471
Imanaka, Hiroshi, 274
Inaba, Satoshi, 349
Inbody, M. A., 198
Indik, R., 454
Ingersoll, D., 198
Ingram, D., 434
Inomata, A., 77, 79
Insley, J., 123
Isaacs, H. S., 58
Isaacs, Nathan D., 205
Isdahl, Wayne, 263
Isenhower, L. D., 404
Ishibashi, Jun-ichiro, 296
Ishii, M., 152, 153
Ishikawa, M., 531
Ithaca, J., 29
Iton, L. E., 104
Ivanov, M. A., 498
Iwasieczko, W., 27
Iyer, A. N., 474
Iyer, S. P., 368

J

Jaanimagi, P. A., 148
Jackman, Charles H., 239
Jackson, C. R., 397
Jackson, J. A., 169
Jackson, K., 37
Jackson, M., 480
Jackson, Teresa L., 311
Jacobs, David K., 330
Jacobs, J. W., 143
Jacobs, R. R., 384
Jacobs, Stanley S., 227
Jacobsen, C., 268
Jacobson, H. M., 91
Jaffe, Richard L., 490
Jager, H. I., 111
Jahnke, Linda, 324
Jahnke, Linda L., 283
Jakosky, Bruce M., 308
Jakowatz, C. V., 130
Jakubczak, J. F., 136
James, B. F., 21
James, R. B., 494
Jamil, S., 172
Jammes, C., 398
Jang, B. W. L., 108
Jangren, Anna, 351
Janik, C., 187
Jankowski, A. F., 197
Janssens, R. V. F., 438
Japaridze, L. A., 34
Jarboe, T. R., 462
Jarrett, D. G., 141
Jarvinen, G., 435
Jasinski, J., 410, 491
Javaux, Emmanuelle J. J. M., 319
Jayaraman, M., 32
Jayatissa, A., 93
Jayne, J. T., 218, 219
Jeffcoate, C. S., 58
Jellinek, J., 46
Jenkins, Adrian, 227
Jenkins, Jon M., 343
Jennings, B., 536
Jennings, R. T., 445
Jenniskens, Peter, 527
Jennison, D. R., 485
Jensen, B., 209
Jensen, B. D., 131
Jensen, C., 494
Jensen, M. P., 398
Jensen, S. A., 184
Jesse, S., 38
Jhabvala, Murzy, 156
Ji, H., 467
Jia,, 416
Jiang, H., 161
Jiang, J. S., 77, 79, 474, 486
Jiang, Y., 152
Jiao, Z., 185
Jimenez, T., 204
Jirsa, J. O., 57
Joachimiak, A., 473
Job, P. K., 382
Jody, B. J., 86
Johansson, E. M., 169
Johnson,, 457
Johnson, C. S., 194
Johnson, Clark M., 283
Johnson, Craig S., 369
Johnson, D. E., 172
Johnson, D. W., 236, 248
Johnson, H. M., 511, 515
Johnson, I., 64
Johnson, J., 425
Johnson, J. R., 292
Johnson, Jeffrey R., 287
Johnson, L., 102
Johnson, M. D., 488
Johnson, R. D., 165
Johnson, S. G., 64, 428
Johnson, W. A., 127
Johnson, W. L., 85
Johnstone, J. A., 458
Joiner, Joanna, 9
Jonah, C. D., 47
Jones, A. D., 275
Jones, B., 470
Jones, E. D., 449, 457, 458, 493
Jones, H., 119
Jones, J. R., 119
Jones, R., 202
Jones, S. A., 192
Jones, T. S., 221
Jonnavithula, S., 147
Joosten, R., 400
Jordan, Mary S., 255
Jorgensen, G., 37

Jorgenson, R. E., 127
Joshi, Ravindra P., 376
Joslyn, C., 374
Jothimurugesan, K., 56, 106
Joyce, P. C., 95, 113
Jusko, M. J., 217
Justice, J. R., 356
Justus, C. G., 22
Justus, C.G., 21

K

Kabadi, V. N., 111
Kad, B. K., 83
Kadam, K., 110
Kadowaki, K., 476
Kadyk, J., 156
Kah, Linda C., 330
Kahaian, A. J., 194
Kahhaleh, K. Z., 57
Kaita, R., 470
Kalantar, D. H., 75, 163
Kalinovsky, Y. L., 498
Kaminska, E., 492
Kaminski, A., 476
Kammer, R., 354
Kamperschroer, J., 413
Kane, J. O., 523
Kang, E., 380
Kanter, E. P., 60, 386, 399
Kaper, H. G., 417
Karandikar, P., 32
Karataglidis, S., 536
Karl, T. R., 244
Karner, D., 206
Karonis, N. T., 123, 356
Karpenko, V. P., 466
Kasamayer, P., 192
Kashgarian, M., 179
Kastenberg, W. E., 227
Kasting, James F., 276, 326, 329, 334
Katarzyna, K., 388
Katonak, D., 433
Katsouleas, T., 466
Katz, B., 261
Katz, Rich, 156
Katzberg, Stephen J., 189
Kaufman, Alan J., 329
Kaufman, Alan Jay, 330
Kaufman, Yoram, 187
Kaufman, Yoram J., 211, 251
Kaun, T. D., 200
Kaushik, D., 367
Kaushik, D. K., 1
Kavaya, Michael J., 128
Kawa, S. Randolph, 239
Kaya, Alpay M., 145
Kebabian, P. L., 248
Keefe, Anthony D., 272
Keefe, Tony, 276
Keenan, Brendan G., 299, 300
Keenan, M. R., 88
Kehm, Karl, 308
Kellar, S. A., 391
Keller, L. P., 268
Keller, Richard M., 324
Kendrick, B., 418
Kennedy, C. R., 94
Kepler, K. D., 194
Kepley, L. J., 50
Kerr, Alastair, 277
Kerr, D. R., 99
Kershaw, D. S., 142
Kessel, C., 462
Kesseler, E., 372
Keune, W., 72
Key, M. H., 160
Key, R. M., 257
Keyes, D. E., 1
Khalil, H., 438
Khare, Bishun N., 306
Khounsary, A., 407, 449
Kieffer, J. A., 106
Kieft, Thomas L., 289
Kiggans, J. O., 166
Kilgroe, J. D., 216
Kilpatrick, J., 100
Kim, B. M., 448, 449
Kim, C., 413
Kim, D. H., 61, 201
Kim, H., 472
Kim, H. J., 126
Kim, J., 45
Kim, K. J., 122, 391, 445, 498
Kim, Paul H., 279
Kim, S., 152, 153, 500
Kim, S. H., 133, 385
Kim, S. M., 362
Kim, Stuart K., 326
Kim, T. H., 45
Kimball, C. W., 475
Kimmons, J. F., 445
Kimura, C. Y., 3
Kinard,, 137
King, D., 37
King, D. B., 138
King, H. A., 29
King, Michael D., 251
King, Roger, 366
Kingon, A. I., 90
Kini, A. M., 493
Kinne, S., 247
Kinoshita, C. M., 110
Kippelen, Bernard, 160
Kirchman, J. A., 501
Kiris, Cetin, 148
Kirk, J., 129
Kirschvink, Joseph L., 304, 330
Kistler, M., 237
Klappenbach, Joel, 335
Klasen, M., 383, 387
Klassen, M., 496
Klazura, G., 245
Klazura, G. E., 180
Klebanoff, L. E., 74
Klein, M., 119
Klein, P. A., 175
Klein, S., 401
Klem,, 161
Klemm, R. A., 484, 485
Klemme, B. J., 80
Kleyner, Igor, 156
Klier, E. M., 120
Klingler, R. J., 193
Klingmann, J. L., 388
Klingner, P., 16
Klock, B. A., 266
Klose, F., 503
Klueh, R. L., 70
Knapp, J. A., 138
Knauth, L. Paul, 309, 322
Knighton, G. C., 145
Knoll, Andrew H., 319, 332
Knoll, G. F., 496
Knupp, P. M., 173
Knuthammar, B., 160
Knyazikhin, Y., 252
Kobayashi, Kensei, 274
Koch, David G., 343
Koch, J. A., 160
Koch, S. W., 454
Kochemasov, G. G., 68
Kochhar, A. K., 218, 221
Koehl, E. R., 91
Koester, C., 23
Koetke, D., 479
Kogut, J. B., 505
Kohlstedt, D. L., 173, 530
Kohlstedt, David L., 233, 234
Kohn, S., 388
Kolb, C. E., 218, 219, 248
Koldenhoven, R., 447
Kolesnichenko, Y. I., 469
Kollgaard, R. I., 524

Kolner, B. H., 445
Kolomiets, A. V., 27
Kolpa, R., 222
Kolstad, C. D., 248
Komashko, A., 421
Komjathy, Attila, 189
Konecni, S., 152, 442
Konecny, R., 139, 408
Koniges, A. E., 356
Konkashbaev, I., 408
Kopasakis, George, 23
Kopasz, J. P., 98
Kopitzke, R., 105
Kortenkamp, Stephen, 349
Kota, C., 427
Kotnour, Tim, 508
Koumoutsakos, Petros, 490
Kowalski, A., 518
Kozlov, A., 61
Kozlowski, M. F., 455
Kozlowski, M. R., 445
Kozubal, M. A., 91
Kozup, S. C., 109
Krafft, G. A., 411
Kraft, M. E., 141
Krainak, Michael A., 456
Kramer, S., 119
Kramlich, J. C., 67, 229, 230, 232
Krasnicki, S., 392
Krassig, B., 399
Kraus, William F., 138
Krauss, A. R., 93
Krenn, C., 34
Kress, J., 502
Kress, M. E., 346
Krieger, A. S., 491
Krisch, A. D., 430
Krishnan, G. S., 169
Krommes, J., 464
Kroposki, B., 196, 209
Kros, J., 216
Krueger, K., 409
Krumpelt, M., 199, 200
Krygowski, T. W., 136
Ku, L. P., 462
Kuchler, V., 516
Kuhlman, Kimberly R., 305
Kukla, G. J., 246
Kulak, R. F., 172
Kullander, F., 160
Kulsrud, R., 467
Kumar, R., 191
Kumar, Sudhir, 328, 330
Kumaran, S. S., 60
Kummerow, Christian, 254
Kump, Lee R., 323, 324, 328
Kung, H. H., 61
Kung, M. C., 61
Kurennoy, S., 403
Kurennoy, S. S., 438, 442
Kursinski, Emil Robert, 9
Kurtz, S. R., 50, 457
Kurz, M. D., 65
Kusubov, A. S., 93
Kuzay, T., 451
Kuznetsov, V. E., 412
Kwak, Dochan, 148, 151
Kwan, J. W., 413
Kwok, W. K., 143
Kwon, S., 425, 488, 494
Kychakoff, G., 27
Kysela, David, 286, 296

L

Labanowski, C., 39
Labouriau, A., 491
Lacerda, A. H., 382
Lackey, Jeffrey D., 25
Lackner, K., 206
Lackner, Klaus, 277
Laenen, E., 497, 505
Lagow, B. W., 72
Lai, B., 449
Lake, James A., 318, 330
Lakeman, C. D. E., 51
Lal, J., 28
Lam, N. Q., 75, 91
Lamphere, P. B., 370
Lampo, E. J., 459
Lanagan, M. T., 79
Lancaster, Vanessa, 288
Landes, S., 464
Lane, David A., 153
Langland, B., 136
Lansky, Amy L., 368
Lanyi, Janos K., 276
LaPorta, C., 203
Larimer, R. M., 400
Larralde, Rosa, 273
Larsen, E., 375
Larsen, E. W., 375
Larson, William E., 357, 517
Lau, K.-M., 240
Lau, William K.-M., 259
Laub, James A., 13
Lauberts, A., 130
Laudal, D. L., 230
Laufer, Alexander, 507
Laulainen, N., 224
Laurent-Muehleisen, S., 537
Lauritsen, T., 439
Laursen, T. A., 376
Lavan, D., 37
LaVan, D. A., 170
Law, K., 39
Lawrence, Timothy W., 25
Lawson, J., 455
Lazarov, R. D., 375
Lebby, Gary, 374
Lebedev, V. A., 411
LeBlanc, B., 470
Lee, Dong-Kye, 279
Lee, E. P., 399
Lee, E. S., 95
Lee, G. S., 101
Lee, K. H., 126
Lee, P. B., 403
Lee, P. L., 475
Lee, R. W., 160
Lee, S. H., 489
Lee, S. R., 449, 493
Lee, S. W., 59
Lee, Timothy J., 66
Lee, W., 395
Lee, Y., 438
Lee, Y. Y., 45
Leeser, M., 355
Leftwich, J., 181
Legan, Brian M., 8
Leger, J. M., 71
Lehman, S. J., 179
Leigh, Dennis, 302
Lelovic, M., 485
Lemke, Kono, 278
Lemke, Kono H., 273
Lemmers, A. J. J. J., 14
Lenkszus, F. R., 497
Lerman, Louis, 310
Leseur, D., 9
Leseur, D. R., 73
Leshin, Laurie A., 311
Lesht, B. M., 180
Leung, K. K., 178
Levin, L., 258
Levy, Matthew, 273
Lewandowski, A., 37
Lewis, J. P., 235
Lewis, M. A., 27
Lewis, R. S., 524, 526
Lewis, Randolph V., 261
Lexa, D., 27
Li, C. K., 396
Li, S. C., 59

Li, Xiao-Fan, 240, 259
Li, Y., 162
Li, Y. H., 215
Liang, Ping, 274, 277
Libby, P., 59
Libby, S. B., 150
Lidia, S. M., 499
Liliental-Weber, Z., 491
Lin, C. D., 423
Lin, J., 51
Lin, J. L., 249
Lin, John K. H., 84
Lin, Ruei-Fong, 247
Lin, S. Y., 135
Lin, Y., 446, 493
Lince, Michael T., 336
Lindahl, P. C., 32
Lindberg, J. W., 185
Linden, Derek S., 138
Lindgren, R., 415
Lindl, J. D., 467, 468
Lindstrom, Marilyn M., 351
Lindzen, Richard S., 237
Linebarger, J. M., 370
Lineberry, J. E., 438
Linker, Jon A., 533
Linkous, C., 105
Lioen, W. M., 360
Lipe,, 137
Lipkin, H. J., 501
Liscum-Powell, J. L., 434
Lisle, John T., 288
Lissauer, Jack J., 343, 521
Lissianski, V. V., 114, 192
Lister, C. J., 381, 394, 422, 438
Littrell, K., 45, 507
Litzinger, T. A., 164
Liu, C., 392
Liu, G. K., 425, 436, 473
Liu, Han-Shou, 534
Liu, M., 86
Liu, X., 378
Livengood, C. D., 28, 53
Llorente, Ignacio M., 365
Lobban, L. L., 105
Lobmeyer, Dennis A., 115, 116
LoDestro, L. L., 462
Loewenstein, Max, 163
Logan, B. G., 468
Logan, C., 500
Logan, Graham A., 323, 326
Lohn, Jason D., 138
Long, R. Q., 105
Longazo, Teresa, 282
Longazo, Teresa G., 311, 318
Loong, C. K., 51, 52
Lopez, D., 143
Lopez, Louis, 368
Lord, S., 244
Lorence, L. J., 434
Loubriel, G. M., 133, 371
Lowe, Donald R., 322, 339
Lowman, Paul D., Jr., 537
Loy, D. A., 29, 42
Loy, R. M., 359
Lu, S. C., 82
Lu, Y., 103
Lucas, Keith, 13
Ludtka, G. M., 68
Lueck, Dale E., 529
Lugo, Samantha Kaj, 287
Luisi, P. Luigi, 269
Lula, J. W., 60
Lum, B. Y., 70
Lumpkin, A. H., 432, 450, 500
Lumsden, J., 171
Luna, Bernadette, 264
Lund, S. M., 384
Lundin, C. D., 69
Luning, J., 140
Luo, J. S., 84
Luqi,, 369
Luther, E., 39
Lutsenko, V. V., 469
Lynch, D., 455
Lynch, M., 410, 425
Lynn, K., 209
Lyons, James R., 288
Lyons, Timothy W., 330
Lyons-Weiler, Maureen, 336
Lysenko, W., 404

M

Ma, Y. H., 103
Macal, C. M., 359
MacCormack, Robert W., 151
MacDonald, P. E., 440
Macek, J. H., 412
Macek, R. J., 433
MacFarland, L., 366
MacFarlane, J. J., 147, 148, 160
Machesky, M., 81
MacIntosh, B., 522
Mackwell, S. J., 530
MacLaren, S. A., 412
Madland, D. G., 420
Mahesh, Ashwin, 254
Maitre, Philippe, 54
Majer, E. L., 236
Majeski, R., 470
Majewski, J., 96
Majkrzak, C. F., 489
Major, B., 213
Majumdar, S., 83, 393
Malcolm, S., 29
Malin, Michael C., 532
Mallinson, R. G., 105
Malone, R., 453
Malsbury, J., 508
Maltman, K., 503
Maly, P. M., 114, 192
Mancho, A.-M., 285
Manes, K., 455
Manginell,, 137
Manginell, R. P., 32
Mani, S. S., 139
Mann, M. K., 99
Manning, Craig E., 331
Manweiler, R., 479
Mar, A., 133, 454
Maran, Stephen Paul, 523
Marcus, D. L., 143
Marcy, Geoffrey W., 343
Margasahayam, Ravi, 24
Maricle, S., 455
Maricle, S. M., 449
Marino, M. A., 181
Marion, B., 196
Marion, J. E., 449
Maris, P., 497, 498
Markov, V. A., 154
Marmo, Jukka, 338
Marnay, C., 204
Marschall, Jochen, 63
Marshak, A., 249
Marshak, Alexander, 251, 252, 253
Marshall, A. M., 216
Marshall, C. L., 51
Marshall, Charles R., 330
Marshall, T. C., 414, 483
Marsman, A. P. L. A., 14
Martens, C., 258
Martin,, 416
Martin, C., 258
Martin, J. P., 224
Martin, K., 28
Martin, Mark W., 321
Martin, R., 435
Martin, R. L., 197
Martin, S. J., 139
Martin, William N., Jr., 374
Martinez, A. L., 151
Martinez, R. L., 434

Martinez-Frias, J., 194
Marumo, Katsumi, 296
Maruyama, Akihiko, 296
Mascarenhas, A., 449
Maser, J., 407
Maslanik, James, 189
Mason, R. J., 74
Massey, T. N., 434
Matsui, Takafumi, 274
Matsuno, Koichiro, 278
Matter, J. C., 434
Mattor, N., 463
Matzke, C. M., 129
Maughan, A. D., 218
Maughan, R. L., 427
Maurice, Patricia, 307
Maxey, L. C., 444
Mayer, T. M., 138
Mayr, Hans G., 534
Mazarik, J., 527
Mazieres, B., 354
Mazzuchi, Thomas A., 169
McArthur, Andrew G., 352
McCarthy, Chris, 347
Mccaughrean, Mark, 345
McClatchy, R. A., 248
McClellan, S. M., 79
McCollough, M. A., 537
McConnell, R., 197
McCormack, Tom, 275, 277
McCreary, D., 153
McCright,, 73
McCullough, B. F., 362
McDonald, G. D., 295
McDonald, Gene D., 312
McDonald, M. J., 357
McDonough, J., 387
McDowell, W., 505
McEachern, R. M., 71
McGee, Thomas J., 220, 247
McGuffin, V. L., 30
McGuire, Steve, 374
McHale, Mary L., 289
McHugh, Martin J., 238
McIlwain, M. E., 171
McInerney, Laura A., 286
McInnes, L. C., 353, 358
McKay, C. P., 533
McKay, Christopher, 325, 347
McKay, Christopher P., 306
McKay, D. S., 339
McKay, David, 314
McKay, David S., 285, 291, 311, 312, 317, 318
McKee, C. F., 250
McKeegan, Kevin D., 282
McKellar, B. H., 422, 424
McKenna, E., 208
McKone, T. E., 227
McLean, M. J., 443
McLean, R. I., 221
McLean, W., 30
McMahan, A. K., 482
McMahon, D., 117
Mcmahon, D., 446
McMahon, J. E., 378
McMichael, G. E., 380, 381
McNary, R., 161
McNulty, I., 449
McNutt, P., 209
Medelius, Pedro J., 157, 517
Meeson, Blanche W., 180
Meier, W. R., 467
Meike, A., 48
Meir, Eli, 327
Meldrum, A., 490
Melendres, C. A., 71
Melton, S., 364
Meltzer, M., 23
Menard, J., 470
Mendelsohn, D. A., 175
Mendelsohn, M. H., 28, 53
Meneghelli, Barry, 116
Meneghelli, Barry J., 115
Menikoff, R., 36
Menzel, W. Paul, 251
Merkle, K. L., 475
Merminga, L., 411
Merrigan, M. A., 151
Mertz, C., 437
Messerli, Mark A., 289
Meyer, DArcy Renee, 290
Meyer, George, 11
Meyer, M. K., 429
Mezei, F., 419
Michael, J. R., 80
Michael, J. V., 60
Michalek, Ted, 22
Michalske, T. A., 138
Michlich, B. J., 434
Mickler, David, 187
Micklich, B., 390
Miglionico,, 416
Mikaelian, K. O., 75
Miley, H. S., 452
Miller, A. W., 104
Miller, D., 77
Miller, D. J., 79, 446, 471, 474
Miller, G. G., 57
Miller, M. E., 386
Miller, Robert J., 14
Miller, S. L., 131, 136
Miller, Scott R., 324
Millot, F., 115
Mills, A. P., 411
Milne, B., 367
Milonni, T., 426
Milos, Frank S., 63
Milovich, J. L., 142
Milton, S. V., 385
Minami, T., 96
Minard, R. D., 275
Minard, Robert D., 276
Minier, L. M., 88
Minnervini, L., 470
Mintz, M., 102
Mintz, M. M., 102
Miralles, C., 209
Mirick, Paul H., 2
Mirkarimi, P. B., 76
Mironova, M., 474
Mitchell, A. R., 101
Mitchell, J. F., 471, 474
Mitsuishi, K., 484
Miyakawa, N., 480
Miyamoto, Michael M., 271
Mizell, Carolyn A., 18
Mizunaga, H., 126
Mkhitarian, L. S., 68
Moch, S., 497
Mock, R. C., 461
Modine, N. R., 457
Moehs, D. P., 390
Moersch, Jeffrey E., 304
Moffat, H. K., 357
Mohammadi, B., 149
Mojzsis, Stephen J., 319, 331
Mol-Dijkstra, J. P., 216
Molina, A., 113, 114, 231
Mollock, G. N., 62
Molvik, A. W., 205
Monroy, Carlos, 156
Montague, S., 136
Montalyo, Michael L., 8
Montano, P. A., 475
Montcalm, C., 76, 155
Monteiro, O. R., 92
Montero, Ruben S., 365
Montgomery, Leslie, 264
Montgomery, Richard, 264
Moon, S. J., 162, 451
Moore, C. B., 62
Moore, William B., 303
Moran, James Joseph, 287
More, R. M., 150

Moreau, Stephane, 239
Morel, J. E., 434
Moreshead, W., 444
Morgan, G., 302
Morgan, M. D., 484
Morgan, S., 266
Morgan, S. B., 4
Moriarty, J. A., 472
Moroz, P. E., 468
Morris, G., 110
Morris, Penny A., 285, 291
Morris, W. L., 92
Morrison, S. E., 505
Morrow, Daniel, 127
Morse, Andy, 302
Morse, J. D., 197
Morss, L. R., 27, 398
Moschetti, T. L., 428
Moser, W. R., 103
Moses, Donald, 8
Moses, G. A., 147
Moses, R. R., 160
Mourad, P., 234
Mouser, R., 455
Mouser, R. P., 445
Moxom, J., 411
Moyeda, D. K., 114
Muccino, Julia C., 284
Muehlhauser, J. W., 209
Mueller, C., 44
Mueller, K. T., 275
Mulligan, J. B., 262
Mumm, D. R., 92
Munoz, Ricardo C., 250
Munsat, T., 470
Muradov, N., 105
Murphy,, 442
Murrah, Michael R., 369
Musick, C. A., 93
Myers, D., 196
Myers, W. Neill, 25
Mynick, H. E., 460

N

Naberejnev, D. G., 429
Nagabhushana, N., 90
Nagasubramanian, G., 198, 207
Nagy, E., 397
Nahum, Laila, 277
Nakotte, H., 382
Nandi, S., 395
Narasimhan, T. N., 149, 188
Natesan, K., 83
Natsagdorj, L., 195
Natschke, D., 32
Navarro, J. P., 124
Navidi, M., 261
Nayfeh, Jamal, 24
Naylor, Guy R., 18
Nealson, K. H., 295
Nealson, K., 315
Nealson, K. H., 295
Nealson, Kenneth H., 305
Nealson, Kenneth L., 283
Necker, G. A., 44
Negri, M. C., 62
Neiderman, E. C., 266
Neil, G., 456
Neil, G. R., 457, 459
Neitzel, D. A., 193
Nelkin, Eric, 225, 234, 256
Nellis, W. J., 53
Nellums, B., 130
Nelson,, 175
Nelson, J. K., 158
Nelson, L. S., 112
Nelson, P. A., 207
Nelson, S. D., 498
Nelson, W. H., 395
Nerad, T. A., 321
Netter, J., 37
Neumark, D. M., 62
Nevins, M. R., 359
New, K., 527
New, Michael H., 276
Newman, Dava J., 264
Newton, E. M., 283
Newton, M., 43
Nguyen, J. H., 235
Nguyen, T. D., 39, 47
Nicholas, K. M., 105
Nichols, B. D., 44
Nichols, R. L., 212
Nicholson, J., 453
Nicol, A. C., 49
Nieh, T. G., 75
Nieman, R. A., 313
Nigam,, 439
Nikitenko, V. I., 446
Nilsen, J., 162
Nilsson, Martin, 275, 277
Nilufer, I. B., 31, 92
Nishiizumi, K., 527
Nitzel, M. E., 184
Nixon, D. D., 352
No, J., 367
Noffke, Nora, 332
Nogues, J. L., 444
Nolting, F., 140
Noon, C. E., 111
Noonan, Kevin W., 2
Norem, J., 393, 408
Norman, M. R., 486
North, M. J., 366
Northam, E. T., 212
Novotny, P. M., 80
Nowroozi, A. A., 181
Nuckolls, J., 531
Nugent, K. A., 447
Nystrand, J., 401
Nystrom, Charles O., 168

O

O, 38, 143, 144, 308, 405, 428
OConnor, Cornelius J., 3
ODay, Peggy, 270
ODay, Peggy A., 284
Odell, Garrett M., 327
Oertel, J., 148
Ohlhausen, J. A., 33
Ohmoto, Hiroshi, 320, 334, 338, 340, 341
Okamoto, P. R., 75, 91
Oldaker, M. E., 466
Olendzenski, Lorraine, 281, 333, 351
Olevsky,, 33
Oliver, B., 79, 407
Olsen, Mark A., 222
Olsen, R., 228
Olsen, R. W., 494
Olsen, T. L., 208
Olson, K., 204
Olsson, Bertil, 347, 351
Olsson, R. J., 143
Omenetto, F., 454
Ono, M., 470
Ono, Shuhei, 334
Ooguri, H., 499
Orasanu, Judith, 263
Orphan, Victoria J., 282
Orr, J. C., 249
Osbourn, G. C., 23
Osgood, R. M., 489
Osterheld, A. L., 162
Osterwald, C., 196
Ottens, Andrew K., 20
Otvos, J. W., 108
Overpeck, J. T., 179
Owen, D., 475

Owusu, Y., 74
Ozawa, M., 52

P

Pace, F., 124
Pace, J. C., 256
Pace, Norman R., 282, 284, 294, 298
Pack, R. T., 418
Padro, C. E. G., 101
Paez,, 176
Paez, T. L., 377
Page, P., 409, 506
Page, P. R., 425
Page, R. H., 162
Pagoria, P. F., 101
Paige, F. E., 397
Palfey, W., 41
Palmer, Richard L., 266
Palmiotti, G., 390
Panagiotopoulos, A. Z., 31
Panek, J., 480
Papadopoulos, P. E., 153
Papka, M. E., 143
Pardo, R. C., 390
Pardyjak, E. R., 210, 231
Parikh, Stavan M., 365
Parish, T. A., 420
Parizzi, A. A., 503
Park, Chul, 239
Park, I. J., 156
Parker, D., 120
Parker, G., 478
Parker, J. K., 74
Parkhutik, V., 482
Parks, R. C., 262
Parrish, Clyde F., 529
Parsa, Z., 398, 411, 414, 423, 424, 483
Parsignault, D. R., 491
Parson, E. A., 241
Pascucci, V., 364
Paskoff, Glenn, 263
Patten, Brian M., 522
Patterson, D., 321
Patterson, David J., 352
Patterson, Emily S., 519
Patterson, Michael J., 26
Patton, J. M., 149
Paulius, L. M., 143
Pautz, J., 97
Pavlov, Alex A., 329
Pavlov, Alexander, 334
Payne, J. E., 484
Payne, Meredith C., 313
Payne, S. M., 184
Pearlstein, L. D., 462
Pearson, J. E., 79
Peebles, D. E., 33
Peet, A. W., 499
Pegion, P., 237
Pehl, J., 121
Peikrishvili, A. B., 34
Pelfrey, Joy W., 118
Pellin, M. J., 524, 526
Peltier, W. Richard, 234
Penfield, Robin, 276
Penner, J. E., 210
Pennington, D., 160
Pepin, J. E., 174
Percus, A., 373
Perez-Mendez, V., 156
Perkins, L. J., 468
Perkins, S., 223, 354
Perlado, M. J., 43
Perry, F. V., 179
Perry, M. D., 421
Perry, R. L., 417
Perry, Randall S., 291
Pershing, D. W., 113, 114, 231
Persily, A. K., 119
Peters, Wanda C., 84
Peters, Warren, 25
Peterson, D. W., 131
Peterson, L. C., 179
Peterson, L. N., 224
Peterson, P. A., 160
Peterson, R. R., 147
Petitt, G. A., 395
Petrasso, R., 396
Petrini, F., 371
Pfarr, Thomas, 522
Pfeifle,, 236
Phaf, L., 505
Phelps, Angela M., 350
Phillips, C. K., 470
Phillips, L., 36
Phillips, Roger J., 308
Piers, M. A., 4
Pierson, Beverly K., 335
Pikaar, A. J., 4
Pikin, A., 424
Pilewskie, Peter, 347
Pillinger, Colin T., 302
Ping Wang, G. A., 160
Piotrowska, A., 492
Pisharody, M., 382
Piwonka, T. S., 74
Pizzarello, S., 313
Pizzarello, Sandra, 311
Plaia, G., 258
Platnick, Steven, 251
Plescia, J. B., 292
Plescia, Jeffrey B., 287
Plohr, Bradley J., 154
Plotkin, S., 103
Plummer, D. W., 457
Podio, A. L., 100
Pohorille, Andrew, 276
Polansky, G., 431
Poli, Paul, 9
Poling, Laura L., 336
Pollaine, S. M., 53
Pollock, Bob, 371
Pollock, E. I., 482
Polosky, M., 361
Polosky, M. A., 452, 457
Pomphrey, N., 462
Poola, R., 214
Poola, R. B., 213
Poole, B. R., 384
Popa Radu, 305
Pope, B. G., 475
Popowski, P., 525
Porter, G. D., 463
Porter, K., 109
Portzer, J. W., 100, 109
Post, Todd, 507
Poston, D. I., 24
Pouchon, M., 83
Povitsky, Alex, 146
Power, J. G., 139, 408
Powers, Charles E., 84
Powers, Janet V., 351
Praine, Ian, 302
Prasad, M. K., 142
Prasad, R., 396
Prelec, K., 424
Price, G. L., 53
Prieto, Manuel, 365
Prime, M., 42, 82
Pringault, Olivier, 287
Prinja, A. K., 434
Priscu, John C., 288
Pritchett, J. W., 191
Probasco, K. M., 190
Prokop, H., 387
Pruess, K., 47
Prufert-Bebout, Lee, 293
Purdom, J., 244
Putsche, V., 101

Q

Qi, N., 396
Qiang, J., 504
Qiant, J., 428
Quinlan, D., 358
Quinn, P. J., 521
Quirk, J. J., 360
Qzyuzer, L., 480

R

Rabbette, Maura, 347
Rabbiolo, G., 364
Rabehseifner, R., 356
Rabitz, H. A., 246
Racine, Stephen C., 66
Radakovich, Jon D., 225
Rader, D. J., 143
Radford, D., 518
Radousky, H., 161
Ragsdale, Stephen W., 271
Rahimian, K., 29
Rakos, C., 111
Ramachandra, A. M., 103
Raman, S., 420
Ramanathan, V., 245
Rambo, P. W., 467
Ramdas, A. K., 472
Randeria, M., 486
Ranganathan, R., 144
Rao, Gopalakrishna M., 205
Rao, K. R. P. M., 64
Rasmussen, Steen, 275, 277
Rath,, 236
Rath, J. S., 100
Rathke, J. W., 193
Raymond, Jason R., 336
Razani, A., 122
Rbinett, R. D., 371
Re, Richard J., 1
Read, M. E., 387
Reagor, D., 127, 128
Reass, W., 402
Reaugh, J. E., 93
Red-Horse, J. R., 377
Redi, M. H., 460, 462
Reece, C., 416, 427, 459
Reedy, E. D., 175
Reel, J. T., 183
Rees, D., 410, 432
Regan, A., 488, 505
Regan, J. J., 60
Rehn, L. E., 72
Reichardt, Jens, 220, 247
Reichardt, Susanne, 220, 247
Reid, R. S., 151
Reifman, J., 129
Reimers, C. E., 257
Reinhardt, C. E., 162
Reinig, W. C., 172
Reis, James E., 522
Reitze, D. H., 52
Remer, Lorraine, 187
Remington, B. A., 75, 488
Ren, Z. F., 489
Renne, D., 196
Resasco, D. E., 105
Reynolds, Amanda C., 337
Reynolds, J. L., 188
Reynolds, K. M., 373
Rezmer, R., 393
Ricardo, Alonso, 314
Richardson, J. W., 52
Richmann, M. K., 27
Rieck, C. T., 484
Rieck, T., 83
Rienecker, Michele M., 259
Rifflet, J. C., 115
Riggs, George A., 241
Rihs, S., 81
Riley, Monica, 274, 275, 277
Ringelberg, D., 48
Rish, J. W., 130
Ritschard, R., 189
Rivera, Eugenio J., 521
Rivers, Natale A., 11
Rivers, Robert A., 11
RizwanUddin,, 147
Roach, D., 10
Robbins, L. L., 316
Roberts, C., 495
Roberts, C. D., 497, 498
Roberts, G. W., 109
Roberts, R. S., 417
Robertson, I. M., 72
Robertson, Michael P., 277
Robin, D., 401
Robinett, R., 372
Robino, C. V., 80
Robinson, C. F., 537
Robinson, J., 520
Robinson, J. A., 33
Robinson, M. A., 430
Rocha, L., 518
Rochez, J. C., 100
Rock, D. R., 235
Rock, D. T., 147
Roco, M. T., 492
Rodacy, P. J., 36
Rodriguez, E. A., 174
Rodriguez, N., 284
Rodriguez, S., 472
Rodrique, G., 161
Roehlsberger, R., 72
Rogers, D., 244
Rogers, J. H., 208
Rogers, M. L., 157
Rognlien, T. D., 463
Roh, Yul, 297
Rohay, A. C., 193
Rohlev, T., 136
Romero, T., 39
Roos, A., 111
Rosato, D. A., 32
Rose,, 457
Rose, E. A., 415, 439
Rosenfield, J. E., 238
Rosenzweig, J., 465
Rosenzweig, J. B., 497
Ross, David S., 273, 278
Ross, E. D., 212
Ross, S., 23, 487
Rote, D. M., 98
Roth, E. P., 198, 207
Roth, Emilie M., 519
Roth, T. C., 112
Rothe, R. E., 443
Rothschild, Lynn, 288
Rouanet, S., 84
Rountree, F. H., 79
Roussel-Dupre, D., 16
Rowe, A., 446
Roy, A. K., 70
Roybal, W., 410, 441
Royston, T. J., 451
Rozanov, A. Yu., 352
Rubenchik, A. M., 421
Rubenchil, A. M., 448
Rubin, J., 34
Rubin, M., 95
Ruby,, 206
Ruckert, T., 72
Rudy, C., 172
Ruffner, J. A., 138
Ruhl, H. A., 183
Ruhl, R. C., 208
Runnegar, Bruce, 337, 340
Runnegar, Bruce N., 330
Ruprecht, W., 69
Ruscic, B., 48
Russell, B. J., 98
Russell, James M., III, 238
Russell, M. J., 184
Russell, S., 441

Rutishauser, David K., 3
Ruzic, D. N., 389
Ryan, E. A., 481
Ryan, J. V., 216
Rybarcyk, L., 433, 438
Rybicki, N. B., 183
Ryckman, S. J., 222
Ryne, R., 504
Ryutov, D. D., 463, 467

S

Sabine, C. L., 257
Saboungi, M. L., 115
Sackos, J., 130
Sacks, E., 132
Sadler, M. E., 404
Saggese, S., 404
Saghatelian, Alan, 267, 278
Sahai, V., 144
Salama, K., 474
Salian, U., 46
Salinger, A. G., 141
Salleo, A., 447
Salomonson, Vincent V., 241
Saloniemi, H., 31
Samuelson, B. C., 459
Sanders, F., 157
Sandford, Scott A., 267, 348
Sandi, G., 195, 196
Sangster, T. C., 466
Sanishvili, R., 473
Santavicca, D. A., 164
Santini, D., 103
Santini, D. J., 211
Santoro, R. J., 45
Santoro, R. T., 67
Sanzo, D. L., 3
Sarathi, P. S., 42
Saricks, C. L., 98, 102, 211
Sarmiento, J. L., 257
Sarofim, A. F., 113, 114, 231
Sarrack, A. G., 169
Sastri, S., 32
Sauter, Barbara J., 362
Sawamura, S., 47
Sawvel, A., 48
Scalettar, R. T., 482
Scapa, Victor, 335
Schaefer, T., 506
Schafer,, 495
Schalm, K., 496
Scharer, J. E., 465
Scharnberg, K., 484
Schein, J., 396
Schelble, Rachel T., 304
Schenck, C. C., 160
Schendel, J., 275
Schikore, D. R., 364
Schindler, Trent, 351
Schlottmann, P., 423
Schlueter, J. A., 493
Schmid, G., 500
Schmidlin, F. J., 212
Schmidt, G., 524
Schmidt, R. D., 101
Schmidt, T., 450
Schmitt,, 58
Schneider, D., 420
Schneider, J., 504
Schneider, S., 85
Schneider, Steven J., 26
Schoeberl, M. R., 238
Schoeler, A., 200
Schoessow, P., 139, 408
Schoessow, P. V., 497
Scholes, B. A., 93
Scholl, A., 140
Schoonen, Martin, 268
Schoonen, Martin A. A., 276
Schrage, D., 140
Schrock, V. E., 146
Schroder, S., 321
Schror, H., 72
Schubert, Siegfried, 247
Schubert, Siegfried D., 237
Schubert, W. K., 88
Schulz, Mark J., 374
Schulze, M., 402
Schuur, C., 393
Schwartz, S., 449, 455
Schwartz, S. E., 245
Schwarz, J. H., 499
Schweitzer, Mary, 314
Scott, B. A., 367
Scott, James, 266
Scott, James H., 294, 306
Scott, T. L., 386
Seama, Nobukazu, 296
Seaman, Nelson L., 250
Sears, S. Kelly, 297
Seeger, P. A., 507
Seidl, P., 412
Seifert, S., 51
Sekar, R., 213
Selkowitz, S. E., 95
Sellers, C., 97
Sellyey, W., 410
Selvamanickam, V., 485
Semones, E., 382
Sena, J. T., 151
Seo, J. W., 140
Seppala, L. G., 450
Sereno, N. S., 385, 500
Sergatskov, D. A., 80
Serkland, D. K., 131
Serre, S. D., 215
Sessler, A. M., 400, 403
Settle, T., 62
Seyfried, William E., 323
Sezgen, O., 204
Sglavo, M., 95
Shack, W. J., 70
Shadoan, Michael, 25
Shadwick, B. A., 403
Shaeffer, D. L., 235
Shaffer, F., 141
Shagam, R. N., 452
Shah, N., 126
Shah, Pinakin M., 205
Shahnam, M., 141
Shaltout, R. M., 42
Shannon, J., 224
Shao, Y., 414, 483
Shao-Horn, Y., 194
Shapiro, A. B., 144
Shapiro, M. D., 397
Shapouri, H., 108, 109
Sharirli, M., 3
Sharma, Anurag, 266, 294
Sharpley, R. C., 182
Shastry, V., 82
Shavers, C., 354
Shaw, M. J., 142
Sheehan, J., 109
Sheehan, L., 451
Sheehan, L. M., 383, 449
Sheffield, R., 504
Sheldon, M. S., 114
Shelton-Davis, C., 437
Shen, Z. X., 391
Shender, Barry S., 263
Shephard, M. S., 359
Shepherd, J. E., 360
Sherby, O. D., 73
Sherman, M. H., 149
Shestakov, A. I., 142
Shie, Chung-Lin, 234, 256
Shields, E. P., 275
Shields, K. D., 211
Shin, Jong-Yeob, 145
Shirkey, Richard C., 362
Shirron, P. J., 480
Shock, Everett L., 290

Short, S. M., 51
Shorter, J. A., 246
Shoura, M. M., 510, 514, 515
Shu, Chi Wang, 377
Shu, D., 451
Shul, R., 117
Shul, R. J., 457
Shuryak, E., 506
Sickafus, K. E., 470
Silberglitt, R., 203
Silk, J., 525
Silva, L. J., 101
Silver, B., 261
Sim, J. W., 360
Simmons, D. F., 137
Simmons, Rickey C., 7
Simon, H., 361
Simon, Horst, 371
Simon, R., 361
Simpson, A. G. B., 321
Sims, Mark R., 302
Sinclair, D. K., 505
Sindelar, A., 203
Singh, A., 510, 511, 512, 513, 514, 515
Singh, M., 102
Singh, S., 511
Singleton, Jeffrey D., 2
Sinha, S. K., 479
Sinha, Surajit, 279
Sisterson, D. L., 214, 244
Sivasambu, M., 41
Sivils, L., 34
Skidmore, J., 162
Slade, B. E., 123
Slattery, D., 105
Sleep, Norman H., 323
Slenes, K., 39
Sliger, R. N., 67, 229, 230, 232
Slingo, J. M., 244
Slinsky, S., 108
Slutter, C. L., 357
Smallwood, D. O., 176
Smirnov, Alexander, 211
Smith, A. B., 389, 440
Smith, A. E., 222
Smith, A. T., 192
Smith, B. F., 1, 353, 358
Smith, D., 393
Smith, D. D., 203, 485
Smith, D. J., 383
Smith, D. L., 429, 434
Smith, David E., 530, 531
Smith, Dennis A., 137, 157
Smith, Eric A., 254
Smith, G. S., 96
Smith, J., 208, 497
Smith, J. L., 72
Smith, K., 223
Smith, Kerry S., 336
Smith, L. E., 496
Smith, M. S., 518
Smith, Norman D., 168
Smith, Peter J. S., 289
Smith, W., 62
Snelgrove, J. L., 429
Sniegowski, J. J., 117, 139
Socolovsky, E. A., 509
Soderlind, P., 46, 472
Soderqvist, J., 397
Sogin, Mitchell L., 300
Sogin, M. L., 321
Sogin, Mitchell, 282
Sogin, Mitchell L., 286, 289, 296, 299, 352
Solomon,, 137
Soltani, Kathy, 267, 278
Somieski, B., 411
Sommargren, G. E., 388
Sommeijer, B. P., 379
Song, Inseok, 348
Sonnendrucker, E., 399
Sorrels, L., 155
Sorroche, E. H., 33
Sosman, L. P., 472
Sotirchos, S. V., 35
Souers, P. C., 51
Southam, Gordon, 311
Southworth, G. R., 186
Southworth, S. H., 399
Sowers, C. H., 486
Spangler, Lee, 38
Sparks, David L., 25
Spath, P. L., 99
Spear, John R., 294
Spencer, B. W., 438
Spencer, Mark N., 532
Sperber, K. R., 244
Spiller, E., 155
Spinhirne, James, 232, 254
Spinka, H., 409, 479
Spivey, J. J., 56, 108
Spoor, P. S., 418
Spore, J. W., 44
Srinivas, S., 46
Stafford, Sherry L., 338
Staggs, K., 43
Stahl, D. A., 282
Staley, James T., 291
Stalker, J. R., 245
Stanford, John L., 222
Stanford, S. A., 524
Stanish, T. K., 52
Stantz, K. M., 371, 372
Staples, B. A., 93
Stapp, H., 502
Starr, David OC., 247
Starr, Stan, 508
Starr, Stanley O., 25
Starrfield, S. G., 524
Stauffer, David R., 250
Stavig, M. E., 175
Stead, R., 126
Steciak, J., 119
Steele, A., 339
Steele, Andrew, 314
Steele, R. A., 444
Steele, W. A., 444
Stein, Brian, 205
Steiner, R., 76
Stelling, P., 170
Stemmer, S., 90
Stence, J., 124
Stenholm, Ingrid, 452
Stephens, G. L., 155
Stephens, T., 491
Sterling, J. P., 36
Stewart, Brian W., 337, 338
Stewart, J. E., 420
Stewart, Jenny, 302
Stickney, B. L., 203
Stiegel, G. J., 94
Stocco, Karen, 351
Stockert, T. D., 356
Stodolsky, F., 98, 223
Stoeffl, W., 429
Stohr, J., 140
Stolbov, S., 474
Stolz, C. J., 383, 386, 446, 449
Stone, C., 358
Stone, D., 461
Stone, L. S., 262
Storey, B. G., 90
Stork, K., 102, 214
Storrie-Lombardi, M. C., 295
Stout, M., 78
Strahan, Susan E., 231
Straight, Christian, 265
Strain, B. R., 219
Strain, R. V., 429
Strangeway, Robert J., 528
Street, R., 151
Streets, D. G., 199
Streiffer, S. K., 90
Streletz, G. J., 366
Strohmayer, Tod E., 537

Stronach, S. L., 127
Stubbins, J. F., 75
Stuckey, J., 91
Stulen, R., 158
Sturchio, N. C., 81, 102
Sturge, M. D., 489
Styf, Jorma R., 263
Suarez, M., 237
Suewattana, M., 460
Sugita, Seiji, 274
Sui, C.-H., 240
Sui, Chung-Hsiung, 259
Suits, Neil S., 329
Sula, M. J., 211
Sullivan, C. T., 452
Sullivan, R., 95
Sullivan, Z., 505
Sumait, N., 217
Suman, A. W., 166
Sumant, A., 93
Summons, Roger E., 279, 283, 323, 326
Sun, H., 295
Sun, J., 144, 234
Sun, X., 152
Sund, R., 465
Sundaram, V., 484
Sundaresan, Mannur J., 374
Sundelin, R., 36, 427
Suratwala, T., 443
Suratwala, T. I., 444
Surdam, R. C., 185
Surek, T., 194
Surh, M., 462
Surma, Jan M., 529
Suszcynski, D. M., 249
Suszcynsky, D., 252
Suuberg, E. M., 56
Suzuki, S., 52
Swanson, Ted, 22
Sweby, P. K., 379
Sweeney, D. W., 158
Sweeney, J. J., 178
Sweet, J. N., 131
Swider, W., 491
Swift, G. W., 418
Switzer, Christopher, 279
Syn, C. K., 73
Sze, D. K., 393
Szostak, Jack W., 269, 272, 273, 276
Szostak, R., 65
Szymanski, M., 143

T

Tabak, M., 467
Taha, H., 226
Tait, T., 387
Takabatake, T., 382
Takacs,, 444
Takahashi, K., 47
Tallant, D. R., 207
Tallerico, P., 432
Talou, P., 441
Tam, S. W., 84
Tamames, Javier, 279
Tannenbaum,, 418
Tanner, D. B., 52
Tanre, Didier, 187, 251
Tarasov, Lev, 234
Tarver, C. M., 49, 50, 169
Tavares, A. D., 472
Taylor, A., 454
Taylor, C. J., 224
Taylor, Craig D., 285
Taylor, J. A., 249
Taylor, J. R., 448
Taylor, S. E., 108
te Riele, H. J. J., 353
Temple, R. D., 415, 439
ten Dam, A. A., 372
Teng, H., 81
Teo, K. L., 481
Teresco, J. D., 359
Terry, D. J., 363
Teske, Andreas, 286
Teske, Andreas P., 285, 296
teVelthius, S. G. E., 478
Thacker, B. H., 174
Thacker, H., 498
Thakur, R., 367
Theiler, J., 355
Thiemens, Mark H., 311, 322
Thies, M. C., 95, 113
Thissell, W., 77
Thiyagarajan, P., 45, 52, 85, 507
Thomas, G. J., 494
Thomas-Keprta, Kathie, 291, 297, 312
Thomas-Keptra, Kathie L., 318
ThomasKeptra, Kathie L., 304
Thompson, A. M., 218, 221, 222
Thompson, Amanda S., 328
Thompson, D., 458
Thompson, E. L., 32
Thompson, G. E., 58
Thompson, J., 419
Thompson, J. S., 230
Thompson, L. J., 475
Thompson, Louis J., 443
Thompson, P. A., 130
Thompson, Robert Earl, 238
Thomson, J. Michael, 280
Thorsmolle, V., 468
Throop, Henry, 345
Thurman-Keup, R., 390
Tiarenko, Y., 406, 427
Tice, Michael M., 339
Tidman, Derek A., 16
Tiede, D., 45
Tiegs, T. N., 166
Tielens, A. G. G. M., 250
Tikare,, 33
Tipei, S., 417
Tiszauer, D., 117, 446
Tiszauer, D. H., 178
Tobola, Kay, 351
Todreas, N., 440
Tokarcik-Polsky, S., 153
Tolbert, Margaret A., 306
Tom, H., 161
Tomlinson, E. T., 153
Tomlinson, H. L., 98
Tompson, S. R., 517
Toon, Owen B., 306
Toonen, B., 123
Toor, A., 467
Toporski, J., 339
Torczynski, J. R., 143
Torres, L. L., 93
Towne,, 408
Townsend, Jacqueline A., 84
Trahan, M. W., 371, 372
Tran, T. N., 120
Travis, J. R., 44
Travish, G., 447
Traylor, Ryan M., 23
Tree, D. R., 65
Treiman, Allan H., 315
Trejo, Leonard J., 264
Trenholm, A. R., 216
Trexler, E. C., 224
Trottier, C., 435
Trowbridge, L. D., 54
Truchan, T. G., 79
Trujillo, E., 77
Tsapin, A., 315
Tsimring, L. S., 150, 186
Tsoukalas, L. H., 129
Tsunoda, S. I., 124
Tuck, Adrian F., 269
Tucker, B. J., 185
Tucker, George E., 7
Tuecke, S., 123

Tufo, H. M., 143, 353
Tunnell, T. W., 157
Turiel, I., 378
Turner, C., 121
Turner, L., 152
Tuttle, J. G., 480
Tyree, L., 206

U

Uccellini, L., 244
Udranszky, Ingrid, 326
Underwood, D., 392, 409
Unser, Leslee, 350
Urabe, Tetsuro, 296
Ural, E. A., 46
Uras, R. A., 172
Urban, V., 45
Urtiew, P. A., 50
Utterback, E. J., 162
Uttiew, P. A., 169

V

Vaca-Cortes, E., 57
Vaida, Veronica, 269
Vaidya, S., 158
Valachovic, T., 435
Valdez, P. F., 417
Valdiviez, R., 402
Valencia, Alfonso, 280
Valentine, G. A., 179
Valeo, E., 464
Valero, F. P. J., 245
Vali, Hojatollah, 297
van Brummelen, E. H., 146
van de Sluis, E., 372
van der Houwen, P. J., 379
van der Poorten, A. J., 353
van der Veen, W. A., 360
van Hees, W. W. S., 183
Van Mechelen, G., 117
van Sterkenburg, R. P., 372
VanCleave, K. A., 316
vanDam, Cornielious P., 11
Vandemark, Douglas, 234
VanHook, W. A., 88
Varadi, Ferenc, 340
Varnai, Tamas, 251
Vasile, M. J., 118
Vassilevski, P. S., 375
Vaughey, J., 199
Vawter, G. A., 454
Vay, J. L., 412
Vazquez, L., 285
Veers, P. S., 207
Veil, J. A., 118, 200
Velbel, Michael A., 318
Vella, M., 498
Vengosh, A., 179
Venkatapathy, E., 153
Vianco, P. T., 85
Vlasko-Vlasov, V. K., 446, 471
Vogel, C. A., 32
Vogelsonger, Ken, 270
Vohra, Y. K., 387
Von Gunten, M. K., 383, 386
Vondrasek, R., 390
VonWittenau, A., 461
Vossebeld, J., 496
Vyas, A., 102

W

Wagner, J. S., 372
Wagner, R., 393
Wai, C. M., 101
Wainwright, Norman R., 316
Wait, J., 177
Waldhoff, S. T., 199
Walker, Jeffrey J., 298
Walker, R., 502
Walker, R. B., 418
Walkington, P., 10
Walsh, M. A., 473
Walsh, M. E., 108
Walter, B., 178
Walter, Malcolm R., 319, 323
Walters, Robert W., 376
Walther, Jens, 490
Walton, J. J., 210
Walvoort, D. J. J., 181
Wambsganss, M. W., 120, 165
Wang,, 416
Wang, Daniel Y.-C., 328
Wang, F., 400
Wang, H. F., 180, 403
Wang, H. H., 493
Wang, J., 301
Wang, J. H., 489
Wang, J. J., 156
Wang, M. Q., 195
Wang, P., 147, 148
Wang, S., 482
Wang, T., 427
Wang, T. F., 433
Wang, W. C., 242
Wang, X., 129, 199
Wang, X. J., 453
Wang, Y., 488
Wang, Z., 389
Wangler, T., 503
Wangler, T. P., 433
Warmflash, David M., 317
Warne, L. K., 127
Warner, B. E., 30
Warren, S., 262
Warshaw, S. I., 235
Washburn, J., 491
Watanabe, Hidemi, 328
Watanabe, Yumiko, 340
Waters, L., 379
Wattson, Richard B., 532
Wayne, D., 76
Weakley, S. C., 386
Weaver, F. J., 121
Webb, D. J., 86
Webb, Rich, 348
Weber, D. P., 147
Weber, E. R., 481
Weddendorf, Bruce, 167
Wedowski, M., 155
Wegner, P., 455
Wehe, D. K., 496
Wehrey, M., 206
Wei, D., 51
Wei, J., 400
Wei, T. Y. C., 129
Weinberg, Dana, 281
Weinzierl, S., 505
Weir, J. T., 499
Weir, R. J., 100
Weisgerber, W., 46
Weiss, R. F., 258
Welton, Judd, 232, 254
Wenski, E. G., 164
Wentworth, Sue, 312
Wentworth, Susan J., 285, 291, 311, 318
Werder, Thomas, 490
Werin, S., 159
Wesely, M. L., 180
West, T. O., 228
Westall, F., 339
Westall, Frances, 304
Wetherill, George, 349
Whalen, R. T., 261
Wheat, H. G., 57
Wheeler, D. R., 42
Wheeler, M. F., 183
White, A. R., 421
White, C. W., 411
White, J. T., 396
White, R. B., 460, 469, 470

Whitehead, J., 531
Whiteman, David N., 243
Whitestone, Jennifer, 369
Whitfield, R. G., 217
Whitman, P. K., 447
Whorton, M., 223
Wich, Mike, 263
Wiedenhover, I., 438
Wignarajah, Kanapathipillai, 220
Wijmans, J. G., 228
Wilbeck, J., 100
Wilbur, Matthew L., 2
Wilcoxen, Keith M., 281
Wilkerson, Stephen, 16
Wilkes, K. E., 121
Wilkins, Mark L., 154, 175
Willemse, R. C., 87
Willhite, G. P., 99
Williams, F., 59
Williams, G., 223
Williams, G. P., 137, 456
Williams, George J., Jr., 26
Williams, H. C., 353
Williams, M. D., 313
Willison, C. G., 117
Willit, J. L., 438
Wilson, C., 458
Wilson, Cindy L., 289, 298
Wimmer, S. A., 175
Wing, David J., 8
Winkleman, B. C., 495
Winkler, P., 460
Winter, V. L., 359, 371
Wirick, S., 268
Wirsen, Carl O., 285
Wiscombe, W., 252
Wiscombe, W. J., 253
Wiscombe, Warren, 247
Wiser, R., 109
Witte, J. C., 218, 221, 222
Wofsy, Steven C., 232
Wohlberg, C., 91
Wojtsekhowski, B., 415
Wolf, Alexander, 366
Wolf, Stephen W. D., 13
Wolff, Charles L., 534
Wolfire, M. G., 250
Won, M. C., 362
Wong, A., 26
Wong, C. C., 129
Wong, J. N., 448
Wood, L., 531
Wood, R., 433
Wood, Richard M., 2
Woodbury, K. A., 74
Woodle, M. H., 455
Woods, David D., 519
Woods, P. J., 426
Wooldridge, Eve M., 84
Workman, R. L., 395
Worland, V. P., 91
Worley, C., 62
Worsham, S. A., 117
Worsnop, D. R., 218, 219
Wright, A. F., 493
Wright, G. W., 494
Wright, Ian P., 302
Wright, L. L., 107
Wright, R., 107
Wu,, 163, 442
Wu, G., 36
Wu, K., 361, 367
Wu, Q., 153
Wu, Z. L., 386
Wunsch,, 137
Wuosmaa, A. H., 438, 502
Wurtele, J. S., 403
Wynn-Williams, D. D., 283

X

Xiang, Q., 45
Xiao, Shuhai, 330
Xie, D., 390
Xie, M., 399, 401, 466
Xie, S. C., 249
Xie, Z. Q., 400
Xu, J., 411
Xu, T., 47
Xu, W., 472
Xu, X., 396

Y

Yacout, A. M., 356
Yakimenko,, 442
Yakimenko, V., 453
Yakovenko, Y. V., 469
Yakuma, S., 117, 446
Yamada, M., 467
Yamaguchi, Kosei E., 341
Yan, M., 161
Yang,, 439
Yang, B. X., 432, 500
Yang, L. H., 462, 472
Yang, N. Y. C., 494
Yang, Ping, 220
Yang, R. T., 105
Yarus, Mike, 270
Yeager, William T., Jr., 2
Yee, H. C., 379
Yelin, B., 209
Yerganian, S. S., 134
Yio, J. J., 249
Yoder, Hatten S., Jr., 266, 269, 272
Yokobayashi, Yohei, 267, 278
Yokosawa, A., 409
Yost, Richard A., 20
You, H., 482
Young, Robert, 347
Yu,, 89, 163
Yu, C., 435
Yu, D. H., 144
Yu, P. Y., 481
Yun, W., 449
Yung, Yuk, 349
Yusuf, S. M., 489

Z

Zadoks, R. I., 376
Zahnle, Kevin, 323
Zaidi,, 206
Zaidi, S. H., 493
Zaluzec, N. J., 479
Zamansky, V. M., 114, 191, 192
Zare, Richard N., 267
Zarnstorff, M. C., 460
Zasadzinski, J. F., 480
Zavadil, K. R., 138
Zavorotny, Valery U., 189
Zeidman, B., 506
Zentai, G., 487
Zettler, L. A. Amaral, 284
Zettler, L. Amaral, 321
Zettler, Linda A. Amaral, 289, 299, 300
Zganjar, E. F., 427
Zhang, M. H., 249
Zhaxbayeva, Olga A., 281
Zhaxybayeva, Olga, 333, 342
Zhorin, V. V., 473
Zhou, C. Q., 28
Zhou, G., 69
Zhou, J., 110
Zhu, J., 488
Zhuang, H. Z., 425
Zhuang, Z. H., 436
Zielinski, M., 492
Ziemke, J. R., 229
Zika, M., 375
Zika, M. R., 375
Zimmerman, G., 161
Zimmerman, M. E., 530

Ziock, H. J., 206
Zoback, M. D., 188
Zoeller, J. R., 108
Zografos, A. I., 150
Zuber, Maria T., 530
Zuckerman, B., 347
Zuckerman, Ben, 348
Zurek, A., 177
Zurek, W., 526
Zweiback, J., 421
Zygmunt, S. A., 104
Zywicz, E., 39